



Cairo University



# Cairo University International Publications Awards



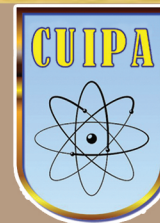
Vol. 8 ( 1 )

May 2014





Cairo University



# Cairo University International Publications Awards

**Vol. 8 Issue 1**

**May. 2014**





# International Publications Awards Cairo University



Issue	I	II	III A, B	IV A, B	V	VI A, B	VII	Vol. 5(1)	Vol. 5(2)	Vol. 6(1) A, B, C
Year	Sep. 2007	Dec. 2007	Oct. 2008	May 2009	Oct. 2009	May 2010	Oct. 2010	May 2011	Oct. 2011	May 2012



**Dear colleagues,**

We are pleased to introduce vol. 8(1) issue of the international publications of Cairo University. It is a further step and distinct contribution, reflecting the scientific ability of staff members, which conforms to international quality standards.

The purpose of issuing these publications is mainly to introduce this work to the academic community, demonstrate the different research abilities of CairoUniversity researchers, and encourage them to increase the quality and quantity of their research.

We would like to assure you that the administration will spare no effort to support and reinforce these goals.

We congratulate all colleagues who were granted the awards for their international publications of the year 2013 and wish them all the best for their future endeavors.

We are also pleased to inform you that this policy will continue to be in effect for the years to come.

.

**Prof. GamalEsmat**

**Vice - President for post-graduate  
studies and research  
Cairo university**

**Prof. GaberNassar**

**President  
Cairo university**



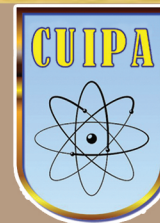
# *Table of Contents*

	Page
<b>Preface</b>	i
<b>1. Basic Sciences Sector</b>	1
1-1 Faculty of Science	3
1-2 Faculty of Agriculture	108
1-3 Faculty of Veterinary medicine	136
1-4 National Institute of Laser Sciences	163
<b>2. Engineering Sciences Sector</b>	183
2-1 Faculty of Engineering	183
2-2 Faculty of Computers and Information	229
2-3 Institute of Statistical Studies and Research	234
<b>3. Medical Sciences Sector</b>	247
3-1 Faculty of Medicine	247
3-2 Faculty of Oral & Dental Medicine	340
3-3 Faculty of Pharmacy	345
3-4 National Cancer Institute	421
3-5 Faculty of Physical Therapy	435
3-6 Faculty of Nursing	437
<b>4. Social Sciences Sector</b>	451
4-1 Faculty of Economics and Political Science	451
4-2 Faculty of Commerce	457
<b>5. Humanity Sciences Sector</b>	465
5-1 Faculty of Arts	465
5-2 Faculty of Archaeology	466
5-3 Faculty of Kindergarten	472
5-4 Institute of African Research and Studies	473
<b>Authors' Index</b>	482





Cairo University



# **(1) Basic Sciences Sector**

**1-1 Faculty of Science**

**1-2 Faculty of Agriculture**

**1-3 Faculty of Veterinary medicine**

**1-4 National Institute of Laser Enhanced Sciences**



CAIRO UNIVERSITY

Publication  
in  
Journals

## Faculty of Science

### Dept. of Astronomy and Meteorology

#### 1. World Meteorological Organization Assessment of the Purported World Record 58°C Temperature Extreme at El Azizia, Libya (13 September 1922)

Khalid I. El Fadli, Randall S. Cervený, Christopher C. Burt, Philip Eden, David Parker, Manola Brunet, Thomas C. Peterson, Gianpaolo Mordacchini, Vinicio Pelino, Pierrem Bessemoulin, José Luis Stella, Fatima Driouech, M. M. Abdel Wahab and Matthew B. Pace

*American Meteorological Society*, 94 (2): 199-204 (2013)  
IF: 6.591

On 13 September 1922, a temperature of 58°C (136.4°F) was purportedly recorded at El Azizia (approximately 40 km south-southwest of Tripoli) in what is now modern-day Libya. That temperature record of 58°C has been cited by numerous world-record sources as the highest recorded temperature for the planet. During 2010–11, a World Meteorological Organization (WMO) Commission of Climatology (CCI) special international panel of meteorological experts conducted an in-depth investigation of this record temperature for the WMO World Archive of Weather and Climate Extremes (<http://wmo.asu.edu/>).

This committee identified five major concerns with the 1922 El Azizia temperature extreme record, specifically 1) potentially problematical instrumentation, 2) a probable new and inexperienced observer at the time of observation, 3) unrepresentative microclimate of the observation site, 4) poor correspondence of the extreme to other locations, and 5) poor comparison to subsequent temperature values recorded at the site. Based on these concerns, the WMO World Archive of Weather and Climate Extremes rejected this temperature extreme of 58°C as the highest temperature officially recorded on the planet. The WMO assessment is that the highest recorded surface temperature of 56.7°C (134°F) was measured on 10 July 1913 at Greenland Ranch (Death Valley), California.

**Keywords:** Azizzia; Maximum temperature; International record.

#### 2. Deep Solar Minimum and Global Climate Changes

Ahmed Abdel Hady

*Journal of Advanced Research*, 4 (3): 209-214 (2013) IF: 3

This paper examines the deep minimum of solar cycle 23 and its potential impact on climate change. In addition, a source region of the solar winds at solar activity minimum, especially in the solar cycle 23, the deepest during the last 500 years, has been studied. Solar activities have had notable effect on palaeoclimatic changes. Contemporary solar activity is so weak and hence expected to cause global cooling. Prevalent global warming, caused by building-up of green-house gases in the troposphere, seems to exceed this solar effect. This paper discusses this issue.

**Keywords:** Deep solar minimum; Solar activity; Climate change; Global cooling.

#### 3. Special Issue on “Heliospheric Physics During and After A Deep Solar Minimum”

Ahmed Abdel Hady

*Journal of Advanced Research*, 4 (3): 2013 1-5 (2013) IF: 3.0

This Special Issue of the Journal of Advanced Research results from the third International Association of Geomagnetism and Aeronomy (IAGA) International Symposium organized in Luxor, Egypt, from 13 to 17 November 2011. The first IAGA Symposium was held October 5–9, 2008, in Cairo and addressed “Space Weather and its Effects on Spacecraft”. The second Symposium was also in Cairo, from 4 to 8 December 2009, and addressed “Solar Wind—Space Environment Interaction”.

**Keywords:** Heliospheric physics; Deep solar minimum.

#### 4. Some Aspects of the Urban Climates of Greater Cairo Region, Egypt

El-Sayed Mohamed Abdel-Hamid Robaa

*International Journal of Climatology*, 33 (15): 3206-3216 (2013)  
IF: 2.886

Rapid urbanization and industrialization over Greater Cairo Region (GCR), Egypt, have resulted in sharp land cover changes. Urban change not only impacts on land cover but also on urban climate. Detailed studies on the effect of urbanization and industrialization processes on climatic elements in GCR have been performed in this study. Five different districts were selected to represent rural, suburban, urban and industrial areas in GCR. The data of monthly mean values of minimum, maximum and mean temperatures, wind speed, relative humidity, cloud amount and rainfall amounts for the period (1990–2010) were used. The results revealed that, for each district, whenever urbanization and/or industrialization increase, the values of minimum, maximum and mean temperatures increase while the values of wind speed, relative humidity, cloud amount and rainfall amounts decrease. The effects of industrialization processes on the climatic elements were found stronger than the effects of urbanization processes. The greatest urban–rural climatic differences were found to be 5.9, 3.1, 3.9 °C, 3.6 kt, 13.9%, 1.1 octas and 7.0 mm for the minimum, maximum and mean temperatures, wind speed, relative humidity, cloud amount and rainfall amounts, respectively, while the greatest industrial–rural climatic differences were found to be 6.7, 4.3, 4.4 °C, 4.4 kt, 17.6%, 1.7 octas and 8.0 mm for the minimum, maximum and mean temperatures, wind speed, relative humidity, cloud amount and rainfall amounts, respectively.

**Keywords:** Urbanization; Industrialization; Urban climates; Temperature; Relative humidity; Wind speed; Cloud amounts; Greater Cairo region; Egypt.

#### 5. Calculating Isotope Concentrations Using Different Schemes of Dispersion Parameters

M. Abdel-Wahab, Khaled S. M. Essa, M. Embaby and Sawsan E. M. Elsaid

*Radiation Protection Dosimetry* 1-7 (2013) IF: 0.909

The investigated work aims to calculate the concentration of different isotopes through short downwind distances. A



theoretical model was designed to calculate the isotope concentration in the wind. The mathematical calculation depends on windspeed, decay distance and the dilution factor to get the concentration of isotopes ( $^{131}\text{I}$ ,  $^{133}\text{I}$ ,  $^{135}\text{I}$  and  $^{137}\text{Cs}$ ) detected in wind at different distances from a nuclear power station. There is a good agreement between the calculated and observed concentrations of  $^{131}\text{I}$ ,  $^{133}\text{I}$ ,  $^{135}\text{I}$  and  $^{137}\text{Cs}$ .

**Keywords:** Isotope concentration; Dispersion parameters.

## 6. Theorems on Null-Paths and Redshift

M. I. Wanas and A. B. Morcos

*Journal of the Korean Astronomical Society* 46: 97-102 (2013)  
IF: 0.909

In the present work, we prove the validity of two theorems on null-paths in a version of absolute parallelism geometry. A version of these theorems has been originally established and proved by Kermak, McCrea and Whittaker (KMW) in the context of Riemannian geometry. The importance of such theorems lies in their applications to derive a general formula for the redshift of spectral lines coming from distant objects. The formula derived in the present work can be applied to both cosmological and astrophysical redshifts. It takes into account the shifts resulting from gravitation, different motions of the source of photons, spin of the moving particle (photons) and the direction of the line of sight. It is shown that this formula cannot be derived in the context of Riemannian geometry, but it can be reduced to a formula given by KMW under certain conditions.

**Keywords:** Null-Geodesics; Riemannian geometry; Absolute parallelism Geometry; Null-Paths; Redshift.

## 7. A Pure Geometric Approach to Stellar Structure

M. I. Wanas and Samah A. Ammar

*Central European Journal of Physics*, 11: 936-948 (2013)  
IF: 0.905

The present work represents a step towards dealing with stellar structure using a pure geometric approach. A geometric field theory is used to construct a model for a spherically symmetric configuration. In this case, two solutions have been obtained for the field equations. The first represents an interior solution which can be considered as a pure geometric one in the sense that the tensor describing the material distributions is not a phenomenological object, but a part of the geometric structure used. A general equation of state for a perfect fluid, is obtained from, and not imposed on, the model. The second solution gives rise to Schwarzschild exterior field in its isotropic form. The two solutions are matched, at certain boundary, to evaluate the constants of integration. The interior solution obtained shows that there are different zones characterizing the configuration: a central radiation dominant zone, a probable convection zone as a physical interpretation of the singularity of the model, and a corona like zone. The model may represent a type of main sequence stars. The present work shows that Einstein's geometrization scheme can be extended to gain more physical information within material distribution, with some advantages.

**Keywords:** Stellar structure; Geometric field theories; Main sequence stars; Absolute parallelism geometry.

## 8. Maximum Crosswind Integrated Ground Level Concentration in Two Stability Classes

M. Abdel-Wahab, Khaled S. M. Essa, M. Embaby and Sawsan E. M. Elsaid

*Mausam*, 64 (4): 655-662 (2013) IF: 0.14

The advection diffusion equation (ADE) is solved in two directions to obtain the crosswind integrated concentration in neutral and unstable conditions. The solution is solved using Laplace transformation technique and considering the wind speed and eddy diffusivity depending on the vertical height. Also the ground level and maximum concentrations are estimated. We use in this model empirical data from Copenhagen (Denmark) to compare between predicted and observed concentration data.

**Keywords:** Advection diffusion equation; Neutral and unstable conditions; Laplace transform; Maximum and predicted normalized crosswind integrated concentrations.

## 9. Satellite Formation Control Using the Approximating Sequence Riccati Equations

Ashraf H. Owis and Morsi A. Amer

*Theory and Applications of Mathematics and Computer Science*, 3 (2): 103-113 (2013)

In this study we develop a reliable algorithm to control the satellite formation using the Approximating Sequence of Riccati Equations (ASRE) minimizing the fuel consumption and the deviation of the orbit from the nominal orbit. The nonlinear Clohessy-Wiltshire (CW) equations of motions are used to describe the motion of the satellite formation about a virtual reference position maintained at the formation center.

The nonlinear dynamics of the system will be factorized in such a way that the new factorized system is accessible. The problem is tackled using the Approximating Sequence Riccati Equations (ASRE) method. The technique is based on Linear Quadratic Regulator (LQR) with fixed terminal state, which guarantees closed loop solution.

**Keywords:** Nonlinear feedback; Linear quadratic regulator; Approximation sequence riccati equation; Satellite formation.

## 10. Solving the Nonlinear Feedback Optimal Control Problem of Satellite Formation

Ashraf H. Owis

*Nonlinear Studies*, 20 (3): 389-400 (2013)

In this paper we present a novel method of solving the nonlinear feedback optimal control of the satellite formation. To get the feedback law, the method of the solution is presented using a new closed loop feedback control algorithm for nonlinear system via dividing the time interval to a number of time steps and transforming the original nonlinear system to a quasi-linear system of state dependent coefficients. The technique is based on Linear Quadratic Regulator, (LQR) with fixed terminal state.

We solve the nonlinear feedback optimal control of the relative motion of satellite formation using the Approximating Sequence Riccati Equation, (ASRE) method.

The accuracy and efficiency of the control technique is verified through numerical simulation dedicated to the problem of the relative motion formation flying.

**Keywords:** Nonlinear; Feedback; Optimal; Satellite formation.

### 11. Acceleration and Particle Field Interactions of Cosmic Rays II: Calculations

Tawfik, A., A. Saleh, M.T. Ghoneim and A.A. Hady Ahmed Abdel Hady

*Physics International*, 4 (1): 2013: 29-36 (2013)

The Ultra High Energy Cosmic Rays (UHECRs) is still a one of the most controversial physical problems, especially that all potential acceleration mechanisms are not entirely able to explain the source of UHECR and their energy scale. Based on our generic acceleration model, that suggests different types of electromagnetic interactions between the cosmic charged particles and the different configurations of the electromagnetic (plasma) fields, UHECR are systematically analyzed. The plasma fields are assumed to vary, either spatially or temporally or both. In this approach, the well-known Fermi accelerations are excluded. But seeking for simplicity, it is assumed that the energy loss due to the different physical processes is negligibly small. The energy available to the plasma sector is calculated in four types of electromagnetic fields. It is found that the drift in a time-varying magnetic field is extremely energetic and the energy scale widely exceeds the Greisen-Zatsepin-Kuzmin (GZK) cutoff. We deduced that the polarization drifts in a time-varying electric field is also able to raise the energy of UHECR to an extreme value.

Thus, this type of generic mechanisms seems to be compatible with the Hillas mechanism. The drift in a spatially-varying magnetic field is almost as strong as the polarization drift. The curvature drift in a non-uniform magnetic field and a vanishing electric field is very weak. It is to be concluded that the studying cosmic charged particle interactions with the different aspects of the cosmic plasmas could be considered as intrinsic sources for UHECR and therefore a remarkable portion of the ultra high energies that are observed in the cosmic rays can be interpreted.

**Keywords:** Greisen-zatsepin-kuzmin (Gzk); Uhecr; Electromagnetic inter-actions.

### 12. Analytical Solution of the Perturbed Orbit-Attitude Motion of a Charged Spacecraft in the Geomagnetic Field

Hani M. Mohammed, Mostafa K. Ahmed, Ashraf Owis and Hany Dwidar

*International Journal of Advanced Computer Science and Applications (Ijacs)*, 4 (3): 272-286 (2013)

In this work we investigate the orbit-attitude perturbations of a rigid spacecraft due to the effects of several forces and torques. The spacecraft is assumed to be of a cylindrical shape and equipped with a charged screen with charge density  $s$ . Clearly the main force affecting the motion of the spacecraft is the gravitational force of the Earth with uniform spherical mass.

The effect of oblate Earth up to  $J_2$  is considered as perturbation on both the orbit and attitude of the spacecraft, where the attitude

of the spacecraft is acted upon by what is called gravity gradient torque.

Another source of perturbation on the attitude of the spacecraft comes from the motion of the charged spacecraft in the geomagnetic field. This motion generates a force known as the Lorentz force which is the source of the Lorentz force torque influencing the rotational motion of the spacecraft. In this work we give an analytical treatment of the orbital-rotational dynamics of the spacecraft.

We first use the definitions of Delaunay and Andoyer variables in order to formulate the Hamiltonian of the orbit-attitude motion under the effects of forces and torques of interest. Since the Lorentz force is a non-conservative force, a potential like function is introduced and added to the Hamiltonian.

We solve the canonical equations of the Hamiltonian system by successive transformations using a technique proposed by Lie and modified by Deprit and Kamel to solve the problem. In this technique we make two successive transformations to eliminate the short and long periodic terms from the Hamiltonian.

**Keywords:** Analytical; Orbit; Attitude.

### 13. Feedback Optimal Control of Low-Thrust Orbit Transfer in Central Gravity Field

Ashraf H. Owis

*International Journal of Advanced Computer Science and Applications (Ijacs)*, 4(4): 158-162 (2013)

Low-thrust trajectories with variable radial thrust is studied in this paper. The problem is tackled by solving the Hamilton- Jacobi-Bellman equation via State Dependent Riccati Equation (STDE) technique devised for nonlinear systems. Instead of solving the two-point boundary value problem in which the classical optimal control is stated, this technique allows us to derive closed-loop solutions.

The idea of the work consists in factorizing the original nonlinear dynamical system into a quasi-linear state dependent system of ordinary differential equations. The generating function technique is then applied to this new dynamical system, the feedback optimal control is solved. We circumvent in this way the problem of expanding the vector field and truncating higher-order terms because no remainders are lost in the undertaken approach. This technique can be applied to any planet-to-planet transfer; it has been applied here to the Earth-Mars low-thrust transfer.

**Keywords:** Feedback; Optimal control; Low-thrust orbit; Central gravity field.

### 14. Lunisolar Invariant Relative Orbits

Walid Ali Rahoma

*American Journal of Applied Sciences*, 10 (4): 307-312 (2013)

The present study deal with constructing an analytical model within Hamiltonian formulation to design invariant relative orbits due to the perturbation of  $J_2$  and the lunisolar attraction. To fade the secular drift separation over the time between two neighboring orbits, two second order conditions that guarantee that drift are derived and enforced to be equal.

**Keywords:** Formation flying; Invariant relative orbits; Secular drifts; Second order conditions; Neighboring orbits; Lunisolar attraction.

### 15. Relative Motion of Formation Flying With Elliptical Reference Orbit

Ashraf H. Owis and Hany R Dwidar

*(Ijarai) International Journal of Advanced Research in Artificial Intelligence*, 2 (6): 80-87 (2013)

In this paper we present the optimal control of the relative motion of formation flying consisting of two spacecrafts. One of the spacecraft is considered as the chief, orbiting the Earth on a Highly Elliptical Orbit (HEO), and the other, orbiting the chief, is considered as the deputy.

The Keplerian relative dynamics of the formation as well as the the second zonal harmonics of the Earth's gravitational field ( $J_2$ ) are studied. To study this perturbative effect the linearized true anomaly varying Tschauner-Hempel equations are augmented to include the effect of  $J_2$ . We solve the nonlinear feedback optimal control of the relative motion using the state dependent Riccati Equation (SDRE). The results are validated through a numerical example.

**Keywords:** Relative; Formation; Elliptical; Orbit.

### 16. Satellite Constellation Reconfiguration Using the Approximating Sequence Riccati Equations

Ashraf H. Owis

*Theory and Applications of Mathematics and Computer Science*, 3 (1): 99-106 (2013)

In this work we study the reconfiguration of a constellation of satellite. In this work we consider the non-linear feedback optimal control of the motion of a spacecraft under the influence of the gravitational attraction of a central body, the Earth in our case, and we would like to transfer the spacecraft from lower circular orbit to a higher one. Both orbits around the Earth are assumed to be circular and coplanar. We use both radial and tangential thrust control. The nonlinear dynamics of the system will be factorized in such a way that the new factorized system is accessible. The problem is tackled using the Approximating Sequence Riccati Equations (ASRE) method. The technique is based on Linear Quadratic Regulator (LQR) with fixed terminal state, which guarantees closed loop solution. The method is tested through GNSS circular constellation.

**Keywords:** Nonlinear feedback; Linear quadratic regulator; Approximation sequence riccati equation; GNSS satellite.

### 17. The Perturbed Motion of Artificial Satellite under of Influence of $J_2$

I. A. Hassan and Z. M. Hayman

*Journal of Basic and Applied Scientific Research*, 3: 1271-1275 (2013)

The authors try to find a good solution of an artificial satellite motion under the influence of  $J_2$ -gravity in terms of KS variables by using Picard's Iterative Method. The result shows that there are many solutions for this problem depends on the initial guess solutions, so the choice of correct/convince initial guess is very difficult. Applications of the method applied on many satellites.

**Keywords:** Satellite; Iterative method; Perturbed motion.

### 18. The Prediction of Motion of an Artificial Satellite

Hayman Zein El-Abdeen Metwally

*Journal of Basic and Applied Scientific Research*, 3: 504-511 (2013)

In this paper the solution of an artificial satellite motion under the influence of  $J_2$ -Earth's gravitational field in terms of Euler parameters that was solved using recurrent power series solution which is one of the semi-analytical solutions. Applications of the method enable anyone to predict the motion of the artificial satellite in any conic section. This expected because the only force affecting on the motion of artificial satellite is Earth's gravitational field.

**Keywords:** Satellite; Semi analytical solution; Euler parameters.

### Dept. of Biophysics

### 19. Improvements in the Order, Isotropy and Electron Density of Glypican-1 Crystals by Controlled Dehydration

Wael Awad, Gabriel Svensson Birkedal, Marjolein M. G. M. Thunnissen, Katrin Manic and Derek T. Logan

*Acta Crystallographica Section D*, 69: 2524-2533 (2013)  
IF: 14.103

The use of controlled dehydration for improvement of protein crystal diffraction quality is increasing in popularity, although there are still relatively few documented examples of success. A study has been carried out to establish whether controlled dehydration could be used to improve the anisotropy of crystals of the core protein of the human proteoglycan glypican-1. Crystals were subjected to controlled dehydration using the HC1 device. The optimal protocol for dehydration was developed by careful investigation of the following parameters: dehydration rate, final relative humidity and total incubation time  $T_{inc}$ . Of these, the most important was shown to be  $T_{inc}$ . After dehydration using the optimal protocol the crystals showed significantly reduced anisotropy and improved electron density, allowing the building of previously disordered parts of the structure.

**Keywords:** Glypican-1; Crystal dehydration; HC1; Optimization; Diffraction anisotropy; Crystal packing.

### 20. Global Structural Motions from the Strain of a Single Hydrogen Bond

Jens Danielsson, Wael Awad, Kadhivel Saraboji, Martin Kurnik, Lisa Lang, Lina Leinartaite, Stefan L. Marklund, Derek T. Logan and Mikael Oliveberg

*Proceedings of the National Academy of Sciences*, 110: 3829-3834 (2013) IF: 9.737

The origin and biological role of dynamic motions of folded enzymes is not yet fully understood. In this study, we examine the molecular determinants for the dynamic motions within the  $\beta$ -barrel of superoxide dismutase 1 (SOD1), which previously were implicated in allosteric regulation of protein maturation and also pathological misfolding in the neurodegenerative disease amyotrophic lateral sclerosis. Relaxation-dispersion NMR, hydrogen/deuterium exchange, and crystallographic data show

that the dynamic motions are induced by the buried H43 side chain, which connects the backbones of the Cu ligand H120 and T39 by a hydrogen-bond linkage through the hydrophobic core. The functional role of this highly conserved H120, H43, T39 linkage is to strain H120 into the correct geometry for Cu binding. Upon elimination of the strain by mutation H43F, the apo protein relaxes through hydrogen-bond swapping into a more stable structure and the dynamic motions freeze out completely.

At the same time, the holo protein becomes energetically penalized because the twisting back of H120 into Cu-bound geometry leads to burial of an unmatched backbone carbonyl group. The question then is whether this coupling between metal binding and global structural motions in the SOD1 molecule is an adverse side effect of evolving viable Cu coordination or plays a key role in allosteric regulation of biological function, or both?

**Keywords:** Allosteric; Local unfolding; Metal binding; Protein aggregation; Structural frustration.

## 21. Enhanced Immunogenicity of A Tricomponent Mannan Tetanus Toxoid Conjugate Vaccine Targeted to Dendritic Cells VIA Dectin-1 by Incorporating $\beta$ -Glucan

Tomasz Lipinski, Amira Fitieh, Joëlle St. Pierre, Hanne L. Ostergaard, David R. Bundle and Nicolas Touret

*The Journal of Immunology*, 198 (8): 4116-4128 (2013)  
IF: 5.52

In a previous attempt to generate a protective vaccine against *Candida albicans*, a  $\beta$ -mannan tetanus toxoid conjugate showed poor immunogenicity in mice. To improve the specific activation toward the fungal pathogen, we aimed to target Dectin-1, a pattern-recognition receptor expressed on monocytes, macrophages, and dendritic cells. Laminarin, a  $\beta$ -glucan ligand of Dectin-1, was incorporated into the original  $\beta$ -mannan tetanus toxoid conjugate providing a tricomponent conjugate vaccine. A macrophage cell line expressing Dectin-1 was employed to show binding and activation of Dectin-1 signal transduction pathway by the  $\beta$ -glucan-containing vaccine.

Ligand binding to Dectin-1 resulted in the following: 1) activation of Src family kinases and Syk revealed by their recruitment and phosphorylation in the vicinity of bound conjugate and 2) translocation of NF- $\kappa$ B to the nucleus. Treatment of immature bone marrow-derived dendritic cells (BMDCs) with tricomponent or control vaccine confirmed that the  $\beta$ -glucan-containing vaccine exerted its enhanced activity by virtue of dendritic cell targeting and uptake.

Immature primary cells stimulated by the tricomponent vaccine, but not the  $\beta$ -mannan tetanus toxoid vaccine, showed activation of BMDCs. Moreover, treated BMDCs secreted increased levels of several cytokines, including TGF- $\beta$  and IL-6, which are known activators of Th17 cells. Immunization of mice with the novel type of vaccine resulted in improved immune response manifested by high titers of Ab recognizing *C. albicans*  $\beta$ -mannan Ag. Vaccine containing laminarin also affected distribution of IgG subclasses, showing that vaccine targeting to Dectin-1 receptor can benefit from augmentation and immunomodulation of the immune response.

**Keywords:** Dectin-1; Fungal infection; Clustering, Fluorescence imaging.

## 22. Polycomb Repressive Complex 2 Contributes to DNA Double-Strand Break Repair

Stuart Campbell, Ismail Hassan Ismail, Leah C. Young, Guy G. Poirier and Michael J. Hendzel

*Cell Cycle*, 12 (6): 2675-2683 (2013) IF: 5.321

Polycomb protein histone methyltransferase, enhancer of Zeste homolog 2 (EZH2), is frequently overexpressed in human malignancy and is implicated in cancer cell proliferation and invasion. However, it is largely unknown whether EZH2 has a role in modulating the DNA damage response. Here, we show that polycomb repressive complex 2 (PRC2) is recruited to sites of DNA damage. This recruitment is independent of histone 2A variant X (H2AX) and the PI-3-related kinases ATM and DNA-PKcs. We establish that PARP activity is required for retaining PRC2 at sites of DNA damage. Furthermore, depletion of EZH2 in cells decreases the efficiency of DSB repair and increases sensitivity of cells to gamma-irradiation. These data unravel a crucial role of PRC2 in determining cancer cellular sensitivity following DNA damage and suggest that therapeutic targeting of EZH2 activity might serve as a strategy for improving conventional chemotherapy in a given malignancy.

**Keywords:** Parp; DNA damage; Polycomb group proteins; Chromatin; Epigenetics.

## 23. Enhancement of the Ocular Therapeutic Effect of Prednisilone Acetate by Liposomal Entrapment

Nihal S. Elbially, Bahaa Mostafa Abdol-Azim, Medhat W. Shafaa, Laila H. El Shazly, Amany H. El Shazly and Wafaa A. Khalil

*Journal of Biomedical Nanotechnology*, 9: 2105-2116 (2013)  
IF: 5.2

Eye drops account for 90% of ophthalmic formulations despite of the rapid precorneal drug loss. Our aim is to test the effect of positive charge induction and the subsequent size reduction on the efficiency of liposomes as ocular drug delivery system for the lipophilic drug prednisolone acetate (PSA). Different formulations of PSA-loaded liposomes, positive multilamellar liposomes (pMLV), positive small (nano-sized) unilamellar liposomes (pSUV) and neutral multilamellar liposomes (nMLV), were prepared. These formulations were characterized by measuring surface charge, size distribution, entrapment efficiency, release rate, and ability to deliver PSA across the cornea. In vitro studies showed that positive charge induction reduces the transcorneal flux (about 1.9-fold lower than nMLV), while the subsequent size reduction results in higher flux (about 1.2-fold higher than nMLV). But in vivo results revealed that pSUV produced more concentrations of PSA in aqueous humor than nMLV ( $P < 0.05$ ) suggesting greater chance for drug penetration, pSUV were more effective than nMLV in this regard ( $P < 0.05$ ). As revealed by in vivo studies and ophthalmic examinations, positive charge induction and the subsequent size reduction increased the efficiency of liposomes as ocular drug delivery system for PSA.

**Keywords:** Liposome; Prednisolone acetate; Entrapment efficiency; Release rate; Transcorneal flux; Uveitis.



## 24. Preparation and Characterization of $\text{SiO}_2$ -Au Nanoshell: in Vivo Study of its Photo-Heat Conversion

Nihal Elbially, Noha Mohamed and Ahmed Soltan Abd Elmonem

*Journal of Biomedical Nanotechnology*, 9: 158-166 (2013)

IF: 5.2

In the event of cancer treatment, photothermal therapy has met successful cancerous cells damage with highly reduced toxicity to normal cells. The prepared GNSs samples have been characterized using transmission electron microscope (TEM), dynamic light scattering, zeta potential and UV-VIS absorption spectroscopy. In-vivo photo-heat conversion of GNSs accumulated in Ehrlich tumor cells inoculated in female balb mice was monitored by measuring tumor tissue temperature as a function of NIR laser exposure time. Resultant heating and therapeutic efficacy were assessed by monitoring tumor growth/regression and tumor cells necrotic percentage. Histopathological examinations for treated and control tumors using light microscope and transmission electron microscopes (TEM) were performed to evaluate the treatment effects. Passively targeted pegylated gold nanoshells were found to have localized photo-heat conversion sufficient to selectively destruct tumor cells. This has been emphasized by the significant decrease in Ehrlich tumor volume for treated groups that administrated either intratumorally (IT) or intravenously (IV) with GNSs. Light microscope examinations revealed high necrotic percentages for both administration routes. TEM images showed degenerated cell membrane and nuclear envelop as well as the appearance of nucleus debris and other cell organelles. This non-invasive protocol showed great promise as a technique for selective cancer photo-thermal therapy.

**Keywords:** Gold nanoshells; Photo-heat conversion; Photo-thermal therapy; Ehrlich tumor; Passive targeting.

## 25. A Small Molecule Inhibitor of Polycomb Repressive Complex 1 Inhibits Ubiquitin Signaling at DNA Double-Strand Breaks

Ismail Hassan Ismail, Darin McDonald, Hilmar Strickfaden, Zhizhong Xu and Michael J. Hendzel

*Journal of Biological Chemistry*, 288: 26944-26954 (2013)

IF: 4.651

Polycomb-repressive complex 1 (PRC1)-mediated histone ubiquitylation plays an important role in aberrant gene silencing in human cancers and is a potential target for cancer therapy. Here we show that 2-pyridine-3-yl-methylene-indan-1,3-dione (PRT4165) is a potent inhibitor of PRC1-mediated H2A ubiquitylation in vivo and in vitro. The drug also inhibits the accumulation of all detectable ubiquitin at sites of DNA double-strand breaks (DSBs), the retention of several DNA damage response proteins in foci that form around DSBs, and the repair of the DSBs. In vitro E3 ubiquitin ligase activity assays revealed that PRT4165 inhibits both RNF2 and RING 1A, which are partially redundant paralogues that together account for the E3 ubiquitin ligase activity found in PRC1 complexes, but not RNF8 nor RNF168. Because ubiquitylation is completely inhibited despite the efficient recruitment of RNF8 to DSBs, our results suggest that PRC1-mediated monoubiquitylation is required for

subsequent RNF8- and/or RNF168-mediated polyubiquitylation. Our results demonstrate the unique feature of PRT4165 as a novel chromatin-remodeling compound and provide a new tool for the inhibition of ubiquitylation signaling at DNA double-strand breaks.

**Keywords:** Chromatin; DNA Damage Response; DNA Repair; Polycomb; Ubiquitylation.

## 26. Non-Thermal Continuous and Modulated Electromagnetic Radiation Fields Effects on Sleep EEG of Rats

Haitham S. Mohammed, Heba M. Fahmy, Nasr M. Radwan and Anwar A. Elsayed

*Journal of Advanced Research*, 4: 181-187 (2013) IF: 3.0

In the present study, the alteration in the sleep EEG in rats due to chronic exposure to low-level non-thermal electromagnetic radiation was investigated. Two types of radiation fields were used; 900 MHz unmodulated wave and 900 MHz modulated at 8 and 16 Hz waves. Animals has exposed to radiation fields for 1 month (1 h/day). EEG power spectral analyses of exposed and control animals during slow wave sleep (SWS) and rapid eye movement sleep (REM sleep) revealed that the REM sleep is more susceptible to modulated radiofrequency radiation fields (RFR) than the SWS. The latency of REM sleep increased due to radiation exposure indicating a change in the ultradian rhythm of normal sleep cycles. The cumulative and irreversible effect of radiation exposure was proposed and the interaction of the extremely low frequency radiation with the similar EEG frequencies was suggested.

**Keywords:** Electromagnetic Radiation; Electroencephalogram; Slow wave sleep; Rapid eye movement sleep.

## 27. Extremely Low-Frequency Magnetic Field Enhances the Therapeutic Efficacy of Low-Dose Cisplatin in the Treatment of Ehrlich Carcinoma

Nihal S. El-Bialy and Monira M. Rageh

*Biomed Research International*, 1-7 (2013) IF: 2.88

The present study examines the therapeutic efficacy of the administration of low-dose cisplatin (cis) followed by exposure to extremely low-frequency magnetic field (ELF-MF), with an average intensity of 10 mT, on Ehrlich carcinoma in vivo. The cytotoxic and genotoxic actions of this combination were studied using comet assay, mitotic index (MI), and the induction of micronucleus (MN). Moreover, the inhibition of tumor growth was also measured. Treatment with cisplatin and ELF-MF (group A) increased the number of damaged cells by 54% compared with 41% for mice treated with cisplatin alone (group B), 20% for mice treated by exposure to ELF-MF (group C), and 9% for the control group (group D). Also the mitotic index decreased significantly for all treated groups (). The decrement percent for the treated groups (A, B, and C) were 70%, 65%, and 22%, respectively, compared with the control group (D). Additionally, the rate of tumor growth at day 12 was suppressed significantly () for groups A, B, and C with respect to group (D). These results suggest that ELF-MF enhanced the cytotoxic activity of cisplatin and potentiate the benefit of using a combination of low-dose cisplatin and ELF-MF in the treatment of Ehrlich carcinoma.

**Keywords:** Extremely low-frequency magnetic field; Cisplatin; DNA; Ehrlich carcinoma.

## 28. Enhancing Antimicrobial Activity for Chitosan by Adding Jojoba Liquid Wax

Osiris W. Guirguis, Mahmoud F. H. AbdElkader and Andrew A. Nasrat

*Materialsletters*, 93: 353-355 (2013) IF: 2.224

The purpose of the present study is to enhance the antimicrobial activity of chitosan. For this reason, thin films of chitosan incorporated with different concentrations of Jojoba liquid wax (JLW) were prepared by using casting technique. The agar disc diffusion method was used to investigate the antimicrobial activity of the films against two different microorganisms namely *Staphylococcus aureus* and *Bacillus subtilis*. The results indicated that as the concentration of JLW increases the antimicrobial activity for *Staphylococcus aureus* and *Bacillus subtilis* increases. Moreover, it is found that the minimum inhibitory concentration (MIC) values for both systems decrease by increasing the amount of the antimicrobial agent Jojoba with chitosan. In conclusion, the data obtained reveal that chitosan has a great potential to improve its antimicrobial activity by incorporating with antimicrobial agent.

**Keywords:** Chitosan; Jojoba liquidwax; Antimicrobial activity; Biomaterials; Thin films; Diffusion.

## 29. Similarity Analysis of Protein Sequences Based on 2D and 3D Amino Acid Adjacency Matrices

Ali El-Lakkani and Seham El-Sherif

*Chemical Physics Letters*, 590: 192-195 (2013) IF: 2.145

This approach presents a 3D amino acid adjacency matrix based on the 2D amino acid adjacency matrix which was proposed by Randic et al. (2008) [1]. Furthermore, a novel numerical method is proposed to measure the degree of similarity based on 2D and 3D adjacency matrices. This new method is applied to nine ND5 proteins of different species. To prove the efficiency of the presented work a correlation with ClustalW and significance analyses are provided. The results show that our work is the most significant among other related works.

**Keywords:** Similarity analysis; Protein sequences; Adjacency matrix.

## 30. Electrical and Photosensing Performance of Heterojunction Device Based on Organic Thin Film Structure

A. A. M. Farag, W.G. Osiris, A. H. Ammara and A. M. Mansour

*Synthetic Metals*, 175: 81-87 (2013) IF: 2.109

In this work, the heterojunction thin films of aluminum phthalocyanine chloride on *N*, *N'*-dioctyl-3,4,9,10-perylenedicarboximide device was fabricated by using thermal evaporation technique under high vacuum ( $\sim 10^{-4}$  Pa). The morphology of the device was characterized by scanning electron microscopy (SEM). The dark current density-voltage ( $J$ - $V$ ), capacitance-frequency ( $C$ - $f$ ) and conductance measurements at

different temperatures in the range 300–425 K were performed to determine the electrical properties of the device. The exponent of the light intensity dependence for the short-circuit photocurrent ( $J_{sc}$ ) of the device indicates the presence of continuous distribution of traps. The device showed improvement in the open circuit voltage as compared to other organic compounds. The photosensitivity of the device was calculated and found to be 3.1 at  $\pm 1$  V under illumination intensity of 100 mW/cm<sup>2</sup>. This suggested that the device shows a photodiode characteristic. The interface state density of the device was determined using the conductance technique and was found to be low which suggested that the interface states at this density range are not effective on the device characteristics which supports the efficient properties for the studied device.

**Keywords:** Aluminum phthalocyanine chloride; *N*, *N'*-dioctyl-3,4,9,10-perylenedicarboximide; Photovoltaic; Photoresponse; Interface state density; Electrical properties.

## 31. Morphological and Macrostructural Studies of Dog Cranial Bone Demineralized With Different Acids

Gehan T. El-Bassyouni, Osiris W. Guirguis and Wafa I. Abdel-Fattah

*Current Applied Physics*, 13: 864-874 (2013) IF: 1.814

Strong and weak acids were chosen for the bone decalcification process. Demineralization of dog cranial bone was carried out using 0.6 M concentration of either of hydrochloric, lactic or citric acid. Consequent morphologic changes were correlated with the developed chemistry, porosity and structure through XRD and FT-IR of the matrices. The dielectric permittivity, loss angle, relaxation dielectric loss as well as a.c.electrical conductivity as functions of frequency and temperature were measured. Zeta potential was evaluated at physiologic pH and temperature and correlated with the developed structures.

The results prove lower dielectric properties of demineralized matrices compared to control and exhibited high dissipation of electric energy with more than one relaxation mechanism. This variation proves that the spectral behavior depended on the nature of the bone matrix which resulted from the phase compositions of bone and its crystallite size. The behavior of the obtained results is attributed to the differences of the demineralizing acids and their consequent actions on the matrices, i.e., the differences in the materials.

**Keywords:** Demineralization; Organic/inorganic acids; Xrd and morphological features; Dielectric properties; Zeta potential.

## 32. DC Conductivity and Dielectric Properties of Maize Starch/Methylcellulose Blend Films

M. F. H. Abd El-Kader and H. S. Ragab

*Ionic*, 19 (2): 361-369 (2013) IF: 1.674

The transient current, electrical conductivity, dielectric constant ( $\epsilon'$ ), and dielectric loss factor ( $\epsilon''$ ) of starch and methylcellulose homopolymers and their blends with various compositions were studied under different conditions. The x-ray diffraction pattern was obtained for individual polymers and 50:50 wt/wt% blend sample to identify both the structure and degree of crystallinity. From transient current, the ionic and electronic transfer number as

well as charge carrier density and drift mobility were determined. The values of activation energy in the temperature range 30–90 °C indicate that the conduction mechanism is due to combined electronic and ionic processes, while in the temperature range 100–160 °C, electronic contribution is predominant. The complex dielectric data of the present samples in an extended frequency and temperature range appear as different relaxation processes, which are connected with polymer dynamics.

**Keywords:** Starch; Methylcellulose; Xrd; Transient current; Electrical conductivity; Dielectric spectroscopy.

### 33. Quantitative Characterization of Fatty Liver Disease Using X-Ray Scattering

Wafaa B. Elsharkawy and Wael M. Elshemey

*Radiation Physics and Chemistry, 92: 14-21 (2013) IF: 1.375*

Nonalcoholic fatty liver disease (NAFLD) is a dynamic condition in which fat abnormally accumulates within the hepatocytes. It is believed to be a marker of risk of later chronic liver diseases, such as liver cirrhosis and carcinoma. The fat content in liver biopsies determines its validity for liver transplantation. Transplantation of livers with severe NAFLD is associated with a high risk of primary non-function. Moreover, NAFLD is recognized as a clinically important feature that influences patient morbidity and mortality after hepatic resection. Unfortunately, there is a lack in a precise, reliable and reproducible method for quantification of NAFLD. This work suggests a method for the quantification of NAFLD. The method is based on the fact that fatty liver tissue would have a characteristic x-ray scattering profile with a relatively intense fat peak at a momentum transfer value of  $1.1 \text{ nm}^{-1}$  compared to a soft tissue peak at  $1.6 \text{ nm}^{-1}$ . The fat content in normal and fatty liver is plotted against three profile characterization parameters (ratio of peak intensities, ratio of area under peaks and ratio of area under fat peak to total profile area) for measured and Monte Carlo simulated x-ray scattering profiles. Results show a high linear dependence ( $R^2 > 0.9$ ) of the characterization parameters on the liver fat content with a reported high correlation coefficient ( $> 0.9$ ) between measured and simulated data. These results indicate that the current method probably offers reliable quantification of fatty liver disease.

**Keywords:** Nafld; X-Ray scattering; Fatty liver; Tissue characterization.

### 34. X-Ray Scattering for the Characterization of Lyophilized Breast Tissue Samples

Wael M. Elshemey, Fayrouz S. Mohamed and Ibrahim M. Khater

*Radiation Physics and Chemistry, 90: 67-72 (2013) IF: 1.375*

This work investigates the possibility of characterizing breast cancer by measuring the X-ray scattering profiles of lyophilized excised breast tissue samples. Since X-ray scattering from water-rich tissue is dominated by scattering from water, the removal of water by lyophilization would enhance the characterization process. In the present study, X-ray scattering profiles of 22 normal, 22 malignant and 10 benign breast tissue samples are measured. The cut-offs of scatter diagrams, sensitivity, specificity and diagnostic accuracy of three characterization parameters (full width at half maximum (FWHM) for the peak at  $1.1 \text{ nm}^{-1}$ , area under curve (AUC), and ratio of 1st to 2nd scattering peak

intensities ( $I_1/I_2\%$ )) are calculated and compared to the data from non-lyophilized samples. Results show increased sensitivity (up to 100%) of the present data on lyophilized breast tissue samples compared to previously reported data for non-lyophilized samples while the specificity (up to 95.4%), diagnostic accuracy (up to 95.4%) and receiver operating characteristic (ROC) curve values (up to 0.9979) for both sets of data are comparable. The present study shows significant differences between normal samples and each of malignant and benign samples. Only subtle differences exist between malignant and benign lyophilized breast tissue samples where  $\text{FWHM} = 0.7 \pm 0.1$  and  $0.8 \pm 0.3$ ,  $\text{AUC} = 1.3 \pm 0.2$  and  $1.4 \pm 0.2$  and  $I_1/I_2\% = 44.9 \pm 11.0$  and  $52.4 \pm 7.6$  for malignant and benign samples respectively.

**Keywords:** X-ray scattering; Breast cancer; Lyophilized tissue; Tissue characterization.

### 35. Scattered Radiation Effects on the Extrinsic Sensitivity and Counting Efficiency of a Gamma Camera

Wael M. Elshemey, Mohamed A. Ghoneim and M. H. Khader

*Applied Radiation and Isotopes, 77: 18-22 (2013) IF: 1.179*

An evaluation of the effect of scattered radiation on the performance of a gamma camera is carried out using a specially designed home-made homogeneous circular planar flood source filled with  $0.2 \pm 0.01 \text{ GBq}$  of  $^{99\text{m}}\text{Tc}$  solution as a scattering medium. The scatter effects are assessed by analyzing the energy spectrum of  $^{99\text{m}}\text{Tc}$  for the scatter fraction and calculating the camera's extrinsic counting efficiency and sensitivity, for five flood source thicknesses (12, 50, 100, 150 and 200 mm) and three source-to-detector distances (0.7, 0.9 and 1.1 m). Results showed an increase in the scatter fraction from 0.29 to 22.96 as the source thickness increased. This increase was associated with a decrease in the extrinsic sensitivity from 121.36 to 49.58 counts/s GBq, and a decrease in counting efficiency as from 3.78 to 1.55%. With the increase in source-to-detector distance, the extrinsic sensitivity decreases from 121.36 to 118.77 counts/s GBq, while the counting efficiency increases from 3.78 to 11.66%. It was found that a source-to-detector distance of  $0.96 \pm 9 \times 10^{-3} \text{ m}$  is a good compromise for an acceptable extrinsic sensitivity and a reasonable counting efficiency.

**Keywords:** Scattered fraction; Gamma camera; Extrinsic counting efficiency; Extrinsic sensitivity.

### 36. Molecular Modeling Comparison of the Performance of NS5b Polymerase Inhibitor (PSI-7977) on Prevalent HCV Genotypes

Abdo A. Elfiky, Wael M. Elshemey, Wissam A. Gawad and Omar S. Desoky

*Protein Journal, 32: 75-80 (2013) IF: 1.126*

The current available treatment for hepatitis C virus (HCV)—the causative of liver cirrhosis and development of liver cancer—is a dual therapy using modified interferon and ribavirin. While this regimen increases the sustained viral response rate up to 40–80 % in different genotypes, unfortunately, it is poorly tolerated by patients. PSI-7977, a prodrug for PSI-7409, is a Non-Structural 5b (NS5b) polymerase nucleoside inhibitor that is currently in phase III clinical trials. The activated PSI-7977 is a direct acting

antiviral (DAA) drug that acts on NS5b polymerase of HCV through a coordination bond with the two  $Mg^{+2}$  present at the GDD active site motif. The present work utilizes a molecular modeling approach for studying the interaction between the activated PSI-7977 and the 12 amino acids constituting a 5 Å region surrounding the GDD active triad motif for HCV genotypes 1a, 2b, 3b and 4a. The analysis of the interaction parameters suggests that PSI-7977 is probably a better DAA drug for HCV genotypes 1a and 3b rather than genotypes 2b and 4a.

**Keywords:** DAA; HCV; NS5b; Molecular modeling; Nucleoside inhibitor; PSI-7977.

### 37. Optical and Thermal Studies of Starch/Methylcellulose Blends

H. S. Ragab and M. F. H. Abd El-Kader

*Physica Scripta*, 87: 1-14 (2013) IF: 1.032

Starch and methylcellulose (MC) homopolymers and their blends were prepared using a casting technique. The samples were investigated by infrared (Fourier transform infrared (IR)), ultraviolet/visible (UV/VIS), differential scanning calorimetry (DSC) and thermogravimetric analysis (TGA). Significant changes in IR spectra of blend samples were observed, which indicated the occurrence of an intermolecular interactions between starch and MC. UV/VIS analyses revealed that the values of the optical band gap decreased with increasing MC content in blend samples. The positions of the investigated samples on the chromaticity diagram and the color parameters, such as  $L^*$ ,  $U^*$ ,  $V^*$ ,  $C^*$ ,  $h_{uc}$  and  $Y_e$ , reflected the presence of a high color gradient and were composition dependent. A single glass transition temperature for each poly-blend sample was observed, which supported the existence of compatibility in such a system. The kinetic thermodynamic parameters, such as activation energy, enthalpy, entropy and Gibbs free energy, were evaluated from thermogravimetric analysis data using the Coats-Redfern relation.

**Keywords:** Optical; Thermal; Starch; Methylcellulose.

### 38. A Miniature Microdrive for Recording Auditory Evoked Potentials from Awake Anurans

Haitham S. Mohammed, Nasr M. Radwan, Wolfgang Walkowiak and Anwar A. Elsayed

*General Physiology and Biophysics*, 32: 381-388 (2013) IF: 0.852

Electrical activity recording from the brains of awake animals is a corner stone in the study of the neurophysiological basis of behavior. To meet this need, a microelectrode driver suitable for the animal of interest has to be developed. In the present study a miniature microdrive was developed specifically for the leopard toad, *Bufo regularis*, however, it can be used for other small animals. The microdrive was designed to meet the following requirements: small size, light weight, simple and easy way of attaching and removing, advancing and withdrawing of microelectrode in the animal brain without rotation, can be reused and made from inexpensive materials. To assess the performance of the developed microdrive, we recorded auditory evoked potentials from different auditory centers in the toad's brain. The potentials were obtained from mesencephalic, diencephalic and

telencephalic auditory sensitive areas in response to simple and complex acoustic stimuli. The synthetic acoustical tones introduced to the toad were carrying the dominant frequencies of their mating calls.

**Keywords:** Anuran; Brain; Microdrive; Auditory; Acoustic stimulus.

### 39. QSAR Properties of Novel Peptidomimetic NS3 Protease Inhibitors

Medhat Ibrahim, Noha A. Saleh, Wael M. Elshemey and Anwar A. Elsayed

*Journal of Computational and Theoretical Nanoscience*, 10: 785-788 (2013) IF: 0.67

NS3 protease is considered as important antiviral target. By using NS5A/NS5B junction sequences for Egyptian genotype 4a (Glu-Asp-Val-Val-Cys-Cys), a new NS3 protease inhibitors were designed with two groups. The first group has hexapeptide binding to cellulose monomer at position 2, 3 or 6 while the second group has hexapeptide binding to cellulose dimer at position 2, 3, 6, 2', 3' or 6'. QSAR descriptors of introduced compounds will be calculated at PM3 method and compared with that of natural substrate. The represented results indicate that the second group compounds especially at position 2, 2' and 6' are more hydrophilic and soluble in polar solutions and may increase the interaction of this class of compounds with the NS3 protease active site.

**Keywords:** Cellulose; Genotype 4a; HCV; Hexapeptide; NS3 protease; QSAR.

### 40. Dielectric and Rheological Properties of Collagen-DPPC Liposomes

Mohsen Mahmoud Mady

*Romanian Journal Biophysics*, 23: 211-219 (2013)

Interaction between liposomes and protein is important for the structure and function of cells. In the present work, the interaction between collagen and dipalmitoyl phosphatidylcholine (DPPC) liposomes was studied using dielectric spectroscopy technique and rheological measurements. Dielectric data indicated that the DPPC liposomes have strong dielectric dispersion in the frequency range of 50 Hz to 5 MHz. The conductivity and relaxation time increased after addition of collagen to DPPC liposomes. The increase in relaxation time might be attributed to increase in the localized charges distribution within the medium confirmed by the conductivity data. The increase in permittivity over the frequency range tested is an indicator of the interaction between protein and liposomal phospholipid. This is either due to the insertion of collagen into the lipid bilayer via its hydrophobic residues or to adsorption causing a protein layer to be located around liposomes.

Interaction between collagen and liposomes increases the liposomal membrane rigidity and increases its microviscosity as indicated from rheological measurements. It was concluded that collagen significantly altered the physical state of liposome membrane, which may be attributed to collagen interaction with liposomes surface and/or by its incorporation within the bilayer membrane.

**Keywords:** Collagen; Liposome; Dipalmitoyl phosphatidylcholine; Dielectric; Rheological.



#### 41. Fast Neutrons Effect on the Dielectric Properties of Poly (Vinyl Alcohol)/Hydroxypropyl Cellulose Blends

Mimouna M. Abutalib and Osiris W. Guirguis

*International Journal of Current Research*, 5 (10): 2840-2849 (2013)

Thin transparent films of poly (vinyl alcohol)/hydroxypropyl cellulose (PVA/HPC) (100/0, 96/4, 92/8, 88/12, 84/16 and 0/100 wt/wt%) blends were prepared by using solution-cast technique. In the present study, the temperature-dependent (in the range 295-390 K) dielectric dispersion was used to probe the molecular mobility of the amorphous phase of the blend systems near the glass transition temperature ( $T_g$ ). The dielectric properties on certain chosen blends (100/0, 92/8 and 88/12 wt/wt%) before and after irradiation with different fast neutron fluencies within the range from 105 to 108 n/cm<sup>2</sup> were investigated. The results noticed that all the samples face to changes in the values of the dielectric permittivity ( $\epsilon'$ ), dielectric loss tangent ( $\tan \delta$ ) and a.c. electrical conductivity ( $\sigma_{ac}$ ). The data also indicated that the measurable changes in the glass transition temperature ( $T_g$ ) may be due to the fact that the position of  $T_g$  is strongly dependent on the molecular weight, purity and water content of the sample. These changes may be attributed to degradation process and/or to cross-linking process either by the presence of HPC with different concentrations or by irradiation with different fast neutron fluencies or both of them. This suggests that, the observed dispersion and the correlated barrier hopping mechanism depend on composition and temperature of blend matrix.

**Keywords:** Poly (vinyl alcohol); Hydroxypropyl cellulose; PVA/HPC blends; Fast neutrons irradiation; Dielectric properties.

#### 42. Macrostructure and Optical Study of PMMA /TiO<sub>2</sub> Nanoparticles Composites

Osiris W. Guirguis Mohamed S.Melegy and Nabawia A.El-Zaher

*Nano Science and Nano Technology and Indian Journal*, 7 (2): 60-65 (2013)

Polymer nanocomposites have elicited extensive research efforts due to their potential to exhibit spectacular properties. In the present work, mixtures of four different concentrations (2.5, 5, 7.5, and 10 wt%) of titanium oxide (TiO<sub>2</sub>) nanoparticles with poly (methyl methacrylate) (PMMA) were prepared. Fourier transform infrared spectroscopy (FTIR) and optical analysis were employed to characterize and reveal the miscibility map and the relationship of the structure properties. From the obtained results, it is clear that the TiO<sub>2</sub> nanoparticles have a great effect on improving the performance properties of PMMA greatly depends on the concentration of nanoparticles. Moreover, the organic parts are attached with the inorganic parts in the PMMA/TiO<sub>2</sub> nanoparticles composites.

**Keywords:** Poly (methyl methacrylate); Titanium oxide; Nanoparticles; FTIR; Tristimulus values; Color parameters.

#### 43. Optical Properties of Poly (Vinyl Alcohol)/Hydroxypropyl Cellulose Blends

Osiris W. Guirguis and Manal T. H. Moselhey

*Materials Science an Indian Journal*, 9 (1): 8-23 (2013)

Transparent films of poly (vinyl alcohol)/hydroxypropyl cellulose (PVA/HPC) blend with different concentrations were prepared by using solution cast technique. Variations in the group coordination in the IR region were followed. The effects of HPC concentrations on the optical characterizations of the films have been done by analyzing the absorbance, transmittance and reflectance spectra in the spectral region 200-2500 nm. The study has been extended to include the changes in the optical parameters including the band tail width and band gap energies for the samples. Moreover, the extinction coefficient (k) has been calculated for the investigated films. As obtained by the FTIR and NIR results, the increase in the concentration of HPC with PVA changed the chemical bonds and hence changed the molecular configuration of PVA. The results indicate that the optical band gap was derived from Tauc's extrapolation and decreases with the HPC contents.

**Keywords:** Poly (Vinyl alcohol); Hydroxypropyl cellulose; FTIR technique; Near infrared analysis; Extinction coefficient; Optical parameters.

#### 44. Optical Studies of Fast Neutron Irradiated Poly (Vinyl Alcohol)/ Hydroxypropyl Cellulose Blends

M. M. Abutalib, Osiris W. Guirguis Nabawia A. Abdel Zaher

*Materials Science an Indian Journal*, 9 (11): 433-444 (2013)

Thin transparent films of poly (vinyl alcohol)/hydroxypropyl cellulose (PVA/HPC) (0/100, 92/8, 88/12, and 0/100 wt/wt %) were prepared by using solution-cast technique. The effects of HPC concentration on the optical characterizations by analyzing the transmittance spectra in the spectral region 200–900 nm as well as the variations in the group coordination by using FTIR technique in the region (4000-1000 cm<sup>-1</sup>) of the prepared PVC/HPC blends have been done before and after irradiation with two fast neutrons fluencies (1 x 10<sup>5</sup> and 1 x 10<sup>7</sup> n/cm<sup>2</sup>).

The study has been extended to include the changes in the optical parameters including the band tail width and band gap energies for the samples. The results noticed that the optical band gap was derived from Tauc's extrapolation and increases with the HPC contents. Also, the results obtained by the FTIR indicate that the increase in the concentration of HPC with PVA changed the chemical bonds and hence changed the molecular configuration of PVA. Moreover, the results obtained by the effect of different weight percent of HPC were compared with that detected by the effect of fast neutrons.

**Keywords:** Poly (Vinyl alcohol); Hydroxypropyl cellulose; Fast neutrons irradiation; Absorption coefficient; Optical parameters; FTIR analysis.

#### 45. Relaxation Dynamics and A.C. Conductivity in Poly (Vinyl Lcohol)/Hydroxypropyl Cellulose

Mimouna M. Abutalib and Osiris W. Guirguis

*International Journal of Current Research*, 5: 2576-2581 (2013)

The frequency-dependent dielectric properties (dielectric permittivity, dielectric loss factor and a.c. electrical conductivity) of blends of poly(vinyl alcohol)/hydroxypropyl cellulose (PVA/HPC) prepared by the solution-cast technique is investigated in the frequency ranges from 1 to 100 kHz to examine a wide range of molecular mobility of the amorphous

phase of the blend systems. The dielectric properties on certain chosen blends before and after irradiation with different fast neutron fluencies in the range from  $10^5$  to  $10^8$  n/cm<sup>2</sup> are also studied. The obtained results noticed that, measureable changes in the behavior and values of the dielectric properties under investigation are detected. These changes may be attributed to degradation and/or cross-linking process either by the presence of HPC with different concentrations or by the irradiation with different fast neutron fluencies or both of them, which suggests that the observed dispersion depends on composition and irradiation of blend matrix.

**Keywords:** Poly (vinyl alcohol); Hydroxypropyl cellulose; PVA/HPC blends; Fast neutrons irradiation; Dielectric properties.

#### 46. Selection of Highly Efficient Small Interference RNA (SiRNA) Targeting Mammalian Genes

Ali El-lakkani, Wissam H. Abd Elgawad and Eman A. Sayed

*Journal of Biophysical Chemistry*, 4 (2): 72-79 (2013)

RNAi is the method of silencing the expression of targeted genes. RNAi applications include gene function analysis and target validation. Designing highly efficient small interference RNA (siRNA) sequence with maximum target specificity for mammalian RNAi is one of important topics in recent years. In this work, a statistical analysis of the information for a large number (3734) of siRNA presented in the database available on the internet is done. This is to improve the design of efficient siRNA molecules. The (3734) siRNAs are classified according to their efficiency to three groups (high efficient, moderate efficient and low efficient). Thirteen properties (positional and thermodynamics) are identified in the high efficient group in the primary statistical study. In the final statistical study, the average weight of each identified property is calculated. A very good linear correlation was found between the average percentage efficiency and the weighted score of siRNA properties. It is found that the most important feature of highly efficient siRNA is the difference in binding energy between the 5' end and the 3' end of the anti-sense strand. The (RISC) activation step is a critical step in RNAi process where the efficiency of this process depends on the instability of the 5' end of the anti-sense strand.

**Keywords:** RNAi; SiRNA; SiRNA Design.

#### 47. Structural, Optical and Thermal Characterization of PVA/2HEC Polyblend Films

G. Attia and M.F.H. Abdel-Kader

*International Journal of Electrochemical Science*, 8: 5672 - 5687 (2013)

Blends of two biodegradable polymer, polyvinyl alcohol (PVA) and 2-hydroxy ethyl cellulose (2HEC) were prepared with different compositions by using cast technique. X-ray diffraction (XRD) scans revealed the semi-crystalline nature of the blends for low concentration of 2HEC up to 50 wt% and the amorphous nature for higher ones. Infrared spectra (IR) of blend samples indicate that there is compatibility between PVA and 2HEC through the formation of hydrogen-bonding between their polar groups. The absorption coefficient spectral analysis revealed the existence of long and wide band tails of the localized states. The absorption edge and band tails were estimated for pure and blend films from their optical absorption spectra. The thermal stability

and thermal behavior of blends were investigated under non isothermal conditions by thermogravimetry (TG) and differential thermal analyses (DTA). A single glass transition temperature for each blend was observed, which supports the existence of compatibility of such system. The kinetic parameters such as activation energy, entropy, and enthalpy and Gibbs energy based on TG data for all samples in first decomposition region were determined using Coats-Redfern relation.

**Keywords:** XRD; IR spectra; UV/visible spectra; Thermal parameters.

#### 48. The Dosimetric Effects of Different Beam Energy on Physical Dose Distributions in IMRT Based on Analysis of Physical Indices

Ismail Eldesoky, Ehab M. Attalla and Wael M Elshemey

*Journal of Cancer Therapy*, 4: 33-43 (2013)

This work aimed at evaluating the effect of 6- and 10-MV photon energies on intensity-modulated radiation therapy (IMRT) treatment plan outcome in different selected diagnostic cases. For such purpose, 19 patients, with different types of non CNS solid tumors, were selected. Clinical step-and-shoot IMRT treatment plans were designed for delivery on a Siemens Oncor accelerator with 82 leafs; multi-leaf collimators (MLCs). To ensure that the similarity or difference among the plans is due to energy alone, the same optimization constraints were applied for both energy plans. All the parameters like beam angles, number of beams, were kept constant to achieve the same clinical objectives.

The Comparative evaluation was based on dose-volumetric analysis of both energy IMRT plans. Both qualitative and quantitative methods were used. Several physical indices for Planning Target Volume (PTV), the relevant Organs at Risk (OARs) as mean dose (Dmean), maximum dose (Dmax), 95% dose (D95), integral dose, total number of segments, and the number of MU were applied. Homogeneity index and conformation number were two other evaluation parameters that were considered in this study.

Collectively, the use of 6 MV photons was dosimetrically comparable with 10 MV photons in terms of target coverage, homogeneity, conformity, and OAR savings. While 10-MV plans showed a significant reduction in the number of MUs that varied between 4.2% and 16.6% (P-value = 0.0001) for the different cases compared to 6-MV. The percentage volumes of each patient receiving 2 Gy and 5 Gy were compared for the two energies. The general trend was that 6-MV plans had the highest percentage volume, (P-value = 0.0001, P-value = 0.006) respectively. 10-MV beams actually decreased the integral dose (from average  $183.27 \pm 152.38$  Gy-Kg to  $178.08 \pm 147.71$  Gy-Kg, P-value = 0.004) compared with 6-MV. In general, comparison of the above parameters showed statistically significant differences between 6-MV and 10-MV groups. Based on the present results, the 10-MV is the optimal energy for IMRT, regardless of the concerns about a potential risk of radiation-induced malignancies. It is recommended that the choice to treat at 10 MV be taken as a risk vs. benefit as the clinical significance remains to be determined on case by case basis.

**Keywords:** 6- and 10-MV photon energies; Intensity-modulated radiation therapy (IMRT); Dose-volumetric analysis.

**Dept. of Botany**

**49. Two Strains of Male-Killing Wolbachia in a Ladybird, *Coccinella Undecimpunctata*, From a Hot Climate**

Sherif Elnagdy, Susan Messing and Michael E. N. Majerus

*Plos One*, 8 (1): 1-9 (2013) IF: 3.73

Ladybirds are a hot-spot for the invasion of male-killing bacteria. These maternally inherited endosymbionts cause the death of male host embryos, to the benefit of female sibling hosts and the bacteria that they contain. Previous studies have shown that high temperatures can eradicate male-killers from ladybirds, leaving the host free from infection. Here we report the discovery of two maternally inherited sex ratio distorters in populations of a coccinellid, *Coccinella undecimpunctata*, from a hot lowland region of the Middle East. DNA sequence analysis indicates that the male killing is the result of infection by *Wolbachia* that the trait is tetracycline sensitive, and that two distinct strains of *Wolbachia* co-occur within one beetle population. We discuss the implications of these findings for theories of male-killing and suggest avenues for future field-work on this system.

**Keywords:** Coccinellidae; Endosymbionts; Inherited bacteria; Reproductive parasite; Sex ratio distorter.

**50. Evaluation of Free and Immobilized *Aspergillus Niger* NRC1ami Pectinase Applicable in Industrial Processes**

Mona A. Esawy, Amira A. Gamal, Zeinat Kamel, Abdel-Mohsen S. Ismail and Ahmed F. Abdel-Fattah

*Carbohydrate Polymers*, 92: 1463-1469 (2013) IF: 3.479

The *Aspergillus niger* NRC1ami pectinase was evaluated according to its hydrolysis efficiency of dry untreated orange peels (UOP), HCl-treated orange peels and NaOH-treated orange peels (HOP and NOP). Pectinase was entrapped in polyvinyl alcohol (PVA) sponge and the optimum pH and temperature of the free and immobilized enzymes were shifted from 4, 40 degrees C to 6, 50 degrees C respectively. The study of pH stability of free and immobilized pectinase showed that the immobilization process protected the enzyme strongly from severe alkaline pHs. The immobilization process improved the enzyme thermal stability to great extent. The unique feature of the immobilization process is its ability to solve the orange juice haze problem completely. Immobilized enzyme was reused 12 times in orange juice clarification with 9% activity loss from the original activity. Maximum reaction rate ( $V_{max}$ ) and Michaelis-Menten constant ( $K_m$ ) of the partially purified form were significantly changed after immobilization.

**Keywords:** *Aspergillus niger* NRC1ami; Pectinase; Citrus pectin; Orange peel; Immobilization; Orange juice clarification.

**51. The Direct Effects of Male Killer Infection on Fitness of Ladybird Hosts (Coleoptera: Coccinellidae)**

S. Elnagdy, M. E. N. Majerus, M. Gardener and L.-J. Lawson Handley

*J. of Evolutionary Biology*, 26 (8): 1816-1825 (2013) IF: 3.479

Male killing bacteria are common in insects and are thought to persist in host populations primarily by indirect fitness benefits to infected females, whereas direct fitness effects are generally assumed to be neutral or deleterious.

Here, we estimated the effect of male killer infection on direct fitness (number of eggs laid, as a measure of fecundity, together with survival) and other life-history traits (development time and body size) in seven ladybird host/male killer combinations. Effects of male killers on fecundity ranged, as expected, from costly to neutral; however, we found evidence of reduced development time and increased survival and body size in infected strains.

Greater body size in *Spiroplasma*-infected *Harmonia axyridis* corresponded to greater ovariole number and therefore higher potential fecundity. To our knowledge, this is the first report of direct benefits of male killer infection after explicitly controlling for indirect fitness effects. Neutral or deleterious fitness effects of male killer infection should not therefore be automatically assumed.

**Keywords:** Coccinellidae; Direct fitness effects; Genetic conflicts; Ladybirds; Male killing bacteria; Selfish elements.

**52. Ability of Ellagic Acid to Alleviate Osmotic Stress on Chickpea Seedlings**

Walid Abu El-Soud, Momtaz Mohamed Hegab, Hamada AbdElgawad, Gaurav Zinta and Han Asad

*Plant Physiology and Biochemistry*, 71: 173-183 (2013) IF: 2.775

Seed germination and growth of seedlings are critical phases of plant life that are adversely affected by various environmental cues. Water availability is one of the main factors that limit the productivity of many crops. This study was conducted to assess the changes in the sensitivity of chickpea seedlings to osmotic stress by prior treatment of chickpea seeds with a low concentration (50 ppm) of ellagic acid. Ellagic acid was isolated and purified from *Padina boryana* Thivy by chromatographic techniques. After ellagic acid treatment, seeds were germinated for 10 days under different osmotic potentials (0, -0.2, -0.4, -0.6 and -0.8 MPa) of polyethylene glycol (PEG) solutions. Ellagic acid treatment accelerated the germination and seedling growth of chickpea under osmotic stress conditions. Consistent with the accelerated growth, ellagic acid-treated seedlings also showed a significant increase in the total antioxidant capacity (FRAP) as well as an increase in the compatible solutes (proline and glycine betaine) content. Additionally, treated seedlings revealed lower lipid peroxidation levels (MDA), electrolyte leakage (EL) and  $H_2O_2$ . Flavonoid and reduced glutathione (GSH) content, and the activity of antioxidant enzymes [catalase (CAT), peroxidase (POX), superoxide dismutase (SOD), glutathione reductase (GR)] and enzymes of the shikimic acid pathway [phenylalanine ammonia lyase (PAL) and chalcone synthase (CHS)] all showed a remarkable increase with ellagic acid pretreatment compared to untreated seedlings especially under mild osmotic stress values (-0.2 and -0.4 MPa). These results suggested that treatment with ellagic acid could confer an increased tolerance of chickpea seedlings to osmotic stress, through reducing levels of  $H_2O_2$  and increasing antioxidant capacity.

**Keywords:** Ellagic acid; Chickpea; Osmotic stress; Oxidative stress; Antioxidants; Phenolics.



### 53. The Japanese Ladybirds, *Coccinula Crotchii* and *Coccinula Sinensis* are Infected With Closely Related Strain of Male-Killing *Flavobacterium*

Sherif Elnagdy, Susan Messing and Michael E. N. Majerus

*Insect Science*, 00: 1-8 (2013) IF: 1.786

Male-killing is 1 of 4 known strategies that inherited parasitic endosymbionts have evolved to manipulate their host's reproduction. In early male-killing, infected male offspring are killed early in embryogenesis. Within the Insecta, male-killing bacteria have been found in a wide range of hosts. The Coccinellidae families of beetles, better known as ladybirds, are particularly prone to male-killer invasion. In samples of the coccinellid, *Coccinula crotchii*, from Japan, a new male-killing bacterium was revealed by phenotypic assay. Molecular genetic analysis revealed the identity to be a tetracycline-sensitive *Flavobacterium* that causes female-biased offspring sex ratio. Furthermore, that *Flavobacterium* strain was found to be closely related to the *Flavobacterium* causing male-killing in the congeneric Japanese coccinellid, *Coccinula sinensis*, which was collected from the same region. However, we found slightly different *Flavobacterium* strains infecting *C. sinensis* from regions with different environmental conditions. This may be an indication of horizontal transmission of male-killing *Flavobacterium* between these 2 ladybird species. Finally, environmental conditions may affect the spread of male-killing bacteria among their hosts.

**Keywords:** *Coccinula crotchii*; *Coccinula sinensis*; Endosymbionts; *Flavobacterium*; Inherited bacteria; Male-Killing; Sex ratio distorter.

### 54. Ecophysiology of the Holoparasitic Angiosperm *Cistanche Phelypaea* (Orobanchaceae) in a Coastal Salt Marsh

Gamal Mohammad Fahmy

*Turkish Journal of Botany*, 37: 908-919 (2013) IF: 1.6

*Cistanche phelypaea* (L.) Cout. (Orobanchaceae) was found parasitising the roots of the succulent shrublets *Arthrocnemum macrostachyum* (Moric.) K.Koch (Chenopodiaceae) in a coastal salt marsh in Qatar. Measurements were conducted to identify soil properties, host, and noninfected plants by soil excavations to expose the haustoria of the parasite attached to the host roots. The water potential, osmotic potential, pressure potential, and chemical analyses were determined in parasite, host, and noninfected plants. Crown diameter and dry mass of the host plants were smaller than in the noninfected plants. A gradient of water potential existed between the host root and the underground tuberous body of the parasite. Potassium was the major cation found in the parasite, while sodium was dominant in the host and noninfected plants. The nitrogen, soluble sugars, total amino acids, and starch contents of the parasite were higher than those of the host and noninfected plants. The high ratio of  $K^+$  to  $Ca^{2+}$  in the parasite indicates that it is phloem-feeding. The high nutrient element contents and metabolic products in the parasite are possibly related to the creation of osmotic and water potential gradients between the host and *C. phelypaea*.

**Keywords:** *Cistanche phelypaea*; *Arthrocnemum macrostachyum*; Water potential; Osmotic potential; Salt marsh; Qatar.

### 55. Weed Flora in the Reclaimed Lands along the Northern Sector of the Nile Valley in Egypt

Monier Abd El-Ghani, Ashraf Soliman, Rim Hamdy and Ebtesam Bennoba

*Turkish Journal of Botany*, 37: 464-488 (2013) IF: 1.6

Deserts comprise about 95% of the total land surface of Egypt; therefore, their potential for production must be assessed. Weed communities are mainly affected by the environment, and studies may increase our knowledge of the relationship among the weed flora, soil properties, crop rotation, soil management, fertiliser usage, and weed control. The area under study is one of the most recently reclaimed lands. The recorded 150 species in the monitored 19 sites were distributed within 33 families. The species-rich families were:

Poaceae (31), Asteraceae (23), Brassicaceae (13), Chenopodiaceae (12), and Fabaceae (12). Chorological analysis revealed that the widely distributed species belonging to cosmopolitan, palaetropical, and pantropical chorotypes constituted about 39.3% of the recorded flora.

Pure Mediterranean species were very poorly represented, while biregional and triregional Mediterranean chorotypes constituted 28%. Saharo-Arabian chorotypes, either pure or penetrated into other regions, constituted 32%. Ubiquitous species with wide amplitude were *Cynodon dactylon* (L.) Pers. and *Sonchus oleraceus* L. Species richness varied from one crop to another. The winter weeds represented the main bulk of the recorded species within each crop, desert perennials exhibited notable variations, and margin species were the lowest.

Redundancy analysis demonstrated the effect of soil organic matter, coarse sand, fine sand, silt, and soil saturation point on the spatial distribution of weed communities. The species-environment correlations were higher for the 4 axes, explaining 64.1% of the cumulative variance. The variations in soil pH, bicarbonates, ammonia, silt, and sulphate contents classified the vegetation into 4 site (vegetation) groups. Application of cluster analysis of species in crop-orchard farmlands resulted in 4 floristic groups (A-D). The weed species of the 2 winter crops, Egyptian clover and wheat, separated in Group A, tomato (winter/summer crop) in Group B, maize as a summer crop in Group C, and weeds of olive orchards and vineyards in Group D. This demonstrated high significant correlations between the olive and vineyard orchards ( $P < 0.01$ ), and between the 2 winter crops, wheat and clover.

**Keywords:** Weed flora; Egypt; Agroecology; Cropping system; Spatial distribution; Winter crops; Orchards; Summer crops.

### 56. Purification and Characterization of Trehalase from Seeds of Chickpea (*Cicer Arietinum* L.)

Maimona Kord, Elhusseiny Youssef, Hanaa Elbadawy Ahmed and Ebtesam Qaid

*Turkish Journal of Biology*, 37: 661-669 (2013) IF: 0.914

In the present study, trehalase was purified and characterized from the seeds of *Cicer arietinum* L. 'Giza 1'. Crude extract was prepared and purified for electrophoretic homogeneity using ammonium sulfate, chromatography on DEAE-cellulose, CM Sepharose, and Sephadex G-200. The final specific activity was 7 U/mg proteins, with 232-fold purification. The purified enzyme exhibited its pH optimum at 5.5. The optimum temperature was

60 °C. The determined  $K_m$  value was 3.64 mM trehalose. The enzyme activity was stimulated by 20 mM  $Mn^{2+}$ ,  $Ni^{2+}$ , or  $Co^{2+}$ , while it was inhibited by 20 mM  $Na^+$ ,  $K^+$ ,  $Li^+$ ,  $Ca^{2+}$ ,  $Zn^{2+}$ ,  $Cu^{2+}$ , or  $Fe^{3+}$ .  $Zn^{2+}$  proved to be a noncompetitive inhibitor, while mannitol and validamycin A proved to be competitive inhibitors. The inhibition constants ( $K_i$ ) of  $Zn^{2+}$ , mannitol, and validamycin A were 7 mM, 9 mM, and 4 nM, respectively. The molecular mass of the native enzyme was 223 kDa by gel filtration. SDS-PAGE indicated that the enzyme consisted of 6 identical subunits with a molecular mass of 38 kDa.

**Keywords:** Cicer arietinum; Trehalase; Trehalose; Purification; Molecular mass; Validamycin A.

### 57. Purification of Antioxidant Protein Isolated from Peganum Harmala and its Protective Effect against $CCl_4$ Toxicity in Rats

Hanaa Ahmed, Helal Abu El Zahab and Gamia Alswiai

*Turkish Journal of Biology*, 37: 39-48 (2013) IF: 0.914

The present study was conducted to determine the protective effect of the purified protein from seeds of Peganum harmala against carbon tetrachloride ( $CCl_4$ )-induced toxicity in male albino rats. The purification steps included ammonium sulfate fractionation and chromatography on DEAE-cellulose, CM-Sephadex, and Superdex 75 columns. The molecular mass of the purified protein was 132 kDa by gel filtration technique; it consisted of 2 subunits with molecular masses of 30.199 kDa and 38.018 kDa by SDS-PAGE.

Results of the dose-dependent experiment with purified protein prior to  $CCl_4$  administration were higher at 4 mg/kg body weight. The antioxidant activity of the purified protein was determined in vitro by DPPH radical scavenging test. Administration of  $CCl_4$  significantly increased the activities of alanine aminotransferase, aspartate aminotransferase, and alkaline phosphatase in serum.

However, a significant decrease in the level of total serum protein as well as the activities of superoxide dismutase, catalase, and reduced glutathione in liver tissues, and a significant increase in malondialdehyde level, were recorded. Pretreatment with 4 mg/kg body weight of the purified protein significantly altered the deteriorating damage induced by  $CCl_4$  toxicity to a near normal range, which was similar to treatment with vitamin C. These results suggest that the purified protein possesses a protective effect against  $CCl_4$ -induced toxicity and probably acts as an antioxidative defense through free radical scavenging activity.

**Keywords:** Peganum harmala;  $CCl_4$ ; Hepatic toxicities; Alanine aminotransferase; Aspartate aminotransferase; Alkaline phosphatase; Superoxide dismutase; Catalase; Glutathione; Malondialdehyde.

### 58. Isolation of Aureobasidium Pullulans and the Effect of Different Conditions for Pullulanase and Pullulan Production<sup>1</sup>

Hani Moubasher, Salwa S. Wahsh and Nabil Abo El-Kassem

*Microbiology*, 82: 155-161 (2013) IF: 0.649

Isolation and production of pullulanase by a new Aureobasidium pullulans isolate from the Fayoum Governorate (AUMC 2997) which was identified by the Assiut University Mycological Center was investigated. Another isolate from the Aswan Governorate

(AUMC 1695) was kindly provided by the Assiut University Mycological Center. Acetone 2× gave better results for the precipitation of protein than 80% ammonium sulfate in the case of the media containing yeast extract. Very low protein production occurred in media without yeast extract. No enzyme production occurred in the first two days and the production of the enzyme started on the third day. Statistical analysis determined that the optimum conditions for the production of pullulanase were: incubation at 25°C for 5 days, pH 5.5, with sucrose as carbon source at 100 g/L and sodium nitrate as nitrogen source at 2 g/L. Addition of manganese chloride to the medium (1, 2 and 3 g/L) caused inhibition of pullulanase. Also, while the lowest pullulan + pigment concentrations were attained at the fifth day, pH 5.5, at 15°C, 100 g/L sucrose, 2 g/L nitrogen sources, the pullulan + pigment production increased with increasing the concentrations of manganese chloride.

**Keywords:** Pullulanase; Pullulan; Aureobasidium pullulans.

### 59. Molecular Differentiation between Aflatoxinogenic and Non-Aflatoxinogenic Strains of Aspergillus Flavus and Aspergillus Parasiticus

H. A. Moubasher, A. Abu Taleb and H. H. Senousy

*Microbiology*, 82: 642-646 (2013) IF: 0.649

Three types of media and a multiplex PCR procedure with a set of four primers were used to differentiate between aflatoxinogenic and non-aflatoxinogenic strains of Aspergillus flavus and Aspergillus parasiticus. Four sets of primers were the aflR, nor-1, ver-1, and omt-A genes of the aflatoxin biosynthetic pathway. Multiplex PCR showed that the four aflatoxinogenic strains gave a quadruplet pattern, indicating the presence of all the genes involved in the aflatoxin biosynthetic pathway which encode for the products. Non-aflatoxinogenic strains gave varying results with two, three, or four banding patterns. A banding pattern in seven non-aflatoxinogenic strains resulted in non-differentiation between these and aflatoxinogenic strains.

**Keywords:** Aflatoxinogenic; Non-aflatoxinogenic; Aspergillus flavus; Aspergillus parasiticus; PCR; aflR; Norsolonic acid;  $\alpha$ -Ketoreductase; O-methyltransferase A genes.

### 60. Impact of Mulching With Calotropis Procera Decne. Leaves on Seedling Emergence and Growth of Parkinsonia Aculeate L

Sanaa A. I. moussa and Hanaa K.Galal

*Wulfenia*, 20 (2): 286-299 (2013) IF: 0.467

In order to assess the magnitude of suppressing capability of Calotropis procera Decne on Parkinsonia aculeate L., the present study was conducted. The idea was quoted from the visual observation of the later as a desert weed of rare occurrence concomitant to the former in its communities. The investigation aims at elucidating the effect of organic mulching on the seed germination and growth of Parkinsonia. In a greenhouse potted experiment, Parkinsonia seeds were subjected to three mulch rates (1.5, 3 & 6 ton ha<sup>-1</sup>) of Calotropis Leaf Dry matter (CLD). The results showed that organic mulches significantly affected the final seed germination as well as the germination rate of Parkinsonia. Organic mulching also encouraged the R/S ratio (at bases of length), only at the mature vegetative stage. On bases of

dry weight, R/S ratio was inhibited; particularly at the rates (1.5 & 6 ton ha<sup>-1</sup>) at the juvenile stage. There was a decrease of the leaves numbers of mulched plants compared to the non-mulched ones. The Parkinsonia leaf area and average dry weight decreased at the intermediate rate of 3 ton ha<sup>-1</sup>, especially at the juvenile stage. Specific leaf area (SLA) decreased at all mulch rates; particularly at juvenile stage.

**Keywords:** Mulching; Seedling emergence; Growth parameters; Calotropis; Parkinsonia.

### 61. Molecular Characterization of Glyceraldehyde-3-Phosphate Dehydrogenase (Gapdh) Gene from *Aspergillus Fumigatus*

Tarek A. A. Moussa, Dalia M. Ali, Neveen M. Khalil and Fatma A. Mostafa

*Journal of Food, Agriculture and Environment*, 11(3.4): 235-241 (2013) IF: 0.435

First-strand cDNA was reverse transcribed from mRNA of *Aspergillus fumigatus* mycelium culture. The nucleotide sequence of gapdh was found to contain an ORF of 1083 bp, capable of coding for a protein of 360 amino acid residues. The signal peptide was predicted to be 19 amino acids in length.

The alignment of sequence analysis of this fragment with the previously determined nucleotide sequence led to the definition of the gene (gapdh -cDNA, accession no. AB683056). Sequence analysis revealed the presence of a potential site for substrate binding (ASCTTNCV) at position 172-179. Amino acids potentially associated with catalysis were found at amino acid positions 174 (C) and 201 (H). Potential phosphorylation sites were located at positions 13-21, 204-212, 219-227, 272-280 and 339-346. The amino acid residues at positions 7 (D) and 311 (N) corresponded to the putative NAD<sup>+</sup> binding sites. Amino acids at positions 145 (S), 150 (T), 204 (T) and 205 (R) were found to be probable sites for inorganic phosphate binding. Positions 180 and 222 were found to be amino acid residues that putatively related to the binding of the phosphate from the substrate (T and R). The calculated molecular weight of deduced polypeptide is 38.7 kDa, and the estimated isoelectric point (pI) is 7.28. The deduced amino acid sequence revealed the most abundant amino acid was alanine followed by leucine, whereas the rare amino acids are methionine followed by tryptophan.

**Keywords:** *Aspergillus fumigatus*; Glyceraldehyde-3-phosphate dehydrogenase gene; Signal peptide; Putative sites.

### 62. Antimicrobial Activities of Some Alkaliphilic and Alkaline-Resistant Microorganisms Isolated from Wadi Araba, the Eastern Desert of Egypt

Wael N. Hozzein, Mohamed Ibrahim A. Ali and Maged S. Ahmed

*Life Science Journal*, 10: 1823-1828 (2013) IF: 0.165

Thirty soil samples from different six localities representing Wadi Araba, Egypt were collected for isolation of alkaliphilic and alkaline-resistant microorganisms as a possible source of new antimicrobial compounds.

The climatic factors and soil analysis of the study area are given. The soil samples were sandy and varied from slightly to moderate alkaline, and also from non-saline to slightly saline. The number

of microbial colonies from the different soil samples varied from 10<sup>2</sup> to 10<sup>4</sup> CFU/g of soil. It was obvious that the viable microbial counts were affected by the organic matter content and the pH of the soil. A total of 117 alkaliphilic and alkaline-resistant microorganisms were isolated. Among them, 73 isolates were bacteria, 40 isolates were actinomycetes and the remaining 4 isolates were fungi. The purified alkaliphilic and alkaline-resistant microorganisms were investigated for their antimicrobial activities and the results revealed that 23 isolates of bacteria, 22 isolates of actinomycetes and two fungal isolates have antimicrobial activities. Therefore, the results recommended the screening of extremophiles as possible source of new secondary metabolites.

**Keywords:** Antimicrobial activities; Alkaliphilic; Alkaline-resistant; Microorganisms; Desert soil.

### 63. Biogenic Silver Nanoparticles by *Aspergillus Terreus* as a Powerful Nanoweapon against *Aspergillus Fumigatus*

Neveen M. Khalil

*African Journal of Microbiology Research*, 7 (50): 5645-5651 (2013)

In the past few decades, nanoparticles have emerged as a field in biomedical research. Four isolated *aspergillus* species were tested for extracellular synthesis of silver nanoparticles using their cell free filtrate (CFF). Silver nanoparticles of the most potent producer, *Aspergillus terreus*, were further characterized. Transmission electron microscope (TEM) and atomic force microscope (AFM) revealed their spherical shape, homogeneity and size range between 20 and 140 nm. X-ray diffraction (XRD) showed the crystalline nature of the biogenic silver nanoparticles. Fourier transform infra-red (FTIR) spectroscopic analysis indicated that the coordination behaviors between amino groups of the secreted fungal proteins and other functional groups present in the CFF may be liable for the reduction of silver ions to form stabilized protein-capped silver nanoparticles. They were stable in aqueous solution for four months of storage at room temperature under dark conditions. The biogenic silver nanoparticles showed remarkable antifungal activity against the human pathogenic fungus *A. fumigatus*. The spore cell wall, plasma membrane and the inner constituents were damaged as shown by TEM. Furthermore, comet assay proved high breakage of DNA.

**Keywords:** Silver nanoparticles; Biosynthesis; Fungi; Antifungal; Comet assay.

### 64. Potential of Antagonistic Yeast Strains As Biocontrol Agents against Root Rot Disease in Tomato

Zeinab Kamel and Nermin Housam Abd El-Moniem

*International Journal of Advanced Research*, 1:2320-5407 (2013)

The present study was conducted to evaluate the efficacy of the sixty plant growth promoting yeasts isolated from rhizosphere of healthy plants were tested for controlling tomato root rot disease caused by *Fusarium solani*, *Rhizoctonia solani* and *Pythium aphanidermatum* under greenhouse conditions. Their growth promoting activities on tomato were also tested. The bioagents were applied as seed dressing and as soil drenching treatments.



All bioagent treatments were significantly reduced disease severity of tomato root rot relative to the infested control plants inoculated with the pathogen only. The highest survival rates in pots (82.6 %), (84.1 %) and (82.6 %) were achieved by Y1, Y2 and Y3 respectively compared to infested control. The highest root dry weights in pots (0.3657 g/plant), (0.3455 g/plant) and (0.3946 g/plant) were achieved by Y1, Y2 and Y3 respectively compared to infested control. The most potent three bioagents with high antagonistic activity against phytopathogens were identified using phenotypic and genotypic techniques as *Candida tropicalis* (Castellani) Berkhout (Y1), *Pichia caribaea* Phaff (Y2) and *Geotrichum candidum* Link (Y3). These three bioagents were tested for lytic activity and the results revealed that *Candida tropicalis*, *Pichia caribaea* and *Geotrichum candidum* showed high chitinolytic activity while only *Geotrichum candidum* showed proteolytic activity and none of them showed phospholipolytic activity. The results indicate that application of *Candida tropicalis*; *Pichia caribaea* and *Geotrichum candidum* have potential as plant promoters and may be useful for biocontrolling soil-borne fungal plant pathogens causing root rot disease of tomato in the field. The use of biological agents to control soil plant pathogenic fungi is an attractive possibility. Successful application of the antagonistic yeast bioagents could become promoting natural antimicrobial agents, may be provide a protection against root rot plant fungal pathogens and may be useful as an eco-friendly manner and sustainable agriculture.

**Keywords:** Antagonists; Tomato root rot; Biological control; *Candida tropicalis*; *Pichia caribaea*; *Geotrichum candidum*.

## 65. Antioxidant Compounds Assays of Determination and Mode of Action

Emad A. Shalaby and Sanaa M. M. Shanab

*African Journal of Pharmacy and Pharmacology*, 7 (10): 528-539 (2013)

The human body uses an antioxidant defense system to neutralize the excessive levels of reactive oxygen species. This system consists of enzymatic and non enzymatic antioxidants, catalase, peroxidase, and superoxide dismutase and glutathion s-transferase as major defense enzymes. However, ascorbic acid, tocopherol, and phenolic compounds are considered as examples for non-enzymatic antioxidants. Increasing research on natural antioxidants in foods and development of new assays has prompted critical reflection on the field. It has been common practice to identify health benefits from antioxidant activity on the cellular level with antioxidant capacity of food measured in vitro. The use of antioxidants and their positive effects on food quality has been demonstrated in a large variety of foods and beverages using various methods for detection of lipid and protein oxidation or various assays based on electron transfer or hydrogen-atom transfer. There is a need for screening studies in order to identify the mode of action of different antioxidant compounds (enzymatic and non-enzymatic in addition, comparing between synthetic and natural antioxidant compounds) by different assays, in addition to highlighting the advantage and disadvantage of it. Some of these assays depend on hydrogen atom transfer methods or electron transfer methods in addition, metal chelating compounds and free radical scavenging activity.

**Keywords:** Synthetic and natural antioxidant compounds; Assays; Mechanism.

## 66. Seed Germination Vigor and Growth Parameters of Fenugreek (*Trigonella Foenum-Graecum* L.) as Affected by *Calotropis Procera* Decne. Organic Mulch

Sanaa A. I. Moussa

*Archives Des Sciences*, 66 (6): 341-353 (2013)

In order to assess the magnitude of the suppressing capability of *Calotropis procera* Decne on *Trigonella foenum-graecum* L., the present study was conducted. The idea was quoted from the visual observation of the former inside and around the cropfields of the later. The investigation aims at elucidating the effect of organic mulching on the seed germination and growth of *Trigonella*. In a greenhouse potted experiment, *Trigonella* seeds were subjected to three mulch rates (1.5, 3 & 6 ton ha<sup>-1</sup>) of *Calotropis* Leaf Dry matter. The results showed that organic mulches significantly affected the final seed germination as well as the germination rate of *Trigonella*. It also encouraged the leaves numbers as well as the leaf area of plants, at both lower and higher rates. On contrary, the intermediate mulching rate rendered both mentioned criteria. Obvious increase in average leaf dry weight per plant occurred at all mulch rates, compared with the non-mulched treatments. Specific leaf area values of highly mulched treatment exceeded that of non-mulched one. The most prominent result was the mortality of all plants, 41 days after planting at all mulched treatments. Generally, we might go to a conclusion that *Calotropis procera* mulch suppresses the seed germination as well as the germination rate of *Trigonella*, compared to the non-mulched treatment. Even the germination rate was affected so that it became faster with increasing the mulch rate. Only the highest mulch rate (6 ton ha<sup>-1</sup>) accompanied with the high R/S ratio; relying on the bases of length. There was a correlation between the numbers of leaves and the leaf area of *Trigonella* plants, especially at (1.5 & 6 ton ha<sup>-1</sup>) mulch rates when either parameter is enhanced. On contrary, both criteria were correlatively delayed at the intermediate (3 ton ha<sup>-1</sup>) mulch rate. Death of plants occurred after the age of 41 days. Certainly, this trait may be a result of releasing out poisonous allelopathic compounds in *Calotropis* which have great competitive abilities on *Trigonella* growth.

**Keywords:** *Calotropis*; Fenugreek; Growth criteria; Mulching rate.

## 67. Synergistic Interactions between Plant Extracts, Some Antibiotics and/or Their Impact upon Antibiotic-Resistant Bacterial Isolates

M. E. A. Dawoud, Y. A. Mawgoud and T. M. Gouda Dawoud

*African Journal of Biotechnology*, 12: 3835-3846 (2013)

In this study, the antibacterial activities of medicinal plant extracts [of *Rehum palmatum* (R), *Cassia angustifolia* (C), *Glycyrrhiza glabra* (G), *Chichorium intybus* (Ch), and *Matricaria chamomilla* (M)], on antibiotic-resistant isolates (*Staphylococcus aureus* and *Alcaligenes xylosoxidans*) collected from clinical samples, pharmaceutical products, and different hospital water drains was detected (single, combined extract). This investigation shows that the extracts of *G. glabra*, *R. palmatum* and *C. angustifolia* and their combination with the selected antibiotic, variously inhibited the growth of the bacterial isolates. The

methanol extraction ingredients recorded the maximum Inhibition Zone Diameter (mm IZD); 18.8/R, 12.6/C and 12.8/G plants. Prominent synergism occurred between plants extract mixture and Gentamycin, Ceftasidine, Tobramycin, Cefoperazone and Spictinomycin (GD) antibiotics.

Rehum plant extract was the most potent antibacterial agent against *S. aureus* and *A. xylosoxidans*, especially when extracted with methanol solvent.

**Keywords:** Synergism; Antagonism; Glycyrrhiza glabra; Rehum palmatum; Cassia angustifolia; Antibiotic-resistant bacteria; Staphylococcus aureus; Alcaligenes xylosoxidans; Hospitals drain; Clinical samples; Volatile oils; Total flavonoids.

#### 68. Trehalose Accumulation in Wheat Plant Promotes Sucrose and Starch Biosynthesis

Hanaa E. Ahmed, Elhusseiny A. Youssef, Maimona A. Kord and Ebtesam A. Qaid

*Jordan Journal of Biological Sciences*, 6: 143-150 (2013)

Seeds of *Triticum aestivum* L. (cv. Sakha 93) were sown in pots and grown under controlled conditions in growth chamber. The plants were irrigated with half strength of Hoagland solution without or with 10 or 30  $\mu$ M validamycin A, a potent inhibitor of trehalase. Plants were collected at three different stages of growth (17, 24 and 31 DAP). Validamycin A decreased the activity of trehalase which leads to the accumulation of trehalose in shoot and root of wheat plants. Raising trehalose level in the plant tissues was accompanied by increase in the sucrose content and starch content of the shoot. The increased contents in sucrose and starch were mainly attributed to the increased levels of trehalose. The effect of trehalose on the sucrose degrading enzymes (alkaline and acid invertases and sucrose synthase) showed stimulation of alkaline invertase activity and inhibition of acid invertase and sucrose synthase. The opposite behavior of sucrose degrading enzymes suggests a regulation mechanism controlling the sucrose pool.

**Keywords:** Trehalose; Trehalose -6-Phosphate; Carbohydrate; *Triticum aestivum*; Trehalase; Invertase; Sucrose synthase; Validamycin.

#### Dept. of Chemistry

#### 69. A Liquid Crystalline Phase with Uniform Tilt, Local Polar Order and Capability of Symmetry Breaking

Mohamed Alaasar, Marko Prehm, Mamatha Nagaraj, Jagdish K. Vij and Carsten Tschierske

*Advanced Materials*, 25: 2186-2189 (2013) IF: 14.829

A new liquid crystalline (LC) phase with uniform tilt, local polar order and capability of symmetry breaking is found for a bent-core mesogen combining a 4-cyanoresorcinol unit with two azobenzene wings. The combination of local polar order and long range synclinic tilt in this SmCsPR phase leads, under special conditions, to macroscopic domains with opposite chirality, though the molecules themselves are achiral.

**Keywords:** Liquid crystals; Chirality; Self-assembly; Bent-core Mesogens; Symmetry breaking.

#### 70. Bilayer Molecular Electronics: All-Carbon Electronic Junctions Containing Molecular Bilayers Made With "Click" Chemistry

Sayed Youssef Sayed, Akhtar Bayat, Mykola Kondratenko, Yann Leroux, Philippe Hapiot and Richard L. McCreery

*Journal of the American Chemical Society*, 135: 12972-12975 (2013) IF: 10.677

Bilayer molecular junctions were fabricated by using the alkyne/azide "click" reaction on a carbon substrate, followed by deposition of a carbon top contact in a crossbar configuration. The click reaction on an alkyne layer formed by diazonium reduction permitted incorporation of a range of molecules into the resulting bilayer, including alkane, aromatic, and redox-active molecules, with high yield (>90%) and good reproducibility. Detailed characterization of the current-voltage behavior of bilayer molecular junctions indicated that charge transport is consistent with tunneling, but that the effective barrier does not strongly vary with molecular structure for this series of molecules studied.

**Keywords:** Bilayer; Molecular Junction.

#### 71. Scalable Fabrication of High-Power Graphene Micro-Supercapacitors for Flexible and On-Chip Energy Storage

Maher El-Kady and Richard B. Kaner

*Nature Communications*, 4:1475: 1-10 (2013) IF: 10.015

The rapid development of miniaturized electronic devices has increased the demand for compact on-chip energy storage. Microscale supercapacitors have great potential to complement or replace batteries and electrolytic capacitors in a variety of applications. However, conventional micro-fabrication techniques have proven to be cumbersome in building cost-effective micro-devices, thus limiting their widespread application. Here we demonstrate a scalable fabrication of graphene micro-supercapacitors over large areas by direct laser writing on graphite oxide films using a standard LightScribe DVD burner. More than 100 micro-supercapacitors can be produced on a single disc in 30 min or less. The devices are built on flexible substrates for flexible electronics and on-chip uses that can be integrated with MEMS or CMOS in a single chip. Remarkably, miniaturizing the devices to the microscale results in enhanced charge-storage capacity and rate capability. These micro-supercapacitors demonstrate a power density of  $\sim 200 \text{ W cm}^{-3}$ , which is among the highest values achieved for any supercapacitor.

**Keywords:** Supercapacitor; Micro-scale; High-power; Graphene; On-chip energy storage.

#### 72. 4-Cyanoresorcinol-Based Bent-Core Mesogens with Azobenzene Wings: Emergence of Sterically Stabilized Polar Order in Liquid Crystalline Phases

Mohammed Alaasar, Marko Prehm, Kathrin May, Alexey Eremin and Carsten Tschierske

*Advanced Functional Materials*, 24 (12): 1703-1717 (2013) IF: 9.765

A new series of azobenzene containing bent-core molecules incorporating 4-cyanoresorcinol as the central core unit exhibiting cybotactic nematic, rectangular, columnar, and different types of tilted smectic (SmC) phases are synthesized. The mesophase behavior and phase structures are characterized in bulk and freely suspended films using a variety of experimental techniques. Depending on the chain length and temperature a series of different mesophases is observed in these compounds, ranging from cybotactic nematic via paraelectric SmC phases, polarization randomized SmC<sub>s</sub>P<sub>R</sub> phases to ferroelectric and antiferroelectric SmC phases, associated with increasing size and correlation length of the polar domains. Spontaneous formation of chiral domains is observed in the paraelectric SmC and the SmC<sub>s</sub>P<sub>R</sub> phases and discussed in relation with superstructural chirality, bend elastic constants, and surface effects.

**Keywords:** Liquid crystals; Ferroelectricity; Phase transitions; Chirality; Bent-core mesogens.

### 73. A New Room Temperature Dark Conglomerate Mesophase Formed by Bent-Core Molecules Combining 4-Iodoresorcinol With Azobenzene Units

Mohamed Alaasar, Marko Prehma and Carsten Tschierske

*Chemical Communications*, 49: 11062-11064 (2013) IF: 6.378

The first bent-core molecules comprising 4-iodoresorcinol as the central core unit and incorporating azobenzene units have been synthesized. A new type of dark conglomerate phase (DC phase) is observed, which remains over a wide temperature range down to room temperature without crystallization.

**Keywords:** Bent-core liquid crystals; Azobenzene; 4-iodoresorcinol; New dark conglomerate phase.

### 74. Rheological Behavior of Environmentally Friendly Castor Oil-Based Waterborne Polyurethane Dispersions

Samy A. Madbouly, Ying Xia and Michael R. Kessler

*Macromolecules*, 46: 4606-4616 (2013) IF: 5.521

Novel biorenewable, waterborne, castor oil-based polyurethane dispersions (PUDs) were successfully synthesized via homogeneous solution polymerization in methyl ethyl ketone followed by solvent exchange with water. Small-amplitude oscillatory shear flow experiments were used to systematically investigate the rheological behavior of these environmentally friendly, biorenewable, aqueous dispersions as a function of angular frequency, solid content, and temperature. In addition, the morphology of the dispersions was investigated at 60 °C for different time intervals using transmission electron microscopy (TEM). The solid content and temperature were found to significantly affect the rheological behavior of the PUDs. The composition dependency of the complex viscosity ( $\eta^*$ ) was found to be well described by the Krieger–Dougherty equation. Thermally induced gelation was observed for PUDs with a solid content  $\geq 27$  wt %. Although the viscoelastic behavior of the PUDs was well described by the time–temperature superposition (TTS) principle in a temperature range lower than the gel point, TTS failed to represent the behavior of the PUDs at temperatures near the critical gel point. The real time gelation behavior was also studied for different solid contents of PUDs under isothermal

conditions over a wide range of angular frequencies. Furthermore, both  $G'$  and  $G''$  showed a power law relationship with the angular frequency at the gel point, with critical power law exponents similar to those predicted theoretically by percolation theory. Aggregation and interconnection of the nano-PU particles caused the formation of fractal gels at a critical temperature, as confirmed by TEM.

**Keywords:** Rheology; Biorenewable; Castor oil-based polyurethane dispersions; Critical gel point.

### 75. Amperometric Glucose Sensor Based on Nickel Nanoparticles/Carbon Vulcan XC-72R

Randa Mohammed Abdel Hameed

*Biosensors and Bioelectronics*, 47: 248-257 (2013) IF: 5.437

A stable non-enzymatic glucose sensor was constructed by chemical deposition of nickel nanoparticles on carbon Vulcan XC-72R using microwave irradiation technique. The mode and time of microwave irradiation during nickel salt reduction were varied. This was found to affect the morphology of formed Ni/C powder as evidenced by TEM analysis. Nickel nanoparticles aggregation becomes more serious at longer microwave irradiation times. The electrocatalytic activity of different Ni/C samples towards glucose oxidation was studied in KOH solution by employing cyclic voltammetry and chronoamperometry techniques. Ni/C sample, prepared by pulse mode with total operating time of 150 s, showed the highest oxidation current density. An excellent sensitivity value of  $1349.7 \mu\text{A mM}^{-1} \text{cm}^{-2}$  with a detection limit of  $0.232 \mu\text{M}$  was gained by Ni/C sensor. It also exhibits good reproducibility and long-term stability, as well as high selectivity with insignificant interference from ascorbic acid.

**Keywords:** Glucose; Non-enzymatic sensor; Nickel nanoparticles; Carbon black; Microwave irradiation; Chemical synthesis.

### 76. An Electrocatalytic Oxygen Reduction by Copper Nanoparticles-Modified Au (100)-Rich Polycrystalline Gold Electrode in 0.5 M KOH

Mohamed I. Awad and Takeo Ohsaka

*Journal of Power Sources*, 226: 306-312 (2013) IF: 4.675

The electrocatalytic oxygen reduction reaction (ORR) at copper nanoparticles (nano-Cu) modified Au (100)-rich polycrystalline gold electrode (nano-Cu/Aur) in 0.5 M KOH is studied using cyclic and rotating disk voltammetry. The nano-Cu/Aur with a relatively enriched free Au(100) facet compared with the bare poly-Au electrode is prepared by a controlled electrodeposition of nano-Cu only on the Au(111) facet of the poly-Au electrode the other low-index facets (i.e., Au(100) and Au(110)) of which are previously covered with the self-assembled monolayer of cysteine. The electrocatalytic behavior of the nano-Cu/Aur is compared with those of the bare Au and the copper nanoparticles-modified gold electrodes (nano-Cu/Au) in which the nano-Cu is directly electrodeposited onto the poly-Au electrode. The nano-Cu/Aur shows a remarkable electrocatalysis, comparable to that of the platinum electrode, toward the ORR i.e., the ORR proceeds exclusively via a 1-step 4-electron reduction pathway at ca. 20–65 mV more positive potentials than at the bare Pt electrode, while

the ORR at the nano-Cu/Au proceeds via a two-electron pathway. X-ray diffraction spectra confirms the relative enrichment of nano-Cu/Aur electrode in Au(100) facet. The relative enrichment in the free Au(100) facet of the nano-Cu/Aur electrode is thought to be behind the extraordinary electrocatalytic activity.

**Keywords:** Nanoparticles; Oxygen reduction; Gold; Copper; Electrocatalysis.

### 77. Enhanced Glucose Electrooxidation at a Binary Catalyst of Manganese and Nickel Oxides Modified Glassy Carbon Electrode

S.M. El-Refaei, M. M. Saleh and M.I. Awad

*Journal of Power Sources*, 223: 125-128 (2013) IF: 4.675

A novel binary electrocatalyst fabricated from manganese and nickel oxides nanoparticles ( $\text{MnO}_x$  and  $\text{NiO}_x$ ), prepared by electrodeposition, is proposed as an anode for an amplified electrochemical oxidation of glucose in NaOH solutions. Cyclic voltammetry and scanning electron microscopy images were used to characterize these electrocatalysts. It has been found that the electrocatalytic activity critically depends on the order of the deposition of the two oxides. The  $\text{NiO}_x/\text{MnO}_x/\text{GC}$  electrode ( $\text{MnO}_x$  deposited first) showed a superior electrocatalytic activity towards glucose oxidation compared to  $\text{NiO}_x/\text{GC}$ ,  $\text{MnO}_x/\text{GC}$  or  $\text{MnO}_x/\text{NiO}_x/\text{GC}$  electrodes ( $\text{NiO}_x$  deposited first). The extraordinary activity obtained at the  $\text{NiO}_x/\text{MnO}_x/\text{GC}$  electrode is attributed to the compilation of the better adsorption of glucose molecules on the  $\text{MnO}_x$  sites and the increase of conductivity of the  $\text{NiO}_x$  due to the increase of  $\text{Ni}^{3+}$  content. The results lead us to conclude that there is a synergism between the two oxides towards the electrooxidation of glucose.

**Keywords:** Glucose; Manganese oxide; Nickel oxide; Fuel cell; Nano.

### 78. Impact of Acrylonitrile Poisoning on Oxygen Reduction Reaction at Pt/C Catalysts

Mohamed S. El-Deab, Fusao Kitamura and Takeo Ohsaka

*Journal of Power Sources*, 229: 65-71 (2013) IF: 4.675

This study addresses the poisoning effect of acrylonitrile (AcN) on the catalytic activity of a Pt/C catalyst modified GC disk electrode toward the oxygen reduction reaction (ORR) in  $\text{O}_2$ -saturated 0.1 M  $\text{HClO}_4$  solution. A significant retarding effect of AcN on the catalytic performance of the Pt/C catalyst toward the ORR is observed. For instance, the presence of 1 ppm AcN in solution causes a cathodic shift of the half-wave potential of the ORR by ca. 85 mV with the formation of hydrogen peroxide (2-electron reduction product of  $\text{O}_2$ ). Similar Tafel slopes (close to  $-68 \text{ mV dec}^{-1}$ ) are obtained at the unpoisoned and the poisoned Pt/C catalysts at low current density region. Whereas, a larger Tafel slope (ca.  $-228 \text{ mV dec}^{-1}$ ) is observed at the poisoned catalyst than that obtained at the unpoisoned Pt/C catalyst (ca.  $-128 \text{ mV dec}^{-1}$ ) at high current density region. The adsorption of AcN on the surface of the Pt/C is believed to alter its work function ( $\Phi$ ) in such a way that deteriorates its catalytic activity. The recovery of the performance of the Pt/C catalyst is achieved by employing a few potential cycles between the onset potentials of the hydrogen and the oxygen evolution reactions.

**Keywords:** Nanoparticles; Fuel cells; Oxygen reduction; poisoning effect; Hydrocarbon impurities.

### 79. Ni-P and Ni-Mo-P Modified Aluminium Alloy 6061 as Bipolar Plate Material for Proton Exchange Membrane Fuel Cells

Amani E. Fetohi, R. M. Abdel Hameed and K. M. El-Khatib

*Journal of Power Sources*, 240: 589-597 (2013) IF: 4.675

Aluminium alloy 6061 (AA6061) is coated with Ni-P and Ni-Mo-P using electroless and electroplating techniques. Coated substrates were characterized using scanning electron microscopy and energy dispersive X-ray analysis. Potentiodynamic polarization technique is applied to investigate the corrosion resistance characteristics of coated AA6061 in (0.5 M  $\text{H}_2\text{SO}_4$  + 2 ppm HF) solution. Coating AA6061 with Ni-P and Ni-Mo-P shifts its corrosion potential towards more positive values and lowers the corresponding current density values. The stability of prepared coatings under simulated cathode condition in PEM fuel cells is tested in air-saturated solution at +160 mV versus (mercury/mercury sulphate electrode (MMS)) for 5 h. After 40 min from starting the polarization test, Ni-P coating is found to be more stable than Ni-Mo-P. Ni-P and Ni-Mo-P coated AA6061 show a lowered ICR value at a compaction force of 140  $\text{N cm}^{-2}$  by 2.22 and 1.88 times, respectively when compared to bare aluminium alloy.

**Keywords:** Bipolar plate; Polymer electrolyte membrane fuel cells; Nickel-phosphorous; Nickel-molybdenum-phosphorous; Potentiodynamic polarization technique.

### 80. Dissolution Testing and Potentiometric Determination of Famciclovir in Pure, Dosage Forms and Biological Fluids

Mohamed S. Rezk and Rasha M. El Nashar

*Bioelectrochemistry*, 89: 26-33 (2013) IF: 3.947

The performance characteristics of two new plastic membrane ion selective electrodes (ISEs) used for the determination of famciclovir (Fcv) based on the ion associate of Fcv with phosphotungstic acid (PTA) or phosphomolybdic acid (PMA) is described. Different experimental conditions as type of plasticizer to be incorporated in the membrane, life span, effect of soaking, pH, temperature, and interferences were studied.

Both electrodes showed similar performance under these conditions, exhibiting Nernstian slopes of  $S(\text{Fcv-PTA}) = 58.60 \pm 0.84 \text{ mV/decade}$  and  $S(\text{Fcv-PMA}) = 58.77 \pm 0.68 \text{ mV/decade}$  within a usable concentration range of  $10^{-5}$ – $10^{-2}$  [Fcv/M] at 298/K. Famciclovir was assayed potentiometrically in its pure solution, pharmaceutical preparations and biological fluids (urine and plasma) using proposed electrodes under batch and flow injection analysis (FIA) conditions with a recovery % ranging between 96.76% and 102.83% having RSD of 0.66%–1.81%. The electrodes were also successfully applied in the determination of the dissolution profile of Fcv tablets and the results came in agreement with the validated results of the HPLC method obtained from the quality control unit of the company producing the tablets.

**Keywords:** Flow injection analysis; Dissolution testing; Famciclovir; Ion-selective electrodes.



### 81. Unravelling the Interplay of Crystal Structure and Electronic Band Structure of Tantalum Oxide (Ta<sub>2</sub>O<sub>5</sub>)

Ramy Nashed, Walid M. I. Hassan, Yehea Ismailc and Nageh K. Allam

*Physical Chemistry Chemical Physics (Pccp)*, 15: 1352-1357 (2013) IF: 3.829

The band structure and bandgap of Ta<sub>2</sub>O<sub>5</sub> are extremely controversial issues. Herein, the use of a hybrid functional reduces the error in bandgap estimation from 95% to 5% resulting in a bandgap of 3.7 eV. This is expected to help controlling the electronic and structural properties of the material.

**Keywords:** Crystal structure; Electronic band structure; Tantalum oxide.

### 82. Silver (I) Complexes as Precursors to Produce Silver Nanowires: Structure Characterization, Antimicrobial Activity and Cell Viability

Nadia Emam Aly El-Gamel

*Dalton Transactions*, 42: 9884-9892 (2013) IF: 3.806

In this contribution a simple method has been employed to synthesis silver nanowires by thermal decomposition of silver complexes. Nanowires are the product of possible chemical reduction of metallic silver residue that remains after the thermal degradation process. Silver (I) complexes of quinolone antibacterial drugs sparfloxacin [Ag (SPHX)<sub>2</sub>·NO<sub>3</sub>]·3H<sub>2</sub>O (1) and enrofloxacin [Ag(ENRX)<sub>2</sub>·NO<sub>3</sub>]·2H<sub>2</sub>O (2) have been prepared and structurally characterized. In the literature the carboxylate and the carbonyl oxygen atoms were the most predominant coordination sites used for quinolones.

The resulted complexes presented the drugs as monodentate ligands; however sparfloxacin displayed different behaviour than enrofloxacin. Sparfloxacin coordinated through the nitrogen atom of the piperazine ring, while enrofloxacin coordinated through carboxylate oxygen. Antimicrobial and antifungal activities of the reported complexes are evaluated using a modified Kirby–Bauer disc diffusion and MIC methods. High significant antimicrobial activity is recorded especially against *Escherichia coli* and *Aspergillus flavus*. In vitro cytotoxicity of the complexes is measured using MTT assay.

The analysis of the cell test showed that the selected complexes displayed no significant cytotoxic response which opens up opportunities for creating further advances in therapeutic challenges. The functional diversity of the prepared silver complexes as precursors of producing nanowires is a subject of high interest in the field of material science.

The prepared complexes represent a unique capability when set in the context of biomaterials for therapeutic actions and material engineering. This work provides insight into the mutual amenability of the prepared complexes which can be used to influence both cell–biomaterials interactions and in technical research community.

**Keywords:** Silver (I) complexes; Enrofloxacin; Sparfloxacin; Biological activity; Cell test.

### 83. Electrocatalysis by Design: Enhanced Electrooxidation of Formic Acid at Platinum Nanoparticles–Nickel Oxide Nanoparticles Binary Catalysts

Gumaa A. El-Nagar, Ahmad M. Mohammad, Mohamed S. El-Deab and Bahgat E. El-Anadoul

*Electrochimica Acta*, 94: 62-71 (2013) IF: 3.777

This study addresses the electrocatalytic oxidation of formic acid (FA) at binary catalysts composed of Pt nanoparticles (nano-Pt) and nickel oxide nanoparticles (nano-NiO<sub>x</sub>) electrodeposited onto glassy carbon (GC) electrodes. Pt electrode shows two oxidation peaks at ca. 0.25 and 0.65 V vs. Ag/AgCl/KCl (sat.) corresponding to the direct (View the Math ML source, favorable) and indirect (View the Math ML source, unfavorable) oxidation pathways of FA, respectively. Nano-Pt/GC electrode shows a significantly higher catalytic activity toward FA oxidation than the bulk Pt electrode. Interestingly, further modification of the nano-Pt/GC electrode with nano-NiO<sub>x</sub> leads to a superb enhancement of View the Math ML source with a concurrent suppression of View the Math ML source. The catalytic activity of the various modified GC electrodes is probed by the ratio of View the MathML source. This ratio increases from 0.2 at bulk Pt to 1.4 at nano-Pt/GC (i.e., ca. 7 times higher), and jumps up to more than 20 at the binary nano-NiO<sub>x</sub>/nano-Pt modified GC electrode, reflecting the superiority of the latter electrode toward FA oxidation to CO<sub>2</sub>. While nano-Pt furnishes a suitable base for FA adsorption, nano-NiO<sub>x</sub> acts as a catalytic mediator which facilitates the charge transfer during the direct oxidation of FA. The influence of the deposition sequence and the loading level of both species (i.e., Pt and NiO<sub>x</sub>) on the catalytic activity of the binary catalyst are investigated.

**Keywords:** Electrocatalysis; Nickel oxide nanoparticles; Platinum nanoparticles; Fuel cells.

### 84. Electrocatalytic Glucose Oxidation at Binary Catalyst of Nickel and Manganese Oxides Nanoparticles Modified Glassy Carbon Electrode: Optimization of the Loading Level and Order of Deposition

Sayed M. El-Refaei, M.I. Awad, B.E. El-Anadoul and M.M. Saleh

*Electrochimica Acta*, 92: 460-467 (2013) IF: 3.777

This work addresses the electrocatalytic activity of a new catalyst composed of nickel and manganese binary oxides, prepared by electrodeposition, towards glucose electro-oxidation in alkaline medium. Cyclic voltammetry, scanning electron microscopy (SEM) and energy-dispersive X-ray spectroscopy (EDX) were used to characterize those electrocatalysts. It has been found that the electrocatalytic activity critically depends on the loading level and the order of deposition of the two oxides; the NiO<sub>x</sub>/MnO<sub>x</sub>/GC electrode (MnO<sub>x</sub> deposited first) showed an excellent electrocatalytic activity and stability towards glucose oxidation compared to NiO<sub>x</sub>/GC, MnO<sub>x</sub>/GC or MnO<sub>x</sub>/NiO<sub>x</sub>/GC electrodes (NiO<sub>x</sub> deposited first). At the present work conditions, it has found that, the optimum loading level is 60 cycles of MnO<sub>x</sub> followed by 10 minutes deposition of nickel. At this loading level,

**Keywords:** Glucose; Manganese oxide; Nickel oxide; Fuel cell; Nanoparticles.

## A. M. Ghonim, B. E. El-Anadouli and M. M. Saleh

Electrochimica Acta, 114: 713-719 (2013) IF: 3.777

The purpose of the anodic oxidation is to manipulate the GC surface such that it gives higher surface concentration of C–O functional groups and higher surface area which leads to an extraordinary increase in the activity of NiOx towards glucose electrooxidation. Glucose electrooxidation is conducted in alkaline medium at GC/NiOx (GC is untreated) and GC<sub>ox</sub>/NiOx (GC is treated) electrodes. Cyclic voltammetry (CV), scanning electron microscopy (SEM) and energy dispersive X-ray spectroscopy (EDX) are used for characterization of the above electrodes. The GC<sub>ox</sub>/NiOx shows an excellent electrocatalytic activity toward glucose oxidation compared to GC/NiOx. The enhancement of the electrocatalytic activity obtained at the GC<sub>ox</sub>/NiOx is discussed in the light of the obtained differences in characteristics of GC<sub>ox</sub>/NiOx and increase in the surface concentration of C–O functional groups.

**Keywords:** GC; Oxidized; Nickel oxide; Nanoparticles; Glucose.

## Ghada M. Abd El-Hafez and Waheed A. Badawy

*Electrochimica Acta*, 108: 860-866 (2013) IF: 3.777

interface. The corrosion inhibition process is based on the adsorption of the amino acid molecules on the alloy surface, and the adsorption follows the Langmuir adsorption isotherm. The free energy of adsorption of the different amino acids on the alloy surface was in the range of  $\approx -35 \text{ kJ mol}^{-1}$ , which reveals a strong physical adsorption of the inhibitor molecules on the metallic surface.

**Keywords:** Amino acids; Corrosion inhibition; Copper alloys; Impedance; Polarization.

## A. Khamis, Mahmoud M. Saleh, Mohamed I. Awad and B.E. El-Anadouli

*Corrosion Science*, 74: 83-91 (2013) IF: 3.615

The synergistic effect of N-hexadecylpyridinium bromide (PyC<sub>16</sub>Br) and different sodium halides on the corrosion of mild steel in 0.5 M H<sub>2</sub>SO<sub>4</sub> solution has been investigated using electrochemical methods, X-ray diffraction (XRD) and scanning electron microscope (SEM). Experimental results showed that the protection efficiency ( $P_{\text{icor}}$ ) of PyC<sub>16</sub>Br improved at either considerable high concentration near its critical micelle concentration (CMC) or in the presence of the different halides with different extents. The synergism parameter ( $S_b$ ) is found to be greater than unity indicating high  $P_{\text{icor}}$ . Corrosion products phases and surface morphology were studied using XRD and SEM, respectively.

**Keywords:** A. Mild steel; B. polarization; B. SEM; B. XRD; C. acid inhibition.

## A. Khamis, M.M. Saleh and M.I. Awad

*Corrosion Science*, 66: 343-349 (2013) IF: 3.615

The synergistic inhibitory action of cetylpyridinium chloride (CPC) and different halides on the corrosion of mild steel in 0.5 M  $\text{H}_2\text{SO}_4$  has been investigated using electrochemical methods and scanning electron microscopy (SEM). Experimental results showed that the protection efficiency ( $P_{\text{icor}}$ ) of CPC improved in the presence of the different halides with different extents. Chemisorption was proposed from the trend of  $P_{\text{icor}}$  and the values of  $\Delta G_{\text{ads}}^{\text{fl}}$ . The synergism parameter is found to be greater than unity indicating that the enhanced  $P_{\text{icor}}$  caused by the addition of the halides to the CPC is due to a co-operative adsorption of both species.

**Keywords:** A-Mild steel; B- polarization; B- sem; C- acid Corrosion; C- acid inhibition.

## 89. Cathodic Hydrogen Evolution on Molybdenum in NaOH Solutions

W.A. Badawy, H. E. Feky, N. H. Helal and H. H. Mohammed

*International Journal of Hydrogen Energy*, 38: 9625-9632 (2013)  
IF: 3.548

The general electrochemical behavior of molybdenum was investigated in sodium hydroxide solutions of different concentrations. The investigations were concentrated on the hydrogen evolution reaction on the metal surface. The effect of alkali concentration, cathodic potential and temperature on the rate of hydrogen evolution was evaluated. The results were compared with those obtained on copper or platinum metals. Different electrochemical techniques were used. Impedance measurements under open circuit conditions and under cathodic polarization were carried out. The experimental impedance data were fitted to theoretical data according to a proposed model for the electrode/electrolyte interface. The results have shown that molybdenum can be considered a good candidate for the cathodic hydrogen on a large scale and for long use.

**Keywords:** Molybdenum; Electrochemical techniques; Hydrogen evolution; Impedance measurements; Sodium hydroxide.

## 90. Synthesis and Characterization of Novel Series of Fe (II)-Mixed Ligand Complexes Involving 2,2'-Bipyridyl Ligand

Ahmed A. Soliman, Mina A. Amin, Ahmed A. El-Sherif, Saliha Ozdemir, Canan Varlikli and Ceylan Zafer

*Dyes and Pigments*, 99: 1056-1064 (2013) IF: 3.532

Mixed ligand complexes of Fe(II) with 2,2'-Bipyridyl (bipy) and some aromatic amines (L) (L  $\frac{1}{4}$  3,4- diamino benzoic acid (DABA), 2-hydazinopyridine (hzpy) or 4-chloro-o-phenylenediamine (4-Cl-o-PDA) have been synthesized and characterized using IR, Mass, and UV-Vis spectrometry, magnetic susceptibility and thermal analysis. The complexes have been proved to have an octahedral geometry with equilibrium between high spin and low spin states which is reflected from the values of the  $m_{eff}$  (3.34e4.09). The electrochemical properties of these complexes have been studied using cyclic voltammetry.

The structure of the Fe(II)-complexes have been geometrically optimized using parameterized PM3 semiempirical method. The photovoltaic performances of the complexes have been tested.

**Keywords:** Fe (II) complexes; Thermal stability; Photophysics; Magnetic susceptibility; Cyclic voltammetry and mo calculations.

## 91. Benzofuran Derivatives: A Patent Review

Kamal Mohamed Dawood

*Expert Opinion Therapeutic Patents*, 23: 1133-1156 (2013)  
IF: 3.525

**Introduction:** Benzofuran moiety constitutes the core of several interesting pharmacologically active natural products. Benzofurans are among feasible potent active inhibitors against many diseases, viruses, microbes, fungus and enzymes. Several series of therapeutically important synthetic and naturally occurring benzofuran-containing compounds are reported in this chapter.

**Areas covered:** The current chapter focuses on the recent applications of benzofuran scaffolds and their wide range of biological activities during 1999 -- 2012. The pharmacological areas covered included anti-inflammatory, antitumor, cytotoxic, antimicrobial, antitubercular, antioxidant, antiplasmodial, trypanocidal and insecticidal activities as well as enzyme inhibitory, HCV and HIV inhibitory activities.

**Expert opinion:** The results reported in the chapter indicate that some benzofuran derivatives may be useful as potent drugs. From the structure-activity relationship (SAR), the presence of certain functions like -OH, -OMe in the benzofuran derivatives contributed greatly in increasing the potency of their therapeutic activities when compared with standards. For example, presence of the -OH and -OMe have made some benzofuran compounds more potent HIV-RT inhibitory activity than the standard atavirdine, and more potent antitumor agent when compared with standards (fluorouracil, doxorubicin and cytarabine). In addition, the enzyme aromatase CYP19 inhibitory activity of benzofurans having -OH and -OMe were greater than that observed for the reference arimidex.

**Keywords:** Anti-inflammatory; Antimicrobial; Antitumor; Benzofurans; Cytotoxic; HCV; HIV inhibitory.

## 92. Synthesis of Some New Pyrazole-Based 1,3-Thiazoles and 1,3,4-Thiadiazoles As Anticancer Agents

Kamal M. Dawood, Taha M.A. Eldebss, Heba S.A. El-Zahabi, Mahmoud H. Yousef and Peter Metz

*European Journal of Medicinal Chemistry*, 70: 740-749 (2013)  
IF: 3.499

N-(4-(Pyrazol-4-yl)thiazol-2-yl)-N'-phenylthiourea derivative 2 was synthesized and then treated with variety of hydrazonoyl chlorides under basic condition at reflux to afford the corresponding 2-(4-(pyrazol-4-yl)thiazol-2-ylimino)-1,3,4-thiadiazole derivatives 6, 10a-e and 17a-e. Reaction of 2 with ethyl chloroacetate and with 3-chloro-2,4-pentanedione gave the thiazolidin-4-one 22 and 1,3-thiazole 25 derivatives, respectively. Condensation of thiazolidin-4-one 22 with aldehydes gave their 5-arylidene derivatives 23a-f. Most of the synthesized compounds were tested for anticancer activity against human hepatocellular carcinoma HepG2, human breast cancer MCF-7 and human lung cancer A549. Their SAR was studied and variously affected by the electronic factor of electron donating and withdrawing groups. Many of the tested compounds showed moderate to high anticancer activity.

**Keywords:** Pyrazole; 1,3-Thiazole; 1,3-Thiazolidin-4-One; 1,3,4-Thiadiazole; Anticancer activity.

## 93. Design, Synthesis and Molecular Modeling Studies of Some Heterocyclic Compounds Derived From the Suzuki-Coupling of 6-Bromo-1,3,4-Oxadiazine Together With Their Antitumor and Anti-Leishmanial Evaluations

Rafat M. Mohareb, Sherif M. Sherif and Adel Abou Elkair

*Current Organic Chemistry*, 17: 1910-1918 (2013) IF: 3.039

The reaction of cyanoacetylhydrazine (1) with 3-(2-bromoacetyl)-2H-chromen-2-one (2) in 1,4-dioxan gave the

hydrazidehydrazone derivative (3). The latter compound was cyclized to the 1,3,4-oxadiazine derivative 4, its 4-bromo derivative underwent a series of cross coupling reactions together with [4+2] cycloaddition reactions with either acrylonitrile or ethyl acrylate to afford the pyran derivatives 10a and 10b, respectively. The antitumor evaluation of the newly synthesized products against three cancer cell lines, namely breast adenocarcinoma (MCF-7), non-small cell lung cancer (NCI-H460) and CNS cancer (SF-268) were recorded. Four of the synthesized compounds namely 7c, 10a, 11a and 12b showed high inhibitory effects. Moreover, the anti-leishmanial activity of the newly synthesized product was tested on Leishmania donovani amastigotes showed that some compounds have high activity.

**Keywords:** Cross coupling; Hydrazide-hydrazone; 1,3,4-oxadiazine; Coumarin; Anti-tumor.

#### 94. Factors Affecting Hydrogen Production from Rice Straw Wastes in A Mesophilic Up-flow Anaerobic Staged Reactor

A. Tawfik, A. Salem, M. El-Qelish, A. A. Fahmi and M. E. Moustafa

*Renewable Energy*, 50: 402-407 (2013) IF: 2.989

Anaerobic biodegradation of rice straw wastes for  $H_2$  production via mesophilic up-flow anaerobic staged reactor (UASR) was investigated. Two batch experiments were carried out. The 1st experiment was conducted to assess the effect of pre-acidification process on  $H_2$  production rate ( $R_m$ ). The results showed that the maximum  $R_m$  of 136.64 mL $H_2$ /h was achieved for pre-acidified (0.72%) rice straw waste, which was approximately 28.64-fold greater than that in untreated rice straw. The  $H_2$  content in the biogas was 52.0% and there was no significant methane observed in this study. The pre-acidified rice straw was used for subsequent experiments concerning the influences of environmental factors such as pH, contact time, and substrate concentration on  $H_2$  yield (HY). Trends indicate that both high and low-end pH is unfavorable and substrate concentration of 30 g COD/l and contact time of 30 h is recommended for  $H_2$  production from pre-acidified rice straw.

**Keywords:** Hydrogen; Rice straw; Ph; Acidification; Substrate.

#### 95. Potential Use of Novel Modified Fishbone for Anchoring Hazardous Metal Ions from Their Solutions

Ehab M. Zayed, Hesham H. Sokker, Hassan M. Albishri and Ahmad M. Farag

*Ecological Engineering*, 61: 390-393 (2013) IF: 2.958

Bones obtained from Mullet fish in the Red Sea were grafted with acrylic acid by radiation-induced polymerization and were used as natural sorbents in the removal of lead and cadmium ions which are considered as major pollutants in the wastewater. The removal efficiency of the adsorbent was investigated as a function of pH, contact time, initial metal ion concentration, and adsorbent dose. The maximum adsorption capacities of lead and cadmium ions were 855 mg/g and 785 mg/g, respectively at optimum conditions. The kinetic studies of adsorption for lead and cadmium ions were found to obey a pseudosecond-order model

and the adsorption of both ions was found to fit the Langmuir isotherm. The grafted fishbone was effectively used as a sorbent for the removal of  $Pb^{2+}$  and  $Cd^{2+}$  ions from aqueous solution.

**Keywords:** Fishbone; Grafted fishbone; Removal of hazardous metal ions; Radiation-induced grafting polymerization.

#### 96. A New Validated Potentiometric Method for Batch and Continuous Quality Control Monitoring of Oseltamivir Phosphate (Taminil) in Drug Formulations and Biological Fluids

Saad S. M. Hassan, Rasha M. EL-Nashar and Aliaa S. M. El-Tantawy

*Electroanalysis*, 25: 408-416 (2013) IF: 2.817

A new validated potentiometric method is described for batch and continuous quality control monitoring of the drug oseltamivir phosphate (Taminil) (OST). The method involves the development of a potentiometric sensor responsive to the drug based on the use of the ion-association complex of (OST<sup>+</sup>) cation with phosphomolybdate anion (PMA<sup>-</sup>) as an electroactive material in a poly(vinyl chloride) matrix membrane plasticized with *o*-nitrophenyloctyl ether (*o*-NPOE). Optimization of the performance characteristics of the sensor is described. A membrane incorporating the OST-PMA-NPOE complex in a tubular flow through detector is used in a two channel flow injection set up for continuous monitoring of the drug at a frequency of ~30 samples h<sup>-1</sup>. The sensor shows fast near-Nernstian response for OST over the concentration range 5.2×10<sup>-3</sup>–0.8×10<sup>-2</sup> M (21.34 µg mL<sup>-1</sup>–3.23 mg mL<sup>-1</sup>) with a detection limit of 9.1×10<sup>-6</sup> M (3.73 µg mL<sup>-1</sup>) over the pH range 4.6–6.1. The sensor displays good selectivity for OST drug over some basic drugs, inorganic cations, excipients and diluents commonly used in the drug formulations. Validation of the assay method is tested by measuring the lower detection limit, range, linearity, bias, trueness, accuracy, precision, and between-day-variability, within day reproducibility, selectivity and ruggedness (robustness). The results reveal good potentiometric performance of the proposed sensor for determination of OST in pharmaceutical capsules and in biological fluid matrices as well as for testing the dissolution profile of the drug and drug homogeneity.

**Keywords:** Oseltamivir phosphate; Flow injection analysis; Pharmaceutical analysis; Potentiometric sensors; Method validation; Poly (vinyl chloride) membrane.

#### 97. The Knoevenagel Reactions of Pregnenolone with Cyanomethylene Reagents: Synthesis of Thiophene, Thieno [2,3-B] Pyridine, Thieno [3,2-D] Isoxazole Derivatives of Pregnenolone and Their In Vitro Cytotoxicity Towards Tumor and Normal Cell Lines

Rafat M. Mohareb, Nahed N.E. El-Sayed and Mahmoud A. Abdelaziz

*Steroids*, 78: 1209-1219 (2013) IF: 2.803

The reaction of pregnenolone with either 2-aminoprop-1-ene-1,1,3-tricarbonitrile or 3-oxo-3-phenylpropanenitrile gave the Knoevenagel condensation products **3** and **6**, respectively. Separation of the E and Z isomeric compounds of **3** and **6** together with their structure elucidation were carried out. Some



chemical transformations of the latter products were carried out and the cytotoxicity of the newly obtained products was evaluated against some cancer cell lines and a human normal cell line. The results indicated that compounds **15**, **17a**, **18** and **20e** among the tested compounds showed the highest cytotoxicity against the cancer cell lines.

**Keywords:** Pregnenolone; Cyanomethylene; Thiophene; Fused thiophene; Cytotoxicity.

## 98. Theoretical Investigation of the Dispersion Interaction in Argon Dimer and Trimer

Abdullah H. Quasti and Walid I. Hassan

*Journal of Biophysical Chemistry*, 4: 91-101 (2013) IF: 2.771

The ultimate aim of the present work is to establish an acceptable level of computation for the van der waals (vdw) complexes that is able to pick up appreciable amount of dispersion interaction energy, reproduce the equilibrium separation within the acceptable limits and at the same time cost and time effective. In order to reach this aim vdw clusters where pure isotropic dispersion interaction occur, namely, Ar dimer and trimer were investigated. Computations using different basis sets and at different levels of theory have been carried out. Three basis sets, namely, the 6-31++G\*\*, the 6-311++G\*\* and the aug-cc-pvdz basis set, were found superior to all other basis sets used. The high performance and relative small CPU time of the 6-31++G\*\* basis set make it a good candidate for use with large vdw clusters, especially those of interest in biology. Three compound methods were applied in the present work, namely G1, G2 and G2 Moller-Plesset (MP2) and the complete basis set method, CBS-Q. These methods failed to detect the attraction dispersion interaction in the dimer. The predicted repulsive interaction seems dominant in all these methods. Some of the recently developed Density Functional Theory (DFT) methods that were parameterized to account for the dispersion interaction were also evaluated in the present work. Results come to the conclusion that, in contrast to the claims made, state-of-the-art Density Functional Theory methods are incapable of accounting for dispersion effects in a quantitative way, although these methods predict correctly the inter-atomic separations and are thus considered a real improvement over the conventional methods. BS-SE has been computed, analyzed and discussed.

**Keywords:** Vdwclusters; Dispersion interaction; Argon dimer and trimer; Ab initio computation; Density functional Theory.

## 99. Novel Terephthaloyl Thiourea Cross-Linked Chitosan Hydrogels as Antibacterial and Antifungal Agents

Nadia Ahmed Mohamed and Noura Yahya Al-mehbad

*International Journal of Biological Macromolecules*, 57: 111-117 (2013) IF: 2.596

Four novel terephthaloyl thiourea chitosan (TTU-chitosan) hydrogels were synthesized via a cross-linking reaction of chitosan with different concentrations of terephthaloyl diisothiocyanate. Their structures were investigated by elemental analyses, FTIR, SEM and X-ray diffraction. The antimicrobial activities of the hydrogels against three species of bacteria (*Bacillus subtilis*, *Staphylococcus aureus* and *Escherichia coli*) and

three crop-threatening pathogenic fungi (*Aspergillus fumigatus*, *Geotrichum candidum* and *Candida albicans*) are much higher than that of the parent chitosan. The hydrogels were more potent in case of Gram-positive bacteria than Gram-negative bacteria. Increasing the degree of cross-linking in the hydrogels resulted in a stronger antimicrobial activity.

**Keywords:** Chitosan; Terephthaloyl diisothiocyanate; Cross-linking; Hydrogels; Synthesis; Antimicrobial activity.

## 100. Quaternized N-Substituted Carboxymethyl Chitosan Derivatives as Antimicrobial Agents

Nadia A. Mohameda, Magdy W. Sabaa, Ahmed H. El-Ghandour, Marwa M. Abdel-Aziz and Omayma F. Abdel-Gawad

*International Journal of Biological Macromolecules*, 60: 156-164 (2013) IF: 2.596

Introduction of quaternary ammonium moieties into N-substituted carboxymethyl chitosan (N-substituted CMCh) derivatives enhances their biological activity. Several derivatives of CMCh having a variety of N-aryl substituents bearing either electron-donating or electron withdrawing groups have been synthesized by the reaction between amino group of CMCh with various aromatic aldehydes under acidic conditions, followed by reduction of the produced Schiff base derivatives with sodium cyanoborohydride. Each of the reduced derivatives was further quaternized using N-(3-chloro-2-hydroxy-propyl) trimethylammonium chloride (Quat-188). The resulting quaternized materials were characterized by FTIR and <sup>1</sup>H NMR spectroscopy. Their antibacterial activities against *Streptococcus pneumoniae* (*S. pneumonia*, RCMB 010010), *Bacillus subtilis* (*B. subtilis*, RCMB 010067), as Gram positive bacteria and against *Escherichia coli* (*E. coli*, RCMB 010052) as Gram negative bacteria and their antifungal activities against *Aspergillus fumigatus* (*A. fumigates*, RCMB 02568), *Geotrichum candidum* (*G. candidum*, RCMB 05097), and *Candida albicans* (*C. albicans*, RCMB 05031) were examined using agar disk diffusion method. The results indicated that all the quaternized derivatives showed better antimicrobial activities than that of CMCh. These derivatives are highly potent against Gram positive bacteria compared to Gram negative bacteria. This is illustrated for example as the values of minimum inhibitory concentration (MIC) of Q4NO<sub>2</sub>-BzCMCh against *B. subtilis* and *S. pneumonia* were 6.25 and 12.5 µg/mL, respectively corresponded to 20.0 µg/mL against *E. coli*. The antimicrobial activity of quaternized N-aryl CMCh derivatives affected by not only the nature of the microorganisms but also by the nature, position and number of the substituent groups on the phenyl ring. Thus while the derivatives with groups of electron withdrawing nature show higher inhibition zone diameter and lower MIC values relative to that of those having electron-donating nature, the non-substituted derivative lies between these two extremes. Antibacterial activities of Q4NO<sub>2</sub>-BzCMCh, Q3Cl-BzCMCh and Q3Br-BzCMCh against *E. coli* are nearly equivalent to that of the standard drug Gentamycin. Q3Br-BzCMCh emerged almost equivalent antibacterial activity to Ampicillin against *S. pneumonia*.

**Keywords:** Quaternized n-substituted carboxymethyl; Chitosan derivatives; Antibacterial activity; Antifungal activity; Structure-activity relationship.

### 101. Determination of the Design Space of the HPLC Analysis of Water-Soluble Vitamins

Hebatallah A. Wagdy, Rasha S. Hanafi, Rasha M. El-Nashar and Hassan Y. Aboul-Enein

*Journal of Separation Science*, 36: 1703-1710 (2013) IF: 2.591

Analysis of water-soluble vitamins has been tremendously approached through the last decades. A multitude of HPLC methods have been reported with a variety of advantages/shortcomings, yet, the design space of HPLC analysis of these vitamins was not defined in any of these reports. As per the food and drug administration (FDA), implementing the quality by design approach for the analysis of commercially available mixtures is hypothesized to enhance the pharmaceutical industry via facilitating the process of analytical method development and approval. This work illustrates a multifactorial optimization of three measured plus seven calculated influential HPLC parameters on the analysis of a mixture containing seven common water-soluble vitamins ( $B_1$ ,  $B_2$ ,  $B_6$ ,  $B_{12}$ , C, PABA, and PP). These three measured parameters are gradient time, temperature, and ternary eluent composition (B1/B2) and the seven calculated parameters are flow rate, column length, column internal diameter, dwell volume, extracolumn volume, %B (start), and %B (end).

The design is based on 12 experiments in which, examining of the multifactorial effects of these 3 + 7 parameters on the critical resolution and selectivity, was carried out by systematical variation of all these parameters simultaneously. The 12 basic runs were based on two different gradient time each at two different temperatures, repeated at three different ternary eluent compositions (methanol or acetonitrile or a mixture of both). Multidimensional robust regions of high critical  $R_s$  were defined and graphically verified. The optimum method was selected based on the best resolution separation in the shortest run time for a synthetic mixture, followed by application on two pharmaceutical preparations available in the market. The predicted retention times of all peaks were found to be in good match with the virtual ones. In conclusion, the presented report offers an accurate determination of the design space for critical resolution in the analysis of water-soluble vitamins by HPLC, which would help the regulatory authorities to judge the validity of presented analytical methods for approval.

**Keywords:** 3D-modeling software; Method development; Quality by design (QbD); Water-soluble vitamins.

### 102. Poisoning Effect of Selected Hydrocarbon Impurities on the Catalytic Performance of Pt/C Catalysts towards the Oxygen Reduction Reaction

Mohamed S. El-Deab, Fusao Kitamura and Takeo Ohsaka

*Journal of the Electrochemical Society*, 160: 651-658 (2013) IF: 2.588

This study addresses the oxygen reduction reaction (ORR) at a typical carbon supported Pt (Pt/C) catalyst in the presence of some hydrocarbon impurities. The activity of Pt/C catalyst decreases in the presence of a few ppm concentrations of impurities (vinyl acetate (VA) > propionic acid (PA) > toluene (Tol) > triethyl amine (TEA)) in 0.1 M  $HClO_4$  solution, as revealed by a negative shift in the half-wave potential of the ORR together with the formation of  $H_2O_2$ . Tafel plots for the ORR with

similar slopes were obtained at the unpoisoned and the poisoned Pt/C catalysts indicating that the ORR proceeds via a similar rate-determining step (albeit with a lower kinetic current). The increase of % $H_2O_2$  at the poisoned Pt/C catalyst indicates that the hydrocarbon impurities act as site-blocking species which decreases the number of active sites necessary for the favorable parallel adsorption of  $O_2$  molecules to affect a 4-electron ORR. The order of activity loss by the hydrocarbon impurities is in line with the dipole moment of each molecule. The recovery of the catalytic activity of the poisoned Pt/C catalysts is achieved by employing a few potential cycles between the onset potentials of hydrogen and oxygen evolution reactions.

**Keywords:** Oxygen reduction; Pt nanoparticles; Fuel cells; Impurities; Electrocatalysis.

### 103. The Electrochemistry and Determination of Some Neurotransmitters at SrPdO<sub>3</sub> Modified Graphite Electrode

Nada F. Atta, Shimaa M. Ali, Ekram H. El-Ads and A. Galal

*Journal of the Electrochemical Society*, 160: 3144-3151 (2013) IF: 2.588

Graphite/SrPdO<sub>3</sub> was utilized for the sensitive determination of some neurotransmitters, namely dopamine (DA), epinephrine (EP), norepinephrine (NE), serotonin (ST), 3,4-dihydroxyphenylacetic acid (DOPAC) and L-dopa. Graphite/SrPdO<sub>3</sub> exhibited higher electrocatalytic activity toward the studied neurotransmitters compared to bare graphite. It was confirmed that graphite electrode was more suitable substrate for immobilization of SrPdO<sub>3</sub> perovskite compared to other surfaces. Moreover, simultaneous determinations of L-dopa, ascorbic acid (AA) and uric acid (UA) or ST were achieved with large peak potential separation. The linear response for L-dopa was obtained in the range of 0.6  $\mu\text{mol L}^{-1}$  to 9  $\mu\text{mol L}^{-1}$  with correlation coefficient 0.996 and detection limit 1.63  $\text{nmol L}^{-1}$ . The proposed composite sensor exhibited high reproducibility, enhanced sensitivity, selectivity, anti-interference ability, unique long-term stability (over two months) and applicability in the human urine samples with satisfying results.

**Keywords:** Nano-structured perovskites; Sensors; Neurotransmitters; Human blood; Graphite electrodes.

### 104. Synthesis and Antimicrobial Activity of Some New Thieno [2,3-*b*] Thiophene Derivatives

Yahia Nasser Mabkhot, Nabila Abdelshafy Kheder and Ahmad M. Farag

*Molecules*, 18: 4669-4678 (2013) IF: 2.428

A series of thieno [2,3-*b*] thiophene moiety-containing bis-cyanopyrazoles 5a-c, bis-aminopyrazole 9 and bis-pyridazine derivatives 11 were synthesized and evaluated in vitro for their antimicrobial potential. The antimicrobial activity of some selected products was evaluated and showed good results. 5,5'-(3,4-Dimethylthieno[2,3-*b*]thiophene-2,5-diyl)bis(3-acetyl-1-(4-chlorophenyl)-1H-pyrazole-4-carbonitrile) (5d) was found to be more potent than the standard drug amphotericin B against *Geotrichum candidum* and equipotent to amphotericin B against *Syncephalastrum racemosum*. In addition, it was found to be equipotent to the standard drug Penicillin G against *Staphylococcus aureus*.

Moreover, it was more potent than the standard drug streptomycin against *Pseudomonas aeruginosa* and *Escherichia coli*.

**Keywords:** Thieno [2,3-*b*] thiophene; Nucleophilic addition; Hydrazonoyl halides; Bis-pyrazole; Antimicrobial activity.

### 105. Synthesis and Characterization of Carboxymethyl Chitosan Nanogels for Swelling Studies and Antimicrobial Activity

Reem K. Farag and Riham R. Mohamed

*Molecules*, 18: 190-203 (2013) IF: 2.428

Nanogels of a binary system of carboxymethyl chitosan (CMCh) and poly- (vinyl alcohol) PVA were successfully synthesized by a novel in situ process. They were also characterized by various analytical tools like Fourier transform infrared spectroscopy (FTIR), transmission electron microscopy (TEM) and X-ray diffraction (XRD). They were studied for their unique swelling properties in water and different pH solutions. They were also investigated for their great ability to capture or isolate bacteria and fungi from aquatic environments.

**Keywords:** Carboxymethyl chitosan; Poly (vinyl alcohol); Nanogels; Antimicrobial activity; Swelling ability.

### 106. Broadband Dielectric Relaxation Spectroscopy of Functionalized Biobased Castor Oil Copolymer Thermosets

Samy A. Madbouly, Ying Xia and Michael R. Kessler

*Macromolecular Chemistry and Physics*, 214: 2891-2902 (2013) IF: 2.386

Novel biorenewable copolymer thermosets are successfully synthesized by the ring-opening metathesis polymerization (ROMP) of norbornenyl-functionalized castor oil (NCO) and norbornenyl-functionalized castor oil alcohol (NCA) with controlled amounts of 0.8 and 1.8 norbornene rings per fatty acid chain, respectively. The NCO and NCA monomers are mixed in different concentrations and simultaneously polymerized via ROMP using Grubbs catalyst. Broadband dielectric relaxation spectroscopy (BDRS) is used to investigate the molecular dynamics of the fully cured copolymer thermosets over a wide range of frequencies ( $5 \times 10^{-2}$  to  $0.5 \times 10^7$  Hz) at different constant temperatures ( $-70$  to  $125$  °C). Four phenomena, namely  $\alpha$ -,  $\beta$ -, and  $\gamma$ -relaxation processes and ionic conductivity are observed for all the measured samples.

**Keywords:** Copolymer thermosets; Norbornenyl-functionalized castor oil; Dielectric relaxation spectroscopy; Ionic conductivity.

### 107. Electrodeposited Nanostructured Pt–Ru Co-Catalyst on Graphene

Hagar K. Hassan, Nada F. Atta and Ahmed Galal

*Journal of Solid State Electrochemistry*, 17: 1717-1727 (2013) IF: 2.279

The electrochemical oxidation of formaldehyde over graphene surfaces modified with Pt–Ru cocatalyst is presented. Graphene was chemically converted from graphite and Pt–Ru co-catalyst was electrochemically deposited using cyclic voltammetry. The

hybrid surface is prepared using “green approaches” and displayed electrocatalytic activity towards formaldehyde in the form of current oscillations. The current oscillations that were mainly due to adsorption/desorption of carbonaceous oxidative products are a factor of several parameters such as the concentrations of both formaldehyde and supporting electrolyte in solution, the amount of catalyst loading, scan rate of potential, upper potential limit, and the temperature change. CCG/Pt–Ru exhibited higher electrocatalytic activity toward formaldehyde electro-oxidation, and intense electrochemical current oscillations were obtained at relatively low HCHO concentrations compared to other work mentioned in literature for CCG/Pt–Pd.

**Keywords:** Chemically converted graphene; Pt-Ru; Co-Catalyst; Formaldehyde electro-oxidation; Electrochemical current oscillations; Fuel cells.

### 108. Enhanced Electrolytic Generation of Oxygen Gas at Binary Nickel Oxide-Cobalt Oxide Nanoparticle-Modified Electrodes

Ibrahim M. Sadiq, Ahmad M. Mohammad Mohamed E. El-Shakre, Mohamed S. El-Deab and Bahgat E. El-Anadoul

*Journal of Solid State Electrochemistry*, 17: 871-879 (2013) IF: 2.279

This study addresses the enhancement of the oxygen evolution reaction (OER) on glassy carbon, Au, and Pt electrodes modified with binary catalysts composed of nickel oxide nanoparticles (nano-NiO<sub>x</sub>) and cobalt oxide nanoparticles (nano-CoO<sub>x</sub>). Binary NiO<sub>x</sub>/CoO<sub>x</sub>-modified electrodes (with NiO<sub>x</sub> initially deposited) show a high catalytic activity and a marked stability which far exceeds that obtained at the individual oxide-modified electrodes. This enhancement is demonstrated by a marked negative shift (more than ca. 600 mV) in the onset potential of the OER compared to that obtained at the unmodified electrodes. The modified electrodes show a significantly higher long-term stability, over a period of 5 h of continuous electrolysis, without any significant loss of activity towards the OER in alkaline medium. The influence of the solution pH, the loading level, and sequence of deposition of each oxide on the electrocatalytic activity of the modified electrodes is addressed with an aim to maximize the catalytic activity of the modified electrodes towards the OER. SEM imaging is used to disclose the size and morphology of the fabricated nano-NiO<sub>x</sub> and nano-CoO<sub>x</sub> binary catalysts at the electrode surface.

**Keywords:** Nanostructures; Water electrolysis; Binary catalysts; Metal oxides; Electrocatalysis.

### 109. Multiclass Analysis on Repaglinide, Flubendazole, Robenidine Hydrochloride and Danofloxacin Drugs

Taleb T. Al-Nahary, Mohamed Abdel Nabi El-Ries, Gehad G. Mohamed, Ali Kamal Attia, Yahia Nasser Mabkhot, Michelyne Haroun and Assem Barakat

*Arabian Journal of Chemistry*, 6: 131-144 (2013) IF: 2.266

The drugs under study; repaglinide (Repag), flubendazole (Flu), robenidine hydrochloride (Roben) and danofloxacin (Dano) are antidiabetic, anthelmintic, anticoccidial, and antibiotic drugs. In the present study, they are investigated using electron impact

mass spectral (EI-MS) fragmentation at 70 eV, in comparison with thermal analyses measurements (TGA/DrTGA and DTA) and molecular orbital calculation (MO). Semi-empirical MO calculation, AM1 procedure, has been carried out on Repag, Flu, Roben and Dano both as neutral molecules (in TA) and the corresponding positively charged species (in MS). The calculated MO parameters include bond length, bond order, charge distribution on different atoms and heat of formation. The fragmentation pathways of Repag, Flu, Roben and Dano in EI-MS led to the formation of important primary and secondary fragment ions. The mechanism of formation of some important daughter ions can be illuminated from comparing with that obtained using mass spectrometer through the accurate mass measurement determination.

The MO provides a base for fine distinction among sites of initial bond cleavage and subsequent fragmentation of drug molecules in both thermal analysis and MS techniques. The activation thermodynamic parameters, such as, (activation energy  $E^*$ ), (enthalpy  $\Delta H^*$ ), (entropy  $\Delta S^*$ ) and (Gibbs free energy  $\Delta G^*$ ) are calculated from the DrTGA curves using Coats–Redfern and Horowitz–Mitzger methods.

**Keywords:** Repag; Flu; Roben and dano; Ei-ms spectrometry; Thermal analyses; Molecular orbital calculation (MOC).

#### 110. Validated Voltammetric Method for the Determination of Some Antiprotozoa Drugs Based on the Reduction at an Activated Glassy Carbon Electrode

H. M. Elqudaby, Gehad G. Mohamed, F.A. Ali and Sh. M. Eid  
*Arabian Journal of Chemistry*, 6: 327-333 (2013) IF: 2.266

A sensitive electrochemical procedure based on reduction of secnidazole (I), tinidazole (II) and ornidazole (III) at a glassy carbon electrode (GCE) was introduced. A study of the variation of the peak current with solution variables such as pH, ionic strength, concentration of drugs, possible interference, and instrumental variables such as scan rate, pulse amplitude, preconcentration time, accumulation potential, has resulted in the optimization of the reduction signal for analytical purposes. Linear calibration plots were obtained over the concentration ranges of 50–800, 50–750  $\mu\text{g mL}^{-1}$  for I, and both (II, III) respectively, in Britton–Robinson buffer of pH 7.

The relative standard deviations of five replicate measurements of 1.0 and 10.0  $\mu\text{g mL}^{-1}$  of I, II and III concentrations were 4.7%, 4.9% and 5.3%, and 2.2%, 2.6% and 2.8%, respectively. The limits of detection (LOD) for I, II and III were found to be  $2 \times 10^{-10}$ ,  $3 \times 10^{-10}$  and  $2.5 \times 10^{-10}$  mol  $\text{L}^{-1}$  and limits of quantification (LOQ) for I, II and III were found to be  $4.0 \times 10^{-8}$ ,  $1.2 \times 10^{-8}$  and  $4.4 \times 10^{-8}$  mol  $\text{L}^{-1}$ , respectively. The optimal conditions were:  $E_{\text{acc}} = -0.9$  V,  $t_{\text{acc}} = 30$  s, scan rate = 20 mV  $\text{s}^{-1}$ , pulse-height = 90 mV and Britton–Robinson buffer of pH 7. The method was applied for the determination of the cited drugs both in raw materials and in pharmaceutical preparations with satisfactory results and compared with the official reference method. Complete validation of the proposed method was also done.

**Keywords:** Pharmaceutical preparations; Antiprotozoa; Voltammetry; Activated glassy carbon electrode.

#### 111. Maleic Diamides as Photostabilizers for Polystyrene

Samira T. Rabie, Ahmed E. Ahmed, Magdy W. Sabaa and M. A. Abd El-Ghaffar

*Journal of Industrial and Engineering Chemistry*, 19: 1869-1878 (2013) IF: 2.145

Some condensation maleic diamide adducts were prepared, characterized, and evaluated as photostabilizers for polystyrene. The potency of these diamides was determined by measuring the extent of weight loss (%), formed gel as well as the average molecular weights MV of the soluble fractions of the degraded polymers. The results indicated a good stabilizing effect of these products compared with the commercial UV absorber, phenyl salicylate. FTIR spectra of both neat and photoirradiated stabilized polystyrene gave an explanation of some photodegraded products of polystyrene. A probable radical mechanism is proposed to account for the stabilizing action of the diamide derivatives as photostabilizers.

**Keywords:** Polystyrene; Photodegradation; Diamides; Photostabilizers.

#### 112. Synthesis, Morphology and Thermal Properties of Polyurethanes Nanocomposites Based on Poly (3-Hydroxybutyrate) and Organoclay

H. F. Naguib, M. S. Abdel Aziz and G. R. Saad

*Journal of Industrial and Engineering Chemistry*, 19: 56-62 (2013) IF: 2.145

Segmented poly (ester-ether urethane) s/organoclay nanocomposites based on bacterial poly(3-hydroxybutyrate) (PHB) and poly( $\epsilon$ -caprolactone)-b-poly(ethylene glycol)-b-poly( $\epsilon$ -caprolactone) (PCL-PEG-PCL triblock copolymer) with Cloisite® 30B organoclay (C30B) were prepared by solution intercalation method. XRD, SEM and TEM results showed good dispersion of clay particles in polyurethane matrix. The presence of C30B increased  $T_g$  of PCL-PEG-PCL soft segments and the crystallization rate of PHB and PCL-PEG-PCL segments. C30B caused an enhancement in polyurethanes thermal stability and had an accelerating effect upon the main thermal decomposition of the polymer matrix as indicated by the lower activation energy ( $E_a$ ) of decomposition compared to virgin materials, estimated using Kissinger–Akahira–Sunose isoconversional method.

**Keywords:** Activation energy; Cloisite® 30B nanocomposites; Poly (3-Hydroxybutyrate); Poly (ester-ether urethane) s; Thermal degradation.

#### 113. The Dissociative Ionization of $\text{CO}_2$ in the 800 Nm Intense Laser Field Using Time-of-Flight (TOF) Mass Spectrometry

Mohamed El-Sayed El-Shkra

*International Journal of Mass Spectrometry*, 336: 37-42 (2013) IF: 2.142

The dissociation of carbon dioxide in an intense ( $10^{13}$ – $10^{14}$  W/ $\text{cm}^2$ ) femtosecond laser field has been investigated. The stepwise nature of the dissociation has been verified experimentally by analyzing the time-of-flight mass spectroscopic



patterns at different laser intensities. The experimental identification shows that if the laser intensity is gradually increased  $\text{CO}_2^+$  is first formed, followed by a dissociation of one of the C–O bonds. Further increase of the laser intensity leads to the dissociation of the second C–O bond. Only  $\text{O}^+$  fragment ion shows anisotropic angular distribution.

**Keywords:** Dissociative ionization; Intense laser field; Femtosecond laser pulses; Carbon dioxide; Anisotropic angular distribution.

#### 114. Effects of Blending on the Molecular Dynamics of Highly Interacting Binary Polymer Blends of Poly (Methyl Methacrylate) and Poly [Styrene-Co-(Maleic Anhydride)]

Samy Abbas Madbouly

*Polymer International*, 62: 1659-1666 (2013) IF: 2.125

The molecular dynamics and miscibility of highly interacting binary polymer blends of poly(methyl methacrylate) (PMMA) and poly[styrene-co-(maleic anhydride)] random copolymer with 8 wt% maleic anhydride content (SMA) were investigated as a function of composition over a wide range of frequency ( $10^{-2}$ – $10^6$  Hz) at different constant temperatures (30–160 °C). Only one common glass relaxation process ( $\alpha$ -process) was detected for all measured blends, and its dynamics and broadness were found to be composition dependent. The existence of only one common  $\alpha$ -relaxation process located at a temperature range between those of the pure polymer components indicated the miscibility of the two polymer components over the entire range of composition. The miscibility was also confirmed by measuring the glass transition temperatures of the blends,  $T_g$ , using differential scanning calorimetry. The composition dependence of  $T_g$  of the blends showed a positive deviation from the linear mixing rule and well described by the Gordon–Taylor–Kwei equation. The relaxation spectrum of the blends was resolved into  $\alpha$ - and  $\beta$ -relaxation processes using the Havriliak–Negami (HN) equation and ionic conductivity. The dielectric relaxation parameters obtained from HN analysis, such as broadness of relaxation processes, maximum frequency,  $f_{\text{max}}$ , and dielectric strength,  $\Delta\epsilon$  (for the  $\alpha$ - and  $\beta$ -relaxation processes), were found to be blend composition dependent. The kinetics of the  $\alpha$ -relaxation process of the blends were well described by the Meander model, while an Arrhenius-type equation was used to evaluate the molecular dynamics of the  $\beta$ -relaxation process. Blending of PMMA and SMA was found to have a considerable effect on the kinetics and broadness of the  $\beta$ -relaxation process of PMMA, indicating that the strong interaction and miscibility between the two polymer components could effectively change the local environment of each component in the blend.

**Keywords:** Polymer blend; Miscibility; Molecular dynamics; Relaxation process.

#### 115. A Study of Calcium Carbonate/Multiwalled-Carbon Nanotubes/Chitosan Composite Coatings on Ti–6Al–4V Alloy for Orthopedic Implants

Rasha A. Ahmed, Amany M. Fekry and R. A. Farghali

*Applied Surface Science*, 285(B): 309-316 (2013) IF: 2.112

In an attempt to increase the stability, bioactivity and corrosion resistance of Ti–6Al–4V alloy, chitosan (CS) biocomposite coatings reinforced with multiwalled-carbon nanotubes (MWCNTs), and calcium carbonate ( $\text{CaCO}_3$ ) for surface modification were utilized by electroless deposition. Scanning electron microscope (SEM), Fourier transform infrared spectroscopy (FTIR) reveals the formation of a compact and highly crosslinked coatings. Electrochemical techniques were used to investigate the coats stability and resistivity for orthopedic implants in simulated body fluid (SBF). The results show that  $E_{\text{st}}$  value is more positive in the following order:  $\text{CaCO}_3/\text{MWCNTs}/\text{CS} > \text{CS}/\text{MWCNTs} > \text{CS} > \text{MWCNTs}$ . The calculated  $i_{\text{corr}}$  was  $0.02 \text{ nA cm}^{-2}$  for  $\text{CaCO}_3/\text{MWCNTs}/\text{CS}$  which suggested a high corrosion resistance.

**Keywords:** Carbon nanotube; Chitosan; Calcium carbonate; Electrochemical impedance.

#### 116. One-Pot Synthesis of 5-Unsubstituted-6-Aroyl [1,2,4]Triazolo[1,5-A]Pyrimidine Utilizing Biginelli-Like Multicomponent Reaction of Enaminones With 3-Amino-1,2,4-Triazole as the Urea Component

Huwaida M. E. Hassaneen and Ismail A. Abdelhamid

*Current Organic Synthesis*, 10 (6): 953-955 (2013) IF: 2.038

A novel and facile Biginelli-like assembly employing enaminones, aldehydes and 3-amino-1,2,4-triazole has been developed, which provides a novel synthesis of new 5-unsubstituted-6-aroyl-[1,2,4]triazolo[1,5-a]pyrimidine derivatives

**Keywords:** 3-Amino-1,2,4-triazole; Enamines; Biginelli-like; 6-Aroyl-[1,2,4]Triazolo[1,5-a]Pyrimidine; Pyrimidine-2-thione; 4-aryl-7-Thioxo-3,4,7,8-tetrahydropyrimido[4,5-D]Pyrimidine-2,5 (1H,6H) -dione.

#### 117. Synthesis and Characterization of Poly ([1,2,4] triazolyl- and [1,2,4]triazolo[3,4- b][1,3,4] Thiadiazinylsulfanylmethyl) Arenes: Novel Multi-Armed Molecules

Ahmed H. M. Elwahy, Radwan M. Sarhan and Mohamed A. Badawy

*Current Organic Synthesis*, 10: 786-790 (2013) IF: 2.038

A synthesis of novel three-, four-, and sixfold branched triazoles 3-5 and triazolothiadiazines 7, 8 and 10, which are linked to a benzene core via sulfanylmethylene spacers was reported. The reaction proceeded via initial treatment of the appropriate poly (bromomethyl) arenes 2 with the corresponding equivalents of 4-amino-4H-1,2,4-triazoles 1 in refluxing ethanolic KOH to give poly(triazolyl)arenes 3-5. Subsequent reaction of 4b and 5b with phenacyl bromide in refluxing DMF-ethanol mixture afforded poly (triazolothiadiazinyl) arenes 7 and 8, respectively. Compounds 7 and 8 were alternatively obtained by the reaction of 2b and 2c with 6-phenyl-7H-[1,2,4]triazolo[3,4-b][1,3,4]thiadiazine 3-thiol 9 in refluxing EtOH/DMF containing KOH. Similarly, threefold substitution of 2a with three equivalents of 9 afforded 10 in good yield.

**Keywords:** Poly (bromomethyl) arenes; Alkylation; Cyclization; Triazoles; Triazolo-thiadiazines.

**118. Synthesis of Furo-, Pyrrolo-, and Thieno-Fused Heterocycles by Multi-Component Reactions (Part 1)**

Mohamed R. Shaabana and Ahmed H. M. Elwahy

*Current Organic Synthesis*, 10: 425-466 (2013) IF: 2.038

Development of efficient routes to many kinds of fused heterocycles is an attractive area of research since these compounds constitute one of the most interesting divisions of organic chemistry. A majority of the compounds produced by nature as well as significant numbers of compounds synthesized in the industrial sector each year have heterocyclic rings as part of their structures. This review survey research works on the specific synthesis of furo-, pyrrolo-, and thieno-fused heterocycles by multi-component reactions over the last ten years. Different approaches for the synthesis of such systems are discussed.

**Keywords:** Multicomponent reactions; Furan; Pyrrole; Thiophene and fused heterocycles.

**119. Electronic Structure and Decomposition Reaction Mechanism of Cyclopropanone, Phenylcyclopropanone and Their Sulfur Analogues: A Theoretical Study**

Shabaan A. K. Elroby, Saadullah G. Aziz and Rifaat Hilal

*Journal of Molecular Modeling*, 19: 1339-1353 (2013) IF: 1.984

The electronic structure, the origin of the extraordinary stability and the reaction mechanisms of the decomposition reaction of the three-membered ring cyclopropanone (IO), its phenyl derivative (IIO) and its sulfur analogues (IS and IIS) have been investigated at the B3LYP/6-311+G\*\* level of theory. All critical points on the reaction surface, reactants, transition states and intermediates were determined. Reaction rate constants and half-lives have been computed. Natural bond orbital (NBO) analysis has been used to investigate the type and extent of interaction in the studied species. Results indicate that the decomposition reaction occurs via a stepwise mechanism, with the formation of a short-lived intermediate. The characters of the intermediates for the decomposition of IIO and IIS are different. In case of IIO decomposition, the intermediate structure is of prevailing zwitterionic character, whereas that for the decomposition of IIS is of prevailing carbenic character. Solvent effects are computed, analyzed and discussed.

**Keywords:** Density functional theory; Phenylcyclopropanone; Natural bond orbital; Zwitterion; Decomposition reaction.

**120. Chelating Behavior, Thermal Studies and Biocidal Efficiency of Tioconazole and its Complexes with Some Transition Metal Ions**

Gehad Genidy Mohamed

*Journal Thermal Analysis and Calorimetry*, 111: 173-181 (2013) IF: 1.982

New seven metal complexes of tioconazole drug with the general formulae  $[MCl_2(L)_2(H_2O)_x] \cdot yH_2O$  (where,  $x = 0$  and  $y = 1$  for  $M = Mn(II)$  or  $x = 2$ ,  $y = 2$  for  $M = Co(II)$ ), and  $x = 0$ ,  $y = 3$  for  $M = Cu(II)$ ,  $Ni(II)$ ,  $Zn(II)$ ) and  $[MCl_2(L)_2(H_2O)_2]Cl \cdot 3H_2O$  (where  $M = Cr(III)$  and  $Fe(III)$ ) have been prepared and characterized

based on elemental analyses, IR, magnetic moment, molar conductance, and thermal analyses techniques. From molar conductance data bivalent metal chelates are non-electrolytes while  $Cr(III)$  and  $Fe(III)$  chelates are electrolytes and of 1:1 type. According to the IR spectral data, TCNZ is coordinated to the metal ions in a neutral unidentate manner with N donor site of the imidazole-N. All the complexes are octahedral except  $Mn(II)$  complex has tetrahedral structure. TCNZ drug and its metal complexes were also screened for their biological activity.

**Keywords:** Tioconazole metal complexes; Spectroscopic studies; Magnetic moment; Thermal analyses; Biological activity.

**121. Effect of Organically Modified Montmorillonite Filler on the Dynamic Cure Kinetics, Thermal Stability, and Mechanical Properties of Brominated Epoxy/Aniline Formaldehyde Condensates System**

Gamal R. Saad, Hala F. Naguib and Said A. Elmenyawy

*Journal of Thermal Analysis and Calorimetry*, 111: 1409-1417 (2013) IF: 1.982

Nanocomposites, based on tetrabromo-bisphenol-A epoxy and aniline formaldehyde condensates, containing 5 and 10 % organically modified montmorillonite (O-MMT), were prepared. The morphologies of these nanocomposites were studied by X-ray diffraction (XRD) and scanning electron microscopy (SEM). The influences of O-MMT on the dynamic cure kinetics, thermal stability, and mechanical properties were investigated by differential scanning calorimetry, thermogravimetric analysis, and non-destructive ultrasonic testing techniques. The XRD and SEM results indicated a good dispersion of O-MMT within the epoxy matrix. The relation between the activation energy,  $E_a$ , and the degree of cure,  $\alpha$ , for the examined systems was obtained by applying model-free isoconversional Kissinger-Akahira-Sunose method. As  $\alpha$  increases,  $E_a$  increases gradually, almost independent of the amount of O-MMT. The dynamic cure kinetics of the neat epoxy system as well as its nanocomposites were described by Šesták-Berggren, [SB ( $m, n$ )], autocatalytic model. The O-MMT enhances the thermal stability of the examined epoxy system. The results of the mechanical properties indicated that the addition of O-MMT enhances the Young's and shear elastic modulus and microhardness. The values of these parameters increase with increasing O-MMT loading.

**Keywords:** Epoxy nanocomposites; Dynamic cure kinetics; Kissinger method; SB ( $M, N$ ) model; Thermal stability; Elastic modulus; Microhardness.

**122. Novel Self-dyed Wholly Aromatic Polyamide-Hydrazides Covalently Bonded With Azo Groups in Their Main Chains**

Part 2. Thermal Characteristics

Nadia A. Mohamed, Mohammad H. Sammour and Ali M. Elshafai

*Journal of Thermal Analysis and Calorimetry*, 114: 859-871 (2013) IF: 1.982

Thermal characteristics of several novel self-dyed wholly aromatic polyamide-hydrazides covalently bonded with azo groups in their main chains and containing *o*-hydroxy group as a substituent group in the aryl ring of the aminohydrazide part of

the polymers have been investigated in nitrogen and in air atmospheres using differential scanning calorimetry, thermogravimetric analyses, infrared spectroscopy, and elemental analyses. The effect of introducing different predetermined proportions of *para*- and *meta*-phenylene moieties into the backbone chain of the polymers on their thermal characteristics has been evaluated. Azopolymers having different molecular masses of all *para*-oriented phenylene type units were also thermally characterized. These polymers were prepared by a low temperature solution polycondensation reaction of either 4-amino-3-hydroxybenzhydrazide or 3-amino-4-hydroxybenzhydrazide with an equimolar amount of either 4,4'-azodibenzoyl chloride (4,4'ADBC), 3,3'-azodibenzoyl chloride (3,3'ADBC), or mixtures of various molar ratios of 4,4'ADBC and 3,3'ADBC in anhydrous *N,N*-dimethyl acetamide containing 3 %  $\text{m v}^{-1}$  LiCl as a solvent at  $-10^\circ\text{C}$ . All the polymers have the same structural formula except the mode of linking phenylene units in the polymer chain. The content of *para*- and *meta*-phenylene moieties was varied within these polymers so that the changes in the latter were 10 mol% from polymer to polymer, starting from an overall content of 0–100 mol%. The results reveal that these polymers are characterized by high thermal stability and could be cyclodehydrated into linear aromatic polymers with alternating 1,3,4-oxadiazole and benzoxazole structural units within the same polymer approximately in the region of 200–480  $^\circ\text{C}$ , either in nitrogen or in air atmospheres by losing water from the hydrazide and *o*-hydroxybenzamide groups, respectively. Along with the cyclodehydration, the polymer may lose molecular nitrogen from the azo groups. This is not a true degradation, but rather a thermochemical transformation reaction of the evaluated polymers into the corresponding poly(1,3,4-oxadiazolyl-benzoxazoles). The resulting poly(1,3,4-oxadiazolyl-benzoxazoles) start to decompose in the temperature range above 330–560  $^\circ\text{C}$ , either in nitrogen or in air atmospheres without mass loss at a lower temperature. The thermal and thermo-oxidative stabilities of the polymers are affected by the nature and amount of arylene groups incorporated into their chains, being higher for polymers with greater content of *para*-oriented phenylene rings, which permits more interchain hydrogen bonds as a result of greater chain symmetry, packing efficiency, and rod-like structure. Increasing the content of *para*-oriented phenylene rings leads to a strong improvement in both the initial decomposition temperature as well as in the residual mass at a particular temperature. The stability of the polymers was found to be independent of their molecular masses. This confirms that high thermal stability is not a polymer property which would depend upon the length of its macromolecular chains, but rather upon its chemical structure in which all and every atomic group contributes by its own thermal stability to the macroscopic properties of the whole polymer.

**Keywords:** Azopolyamide-hydrazides; Differential scanning calorimetry; Poly (1,3,4-oxadiazolyl-benzoxazoles); Thermal characteristics; Thermogravimetric analyses.

### 123. Synthesis, Characterization, and Thermal Investigation of Some Transition Metal Complexes of Benzopyran-4-one Schiff Base as Thermal Stabilizers for Rigid Poly (Vinyl Chloride) (PVC)

Nora S. Abdel-Kader and Riham R. Mohamed

*Journal of Thermal Analysis and Calorimetry*, 114: 603-611 (2013) IF: 1.982

New metal complexes of Schiff base (PB) prepared from condensation reaction of 2-aminopyridine and 6-formyl-5,7-dihydroxy-2-methylbenzopyran-4-one with metal ions; Mn(II), Co(II), Ni(II), and Cu(II) are prepared. Different analysis tools like elemental analyses, FTIR, thermal analysis, conductivity, electronic spectra, and magnetic susceptibility measurements are all used to elucidate the structures of the newly prepared metal complexes. The free Schiff base (PB) has been examined as thermal stabilizer and co-stabilizer for rigid PVC in air, at 180  $^\circ\text{C}$ . Its high stabilizing efficiency is detected by its high induction period value ( $T_s$ ) when compared with some of the common reference stabilizers used industrially, such as dibasic lead carbonate and calcium-zinc stearate (Ca-Zn soap). Blending Schiff base or its metal complexes with Mn (II), Co(II), Ni(II), and Cu(II) ions with the reference stabilizers in different ratios had a synergistic effect on the induction period (thermal stability). The stabilizing efficiency is attributed at least partially to the ability of the stabilizer to be incorporated in the polymeric chains, thus disrupting the chain degradation process.

**Keywords:** Schiff bases; Transition metal complexes; PVC; Stabilizer; Induction period; Degradation.

### 124. Design and Synthesis of Novel Complexes Containing *N*-Phenyl-1*H*-Pyrazole Moiety: Ni Complex as Potential Antifungal and Antiproliferative Compound

Nadia E.A. El-Gamel and Thoraya A. Farghaly

*Spectrochimica Acta Part A: Molecular and Biomolecular Spectroscopy*, 115: 469-475 (2013) IF: 1.977

Cu(II) (1), Ni(II) (2), Cr(III) (3) and Fe(III) (4) complexes with 3-acetyl-4-benzoyl-1-phenyl-1*H*-pyrazole (L<sub>1</sub>) were prepared and structurally characterized. Usual coordination of L<sub>1</sub> was achieved through nitrogen of pyrazole moiety and carbonyl acetyl group. Electronic spectra of the complexes indicate that the geometry of the metal center was six coordinate octahedral. In vitro antimicrobial activity of the ligand and complex compounds was screened in terms of antibacterial effect on *Staphylococcus aureus* (Gram-positive), *Escherichia coli* (Gram-negative) and antifungal effect on the fungi *Aspergillus flavus* and *Candida albicans* using the modified Kirby-Bauer disc diffusion and minimum inhibitory concentrations (MIC) methods. Ni(II) complex (2) exhibited remarkable antifungal inhibition against *Candida albicans* equal to the standard antifungal agent. To continue our study some structural modifications are formed by adding 4-fluoro-benzoyl moiety to L<sub>1</sub> in different forms to produce different ligands, 3-acetyl-4-(4-fluorobenzoyl)-1-phenyl-1*H*-pyrazole (L<sub>2</sub>) and 3-[(3-acetyl-1-phenyl-1*H*-4-pyrazolyl) carbonyl]-1-phenyl-4-(4-fluorobenzoyl)-1*H*-pyrazole (L<sub>3</sub>), Ni complexes (5 and 6) are prepared and comparable in vitro antimicrobial study is evaluated. In vitro cytotoxicity of the Ni(II) complex (2) is studied using MTT assay. The analysis of the cell test showed that (2) displayed quite small cytotoxic response at the higher concentration level which indeed would further enable us for more opportunities in therapeutic and biomedical challenges. Both of the capability as a potent in vitro antifungal agent and the cell test analysis show Ni(II) complex (2) as a promising material in the translation of observed in vitro biological phenomenon into clinical therapies settings.

**Keywords:** Pyrazole derivatives; Spectroscopic characterization; Thermal studies; *Candida albicans*; Antifungal activity.

### 125. Bivalent Transition Metal Complexes of Cetirizine: Spectroscopic, Equilibrium Studies and Biological Activity

Ahmed A. El-Sherif, Mohamed M. Shoukry and Lamis O. Abobakr

*Spectrochimica Acta Part A: Molecular and Biomolecular Spectroscopy*, 112: 290-300 (2013) IF: 1.977

Metal complexes of cetirizine.2HCl (CTZ = 2-[2-[4-[(4-chlorophenyl)phenyl methyl]piperazine-1-yl]-ethoxy]acetic acid, dihydrochloride have been prepared and characterized by elemental analyses, IR, solid reflectance, magnetic moment, molar conductance, and UV-Vis spectra. The analytical data of the complexes show the formation of 1:2 [M:L] ratio, where M represents Ni(II), Co(II) and Cu(II) ions, while L represents the deprotonated CTZ ligand. IR spectra show that CTZ is coordinated to the metal ions in a monodentate manner through carboxylate-O atom. Protonation equilibria of CTZ and its metal complexation by some divalent metal ions were determined in aqueous solution at constant ionic strength (0.1 M NaCl) using an automatic potentiometric technique. Thermodynamic parameters for the protonation equilibria of CTZ were calculated and discussed. The stability order of M (II)-CTZ complexes were found to obey  $Mn^{2+} < Co^{2+} < Ni^{2+} < Cu^{2+}$ , in accordance with the Irving-Williams order. The concentration distribution of the complexes in solution is evaluated as a function of pH. The CTZ ligand and its metal complexes were screened for their biological activity against bacterial species (*Bacillus subtilis* RCMB 010067, *Staphylococcus aureus* RCMB 010028, *Pseudomonas aeruginosa* RCMB 010043, and *Escherichia coli* RCMB 010052) and fungi as (*Aspergillus flavus* RCMB 02568, *Penicillium italicum* RCMB 03924, *Candida albicans* RCMB 05031 and *Geotricum candidum* RCMB 05097). The activity data show that the metal complexes have antibacterial and antifungal activity more than the parent CTZ ligand against one or more bacterial or fungi species. MIC was evaluated for the isolated complexes.

**Keywords:** Cetirizine; Stability constants; Potentiometry speciation; Electronic spectra; Biological activity.

### 126. Cr (III), Mn(II), Fe(III), Co(II), Ni(II), Cu(II) and Zn (II) New Complexes of 5-Aminosalicylic Acid: Spectroscopic, Thermal Characterization and Biological Activity Studies

Madiha H. Soliman and Gehad G. Mohamed

*Spectrochimica Acta Part A: Molecular and Biomolecular Spectroscopy*, 107: 8-15 (2013) IF: 1.977

The complexing behavior of mesalazine (5-aminosalicylic acid; 5-ASA) towards the transition metal ions namely, Cr(III), Mn(II), Fe(III), Co(II), Ni(II), Cu(II) and Zn(II) have been examined by elemental analyses, magnetic measurements, electronic, IR and <sup>1</sup>H NMR. Thermal properties and decomposition kinetics of all complexes are investigated. The interpretation, mathematical analyses and evaluation of kinetic parameters of all thermal decomposition stages have been evaluated using Coats-Redfern equation. The free ligand and its metal complexes have been tested in vitro against *Aspergillus fumigatus* and *Candida albicans* fungi and *Pseudomonas aeruginosa*, *Escherichia coli*, *Bacillus*

subtilis and *Staphylococcus aureus* bacteria in order to assess their antimicrobial potential. The results indicate that the metal complexes are also found to have more antimicrobial activity than the parent 5-ASA drug.

**Keywords:** 5-Aminosalicylic acid; Spectral studies; Transition metal complexes; Thermal analyses; Biological activity.

### 127. Extractive Determination of Ephedrine Hydrochloride and Bromhexine Hydrochloride in Pure Solutions, Pharmaceutical Dosage form and Urine Samples

N. T. Abdel-Ghani, M. S. Rizk and M. Mostafa

*Spectrochimica Acta Part A: Molecular and Biomolecular Spectroscopy*, 111: 131-141 (2013) IF: 1.977

Simple, rapid, sensitive, precise and accurate spectrophotometric methods for the determination of ephedrine hydrochloride (E-HCl) and bromhexine hydrochloride (Br-HCl) in bulk samples, dosage form and in spiked urine samples were investigated. The methods are based on the formation of a yellow colored ion-associates due to the interaction between the examined drugs with picric acid (PA), chlorophyllin coppered trisodium salt (CLPH), alizarin red (AR) and ammonium reineckate (Rk) reagents. A buffer solution had been used and the extraction was carried out using organic solvent, the ion associates exhibit absorption maxima at 410, 410, 430 and 530 nm of (Br-HCl) with PA, CLPH, AR and Rk respectively; 410, 410, 435 and 530 of (E-HCl) with PA, CLPH, AR and Rk respectively. (E-HCl) and (Br-HCl) could be determined up to 13, 121, 120 and 160; 25, 200, 92 and 206  $\mu\text{g mL}^{-1}$ , using PA, CLPH, AR and Rk respectively. The optimum reaction conditions for quantitative analysis were investigated. In addition, the molar absorptivity, Sandell sensitivity were determined for the investigated drug. The correlation coefficient was  $\geq 0.995$  ( $n = 6$ ) with a relative standard deviation (RSD)  $\leq 1.15$  for five selected concentrations of the reagents. Therefore the concentration of Br-HCl and E-HCl drugs in their pharmaceutical formulations and spiked urine samples had been determined successfully.

**Keywords:** Bromhexine hydrochloride; Ephedrine hydrochloride; Chlorophyllin; Coppered trisodium salt; Ammonium reineckate; Alizarin red; Picric acid.

### 128. Novel Ni (II) and Zn(II) Complexes Coordinated by 2-Arylaminomethyl-1H-Benzimidazole: Molecular Structures, Spectral, DFT Studies and Evaluation of Biological Activity

Nour T. Abdel-Ghani, Maha F. Abo El-Ghar and Ahmed M. Mansour

*Spectrochimica Acta Part A: Molecular and Biomolecular Spectroscopy*, 104: 134-142 (2013) IF: 1.977

$[NiL^{1,2}Cl_2(OH_2)_3] \cdot zH_2O$  and  $[ZnL^{1,2}(CH_3CO_2)_2]$  ( $L^1 = (1H\text{-benzimidazol-2-ylmethyl})\text{-N-phenyl amine}$ ,  $z = 0$  and  $L^2 = 2\text{-}[(1H\text{-Benzimidazol-2-ylmethyl})\text{-amino}]\text{-benzoic acid methyl ester}$ ,  $z = 1$ ) complexes have been synthesized and characterized by a variety of physico-chemical techniques. The central Ni(II) ion is coordinated by only the pyridine-type nitrogen ( $N_{pv}$ ) of benzimidazole ring, three water molecules and two chlorido ligands forming a distorted octahedral geometry. Five coordinated



zinc complexes were obtained, where the coordination sphere of zinc ion is made up of secondary amino group ( $\text{NH}_{\text{sec}}$ ),  $\text{N}_{\text{ov}}$  and two acetate groups, one acts as a unidentate and the other as a bidentate. A theoretical DFT/UB3LYP method combined with LANL2DZ basis set shows that all the metal–ligand bonds are of the  $\text{L} \rightarrow \text{M}$  type. Electronic structures have been calculated using TD-DFT method. The antibacterial activity of  $\text{NiL}^2$  complexes decreases by the introduction of  $\text{COOCH}_3$  group in the ortho-position of the aniline moiety.

**Keywords:** Benzimidazole; Hydrogen bond; TD-DFT; NBO; Antimicrobial.

### 129. Spectroscopic and Density Functional Theory Investigation of Novel Schiff Base Complexes

Walid M.I. Hassan, Ehab M. Zayed, Asmaa K. Elkholy, H. Moustafa and Gehad G. Mohamed

*Spectr Ochimica Acta Part A: Molecul Ar and Biomo Lecular Spectroscopy*, 103: 378-387 (2013) IF: 1.977

Novel Schiff base ( $\text{H}_2\text{L}$ , 1,2-bis[(2-(2-mercaptophenylimino) methyl)phenoxy] ethane) derived from condensation of bisaldehyde and 2-aminothiophenol was prepared in a molar ratio 1:2. The ligand and its metal complexes are fully characterized with analytical and spectroscopic techniques. The metal complexes with Cr(III), Mn(II), Fe(III), Co(II), Ni(II), Cu(II), Zn(II) and Th(IV) have been prepared and characterized by elemental analyses, IR and  $^1\text{H}$ -NMR spectroscopy, thermal and magnetic measurements. The results suggested that the Schiff base is a bivalent anion with hexadentate OONNSS donors derived from the etheric oxygen (O, O'), azomethine nitrogen (N, N') and thiophenolic sulphur (S, S'). The formulae of the complexes were found to be  $[\text{ML}]\cdot x\text{H}_2\text{O}$  ( $\text{M} = \text{Mn(II)} (x = 0)$ ,  $\text{Co(II)} (x = 1)$ ,  $\text{Ni(II)} (x = 1)$ ,  $\text{Cu(II)} (x = 2)$  and  $\text{Zn(II)} (x = 0)$ ) and  $[\text{ML}]\cdot n\text{Cl}$  ( $\text{M} = \text{Cr(III)} (n = 1)$ ,  $\text{Fe(III)} (n = 1)$  and  $\text{Th(IV)} (n = 2)$ ). The thermogravimetric analysis of the complexes shows metal oxide remaining as the final product at 700–1000 °C. Density functional theory at the B3LYP/6-31G\* level of theory was used to investigate molecular geometry, Mulliken atomic charges and energetics. The synclinal-conformer was found to be responsible for complex formation. The calculation showed that ligand has weak field. Structural deformation and the dihedral angles rotation during complexation were investigated. The binding energy of each complex was calculated. The calculated results are in good agreement with experimental data.

**Keywords:** Schiff base metal complexes; Bisaldehyde; 2-Aminothiophenol; Spectroscopy; Thermal; DFT theoretical investigation.

### 130. Synthesis, Spectroscopic, Thermal and DFT Calculations of 2-(3-Amino-2-Hydrazono-4-Oxothiazolidin-5-Yl) Acetic Acid Binuclear Metal Complexes

Walid M. I. Hassan, M. A. Badawy, Gehad G. Mohamed, H. Moustafa and Salwa Elramly

*Spectr Ochimica Acta Part A: Molecul Ar and Biomo Lecular Spectroscopy*, 111: 169-177 (2013) IF: 1.977

The binuclear complexes of 2-(3-amino-2-hydrazono-4-oxothiazolidin-5-yl) acetic acid ligand (HL) with Fe(III), Co(II),

Ni(II), Cu(II) and Zn(II) ions were prepared and their stoichiometry was determined by elemental analysis. The stereochemistry of the studied series of metal complexes was established by analyzing their infrared,  $^1\text{H}$  NMR spectra and the magnetic moment measurements. According to the elemental analysis data, the complexes were found to have the formulae  $[\text{Fe}_2\text{L}(\text{H}_2\text{O})_8]\text{Cl}_5$  and  $[\text{M}_2\text{L}(\text{H}_2\text{O})_8]\text{Cl}_3$  ( $\text{M} = \text{Co(II)}$ ,  $\text{Ni(II)}$ ,  $\text{Cu(II)}$  and  $\text{Zn(II)}$ ). The present analyses demonstrate that all metal ions coordinated to the ligand via O(9), O(11), N(16) and N(18) atoms. Thermal decomposition studies of the ligand–metal complexes have been performed to verify the status of water molecules present in these metal complexes and their general decomposition pattern. Density Functional Theory (DFT) calculations at the B3LYP/6-31G\* level of theory have been carried out to investigate the equilibrium geometry of the ligand and complexes. Moreover, charge density distribution, extent of distortion from regular geometry, dipole moment and orientation have been performed and discussed.

**Keywords:** DFT-calculations; 1,3-Thiazole complexes; IR; Thermal analysis; Solid reflectance.

### 131. Effect of Alkoxy-chain Length Proportionation on the Mesophase Behaviour of Terminally Di-Substituted Phenylazo Phenyl Benzoates

H. A. Ahmed, M. M. Naoum and G. R. Saad

*Liquid Crystals*, 40: 914-921 (2013) IF: 1.959

A series of 4-alkoxyphenylazo-4'-phenyl-4''-alkoxybenzoates bearing two terminal alkoxy groups ( $\text{I } m + n$ ), where  $m$  and  $n$  denote the number of carbon atoms in the alkoxy groups attached to the phenylazo and benzoate moieties, respectively, was synthesised, and the molecular structures were established via elemental analyses, IR, NMR and mass spectroscopy. First, the thermal transitions and mesophase characteristics of any two isomeric molecules, having the same molecular length but with differently proportionated alkoxy groups, were investigated by differential scanning calorimetry and polarised-light microscopy. All compounds investigated proved to have a wide smectic C and nematic liquid crystalline ranges, except for the lower homologous ( $\text{I } 6 + 8$  and  $\text{I } 8 + 6$ ) where they are purely nematogenic. Mesophases were confirmed by the miscibility method, using dodecyloxybenzoic acid as the mesophase reference. Second, the mesophase behaviours of binary mixtures of isomeric compounds, bearing the same total alkoxy-chain length ( $m + n$ ) but differ in the individual values of  $m$  and  $n$ , were studied and discussed. It was found that the smectic C and nematic phases behaved ideally in their binary mixture with the 4-alkoxy benzoic acid, independent of either  $n$  or  $m$ .

**Keywords:** Liquid crystals; 4-Alkoxyphenylazo--4'-Phenyl-4''-Alkoxybenzoates; Phase transitions; Binary phase diagrams.

### 132. Influence of Halogen Substituent on the Mesomorphic Properties of Five-ring Banana-Shaped Molecules with Azobenzene Wings

M. Alaasar, M. Prehm and C. Tschierske

*Liquid Crystals*, 40: 656-668 (2013) IF: 1.959

Three new series of bent-shaped molecules with 4-chlororesorcinol, 4-bromoresorcinol or 4-fluororesorcinol as the

central unit, and azobenzene with different alkoxy chain length as side arms were synthesised. The mesophase behaviour was investigated by polarising optical microscopy, and differential scanning calorimetry. A representative example has also been characterised by X-ray diffraction (XRD) studies. It is found that almost all of the materials prepared are monotropic liquid crystalline. Depending on the substituent at the central unit and on the chain length nematic phases, B<sub>6</sub> phases, a B<sub>4</sub>-like dark conglomerate phase and a modulated/undulated anticlinic SmC phase were found. As a unique feature, upon reducing the chain length a transition from nematic to B<sub>6</sub>-type smectic phases was observed, which is reverse to usually observed phase sequences. The UV-vis absorption spectroscopy was also performed to study the effect of light-induced trans-cis-isomerisation on the prepared compounds.

**Keywords:** Bent-core liquid crystals; Azobenzene; Nematic phase; Anticlinic SmC Phase; B<sub>6</sub> Phases; B<sub>4</sub>-like dark conglomerate phase.

### 133. Predictability of Enantiomeric Chromatographic Behavior on Various Chiral Stationary Phases Using Typical Reversed Phase Modeling Software

Hebatallah A. Wagdy, Rasha S. Hanafi, Rasha M. El-Nashar and Hassan Y. Aboul-Enein

*Chirality*, 25: 506-513 (2013) IF: 1.894

Pharmaceutical companies worldwide tend to apply chiral chromatographic separation techniques in their mass production strategy rather than asymmetric synthesis. The present work aims to investigate the predictability of chromatographic behavior of enantiomers using DryLab HPLC method development software, which is typically used to predict the effect of changing various chromatographic parameters on resolution in the reversed phase mode. Three different types of chiral stationary phases were tested for predictability: macrocyclic antibiotics-based columns (Chirobiotic V and T), polysaccharide-based chiral column (Chiralpak AD-RH), and protein-based chiral column (Ultron ES-OVM). Preliminary basic runs were implemented, and then exported to DryLab after peak tracking was accomplished. Prediction of the effect of % organic mobile phase on separation was possible for separations on Chirobiotic V for several probes: racemic propranolol with 97.80% accuracy; mixture of racemates of propranolol and terbutaline sulphate, as well as, racemates of propranolol and salbutamol sulphate with average 90.46% accuracy for the effect of percent organic mobile phase and average 98.39% for the effect of pH; and racemic warfarin with 93.45% accuracy for the effect of percent organic mobile phase and average 99.64% for the effect of pH. It can be concluded that Chirobiotic V reversed phase retention mechanism follows the solvophobic theory.

**Keywords:** Predictability of enantiomeric separations; Drylab; Chirobiotic V; Chirobiotic T; Chiralpak AD-RH; Ultron ES-OVM.

### 134. Magnetite-hematite Nanoparticles Prepared by Green Methods for Heavy Metal Ions Removal from Water

M.A. Ahmeda, S.M. Ali, S.I. El-Deka and A. Galal

*Materials Science and Engineering*, 178:744-751 (2013) IF:1.846

Mixed magnetite-hematite nanoparticles were synthesized via different routes such as, coprecipitation in air and N<sub>2</sub> atmosphere, citrate-nitrate, glycine-nitrate and microwave-assisted citrate methods. The prepared samples were characterized by X-ray diffraction (XRD), high resolution transmission electron microscope (HRTEM), BET measurements and magnetic hysteresis. XRD data showed the formation of magnetite-hematite mixture with different compositions according to the synthesis method. The particle size was in the range of 4–52 nm for all the prepared samples. From HRTEM micrographs, it was found that, the synthesis method affects the morphology of the prepared samples in terms of crystallinity and porosity. The magnetite-hematite mixture was employed as a sorbent material for removal of some heavy metal ions from water such as lead(II), cadmium(II) and chromium(III). The effects of pH value and the contact time on the adsorption process were studied and optimized in order to obtain the highest possible adsorption efficiency of the magnetite-hematite mixture. The effect of the synthesis method of the magnetite-hematite mixture on the adsorption process was also investigated. It was found that samples prepared by the coprecipitation method had better adsorption efficiency than those prepared by other combustion methods.

**Keywords:** Magnetite-hematite; Nanoparticles; Microwave; Adsorption; Water decontamination.

### 135. Synthesis and Characterization of Some Chelating Polymers Bearing Maleic Acid and/or Sodium Maleate Moieties for Removal of Some Toxic Heavy Metal Ions

Mahmoud Abd El-Ghaffar, Noha Elhalawany, Elsayed Ahmed and Magdy Sabaa

*Clean Techn Environ Policy*, 15: 1013-1021 (2013) IF: 1.827

Chelating copolymers (CCPs) bearing carboxylic acid and/or carboxylate moieties based on ethyl methacrylate in the absence and in the presence of divinyl benzene as a crosslinker were prepared via new emulsion copolymerization route. The obtained CCPs were characterized by (FT-IR, <sup>1</sup>HNMR, TEM, GPC, and TGA). Furthermore, the prepared CCPs have been tested as adsorbents for various toxic heavy metal ions. They showed higher sorption capacities toward transition metal ions such as (Co(II) and Ni(II)) and much less sorption capacity for (Cd(II) and Pb(II)). The optimum conditions for metal ion uptake such as time, pH, and comonomer concentrations of different weight percent (wt%) as well as the sorption kinetics were investigated. A high recovery about 90–93 % was obtained using HCl as an eluent agent.

**Keywords:** Chelating copolymers; Adsorbents; Emulsion copolymerization; Metal ion uptake.

### 136. Experimental and Quantum Chemical Studies of Sulfamethazine Complexes with Ni (II) and Cu (II) Ions

Ahmed Moustafa Mansour

*J. of Coordination Chemistry*, 66:7: 1118-1128 (2013) IF: 1.801

[Ni(SZ)Cl(H<sub>2</sub>O)<sub>3</sub>].2H<sub>2</sub>O and [Cu (SZ)(NO<sub>3</sub>)(H<sub>2</sub>O)<sub>2</sub>].2H<sub>2</sub>O  
(HSZ = 4-amino-N-(4,6-dimethyl-2-pyrimidinyl)

benzenesulfonamide, sulfamethazine) have been synthesized and characterized by experimental and theoretical methods at the DFT/B3LYP/LANL2DZ level of theory. Ni(II) is coordinated by sulfonamidic (N15) and pyrimidic (N23) of the sulfamethazine drug, three water molecules, and one chloride forming a distorted octahedral geometry, while the Cu(II) complex has a square pyramidal geometry with the same ligand N,N active binding sites. Natural bond orbital (NBO) analysis of CuSZ reveals the participation of the coordinated  $\text{NO}_3^-$  triple H-bonds of different strengths with hydrated water molecules,  $\text{LP}(2)\text{O}33 \rightarrow \sigma^*(\text{O}45-\text{H}46)$ ,  $\text{LP}(2)\text{O}40 \rightarrow \sigma^*(\text{O}45-\text{H}44)$ , and  $\text{LP}(2)\text{O}38 \rightarrow \sigma^*(\text{O}48-\text{H}47)$ . The voltammogram of NiSZ shows one cathodic and one anodic peak. The complexes and NaSZ were screened for their antibacterial activity.

**Keywords:** Sulfamethazine; Antimicrobial; LANL2DZ; TD-DFT; Electrochemical.

### 137. Review: Protonation, Complex-Formation Equilibria, and Metal-Ligand Interaction of Salicylaldehyde Schiff Bases

Ahmed A. El-Sherif and Mutlaq S. Aljahdali

*Journal of Coordination Chemistry*, 66: 3423-3468 (2013)

IF: 1.801

Schiff bases (SBs) are aldehyde- or ketone-like compounds in which the carbonyl group is replaced by an imine or azomethine. In spite of the large interest always shown in the coordination properties of Schiff base ligands and the attention paid in recent years to the possible variable biological activities of their metal complexes, studies dealing with protonation and formation equilibria of Schiff bases and their complexes are still very rare. Thus, the importance of the determination of the equilibrium constants of Schiff bases and their complex formation equilibria is of paramount importance to understand the complicated biological reactions like transamination, racemization and decarboxylation. The 33 ligands considered herein include salicylaldehyde/substituted salicylaldehyde SBs and salicylaldehyde/ substituted salicylaldehyde amino acid SBs. This article is focused on protonation and complex-formation equilibria of salicylaldehyde or substituted salicylaldehyde SBs and salicylaldehyde amino acid SBs in aqueous and nonaqueous solutions, taking into account also the structure-activity correlation of SBs and their metal(II) complexes based on their stability constants. Activity of SBs enhances upon complexation and the order of activity is nearly in accord with the order of the formation constants of metal ions. The few enthalpy and entropy changes available for such protonation and complex-formation reactions are reported and discussed.

**Keywords:** Schiff bases; Protonation equilibria; Complex formation; Salicylaldehyde; Amino acid schiff bases.

### 138. Speciation Studies of Diorganotin (IV) Complexes With 3,3-Bis (1-Methylimidazol-2-Yl) Propionate-Displacement Reaction by DNA Constituents

Mohamed M. Shoukry and Safaa S. Hassan

*The Scientific World Journal*, 1-7: (2013) IF: 1.73

The interaction of 3,3-bis(1-methylimidazol-2-yl)propionate (BIMP) with dimethyltin(IV) dichloride (DMT), dibutyltin(IV) dichloride (DBT), and diphenyltin(IV) dichloride (DPT) is investigated at 25°C and 0.1M ionic strength in water for dimethyltin (IV), and in a 50% dioxane-water mixture for dibutyltin(IV) and diphenyltin(IV). The stepwise formation constants of the 1 : 1 and 1 : 2 complexes formed in solution are calculated from potentiometric measurements using the nonlinear least-square program MINQUAD-75. The concentration distribution of the various complex species is evaluated as a function of pH. Displacement reactions of the coordinated 3,3-bis(1-methylimidazol-2-yl)propionate by inosine and inosine-5'-monophosphate are investigated from calculations based upon equilibrium properties.

**Keywords:** 3,3-bis (1-Methylimidazol-2-Yl) propionate; Diorganotin (IV).

### 139. Coordination Behavior of Sulfamethazine Drug towards Ru (III) and Pt (II) Ions: Synthesis, Spectral, DFT, Magnetic, Electrochemical and Biological Activity Studies

Ahmed Moustafa Mansour

*Inorganica Chimica Acta*, 394: 436-445 (2013) IF: 1.687

Ru(III) and Pt(II) complexes of sulfamethazine drug have been synthesized as antibacterial agents, aiming to enhance the biological activity of sulfamethazine drug against resistance development of some organisms and to throw more light about the debatable coordination behavior of sulfamethazine, and their structures were elucidated by several experimental and theoretical tools.

Sulfamethazine acts as a bidentate ligand through sulfonamidic (N15) and pyrimidic (N23) nitrogen atoms. AC magnetic susceptibility measurements of RuIII complex showed anti-ferromagnetic behavior in 80–212 K with a Néel temperature at 128 K. Electrochemical studies revealed that  $-\text{NH}_2$  and  $-\text{SO}_2$  groups remain intact in complex formation.

Antibacterial activity and structural activity relationship (SAR) showed that activity decreases with complex formation due to increase the energy of lowest unoccupied molecular orbital ( $E_{\text{LUMO}}$ ), dipole moment, and charge on sulfonamidic nitrogen (N15) as a result of formation of covalent M-sulfonamidic bond, which in turn suppress the activity.

**Keywords:** Sulfamethazine; Antimicrobial; DFT; Magnetic; LANL2DZ; MEP.

### 140. Synthesis, Characterization, Molecular Modeling and Biological Activity of Mixed Ligand Complexes of Cu (II), Ni (II) and Co (II) Based on 1,10-Phenanthroline and Novel Thiosemicarbazone

M. Aljahdali and Ahmed A. EL-Sherif

*Inorganica Chimica Acta*, 407: 58-68 (2013) IF: 1.687

A combined experimental and computational study of novel mixed ligand Cu(II), Ni(II) and Co(II) complexes of 2-(1-(2-phenyl-hydrazono)-propan-2-ylidene) hydrazine-carbothioamide (TPHP) and 1,10-phenanthroline (1,10-Phen) have been synthesized. The complexes have been characterized by elemental

analyses, IR, solid reflectance, magnetic moment,  $^1\text{H}$ NMR and molar conductance. Spectral data showed that the 1,10-phenanthroline acts as neutral bidentate ligand coordinating to the metal ion through two nitrogen donor atoms and thiosemicarbazone acts as monobasic tridentate coordinating through two imine-N and thiolate sulphur groups. The geometry of the studied M(II) complexes has been fully optimized using parameterized PM3 semiempirical method. It was observed that the M–S bond length is longer than that of M–Cl in the isolated complexes and the M–N bond length is shorter than that of M–Cl. Also, valuable information is obtained from calculations of molecular parameters for all complexes including net dipole moment of the metal complexes, values of binding energy, which proved that the complexes are more stable than the free ligand.

The metal chelates have been screened for their antimicrobial activities using the disc diffusion method against different selected types of bacteria ( $G^+$ : *Bacillus subtilis* RCMB 010067, *Staphylococcus aureus* RCMB 010028);  $G^-$ : *Pseudomonas aeruginosa* RCMB010043, *Escherichia coli* RCMB 010052) and fungi (*Aspergillus flavus* RCMB 02568, *Penicillium italicum* RCMB 03924, *Candida albicans* RCMB 05031, *Geotricum candidum* RCMB 05097). Finally, structure–activity relationship studies were investigated with the aim to correlate physico-chemical properties that may be related to the antimicrobial action of the studied compounds. Protonation constant of (TPHP) ligand and stability constants of its M(II) complexes were determined by potentiometric titration method in 70%:30% DMSO–water mixture at 0.1 mol dm $^{-3}$ NaCl.

**Keywords:** Thiosemicarbazone; 1,10-phenanthroline; Transition metals; Quantum calculations; Biological activity.

#### 141. What Happens When (1H-Benzimidazol-2-ylmethyl)-N-Phenyl Amine is Added To Copper (II) Acetate? Spectroscopic, Magnetic, and DFT Studies

Ahmed Moustafa Mansour

*Inorganica Chimica Acta*, 408: 186-192 (2013) IF: 1.687

On performing a reaction between (1H-benzimidazol-2-ylmethyl)-N-phenyl amine (H $_2$ L) and copper (II) acetate in methanol, a green ‘paddle-wheel’ copper (II) complex, [Cu $_2$ (CH $_3$ COO) $_4$ (H $_2$ L) $_2$ ] (1), was separated after about 5 min. The two Cu atoms are separated by 2.852 Å and bridged by four bidentate acetate groups with Cu–O distance of 2.012–2.043 Å as calculated by DFT/B3LYP method. As the reflux continues, the reaction mixture was rapidly turned brown, and a polymeric complex, {[Cu $_2$ (CH $_3$ COO) $_3$ (H $_2$ O) $_2$ (HL)]} $_n$  (2), was separated. In complex 2, the benzimidazole ligand serves as a bridge between dimeric Cu $_2$  (CH $_3$ COO) $_3$ (H $_2$ O) $_2$  units via the benzimidazole moiety. The anionic effect was established by comparing complexes (1) and (2) with [Cu(H $_2$ L) $_2$ (OH) $_2$ Cl]Cl (3). Variable temperature magnetic susceptibility measurements of compound 2 showed occurrence of large anti-ferromagnetic interactions caused by the presence of syn–syn conformation of bridged acetate groups in terms of direct interaction, and  $\pi$ – $\pi$  super exchange pathway of the benzimidazolate moiety.

**Keywords:** Copper (II) acetate; Benzimidazole; Paddle-wheel; EPR, TD-DFT; Magnetic.

#### 142. Potentiometric Determination of Stability Constants and Thermodynamic Data for Dimethyltin (IV) Dichloride Complexes with Iminobis (Methylphosphonic Acid) in Water and Dioxane–Water Mixtures

M. Aljahdali, Claudia Foti, Ahmed A. El-Sherif, Mahmoud M. A. Mohamed, Ahmed A. Soliman and Obaid S. Al Ruqi

*Monatshefte Für Chemie - Chemical Monthly*, 144: 1467-1480 (2013) IF: 1.629

The interaction of dimethyltin (IV) (DMT) with iminobis (methylphosphonic acid) (IDP) was investigated at 25 °C and ionic strength 0.1 mol dm $^{-3}$  NaCl using the potentiometric technique.

The formation constants of the complexes formed in solution were calculated using the non-linear least-squares program MINQUAD-75. The stoichiometry and stability constants for the complexes formed are reported. The results showed the formation of 110, 111, 112, 11-1, and 11-2 for DMT–IDP complexes. The concentration distribution of the various complex species was evaluated. The effect of dioxane as a solvent on the hydrolysis of DMT and both the protonation and the formation constants of DMT complexes with IDP was discussed. The thermodynamic parameters  $\Delta H^\circ$  and  $\Delta S^\circ$  were calculated from the temperature dependence of the equilibrium constants. The effect of ionic strength on the hydrolysis of DMT, the protonation of IDP, and the formation constants of DMT–IDP complexes was also discussed.

**Keywords:** Dimethyltin (IV); Iminobis (methylphosphonic acid); Stability; Speciation; Hydrolysis; Ionic strength; Thermodynamics.

#### 143. Synthesis, Anticancer, and Antimicrobial Activities of Some New Antipyrine-based Heterocycles

Sayed M. Riyadh, Nabila A. Kheder and Ahlam M. Asiry

*Monatshefte Für Chemie - Chemical Monthly*, 144: 1559-1567 (2013) IF: 1.629

A facile and convenient synthesis of [1,2,3]triazole, [1,2,4]triazolo[5,1-*c*][1,2,4]triazine, and pyrazolo[5,1-*c*][1,2,4]triazine derivatives incorporating an antipyrin-4-yl or antipyrin-4-ylcarboxamide moiety via the versatile, readily accessible 2-cyano-*N*-(1,5-dimethyl-3-oxo-2-phenyl-2,3-dihydro-1H-pyrazol-4-yl)acetamide is described. Structures of the synthesized compounds were elucidated by means of IR,  $^1\text{H}$  NMR,  $^{13}\text{C}$  NMR, and mass spectral data. The biological activity of the newly synthesized compounds was examined and some of them were found to possess anticancer and antimicrobial activities.

**Keywords:** Mass spectroscopy; Cyclizations; Heterocycles; NMR Spectroscopy.



#### 144. Thermal Studies, Structural Characterization, and Antimicrobial Evaluation of Coordinated Metal Complexes Containing Salen Moiety

Nadia Emam Aly El-Gamel

*Monatshefte Für Chemie - Chemical Monthly*, 144: 1627-1634 (2013) IF: 1.629

Using the bidentate ligand N,N'-bis(2-methoxybenzylidene) ethylenediamine salen Schiff base, Cu(II), Cr(III), and La(III) complexes were prepared and structurally characterized using several physicochemical techniques. The thermal behavior of the synthesized complexes was investigated using simultaneous thermogravimetry (TG) and differential thermal analysis (DTA) techniques. The geometrical configurations of the complexes are proposed to be octahedral. Antimicrobial and antifungal activities of the reported complexes were tested and evaluated in vitro using modified Kirby–Bauer disc diffusion and minimum inhibitory concentration methods. The prepared complexes show remarkable antimicrobial activity; in particular, the Cr(III) complex exhibits potential inhibition against *Escherichia coli*, *Staphylococcus aureus*, and *Candida albicans*. On the other hand, the lanthanum complex presents higher in vitro antimicrobial activity when compared with the copper complex. In vitro antimicrobial activity assays indicate that the novel complexes might serve as promising candidates for new therapeutic agents.

**Keywords:** Salen; Metal complexes; Spectroscopic studies; Simultaneous thermal analysis (TG/DTA); Antimicrobial activity.

#### 145. Antitumor and Antileishmanial Evaluation of Novel Heterocycles Derived from Quinazoline Scaffold: A Molecular Modeling Approach

Daisy H. Fleita, Rafat M. Mohareb and Ola K. Sakka

*Medicinal Chemistry Research*, 22: 2207-2221 (2013) IF: 1.612

Novel thiazole, pyrimidine and benzylidene derivatives derived from quinazoline scaffold have been synthesized. The antitumor evaluation of the newly synthesized products against three cancer cell lines namely breast adenocarcinoma (MCF-7), non-small cell lung cancer (NCI-H460), and CNS cancer (SF-268) showed that the benzylidene–quinazoline derivative 12a showed remarkable activity against all three cell lines. The thiazolo-quinazoline derivative 10 showed greater activity than the control against breast adenocarcinoma (MCF-7) with a concentration of 0.01 IM. Moreover, the antileishmanial activity of the newly synthesized products tested on *Leishmania donovani* amastigotes showed that compounds 4, 14, and 18 had very promising activity.

**Keywords:** Quinazolines; Thiazole; Pyrimidine; Antitumor; Antileishmanial.

#### 146. New Approaches for the Synthesis of Pyrazole, Thiophene, Thieno [2,3-*b*] Pyridine, and Thiazole Derivatives Together With Their Anti-Tumor Evaluations

Rafat M. Mohareb, Amira E. M. Abdallah and Mahmoud A. Abdelaziz

*Medicinal Chemistry Research*, 22: 1-16 (2013) IF: 1.612

The reaction of cyanoacetylhydrazine (1) with acetylchloride (2) gave the N-acyl derivative 3. The latter underwent ready cyclization in sodium ethoxide to give the pyrazole derivative 4 which was the key compound for the synthesis of thiophene, thieno[2,3-*b*]pyridine, and thiazole derivatives. The anti-tumor evaluations of the newly synthesized products against the three human tumor cell lines, namely, breast adenocarcinoma (MCF-7), non-small cell lung cancer (NCI-H460), and CNS cancer (SF-268), were studied. Some of these compounds were found to exhibit much higher inhibitory effects toward the three tumor cell lines than the reference doxorubicin. Molecular modeling of the four compounds 12c, 12f, 16a, and 16d, which showed the maximum inhibitory effect, were done.

**Keywords:** Pyrazole; Thiophene; Thieno [2,3-*b*]; Pyridine thiazole; Anti-tumor.

#### 147. New Route for Synthesis, Spectroscopy, and X-Ray Studies of 2-[aryl-(6'-hydroxy-4',4'-dimethyl-2'-Oxocyclohex-6'-enyl)methyl]-3-hydroxy-5,5-Dimethylcyclohex-2-enone and 1,8-Dioxooctahydro-Oxanthenes and Antitumor Evaluation

Fatima Al-Omran, Rafat M. Mohareb and Adel Abou El-Khair

*Medicinal Chemistry Research*, 22: 1-13, (2013) IF: 1.612

Treatment of 1-(benzothiazol-2-yl-thio)-acetonitrile 1 with 5,5-dimethyl-1,3-cyclohexanedione-(dimedone) 2 and aromatic aldehyde 3a, b in refluxing ethanol containing a catalytic amount of piperidine lead to bisdimedone derivatives 5a and b in short periods of times with excellent yields and not 4H-chromen-5(6H)-one derivatives 8. The compound 5a was then cyclized to 1,8-dioxo-octahydroxanthene derivative 6. The structures of the synthesized compounds were elucidated by elemental analysis <sup>1</sup>H NMR and <sup>13</sup>C NMR spectra, COSY, HSQC, HMBC, MS, and X-ray crystallographic investigations.

The cytotoxicity of the synthesized compounds 5a, b, and 6 were studied and evaluated. Three human tumor and three normal cell lines, namely as breast adenocarcinoma (MCF-7), non-small cell lung cancer (NCI-H460) and CNS cancer (SF-268), human fibroblast (WI-38), normal prostate epithelial cells, and normal colon mucosal, NCM 460 cells, respectively. The tested compounds were found to exhibit higher inhibitory effects toward the tumor and normal cell lines than the reference drug, doxorubicin.

**Keywords:** Bisdimedone; 1,8-Dioxo-octahydroxanthene; Knoevenagel condensation; Michael addition; Cytotoxicity.

#### 148. Azoles and Bis-azoles: Synthesis and Biological Evaluation as Antimicrobial and Anti-cancer Agents

Nabila Abdelshafy Kheder, Sayed Mohamed Riyadh and Ahlam Maade Asiry

*Chemical and Pharmaceutical Bulletin*, 61: 504-510 (2013) IF: 1.564

Novel hydrazoneyl halides 3, 5 and bis-hydrazoneyl halides 7, 9 were synthesized. The synthetic utility of bis-hydrazoneyl halide 7 was explored to prepare novel bis-azole 13 with antipyrene moiety. On the other hand, [1,3,4]thiadiazol-2(3*H*)-ylidene 17 and thiazol-2(3*H*)-ylidene 21 derivatives, with antipyrene moiety, were prepared from the reaction of 3-mercapto-3-

(phenylamino)acrylamide derivative 10 with N-phenyl benzenecarbohydrazonoyl chloride (14) and 3-(2-bromoacetyl)-2H-chromen-2-one (18), respectively. The structures of the isolated products were confirmed by spectral data (IR, <sup>1</sup>H-NMR, <sup>13</sup>C-NMR, MS) and elemental analyses. The anti-cancer activity of the synthesized products against the colon carcinoma (HCT) cell line was determined and the results revealed promising activity of compound 3. In addition, the antimicrobial activity of some selected products was evaluated. The results proclaimed that compounds 9, 17, and 21 have high antibacterial activity against Gram-positive bacteria (SA, BS) and Gram-negative bacteria (PA, EC).

**Keywords:** Anti-cancer activity; Antimicrobial activity; Antipyrine; Azole; Bis-azole.

#### 149. Synthesis, Tautomeric Structures, and Antitumor Activity of New Perimidines

Thoraya A. Farghaly and Huda K. Mahmoud

*Arch. Pharm. Chem. Life Sci*, 346: 392-402 (2013) IF: 1.54

New series of perimidine derivatives and fused perimidines were derived from the reaction of ketene amins 1 and 2 with diazotized anilines or hydrazonoyl chlorides. In addition, 8,10-disubstituted-[1,2,4]triazolo[4,3-a]perimidines (20a-m) were prepared through the reaction of perimidine-2-thione (15) with hydrazonoyl chlorides. The structures of the newly synthesized compounds were established on the basis of spectral data and elemental analyses. Some products were investigated for their antitumor activities against the human breast cancer cell line MCF-7 and the liver carcinoma cell line HEPG-2, and the results of some derivatives showed promising activity.

**Keywords:** [1,2,4]Triazolo[4,3-a]Perimidine; Antitumor activity; Hydrazone; Ketene aminal; Perimidines; Pyrrolo- [1,2-a] Perimidine-10-one.

#### 150. Site-Selective Reactions of Hydrazonoyl Halides with Cyanoacetic Hydrazide and its N-Aryldene Derivatives and Anti-aggressive Activity of Prepared Products

Ahmad Sami Shawali, Thoraya A. Farghaly, Shadia M. Hussein and Mohamed M. Abdalla

*Archives Pharmacol Research*, 36: 694-701 (2013) IF: 1.538

Reactions of hydrazonoyl halides with cyanoacetic hydrazide and its N-aryldene derivatives proceeded site-selectively and afforded the respective pyrazolo[3,4-d]pyridazine and aldehyde N-(1-aryl-3-acetyl-4-cyanopyrazol-5-yl)hydrazone derivatives. The structures of the products were elucidated on the basis of their spectral and elemental analyses. The anti-aggressive activity of the compounds prepared was screened.

**Keywords:** Site-selectivity; Hydrazonoyl halides; Pyrazoles; Pyrazolo [3,4-d] Pyridazines; Anti-aggressive activity.

#### 151. Synthesis of Pyrido [2,3-d][1,2,4]Triazolo[4,3-a]Pyrimidin-5-Ones as Potential Antimicrobial Agents

Thoraya A. Farghaly and Huwaida M. E. Hassaneen

*Archives of Pharmacol Research*, 36(5): 564-572 (2013) IF: 1.538

Synthesis of new derivatives of pyrido[2,3-d][1,2,4]triazolo[4,3-a]pyrimidin-5-one via reaction of 7-(4-bromophenyl)-1,2-dihydro-5-(4-fluorophenyl)-2-thioxopyrido[2,3-d]pyrimidin-4(3H)-one with hydrazonoyl chlorides or reaction of 2-hydrazinopyrido[2,3-d]pyrimidin-4(3H)-one with different aldehydes followed by cyclization of the products. All the newly synthesized compounds were evaluated for their antimicrobial activities and also their minimum inhibitory concentration against most of test organisms was performed. Amongst the tested compounds displayed excellent activity against all the tested microorganisms except SR and PA.

**Keywords:** Pyrido [2,3-d] [1,2,4] triazolo[4,3-a] pyrimidin-5-ones; Hydrazonoyl chlorides; Antimicrobial activity.

#### 152. Charge Transfer Complexes of 2-Arylaminomethyl-1H-Benzimidazole With 2,3-Dichloro-5,6-Dicyano-1,4-Benzoquinone: Experimental and DFT Studies

Ola R. Shehab and Ahmed M. Mansour

*Journal of Molecular Structure*, 1047: 121-135 (2013) IF: 1.404

Two new charge transfer complexes ( $L^{1,2} \rightarrow DDQ$ ;  $L^1 = (1H\text{-benzimidazol-2-ylmethyl})\text{-N-phenyl amine}$ ,  $L^2 = (1H\text{-benzimidazol-2-ylmethyl})\text{-(4-nitro-phenyl)-amine}$   $DDQ = 2,3\text{-dichloro-5,6-dicyano-1,4-benzoquinone}$ ) have been synthesized and characterized by a variety of physico-chemical techniques. The experimental studies were complemented by quantum chemical calculations at DFT/B3LYP level of theory. Electronic structures were investigated by TD-DFT method and the descriptions of frontier molecular orbitals and the relocation of the electron density were determined. Stability of the molecule arises from hyperconjugative interactions, charge delocalization and hydrogen bonding has been analyzed using natural bond orbital (NBO) analysis. <sup>1</sup>H NMR chemical shifts were computed at B3LYP/6-311+G(2d,p) level of theory by Gauge-invariant atomic orbital (GIAO) in DMSO as a solvent using the polarizable continuum model (PCM). Photometric titration was carried out to shed more light about the stoichiometry of the formed complexes in the solution. Spectral data were analyzed in terms of formation constant, molar extinction coefficient, oscillator strength, dipole moment, standard free energy, and ionization potential.

**Keywords:** Benzimidazole; DDQ; TD-DFT; PCM; NBO; Charge transfer.

#### 153. Hydrogen-Bond Effect, Spectroscopic and Molecular Structure Investigation of Sulfamethazine Schiff-Base: Experimental and Quantum Chemical Calculations

Ahmed M. Mansour and Nour El-deen T. Abdel-Ghani

*Journal of Molecular Structure*, 1040: 226-237 (2013) IF: 1.404

Comprehensive theoretical and experimental structural studies on N- (4,6-dimethyl-pyrimidin-2-yl)-4-[(2-hydroxy-benzylidene)-amino]benzenesulfonamide (SMS) have been carried out by elemental analysis, FT IR, <sup>1</sup>H NMR, UV-Vis. and MS. Optimized molecular structure and harmonic vibrational frequencies have been investigated by DFT/B3LYP and HF methods combined with 6-31G(d) basis set. Stability of the molecule arises from hyperconjugative interactions, charge delocalization and intramolecular hydrogen bond has been analyzed using natural bond orbital (NBO) analysis. Electronic structures were discussed by TD-DFT method and the descriptions of frontier molecular orbitals and the relocation of the electron density were determined. <sup>1</sup>H NMR chemical shifts were computed by Gauge-invariant atomic orbital (GIAO) method in both gas and DMSO media, using the polarizable continuum model (PCM). Structure-activity relationship has been used to correlate biological activity with some appropriate quantum descriptors such as  $E_{\text{HOMO}}$ ,  $E_{\text{LUMO}}$ , energy gap, dipole moment ( $\mu$ ), global hardness ( $\eta$ ), softness ( $S$ ), electrophilicity index ( $\omega$ ), molecular polarizability ( $\alpha$ ), Mulliken electronegativity ( $\chi$ ), Mulliken charge ( $Q_i$ ) and molecular electrostatic potential (MEP).

**Keywords:** Sulfamethazine; TD-DFT; Hydrogen bond; NBO; MEP; SAR.

#### 154. Molecular Structure and Spectroscopic Properties of Novel Manganese (II) Complex with Sulfamethazine Drug

Ahmed Moustafa Mansour

*Journal of Molecular Structure*, 1035: 114-123 (2013) IF: 1.404

[MnLCl(H<sub>2</sub>O)<sub>3</sub>]·H<sub>2</sub>O complex (HL = 4-amino-N-(4,6-dimethyl-2-pyrimidinyl)benzenesulfonamide, sulfamethazine) has been synthesized and characterized by elemental analysis, TG/DTA, MS, FT-IR, UV-Vis, magnetic, electrochemical, and X-ray powder diffraction. The experimental studies were complemented by quantum chemical calculations at DFT/B3LYP level of theory. Sulfamethazine behaves as a mono-negatively bidentate ligand and interacts with Mn(II) ion through sulfonamidic (N15) and pyrimidic (N23) nitrogen atoms. Electronic structures were investigated using TD-DFT method and the descriptions of frontier molecular orbitals and the relocation of the electron density were determined. The voltammogram of NaL shows one irreversible one-electron process due to oxidation of p-amino group, and one anodic peak characteristic of reduction of single bondSO<sub>2</sub> group. The synthesized complex, in comparison to the parent drug, was screened for its antibacterial activity.

**Keywords:** Sulfamethazine; DFT; Electrochemical; NBO; MEP; Antibacterial.

#### 155. Single Crystal, Spectral, Computational Studies and in Vitro Cytotoxicity of 2-Chloro-3-Formyl pyrido[2,1-a]Isoquinoline-1-Carbonitrile Derivative

Ahmed M. Mansour, Hamdi M. Hassaneen, Yasmin Sh. Mohammed and Nour El-deen T. Abdel-Ghani

*Journal of Molecular Structure*, 1045: 180-190 (2013) IF: 1.404

In the present work, comprehensive theoretical and experimental structural studies on 2-chloro-3-formyl-9,10-dimethoxy-4-oxo-6,7-dihydro-4H-pyrido[2,1-a]isoquinoline-1-carbonitrile (PQC)

have been performed using spectral methods and X-ray crystallography. PQC crystallizes in monoclinic crystal system of P2<sub>1</sub>/c space group with  $a = 23.5106$  (6) Å,  $b = 17.7940$  (4) Å,  $c = 7.2843$  (2) Å and  $\beta = 90.1421$  (9)°. The unit-cell is built by two molecules of different conformations. The two molecules are not coplanar and they are linked to each other through double intermolecular hydrogen bonds of different strength. Optimized molecular structure and harmonic vibrational frequencies have been investigated at DFT/B3LYP and HF level of theory combined with 6-31G(d) basis set. Stability, arises from hyperconjugative interactions, charge delocalization and H-bond, has been analyzed using natural bond orbital (NBO) analysis. Electronic structures were discussed by time-dependent density functional theory. Descriptions of frontier molecular orbitals and the relocation of the electron density were determined. <sup>1</sup>H NMR chemical shifts were computed by using Gauge-invariant atomic orbital method in both gas and DMSO media, using the polarizable continuum model. The cytotoxicity assay was performed against three-cell lines, breast cancer (MCF7), colon Carcinoma (HCT) and human hepatocellular Carcinoma (HepG2).

**Keywords:** Pyrido [2,1-a]Isoquinoline; Crystal structure; Antitumor; NBO; PCM; GIAO

#### 156. An Efficient Synthesis of Novel Benzo-Fused Macrocyclic Dilactams

Ahmed E. M. Mekky, Ahmed A. M. Ahmed and Ahmed H. M. Elwahy

*Helv Chim Acta*, 96: 1290-1297 (2013) IF: 1.383

A facile synthetic approach was adopted towards the synthesis of benzo-fused macrocyclic lactams 2a–2g via the base-catalyzed condensation reaction of 2,2'-[alkanediylbis (oxy)]bis [benzaldehydes] 3a–3c with N,N'-substituted bis[2-cyanoacetamide] derivatives 7a–7c (Scheme 2). The latter compounds were obtained by the reaction of the appropriate diamines 6a–6c with ethyl 2-cyanoacetate (4). Attempts to prepare the oxaza macrocycles 2 by alternative pathways were also investigated. The novel pyrazolo-fused macrocycles 13a and 13b were obtained in 48 and 52% yield, respectively, upon treatment of 2d and 2g with NH<sub>2</sub>NH<sub>2</sub>·H<sub>2</sub>O at 100° (Scheme 4).

**Keywords:** Bis aldehydes; Bis amines; Bis cyanoacetamides; Macrocycles; Cyclocondensation.

#### 157. Synthesis of Novel Palladacycles Inhibitors of the Cathepsin B Activity and Antitumoral Agents

Abdel-Sattar S Hamad Elgazwy, Mohamed R Shehata, Myssoune Y Zaki, Dalia H S Solima and Marwa M Elbakkry

*Medicinal Chemistry*, 3: 254-261 (2013) IF: 1.373

The reaction of 2-bromo-3,4,5-trimethoxybenzaldehyde 1 with Pd(dba)<sub>2</sub>; dba=dibenzylideneacetone in the presence of a stoichiometric amount of nitrogen donor ligands, such as N,N,N',N'-tetramethyl-ethane-1,2-diamine (TMEDA), 2,2'-bipyridine (bpy) 4,4'-dimethyl-2,2'-bipyridine (dmbpy) and an 1,10-phenanthroline (Phen), should be added to with equimolar ratio in degassed acetone under nitrogen to give mononuclear s-aryl palladium (II) complexes cis-[2-Pd{C<sub>6</sub>H(CHO)-6-(OMe)<sub>3</sub>-3,4,5}BrL<sub>2</sub>] 3a-d, where L<sub>2</sub>=TMEDA (3a); L<sub>2</sub>=bpy (3b); L<sub>2</sub>=dmbpy (3c); L<sub>2</sub>=Phen (3d) in good yields 48-65%. The

reaction of the synthesized five-membered C,N-palladacycle  $\text{cis-[2-Pd}\{\text{C}_6\text{H}(\text{CHO})\text{-6-(OMe)}_3\text{-3,4,5}\}\text{BrL}_2\text{]}$  3a-d, where  $\text{L}_2=\text{TMEDA}$  (3a);  $\text{L}_2=\text{bpy}$  (3b);  $\text{L}_2=\text{dmbpy}$  (3c);  $\text{L}_2=\text{Phen}$  (3d), with an 1-naphthylisocyanates ( $\text{C}_{10}\text{H}_7\text{-NCO}$ ) and an 1-naphthylisothiocyanates ( $\text{C}_{10}\text{H}_7\text{-NCS}$ ), leads to the formation of novel palladacycle 4a-d and 5a-d, which was characterized in solution by  $^1\text{H}$  NMR spectroscopy. The solid products were characterized by satisfactory elemental analysis and spectra studies. All the resulting complexes 3a-d, 4a-d and 5a-d were tested in vitro against a number of cell lines. For example, it inhibited K562 leukaemia cells with an  $\text{IC}_{50}$  value in the range of (3.00 - 4.3)  $\mu\text{M}$  (1h exposure) and displayed cathepsin B inhibitory action with an  $\text{IC}_{50}$  value in the range of (0.045-0.055  $\mu\text{M}$ ).

**Keywords:** Palladium complexes; 1-Naphthyl isocyanate; Isothiocyanate; Palladacycles.

### 158. Conformational Preference and Mechanism of Decarboxylation of Levodopa. A Quantum Dynamics/Quantum Mechanics Study

Shabaan A. K. Elroby, Ashour A. Ahmed and Rifaat H. Hilal

*International Journal of Quantum Chemistry*, 113: 1966-1974 (2013) IF: 1.306

The present study addresses the conformational preferences and the mechanism of decarboxylation of levodopa (LD). LD is used to increase dopamine concentrations in the treatment of Parkinson's disease. LD crosses the protective blood-brain barrier, where it is converted into dopamine by the process of decarboxylation. Molecular dynamics simulation has been carried out at the DFT/6-31++G level of theory to identify the global minimum structure of LD. Conformational preferences of the amino acid side chain of LD has been investigated at the B3LYP/6-311++G\*\* level of theory. Fourier transform analysis has been performed to identify the origin of the rotational barriers. Electrostatic dipole moment and bond interactions underlie the observed potential energy barriers for rotation of the amino acid side chain of LD. The vital biological process of decarboxylation of LD has been examined in the gas phase and in aqueous solution. Without the presence of water, there is only one possible route for the decarboxylation of LD. In this concerted mechanism, a proton transfer and breakage of the  $\text{C}_{10}\text{—C}_{18}$  bond, take place simultaneously ( $\Delta E^\ddagger = 73.2$  kcal/mol). In solution, however, two possible decarboxylation routes are available for LD. The first involve the formation of a zwitterionic intermediate ( $\Delta E^\ddagger = 72.4$  kcal/mol). The zwitterionic form of LD have been localized using explicitly bound water molecules to model short-range solvent effects and self-consistent reaction field polarized continuum model to estimate long-range solvent interactions. The second route involve the formation of a cyclic structure in which a water molecule acts as a bridge linking the anticarboxylic hydrogen and  $\alpha$ -position carbon atom ( $\Delta E^\ddagger = 59.8$  kcal/mol). Natural bond orbital (NBO) analysis reveals that the conformational and overall stability of the amino acid side chain is facilitated by the antiperiplanar interactions between the phenyl moiety  $\text{C—H}$  and  $\text{C—C}$  bonds and  $\text{C—X}$  bonds of the amino acid side chain. However, much of the major donor-acceptor interactions is of the lone pair type and is localized within the amino acid side chain itself. Results of the present work reveal that NBO data reflect nicely and identify clearly reaction coordinates at the transition species.

**Keywords:** levodopa; Conformational preference; Mechanism of decarboxylation; Molecular dynamics/qM; Density functional theory.

### 159. Structure and Cooperativity of the Hydrogen Bonds in Sodium Dihydrogen Triacetate

Ashour A. Ahmed, Oliver Kühn, Rifaat H. Hilal and Mohamed F. Shibl

*International Journal of Quantum Chemistry*, 113 (9): 1394-1400 (2013) IF: 1.306

Geometry and energetics of low energy conformers of sodium dihydrogen triacetate (SDHTA) and its anion are studied using density functional theory (DFT) at the Becke, Lee-Yang-Parr hybrid functional (BLYP) and Becke, three-parameter, Lee-Yang-Parr hybrid functional (B3LYP) levels. For both cases, two structures of comparable energy are found, which have different symmetry with respect to the two hydrogen bonds (HBs). DFT-based Born-Oppenheimer molecular dynamics simulations are performed for SDHTA, which show that both structures are visited at room temperature conditions. The trajectory analysis further reveals that the two HBs behave anticooperative, that is, on average elongation of one HB is accompanied by a compression of the other one. This is in accord with nuclear magnetic resonance (NMR) experimental studies for a similar counter ion-dihydrogen triacetate complex.

**Keywords:** Hydrogen bonds; Cooperative dynamics; Density functional theory; Molecular dynamics.

### 160. Plastic Membrane, Carbon Paste and Multiwalled Carbon Nanotube Composite Coated Copper Wire Sensors for Determination of Oxeladin Citrate Using Batch and Flow Injection Techniques

Sayed I. M. Zayed and Yousry M. Issa

*Journal Of Brazilian Chemical Society*, 24: 585-594 (2013) IF: 1.283

The fabrication and performance characteristics of three novel potentiometric sensors for the determination of oxeladin citrate are described. The proposed sensors include a PVC plastic membrane sensor, a carbon paste sensor and a multiwalled carbon nanotube (MWCNT) composite coated copper wire sensor. The sensors are based on the oxeladin-phosphotungstate ion associate as electroactive material and dibutyl phthalate as solvent mediator. The developed sensors exhibited near nernstian slopes of  $58.00 \pm 0.22$ ,  $55.00 \pm 0.69$  and  $57.8 \pm 0.13$  mV concentration decade<sup>-1</sup> at 25 °C, in the concentration ranges  $5.96 \times 10^{-6}$  -  $1.00 \times 10^{-2}$ ,  $1.96 \times 10^{-5}$  -  $1.00 \times 10^{-2}$  and  $3.98 \times 10^{-6}$  -  $1.00 \times 10^{-2}$  mol L<sup>-1</sup> oxeladin citrate with limits of detection of  $4.14 \times 10^{-6}$ ,  $8.58 \times 10^{-6}$  and  $2.51 \times 10^{-6}$  mol L<sup>-1</sup> oxeladin citrate for plastic membrane, carbon paste and MWCNT composite coated copper wire sensors, respectively. The proposed sensors exhibit good selectivity for oxeladin with respect to a large number of inorganic cations, sugars, amino acids and vitamins. The developed sensors were successfully applied for the potentiometric determination of oxeladin citrate in the pharmaceutical preparation (Paxeladine® capsules) in batch and flow injection conditions. The sensors were also applied for the



determination of oxeladin citrate in human urine samples by using the standard addition method.

**Keywords:** Oxeladin citrate; Potentiometry; Flow injection; Pharmaceutical.

### 161. Stability-indicating Methods for the Determination of Candesartan Cilexetil in Bulk Drug and Pharmaceutical Formulations

Yousry Moustafa Issa

*Journal of Aoa C International*, 96: 580-568 (2013) IF: 1.233

Two stability-indicating methods were developed for the determination of candesartan cilexetil in the presence of its degradation products. The first method uses isocratic RP-HPLC with an Agilent C18 column. The mobile phase was phosphate buffer (pH = 2.8 ± 0.1)-acetonitrile (60 + 40, v/v). The flow rate was 2.0 mL/min, and the UV detection was at 254 nm. The second method depends on TLC-densitometric measurements of drug spots at 254 nm. The separation was carried out on silica gel 60 F254 plates using ethyl acetate-methanol-toluene-ammonia 33% (40 + 25 + 20 + 2, v/v/v/v) mobile phase. The methods were validated according to U.S. Pharmacopeia guidelines, and the acceptance criteria for accuracy, precision, linearity, specificity, robustness, LOD, LOQ, and system suitability were met in all cases. Linear ranges of the methods were 10.0–200.0 µg/mL and 1.0–9.0 µg/spot for HPLC and TLC, respectively. The proposed methods were successfully applied to the drug in bulk powder, in laboratory-prepared mixtures with its degradation products, and in commercially available tablets. The results were compared statistically at the 95% confidence level with each other. There were no significant differences between the mean recovery and precision of the two methods.

**Keywords:** Stability indicating method; RP HPLC; TLC.

### 162. Reaction of Hydrazonoyl Halides with Bis-Enaminones: A Convenient Route for Synthesis of Novel Polyaza-Terheterocycles

Ahmad Sami Shawali and Adel J. M. Haboub

*Journal of Heterocyclic Chemistry*, 50: 17-22 (2013) IF: 1.224

New bis (pyrazolylenaminones) were prepared in good yields. Their synthetic utilities as precursors for regioselective synthesis of novel bis(hetarylpyrazoles) were also investigated. The mechanisms and selectivities observed in the studied reactions were discussed.

**Keywords:** Bis pyrazolylenaminones; Regioselectivity.

### 163. Synthesis of New Indeno [1,2-c]Pyrazole-Based Heterocycles and Evaluation of Their Protective Effect Against DNA Damage Induced by Bleomycin-Iron

Bahira Hegazi, Hassan Abdel-Gawad, Hanan A. Mohamed, Farid A. Badria and Ahmad M. Farag

*Journal of Heterocyclic Chemistry*, 50: 355-360 (2013) IF: 1.224

Reaction of potassium 2-(1-phenyl-1,4-dihydroindeno[1,2-c]pyrazole-3-carbonyl)hydrazine carbodithioate (2) with

hydrazine hydrate, phenacyl bromides, and hydrazonoyl chlorides afforded the corresponding 1,2,4-triazole, 1,3-thiazole, and 1,3,4-thiadiazole derivatives 3, 5, and 7, respectively. Reaction of 3-mercapto-4-amino-1,2,4-triazole 3 with phenacyl bromides 4a-c and hydrazonoyl chlorides 6a,b afforded the corresponding 1,2,4-triazolo[3,4-b]-1,3,4-thiadiazine derivatives 10a-c and 13a,b, respectively, whereas its reaction with 2-chloro-N-arylacetylamide derivatives 11a-d afforded the corresponding 2-(4-amino-5-(1-phenyl-1,4-dihydroindeno[1,2-c]pyrazol-3-yl)-4H-1,2,4-triazol-3-ylthio)-N- arylacetamide derivatives 12a-d.

All of the new compounds were tested for their protection activity against DNA damage induced by bleomycin-iron complex. Compounds 7a and b showed the highest protection activity through diminishing chromogen formation between the damaged DNA and thiobarbituric acid.

**Keywords:** New indeno[1,2-c] pyrazole; DNA damage; Bleomycin-iron, 1,3,4-thiadiazole; 1,2,4-triazole; Hydrazonoyl chlorides.

### 164. Impact of Composition and Fabrication Method of the Corrosion Behavior of Tungsten Heavy Alloys in Aqueous Solutions

Z. Abdel Hamid and H. B. Hassan

*Surface and Interface Analysis*, 45: 1830-1837 (2013) IF: 1.22

Tungsten heavy alloys (WHAs) are kind of composite materials; these alloys provide a unique combination of properties such as high density, excellent mechanical properties and good corrosion resistance that making them increasingly attractive in many practical applications. In this work, the corrosion behavior of the investigated tungsten heavy alloys with the composition of (95% W-3.5% Ni-1.5% Fe), (93% W-4.5% Ni-1.0% Fe-1.5% Co) and (90% W-6% Ni-4% Cu) fabricated by either chemical or mechanical technique has been evaluated through potentiodynamic polarization measurements in different aqueous solutions of 0.6M NaCl, 0.1M HCl and 0.1M NaOH. The extent of the corrosion has been illustrated by examining the surfaces of WHAs before and after the corrosion test using SEM. It includes general dissolution, localized attack of the binder phase and tungsten grain loss, where the extent of each of these depends on the fabrication technique and the alloy composition as well as the pH of the medium.

**Keywords:** Tungsten heavy alloys (Whas); Corrosion resistance; Chemical reduction; Electrochemical measurements; Powder.

### 165. The Electrocatalytic Behavior of Electrodeposited Ni-Mo-P Alloy Films towards Ethanol Electrooxidation

H. B. Hassana and Z. Abdel Hamid

*Surface and Interface Analysis*, 45: 1135-1143 (2013) IF: 1.22

Ternary Ni-Mo-P thin films have been electrodeposited from citrate-based electrolyte onto graphite substrates for application as anode catalysts for ethanol electrooxidation. The operating deposition parameters were optimized to produce Ni-Mo-P alloy films of outstanding catalytic activity. The phase structure of the deposits was evaluated employing X-ray diffraction technique. Morphology and chemical composition of the deposited alloy films were studied using scanning electron microscopy and

energy-dispersive X-ray analysis, respectively. The results demonstrated that the rate of Ni–Mo–P deposition increases with increasing the ammonium molybdate concentration in the plating electrolyte up to 10 g l<sup>-1</sup>. Also, the amount of Mo in the deposits increases with increasing the ammonium molybdate concentration up to 7.5 g l<sup>-1</sup>, and the maximum Mo content in the film was 9.1 at.%. The catalytic activity of Ni–Mo–P/C alloy films has been evaluated towards electrooxidation of ethanol in 1.0 M NaOH solution by using cyclic voltammetry and chronoamperometry. The catalytic performance of the prepared anodes as a function of the amount of Mo was studied. The results showed an increase in the oxidation peak current density of ethanol with increasing the Mo at.% in the deposited alloy films. Additionally, Ni–Mo–P/C electrodes displayed significantly improved catalytic activity and stability towards electrooxidation of ethanol compared with that of Ni–P/C electrode.

**Keywords:** Electrodeposition; Ni–Mo–P alloy; Electrooxidation; Ethanol; DfCs; Fuel cell.

#### 166. Synthesis and anti-tumor evaluation of novel hydrazide and hydrazide-hydrazone derivatives

Wardakhan W.W., El-Sayed N.N. and Mohareb R.M.

*Acta Pharmaceutica*, 63: 45-57 (2013) IF: 1.162

The reaction of cyclopentanone with cyanoacetylhydrazine gave 2-cyano-2-cyclopentylideneacetohydrazide (1). Treatment of compound 1 with elemental sulphur in the presence of triethylamine afforded 2-amino-5,6-dihydro-4H-cyclopenta[b]thiophene-3-carbohydrazide (2), which in-turn formed the corresponding intermediate diazonium salt. The latter was coupled with either ethyl cyanoacetate or ethyl acetoacetate to form 2-cyano-2-(3-(hydrazinecarbonyl)-5,6-dihydro-4H-cyclopenta[b]thiophen-2-yl)hydrazono) acetate (3) and ethyl 2-(2-(3-(hydrazinecarbonyl)-5,6-dihydro-4H-cyclopenta[b]thiophen-2-yl)hydrazono)-3-oxobutanoate (4), respectively. On the other hand, the reaction of compound 1 with either benzaldehyde or acetophenone afforded N'-benzylidene-2-cyano-2-cyclopentylideneacetohydrazide (7) and 2-cyano-2-(2-cyclopentylidene)phenylacetohydrazide (10), respectively. Moreover, compound 1 was used to synthesize 2-cyano-2-cyclopentylidene- N'-(arylthiazol-2(3H)-ylidene)acetohydrazides (6a,b), 2-(2-benzylidenecyclopentylidene)-2-cyanoacetohydrazide (8), 2-amino-N'-benzylidene-5,6-dihydro-4H-cyclopenta[b]thiophene-3-carbohydrazide (9), 2-cyano-2-(2-phenylhydrazono)cyclopentylidene)acetohydrazide (11), N'-(1-chloropropan-2-ylidene)-2-cyano-2-cyclopentylideneacetohydrazide (12), and 2-cyclopentylidene-3-(3,5-disubstituted-1H-pyrazol-1-yl)-3-oxopropanenitriles (13a,b) through its reaction with the respective reagents. Antitumor evaluation of the newly synthesized compounds against the three human tumor cells lines, namely, breast adenocarcinoma (MCF-7), non-small cell lung cancer (NCI-H460) and CNS cancer (SF-268) showed that some of the described compounds exhibited higher inhibitory effects towards the three tumor cell lines than the reference compound doxorubicin.

**Keywords:** Hydrazide; Hydrazide-hydrazone; Thiophene; Pyrazole; Antitumor.

#### 167. New Approaches for the Synthesis of Thiophene Derivatives with Anti-tumor Activities

Rafat M. Mohareb, Nermeen S. Abbas and Rehab A. Ibrahim

*Acta Pharm.* 63: 45-57 (2013) IF: 1.135

The reaction of either cyclohexanone or cyclopentanone with cyanoacetylhydrazine and elemental sulfur gave the 2-aminocycloalkeno[b]thiophene derivatives 3a and 3b, respectively. The latter compounds reacted with either aromatic benzaldehydes or active methylene reagents to give the Schiff's bases 5a-d and the pyrazole derivatives 7a-d and 9a-d, respectively. On the other hand, the reaction of 3-oxo-N-p-tolylbutanamide (10) with either of malononitrile or ethyl cyanoacetate gave the thiophene derivatives 13a and 13b, respectively. Compounds 13a,b were subjected to a series of heterocyclization reactions to give heterocyclic derivatives. Their cytotoxicity against the three human tumor I cells lines, namely breast adenocarcinoma (MCF-7), non-small cell lung cancer (NCI-H460) and CNS cancer (SF-268) together against the normal human cell line namely the normal fibroblast cells WI 38 were measured.

**Keywords:** Hydrazide-hydrazone; Thiophene; Pyrazole; Arylhydrazone; Antitumor activity.

#### 168. Complex Formation Equilibria of Unusual Seven Coordinate Fe (III) Complexes with DNA Constituents

M. Aljahdali, A. A. El-Sherif, M. M. Shoukry, W. M. Hosny and M. G. Abd-Elmoghny

*Journal of Solution Chemistry*, 42: 1663-1679 (2013) IF: 1.128

Seven-coordinate Fe(III) complexes [Fe(dapsox)(H<sub>2</sub>O)<sub>2</sub>]<sup>+</sup>, where [dapsox = 2,6-diacetylpyridine-bis(semioxamazide)] is an equatorial pentadentate ligand with five donor atoms (2O and 3N), were studied with regard to their acid-base properties and complex formation equilibria. Stability constants of the complexes and the pK<sub>a</sub> values of the ligands were measured by potentiometric titration. The interaction of [Fe(dapsox)(H<sub>2</sub>O)<sub>2</sub>]<sup>+</sup> with the DNA constituents, imidazole and methylamine·HCl were investigated at 25 °C and ionic strength 0.1 mol·dm<sup>-3</sup> NaNO<sub>3</sub>. The hydrolysis constants of the [Fe(dapsox)(H<sub>2</sub>O)<sub>2</sub>]<sup>+</sup> cation (pK<sub>a1</sub> = 5.94 and pK<sub>a2</sub> = 9.04), the induced ionization of the amide bond and the formation constants of the complexes formed in solution were calculated using the nonlinear least-squares program MINQUAD-75. The stoichiometry and stability constants for the complexes formed are reported. The results show the formation of 1:1 and 1:2 complexes with DNA constituents supporting the hepta-coordination mode of Fe(III). The concentration distributions of the various complex species were evaluated as a function of pH. The thermodynamic parameters ΔH° and ΔS° calculated from the temperature dependence of the equilibrium constants were investigated for interaction of [Fe(dapsox)(H<sub>2</sub>O)<sub>2</sub>] with uridine

**Keywords:** Complex formation equilibria; Fe (III); DNA Stability constants; 2,6-diacetylpyridine; Speciation.

### 169. Electrochemical Behavior and Stability of Cu-Al-Ni Alloys in NaOH Solutions

Waheed A. Badawy, Mohammed M. El-Rabiei, Nadia H. Helal and Hashem M. Nady

*Zeitschrift Für Physikalische Chemie*, 227: 1059-1071 (2013)  
IF: 1.128

The electrochemical behavior of copper-aluminum-nickel alloy with different Ni content in sodium hydroxide solutions was investigated. The alloys are usually used as tubes and reservoirs in basic solutions for the production of salts from marine solutions. The role of the Ni-content on the corrosion resistance of the alloy was evaluated. Different electrochemical methods were used. The increase of the nickel content in the alloy and increased immersion time in the solution improve the alloy stability due to the formation of a stable passive film. The experimental impedance data were fitted to theoretical data. The results of these experiments are discussed in reference to potential-pH (Pourbaix) diagrams. Surface morphology and barrier film constituents were examined by SEM.

**Keywords:** Alloys; Corrosion; Electrochemical techniques; Passivation; SEM.

### 170. Electropolymerization of Aminoanthraquinone from H<sub>2</sub>SO<sub>4</sub>/Acetonitrile Mixed Solvent – Polymer Film Characterization and its Use as Analytical Sensor

Waheed A. Badawy, Khaled M. Ismail and Shymaa S. Medany

*Zeitschrift Für Physikalische Chemie*, 1-17 (2013) IF: 1.128

Polyaminoanthraquinone, PAAQ, films were prepared potentiodynamically and potentiostatically from acetonitrile/sulfuric acid mixed solvent. Series of investigations have been carried out in which the mixed solvent ratio, type of substrate, electrochemical technique, potential scan range, scan rate and number of cycles were investigated in order to optimize the electropolymerization process. The potentiodynamic technique using glassy carbon, GC, substrates provides more stable films and useful information about the electropolymerization process from the mixed solvent. The suitable monomer concentration was 5.0mM of 1-amino-9, 10-anthraquinone dissolved in 4.0M H<sub>2</sub>SO<sub>4</sub>/ACN mixed solvent with a volume ratio 7 : 3. The most suitable potential scan range was from -0.5 to +1.4 V at a scan rate of 100mVs<sup>-1</sup>. The effect of the scan repetition i. e. the thickness of the prepared polymer films on the electroanalytical performance of the modified electrode was investigated and discussed. The kinetics of electropolymerization process was investigated and the reaction was found to be first order with respect to the monomer concentration and of negative order with respect to sulfuric acid. The formed films were used successfully as analytical sensors for ascorbic acid, catechol, Ce III ions, dopamine, epinephrine, p-aminophenol and pyrogallol. The determination is based on the construction of a calibration curve for each analyte using the values of the oxidation peak currents in the cyclic voltammogram obtained by the PAAQ modified electrode in each case. The data were compared with the data obtained previously by the same films prepared in non-aqueous and aqueous media. The significance of the analytical performance of the formed films

with respect to the state-of-the-art was investigated and discussed. The use of the mixed solvent, beside its effectiveness as analytical sensor, has limited the effect of hazardous organic solvent.

**Keywords:** Polymers; Thin films; Electrochemical techniques; Electrochemical properties.

### 171. Modified Screen-Printed Electrode for Potentiometric Determination of Copper (II) in Water Samples

Tamer Awad Ali, Gehad G. Mohamed, Maher M. I. El-Dessouky, Salwa M. Abou El-Ella and Rabab T. F. Mohamed

*J. Solution Chem*, 42 (6): 1336-1354 (2013) IF: 1.128

Modified screen printed (SPE) and carbon paste electrodes (CPE) with phenanthroline-tetraphenyl borate ionophore [Phen:TPB] were fabricated for the determination of copper(II). The modified electrodes have linear responses over a wide concentration range ( $1 \times 10^{-6}$ – $1 \times 10^{-2}$  mol·L<sup>-1</sup>) of copper(II) ion at 25 °C with divalent cationic slopes of  $29.85 \pm 0.58$  and  $29.45 \pm 0.81$  mV·decade<sup>-1</sup> and exhibit a detection limit of  $1 \times 10^{-6}$  mol·L<sup>-1</sup> for SPE and CPE. The selectivity coefficient was measured using the match potential method in acetate buffer of pH = 4.2. The modified SPE and CPE sensors show high selectivity and sensitivity for determination of copper(II) and also show stable and reproducible response over a period of five and three months for SPE and CPE sensors, respectively. This method can be used for determination of copper(II) in water, soil, plant and fish tissue samples and the results obtained agreed with those obtained with atomic absorption spectrometer (AAS).

**Keywords:** Screen printed ion selective electrode; Modified carbon paste electrode; Copper sulfate; Potentiometric titration; Water samples.

### 172. Potentiometric and Thermodynamic Studies of Binary and Ternary Transition Metal (II) Complexes of Imidazole-4-Acetic Acid and Some Bio-Relevant Ligands

M. Aljahdali, Ahmed A. El-Sherif, Mohamed M. Shoukry and Seham E. Mohamed

*Journal of Solution Chem*, 42: 1028-1050 (2013) IF: 1.128

Proton-ligand association constants of imidazole-4-acetic acid (IMA) were determined potentiometrically in aqueous solution at different temperatures in the range 15–35 °C. The stepwise stability constants of IMA with some selected bivalent transition metal ions were also determined in 0.1 mol·dm<sup>-3</sup> NaNO<sub>3</sub>. The stability of the complexes follows the trend Cu<sup>2+</sup> > Ni<sup>2+</sup> > Co<sup>2+</sup> > Mn<sup>2+</sup>, which is in agreement with the Irving-Williams order of the metal ions. The thermodynamic parameters for Cu(II)–IMA complex formation were derived and discussed. The ternary complexes Cu(IMA)L (IMA = imidazole-4-acetic acid, HL = amino acid, amides or DNA constituents) have been investigated. Ternary complexes of amino acids or amides are formed by a simultaneous mechanism. Amino acids form the complex Cu(IMA)L, whereas amides form two complex species Cu(IMA)L and Cu(IMA)(LH<sub>-1</sub>). The DNA constituents form both 1:1 and 1:2 complexes. The stabilities of ternary complexes are quantitatively compared with their corresponding binary

complexes. The concentration distribution of the complexes in solution was evaluated as a function of pH.

**Keywords:** Imidazole-4-acetic acid (IMA); Amino acids; Amides; DNA constituents; Potentiometry; Thermodynamics.

### 173. Potentiometry, Stability and Thermodynamics of Diethyltin (IV) Dichloride with Some Selected Biomolecules

Mutlaq S. Aljahdali, Abeer T. Abdelkarim and Ahmed A. El-Sherif

*Journal of Solution Chemistry*, 42: 2240-2266 (2013) IF: 1.128

The interaction of diethyltin(IV), DET, with selected bioligands having a variety of model functional groups was investigated at 25 °C and ionic strength 0.1 mol·dm<sup>-3</sup> NaCl using the potentiometric technique. The hydrolysis constants of the DET cation and the formation constants of the complexes formed in solution were calculated using the MINIQUAD-75 program. The stoichiometry and stability constants for the complexes formed are reported. The results show the formation of 1:1 and 1:2 complexes with amino acids and DNA constituents. The dicarboxylic acids form 1:1 complexes. The peptides form both 1:1 complexes and the corresponding deprotonated amide species [Et<sub>2</sub>Sn (LH<sub>-1</sub>)] (1:1). The participation of different ligand functional groups in binding to organotin is discussed. The concentration distributions of the various complex species were evaluated as a function of pH. The standard thermodynamic parameters  $\Delta H^\circ$  and  $\Delta S^\circ$ , calculated from the temperature dependence of the equilibrium constants, were investigated for the interaction of DET with thymine as a representative example of DNA constituents. The effect of ionic strength and solvent on hydrolysis constants of DET, protonation equilibria of thymine and its complex formation with DET were investigated and discussed.

**Keywords:** Complex formation equilibria; Diethyltin (IV); DNA peptides; Amino acids; Speciation.

### 174. Protonation Equilibria of Some Selected $\alpha$ -Amino Acids in DMSO–water Mixture and their Cu (II) Complex

Ahmed A. El-Sherif, Mohamed M. Shoukry and Mohamed M. A. Abd-Elgawad

*Journal of Solution Chemistry*, 42: 412-427 (2013) IF: 1.128

The protonation constants of some  $\alpha$ -amino acids (glycine (Gly), l-alanine (Ala), l-valine (Val), l-serine (Ser), l-leucine (Leu) and l-isoleucine (Ile)) were studied in water and DMSO–water solution mixtures containing 30, 50 and 70 vol-% DMSO; in addition the complex formation equilibria of their copper(II) complexes were studied by potentiometric technique using a combined pH electrode system calibrated in concentration units of the hydrogen ion at 25  $\pm$  0.1 °C under a nitrogen atmosphere, and at an ionic strength of 0.10 mol·dm<sup>-3</sup> NaNO<sub>3</sub>. The protonation constants and the overall stability constants of copper(II) complexes were influenced by changes in solvent composition, and their variations are discussed in terms of solvent and structural properties.

**Keywords:** Amino acids; Protonation equilibria; Potentiometry; DMSO–water mixtures; Speciation; Copper (II).

### 175. Polyester Condensation Adducts as Novel Photostabilizers for Polystyrene

Magdy W. Sabaa, Samira T. Rabie, Mahmoud A. Abd-El-Ghaffar and Ahmed E. Ahmed

*J. Vinyl Addit. Technol.*, 19: 293-301 (2013) IF: 1.107

Polycondensation adducts formed by the reaction of maleic anhydride with some Polyalcohols, namely, phloroglucinol, glycerol, and ethylene glycol, were prepared, characterized, and investigated as photostabilizers for polystyrene. Their Photostabilizing effectiveness was evaluated by measuring the extent of weight loss (%), the amount of gel formed as well as the viscosity average molecular weight of the soluble fractions of the degraded polymer. The results indicated better stabilizing effects of these stabilizers compared with that of the UV absorber, phenyl salicylate. A synergistic effect was achieved when the investigated photostabilizers were mixed with phenyl salicylate in a weight ratio of 1:1, and a radical mechanism is proposed to account for the action of the polycondensation adducts as photostabilizers.

**Keywords:** Polyester; Condensation; Photostabilizer.

### 176. Synthesis and Quantum Calculations of 1,3-Thiazoles and 1,3,4-Thiadiazole Derivatives Via Pyridinyliothiureas

Kamal M. Dawood, Adel A. Mohamed, Mansour A. Alsenoussi and Ibrahim H. Ibrahim

*Journal of Sulfur Chemistry*, 34: 383-394 (2013) IF: 1.101

In this study, the reaction of 4- and 2-aminopyridines with phenyl isothiocyanate afforded the corresponding 1-phenyl-3-(pyridin-4-yl)thiourea 1 and its pyridin-2-yl analog 20. The reaction of 1 with ethyl chloroacetate gave 3-phenyl-2-(pyridin-4-ylimino)thiazolidin-4-one (3B), which upon a condensation reaction with aldehydes furnished 5-benzylidene derivatives 4a–c. Compounds 1 and 20 underwent heterocyclization upon their reaction with hydrazonoyl chloride 5 and gave the corresponding 1,3,4-thiadiazoles 8 and 22; however, the treatment of 1 and 20 with hydrazonoyl chloride 10 afforded the corresponding 1,3-thiazoles 14 and 25. The quantum calculations were studied using the density functional theory of the starting materials and some products.

**Keywords:** Pyridines; 1,3,4-thiadiazoles; 1,3-thiazoles; Molecular orbital calculations; Density functional theory.

### 177. A Facile Green Synthesis and Anti-Cancer Activity of Bis-Arylhydrazononitriles, Triazolo[5,1-C][1,2,4]Triazine, and 1,3,4-Thiadiazolines

Sobhy Mohamed Gomaa

*Heterocycles*, 87: 1109-1120 (2013) IF: 1.077

Coupling of 2-cyanoacetyl-1-methyl-1H-pyrrole (1) with diazonium salts of 1,4-benzenediamine (2), 2,6-dichlorobenzene-1,4-diamine (4), and benzidine (6) afforded bis arylhydrazononitriles 3, 5, and 7, respectively. Also, coupling of 1 with [1,2,4]triazole-3-diazonium sulfate (8) gave the respective [1,2,4]triazolo[5,1-c][1,2,4]triazine derivative 11. On the other hands, treatment of 2-[(1-methyl-1H-pyrrol-2-yl)carbonyl]-3-



mercapto-3-(phenylamino)acrylonitrile (12) with hydrazonoyl chlorides 13a-h in dioxane, in the presence of chitosan as eco-friendly heterogeneous basic catalyst, under microwave irradiation furnished 1,3,4-thiadiazolines 16a-h, incorporating pyrrole moiety. The anti-cancer activities of the synthesized products were determined against the colon carcinoma (HCT), human laryngeal carcinoma (Hep-2), human medulloblastoma (Daoy), human breast adenocarcinoma (MCF-7), and human colon adenocarcinoma (WiDr) cell lines.

**Keywords:** 1,3,4-Thiadiazolines; Triazolo [5,1-C] triazine; Coupling; Hydrazonoyl halides; Anticancer activity.

#### 178. Synthetic Utility of Ethylenethiosemicarbazide Synthesis and Anticancer Activity of 1,3-Thiazines and Thiazoles With Imidazole Moiety

Sobhi M. Gomha, Sayed M. Riyadh, Ikhlass M. Abbas and Mohammed A.

*Heterocycles*, 87: 341-356 (2013) IF: 1.077

Reactions of ethylenethiosemicarbazide **3** with DMAD **4** or substituted methylenemalononitriles **8** gave thiazolidin-4-one **6** or 1,3-thiazine derivatives (**10**, **11**), respectively. Also, treatment of **3** with hydrazonoyl halides 12a-i,  $\alpha$ -haloketones **15a-d**, and chloroacetic acid **18** afforded the corresponding arylazothiazoles **14a-i**, thiazoles **17a-d**, and thiazolin-4-one derivative **20**, respectively. The structures of the synthesized products were confirmed by IR,  $^1\text{H}$  NMR,  $^{13}\text{C}$  NMR and mass spectral techniques. The anticancer activity of the selected products against the colon carcinoma cell line (HCT-116) was determined and the results revealed promising activity of compound **6**.

**Keywords:** Ethylenethiosemicarbazide; 1,3-Thiazines; Thiazoles.

#### 179. 2-Keto-3-Mercaptocinchoninic Acids as Precursors for Novel Thiazino [6,5-C]Quinoline-1,5-Dione Derivatives

Nadia Hanafy Metwally

*Synthetic Communications*, 43: 398-405 (2013) IF: 1.06

2-Keto-3-mercaptocinchoninic acid derivatives 1a and b react with Schiff's bases 2a-d in toluene at refluxing temperature to give thiazino[6,5-c]quinoline derivatives 4a-h. Also, refluxing of 1a and b with arylazomalononitriles 5a-d in acetic acid afforded the thiazolo[6,5-c]quinoline derivatives 7a-d. The structure of all the newly synthesized products was confirmed based on elemental and spectral data.

**Keywords:** Arylazomalononitriles; 2-keto-3-mercaptocinchoninic acid Derivatives; Schiff'S Bases; Thiazino [6,5-C] quinoline derivatives.

#### 180. Design and Synthesis of Some New Pyrazolo[1,5-a]pyrimidines, Pyrazolo[5,1-c] Triazines, Pyrazolo[3,4-d]pyridazines, and Isoxazolo[3,4-d]pyridazines Containing the Pyrazole Moiety

Abdou O. Abdelhamid, Abdelgawad A. Fahmi and Karema N. M. Halim

*Synthetic Communications*, 43: 1101-1126 (2013) IF: 1.06

Pyrazolo[1,5-a]pyrimidines, pyrazolo[5,1-c]triazines, [1,2,4] triazolo [4,3-a]pyrimidine, [1,2,4]triazolo[3,4-c][1,2,4]triazine, pyrazolo[3,4-d]pyridazines, and isoxazolo[3,4-d]pyridazines were prepared from 3-(3-(dimethylamino)acryloyl)-1-aryl-5-diphenyl-1H-pyrazole-5-carbonitrile with each of hydrazonoyl halides, hydroximoyl chlorides, heterocyclic amines, and diazotized heterocyclic amines. All the newly synthesized compounds were confirmed by elemental analyses, spectral data, and alternative synthetic routes whenever possible.

**Keywords:** Isoxazolo [3,4-D] pyridazines; Pyrazolo[1,5-A] pyrimidines; Pyrazolo[3,4-D] pyridazines.

#### 181. Microwave-assisted Synthesis of 5-Arylbenzofuran- 2-Carboxylates Via Suzuki Coupling Using a 2-Quinolinealdoxime-Pd (II) -Complex

Kamal M. Dawood, Ahmad M. Farag, Moteaa M. El-Defar, Michael Gardiner and Hatem A. Abdelaziz

*Arkivoc*, (3): 210-226 (2013) IF: 1.057

A new quinoline-based Pd(II)-complex was synthesized and its structure was established by single crystal X-ray analysis. Applications of the obtained complex as a precatalyst in Suzuki-Miyaura C-C cross-coupling reactions of 4-bromoacetophenone and 5-bromobenzofuran-2-carboxylate esters with several aryl- and heteroarylboronic acids were investigated. The catalytic activity of the Pd(II)-precatalyst under microwave irradiating conditions was evaluated.

**Keywords:** Quinolines; Benzofurans; Palladium catalysis; Microwave; Suzuki reactions.

#### 182. Synthesis of New Functionalized Derivatives of 1,2,4-Triazolo[4',3':2,3][1,2,4]Triazino[5,6-b]Indole

Sobhi M. Gomha and Hatem A. Abdel-Aziz

*Journal of The Serbian Chemical Society*, 78: 1119-1125 (2013) IF: 0.912

New functionalized 1,2,4-triazolo[4',3':2,3][1,2,4]triazino[5,6-b] indole derivatives were synthesized via reaction of the hydrazonoyl halides with 2,4-dihydro-3H-1,2,4-triazino[5,6-b] indole-3-thione or its 3-methylthio derivative. The mechanism and the regioselectivity of the studied reactions are discussed.

**Keywords:** Hydrazonoyl Halides; 1,2,4-Triazino[5,6-b]Indole-3-Thione; Hydrazonothioates.

#### 183. A Novel Route to Isoquinoline[2,1-g][1,6] Naphthyridine, Pyrazolo[5,1-a] Isoquinoline and Pyridazino[40,50:3,4]Pyrazolo[5,1-a]Isoquinoline Derivatives with Evaluation of Antitumor Activities

Hamdi M. Hassaneen, Wagnat W. Wardkhan and Yasmin Sh. Mohammed

*Zeitschrift Für Naturforschung B*, 68b (2013): 895-904 (2013) IF: 0.899

(E) -2- Chloro-3- (2-cyanovinyl) -9,10- dimethoxy-4-oxo-6,7 dihydro-4H-pyrido[2,1- $\alpha$ ] isoquinoline-1-carbonitrile (**5**) was obtained by treatment of the 2-chloro-3-formylpyrido[2,1-

$\alpha$ ]isoquinoline derivative **3** with 2-(triphenylphosphoranylidene) acetonitrile (**4**). Treatment of **5** with sodium azide afforded the corresponding azido compound **6** which could be reduced by sodium dithionite to compound **7**. A novel isoquinolino[2,1-g][1,6]naphthyridine derivative **11** was obtained by the reaction of phenyl isothiocyanate with the phosphorane compound **8**, which was prepared by the reaction of compound **6** with triphenylphosphine. Treatment of **5** with amines **12a-c** and thiophenols **14a-c** in refluxing ethanol afforded the corresponding substitution products **13a-c** and **15a-c**, respectively. Also, the reaction of **1** with  $\alpha$ -oxo hydroxamoyl chlorides **16** was reinvestigated, and the synthesized pyrazoloisoquinolines **19a-f** and pyridazinopyrazoloisoquinolines **20a, e** were screened for their *in vitro* antitumor activities.

**Keywords:** Isoquinoline-1- acetonitrile; Naphthyridines; Pyrazoloisoquinolines; Pyridazinopyrazoloisoquinolines; Hydroxamoyl chlorides; Antitumor activity.

#### 184. New Synthetic Strategy for Novel 6-Arylazo-5-Methyl-3-Aryl-thiazolo [2,3-c]-[1,2,4]Triazoles and Study of their Solvatochromic Properties

Ahmad Sami Shawali and Mohie Eldin Moustafa Zayed

*Turkish Journal of Chemistry*, 37: 413-421 (2013) IF: 0.888

Two series of 6-arylazothiazol [2,3- c][1,2,4]triazoles were prepared via oxidative cyclization of the respective aldehyde N-(5-arylazo-4-methylthiazol-2-yl)-hydrazones. The structures of the latter hydrazone precursors and the azo compounds were confirmed by spectral and elemental analyses. The solvatochromism of the title azo dyes is evaluated by means of the Kamlet-Taft equation and discussed.

**Keywords:** Arylazoheterocycles; Thiazole; 1,5-electrocyclization; Solvatochromism; Hydrazonoyl halides 1.

#### 185. Simultaneous Removal of Aluminum, Iron, Copper, Zinc, and Lead from Aqueous Solution Using Raw and Chemically Treated African Beech Wood Sawdust

Nour El-deen Tawfik Abdel-Ghani, Ghadir A. El-Chaghaby and Farag S. Hela

*Desalination and Water Treatment*, 51: 3558-3575 (2013) IF: 0.852

The present study investigates the use of raw and chemically modified African beech sawdust for the simultaneous removal of aluminum, iron, copper, zinc, and lead from aqueous solution. Batch adsorption studies were carried out at different operational conditions including: contact time, solution pH, metal ions concentrations, and adsorbents loading weights. The adsorption reached its equilibrium after a contact time of 240 min. The point of pH zero charge was found to be between 4 and 6.5 for raw and chemically treated sawdust, respectively.

The spontaneous nature of the adsorption reaction was confirmed by the thermodynamic studies. The properties of the prepared adsorbents were characterized by TGA, FTIR, and SEM analysis. The kinetic and equilibrium studies suggested that the experimental data best fitted the pseudo-second-order kinetic and the Langmuir isotherm models, respectively. The recovery of the

adsorbed ions was successfully achieved using different desorption solutions.

**Keywords:** Adsorption; African beech; Langmuir; Pseudo-Second-Order Kinetic; Desorption.

#### 186. Intermolecular Interaction in the Benzene-Ar<sub>n</sub> and Benzene Dimer Van Der Waals Complexes: DFT Analysis of the Charge Distribution and Electric Response Properties

Rifaat H. Hilal, Walid M. I. Hassan, Abdulrahman Alyoubi, Saadullah G Aziz and Shabaan A. K. Elroby

*Indian Journal of Chemistry*, 52: 19-27 (2013) IF: 0.648

The performance of the DFT/B-97-D and ?B97-D methods to reproduce the isotropic non-bonded interaction and the electric response properties in the benzene-argon and the p-p interaction in the benzene dimer have been studied. The PES for the interaction of benzene and argon with all possible Ar<sub>n</sub>-benzene (n = 1, 2) conformations has been explored. Results indicate that the ?B97-XD method is capable of reproducing well positions and depths for the studied benzene-Ar and benzene-benzene clusters to a high degree of accuracy and compare well with the experimental and best benchmark calculations. Satisfactory results have also been obtained for the benzene-X (X = He, Ne and Kr) clusters. The features of the charge density distributions of the studied benzene-Ar van der Waal complexes have been analyzed by calculating the dipole and higher multipole moments and the static polarizability, its anisotropic part and the interaction polarizability. Trends and relationships to the dispersion interaction energy are suggested. Natural bond orbital analyses of the benzene-Ar<sub>n</sub> vdw complexes show clearly that all carbon valence orbitals are over-populated by about 21% at the expense of the hydrogen atoms valence orbitals. These data also indicate that argon behaves as electron donor in the Ar-benzene vdw complex, and hence, the slight positive charge on argon is at on the expense of its valence (non-bonding) p-orbitals.

**Keywords:** Theoretical chemistry; Density functional calculations, *Ab initio* calculations; Dispersion interactions; Van der waals clusters; Benzene-argon clusters; Benzene-benzene clusters.

#### 187. Substituted 4,5,6,7-Tetrahydroindoles and their Fused Derivatives. Synthesis and Cytotoxic Activity Towards Tumor and Normal Human Cell Lines

R. M. Mohareb and M. A. Abdelaziz

*Chemistry of Heterocyclic Compounds*, 49: 1212-1223 (2013) IF: 0.634

This work has been carried out to explore the reaction of 2-cyanoacetohydrazide with cyclohexanone to form 4,5,6,7-tetrahydroindole derivatives. 2-Hydroxy-4,5,6,7-tetrahydro-1H-indole-3-carbonitrile was used as the starting material for a series of novel heterocyclic products containing fused oxazine, pyran, pyrazole, pyridazine, and thiophene rings. The antitumor activity evaluation of the newly synthesized compounds against three human tumor cells lines, breast adenocarcinoma (MCF-7), non-small cell lung cancer (NCI-H460), and CNS cancer (SF-268), and with normal fibroblast cells (WI 38) showed that some of these compounds exhibit much higher inhibitory effects towards

the three tumor cell lines than the reference drug doxorubicin while being minimally active towards normal cells.

**Keywords:** Indoles; Pyrans; Pyrazoles; Thiophenes; Antitumor activity.

### 188. Synthesis and Applications of New Bifunctional Dyes Bis (Monochlorotriazine) Based on Tetrahydrobenzo[b] Thiophene Moiety

Fatma Ali Mohamed and Rafaat Melad Mohareb

*Pigment & Resin Technology*, 42: 264-270 (2013) IF: 0.616

The purpose of this paper is to synthesise, characterise and find out properties of some new bifunctional dyes bis (monochlorotriazine) using tetrahydrobenzo[b]thiophene systems as the chromophoric moiety, bearing good colour strength, lightfastness, and other favourable properties.

Design/methodology/approach – The novel reactive dyes were prepared, containing bis monochlorotriazine as reactive groups. The dye is synthesised by diazotization and coupling reactions. Firstly the authors synthesised the ethyl 2-amino 4,5,6,7-tetrahydrobenzo[b]thiophen-3-carboxylate chromophoric moiety compound which in turn underwent diazotization and coupling then diazotized and coupled reaction with either 1-amino-8-naphthol-3,6-disulphonic acid (H-acid) and or 2-amino-8-naphthol-6-sulphonic (g acid) to give the monoazo dye intermediates compounds. The latter products reacted with 2,4,6-trichloro-1,3,5-triazine in 1:1 molar ratio afforded, via nucleophilic displacement when subjected to condensation 2,4,6-trichloro-1,3,5-triazine in 1:1 molar ratio afforded via nucleophilic displacement, which reacted with 1,4-phenylenediamine in 2:1 molar ratio to give reaction with the 1,4-phenylenediamine in 2:1 molar ratio, the bisazobifunctional bismonochlorotriazine reactive dyes. bisazo bifunctional bismonochlorotriazine reactive dyes thus yielding the new target reactive. The synthesised dyes were applied onto cotton fabric under the typical exhaust dyeing conditions and their dyeing properties were investigated. Findings – The results assessed for dyeing indicate high quality dyeing properties. However, the homobifunctional (bis MCT) dyes showed higher exhaustion and fixation values, colour yield and fastness properties.

Practical implications – The described method showed the synthesis of bis monochlorotriazines derived from the tetrahydrobenzo[b]thiophene derivative 3 followed by their application towards cotton fabric.

Social implications – Social implications are to prepare new reactive dyes having higher fastness and uses for dyeing cotton which is the commonest fabric use.

**Keywords:** Reactive dyes; Cyclohexanone; Bismonochlorotriazine; Tetrahydrobenzo [B]Thiophene; Dyeing; Cotton fabric; Dyes; Cotton.

### 189. A Convenient Synthesis of Some New Thiazole and Pyrimidine Derivatives Incorporating a Naphthalene Moiety

Sobhi M. Gomhaa and Mohamed G. Badrey

*Journal of Chemical Research*, 2: 86-90 (2013) IF: 0.596

The reaction of 2-[1-(naphthalen-2-yl) ethylidene] hydrazinecarbothioamide with hydrazonoyl halides afforded new

thiazole derivatives, whilst reaction with compounds containing an activated double bond such as ethoxymethylenemalononitrile and benzylidenemalononitrile yielded the respective pyrimidine derivatives. A 4-thiazolidin-4-one was obtained by reaction of the hydrazinecarbothioamide with ethyl bromoacetate. Subsequent condensation of the thiazolidinone with aromatic aldehydes afforded the corresponding arylidene derivatives. Treatment of the hydrazinecarbothioamide with dimethyl acetylenedicarboxylate resulted in the formation of a (methoxycarbonylmethylidene) thiazolinone. Reaction of the hydrazinecarbothioamide with 2-chloro-1,3-dicarbonyl compounds gave the respective thiazole derivatives. The structures of the newly synthesised compounds were confirmed by their elemental analysis and spectral data.

**Keywords:** Thiazoles; Thiosemicarbazide; Hydrazonoyl halides.

### 190. An Efficient Synthesis of Functionalised 2-(Heteroaryl)-3H-Benzo [f] Chromen-3-Ones and Antibacterial Evaluation

Sobhi M. Gomhaa and Hassan M. Abdel-Aziz

*Journal of Chemical Research*, 5: 298-303 (2013) IF: 0.596

An efficient synthesis of 19 2-(heteroaryl)-3H-benzo[f]chromen-3-ones is described via reaction of 2-(3-hydroxyacryloyl)-3H-benzo[f]chromen-3-one with various heterocyclic amines and active methylene compounds. The synthesized compounds, 18 of which are novel, were characterised on the basis of their elemental analysis and spectral data. Eight of the synthesised products were evaluated as antibacterial agents.

**Keywords:** 2-acetyl-3H-benzo[f]chromen-3-one; Pyrazolopyrimidines; Triazolopyrimidines; Tetrazolopyrimidines; Pyrimidopyrimidines.

### 191. Synthesis and Tautomeric Structure of 3,7-Bis (Arylazo)-2,6-Dimethyl-1H- Imidazo[ 1,2-b] Pyrazoles

Ahmad Sami Shawali, Magda A. Abdallah, Mohamed R. Shehata and Mohamed Kandil

*Journal of Chemical Research*, 37: 128-131 (2013) IF: 0.596

Three series of 3,7-bis(arylazo)-2,6-dimethyl-1H-imidazo[1,2-b] pyrazoles were prepared starting from N-aryl-2-oxopropanehydrazonoyl chlorides. The acid dissociation constants pKa were determined and correlated with the Hammett equation. The results of such correlations together with the spectroscopic data indicated that the title compounds exist predominantly in the 1H-bis (arylazo) form.

**Keywords:** Hydrazonoyl halides; Azo compounds; Pyrazoles; Imidazo [1,2-b] pyrazoles.

### 192. Effect of as, Cu and Sb Impurities on Performance of Pb-Ca-Sn Grids of Lead-Acid Batteries

A. G. Gad-Allah, S. A. Salih, A. A. Mokhtar and H. A. Abd El-Rahman

*Material Wissenschaft Und Werkstoff Technik*, 44(10): 832-838 (2013) IF: 0.505

The performance of Pb-ca-Sn grids of lead acid batteries made from recycled lead in 4M H<sub>2</sub>SO<sub>4</sub> in the absence and presence of traces of Cu, As and Sb as potential impurities in the recycling process at 0.1% level is investigated by electrochemical methods. the study includes the effect of each impurity and impurities combined on the alloy corrodibility, the efficiency of PbO<sub>2</sub> formation, the rate of the self discharge and the hydrogen evolution reaction (HER) and oxygen evolution reaction (OER). the results show that individual impurity enhances the corrosion resistance but increases the anode corrosion and the self discharge rate. Impurities play opposite effect on hydrogen evolution reaction and oxygen evolution reaction either individually or combined. Concerning water loss problem, the harmful effect of individual impurity on increasing oxygen evolution reaction is compensated by their suppression of hydrogen evolution reaction, the impurities combined suppress effectively both hydrogen evolution reaction and oxygen evolution reaction relative to alloy without any impurity. Sb has the highest harmful effects on oxygen evolution reaction and the self discharge but it is the best in the suppression of hydrogen evolution reaction. the impurities combined relatively improve the general corrosion resistance, the anodic corrosion resistance and self discharge. The study supports higher tolerance levels of Cu, As and Sb in Pb-ca-Sn grids, especially when present combined than the recommended levels in the industry standards.

**Keywords:** Pb-Ca-Sn Alloys; Lead acid batteries; Acid corrosion; Recycled lead.

### 193. Synthesis and Spectroscopic Characterization of Indomethacin–Cd (II), Ce (III), and Th (IV) Complexes: IR, <sup>1</sup>H NMR, Thermal, and Biological Studies

Moamen S. Refat, Gehad G. Mohamed, Mohamed Y. S. Ibrahim, Hamada M. A. Killa and Hammad Fetooh

*Russian Journal of General Chemistry*, 83(12): 2479-2487 (2013) IF: 0.432

Solid complexes have been prepared and characterized by IR, UV-Vis, elemental analysis, and <sup>1</sup>H NMR. Indomethacin forms complexes with Cd(II), Ce(III), and Th(IV) ions in molar ratios (ligand : metal) (2 : 1), (3 : 1), and (4 : 1), respectively. The IR spectra of the complexes suggest that the Indomethacin behaves as a monobasic monodentate ligand coordinated to the metal ions via the deprotonated carboxylate group. Prepared complexes exhibit higher antimicrobial activity against several microorganisms, compared to free ligand.

**Keywords:** Charge transfer complexes; Indomethacin; Spectroscopy.

### 194. Spectrophotometric Determination of Sildenafil Citrate Drug in Tablets. Spectroscopic Characterization of the Solid Charge Transfer Complexes

M.S. Refat, G.G. Mohamed and A. Fathi

*Bulgarian Chemical Communications*, 2: 250-262 (2013) IF: 0.32

The purpose of this study is to propose sensitive, accurate and reproducible methods for the determination of sildenafil citrate in pure pharmaceutical preparations. Sildenafil citrate is determined

spectrophotometrically via charge-transfer complex formation. This includes the use of some  $\pi$ -acceptors as 2,3-dichloro-5,6-dicyano-p-benzoquinone (DDQ) and 3,6-dichloro-2,5-dihydroxy-p-benzoquinone (p-CLA). The proposed methods can be used for routine analysis of the suggested drugs in pharmaceutical preparations. The solid ions of the CT complexes from the reaction of DDQ and p-CLA as  $\pi$ -acceptors with sildenafil citrate as donor are isolated and the formed CT complexes are characterized via elemental analyses, IR, <sup>1</sup>H NMR and mass spectrometric studies.

**Keywords:** Sildenafil citrate; DDQ; p-CLA; Spectrophotometry; Charge transfer complexes.

### 195. Electrochemical Performance of Grids of Lead-Acid Batteries Made from Pb-0.8%Ca-1.1%Sn Alloys Containing Cu, as and Sb Impurities in the Presence of Phosphoric Acid

H.A. Abd El-Rahman, A.G. Gad-Allah, S.A. Salih and A. M. Abd El-Wahab

*Afinidad*, 70 (564): 295-304 (2013) IF: 0.145

Electrochemical performance of grids of lead-acid batteries manufactured from Pb-0.8%Ca-1.1%Sn alloys containing Cu, As and Sb impurities at 0.1 wt% level were studied in 4.0 M H<sub>2</sub>SO<sub>4</sub> without and with 0.4 M H<sub>3</sub>PO<sub>4</sub>. The presence of impurities in the alloy or addition of H<sub>3</sub>PO<sub>4</sub> was found to suppress the corrosion rate. H<sub>3</sub>PO<sub>4</sub> increased the rates of both hydrogen and oxygen evolution reactions at high overpotentials for all alloys. Except for Cu-containing alloy, H<sub>3</sub>PO<sub>4</sub> had a slight positive effect on PbO<sub>2</sub> formation.

The self-discharge of PbO<sub>2</sub> under polarization or opencircuit conditions increased in the presence of H<sub>3</sub>PO<sub>4</sub> but the positive grid corrosion decreased, except for the As-containing alloy. Impurity-containing alloys showed significantly lower self-discharge rate in the presence of H<sub>3</sub>PO<sub>4</sub> than in its absence. Impedance measurement was able to detect and quantify the formation of the highly insulating inner PbO layer beneath the outer PbSO<sub>4</sub> layer and its transformation to the conducting PbO<sub>2</sub>, during the oxidation of alloys under constant current conditions. H<sub>3</sub>PO<sub>4</sub> significantly enhanced the formation of PbO in the presence of impurities, especially Sb.

**Keywords:** Pb-Ca-Sn Alloys; Lead-acid batteries; Recycled lead; Phosphoric acid.

### 196. Sensitive and Selective Extractive Determination of Citalopram Hydrobromide in Pure Solutions, Pharmaceutical Dosage Form and Urine Samples

Nour El-deen T. Abdel-Ghani, M. S. Rizk and M. Mostafa

*Analytical Chemistry an Indian Journal*, 12 (9): 338-346 (2013)

Simple, rapid, sensitive, precise and accurate spectrophotometric methods for the determination of antidepressant drug CitalopramHydrobromide (C-HBr) in bulk samples, dosage form and in spiked urine samples were investigated. The methods are based on the formation of a yellow colored ion-associates due to the interaction between the examined drug (C-HBr)withPicric acid (PA),Bactophenol red (BPR),Alizarin red (AR), Bromothymol blue (BTB) reagents. A buffer solution had been



used and the extraction was carried out using chloroform, the ion associates exhibit absorption maxima at 410, 403, 432 and 415 nm for PA, BPR, AR and BTB respectively. (C-HBr) can be determined up to 35, 58, 85 and 40  $\mu\text{g mL}^{-1}$ , respectively.

The optimum reaction conditions for quantitative analysis were investigated. In addition the molar absorptivity, Sandell sensitivity was determined for the investigated drug. The correlation coefficient was  $\geq 0.995$  ( $n=6$ ) with a relative standard deviation (RSD)  $\leq 1.15$  for five selected concentrations of the reagents. Therefore the concentration of C-HBr drug in its pharmaceutical formulations and spiked urine samples had been determined successfully.

**Keywords:** Citalopram hydrobromide; Bactrophenol red; Bromothymol blue; Alizarin red; Picric acid.

### 197. A Convenient Route for Synthesis of New Benzimidazole-Based Heterocycles

Taha Mohammed Abdallah Eldebss and Ahmad Mahmoud Farag

*Iranian Journal of Organic Chemistry*, 5 (2): 1005-1013 (2013)

Reaction of 2-bromo-1-(1-methyl-1H-benzo[d]imidazole-2-yl) ethanone (1) with dimethylsulfide afforded the corresponding sulfonium bromide derivative 2. Coupling of compound 2 with diazotized aromatic amines or with the corresponding N-nitrosoacetanilide derivatives afforded the corresponding hydrazoneyl bromides derivatives 5a-c in good yields. Reaction of 2-bromo-1-(1-methyl-1H-benzo[d]imidazole-2-yl) ethanone (1) with potassium thiocyanate afforded the corresponding 1-(1-methyl-1H-benzo[d]imidazole-2-yl)-2-thiocyanatoethanone (6) that reacts with diazotized aromatic amines or with the corresponding N-nitrosoacetanilide derivatives to afford the corresponding iminothiadiazole derivatives 8a-c. Compounds 8a-c were converted into the corresponding N-acetylthiadiazole, N-nitrosothiadiazole, and thiadiazolone derivatives 9a-c, 10a-c and 11a-c, respectively upon treatment with acetyl chloride, sodium nitrite in presence of acetic acid and refluxing in ethanolic HCl respectively. Reaction of compound 6 with aromatic amines afforded the corresponding arylaminothiazole derivatives 14a-c. Coupling of compound 6 with diazotized anthranilic acid (or methyl anthranilate) and with diazotized anthranilonitrile afforded the corresponding thiadiazolo [3,2-a] quinazoline imine derivative 21a and thiadiazolo [3,2-a] quinazolinone derivative 21b, respectively.

**Keywords:** Benzimidazole; Thiadiazole; Thiazole; Thiadiazolo [3,2-a] quinazoline; Oxazole.

### 198. A Facile Synthesis of Pyrido[2',3':3,4] Pyrazolo [1,5-a]Pyrimidine and Pyrido[2',3':3,4]Pyrazolo[5,1-c][1,2,4]Triazine Bearing A Thiophene Moiety

Tilal Elsaman, Mohamed Fares, Hatem A. Abdel-Aziz, Mohamed I. Attia, Hazem A. Ghabbour and Kamal M. Dawood

*Journal of Chemistry*, 2013; 1-7: (2013)

Pyridinone derivative 8 was synthesized and transformed into the respective chloropyridine 9, which was allowed to react with hydrazine hydrate to afford pyrazolo[3,4-b] pyridin-3-amine derivative 11. Compound 11 was used as a key intermediate for a facile synthesis of the title compounds 14, 15, 17, 21a,b, and 24a-c where the reaction of 11 with some 1,3-dielectrophiles resulted

in the formation of pyrido[2',3':3,4]pyrazolo[1,5-a]pyrimidines 14, 15, and 17, whereas diazotization of compound 11 gave the respective diazonium salt 18 which was coupled with some active methylene-containing compounds to give the corresponding hydrazones 19a,b and 22a-c. Cyclization of the latter hydrazones yielded the pyrido[2',3':3,4]pyrazolo[5,1-c][1,2,4]triazines 21a,b and 24a-c, respectively.

**Keywords:** Thiophene; Pyridones; Pyrazolo [3,4-b] pyridines; Hydrazones; Cyclization.

### 199. Ab Initio Density Functional Theory Investigation of the Interaction between Carbon Nanotubes and Water Molecules during Water Desalination Process

Loay A. Elalfy, Walid M. I. Hassan and Wael N. Akl

*Journal of Chemistry*, 813592: 1-6 (2013)

Density functional theory calculations using B3LYP/3-21G level of theory have been implemented on 6 carbon nanotubes (CNTs) structures (3 zigzag and 3 armchair CNTs) to study the energetics of the reverse osmosis during water desalination process. Calculations of the band gap, interaction energy, highest occupied molecular orbital, lowest unoccupied molecular orbital, electronegativity, hardness, and pressure of the system are discussed. The calculations showed that the water molecule that exists inside the CNT is about 2-3 Å away from its wall. The calculations have proven that the zigzag CNTs are more efficient for reverse osmosis water desalination process than armchair CNTs as the reverse osmosis process requires pressure of approximately 200 MPa for armchair CNTs, which is consistent with the values used in molecular dynamics simulations, while that needed when using zigzag CNTs was in the order of 60 MPa.

**Keywords:** Ab initio density functional theory.

### 200. Biochemical Studies on the Effect of Nano Particles of Some Nutrients on Apoptosis Modulation of Breast Cancer Cells in Experimental Animals

Afaf Ezzat, Abdou O. Abdelhamid, A. I. Amin, Amal S. Abd El Azeem, Mohamed F. R. Fouda and Dina M. Mohammed

*Journal of Applied Sciences Research*, 9 (1): 658-665 (2013)

The effect of alternative compounds of some nano nutrients, their potential to induce apoptosis in breast cancer cells and the inhibitory effect of nano particles on development of induce toxic material of mammary tumor in experimental animals were studied. Experimental animals in this study include (42 rats) which induced breast cancer by injected a single dose of MNU intraperitoneally. Two weeks after MNU treatment, a time by which the animals had recovered from MNU-induced toxicity, the rats were divided into 7 groups (6 for each). A group of injected animals fed on the basal synthetic diet that served as control. Injected animals (6 groups) fed on the basal synthetic diet supplemented with nano particles nutrients (ascorbic acid, folic acid, methionine and niacin) group of (I), or with nano curcumin (group II), or with nano green tea (group III) or with nano yeast (group IV). Groups of (V) and (VI) fed on the basal synthetic diet supplemented with nano curcumin or yeast. At the end of experiments (6 months), apoptosis, TNF, total antioxidants, lipid peroxidation, folic acid, B12 and vitamin C were determined. The

results of nano-nutrients and their impact on biochemical parameters showed high levels of vitamin C in all groups except for a group of (I and II) which observed by low levels of total antioxidants.

Also observed increasing level of folic acid and B12 in most groups especially a group of (V and VI) a source of curcumin and yeast. Groups (III and VI) which containing yeast were appeared rise in level of TNF in a group of (III) as well as a group of (VI) as well to increase level of apoptosis in the same group. The nano yeast as a natural source of vitamin B complex may be gave best result because it might have helped retention the cell folic acid and B12 contrary what happened in other the nano treatment groups compared with normal treatments.

**Keywords:** Rats; Apoptosis; Breast cancer; Nano particles; Nutrients; Mammary tumor.

### 201. Chemically Modified Carbon Paste Sensor for Potentiometric Determination of Doxycycline Hydrochloride in Batch and FIA Conditions

Y. M. Issa, H. M. Abdel-Fattah and N. B. Abdel-Moniem

*Int. J. Electrochem. Sci.*, 8: 9578 -9592 (2013)

The utility of carbon paste electrode for the determination of doxycycline HCl modified with doxycycline-tetraphenylborate ion-pair (in both batch and flow injection analysis (FIA) modes) is demonstrated. The electrode revealed a Nernstian response over a wide concentration range ( $1.99 \times 10^{-5}$  -  $3.19 \times 10^{-3}$  mol L<sup>-1</sup>). The detection limit of this sensor is  $1.33 \times 10^{-5}$  mol L<sup>-1</sup>. The best performance was obtained with carbon paste composition of 3% doxycycline-tetraphenylborate, 48.5% graphite and 48.5% dibutyl phthalate (DBP).

The sensor exhibits a very fast response time (9 s) and good selectivity in presence of inorganic cations, sugars and aminoacids. The proposed sensor shows a great improvement in comparison with other previously reported sensors. The sensor was successfully applied to monitoring of doxycycline in pure solution and pharmaceutical formulation (vibramycin and farcodoxin capsules) with recovery ranges from 97.30 - 105.37% and coefficient of variation from 0.54 to 2.40%.

**Keywords:** Doxycycline; Carbon paste electrode; Potentiometry.

### 202. Cytotoxicity of Novel 4,5,6,7-Tetrahydrobenzo [b]Thiophene Derivatives and their Uses as Anti-Leishmanial Agents

Rafat M. Mohareb and Abdelgawad A. Fahmy

*Eur. Chem. Bull.*, 2: 545-553 (2013)

This work has been carried out to investigate some reactions of 4,5,6,7-tetrahydrobenzo[b]thiophene derivatives 1a,b to give synthesis a series of novel heterocyclic products like N-ethoxymethino derivatives (2a, 2b), N-phenylaminomethino derivatives (3a, 3b), hydrazine derivatives (5a-d), pyrazole derivatives (7a-d, 10a-d, 11a, 11b) and N-methinonitrilo derivatives (9a-d). The antitumor evaluation of the newly synthesized compounds against the three human tumor cells lines namely breast adenocarcinoma (MCF-7), non-small cell lung cancer (NCI-H460) and CNS cancer (SF-268) showed that some of these compounds exhibit much higher inhibitory effects towards the three tumor cell lines than the positive control

doxorubicin. Moreover, they were tested against normal cells namely diploid normal human fibroblast (WI-38), Normal prostate epithelial cells (PrEC) and normal human mucosal epithelial cells (NCM 460). The anti-leishmanial evaluations of the obtained compounds were also performed. Compounds 7d and 10b were the most active towards tumor cell lines while compounds 3a, 3b, 9b and 9d were the most active compounds as anti-leishmanial. Docking of these most active compounds was demonstrated.

**Keywords:** Tetrahydrobenzo [b] thiophene; Pyrazole; Human tumor cell lines; Normal cell lines; Anti-leishmanial agents.

### 203. Ecofriendly Regioselective One-Pot Synthesis of Chromeno [4,3-d][1,2,4] Triazolo[4,3-a] Pyrimidine Derivatives

Sobhi Mohamed Gomha and Mohamed Gomaa Badrey

*European Journal of Chemistry*, 4: 180-184 (2013)

methylthio derivative (7) with hydrazonoyl halides (2) in dioxane under ultrasound irradiation in the presence of chitosan yielded chromeno[4,3-d][1,2,4]triazolo[4,3-a]pyrimidine derivatives (5a-r). On the other hand, the reaction of compound 1 with the appropriate active chloromethylene compounds (9b, h and m) followed by coupling the products with benzenediazonium chloride afforded the azo coupling products which converted in situ to compound 5.

The reaction mechanism was proposed and the structure of the newly synthesized compounds were established on the basis of spectral data (Mass, IR, <sup>1</sup>H and <sup>13</sup>C NMR) and elemental analyses.

**Keywords:** Chitosan; Hydrazonoyl halides; Ultrasound irradiation; Active chloromethylene; Benzopyranopyrimidine; Chromeno [4,3-D] [1,2,4] triazolo[4,3-A] pyrimidine.

### 204. Efficient Catalytic Synthesis, Characterization and Antimicrobial Evaluation of 1,4-Bis(6-Substituted-7-(2-Arylhydrazono)-7H-[1,2,4]Triazolo [3,4-B][1,3,4]Thiadiazin-3-Yl)Benzene Derivatives Using Chitosan

Sobhy M. Gomaa

*International Journal of Pharmacy and Pharmaceutical Sciences*, 5 (2): 42-45 (2013)

The reaction of 5, 5'-(1, 4-phenylene)bis(4-amino-3-mercapto-4H-1,2,4-triazole) 1 with hydrazonoyl halides 2A,B gave a new series of 1,4-bis (6-substituted-7- (2-arylhydrazono) -7H-[1,2,4] triazolo[3,4-b][1,3,4]thiadiazin-3-yl)benzene derivatives 4a-j. An alternate method to synthesize 4a-j was described. The structures of new compounds 4a-j were established on the basis of their elemental analysis and IR, <sup>1</sup>H NMR, [<sup>13</sup>C NMR and mass spectral data. All the title compounds were evaluated for their in vitro antimicrobial activity. All the compounds exhibited moderate to significant antibacterial and antifungal activities.

**Keywords:** Triazolo [3,4-B][1,3,4] thiadiazines; Hydrazonoyl halides; Antimicrobial activities.

## 205. Efficient Syntheses of Some New Pyridine Based Heterocycles

Ahmad M. Farag, Nabila A. Kheder and Kamal M. Dawood

*International Journal of Modern Organic Chemistry*, 2(1): 26-39 (2013)

A facile and convenient synthesis of a series of 1,2,4-triazolo[5,1-c][1,2,4]triazine, 1,3,4-thiadiazole, thiazolidine, and pyrido[1,2-a]pyrimidine derivatives incorporating pyridine moiety via the versatile, readily accessible 2-cyano-N-(pyrid-2-yl)acetamide are described.

**Keywords:** Pyridine; 1,2,4-triazolo[5,1-c][1,2,4]triazine; 1,3,4-Thiadiazole; Thiazolidine; Pyrido[1,2-a] pyrimidine.

## 206. Electrochemical Behavior of Maraging Steel in Chloride Containing Environment

Fakiha El-Taib Heakal, G. A. El-Mahdy, M. M. Hegazy, Hussam E. Mahmoud, A. M. Fathy and F. M. Sayed

*International Journal of Electrochemical Science*, 8 (2): 2816-2825 (2013) IF: 3.729

Electrochemical behavior of aged and solution treated maraging steel have been investigated, in NaCl using open circuit potential (OCP) and potentiodynamics measurements. OCP shifts to more noble value during initial stage of immersion followed by slow shift in potential during the middle stage of immersion and eventually attain a steady state of potential during the last stage of monitoring. Various properties, such as, mechanical properties and corrosion resistance were investigated for aged and solution treated steel. Aging the maraging steel improving the mechanical properties and enhances the corrosion process. Maraging steel exhibits better passivity during polarization at low NaCl concentration and the passive region is broader than at higher concentration.

**Keywords:** Maraging steel; Polarization; Open circuit potential; Tensile properties.

## 207. Electrochemical Behavior of Titanium in Saline Media Containing Alga Dunaliella Salina and Its Secretions

Fakiha El-Taib Heakal, M. M. Hefny and A. M. Abd El-Tawab

*International Journal of Electrochemical Science*, 8 (4): 4610-4630 (2013)

The present work shows how to make use of cell biology in corrosion control of technical titanium in highly saline solutions. Besides, it opens the door towards correlating cell secretions with corrosion parameters when live cells are adsorbed on the surface. Generally, the corrosion current density ( $j_{\text{corr}}$ ,  $\mu\text{A}/\text{cm}^2$ ) decreases in media containing alga Dunaliella Salina over the density range of  $\rho_c = 0.1-1.0 \times 10^5$  cell/ml and then appears to approach a stabilized value. Results on the effect of glycerol and  $\beta$ -carotene secreted by the alga revealed that glycerol has no effect on the corrosion performance of technical titanium, while  $\beta$ -carotene can effectively mitigate the dissolution process of the sample. The increase in the total resistance ( $R_t/\Omega \text{ cm}^2$ ) of the film assigns the inhibition extent due to sealing effect of the surface by  $\beta$ -carotene

molecules and hence higher corrosion resistance for titanium. The inhibition mechanism is likely occurred via physical adsorption on the electrode surface following Temkin isotherm. This mostly happens through the conjugate system of the double bonds in the inhibitor molecular formula. Effect of pH of sulfate solution on the degree of surface coverage by  $\beta$ -carotene indicated that a maximum inhibition efficiency of  $\sim 90\%$  is achieved at pH around 7.0.

**Keywords:** Technical titanium; Alga dunaliella salina;  $\beta$ -carotene; EIS; Neutral and acidic corrosion.

## 208. Electrochemical Study and Biological Activity of AZ91E Alloy in Hank's Solution

Wafaa M. Hosny and M. A. Ameer

*International Journal of Electrochemical Science*, 8: 8371-8387 (2013)

The electrochemical behavior of AZ91E alloy was investigated in Hank's solution at 37°C. The behavior of the alloy was studied with immersion time by using electrochemical impedance spectroscopy (EIS) and potentiodynamic tests. Also, the effect of adding different concentrations of a commercial drug, known as salicylhydroxamic acid (Sham), as inhibitor, in Hank's solution was studied. The corrosion was inhibited by addition of salicylhydroxamic acid that reacts with AZ91E alloy and forms a protective film on the surface at different concentration (0.01-1mM). The results were confirmed by surface examination via scanning electron microscope. The stability constant values of the binary complexes between salicylhydroxamic acid and metal ions Mg(II), Al(III) and Zn(II) formed in solution were investigated potentiometrically. The antimicrobial activity of these complexes has been screened against two Gram-positive and two Gram-negative bacteria and other bacteria. Antifungal activity against two different fungi has been evaluated and compared with reference drug.

**Keywords:** AZ91E Alloy; EIS; Potentiodynamic; SEM; Hank'S solution; Biological activity.

## 209. Equilibrium Study and Biological Activity of Cu (II) With Polyvinyl Alcohol (PVA) and Some Amino Acids and DNA

Perihan A. Khalaf-Alaa and Wafaa M. Hosny

*Journal of Advances in Chemistry*, 3 (3): 264-277 (2013)

This study presents the acid-base equilibrium of polyvinyl alcohol (PVA). The stability constant values of the binary and ternary complexes formed in solution among polyvinyl alcohol, Cu(II), some amino acids and DNA were determined potentiometrically. The stability constants of the complexes are determined and the concentration distribution diagrams of the complexes are evaluated. The ligand and their metal chelates have been screened for their antimicrobial activities using the disc diffusion method against the selected bacteria and fungi. Binary and ternary complexes of copper (II) involving polyvinyl alcohol (PVA) and various biologically relevant ligands containing different functional groups, were investigated. The ligands (L) are amino acids and DNA constituents. The ternary complexes of amino acids and DNA are formed by simultaneous and stepwise reactions respectively.

The results showed the formation of Cu (PVA) (L) complexes with amino acids and DNA. Amino acids form both Cu (PVA) (L) complexes and the corresponding protonated Cu (PVA) (LH) and deprotonated species Cu (PVA) (LH<sub>1</sub>). The ternary complexes of copper (II) with (PVA) and DNA are formed in a 1stepwise process, whereby binding of copper (II) to (PVA) is followed by ligation of the DNA components. DNA constituents form 1:1 complexes with Cu (PVA). The stability of these ternary complexes was quantitatively compared with their corresponding binary complexes in terms of the parameter  $\Delta \log_{10} K$ . The values of  $\Delta \log_{10} K$  indicate that the ternary complexes containing aromatic amino 1010acids were significantly more stable than the complexes containing alkyl- and hydroxyl alkyl substituted amino acids. The concentration distribution of various complex species formed in solution was also evaluated as a function of pH. The antimicrobial activities using the disc diffusion method against some selected bacteria and fungi. The activity data show that the metal complexes are found to have antibacterial and antifungal activity.

**Keywords:** Copper (II); PVA; Amino acids; DNA constituents; Stability constant.

## 210. Evaluation of New, Triazoloisoquinoline and Pyrazolopyridazine Compounds Against the Desert Locust *Schistocerca Gregaria* (Orthoptera: Acridiidae)

Hamdy M. Hassanain and Mamdouh I. Nassar

*International Journal of Entomological Research*, 1 (1): 42-47 (2013)

The present study deals with the bioactivities of 3-Acetyl [1,2,4]triazolo[3,4-*a*] isoquinoline was used to prepare a novel enaminone 5. Reactions of 5 with hydrazonoyl halides 6 gave triazoloisoquinolines 10 with a carbonylpyrazole as a side chain. Hydrazinolysis of 10 gave the pyrazolopyridazines 12. Bioactivity of these compounds was applied on 4th nymphal instar of the desert locust *Schistocerca gregaria*. Results clearly showed that the compound 12b was the most effective against 4<sup>th</sup> nymphal instars, while the compound 12a has the lowest effect. Meanwhile the chemical compounds, 10b and 10a were intermediate bioactive. In order of toxicity the lethal concentration was 0.31, 0.37, 0.46, and 0.57 of the chemical compounds 12b, 10b, 10a and 12a respectively. On the other hand some deformation of the treated nymphs was observed by the effect of different chemical compounds due to molting inhibition for the next stages.

**Keywords:** [1,2,4] Triazolo [3,4-*a*] isoquinolines; Enaminones; Hydrazinolysis; Hydrazonoyl chlorides; Cycloaddition reactions; Bioactivities study; Desert locust; *Schistocerca gregaria*.

## 211. In Situ Modified Screen Printed and Carbon Paste Ion Selective Electrodes for Potentiometric Determination of Naphazoline Hydrochloride in its Formulation

Gehad G. Mohamed, F. A. Nour El-Dien, Eman Y. Z. Frag and Marwa El-Badry Mohamed

*Journal of Pharmaceutical Analysis*, 3(5): 367-375 (2013)

The construction and performance characteristics of new sensitive and selective in situ modified screen printed (ISPE) and carbon

paste (ICPE) electrodes for determination of naphazoline hydrochloride (NPZ-HCl) have been developed. The electrodes under investigation show potentiometric response for NPZ-HCl in the concentration range from  $7.0 \times 10^{-7}$  to  $1.0 \times 10^{-2}$  M at 25 °C and the electrode response is independent of pH in the range of 3.1–7.9. These sensors have slope values of  $59.7 \pm 0.6$  and  $59.2 \pm 0.2$  mV decade<sup>-1</sup> with detection limit values of  $5.6 \times 10^{-7}$  and  $5.9 \times 10^{-7}$  M NPZ-HCl using ISPE and ICPE, respectively. These electrodes show fast response time of 4–7 s and 5–8 s and exhibits lifetimes of 28 and 30 days for ISPE and ICPE, respectively. Selectivity for NPZ-HCl with respect to a number of interfering materials was also investigated. It was found that there is no interference from the investigated inorganic cations, anions, sugars and other pharmaceutical excipients. The proposed sensors were applied for the determination of NPZ-HCl in pharmaceutical formulation using the direct potentiometric method. It showed a mean average recovery of 100.2% and 102.6% for ISPE and ICPE, respectively. The obtained results using the proposed sensors were in good agreement with those obtained using the official method. The proposed sensors show significantly high selectivity, response time, accuracy, precision, limit of detection (LOD) and limit of quantification (LOQ) compared with other proposed methods.

**Keywords:** ISPE and ICPE; Potentiometry; Naphazoline hydrochloride; Eye drops.

## 212. In-Vitro Antimicrobial and Antifungal Activity of Pyrimidine and Pyrazolo-[1, 5-a] Pyrimidine

Christina Y. Ishak, Nadia H. Metwally and Hajir Ibrahim Wahbi

*International Journal of Pharmaceutical and Phytopharmacological Research (EIJPPR)*, 2: 407-411 (2013)

In the present study, we have carried out the synthesis of pyrazolo-[1, 5-a] pyrimidine and pyrimidine derivatives and were investigated for their in vitro antimicrobial and antifungal activities. The results revealed that some of tested compounds possess potent antimicrobial and anti-fungal activities.

**Keywords:** Hetaryl chalcones; Pyrazolo [1, 5-a] pyrimidine; Pyrimidine; Antimicrobial and anti-fungal activities.

## 213. Isolation and Structure Elucidation of Acetyl Cholinesterase Inhibitor from *Gyrostoma Helianthus* of the Red Sea, Egypt

M. N. Gomaa, A. M. Farag, A. M. Ayesh and M. A. Embaby

*Middle-East Journal of Scientific Research*, 14: 1569-1575 (2013)

The present study was carried out to isolate, purify and elucidate the structure of low molecular weight bioactive compounds from sea anemone, *Gyrostoma helianthus* of the Red Sea environment. The obtained results indicated that the ethanolic crude extract of the sea anemone, *Gyrostoma helianthus* showed inhibition activity against acetylcholinesterase (AChE). The 0.5kD fraction inhibited the activity of AChE that indicated the presence of low molecular weight active compound(s) of less than 0.5kD. Two active fractions were obtained after BioGel P2 fractionation of the 0.5kD of the *Gyrostoma helianthus*. The first active fraction inhibited the activity of the acetylcholinesterase, while the other fraction was not. HPLC technique aided by semipreparative

columns was used to isolate the target compounds in a pure form for the structure elucidation, one dimensional NMR analysis ( $^1\text{H}$  and  $^{13}\text{C}$ -NMR) and DEPT were carried out to elucidate the structure of the isolated compound which tentatively identified as N,N'-bis-(1-methyl-pyridin-2-yl)-hydrazine.

**Keywords:** Sea anemone; Gyrostoma helianthus; Red sea; Structure elucidation; Acetylcholinesterase (Ache) Inhibitor.

#### 214. Metallic Nanomaterials as Drug Carriers to Decrease Side Effects of Chemotherapy (In Vitro: Cytotoxicity Study)

Samah A. Loutfy, Mona Bakr Mohamed, Nour Tawfik Abdel-Ghani, Nadia Al-Ansary, Wafaa A. Abdulla, Ola M. El-Borady, Yasmein Hussein and M. Hossam Eldin

*Journal of Nanopharmaceutics and Drug Delivery*, 1: 1-12 (2013)

**Background:** Toward designing new class of desired physicochemical properties of metallic nanomaterials such as spherical gold and silver nanoparticles capped with citrate to be used as a drug delivery system for anticancerous drug like 6-Mercaptopurine (6-MP) against human breast cancer. This could increase curative effect of potent drug and lower side effects of high dose of anticancerous drug. Methods: Full characterization for the prepared nanoparticles and drugs loaded nanoparticles was performed by TEM. Human breast cancer cell line (MCF-7) was maintained in the laboratory. Colourimetric cytotoxicity assay was established and standardized for testing all engineered nanomaterials.

**Results:** Alteration of cell morphology was observed after treatment of MCF-7 with concentrated solution of silver nanoparticles (AgNPs) and 6-MP@AgNPs ( $10^{-3}$  M) capped with citrate after 24 hrs of cells exposure. Also, such concentration of AgNPs exhibited more aggressive cytotoxic effect than that exerted by AuNPs after 24 hrs of cell exposure (viability was 30% vs. 83 for both AgNPs and AuNPs, respectively). The concentrated solution of gold composite ( $10^{-3}$  M of 6-MP@AuNPs) exhibited double cytotoxic effect than that exerted by each of free 6-MP or AuNPs, after 24 hrs of cell exposure (43% viability for gold composite vs. 92% and 83% for both 6-MP and AuNPs, respectively). The effect of capping materials has been tested via investigating the cytotoxicity of AgNPs capped with lactose compared to that which capped with citrate. Our results indicate that Ag NPs capped with lactose is much more safer on cells than that capped with citrate. The antiproliferative activity of tested nanomaterials against breast cancer was notable at different concentrations, for example, at 25 M, gold composite showed aggressive cytotoxic effect than that exerted by silver composite capped with lactose (viability 59% vs. 80%), but smaller molar ratio of 6-MP used for synthesis silver composite may be useful as a safer drug carrier against human breast cancer.

**Conclusion:** Our engineered metallic nanoparticles provided a flexible platform for enhancing anticancerous activity of 6-MP against human breast cancer. Silver nanocomposite capped with lactose may be useful as a drug carrier for 6-MP minimizing its side effect more than gold nanoparticles capped with citrate, but this require further studies.

**Keywords:** Metallic nanoparticles as a drug delivery system; 6-mercaptopurine; Cytotoxicity; MCF-7.

#### 215. One Pot Synthesis of Pyridine, Thiazolidine, Pyrazole and 2, 3-Dihydro-1, 3, 4-Thiadiazole Derivatives under Solvent-free Condition

Anhar Abdel-Aziem and Abdou Osman Abdelhamid

*International Journal of Advanced Research*, 1 (9): 717-728 (2013)

Claisen condensation of 2-acetylbenzofuran and 1,3-diphenyl-1H-pyrazole-4-carbaldehyde 2 gave chalcone 3 which was exploited as a starting material for the syntheses of hitherto unknown different types of new heterocyclic compounds incorporating the benzofuran moiety via the reaction with various active methylene compounds. On the other hand, several new thiadiazolines, pyrazoles and pyrazolo[3,4-d] pyridazine were synthesized by the reaction of 3-(benzofuran-2-yl)-3-oxopropanenitrile 12 with a-halo ketone, a-halo ester and hydrazonoyl halides.

**Keywords:** 2-Acetylbenzofuran; Hydrazonoyl halides; Pyridins; 1,3-Thiazoles; Solvent-free.

#### 216. Potentiometric Determination of Ranitidine Hydrochloride Utilizing Modified Carbon Paste Electrodes

Gehad G, Mohamed, M. M. Khalil, E. Y. Z. Frag and Gamal M. Abed El Aziz

*International Journal of Current Pharmaceutical Research*, 5(2): 72-79 (2013)

Sensitive potentiometric method is reported in this work for the determination of ranitidine hydrochloride (RNH) in pure form and pharmaceutical preparation using modified carbon paste (MCPE) and insitu carbon paste (ICPE) electrodes. The MCPE and ICPE electrodes are based on ranitidine-tetraphenyl borate ion pair (RNH-TPB) and sodium tetraphenyl borate ion pairing reagent (Na TPB), respectively, by using tricresyl phosphate (TCP) as plasticizer. The MCPE and ICPE electrodes exhibit suitable response to RNH in the concentration range from  $1 \times 10^{-6}$  to  $1 \times 10^{-2}$  mol L $^{-1}$ . The slope of the electrodes were  $56.8 \pm 1.4$  and  $57.9 \pm 1.65$  mV decade $^{-1}$  over the pH range 3-8 and 3-9 for MCPE and ICPE electrodes, respectively.

Selectivity coefficients of RNH relative to a number of potential interfering substances were investigated. The MCPE and ICPE electrodes showed fast response time of 4 and 3.5 sec, respectively, and were used over a period of two months with good reproducibility. The sensors were applied successfully to determine RNH in pure and pharmaceutical preparations.

**Keywords:** Ranitidine hydrochloride; MCPE; ICPE; Potentiometry; Ion selective electrodes.

#### 217. Potentiometric Study and Biological Activity of Some Metal Ion Complexes of Polyvinyl Alcohol (PVA)

Wafaa M. Hosny and Perihan A. Khalaf-Alaa

*International Journal of Electrochemical Science*, 8: 1520-1533 (2013)

The acid-base equilibrium of polyvinyl alcohol (PVA) is investigated. The stability constant values of the binary



complexes between PVA and metal ions Cu(II), Co(II), Ni(II) and Zn(II) formed in solution were investigated potentiometrically. The relationships between the properties of the studied central metal ions as ionic radius, electronegativity, atomic number, and ionization potential of the formed complexes were investigated and give information about the nature of chemical bonding in complexes and make possible the calculation of unknown stability constants. Cu<sup>II</sup> and Ni<sup>II</sup> complexes with PVA are isolated as solid complexes and characterized by chemical and physical methods, and their general formula [ML.nH<sub>2</sub>O]2H<sub>2</sub>O, where M = Cu<sup>II</sup> and Ni<sup>II</sup>, L = PVA, and n = 2 and 4 for Cu<sup>II</sup> and Ni<sup>II</sup> respectively. The ligand and their metal chelates have been screened for their antimicrobial activities using the disc diffusion method against the selected bacteria and fungi.

**Keywords:** Polyvinyl alcohol (PVA); Metal complexes; Potentiometry; Ir spectra; Antimicrobial activities.

### 218. Preparation and Characterization of Nanoparticles Modified Chitosan Sensor and its Application for the Determination of Heavy Metals from Different Aqueous Media

Rasha A. Ahmed and A. M. Fekry

*International Journal of Electrochemical Science*, 8: 6692 - 6708 (2013)

A biosensor electrode based on the incorporation of super nanoparticles paramagnetic iron oxide ( $\alpha$ -Fe<sub>3</sub>O<sub>4</sub>) in chitosan (CS) film coated on platinum electrode, was developed for the determination and removal of heavy metals.

The morphological properties of the homogenous  $\alpha$ -Fe<sub>3</sub>O<sub>4</sub>/CS nanocomposite were studied with scanning electron microscopy (SEM), Energy Dispersive X-ray analysis (EDX), and thermal gravimetric analysis (TGA). The morphological results indicate the successful formation of  $\alpha$ -Fe<sub>3</sub>O<sub>4</sub>/CS nanocomposite and high stability of the film. The  $\alpha$ -Fe<sub>3</sub>O<sub>4</sub>/CS nanocomposite showed a great efficiency for the determination of As, Pb, and Ni ions from aqueous solution using various electrochemical techniques. The presence of  $\alpha$ -Fe<sub>3</sub>O<sub>4</sub> nanoparticles results in increased active surface area and enhanced electron transfer. Results showed that this novel  $\alpha$ -Fe<sub>3</sub>O<sub>4</sub>/CS nanocomposite was successfully applied for sewage water and human urine samples with very low detection limit.

**Keywords:** Sensor;  $\alpha$ -Fe<sub>3</sub>O<sub>4</sub>; Impedance; CV; Heavy metals.

### 219. Reactions and Antimicrobial Activity of (3-(3-(4-Methoxyphenyl) Acryloyl)-2H-Chromen-2-one

Marwa Sayed El-Gendy, Anhar Abdel-Aziem and Abdou Osman Abdelhamid

*International Journal of Advanced Research*, 1 (10): 557-568 (2013)

Several pyridines derivatives, pyrazolines were synthesized via reaction of 3-(3-(4-methoxyphenyl) acryloyl)-2H-chromen-2-one with different reagents. Structures of newly synthesized were confirmed by elemental analysis, spectral data, chemical transformation and alternative synthetic route whenever possible. Also, the newly synthesized were screen towards some microorganism.

**Keywords:** Coumaines; Pyrazolines; Pyridines; Hydrazonoyl halides; Carbamates; Urea.

### 220. Regioselective Synthesis of Some Functionalized 3,4'-Bis-(Pyrazolyl) Ketones and Chemoselectivity in their Reaction With Hydrazine Hydrate

Hamdy M. Hassanain and Ahmad Sami Shawali

*European Journal of Chemistry*, 4 (2): 102-109 (2013)

A new enamino ester, (E)-ethyl 3-(dipropylamino)acrylate, was prepared and used for synthesis of various pyrazole derivatives, 4a-k and 5a-d. Other new enaminone, (E)-ethyl 3-(3-(dimethylamino) acryloyl) -1- (4-nitrophenyl) -1H-pyrazole-4 carboxylate (8), was also prepared from compound 4a and utilized as precursor for synthesis of different functionalized 3,4'-bis-pyrazolyl ketones 9a-c, 10a-c. The site selectivity in hydrazinolysis of the latter was studied. The structures of the products namely pyrazolo[3,4-d]pyridazine derivatives 11(13) were confirmed by spectral and elemental analyses and by alternate unambiguous synthesis.

**Keywords:** Enaminones; Enamino esters; Regioselectivity; Chemoselectivity; Hydrazonoyl halides; Pyrazolo [3,4-d] Pyridazines.

### 221. Self-Assembling of Gold Nanoparticles Array for Electro-Sensing Applications

Islam M. Al-Akraa, Ahmad M. Mohammad, Mohamed S. El-Deab and Bahgat E. El-Anadouli

*International Journal of Electrochemical Science*, 8: 458-466 (2013)

A colloidal solution of citrate-stabilized gold nanoparticles (AuNPs) with an average size of ca. 2.6 nm has been prepared, characterized and further implemented in electro-sensing applications. This colloidal solution of AuNPs has been prepared via the reduction of NaAuCl<sub>4</sub> with sodium tetrahydroborate (NaBH<sub>4</sub>) using trisodium citrate as a stabilizer. The optical properties of this solution have been studied with UV-Vis spectroscopy.

Next, these AuNPs have been immobilized onto a polycrystalline Au (poly-Au) electrode with the assistance of benzenedimethanethiol (BDMT), which served as a binder. Attention has been taken to ensure the formation of a compact impermeable layer of BDMT on poly-Au electrode, in order isolate the ploy-Au surface from participating in the upcoming applications. Interestingly, the AuNPs-modified Au electrode has shown a better sensing capability for ascorbic acid than that of the bare poly-Au, which opens opportunities for future designing of nanoparticles-based biological sensors.

**Keywords:** Gold nanoparticles; Optical properties; Self-assembly; Benzenedimethanethiol; Ascorbic acid.

## 222. Spectrophotometric Determination of Distigmine Bromide, Cyclopentolate Hcl, Diaveridine Hcl and Tetrahydrozoline Hcl VIA Charge Transfer Complex Formation with DDQ Reagent

M.S. Rizk, Eman Y.Z. Frag, Gehad G. Mohamed and Ayman A. Tamam

*International Journal of Research in Pharmacy and Chemistry*, 3(2): 168-183 (2013)

In this work, distigmine bromide, cyclopentolate hydrochloride, diaveridine hydrochloride and tetrahydrozoline hydrochloride were chosen to study their properties from the analytical point of view. The purpose of this investigation was directed to propose sensitive, accurate and reproducible methods of analysis that can be applied to determine these drugs in pure form and pharmaceutical preparations. The studied work with the spectrophotometric determination of distigmine bromide, cyclopentolate hydrochloride, diaveridine hydrochloride and tetrahydrozoline hydrochloride via charge-transfer complex formation. This includes the utility of p-acceptor like 2,3-dichloro-5,6-dicyanobenzoquinon (DDQ) for estimation of distigmine bromide, cyclopentolate hydrochloride, diaveridine hydrochloride in their pure and in pharmaceutical preparations.

**Keywords:** Distigmine bromide; Cyclopentolate hydrochloride; Diaveridine hydrochloride.

## 223. Spectrophotometric Studies Using Ion-Pair Formations of Ranitidine Hydrochloride in Pure and in Pharmaceutical Forms with Some Dyestuff Reagents

M. M. Khalil, E. Y. Z. Frag, Gehad G. Mohamed and Gamal M. Abed el Aziz

*Journal of Applied Pharmaceutical Science*, 3(4): 92-98 (2013)

Simple, rapid and sensitive spectrophotometric procedure is suggested for the determination of ranitidine hydrochloride (RNH) drug in pure form and in pharmaceutical formulations. The method was based on the ion-pair formations of RNH with different dyestuff reagents such as methyl orange (MO), bromocresol purple (BCP), eriochrome cyanine R (ECR) and alizarine red S (ARS). The obtained ion-pairs were measured spectrophotometrically at 408, 420, 330 and 326 nm by using BCP, MO, ECR and ARS reagents, respectively. Beer's plots were linear in the concentration range of 5-200, 20-350, 10-150 and 10-180 µg mL<sup>-1</sup> RNH, with correlation coefficients not less than 0.9991, 0.9996, 0.9993 and 0.999 using BCP, MO, ECR and ARS reagents, respectively. The Sandell sensitivity was found to be 0.813, 0.462, 0.541 and 0.630 µg cm<sup>-2</sup> for BCP, MO, ECR and ARS, respectively. Standard deviation (SD = 0.024-0.028, 0.018-0.023, 0.016-0.021 and 0.023-0.029) and relative standard deviation (RSD% = 0.123-0.943, 0.0102-0.82, 0.118-0.145 and 0.132-0.178%) (n = 4) values using BCP, MO, ECR and ARS reagents, respectively, were obtained. These results were also confirmed with percent recovery of 99.78-100.52%, 99.86-101.12%, 99.82-100.31% and 100.18-101.25% for BCP, MO, ECR and ARS reagents, respectively. This method was successfully applied for determination of RNH in aciloc tablet. The calculated t- and F- values (95% confidence limit) indicate no

significant differences between the proposed and official methods.

**Keywords:** Ranitidine hydrochloride; BCP; MO; ECR; ARS; ion pair formation; Spectrophotometry.

## 224. Synthesis, Reactions of 3-Oxo-3-(3-Oxo-3h-Benzo [f] Chromen-2-Yl)-2- (2-Phenylhydrazono) Propanal, and Investigation of their Antitumor Activity

Sobhy M. Gomaa and Hassan M. Abdel-aziz

*World Journal of Pharmacy and Pharmaceutical Sciences*, 2 (5): 2341-2354 (2013)

Heteroarylhydrazonals were prepared from coupling of sodium salt of 2-(3-hydroxyacryloyl)-3H-benzo [f] chromen-3-one with various diazotized heterocyclic amines. Treatment of heteroarylhydrazonals, with 2-cyanoacetamide, 3-oxo-3-phenylpropanenitrile, ethylcyanoacetate, and α-haloketones afforded the corresponding pyridazinone, pyridine, and pyrazole derivatives, respectively. The synthesized compounds were characterized on the basis of their elemental analysis and spectral data. All the newly synthesized compounds were evaluated for their antitumor activities against the human breast cancer cell line MCF-7 and the liver carcinoma cell line HEPG-2, and the results of some derivatives showed promising activity.

**Keywords:** Coupling reaction; Pyrazolotriazine; Triazolotriazine; Benzoimidazotriazine pyridazinone; Antitumor evaluation.

## 225. Synthesis and Antifungal Evaluation of Some New Heterocycles Incorporating Naphthalene Moiety

Sobhi M. Gomha and Mohamed G. Badrey

*International Journal of Advanced Research*, 1(9): 439-446 (2013)

The reaction of 2-cyano-N'-(1-(naphthalen-2-yl) ethylidene) acetohydrazide 1 with the aromatic aldehydes afforded the corresponding arylidene derivatives 3a-e. Refluxing of the latter product 3a with hydrazine hydrate gave the aminopyrazole derivative 4. Compound 1 was utilized as key intermediate for the synthesis of some new 1,2-dihydropyridine 7 and 2,3-dihydrothiazole 8 derivatives. Treatment of 8 with triethylorthoformate in acetic anhydride yielded 2,3-dihydrothiazolo[4,5-d]pyrimidinone 9. Moreover, reaction of 1 with phenyl isothiocyanate gave the corresponding thioacetanilide 10. The latter compound 10 was used for the synthesis of thiadiazole 12. The structures of all new compounds were elucidated on the basis of elemental analysis and spectral data. Twelve of the synthesized products were evaluated as antifungal agents.

**Keywords:** 2-Cyanoacetohydrazide; Aminopyrazole; 1, 2-dihydropyridine; 2,3-dihydrothiazole and antifungal activity.

## 226. Synthesis and Antimicrobial Activity of 5-Arylazothiazoles, 2,3-Dihydro-1,3,4-Thiadiazoles and Triazolo[4,3-*a*]Pyrimidine Derivatives

Abdou O. Abdelhamid, Abdelgawad A. Fahmi and Amna A. M. Alsheflo

*International Journal of Advanced Research*, 1 (8): 568-586 (2013)

2,3-Dihydro-1,3,4-thiadiazoles, and triazolino[4,3-*a*] pyrimidines, were synthesized from the reactions of methyl (or benzyl) carbodithioate and pyrimidine-2-thione derivatives with C-benzofuran-2-oyl-N-phenylhydrazonoyl bromide. The structures of all the newly synthesized compounds were confirmed by elemental analyses, spectral data, and alternative routes synthesis whenever possible. Also, the newly synthesized compounds were tested towards different types of bacteria.

**Keywords:** Chalcones; Hydrazonoyl bromide; Nitrilimines; 5-Arylazothiazoles; 1,3,4-Thiadiazoles; Pyrimidine-2-thione; Triazolino [4,3-*a*] pyrimidines.

## 227. Synthesis and Antimicrobial Activity of Some New 1,2-Bis-[1,3-Thiazolidin-3-Yl] Ethane Derivatives

Kamal Mohamed Dawood and Hussein Khalaf-Allah Abu-Deif

*European Journal of Chemistry*, 4: 277-284 (2013)

1,2-Bis-(2-(phenylimino)-4-oxo-1,3-thiazolidin-3-yl)ethane (4) was synthesized and its reaction with various aldehydes afforded the novel 5-arylidene derivatives 5a-e and 7. Reaction of 4 with phenyl isothiocyanate in the presence of potassium hydroxide, followed by addition of two equivalents of *a*-halo ketones furnished the corresponding 1,2-bis-[5-(thiazolidin-2-ylidene)thiazolidin-3-yl]ethane derivatives 10, 14a-c, and 17a,b. The structures of the newly synthesized compounds were established by elemental and spectral analyses. Compounds 5a-e, 7, 10, 14a-c and 17a were screened for their antimicrobial activity against eight microorganisms. All compounds showed high antibacterial and antifungal activities against all the test microorganisms except *E. coli* and *C. albicans*. The MIC of the active compounds was also evaluated, where; compounds 10 and 17a were more potent active (minimum inhibitory concentration 0.49 and 0.98 µg/mL, respectively) against *S. racemosum* than Amphotericin B (MIC 1.95 µg/mL).

**Keywords:** Antifungal; Bis-thiourea; Antibacterial; A-Halo ketones; Bis-thiazolidinones; 1,3-Thiazolidin-4-one.

## 228. Synthesis and Antimicrobial Activity of Some Pyrazolo[3',4':4,5]Pyrimido[1,2-b][1,2,4] Triazino [5,4-f] [1,2,4,5]Tetrazinone Derivatives

Sobhi M. Gomha and Hatem A. Abdel-Aziz

*International J. of Advanced Research*, 1 (7): 450-457 (2013)

In the present study, Preparation of a novel series of 2-(2-heteroaroylhydrazono)-N'-(4-fluorophenyl)propanehydrazonoyl chloride (4a-d), which is used as a key intermediate in the synthesis of a novel series of pyrazolo[3',4':4,5]pyrimido[1,2-b][1,2,4]triazino[5,4-f][1,2,4,5]tetrazin-11(8H)-one derivatives

(10a-d), via its reaction with 5-amino-1-phenyl-6-thioxopyrazolo [3,4-d]pyrimidin-4-one (5) in dioxane in the presence of TEA under reflux followed by dehydrative cyclization in boiling pyridine was described. The structures of all the newly synthesized heterocyclic compounds were established by considering elemental analysis, spectral data and an alternative synthetic route. The antimicrobial activity of some selected products was evaluated and showed good results.

**Keywords:** Benzohydrazide; Hydrazonoyl halides; 5-Amino-1-Phenyl-6-Thioxopyrazolo[3,4-d]Pyrimidin-4-One; Pyrazolo[3,4-d]Pyrimido[1,2-b][1,2,4,5]Tetrazin-6-One; Antimicrobial activity.

## 229. Synthesis and Antimicrobial Evaluations of New Bioactive Dyes and their Cyclized Derivatives Synthesized from 4,5,6,7-Tetrahydrobenzo[b]-Thiophene

Rafat M. Mohareb, Amira E. M. Abdallah, Maher H. E. Helal and Heba Allah N. A. Mohammed

*Eur. Chem. Bull.*, 2: 618-628 (2013)

The reaction of 3-cyano-2-diazo-4,5,6,7-tetrahydrobenzo [b]thiophene (1) with active methylene reagents 2a-e gave the respective hydrazone derivatives 3a-e. The reactivity of the latter derivatives towards different chemical reagents was studied. The antimicrobial activity of the newly obtained products was studied and evaluated in terms of minimal inhibitory concentration (MIC) in µg mL<sup>-1</sup>. The results showed that compounds 3b, 7a and 15a are the most active compounds towards *E. coli* ECT 101; compounds 5f, 13b, 17a and 23 are active towards *B. Cereus* CECT 148; while 10, 19a and 19b towards *B. subtilis* CECT 498 and 3c, 5c and 13b towards *C. albicans* CECT 1394.

**Keywords:** Tetrahydrobenzo [b] thiophene; Pyridazines; Pyrazoles; Antimicrobial activity.

## 230. Synthesis and Antiviral Evaluation of Some New Thieno [2,3-*d*] Pyrimidine Sglycosides

Nasser A. Hassan, Ahmad S. Shawali, Kh. M. Abu-Zied and Dalia A. Osman

*Journal of Applied Sciences Research*, 9: 833-842 (2013)

Several thioglycosides of the thieno[2,3-*d*] pyrimidine ring system were prepared from the reaction of 2-mercapto-3-substituted-1,2,3,5,6,7,8,9-octahydro-4*H*-cyclohepta (Attia et al 1997 and Rashad et al 2005) thieno[2,3-*d*] pyrimidin-4-one with 2,3,4,6-tetra-O-acetyl- $\alpha$ -D-glucopyranosyl bromide. Their structural elucidation is reported and also some of the products were screened for their antiviral activity.

**Keywords:** Cyclohepta [4,5]thieno[2,3-*d*]pyrimidin-4-One; S-Glycosides; 2,3,4, 6-Tetra-O-acetyl-A-dglucopyranosyl bromide; Antiviral evaluation.

## 231. Synthesis and Characterization of Nano-Structure TiO<sub>2</sub> Thin Film Prepared by Sol-Gel Spin Coating Method

N. M. Amin, Y. M. Issa, I. K. Battisha and M. M. El-Husseiny

*Journal of Applied Sciences Research*, 9(3): 1960-1965 (2013)

Titanium dioxide thin films have been synthesized by sol-gel spin coating technique on glass substrate. The prepared thin films have been submitted to different annealing temperature ranging from 300 upto 500 °C. The effects of annealing temperatures on the structural and optical properties of thin films were investigated. The films were characterized by different techniques: X-ray diffraction (XRD), UV-visible spectroscopy, scanning electron microscope (SEM) and transmission electron microscopy (TEM). The characterization studies revealed that the films are crystallized into nano-structured anatase phase. The crystallite sizes obtained from XRD annealed at 300, 400 and 500 °C are found to be about 159.34, 76.95 and 17.61 nm respectively. The crystallite size of TiO<sub>2</sub> thin films decreased with increasing annealing temperature. The mentioned data were confirmed by TEM, which revealed the presence of TiO<sub>2</sub> nano-particle of about (~3-4 nm). The optical measurement showed the direct band gap at 4.27, 4.28 and 4.37 eV for 300, 400 and 500 °C, respectively. The TiO<sub>2</sub> thin films have higher transparency in the visible range at 500 °C. SEM image of films annealed showed nano-crystalline structure of TiO<sub>2</sub> particles and they are approximately in spherical forms.

**Keywords:** Nano-structure TiO<sub>2</sub> film; Sol-gel; Optical properties; Anatase; XRD; TEM and SEM.

### 232. Synthesis and Characterization of Some Sulfadryugs Azodyes, Potentiometric Studies of the Synthesized Dyes and their Fe (III) Complexes

Aida L. El-Ansary, Hussein M. Abd El-Fattah, Nora S. Abdel-Kader and Aya M. Farghaly

*Communications in Inorganic Synthesis, 1: 16-18 (2013)*

New sulfa drugs azo dyes (HL<sub>1</sub>, HL<sub>2</sub>, HL<sub>3</sub>, HL<sub>4</sub> and HL<sub>5</sub>) were prepared by the coupling of 6-formyl-7-hydroxy-5-methoxy-2-methylbenzopyran-4-one with the sulfa drugs (sulfadiazine, sulfapyridine, sulfamethoxazole, sulfadiazine, sulfathiazole). The five prepared ligands were characterized by elemental analysis, infrared, mass spectra, and <sup>1</sup>H-NMR spectra. The ionization constants of the ligands and stability constants of their Fe (III) complexes were determined potentiometrically in ethanol-water media at 25°C. HL<sub>1</sub> ligand has two pK<sub>a</sub> values while the other ligands (HL<sub>2</sub>, HL<sub>3</sub>, HL<sub>4</sub> and HL<sub>5</sub>) have one pK<sub>a</sub> value. All the ligands form 1:1 metal chelates.

**Keywords:** Azo dyes; Sulfa drugs; Benzopranes; Potentiometry; Fe (III).

### 233. Synthesis and in Vitro Anti-Breast Cancer Activity of Some Novel 1,4-Dihydropyridine Derivatives

Hassan M. Abd El Aziz and Sobhi M Gomha

*International Journal of Pharmacy and Pharmaceutical Sciences, 5: 183-189 (2013)*

**Objective and methods:** Reaction of cyanoacetohydrazide with different aromatic and heteroaromatic ketones yielded the corresponding hydrazones, which reacted with ketene dithioacetal in presence of KOH at room temperature to give pyridinedicarbonitrile derivatives. The latter compounds refluxed with hydrazine hydrate to give pyrazolo [4,3-c] pyridinecarbonitrile derivatives.

**Results:** The structures of the newly synthesized compounds were confirmed by elemental analysis, IR, <sup>1</sup>H NMR, <sup>13</sup>C NMR and mass spectral data. Nine compounds of the newly synthesized compounds were evaluated for their in-vitro anticancer activity against human breast cancer cell line (MCF-7).

**Conclusion:** The results revealed that all such compounds exhibited lower activity in relation to the reference drug doxorubicin.

**Keywords:** Hydrazones; Ketene dithioacetal; Pyridine dicarbonitrile; Pyrazolo[4,3-C] pyridine; Anti-breast activity.

### 234. Synthesis of New Pyrazolo [1,5-a]Pyrimidine, Triazolo[4,3-a] Pyrimidine Derivatives and Thieno[2,3-b]Pyridine Derivatives from Sodium 3-(5-Methyl-1-Phenyl-1H-Pyrazol-4-Yl)-3-Oxoprop-1-En-1-olate

Abdou O. Abdelhamid and Sobhi M. Gomha

*Journal of Chemistry, 2013: 1-7 (2013)*

Condensation of sodium 3-oxo-3-(1-phenyl-1H-pyrazol-4-yl)prop-1-en-1-olate (2) with several heterocyclic amines, cyanoacetamide, cyanothioacetamide and 2-cyanoacetohydrazide to give pyrazolo[1,5-a] pyrimidines (5a-d), pyrido[2',3':3,4] pyrazolo[1,5-a] pyrimidine (9), benzo[4,5]imidazo[1,2-a]pyrimidine (10), [1,2,4]triazolo[1,5-a]pyrimidine (11) and pyridine derivatives (12-14). Also, thieno[2,3-b] pyridines (15-18) were synthesized via pyridinethione (13) with a-halo ketones and a-halo ester. Structures of the newly synthesized compounds were elucidated by elemental analysis, spectral data, alternative synthetic routes and chemical transformation whenever possible.

**Keywords:** Pyrazoles; Pyrazolo[1,5-A]Pyrimidines; Triazolo[1,5-A] Pyrimidines; Thieno[2,3-B] Pyridines; Pyrido [2',3':3,4] Pyrazolo[1,5-A]Pyrimidine.

### 235. Synthesis of Some New Azolotriazine, 4-Arylazopyrazole and Pyridine Derivatives Containing 1,2,3-Triazole Moiety

Abdou O. Abdelhamid, Nadia A. Abdel-Riheem, Tamer T. El-Idreesy and Huda R. M. Rashdan

*International Journal of Advanced Research, 1 (9): 729-745 (2013)*

Pyrazolo[5,1-c]triazines, [1,2,4] triazolo[4,3-c] triazine, benzo[4,5]-imidazo[2,1-c] [1,2,4] triazine, pyridine, urea and carbamate derivatives containing 1,2,3-triazole moiety were synthesized in a good yields via sodium salt of 3-hydroxy-1-(5-methyl-1-phenyl-1H-1,2,3-triazol-4-yl) prop-2-en-1-one. The newly synthesized derivatives were elucidated by elemental analysis, spectral data and alternative synthetic routes whenever possible.

**Keywords:** Pyrazolo [5,L-c] triazines; [L,2,4]triazolo[4,3-c] triazine; Pyridines; Carbamates; 1,2,3-triazole.

### 236. Synthesis of Some New Fused Azolopyrimidines, Azolotriazines and Pyridines Containing Coumarines Moieties

Abdou O. Abdelhamid, Abdelgawad A. Fahmi and Abeer Al-Bahlol Ali

*International Journal of Advanced Research*, 1(8): 627-644 (2013)

Pyrazolo[1,5-*a*]pyrimidines, [1,2,4] triazolo[4,3-*a*] pyrimidines, benzo[4,5]-imidazo [1,2-*a*] pyrimidines, pyrazolo [5,1-*c*][1,2,4] triazines, Triazolo[3,4-*c*][1,2,4]-triazines, benzo[4,5]imidazo[2,1-*c*][1,2,4]triazines, pyridenes are synthesized from each of 3-(3-(dimethylamino) acryloyl)-2H-chromen-2-one, and 2-(3-(dimethylamino) acryloyl)-3H-benzo[*f*]chromen-3-one and various reagents. The newly synthesized compounds were elucidated by elemental analysis, spectral data, chemical transformation and alternative synthetic route whenever possible.

**Keywords:** Pyrazolo[1,5-*a*] pyrimidines; Triazolo [4,3-*a*] pyrimidines; Benzo [4,5]-imidazo [1,2-*a*]-pyrimidines; Pyrazolo[5,1-*c*][1,2,4]-triazines; Benzo [*f*] chromene-3-one; Chromen-2-one.

### 237. Synthesis, Reactions and Biological Evaluation of 3-Amino-6- (Subs.) Thieno [2,3-*b*] Pyridine-2-Carbohydrazides

Fawzy A. Attabya, Ahmed H. El-Ghandour, Abdelwahed R. Sayed, Ashraf A. El Bassuony and Ahmed A. M. El-Reedy

*Current Bioactive Compounds*, 9: 167-181 (2013)

A new and efficient method for the preparation of 3-amino-6-thieno[2,3-*b*]pyridine-2-carbohydrazides and pyrido [3',2':4,5] thieno[3,2-*d*]pyrimidinones from one-pot synthesis has been accomplished using 3-amino-6-thieno[2,3-*b*]pyridines with hydrazine hydrate in ethanol under reflux. This new protocol has the advantages of easy availability and high to excellent yields, simple experimental and work-up procedure. The synthesized compounds were confirmed through spectral characterization using IR, <sup>1</sup>H NMR, mass spectra and elemental analyses.

**Keywords:** Thienopyridines; Pyridinethiones pyridothienopyrimidinones; Thienopyridineoxadiazoles; Pyrazolothienopyridinone.

### 238. Synthesis, Structure Activity Relationships and Biological Activity Evaluation of Novel Spirocyclic Thiazolidin-4-ones as Potential Anti-Breast Cancer and Epidermal Growth Factor Receptor Inhibitors

D. H. Fleita, O. K. Sakka and R. M. Mohareb

*Drug Research*, 63: 1-8 (2013)

A series of triazaspiro [4.5]dec-8-ene benzyldine derivatives containing thiazolidinone ring system (6-18) have been designed, synthesized and their biological activities evaluated as potential epidermal growth factor receptor inhibitors. Among them, 9-amino-2-(4-nitrobenzylidene)-3-oxo-4- phenyl-7-thioxo-1-thia-4,6,8-triazaspiro[4.5] dec-8-ene-10-carbonitrile (18) displayed the most potent inhibitory activity (IC<sub>50</sub> = 6.355 μM).

Antiproliferative assay results indicated that compound 18 exhibited moderate antiproliferative activity against MCF-7 cell line in vitro; with GI<sub>50</sub> value of 30.6 μM. In addition, compounds 7 and 15 displayed the highest antiproliferative activity at a common GI<sub>50</sub> value of 10.8 μM. Docking simulation was performed to determine the probable binding model and to pursue information regarding the activity of compound 18. Based on the preliminary results, compound 18 could be used as an attractive building block for designing potential epidermal growth factor receptor inhibitors.

**Keywords:** Spiro-thiazolidin-4-one; Egfr; Antiproliferative; Structure activity relationship.

### 239. Synthesis of Some Fused Heterocyclic Compounds Based on 1-(1-Benzofuran-2-Yl)-3-(Furan-2-Yl) Prop-2-En-1-one

Azza M. Abdel-Fattah, Fawzy A. Attaby and Labeeb M. Shaif

*International Journal of Scientific and Engineering Research*, 4(11): 1831-1839 (2013)

1-(1-Benzofuran-2-yl)-3-(furan-2-yl) prop-2-en-1-one (3) reacted with 2-cyanoethanethioamide (4) to afford the corresponding 6-(1-benzofuran-2-yl)-4-(furan-2-yl) -2-thioxo-1,2-dihydropyridine-3-carbonitrile (5). The synthetic potentiality of compound 5 was investigated in the present study via its reactions with several active-hydrogen containing compounds aiming to synthesize each of thieno[2,3-*b*]pyridine derivatives 8a,b, 11, 14a,b, 17, 20, 23; 3-aminothieno[2,3-*b*]pyridine-2-carbohydrazide derivative 24 which used in turn, to prepare (1H-pyrazol-1-yl)carbonyl-thieno[2,3-*b*]pyridin-3-amine 26, N-phenylmethylenethieno[2,3-*b*]pyridine-2-carbohydrazide 31, pyrido[3',2':4,5]thieno[3,2-*d*]pyrimidinone derivatives 33, 35, 38a,b and pyrazolo [3',4':4,5] thieno[2,3-*b*]pyridine-3-one derivative 40. The structures of the newly synthesized heterocyclic compounds were elucidated by considering the data of both elemental and spectral data.

**Keywords:** 2-Cyanoethanethioamide; Pyridothienopyrimidinones; N-Phenylmethylenethienopyridin-2-Carbohydrazides; 2-Thioxopyridine-3-Carbonitrile.

### 240. Utility of 2-Amino-4,5,6,7-Tetrahydrobenzo [B]Thiophene-3-Carboxylic Acid in the Synthesis of Novel Thieno[2,3-*B*] [1,2,4]Triazepinones and Thieno [2,3-*D*][1,3,4]Thiadiazolo[2,3-*B*]Pyrimidinones

Sobhy M. Gomha and Hassan M. Abd El Aziz

*Journal of Engineering Research and Application*, 3 (5): 694-700 (2013)

A new series of thienothiadiazolopyrimidinone 4 was prepared via the reaction of hydrazonoyl chlorides 2 with 2-amino-tetrahydrobenzo[*b*]thiophene-3-carboxylic acid 1 followed by cyclization with 1,1'-carbonyldiimidazole. Furthermore, benzothienothiadiazolo pyrimidinone derivatives 11a-c were prepared. The structure of the newly synthesized compounds were established on the basis of spectral data (Mass, IR, <sup>1</sup>H and <sup>13</sup>C NMR) and elemental analyses.

**Keywords:** Hydrazonoyl halides; 2-Amino-tetrahydrobenzo [b] Thiophene-3-Carboxylic acid; Thienothiadiazolo- pyrimidinone; Thienothiadiazolopyrimidinone.



#### 241. Utilization of Phosphotungstic Acid in the Conductometric Determination of Loperamide Hydrochloride and Trimebutine Antidiarrhea Drugs

Hoda M. Elqudaby, Gehad G. Mohamed and Ghada M.G. El Din

*Journal of Pharmacy Research*, 7: 686-691 (2013)

**Aim:** Phosphotungstic acid (PTA), was used as titrant for the conductometric determination of loperamide hydrochloride (LOP.HCl) and trimebutine (TB) antidiarrhea drugs through ion-associated complex formation.

**Method:** The effect of the reagent concentration, temperature, molar combining ratio, and the solubility products of the formed ion-associates were studied and calculated.

**Results:** The suggested method was applied for the determination of loperamide hydrochloride and trimebutine in their pure form and pharmaceutical preparations with mean recovery values of 99.67 and 99.47 % for loperamide hydrochloride in pure form and in Imodium capsule, respectively, and 99.88 and 99.04 % for trimebutine in pure form and in Triton tablets, respectively. Relative standard deviation was less than 1.0%. The accuracy of the method was indicated by excellent recovery while low standard deviation supported the precision of the method. The sensitivity of the proposed method was discussed and the results were compared with the pharmacopeial methods.

**Conclusion:** The proposed procedure was simple, rapid, sensitive, and accurate and can be applied for the routine measurements of the cited drugs.

**Keywords:** Loperamide hydrochloride; Trimebutine; Conductometric titration; Phosphotungstic acid.

#### 242. Validated Spectrophotometric Methods for Determination of Escitalopram Through Study of Charge Transfer and Ion Pair Complexation

A.L. El-Ansary, N.N. Salama, F.M. Abu Attia, H.B. Hassib and M.A. Mohamed

*Journal of Chimica Acta*, 2: 119-128 (2013)

Two simple and sensitive spectrophotometric methods were developed and validated for quantitative determination of escitalopram (Esc). The first method is based on the formation of charge-transfer complexes between the drug as n-donor and 2,3-dichloro-5,6-dicyano-p-benzoquinone (DDQ), 7,7,8,8-tetracyanoquinodimethane (TCNQ), tetracyanoethylene (TCNE) and p-chloranilic acid (p-CA) as  $\pi$ -acceptors to give highly colored complex species. The products exhibit absorption maxima at 456, 841, 413 and 518 nm in acetonitrile for DDQ, TCNQ, TCNE and p-CA, respectively. Beer's law was obeyed in the range of 8.28–373.00  $\mu\text{g mL}^{-1}$ . Moreover, kinetic spectrophotometry was adopted for analysis of Esc with TCNE, using initial rate and fixed time methods. The second method is based on the formation of yellow ion-pair complexes between escitalopram and four sulphonphthalein acid dyes, namely; bromocresol purple (BCP), bromophenol blue (BPB), bromocresol blue (BCB), and bromocresol green (BCG) in chloroform. The formed complexes are measured at 407, 413, 415 and 416 nm for BCP, BPB, BCB and BCG, respectively. Under the optimum reaction conditions, linear relationships with good correlation coefficients (0.9996 - 0.9999) are found between absorbance of the formed complexes and concentrations of

escitalopram in the range of 2.07–41.44  $\mu\text{g mL}^{-1}$ . Spectral characteristics and stability constants of the formed ion associates are discussed in terms of the nature of donor and acceptor molecular structures. The molar absorptivities and association constants for the colored complexes were evaluated using the Benesi-Hildebrand equation. The proposed methods were successfully applied for determination of the drug in tablets with good accuracy and precision.

**Keywords:** Escitalopram; Charge transfer complexes; Kinetic spectrophotometry; Ion pair complexes; Acid dyes.

#### Dept. of Entomology

#### 243. Scanning Electron Microscopy of the Four Larval Instars of the Lymphatic Filariasis Vector Culex Quinquefasciatus (Say) (Diptera: Culicidae)

Fatma K. Adham, Heinz Mehlhorn and Abeer S. Yamany

*Parasitology Research*, 112: 2307-2312 (2013) IF: 2.852

Since *Culex pipiens quinquefasciatus* is the main vector of lymphatic filariasis in tropics and subtropics, the identification and quantification of the mosquito is an important task. Scanning electron microscopy reveals that morphological changes during larval development as the number of comb scale varies greatly and their complexity increases from first to the fourth instar. Also, their structures are more complex with a varying number of subapical denticles. The amount of pecten shows modifications at different larval instars with regard to the number and complexity of their spines. The pecten teeth increase in their number and complexity during larval development from the first to the fourth instar. The ventral brush of the abdominal segment X in the first and second instars is composed of two respectively three pairs of setae while the third and fourth instars have four pairs of sturdy setae.

**Keywords:** *Culex quinquefasciatus*; Four larval instars; Electron microscopy.

#### 244. Infectivity of Metarhizium Anisopliae (Hypocreales: Clavicipitaceae) to Phlebotomus Papatasi (Diptera: Psychodidae) Under Laboratory Conditions

Alia Zayed, Mustafa M. Soliman and Mohamed M. El-Shazly

*Journal of Medical Entomology*, 50: 796-803 (2013) IF: 1.857

Susceptibility of *Phlebotomus papatasi* Scopoli (Diptera: Psychodidae) larvae to the entomopathogenic fungus *Metarhizium anisopliae* (Metschnikoff) Sorokin (Ma79) (Hypocreales: Clavicipitaceae) was evaluated at two different temperatures. The ability of the fungus to reinfect healthy sand flies was followed up for  $\approx 20$  wk and the effect of in vivo repassage on the enhancement of its virulence was assessed. The fungus reduced the adult emergence at  $26 \pm 1^\circ\text{C}$  when applied to larval diet. Six spore concentrations were used in the bioassays ranging from  $1 \times 10^6$  to  $5 \times 10^8$  spores/ml. Mortality decreased significantly when the temperature was raised to  $31 \pm 1^\circ\text{C}$  at all tested concentrations. Fungus-treated vials were assayed against sand fly larvae at different time lapses without additional reapplication of the fungus in the media to determine whether the level of inocula persisting in the media was sufficient to reinfect healthy sand

flies. Twenty weeks postapplication, there were still enough infectious propagules of Ma79 to infect 40% of *P. papatasi* larvae. A comparison between the infectivity of 10 subsequent in vitro cultures and the host-passed inocula of the fungus against sand fly larvae was conducted. Mortalities of *P. papatasi* larvae changed significantly when exposed to inocula passed through different insects. Presented data can provide vector control decision makers and end users with fundamental information for the introduction and application of *M. anisopliae* as an effective control agent against the main cutaneous leishmaniasis old-world vector *P. papatasi*.

**Keywords:** Sand flies; *Metarhizium anisopliae*; Biological control; Fungal persistence.

#### 245. A Review of the Family Eucharitidae (Hymenoptera: Chalcidoidea) of Egypt

Neveen S. Gadallah, Yusuf A. Edmardash and John M. Heraty

*Zootaxa*, 3717(3): 389-394 (2013) IF: 0.974

The species of Eucharitidae (Hymenoptera: Chalcidoidea) of Egypt are reviewed. Three species of *Eucharis* Westwood are reported, *Eucharis* (*Eucharisca*) *bytinskisalzi* Boucek, *E. (Psilogastrellus)* *cuprea* (Blanchard) and *E. (Psilogastrellus)* *punctata* Förster. Primary type material of *E. bytinskisalzi* and *E. cuprea* is illustrated through macrophotography and a key to separate the three species is provided. *Eucharis bytinskisalzi* is listed as a new record for the Egyptian fauna.

**Keywords:** *Eucharis* (*eucharisca*) *bytinskisalzi*; New record; Faunistic list.

#### 246. A Study on the Dynamics of Aedes caspius larval Uptake and Release of Novel Haematoporphyrin

T. A. El-Tayeb, N. M. Abd El-Aziz and H. H. Awad

*African Entomology*, 21(1): 15-23 (2013) IF: 0.969

Haematoporphyrin efficiency on *Aedes caspius* increased the larval mortality with the increase of haematoporphyrin formulation (HPF) concentration ( $1 \times 10^3$  M/l). Larval mortality increased with increase the solar simulator light irradiances ( $350\text{--}650$  W/m<sup>2</sup>) and exposure times (45 min). Dynamics of HPF accumulation and release as a function of time feeding and consumption was investigated using confocal laser scanning microscopy (CLSM). HPF accumulation in the larval body reached its maximum level after incubation for 12 h. Remaining HPF concentration decreased as the time elapsed reaching its minimal level after 15 h of HPF removal from the treatment medium.

**Keywords:** Mosquitoes; Porphyrin; Solar irradiances; CLSM.

#### 247. Impact of Farnesol on the Food Consumption and Utilization, Digestive Enzymes and Fat Body Proteins of the Desert Locust Schistocerca Gregaria Forskål (Orthoptera: Acrididae)

H. H. Awad, N. A. Ghazawy and K. M. Abdel Rahman

*African Entomology*, 21(1): 126-131 (2013) IF: 0.969

The food consumption, nutritional indices and the digestive enzymes (protease, invertase, amylase, trehalase and chitinase) of *Schistocerca gregaria* were affected by treatment with farnesol. Treated insects oviposited fewer eggs. The total haemolymph and midgut protein significantly increased in farnesol-treated insects as compared with the control. Protein profiles in the fat body of treated females showed a significant ( $P < 0.05$ ) change compared with the control females. This change in the intensity might reflect the decline in the synthesis or the increase in the utilization of this protein.

**Keywords:** Grasshoppers; Locusts; Terpenes; Consumption indices; Fecundity.

#### 248. Pathogenicity, Yield and DNA Genome Pattern of the Entomopathogenic Virus Spodoptera Littoralis Multicapsid Nucleopolyhedrovirus (SpliMNPV) to Spodoptera Littoralis (Boisduval) Under the Impact of Environmental Stress

E. H. Shaurub, A. A. Abd El-Wahab and N. M. Abd El-Aziz

*African Entomology*, 21(2): 221-230 (2013) IF: 0.969

The effect of temperature, ultraviolet (UV) radiation and sunlight on the pathogenicity, yield and DNA genome pattern of the entomopathogenic virus SpliMNPV to the Egyptian cotton leafworm *Spodoptera littoralis* (Boisduval) was studied. The viral pathogenicity in terms of larval mortality, and yield in terms of polyhedral inclusion bodies/g larval body weight, significantly increased with the increase of temperature; with optimal temperature of 30 °C for viral yield. However, the pathogenicity significantly decreased with the increase of the exposure period, under the stress of both UV radiation and sunlight, in case of non-shielded exposed viral samples. In contrast, sunlight and UV had no significant effect on the viral pathogenicity in shielded exposed samples. The viral yield significantly decreased with the increase of the exposure period to UV radiation. The same pattern also held true for the exposure to sunlight in case of non-shielded exposed samples without using a UV filter. The viral DNA genome pattern was not affected under the stress of temperature, UV-radiation (shielded samples), sunlight using a UV filter (shielded or non-shielded samples), and sunlight without using a UV filter (shielded samples). Whereas, the intensity of the viral DNA, in non-shielded samples, decreased gradually with the increase of the exposure period to UV radiation and sunlight without using a UV filter.

**Keywords:** *Spodoptera littoralis*; Nucleopolyhedroviruses; Pathogenicity; Viral yield; Viral DNA, Temperature; Ultraviolet radiation; Sunlight.

#### 249. Antibacterial Activity of Lysozyme in the Desert Locust, Schistocerca Gregaria (Orthoptera: Acrididae)

Amr A. Mohamed, Mohamed Elmogy, Moataza A. Dorrah, Hesham A. Yousef and Taha T. M. Bassal

*European Journal of Entomology*, 110 (4): 559-565 (2013) IF: 0.918

The ability of biocontrol agents to overcome the immune defense of pests is a crucial issue. This is the first study of lysozyme activity as an inducible humoral component of the defense of

*Schistocerca gregaria*, which depends on the recognition of the elicitor molecules of pathogens and not on epidermal wounding or a spiking effect. The level of lysozyme activity in fat body, haemocytes and haemolymph plasma of naïve and immunologically challenged 5<sup>th</sup> instar *S. gregaria* was evaluated using the zone of inhibition test against *Micrococcus lysodeikticus*. Various Gram-positive and Gram-negative bacteria as well as peptidoglycans (PGN) and lipopolysaccharides (LPS) of bacterial cell walls induce and increase in the level of lysozyme activity. *Escherichia coli* induced an increase in the level of activity of lysozyme in the fat body, haemocytes and plasma, but not in mid gut epithelium, 6-12 h after an immunological challenge and then it decreased to the constitutive level after 72 h. This study revealed that in *S. gregaria* there is a constitutive and a bacteria-inducible level of lysozyme activity, which protects it against infection by both Gram-negative and Gram-positive bacteria.

**Keywords:** Orthoptera; Acrididae; *Schistocerca gregaria*; Antibacterial; Lysozyme; *Escherichia coli*; Haemocytes.

## 250. A Preliminary Study on the Insect Fauna of Al-Baha Province, Saudi Arabia, With Descriptions of Two New Species

Magdi S. El-Hawagry, Mohammed W. Khalil, Mostafa R. Sharaf, Hassan H. Fadl and Abdulrahman S. Aldawood

*Zookeys*, 274: 1-88 (2013) IF: 0.864

A preliminary study was carried out on the insect fauna of Al-Baha Province, south-western part of Saudi Arabia. A total number of 582 species and subspecies (few identified only to the genus level) belonging to 129 families and representing 17 orders were recorded. Two of these species are described as new, namely: *Monomorium sarawatensis* Sharaf & Aldawood, sp. n. [Formicidae, Hymenoptera] and *Anthrax alruqibi* El-Hawagry sp. n. [Bombyliidae, Diptera]. Another eight species are recorded for the first time in Saudi Arabia, namely: *Xiphoceriana arabica* (Uvarov, 1922) [Pamphagidae, Orthoptera], *Pyrgomorpha conica* (Olivier, 1791) [Pyrgomorphidae, Orthoptera], *Catopsilia florella* (Fabricius, 1775) [Pieridae, Lepidoptera], *Anthrax chionanthrax* (Bezzi, 1926) [Bombyliidae, Diptera], *Spogostylum near tripunctatum* Pallas in Wiedemann, 1818 [Bombyliidae, Diptera], *Cononedys dichromatopa* (Bezzi, 1925) [Bombyliidae, Diptera], *Mydas* sp. [Mydidae, Diptera], and *Hippobosca equina* Linnaeus, 1758 [Hippoboscidae, Diptera]. Al-Baha Province is divided by huge and steep Rocky Mountains into two main sectors, a lowland coastal plain at the west, known as "Tihama", and a mountainous area with an elevation of 1500 to 2450 m above sea level at the east, known as "Al-Sarat or Al-Sarah" which form a part of Al-Sarawat Mountains range. Insect species richness in the two sectors (Tihama and Al-Sarah) was compared, and the results showed that each of the two sectors of Al-Baha Province has a unique insect community. The study generally concluded that the insect faunal composition in Al-Baha Province has an Afrotropical flavor, with the Afrotropical elements predominant, and a closer affiliation to the Afrotropical region than to the Palearctic region or the Eremic zone. Consequently, we tend to agree with those biogeographers who consider that parts of the Arabian Peninsula, including Al-Baha Province, should be included in the Afrotropical region rather than in the Palearctic region or the Eremic zone.

**Keywords:** Palaearctic; Afrotropical; Eremic; List; Insect species; Arabian peninsula; Tihama; Al-Sarah; Al-Sarawat mountains; New species.

## 251. The Digger Wasps of Saudi Arabia: New Records and Distribution, With A Checklist of Species (Hym: Ampulicidae, Crabronidae and Sphecidae)

Neveen S. Gadallah, Hathal M. Al Dhafer, Yousif N. Aldryhim, Hassan H. Fadl and Ali A. Elgharbawy

*North-Western Journal of Zoology*, 9(2): 345-364 (2013)

IF: 0.706

The "sphecids" fauna of Saudi Arabia (Hymenoptera: Apoidea) is listed. A total of 207 species in 42 genera are recorded including previous and new species records. Most Saudi Arabian species recorded up to now are more or less common and widespread mainly in the Afrotropical and Palaearctic zoogeographical zones, the exception being *Bembix buettikeri* Guichard, *Bembix hofufensis* Guichard, *Bembix saudi* Guichard, *Cerceris constricta* Guichard, *Oxybelus lanceolatus* Gerstaecker, *Palarus arabicus* Pulawski in Pulawski & Prentice, *Tachytes arabicus* Guichard and *Tachytes fidelis* Pulawski, which are presumed endemic to Saudi Arabia (3.9% of the total number of species). General distribution and ecozones, and Saudi Arabian localities are given for each species. In this study two genera (*Diodontus* Curtis and *Dryudella* Spinola) and 11 species are newly recorded from Saudi Arabia.

**Keywords:** Ampulicidae; Crabronidae; Sphecidae; Faunistic list; New records; Saudi Arabia.

## 252. Some Biological Parameters and Morphological Descriptions Study on the Milkweed Bug, *Spilostethus Pandurus* Scop., (Hemiptera: Lygaeidae)

Hanan H. Awad, Heba A. S. Elelimy, Aziza H. Omar and Afaf A. Meguid

*Wulfenia Journal*, 20(5): 169--187, (2013) IF: 0.467

The milkweed bug, *Spilostethus pandurus*, is an agricultural pest in Egypt and some other tropical and subtropical areas. The objective of the present work is to clarify some biological parameters and morphological descriptions to emphasize the future researches from the ecological view point to the physiological study, biochemical study and control programs, integrated pest management program, study. Adult emergence of *S. pandurus* in summer season was higher than that in winter season. The increased longevity of *S. pandurus* was associated with prolonged rate of sexual maturation and low mean daily fecundity and that the life span increased during the cold months of the year and decreased during the hot summer and the males lived longer than females. The morphological descriptions of the adult and immature stages of *S. pandurus* were agreed with the taxonomic illustrations.

**Keywords:** Milkweed bug; Biology; Development; Morphology.

### 253. Taxonomic Revision of the Genus *Gynecaptera* Skorikov, 1935 from Egypt, With Description of a New Species (Hymenoptera: Bradynobaenidae, Aptergyninae)

Ahmed M. Soliman and Neveen S. Gadallah

*Zoology In The Middle East*, 59:3: 273-279 (2013) IF: 0.434

The genus *Gynecaptera* Skorikov (Bradynobaenidae: Aptergyninae) is revised from Egypt, based on specimens collected from the Sinai Peninsula and those deposited in Egyptian insect collections as well as recorded data from the literature. Three species were previously recorded from Egypt, *G. alexandri* (Invrea), *G. alfieri* (Invrea) and *G. trimaculata* (Skorikov). *Gynecaptera sinaitica* sp. n. is described here. An illustrated key and a faunistic list comprising all *Gynecaptera* species recorded from Egypt are also given.

**Keywords:** Aptergyninae; *Gynecaptera*; New species; Egypt.

### 254. An Annotated Catalogue of the Iranian Agathidinae and Brachistinae (Hymenoptera: Braconidae)

Neeven S. Gadallah and H. Ghahari

*Linzer Biologische Beiträge*, 45(2): 1873-1901 (2013)

The fauna of Iranian Agathidinae and Brachistinae (Hymenoptera: Braconidae) is summarized in this paper, and synonyms and distribution data are given.

In total 28 species of Agathidinae from nine genera *Agathis* LATREILLE, *Bassus* Fabricius, *Camptothrips* ENDERLEIN, *Coccygaster* SAUSSURE, *Cremonops* FÖRSTER, *Disophrys* FÖRSTER, *Earinus* WESMAEL, *Leptopylus* FÖRSTER, *Therophilus* WESMAEL, and 17 species of Brachistinae from four genera *Eubazus* NEES von ESENBECK, *Foersteria* SZÉPLIGETI, *Schizoprymnus* FÖRSTER, *Triaspis* HALIDAY are listed from the fauna of Iran. Two species of Brachistinae, *Triaspis pallipes* (NEES) and *Eubazus* (Brachistes) *minutus* (RATZEBURG) are newly recorded from Iran. Host records are also given for each species whenever available.

**Keywords:** Hymenoptera; Braconidae; Agathidinae; Brachistinae; Catalogue; Iran.

### 255. An Annotated Catalogue of the Iranian Cheloninae (Hymenoptera: Braconidae)

N.S. Gadallah and H. Ghahari

*Linzer Biologische Beiträge*, 45(2): 1921-1943 (2013)

In the present study a catalogue of the Iranian Cheloninae (Hymenoptera: Braconidae) is given. It is based on a detailed study of all available published data. In total 48 species from 4 genera including, *Ascogaster* WESMAEL (4 species), *Chelonus* PANZER (32 species), *Phanerotoma* WESMAEL (11 species) and *Phanerotomella* SZÉPLIGETI (1 species) of two tribes (Chelonini and Phanerotomini) are presented. Three species may be endemic to the Iranian fauna, *Chelonus* (Chelonus) *iranicus* TOBIAS, *Chelonus* (Chelonus) *setaceus* PAPP and *Chelonus* (Microchelonus) *iranicus* TOBIAS. A faunistic list with synonyms, host records and distribution data is provided.

**Keywords:** Hymenoptera; Ichneumonoidea; Braconidae; Cheloninae; Catalogue; Distribution; Host; Iran.

### 256. The Potential of Natural Venom of *Apis mellifera* for the Control of Grains Weevil Adults (*Sitophilus granarius*- Coleoptera- Curculionidae)

Mamdouh Ibrahim Nassar

*International Journal of Entomological Research*, 1(1): 25-31 (2013)

The natural venom of honey bees, *Apis mellifera* was applied for the control of *Sitophilus granarius* adults. Five dose levels of 1.1, 2.4, 3.7, 5.0, and 6.3 µg/insect of bee venom were tested against the adult stage of *S. granarius*. The adult mortality increased gradually and this parameter correlated with an increase in the doses of bee venom. Higher and lower mortalities were 94.3 and 20.2% after 72 hr of adult treatment with the doses of 6.3 and 1.1 µg/insect of bee venom, respectively. The LD<sub>50</sub> value of the venom was 3.9 and 3.3 µg/insect after 24 and 72 hr of adult treatment, respectively. Chemical survey of the active fraction number 10 of the venom indicated the presence of 5.47% carbon (C), 17.96% oxygen (O), 68% nitrogen (N) and 8% hydrogen (H) by using elementary analysis. Also spectrophotometer screening of the active venom fraction by using UV, IR, and MS spectrum proved the molecular weight of the active toxic components was 2847.7 MW. The chemical components of the active fraction (no. 10) supported the presence of aromatic chain attached to the functional groups of amine (NH), carboxylic (COH), and carbonyl (CO). These analyses supported the empirical chemical formula of the biological active fraction of the bee venom, which is, C<sub>31</sub>H<sub>228</sub>N<sub>38</sub>O<sub>32</sub>.

**Keywords:** Natural toxins; Bee venom; Insect control; Cereals weevils.

### 257. Ultrastructural Study on the Midgut Regions of the Milkweed Bug, *Spilostethus pandurus* Scop., (Hemiptera: Lygaeidae)

Afaf A. Meguid, Hanan H. Awad, Aziza H. Omar and Heba A.S. Elelimy

*Asian Journal of Biological Sciences*, 6(1): 54-66 (2013)

The present study aims to investigate the morphological, histological and cytological changes among the four midgut regions of *Spilostethus pandurus* adult. The adults were dissected to examine the four midgut regions. The cellular structure of the midgut was clarified by means of light and electron microscopy. The midgut consists of a single layered epithelium of two cell types. Most cells were binucleated and this may be due to active digestive properties. The midgut region has no peritrophic membrane but has internally a perimicrovillar membrane. The electron dense glycocalyx layer separates the plasma membrane from an outer or perimicrovillar membrane which is produced continuously into the midgut lumen, possibly also from secretory lysosome-like vesicles. The lysosomes and large amounts of rough endoplasmic reticulum indicate that the second, third and fourth midgut regions play a role in food digestion. The lipid in the second midgut region suggests that this region plays only a minor role in lipid absorption and energy storage. The distribution

of different cell types in *S. pandurus* midgut could be correlated with the physiology of digestion and absorption.

**Keywords:** *Spilostethus pandurus*; Midgut; Morphology; Histology; Ultrastructural.

#### Dept. of Geology

### 258. Mineral Evolution and Processes of Ferruginous Microbialite Accretion—An Example from the Middle Eocene Stromatolitic and Ooidal Ironstones of the Bahariya Depression, Western Desert, Egypt

W. Salama, M. M. El Aref and R. Gaupp

*Geobiology*, 11: 15-28 (2013) IF: 3.042

Peritidal ferruginous microbialites form the main bulk of the Middle Eocene ironstone deposits of the Bahariya Depression, Western Desert, Egypt. They include ferruginous stromatolites and microbially coated grains (ferruginous oncoids and ooids). Their internal structures reveal repeated cycles of microbial and Fe oxyhydroxide laminae. The microbial laminae consist of fossilised neutrophilic filamentous iron-oxidising bacteria. These bacteria oxidised the Fe(II)-rich acidic groundwater upon meeting the marine water at an approximately neutral pH. The iron oxyhydroxide laminae were initially precipitated as amorphous iron oxyhydroxides and subsequently recrystallised into nanocrystalline goethite during early diagenesis. Organic remains such as proteinaceous compounds, lipids, carbohydrates and carotenoids are preserved and can be identified by Raman spectroscopy. The ferruginous microbialites were subjected to post-depositional subaerial weathering associated with sea-level retreat and subsurface alteration by continued ascent of the Fe(II)-rich acidic groundwater. At this stage, another iron-oxidising bacterial generation prevailed in the acidic environment. The acidity of the groundwater was caused by oxidation of pyrite in the underlying Cenomanian Bahariya formation. The positive iron isotopic ratios and presence of ferrous and ferric iron sulphates may result from partial iron oxidation along the redox boundary in an oxygen-depleted environment.

**Keywords:** Microbialites; Ironstones; Bahariya depression; Egypt.

### 259. Syn-eruptive/inter-eruptive Relationships in Late Neoproterozoic Volcano-sedimentary Deposits of the Hamid Area, North Eastern Desert, Egypt

Ezz El Din Abdel Hakim Khalaf

*Bulletin of Volcanology*, 75: 1-31 (2013) IF: 2.653

Nonmarine volcano-sedimentary successions in the Late Neoproterozoic Hamid Basin were studied in order to examine the distinctive characteristics of accumulation during syn-eruptive and inter-eruptive periods in a depocenter associated with active volcanism and both extensional and dextral strike-slip tectonics. In particular, the syn-rift fill in this area comprises a wide range of compositions and transport and depositional processes in which lava flows coexist with pyroclastic and epiclastic deposits in the same accumulation space. Seven different accumulation units were identified in the syn-rift fill: (1) polymictic alluvial fan units, (2) fluvial braid plain units, (3) lacustrine units, (4) coherent volcanic bodies/shallow intrusion units, (5) pyroclastic

fall units, (6) phreatomagmatic volcanic units, and (7) pyroclastic density current units. These deposits are organized into several stratal packages with contrasting geometries. Analysis of these units and the relationships between them provided insights into the evolution of the syn-rift sedimentary environments and permitted identification of different stages of effusive activity, explosive activity, and relative quiescence, determining syn-eruptive and inter-eruptive rock units. These units provide important clues to the distribution of, and temporal changes in, accommodation space, and hence the configuration and structural evolution of the Hamid Basin. Two accumulation stages were defined. The underfilled stage occurs when the material supplied to the depocenter during the eruptive events is not enough to level the existing topography, allowing the development of high-gradient alluvial systems during the next inter-eruptive period. The overfilled stage occurs when extensive pyroclastic density current deposits choke the accumulation space during syn-eruptive periods, causing low-gradient sedimentary systems to develop during the subsequent inter-eruptive periods. The Hamid Basin is thus interpreted to have been hybrid in nature, influenced by the dynamic changes of the basin-margin faults, which were either normal or strike-slip.

**Keywords:** Volcanic rifts; Syn-eruptive; Inter-eruptive.

### 260. Tectonostratigraphy and Depositional History of the Neoproterozoic Volcano-Sedimentary Sequences in Kid Area, Southeastern Sinai, Egypt: Implications for Intra-Arc to Foreland Basin in the Northern Arabian–Nubian Shield

Ezz El Din A. Khalaf and M. A. Obeid

*Journal of Asian Earth Sciences*, 73: 473-503 (2013) IF: 2.379

This paper presents a stratigraphic and sedimentary study of Neoproterozoic successions of the South Sinai, at the northernmost segment of the Arabian–Nubian Shield (ANS), including the Kid complex. This complex is composed predominantly of thick volcano-sedimentary successions representing different depositional and tectonic environments, followed by four deformational phases including folding and brittle faults ( $D_1$ – $D_4$ ). The whole Kid area is divisible from north to south into the lower, middle, and upper rock sequences. The higher metamorphic grade and extensive deformational styles of the lower sequence distinguishes them from the middle and upper sequences. Principal lithofacies in the lower sequence include thrust-imbricated tectonic slice of metasediments and metavolcanics, whereas the middle and upper sequences are made up of clastic sediments, intermediate-felsic lavas, volcanoclastics, and dike swarms. Two distinct Paleo- depositional environments are observed: deep-marine and alluvial fan regime. The former occurred mainly during the lower sequence, whereas the latter developed during the other two sequences. These alternations of depositional conditions in the volcano-sedimentary deposits suggest that the Kid area may have formed under a transitional climate regime fluctuating gradually from warm and dry to warm and humid conditions. Geochemical and petrographical data, in conjunction with field relationships, suggest that the investigated volcano-sedimentary rocks were built from detritus derived from a wide range of sources, ranging from Paleoproterozoic to Neoproterozoic continental crust. Deposition within the ancient Kid basin reflects a complete basin cycle from rifting and passive margin development, to intra-arc and foreland basin development



and, finally, basin closure. The early phase of basin evolution is similar to various basins in the Taupo volcanics, whereas the later phases are similar to the Cordilleran-type foreland basin. The progressive change in lithofacies from marine intra-arc basin to continental molasses foreland basin and from compression to extension setting respectively, imply that the source area became peneplained, where the Kid basin became stabilized as sedimentation progressed following uplift. The scenario proposed of the study area supports the role of volcanic and tectonic events in architecting the facies and stratigraphic development.

**Keywords:** Egypt; Wadi kid volcanics; Lithostratigraphy; Depositional environment; Tectonic evolution.

### 261. Petrology and Geochemistry of the Tertiary Suez Rift Volcanism, Sinai, Egypt

N.A. Shallaly, C. Beier, K.M. Haase and M. S. Hammed

*Journal of Volcanology and Geothermal Research*, 267: 119-137 (2013) IF: 2.193

The Tertiary basaltic rocks of Southwestern Sinai, situated along the Wadi Nukhul–Wadi Matullah–Wadi El Tayiba join, were selected to study the Gulf of Suez rift related-lavas and their geochemical and petrological relation with the rifting process. Whole rock samples were studied petrographically and analysed for major and trace elements. The samples from dykes, sills and flows from multiple magmatic events display a large variety in texture and in modal mineral compositions. They range from olivine dolerites and olivine-bearing basalts to vitrophyric, texturally heterogeneous basalts and crystal lithic tuffs. The transitional tholeiitic basalts display low compatible element concentrations and an enrichment of the whole spectrum of the incompatible elements. Major, trace and Rare Earth Element data suggest that the melts formed by 5% melting of mantle peridotite at the spinel–garnet transition zone (80–90km depth), in the presence of 2–4% residual garnet. During the melt ascent, the fractionating phases were olivine, clinopyroxene and, to a lesser extent, plagioclase.

Thermobarometric calculations indicate the presence of two crystallization levels beneath the Gulf of Suez rift: a shallower stage at 15–20km and a deeper stage at depths of 25–30km. The mantle source consists of streaks and blobs of enriched mantle, preserved in the geochemical signatures of these rocks. The enriched mantle sources melted preferentially compared to the surrounding ambient mantle and thus led to a preferential enrichment of the sources of the Gulf of Suez rift.

**Keywords:** Gulf of Suez rift; Geochemistry; Thermobarometry; Basalt; Petrology; Egypt.

### 262. Holocene Paleoenvironmental, Paleoclimatic and Geoarchaeological Significance of the Sheikh El-Obeiyid Area (Farafra Oasis, Egypt)

Mohamed A. Hamdan and Giulio Lucarini

*Quaternary International*, 302: 154-168 (2013) IF: 1.962

The present paper focuses on the combination of archaeological and geological data sets in order to obtain a synthesis of Holocene occupational and environmental history in the Sheikh El-Obeiyid region of the Farafra Depression, Egypt. In this region, the Epipalaeolithic and Saharan Pastoral Neolithic sites are

distributed along different landscape elements of the Sheikh El-Obeiyid Plateau, escarpment and Bir El-Obeiyid Depression, respectively. Three phases of playa formation were recorded at the Bir El-Obeiyid basin and at the top of the Sheikh Obeiyid Plateau, corresponding to humid conditions during the early/mid Holocene. The  $^{14}\text{C}$  dates obtained from the excavated hearths at Sheikh El-Obeiyid indicate the presence of three occupation phases, confirmed by the different characteristics of the lithic assemblages and playa generations: P<sub>I</sub>, P<sub>II</sub>, and P<sub>III</sub>. Early Holocene occupation is associated with lithic artefacts of high blade and microlithic index and backed retouched tools.

The Middle Holocene is represented by two occupations: the early and late middle Holocene. The former is linked with bifacial knives, gouges, discoidal side scrapers, tools with foliated retouch, and lens-shaped arrowheads. The last horizon points to a final Middle Holocene exploitation phase of the area, probably by small groups of herders who periodically visited the region when the climate had already started to deteriorate. The Sheikh El-Obeiyid Village lies on the second erosion surface of the Northern Plateau. It is characterised by 30 circular or elliptical structures, of various sizes, grouped together and located near the edge of the terrace, commanding the Bir El-Obeiyid playa below. Radiocarbon dating of charcoal recovered from the structures indicates that the village was used between  $7930 \pm 123$  and  $7930 \pm 144$  cal. BP.

**Keywords:** Farafra; Playa; Geoarchaeology; Holocene; Egypt.

### 263. Palynology and Genetic Sequence Stratigraphy of the Reservoir Rocks (Cenomanian, Bahariya Formation) in the Salam Oil Field, North Western Desert, Egypt

Sameh S. Tahoun and Omar Mohamed

*Cretaceous Research*, 45: 342-351 (2013) IF: 1.63

Twenty-eight samples from the Bahariya Formation of the Salam-17 Well in the north Western Desert were palynologically investigated. These samples are of Cenomanian age. Fair diversity and fair to moderately preserved palynomorph assemblage has been recovered.

Among them, the dinoflagellate cysts showed very poor diversity and abundance. Four miospore zones have been informally identified in the lower Cenomanian. Various palynofacies criteria, adopted from previous publications (e.g. relative particle abundance data, brown to black wood ratio, equi-dimensional to lath-shaped black wood ratio, average size of phytoclasts and spores/pollen ratio) are applied as alternative indicators to monitor the proximal–distal trends instead of the marine palynomorphs-based parameters. The method can be applied in the Egyptian Western Desert to overcome the rarity and absence of dinoflagellate cysts in the recovered organic residues. The palynofacies study of the section demonstrates a predominantly regressive phase, characterized by deltaic, distributary or tidal channels, interrupted by short-lived marine incursions. The palynofacies trends within the studied succession indicate six genetic sequences informally described as Genetic Stratigraphic Sequences A through F.

**Keywords:** Genetic sequences; Palynofacies; Cenomanian; Bahariya formation; North western desert.

#### 264. *Stephanodiscus* Ehr. Species from Holocene Sediments in the Faiyum Depression (Middle Egypt)

R.J. Flower, K. Keatings, M.A. Hamdan and F.A. Hassan

*Phytotaxa*, 127 (1): 66-80 (2013) IF: 1.295

Lake Qarun in the Egyptian Faiyum Depression is the shrunken remnant of a much larger lake. To investigate the sedimentary history of the former lake, several continuous lacustrine sediment cores were collected from now terrestrial locations within the basin. The suitability of these sediments for reconstructing past environmental changes was first assessed by describing the gross stratigraphies of three core sequences and secondly by evaluating taxonomic issues concerning sedimentary diatom species within the genus, *Stephanodiscus* Ehr. The stratigraphic descriptions show basal sections comprised of either coarse sand or weathered Eocene limestone overlain by lacustrine sediments. Lower sections of the lacustrine sediments are diatom marls, and, in the two lakeside cores, these are laminated. These sections indicate that the lake initially formed by rapid infilling to a considerable depth with freshwater and the diatom-rich marls containing abundant *Stephanodiscus* and *Aulacoseira* Thwaites species. A new species and variety of *Stephanodiscus*, *S. neoaegypticus* and *S. neoaegypticus* var. *fekrii*, are described from the marl section in one core. Another species, *S. galileenis* Håkansson & Erhlich, was also present and is re-evaluated with reference to the published description. The importance of establishing a sound taxonomic foundation for palaeolimnological studies of Lake Qarun is stressed.

**Keywords:** Faiyum; Lake Qarun; Diatoms; Holocene; Paleoclimate.

#### 265. Variations in Eruptive Style and Depositional Processes of Neoproterozoic Terrestrial Volcano-sedimentary Successions in the Hamid Area, North Eastern Desert, Egypt

Ezz El Din Abdel Hakim Khalaf

*Journal of African Earth Science*, 83: 74-103 (2013) IF: 1.229

Two contrasting Neoproterozoic volcano-sedimentary successions of ca. 600 m thickness were recognized in the Hamid area, Northeastern Desert, Egypt. A lower Hamid succession consists of alluvial sediments, coherent lava flows, pyroclastic fall and flow deposits. An upper Hamid succession includes deposits from pyroclastic density currents, sills, and dykes. Sedimentological studies at different scales in the Hamid area show a very complex interaction of fluvial, eruptive, and gravitational processes in time and space and thus provided meaningful insights into the evolution of the rift sedimentary environments and the identification of different stages of effusive activity, explosive activity, and relative quiescence, determining syn-eruptive and inter-eruptive rock units.

The volcano-sedimentary deposits of the study area can be ascribed to 14 facies and 7 facies associations: (1) basin-border alluvial fan, (2) mixed sandy fluvial braid plain, (3) bed-load-dominated ephemeral lake, (4) lava flows and volcanoclastic, (5) pyroclastic fall deposits, (6) phreatomagmatic volcanic deposits, and (7) pyroclastic density current deposits. These systems are in part coeval and in part succeed each other, forming five phases of basin evolution: (i) an opening phase including

alluvial fan and valley flooding together with lacustrine period, (ii) a phase of effusive and explosive volcanism (pulsatory phase), (iii) a phase of predominant explosive and deposition from base surges (collapsing phase), and (iv) a phase of caldera eruption and ignimbrite-forming processes (climactic phase). The facies architecture records volcanic activity from mainly phreatomagmatic eruptions, producing large volumes of lava flows and pyroclastics (pulsatory and collapsing phase), to highly explosive, pumice-rich plinian-type pyroclastic density current deposits (climactic phase). Hamid area is a small-volume volcano, however, its magma compositions, eruption styles, and interruptive breaks suggest that it closely resembles a volcanic architecture commonly associated with large, composite volcanoes.

**Keywords:** Hamid area; Volcano-sedimentary successions; Vent; Eruption column dynamics.

#### 266. Diagenetic Evolution of the Volcaniclastic Deposits: An Example from Neoproterozoic Dokhan Volcanics in Wadi Queih Basin, Central Eastern Desert, Egypt

Ezz El Din Abdel Hakim Khalaf

*Arabian Journal of Geosciences*, (2013) IF: 0.74

Wadi Queih basin hosts a ~2,500-m thick Neoproterozoic volcanoclastic successions that unconformably lie over the oldest Precambrian basement. These successions were deposited in alluvial fan, fluvial, lacustrine, and aeolian depositional environments. Diagenetic minerals from these volcanoclastic successions were studied by X-ray diffractometry, scanning electron microscopy, and analytical electron microscopy. The diagenetic processes recognized include mechanical compaction, cementation, and dissolution.

Based on the framework grain-cement relationships, precipitation of the early calcite cement was either accompanied or followed by the development of part of the pore lining and pore-filling clay cements. Secondary porosity development occurred due to partial to complete dissolution of early calcite cement and feldspar grains. In addition to calcite, several different clay minerals including kaolinite, illite, and chlorite with minor smectite occur as pore-filling and pore-lining cements. Chlorite coating grains helps to retain primary porosity by retarding the envelopment of quartz overgrowths. Clay minerals and their diagenetic assemblages have been distinguished between primary volcanoclastics directly produced by pyroclastic eruptions and epiclastic volcanoclastics derived from erosion of the pre-existing volcanic rocks. Phyllosilicates of the epiclastic rocks display wider compositional variations owing to wide variations in the mineralogical and chemical compositions of the parent material. Most of the phyllosilicates (kaolinite, illite, chlorite, mica, and smectite) are inherited minerals derived from the erosion of the volcanic basement complex, which had undergone hydrothermal alteration. Smectites of the epiclastic rocks are beidellite-montmorillonite derived from the altered volcanic materials of the sedimentary environment. Conversely, phyllosilicate minerals of the pyroclastic rocks are dominated by kaolinite, illite, and mica, which were formed by pedogenetic processes through the hydrothermal influence.

**Keywords:** Volcaniclastic sediments; Queih basin.

## 267. Sedimentological Characteristics and Geochemical Evolution of Nabq Sabkha, Gulf of Aqaba, Sinai, Egypt

Osama Elsayed Attia

*Arabian Journal of Geosciences*, 6 (6): 2045-2059 (2013)

IF: 0.74

Nabq sabkha exists 16 km north of Sharm El Sheikh City occupying the low land topography in the alluvial fan zone along the coastal area, Gulf of Aqaba, Sinai, Egypt. The long axis of the sabkha trends NW–SE receiving water from two different sources: meteoric water drained from the surrounding mountainous area and seawater seepage. Field observations help to divide the area into raised beach, hill slopes, sabkha basin, and coastal area. The sabkha basin can be subdivided from its center outward into (1) basin center hypersaline lake flourished with microbial mat and precipitation of halite as rafts, cumulates, and chevrons, (2) saturated saline sand and/or mud flat zone with the extensive growth of gypsum and halite crystals growing displacively as well as different forms of petee structures, and (3) an elevated marginal dry zone with tepee structures. Mineralogical analysis reveals that quartz, halite, and gypsum are the dominant minerals with subordinate amount of aragonite, anhydrite, thenardite, and/or polyhalite. In addition, clay minerals in the mudflat zone are presented by illite and smectite, indicating derivation of soil from the surrounding basement rocks.

Chemical analysis of the collected brine samples reveals alkali character in the saline lake (pH07.6) and high concentrations of  $\text{Na}^+$  (680 meq/l),  $\text{Cl}^-$  (940 meq/l),  $\text{Mg}^{2+}$  (208 meq/l),  $\text{Ca}^{2+}$  (70 meq/l),  $\text{SO}_4^{2-}$  (30 meq/l), and  $\text{HCO}_3^-$  (6 meq/l). The high salinity values are due to the aridity of the area, which favors precipitation of halite. Using comparative sedimentological, chemical, and mineralogical methods between such modern and ancient evaporitic environments and by detailed field, petrographic and mineralogical studies of modern evaporite environments help to interpret paleo-depositional environments of ancient evaporites sequences still in debate.

**Keywords:** Nabq sabkha; Sedimentology; Evaporites.

## 268. Foraminiferal Biostratigraphy of the Pliocene-Pleistocene Deep Marine Offshore, North Nile Delta, Egypt

Nabil M. Aboul Ela, Samy A. Mohamed and Ahmed Z. Ibrahim

*Micropaleontology*, 59: 285-304 (2013) IF: 0.706

A high resolution biostratigraphic analysis of the Pliocene–Pleistocene sequence of the offshore Nile Delta region in West Nile Delta Deep Marine Concession (WDDM), in which 29 planktonic foraminiferal species belonging to 8 genera and 51 benthic foraminiferal species belonging to 40 genera were identified, allowed the recognition of seven foraminiferal zones and two subzones. These are as follows: Sphaeroidinellopsis Acme Zone (MP11), Globorotalia margaritae Zone (MP12), Globorotalia puncticulata/Globorotalia margaritae Zone (MP13), Sphaeroidinellopsis s.l. Zone (MP14), Globorotalia puncticulata Subzone (MP14a), Globorotalia planispira Subzone (MP14b), Globigerinoides elongatus Zone (MP15), Globorotalia inflata Zone (MP16) and Hyaline balthica Zone.

**Keywords:** Pliocene; Pleistocene; Foraminifera; Biostratigraphy; Nile delta.

## 269. Geochemical Characterization of Middle Eocene Sediments in Helwan Area, Greater Cairo, Egypt

Mohamed Mohamed El Kammar

*Life Science Journal*, 10(11s): 170-178, (2013) IF: 0.165

The Middle Eocene sediments of Qurn and Wadi Garawi formations exposed in the area east of Helwan have been categorized on geochemical basis. Major oxides and trace elements, including the REE, were determined by ICP-MS. This work focuses on the role of the clastic admixture and diagenetic processes on the geochemistry of the marine carbonates. The normalization of the clay-rich limestone to the almost pure limestone points to the significant role of clay admixture as prominent accumulator of trace elements, especially Cu, Pb, Ni, U, Th and REE. The analyzed sediments were generally depleted in Ce, suggesting an influential role of marine conditions, especially when clayey and ferruginous materials are not abundant. The marine versus terrestrial character was best documented by the Y/Ho ratio in the studied sediments. Heavy metals such as Cr, V and as were scavenged by the ferruginous material. The recrystallization of carbonate leads to purification of carbonate sediments, hence, the depletion in content of most major and trace elements. The REE pattern of the recrystallized carbonate displayed clear tetrad effect.

**Keywords:** REE; Geochemistry; Maadi group; Limestone; Eocene; Egypt.

## 270. The Environmental Impact on the Hydrogeochemical Characterization of the Kurkar Aquifer System, Gaza Strip, Palestine

Naglaa S. Mohamed, Ahmed N. Shahin, Ahmed M. El-Kammar

*Life Science Journal*, 10(11s): 158-169 (2013) IF: 0.165

The Gaza strip is suffering groundwater deterioration as a result of high population density where the outflow exceeds inflow by about 20 Mm<sup>3</sup>/y. This quantity of water is believed to be replaced by deep seawater intrusion and/or upconing of deep brines in the southern areas or by anthropogenic wastewater. Large cones of depression have been formed over the last 40 years within the Gaza, Khan Younis, and Rafah governorates. The salinity increases in the northwestern and the southeastern parts of Gaza Strip. Nitrate and chloride exceed the WHO maximum permissible limits and are considered as the major pollutants of the aquifer, their high concentration values are attributed to agricultural activity and leaked wastewaters as well as the scarcity of the resource. The cluster analysis (Q-mode) classified the data into 5 clusters and 3 independent cases depending upon salinity and nitrate concentrations. The rotated factor analysis identified 3 factors. The AquaChem program clarified that the study area was supersaturated with calcite and dolomite and undersaturated with gypsum and anhydrite minerals. In general, the groundwater was unsuitable for drinking according to their TDS and NO<sub>3</sub> contents. The groundwater can be used in permeable soils for irrigation purposes.

**Keywords:** Environmental assessment; Hydrogeology; Hydrogeochemistry; Modeling; Gaza strip.

### 271. The Archaeological Mission of “L’Orientale” in the Central-eastern Desert of Egypt

Marco Barbarino, Andrea Manzo, Mohamed Hamdan and Yaser Abd el-Rahman

*Newsletter Di Archeologia CISA*, 4: 47-156 (2013)

The Italian project in the Central-Eastern Desert - promoted by the Italian Embassy in Egypt and directed by Irene Bragantini - is a joint project of different Italian and Egyptian institutions (Università degli Studi di Napoli “L’Orientale”, University of Cairo, Faculty of Geology, and University of Helwan, Faculty of Archaeology), and is aimed at investigating the central area of the Eastern Desert<sup>1</sup>. The cooperation between archaeologists and geologists aims at conducting a geoarchaeological survey of the region, in order to investigate the natural resources, the exploitation in the different periods, and the economic and commercial potential of the area. The methodology we want to follow and the problems we will be confronted with, demand in fact the cooperation of different scientific fields in order to reconstruct a geo-economic landscape.

**Keywords:** Wadi gasus; Archaeology; Precambrian rocks; Gold mines.

#### Dept. of Geophysics

### 272. Detection of Magnetically Susceptible Dyke Swarms in a Fresh Coastal Aquifer

Mohamed hasan mahmoud khalil

*Pure and Applied Geophysics*, 170(8): 1-17 (2013) IF: 1.617

Groundwater constitutes the main source of freshwater in Shalatein, on the western coast of the Red Sea, in Egypt. The fresh aquifer of Shalatein is intensively dissected by shallow and deep faults associated with the occurrence of dykes and/or dyke swarms. In this context, synthesis of electrical resistivity, ground magnetics, and borehole data was implemented to investigate the freshwater aquifer condition, locate the intrusive dykes and/or dyke swarms, and demarcate the potential freshwater zones. Nine Schlumberger VES's with maximum current electrode half-spacing (AB/2) of 682 m were conducted. The subsurface was successfully delineated by general four layers. The fresh aquifer of the Quaternary and Pre-Quaternary alluvium sediments was effectively demarcated with true resistivities ranged from 30 to 105 Om and thickness ranged between 20 and 60 m. A ground magnetic survey comprised 35 magnetic profiles, each 7 km in length. Magnetic data interpretation of the vertical derivatives (first and second order), downward continuation (100 m), apparent susceptibility (depth of 100 m), and wavelength filters (Butterworth high-pass of wavelengths <100 m and Band-Pass of wavelengths 30–100 m) successfully distinguished the near surface structure with five major clusters of dyke swarms, whereas filters of the upward continuation (300 m) and Butterworth low-pass (wavelengths >300 m) clearly reflected the deep-seated structure. The computed depth by the 3D Euler deconvolution for geological contacts and faults (SI = 0) ranged from 14 to 545 m, whereas for dyke and sill (SI = 1), it ranged from 10 to 1,095 m. The western part of the study area is recommended as a potential freshwater zone as it is characterized by depths >100 m to the top of the dykes, higher thickness of the fresh aquifer (45–60 m), depths to the top of the fresh aquifer

ranging from 25 to 40 m, and higher resistivities reflecting better freshwater quality (70–105 Ωm).

**Keywords:** Dyke swarms; Around magnetics; Ves; Vertical derivatives; Apparent susceptibility; Wavelength filters; Continuation filters; 3Deuler deconvolution.

### 273. Inversion Approach to Estimate Acoustic Impedance from Petrophysical Data in Absence of Density and Sonic Logs

Walid M. Mabrouk and Ahmed M. Hassan

*Journal of Petroleum Science and Engineering*, 110: 1-6 (2013) IF: 0.997

Acoustic impedance is an important parameter for seismic and direct geologic interpretation and can be defined as the product of density and velocity, in the absence of density data or if the well suffers from a rough hole condition and/or irregularities, and also in absence of velocity or sonic data, another approach to determine such an important parameter must be used.

This paper aims to introduce a new definition for the acoustic impedance by introducing a formula for estimating such a parameter from Neutron log and also contains the effect of matrix and fluid. This formula depends mainly upon the density response equation, the elastic definition of the impedance and on Raigal-clemenceau et al. (1988) equation.

Test and application of the suggested approach in two intervals from different wells in the Gulf of Suez Basin of Egypt reflect how far such treatment is more or less reliable and accurate.

**Keywords:** Seismic impedance; Acoustic impedance.

### 274. New Method to Calculate the Formation Water Resistivity ( $R_w$ )

Walid M. mabrouk, Khaled S. Soliman and Samar S. Anas

*Journal of Petroleum Science and Engineering*, 104: 49-52 (2013) IF: 0.997

One of the most important parameters needed to calculate hydrocarbon in place from wireline logs is the resistivity of connate water ( $R_w$ ) in a formation of interest. Connate water or interstitial water is the water, uncontaminated by drilling mud that saturates the porous formation rock. The resistivity of this formation water is an important interpretation parameter since it is required for the calculation of saturations (water and/or hydrocarbon) from the basic resistivity logs. The most accurate method of determining this value is by measuring the resistivity or chemical composition of uncontaminated connate water produced from the formation. In case that the formation does not produce any connate water, e.g., deep basin and tight gas plays, or the produced water is contaminated it is difficult to determine accurate  $R_w$  necessary for reliable hydrocarbon-in-place calculation from logs. This paper presents a numerical method to determine connate water resistivity from the true formation resistivity. The method was tested using synthetic and real field data to ensure its ability in determining formation water resistivity.

**Keywords:** Archie equation; Connate water resistivity; Formation resistivity parameters  $R_w$ - $R_t$ .

**275. Petrophysical Analysis for Ammonite-1 Well, Farafra Area, Western Desert, Egypt**

Ahmed M. Hassan, Walid M. Mabrouk and Khamis M. Farhoud

*Arabian Journal of Geosciences*, 2013: -, (2013) IF: 0.740

The purpose of this paper is mainly twofold: (1) to introduce a complete review on the major petrophysical parameters and (2) to design a work flow for the qualitative and quantitative interpretation of any well logging data and applying this work flow on Ammonite-1 well in the Western Desert, Egypt. Finally, the formation rock model will be created so that at each depth the volume of shale, matrix, water, and hydrocarbon could be determined. This model provides direct method for quantitative interpretation for the petrophysical parameters such as shale, porosity ( $\phi$ ), and saturation ( $S_w$  and  $S_h$ ) which are the most important for the geologists, geophysicists, petrophysicists, and engineers.

**Keywords:** Ammonite-1 well; Formation rock model; Petrophysical parameters.

**276. A Least-Squares Window Curves Method to Interpret Gravity Data Due to Dipping Faults**

E. M. Abdelrahman, K. S. Essa and E. R. Abo-Ezz

*J. of Geophysics and Engineering*, 10 (9pp): (2013) IF: 0.721

We have developed a least-squares method to determine simultaneously the depth and the dip angle of a buried fault from first moving average residual gravity anomalies using filters of successive window lengths. The method involves using a relationship between the depth and the dip angle of the source and a combination of windowed observations. The relationship represents a family of curves (window curves). For a fixed window length, the depth is determined for each dip angle value by solving one nonlinear equation of the form  $f(z) = 0$  using the least-squares method. The computed depths are plotted against the dip angle values representing a continuous curve. The solution for the depth and the dip angle of the buried fault is read at the common intersection of the window curves. The method involves using a dipping faulted thin slab model convolved with the same moving average filter as applied to the observed data. As a result, this method can be applied to residuals as well as to measured gravity data. The method is applied to theoretical data with and without random errors. The validity of the method is tested on gravity data from Egypt. In all cases examined, the model parameters obtained are in good agreement with the actual ones and with those given in the published literature.

**Keywords:** Gravity dipping faults; Depth and dip angle solutions; Least-squares method; Window curves method.

**277. Gravity Interpretation of Dipping Faults Using the Variance Analysis Method**

Khalid Sayed Essa

*Journal of Geophysics and Engineering*, 10 (7PP): (2013) IF: 0.721

A new algorithm is developed to estimate simultaneously the depth and the dip angle of a buried fault from the normalized gravity gradient data. This algorithm utilizes numerical first

horizontal derivatives computed from the observed gravity anomaly, using filters of successive window lengths to estimate the depth and the dip angle of a buried dipping fault structure. For a fixed window length, the depth is estimated using a least-squares sense for each dip angle. The method is based on computing the variance of the depths determined from all horizontal gradient anomaly profiles using the least-squares method for each dip angle. The minimum variance is used as a criterion for determining the correct dip angle and depth of the buried structure. When the correct dip angle is used, the variance of the depths is always less than the variances computed using wrong dip angles. The technique can be applied not only to the true residuals, but also to the measured Bouguer gravity data. The method is applied to synthetic data with and without random errors and two field examples from Egypt and Scotland. In all cases examined, the estimated depths and other model parameters are found to be in good agreement with the actual values.

**Keywords:** Normalized gravity gradient anomaly; Dipping fault; Depth; Dip angle.

**278. A New Approach to Semi-infinite Thin Slab Depth Determination from Second Moving Average Residual Gravity Anomalies**

El-Sayed M. Abdelrahman and Khalid S. Essa

*Exploration Geophysics*, 44(3): 185-191 (2013) IF: 0.667

In this paper, we have developed a new least-squares minimisation approach to determine the depth of a buried faulted structure approximated by a 2D semi-infinite horizontal slab from second moving average residual gravity anomalies. The problem of depth determination has been transformed into a problem of finding the solution to a nonlinear equation of the form  $z = f(z)$ . The method can be applied not only to residuals but also to observed data. The method overcomes the problems associated with determining the depth from successive horizontal derivative anomalies obtained from 2D gravity data using filters of successive graticule spacings. The method is applied to theoretical data with and without random errors and is tested on a field example from Egypt. In all cases, the depth solution obtained is in good agreement with the actual depth.

**Keywords:** Faults; Gravity interpretation; Least-squares method; Second moving average method.

**Dept. of Mathematics****279. Higgs Vacuum Stability in the B-L Extended Standard Model**

Alakabha Datta, A. Elsayed, S. Khalil and A. Moursy

*Physical Review, D* 88: (2013) IF: 4.691

We study vacuum stability of B-L extension of the Standard Model (SM) and its supersymmetric version. We show that the generation of nonvanishing neutrino masses through TeV inverse seesaw mechanism leads to a cutoff scale of SM Higgs potential stability of order  $10^5$  GeV. However, in the nonsupersymmetric B-L model, we find that the mixing between the SM-like Higgs boson and the B-L Higgs boson plays a crucial role in alleviating the vacuum stability problem. We also provide the constraints of stabilizing the Higgs potential in the supersymmetric B-L model.

**Keywords:** Vacuum stability; Supersymmetric B-L model.



## 280. Right-Handed Sneutrino-antisneutrino Oscillations in a TeV Scale Supersymmetric B-L Model

A. Elsayed, S. Khalil, S. Moretti and A. Moursy

*Physical Review, D* 87 (2013) IF: 4.691

We explore right-handed sneutrino-antisneutrino mixing in a TeV-scale B-L extension of the Minimal Supersymmetric Standard Model, where a type-I seesaw mechanism of light neutrino mass generation is naturally implemented. The constraints imposed on the mass splitting between a heavy right-handed sneutrino and the corresponding antisneutrino by the experimental limits set on the light neutrino masses are investigated. We also study direct pair production of such right-handed sneutrinos at the Large Hadron Collider and their decay modes, emphasizing that their decay into same-sign dilepton pairs is a salient feature for probing these particles at the CERN machine. Finally, the charge asymmetry present in such same-sign dilepton signals is also analyzed and confirms itself as a further useful handle to extract information about the oscillation dynamics.

**Keywords:** Sneutrino-antisneutrino mixing; Large hadron collider; Same-sign dilepton.

## 281. TeV Scale Leptogenesis in B-L Model With Alternative Cosmologies

W. Abdallah, D. Delepinec and S. Khalil

*Physics Letters B*, 725: 361-367 (2013) IF: 4.569

In TeV scale B-L extension of the standard model with inverse seesaw, the Yukawa coupling of right-handed neutrinos can be of order one. This implies that the out-of-equilibrium condition for leptogenesis within the standard cosmology is not satisfied. We provide two scenarios for overcoming this problem and generating the desired value of the baryon asymmetry of the Universe. The first scenario is based on the extra-dimensional braneworld effects that modify the Friedman equation. We show that in this case the value of the baryon asymmetry of the Universe constrains the five-dimensional Planck mass to be of order 100 TeV. In the second scenario a non-thermal right-handed neutrino produced by the decay of a heavy moduli is assumed. In this case, we emphasize that it is possible to generate the required baryon asymmetry of the Universe for TeV scale right-handed neutrinos.

**Keywords:** Leptogenesis; Inverse seesaw; Extra-dimensional braneworld.

## 282. The Role of the Bacterial Mismatch Repair System in SoS-induced Mutagenesis: A theoretical Background

Oleg V. Belov, Ochbadrakh Chuluunbaatar, M. I. Kapralov and N. H. Sweilam

*Journal of Theoretical Biology*, 332: 30-41 (2013) IF: 2.496

A theoretical study is performed of the possible role of the methyl directed mismatch repair system in the ultraviolet-induced mutagenesis of *Escherichia coli* bacterial cells. For this purpose,

mathematical models of the SOS network, translesion synthesis and mismatch repair are developed. Within the proposed models, the key pathways of these repair systems were simulated on the basis of modern experimental data related to their mechanisms. Our model approach shows a possible mechanistic explanation of the hypothesis that the bacterial mismatch repair system is responsible for attenuation of mutation frequency during ultraviolet-induced SOS response via removal of the nucleotides misincorporated by DNA polymerase V (the UmuD<sub>2</sub>C complex).

**Keywords:** SOS response; Mismatch repair; UV mutagenesis Mathematical Modeling Method.

## 283. New Algorithms for Solving High Even-order Differential Equations using third and Fourth Chebyshev-galerkin Methods

E.H. Doha, W.M. Abd-Elhameed and M.A. Bassuony

*Journal of Computational Physics*, 236: 563-579 (2013) IF: 2.138

This paper is concerned with spectral Galerkin algorithms for solving high even-order two point boundary value problems in one dimension subject to homogeneous and nonhomogeneous boundary conditions. The proposed algorithms are extended to solve two-dimensional high even-order differential equations. The key to the efficiency of these algorithms is to construct compact combinations of Chebyshev polynomials of the third and fourth kinds as basis functions. The algorithms lead to linear systems with specially structured matrices that can be efficiently inverted. Numerical examples are included to demonstrate the validity and applicability of the proposed algorithms, and some comparisons with some other methods are made.

**Keywords:** Spectral-galerkin method; Chebyshev polynomials of the third and fourth kinds; High even-order two point boundary value problems.

## 284. Exact Solutions of Space Dependent Korteweg-de Vries Equation by the Extended Unified Method

Hamdy I. Abdel-Gawad, Nasser S. Elazaby and Mohamed Osman

*Journal of the Physical Society of Japan*, 82 (4): (2013) IF: 2.087

Recently the unified method for finding traveling wave solutions of nonlinear evolution equations was proposed by one of the authors (HIAG). It was shown that, this method unifies all the methods being used to find these solutions. In this paper, we extend this method to find a class of formal exact solutions to Korteweg-de Vries equation with space dependent coefficients.

**Keywords:** Exact solution; Extended unified method; Korteweg-de Vries equation; Variable coefficients.

## 285. Numerical Solution of Some Types of Fractional Optimal Control Problems

Nasser Hassan Sweilam, Tamer Mostafa Al-Ajami and Ronald H.W. Hoppe

*The Scientificworld Journal*, (2013) IF: 1.73

We present two different approaches for the numerical solution of fractional optimal control problems (FOCPs) based on a spectral method using Chebyshev polynomials. The fractional derivative

is described in the Caputo sense. The first approach follows the paradigm “optimize first, then discretize” and relies on the approximation of the necessary optimality conditions in terms of the associated Hamiltonian. In the second approach, the state equation is discretized first using the Clenshaw and Curtis scheme for the numerical integration of nonsingular functions followed by the Rayleigh-Ritz method to evaluate both the state and control variables. Two illustrative examples are included to demonstrate the validity and applicability of the suggested approaches.

**Keywords:** Fractional optimal control problems; Spectral method using Chebyshev polynomials.

## 286. On the Approximate Solutions for System of Fractional Integro-differential Equations Using Chebyshev Pseudo-spectral Method

M. M. Khader and N. H. Sweilam

*Applied Mathematical Modelling*, 37: 9819-9828 (2013)

IF: 1.706

In this paper, we implement Chebyshev pseudo-spectral method for solving numerically system of linear and non-linear fractional integro-differential equations of Volterra type.

The proposed technique is based on the new derived formula of the Caputo fractional derivative. The suggested method reduces this type of systems to the solution of system of linear or non-linear algebraic equations. We give the convergence analysis and derive an upper bound of the error for the derived formula. To demonstrate the validity and applicability of the suggested method, some test examples are given. Also, we present a comparison with the previous work using the homotopy perturbation method.

**Keywords:** Chebyshev pseudo-spectral method; Systems of fractional integro-differential; Equations of Volterra type; Caputo fractional derivative; Convergence analysis

## 287. Numerical and Analytical Study for Fourth-order Integro-differential Equations Using a Pseudospectral Method

N. H. Sweilam, M. M. Khader and W. Y. Kota

*Mathematical Problems in Engineering*, 1-7 (2013) IF: 1.383

A numerical method for solving fourth-order integro-differential equations is presented. This method is based on replacement of the unknown function by a truncated series of well-known shifted Chebyshev expansion of functions. An approximate formula of the integer derivative is introduced. The introduced method converts the proposed equation by means of collocation points to system of algebraic equations with shifted Chebyshev coefficients. Thus, by solving this system of equations, the shifted Chebyshev coefficients are obtained. Special attention is given to study the convergence analysis and derive an upper bound of the error of the presented approximate formula. Numerical results are performed in order to illustrate the usefulness and show the efficiency and the accuracy of the present work.

**Keywords:** Fourth-order Integro-differential equations; Pseudospectral method; Chebyshev polynomials.

## 288. On Shifted Jacobi Spectral Approximations for Solving Fractional Differential Equations

E.H. Doha, A.H. Bhrawy, D. Baleanu and S.S. Ezz-Eldien

*Applied Mathematics and Computation*, 219: 8042-8056 (2013) IF: 1.349

In this paper, a new formula of Caputo fractional-order derivatives of shifted Jacobi polynomials of any degree in terms of shifted Jacobi polynomials themselves is proved. We discuss a direct solution technique for linear multi-order fractional differential equations (FDEs) subject to nonhomogeneous initial conditions using a shifted Jacobi tau approximation. A quadrature shifted Jacobi tau (Q-SJT) approximation is introduced for the solution of linear multi-order FDEs with variable coefficients. We also propose a shifted Jacobi collocation technique for solving nonlinear multi-order fractional initial value problems. The advantages of using the proposed techniques are discussed and we compare them with other existing methods. We investigate some illustrative examples of FDEs including linear and nonlinear terms. We demonstrate the high accuracy and the efficiency of the proposed techniques.

**Keywords:** Multi-term fractional differential equations; Nonlinear fractional initial value problems; Spectral methods; Shifted Jacobi polynomials; Jacobi-gauss-lobatto quadrature; Caputo derivative.

## 289. Variational Principle for Zakharov-shabat Equations in Two-dimensions

M. A. Helal, A. R. Seadawy and R.S. Ibrahim

*Applied Mathematics and Computation*, 219: 5635-5648 (2013) IF: 1.349

We study the corresponding scattering problem for Zakharov and Shabat compatible differential equations in two-dimensions, the representation for a solution of the nonlinear Schrödinger equation is formulated as a variational problem in two-dimensions. We extend the derivation to the variational principle for the Zakharov and Shabat equations in one-dimension. We also developed an approximate analytical technique for finding discrete eigenvalues of the complex spectral parameters in Zakharov and Shabat equations for a given pulse-shaped potential, which is equivalent to the physically important problem of finding the soliton content of the given initial pulse. Using a trial function in a rectangular box we find the functional integral. The general case for the two box potential can be obtained on the basis of a different ansatz where we approximate the Jost function by polynomials of order  $n$  instead of a piecewise linear function. We also demonstrated that the simplest version of the variational approximation, based on trial functions with one, two and  $n$ -free parameters respectively, and treated analytically.

**Keywords:** Partial differential equations; Calculus of variations; Canonical formalism; Lagrangians; Variational principles.

## 290. A Jacobi Collocation Method for Solving Nonlinear Burgers-type Equations

E. H. Doha, D. Baleanu, A. H. Bhrawy and M. A. Abdelkawy

*Abstract and Applied Analysis*, (2013) IF: 1.102

We solve three versions of nonlinear time-dependent Burgers-type equations. The Jacobi-Gauss-Lobatto points are used as collocation nodes for spatial derivatives. This approach has the advantage of obtaining the solution in terms of the Jacobi parameters  $\alpha$  and  $\beta$ . In addition, the problem is reduced to the solution of the system of ordinary differential equations (SODEs) in time. This system may be solved by any standard numerical techniques. Numerical solutions obtained by this method when compared with the exact solutions reveal that the obtained solutions produce high-accurate results. Numerical results show that the proposed method is of high accuracy and is efficient to solve the Burgers-type equation. Also the results demonstrate that the proposed method is a powerful algorithm to solve the nonlinear partial differential equations.

**Keywords:** Collocation method; Burgers equations.

### 291. New Spectral Second Kind Chebyshev Wavelets Algorithm for Solving Linear and Nonlinear Second-order Differential Equations Involving Singular and Bratu Type Equations

W. M. Abd-Elhameed, E. H. Doha and Y. H. Youssri

*Abstract and Applied Analysis*, (2013) IF: 1.102

A new spectral algorithm based on shifted second kind Chebyshev wavelets operational matrices of derivatives is introduced and used for solving linear and nonlinear second-order two-point boundary value problems. The main idea for obtaining spectral numerical solutions for these equations is essentially developed by reducing the linear or nonlinear equations with their initial and/or boundary conditions to a system of linear or nonlinear algebraic equations in the unknown expansion coefficients. Convergence analysis and some efficient specific illustrative examples including singular and Bratu type equations are considered to demonstrate the validity and the applicability of the method. Numerical results obtained are compared favorably with the analytical known solutions.

**Keywords:** Second kind chebyshev wavelets; Operational matrix.

### 292. On Finslerized Absolute Parallelism Spaces

Nabil L. Youssef, Amr M. Sid-Ahmed and Ebtsam H. Taha

*International Journal of Geometric Methods in Modern Physics*, 10 (7): (21 Pages) (2013) IF: 0.951

The aim of this paper is to construct and investigate a Finsler structure within the framework of a Generalized Absolute Parallelism (GAP)-space. The Finsler structure is obtained from the vector fields forming the parallelization of the GAP-space. The resulting space, which we refer to as a Finslerized absolute parallelism (parallelizable) space, combines within its geometric structure the simplicity of GAP-geometry and the richness of Finsler geometry, hence is potentially more suitable for applications and especially for describing physical phenomena. A study of the geometry of the two structures and their interrelation is carried out. Five connections are introduced and their torsion and curvature tensors derived. Some special Finslerized parallelizable spaces are singled out. One of the main reasons to introduce this new space is that both absolute parallelism and Finsler geometries have proved effective in the formulation of physical theories, so it is worthy to try to build a more general

geometric structure that would share the benefits of both geometries.

**Keywords:** Pullback bundle; Nonlinear connection; Finsler space; Generalized absolute parallelism space; Generalized lagrange space; Landsberg space; Berwald space; Minkowskian space; Riemannian space.

### 293. Teleparallel Lagrange Geometry and a Unified Field Theory: Linearization of the Field Equations

M. I. Wanas, Nabil L. Youssef and A. M. Sid-Ahmed

*International Journal of Geometric Methods in Modern Physics*, 10 (3): (2013) IF: 0.951

This paper is a natural continuation of our previous paper: "Teleparallel Lagrange geometry and a unified field theory, Class. Quantum Grav. 27 (2010) 045005 (29 pp)". In this paper, we apply a linearization scheme on the field equations obtained in the above-mentioned paper. Three important results under the linearization assumption are accomplished. First, the vertical fundamental geometric objects of the EAP-space lose their dependence on the positional argument  $x$ . Secondly, our linearized theory in the Cartan-type case coincides with the GFT in the first-order of approximation. Finally, an approximate solution of the vertical field equations is obtained.

**Keywords:** Extended absolute parallelism geometry; Euler-lagrange equations; Generalized field theory; Extended teleparallel unified field theory; Linearization; Cartan-type case.

### 294. Numerical Approximations for Fractional Diffusion Equations Via a Chebyshev Spectral-tau Method

Eid H. Doha, Ali H. Bhrawy and Samer S. Ezz-Eldien

*Central European Journal of Physics*, 11(10): 1494-1503 (2013) IF: 0.905

In this paper, a class of fractional diffusion equations with variable coefficients is considered. An accurate and efficient spectral tau technique for solving the fractional diffusion equations numerically is proposed. This method is based upon Chebyshev tau approximation together with Chebyshev operational matrix of Caputo fractional differentiation. Such approach has the advantage of reducing the problem to the solution of a system of algebraic equations, which may then be solved by any standard numerical technique. We apply this general method to solve four specific examples. In each of the examples considered, the numerical results show that the proposed method is of high accuracy and is efficient for solving the time-dependent fractional diffusion equations.

**Keywords:** Fractional diffusion equations; Spectral tau technique; Operational matrix; Shifted chebyshev polynomials.

### 295. Numerical Simulations for the Space-time Variable Order Nonlinear Fractional Wave Equation

Nasser Hassan Sweilam and Taghreed Abdul Rahman Assiri

*Journal of Applied Mathematics*, (2013) IF: 0.834

The explicit finite-difference method for solving variable order fractional space-time wave equation with a nonlinear source

terms considered. The concept of variable order fractional derivative is considered in the sense of Caputo. The stability analysis and the truncation error of the method are discussed. To demonstrate the effectiveness of the method, some numerical test examples are presented.

## 296. On Concircularly Recurrent Finsler Manifolds

Nabil L. Youssef and A. Soleiman

*Balkan Journal of Geometry and Its Applications*, 18 (1): 101-113 (2013) IF: 0.806

Two special Finsler spaces have been introduced and investigated, namely  $R^h$ -recurrent Finsler space and concircularly recurrent Finsler space. The defining properties of these spaces are formulated in terms of the first curvature tensor of Cartan connection. The following three results constitute the main object of the present paper: (i) a concircularly flat Finsler manifold is necessarily of constant curvature (Theorem A); (ii) every  $R^h$ -recurrent Finsler manifold is concircularly recurrent with the same recurrence form (Theorem B); (iii) every horizontally integrable concircularly recurrent Finsler manifold is  $R^h$ -recurrent with the same recurrence form (Theorem C). The whole work is formulated in a coordinate-free form.

**Keywords:** Cartan connection; Concircular curvature tensor; Concircularly flat; Concircularly recurrent Finsler manifold;  $R^h$ -recurrent Finsler manifold;  $R^h$ -symmetric Finsler manifold.

## 297. New Spectral-galerkin Algorithms for Direct Solution of High Even-order Differential Equations Using Symmetric Generalized Jacobi Polynomials

E. H. Doha, W. M. Abd-Elhameed and A. H. Bhrawy

*Collectanea Mathematica*, 64 (3): 373-394 (2013) IF: 0.786

A family of symmetric generalized Jacobi polynomials (GJPs) is introduced and used for solving high even-order linear elliptic differential equations in one variable by the Galerkin method. Some efficient and accurate algorithms are developed and implemented for solving such equations. The use of GJPs leads to a simplified analysis, more precise error estimates and very efficient numerical algorithms. The methods lead to linear systems with specially structured matrices that can be efficiently inverted. Two numerical examples are presented aiming to demonstrate the accuracy and the efficiency of the proposed algorithms.

**Keywords:** Spectral-galerkin method; Generalized Jacobi Polynomials; Nonhomogeneous Dirichlet conditions; Even high-order equations.

## 298. Existence and Uniqueness of Solutions of Hahn Difference Equations

Alaa Eldeen Hamza and Samah M Ahmed

*Advances in Difference Equations*, 1/316: 1-15, (2013) IF: 0.76

Hahn introduced the difference operator  $D_{q,\omega}f(t) = (f(qt + \omega) - f(t))/(t(q - 1) + \omega)$  in 1949, where  $0 < q < 1$  and  $\omega > 0$  are fixed real numbers. This operator extends the classical difference

operator  $\Delta_{\omega}f(t) = (f(t + \omega) - f(t))/\omega$  as the Jackson  $q$ -difference operator  $D_qf(t) = (f(qt) - f(t))/(t(q - 1))$ .

In this paper, we present new results of the calculus based on the Hahn difference operator. Also, we establish an existence and uniqueness result of solutions of Hahn difference equations by using the method of successive approximations.

**Keywords:** Hahn difference operator; Jackson  $q$ -difference operator.

## 299. A Global Approach to Absolute Parallelism Geometry

Nabil L. Youssef and Waleed A. Elsayed

*Reports on Mathematical Physics*, 72: 1-23 (2013) IF: 0.756

In this paper we provide a global investigation of the geometry of parallelizable manifolds (or absolute parallelism geometry) frequently used in applications. We discuss different linear connections and curvature tensors from a global point of view. We give an existence and uniqueness theorem for a remarkable linear connection, called the canonical connection. Different curvature tensors are expressed in a compact form in terms of the torsion tensor of the canonical connection only. Using the Bianchi identities, some interesting identities are derived. An important special fourth-order tensor, which we refer to as Wanas tensor, is globally defined and investigated. Finally a "double-view" for the fundamental geometric objects of an absolute parallelism space is established: The expressions of these geometric objects are computed in the parallelization basis and are compared with the corresponding local expressions in the natural basis. Physical aspects of some geometric objects considered are pointed out.

**Keywords:** Absolute parallelism geometry; Parallelization vector field; Parallelization basis; Canonical connection; Dual connection, Bianchi identities, Wanas tensor.

## 300. Numerical Study for the Fractional Differential Equations Generated by Optimization Problem Using Chebyshev Collocation Method and FDM

M. M. Khader, N. H. Sweilam and A. M. S. Mahdy

*Applied Mathematics and Information Sciences, an International Journal*, 7: 2011-2018 (2013) IF: 0.731

This paper is devoted with numerical solution of the system fractional differential equations (FDEs) which are generated by optimization problem using the Chebyshev collocation method. The fractional derivatives are presented in terms of Caputo sense. The application of the proposed method to the generated system of FDEs leads to algebraic system which can be solved by the Newton iteration method. The method introduces a promising tool for solving many systems of non-linear FDEs. Two numerical examples are provided to confirm the accuracy and the effectiveness of the proposed methods. Comparisons with the fractional finite difference method (FDM) and the fourth order Runge-Kutta (RK4) are given.

**Keywords:** Non-linear programming; Penalty function; Dynamic system; Caputo fractional derivatives; Chebyshev approximations; Finite difference method; Runge-kutta method.

### 301. A Note on “Sur Le Noyau De L’Opérateur De Courbure D’Une Variété Finslérienne” [C. R. Acad. Sci. Paris, T. 272 (1971), 807-810]

Nabil L. Youssef and Salah G. Elgend

*Comptes Rendus Mathématiques, Ser. I*, 351: 829-832 (2013)  
IF: 0.477

In this note, adopting the pullback formalism of global Finsler geometry, we show by a counter example that the kernel  $Ker_R$  of the h-curvature  $R$  of the Cartan connection and the associated nullity distribution  $N_R$  do not coincide, contrary to a result of Akbar-Zadeh (given in the article that appears in the title). We also give sufficient conditions for  $Ker_R$  and  $N_R$  to coincide.

**Keywords:** Kernel distribution; Nullity distribution; Pullback formalism.

### 302. Approximate Solutions for the Fractional Advection–dispersion Equation Using Legendre Pseudo-spectral Method

M. M. Khader and N. H. Sweilam

*Computational and Applied Mathematics*, 3: 1-12 (2013)  
IF: 0.452

Fractional differential equations have recently been applied in various areas of engineering, science, finance, applied mathematics, bio-engineering and others. Fractional advection–dispersion equation (FADE) is used in groundwater hydrology to model the transport of passive tracers carried by fluid flow in a porous medium and for modeling transport at the Earth surface. In this paper, an efficient numerical method for solving FADE is considered.

The fractional derivative is described in the Caputo sense. The method is based on Legendre approximations. The properties of Legendre polynomials are utilized to reduce FADE to a system of ODEs, which is solved using the finite difference method. Moreover, the convergence analysis and an upper bound of the error for the derived formula are given. Numerical solutions of FADE are presented and the results are compared with the exact solution.

**Keywords:** Fractional advection–dispersion equation; Caputo fractional derivative; Finite difference method; Legendre pseudo-spectral method; Convergence analysis.

### 303. Efficient Jacobi–gauss Collocation Method for Solving Initial Value Problems of Bratu Type

E. H. Doha, A. H. Bhrawy, D. Baleanu and R. M. Hafez

*Computational Mathematics and Mathematical Physics*, 53.9: 1292-1302 (2013) IF: 0.408

In this paper, we propose the shifted Jacobi–Gauss collocation spectral method for solving initial value problems of Bratu type, which is widely applicable in fuel ignition of the combustion theory and heat transfer. The spatial approximation is based on shifted Jacobi polynomials  $J_n^{(\alpha, \beta)}(x)$  with  $\alpha, \beta \in (-1, \infty)$ ,  $x \in [0, 1]$  and  $n$  the polynomial degree. The shifted Jacobi–Gauss points are used as collocation nodes. Illustrative examples have been discussed to demonstrate the validity and applicability of the

proposed technique. Comparing the numerical results of the proposed method with some wellknown results show that the method is efficient and gives excellent numerical results.

**Keywords:** Bratu-type equations; Second-order initial value problems; Collocation method, Jacobi-gauss quadrature; Shifted Jacobi polynomials.

### 304. Rad-projective and Strongly Rad-projective Modules

Ismail Amin, Yasser Ibrahim and Mohamed Yousif

*Communications in Algebra* 41 (6): 2174-2192 (2013) IF: 0.356

We introduce the dual notion to soc-injectivity, namely rad-projective and strongly radprojective modules. Several interesting results and applications on the new notion are obtained.

**Keywords:** Injective and projective modules; Rad-projective and strongly rad-projective modules; Soc-injective modules.

### 305. Efficient Spectral-Petrov-Galerkin Methods for Third- and Fifth-order Differential Equations Using General Parameters Generalized Jacobi Polynomials

W.M. Abd-Elhameed

*Quaestiones Mathematicae*, 36: 15-38 (2013) IF: 0.224

Two new families of general parameters generalized Jacobi polynomials are introduced. Some efficient and accurate algorithms based on these families are developed and implemented for solving third- and fifth-order differential equations in one variable subject to homogeneous and nonhomogeneous boundary conditions using a dual Petrov-Galerkin method. The use of general parameters generalized Jacobi polynomials leads to simplified analysis, more precise error estimates and well conditioned algorithms. The method leads to linear systems with specially structured matrices that can be efficiently inverted. Numerical results indicating the high accuracy and effectiveness of the proposed algorithms are presented.

**Keywords:** Dual-petrov- galerkin method; General parameters generalized jacobi polynomials; Nonhomogeneous dirichlet conditions.

### 306. A New Model for Context-oriented Programs

Mohamed A. El-Zawawy and Eisa A. Aleisa

*Life Science Journal-acta Zhengzhou University Overseas Edition*, 10(2): 2515-2523 (2013) IF: 0.165

Context-oriented programming (COP) is a new technique for programming that allows changing the context in which commands execute as a program executes. Compared to object-oriented programming (aspect-oriented programming), COP is more flexible (modular and structured). This paper presents a precise syntax-directed operational semantics for context-oriented programming with layers, as realized by COP languages like ContextJ\* and ContextL. Our language model is built on Java enriched with layer concepts and activation and deactivation of layer scopes. The paper also presents a static type system that guarantees that typed programs do not get stuck. Using the means



of the proposed semantics, the mathematical correctness of the type system is presented in the paper.

**Keywords:** Context-oriented programming; Operational semantics; Type systems; Layers activation and deactivation.

### 307. Distributed Data and Programs Slicing

Mohamed A. El-Zawawy

*Life Science Journal-acta Zhengzhou University Overseas Edition*, 10(4): 1361-1369 (2013) IF: 0.165

This paper presents a new technique for data slicing of distributed programs running on a hierarchy of machines. Data slicing can be realized as a program transformation that partitions heaps of machines in a hierarchy into independent regions. Inside each region of each machine, pointers preserve the original pointer structures in the original heap hierarchy. Each heap component of the base type (e.g., the integer type) goes only to a region of one of the heaps. The proposed technique has the shape of a system of inference rules. In addition, this paper presents a simply structure type system to decide type soundness of distributed programs. Using this type system, a mathematical proof that the proposed slicing technique preserves typing properties is outlined in this paper as well.

**Keywords:** Distributed data; Distributed programs; Data slicing; Programs slicing; Type systems; Program transformation.

### 308. Exact Solutions of Space-Time Dependent Korteweg-De Vries Equation by the Extended Unified Method

H.I. Abdel-Gawad, Mohamed Osman and Nasser S. Elazab

*Life Science Journal*, 10 (2): 2598-2604 (2013) IF: 0.165

Recently the unified method for finding traveling wave solutions of nonlinear evolution equations was proposed by one of the authors. It was shown that, this method unifies all the methods being used to find these solutions. In this paper, we extend this method to find a class of formal exact solutions to Korteweg-de Vries (KdV) equation with space-time dependent coefficients. A new class of multiple-soliton or wave trains is obtained.

**Keywords:** Exact solution; Extended unified method; Korteweg-de vries equation; Variable coefficients.

### 309. A Concircular $\pi$ -Vector Fields and Special Finsler Spaces

Nabil L. Youssef and Amr Soleiman

*Advances in Pure Mathematics*, 3: 282-291 (2013)

The aim of the present paper is to investigate intrinsically the notion of a concircular  $\pi$ -vector field in Finsler geometry. This generalizes the concept of a concircular vector field in Riemannian geometry and the concept of concurrent vector field in Finsler geometry. Some properties of concircular  $\pi$ -vector fields are obtained. Different types of recurrence are discussed. The effect of the existence of a concircular  $\pi$ -vector field on some important special Finsler spaces is investigated. Almost all results obtained in this work are formulated in a coordinate-free form.

**Keywords:** Finsler manifold; Cartan connection; Concurrent  $\pi$ -vector field; Concircular  $\pi$ -vector field; Special finsler space; Recurrent finsler space.

### 310. A Quantitative Model of Bacterial Mismatch Repair as Applied to Studying Induced Mutagenesis

O. V. Belov, O. Chuluunbaatar, M. I. Kapralov and N. H. Sweilam

*Physics of Particles and Nuclei Letters*, 10: 587-596 (2013)

The paper presents a mathematical model of the DNA mismatch repair system in *Escherichia coli* bacterial cells. The key pathways of this repair mechanism were simulated on the basis of modern experimental data. We have modeled in detail five main pathways of DNA misincorporation removal with different DNA exonucleases. Here we demonstrate an application of the model to problems of radiation-induced mutagenesis.

**Keywords:** Mathematical model of the DNA mismatch repair system in *Escherichia coli*; Problems of radiation.

### 311. Characterizations of Stability of First Order Linear Hahn Difference Equations

Alaa E. Hamza, A. S. Zaghrout and S. M. Ahmed

*Journal of Advances in Mathematics*, 5: 677-687 (2013)

Hahn introduced the difference operator in 1949. This operator extends the classical difference operator as well as Jackson  $q$ -difference operator. In this paper, our objective is to establish characterizations of many types of stability, like (uniform, uniform exponential,  $h$ -) stability of first order linear Hahn difference equations. At the end, we give two illustrative examples.

**Keywords:** Hahn difference operator; Jackson  $Q$ -difference operator.

### 312. Computing the Missing Dark Energy of a Clopen Universe which is its Own Multiverse in Addition to Being both Flat and Curved

M.S. El Naschie, L. Marek-Crnjac, Ji-Huan He and Mohamed Atef Helal

*Fract Spacetime Noncommut. Geom. Quant. High Energ. Phys.*, 3 (1): 3-10 (2013)

We approach the problem of the mysteriously missing hypothetical dark energy of the universe from first principles. For that purpose we fuse the large structure as well as the quantum scale of spacetime together and model it using certain Calabi-Yau manifold. That way we derive a rescaled energy-mass special relativity equation which includes quantum effects. The missing energy predicted by this equation is in astonishing, almost perfect agreement with the cosmological measurement of WMAP and supernova analysis. The rationale behind the basic idea of the proposed theory is simply put as follows: Einstein's special relativity and consequently his equation  $E = mc^2$  may be considered from the view point of high energy particle physics as a one dimensional theory, i.e. a theory based upon a single elementary particle, the photon. On the other hand the simplest

and yet extremely successful standard model of quantum field theory relies on a minimum of 12 particles of which the photon is just one. It is therefore reasonable to assume that the Newtonian expression for kinetic energy  $E = mv^2 / 2$  could be reduced following a principle of scale relativity by the ratio of one to  $12-1=11$ . This fact also follows from Rayleigh theorem on Eigenvalues which state that restricting the number of generalized coordinates leads to an upper bound rather than a lower bound and lower proper minimization of energy. In other words the maximum quantum relativity approximate magnitude of the energy is  $E = (1/2) (1/11) (mc^2)$  when  $v = c$ . Compared to the result of the classical special theory of relativity, this is a reduction of nearly 95.45% and matches almost perfectly the cosmic measurements.

The present work claims to give the above qualitative arguments a precise topological foundation using various advanced mathematics and topological theorems. In addition we give a rational ground to the intrinsic dialectic nature of spacetime. In particular we reason that spacetime is both open and closed i.e. clopen in the topological sense as well as being both flat and curved in a way which related the 22 compactified dimensions of bosonic string theory to Einstein's cosmological constant.

**Keywords:** Dark energy; Quantum gravity; Calabi yau manifold; Lorentz transformation; Dark extra dimensions; Yang-mills theory.

### 313. Dark Energy Explained Via the Hawking-hartle Quantum Wave and the Topology of Cosmic Crystallography

Mohamed S. El Naschie and Atef Helal

*Int. Journal of Astronomy and Astrophysics*, 3: 318-343 (2013)

The aim of the present paper is to explain and accurately calculate the missing dark energy density of the cosmos by scaling the Planck scale and using the methodology of the relatively novel discipline of cosmic crystallography and Hawking-Hartle quantum wave solution of Wheeler-DeWitt equation. Following this road we arrive at a modified version of Einstein's energy mass relation  $E = mc^2$  which predicts a cosmological energy density in astonishing accord with the WMAP and supernova measurements and analysis. We develop non-destructively what may be termed super symmetric Penrose fractal tiling and find that the isomorphic length of this tiling is equal to the self affinity radius of a universe which resembles an 11 dimensional Hilbert cube or a fractal M-theory with a Hausdorff dimension  $D_F^{(11)} = 11 + \phi^5$  where  $\phi = (\sqrt{5} - 1)/2$ . It then turns out that the correct maximal quantum relativity energy-mass equation for intergalactic scales is a simple relativistic scaling, in the sense of Weyl-Nottale, of Einstein's classical equation, namely  $EQR = (1/2)(1/D_F^{(11)}) mc^2 = 0.0450849 mc^2$  and that this energy is the ordinary measurable energy density of the quantum particle. This means that almost 95.5% of the energy of the cosmos is dark energy which by quantum particle-wave duality is the absolute value of the energy of the quantum wave and is proportional to the square of the curvature of the curled dimension of spacetime namely  $(26+k-4)^2$  where  $k = 2\phi^5$  and  $\phi^5$  is Hardy's probability of quantum entanglement. Because of the quantum wave collapse on measurement this energy cannot be measured using our current technologies. The same result is obtained by involving all the 17 Stein spaces corresponding to 17 types of the wallpaper groups as well as the  $230-11=219$  three dimensional crystallographic group

which gives the number of the first level of massless particle-like states in Heterotic string theory. All these diverse subjects find here a unified view point leading to the same result regarding the missing dark energy of the universe, which turned out to be synonymous with the absolute value of the energy of the Hawking-Hartle quantum wave solution of Wheeler-DeWitt equation while ordinary energy is the energy of the quantum particle into which the Hawking-Hartle wave collapse at cosmic energy measurement. In other words it is in the very act of measurement which causes our inability to measure the "Dark energy of the quantum wave" in any direct way. The only hope if any to detect dark energy and utilize it in nuclear reactors is future development of sophisticated quantum wave non-demolition measurement instruments.

**Keywords:** Doubly special relativity; Week's manifold; Experimental test of Einstein's relativity; Witten's m-Theory; Ordinary energy of the quantum particle; Hawking-hartle wave of cosmos; Crystallographic symmetry groups; Revising special relativity.

### 314. Exact Solution of Time Dependent Korteweg-De Vries Equation by the Extended Unified Method

H. I. Abdel-Gawad, Mohamed Osman and Nasser S. Elazab

*International Journal of Soft Computing and Engineering (Ijsce)*, 3 (1) 59-63 (2013)

Recently the unified method for finding traveling wave solutions of nonlinear evolution equations was proposed by the first author. It was shown that, this method unifies all the methods being used to find these solutions. In this paper, we extend this method to find a class of formal exact solutions to Korteweg-de Vries equation with time dependent coefficients. A new class of multiple-soliton or wave trains is obtained.

**Keywords:** Exact solution; Extended unified method.

### 315. Exact Solutions of Space and Time Dependent Burgers Equation by the Extended Unified Method

H. I. Abdel-Gawad, Mohamed Osman and Nasser S. Elazab

*Int. Journal of Basic and Applied Sciences*, 13 (1) 65-68 (2013)

Recently the unified method for finding traveling wave solutions of nonlinear evolution equations was proposed by the first author. It was shown that, this method unifies all the methods being used to find these solutions. In this paper, we extend this method to find a class of formal exact solutions to Burgers equation with space- time dependent coefficients. A new class of solutions is obtained.

**Keywords:** Exact Solution, Extended Unified Method, Burgers Equation, Variable Coefficients.

### 316. Explicit Finite Difference Method for the Fractional Non-linear Wave Equation with the Riesz Fractional Derivative

N. H. Sweilam and T. A. Assiri

*International Journal of Mathematics and Computer Applications Research (Ijmcra)*, 3: 193-202 (2013)

In this paper, the explicit finite difference method (EFDM) for solving nonlinear fractional wave equation is considered. The stability and convergence of the method are discussed by means of Greshgorin theorem and using the stability matrix analysis. Numerical studies for a model are presented to confirm the accuracy and the effectiveness of the proposed method. The obtained results are compared with exact solutions. It is found that the proposed method is simple and efficient for such nonlinear problem.

**Keywords:** Explicit finite difference method; Fractional wave equation; Riesz fractional derivative; Stability matrix analysis; Greshgorin theorem.

### 317. Lyapunov Stabilizability for Nonlinear Dynamic Control Systems on Time Scales

Alaa E. Hamza and M. H. Abu-Risha

*Applied Mathematical Sciences*, 7 (71): 3497 -3510 (2013)

In this paper we use an appropriate Lyapunov function and derive sufficient conditions for the nonlinear dynamic control system

$x^\Delta(t) = A(t)x(t) + B(t)u(t) + f(t, x(t), u(t))$ ,  $t \in T$  on a time scale  $T$  to be uniformly stabilizable, uniformly exponentially stabilizable, and  $h$ -stabilizable. Here,  $A : T \rightarrow \mathbb{R}^{n \times n}$  is an  $n \times n$  matrix valued function and  $B : T \rightarrow \mathbb{R}^{n \times m}$  is an  $n \times m$  matrix valued function,  $m \leq n$ . By way of illustration we give numerical examples.

**Keywords:** Uniformly Stabilizable, Uniformly Exponentially Stabilizable,  $h$ -Stabilizable, Dynamical Control System, Time Scales.

### 318. On the Numerical Solution for the Fractional Wave Equation Using Legendre Pseudospectral Method

M. M. Khader, N. H. Sweilam and T.A. Assiri

*Int. J. of Pure and Applied Mathematics*, 84 (4): 307-319 (2013)

Fractional differential equations have recently been applied in various areas of engineering, science, finance, applied mathematics, bio-engineering and others. However, many researchers remain unaware of this field. In this paper, an efficient numerical method for solving the fractional wave equation (FWE) is considered. The fractional derivative is described in the Caputo sense. The method is based upon Legendre approximations. The properties of Legendre polynomials are utilized to reduce FWE to a system of ordinary differential equations, which solved using the finite difference method (FDM). Numerical solutions of FWE are presented and the results are compared with the exact solution.

**Keywords:** Fractional wave equation; Caputo derivative; Finite difference method; Legendre pseudospectral method.

### 319. On the Variational Approach for Analyzing the Stability of Solutions of Evolution Equations

Hamdy I. Abdel-Gawad and M. S. Osman

*Kyungpook Math. J.*, 53: 661-680 (2013)

The eigenvalue problems arise in the analysis of stability of traveling waves or rest state solutions are currently dealt with,

using the Evans function method. In the literature, it had been shown that, use of this method is not straightforward even in very Simple examples Here an extended "variational" method to solve the eigenvalue problem for the higher order differential equations is suggested. The extended method is matched to the well known variational iteration method. The criteria for validity of the eigenfunctions and eigenvalues obtained are presented. Attention is focused to find eigenvalue and eigenfunction solutions of the Kuramoto-Sivashinsky and (K[p,q]) equation.

**Keywords:** An extended variational method; Stability analysis-traveling wave.

### 320. Stability Analysis Solutions for the Fourth-order Nonlinear Ablowitz-kaup-Newell-Segur Water Wave Equation

Mohamed Atef Helal

*Applied Mathematical Sciences*, 7: 3355-3365 (2013)

Ablowitz-Kaup-Newell-Segur (AKNS) hierarchy appears naturally in the model besides a string equation. The Korteweg-de Vries hierarchy is contained in the AKNS hierarchy as a reduction, and therefore appears in the model before one takes the double scaling limit. The AKNS hierarchy is a complexified version of the Nonlinear Schrödinger (NLS) hierarchy and also contains the modified Korteweg-de Vries hierarchy. By using the extended auxiliary equation method, we obtained some new soliton like solutions for the two-dimensional fourth-order nonlinear (AKNS) equation with variable coefficient. These solutions include symmetrical, non-symmetrical kink solutions, bell-shaped solitary wave solutions, solitary wave solutions and traveling wave solutions. The stability analysis for these solutions is discussed.

**Keywords:** Stability analysis; Nonlinear; Akns equation.

### 321. Structural and Diffusional Study of Pure Ethanol and Water on Pt (111) Surface Using Molecular Dynamics Simulation

Kholmirzo Kholmurodov, Ermuhammad Dushanov, Kenji Yasuoka, Hagar Hassan Ahmed Galal and Nasser Sweilam

*European Chemical Bulletin*, 2(5): 247-254 (2013)

Molecular dynamics simulations were performed on ethanol-water-Pt system for studying the structural and diffusion behavior of both ethanol and water molecules on the surface of Pt (111). This work is concerned with the differences between pure liquids and solutions in their diffusional behavior. The self-diffusion coefficients and activation energies of diffusion of pure ethanol and water on Pt (111) surface were calculated and compared with the corresponding values of their mixtures. The results showed that the values of both the diffusion coefficients and activation energies are strongly affected by the purity of chemical species under investigation. A comparison between two different metal surfaces was also investigated and the results revealed that the nature of metal surface has a strong effect on the adsorption and diffusional behaviour of liquids based on their affinity towards a specific type of surfaces in addition to the hydrophobicity and hydrophilicity of the metal surface.

**Keywords:** Molecular dynamics simulation; Ethanol; Water; Pt (111); Diffusion coefficient; Activation energy of diffusion.

### 322. The Three Page Guide to the Most Important Results of M. S. El Naschie'S Research in E-infinity Quantum Physics and Cosmology

Mohamed A. Helal, L. Marek-crnjac and Ji-huan He

*Open Journal of Microphysics*, 3: 141-145 (2013)

In this short survey, we give a complete list of the most important results obtained by El Naschie's E-infinity Cantorian space-time theory in the realm of quantum physics and cosmology. Special attention is paid to his recent result on dark energy and revising Einstein's famous formula  $E = mc^2$

**Keywords:** Review of e-infinity; Summary of cantorian space-time; El naschie nottale and ord fractal space-time; Rindler space-time; Revising einstein theory; Dark energy revealed.

### 323. Theory of Linear Hahn Difference Equations

Alaa Eldeen Hamza and S. M. Ahmed

*Journal of Advances in Mathematics*, 4: 440-461 (2013)

Hahn introduced the difference operator,  $(\Delta f)(t) = f(t+1) - f(t)$  in 1949, where  $0 < q < 1$  and  $\omega > 0$  are fixed real numbers. This operator extends the classical difference operator  $\Delta f(t) = f(t+1) - f(t)$  as well as Jackson  $q$ -difference operator  $(\Delta_q f)(t) = f(qt) - f(t)$ . In this paper, our target is to give a rigorous study of the theory of linear Hahn difference equations of the form We introduce its fundamental set of solutions when the coefficients are constant and the Wronskian associated with the Hahn operator.

Hence, we obtain the corresponding Liouville's formula. Also, we derive solutions of the first and second order linear Hahn difference equations with non-constant coefficients. Finally, we present the analogues of the variation of parameter technique and the annihilator method for the non-homogeneous case.

**Keywords:** Hahn difference operator; Jackson Q-difference operator.

### 324. Uniform Exponential Stabilizability of Dynamic Control Equations on Time Scales

Alaa Eldeen Hamza and Nada A. Laabi

*Int. J. Contemp. Math. Sciences*, 8: 469- 480, (2013)

In this paper the uniform exponential stablizabeth of the non-linear dynamic control systems of the form

$$x^\Delta(t) = Ax(t) + Bu(t) + f(x(t), u(t), t), t \in \mathbb{T}^+ \cap \mathbb{R}$$

on a time scale  $\mathbb{T}^+$  is investigated. Here  $A \in \mathbb{R}^{n \times n}$  and  $B \in \mathbb{R}^{n \times m}$  are constant matrices,  $(m \leq n)$  and  $f(x, u, t) : \mathbb{R}^n \times \mathbb{R}^m \times \mathbb{T}^+ \rightarrow \mathbb{R}^n$  satisfies Lipschitz condition with respect  $x$ . We find a suitable matrix  $K$ , which leads to make the feedback nonlinear dynamic equation is uniformly exponentially stabilizable. An illustrative example is presented to show the effectiveness of the theoretical results.

**Keywords:** Uniform exponential stabilizability; Dynamic equation; Time scales.

### Dept. of Physics

### 325. Measurement of the azimuthal anisotropy of neutral pions in PbPb collisions at $\sqrt{s}(\text{NN}) = 2.76 \text{ TeV}$

S. Chatrchyan, Ali Yehia Ellithi et al

*Physical Review Letters*, 110: (2013) IF: 7.943

First measurements of the azimuthal anisotropy of neutral pions produced in PbPb collisions at a center-of-mass energy of  $\sqrt{s}(\text{NN}) = 2.76 \text{ TeV}$  are presented. The amplitudes of the second Fourier component ( $v_2$ ) of the neutral pion azimuthal distributions are extracted using an event-plane technique. The values of  $v_2$  are studied as a function of the neutral pion transverse momentum ( $p_T$ ) for different classes of collision centrality in the kinematic range  $1.6 < p_T < 8.0 \text{ GeV}$ , within the pseudorapidity interval  $|\eta| < 0.8$ . The CMS measurements of  $v_2(p_T)$  are similar to previously reported neutral pion azimuthal anisotropy results from  $\sqrt{s}(\text{NN}) = 200 \text{ GeV}$  AuAu collisions at RHIC, despite a factor of about 14 increase in the center-of-mass energy. In the momentum range  $2.5 < p_T < 5.0 \text{ GeV}$ , the neutral pion anisotropies are found to be smaller than those observed by CMS for inclusive charged particles.

**Keywords:** Azimuthal anisotropy; Neutral pions; Pb-Pb collisions.

### 326. Evidence for Associated Production of a Single Top Quark and W Boson in PP Collisions at $\sqrt{s} = 7 \text{ TeV}$

S. Chatrchyan, Ali Yehia Ellithi et al

*Physical Review Letters*, 110: 022003-, (2013) IF: 7.9

Evidence is presented for the associated production of a single top quark and W boson in pp collisions at  $\sqrt{s} = 7 \text{ TeV}$  with the CMS experiment at the LHC. The analyzed data corresponds to an integrated luminosity of 4.9 inverse femtobarns. The measurement is performed using events with two leptons and a jet originated from a b quark. A multivariate analysis based on kinematic properties is utilized to separate the  $t$ -bar background from the signal. The observed signal has a significance of 4.0 sigma and corresponds to a cross section of  $16^{+5}_{-4} \text{ pb}$ , in agreement with the standard model expectation of  $15.6^{+1.0}_{-1.2} \text{ pb}$ .

**Keywords:** Top quark; W boson; Pp collision.

### 327. Inclusive Search for Supersymmetry Using Razor Variables in PP Collisions at $\sqrt{s} = 7 \text{ TeV}$

S. Chatrchyan, Ali Yehia Ellithi et al

*Physical Review Letters*, 111: 081802-, (2013) IF: 7.9

An inclusive search is presented for new heavy particle pairs produced in  $\sqrt{s} = 7 \text{ TeV}$  proton-proton collisions at the LHC using  $4.7^{+0.1}_{-0.1} \text{ fb}^{-1}$  of integrated luminosity. The selected events are analyzed in the 2D razor space of  $M_R$ , an event-by-event indicator of the heavy particle mass scale, and  $R$ , a dimensionless variable related to the missing transverse energy. The third-generation sector is probed using the event heavy-flavor content. The search



is sensitive to generic supersymmetry models with minimal assumptions about the superpartner decay chains. No excess is observed in the number of events beyond that predicted by the standard model. Exclusion limits are derived in the CMSSM framework as well as for simplified models. Within the CMSSM parameter space considered, gluino masses up to 800 GeV and squark masses up to 1.35 TeV are excluded at 95% confidence level depending on the model parameters. The direct production of pairs of top or bottom squarks is excluded for masses as high as 400 GeV.

**Keywords:** PP collision; Super symmetry.

### 328. Measurement of Associated Production of Vector Bosons and Top Quark-Antiquark Pairs in PP Collisions at $\sqrt{s} = 7$ TeV

S. Chatrchyan, Ali Yehia Ellithi et al

*Physical Review Letters*, 110: 172002 (2013) IF: 7.9

The first measurement of vector-boson production associated with a top quark-antiquark pair in proton-proton collisions at  $\sqrt{s} = 7$  TeV is presented. The results are based on a data set corresponding to an integrated luminosity of 5.0 fb<sup>-1</sup>, recorded by the CMS detector at the LHC in 2011. The measurement is performed in two independent channels through a trilepton analysis of ttZ events and a same-sign dilepton analysis of ttV (V = W or Z) events. In the trilepton channel a direct measurement of the ttZ cross section  $\sigma(\text{ttZ}) = 0.28 (-0.11) (+0.14)$  (stat)  $(-0.03) (+0.06)$  (syst) pb is obtained. In the dilepton channel a measurement of the ttV cross section yields  $\sigma(\text{ttV}) = 0.43(-0.15) (+0.17)$  (stat)  $(-0.07) (+0.09)$  (syst) pb. These measurements have a significance, respectively, of 3.3 and 3.0 standard deviations from the background hypotheses and are compatible, within uncertainties, with the corresponding next-to-leading order predictions of 0.137(-0.016) (+0.012) and 0.306(-0.053) (+0.031) pb.

**Keywords:** Vector boson; Top quark.

### 329. Measurement of the $B_s^0 \rightarrow \mu^+\mu^-$ Branching Fraction and Search for $B^0 \rightarrow \mu^+\mu^-$ with the CMS Experiment

S. Chatrchyan, Ali Yehia Ellithi et al

*Physical Review Letters*, 111: (2013) IF: 7.9

Results are presented from a search for the rare decays  $B_s^0 \rightarrow \mu^+\mu^-$  and  $B^0 \rightarrow \mu^+\mu^-$  in pp collisions at  $\sqrt{s} = 7$  and 8 TeV, with data samples corresponding to integrated luminosities of 5 and 20 fb<sup>-1</sup>, respectively, collected by the CMS experiment at the LHC. An unbinned maximum-likelihood fit to the dimuon invariant mass distribution gives a branching fraction  $B(B_s^0 \rightarrow \mu^+\mu^-) = (3.0^{+1.0}_{-0.9}) \times 10^{-9}$ , where the uncertainty includes both statistical and systematic contributions. An excess of  $B_s^0 \rightarrow \mu^+\mu^-$  events with respect to background is observed with a significance of 4.3 standard deviations. For the decay  $B^0 \rightarrow \mu^+\mu^-$  an upper limit of  $B(B^0 \rightarrow \mu^+\mu^-) < 1.1 \times 10^{-9}$  at the 95% confidence level is determined. Both results are in agreement with the expectations from the standard model.

**Keywords:** Rare decays; PP collision.

### 330. Measurement of the Y(1S), Y(2S), and Y(3S) Polarizations in PP Collisions at $\sqrt{s} = 7$ TeV

S. Chatrchyan, Ali Yehia Ellithi et al

*Physical Review Letters*, 110: 081802-, (2013) IF: 7.9

The polarizations of the Y(1S), Y(2S), and Y(3S) mesons are measured in proton-proton collisions  $\sqrt{s} = 7$  TeV, using a data sample of  $Y(nS) \rightarrow \mu^+\mu^-$  to oppositely charged muon pair decays collected by the CMS experiment, corresponding to an integrated luminosity of 4.9 fb<sup>-1</sup>. The dimuon decay angular distributions are analyzed in three different polarization frames. The polarization parameters  $\lambda_{\theta}$ ,  $\lambda_{\phi}$ , and  $\lambda_{\theta\phi}$ , as well as the frame-invariant quantity  $\tilde{\lambda}$ , are presented as a function of the Y(nS) transverse momentum between 10 and 50 GeV, in the rapidity ranges  $|\text{abs}(y)| < 0.6$  and  $0.6 < |\text{abs}(y)| < 1.2$ . No evidence of large transverse or longitudinal polarizations has been seen in the explored kinematic region.

**Keywords:** Meson polarization; Pp Collision.

### 331. Search for Pair Production of Third-Generation Leptoquarks and Top Squarks in PP Collisions at $\sqrt{s} = 7$ TeV

S. Chatrchyan, Ali Yehia Ellithi et al

*Physical Review Letters*, 110: (2013) IF: 7.9

Results are presented from a search for the pair production of third-generation scalar and vector leptoquarks, as well as for top squarks in R-parity-violating supersymmetric models. In either scenario, the new, heavy particle decays into a tau lepton and a b quark. The search is based on a data sample of pp collisions at  $\sqrt{s} = 7$  TeV, which is collected by the CMS detector at the LHC and corresponds to an integrated luminosity of 4.8 inverse femtobarns. The number of observed events is found to be in agreement with the standard model prediction, and exclusion limits on mass parameters are obtained at the 95% confidence level. Vector leptoquarks with masses below 760 GeV are excluded and, if the branching fraction of the scalar leptoquark decay to a tau lepton and a b quark is assumed to be unity, third-generation scalar leptoquarks with masses below 525 GeV are ruled out. Top squarks with masses below 453 GeV are excluded for a typical benchmark scenario, and limits on the coupling between the top squark, tau lepton, and b quark,  $\lambda_{t\tau b}$  are obtained. These results are the most stringent for these scenarios to date.

**Keywords:** Leptoquarks; Top quarks.

### 332. Search for Pair-Produced Dijet Resonances in Four-Jet Final States in PP Collisions at $\sqrt{s} = 7$ TeV

S. Chatrchyan, Ali Yehia Ellithi et al

*Physical Review Letters*, 110: (2013) IF: 7.9

A search for the pair production of a heavy, narrow resonance decaying into two jets has been performed using events collected in  $\sqrt{s} = 7$  TeV pp collisions with the CMS detector at the LHC. The data sample corresponds to an integrated luminosity of



5.0 inverse femtobarns. Events are selected with at least four jets and two dijet combinations with similar dijet mass. No resonances are found in the dijet mass spectrum. The upper limit at 95% confidence level on the product of the resonance pair production cross section, the branching fractions into dijets, and the acceptance varies from 0.22 to 0.005 pb, for resonance masses between 250 and 1200 GeV. Pair-produced colorons decaying into  $q\bar{q}'$  are excluded for coloron masses between 250 and 740 GeV.

**Keywords:** Dijet resonance; PP Collision.

### 333. Search for Top Squarks in R-Parity-Violating Supersymmetry Using Three or More Leptons and b-Tagged Jets

S. Chatrchyan, Ali Yehia Ellithi et al

*Physical Review Letters*, 111: (2013) IF: 7.9

A search for anomalous production of events with three or more isolated leptons and bottom-quark jets produced in pp collisions at  $\sqrt{s} = 8$  TeV is presented. The analysis is based on a data sample corresponding to an integrated luminosity of 19.5 inverse femtobarns collected by the CMS experiment at the LHC in 2012. No excess above the standard model expectations is observed. The results are interpreted in the context of supersymmetric models with signatures that have low missing transverse energy arising from light top-squark pair production with R-parity-violating decays of the lightest supersymmetric particle. In two models with different R-parity-violating couplings, top-squarks are excluded below masses of 1020 GeV and 820 GeV when the lightest supersymmetric particle has a mass of 200 GeV.

**Keywords:** Squarks; R-parity; Tagged jets.

### 334. Searches for new physics using the $t\bar{t}$ invariant mass distribution in $pp$ collisions at $\sqrt{s} = 8$ TeV

S. Chatrchyan, Ali Yehia Ellithi et al

*Physical Review Letters*, 111: (2013) IF: 7.9

Searches for anomalous top quark-antiquark production are presented, based on  $pp$  collisions at  $\sqrt{s} = 8$  TeV. The data, corresponding to an integrated luminosity of  $19.7 \text{ fb}^{-1}$ , were collected with the CMS detector at the LHC. The observed  $t\bar{t}$  invariant mass spectrum is found to be compatible with the standard model prediction. Limits on the production cross section times branching fraction probe, for the first time, a region of parameter space for certain models of new physics not yet constrained by precision measurements.

**Keywords:** Pp Collision, Top Quark Antiquark.

### 335. Study of the Mass and Spin-Parity of the Higgs Boson Candidate VIA its Decays to Z Boson Pairs

S. Chatrchyan, Ali Yehia Ellithi et al

*Physical Review Letters*, 110: (2013) IF: 7.9

A study is presented of the mass and spin-parity of the new boson recently observed at the LHC at a mass near 125 GeV. An

integrated luminosity of 17.3 inverse femtobarns, collected by the CMS experiment in proton-proton collisions at center-of-mass energies of 7 and 8 TeV, is used. The measured mass in the ZZ channel, where both Z bosons decay to e or mu pairs, is  $126.2 \pm 0.6$  (stat.)  $\pm 0.2$  (syst.) GeV. The angular distributions of the lepton pairs in this channel are sensitive to the spin-parity of the boson. Under the assumption of spin 0, the present data are consistent with the pure scalar hypothesis, while disfavoring the pure pseudoscalar hypothesis.

**Keywords:** Decay of higgs boson; PP Collision.

### 336. Magnetic Properties of Cylindrical Diameter Modulated $\text{Ni}_{80}\text{Fe}_{20}$ Nanowires: Interaction and Coercive Fields

Mohamed Shaker Salem, Philip Sergelius, Rosa M. Corona, Juan Escrig, Detlef Görlitz and Kornelius Nielsch

*Nanoscale*, 5: 3941-3947 (2013) IF: 6.233

Magnetic properties of cylindrical  $\text{Ni}_{80}\text{Fe}_{20}$  nanowires with modulated diameters are investigated theoretically as a function of their geometrical parameters and compared with those produced inside the pores of anodic alumina membranes by pulsed electrodeposition. We observe that the  $\text{Ni}_{80}\text{Fe}_{20}$  nanowires with modulated diameters reverse their magnetization via the nucleation and propagation of a vortex domain wall. The system begins generating vortex domains in the nanowire ends and in the transition region between the two segments to minimize magnetostatic energy generated by surfaces perpendicular to the initial magnetization of the sample. Besides, we observed an increase of the coercivity for the sample with equal volumes in relation to the sample with equal lengths. Finally, the interaction field is stronger in the case of constant volume segments. These structures could be used to control the motions of magnetic domain walls. In this way, these nanowires with modulated diameters can be an alternative to store information or even perform logic functions.

**Keywords:** Porous alumina; Magnetic nanowires.

### 337. Search for New Physics in Events with Same-Sign Dileptons and B Jets in $PP$ Collisions at $\sqrt{s} = 8$ TeV

Ali Yehia Ellithi Kamel

*Journal of High Energy Physics*, 37: (2013) IF: 5.618

A search for new physics is performed using events with isolated same-sign leptons and at least two bottom-quark jets in the final state. Results are based on a sample of proton-proton collisions collected at a center-of-mass energy of 8 TeV with the CMS detector and corresponding to an integrated luminosity of  $10.5 \text{ fb}^{-1}$ . No excess above the standard model background is observed. Upper limits are set on the number of events from non-standard-model sources and are used to constrain a number of new physics models. Information on acceptance and efficiencies is also provided so that the results can be used to confront an even broader class of new.

**Keywords:** PP collision; Higgs particles.

### 338. Crown Graphene Nanomeshes: Highly Stable Chelation-doped Semiconducting Materials

Ahmed A. Maarouf, Razvan A. Nistor, Ali Afzali-Ardakani, Marcelo A. Kuroda, Dennis M. Newns and Glenn J. Martyna

*Journal of Chemical Theory and Computation*, 9: 2398-2403 (2013) IF: 5.389

Graphene nanomeshes (GNMs) formed by the creation of pore superlattices in graphene are a possible route to graphene-based electronics due to their semiconducting properties, including the emergence of fractional electronvolt band gaps. The utility of GNMs would be markedly increased if a scheme to stably and controllably dope them was developed. In this work, a chemically motivated approach to GNM doping based on selective pore-perimeter passivation and subsequent ion chelation is proposed. It is shown by first-principles calculations that ion chelation leads to stable doping of the passivated GNMs—both n- and p-doping are achieved within a rigid-band picture. Such chelated or “crown” GNM structures are stable, high mobility semiconducting materials possessing intrinsic doping-concentration control; these can serve as building blocks for edge-free graphene nanoelectronics including GNM-based complementary metal oxide semiconductor (CMOS)-type logic switches.

**Keywords:** Graphene; Nanomesh; Antidot lattice; Doping; Ion-chelation; First-principles calculations.

### 339. The $\alpha$ Decay Spectroscopic Factor of Heavy and Superheavy Nuclei

Wala Mohamed Seif

*Journal of Physics G: Nuclear and Particle Physics*, 40 (10): (2013) IF: 5.326

The spectroscopic factor which refers to the preformation probability of an  $\alpha$  cluster inside parent radioactive nuclei is investigated. The study is based on the cluster model of a decay that is extended to account for the deformation degrees of freedom. The calculations are carried out for 179 even (Z)-even(N) parent nuclei in the mass region of  $A = 144-294$ . Taking into account the deformations of daughter nuclei, the semi-microscopic calculations of the  $\alpha$ -daughter interaction potential are performed using the Hamiltonian energy density approach in terms of the SLy4 Skyrme-like effective interaction. The calculated potential is then implemented to find both the assault frequency and the penetration probability of the particle by means of the Wentzel-Kramers-Brillouin approximation at different orientations of the deformed daughter. By averaging the obtained decay widths over different orientations, the half-lives of the mentioned  $\alpha$  decays are then estimated. Taking into account the errors on both the released energy and the experimental half-life times, the extracted half-lives are employed in turn to deduce the  $\alpha$  spectroscopic factor. The results show a periodic behaviour of the spectroscopic factor as a function of the charge and neutron numbers characterized by several local maxima and minima. The predicted minima are mainly related to the proton and neutron shell and subshell closures. In addition to the well-known closed shells of the nucleonic numbers 50, 82, and 126, the obtained values of the spectroscopic factor give some evidence for the presence of closed subshells of nucleonic numbers 70, 102 (104) and 152 (150). A simple formula is suggested to roughly estimate the spectroscopic factor in terms of the numbers of protons and

neutrons of the parent nucleus outside its closed shells. The parameters of this formula are fitted to the deduced values of the spectroscopic factor.

**Keywords:** Alpha decay; Preformation factor; Spectroscopic factor; Deformed nuclei; Half-life.

### 340. Interpretation of Searches for Supersymmetry with Simplified Models

S. Chatrchyan, Ali Yehia Ellithi et al

*Physical Review D*, 88: 052017 (2013) IF: 4.691

The results of searches for supersymmetry by the CMS experiment are interpreted in the framework of simplified models. The results are based on data corresponding to an integrated luminosity of 4.73 to 4.98 inverse femtobarns. The data were collected at the LHC in proton-proton collisions at a center-of-mass energy of 7 TeV. This paper describes the method of interpretation and provides upper limits on the product of the production cross section and branching fraction as a function of new particle masses for a number of simplified models. These limits and the corresponding experimental acceptance calculations can be used to constrain other theoretical models and to compare different supersymmetry-inspired analyses.

**Keywords:** PP collision; Supersymmetric particles.

### 341. Measurements of Differential Jet Cross Sections in Proton-Proton Collisions at $\sqrt{s} = 7$ TeV with the CMS detector

S. Chatrchyan, Ali Yehia Ellithi et al

*Physical Review D*, 87: 112002 (2013) IF: 4.691

Measurements of inclusive jet and dijet production cross sections are presented. Data from LHC proton-proton collisions at  $\sqrt{s} = 7$  TeV, corresponding to 5.0 inverse femtobarns of integrated luminosity, have been collected with the CMS detector. Jets are reconstructed up to rapidity 2.5, transverse momentum 2 TeV, and dijet invariant mass 5 TeV, using the anti-kt clustering algorithm with distance parameter  $R = 0.7$ . The measured cross sections are corrected for detector effects and compared to perturbative QCD predictions at next-to-leading order, using five sets of parton distribution functions.

**Keywords:** PP collision; Inclusive jets; Dijet cross section.

### 342. Observation of A Diffractive Contribution to Dijet Production in Proton-Proton Collisions at $\sqrt{s} = 7$ TeV

S. Chatrchyan, Ali Yehia Ellithi et al

*Physical Review D*, 87: 012006- (2013) IF: 4.691

The cross section for dijet production in pp collisions at  $\sqrt{s} = 7$  TeV is presented as a function of  $\xi$ , a variable that approximates the fractional momentum loss of the scattered proton in single-diffractive events. The analysis is based on an integrated luminosity of 2.7 inverse nanobarns collected with the CMS detector at the LHC at low instantaneous luminosities, and uses events with jet transverse momentum of at least 20 GeV. The dijet cross section results are compared to the predictions of

diffractive and nondiffractive models. The low- $x$  data show a significant contribution from diffractive dijet production, observed for the first time at the LHC. The associated rapidity gap survival probability is estimated.

**Keywords:** PP collision; Dijet production.

### 343. Rapidity distributions in exclusive Z+jet and $\gamma$ +jet events in pp collisions at $\sqrt{s}=7$ TeV

S. Chatrchyan, Ali Yehia Ellithi et al

*Physical Review D*, 88: 112009 (2013) IF: 4.691

Rapidity distributions are presented for events containing either a Z boson or a photon with a single jet in proton-proton collisions produced at the CERN LHC. The data, collected with the CMS detector at  $\sqrt{s}=7$  TeV, correspond to an integrated luminosity of  $5.0 \text{ fb}^{-1}$ . The individual rapidity distributions of the boson and the jet are consistent within 5% with expectations from perturbative QCD. However, QCD predictions for the sum and the difference in rapidities of the two final-state objects show discrepancies with CMS data. In particular, next-to-leading-order QCD calculations, and two common Monte Carlo event generators using different methods to match matrix-element partons with parton showers, appear inconsistent with the data as well as with each other.

**Keywords:** PP collision; Rapidity distribution.

### 344. Search for Contact Interactions in $\mu^+ \mu^-$ Events in PP Collisions at $\sqrt{s}=7$ TeV

S. Chatrchyan, Ali Yehia Ellithi et al

*Physical Review D*, 87: (2013) IF: 4.691

Results are reported from a search for the effects of contact interactions using events with a high-mass, oppositely charged muon pair. The events are collected in proton-proton collisions at at  $\sqrt{s}=7$ TeV using the Compact Muon Solenoid detector at the Large Hadron Collider. The data sample corresponds to an integrated luminosity of  $5.3 \text{ fb}^{-1}$ . The observed dimuon mass spectrum is consistent with that expected from the standard model. The data are interpreted in the context of a quark- and muon-compositeness model with a left-handed isoscalar current and an energy scale parameter  $\Lambda$ . The 95% confidence level lower limit on  $\Lambda$  is 9.5 TeV under the assumption of destructive interference between the standard model and contact-interaction amplitudes. For constructive interference, the limit is 13.1 TeV. These limits are comparable to the most stringent ones reported to date.

**Keywords:** PP collision; Contact interactions.

### 345. Search for Contact Interactions Using the Inclusive Jet Pt Spectrum in PP Collisions at $\sqrt{s} = 7$ TeV

S. Chatrchyan, Ali Yehia Ellithi et al

*Physical Review D*, 87: 052017 (2013) IF: 4.691

Results are reported of a search for a deviation in the jet production cross section from the prediction of perturbative quantum chromodynamics at next-to-leading order. The search is conducted using a 7 TeV proton-proton data sample

corresponding to an integrated luminosity of 5.0 inverse femtobarns, collected with the Compact Muon Solenoid detector at the Large Hadron Collider. A deviation could arise from interactions characterized by a mass scale  $\Lambda$  too high to be probed directly at the LHC. Such phenomena can be modeled as contact interactions. No evidence of a deviation is found. Using the CLs criterion, lower limits are set on  $\Lambda$  of 9.9 TeV and 14.3 TeV at 95% confidence level for models with destructive and constructive interference, respectively. Limits obtained with a Bayesian method are also reported.

**Keywords:** PP collision; Contact interactions; Inclusive jet spectrum.

### 346. Search for Fractionally Charged Particles in PP Collisions at $\sqrt{s} = 7$ TeV

S. Chatrchyan, Ali Yehia Ellithi et al

*Physical Review D*, 87: 092008- 092008 (2013) IF: 4.691

A search is presented for free heavy long-lived fractionally charged particles produced in pp collisions at  $\sqrt{s}=7$  TeV. The data sample was recorded by the CMS detector at the LHC and corresponds to an integrated luminosity of 5.0 inverse femtobarns. Candidate fractionally charged particles are identified by selecting tracks with associated low charge measurements in the silicon tracking detector. Observations are found to be consistent with expectations for background processes. The results of the search are used to set upper limits on the cross section for pair production of fractionally charged, massive spin-1/2 particles that are neutral under SU(3)[C] and SU(2)[L]. We exclude at 95% confidence level such particles with electric charge  $\pm 2e/3$  with masses below 310 GeV, and those with charge  $\pm e/3$  with masses below 140 GeV.

**Keywords:** PP collisions; Fractionally charged particles.

### 347. Search for Narrow Resonances Using the Dijet Mass Spectrum in PP Collisions at $\sqrt{s}=8$ TeV

S. Chatrchyan, Ali Yehia Ellithi et al

*Physical Review D*, 87: 114015 (2013) IF: 4.691

Results are presented of a search for the production of new particles decaying to pairs of partons (quarks, antiquarks, or gluons), in the dijet mass spectrum in proton-proton collisions at  $\sqrt{s}=8$  TeV. The data sample corresponds to an integrated luminosity of 4.0 inverse femtobarns, collected with the CMS detector at the LHC in 2012. No significant evidence for narrow resonance production is observed. Upper limits are set at the 95% confidence level on the production cross section of hypothetical new particles decaying to quark-quark, quark-gluon, or gluon-gluon final states. These limits are then translated into lower limits on the masses of new resonances in specific scenarios of physics beyond the standard model. The limits reach up to 4.8 TeV, depending on the model, and extend previous exclusions from similar searches performed at lower collision energies. For the first time mass limits are set for the Randall-Sundrum graviton model in the dijet channel.

**Keywords:** PbPb collision; Dijet mass spectrum.

### 348. Search for New Physics in Final States with a Lepton and Missing Transverse Energy in PP Collisions at the LHC

S. Chatrchyan, Ali Yehia Ellithi et al

*Physical Review D*, 87: 072005 (2013) IF: 4.691

This Letter describes the search for an enhanced production rate of events with a charged lepton and a neutrino in high-energy pp collisions at the LHC. The analysis uses data collected with the CMS detector, with an integrated luminosity of 5.0 inverse femtobarns at  $\sqrt{s} = 7$  TeV, and a further 3.7 inverse femtobarns at  $\sqrt{s} = 8$  TeV. No evidence is found for an excess. The results are interpreted in terms of limits on a heavy charged gauge boson ( $W'$ ) in the sequential standard model, a split universal extra dimension model, and contact interactions in the helicity-nonconserving model. For the last, values of the binding energy below 10.5 (8.8) TeV in the electron (muon) channel are excluded at a 95% confidence level. Interpreting the  $\ell\nu$  final state in terms of a heavy  $W'$  with standard model couplings, masses below 2.90 TeV are excluded.

**Keywords:** PP collision; Charged lepton and neutrino.

### 349. Search for Supersymmetry in Events with Opposite-sign Dileptons and Missing Transverse Energy Using an Artificial Neural Network

S. Chatrchyan, Ali Yehia Ellithi et al

*Physical Review D*, 87: 072001 (2013) IF: 4.691

In this paper, a search for supersymmetry (SUSY) is presented in events with two opposite-sign isolated leptons in the final state, accompanied by hadronic jets and missing transverse energy. An artificial neural network is employed to discriminate possible SUSY signals from a standard model background. The analysis uses a data sample collected with the CMS detector during the 2011 LHC run, corresponding to an integrated luminosity of 4.98 inverse femtobarns of proton-proton collisions at the center-of-mass energy of 7 TeV. Compared to other CMS analyses, this one uses relaxed criteria on missing transverse energy (missing  $E_T > 40$  GeV) and total hadronic transverse energy ( $HT > 120$  GeV), thus probing different regions of parameter space. Agreement is found between standard model expectation and observations, yielding limits in the context of the constrained minimal supersymmetric standard model and on a set of simplified models.

**Keywords:** PP collision; Isolated leptons; Hadronic jets.

### 350. Search for Supersymmetry in Final States with a Single Lepton, b-Quark Jets, and Missing Transverse Energy in Proton-Proton Collisions at $\sqrt{s} = 7$ TeV

S. Chatrchyan, Ali Yehia Ellithi et al

*Physical Review D*, 87: 052006-, (2013) IF: 4.691

A search motivated by supersymmetric models with light top squarks is presented using proton-proton collision data recorded with the CMS detector at a center-of-mass energy of  $\sqrt{s} = 7$  TeV during 2011, corresponding to an integrated luminosity of 4.98 inverse femtobarns. The analysis is based on final states with

a single lepton, b-quark jets, and missing transverse energy. Standard model yields are predicted from data using two different approaches. The observed event numbers are found to be compatible with these predictions. Results are interpreted in the context of the constrained minimal supersymmetric standard model and of a simplified model with four top quarks in the final state.

**Keywords:** Transverse energy; Supersymmetry; PP collision.

### 351. Search for $Z'$ Resonances Decaying to $t\bar{t}$ in Dilepton+jets Final States in pp Collisions at $\sqrt{s} = 7$ TeV

S. Chatrchyan, Ali Yehia Ellithi et al

*Physical Review D*, 87: 027002 (2013) IF: 4.691

A search for resonances decaying to top quark-antiquark pairs is performed using a dilepton+jets data sample recorded by the CMS experiment at the LHC in pp collisions at  $\sqrt{s} = 7$  TeV corresponding to an integrated luminosity of 5.0 fb<sup>-1</sup>. No significant deviations from the standard model background are observed. Upper limits are presented for the production cross section times branching fraction of top quark-antiquark resonances for masses from 750 to 3000 GeV. In particular, the existence of a leptophobic topcolor particle  $Z'$  is excluded at the 95% confidence level for resonance masses  $M_{Z'} < 1.3$  TeV for  $\Gamma_{Z'} = 0.012 M_{Z'}$ , and  $M_{Z'} < 1.9$  TeV for  $\Gamma_{Z'} = 0.10 M_{Z'}$ .

**Keywords:** PP collision;  $Z'$  decay.

### 352. Search for A Narrow, Spin-2 Resonance Decaying to A Pair of Z Bosons in the $Q\bar{Q} L+L$ Final State

S. Chatrchyan, Ali Yehia Ellithi et al

*Physics Letters B*, 718: 1208-1228 (2013) IF: 4.569

Results are presented from a search for a narrow, spin-2 resonance decaying into a pair of Z bosons, with one Z-boson decaying into leptons ( $e^+e^-$  or  $\mu^+\mu^-$ ) and the other into jets. An example of such a resonance is the Kaluza-Klein graviton, GKK, predicted in Randall-Sundrum models. The analysis is based on a 4.9 fb<sup>-1</sup> sample of proton-proton collisions at a center-of-mass energy of 7 TeV, collected with the CMS detector at the LHC. Kinematic and topological properties including decay angular distributions are used to discriminate between signal and background. No evidence for a resonance is observed, and upper limits on the production cross sections times branching fractions are set. In two models that predict Z-boson spin correlations in graviton decays, graviton masses are excluded lower than a value which varies between 610 and 945 GeV, depending on the model and the strength of the graviton couplings.

**Keywords:** Cms; Physics; Kaluza-Klein; Graviton

### 353. Elastic Interaction of Protons with Stable and Exotic Light Nuclei

M. Y. H. Farag, E. H. Esmael and H. M. Maridi

*Physical Review C*, (2013) IF: 3.715

The proton elastic-scattering data on  $^{4,6,8}\text{He}$  and  $^{6,7,9,11}\text{Li}$  nuclei are analyzed over a wide range of incident energies below 160 MeV/nucleon using the single-folding optical model. The real part of the folding optical potential (OP) is calculated using the M3Y nucleon-nucleon interaction and microscopic densities. The Green's function Monte Carlo density is used for the stable nuclei, whereas the large-scale shell model density is used for the exotic nuclei. The high-energy approximation calculation is used for the volume imaginary OP. The spin-orbit and surface imaginary parts of the OP are constructed from the derivatives of the real and volume imaginary parts of the folded potentials, respectively. The volume integrals of the OPs are studied, and it is found that they show clear dependencies on energy and root-mean-square radii. Hence, it can be considered an important constraint for the choice of the optical potential. A new empirical formula is assumed and successfully applied for the real volume integrals. The obtained results of the differential and the reaction cross sections are in good agreement with the available experimental data. In general, this OP with few and limited fitting parameters, which have systematic behavior with incident energy, successfully describes the proton elastic-scattering data with stable and exotic light nuclei at energies below 160 MeV/nucleon.

### 354. Prediction of Nuclear Spin Based on the Behavior of $\alpha$ -Particle Preformation Probability

M. Ismail and A. Adel

*Physical Review C*, 88: (2013) IF: 3.715

A realistic density-dependent nucleon-nucleon (NN) interaction with a finite-range exchange part which produces the nuclear matter saturation curve and the energy dependence of the nucleon-nucleus optical model potential is used to calculate the microscopic  $\alpha$ -nucleus potential in the well-established double-folding model.

The main effect of antisymmetrization under exchange of nucleons between the  $\alpha$  and daughter nuclei has been included in the folding model through the finite-range exchange part of the NN interaction. The  $\alpha$ -decay half-lives have been determined using a microscopic potential within the semiclassical Wentzel-Kramers-Brillouin approximation in combination with the Bohr-Sommerfeld quantization condition. We systematically studied the preformation probability,  $S_\alpha$ , for ten even-even and odd mass heavy nuclei from Po to No isotopes. We found that  $S_\alpha$  has a regular behavior with  $N$  if the  $\alpha$  particle emitted from adjacent isotopes comes from the same energy levels or from a group of levels, assuming that the order of levels in this group is not changed. Sudden increase in  $S_\alpha$  is found when protons and neutrons holes exist below the Fermi levels. Based on the similarity in the behavior of  $S_\alpha$  with the neutron number for two adjacent nuclei, we try to determine the unknown or doubted nuclear spins and parities or at least correlate spins of adjacent nuclei.

**Keywords:** Nuclear spin;  $\alpha$ -particle; Preformation probability.

### 355. Measurement of the Elliptic Anisotropy of Charged Particles Produced in PbPb Collisions at Nucleon-nucleon Center-of-mass Energy = 2.76 TeV

S. Chatrchyan, Ali Yehia Ellithi et al

*Physical Review C*, 87, 014902 (2013) IF: 3.7

The anisotropy of the azimuthal distributions of charged particles produced in PbPb collisions with a nucleon-nucleon center-of-mass energy of 2.76 TeV is studied with the CMS experiment at the LHC. The elliptic anisotropy parameter defined as the second coefficient in a Fourier expansion of the particle invariant yields, is extracted using the event-plane method, two- and four-particle cumulants, and Lee-Yang zeros. The anisotropy is presented as a function of transverse momentum ( $p_t$ ), pseudorapidity ( $\eta$ ) over a broad kinematic range:  $0.3 < p_t < 20$  GeV,  $|\eta| < 2.4$ , and in 12 classes of collision centrality from 0 to 80%. The results are compared to those obtained at lower center-of-mass energies, and various scaling behaviors are examined. When scaled by the geometric eccentricity of the collision zone, the elliptic anisotropy is found to obey a universal scaling with the transverse particle density for different collision systems and center-of-mass energies.

**Keywords:** PP collisions; Elliptic anisotropy.

### 356. Assessment of Strontium Immobilization in Cement-bentonite Matrices

R.O. Abdel Rahman, D.H. A. Zin El Abidin and H. Abou-Shady

*Chemical Engineering Journal*, 228: 772-780 (2013) IF: 3.473

The feasibility of immobilizing strontium in cement-bentonite matrices was investigated by studying the effect of mineralogical phase development on mechanical and containment performances. Within this context, the chemical composition and physical properties of bentonite were determined. Different cement-bentonite waste matrices were prepared and analyzed using XRD technique to trace the changes in phases during the curing period. The mechanical performance of these matrices was evaluated by measuring the compressive strength throughout their curing period and the containment performance was determined by conducting long-term static leaching test then the experimental results were checked against some regulatory limits. The results indicated that the presence of strontium and bentonite did not lead to formation of new hydrated phases. The mechanical performance of the matrices is acceptable and the enhanced compressive strength was attributed to the progression in the formation of cement hydrated phases and the pozzolanic reaction between bentonite and lime in cement-bentonite matrices. The speciation data and phase structures analysis indicated that  $\text{Sr}^{2+}$  containment in cement might be due to Ca substitution in Ettringite structure and cations exchange on Montmorillonite lattice. The mathematical analysis of the long-term leaching results indicated that strontium leaching resulted from a combination of first order reaction and diffusion mechanisms.

**Keywords:** Radioactive waste; Cement; Immobilization; Leaching mechanisms.

### 357. Advanced Imaging Techniques for Characterization of $0.5\text{BaTiO}_3/0.5\text{Ni}_{0.5}\text{Zn}_{0.5}\text{Fe}_2\text{O}_4$ Multiferroic Nanocomposite

M. A. Ahmed, N. Okasha and N.G. Imam

*Journal of Alloys and Compounds*, 557: 130-141 (2013) IF: 2.39

New techniques are used to synthesis and characterize  $0.5\text{BaTiO}_3/0.5\text{Ni}_{0.5}\text{Zn}_{0.5}\text{Fe}_2\text{O}_4$ ; (BTO/NZF) multiferroic nanocomposite. Improved citrate autocombustion preparation technique is used to synthesis ferromagnetic and ferroelectric



phases of the investigated nanocomposite. Atomic force microscope (AFM) is one of the important tools for imaging, measuring, and manipulating matter at the nanoscale. AFM is used at different sample areas to confirm the data obtained from scanning electron microscope (SEM) and transmission electron microscope (TEM). Moreover AFM gives 3D visualization for the surface texture and roughness showing the morphology of the two distinguishes phases. The traditional characterizations techniques have been used such as X-ray diffraction (XRD), Fourier transform infrared spectroscopy (FT-IR) to identify the formation of the two individual phases separately and to study the chemical composition of the prepared nanocomposite respectively.

**Keywords:** Multiferroic nanocomposite; Citrate technique; Afm; Tem; Nanorods.

### 358. Effective Dye Removal and Water Purification Using the Electric and Magnetic $\text{Zn}_{0.5}\text{Co}_{0.5}\text{Al}_{0.5}\text{Fe}_{1.46}\text{La}_{0.04}\text{O}_4$ / Polymer Core-shell Nanocomposites

M.A. Ahmed, Rasha M. Khafagy, Samiha T. Bishay and N.M. Saleh

*Journal of Alloys and Compounds*, 578: 121-131 (2013) IF: 2.39

Flash auto combustion method was successfully used to synthesize nanoparticles of  $\text{Zn}_{0.5}\text{Co}_{0.5}\text{Al}_{0.5}\text{Fe}_{1.46}\text{La}_{0.04}\text{O}_4$ . High resolution transmission electron microscopy (HRTEM) specified the formation of granular nanospheres beside an intermediated phase of nanowires. Polymer-blended magnetic materials were obtained using poly(vinyl pyrrolidone) (PVP), poly(vinyl alcohol) (PVA), poly(vinyl acetate) (PVAc) and Polyethylene Glycol (PEG) as capping agents. This coating strategy controls the agglomeration of ferrite nanoparticles, and produces a well-designed core-shell nano-assembly with enhanced physical properties. XRD and HRTEM confirmed the formation of ferrite as a core surrounded by various polymeric shells. The nanocomposite with PVP shell resulted in increased ac conductivity (s) of about four orders of magnitude higher than that recorded for the pure ferrite. Curie temperature ( $T_C$ ) decreased from 703 K as recorded for the pure ferrite to less than 440 K for the core-shell nanocomposites containing PVA and PVAc. All prepared samples succeeded in purifying inked-water with high efficiency.  $\text{Zn}_{0.5}\text{Co}_{0.5}\text{Al}_{0.5}\text{Fe}_{1.46}\text{La}_{0.04}\text{O}_4$  up-took 76% of the dye content, while the dye-removal efficiency was increased to 90% when  $\text{Zn}_{0.5}\text{Co}_{0.5}\text{Al}_{0.5}\text{Fe}_{1.46}\text{La}_{0.04}\text{O}_4$ /PVP core-shell nanocomposite was applied. These novel results indicate that such series of core-shell nanocomposites are promising candidates in industrial applications such as purifying and recycling of industrial waste water. Moreover, this study emphasized that polymers are good additive to ferrites when blended in the form of core-shell nanocomposite structure.

**Keywords:** Water purification and dye uptake; Recycling of industrial waste water; Ferrite/polymer core-shell nanocomposites; AC conductivity; Magnetic properties.

### 359. Structural, Electric and Magnetoelectric Properties of $\text{Ni}_{0.85}\text{Cu}_{0.15}\text{Fe}_2\text{O}_4$ / $\text{BiFe}_{0.7}\text{Mn}_{0.3}\text{O}_3$ Multiferroic Nanocomposites

Mohamed Ali Ahmed Mohamed

*Journal of Alloys and Compounds*, 578: 303-308 (2013) IF: 2.39

Spinel-perovskite nanocomposites  $[(1-y) (\text{Ni}_{0.85}\text{Cu}_{0.15}\text{Fe}_2\text{O}_4) + y (\text{BiFe}_{0.7}\text{Mn}_{0.3}\text{O}_3)]$ ;  $y = 30\%$ ,  $40\%$ ,  $50\%$ ,  $60\%$  and  $70\%$  were prepared by mixing the two separately single materials. X-ray diffraction measurements confirm the formation of both phases  $\text{Ni}_{0.85}\text{Cu}_{0.15}\text{Fe}_2\text{O}_4$  (NCFO) and  $\text{BiMn}_{0.3}\text{Fe}_{0.7}\text{O}_3$  (BFMO). The magnetoelectric coefficient was measured as a function of applied dc magnetic field. Dielectric constant ( $\epsilon$ ), loss tangent ( $\tan \delta$ ) and ac conductivity (s) were measured as a function of frequency with different temperatures. The  $\epsilon$  and  $\sigma$  of  $\text{Ni}_{0.85}\text{Cu}_{0.15}\text{Fe}_2\text{O}_4$  were improved by introducing  $\text{BiMn}_{0.3}\text{Fe}_{0.7}\text{O}_3$ . Magnetoelectric nanocomposites may have possible applications in magnetic field sensing probes and linear ME devices. The electric hysteresis loops were obtained in ferrite/BFMO composite, but the loops were not really saturated.

**Keywords:** Nanocomposites; Structural properties; Dielectric properties; Conductivity; Magnetoelectric; P-E hysteresis.

### 360. Synthesis, Characterization and Studies on Magnetic and Electrical Properties of $\text{LaAl}_y\text{Fe}_{1-y}\text{O}_3$ Nanomultiferroic

M. A. Ahmed, N. Okasha and B. Hussein

*Journal of Alloys and Compounds*, 553: 308-315 (2013) IF: 2.39

Multiferroic  $\text{LaAl}_y\text{Fe}_{1-y}\text{O}_3$ ;  $0.00 \leq y \leq 0.20$  were successfully synthesized using citrate auto combustion method and their properties were systematically studied. All the samples were crystallized in a perovskite structure. The evaluation of the unit-cell parameters by X-ray diffraction technique revealed that the lattice constants and volume of the unit cell decreased along with increase of Al content, while the Fe-O octahedra became less distorted. The Goldschmidt tolerance factor for the perovskite increases from 0.905 for  $\text{LaFeO}_3$  to 0.914 for  $\text{LaAl}_{0.2}\text{Fe}_{0.8}\text{O}_3$  confirming that the crystal structure is orthorhombic. All the magnetic parameters such as  $\mu_{\text{eff}}$ ,  $\chi_M$ , and magnetization ( $M_{\text{RT}}$ ) decrease as Al content increases, while Néel temperature indicates the highest value (834 K) at  $y = 0.1$ . The magnetic measurements revealed that it has a superparamagnetic behavior with coercive field  $H_c$  nearly zero. Dielectric and activation energy results agree well with the other measurements.

**Keywords:**  $\text{LaAlFeO}_3$ ; Multiferroic; Tolerance factor; Magnetization; Dielectric; Thermoelectric power.

### 361. Two Distinct Phases in the First 13 Seconds of GRB110731A Prompt Emission

Mohammad A. F. Basha

*Astrophysics and Space Science*, 343: 107-116, (2013) IF: 2.064

In this work, the time-resolved BAT/GBM/LAT joint spectral analysis of GRB110731A during the prompt phase from the GBM trigger and up to 13 seconds later showed that, at the very early phase of prompt emission, the emission mechanism is closest to the standard fireball model. This model over-predicts the thermal photospheric emission and used to contradict observations. Lightcurves at different energy bands revealed two distinguishable phases that may come from different regions. First, we have an early phase, which is not detected by LAT, and is dominated by lower energies, which arises from the photospheric emissions without any emissions involved in

dissipation mechanisms and characterized by low Lorentz factor and high radiation efficiency. This is followed by a later phase, having a more complex structure that remarkably follows the same track in all energy bands and is attributed to emissions from internal shocks. This burst is a good candidate to study both thermal and non-thermal emissions, since the two phases can be clearly separated in lightcurve and spectrum. The rapid variation of Lorentz factor and the values of photospheric radii, which are relatively far away from the central engine in Phase 2, are more consistent with the mechanism of collisional heating in baryonic jets. Further information can be obtained by combining more wavelengths with the help of the other detectors.

**Keywords:** Gamma rays: bursts; Gamma rays observations; Radiation mechanism: thermal.

### 362. IR Spectroscopic Analysis of the New Organic Silver Complex $C_{13}H_{13}N_4OAG$

Farouk El-kabbany, S. Taha and M. Hafez

*Spectrochimica Acta Part A: Molecular and Biomolecular Spectroscopy*, 111: 252-259 (2013) IF: 1.977

IR analysis in the frequency range  $400\text{--}4000\text{ cm}^{-1}$  is used here to investigate the changes in different modes of thermally treated new metal complex (diphenyl carbazide silver complex DPCAg,  $C_{13}H_{13}N_4OAG$ ) during the glass transition at  $91\text{ }^{\circ}\text{C}$  and the high temperature phase transition at  $167\text{ }^{\circ}\text{C}$ . These two phase transitions in this new metal compound are studied here by detecting the changes in some IR spectroscopic parameters (e.g., mode shift, band contour, peak height and peak intensity) during the elevation of temperature. All of the vibrations of DPCAg were found to be due to ionic fundamentals  $3311\text{ cm}^{-1}$ ,  $3097\text{ cm}^{-1}$ ,  $3052\text{ cm}^{-1}$ ,  $1677\text{ cm}^{-1}$ ,  $1602\text{ cm}^{-1}$ ,  $1492\text{ cm}^{-1}$ ,  $1306\text{ cm}^{-1}$ ,  $1252\text{ cm}^{-1}$ ,  $887\text{ cm}^{-1}$  and  $755\text{ cm}^{-1}$ . The results obtained can be considered as the first spectroscopic analysis of this new metal complex. These results strongly confirmed that the thermally treated DPCAg transverse a glass transition at  $91\text{ }^{\circ}\text{C}$  and a high temperature phase transition at  $167\text{ }^{\circ}\text{C}$ . Anomalous spectroscopic changes near the glass transition temperature  $T_g$  could be recorded. A temperature dependence of peak intensity of the two modes  $810\text{ cm}^{-1}$  and  $3440\text{ cm}^{-1}$  could be observed beyond  $T_g$ . Also, the high temperature phase modification at  $167\text{ }^{\circ}\text{C}$  showed anomalous change in the spectroscopic parameters before and after the phase transition process. A proposed silver position in the new silver complex DPCAg has been presented.

**Keywords:** Silver complex; IR analysis.

### 363. Improvement of the Physical Properties of Novel (1-Y) $CO_{0.8}Cu_{0.2}Fe_{2.04+}(y)SrTiO_3$ Nanocomposite

M. A. Ahmed, S.F. Mansour and M.A. Abdo

*Materials Research Bulletin*, 48: 1796-1805 (2013) IF: 1.913

Magnetoelectric (ME) nanocomposites  $(1-y)CO_{0.8}Cu_{0.2}Fe_{2.04} + (y)SrTiO_3$  ( $y = 40, 50, 60, 80$  and  $100\%$ ) were prepared by standard ceramic method. Phase formation was checked using X-ray diffraction analysis. Both saturation magnetization ( $M_s$ ) and Curie temperature ( $T_C$ ) decrease with increasing  $SrTiO_3$  content. Temperature dependence of the dielectric constant reveals two maxima, one about  $550\text{ K}$  corresponds to non-stoichiometry and

lattice distortions while the second around  $900\text{ K}$  corresponds to the Curie temperature ( $T_C$ ). The large value of ME output is due to the strain induced by lattice distortion in the ferrite phase by Jahn–Teller ions like Cu. Hence, Jahn–Teller effect in the ferrite leads to polarization in the piezoelectric phase.

**Keywords:** Magnetic materials; Chemical synthesis; X-ray diffraction; Dielectric properties.

### 364. Innovative Methodology for the Synthesis of Ba-M Hexaferrite $BaFe_{12}O_{19}$ Nanoparticles

M. A. Ahmed, N. Helmy and S.I. El-Dek

*Materials Research Bulletin*, 48: 3394-3398 (2013) IF: 1.913

In this piece of work, high quality and homogeneity, barium hexaferrite (BaM)  $BaFe_{12}O_{19}$  nanoparticles were prepared from organometallic precursors for the 1<sup>st</sup> time. This method is based on the formation of supramolecular crystal structure of  $Ba[Fe(H_3NCH_2CH_2NH_3)]Cl_7 \cdot 8H_2O$ . The crystal structure, morphology and magnetic properties of  $BaFe_{12}O_{19}$  at two different annealing temperatures namely  $1000\text{ }^{\circ}\text{C}$  and  $1200\text{ }^{\circ}\text{C}$  were investigated using X-ray diffraction, transmission electron microscope TEM and vibrating sample magnetometry (VSM). The results show that monophasic nanoparticles of hexaferrites were obtained. Nanoparticles of crystallite size  $40\text{--}50\text{ nm}$  distinguished by narrow distribution and excellent homogeneity were obtained with superior magnetic properties which suggested single-domain particles of Ba-M hexaferrite.

**Keywords:** Magnetic materials; Chemical synthesis; X-ray diffraction; Magnetic properties.

### 365. Analysis of Neutronic Parameters for Supercell of Candu Reactor Using Mcnpx Code

Afrah EL-Khawlani, Moustafa Aziz Ibrahim and Ali Ellithi

*Journal of Materials Science and Engineering B*, 3 (8): 550-553 (2013) IF: 1.884

MCNPX code has been used for modeling and simulation of a supercell of CANDU Fuel, the supercell consists of two fuel bundle and adjuster rod. The fuel bundle are burnt in normal operation conditions of CANDU reactors. Natural uranium fuel is used in the model. The multiplication factor of the bundle is calculated during fuel burnup. The concentration of both uranium and plutonium isotopes are analysed in the bundle. The worth of the adjuster rod is calculated. Comparison of multiplication factor and worth of the adjuster rod with the previous published references showed good agreement.

**Keywords:** Candu; Supercell; MCNPX.

### 366. Structural Characterization and Magnetic Properties of Smart $CuCd$ Ferrite/ $LaSrCo$ Manganite Nanocomposites

M. A. Ahmed, Samiha T. Bishay and S. M. Salem-Gaballah

*Journal of Magnetism and Magnetic Materials*, 334: 96-101 (2013) IF: 1.826

Smart nanocomposites  $Cu_{0.7}Cd_{0.3}Fe_2O_4/La_{0.67}Sr_{0.33}Mn_{0.98}Co_{0.02}O_3$  in different weight ratios were prepared and characterized by

different techniques. The parent compounds were prepared by the citrate–nitrate autocombustion method. Phase formation and crystal structure were investigated by X-ray diffraction. Morphological properties of the nanoparticles were studied using high resolution transmission electron microscopy. Thermal dc magnetization curves were measured from 200 to 800 K for the nanocomposites and showed a characteristic peak near the blocking temperature of LaSrCo manganite shifted toward higher temperature with increasing CuCd ferrite percentage. Such behavior was explained in light of granular model of exchange bias. Vibrating sample magnetometer measurements reveal an enhancement in the ferromagnetic properties with increasing ferrite ratio. The prominent anisotropic shift in the M-H hysteresis loop was discussed as a consequence of interfacial magnetic interactions between LaSrCo manganite and CuCd ferrite grains. Correlation between the measured magnetic parameters and ferrite/manganite ratio is reported and discussed.

**Keywords:** Ferrite/manganite; Nanocomposite; Magnetization; XRD; HRTEM; Hysteresis.

### 367. Synthesis of novel $\text{Zn}_x\text{Co}_{1-x}\text{Al}_{0.5}\text{Fe}_{1.46}\text{La}_{0.04}\text{O}_4$ ; $0.0 \leq x \leq 0.6$ Nanowires, and Optimization of Their Transport and Magnetic Properties

M. A. Ahmed, Samiha T. Bishay, Rasha M. Khafagy and N.M. Saleh

*Journal of Magnetism and Magnetic Materials*, 331: 256-263 (2013) IF: 1.826

$\text{Zn}_x\text{Co}_{1-x}\text{Al}_{0.5}\text{Fe}_{1.46}\text{La}_{0.04}\text{O}_4$ ;  $0.0 \leq x \leq 0.6$  nanowires are synthesized for the first time using urea auto-combustion method. X-ray diffraction (XRD) results prove the phase formation, while transmission electron microscope images prove that the flash auto-combustion method is a successful and easy method for obtaining nanowire-bundle filaments in this type of ferrite. At  $x=0.0$ , nano-spheres were obtained with average size  $\approx 22$  nm, while the formation of nanowires started at  $x=0.2$ , at which nanowire-bundle filaments begin to grow on the surface of these nano spheres with average lengths  $\approx 150$  nm and narrow outer diameters with average value  $\approx 22$  nm. The quantity of nanowires increased with increasing Zn-content substitution to reach its maximum quantity at  $x=0.4$ , after which it decreased at  $x=0.5$ . This observation accords well with the inversion point that occurs in the lattice parameters at  $x=0.5$ . The conduction mechanism in the samples of  $x=0.0$  and  $x=0.5$  reveals the quantum mechanical tunneling, while that in the samples of  $x=0.2$  and  $x=0.3$  reveals overlapping large polaron. The Seebeck coefficient for all the investigated samples takes a +ve sign pointing to a p-type conduction. The sample  $\text{Zn}_{0.6}\text{Co}_{0.4}\text{Al}_{0.5}\text{Fe}_{1.46}\text{La}_{0.04}\text{O}_4$  showed paramagnetic behavior, while the sample  $\text{Zn}_{0.4}\text{Co}_{0.6}\text{Al}_{0.5}\text{Fe}_{1.46}\text{La}_{0.04}\text{O}_4$  showed the largest Curie temperature ( $T_C=790$  K), the lowest conductivity ( $\sigma=0.117 \times 10^{-3} \Omega^{-1} \text{cm}^{-1}$ ), and resulted in the formation of the maximum quantity of nanowire-bundle filaments which are characterized by their large surface area, that might result in a unique behavior which has never been obtained within traditional bulk materials or normal nano-spheres. One recommends the use of such sample in nanobuilding structures demanding low conductivity and high Curie temperature.

**Keywords:** Nanowire; Flash auto-combustion synthesis; Transmission electron microscopy; Electrical conductivity; Magnetic property.

### 368. Enhancement of Structural and Thermal Properties of PEO/PVA Blend Embedded With $\text{TiO}_2$ Nanoparticles

F H Abd El-kader, N A Hakeem, I S Elashmawi and A M Ismail

*Indian Journal of Physics*, 87: 983-990 (2013) IF: 1.785

Blend films based on PEO/PVA (50/50 wt%) undoped and doped with different concentration of  $\text{TiO}_2$  nanoparticles are prepared by casting technique. Characteristic properties of the blend films are investigated using Fourier transform infrared, X-ray diffraction (XRD), ultraviolet–visible spectra (UV-Vis), scanning electron microscope (SEM), differential scanning calorimetry (DSC) and thermogravimetric analysis. On the basis of results obtained from IR and DSC data, blends appear to be immiscible. XRD, UV-Vis and TG reveal that 1.0 wt%  $\text{TiO}_2$  is most ordered concentration. SEM reveals that the presence of  $\text{TiO}_2$  leads to changes in the surface morphology and gives rise to crystalline domains with coarse spherulitic structure. It has been seen that spherulites increases with addition of  $\text{TiO}_2$  nanoparticles. TG studies conclude that this concentration has low  $E^*$ ,  $\Delta S^*$  and  $\Delta H^*$ . So, it is more ordering and has low thermal motion. Kinetic thermodynamic parameters such as activation energy, enthalpy, entropy and Gibb's free energy are evaluated from TG data using Coat's–Redfern model.

**Keywords:** Nanocomposites; Fourier transform infrared (FT-IR); X-ray Diffraction (XRD); Optical properties;

### 369. Laser-Induced Breakdown Spectroscopy: Technique, New Features, and Detection Limits of Trace Elements in Al Base Alloy

H. Hegazy, E. A. Abdel-Wahab, F. M. Abdel-Rahim, S. H. Allam and A. M. A. Nossair

*Applied Physics B*, 115 (2): 173-183 (2013) IF: 1.782

Laser-induced breakdown spectroscopy (LIBS) has proven to be extremely versatile, providing multielement analysis in real time without sample preparation. The principle is based on the ablation of a small amount of target material by interaction of a strong laser beam with a solid target. The laser must have sufficient energy to excite atoms and to ionize them to produce plasma. We aimed to improve the LIBS limit of detection (LOD) and the precision of spectral lines emitted from the produced plasma by optimizing the parameters affecting the LIBS technique. LIBS LOD is affected by many experimental parameters such as interferences, self-absorption, spectral overlap, signal-to-noise ratio, and matrix effects. The plasma in the present study is generated by focusing a 6-ns pulsed Nd–YAG laser at the fundamental wavelength of 1,064 nm onto the Al target in air at atmospheric pressure. The emission spectra are recorded using an SE 200 Echelle spectrometer manufactured by the Catalina Corporation; it is equipped with an ICCD camera type Andor model iStar DH734-18. This spectrometer allows time-resolved spectral acquisition over the whole UV-NIR (200–1,000 nm) spectral range. Calibration curves for Cu, Mg, Mn, Si, Cr, and Fe were obtained with linear regression coefficients around 99 % on the average in aluminum standard alloy samples. The determined LOD has very useful improvements for Cu I at 521.85 nm, Si I at 288.15 nm, Mn I at 482.34 nm, and Cr I at 520.84 nm spectral lines. LOD is improved by 83.8 % for Cu, 49 % for Si, 84.3 % for Mn, and 45 % for Cr lower with respect to the previous works.

### 370. Spectral Evolution of Nano-Second Laser Interaction with Ti Target in Air

H. Hegazy, H. A. Abd El-Ghany, S. H. Allam and Th. M. El-Sherbini

*Appl Phys B-Lasers O*, 110 (4): 509- 518 (2013) IF: 1.782

Time-resolved optical emission spectroscopy has been successfully employed to investigate the evolution of plasma produced by the interaction of IR- and visible-pulsed laser beams with a titanium target in ambient air at atmospheric pressure. The characterization of the plasma-assisted pulsed laser ablation of the titanium target is discussed in this study. The emission spectrum produced by the titanium plasma in the wavelength range 200–1,000 nm has been carefully investigated for different experimental conditions. Boltzmann plots have been used in the calculation of the excitation temperature employing Ti II spectral lines at 286.23, 321.71, 325.29, 348.36, and 351.08 nm; this set of lines was tested and proved to be suitable for the measurement of the plasma temperature. The obtained temperature is in good agreement with the one obtained from Ti II spectral lines previously suggested by Hermann et al. [J. Appl. Phys. 77, 2928–2936, 1995, 22]. Moreover, the Stark broadening method has been employed for electron density measurements. In this study, the Stark width of the Ti II spectral line at 350.49 nm was used.

### 371. Size Confinement and Magnetization Improvement by $\text{La}^{3+}$ Doping in $\text{BiFeO}_3$ Quantum Dots

Mohamed Ali Ahmed Mohamed

*Solid State Sciences*, 20: 23-28 (2013) IF: 1.671

Nanometric multiferroic samples  $\text{Bi}_{1-x}\text{La}_x\text{FeO}_3$ ;  $0.05 \leq x \leq 0.40$  were prepared using ceramic method. Structural and magnetic properties were investigated using XRD, TEM, magnetic susceptibility and  $M-H$  loop. The decrease in the lattice parameters is due to the difference between the ionic radii of Bi and La and this effect is compensated by the change in the atomic weight of the two elements which is reflected as a decrease in the density. The obtained results showed that all samples were antiferromagnetic in character. The small values of remnant and saturation magnetization indicated the canted type antiferromagnetism. Maximum coercivity  $H_c = 5265$  Oe was obtained at  $x = 0.25$ . The magnetic susceptibility measurements show its size dependence due to long range spin arrangement. Improvement of the magnetization of  $\text{BiFeO}_3$  is achieved by  $\text{La}^{3+}$  at different doping levels. The obtained quantum dot size of the crystallites enhances their use in spintronic devices.

**Keywords:** Nanometric  $\text{BiFeO}_3$ ; Magnetic quantum dots; Multiferroic; Neel temperature; G-type antiferromagnet.

### 372. Effect of Energy Level Sequences and Neutron-Proton Interaction on $\alpha$ -Particle Preformation Probability

M. Ismail and A. Adel

*Nuclear Physica, A 912: 18-30* (2013) IF: 1.525

A realistic density-dependent nucleon–nucleon ( $NN$ ) interaction with finite-range exchange part which produces the nuclear matter saturation curve and the energy dependence of the nucleon–nucleus optical model potential is used to calculate the preformation probability,  $S_\alpha$ , of  $\alpha$ -decay from different isotones with neutron numbers  $N = 124, 126, 128, 130$  and  $132$ . We studied the variation of  $S_\alpha$  with the proton number,  $Z$ , for each isotone and found the effect of neutron and proton energy levels of parent nuclei on the behavior of the  $\alpha$ -particle preformation probability. We found that  $S_\alpha$  increases regularly with the proton number when the proton pair in  $\alpha$ -particle is emitted from the same level and the neutron level sequence is not changed during the  $Z$ -variation. In this case the neutron–proton ( $n-p$ ) interaction of the two levels, contributing to emission process, is too small. On the contrary, if the proton or neutron level sequence is changed during the emission process,  $S_\alpha$  behaves irregularly, the irregular behavior increases if both proton and neutron levels are changed. This behavior is accompanied by change or rapid increase in the strength of  $n-p$  interaction.

**Keywords:**  $\alpha$ -Particle preformation probability; Finite-range exchange  $NN$  interaction; Odd-mass nuclei.

### 373. Analysis of Target Fragmentation Induced by Relativistic $^{24}\text{Mg}$

A.Abdelsalam, E. A.Shaat, Z. Abou-Moussa, B. M. Badawy and Z. S.Mater

*Radiation Physics and Chemistry*, 91: 1-8 (2013) IF: 1.375

This is an experimental work in which, we focus on the target fragments production in the interactions of 4.5 A GeV/c  $^{24}\text{Mg}$  with emulsion nuclei. For the protons flying in the nuclear emulsion with a kinetic energy up to 400 MeV, the energy–range relations exhibit a power law form. The exponential decay is a characteristic shape of the gray and black particle energy spectra. The SRIM software succeeds to simulate the ionization behavior of the gray and black particles in the nuclear emulsion. The anisotropy factors belonging to the gray and black particle emission systems are always  $\sim 3.5$  and  $1.3$ , respectively, irrespective of the projectile size or energy. In the light of the modified statistical model, the temperatures of the gray and black particle emission systems are predicted as 60 and 6 MeV, respectively. The results indicate that, the target fragmentation system is thermalized and moving towards equilibrium.

**Keywords:** Angular characteristics; Target fragmentation; Ionization behavior of proton in photographic emulsion; Srim predictions.

### 374. Effect of Focusing Conditions and Laser Parameters on the Fabrication of Gold Nanoparticles via Laser Ablation in Liquid

Khaled A. Elsayed, Hisham Imam, M.A.Ahmed and Rania Ramadan

*Optics and Laser Technology*, 45: 495-502 (2013) IF: 1.365

The generation of nanoparticles using pulsed laser ablation has inherent advantages compared to conventional methods, like the purity and stability of the fabricated nanoparticles, aerosols and colloids. This study addresses the influence of laser parameters



such as laser fluence, laser wavelength as well as focusing condition of laser beam on the size and morphology of the gold nanoparticles prepared in de-ionized water by pulsed laser ablation. The optimum conditions at which gold nanoparticles are obtained with controllable average size have been reported as these parameters affected the size, distribution and absorbance spectrum. The effect of laser fluence was studied. The laser fluences were divided into three regions (low, middle and high). A noteworthy change was observed at each region. At low fluences, the size of the nanoparticles decreases as the fluence increases to a certain critical value after which the size of the nanoparticles increases as the fluence increases. Also a significant change in the size distribution of the gold nanoparticles was noticed during the variation of the focusing conditions at gold–water interface

**Keywords:** Gold nanoparticles; Laser ablation; Absorption spectrum; Focusing conditions.

### 375. DC Conduction Mechanism and Dielectric Properties of Poly (Methyl Methacrylate)/ Poly (Vinyl Acetate) Blends Doped and Undoped With Malachite Green

F. H. Abd-Elkader, W. H. Osman and R. S. Hafez

*Physica B: Condensed Matter*, 408: 140-150 (2013) IF: 1.327

Cast thin films of Poly (methyl methacrylate)/Poly (vinyl acetate) blends of different concentrations undoped and doped with malachite green have been prepared and subjected to both dc electrical conduction and dielectric spectroscopy measurements. The analysis of dc electrical conduction data showed that the space charge limited current mechanism has been dominant for Poly (vinyl acetate) while Schottky–Richardson conduction mechanism prevailed for the Poly (methyl methacrylate) and blended samples. The values of field lowering constant  $\beta$  and the thermal activation energy  $\Delta E$  involved in the dc conduction were reported, which provide another support for the suggested Schottky–Richardson mechanism. The increase in current for the blend sample doped with malachite green has been attributed to the formation of charge transfer complexes inside the polyblend matrix. The dielectric constant as a function of temperature for all samples have been calculated which are affected by the composition ratio and the addition of dye. The relaxation peak that appeared in the dielectric loss curve at 347 K for the doped blend sample is related to local dipoles that are present in the dye material. The obtained relaxation process spectra present in the investigated samples were analyzed with the well-known model of Havriliak–Negami

**Keywords:** Polymer blend; DC conduction; I–V characteristic; Schottky–Richardson mechanism; Dielectric spectroscopy; Malachite green.

### 376. (A = 10)-Accompanied Spontaneous Ternary Fission of Californium

M. Ismail, W.M. Seif, A.Y. Ellithi and A.S. Hashem

*Canadian Journal of Physics*, 91:401-410 (2013) IF: 0.902

The ternary fission of  $^{238-256}\text{Cf}$  even-A isotopes is studied in the framework of the three-cluster model within the spherical approximation. The study is confined to those decays in which the accompanied light charged particle is of mass  $A = 10$ .

The most probable ternary fission path is obtained as the one that has a peak in the Q-value and a minimum in the driving potential, with respect to the mass and charge asymmetries. Assuming both equatorial and collinear configurations of the different emissions of the light charged particles with  $A = 10$ , the ternary fission of  $^{252}\text{Cf}$  is found to be most favored with  $^{10}\text{Be}$ .

The predicted favorable fragmentation channels of the  $^{10}\text{Be}$ -accompanied ternary fission of  $^{238-256}\text{Cf}$ , even-A, isotopes are discussed in detail. The closed-shell structure of the produced heaviest fragment is found to play a key role for the detected most favorable channels. A nucleus with a closed neutron shell or even doubly closed shell always appears as the heaviest nucleus in the favored channel of the ternary fission of all mentioned isotopes. As the isospin asymmetry of the isotope increases, the width of its cold fission valley around the symmetric mass region decreases, with more shifting towards the centre of the symmetric region. Neither the most favorable ternary emissions nor the behavior of the ternary fragmentation potential changed with the type of nuclear interaction potential (Yukawa, folding potential with Migdal force, and proximity 77). Also, almost no change is observed according to the method of emission of the fragments (equatorially or collinearly) or when the calculations are performed without inserting the nuclear interaction potential.

**Keywords:** Superheavy nuclei; Spontaneous ternary fission; Three-cluster model.

### 377. Comparative Analysis of Multiplicity of Target Fragments in a Few a GeV $^4\text{He}$ -Emulsion Interactions

A. Abdelsalam, N. Metwalli, S. Kamel, M. Aboullela, B.M. Badawy and N. Abdallah

*Canadian Journal of Physics*, 91(5): 438-443 (2013) IF: 0.902

We report an experimental measurement on the multiplicity of slow target-associated particles in the forward and backward hemispheres in the interactions of  $^4\text{He}$  ions with emulsion nuclei at 2.1A and 3.7A GeV. The results indicate that the target fragment multiplicity does not depend on the incident kinetic energy. The dominant feature characterizing the multiplicity distributions of black and grey particles, in both forward and backward hemispheres, is exponential decay shaped curves, with the exception of the most central collisions and heavy target sizes. The results favor the nuclear limiting fragmentation hypothesis in the energy range beyond 1 GeV.

### 378. Limiting Fragmentation of Target Nucleus at High Energy

M.S. El-Nagdy, A. Abdelsalam, Z. Abou-Moussa and B.M. Badawy

*Canadian Journal of Physics*, 91(9): 737-743 (2013) IF: 0.902

This study discusses features suggestive of a nuclear multifragmentation in the target. A wide range of projectile masses are used ( $A_{\text{proj}} = 1-207$ ) over a large energy region ( $E_{\text{lab}} = 1\text{A}-200\text{A GeV}$ ). In particular, the validity of the nuclear limiting fragmentation hypothesis is focused in the target region. The probability that the target is fragmented forms about 90% from the total inelastic geometrical cross section. The dependence of the target fragmentation cross section on the system size and on



the incident energy is presented. The results are analyzed in the framework of the modified FRITIOF simulation code.

### 379. Studies of Target-Evaporated Particle Production in Forward and Backward Hemispheres in $^{16}\text{O}$ -Emulsion Interactions at 60A and 200A GeV

A. Abdelsalam, S. Kamel, N. Rashed and M. Fayed

*Canadian Journal of Physics*, 91(1): 105-112 (2013) IF: 0.902

The multiplicity distribution of the target-evaporated black particles emitted in the interactions of  $^{16}\text{O}$  beams with emulsion nuclei at 60A and 200A GeV in both the forward and backward hemispheres are examined. The asymmetry parameters, the forward-backward ratios as well as multiplicity distribution moments are evaluated. The investigated scaled variances and the second Mueller moments are observed to indicate the strongly correlated emission of target-evaporated black particles in the forward direction. The ratio of entropy to average multiplicity of target fragments is evaluated, and is found to be energy-independent in both the forward and backward hemispheres.

### 380. The 4d-4P Transitions and Soft X-ray Laser Wavelengths in Si-Like Ions<sup>1</sup>

A. Abou El-Maaref, M.A.M. Uosif, S.H. Allam and Th.M. El-Sherbini

*Canadian Journal of Physics*, 91(11): 981-993 (2013) IF: 0.902

The transitions between 4p and 4d levels have been studied to examine the possibility of laser wavelength production in the soft X-ray region. The oscillator strengths of the transitions  $3p4p (^3S, ^3P, ^3D) \rightarrow 3p4d (^3P^o, ^3D^o, ^3F^o)$  have been calculated using CIV3 code. Using calculated oscillator strengths, the excitation rate coefficients, reduced populations, and gain coefficients for Si-like Ni XV, Zn XVII, Ga XVIII, Ge XIX, and As XX at electron temperatures 1/4, 1/2, and 3/4 the ionization potential have been calculated. The method by Palumbo and Elton has been used in the calculation of laser parameters. The present calculated data show promising values for the production of laser wavelengths in the soft X-ray region. The maximum values of the gain factor lie within the range  $\alpha \sim 10^9 \text{ cm}^{-1}$  and wavelength  $\lambda \leq 469 \text{ \AA}$ .

### 381. Dynamical Change of Surface Diffuseness of Ion-Ion Potential and Its Effect on Fusion Cross-Section

M. Ismail and W. M. Seif

*International Journal of Modern Physics E*, 22 (2): (2013) IF: 0.625

We assume a simple model to describe the ion-ion potential with dynamical change in its surface diffuseness. In particular, this model is used to calculate the heavy-ion fusion cross-section using different values of the surface diffuseness. Both the static and dynamic nuclear Woods-Saxon potentials with diffuseness values ranging between 0.65 fm and 1.3 fm are used to reproduce the fusion cross-sections data of the  $^{19}\text{F} + ^{208}\text{Pb}$  and  $^{16}\text{O} + ^{154}\text{Sm}$  reactions. The results estimate that there are different physical processes which could contribute to the fusion cross-

section with different weights at each energy value. Each of these processes has its own nuclear potential.

**Keywords:** Diffuseness; Fusion reactions; Woods-saxon; Heavy ions; Coupled channels.

### 382. Multiplicity Characteristics in Relativistic $^{24}\text{Mg}$ -Nucleus Collisions

A. Abdelsalam, E. A. Shaat, Z. Abou-Moussa, B. M. Badawy and Z. S. Mater1

*Chinese Physics C*, 37(8): (2013) IF: 0.338

This work is concerned with the analyses of the shower and gray particle production in  $4.5 \text{ A GeV/c } ^{24}\text{Mg}$  collision with emulsion nuclei. The highest particle production occurs in the region of the low impact parameters. While the multiplicity of the shower particles emitted in the forward direction depends on the projectile mass number and energy, the multiplicity of the backward ones shows a limiting behaviour. The source of the emission of the forward shower particles is completely different from that of the backward ones. The target fragments are produced in a thermalized system of emission.

**Keywords:**  $^{24}\text{Mg}$  interactions with emulsion; Forward and backward emission of hadrons; Projectile and target dependence.

### 383. The Effect of Higher-order Mesonic Interactions on the Chiral Phase Transition and the Critical Temperature

M. Abu-Shady and H. M. Mansour

*Ukr.J.Phys.* 58 (10): 925-932 (2013)

In the present work, higher-order mesonic interactions are included in the linear sigma model at finite temperature. The effective potential is minimized in the calculations of the sigma and pion effective masses. The field equations have been solved in the mean-field approximation by using the extended iteration method at finite temperature. The order of chiral phase transition, the effective sigma and pion masses, and the effective mesonic potential are investigated as functions of temperature. We find that the chiral phase transition satisfies the Goldstone theorem below the critical point temperature when the minimization condition is satisfied in the chiral limit. The value of the critical temperature is reduced compared to that of the original model in agreement with lattice QCD results. The modified model is compared to the models in other works.

**Keywords:** Finite-temperature field theory; Chiral symmetry; Meson properties.

### 384. Analysis of Elastic Scattering of Pi-Mesons by Nuclei within the Microscopic Optical Potential

V. K. Lukyanov, E. V. Zemlyanaya, K. V. Lukyanov, Ali El Lithi, Ibrahim Abdulmagead and B. Slowinski

*Bulletin of the Russian Academy of Sciences: Physics*, 77 (4): 427-432 (2013)

The microscopic pion-nucleus optical potential defined by the pion-nucleon scattering amplitude and the density distribution function of the target nucleus is applied to obtain the differential

cross section of the elastic pion-nucleus scattering based on the solution to the relativistic wave equation. This allows one to account for effects of the relativization and distortion by the potential field. Data on  $\pi^\pm$ -meson scattering on  $^{28}\text{Si}$ ,  $^{58}\text{Ni}$ , and  $^{208}\text{Pb}$  nuclei at  $T_{\text{lab}} = 291$  MeV are analyzed and the parameters of the in-medium  $\pi N$ -amplitude are obtained. The parameters are compared with similar parameters for scattering on free nucleons.

**Keywords:** Pion; Elastic scattering; Microscopic optical potential.

### 385. Analysis of Reactivity-Initiated Accident for Control Rods Ejection

Hesham Mansour, Hend M. Saad and M. Aziz

*Journal of Nuclear and Particle Physics*, 3(4): 45-54 (2013)

Understanding of the time-dependent behavior of the neutron population in a nuclear reactor in response to either a planned or unplanned change in the reactor conditions is of great importance to the safe and reliable operation of the reactor. In the present work, the point kinetics equations are solved numerically using the stiffness confinement method (SCM). The solution is applied to the kinetic equation in the presence of different types of reactivities, and is compared with other method. This method is, also used to analyze reactivity induced accidents in two reactors. The first reactor is fueled by uranium and the second is fueled by plutonium. This analysis presents the effect of negative temperature feedback with the addition positive reactivity of the control rods to overcome the occurrence of the control rod ejection accident and damaging of the reactor. Both the power and the temperature pulse following the reactivity- initiated accidents are calculated. The results are compared with previous works and satisfactory agreement is found.

**Keywords:** Reactivity induced accident; Stiffness confinement method; Point kinetic equations; Control rods ejection; Reactivity coefficient; Safety analysis.

### 386. Analysis of Reactivity Induced Accident for Control Rods Ejection with Loss of Cooling

Hend Mohammed El Sayed Saad, Hesham Mohammed Mohammed Mansour and Moustafa Aziz Abd El Wahab

*Journal of Materials Science and Engineering B*, 3 (2): 128-137 (2013)

Understanding of the time-dependent behavior of the neutron population in nuclear reactor in response to either a planned or unplanned change in the reactor conditions, is a great importance to the safe and reliable operation of the reactor. In the present work, the point kinetics equations are solved numerically using stiffness confinement method (SCM). The solution is applied to the kinetics equations in the presence of different types of reactivities and is compared with different analytical solutions. This method is also used to analyze reactivity induced accidents in two reactors. The first reactor is fueled by uranium and the second is fueled by plutonium. This analysis presents the effect of negative temperature feedback with the addition positive reactivity of control rods to overcome the occurrence of control rod ejection accident and damaging of the reactor. Both power and temperature pulse following the reactivity- initiated accidents are calculated. The results are compared with previous works and satisfactory agreement is found.

**Keywords:** Reactivity induced accident; Stiffness confinement method; Point kinetic equations; Control rods ejection; Reactivity coefficient; Safety analysis.

### 387. Antifungal Activity of Zinc Oxide Nanoparticles against Dermatophytic Lesions of Cattle

Eman M. El-Diasty, M.A Ahmed, Nagwa Okasha, Salwa .F. Mansour, Samaa I.El-Dek, Hanaa M. Abd El-Khalek and Mariam H. Youssif

*Romanian Journal of Biophysics*, 23(3): 191-202 (2013)

Ringworm is a fungal and zoonotic infectious disease, caused by different species of dermatophytes. In this study, skin scrapings and hair samples were collected from 50 cattle with clinical symptoms of dermatophytosis. The collected samples were directly examined for fungal elements by direct microscopy. Isolates of Dermatophytes were found to be 14.3% and 26.6% for samples obtained from cow and buffaloes respectively. The distribution of isolates was *Trichophyton mentagrophyte* (33.33%), *Microporum canis* (26.67%), *Candida albicans* (26.67%), *Aspergillus fumigatus* (13.33%) respectively. The antifungal activity of zinc oxide (ZnO) nanoparticles was evaluated for *Trichophyton mentagrophyte*, *Microsporum canis*, *Candida albicans* and *Aspergillus fumigatus*. The largest inhibition in the germination of all the tested fungi was observed at largest ZnO nanoparticles concentration (40 mg/mL).

**Keywords:** ZnO nanoparticles; Hexagonal; Antifungal activity; *Trichophyton mentagrophytes*; *Microsporum canis*; *Candida albicans*; *Aspergillus fumigatus*.

### 388. Bulk Properties of Symmetric Nuclear and Pure Neutron Matter

Khaled Hassaneen and Hesham Mansour

*Journal of Modern Physics*, 4: 37-41 (2013)

We study the equation of state (EOS) of symmetric nuclear and neutron matter within the framework of the Brueckner-Hartree-Fock (BHF) approach which is extended by including a density-dependent contact interaction to achieve the empirical saturation property of symmetric nuclear matter. This method is shown to affect significantly the nuclear matter EOS and the density dependence of nuclear symmetry energy at high densities above the normal nuclear matter density, and it is necessary for reproducing the empirical saturation property of symmetric nuclear matter in a nonrelativistic microscopic framework. Realistic nucleon-nucleon interactions which reproduce the nucleon-nucleon phase shifts are used in the present calculations.

**Keywords:** Symmetric nuclear matter; Equation of state; Three-body force; Symmetry energy.

### 389. Effect of the $\text{La}^{3+}$ Ions Substitution on the Magnetic Properties of Spinal Li-Zn-Ferrites at Low Temperature

Ahmed Ibrahim Ali, Mohamed Ali Ahmed, Nagwa Okasha, Mahmoud Hammam and Jong Yeog Son

*Journal of Materials Research and Technology*, 2 (4): 356-361 (2013)

The effect of  $\text{La}^{3+}$  ions substitution on the magnetic properties of the composition  $\text{Li}_{0.5-0.5x}\text{Zn}_y\text{La}_x\text{Fe}_{2.5-0.5x-y}\text{O}_4$  ( $0.02 \leq x \leq 0.1$ ;  $y = 0.6$ ) was studied. The structure of the samples was investigated using X-ray, SEM and IR. Both of zero field cooled (ZFC) and field cooled (FC) modes magnetization were studied at low temperature range ( $2 \text{ K} \leq T \leq 400 \text{ K}$ ). Magnetization applied field-dependence (M-H) curves were measured at low temperature (5 K). The experimental data revealed that the samples exhibited a phase transition from ferrimagnetic state at low temperature to paramagnetic state at high temperature (400 K). The obtained Curie temperature was shifted to lower value with  $\text{La}^{3+}$ -content. The M-H curves showed that the samples are soft ferromagnetic and it can be an excellent candidate for industrial applications.

**Keywords:** Rare earth-Li-Zn-Ferrite; Low temperature magnetization; IR spectroscopy; DTA analyses; Magnetic hysteresis loop at low temperature.

### 390. Geometrical Formulae for Reaction Cross-Section between Deformed-Deformed Nuclei

M. Y. Ismail, A. Y. Ellithi, H. El Gebaly and A. A. Mohamed

*International Journal of Physics and Research (Ijpr)*, 3 (3): 41-60 (2013)

Three geometrical formulae were suggested for the orientation dependence of  $\sigma_R$  for two interacting deformed nuclei. The reaction cross-section of the interacting pairs ( $^{17}\text{N}$ - $^{17}\text{N}$ ), ( $^{17}\text{N}$ - $^{238}\text{U}$ ) and ( $^{238}\text{U}$ - $^{238}\text{U}$ ), are calculated for these models, for different orientations of their symmetry axes. The results of these calculations are compared with the theoretical calculations obtained by the Glauber optical limit, at incident energy  $E_L/A_p$  MeV per nucleon. The variation of the ratio between the Glauber optical limit and modeled data  $\alpha_{dd}$  with the orientation angles is studied for each interacting pair and the most reasonable formula is suggested. Our second model is the closest to the Glauber approach results of the reaction cross-section. It is very close to the assumed average  $\alpha_{dd} = 1.0$ .

**Keywords:** Reaction cross; Section; Glauber optical limit; Deformed nuclei.

### 391. Natural Radioactivity Assessment and Radiological Hazards in Soils from Qarun Lake and Wadi El Rayan in Faiyum, Egypt

Saher M. Darwish, Samia M. El-Bahi, Amany T. Sroor and Najat F. Arhoma

*Open Journal of Soil Science*, 3 (7): 289-296 (2013)

The activity concentrations of naturally occurring  $^{238}\text{U}$ ,  $^{232}\text{Th}$  and  $^{40}\text{K}$  in surface soils along Qarun Lake and Wadi El Rayan located in Faiyum, Egypt were determined. The measurements were carried out through gamma-ray spectrometry using a coaxial HPGe detector. The results were compared with those reported in the literature. The radiological hazard radium-equivalent activity index, external and internal indices, radioactivity level index, absorbed dose rate, annual effective dose rate and total absorbed dose rate associated with radioactivity in all samples were evaluated and compared with recommended values. Correlation studies between pairs of radionuclides were performed and discussed.

**Keywords:** Natural radioactivity; Radiological hazards; Hpge detector; Gamma-ray spectrometry.

### 392. Neutral Higgs-boson Production in Association with a Pair of Muon-Sneutrino at $e^-e^+$ Linear Colliders

B. Y. Al-Negashi, T. A. El-Azim and I. A. Abdul-Magead

*International Review of Physics*, 7: 259-268 (2013)

The full virtual one loop radiative electroweak corrected cross section,  $\sigma$ , to the  $e^-e^+ \rightarrow \nu\bar{\nu} \mu^+ \mu^- h^0$  channel is presented. The dependence of the ( $s_0$  and  $s$ ) on the  $v_s$  and the other parameters in the framework of Minimal Supersymmetric Standard Model (MSSM) is discussed. The numerical results in each of the SPS 1b and SPS 4 scenarios show clearly that  $s$  are always more than the corresponding  $s_0$ . The  $\Delta\sigma/\sigma_0$  varies in the range of  $[-43\%, 40\%]$  as  $V_s$  goes from 0.5 TeV to 2.5 TeV for SPS 1b scenario and in the range of  $[41\%, 54\%]$  as  $v_s$  goes from 1 TeV to 2.5 TeV for SPS 4 one.

**Keywords:** Light neutral higgs boson particle; Mssm; Muon sneutrino particle.

### 393. Orientation Dependence of the Phase Shift Function for Deformed-Deformed Interacting Pairs

M.Y. Ismail, A.Y. Ellithi, H. EL Gebaly and A.A. Mohamed

*Australian Journal of Basic and Applied Sciences*, 7 (8): 151-162 (2013)

The variation of the phase shift function of the deformed-deformed pairs ( $^{17}\text{N}$ - $^{17}\text{N}$ ), ( $^{17}\text{N}$ - $^{238}\text{U}$ ) and ( $^{238}\text{U}$ - $^{238}\text{U}$ ) with the impact parameter at certain orientations and the effect of the in-medium NN interaction on the phase shift function by using three different approaches are studied. The phase shift function has strong  $\theta$ -dependence at  $b = 6 \text{ fm}$  for the light-heavy pair ( $^{17}\text{N}$ - $^{238}\text{U}$ ). This dependence is sensitive to the volume of the projectile and the orientations of the symmetry axes of the nuclei involved in collision. The dependence is large when the projectile is  $^{238}\text{U}$  and when the orientations are  $\theta_p = \theta_r = 0^\circ$  and  $\theta_T = \theta_r = 90^\circ$ .

**Keywords:** Glauber theory; Phase shift function; Deformed nuclei.

### 394. Radiological Hazards for Marble and Granite Used At Shak El Thouban Industrial Zone in Egypt

Amany T. Sroor, Saher M. Darwish, Samia M. El-Bahi and Mohamed G. Abdel Karim

*Journal of Environmental Protection*, 4: 41-48 (2013)

The background level of radiation in the natural environment surrounds us at all times. Levels of natural occurring radioactivity in marble and granite used at Shak El Thouban industrial zone in Cairo, Egypt have been investigated using HPGe detector through gamma-ray spectrometry. The activity concentration of radionuclides in the  $^{238}\text{U}$ -,  $^{232}\text{Th}$ -series and  $^{40}\text{K}$  has been determined. The average activity concentration of  $^{238}\text{U}$ ,

$^{232}\text{Th}$  and  $^{40}\text{K}$  for marble samples was 23.77 Bq/kg ranged from (10.91 to 45.4), 10.75 Bq/kg ranged from (5.46 to 23.61) and 520.43 Bq/kg ranged from (382.30 to 1132.41), respectively. The  $^{238}\text{U}$ ,  $^{232}\text{Th}$  and  $^{40}\text{K}$  activity concentration for granite samples were 54.31 Bq/kg ranged from (12.04 to 106.34), 113.57 Bq/kg ranged from (23.91 to 270.36) and 7867.51 Bq/kg ranged from (2017.60 to 11436.91), respectively. Concerning the radiological risk, the radium equivalent activity, external and internal radiation hazard indices, the radiation level index and absorbed dose rate were evaluated. The mass exhalation rates of  $^{222}\text{Rn}$  and emanation coefficient have been also calculated. The mass exhalation rate of radon was found to be from 14.86 to 137.13 and 16.48 to 155.26  $\mu\text{Bq/kg}\cdot\text{s}$  for marble and granite samples, respectively. The mean values of the specific activity of  $^{226}\text{Ra}$ , activity of  $^{238}\text{U}$  before and after sealing time and the mass exhalation rate of radon for granite samples are twice that for marble samples. All radiological indices and the mass exhalation rate of radon are lower than the permissible levels for building material in all marble samples, while all granite samples are higher and unsafe and pose a risk to the workers and users of these products due to the emanation of radon that may accumulate by time, especially in closed spaces.

**Keywords:** Radiological hazards; Marble; Granite; Hpge detector; Shak El Thouban.

### 395. Search for Heavy Majorana Neutrinos at LHC Using Monte Carlo Simulation

Hesham M. M. Mansour and Nady Bakhiet

*Open Journal of Microphysics*, 3: 12-17 (2013)

Heavy neutrinos can be discovered at LHC. Many extensions for Standard Model predict by existing of new neutrino has a mass at high energies at LHC. B-L model one of them that predict by existence three heavy (right-handed) neutrinos one per generation, new gauge massive boson and new scalar Higgs boson rather than SM Higgs. In this work we search for heavy neutrino in 4 leptons + missing energy final state events produced in proton-proton collisions at LHC using data produced from Monte Carlo simulation for B-L model at different center of mass energies. We predict that the heavy neutrinos pairs can be produced from  $Z'_{B-L}$  new gauge neutral massive boson decay and then the heavy neutrino pairs can decay to 4 leptons + missing energy final state which give us an indication for new signatures of new physics beyond Standard Model at higher energies at LHC for B-L extension of Standard Model.

**Keywords:** Heavy neutrinos; LHC; B-L model; Monte Carlo; SM.

### 396. Search for High Energy Electrons from New Neutral Massive Gauge Boson Decay in the CMS Detector at the LHC Using Monte Carlo Simulation

Hesham M. M. Mansour and Nady Bakhiet

*Open Journal of Microphysics*, 3: 34-42 (2013)

The existence of new heavy neutral massive boson  $Z'$  is a feature of many extensions of Standard Model models as the two-Higgs-doublet model (2HDM), the Hidden Abelian Higgs Model (HAHM), Left-Right Symmetric Model (LRSM), Sequential Standard Model (SSM) and Baryon number minus Lepton

number Model (B-L). In the present work we search for two high energy electrons produced from decaying heavy neutral massive boson in the events produced in proton-proton collisions at LHC and can be detected by CMS detector. We used the data which is produced from proton-proton collisions by Monte Carlo events generator for different energies at LHC, then we use the angular distribution, invariant mass, combined transverse momentum and combined rapidity distributions for the two high energy electrons produced from decay channel to detect the  $Z'_{B-L}$  signal. B-L extension of the SM model predicts the existence of a  $Z'_{B-L}$  heavy neutral massive boson at high energies. From our results which we had simulated using MC programs for  $Z'_{B-L}$  in the B-L extension of standard model, we predict a possible existence of new gauge  $Z'_{B-L}$  at LHC in the mass range 1 TeV to 1.5 TeV via electrons identification of the two high energy electrons by CMS detector.

**Keywords:** LHC; CMC; Monte Carlo simulation; New boson; Sm; B-L; Gauge boson.

### 397. Search of New Higgs Boson in B-L Model at the LHC Using Monte Carlo Simulation

Hesham M. M. Mansour and Nady Bakhiet

*Open Journal of Microphysics*, 3: 106-113 (2013)

The aim of this work is to search for a new heavy Higgs boson in the B-L extension of the Standard Model at LHC using the data produced from simulated collisions between two protons at different center of mass energies by Monte Carlo event generator programs to find new Higgs boson signatures at the LHC. Also, we study the production and decay channels for Higgs boson in this model and its interactions with the other new particles of this model namely the new neutral gauge massive boson  $Z'_{H-L}$  and the new fermionic right-handed heavy neutrinos  $V_h$ .

**Keywords:** Higgs boson; LHC; B-L model; Monte Carlo; SM; Neutrinos.

### 398. Spectroscopic Measurement of Stark Broadening Parameter of the 636.2 nm Zn I-line

Ashraf M. El Sherbini, Abdel-Nasser Aboulfotouh, Farid Rashid, Sami H. Allam, Ahmed M. Al-Kaoud, Ashraf El Dakroui and Tharwat M. El Sherbini

*Natural Science*, 5(4): 501-507 (2013)

In this article we will present an attempt to measure the Stark broadening parameter of the Zn I-line at 636.23 nm utilizing the optical emission spectroscopy (OES) technique, taking into consideration the possibility of existence of self absorption. This method is standing on comparison of the Lorentzian FWHM and spectral line intensity of the unknown Stark broadening parameter line (Zn I-636.23 nm—in our case) to a well known Stark parameter line (e.g. Zn I-lines at 472.2, 481 and 468 nm) at a reference electron density of  $2.7 \times 10^{17} \text{ cm}^{-3}$  and temperature of 1 eV. We have utilized the emission spectral data acquired from well diagnosed plasma produced by the interaction of Nd: YAG laser at wave-length of 1064 nm with ZnO nanomaterial target in open air. The results indicates that the Stark broadening of the Zn I-line at 636.23 nm is centered at  $5.06 \pm 0.03 \text{ \AA}$  with a 25% uncertainty at the given reference plasma parameters. The knowledge of the Stark broadening parameter of the 636.23 nm

line may be important in the diagnostics of the laser plasma experiments especially in the absence of the  $H_{\alpha}$ -line.

**Keywords:** Stark broadening parameter; LIBS; OES; ZnO; Zinc lines.

### 399. Structural, Optical and Thermal Characterization of ZnO Nanoparticles Doped in PEO/PVA Blend Films

F. H. Abd El-kader, N. A. Hakeem, I. S. Elashmawi and A. M. Ismail

*Australian Journal of Basic and Applied Sciences*, 7 (10): 608-619 (2013)

Solid polymer blend films based on PEO/PVA (50/50 wt/wt %) undoped and doped with different concentration of ZnO nanoparticles were prepared by using casting technique. Structural, optical and thermal studies were performed using X-ray diffraction (XRD), Fourier transform infrared (FT-IR), Ultra violet - visible spectra (UV-VIS), Scanning electron microscope (SEM), Differential scanning calorimetry (DSC) and Thermogravimetric analysis (TGA) and its derivative (DrTG). IR absorption spectra and DSC thermograms indicate that the PEO/PVA undoped blend and doped with ZnO are immiscible. XRD and band tail energy data showed that the incorporation of nano-ZnO into the polymeric system causes decreasing the crystallinity of samples. The kinetic thermodynamic parameters such as activation energy, enthalpy, entropy and Gibbs free energy were evaluated from TG data using Coats' - Redfern relation. SEM analysis indicate that the change of the surface morphology of PEO/PVA/ZnO- nano particles system as phase segregation.

**Keywords:** Nanocomposites; X-Ray diffraction; FT-IR; Optical Properties; DSC; TGA.

### 400. Study of Some Aspects of Reaction Cross-Section between Deformed Nuclei

M. Y. Ismail, A. Y. Ellithi, H. El Gebaly and A. A. Mohamed

*Int. Journal of Physics and Research (Ijpr)* 3 (5): 1-10 (2013)

The reaction cross-section is calculated for three deformed-deformed interacting pairs at range of energy [100-1000 MeV] per nucleon taking into account three approaches of the density dependence of the nucleon-nucleon reaction cross-section, the energy and orientation dependence of the reaction cross-section are studied. We found that, the reaction cross-section  $\sigma_R$  is strongly orientation dependent for the three deformed-deformed interacting pairs. The percentage ratio between the minimum and maximum values of  $\sigma_R$  changes up to 80% for the energy range considered.

**Keywords:** Deformed-deformed interacting pairs; Glauber theory; Nucleon-nucleon interaction.

### 401. Synthesis and Characterization of Cobalt-Doped Nano-Structure Barium Strontium Titanate Prepared by Sol-Gel Process

M.A. Ahmed, M. Kamal, F.G. El Desouky, E. Girgis, I.S.A. Farag and I.K. Battisha

*Journal of Applied Sciences Research*, 9(3): 2432-2438 (2013)

Multiferroic materials possess at least two ferroic properties which make them particularly suitable for multifunctional device applications [Chunqing Wang et al., (2012)]. The purpose of this work was to get onedimensional multiferroics by doping of  $\text{Co}^{2+}$  into ferroelectrics. Multiferroic  $\text{Ba}_{0.9}\text{Sr}_{0.1}\text{Ti}_{0.90}\text{Co}_{0.1}\text{O}_3$  nanoparticle was prepared via a sol-gel method. The magnetic hysteresis loop confirmed the expected enhancing of ferromagnetic properties with a saturation magnetization of 127.58 memu/g, a retentivity of 19.656 memu/g, and a coercivity of 93.951 Oe measured at room temperature. Structural study revealed the tetragonal BST phase by using XRD. The crystallite sizes obtained were 52 and 31 nm for  $\text{Ba}_{0.9}\text{Sr}_{0.1}\text{TiO}_3$  and  $\text{Ba}_{0.9}\text{Sr}_{0.1}\text{Ti}_{0.90}\text{Co}_{0.1}\text{O}_3$ , respectively. The TEM was used to confirm the presence of the nano-structure phase giving 50 and 30 nm, respectively which is agree with that calculated data from XRD.

**Keywords:** Sol gel; SEM; TEM; Multiferroic; Nano-structure; Magnetic hysteresis loop.

### 402. The Hot and Cold Properties of Nuclear Matter

Khaled Hassaneen and Hesham Mansour

*Journal of Nuclear and Particle Physics*, 3 (4): 77-96 (2013)

The properties of nuclear matter at zero and finite temperatures in the frame of the Brueckner theory realistic nucleon-nucleon potentials are studied. Comparison with other calculations is made. In addition we present results for the symmetry energy obtained with different potentials, which is of great importance in astrophysical calculation. Properties of asymmetric nuclear matter are derived from various many-body approaches. This includes phenomenological ones like the Skyrme Hartree-Fock and relativistic mean field approaches, which are adjusted to fit properties of nuclei, as well as more microscopic attempts like the BHF approximation, a Self-Consistent Greens Function (SCGF) method and the so-called Vlowk approach, which are based on realistic nucleon-nucleon interactions which reproduce the nucleon-nucleon phase shifts. These microscopic approaches are supplemented by a density-dependent contact interaction to achieve the empirical saturation property of symmetric nuclear matter. Special attention is paid to behavior of the isovector and the isoscalar component of the effective mass in neutron-rich matter. The nuclear symmetry potential at fixed nuclear density is also calculated and its value decreases with increasing the nucleon energy. In particular, the nuclear symmetry potential at saturation density changes from positive to negative values at nucleon kinetic energy of about 200 MeV. The hot properties of nuclear matter are also calculated using  $T^2$ -approximation method at low temperatures. Good agreement is obtained in comparison with previous theoretical estimates and experimental data especially at low densities.

**Keywords:** Brueckner-hartree-fock approximation; Self-consistent greens function (SCGF) method; Three-body forces; Symmetry energy; Symmetry potential; Effective mass.

### 403. XRF Analysis of Heavy Metals for Surface Soil of Qarun Lake and Wadi El Rayan in Faiyum, Egypt

Samia M. El-Bahi, Amany T. Sroor, Najat F. Arhoma and Saher M. Darwish

*Open Journal of Metal*, 3 (2A) 21-25 (2013)



The environmental pollution with some heavy metals for twenty four surface soil samples collected from Qarun Lake and Wadi El Rayan region in Faiyum, Egypt utilizing X-ray fluorescence (XRF) spectroscopy was measured. The concentrations of 13 elements Cr, Ni, Cu, Zn, Zr, Rb, Y, Ba, Pb, Sr, Ga, V and Nb were determined. The elemental concentrations were compared with the normal values and other studies in different locations from the world. The correlation between elements appears that pollution inside the investigated lake and Wadi result from different sources of contamination present inside them. The results establish a database reference of radioactivity background levels around these regions.

**Keywords:** XRF; Heavy metals; Surface soil; Faiyum.

#### Dept. of Zoology

#### 404. Syndecan-1 Modulates $\beta$ -Integrin-Dependent and Interleukin-6-Dependent Functions in Breast Cancer Cell Adhesion, Migration, and Resistance to Irradiation

Hebatallah Hassan, Burkhard Greve, Mauro S. G. Pavao, Ludwig Kiesel, Sherif A. Ibrahim and Martin Götze

*Federation of European Biochemical Societies Febs*, 280: 2216-2227 (2013) IF: 4.25

Syndecan-1 is a cell surface heparan sulfate proteoglycan with various biological functions relevant to tumor progression and inflammation, including cell-cell adhesion, cell-matrix interaction, and cytokine signaling driving cell proliferation and motility. Syndecan-1 is a prognostic factor in breast cancer, and has a predictive value for neoadjuvant chemotherapy. It is still poorly understood how syndecan-1 integrates matrix-dependent and cytokine-dependent signaling processes in the tumor microenvironment. Here, we evaluated the potential role of syndecan-1 in modulating matrix-dependent breast cancer cell migration in the presence of interleukin-6, and its potential involvement in resistance to irradiation in vitro. MDA-MB-231 breast cancer cells were transiently transfected with syndecan-1 small interfering RNA or control reagents, and this was followed by stimulation with interleukin-6 or irradiation. Cellular responses were monitored by adhesion, migration and colony formation assays, as well as analysis of cell signaling. Syndecan-1 depletion increased cell adhesion to fibronectin. Increased migration on fibronectin was significantly suppressed by interleukin-6, and GRGDSP peptides inhibited both adhesion and migration. Interleukin-6-induced activation of focal adhesion kinase and reduction of constitutive nuclear factor kappaB signaling were decreased in syndecan-1-deficient cells. Focal adhesion kinase hyperactivation in syndecan-1-depleted cells was associated with dramatically reduced radiation sensitivity. We conclude that loss of syndecan-1 leads to enhanced activation of  $\beta$ 1-integrins and focal adhesion kinase, thus increasing breast cancer cell adhesion, migration, and resistance to irradiation. Syndecan-1 deficiency also attenuates the modulatory effect of the inflammatory microenvironment constituent interleukin-6 on cancer cell migration.

**Keywords:** Focal adhesion kinase; Integrin; Interleukin-6 (IL-6); Irradiation resistance; Syndecan.

#### 405. Human Cytomegalovirus Infection Enhances NF- $\kappa$ B/P65 Signaling in Inflammatory Breast Cancer Patients

Mohamed El-Shinawi, Hossam Taha Mohamed, Eslam A. El-Ghonaimy, Marwa Tantawy, Amal Younis, Robert J. Schneider and Mona Mostafa Mohamed

*Plos One*, 8 (2): (2013) IF: 3.73

Human Cytomegalovirus (HCMV) is an endemic herpes virus that re-emerges in cancer patients enhancing oncogenic potential. Recent studies have shown that HCMV infection is associated with certain types of cancer morbidity such as glioblastoma. Although HCMV has been detected in breast cancer tissues, its role, if any, in the etiology of specific forms of breast cancer has not been investigated. In the present study we investigated the presence of HCMV infection in inflammatory breast cancer (IBC), a rapidly progressing form of breast cancer characterized by specific molecular signature. We screened for anti-CMV IgG antibodies in peripheral blood of 49 non-IBC invasive ductal carcinoma (IDC) and 28 IBC patients. In addition, we screened for HCMV-DNA in postsurgical cancer and non-cancer breast tissues of non-IBC and IBC patients. We also tested whether HCMV infection can modulate the expression and activation of transcriptional factor NF- $\kappa$ B/p65, a hallmark of IBC. Our results reveal that IBC patients are characterized by a statistically significant increase in HCMV IgG antibody titers compared to non-IBC patients. HCMV-DNA was significantly detected in cancer tissues than in the adjacent non-carcinoma tissues of IBC and IDC, and IBC cancer tissues were significantly more infected with HCMV-DNA compared to IDC. Further, HCMV sequence analysis detected different HCMV strains in IBC patients tissues, but not in the IDC specimens. Moreover, HCMV-infected IBC cancer tissues were found to be enhanced in NF- $\kappa$ B/p65 signaling compared to non-IBC patients. The present results demonstrated a correlation between HCMV infection and IBC. Etiology and causality of HCMV infection with IBC now needs to be rigorously examined.

**Keywords:** Human cytomegalovirus; Inflammatory breast cancer; Nf- $\kappa$ B/P65.

#### 406. Syndecan-1 (CD138) Modulates Triple-Negative Breast Cancer Stem Cell Properties Via Regulation of LRP-6 and IL-6-Mediated STAT3 Signaling

Sherif A. Ibrahim, Hebatallah Hassan, Laura Vilardo, Sampath Katakam Kumar, Archana Vijaya Kumar, Reinhard Kelsch, Cornelia Schneider, Ludwig Kiesel, Hans Theodor Eich, Ileana Zucchi, Rolland Reinbold, Burkhard Greve and Martin Götze

*Plos One*, 8 (12): (2013) IF: 3.73

Syndecan-1 (CD138), a heparan sulfate proteoglycan, acts as a coreceptor for growth factors and chemokines and is a molecular marker associated with epithelial-mesenchymal transition during development and carcinogenesis. Resistance of Syndecan-1-deficient mice to experimentally-induced tumorigenesis has been linked to altered Wnt-responsive precursor cell pools, suggesting a potential role of Syndecan-1 in breast cancer cell stem function. However, the precise molecular mechanism is still elusive. Here, we decipher the functional impact of Syndecan-1 knockdown using RNA interference on the breast cancer stem cell phenotype

of human triple-negative MDA-MB-231 and hormone receptor-positive MCF-7 cells in vitro employing an analytical flow cytometric approach. Successful Syndecan-1 siRNA knockdown was confirmed by flow cytometry. Side population measurement by Hoechst dye exclusion and Aldehyde dehydrogenase-1 activity revealed that Syndecan-1 knockdown in MDA-MB-231 cells significantly reduced putative cancer stem cell pools by 60% and 27%, respectively, compared to controls. In MCF-7 cells, Syndecan-1 depletion reduced the side population by 40% and Aldehyde dehydrogenase-1 by 50%, respectively. In MDA-MB-231 cells, the CD44(+)CD24(-/low) phenotype decreased significantly by 6% upon siRNA-mediated Syndecan-1 depletion. Intriguingly, IL-6, its receptor sIL-6R, and the chemokine CCL20, implicated in regulating stemness-associated pathways, were downregulated by >40% in Syndecan-1-silenced MDA-MB-231 cells, which showed a dysregulated response to IL-6-induced shifts in E-cadherin and vimentin expression. Furthermore, activation of STAT-3 and NFkB transcription factors and expression of a coreceptor for Wnt signaling, LRP-6, were reduced by >45% in Syndecan-1-depleted cells compared to controls. At the functional level, Syndecan-1 siRNA reduced the formation of spheres and cysts in MCF-7 cells grown in suspension culture. Our study demonstrates the viability of flow cytometric approaches in analyzing cancer stem cell function. As Syndecan-1 modulates the cancer stem cell phenotype via regulation of the Wnt and IL-6/STAT3 signaling pathways, it emerges as a promising novel target for therapeutic approaches.

**Keywords:** Syndecan-1; Cancer stem cells; Flow cytometry.

#### 407. Novel Therapeutic and Prevention Approaches for Schistosomiasis: Review

Rashika A.F. El Ridi and Hatem A. M. Tallima

*Journal of Advanced Research*, 4: 467-478 (2013) IF: 3

Schistosomiasis is a debilitating disease affecting approximately 600 million people in 74 developing countries, with 800 million, mostly children at risk. To circumvent the threat of having praziquantel (PZQ) as the only drug used for treatment, several PZQ derivatives were synthesized, and drugs destined for other parasites were used with success. A plethora of plant-derived oils and extracts were found to effectively kill juvenile and adult schistosomes, yet none was progressed to pre- and clinical studies except an oleo-gum resin extracted from the stem of Commiphora molmol, myrrh, which action was challenged in several trials. We have proposed an essential fatty acid, a component of our diet and cells, the polyunsaturated fatty acid arachidonic acid (ARA) as a remedy for schistosomiasis, due to its ability to activate the parasite tegument-bound neutral sphingomyelinase, with subsequent hydrolysis of the apical lipid bilayer sphingomyelin molecules, allowing access of specific antibody molecules, and eventual worm attrition. This concept was convincingly supported using larval and adult *Schistosoma mansoni* and *Schistosoma haematobium* worms in in vitro experiments, and in vivo studies in inbred mice and outbred hamsters. Even if ARA proves to be an entirely effective and safe therapy for schistosomiasis, it will not prevent reinfection, and accordingly, the need for developing an effective vaccine remains an urgent priority. Our studies have supported the status of *S. mansoni* calpain, glutathione-S-transferase, aldolase, triose phosphate isomerase, glyceraldehyde 3-phosphate dehydrogenase, enolase, and 2-cys peroxiredoxin as vaccine candidates, as they are larval excreted-secreted products

and, contrary to the surface membrane molecules, are entirely accessible to the host immune system effector elements. We have proposed that the use of these molecules, in conjunction with Th2 cytokines-inducing adjuvants for recruiting and activating eosinophils and basophils, will likely lead to development and implementation of a sterilizing vaccine in a near future.

**Keywords:** *Schistosoma mansoni*; *Schistosoma haematobium*; Schistosomicides; Arachidonic acid; Excretory-secretory products; Type 2 adjuvants.

#### 408. Developmental Stages of Hepatozoon seurati (Laveran and Pettit 1911) Comb. Nov., A Parasite of the Corned Viper Cerastes cerastes and the Mosquito Culex pipiens from Egypt

Kareem Morsy, Abdel Rahman Bashtar, Fathy Abdel Ghaffar, Saleh Al Quraishy, Salam Al Hashimi, Ali Al Ghamdi and Mohammed Shazly

*Parasitology Research*, 112: 2533-2542 (2013) IF: 2.852

Developmental stages of *Hepatozoon seurati* (Laveran and Pettit 1911) comb. nov. are described from the tissues of the corned viper *Cerastes cerastes*, and from the vector *Culex pipiens*. The parasite described in the present study is firstly recorded as *Haemogregarina seurati* (Laveran and Pettit 1911) in the same host. After demonstration of the sporogonous development in the mosquito vector (*C. pipiens*) which showed all characteristics of the genus *Hepatozoon* (large oocysts containing many sporocysts producing numerous sporozoites), the parasite should be transferred into the genus *Hepatozoon*. The infected erythrocytes measured  $20 \pm 0.95 \times 7.3 \pm 0.85 \mu\text{m}$ ; while uninfected cells measured  $13.3 \pm 1.04 \times 7.5 \pm 0.16 \mu\text{m}$ . Hypertrophy and faintly stained cytoplasm are mostly occurred in infected erythrocytes. Blood stages of the parasite were found exclusively in the erythrocytes in two forms: (1) small trophozoites ( $10.0 \pm 0.52 \times 3.0 \pm 0.4 \mu\text{m}$ ) and (2) long (mature) sausage-shaped ( $16.5 \pm 1.5 \times 3.5 \pm 0.4 \mu\text{m}$ ). Merogony occurred in the endothelial cells of the blood capillaries of lung, liver, and spleen. Mature meronts was  $27.6 \pm 0.7 \times 17.5 \pm 0.5 \mu\text{m}$  in diameter and contained 20-35 merozoites (averaged in 26). These merozoites measured  $16.5 \pm 1.5 \times 3.5 \pm 0.4 \mu\text{m}$ . Syzygy and gamogony occurred in the mosquito myxocoel till the 5th day post-infection (p.i.) while sporogony took place after 15 days p.i. On the third day p.i., a large spherical macrogamete of  $29.0 \pm 0.8 \times 20.5 \pm 0.6 \mu\text{m}$  containing a distinct nucleus in association with a single microgamete were observed. The microgamete was pyriform measured  $8 \pm 0.2 \mu\text{m}$  in length. It had a prominent nucleus and a long flagellum of at least  $20.4 \pm 1.3 \mu\text{m}$  in length. Fertilization occurred on the 3rd to the 4th days p.i. and the formed zygote developed into an oocyst in which repeated mitotic divisions with centripetal invaginations occurred producing sporoblasts. After sporulation, each sporoblast termed as sporocyst, and contained 18 banana-shaped sporozoites measured  $14.0 \pm 1.6 \times 3.2 \pm 0.6 \mu\text{m}$ . Experimental transmission was successful by intraperitoneal inoculation of the infective stages (sporozoites) to uninfected vipers and led to the appearance of blood stages after 5-6 weeks.

**Keywords:** *Hepatozoon seurati*; *Cerastes cerastes*; *Culex pipiens*.

#### 409. First Identification of Four Trypanorhynchid Cestodes: *Callitetrarhynchus Speciosus*, *Pseudogrillotia Sp.* (Lacistorhynchidae), *Kotorella Pronosoma* and *Nybelinia Bisulcata* (Tentaculariidae) from Sparidae and Mullidae Fish

Kareem Morsy, Abdel-Rahman Bashtar, Fathy Abdel-Ghaffar, Saleh Al Quraishy, Ali Al Ghamdi and Nesma Mostafa

*Parasitology Research*, 112: 2523-2532 (2013) IF: 2.852

Four previously unrecognized trypanorhynchids are described based on fish specimens from Sparidae and Mullidae host fish of the Red Sea. From September 2010 to June 2011, 66 specimens of the sea bream *Pagrus pagrus* (F: Sparidae) and 43 of the red mullet *Mullus barbatus* (F: Mullidae) were purchased from markets in the Suez and Hurgada cities of the Red Sea. The fishes were measured, and their organs investigated for helminth infections. Forty-one (37.6 %) out of the 109 fish specimens investigated were parasitized with Trypanorhyncha metacestodes, identified as *Callitetrarhynchus speciosus* Linton 1897, *Pseudogrillotia sp.*

*Dollfus* 1969, *Kotorella pronosoma* Stossich 1901 from *P. pagrus*, and *Nybelinia bisulcata* Linton 1889 from *M. barbatus* in the mesentery and peritoneal cavity, with prevalences of 16.5, 11.0, 6.0, and 12.0 %. All of these larval stages were encapsulated larvae in blastocysts. *C. speciosus* is characterized by an elongated scolex, two bothria, a long postbulbosa, and four elongated bulbs. *Pseudogrillotia sp.* possesses a scolex with two lateral patelliform bothridia; posterior margins are free, not notched. A long sheath was observed, which was irregularly coiled when tentacles invaginated. *N. bisulcata* possesses an acraspedote scolex with four bothridia, which are broad, bean-shaped.

The tentacles are spirally coiled, supplied with hooks with abruptly turned points. The four tentacles sheaths rose from scolex as two anterior (front) and two posterior (back) which overlap at the apices of bulbs. *K. pronosoma* is characterized by a short body with a craspedote scolex and four bothridia. The tentacles are short and emerge pairwise. The presence of Trypanorhyncha metacestodes in the muscles does not represent a risk of infection for humans. They have a negative effect on fish esthetics. The repugnant aspect and the prohibition for commercial use by sanitary inspectors, however, cause consumer rejection. Parasites of the order Trypanorhyncha have been recorded in these host fishes for the first time.

**Keywords:** Trypanorhynchids; *Callitetrarhynchus speciosus*; *Pseudogrillotia Sp.*; *Kotorella pronosoma*; *Nybelinia bisulcata*.

#### 410. Morphological and Molecular Characterization of *Lecithochirium Grandiporum* (Digenea: Hemiuridae) Infecting the European Eel *Anguilla Anguilla* as A New Host Record in Egypt

Fathy Abdel-Ghaffar, Abdel-Rahman Bashtar, Heinz Mehlhorn, Rewaida Abdel-Gaber and Rehab Saleh

*Parasitology Research*, 112: 3243-3250 (2013) IF: 2.852

In the present study, the morphological and molecular characterization of *Lecithochirium grandiporum*, a digenetic trematode infecting the European eel *Anguilla anguilla* (Family (F): Anguillidae), were described for the first time from Burullus

Lake, Kafr El-Sheikh Governorate, Egypt. Twenty-five out of 60 specimens (infection rate of 41.66 %) were found to be naturally infected. Infection was recorded as small worms attached to the inner wall of the intestine of host fish. Adult worms measured  $1.59 \pm 0.20$  (1.3–1.85) mm long and  $0.3 \pm 0.02$  (0.29–0.48) mm wide for everted specimens with a smaller oral sucker measuring  $0.15 \pm 0.02$  (0.13–0.18) mm, and a larger ventral sucker which was  $0.16 \pm 0.02$  (0.14–0.25) mm. Our results recorded morphological differences as smaller dimensions of different body parts and the smaller oral/ventral sucker ratio between *Lecithochirium fusiforme* and *L. grandiporum*. Also, the phylogenetic position of the worm was determined by molecular characterization of their 18 SSU rDNA. Results were compared with those of previously recorded species on the Gene Bank. It was found that the present species coincide with those belonging to genus *Lecithochirium*. Comparison of the nucleotide sequences and divergence showed that the SSU rDNA gene of this *Lecithochirium* species revealed 92 % sequence identity with *L. fusiforme* (accession no. DQ413192) differing in 26 nucleotides with lower divergence value. According to these results, this study indicated that the present species is recorded as *L. grandiporum* with accession no. KC166146 as a parasite with new host and locality records in Egypt.

**Keywords:** *Lecithochirium*; Anguillidae; Morphological; Molecular characterization.

#### 411. Morphological and Phylogenetic Analysis of *Echinocephalus Carpiae* N. Sp. (Nematoda: Gnathostomatidae) Infecting the Common Carp *Cyprinus Carpio* Inhabiting Burullus Lake—A New Host Record in Egypt

Fathy Abd el-Ghaffar, Abdel-Rahman Bashtar, Heinz Mehlhorn, Rewaida Abdel-Gaber, Saleh Al Quraishy and Rehab Saleh

*Parasitology Research*, 112: 4021-4028 (2013) IF: 2.852

The present study described a new species of the genus *Echinocephalus* that was isolated from the intestine of the common carp *Cyprinus carpio* inhabiting Burullus Lake, Kafr el-Sheikh Governorate, Egypt. Thirty-two out of 70 examined specimens (45.71 %) were found to be naturally infected. The adult male worms were elongated and measured  $0.79\text{--}0.85$  mm ( $0.81 \pm 0.02$ ) in length and  $0.21\text{--}0.32$  mm ( $0.28 \pm 0.002$ ) in width, while females reached  $0.89\text{--}0.98$  mm ( $0.9 \pm 0.02$ ) long and  $0.25\text{--}0.38$  mm ( $0.28 \pm 0.002$ ) wide. The reported species are investigated microscopically, genetically, and compared with previous related ones.

The present study recorded this new nematode parasite as *Echinocephalus carpiae* with accession no. KC493258, inhabiting new host and locality records in Egypt. It is especially characterized by short body length, cephalic bulb with few (six to eight) multiple rows of spines, clear annulated cuticle, and new genetic sequences, which identify the paraphyly of *Gnathostomatinae*.

**Keywords:** *Echinocephalus*; Nematode; Morphological study; Molecular study.

#### 412. Morphological and Phylogenetic Description of A New Xenoma-Inducing Microsporidian, *Microsporidium Aurata* Nov. Sp., Parasite of the Gilthead Seabream *Sparus Aurata* from the Red Sea

Kareem Morsy, Abdel Rahman Bashtar, Fathy Abdel-Ghaffar and Saleh Al-Quraishy

*Parasitology Research*, 112: 3905-3915 (2013) IF: 2.852

A new species of Microsporidia found in the marine teleost *Sparus aurata* collected from Hurghada coasts along the Red Sea, Egypt was described based on light and ultrastructural studies. Twenty three (30.6%) out of 75 of the examined fish were parasitized with a microsporidian parasite. Numerous macroscopic whitish cysts embedded in the peritoneal cavity were observed to infect many organs of the body including muscles, connective tissues, and the intestinal epithelium. The infection was developed as tumor-like masses of often up to 5 mm in diameter inducing an enormous hypertrophy to the infected organs. Fresh spores appeared mostly ovoid to pyriform in shape reaching a size of  $1.7 \pm 0.5$  ( $1.5-2.5$ )  $\mu\text{m} \times 1.3 \pm 0.4$  ( $1-2$ )  $\mu\text{m}$ ; they possessed a large vacuole at the posterior end. These spores were located within a sporophorous vesicle which was bound by a thick amorphous wall. The ultrastructural features support the placement of the present species within the genus *Microsporidium*. The developmental stages were enclosed within a xenoma structure that was bounded by a double-layered cyst wall. The life cycle of the microsporidian pathogen described herein included four stages: proliferation (merogony), sporogony, sporoblast, spores, and liberation. Mature spores appeared electron dense, uninucleate, and were ellipsoidal in shape. At the anterior end of the spore, the anchoring disk was found in a central position. There was a definite number (5-11) of turns of the polar tube. A 538-bp region of the SSU rDNA gene of the studied species was sequenced (GenBank accession number: KF0220444). Multiple sequence alignment calculated a high degree of similarity (>92%) with six microsporidian species. The most closely related sequence was provided by the GenBank entry AF151529 for *Microsporidium prosopium* isolated from *Hyperoplus lanceolatus* differing in 67 nucleotide positions in its SSU rDNA with the highest percentage of identity (97.2%) and the lowest divergence value (0.20). Variations in the morphology of the spores and developmental stages between the two species revealed that the two species are different. The site of infection in the host and description of the onset of parasite development are strong criteria for the placement of the microsporidian parasite of the fish *S. aurata* within the genus *Microsporidium* as a new species, and we propose to name it *Microsporidium aurata* nov. sp.

**Keywords:** *Microsporidium aurata* NOV. Sp.; Microsporidia; *Sparus aurata*; Red Sea; Light and ultrastructural study.

#### 413. New Host and Locality Records of Two Nematode Parasites *Dujardinascaris Mujibii* (Heterocheilidae) and *Hysterothylacium Aduncum* (Anisakidae) from the Common Seabream *Pagrus Pagrus*: A Light and Scanning Electron Microscopic Study

Kareem Morsy, Abdel-Rahman Bashtar, Fathy Abdel-Ghaffar and Nesma Mostafa

*Parasitology Research*, 112: 807-815 (2013) IF: 2.852

In the present study, the morphology and morphometric characterization of *Dujardinascaris mujibii* (Heterocheilidae) and *Hysterothylacium aduncum* (Anisakidae), new nematode parasites infecting the sea bream *Pagrus pagrus* (Osteichthyes, Sparidae), were described for the first time from the Gulf of Suez and Hurghada City of the Red Sea, Egypt. Ninety-eight (70 %) and 62 (44.2 %) out of 140 of the examined fish were naturally infected with these nematodes, respectively. The infection was investigated macroscopically by the occurrence of these parasites in the flesh, stomach, intestines, as well as their body cavities as adult and larval stages. *D. mujibii* is characterized by an elongated body with a length of  $36.4 \pm 3$  (23-38) mm (female) and  $20 \pm 3.0$  (17-24) mm (males); the head is provided with three prominent lips each with four teeth like structures and the apical lip is embossed with a regular zigzag pattern as revealed by SEM. Interlabia were present, with prominent grooves. Juvenile stage is smaller than adults and provided with a spiny mucron. *H. aduncum* was small, measured  $22.5 \pm 2.0$  (20.0-24.3) mm in length (female) and  $16.3 \pm 2.0$  (14.5-17.4) mm (male). The head region bears three large lips which were clearly separated from each other, with the apical one having two rounded ends and the space between the two adjacent lips occupied by very prominent interlabia. The present study represents new host and locality records from *P. pagrus* fish in Egypt.

**Keywords:** *Dujardinascaris mujibii*; *Hysterothylacium aduncum*; *Pagrus pagrus*; Light and ultrastructural study.

#### 414. *Thelohanellus Niloticus* Sp. Nov. (Myxozoa: Myxosporea), A Parasite of the Nile Carp *Labeo Niloticus* from the River Nile, Egypt

Fathy Abdel-Ghaffar, Kareem Morsy, Abdel-Rahman Bashtar, Sahar EL-Ganainy and Shams Gamal

*Parasitology Research*, 112: 379-383 (2013) IF: 2.852

In the present study, the morphology and morphometric characterization of *Thelohanellus niloticus* sp. nov., a new myxozoan belonging to genus *Thelohanellus* Kudo, 1933 (Myxosporea, Bivalvulida) infecting the gills of *Labeo niloticus* (Osteichthyes, Cyprinidae), were described for the first time from the River Nile at El-Minia Governorate, Egypt. Forty-one out of 78 (52.6 %) of the examined fish were infected. The infection was observed as irregular, milky whitish, cyst-like plasmodia (up to 0.8 mm in diameter) attached to the gill filaments of the host fish. These plasmodia contained tear-shaped myxospores with slightly tapering anterior and rounded posterior ends. Each spore has a single pyriform polar capsule. Spores measured about  $23.3 \pm 0.3$  (20.4-27.1)  $\mu\text{m}$  long and  $13.4 \pm 0.4$  (11.5-14.2)  $\mu\text{m}$  wide. The polar capsule was  $11.7 \pm 0.3$  (9.2-12.5)  $\mu\text{m}$  long and  $4.7 \pm 0.3$  (3.5-6.2)  $\mu\text{m}$  wide, containing a polar filament coiled perpendicular to the longitudinal axis of the spore body making eight turns. Occasionally, an oblong, irregular-shaped mass of protoplasm with a slightly oval nucleus (1.4  $\mu\text{m}$  in diameter) and a small iodophilous vacuole measured  $0.85 \pm 0.2$   $\mu\text{m}$  (0.73-1.2  $\mu\text{m}$ ) were observed in the spore. Due to the lack of the second polar capsule characterizing *Myxobolus* sp., the present parasite is placed within the genus *Thelohanellus*. Based on morphological differences (compared with other members of *Thelohanellus* Kudo, 1933) and the host specificity, this species is described as a new one of the genus *Thelohanellus* recorded for the first time in Egypt.

**Keywords:** *Thelohanellus*; *Myxobolus*; Osteichthyes.



#### 415. Alterations in Monoamines Level in Discrete Brain Regions and Other Peripheral Tissues in Young and Adult Male Rats during Experimental Hyperthyroidism

Hassan W.A., Rahman T.A., Aly M.S. and Shahat A.S

*International Journal of Developmental Neuroscience*, 31 (5): 311-318 (2013) IF: 2.692

The present study was conducted to investigate the effect of experimentally-induced hyperthyroidism on dopamine (DA), norepinephrine (NE) and serotonin (5-HT) levels in different brain regions as well as in blood plasma, cardiac muscle and adrenal gland of young and adult male albino rats (60 rats of each age). Hyperthyroidism was induced by daily s.c. injection of L-thyroxine (L-T<sub>4</sub>, 500 µg/kg body wt.) for 21 consecutive days. Induction of hyperthyroidism caused a significant elevation in DA and 5-HT levels in most of the tissues studied of both young and adult animals after 7, 14, and 21 days. NE content significantly decreased after 21 days in most of the brain regions examined and after 14 and 21 days in blood plasma of young rats following hyperthyroidism. In adult rats, NE content decreased after 14 and 21 days in cardiac muscle and after 21 days only in adrenal gland. It may be suggested that the changes in monoamines level induced by hyperthyroidism may be due to disturbance in the synthesis, turnover and release of these amines through the neurons impairment or may attributed to an alteration pattern of their synthesis and/or degradative enzymes or changes in the sensitivity of their receptors.

**Keywords:** Thyroid Hormones Hyperthyroidism Development Monoamines Catecholamine Serotonin

#### 416. Impact of Experimental Hypothyroidism on Monoamines Level in Discrete Brain Regions and Other Peripheral Tissues of Young and Adult Male Rats

Hassan W.A., Aly M.S., Rahman T.A. and Shahat A. S

*International Research Journal of Natural Sciences (Irnjs)*, 31: 225-233 (2013) IF: 2.692

The levels of dopamine (DA), norepinephrine (NE) and serotonin (5-HT) in different brain regions as well as in blood plasma, cardiac muscle and adrenal gland of young and adult male albino rats were measured following experimentally induced hypothyroidism. Hypothyroidism induced by daily oral administration of propylthiouracil (PTU, 5mg/kg body wt) caused a significant reduction in DA levels in most of the tissues examined of both young and adult rats after 21 and 28 days, in NE levels after all the time intervals studied in young rats, and after 21 and 28 days in adult rats. 5-HT exhibited a significant reduction in the selected brain regions and blood plasma after 21 and 28 days and in cardiac muscle after all the time intervals in the two age groups of animals. It may be suggested that the changes in monoamine levels induced by hypothyroidism may be due to disturbance in the synthesis and release of these amines through the neurons impairment or may be due to an alteration pattern of their synthesizing and/or degradative enzymes.

**Keywords:** Hypothyroidism Propylthiouracil Development Neurotransmitters Catecholamines Serotonin.

#### 417. Evaluation of the Role of the Antioxidant Silymarin in Modulating the in Vivo Genotoxicity of the Antiviral Drug Ribavirin in Mice

Magda M. Noshay, Nahed A. Hussien and Akmal A. El-Ghor

*Mutation Research*, 752: 14-20 (2013) IF: 2.22

Ribavirin (1-β-d-ribofuranosyl-1,2,4-triazole-3-carboxamide) is a widely used broad-spectrum antiviral drug. Recently, several reports revealed genotoxic effects of ribavirin in vivo and in vitro, which were correlated with the production of reactive oxygen species (ROS). This study aimed to evaluate the genotoxicity of ribavirin and to investigate the role of the natural antioxidant silymarin to modulate this genotoxicity. Male albino mice (age, 8-10 weeks) were injected intraperitoneally (i.p.) with ribavirin at three dose levels (20, 75 and 130 mg/kg bw) either in a single injection (acute treatment) or in multiple injections on five consecutive days (sub-acute treatment). Other comparable groups were treated with silymarin (70 mg/kg bw) 1h before the injection with ribavirin. Mice were sacrificed at different sampling times (24, 48 and 72 h) after the last ribavirin treatment. Micronucleus (MN) and single-strand conformation polymorphism (SSCP) assays were used to assess genotoxic and cytotoxic effects of ribavirin and to evaluate the protective effect of the pre-treatment with silymarin. Our results reveal genotoxic and cytotoxic effects of ribavirin in the MN assay. Pre-treatment with silymarin reduced the toxicity of ribavirin. In the SSCP assay, ribavirin treatment did not induce any mutations in the two selected sites in the D-loop of mitochondrial DNA (mtDNA).

**Keywords:** Ribavirin; Silymarin; Genotoxicity; Micronucleus test; SSCP assay.

#### 418. The Anticonvulsant Effect of Cooling in Comparison to A-Lipoic Acid: A Neurochemical Study

Yasser A. Khadrawy, Heba S. AboulEzz Nawal A. Ahmed and Haitham S. Mohammed

*Neurochem Research*, 38: 906-915 (2013) IF: 2.125

Brain cooling has pronounced effects on seizures and epileptic activity. The aim of the present study is to evaluate the anticonvulsant effect of brain cooling on the oxidative stress and changes in Na<sup>+</sup>, K<sup>+</sup>-ATPase and acetylcholinesterase (AChE) activities during status epilepticus induced by pilocarpine in the hippocampus of adult male rat in comparison with a-lipoic acid. Rats were divided into four groups: control, rats treated with pilocarpine for induction of status epilepticus, rats treated for 3 consecutive days with a-lipoic acid before pilocarpine and rats subjected to whole body cooling for 30 min before pilocarpine. The present findings indicated that pilocarpine-induced status epilepticus was accompanied by a state of oxidative stress as clear from the significant increase in lipid peroxidation (MDA) and superoxide dismutase (SOD) and significant decrease in reduced glutathione and nitric oxide (NO) levels and the activities of catalase, AChE and Na<sup>+</sup>, K<sup>+</sup>-ATPase. Pretreatment with a-lipoic acid ameliorated the state of oxidative stress and restored AChE to nearly control activity. However, Na<sup>+</sup>, K<sup>+</sup>-ATPase activity showed a significant decrease. Rats exposed to cooling for 30 min before the induction of status epilepticus revealed significant increases in MDA and NO levels and SOD activity. AChE returned to control value while the significant decrease in Na<sup>+</sup>,



K<sup>+</sup>-ATPase persisted. The present data suggest that cooling may have an anticonvulsant effect which may be mediated by the elevated NO level. However, brain cooling may have drastic unwanted insults such as oxidative stress and the decrease in Na<sup>+</sup>, K<sup>+</sup>-ATPase activity.

**Keywords:** Brain cooling; Alpha-lipoic acid; Hippocampus; Epilepsy; Oxidative stress.

#### 419. Superoxide Dismutases from Larvae of the Camel Tick *Hyalomma Dromedarii*

Mahmoud A. Ibrahim, Mona M. Mohamed, Abdel-Hady M. Ghazy and Hassan M. M. Masoud

*Comparative Biochemistry and Physiology Part B: Biochemistry and Molecular Biology*, 164(3): 221-228 (2013) IF: 2.069

Three superoxide dismutases (EC 1.15.1.1) (TLSOD1, TLSOD2 and TLSOD3) were purified from larvae of the camel tick *Hyalomma dromedarii* by ammonium sulfate precipitation, ion exchange and gel filtration columns. SDS-PAGE revealed that the subunit molecular masses of the SODs are 40±2 kDa, 67±1.5 kDa and 45±2.6 kDa for TLSOD1, TLSOD2 and TLSOD3, respectively. TLSOD1 and TLSOD2 are monomeric proteins, while TLSOD3 isoenzyme exhibits dimeric structure with native molecular mass of 90 kDa. The pI values are estimated at pH 8.0, pH 7.2 and pH 6.6 for the three SODs which displayed pH optima at 7.6, 8.0 and 7.8, respectively. CuCl<sub>2</sub> and ZnCl<sub>2</sub> increase the activity of TLSOD2 and TLSOD3, while MnCl<sub>2</sub> increases the activity of TLSOD1. KCN inhibits the activity of TLSOD2 and TLSOD3, while a remarkable resistance of TLSOD1 isoenzyme was detected. TLSOD1 is suggested to be a manganese containing isoenzyme while TLSOD2 and TLSOD3 are suggested to be copper/zinc-containing isoenzymes. These results indicate the presence of three different forms of SODs in the larval stage of camel tick. This finding will contribute to our understanding of the physiology of these ectoparasites and the development of non-traditional methods to control them.

**Keywords:** Superoxide dismutase; Camel tick larvae; Purification and characterization.

#### 420. Risk Assessment and Toxic Effects of Metal Pollution in Two Cultured and Wild Fish Species from Highly Degraded Aquatic Habitats

Wael A. Omar, Khalid H. Zaghloul, Amr A. Abdel-Khalek and S. Abo-Hegab

*Archives of Environmental Contamination and Toxicology*, 65: 753-764 (2013) IF: 2.012

Lake Qaroun is an inland lake at the lowest part of El-Fayoum depression, Egypt. It receives agricultural and domestic non-treated drainage waters, which are also used for aquaculture in Qaroun area. The results of the present study aimed to provide comparable data between wild (collected from Lake Qaroun) and cultured (collected from Qaroun fish farms and the reference site) Nile tilapia *Oreochromis niloticus* and mullet *Mugil cephalus*, as indicators of natural and anthropogenic impacts on aquatic ecosystem as well as to evaluate the human hazard index associated with fish consumption. Metal concentrations in fish tissues showed a species-specific bioaccumulation pattern. Statistically significant differences were observed in the mean

metal concentrations with lower bioavailability in *M. cephalus* compared with *O. niloticus* in internal vital organs (liver, kidney, and muscle) but much higher in external organs (gill and skin). Histopathological alterations and evident damages were observed in gill, liver, and kidney of both species collected from Lake Qaroun and Qaroun fish farms compared with those from the reference site. The results showed significant increase of plasma aspartate aminotransferase and alanine aminotransferase activity as well as creatinine and uric acid concentration in both fish species from polluted locations. The human health hazard index showed that the cumulative risk greatly increases with increasing fish consumption rate, thus yielding an alarming concern for consumer health.

**Keywords:** Risk assessment; Toxicity; Metal pollution; Fish.

#### 421. Assessing the Level of Breast Cancer Awareness among Recently Diagnosed Patients in Ain Shams University Hospital

Mohamed El-Shinawi, AlMoataz Bellah Youssef, Mohammad Alsara, Mohamed K. Aly, Mohamed Mostafa, Ahmed Yehia, Marc Hurlbert, Reda Abd El-Tawab and Mona M. Mohamed

*The Breast*, 22 (6): 1210-1214 (2013) IF: 1.976

Breast cancer is the leading female malignancy among Egyptian women. The majority of Egyptian breast cancer patients present at late stages of the disease with a large tumor size compared to Western countries. Low breast cancer awareness, social and cultural factors were suggested to play crucial role in late presentation of breast cancer among Egyptians. The aim of our present study is to establish a questionnaire-based survey that can assess levels of breast cancer awareness among Egyptians. Patients enrolled were interviewed and answered 60 questions related to knowledge, symptoms, risk factors, prevention and management options of breast cancer. We evaluated our interactions with breast cancer patients and defined the level of awareness gained from education and culture of Egyptian women. Our results described that Egyptian breast cancer patients lack knowledge about their illness and condition. The lowest levels of awareness were related to age, education and culture. We concluded that breast cancer public awareness and women education programs covering factors identified in our study is warranted among Egyptian population.

**Objective:** To assess breast cancer awareness among recently diagnosed breast cancer Egyptian patients.

**Subjects and Methods:** Among 289 interviewed breast cancer patients we enrolled 45 patients who fulfilled the study inclusion criteria. Participants were asked to answer a validated 60-item questionnaire that inquires about socio-demographic characteristics, knowledge of breast cancer symptoms, risk factors, symptoms, prevention, general management and willingness to participate in awareness campaigns. The average of interview time was about 45 min, depending on patient's age and education level.

**Results:** The mean age of included patients was 48.2 ± 10.19 years. Geographical distribution revealed that 66.7% patients were from Cairo and the rest were from other governorates, including Aswan, Sharqia, Mansora, Qena, Kalyobia, Elminya and Sohag. Among interviewed patients 85% were non-working housewives, 42.2% of them were illiterate. Questions about knowledge of breast cancer revealed that 53.33% of patients knew an acquaintance with breast cancer; however, they spent a median

time of 3 months to seek medical advice after recognizing the first symptom with a delay range between a month and 72 months. We found that 73% of the participants presented to a physician with the same first recognized symptom and 75.6% didn't think of cancer then as a possible diagnosis. Total breast cancer knowledge scores had an average of 13.3 (out of 35 knowledge points), with 93% of the patients recognizing "painless breast mass" as a breast cancer symptom and 44% only recognized the concept of breast self examination. Interestingly, 61.4% identified breastfeeding as a risk factor for breast cancer, 60% did not recognize mammography as an early detection method, and 57.7% agreed that clinical breast examination (CBE) is important for early detection. Regarding management, 75% said breast cancer was potentially curable and 60% said medical care could be helpful regardless the age of presentation.

**Conclusion:** Egyptian breast cancer patients knew little about their condition. Less awareness was related to age and education level. Low knowledge of risk factors, early detection and management of breast cancer should be addressed by designing patient education programs, where less educated patients are supported by health care professionals to participate in the management of breast cancer. Moreover, we found that 67% and 97% of enrolled breast cancer patients were willing as well to participate in spreading awareness among their community and among their own families, respectively.

**Keywords:** Awareness; Breast Cancer; Early detection; Egypt; Egyptian; Questionnaire; Recently diagnosed; Risk factors.

#### 422. Vaccine-Induced Protection against Murine Schistosomiasis *Mansoni* with Larval Excretory-Secretory Antigens and Papain or Type-2 Cytokines

Rashika El Ridi and Hatem Tallima

*Journal of Parasitology*, 99(2): 194-202 (2013) IF: 1.321

*Schistosoma mansoni* glyceraldehyde 3-phosphate dehydrogenase (SG3PDH), peroxiredoxin (TPX), and other larval excretory-secretory products (ESP) essentially induce T helper (Th) 1 and Th17 immune responses during a non-protective natural infection. Such an immune environment promotes production of nitric oxide and hydrogen peroxide by interferon- $\gamma$ -activated monocytes and interleukin (IL)-17-mediated recruitment and activation of neutrophils; however, it also likely prevents engagement of eosinophils and basophils in the hunt for developing larvae. We reasoned that polarizing ESP-induced immune responses toward a Th2 phenotype, via the use of cysteine proteases or type-2 cytokines, would lead to almost total parasite elimination. Accordingly, outbred mice were immunized with 10 $\mu$ g recombinant SG3PDH and 15 $\mu$ g TPX-derived peptide together with 10 $\mu$ g papain, or 200 ng thymic stromal lymphopoietin, IL-25, or IL-33 as an adjuvant. Two weeks later, untreated mice, adjuvant controls, and immunized mice were challenged with 100 or 125 cercariae. Results of 6 experiments indicated that these formulations elicited IgM, IgG1, and IgA specific antibodies, and an increase in ex vivo spleen cells release of IL-4 and IL-5 correlated with highly significant (up to  $P < 0.0001$ ) reduction of 62 to 78% in challenge worm burden. Improvement of ESP selection, singly or in a combination, and immunization regimen, namely ESP and type-2 cytokine dose and injection site and schedule, could lead to a sterilizing schistosomiasis vaccine in the foreseeable future.

**Keywords:** *Schistosoma mansoni*; Glyceraldehyde 3-phosphate dehydrogenase (Sg3pdh).

#### 423. Hypoglycemic and Antioxidative Effects of Fenugreek and Termis Seeds Powder in Streptozotocin-Diabetic Rats

M. Marzouk, A.M. Soliman and T.Y. Omar

*European Review For Medical and Pharmacological Sciences*, 17: 559-565 (2013) IF: 1.093

**Background and Objectives:** Diabetes mellitus is a heterogeneous disease characterized by altered cellular metabolism. So, many traditional herbs are being used by diabetic patients to control this disease. In the present study, an attempt has been made to investigate the anti-diabetic and antioxidative effects of water suspension of Fenugreek (F), and Termis (T) seeds powder and their mixture (M) that were studied in Streptozotocin (STZ)-induced diabetic rats.

**Materials and Methods:** Experimental diabetes was induced by injection a single dose of STZ (50 mg/kg, i.p.). Adult male albino rats were divided into five groups; normal control, diabetic control, diabetic-F supplement (1 g/kg b.wt.), diabetic- T supplement (1 g/kg b.wt.) and diabetic-M supplement 1 g/kg b.wt. of each seed powder concurrently for 30 days. Serum glucose, insulin, lipid profile, activities of serum marker enzymes of liver function as well as liver and muscle glycogen content were measured. The oxidative stress was assessed by blood reduced glutathione (GSH) content and enzyme activities of glutathione-S-transferase (GST) and catalase (CAT) in plasma.

**Results:** The increase in serum glucose, total lipid, triglycerides, total cholesterol, AST, ALT, ALP and decreased insulin, plasma, GSH, GST, CAT, as well as liver and muscle glycogen content were the salient features recorded in diabetic control rats. The F, T and M supplements significantly reverted the levels of the studied metabolites and enzymes activities to near normal control values. Co-administration of F and T seeds powder was considered as an effective agent in modulating the alterations in total lipid, AST, ALT, GSH and muscle glycogen.

**Conclusions:** Our data suggest that F, T and M seeds powder supplementation may be beneficial for preventing diabetic complications in this animal model.

**Keywords:** Fenugreek; Termis; Streptozotocin; Diabetic rats; Hypoglycemia; Antioxidant enzymes.

#### 424. The Effect of Pulsed Electromagnetic Radiation from Mobile Phone on the Levels of Monoamine Neurotransmitters in Four Different Areas of Rat Brain

H.S. Aboul Ezz, Y.A. Khadrawy, N.A. Ahmed, N.M. Radwan and M.M. El Bakry

*European Review for Medical and Pharmacological Sciences*, 17: 1782-1788 (2013) IF: 1.093

**Background:** The use of mobile phones is rapidly increasing all over the world. Few studies deal with the effect of electromagnetic radiation (EMR) on monoamine neurotransmitters in the different brain areas of adult rat.

**Aim:** The aim of the present study was to investigate the effect of EMR on the concentrations of dopamine (DA), norepinephrine

(NE) and serotonin (5-HT) in the hippocampus, hypothalamus, midbrain and medulla oblongata of adult rats.

**Materials And Methods:** Adult rats were exposed daily to EMR (frequency 1800 MHz, specific absorption rate 0.843 W/kg, power density 0.02 mW/cm<sup>2</sup>, modulated at 217 Hz) and sacrificed after 1, 2 and 4 months of daily EMR exposure as well as after stopping EMR for 1 month (after 4 months of daily EMR exposure). Monoamines were determined by high performance liquid chromatography coupled with fluorescence detection (HPLC-FD) using their native properties.

**Results:** The exposure to EMR resulted in significant changes in DA, NE and 5-HT in the four selected areas of adult rat brain.

**Conclusions:** The exposure of adult rats to EMR may cause disturbances in monoamine neurotransmitters and this may underlie many of the adverse effects reported after EMR including memory, learning, and stress.

**Keywords:** Electromagnetic radiation; Dopamine; Norepinephrine; Serotonin; Brain areas.

#### 425. Efficacy Evaluation of the Protein Isolated from Peganum Harmala Seeds as an Antioxidant in Liver of Rats

Amel M Soliman, Helal S Abu-El-Zahab and Gamiaa A Alswiai  
*Asian Pacific Journal of Tropical Medicine*, 6 (4): 285-295 (2013) IF: 0.502

**Objective:** The present study aimed to evaluate the curative effect of the 132 KD protein isolated from the seeds of Peganum harmala L. against carbon tetrachloride (CCl<sub>4</sub>) induced oxidative stress in rats.

**Methods:** Animals were post treated intraperitoneally with 132 KD isolated protein at doses of 4 and 8 mg/kg body weight and bovine serum albumin (BSA) (8 mg / kg body weight) as well as vitamin C (250 mg/kg body weight p.o) for 7 days after they challenged with CCl<sub>4</sub> orally (1 ml/kg body weight) in olive oil (50%) for 2 days.

**Results:** The purified protein from seeds of Peganum harmala plant showed in vitro antioxidant activity with DPPH assay. Administration of CCl<sub>4</sub> induced induction in serum aminotransferases (AST,ALT), alkaline phosphatase (ALP), lipid profile parameters and liver malondialdehyde (MDA) and decrease in serum total protein, liver superoxide dismutase (SOD), catalase (CAT), and reduced glutathione (GSH) levels. 132 KD protein treatment of rats post CCl<sub>4</sub> intoxication successfully alleviated the toxic effects of CCl<sub>4</sub>.

**Conclusion:** The isolated protein possessed strong antioxidant activity comparable to that of BSA (negative control) and vitamin C (positive control).

**Keywords:** Carbon tetrachloride; Peganum harmala; Oxidative stress; 132KD isolated protein.

#### 426. Pathological Mechanisms of Liver Injury Caused by Oral Administration of Bisphenol A

Rehab M. Hussein and Jehane I. Eid

*Life Science Journal*, 10: 663-673 (2013) IF: 0.165

Bisphenol A (BPA) is a widely produced, endocrine disrupting compound that is pervasive in the environment. BPA is a contaminant with increasing exposure to it and exerts both toxic and estrogenic effects on mammalian cells. Due to variability in

study design, the disruptive effects of BPA have been proven difficult to experimentally replicate. BPA exposure causes oxidative stress leading to inflammation in the liver. However, its precise mechanisms are not fully elucidated. This study was designed to assess the molecular, biochemical and histological alterations behind inflammation and hepatic injury caused by BPA. We investigated the disruptive hepatotoxic actions of oral exposure to BPA by measuring changes in oxidative stress, cytokine expression and histopathology in the liver tissue of mice. Swiss albino mice were exposed to BPA via drinking water at doses of 1/50, 1/40, 1/30, 1/20 and 1/10 LD50 (48, 60, 80, 120 and 240 mg/kg b.w. respectively) for three weeks. Oral exposure to BPA caused dose-related hepatotoxic effects, including oxidative stress in terms of increase lipid peroxidation and decrease catalase antioxidant enzyme. The mRNA levels of liver pro-inflammatory cytokines IL-6, and IL-1 $\beta$  were up-regulated in a dose dependant manner by BPA. Our data demonstrated that BPA exposure causes liver injury, which is associated with remarkable inflammatory response, oxidative stress, and histopathological alterations

**Keywords:** Bisphenol A; Hepatotoxicity; Inflammatory cytokines; Kupffer cells; Oxidative stress.

#### 427. Alterations in the Fatty Acid Profile, Antioxidant Enzymes and Protein Pattern of Biomphalaria Alexandrina Snails Exposed to the Pesticides Diazinon and Profenofos

Fayez A. Bakry, Karem El-Hommosany, M. S. Abd El-Atti and Somaya M. Ismail

*African Journal of Pharmacy and Pharmacology*, 7 (37): 2603-2612 (2013)

The use of pesticides is widespread in agricultural activities. These pesticides may contaminate the irrigation and drainage systems during agricultural activities and pests' control and then negatively affect the biotic and abiotic component of the polluted water courses. The present study aimed to evaluate the effect of the pesticides diazinon and profenofos on some biological activities of Biomphalaria alexandrina snails such as fatty acid profile, some antioxidant enzymes like thioredoxin reductase (TrxR), sorbitol dehydrogenase (SDH), superoxide dismutase (SOD), catalase (CAT) as well as glutathione reductase (GR) and lipid peroxidation (LP) and protein patterns in snails' tissues exposed for 4 weeks to LC10 of diazinon and profenofos. The results showed that the two pesticides caused considerable reduction in survival rates and egg production of treated snails. Identification of fatty acids composition in snails' tissues treated with diazinon and profenofos pesticides was carried out using gas liquid chromatography (GLC). The results declared alteration in fatty acid profile, fluctuation in percent of long chain and short chain fatty acid contributions either saturated or unsaturated ones and a decrease in total lipid content in tissues of snails treated with these pesticides. The data demonstrate that, there was a significant inhibition in the activities of tissues SOD, CAT, GR, TrxR and SDH in tissues of treated snails while a significant elevation was detected in lipid peroxidation as compared to the normal control. On the other hand, the electrophoretic pattern of total protein showed differences in number and molecular weights of protein bands due to snails' treatment. It was concluded that the residues of diazinon and profenofos pesticides in aquatic environments have toxic effects on B. alexandrina snails.

**Keywords:** Snails; Pesticides; Antioxidants; Enzymes; Fatty acids; Proteins; Biochemistry.

#### 428. Anatomical, Histological and Histochemical Adaptations of the Avian Alimentary Canal to their Food Habits: II- *Elanus Caeruleus*

Hamida Hamdi, Abdel-Wahab El-Ghareeb, Mostafa Zaher and Fathia AbuAmod

*International Journal of Scientific and Engineering Research*, 4 (10): 1355-1364 (2013)

This study was the second in a series of studies aiming at establishing a connection between the food habits of aves and the anatomical, histological and histochemical structures of their alimentary tract. In this study, the gross anatomy, histology and histochemistry of the digestive system of the black-winged kite, *Elanus caeruleus*, a carnivorous bird, have been investigated. This study has revealed that, the oesophagus was relatively long with poorly developed crop; the simple stomach is differentiated into a glandular proventriculus and a muscular ventriculus or gizzard. The small intestine is divided into duodenum, and ileum. The large intestine contains a very small pair of ceca called, lymphoid ceca and a short rectum. The internal mucous glands of the oesophagus keep the surface of the tube moist and slimy and thereby facilitate the passage of the food. The differences in the proventriculus structure may also be related to diet. The present study revealed that the alimentary tract shows the usual four laminae; serosa, muscosa, submucosa and mucosa. The oesophageal mucosa is thrown into numerous longitudinal folds. The mucosa of the oesophagus is lined with stratified squamous keratinized epithelium. The oesophageal glands were of the simple tubule alveolar type. The proventricular mucosa is thrown into numerous folds of different depths which are lined by simple columnar epithelium. The proventricular glands were simple tubular to simple branched tubular glands. A thin layer of gastric keratinoid material is found in the ventriculus. The goblet cells gradually increase in frequency from the duodenum to the rectum. The lamina propria contains diffuse lymphatic tissue and the muscularis mucosa is well developed, and extends into the stroma of the villi. Also, the histochemical studies revealed that PAS positive matter was found in the entire alimentary tract. The oesophageal glands have acid mucopolysaccharide secretions. While gastric glands of stomach, the thin koilin layer, the goblet cells and crypts of Lieberkühn have acid and neutral mucopolysaccharide secretions. Proteins and nucleic acid was observed in the different regions of the alimentary canal.

**Keywords:** Anatomical; Histological; Alimentary tract.

#### 429. Antiosteoporotic Effect of *Coelatura Aegyptiaca* Shell Powder on Ovariectomized Rats

Amany A. Sayed, Amel M. Soliman, Sohair R. Fahmy and Mohamed Marzouk

*African Journal of Pharmacy and Pharmacology*, 7 (34): 2406-2416 (2013)

The efficacy of *Coelatura aegyptiaca* shell powder (CES, 500 mg/kg BW) was evaluated as a calcium supplement in ovariectomized (OVX) rats for ten weeks of treatment. The biochemical components and the antioxidant properties of the

shell powder were determined. The bone mineral density (BMD), bone mineral content (BMC), calcium (Ca) and phosphorus (P) contents in serum and bone, serum total alkaline phosphatase (TALP) and bone alkaline phosphatase (BALP), serum calcitonin and parathyroid (PTH) hormones were determined. Furthermore, some of the oxidative stress markers [malondialdehyde (MDA), superoxide dismutase (SOD), glutathione peroxidase (GPx) and total antioxidant capacity (TAC)] were estimated in bone. The current study revealed that CES contained 19.38% Ca, 0.315% P as well as some of antioxidant amino acids which have a potent antioxidant activity against 1,1-diphenylpicrylhydrazyl (DPPH) free radical. Administration of CES to OVX rats increased BMD, BMC, tibial Ca and P contents and BALP activity, as compared to OVX rats. An ameliorative effect was recorded in the levels of calcitonin, PTH, MDA, SOD, GPx and TAC subsequent to CES administration to OVX rats. This ameliorative effect of CES powder against osteoporosis may be attributed to its antioxidant efficacy and/or to its Ca content. In conclusion, CES may have the potential to develop a clinically useful anti-osteoporotic agent, since its effect was comparable with alendronate (6.5 mg/kg BW/week).

**Keywords:** Ovariectomized rats; *Coelatura aegyptiaca* shell; Calcium supplement; 1,1-diphenylpicrylhydrazyl (DPPH); Oxidative stress markers.

#### 430. Biochemical Variability between Two Egyptian *Stenodactylus* Species (Reptilia: Gekkonidae) Inhabiting North Sinai

Mohamed A. M. Kadry and Sayed A. M. Amer

*Advances in Bioscience and Biotechnology*, 4: 974-978 (2013)

Polyacrylamide gel electrophoreses for malate dehydrogenase (Mdh) and beta-esterase ( $\beta$ -Est) isoenzymes were conducted for biochemical differentiation between two *Stenodactylus* gekkonid species inhabiting North Sinai of Egypt. Total lipids and proteins of liver and muscle tissues in both species were also analyzed. A total of three Mdh isoforms were recorded in the analysis, in which the activity of Mdh-2 and Mdh-3 seemed to be higher in *S. petrii* than in *S. sthenodactylus*. This high activity could be supported by the significant increase in the total lipids and proteins in liver and muscle tissues of the species. It may thus be reasonable to suppose that *S. petrii* is more active, energetic and adaptable in the desert habitat than *S. sthenodactylus*.  $\beta$ -Est showed six fractions in *S. petrii* and only one fraction in *S. sthenodactylus*. It is therefore noticeable that  $\beta$ -Est is more highly expressed in *S. petrii* than in *S. sthenodactylus*.

**Keywords:** Electrophoreses; Physiological ecology; Geckos; Isoenzymes; Lipids; Proteins.

#### 431. Chlorophyllin Protects Against Cisplatin and 5-Fluorouracil Regimen Induced Genotoxicity and Cytotoxicity without Affecting their Antitumor Activity

Magda M. Noshay and Hanan R. Hamad

*Academic Journal of Cancer Research* 6 (2): 90-98 (2013)

Two combination therapies based on cisplatin and 5-fluorouracil might improve treatment efficacy for several types of

malignancies, but at risk of increasing toxicity. The possible protective effects of chlorophyllin (CHL) against the genotoxicity and cytotoxicity of the widely used cisplatin (CIS) and 5-fluorouracil (5-FU) regimen were evaluated. Mice were injected i.p. with CIS (6 mg/kg b.w.) and 5-FU (10 mg/kg b.w.) while CHL (2, 4 and 6 mg/kg b.w.) was administered as single i.p. injection 1 hour before the treatment with the two anticancer drugs. The results showed that CHL administered at dose levels of 2, 4 and 6 mg/kg b.w. 1h before the treatment with CIS and 5-FU did not induce any significant change in the antitumor activity of CIS and 5-FU combination. Moreover, CHL pretreatment significantly decreased the levels of chromosomal aberrations and micronuclei induced by CIS and 5-FU treatment in mice bone marrow cells. In addition, CHL pretreatment markedly restored the mitotic activity of bone marrow cells that had been suppressed by the two anticancer drugs in a dose-dependent manner. It could be concluded that CHL acts as a potent protective agent against the genotoxicity and cytotoxicity of CIS and 5-FU combination without affecting their antitumor activity.

This protective effect of CHL may be attributed to free radicals scavenging ability of CHL. Therefore, more and extensive studies on the possibilities of using CHL supplement in cancer patients treated with cisplatin + 5-FU regimen are recommended.

**Keywords:** Anticancer drugs; Antitumor activity; Chlorophyllin; Cisplatin and 5-fluorouracil regimen; Genotoxicity.

#### 432. Diagnostic Potential of Target Giardia Lamblia Specific Antigen for Detection of Human Giardiasis Using Coproantigen Sandwich ELISA

Kamel, D., A. Farid, E. Ali, I. Rabia, M. Hendawy and E. A. M. Amir

*World Journal of Medical Sciences*, 9: 113-122 (2013)

Giardiasis is endemic in all regions of the world. Giardia lamblia (G. lamblia) cysts are spread in Egypt via the fecal-oral route, through ingestion of the cyst with contaminated food or water. The symptoms of giardiasis vary from the asymptomatic passage of cysts to chronic diarrhea, malabsorption and weight loss.

Although microscopy has the advantage of low cost and ability to simultaneously detect other gastrointestinal parasite, the limitation of this method is that G. lamblia cysts are small and similar to many pseudoparasites. This study aimed to verify the advantages and disadvantages of enzyme-linked immunoassaying versus microscopy for diagnosing G. lamblia in human. The 65 kDa glycoprotein Giardia specific antigen (GSA-65 kDa) is considered to be an antigen of interest. It is shared by cysts and trophozoites of G. Lamblia as determined by sodium dodecyl sulfate-polyacrylamide gel electrophoresis (SDS-PAGE) analysis and immunoblotting and very specific to this parasite. Sandwich ELISA was more sensitive (95.12%) than ordinary parasitological diagnosis (78.05% for direct smear or 85.36% for MIFC method). Also, the NPV of sandwich ELISA (95.12%) is higher than that of parasitological procedure (82.35% for direct smear or 87.5% for MIFC method). On the other hand, the specificity (92.85%) and PPV (92.85%) of sandwich ELISA is lesser than that of parasitological procedure (100% and 100%, respectively). Sandwich ELISA, using purified anti-GSA-65 kDa IgG pAb, is recommended as a diagnostic test for Giardia spp. diagnosis more than ordinary microscopy methods.

**Keywords:** Giardia lamblia; Diagnosis; Coproantigen; Sandwich elisa.

#### 433. Effect of Zingiber Officinal (Ginger) on Electrophoresis Analysis and Biochemical Aspects of Biomphalaria Alexandrina Snails Infected With Schistosoma Mansoni

Fayez A.Bakry, Abd El-Atti M. S. and Somaya M. Ismail

*International Journal of Scientific and Engineering Research*, 4 (11): 1147-1154 (2013)

Schistosomiasis is an important parasitic disease that infects humans. Schistosoma mansoni is one of the main species of schistosomes infecting humans. Biomphalaria alexandrina snails, act as an intermediate hosts and play a major role in the transmission of schistosomes. The effect of Zingiber officinal (ginger) on the survival rate, egg production, electrophoresis analysis, biochemical aspects of B. alexandrina snails infected with S. mansoni were studied. The obtained result showed that a rapid decline in survival rate and egg production of infected snails with S. haematobium exposed to ginger. The present results also, showed that the glucose concentrations in uninfected and infected snails exposed to ginger were increased in hemolymph, while soft tissue glycogen decreased. The activities of glycogen phosphorylase, succinate dehydrogenase (SDH) and glucose-6-phosphatase in homogenate of snail's tissues of uninfected and infected snails exposed to ginger were reduced ( $P < 0.001$ ) in re-sponse to infection and exposure to ginger. Qualitative and quantitative effects on the protein patterns have been revealed for uninfected and infected snails exposed to ginger. The electrophoresis pattern of total protein showed differences in number and molecular weights of protein bands.

**Keywords:** Biomphalaria alexandrina snails; Schistosoma mansoni; Zingiber officinal (ginger).

#### 434. Immunodiagnosis of Fascioliasis Using Sandwich Enzyme-Linked Immunosorbent Assay for Detection of Fasciola Gigantica Paramyosin Antigen

Hany Mohamed Adel Abou-Elhakam, Ibraheem Rabia Bauomy, Somaya Osman El Deeb and Azza Mohamed El Amir

*Tropical Parasitology*, 3 (1): 44-52 (2013)

Many immunological techniques have been developed over years using the different Fasciola antigens for diagnosis of parasitic infection and to replace the parasitological techniques, which are time consuming and usually lack sensitivity and reproducibility. In this study, Fasciola gigantica paramyosin (Pmy) antigen was early detected in cattle sera using sandwich enzyme-linked immunosorbent assay (ELISA), to evaluate the Pmy antigen performance in diagnosis. This work was conducted on 135 cattle blood samples, which were classified according to parasitological investigation into, healthy control (30), fascioliasis (75), and other parasites (30) groups. The sensitivity of Sandwich ELISA was 97.33%, and the specificity was 95%, in comparison with parasitological examination, which recorded 66.66% sensitivity and 100% specificity, respectively. It was clear that the native F. gigantica Pmy is considered as a powerful antigen in early immunodiagnosis of fascioliasis, using a highly sensitive and specific sandwich ELISA technique.

**Keywords:** Enzyme-linked immunosorbent assay; Fasciola gigantica; Paramyosin; Polyclonal antibodies; Sensitivity; Specificity.



### 435. Impact of Plant Extracts as Molluscicides Agent against Biomphalaria Alexandrina Snails Andschistosoma Mansoni

Fathy Abdel-Ghaffar, Fayez A. Bakry and Samir A. Taha

*Int. J. of Scient. and Engine. Research*, 4 (11): 420-426 (2013)

In the present study, the efficacy of 6 different species of medicinal plants belonging to 5 different families against *Biomphalaria alexandrina* snails and *Schistosoma mansoni* stages were examined. During screening test of water suspension and methanol extract, results revealed that *Oreopanax reticulatum* (Family: Araliaceae) had the strongest molluscicidal activity against *Biomphalaria alexandrina* snails followed by *Azadirachta indica* A juss (Maliaceae) and *Dizygotheca kerchoviana* (F: Araliaceae). Methanol extracts revealed more molluscicidal potency as compared to water suspension. Also, the effect of methanol extracts of *Oreopanax reticulatum*, *Azadirachta indica* A juss (Maliaceae) and *Dizygotheca kerchoviana* on the survival rate and cercarial production of *Biomphalaria alexandrina* infected with *Schistosoma mansoni*, as well as on free living stages of *Schistosoma mansoni* (miracidia, cercariae and worm) were studied. The results show that the sublethal concentrations of methanol extract of these plants caused a considerable reduction in the survival rate of the snails and in the infectivity of *Schistosoma mansoni* miracidia to the snail. Reduction in the number of cercariae per snail during the patent period and in the period of cercarial shedding was also, observed. The pre patent shortened. The mortality rate of miracidia and cercariae and adult worms were elevated gradually by increasing the exposure period to methanol extract of these plants.

**Keywords:** Plant extracts; Molluscicidal; *Schistosoma mansoni*; *Biomphalaria alexandrina*.

### 436. Impact of the Residue of Deltamethrin and Endosulfan Pesticides on Biochemical Toxicity and Some Neurotransmitter Contents in Different Brain Areas of Male Albino Mice

Somaya M. Ismail, Azza A. Said and Samira M. El-Sayad

*Journal of Research in Biology*, 3 (4): 954-966 (2013)

Evaluating the action of the residues of pesticides on non-target organisms has been of interest to many researchers. The present study aimed to evaluate the pesticides deltamethrin and endosulfan on biochemical toxicity and some neurotransmitter contents in different brain areas of male albino mice. The results showed that the daily oral administration of deltamethrin and endosulfan caused a significant decrease in neurotransmitter contents (NE, DA and GABA) in most of the tested brain areas (cerebellum, striatum, cerebral cortex, hypothalamus, brain stem and hippocampus). On the other hand a gradual significant reduction, ALT, AST and ALP enzyme activities, while the glucose level and acid phosphatase increase were observed in serum of mice treated with deltamethrin and endosulfan for two weeks. Also, this study has a significant inhibition in the activities of enzymes in liver tissues of treated mice including glutathione reductase. Meanwhile, the activity of lipid peroxide, glycolytic (PK, PFK and GPI) and gluconeogenic enzyme activities (F-1, 6-D-Pase) were significantly increased in liver tissues of treated mice in response to treatment. Additionally,

total protein and glycogen content showed a significant reduction in liver tissues of mice treated with deltamethrin and endosulfan for two weeks. It was concluded that the pollution of the aquatic environment by deltamethrin and endosulfan pesticides, would adversely affect the metabolism of the mice.

**Keywords:** Deltamethrin; Endosulfan pesticide; Laboratory-bred strain swiss albino male mice; Neurotransmitter contents (NE, D A and GABA).

### 437. Importance of Schistosoma Mansoni Thioredoxin Glutathione Reductase 1- Evaluation of its Role in Schistosomiasis Diagnosis in Human

A. El Gendy, I. Rabie, S. El Deeb and A.M. El Amir

*Journal of Medical Sciences*, 13 (8): 635-646 (2013)

*Schistosoma* parasite continued to be the focus of solicitude investigators to control the prevalence of the parasite. Efforts are needed for sensitive and accurate diagnosis that can be utilized to rapidly map the prevalence of the disease. Our study aimed to benefit from the necessity of the *S. mansoni* for the enzyme thioredoxin/glutathione reductase (TGR), in utilization of the enzyme as target antigen and to evaluate its efficacy in the diagnosis of *S. mansoni* infection patients. For reach the our goal, affinity chromatographic method has been utilized for isolation of TGR antigen from *S. mansoni* adult worm and employ this antigen for production of pAb for schistosomiasis by immunized rabbits. The pAb used in the efficacy evaluation of the purified pAb of TGR antigen in the diagnosis of *S. mansoni* in serum and urine of infected individual by indirect ELISA. Our study, introduced a high diagnostic efficiency for the sandwich ELISA for detection of SmTGR antigen when applied to individuals with low or high worm burden in both serum and urine (89.73% and 87.02%, respectively). Sandwich ELISA revealed that this antigen can be relied on as a diagnostic target antigen in serum and urine.

**Keywords:** *S. Mansoni* diagnosis; Sandwich ELISA; Thioredoxin/glutathione reductase.

### 438. In Vitro Antioxidant, Analgesic and Cytotoxic Activities of Sepia Officinalis Ink and Coelatura Aegyptiaca Extracts

Sohair Ramadan Fahmy and Amel M. Soliman

*African J. of Phar. and Pharmacology*, 7 (22): 1512-1522 (2013)

The present study aims to evaluate the antitumor, antioxidant and anti-inflammatory activities of two molluscan extracts, *Sepia officinalis*, ink extract (IE) and *Coelatura aegyptiaca* extract (CE). The antioxidant activities of both extracts were evaluated using 1,1- diphenyl-2-picrylhydrazyl (DPPH) scavenging and lipid peroxidation assays. The analgesic effects were evaluated using the writhing, hot plate and formalin tests. Cytotoxicity assay was performed using sulphorhodamine B (SRB) method on hepatocellular carcinoma (HepG2) cell lines. The IE extract exhibited dose dependent radical scavenging activity. The two tested extracts showed inhibition of thiobarbituric acid-reactive substances (TBARAS) at all concentrations, with an IC<sub>50</sub> value of 176.77 and 177.23 (µg/ml), respectively. IE and CE extracts showed analgesic action by inhibiting the acetic acid-induced writhing. IE exhibited significant anti-nociceptive actions in mice by increasing the latency period in the hot-plate test. Both extracts

significantly decreased the time of paw lickings in both early and late phases. Furthermore, IE and CE showed cytotoxic activities HepG2 cell lines with IC50 value of 67 and 49.24 µg/ml, respectively. In conclusion, IE and CE extracts have antioxidant, anti-inflammatory and cytotoxic properties and can be considered as promising anticancer drugs.

**Keywords:** Sepia ink; Coelatura aegyptiaca; Antioxidant; Anti-inflammatory; Cytotoxicity.

#### 439. In Vitro Study of A Bacterial Polysaccharides Anti Cancer

Faten S. Bayoumi, Azza M. El Amir, El Deeb S.O., Hassan Abd el Zaher and Haia M.A

*Journal of Applied Sciences Research*, 9 (3): 2007-2018 (2013)

**The aim** of this study was to evaluate in vitro anti-cancerous and immunomodulatory potential of the purified bacterial polysaccharide (Bacillus subtilis sulphated levan; BSL). The antipromotion and antiprogession activities of BSL were assayed through a series of tests using cell line (Hep-G2 cells) and RAW macrophage 264.7 cells. Evaluation of different macrophage functions which include macrophage proliferation rate and levels of nitrous oxide (NO), Tumor necrosis factor- $\alpha$  (TNF- $\alpha$ ) and Cyclooxygenase-2 (COX-2) generated from lipopolysaccharide (LPS) stimulated RAW macrophage 264.7 cells. Estimation of DNA fragmentation and cytotoxicity against human tumor cell line (Hep-G2 cells) illustrated its anti-progression activity. Statistical results showed that BSL inhibited NO production from LPS-stimulated macrophages and increased macrophages proliferation rate. BSL could be recognized as a significant COX-2 and TNF- $\alpha$  inhibitor. So it is evident that BSL is a potent anti-inflammatory agent. Furthermore, BSL was a significant DNA fragmentation inhibitor and its cytotoxicity assessed against Hep-G2 cells demonstrated its anti-progression activity.

**Conclusion:** BSL proved to be a potent antipromotion and antiprogession drug against cancerous cells.

**Keywords:** Macrophage; Immunomodulatory properties; Hepatocellular carcinoma; Carcinogenesis.

#### 440. New Digenean Parasite Infecting the Freshwater Fish, Clarias Gariepinus with Special Reference to its Tegumental Ultrastructure

Elsayed, M. Bayoumy, Sayed Abd El-Monem and M.S. Abd El-Atti

*World Applied Sciences Journal*, 26 (8): 1046-1052 (2013)

The following Lepocreadiid species are described. Fifty Clarias gariepinus fish samples were collected from Giza Province, Egypt, during the period from October 2010 to January 2011. It is found that, 12 out of 50 (24.5 %) fish were found to be naturally infected with a new species (Pseudoholorchis clarii) that is named according to the host harboring this parasite which is distinguished from other species of the same genus by some interspecific variations. The tegument of the present species consists of an outer syncytial layer which is folded into a series of ridges and grooves. The syncytial layer (external layer) is connected to the nucleated internal region across the fibrous discontinuous middle layer. The folds are interrupted by numerous cuticular spines; each one is enclosed at the apex and at the base by the corresponding unit membrane. The inner

nucleated layer is consisted of epidermal cells arranged in two levels. The cells are conical in shape and have a large nucleus with prominent nucleoli. Large vacuoles are also observed between the epidermal cells containing granules of different shapes and sizes.

**Keywords:** Parasites; Digenea; pseudoholorchis clarii; Transmission-electron microscope; Freshwater fish; Clarias gariepinus.

#### 441. Overview on Cysteine Protease Inhibitors as Chemotherapy for Schistosomiasis Mansoni in Mice and Also its Effect on the Parasitological and Immunological Profile

Farid A., Malek A.A., Rabie I., Helmy A. and El Amir A.M.

*Pakistan J. of Biological Sciences*, 16 (24): 1849-1861 (2013)

The present study evaluated the use of 3 types of Cysteine Protease Inhibitors (CPIs) with praziquantel (PZQ) as chemotherapy against schistosomiasis mansoni in mice. All groups were going to assessment of fluromethylketone (FMK), Vinyl Sulfone (VS) and Sodium Nitro Prussid (SNP) by measurement of parasitological, immunological and histological parameters. In our study, the ova count/gm liver or intestine on with PZQ treatment showed 99.1 and 95.2% Percent Reduction (PR), respectively compared to control group. The most effective CPI was FMK when combined with PZQ recording 99.8 and 99.6% PR for liver and intestine, respectively. Regarding to the oogram pattern, FMK, VS and SNP treatment either at 3 or 5 wk PI revealed marked decrease in the immature and mature ova counts and an increase of the dead ova percentages. The effect of CPIs was studied on the PR of Mean Granuloma Diameter (MGD) and Mean Granuloma Number (MGN) of infected treated groups compared to infected control and PZQ treated groups. FMK treatment proved to be highly was effective against S. mansoni in mice disintegrating ova and reduction in granulomatous size and numbers. The microscopic examination of liver sections of infected mice showed a large cellular granuloma with living central ova. sections of Infected mice liver treated with FMK or VS alone or combined with PZQ showed a great reduction in granuloma size as small cellular granuloma with central degenerated ova. We observed that these CPIs alone or combined with PZQ could effectively block schistosomal activity and prevented its growth and differentiation. Briefly, the best schistosomicidal effect of CPIs, that gained by drug administration orally in a dose of 50 mg kg<sup>-1</sup> mouse, was observed with FMK. This was followed by VS and lastly with SNP. These results gave evidence that CPIs can selectively arrest parasite replication without untoward toxicity to the host.

**Keywords:** Praziquantel; Fluromethylketone; Vinyl sulfone; Sodium nitro prussid; Egg profile; Granuloma.

#### 442. Protection against Fasciola Gigantica Using Paramyosin Antigen as a Candidate for Vaccine Production

Abou-Elhakam H., Rabee I., El Deeb S. and El Amir A.

*Pakistan J. of Biological Science*, 16 (22): 1449-1458 (2013)

Yet no vaccine to protect ruminants against liver fluke infection has been commercialized. In an attempt to develop a suitable

vaccine against *Fasciola gigantica* (*F. gigantica*) infection in rabbits, using 97 kDa Pmy antigen. It was found that, the mean worm burdens and bile egg count after challenge were reduced significantly by 58.40 and 61.40%, respectively. On the other hand, immunization of rabbits with Pmy induced a significant expression of humoral antibodies (IgM, total IgG, IgG1, IgG2 and IgG4) and different cytokines (IL-6, IL-10, L-12 and TNF-alpha). Among Ig isotypes, IgG2 and IgG4 were most dominant Post-infection (PI) while, recording a low IgG1 level. The dominance of IgG2 and IgG4 suggested late T helper1 (Th1) involvement in rabbit's cellular response. While, the low IgG1 level suggested Th2 response to adult *F. gigantica* worm Pmy. Among all cytokines, IL-10 was the highest in rabbits immunized with Pmy PI suggesting also the enhancement of Th2 response. It was clear that the native *F. gigantica* Pmy is considered as a relevant candidate for vaccination against fascioliasis. Also, these data suggested the immunoprophylactic effect of the native *F. gigantica* Pmy which is mediated by a mixed Th1/Th2 response.

**Keywords:** Fasciola; Antigens; Vaccines; Fascioliasis prevention; Immunization; Humoral immunity; Cytokines.

#### 443. Protective Effects of Vitamin C against Biochemical Toxicity Induced by Malathion Pesticides in Male Albino Rat

Somaya Mostafa Ismail

*Journal of Evolutionary Biology Research*, 5 (1): 1-5 (2013)

Malathion is a chemical pesticide, commonly used by Egyptian farmers; however, its contamination of water sources has become an important issue. It is suggested that the role of vitamin C in alteration of enzymes responsible for energy metabolism was induced by administration of Malathion. The effect of malathion and malathion with vitamin C on some enzymes in the rat were recorded in the present study. Significant increases in the level of hepatic enzymes (alanine aminotransferase, aspartate aminotransferase, alkaline phosphatase, and gamma glutamyl transpeptidase) were recorded. Furthermore, renal markers such as urea, cholesterol and creatinine were increased in rats treated with malathion. Additionally, serum triglyceride was significantly decreased. No significant changes were observed in total protein, albumin and bilirubin in all treated groups as compared to the control. The present results showed that a significant ( $p < 0.001$ ) decrease in glycolytic enzymes (hexokinase, pyruvatekinase, glucose phosphate isomerase and phosphofructokinase) were observed in treated groups, and lactate dehydrogenase enzyme activity also showed significant ( $p < 0.01$ ) reduction. Co-administration of vitamin C to the groups restored all the parameters cited above to near-normal values. Therefore, the present investigation revealed that vitamin C appeared to be a promising agent for protection against malathion-induced toxicity.

**Keywords:** Malathion pesticide; Male albino rat; Biochemical toxicity.

#### 444. Study of the Efficacy of Cysteine Protease Inhibitors Alone or Combined with Praziquantel as Chemotherapy for Mice Schistosomiasis Mansoni

Farid A., Ismail A., Rabee I. and Zalat R. El Amir A.

*International Journal of Medical, Pharmaceutical Science and Engineering*, 7 (12): 487-494 (2013)

This study was designed for assessment of 3 types of Cysteine protease inhibitors (CPIs) fluromethylketone (FMK), vinyl sulfone (VS) and sodium nitro prussid (SNP), to define which of them is the best for curing *S. mansoni* infection in mice? In vitro, treated *S. mansoni* adult worms recorded a mortality rate after 1 hr of exposure to 500 ppm of FMK, VS and SNP as 75, 70 and 60%, respectively. FMK+PZQ treatment recorded the maximum reduction in worm burden (97.2% at 5 wk PI). VS treatment alone or combined with PZQ increases IgM, total IgG, IgG2 and IgG4 levels. In EM study, the completely implanted spines were reported in the degenerated tegument of adult worms in all groups treated with CPIs.

VS+PZQ Treatment increased Igs levels but, its effect was different on worm reduction. So, it is not enough to eliminate the infection and FMK+PZQ considered the antischistosomal drug of choice.

**Keywords:** Praziquantel; Fluromethylketone; Vinyl sulfone; Sodium nitro prussid.

#### 445. Ultrastructural Studies on the Tongue of Some Egyptian Lizards 1-Scincine Lizards Chalcides Ocellatus and Chalcides Sepsoides (Lacertilia, Scincidae)

Osama Mohamed M Sarhan and Rehab M Hussein

*Cytology and Hstology*, 4: 165-175 (2013)

Tongues of Egyptian lizards *Chalcides ocellatus* and *Chalcides sepsoides* are investigated under scanning and transmission electron microscope. Their tongues are divided into tip, anterior, middle and posterior regions. In *C. ocellatus*, the tip region is bifurcated and protected with strong, non-papillosed, keratinized epithelium. The lingual papillae are separating with wide trenches except in the middle region. Papillae of the anterior and posterior regions have serrated and imbricated ends oriented in the posterior direction. The surface epithelia are studded by tiny or reticular microvilli. Ultra-sections show that the imbricated portions have goblet cells rich in numerous secretory granules. The lamina propria of each papilla is provided with striated muscle fibers. The distribution and orientation of the lingual muscle fibers prove that the tongue is adapted for snipping, masticate and swallowing their prey. In *C. sepsoides* tongue, the tip region is slightly bifurcated. All lingual papillae have different shapes with narrow moats separating between them. Those of the anterior and posterior regions have free ends overlapped towards the anterior or posterior directions, respectively, while that of the middle region is not imbricated. The surface epithelia of the tongue has dispersed or aggregated microvilli. In the tongue of the *C. sepsoides*, new structures are described for the first time. At its ventral aspect, there is an accessory lingual muscle formed of numerous muscle fibers orient to the vertical, transverse or longitudinal directions. These orientations prove that the tongue is able to mash and suck the prey's sherbets. At the end of the posterior region, there is a ciliated concave depression hosting a laryngotracheal organ, which has T-shaped crevice precedent by large fleshy highly ciliated lip supported by inflexible folds.

**Keywords:** Tongue; Ultrastructure; Egyptian lizards; Scincidae.

## Faculty of Agriculture

### Dept. of Agricultural Biochemistry Section

#### 446. Bioactive Compounds and Antioxidant Activity of fresh and Processed white Cauliflower

Fouad A. Ahmed and Rehab F. M. Ali

*Biomed Research International*, 1-9 (2013) IF: 2.88

Brassica species are very rich in health-promoting phytochemicals, including phenolic compounds, vitamin C, and minerals. The objective of this study was to investigate the effect of different blanching (i.e., water and steam) and cooking (i.e., water boiling, steam boiling, microwaving, and stir-frying) methods on the nutrient components, phytochemical contents (i.e., polyphenols, carotenoids, flavonoid, and ascorbic acid), antioxidant activity measured by DPPH assay, and phenolic profiles of white cauliflower. Results showed that water boiling and water blanching processes had a great effect on the nutrient components and caused significant losses of dry matter, protein, and mineral and phytochemical contents. However, steam treatments (blanching and cooking), stir-frying, and microwaving presented the lowest reductions. Methanolic extract of fresh cauliflower had significantly the highest antioxidant activity (68.91%) followed by the extracts of steam-blanching, steam-boiled, stir-fried, and microwaved cauliflower 61.83%, 59.15%, 58.93%, and 58.24%, respectively. HPLC analysis revealed that the predominant phenolics of raw cauliflower were protocatechuic acid (192.45), quercetin (202.4), pyrogallol (18.9), vanillic acid (11.90), coumaric acid (6.94), and kaempferol (25.91) mg/100 g DW, respectively.

**Keywords:** Polyphenols; Carotenoids; Flavonoid; Ascorbic acid.

#### 447. Predicting in Silico Which Mixtures of the Natural Products of Plants Might Most Effectively Kill Human Leukemia Cells?

Hany A. El-Shemy, Khalid M. Aboul-Enein and David A. Lightfoot

*Evidence-Based Complementary and Alternative Medicine*, Article Id 801501: 801501-801510 (2013) IF: 1.722

The aim of the analysis of just 13 natural products of plants was to predict the most likely effective artificial mixtures of 2-3 most possible natural products on leukemia cells from over 364 possible mixtures. The natural product selected included resveratrol, honokiol, chrysin, limonene, cholecalciferol, cerulenin, aloe emodin, and salicin and had over 600 potential protein targets. Target profiling used the Ontomine set of tools for literature searches of potential binding proteins, binding constant predictions, binding site predictions, and pathway network pattern analysis. The analyses indicated that 6 of the 13 natural products predicted binding proteins which were important targets for established cancer treatments. Improvements in effectiveness were predicted for artificial combinations of 2 or 3 natural products. That effect might be attributed to drug synergism rather than increased numbers of binding proteins bound (dose effects). Among natural products, the combinations of aloe emodin with mevinolin and honokiol were predicted to be the most effective combination for AML-related predicted binding proteins. Therefore, plant extracts may in future provide more effective

medicines than the single purified natural products of modern medicine, in some cases.

**Keywords:** Natural products; Potential protein; Dose effects.

#### 448. Pharmacological evaluation of some novel synthesized compounds derived from spiro (cyclohexane-1,2'-thiazolidines)

Eman M. Flefel, Hayam H. Sayed, Ahmed I. Hashem, Emad A. Shalaby, Walaa El-Sofany and Farouk M. E. Abdel-Megeid

*Med Chem Res*, 1-14 (2013) IF: 1.612

A series of novel spiro(cyclohexane-1,2'-thiazolidine) derivatives 1-5 and spiro(cyclohexane-1,2'-thiazolo-pyridine) derivatives 6-14 were synthesized. Arylidene thiazolidine derivative 2b was reacted with hydroxylamine hydrochloride, hydrogen peroxide or ethyl cyanoacetate to give spiro(cyclohexane-1,2'-thiazolidine), and spiro(cyclohexane-1,2'-thiazole) derivatives 15-17. Moreover, some of the newly prepared products were screened for their antibacterial, antioxidant, and anticancer activities, and some of them showed moderate to good biological activities. The results showed that the compounds 9, 7a, and 8 have the highest antioxidant activity (92.52, 85.00, and 84.61 %, respectively at 100 µg/mL) when compared with butylated hydroxyl toluene as a standard (93.6 %). Also, the compound 9 showed the highest anticancer activity against two cell lines (MCF-7 and HepG2); **Keywords:** Spiro (cyclohexane-1,20-thiazolidine); Spiro (cyclohexane-1,20-thiazolo-pyridine); Antimicrobial; Antioxidant; Anticancer activity.

#### 449. Antiherpetic Efficacy of Aqueous Extracts of the Cyanobacterium Arthrospira Fusiformis from Chad

M. Sharaf, A. Amara, A. Aboul-Enein, S. Helmi, A. Ballot and P. Schnitzler

*Die Pharmazie- an International Journal of Pharmaceutical Sciences*, 68: 376-380 (2013) IF: 0.962

Natural substances offer interesting pharmacological perspectives for antiviral drug development with regard to broad spectrum antiviral properties and novel modes of action. Drugs currently used to treat cutaneous or genital herpetic infections are effective in limiting disease, but the emergence of drug-resistant viruses in immunocompromised individuals can be problematic. A nontoxic cyanobacterium *Arthrospira* strain from Chad has been characterized by sequence analysis of the intergenic spacer region of the phycocyanine gene. This cyanobacterium was identified as *Arthrospira fusiformis* by phylogenetic tree analysis. The antiherpetic activity of crude aqueous extracts from the *A. fusiformis* isolate was determined. Antiviral efficacy against herpes simplex virus of cold water extract, hot water extract and phosphate buffer extract was assessed in plaque reduction assays and their mode of antiherpetic action was analysed. In virus suspension assays, cold water extract, hot water extract and phosphate buffer extract inhibited virus infectivity by 54.9%, 64.6%, and 99.8%, respectively, in a dose-dependent manner. The mode of antiviral action was determined by addition of cyanobacterial extracts separately at different time periods during the viral infection cycle. Extracts of *A. fusiformis* strain clearly inhibited herpesvirus multiplication before and during virus infection of host cells. The phosphate buffer extract of the

A. fusiformis strain affected freeherpes simplex virus prior to infection of host cells and inhibited intracellular viral replication. It is concluded, that Arthrospira compounds warrant further investigation to examine their potential role in the treatment of herpetic infections.

**Keywords:** Antiherpetic; Arthrospira fusiformis; Antiviral.

#### 450. Effect of Gamma Radiation on the Lipid Profiles of Soybean, Peanut and Sesame Seed Oils

A.M.R. Afify, M.M. Rashed, A.M. Ebtesam and H.S. El-Beltagi

*Grasas Y Aceites*, 64: 356-368 (2013) IF: 0.74

Seeds of soybean, peanut, and sesame were exposed to various doses of gamma irradiation (0.0, 0.5, 1.0, 2.0, 3.0, 5.0 and 7.5 kGy). Fatty acid and unsaponifiable profiles of the extracted oils were separated by gas chromatography mass spectroscopy. The results demonstrated that the ratios of unsaturated to saturated total fatty acids (TU/TS) and total hydrocarbons to sterols (TH/TS<sub>t</sub>) were significantly altered upon irradiation. These changes were clearly observed in the oil extracted from irradiated sesame seeds compared with the oils from irradiated peanuts and soybean. The major change in fatty acid composition was the decrease in the quantity of unsaturated fatty acids (C18:1 and C18:2) in all cases. In contrast, the sterol fractions such as cholesterol, campesterol, stigmasterol and  $\beta$ -sitosterol levels of irradiated seeds were generally lower than that of the un-irradiated seeds.

**Keywords:** Fatty acid; Gamma irradiation; Hydrocarbon; Oil seeds; Sterol.

#### 451. Structural Characterization and Biological Activity of Sulfolipids from Selected Marine Algae

F.K. El Baz, G.S. El Baroty, H.H. Abd El Baky, O.I. Abd El-Salam and E.A. Ibrahim

*Grasas Y Aceites*, 64 (5): 561-571 (2013) IF: 0.74

The sulfolipid classes (SLs) in the total lipids of five species of marine algae, two species of Rhodophyta (*Laurenciapopilliose*, *Galaxoura cylindrica*), one species of Chlorophyta (*Ulva fasciata*), and two species of Phaeophyta (*Dilophysfasciola*, *Taonia atomaria*) were separated and purified on DEAE-cellulose column chromatography. The SLs component was identified by IR, gas chromatography MS/MS and liquid chromatography MS/MS. The level of SLs contents varied from 1.25% (in *L. papillose*) to 11.82% (in *D. fasciola*) of the total lipid contents. However, no significant differences in sulfate content (0.13 – 0.21%) were observed among all these algae species. All SLs were characterized by high contents of palmitic acid (C<sub>16:0</sub>), which ranged from 30.91% in *G. cylindrica* to 63.11% in *T. atomaria*. The main constituents of algal sulfolipids were identified as sulfoquinovosyl-di-acylglycerol and sulfoquinovosyl acylglycerol. The sulfolipids of different algal species exhibited remarkable antiviral activity against herpes simplex virus type 1 (HSV-1) with an IC<sub>50</sub> ranging from 18.75 to 70.2  $\mu$ g mL<sup>-1</sup>. Moreover, algal sulfolipid inhibited the growth of the tumor cells of breast and liver human cancer cells with IC<sub>50</sub> values ranging from 0.40 to 0.67  $\mu$ g mL<sup>-1</sup> for human breast adenocarcinoma cells (MCF7).

**Keywords:** Antibacterial; Anticancer; Antiviral; Cells; Hepg2; HSV-1; Marine algae; MCF7; Sulfolipids.

#### 452. White Bean Seeds and Pomegranate Peel and Fruit Seeds as Hypercholesterolemic and Hypolipidemic Agents in Albino Rats

By E.A. Abdel-Rahim, H.S. El-Beltagi and R.M. Romela

*Grasas Y Aceites*, 64 (1): 50-58 (2013) IF: 0.74

This study was carried out to evaluate the effects of soaked white bean seeds, pomegranate seeds and dried peels and their mixtures on the lipid profiles of rats suffering from hyperlipidemia and hypercholesterolemia. The chemical compositions of dried soaked beans and pomegranate (seeds and peels) were determined on dry matter which amounted to good values for proteins, lipids, crude fiber and phenols. Also, the phenol contents of pomegranate seeds and peels showed 16 compounds varying in amount between them. It was noticed that catechin and phenol are the dominating compounds. The obtained results showed a good hypolipidemic ability for soaked bean seeds and pomegranate (seeds, peels and their mixtures) as well as their mixtures. A bean seeds diet produced a general improvement in the clinical status of blood lipid profile (total lipids, triglycerides, cholesterol, HDL-c, LDL-c and VLDL-c), liver function (ALT, AST and bilirubin), kidneys function (uric acid, urea and creatinine), blood lipid peroxidation and antioxidant enzymes (SOD and CAT) by which hyperlipidemia and hypercholesterolemia were reduced. The mixed diet had the best influence concerning biological studies than the other treatments which used bean seeds and pomegranate (seeds and peels) alone.

**Keywords:** Hypercholesterolemia; Hypolipidemia; Pomegranate (*punica granatum*); White bean (*phaseolus vulgaris* L.).

#### 453. Alleviation of Cadmium Toxicity in Pisum Sativum L. Seedlings by Calcium Chloride

Hossam S. El-Beltagi and Heba I. Mohamed

*Notulae Botanicae Horti Agrobotanici Cluj-Napoca*, 41(1): 157-168 (2013) IF: 0.59

The present investigation was carried out to study the role of calcium chloride in enhancing tolerance and reducing cadmium toxicity in pea seedlings. Some treatment with 1 and 5 mM CaCl<sub>2</sub> mitigated cadmium stress by increasing antioxidant enzyme activities: catalase (CAT), peroxidase (POD) and polyphenol oxidase (PPO), as well as by elevating contents of ascorbic acid (ASA), tocopherol and carotenoids. On the other hand, total carbohydrate and total soluble proteins decreased with increasing cadmium concentrations in comparison with control plants. However, total phenol, total free amino acids, proline and lipid peroxidation increased with increasing concentrations of cadmium acetate. Electrophoretic studies of protein revealed that cadmium treatments alone or in combination with calcium chloride were associated with the disappearance of some bands or appearance of new bands in pea seedlings. Electrophoretic studies of  $\alpha$ -esterase,  $\beta$ -esterase and acid phosphatase isozymes showed wide variations in their intensities and densities.

**Keywords:** Antioxidant enzymes; Cadmium toxicity; Calcium; Non enzymatic antioxidants; Oxidative stress; Pisum sativum.



#### 454. Comparison of Antioxidant and Antimicrobial Properties for Ginkgo Biloba and Rosemary (Rosmarinus officinalis L.) from Egypt

Hossam S. El-Beltagi and Mona H. Badawi

*Notulae Botanicae Horti Agrobotanici Cluj-Napoca*, 41(1): 126-135 (2013) IF: 0.59

The widespread use of medicinal plants for health purposes has increased dramatically due to their great importance to the public health. In this study levels of phenolic, flavonoid contents of Ginkgo biloba and Rosmarinus officinalis from Egypt were determined. HPLC was used to identify and quantify the phenolic compounds in selected plants. The plant extracts were evaluated for their antioxidant activities using various antioxidant methodologies, (i) scavenging of free radicals using 2, 2-diphenyl-1-picrylhydrazyl, (ii) metal ion chelating capacity, and (iii) scavenging of superoxide anion radical. The antimicrobial activity of both plant's extracts were evaluated against a panel of microorganisms by using agar disc diffusion method. The total phenolic content (75.30 and 98.31 mg/g dry weight in G. biloba and R. officinalis, respectively) was significantly ( $p < 0.05$ ) different. Among the identified phenolic compounds, quercetin, kaempferol and caffeic acid were the predominant phenolic compounds in Ginkgo biloba, whereas carnosic acid, rosmarinic acid, narinigen and hispidulin were the predominant phenolic compound in Rosmarinus officinalis leaves. The antioxidant activity increased with the concentration increase. The R. officinalis was more active than G. biloba extract against Gram-negative bacteria. This study reveals that the consumption of these plants would exert several beneficial effects by virtue of their antioxidant and antimicrobial activities.

**Keywords:** Antimicrobial activity; Antioxidant activity; Ginkgo biloba; Phenolic compounds; Rosmarinus officinalis.

#### 455. Physiological and Biochemical Effects of $\gamma$ -Irradiation on Cowpea Plants (Vigna Sinensis) Under Salt Stress

Hossam S. El-Beltagi, Heba I. Mohamed, Abdel Haleem M.A. Mohammed, Laila M. Zaki and Asmaa M. Mogazy

*Notulae Botanicae Horti Agrobotanici Cluj-Napoca*, 41(1): 104-114 (2013) IF: 0.59

Soil salinity is one of the most severe factors limiting growth and physiological response in cowpea plants. In this study, the possible role of  $\gamma$ -irradiation in alleviating soil salinity stress during plant growth was investigated. Increasing salinity in the soil (25, 50, 100 and 200 mM NaCl) decreased plant growth, photosynthetic pigments content, total carbohydrate content and mineral uptake compared to control, while increased total phenol content, proline, total free amino acids and lipid peroxidation. Seed irradiation with gamma rays significantly increased plant growth, photosynthetic pigments, total carbohydrate, total phenol, proline, total free amino acids and the contents of N, P,  $K^+$ ,  $Ca^{+2}$  and  $Mg^{+2}$  compared to non irradiated ones under salinity. On the other hand, irradiation with gamma rays decreased lipid peroxidation,  $Na^+$  and  $Cl^-$  contents which may contribute in part to activate processes involved in the alleviation of the harmful effect of salt at all concentrations used (25, 50 and 100 mM) except at the high concentration (200 mM). Electrophoretic

studies of  $\alpha$ -esterase,  $\beta$ -esterase, polyphenol oxidase, peroxidase and acid phosphatase isozymes showed wide variations in their intensities among all treatments.

**Keywords:** Cowpea; Gamma rays; Isozyme; Lipid peroxidation; Salt stress.

#### 456. Reactive Oxygen Species, Lipid Peroxidation and Antioxidative Defense Mechanism

Hossam S. El-Beltagi and Heba I. Mohamed

*Notulae Botanicae Horti Agrobotanici Cluj-Napoca*, 41(1): 44-57 (2013) IF: 0.59

Lipid peroxidation can be defined as the oxidative deterioration of lipids containing any number of carbon-carbon double bonds. Lipid peroxidation is a well-established mechanism of cellular injury in both plants and animals, and is used as an indicator of oxidative stress in cells and tissues. Lipid peroxides are unstable and decompose to form a complex series of compounds including reactive carbonyl compounds. The oxidation of linoleates and cholesterol is discussed in some detail. Analytical methods for studying lipid peroxidation were mentioned. Various kinds of antioxidants with different functions inhibit lipid peroxidation and the deleterious effects caused by the lipid peroxidation products.

**Keywords:** Antioxidants; Cholesterol; Fatty acids; Lipid peroxidation.

#### 457. Comparison of Dpph and Abts Assays for Determining Antioxidant Potential of Water and Methanol Extracts of Spirulina Platensis

Emad A. Shalaby and Sanaa M. M. Shanab

*Indian Journal of Geo-Marine Sciences (Ijms)*, 42 (5): 556-564 (2013) IF: 0.183

Present research was to evaluate and compare the antiradical and antioxidant activities of extracts from Spirulina platensis. In the present study, three extracts (Water, absolute methanol and 50% methanol in water) were analyzed for the total phenolic compounds, phycobiliprotein content: Antiradical and antioxidant activities were evaluated using 2,2-diphenyl-1-picrylhydrazyl (DPPH•) and 2,2-azinobis (3-ethylbenzothiazoline-6-sulfonic acid) (ABTS) radical scavenging methods at 100 and 200  $\mu$ g/mL. Results revealed that, absolute methanol extract recorded the highest number of antiradical units 1 mg extract followed in descending order by that of water while the lowest number was that of aqueous methanol (against DPPH and ABTS radical methods) and these correlated with chemical constituents of extract from phenolic and phycobiliprotein compounds. It is elucidated that selection of the cyanobacterium (Spirulina platensis) very important for consumer's health, as it is considered as potential sources of dietary antioxidants.

**Keywords:** Spirulina platensis; Antioxidant; Antiradical; DPPH; ABTS; Phenolic compounds.

#### 458. Anticancer Activity of Some Commercial Antihypertensive Drugs by Neutral Red Assay

Fathia Z.El Sharkawi, Hany A.El Shemy and Hussein.Khaled

*Life Sci J.*, 10 (1): 609-613 (2013) IF: 0.165

Lisinopril, propranolol and nifedipine are three commercial drugs used clinically for the management of hypertension, angina pectoris, and cardiac arrhythmias. It has been reported that these drugs have inhibitory effects on some cancer cells. In the current study the cytotoxicity of these drugs was evaluated against HeLa, HepG2, MCF-7 and EACC transformed cell lines using Neutral Red and Trypan Blue assay methods. The three drugs showed a cytotoxicity against HeLa, HepG2 and MCF-7 cells with different potentiality. Lisinopril was the most potent cytotoxic drug against HepG2 cells with  $IC_{50} = 33.8 \pm 88.4 \mu\text{g/ml}$  at the concentration of 300  $\mu\text{g/ml}$ ; while Nifedipine was the most active one against HeLa cells with  $IC_{50} = 130 \pm 58.4 \mu\text{g/ml}$  at a concentration of 300  $\mu\text{g/ml}$ . Propranolol was the most active against MCF7 cells  $IC_{50}$  of  $78.0 \pm 121.4 \mu\text{g/ml}$  at a concentration of 3000  $\mu\text{g/ml}$ . The three used drugs inhibited the growth of EACC cells and propranolol showed highest inhibitory activity; it inhibited 97.7% of cell growth at a concentration of 300  $\mu\text{g/ml}$  and 100% inhibition at a concentration of 3000  $\mu\text{g/ml}$ . Lisinopril and nifedipine showed a lower rate of growth inhibition of 18.28% and 11.40% respectively at a concentration of 3000  $\mu\text{g/ml}$ . In conclusion: At these high concentrations, the three tested drugs are lethal in vitro to cancer cells of endometrial, cervical, hepatic, and breast origin. Further animal studies are required to confirm this conclusion.

**Keywords:** Lisinopril; Propranolol; Nifedipine; Cell lines; In vitro chemosensitivity.

#### 459. Characterization of Egyptian Moringa Peregrine Seed Oil and Its Bioactivities

Hanaa H. Abd El Baky and Gamal S. El-Baroty

*International Journal of Management Sciences and Business Research*, 2 (7): 98-108 (2013)

The seed oil of Egyptian Moringa peregrina (Forssk) was extracted with a mixture of dichloromethane/methanol (1:1, v/v). The oil was examined with respect to physicochemical properties, unsaponifiable (UnSap) and fatty acids profiles, tocopherols and phenolic contents, anticancer and antioxidant activities. Moringa oil (MO) showed a better overall quality, its acid, peroxide, iodine, saponification values were 0.02 mg KOH/g oil, 0.01 meq O<sub>2</sub>/kg oil, 67 I<sub>2</sub> g/100 g oil and 177 mg KOH/g. The Un-Sap of MO was found to contain high amounts of hydrocarbon fraction C<sub>12</sub> to C<sub>32</sub> and phytoesterol fractions were found rich in campesterol, clerosterol and  $\beta$  sitosterol compounds. The major fatty acids were identified as oleic (C<sub>18</sub>:1  $\omega$ 9, 65.36%) and linoleic (C<sub>18</sub>:3  $\omega$ 6, 15.32%). Tocopherols and phenolic in oil accounted for 20.35 and 48.31 mg/100 g. The Moringa oil showed high growth inhibition against three human cancer cell lines, breast adenocarcinoma (MCF-7), hepatocellular carcinoma (Hep-G2), and colon carcinoma (HCT-116), with  $IC_{50}$  values of 2.92, 9.40 and 9.48  $\mu\text{g/ml}$ , respectively. The MO showed remarkable antioxidant activity, compared with that of commonly used antioxidants (?-tocopherol, BHT and BHA) as determined by five antioxidant assays (includes, free radical scavenging of DPPH, ABTS, .OH, anion-scavenging capability and reducing power. These results strongly suggested its potential use MO as non-conventional seed crop for high quality oil and as candidate in the area of natural anticancer and antioxidant compounds.

**Keywords:** Moringa peregrina; Seed oil; Anticancer; Fatty acid; Antioxidant activity.

#### 460. Effect of Solanum Nigrum Linn Against Lambda Cyhalothrin-Induced Toxicity in Rats

Marwa M Abd Elkawy, Ghada Z A Soliman and Emam Abd-El Mobd'ea Abd-El Rehim

*Journal of Pharmacy and Biological Sciences*, 5 (5): 55-62 (2013)

Lambda-cyhalothrin is a type II pyrethroid insecticide and may cause liver damage. Solanum nigrum may act as hepatoprotective agent; therefore we aimed to study the effect of solanum nigrum (dried fruits or its ethanolic extract) against lambda cyhalothrin toxicity in rats. Materials and Methods: Thirty three male Sprague Dawley rats were divided into 6 groups (G1: normal; G2 & 3: normal treated with ethanolic extract of the dried fruits, and dried fruits respectively; G4: normal rats intoxicated with Lambda cyhalothrin; G5 & 6: as G2 & 3 but intoxicated with lambda cyhalothrin. At the end of the experiment (6 weeks), the rats were sacrificed and blood was taken for the determination of AST, ALT, Alk Ph, LDH, Hb, Hct, MCH, MCHC and RBC count. Lactate dehydrogenase (LDH) was measured in serum and brain. Results and Discussion: A significant decrease in body weight, Hb and Hct level was observed in G4 (Lambda cyhalothrin intoxicated rats). The intoxicated groups (G 5 & 6) treated with ethanolic extract or dried fruits of Solanum nigrum showed an improvement of body weight, Hb and Hct where a significant increase compared to G4 but still significantly lower than G1 was observed trying to return to normal or near normal level. A significant increase in AST, ALT and Alk Ph level was observed in G4. Group 5 & 6 showed an improvement of AST, ALT and Alk Ph level where a significant decrease compared to G4, but still significantly higher than G1, was observed trying to return to normal or near normal.

**Keywords:** Solanum nigrum; Hepatoprotective; Rats; Lambda cyhalothrin.

#### 461. Evaluation of Carrot Pomace (Daucus Carota L.) As Hypocholesterolemic and Hypolipidemic Agent on Albino Rats

Abd El-Moneim M.R. Afif, Ramy R. M. Romeilah, Mahmoud M.H. Osfor and Amir S. M. Elbahnasawy

*Not Sci Biol*, 5: 7-14 (2013)

The current study examined the attenuating influence of dietary carrot pomace powder (CaPP) on hypercholesterolemia and various oxidative stress-associated with biochemical parameters in hypercholesterolemic rats. Thirty two male albino rats weighing  $110 \pm 10$  g were divided into four groups, the first group received the basal diet only and served as (negative control), the second group received the hypercholesterolemic diet and served as positive control, the other groups received hypercholesterolemic diet supplemented with 10%, 20% CaPP for six weeks. The obtained results revealed that groups supplemented with 10% and 20% CaPP significantly decrease total lipid, total cholesterol, triglycerides, low density lipoprotein cholesterol, liver enzymes: alanine aminotransferase, aspartate aminotransferase compared to positive and negative groups. Organs weight, body weight gain significantly decreased compared with positive control. Moreover dietary carrot pomace powder can used to reduce the body weight and reducing hypercholesterolemic complications. In addition, dietary carrot

pomace powder serves to improve the blood picture and to reduce the blood glucose level in hypercholesterolemic rats and could use in obese people for body loss. Data of kidney function (Urea) record an increase in CaPP 20% level ( $26.9 \pm 2.96$ ) but this increase was non significant with the negative control group ( $26.6 \pm 3.1$ )

**Keywords:** Daucus carota; Hypercholesterolemia; Kidney Function; Obese people.

#### 462. Healthy Benefit of Microalgal Bioactive Substances

Abd El Baky H. H. and El-Baroty G. S.

*Journal of Aquatic Science, 1 (1): 11-23 (2013)*

Microalgae have been widely used as novel sources of bioactive substances. Along with this trend, the possibility of replacing synthetic preservatives with natural ones is receiving much attention. In general, microalgae are rich in various phytochemicals like carotenoids, phycocyanine, phenolics, amino acids, polyunsaturated fatty acids, and sulphated polysaccharides. These compounds are providing excellent various biological actions including, antioxidant, antimicrobial, antiviral, antitumoral, anti-inflammatory and anti-allergy effects. Their healthy benefit seemed to be due to different biochemical mechanisms. However, some microalgae species such as Chlorella, Spirulina and Dunaliella species have been used in several areas in nutraceutical, pharmaceutical, cosmetics, nutrition and functional quality of foods. In 2006, World Health Organization has been described Spirulina as one of the greatest super-foods on earth serving as an example of the potential of microalgae. This review provides background on current and future uses of microalgae as novel source of health promoting compounds.

**Keywords:** Microalgae; Antioxidant; Nutrition; Biological activities; Functional food.

#### 463. Impact of Pre-Treatments on the Acrylamide Formation and Organoleptic Evolution of Fried Potato Chips

Samir Abdel-Monem Ahmed Ismial, Rehab Farouk Mohammed Ali, Mohsen Askar and Wafaa Mahmoud Samy

*American Journal of Biochemistry and Biotechnology, 9: 90-101 (2013)*

The main objective of this investigation was to study the effect of different pre-frying treatments on reduction of acrylamide formation of fried potato. Moreover; the impact of different phenol compounds and leaves on acrylamide formation was evaluated. In addition, the effects of these treatments on the sensorial quality of fried potato chips were studied. Results showed that blanching process caused significant decreases in acrylamide content of fried potato. The highest decrease was observed for those samples blanched in  $MgCl_2$  (0.1 M), L-cysteine (0.05 M) and 0.01 M of citric acid solutions, 97.97, 97.17 and 93.43%, respectively. Soaking of potato slices in water or different solutions significantly reduced the formation of acrylamide. The decreases in acrylamide content ranged from 61.61 to 97.47%. Soaking in crude, semi-purified asparaginase solutions, blanching in hot water plus immersing in the enzyme solutions and soaking in

phenolic acid solutions caused significant reduction in the formation of acrylamide of potato chips. Addition of fresh leaves into frying oil significantly influenced acrylamide formation. Oregano, rosemary, bamboo, guava and olive leaves caused the greatest reductions. Potato slices blanched in distilled water at  $65^\circ C$ , NaCl,  $MgCl_2$  and 0.1 M glutamine had significantly the highest scores of overall acceptability.

**Keywords:** Acrylamide; Potato; Blanching; Soaking; Protein; Antioxidants.

#### 464. in Vitro Clonal Propagation, Caffeic Acid Production and Rapid Analysis of Some Varieties of Echinacea Purpurea Plant

Ahmed M. Aboul-Enein, abd El-Moneim M. Afify, Mohamed R. Rady, Saber F. Hedawy and Mona M. Ibrahim

*Journal of Applied Sciences Research, 9: 843-851 (2013)*

An efficient multiple shoot has been developed for three varieties of Echinacea purpurea using shoot tip explant. Multiple shoots originated when shoot tip cultured on MS-medium supplemented with 0.5 mg/L BA and different concentrations of NAA. Optimum shoot multiplication was observed on MS-medium containing 0.5 mg/L BA for the three varieties. The best results for rooting experiment were obtained with MS-basal medium for Rubinstern variety, however in Double decker and Baby swan white varieties, the addition of IBA to the medium improve rooting. Analysis of caffeic acid derivatives in the dried flowering tops of in vivo Echinacea varieties and produced in vitro plants Echinacea varieties indicated that the total caffeic acid derivatives were higher in the dried flowering tops of in vivo Echinacea varieties in comparison with produced in vitro plants Echinacea varieties. Whereas HPLC analysis of caffeic acid and chicoric acids which the most important compounds in the caffeic acid derivatives showed that the higher productivity of caffeic and chicoric acids were recorded in the in vitro plants Echinacea varieties compared to the dried flowering tops of in vivo Echinacea varieties. The Data of RAPD-based DNA fingerprint analysis revealed that the highest percentage of polymorphism (22.2%) was recorded with B4 primer.

**Keywords:** Echinacea; Multiplication; Caffeic acid derivatives; Rapid; Medicinal plants.

#### 465. Jatropha Curcas (Linn) Seed Ethanolic Extract Possess Antifungal Activity against Phytophthora Infestans and Stimulates Potato Resistant Response

G.M.G. Shehab, O.K. Ahmed and M.A. Ahmad

*Journal of Biological and Chemical Research, 30 (2): 929-941 (2013)*

Medicinal plants have shown great potential in controlling many diseases and appear to be one of the alternatives of synthetic pesticides for controlling plant diseases. In the present study, the in vitro antifungal activity of crude ethanolic extract of Jatropha curcas seed against Phytophthora infestans and its protective effect against late blight disease were investigated. Phytochemical screening of jatropha seed ethanolic extract showed considerable proportions of phenolic compounds, flavonoids and glycosides and reasonable amounts of steroids, tannins and terpenoids. Using the supplemented media technique,

concentrations ranging from 50 – 200 mg/ml of the ethanolic extract were tested against *P. infestans*. The growth of the fungus was significantly inhibited by all used concentrations of the crude extract. The highest crude concentration 200 mg/ml showed significantly the highest mycelia growth inhibition ( $92.03 \pm 1.02$  %) which was comparable to the fungicide positive control (0.1% Dithane M 45). The effects of the ethanolic extract treatment on the activity of the antioxidant enzymes (POD, SOD, APX and CAT) as well as PAL activity during the interaction between potato plants and *P. infestans* were investigated. Spraying the plants with 200 mg/ml crude extract induced the activity of the antioxidant enzymes as well as PAL activity compared to the positive and negative controls. The results of the present study highlight the possibility to reduce *P. infestans* infection in the potato production fields by using plant natural products like jatropha crude extracts. **Keywords:** Antifungal activity, Antioxidant enzymes, *Jatropha curcas*, late blight, *Phytophthora infestans*, Potato. Abbreviations: APX, ascorbate peroxidase; AT, catalase; PAL, Phenylalanine ammonia-lyase; POD, peroxidase; ROS, reactive oxygen species; and SOD, superoxide dismutase. **Keywords:** Antifungal activity; Antioxidant enzymes; *Jatropha curcas*; Late blight; *Phytophthora*.

#### 466. Leadership Skills in Higher Education

Hany R. Alalfy, Ibrahim S. Al-Aodah and Emad A. Shalaby

*Mediterranean Journal of Social Sciences*, 4 (2): 475-480 (2013)

Universities all over the world are facing significant new challenges and some fascinating opportunities in an increasingly competitive global context. The continuing under representation of human skills at more senior and management levels of the international higher education sector is receiving renewed attention with the recognition that neither institutions nor the countries in which they are located can afford to continue neither to overlook their management abilities nor to neglect their leadership potential. The present study aims to clarify Leaders in management education face diverse challenges in today's competitive and changing environment. Moreover, How can take the decision with high quality (Decision quality).

**Keywords:** Faculties; Skills; Leadership; Decision.

#### 467. Preparation and Characterization of Protein Isolate and biodiesel from Garden Cress Seed

Rehab Farouk Mohammed Ali

*European Journal of Chemistry*, 4: 85-91 (2013)

Garden cress (Gc) seeds were analyzed for proximate composition and mineral content. The protein isolate (PI) was evaluated for chemical composition, mineral content, amino acid composition, biological values and some functional properties. The seed oil was evaluated for fatty acid profile; tocopherols and some of physicochemical properties were studied. Seeds were found to contain 29.11% oil and 25.12% protein. Phosphorus, magnesium and calcium constituted the major minerals of the seeds. The protein efficiency ratio (PER) of PI was 2.37. PI was found to possess relatively high values of water and fat absorption capacity, emulsification capacity and foam capacity. The fatty acid profile showed that linolenic acid (41.17%) and oleic acid (26.42%) were the major unsaturated fatty acids, whereas palmitic acid was the major saturated acid. Total tocopherol content of

Garden cress oil was 150.46 mg/100 g oil. The physicochemical characteristics of oil and biodiesel meet the norm specifications.

**Keywords:** Seed; Biodiesel; Erucic acid; Amino acid; Triglycerides; garden cress.

#### 468. Protective Effects of Red Grape Seed Extracts on DNA, Brain and Erythrocytes against Oxidative Damage

Hazem Mohamed Mahmoud Hassan

*Global Journal of Pharmacology*, 7: 241-248 (2013)

The aim of this study was to investigate the protective role of red grape seed extracts (GSEs) against oxidative damage on DNA, brain and erythrocytes in vitro. In this study, the protective effects of two GSEs (water and ethanol) on free radical mediated DNA-sugar damage, Fe<sup>2+</sup>-induced lipid peroxidation in brain and H<sub>2</sub>O<sub>2</sub> induced hemolysis and lipid peroxidation of erythrocytes were determined. The results revealed that the presence of various concentrations of each grape seed extract in the reaction mixture prevented the free radical-mediated DNA-sugar damage in a dose dependently. Similarly, GSEs caused a significant decrease in Fe<sup>2+</sup>-induced lipid peroxidation in rat brain tissues in a dose dependent manner. Both GSEs at different concentrations suppressed H<sub>2</sub>O<sub>2</sub>-induced hemolysis of rat erythrocytes in a concentration-dependent manner. Pre-treatment of cells with GSEs, however, prevented the phospholipid oxidative alteration in a concentration-dependent manner. Noteworthy, the ethanol grape seed extract (EGSE) was more effective than water grape seed extract (WGSE) against oxidative damage of DNA, brain and erythrocytes. In conclusion, the results demonstrated that GSEs protected DNA, brain and erythrocytes against oxidative stress and it could be used as a valuable food supplement or a nutraceutical product.

**Keywords:** Brain; DNA; Erythrocytes; In vitro; Oxidative damage Red grape seeds.

#### 469. Proximate Compositions, Phytochemical Constituents, Antioxidant Activities and Phenolic Contents of Seed and Leaves Extracts of Egyptian Leek (*Allium Ampeloprasum* Var. *Kurrat*)

Fouad Abd El-Rehem Ahmed Abd El-Rehem and Rehab Farouk Mohammed Ali

*European Journal of Chemistry*, 4: 185-190 (2013)

Leeks (*Allium ampeloprasum* var. *kurrat*.) are the most commercially produced vegetables in the world. The seed and leaves were analyzed for proximate composition and mineral content. Phytochemical screening, total polyphenols, total flavonoids, tannins, radical scavenging activity by DPPH (2,2-diphenyl-1-picrylhydrazyl), total antioxidant activities and phenolic profile of various extracts of Egyptian leek were screened and investigated. The seed is good source of fat and protein, whereas the leaves are good source of crude fiber and ash. Both seed and leaves contain substantial quantities of potassium, calcium, and phosphorus. Methanolic and ethanolic extracts of seeds and leaves were found to contain alkaloids, steroid, terpenoid, flavonoid, tannins, saponine, reducing sugar, proteins and oil. The highest values of total phenolic, flavonoid, tannin, radical scavenging and antioxidant activities were

observed for methanolic and ethanolic extracts of seed and leaves. HPLC analysis results showed that certain phenolic compounds; gallic, coumaric, caffeic, tannic, vanillic, chlorogenic, kaempferol, and quercetin exist in methanolic extracts of both seed and leaves at different levels. These results suggested that *Allium ampeloprasum* phenolic compounds could be used as a natural antioxidant.

**Keywords:** Leek; Leaf; Seed; Antioxidant activities; 2,2-Diphenyl-1-picrylhydrazyl; *Allium ampeloprasum* var; Kurrat.

#### 470. Role of Development and Accreditation Deanship for Qualification of Hail Faculties, Saudi Arabia for Local Accreditation

Hany R. Alalfy, Ibrahim S. Al-Aodah and Emad A. Shalaby

*Greener Journal of Educational Research*, 3(3): 123-133 (2013)

Quality education is a prerequisite to gain access to knowledge which guarantees economic development. This makes the condition of higher education in Saudi Arabia a very critical issue. The present work aimed to discuss the quality movement of Hail University, Particularly, the efforts of Deanship of Development and Quality (DQD) in setting up NCAAA standards (National Commission for Academic Accreditation and Assessment). In the process, the authors identify the steps for technical support e.g.: Workshops, Site visits and meetings in addition, design of different action plans for quality assurance activities and accreditation approach. The results revealed that, 90% from Hail Faculties achieved most of DQD requirements except Community and Engineering Faculties.

**Keywords:** Quality assurance; Accreditation; Hail university; DQD.

#### 471. Semi-modified carrot diet alleviates the toxicity effects of dimethoate in albino rats

Osama K. Ahmed, Gaber M.G. Shehab and Yasmin E. Abdel-Mobdy

*Australian Journal of Basic and Applied Sciences*, 7(14): 554-561 (2013)

**Background:** Dimethoate is an effective organophosphate pesticide that used heavily against a broad range of insects and mites and is also used indoor to control house flies. Investigators have shown that dimethoate has immunotoxicologic effects and carcinogenic potential. Moreover, it has been shown to cause adverse reproductive effects in rats

**Objective:** The current study was conducted to evaluate the toxicity effects of dermal and oral administration of the technical (TD) and the formulated dimethoate (FD) in rats and the possibility of alleviating the toxicity effects by semi-modified diet of carrot as a source of antioxidant agents.

**Results:** Ten groups of albino rats were used in this experiment. Five groups of them fed on standard diet (SD-groups) and the other five fed on semi-modified carrot diet (15% carrot) (MD-groups). In each of these previous groups (SD & MD); one group untreated (served as negative control), the second group ingested orally with TD, the third group ingested orally with FD, the fourth group administered dermally with TD and the fifth group administered dermally with FD. Body weight gain, feed intake, feed efficiency, organs weight, liver glycogen, blood sugar,

thyroid hormones (T4 and T3) and lipid profile were estimated. The results revealed that, the treatment with 1/25 LD50 of technical and formulated dimethoate insecticide reduced the values of body weight gain, feed efficiency and body weight gain ratio compared to the control animals. The reduction was higher in the animals treated with the formulated dimethoate compared to the animals treated with the technical dimethoate. In both cases, the oral administration was more effective than the dermal administration. On the other hand, the liver, kidney, heart and spleen weight of the treated animals were higher than the control. The increment of organ weight was higher in formulated dimethoate treated animals compared to the technical treated animals and the oral administration was more effective than the dermal administration. The biochemical analysis showed that the treatment with technical or formulated dimethoate increased the blood glucose level and the thyroid hormones (T3 and T4), while the treatment decreased the liver glycogen contents, total lipids, total cholesterol and total phospholipids. In the same manner, the effect of the formulated dimethoate was more pronounced than the technical dimethoate and the oral ingestion was more effective than the dermal administration. Feeding the animals on the semi-modified carrot diet (15% dried carrot) alleviated the harmful effects of the insecticide, indicated by returning the values of the estimated parameters around the normal values.

**Conclusion:** it can be concluded that, carrot has the potential to reduce the harmful toxicity of dimethoate, thus can be recommended to dimethoate producers, pesticide workers and farm owners, whom expose to this insecticide risk

**Keywords:** Carro; Dimethoate; Organophosphate; Pesticides; Toxicity.

#### 472. Stimulating of Biodegradation of Oxamyl Pesticide by Low Dose Gamma Irradiated Fungi

Abd El-Moneim M.R. Afify, Mohamed A Abo-El-Seoud, Ghada M. Ibrahim and Bassam W Kassem

*J. Plant Pathol. Microb*, 4: 1-5 (2013)

This investigation has been conducted to study the possibility of stimulating *Trichoderma* spp with low dose gamma radiation for biodegradation of Oxamyl pesticides. Fungi strains capable for biodegradation of oxamyl are identified as *Trichoderma* spp., including *T. harzianum*, *T. viride*, *Aspergillus niger*, *Fusarium oxysporum* and *Penicillium cyclopium*. The results indicated that *Trichoderma* spp. used Oxamyl as source of carbon and nitrogen and possesses enzyme(s), which acts on amide and ester bond in Oxamyl structure. Degradation of oxamyl was 72.5% within 10 days of incubation by *T. harzianum* strain. It is very important to note that degradation of oxamyl 82.05% within 10 days of incubation by *T. viride* strain. This indicated that the isolates of *Trichoderma* spp. were potentially useful for oxamyl bioremediation. The biomass of *Trichoderma* spp strain were increased and reached its maximum at 250 Gy by 21.97 and 40.0 when using *Trichoderma* spp., as well as *T. viride*, respectively. As a general trends the gamma radiation over than 0.25 KGr reduce the growth of *Trichoderma* spp by 50.27 and 38.13, using *Trichoderma* spp. as well as *T. viride*, respectively.

**Keywords:** Oxamyl; *Trichoderma harzianum*; *Trichoderma viride*; Biodegradation; Gamma-irradiation.



**Dept. of Agricultural Botany****473. Six-Rowed Spike4 (Vrs4) Controls Spikelet Determinacy and Row-Type in Barley**

Ravi Koppolu, Nadia Anwar, Shun Sakuma, Akemi Tagiri, Udda Lundqvist, Mohammad Pourkheirandish, Twan Rutten, Christiane Seiler, Axel Himmelbach, Ruvini Ariyadasa, Helmy Mohamad Yousse, Nils Stein, Nese Sreenivasulu, Takao Komatsuda and Thorsten Schnurbusch

*Proceedings of the National Academy of Sciences of the United States of America*, 110 (32): 13198-13203 (2013) IF: 9.737

Inflorescence architecture of barley (*Hordeum vulgare* L.) is common among the Triticeae species, which bear one to three singleflowered spikelets at each rachis internode. Triple spikelet meristem is one of the unique features of barley spikes, in which three spikelets (one central and two lateral spikelets) are produced at each rachis internode. Fertility of the lateral spikelets at triple spikelet meristem gives row-type identity to barley spikes. Sixrowed spikes show fertile lateral spikelets and produce increased grain yield per spike, compared with two-rowed spikes with sterile lateral spikelets. Thus, far, two loci governing the row-type phenotype were isolated in barley that include Six-rowed spike1 (Vrs1) and Intermedium-C. In the present study, we isolated Sixrowed spike4 (Vrs4), a barley ortholog of the maize (*Zea mays* L.) inflorescence architecture gene RAMOSA2 (RA2). Eighteen coding mutations in barley RA2 (HvRA2) were specifically associated with lateral spikelet fertility and loss of spikelet determinacy. Expression analyses through mRNA in situ hybridization and microarray showed that Vrs4 (HvRA2) controls the row-type pathway through Vrs1 (HvHox1), a negative regulator of lateral spikelet fertility in barley. Moreover, Vrs4 may also regulate transcripts of barley SISTER OF RAMOSA3 (HvSRA), a putative trehalose-6-phosphate phosphatase involved in trehalose-6-phosphate homeostasis implicated to control spikelet determinacy. Our expression data illustrated that, although RA2 is conserved among different grass species, its down-stream target genes appear to be modified in barley and possibly other species of tribe Triticeae.

**Keywords:** Vrs4; Ra2; Barley Fertility; Barley row-type; Spikelet determinacy.

**474. AtMBP-1, an Alternative Translation Product of LOS2, affects abscisic acid Responses and is Modulated by the E3 Ubiquitin Ligase Atsap5**

Miyoung Kang, Haggag Abdelmageed, Seonghee Lee, Angelika Reichert, Kirankumar S. Mysore and Randy D. Allen

*The Plant Journal*, 76: 481-493 (2013) IF: 6.582

The LOS2 gene in *Arabidopsis* encodes an enolase with 72% amino acid sequence identity with human ENO1. In mammalian cells, the a-enolase (ENO1) gene encodes both a 48 kDa glycolytic enzyme and a 37 kDa transcriptional suppressor protein that are targeted to different cellular compartments. The tumor suppressor c-myc binding protein (MBP-1), which is alternatively translated from the second start codon of ENO1 transcripts, is preferentially localized in nuclei while a-enolase is found in the cytoplasm. We report here that an *Arabidopsis* MBP-1-like protein (AtMBP-1) is alternatively translated from full-length LOS2 transcripts using a second start codon. Like

mammalian MBP-1, this truncated form of LOS2 has little, if any, enolase activity, indicating that an intact N-terminal region of LOS2 is critical for catalysis. AtMBP-1 has a short half-life in vivo and is stabilized by the proteasome inhibitor MG132, indicating that it is degraded via the ubiquitin-dependent proteasome pathway. *Arabidopsis* plants that over-express AtMBP-1 are hypersensitive to abscisic acid (ABA) during seed germination and show defects in vegetative growth and lateral stem development. AtMBP-1 interacts directly with the E3 ubiquitin ligase AtSAP5 and co-expression of these proteins resulted in destabilization of AtMBP-1 in vivo and abolished the developmental defects associated with AtMBP-1 over-expression. Thus, AtMBP-1 is as a bona fide alternative translation product of LOS2. Accumulation of this factor is limited by ubiquitin-dependent destabilization, apparently mediated by AtSAP5.

**Keywords:** LOS2; AtMBP-1; Alternative translation; Abscisic acid signaling

**475. Two Closely Linked Tomato Hkt Coding Genes are Positional Candidates for the Major Tomato Qtl Involved in Na<sup>+</sup>/K<sup>+</sup> Homeostasis**

Maria José Asins, Irene Villalta, Mohamed M. Aly, Raquel Olías, Paz Álvarez De Morales, Raúl Huertas, Jun Li, Noelia Jaime-Pérez, Rosario Haro, Verónica Raga, Emilio A. Carbonell and Andrés Bolver

*Plant, Cell and Environment*, 36: 1171-1191 (2013) IF: 5.135

The location of major quantitative trait loci (QTL) contributing to stem and leaf [Na<sup>+</sup>] and [K<sup>+</sup>] was previously reported in chromosome 7 using two connected populations of recombinant inbred lines (RILs) of tomato. HKT1;1 and HKT1;2, two tomato Na<sup>+</sup> selective class I-HKT transporters, were found to be closely linked, where the maximum logarithm of odds (LOD) score for these QTLs located. When a chromosome 7 linkage map based on 278 single-nucleotide polymorphisms (SNPs) was used, the maximum LOD score position was only 35 kb from HKT1;1 and HKT1;2. Their expression patterns and phenotypic effects were further investigated in two near-isogenic lines (NILs): 157-14 (double homozygote for the *cheesmaniae* alleles) and 157-17 (double homozygote for the *lycopersicum* alleles). The expression pattern for the HKT1;1 and HKT1;2 alleles was complex, possibly because of differences in their promoter sequences. High salinity had very little effect on root dry and fresh weight and consequently on the plant dry weight of NIL 157-14 in comparison with 157-17. A significant difference between NILs was also found for [K<sup>+</sup>] and the [Na<sup>+</sup>]/[K<sup>+</sup>] ratio in leaf and stem but not for [Na<sup>+</sup>] arising a disagreement with the corresponding RIL population. Their association with leaf [Na<sup>+</sup>] and salt tolerance in tomato is also discussed.

**Keywords:** *Solanum cheesmaniae*; *Solanum lycopersicum*; Candidate gene analysis; HKT1-like genes; K<sup>+</sup>; Na<sup>+</sup> Concentration.

**476. Knockouts of *Physcomitrella patens* CHX1 and CHX2 Transporters Reveal High Complexity of Potassium Homeostasis**

Shady Mohamed Ossama Abdel Mottaleb Shady A. Mottaleb, Alonso Rodríguez-Navarro and Rosario Haro

*Plant and Cell Physiology*, 54 (9): 1455-1468 (2013) IF: 4.13

This study aims to increase our understanding of the functions of CHX transporters in plant cells using the model plant *Physcomitrella patens*, in which four CHX genes have been identified, PpCHX1–PpCHX4. Two of these genes, PpCHX1 and PpCHX2, are expressed at approximately the same level as the PpACT5 gene, but the other two genes show an extremely low expression. PpCHX1 and PpCHX2 restored growth of *Escherichia coli* mutants on low K<sup>+</sup>-containing media, suggesting that they mediated K<sup>+</sup> uptake that may be energized by symport with H<sup>+</sup>. In contrast, these genes suppressed the defect associated with the *kha1* mutation in *Saccharomyces cerevisiae*, which suggests that they might mediate K<sup>+</sup>/H<sup>+</sup> antiport. PpCHX1–green fluorescent protein (GFP) fusion protein transiently expressed in *P. patens* protoplasts co-localized with a Golgi marker. In similar experiments, the PpCHX2–GFP protein appeared to localize to tonoplast and plasma membrane. We constructed the Ppchx1 and Ppchx2 single mutant lines, and the Ppchx2 Pphak1 double mutant. Single mutant plants grew normally under all the conditions tested and exhibited normal K<sup>+</sup> and Rb<sup>+</sup> influxes; the Ppchx2 mutation did not increase the defect of Pphak1 plants. In long-term experiments, Ppchx2 plants showed slightly higher Rb<sup>+</sup> retention than wild-type plants, which suggests that PpCHX2 mediates the transfer of Rb<sup>+</sup> either from the vacuole to the cytosol or from the cytosol to the external medium in parallel with other transporters. The distinction between these two possibilities is technically difficult. We suggest that K<sup>+</sup> transporters of several families are involved in the pH homeostasis of organelles by mediating either K<sup>+</sup>/H<sup>+</sup> antiport or K<sup>+</sup>–H<sup>+</sup> symport.

**Keywords:** CHX Transporters; Endomembranes; Potassium fluxes.

#### 477. Rnai Based Simultaneous Silencing of All Forms of Light-Dependent NADPH: Protochlorophyllide oxidoreductase Genes Result in the Accumulation of Protochlorophyllide in Tobacco (*Nicotiana Tabacum*)

Neveen Bahaa El-Din T. Shawky

*Plant Physiology and Biochemistry*, 71: 31-36 (2013) IF: 2.775

Conversion of protochlorophyllide (Pchl<sub>id</sub>) into chlorophyllide (Chl<sub>id</sub>), a key step in chlorophyll biosynthesis, is mediated by a light-dependent NADPH:protochlorophyllide oxidoreductase (POR). POR exists in multiple isoforms that share high degree of homology. RNAi-mediated gene silencing approach was used to suppress the expression of POR genes in order to study its role in the Chl<sub>s</sub> biosynthesis in tobacco (*Nicotiana tabacum* L.). The transgenic plants were devoid of chlorophyll pigments and resembled albino plants. Northern blot analysis confirmed the degradation of POR transcripts into 21e23 bp fragments. Pigment analysis showed the accumulation of various intermediate compounds of Chl<sub>s</sub> biosynthesis pathway including Pchl<sub>id</sub>. However, no trace of chlorophyll was observed. As compared to wild type, POR-silenced plants accumulated larger (60%) amounts of Pchl<sub>id</sub> from its endogenous substrate. When leaf discs of WT and POR-silenced plants were treated with exogenous ALA both WT and POR-silenced plants accumulated large amounts of tetrapyrrolic intermediates demonstrating that Pchl<sub>id</sub> biosynthesis potential was not suppressed in POR-silenced plants. Upon illumination, WT plants photo-transformed large amounts of Pchl<sub>id</sub> to Chl<sub>id</sub>. However, POR-silenced

plants almost completely failed to do so. Results demonstrate that the antisense approaches to drop expression of individual POR isoforms have provided valuable insights into the role of distinct PORs during greening. Moreover, data illustrate that the POR is the only enzyme that can convert the Pchl<sub>id</sub> to Chl<sub>id</sub> and there is no alternate enzyme that can substitute the POR in higher plants. Thus, this investigation describes ideal mechanism for the silencing of POR isozymes in tobacco.

**Keywords:** Chlorophyll biosynthesis; Protochlorophyllide; Light-dependent NADPH:pchl<sub>id</sub> oxidoreductases (POR); Silencing; Gene silencing.

#### 478. Anatomical Structures of Vegetative and Reproductive organs of *Senna occidentalis* (Caesalpinaceae)

Mohamed Abdel Aziz Ahmed Nassar, Hassan Ramadan Hassan Ramadan and Hend Mohammad S. Ibrahim

*Turkish Journal of Botany*, 37: 542-552 (2013) IF: 1.6

The current investigation is concerned with the histological features of *Senna occidentalis* (L.) Link (coffee senna plant). The anatomical structure of different vegetative and reproductive organs was investigated weekly or fortnightly, according to the investigated organ, throughout the growing season. Organs studied included the main root, main stem (represented by shoot apex, apical, and median internodes), different foliage leaves developed on the main stem and on lateral shoots (including lamina and petiole), epidermal peel and trichomes, flower buds, fruits, and seeds. Histological features of various organs of the coffee senna plant were analysed microscopically and photomicrographed. Moreover, ultrastructural features of the seed coat were investigated by scanning electron microscope.

**Keywords:** *Senna*; Caesalpinaceae; Anatomy; Vegetative organs; Reproductive organs.

#### 479. 24-Epibrassinolide Alleviates Salt-Induced Inhibition of Productivity by Increasing Nutrients and Compatible Solutes Accumulation and Enhancing Antioxidant system in Wheat (*Triticum Aestivum* L.)

Neveen B. Talaat and Bahaa T. Shawky

*Acta Physiologia Plantarum*, 35: 729-740 (2013) IF: 1.305

Two wheat (*Triticum aestivum* L.) cultivars, Sids 1 and Giza 168, were grown under non-saline or saline conditions (4.7 and 9.4 dS m<sup>-1</sup>) and were sprayed with 0.00, 0.05 and 0.10 mg l<sup>-1</sup> 24-epibrassinolide (EBL). Salt stress markedly decreased plant productivity and N, P, and K uptake, particularly in Giza 168. A follow-up treatment with 0.1 mg l<sup>-1</sup> EBL detoxified the stress generated by salinity and considerably improved the above parameters, especially in Sids 1. Organic solutes (soluble sugars, free amino acids, proline and glycine betaine), antioxidative enzymes (superoxide dismutase, peroxidase, catalase and glutathione reductase), antioxidant molecules (glutathione and ascorbate) and Ca and Mg levels were increased under saline condition, and these increases proved to be more significant in salt-stressed plants sprayed with EBL, particularly at 0.1 mg l<sup>-1</sup> EBL with Sids 1. Sodium concentration, lipid peroxidation, hydrogen peroxide content and electrolyte leakage were increased

under salt stress and significantly decreased when 0.1 mg l<sup>-1</sup> EBL was sprayed. Clearly, EBL alleviates salt-induced inhibition of productivity by altering the physiological and biochemical properties of the plant.

**Keywords:** 24-Epibrassinolide; Wheat; Salt stress.

#### 480. Modulation of nutrient acquisition and polyamine pool in salt-stressed Wheat (*Triticum aestivum* L.) Plants inoculated with arbuscular mycorrhizal fungi

Neveen B. Talaat and Bahaa T. Shawky

*Acta Physiologiae Plantarum*, 35: 2601-2610 (2013) IF: 1.305

Two wheat (*Triticum aestivum* L.) cultivars, Sids 1 and Giza 168, were grown under non-saline or saline conditions (4.7 and 9.4 dS m<sup>-1</sup>) with and without arbuscular mycorrhizal fungi (AMF) inoculation. Salt stress considerably decreased root colonization, plant productivity and N, P, K<sup>+</sup>, Fe, Zn and Cu concentrations, while it increased Na<sup>+</sup> level, particularly in Giza 168. Mycorrhizal colonization significantly enhanced plant productivity and N, P, K<sup>+</sup>, Fe, Zn and Cu acquisition, while it diminished Na<sup>+</sup> uptake, especially in Sids 1. Salinity increased putrescine level in Giza 168, however, values of spermidine and spermine increased in Sids 1 and decreased in Giza 168. Mycorrhization changed the polyamine balance under saline conditions, an increase in putrescine level associated with low contents of spermidine and spermine in Giza 168 was observed, while Sids 1 showed a decrease in putrescine and high increase in spermidine and spermine. Moreover, mycorrhizal inoculation significantly reduced the activities of diamine oxidase and polyamine oxidase in salt-stressed wheat plants. Modulation of nutrient acquisition and polyamine pool can be one of the mechanisms used by AMF to improve wheat adaptation to saline soils. This is the first report dealing with mycorrhization effect on diamine oxidase and polyamine oxidase activities under salt stress.

**Keywords:** Arbuscular mycorrhiza; Salinity; Wheat; Productivity; Nutrient acquisition; Polyamines pool.

#### 481. Comparative Systematic Studies of *Astragalus* in Flora of Arab Republic of Egypt and Syrian Arab Republic: Seed Features and Germination

El-Sahhar, K. F., Emara, Kh. S. and Ali, W.A.

*Research Journal of Agriculture and Biological Sciences*, 9 (2): 79-88 (2013)

This paper is the first of a series of studies which aimed at comparing the differences in characters of the same species of some *Astragalus* plant species, originated from the flora of Egypt and their corresponding species in the flora of Syria, when grown under the Egyptian habitat, to evaluate the effect of variation in origin of species on plant characters. Three species were chosen for this study; namely, *Astragalus annularis* L., *A. boeticus* L. and *A. hamosus* L. The present study dealt with seed morphology, seed surface sculptures by means of Scanning Electron Microscope (SEM), anatomical characters of seed, physico-mechanical features of seeds, in addition to germination tests. Data of all the above mentioned seed characters were coded and applied in numerical analysis by using a Single Linkage Clustering technique, which represents the similarity or

dissimilarity of studied species in a form of dendrogram, which reflected that, *A. annularis* is the most influenced species by variation of habitat, as Egyptian and Syrian genotypes of it split away in two different clusters of the numerical analysis. However, both genotypes of *A. boeticus* of different origins, Egypt and Syria, are more close to each other compared with other studied species.

**Keywords:** *Astragalus*; Flora of Egypt; Flora of Syria; Germination; Habitat; seed.

#### 482. Comparative Systematic Studies of *Astragalus* in Flora of Arab Republic of Egypt and Syrian Arab Republic: Plant Morphology, SEM of Lamina Surface and SDS-Page of Proteins

El-Sahhar, K.F., Emara, Kh. S. and Ali, W.A.

*Research Journal of Agriculture and Biological Sciences*, 9 (6): 271-286 (2013)

This paper is the second of a series of studies which aimed at comparing the differences in characters of the same species of some *Astragalus* plant species, originated in the flora of Egypt and their correspondent species in the flora of Syria, when grown under the Egyptian habitat. It was intended to evaluate the effect of variation in origin of species on plant characters. Three species were chosen for this study; namely, *Astragalus annularis* Forssk; *A. boeticus* L. and *A. hamosus* L. The present study dealt first with the morphology of the vegetative growth including various characters of root, stem, and leaf lamina and petiole; second with reproductive growth; i.e., inflorescence, flower and fruit. Surface of lamina samples were studied by means of Scanning Electron Microscopy (SEM). In addition, plant proteins fractioning was carried out through SDS-PAGE. Finally, a dendrogram representing the level of similarity in which the studied species have been shared was constructed, following numerical analysis. Results obtained proved that various tested characters responded in varied manners according to their flora and habitat conditions. However, numerical phenetic analysis confirmed that *A. annularis* and *A. hamosus* split away in clusters process not count on kinship relation, but depends mainly on seed origin (flora). In the mean time, *A. boeticus* split away in two remote clusters, where that procured from flora of Egypt biased to group of Syrian origin, and the latter grouped with Egyptian cluster. This reveals the sensitivity of *A. boeticus* to variation of habitat more than the other two species.

**Keywords:** *Astragalus*; Flora of Egypt; Flora of Syria; Morphology; SEM; SDS-Page of proteins.

#### 483. Vascular Development and Transition in the Seedling of *Lupinus albus* L

Abdel-Fattah I. El-Shaarawi, Sawsan M. Abou-Taleb and Hind S. Mohamed

*Indian Streams Research Journal*, 3: 1-9 (2013)

Transverse sections made in seedling of lupine (*Lupinus albus* L.) were examined by light microscope to study the development and transition of the vascular system. Vascular transition occurred in the root. It started few centimeters below the soil surface, and completed at the basal (superior) end of the root. No rotation was observed during the transition of vascular tissues from exarch

radial to endarch collateral arrangement, but the protoxylem elements differentiated gradually on the inner side of metaxylem. Although vascular transition is completed at the base of the root, the vascular system of the hypocotyl axis showed differential structure at the different levels of the hypocotyl. Development and course of the leaf traces indicate that there is continuity between the vascular system of the hypocotyl and that of the epicotyl. Regardless the phase of transition; the fascicular cambium was established between the primary phloem and metaxylem. The development and activity of interfascicular cambium varied to some extent according to the level of seedling axis.

**Keywords:** *Lupinus albus* L; Vascular development; Transition.

#### Dept. of Agricultural Microbiology

##### 484. Diversity of Bacteria Nesting the Plant Cover of North Sinai Deserts, Egypt

Amira L. Hanna, Hanan H. Youssef, Wafaa M. Amer, Mohammed Monib, Mohammed Fayez and Nabil A. Hegazi

*Journal of Advanced Research*, 4: 13-26 (2013) IF: 3

North Sinai deserts were surveyed for the predominant plant cover and for the culturable bacteria nesting their roots and shoots. Among 43 plant species reported, 13 are perennial (e.g. *Fagonia* spp., *Pancretium* spp.) and 30 annuals (e.g. *Bromus* spp., *Erodium* spp.). Eleven species possessed rhizo-sheath, e.g. *Cyperus capitatus*, *Panicum turgidum* and *Trisetaria koelerioides*. Microbiological analyses demonstrated: the great diversity and richness of associated culturable bacteria, in particular nitrogen-fixing bacteria (diazotrophs); the majority of bacterial residents were of true and/or putative diazotrophic nature; the bacterial populations followed an increasing density gradient towards the root surfaces; sizeable populations were able to reside inside the root (endospheres) and shoot (endophyllosphere) tissues. Three hundred bacterial isolates were secured from studied spheres. The majority of nitrogen-fixing bacilli isolates belonged to *Bacillus megaterium*, *Bacillus pumilus*, *Bacillus polymyxa*, *Bacillus macerans*, *Bacillus circulans* and *Bacillus licheniformis*. The family Enterobacteriaceae represented by *Enterobacter agglomerans*, *Enterobacter sakazakii*, *Enterobacter cloacae*, *Serratia odorifera*, *Serratia liquefaciens* and *Klebsiella oxytoca*. The non-Enterobacteriaceae population was rich in *Pantoea* spp., *Agrobacterium radiobacter*, *Pseudomonas vesicularis*, *Pseudomonas putida*, *Stenotrophomonas maltophilia*, *Ochrobactrum anthropi*, *Sphingomonas paucimobilis* and *Chryseomonas luteola*. *Gluconacetobacter diazotrophicus* were reported inside root and shoot tissues of a number of tested plants. The dense bacterial populations reported speak well to the very possible significant role played by the endophytic bacterial populations in the survival, in respect of nutrition and health, of existing plants. Such groups of diazotrophs are good candidates, as bio-preparates, to support the growth of future field crops grown in deserts of north Sinai and irrigated by the water of El-Salam canal.

**Keywords:** North Sinai; Desert ecosystems; Xerophytes; Culturable bacteria; Rhizospheric microorganisms (RMOs); Diazotrophs; Rhizosphere.

#### Dept. of Agricultural Zoology and Nematology

##### 485. Potentials of Aquaculture Effluents on Nematode Management: 1- Effect of Tilapia Effluents on Two Nematode Species and Cowpea Growth

H. H. Kesba, M. A. El-Helaly, S. Abdel Ghanny and A. Suloma

*The Journal of Animal and Plant Sciences*, 23 (1): 281-289 (2013) IF: 0.638

This study was conducted to investigate the effect of tilapia effluents on infectivity, development and reproduction of *M. incognita* and *R. reniformis* on five strains of cowpea and its impact on plant growth under greenhouse conditions. Unfertilized tilapia pond with complete diet (T4) was the best treatment which significantly reduced all *M. incognita* criteria (no. of galls, embedded stages, egg masses, build up and eggs/egg mass) on cowpea strains 1, 2 & 4. Biofloc tanks (T5) was significantly efficient on cowpea strain 3. Low organic fertilized tilapia pond (T2) reduced nematode criteria on strain 5 without significant differences in build up when compared with high inorganic fertilized tilapia pond (T1) & high organic fertilized tilapia pond (T3). On the other hand, T4 significantly reduced build up of *R. reniformis* on cowpea strains 1 & 4. T5 significantly decreased reniform nematode reproduction on strains 2 & 3. However, all treatments failed to reduce nematode criteria on strain 5. In general, all treatments ameliorated cowpea growth parameters and improved plant content of NPK except on strains 1 and 5. Integrating aquaculture-agriculture system (IAA) has an additional benefit which makes the fish waste and algae productions have the potential to decrease the nematode populations and improve plant growth.

**Keywords:** Cowpea; Irrigation; *M. incognita*; *R. reniformis*; Tilapia effluents.

##### 486. Host Penetration and Emergence Patterns of the Mosquito-Parasitic Mermithids *Romanomermis Iyengari* and *Strelkovimermis Spiculatus* (Nematoda: Mermithidae)

Manar M. Sanad, Muhammad S. M. Shamseldean, Abd-Elmoneim Y. Elgindi and Randy Gaugler

*Journal of Nematology*, 45 (1): 30-38 (2013) IF: 0.3

*Romanomermis iyengari* and *Strelkovimermis spiculatus* are mermithid nematodes that parasitize mosquito larvae. We describe host penetration and emergence patterns of *Romanomermis iyengari* and *Strelkovimermis spiculatus* in laboratory exposures against *Culex pipiens pipiens* larvae. The mermithid species differed in host penetration behavior, with *R. iyengari* juveniles attaching to the host integument before assuming a rigid penetration posture at the lateral thorax (66.7%) or abdominal segments V to VIII (33.3%). *Strelkovimermis spiculatus* attached first to a host hair in a coiled posture that provided a stable base for penetration, usually through the lateral thorax (83.3%). Superparasitism was reduced by discriminating against previously infected hosts, but *R. iyengari*'s ability to avoid superparasitism declined at a higher inoculum rate. Host emergence was signaled by robust nematode movements that induced aberrant host swimming. Postparasites of *R. iyengari* usually emerged from the lateral prothorax (93.2%), whereas *S.*

spiculatus emergence was peri-anal. In superparasitized hosts, emergence was initiated by males in *R. iyengari* and females in *S. spiculatus*; emergence was otherwise nearly synchronous. Protandry was observed in *R. iyengari*. The ability of *S. spiculatus* to sustain an optimal sex ratio suggested superior self-regulation. Mermithid penetration and emergence behaviors and sites may be supplementary clues for identification. Species differences could be useful in developing production and release strategies.

**Keywords:** *Culex pipiens pipiens*; Insect-parasitic; Host emergence; Host penetration; Mermithid; Mermithidae; Mosquito; Nematode behavior; *Romanomermis iyengari*; *Strelkovimermis spiculatus*.

#### Dept. of Agronomy

### 487. Effect of Air Injection under Subsurface Drip Irrigation on Yield and Water Use Efficiency of Corn in a Sandy Clay Loam Soil

Mohamed Abuarab, Ehab Mostafa and Mohamed Ibrahim

*Journal of Advanced Research*, 4: 493-499 (2013) IF: 3

Subsurface drip irrigation (SDI) can substantially reduce the amount of irrigation water needed for corn production. However, corn yields need to be improved to offset the initial cost of drip installation. Air-injection is at least potentially applicable to the (SDI) system. However, the vertical stream of emitted air moving above the emitter outlet directly toward the surface creates a chimney effect, which should be avoided, and to ensure that there are adequate oxygen for root respiration. A field study was conducted in 2010 and 2011, to evaluate the effect of air-injection into the irrigation stream in SDI on the performance of corn. Experimental treatments were drip irrigation (DI), SDI, and SDI with air injection. The leaf area per plant with air injected was 1.477 and 1.0045 times greater in the aerated treatment than in DI and SDI, respectively. Grain filling was faster, and terminated earlier under air-injected drip system, than in DI. Root distribution, stem diameter, plant height and number of grains per plant were noticed to be higher under air injection than DI and SDI. Air injection had the highest water use efficiency (WUE) and irrigation water use efficiency (IWUE) in both growing seasons; with values of 1.442 and 1.096 in 2010 and 1.463 and 1.112 in 2011 for WUE and IWUE respectively. In comparison with DI and SDI, the air injection treatment achieved a significantly higher productivity through the two seasons. Yield increases due to air injection were 37.78% and 12.27% greater in 2010 and 38.46% and 12.5% in 2011 compared to the DI and SDI treatments, respectively. Data from this study indicate that corn yield can be improved under SDI if the drip water is aerated.

**Keywords:** Drip irrigation; Subsurface drip irrigation; Air injection; Corn; Wue.

### 488. Air Velocity Measurements Using Ultrasonic Anemometers in the Animal Zone of A Naturally Ventilated Dairy Barn

Merike Fiedler, Werner Berg, Christian Ammon, Christiane Loebstin, Peter Sanftleben, Mohamed Samer, Kristina von Bobrutski, Alaa Kiwan and Chayan K. Saha

*Biosystems Engineering*, 116 (3): 276-285 (2013) IF: 1.357

Air velocity measurements were collected from one horizontal plane across the entire animal occupied zone (AOZ) floor area of a dairy barn. Data recorded from the undisturbed approaching airflow (25° deviation from normal to the sidewall of the building) and an approach flow disturbed by obstacles (surrounding buildings) in front of the barn (at an incident angle of 20° from normal to the building facade) were analysed. The 96.2 m long, 34.2 m wide and 10.7 m high (ridge) building had open sidewalls, wind protecting nets and large openings in both gable walls. The barn, with a loose housing system with freestalls, accommodated 364 dairy cows. The outside temperatures were between 10 and 20 °C, and the outside wind speeds were between 0.7 and 3.9 m s<sup>-1</sup>. The air speed in the AOZ varied from 0.2 to 1.4 m s<sup>-1</sup>. Differences between single areas inside the barn were large and led to different climatic conditions for different animal groups. The undisturbed approaching airflow (at an incident angle of 25° from normal) resulted in a heterogeneous airflow pattern inside the barn with no defined outlet. This airflow pattern was probably influenced by the surrounding buildings on the leeward. In contrast, the disturbed approaching airflow (with obstacles at the windward side) resulted in a homogeneous flow pattern with a lower airflow. A linear model showed that only the interaction between the outside wind speed and the outside wind direction significantly influenced the inside air velocity. Long term measurements at or above the AOZ are needed to complement existing data.

**Keywords:** Air velocity; Ultrasonic anemometers; Animal zone; Natural ventilation; Dairy barn.

### 489. Emissions Inventory of Greenhouse Gases and Ammonia from Livestock Housing and Manure Management

Mohamed Samer

*Agricultural Engineering International: Cigr Journal*, 15 (3): 29-54 (2013)

An emission inventory is a database on the amount of pollutants released into the atmosphere. The anthropogenic emissions of air pollutants and greenhouse gases are detrimental to the environment and the ecosystems. Therefore, reducing emissions is crucial. One key issue is to inventory these emissions, and consequently databases on anthropogenic emissions will be available for making decisions on implementing suitable mitigation strategies. Such investigations aim at developing national emissions inventory for domestic livestock and to identify possible abatement techniques in order to reduce these emissions. Therefore, the objectives of this study are to introduce and define the emissions inventories, review the emission inventory guides, introduce the relation between the emissions inventory and livestock buildings and manure stores and the relevant emission factors and algorithms, review the tools for processing the emissions inventories (e.g. models, software), show the evaluation and improvement methods of emissions inventories, review the emissions abatement techniques, and present examples and paradigms of available national emissions inventories for several countries.

**Keywords:** Emissions inventory; Greenhouse gases; Methane; Nitrous oxide; Ammonia; particulate matter; Livestock buildings; Manure; Emission factors; Emissions abatement techniques.



#### **490. Software for Planning Loose Yards and Designing Concrete Constructions for Dairy Farms in Arid and Semi-Arid Zones**

Mohamed Samer

*Emirates Journal of Food and Agriculture*, 25: 238-249 (2013)

To plan and design dairy housing, several calculations should be made; this requires time and efforts, with the possibility of making mistakes. The objectives of this paper are to develop a tool to assist the designers in planning and designing dairy housing in arid and semi-arid zones, to save time and efforts, and to provide a new design model. Two mathematical models were developed to plan and design corral systems and the required concrete constructions. Subsequently, an electronic spark map (decision tree) was developed for each mathematical model, and then the mathematical models were integrated into the electronic spark maps. Afterwards, C# (C Sharp) programming language was used to develop the software by integrating the electronic spark maps, and making the user interface. The developed software is able to plan and design the housing system (corrals system), specify corrals and house dimensions, and compute the required amounts of construction materials (iron rods, cement, sand, and gravels) to build the required concrete base. Furthermore, it calculates the capital investment and the fixed, variable, and total costs of the construction. Data of 6 dairy farms were used to validate the model, and to evaluate the software. The differences between actual and calculated values were determined, and the standard deviations were calculated. The coefficients of variation (COVs) range between 3% and 7%.

**Keywords:** Arid zones, Dairy farms; Loose yards, Mathematical modeling; Precision livestock farming.

#### **491. Towards the Implementation of the Green Building Concept in Agricultural Buildings: A Literature Review**

Mohamed Samer

*Agricultural Engineering International: Cigr Journal*, 15 (2): 25-46 (2013)

The "Green Building" is an interdisciplinary theme, where the green building concept includes a multitude of elements, components and procedures which diverge to several subtopics that intertwined to form the green building concept. Generally, the green building is considered to be an environmental component, as the green building materials are manufactured from local eco-sources, i.e. environmentally friendly materials, which are then used to make an eco-construction subject to an eco-design that provides a healthy habitat built on the cultural and architectural heritage in construction while ensuring conservation of natural resources. This ensures disassembling the building components and materials, after a determined building lifetime, to environmentally friendly materials that can be either re-used or recycled. During their lifecycle, the green buildings minimize the use of resources (energy and water); reduce the harmful impact on the ecology, and provide better indoor environment. Green buildings afford a high level of environmental, economic, and engineering performance. These include energy efficiency and conservation, improved indoor air quality, resource and material efficiency, and occupant's health and productivity. This study

focuses on defining green buildings and elaborating their interaction with the environment, energy, and indoor air quality and ventilation. Furthermore, the present study investigates the green building materials (e.g. biocement, eco-cement and green concrete), green designs, green roofs, and green technologies. Additionally, the present study highlights the green buildings rating systems, the economics of green buildings, and the challenges that face the implementation. Eventually, the interdependency between the green buildings and agriculture has been discussed.

**Keywords:** Green building; Agricultural buildings; Biocement; Eco-cement; Green concrete; Green roofs; Low-energy building; Zero-carbon building; Eco-construction.

#### **Dept. of Animal Production**

#### **492. RNA Deep Sequencing Reveals Novel Candidate Genes and Polymorphisms in Boar Testis and Liver Tissues with Divergent Androstenone Levels**

Asep Gunawan, Sudeep Sahadevan, Christiane Neuhoﬀ, Christine Große-Brinkhaus, Ahmed Gad, Luc Frieden, Dawit Tesfaye, Ernst Tholen, Christian Looft, Muhammad Jasim Uddin, Karl Schellander and Mehmet Ulas Cinar

*Plos One*, 8: 1-15 (2013) IF: 3.73

Boar taint is an unpleasant smell and taste of pork meat derived from some entire male pigs. The main causes of boar taint are the two compounds androstenone (5 $\alpha$ -androst-16-en-3-one) and skatole (3-methylindole). It is crucial to understand the genetic mechanism of boar taint to select pigs for lower androstenone levels and thus reduce boar taint.

The aim of the present study was to investigate transcriptome differences in boar testis and liver tissues with divergent androstenone levels using RNA deep sequencing (RNA-Seq). The total number of reads produced for each testis and liver sample ranged from 13,221,550 to 33,206,723 and 12,755,487 to 46,050,468, respectively.

In testis samples 46 genes were differentially regulated whereas 25 genes showed differential expression in the liver. The fold change values ranged from -4.68 to 2.90 in testis samples and -2.86 to 3.89 in liver samples. Differentially regulated genes in high androstenone testis and liver samples were enriched in metabolic processes such as lipid metabolism, small molecule biochemistry and molecular transport.

This study provides evidence for transcriptome profile and gene polymorphisms of boars with divergent androstenone level using RNA-Seq technology. Digital gene expression analysis identified candidate genes in flavin monooxygenase family, cytochrome P450 family and hydroxysteroid dehydrogenase family. Moreover, polymorphism and association analysis revealed mutation in IRG6, MX1, IFIT2, CYP7A1, FMO5 and KRT18 genes could be potential candidate markers for androstenone levels in boars. Further studies are required for proving the role of candidate genes to be used in genomic selection against boar taint in pig breeding programs.

**Keywords:** RNA deep sequencing; Androstenone; Boar.

### 493. Embryo Gene Expression in Response to Maternal Supplementation with Glycogenic Precursors in the Rabbit

M. Arias-Álvarez, R.M. García-García, P.L. Lorenzo, A. Gutiérrez-Adán, O.G. Sakr, A. González-Bulnes and P.G. Rebollar

*Animal Reproduction Science*, 142: 173-182 (2013) IF: 1.897

Disturbing maternal metabolism during the first pregnancy and postpartum period is associated with sub fertility in rabbit does. Nutritional strategies can be used during those periods and its effects to improve reproductive management may affect periconceptional events and early embryo development. Our goal was to elucidate if treatment with a glycogenic precursor such as propylene glycol (PG) could affect the maternal metabolic profile, follicular and oocyte quality and gene expression patterns in early embryos. Rabbit does were supplemented with 2.5% (v/v) PG from either mid-pregnancy and for 25 days of lactation (PG-GL group); only during lactation (PG-L group); or were not treated (control group). Ovarian parameters and embryos were studied at the end of treatment. At parturition serum non-esterified fatty acid concentrations increased whilst insulin decreased in all groups. Maternal feed intake was reduced in PG-supplemented does but glycaemia was maintained during the experimental period. When PG was suppressed, blood insulin immediately increased in PG-groups, but no differences in follicular population, follicular atresia, and nuclear and cytoplasmic oocyte maturation were observed compared with non-treated animals. Although embryo development was similar among groups, mRNA of SLC2A4, INSR, IGF1R, PLAC8, COX2 and IGF2R were up regulated in the blastocysts of PG-GL does. Transcripts of SOD1 were lower in PG-L embryos; but NOS3 and TP53 were similar among groups. PG did not affect the maternal metabolic profile during the postpartum period, nor the ovarian response or number of embryos developed. Nonetheless, PG supplied from mid-pregnancy modified mRNA transcripts involved in some important developmental and metabolic events in the blastocysts of those females. More experiments are needed to elucidate the physiological consequence of these results.

**Keywords:** Propylene glycol; Follicle; Oocyte; Maternal-embryo interaction; Rabbit.

### 494. Dietary L-Arginine Supplementation Reduces Abdominal Fat Content by Modulating Lipid Metabolism in Broiler Chickens

A. M. Fouad, H. K. El-Senousey, X. J. Yang and J. H. Yao

*Animal*, 7: 1239-1245 (2013) IF: 1.648

This study investigated the effects of different levels of dietary L-arginine (L-Arg) supplementation on the abdominal fat pad, circulating lipids, hepatic fatty acid synthase (FAS) gene expression, gene expression related to fatty acid  $\beta$ -oxidation, and the performance of broiler chickens. We tested whether the dietary L-Arg levels affected the expression of genes related to lipid metabolism in order to reduce body fat deposition. A total of 192 broiler chickens (Cobb 500) aged 21 days with an average BW of 920 g were randomly assigned to four groups (six broilers per replicate and eight replicates per treatment). The control group was fed a basal diet, whereas the treatment groups were fed basal diets supplemented with 0.25%, 0.50%, or 1.00%

L-Arg for 3 weeks. The average daily feed intake, average daily gain and feed: gain ratio were not affected by the dietary L-Arg levels. However, chickens supplemented with L-Arg had lower abdominal fat content, plasma triglyceride (TG), total cholesterol (TC) concentrations, hepatic FAS mRNA expression and increased heart carnitine palmitoyl transferase 1 (CPT1) and 3-hydroxyacyl-CoA dehydrogenase (3HADH) mRNA expression. These findings suggest that the addition of 0.25% L-Arg may reduce the plasma TC concentration by decreasing hepatic 3-hydroxy-3-methylglutaryl-CoA reductase mRNA expression. This may lower the plasma TG and abdominal fat content by suppressing hepatic FAS mRNA expression and enhancing CPT1 and 3HADH (genes related to fatty acid  $\beta$ -oxidation) mRNA expression in the hearts of broiler chickens.

**Keywords:** L-Arginine; Chickens; Fatty acid  $\beta$ -oxidation; Fatty acid synthase.

### 495. In Vitro Development Rate of Preimplantation Rabbit Embryos Cultured with Different Levels of Melatonin

Gamal Mohamed Kamel Mehaisen and Ayman Moustafa Saeed

*Zygote*, First View Article: 1-5 (2013) IF: 1.5

This study aimed to investigate the effect of melatonin supplementation at different levels in culture medium on embryo development in rabbits. Embryos of 2–4 cells, 8–16 cells and morula stages were recovered from nulliparous Red Baladi rabbit does by laparotomy technique 24, 48 and 72 h post-insemination, respectively. Normal embryos from each stage were cultured to hatched blastocyst stages in either control culture medium (TCM-199 + 20% fetal bovine serum) or control supplemented with melatonin at  $10^{-3}$  M,  $10^{-6}$  M or  $10^{-9}$  M. No effect of melatonin was found on development of embryos recovered at 24 h post-insemination. The high level of melatonin at  $10^{-3}$  M adversely affected the in vitro development rates of embryos recovered at 48 h post-insemination (52 versus 86, 87 and 80% blastocyst rate; 28 versus 66, 78 and 59% hatchability rate for  $10^{-3}$  M versus  $10^{-9}$  M,  $10^{-6}$  M and control, respectively,  $P < 0.05$ ). At the morula stage, melatonin at  $10^{-3}$  M significantly increased the in vitro development of embryos (92% for  $10^{-3}$  M versus 76% for control,  $P < 0.05$ ), while the hatchability rate of these embryos was not improved by melatonin (16–30% versus 52% for melatonin groups versus control,  $P < 0.05$ ). Results show that a moderate level of melatonin ( $10^{-6}$  M) may improve the development and hatchability rates of preimplantation rabbit embryos. The addition of melatonin at a  $10^{-3}$  M concentration enhances the development of rabbit morulae but may negatively affect the development of earlier embryos. More studies are needed to optimize the use of melatonin in in vitro embryo culture in rabbits.

**Keywords:** Embryos; In vitro development; Melatonin; Rabbits.

### 496. Effect of Bovine Ovarian Tissue Vitrification on the Structural Preservation of Antral Follicles

MS Faheem, I Carvalhais, E Baron and F Moreira da Silva

*Reproduction in Domestic Animals*, 48: 774-780 (2013) IF: 1.392

This study was performed to evaluate the structural preservation of antral follicles after bovine ovarian tissue vitrification using histological analysis. Ovaries ( $n = 30$ ) of slaughtered cows were

cut into small fragments using a scalpel blade, and the ovarian tissues were randomly assigned to vitrification using 15% dimethyl sulphoxide (DMSO) and 15% ethylene glycol (EG) and fresh tissues (control) groups. For histological evaluations, fresh and post-thawing ovarian tissues were immediately fixed, serially sectioned into 5- $\mu$ m sections and stained with haematoxylin and eosin (H&E).

Nine serial sections per fragment were subjected for morphological assessment. The diameter of the antral follicles was determined and classified into four groups: 1 (1 mm), 2 (>1–2 mm), 3 (>2–3 mm) and 4 (>3–4 mm). Then, follicular morphology was evaluated in relation to atresia and categorized into seven grades: Grade A (healthy follicle); Grades B, C and D (early atresia); Grades E and F (moderate atresia); and Grade G (advanced atresia). The results revealed that small diameters of antral follicles (1 and 2 mm) were more susceptible for cryoinjury. The normal follicular morphology (Grade A) was not affected by vitrification throughout follicle diameters. Nevertheless, some damage features were monitored after vitrification. In conclusion, the morphological structure of bovine antral follicles could be successfully preserved by ovarian tissue vitrification.

**Keywords:** Vitrification of bovine ovarian tissue.

#### 497. Meat and Bone Meal as a Potential Source of Phosphorus in Plant-Protein-Based Diets for Nile Tilapia (*Oreochromis Niloticus*)

Ashraf Suloma, Rania S. Mabroke and Ehab R. El-Haroun

*Aquaculture International*, 21: 375-385 (2013) IF: 1.037

A growth trial was conducted to evaluate meat and bone meal (MBM) as a source of Phosphorus (P) for Nile tilapia fed with plant-based diets on growth, and the efficiency of P utilization. Four isonitrogenous and isoenergetic diets were formulated. A plant-based diet, deficient in P (0.45 % diet, no P added), was used as the basal diet.

Three levels of MBM were substituted for cornstarch in the base diet to produce experimental diets containing MBM<sub>0.56</sub>, MBM<sub>0.67</sub>, or MBM<sub>0.78</sub>% P. These diets were fed (to apparent satiation) to Nile tilapia (initial body weight = 1.53  $\pm$  0.01 g) for eight weeks. Weight gain (WG), specific growth rate (SGR), feed conversion ratio (FCR, feed:gain), whole-body P concentration (WBPC), protein retention (PR), and retained phosphorus (RP) increased significantly ( $P \leq 0.05$ ), with the increasing dietary P levels coming from MBM. Diets containing MBM<sub>0.78</sub> produced significantly greater WG, SGR, WBPC, PR, and RP compared to other experimental diets ( $P \leq 0.05$ ). The linear regression analysis revealed a positive correlation between the WG, WBPC, RP, and dietary P levels coming from MBM of Nile tilapia. These results indicate that MBM has an additional value as a source of P and can serve as a potential source of supplemental P for Nile tilapia fed plant-protein-based diets.

**Keywords:** Meat; Bone meal; Phosphorus; Growth performance; Retained phosphorus; Nile tilapia.

#### 498. The Effect of Stocking Different Ratios of Nile Tilapia *Oreochromis Niloticus*, Striped Mullet *Mugil Cephalus*, and Thinlip Grey Mullet *Liza Ramada* in Polyculture Ponds on Biomass Yield, Feed Efficiency and Production Economics

Al-Azab Tahoun, Ashraf Suloma, Yasser Hammouda, Hanan Abo-State and Ehab EL-Haroun

*North American J. of Aquaculture*, 75: 548-555 (2013) IF: 0.755

To evaluate the effect of stocking different ratios of Nile tilapia *Oreochromis niloticus* with stripped mullet *Mugil cephalus* and thin-lipped mullet *Liza ramada* on production characteristics and economic returns at brackish water ponds, a 180-d trial was done to evaluate the effect of stocking different ratios of Nile Tilapia *Oreochromis niloticus*, Striped Mullet *Mugil cephalus*, and Thinlip Grey Mullet *Liza ramada* on production and economic return in brackish-water ponds. The trial was conducted in twelve 3,000-m<sup>2</sup> earthen ponds with four treatments (3 ponds/treatment): Nile Tilapia alone (100% Nile Tilapia, monoculture group [MG]); 75% Nile Tilapia and 25% Thinlip Grey Mullet (polyculture group 1 [PG1]); 75% Nile Tilapia, 12.5% Thinlip Grey Mullet, and 12.5% Striped Mullet (PG2); and 75% Nile Tilapia and 25% Striped Mullet (PG3). Fish were fed a commercial diet containing 25% crude protein twice per day. The efficiency of feed utilization was determined in terms of feed conversion ratio (FCR; feed intake/weight gain). Polyculture group 3 had the best FCR, whereas the FCR results did not differ significantly among the MG, PG1, and PG2 treatments. In addition, PG3 had the highest total yield (3,350.3 kg/pond<sup>-1</sup>), followed in descending order by PG2 (3,234.4 kg/pond<sup>-1</sup>), PG1 (3,078.4 kg/pond<sup>-1</sup>), and MG (2,856.3 kg/pond<sup>-1</sup>). The PG3 treatment achieved the highest net financial return, followed by PG2, PG1, and MG. This study indicates that tilapia-mullet polyculture may improve the efficiency with which natural food resources are used within the system, resulting in better environmental quality, system sustainability, feed utilization, and net financial return.

**Keywords:** Nutrition; Culture; Production economics; Feed utilization efficiency; Polyculture; Nile tilapia; Mullet.

#### 499. Dietary Alpha Lipoic Acid Improves Body Composition, Meat Quality and Decreases Collagen Content in Muscle of Broiler Chickens

H. K. El-Senousey, A. M. Fouad, J. H. Yao, Z. G. Zhang and Q. W. Shen

*Asian-Australasian Journal of Animal Sciences*, 26 (3): 394-400 (2013) IF: 0.643

A total of 192 broiler chicks were used to evaluate the influence of dietary  $\alpha$ -lipoic acid (ALA) on growth performance, carcass characteristics and meat quality of broiler chickens with the purpose of developing a strategy to prevent the occurrence of pale, soft, and exudative (PSE) meat and to improve the meat quality of broilers. At 22 d of age, birds were allocated to 4 ALA treatments (0, 400, 800, and 1200 ppm). The results showed that dietary ALA significantly decreased average feed intake (AFI), average daily gain (ADG), final live body weight (BW) and carcass weight ( $p < 0.05$ ), while no difference in feed conversion ratio (FCR) was detected among chickens fed with and without ALA. Abdominal fat weight significantly decreased ( $p < 0.05$ ) for

broilers fed 800 and 1200 ppmALA. However when calculated as the percentage of carcass weight there was no significant difference between control and ALAtreatments. Meat quality measurements showed that dietary ALA regulated postmortem glycolysis and improved meat quality as evidenced by increased muscle pH and decreased drip loss of meat ( $p<0.05$ ). Although ALA did not change the tenderness of meat as indicated by meat shear force, dietary ALA decreased collagen content and mRNA expression of COL3A1 gene ( $p<0.05$ ). In conclusion, the results indicate that dietary ALA may contribute to the improvement of meat quality in broilers

**Keywords:** Broiler chickens; A-Lipoic acid; Pse meat; Col3a1 gene.

### 500. Evaluation of Meat and Bone Meal and Mono-Sodium Phosphate as Supplemental Dietary Phosphorus Sources for Broodstock Nile Tilapia (*Oreochromis Niloticus*) Under the Conditions of Hapa-in- Pond System

Rania S. Mabroke, Azab M. Tahoun, Ashraf Suloma and Ehab R. El-Haroun

*Turkish Journal of Fisheries and Aquatic Sciences*, 13: 11-18 (2013) IF: 0.591

An experiment was conducted to evaluate if phosphorus (P) supplement is required in Nile tilapia *Oreochromis niloticus* broodstock diet under hapa-in-pond system. Seven isonitrogenous (33% crude protein), isocaloric (4400 kcal kg<sup>-1</sup>) diets were formulated. A corn-soybean meal based diet, deficient in P, was used as the basal diet. Three levels of meat and bone meal (MBM), and mono-sodium phosphate (MSP) were substituted for corn-starch in the basal diet to produce experimental diets containing 0.56, 0.67, or 0.78% P. Males and females with mean body weights of (270±1.52 g) and (250±1.17 g), respectively, were stocked at a density of 4 fish m<sup>-1</sup>, (8 fish hapa-1) with a male: female ratio of 1:3. Irrespective of P source, it was observed that, increasing P level significantly ( $P=0.05$ ) increased broodstock fecundity. Spawning performance and egg weight were not significantly affected by dietary P source. However, dietary MBM increased the absolute fecundity and total egg production ( $P=0.05$ ) compared to the MSP diets. While, broodstock fed MSP diets showed the highest egg weight. This result revealed that Nile tilapia broodfish reared in the green water under hapa-in-pond system require a source of dietary P for optimum spawning performance.

**Keywords:** Phosphorus; Nile tilapia broodstock; Hapa-in pond; Reproductive performance.

### 501. Development of Transgenic Chickens by Sperm-mediated gene transfer

Essam A. El-Gendy, Marwa M. Ahmed and Shoukry M. El-Tantawy

*African Journal of Biotechnology*, 12 (19): 2755-2763 (2013)

An experiment was carried out to develop transgenic chickens using sperm incubated with exogenousDNA. Two random bred lines of chickens were used as parental flocks, and the plasmid pUC18 was used as the exogene. Lipofectin was also used to facilitate the sperm cell uptake of the plasmid. Hens were

inseminated with the semen that was subjected to different treatments and their eggs were hatched. Polymerase chain reaction (PCR) was performed on spermatozoa and blood genomes of the parental flocks and on blood genomes of the progeny. The plasmid DNA was recognized in spermatozoa of both lines in most of the treatments with different amplification rates. However, plasmidDNA was highly fused into the sperm cells when it was introduced in a complex with lipofectin. Also, the plasmid DNA band was highly amplified in the progeny which resulted from sperm cells incubated with the plasmid and lipofectin at 5% concentration. The results reveal the success of the development of F1 chickens by sperm-mediated gene transfer (SMGT). The positively detected SMGT-derived offspring formed 40.0 to 50.0% of the F1 generation.

**Keywords:** Rooster spermatozoa; Lipofectin; Sperm-mediated gene transfer-derived offspring; Sperm-mediated.

### 502. Evaluation of Olive and Palm Byproducts in Feeding Camels

Adel Eid Mohamed Mahmoud and H. M. El-Bana

*Pakistan Journal of Nutrition*, 12 (9): 879-885 (2013)

Metabolism trials were carried out using four mature males of Sudanese camels; *Camelus dromedaries* to evaluate the nutritive value of date stone (DS) and olive cake (OC), palm leaves (PL) and barley grains (BG) or their mixture. Results indicated that barley grains showed significantly ( $p<0.05$ ) higher digestibility and nutritive value in all nutrients except for EE and ADF compared with either olive cake or date stone. In addition, DS showed better digestibility in all nutrients compared with OC except for EE digestibility. The ration contained BG plus DS recorded the highest digestibility for DM, OM, CP, CF and NFE. While, the ration contained BG plus OC recorded higher digestibility for NDF and ADF. No significant differences were detected in dry matter intake expressed as DMI g/W<sup>0.75</sup> by camels fed different either tested feeds or rations. The water intake increased with animals fed DS being 8.42 L compared with BG and OC being 7.58 and 6.92 L, respectively. Also, results showed that animals consumed the ration contained BG plus DS recorded the highest water intake being 8.33 L. Feeding on BG led up to significant ( $p<0.05$ ) decrease in pH values compared with other feeds after 3 and 5 h. No significant differences in ammonia nitrogen concentration at 5 h post feeding with all feeds. The BG plus DS mixture gave the lowest concentration of rumen ammonia content at the three times. While, BG with PL mixture showed the highest value of rumen ammonia content at the three times. It could be concluded that date stone and olive cake used to feed camel as substitution of barley grains without any adverse effect.

**Keywords:** Olive cake, Date stone; Palm leaves; Camels.

### 503. Influence of Dietary Enzymes Prepared at Ensiling (Zado®) From Hatch to 42 Days of Age on Productivity, Slaughter Traits and Blood Constituents in Broiler Chickens

Hosam Mohamed Safaa Mohamed Ali

*International Journal of Poultry Science*, 12 (9): 529-537 (2013)

480 Cobb-500 broiler chicks at one-day old were used to study the effects of exogenous xylanases, cellulases, protease and a-

amylase enzyme preparations at ensiling (ZADO®) on the productive performance, slaughter traits and blood metabolites. Chicks were divided randomly into 4 treatments (broiler basal diets supplemented with 0, 2, 4 and 6‰ with ZADO®) and housed on deep litter at an open house system under commercial conditions. Each treatment replicated 4 times (30 chicks per replicate). Basal diet contained 23.1% CP and 3,103 kcal AME/kg for the starter diet (0–21 d) and 20.0% CP and 3,207 kcal AME/kg for the finisher diet (21–42 d). Results indicated that broiler productivity improved in response to dietary 4 or 6‰ ZADO®. Feed conversion ratio was 1.948, 1.903, 1.758 and 1.678 for birds fed diet supplemented with 0, 2, 4 and 6‰ ZADO® ( $P=0.0007$ ), respectively. In addition, birds fed diet supplemented with 6‰ ZADO® recorded higher dressing and immune organs relative weights at 42 days of age than other treatments ( $P<0.05$ ). Moreover, enzyme supplementation increased significantly plasma total protein ( $P=0.0040$ ) and globulin ( $P=0.0131$ ) at 42 days of age. Also, dietary 6‰ ZADO® decreased plasma cholesterol ( $P=0.0466$ ) and increased HDL:Total-cholesterol ratio ( $P=0.0040$ ). It could be concluded that ZADO® supplementation to broiler diets improved broiler productivity and might improve immunity. Moreover, dietary 6‰ ZADO® has a favor effects on lipid metabolism. It could be recommended from this study to supplement 4‰ or more of ZADO® to broiler diets up to 42 days of age.

**Keywords:** ZADO® enzyme complex; Broiler performance; Slaughter traits; Blood biochemical characteristics.

#### 504. Influence of Egg Storage Time on Egg Quality, Hatchability and Chick Quality Traits of Commercial and Egyptian Local Broiler Breeders

Safaa H.M., Sobhy H.N. and Elsemary M.S.A.

*Australian Journal of Basic and Applied Sciences*, 7 (13): 154-163 (2013)

1,680 eggs were used to investigate the effect of egg storage time (EST) on egg quality, hatchability and chick quality traits of Hubbard (HU), Cairo B-2 (B2) and Fayoumi (FA) broiler breeders (48 wk of age). The HU are commercial broiler breeders, B2 is a new Egyptian broiler cross-line between Arbor Acres males and Egyptian native White Baladi females in the 8th generation and FA is an Egyptian native breed. There were 12 groups (4 replicates per group) arranged factorially with 3 broiler breeders (HU, B2 and FA) and 4 ESTs (0, 3, 7 and 10 d). Fertility rates were 94.6, 89.2, and 84.8% for HU, B2, and FA, respectively. No interaction effects were detected for all traits except for Haugh units that were in between FA's eggs values (the highest) and B2's eggs values (the lowest) for all ESTs except for 10 d that, the values of Haugh units decreased faster in HU's eggs than other breeders' ones. Results indicated that HU fresh egg and chick weights (71.8 and 46.6 g) were higher than FA (52.1 and 33.4 g) and B2 (67.1 and 43.4 g) were intermediate, respectively ( $P<0.0001$ ). The same trend was observed in hatchability (88.5 vs. 82.3 vs. 74.2%) for HU, B2 and FA, respectively. Increasing EST to 7 or 10 d negatively ( $P<0.0001$ ) affected egg weight (63.8, 63.0, 61.7 and 60.9 g), hatchability rate (84.2, 83.3, 80.3 and 78.9%) and chick weight (42.2, 41.6, 40.6 and 40.0 g). However, egg shape index, yolk color, shell thickness, clear eggs, piping eggs, embryonic mortality, mortality rate at hatch, percentage of culled chicks at hatch and chick navel quality were not affected by increasing EST up to 10 d. To conclude, HU, B2 and FA

breeds were different in egg weights, egg Haugh units, yolk index, yolk color, shell thickness, fertility, hatchability, late embryonic mortality (19-21 d of incubation), one-d-old chick weights and chicken mortality rates at hatch. Also, EST for 7 d or more was not recommended for these breeds.

**Keywords:** Breed; Egg storage time; Egg quality; Hatchability; Chick quality.

#### 505. Response of Growing Bulls Fed Ration Containing Different Levels of Citrus Pulp

A.M. Abdel Gawad, A.E.M. Mahmoud and Y.H.Al Slibi

*World Applied Sciences Journ*, 28 (10): 1475-1480 (2013)

**The objective** of this study was to assess the compared between corn silage and citrus pulp silage in two levels on nutrients digestibility, growth performance and blood metabolites of beef cattle. Thirty male, crossbred bulls (Friesian x Baladi) averaged 235 kg live body weight, 14-15 months old were divided into 3 groups of 10 animals in each according to live body weight. Animals in the control group or ration C) were fed 30% corn silage plus 70% concentrate feed mixture (CFM), while, the experimental animals were fed T1) 30% citrus pulp silage plus 70% CFM and T2) 45% citrus pulp silage plus 55% CFM. The experiment lasted for 120 days.

**Results** indicated that no significant ( $p>0.05$ ) differences observed among experimental groups in dry matter (DM), organic matter (OM), crude protein (CP) nitrogen free extract (NFE), acid detergent fiber (ADF), cellulose and hemicelluloses digestibilities. Crude fiber (CF) digestibility was significantly ( $p<0.05$ ) increase for bulls fed control rations when compared with those fed the T1 and T2. Moreover, there were significantly ( $p<0.05$ ) different between T1 and T2 rations. Ether extract digestibility was significantly ( $p<0.05$ ) among all the experimental rations. The highest value was observed for bulls fed control ration then followed by T1 and T2. The corresponding values were 84.02, 78.48 and 71.11%, respectively. Neutral detergent fiber digestibility was significantly ( $p<0.05$ ) higher for bulls fed control ration than those fed T1 and T2. Bulls fed control and T1 rations recorded significant ( $p<0.05$ ) increase of TDN compared to those fed T2 rations. The corresponding values were 73.14, 72.56 and 68.61%, respectively. Digestible crude protein was significantly ( $p<0.05$ ) increase for bulls fed T1 compared with the T2, however there was insignificantly ( $p>0.05$ ) differences with those fed the T2 ration. Dry matter intake (DMI) was significantly ( $p<0.05$ ) difference among the different experimental rations. Data indicated that bulls fed T2 recorded the lowest dry matter intake. Insignificant ( $p>0.05$ ) differences in average daily gain (ADG) among treatments were detected. The highest average daily gain had been recorded with bulls fed T1, while the lowest average daily gain was recorded with bulls fed T2. The values were 1.15 and 1.02 Kg respectively. Blood parameters such as hemoglobin, hematocrit, total protein, urea, creatinine, triglycerides and cholesterol, did not record any significant differences among experimental animals. Meanwhile, cholesterol concentration was significantly ( $p<0.05$ ) increase for bulls fed T1 compared with those fed control group, with insignificant ( $p>0.05$ ) difference for T2.

**In conclusion**, corn silage could be replaced by citrus silage in beef cattle rations without any adverse effects on nutrients digestibility, blood parameters and growth performance.

**Keywords:** Bulls citrus pulp; Silage; Intake; Performance growth.



### 506. Agronomical Evaluation of Six Soybean Cultivars Using Correlation and Regression Analysis Under Different Irrigation Regime Conditions

Ashraf A. Abd El-Mohsen, Gamalat O. Mahmoud and Sayed A. Safina

*Journal of Plant Breeding and Crop Science*, 5 (5): 91-102 (2013)

Two field experiments were conducted during summer seasons of 2011 and 2012 to study the effect of irrigation regimes at different growth stages on seed, oil and protein yields of soybean cultivars. The interrelationships among seed yield ha<sup>-1</sup> and its attributes through simple correlation and stepwise regression analysis were evaluated. The results indicated that the percentages of oil and protein in these seeds were significantly affected by water regimes and caused a decrease in oil percentage and increase in protein percentage. In addition, both oil and protein output per unit area was significantly reduced, as water regimes increased. The results showed that skipping irrigation during vegetative, flowering and pod filling stages had no effect on economic yield and save 14% from total irrigation costs of soybean production, but skipping two or three irrigations during vegetative, flowering and pod filling stages had effect on economic yield of soybean production under the environmental conditions of Giza region. Results revealed that Giza 111 proved to be the best cultivar followed by Giza 21 among the six cultivars included in the test under different water regime. Simple correlation analysis indicated that seed yield ha<sup>-1</sup> was positively correlated with number of branches plant<sup>-1</sup>, number of pods plant<sup>-1</sup>, 1000-seed weight and seed yield plant<sup>-1</sup>. Stepwise regression procedure indicated that number of branches plant<sup>-1</sup>, number of pods plant<sup>-1</sup> and number of seeds pod<sup>-1</sup>, were the most important characters affecting seed yield ha<sup>-1</sup>. Combined analysis of variance (ANOVA) showed that effect of irrigation regimes, cultivars and irrigation regimes × cultivars on seed, oil and protein yield were significant.

**Keywords:** Soybean; Skipping Irrigations; Cultivars; Seed Yield; Oil Yield; Protein Yield; Correlation; Regression.

### 507. Comparing the Relative Efficiency of two Experimental Designs in wheat Field Trials

Ashraf A. Abd El-Mohsen and Samir R. Abo-Hegazy

*Scientific Research and Review Journal*, 1 (3): 101-109 (2013)

This investigation was conducted in 2010/11 and 2011/12 growing seasons at the experimental farm of the Faculty of Agriculture, Cairo University, Giza, Egypt. Twenty Egyptian bread wheat cultivars were evaluated in an alpha lattice design with three replications for nine characters. The aim was to compare the relative efficiency of two experimental designs based on error mean squares. In field trials, variation in soil fertility can result in substantial heterogeneity within blocks and thus, poor precision in treatment estimates resulted. For this purpose, two datasets were analyzed according to alpha lattice design and randomized complete blocks design (RCBD). For the two trials, alpha lattice design exhibited more efficient than randomized complete blocks design in reducing both the error mean squares and the coefficient of variation consequently, an efficient estimation of treatment differences, than RCBD. Average estimated relative efficiency (RE) was 9.5, 28.5, 30.0, 22.5, 40.0, 30.5, 35.0 and 28.5% for plant height, number of tillers plant<sup>-1</sup>,

spike length, number of spikelets spike<sup>-1</sup>, number of grains spike<sup>-1</sup>, 1000-grain weight, grain yield plant<sup>-1</sup> and grain yield feddan<sup>-1</sup>, respectively, indicating that the high precision to estimate treatment effects is gained significantly from using an alpha lattice design instead of RCBD. Whereas RE value of 0.98 for days to 50% heading indicated that the precision of both alpha lattice design and RCBD was similar. Mean rank comparisons for both RCBD and alpha lattice design were performed. The ranks were not constant across the experiments. The results showed that the traditional RCBD should be replaced by alpha lattice in the agricultural field trials when the number of treatments to be tested in an experiment increases to more than ten, where a homogeneous block is quite difficult to find in field experiments.

**Keywords:** Alpha lattice design; Rcbd; Coefficient of variation; Efficiency; Error mean squares; Relative standard error difference; Wheat; Yield trials.

### 508. Comparison of Some Statistical Techniques in Evaluating Sesame Yield and its Contributing Factors

Ashraf Abd El-Aala Abd El-Mohsen

*Scientia Agriculturae*, 1 (1): 8-14 (2013)

Two field experiments were carried out in a commercial field at Abo Rawash village, Giza governorate, Egypt during 2004 and 2005 seasons to compare five statistical procedures including: simple correlation, path analysis, multiple linear regression, stepwise regression and factor analysis were in determining the relationship between sesame seed yield and its contributing traits. Thirty sesame genotypes were used for this purpose.

The studied characters were: flowering date, plant height, stem height to the first capsule, fruiting zone length, number of capsules on main stem, number of capsules per plant, capsule density on main stem, 1000-seed weight and seed yield per plant. The most important results can be summarized as follows: 1.

The simple correlation coefficients and path analysis of yield components revealed that components with the highest positive correlation to yield also had the highest positive direct effect to yield i.e., number of capsules on main stem and number of capsules per plant. Path analysis showed that, the residual effect (0.433) was high in magnitude which shows that some other important yield contributing characters which contribute to yield have to be included. 2. Stepwise multiple regression analysis showed that 77.25% of the total variation in seed yield could be explained by the variation in number of capsules per plant and flowering date in sesame.

The linear regression equation was  $(Y) = 10.951 - 0.110 X_1 + 0.114 X_7$ , where Y, X<sub>1</sub> and X<sub>7</sub> represent seed yield per plant, flowering date and number of capsules per plant, respectively. 3. Besides, coefficient of determination (R<sup>2</sup>), adjusted R-squared statistic and standard error of estimate values, mean absolute error (MAE) and Durbin-Watson (DW) statistic test showed no significant differences between the full model regression and stepwise multiple regression analysis technique. However, the efficiency expressed is due to the reduction in number of variables in the fitted model from all variables (full model regression) to two variables only (stepwise multiple regression).

**Keywords:** Sesame trait Interrelationships statistical techniques simple correlation; Path analysis; Multiple linear regression; Stepwise regression; Factor analysis.

## 509. Correlation and Regression Analysis in Barley

Ashraf Abd El-Aala Abd El-Mohsen

*Scientific Research and Review Journal*, 1 (3): 88-100 (2013)

Two field experiments were carried out at the Experimental Station, Faculty of Agriculture, Cairo University, during the two successive winter seasons of 2008/09 and 2009/10. Six cultivars were grown in a randomized complete blocks design with three replications and evaluated for eight characteristics. Combined analysis of variance was done from the mean data obtained for each characteristic over two seasons and correlation and regression analysis were carried out to better understand the relationship between yield and some yield components. Results indicated that seasons significantly affected all traits and interaction between seasons and cultivars was also significant. Highly significant differences and adequate genetic variability were observed among cultivars for all the eight characters. The results of the correlation coefficients of traits with grain yield revealed that the grain number per spike ( $r=0.84^{**}$ ), grain weight/spike ( $0.87^{**}$ ), 1000-grain weight ( $r=0.88^{**}$ ), number of spikes per square meter ( $r=0.68^{*}$ ) and spike length ( $r=0.67^{*}$ ) had the highest significant positive correlation with grain yield, indicating dependency of these characters on each other. Heading date was negatively and highly correlated with number of spikes per square meter ( $r=-0.58^{*}$ ), number of grains per spike ( $r=-0.87^{**}$ ), grain weight per spike ( $r=-0.89^{**}$ ), thousand grain weight ( $r=-0.87^{**}$ ) and spike length ( $r=-0.75^{**}$ ). The criteria used in identifying the best subsets are based on monotone functions of the residual sum of squares (RSS) such as  $R^2$ , adjusted  $R^2$  and Mallows' Cp. Results revealed that the best subset regression model, based on the three different criteria, the predicted equation for barley grain yield per fed (Y) was  $Y = 3.12 - 0.006x_1 - 0.019x_2 + 0.0007x_3 + 0.020x_6 - 0.149x_7$ . The simplified results from best subset regression analysis show that the highest coefficient of determination ( $R^2=96.5\%$ ), adjusted  $R^2$  (93.6%) and lowest Mallows' conceptual predictive (Cp) value (5.8), and has five-independent variable model with all variables except number of grain per spike ( $X_4$ ) and grain weight per spike ( $X_5$ ). The Best Subset Multiple Regression analysis indicates that adding the variable number of grain per spike ( $X_4$ ) and grain weight per spike ( $X_5$ ) does not improve the fit of the model.

**Keywords:** Barley; Best subset regression; Correlation; Grain yield; Components; Mallows' Cp; Multiple regression analysis; Regression analysis.

## 510. Genetic Behavior of Grain Yield and Its Components in Barley Crosses Under Water Stress and Non-Stress Conditions

F. F. Saad, A. A. Abd El-Mohsen, M. A. Abd El-Shafi and I. H. Al-Soudan

*Scientia Agriculturae*, 1 (2): 45-55 (2013)

Twenty one diallel crosses among seven Egyptian barley cultivars showing clear differences in reaction to drought were made and evaluated under full and stress irrigation regimes at the Experimental Station, Faculty of Agriculture, Cairo University, Giza Governorate, Egypt during 2011/2012 and 2012/2013 seasons. The objective was to estimate the mode of gene action in the inheritance, combining ability effects and heterosis for studied traits.

Water stress caused significant reductions in all studied traits; with number of spikes per plant of F1's showing maximum reduction (43.07%). Genotypic differences were found in all traits under both irrigation treatments. Giza 123, Giza 126 and F1 cross Giza 126 X Giza 2000 were early maturing as well as having high yielding ability. Giza 2000 X Giza 130 and Giza 129 X Giza 125 had the best yield under both irrigation regimes and the lowest reduction due to drought besides its intermediate earliness. Some crosses showed significant desirable heterobeltiosis for all studied traits under both irrigation regimes. It is interesting to mention that the high positive heterobeltiosis in grain yield/plant was associated with high positive heterobeltiosis in No. S/P and 100-KW for Giza 126 X Giza 2000 and Giza 130 X Giza 131 under stress and non-stress conditions, respectively. The crosses showing the best heterobeltiosis could be recommended to improve the respective traits. Both general (GCA) and specific (SCA) combining ability variances were significant for most studied traits under both irrigation regimes, indicating the importance of additive and non-additive genetic variances in determining the performance of these traits. The best general combiners were Giza 126 for 100-KW and GY/P and Giza 125 for PH, No. K/S. and GY/P under both irrigation regimes. The best F1 cross in SCA effect for 100-KW, No. K/S and GY/P was Giza 126 X Giza 2000 under both irrigation regimes.

**Keywords:** Barley *Hordeum Vulgare* L. General Combining Ability (Gca) Specific Combining Ability (Sca) Heterobeltiosis Grain Yield And Its Components.

## 511. Impact of Temperature Fluctuation on Yield and Quality Traits of Different Safflower Genotypes

Reda Shabana, Ashraf A. Abd El Mohsen, Hasnaa, A. H. Gouda and Hoda S. Hafez

*Scientific Research and Review Journal*, 1 (3): 74-87 (2013)

Growth and development of safflower are affected by different uncontrollable environmental conditions. Oil contents of safflower are largely influenced by temperature fluctuations. Temperature variations in the field can be created by sowing crops at different dates in the season. The objective of this work was to investigate the effect of different planting dates (i.e., 1st November, 15th November and 1st December), and thermal temperatures (growing degree days, GDD) on yield and quality traits of four genotypes (two local land races, i. e. G 21 and G 81 and two exotic genotypes from Cyprus i. e. G 45 and G 48) and a commercial cultivar (Giza 1). Six environments were created (three different planting dates during 2006/07 and 2007/08). The experimental design was a randomized complete blocks design with three replications. Safflower genotypes exhibited significant differences for seed, oil and protein yields, oil content, heat units accumulation and fatty acids composition. Seed yield was positively correlated ( $r=0.97^{**}$ ) with growing degree days (GDD) to maturity. The results showed that the seed, oil and protein yield, decreased significantly as the planting dates were delayed. Linear regression equation revealed that increases of one unit (15-day interval) than the optimum date decreased yield by 29.64 kg/fed.

The first planting date (1 November) produced the highest seed yield (581.70 kg/fed), whereas the third planting date (1 December) produced the lowest seed yield (522.42 kg/fed). The first planting date yielded the highest average oil yield compared to the other planting dates. Although a positive linear relationship

was achieved between accumulated heat units during the period of oil synthesis and until physiological maturity, the R<sup>2</sup> value was very low. The average values of oil content were highest in seeds for genotype G 45 (34.21%). Giza 1 had on average the lowest oil content (29.55%). High linoleic acid was dominant in all the five safflower genotypes. Pronounced variation in the main unsaturated fatty acids of oil (linoleic and oleic) was obvious in different environments and was very high. The linear association between heat units and concentration of either oleic or linoleic acid was also discussed.

**Keywords:** Safflower, Planting Date, Varying Environments, Temperature, Correlation, Regression, Coefficient Of Determination, Heat Units Accumulation, Seed Yield, Oil Content, Fatty Acids.

### 512. Modeling the Influence of Nitrogen Rate and Plant Density on Seed Yield, Yield Components and Seed Quality of Safflower

Ashraf A. Abd El- Mohsen and Gamalat O. Mahmoud

*American Journal of Experimental Agriculture*, 3 (2): 336-360 (2013)

To study the effect of nitrogen rate and plant density at different levels on yield, yield components and quality traits of safflower (cv. Giza 1) an experiment was conducted as split plot design in randomized complete block design arrangement with three replications, during the successive seasons 2010/11 and 2011/12. The factors consisted of four levels of nitrogen (0, 40, 80 and 120 kg N ha<sup>-1</sup>) and four different densities (80,000, 100,000, 133,000 and 200,000 plants ha<sup>-1</sup>). Different statistical analyses such as ANOVA, polynomial regression, correlation, and stepwise multiple linear regression were used. The multiple statistical procedures showed that the main effects of nitrogen rate and plant density levels were significant ( $P = 0.01$ ) for yield and yield components studied. A rise in nitrogen rate and plant density increased seed and oil yield, whereas plant height, number of branches plant<sup>-1</sup>, number of heads plant<sup>-1</sup>, seed yield plant<sup>-1</sup> and 1000-seed weight decreased as plant density increased. In general, the highest plant density (200,000 plants ha<sup>-1</sup>) and the nitrogen level (80 kg ha<sup>-1</sup>) was the best treatment in this research to attain high safflower seed yield under environmental conditions of Giza Governorate, Egypt. Polynomial models of seed, oil yield and yield components based on the ANOVA were fitted. Polynomial regression analysis indicated that the relationship between the nitrogen amount applied and safflower seed, oil yield and yield components could be defined by using a quadratic function. Also, the results revealed that, yield and yield components were significantly affected by plant density in linear responses. Correlation analysis showed a positive and significant correlation between seed yield ha<sup>-1</sup> and each of number of heads plant<sup>-1</sup>, seed yield plant<sup>-1</sup>, number of branches plant<sup>-1</sup> and 1000-seed weight. Stepwise regression analysis showed that number of heads plant<sup>-1</sup> explained 45.57% and along with seed yield plant<sup>-1</sup>, number of branches plant<sup>-1</sup> and 1000-seed weight explained 81.63% of total variations for seed yield (kg ha<sup>-1</sup>).

**Keywords:** Safflower; Nitrogen fertilizer; Plant density; Statistical models; Polynomial regression; Correlation; Stepwise regression.

### 513. Optimizing and Describing the Influence of Planting Dates and Seeding Rates on Flax Cultivars Grown Under Middle Egypt Region Conditions

Ashraf A. Abd El-Mohsen, Amany M. Abdallah and Gamalat O. Mahmoud

*Journal of Applied Sciences Research*, 9 (7): 4174-4185 (2013)

Cultivar selection, time of planting and seeding rate is important factors that influence flax growth and yield variables. The objectives of this study were to evaluate the effects of planting date, seeding rate and their interactions on yield and yield components of two flax cultivars. Cultivars, planting date and seeding rate had significant effects on flax yield and yield components. In general, the interaction between planting date and seeding rate and between planting date and cultivar was non significant. Results indicated that, no interaction occurred between cultivar and each of planting date and seeding rate suggesting that planting date and seeding rate affected the cultivars similarly. The two tested cultivars exhibited significant differences for almost traits. The early planting on November 15 was superior to the other two dates on November 30 and December 15 for seed yield and yield components and straw, fiber yield and related traits. Maximum seed, oil, straw and fiber yields ha<sup>-1</sup> was produced when seeding rate was applied at the rate of 180 kg ha<sup>-1</sup>. Therefore, early planting time November 15 with seeding rate 180 kg ha<sup>-1</sup> is recommended to obtain higher yield of flax cultivars Sakha 1 and Sakha 2. Significant linear relationship between planting dates and each of seed and oil yield provides the clue that these traits are dependent upon planting dates. Linear regression for planting date suggested that increase in one unit (15 days delaying) of planting date lead to decreased seed and oil yield by 162.7 kg ha<sup>-1</sup> and 63.66 kg ha<sup>-1</sup>, respectively. Regression analysis indicated that seed and fiber yields was positively correlated with seeding rates ( $r = 0.99$  and  $r = 0.99$ ) and increased linearly when the seeding rates increased from 140 to 180 kg ha<sup>-1</sup>. Finally coefficients of regression results suggest that an increase by one unit (20 kg ha<sup>-1</sup>) of seeding rate lead to increase seed and fiber yields by 62.55 kg ha<sup>-1</sup> and 249.5 kg ha<sup>-1</sup>, respectively.

**Keywords:** Flax; Cultivar; Planting date; Seeding rate; Regression analysis; Yield; quality traits.

### 514. Parametric Statistical Methods for Evaluating Barley Genotypes in Multi-Environment Trials

Fawzy F. Saad, Ashraf A. Abd El-Mohsen and Ismaeil H. Al-Soudan

*Scientia Agriculturae*, 1 (2): 30-39 (2013)

The current study aimed at assessing twelve genotypes of barley in a randomized complete blocks design with 3 replications across 8 environments (the combinations of 2 years x 2 locations x 2 sowing dates) during 2008/2009-2009/2010 seasons in Egypt. Significant differences were observed among barley genotypes for heading date, grain filling, number of spike/m<sup>2</sup>, spike length, thousand grain weight and grain yield (ardab/fed). Combined analysis of variance of grain yield of twelve genotypes tested in eight environments showed highly significant ( $p < 0.01$ ) differences between the genotypes, between environments and for GEI, of all traits under study, suggesting differential response of genotypes across testing environments and the validity of stability analysis.

To quantify yield stability, six parametric stability statistics were calculated (bi, S<sub>2</sub>di, Ri<sub>2</sub>, Wi<sub>2</sub>, S<sub>2</sub>i and CVi). According to the stability parameters, for grain yield of barley genotypes, the results revealed that genotypes Giza 123, Giza 129, Giza 127, G4, G2, G6 and G8 were more stable genotypes for 7, 7, 7.5, 4, 4 and 4 out of all 7 stability statistics used, respectively. Thus, these genotypes would be considered to be more stable than others for these statistics. This implies therefore that these genotypes are of low contribution to the genotypic by environment interaction. These genotypes may be utilized as donor parents for stability in barley improvement programs, and could be recommended to be as commercial stable high yielding cultivars. Highly significant rank correlations coefficient were found among S<sub>2</sub>di, W<sub>2</sub>i and Ri<sub>2</sub> implying their close similarity and effectiveness in detecting stable genotypes and they are equivalent in measuring stability. Hence any one of these parameters could be used to describe genotypes stability. Our results showed that high-yielding genotypes can differ in yield stability, and suggest that yield stability and high grain yield is not mutually exclusive.

**Keywords:** Barley; Grain yield; Parametric stability statistics; Genotype by environment interaction; Spearman's rank correlations.

#### 515. Predicting the Effect of Temperature on Leaf Appearance in Seven Spring Bread Wheat Genotypes

Mohamed A. Abd El-Shafi and Ashraf A. Abd El-Mohsen

*Scientific Research And Review Journal*, 1 (2): 46-51 (2013)

Field experiments were conducted at the Faculty of Agriculture, Cairo University, Agriculture Experiment and Research Station, during two successive seasons starting with 2010/2011 in Giza, Egypt. The study aimed to determine the effect of temperature (by sowing dates) on leaf appearance and growth of seven spring bread wheat genotypes. Linear response was found between rate of leaf appearance and thermal time. Phyllochron ranged between 108°C d and 122°C d. Mean final leaf number on the main stem ranged from 8.5 to 11.5 and it was highly correlated with thermal time ( $r=0.99^{**}$ ). Genetic constitution of genotypes had larger effect on number of leaves per main-stem than temperature. These results suggest that, to model leaf appearance and canopy development in wheat, genotypic coefficients of phyllochron need to be determined in relation to growing environment temperature.

**Keywords:** Phyllochron; Leaf number; Thermal time; *Triticum aestivum* L.

#### 516. Sowing Dates and Nitrogen Fertilizer Levels Effect on Grain Yield and Its Components of Different Wheat Genotypes

E.M.S. Gheith, Ola Z. El-Badry and S.A. Wahid

*Research Journal of Agriculture and Biological Sciences*, 9 (5): 176-181 (2013)

Two field experiments were conducted at Experimental Research Center, Faculty of Agriculture, Cairo University, Egypt during 2011/2012 and 2012/2013 seasons to determine the effect of different sowing dates and nitrogen levels on growth and grain yield and its components of some wheat genotypes. Wheat crop genotypes responded differently to the three factors for various

characters (number of spikes/m<sup>2</sup>, spike length, grain weight/spike, 1000-grain weight, harvest index and grain yield/fed.) produced the highest values at early sowing (25 November) as well as at 100 kg N/fed. in both seasons. Late sowing (December) and low nitrogen application significantly declined yielding capacity of wheat genotypes. Either L.R.-62 or Sids 1 produced highest grain yield performed better in term of grain yield as compared to other genotypes in both seasons, respectively. Moreover, all tested genotypes produced highest grain yield when planted early in 25 November and application of 100 kg N/fed.

**Keywords:** Wheat; Sowing dates; Nitrogen fertilization; Genotypes; Grain yield.

#### Dept. of Dairy Sciences

#### 517. Growth of Adjunct *Lactobacillus Casei* in Cheddar Cheese Differing in Milk fat Globule Membrane Components

Aleksandra Martinovic, Kim Marius Moe, Ehab Romeih, Bashir Aideh, Finn K. Vogensen, Hilde Østlie and Siv Skeie

*International Dairy Journal*, 31: 70-82 (2013) IF: 2.333

The effect of two adjunct *Lactobacillus casei* strains on the lactobacilli population of low-fat Cheddar cheese is described. The adjuncts, added at a low initial number, differed in their ability to utilize components of the milk fat globule membrane (MFGM); these were controlled by addition of butter milk powder or skim milk powder. The most diverse microbial composition was revealed at the start of cheese ripening and became more uniform in the later stages. The microorganisms present at the start influenced the lactobacilli population during ripening, but the adjuncts did not dominate the microflora in the cheese. A higher content of MFGM components in the cheese seemed to influence the lactobacilli population and the composition of free amino acids during ripening. The low initial numbers of lactobacilli resulted in comparatively large distances of separation between these cells in fresh cheese; electron micrographs of ripened cheese showed large clusters of clearly elongated lactobacilli.

**Keywords:** Cheddar; *Lactobacillus casei*; Milk-fat globule membrane components.

#### 518. Effect of Milk Proteins on Physical and Chemical Characteristics of Crispy Puff Snacks

Ismail Hussein Abd El-Ghany, Mohamed Abdelghany El-Asser, Khalid Said Nagy and Ahmed Ali Abd El-Maksoud

*Journal of Agricultural Science and Technology*, 3: 633-645 (2013) IF: 0.685

Dairy proteins included sweet whey solids (SWS), whey protein concentrate (WPC), milk protein concentrate (MPC) or sodium caseinate (SC) at level of 10% by weight were extruded with corn, rice, oat flour and other ingredients in a twin screw extruder. The functional properties and textural of crispy balls snacks (CBS) have been studied. The results showed that different protein types were significantly affected on functional and chemical properties of extrudate. The bulk density of CBS-SC was the lowest due to the highest expansion, while CBS-WPC retained the most water in the product, whereas, the maximum



value of water solubility index was obtained in the CBS-CWP. Results also showed that protein digestibility value of extrudates had higher than non-extruded products. Color analysis of CBS-SC and CBS-SWS products had the highest  $\Delta E$  values ( $P = 0.05$ ), whereas CBS-SWS was statistically higher than CBS-SC in rank. Also, it was noticed that CBS-SWS had the highest value of browning index. The hardness of all extrudates products was desirable for expanded crispy where ranged from 17.3 N to 12.18 N. Generally, MPC and SC incorporated with cereal flour had acceptable quality characteristics and improved significantly the functional and texture properties of crispy balls products.

**Keywords:** Extrusion; Sodium caseinate; Whey protein concentrate; Functional properties; Crispy product.

#### *Dept. of Economic Entomology and Insecticides*

##### **519. Natural Enemies of the South American Moth, Tuta Absoluta, in Europe, North Africa and Middle East, and Their Potential Use in Pest Control Strategies**

Lucia Zappala, Antonio Biondi, Alberto Alma, Ibrahim J. Al-Jboory, Judit Arno, Ahmet Bayram, Anar's Chailleux, Ashraf El-Arnaouty, Dan Gerling, Yamina Guenaoui, Liora Shaltiel-Harpaz, Gaetano Siscaro, Menelaos Stavrinos, Luciana Tavella, Rosa Vercher Aznar, Alberto Urbaneja and Nicolas Desneux

*Journal of Pest Science*, 86: 635-647 (2013) IF: 2.174

The South American tomato leafminer, *Tuta absoluta* Meyrick (Lepidoptera: Gelechiidae), is an invasive Neotropical pest. After its first detection in Europe, it rapidly invaded more than 30 Western Palaearctic countries becoming a serious agricultural threat to tomato production in both protected and open-field crops. Among the pest control tactics against exotic pests, biological control using indigenous natural enemies is one of the most promising. Here, available data on the Afro-Eurasian natural enemies of *T. absoluta* are compiled. Then, their potential for inclusion in sustainable pest control packages is discussed providing relevant examples. Collections were conducted in 12 countries, both in open-field and protected susceptible crops, as well as in wild flora and/or using infested sentinel plants. More than 70 arthropod species, 20 % predators and 80 % parasitoids, were recorded attacking the new pest so far. Among the recovered indigenous natural enemies, only few parasitoid species, namely, some eulophid and braconid wasps, and especially mirid predators, have promising potential to be included in effective and environmentally friendly management strategies for the pest in the newly invaded areas. Finally, a brief outlook of the future research and applications of indigenous *T. absoluta* biological control agents is provided.

**Keywords:** Biological control; Generalist predators; Integrated pest management; Invasive species; Parasitoid community; Western palaearctic.

##### **520. Determination of etoxazole residues in fruits and vegetables by SPE Clean-up and HPLC-DAD**

Malhat F., Badawy H., Barakat D. and Saber A.

*Journal of Environmental Science and Health, Part B: Pesticides, Food Contaminants and Agricultural Wastes*, 48 (5): 331-335 (2013) IF: 1.211

A method for determination of etoxazole residues in apples, strawberries and green beans was developed and validated. The analyte was extracted with acetonitrile from foodstuff and a charcoal-celite cartridge was used for clean-up of raw extracts. Reversed phase high performance liquid chromatography with photodiode array detector (HPLC-DAD) was used for the determination and quantification of etoxazole residues in the studied samples. The calibration graphs of etoxazole in a solvent or three blank matrixes were linear within the tested intervals 0.01–2 mg L<sup>-1</sup>, with correlation coefficient of determination >0.999. The combined solid phase extraction (SPE) clean-up and the chromatographic method steps were sensitive and reliable for simultaneous determination of etoxazole residues in the studied samples. The average recoveries of etoxazole in the tested foodstuffs were between 93.4 to 102% at spiking levels of 0.01, 0.10, and 0.50 mg kg<sup>-1</sup>, with relative standard deviations ranging from 2.8 to 4.7%, in agreement with directives for method validation in residue analyses. The limit of detection (LOD) of the HPLC-DAD system was 100 pg. The limit of quantification of the entire method was 0.01 mg kg<sup>-1</sup>.

**Keywords:** Etoxazole in food stuff; Solid phase extraction; HPLC-DAD.

##### **521. Preliminary Molecular Identification of a Predatory Bug, Orius Albidipennis, Collected From Ornamental Plants**

Samy M. Sayed, Metwally M. Montaser, G. Elsayed and Sayed A.M. Amer

*Journal of Insect Science*, 13: 1-8 (2013) IF: 0.875

*Orius albidipennis* (Reuter) (Hemiptera: Anthoridae) is a generalist predator used for biological control of insects attacking ornamental plants. Molecular identification of this species using internal transcribed spacer 1 (ITS1) of ribosomal DNA was conducted for the first time.

The complete sequence of ITS1 and fragments of its flanking 18S and 5.8S rDNA genes are reported herein. The estimated length of ITS1 of *O. albidipennis* was 305 bp. This spacer was nearly identical to its counterpart of *Orius* sp-Taif strain in spite of the difference in their length.

The phylogenetic relationships were determined using the maximum-likelihood method supported with strong bootstrap probabilities clustering of both taxa together. Further molecular markers could be useful to identify the Taif strain and support its sister relationship to the Egyptian *O. albidipennis*.

**Keywords:** biological control; ITS1; Molecular identification; Ribosomal DNA.

##### **522. Altered Gene Expression: Induction/Suppression in Leek Elicited by Iris Yellow Spot Virus Infection (IYSV) Egyptian Isolate**

Elsayed Elsayed Hafez, Ahmed A. Abdelkhalek, Abeer Salah El-Deen Abd El-Wahab and Fatma Hassan Galal

*Biotechnology and Biotechnological Equipment*, 27 (5): 4061-4068 (2013) IF: 0.622

Leek (*Allium porrum*) has become one of the major leafy vegetable crops in Egypt and all over the world. Iris yellow spot virus (IYSV) was observed on leek plants in eight different governorates in Egypt, in fields near to onion fields. The



symptoms in infected leek plants included yellowish or tan diamond-shaped or irregularly shaped lesions on leaves and flower stalks. Necrotic areas developed on leaves, and some plants had elongated brown lesions or brown flecks resembling thrips injury. Moreover, thrips larvae and adults feed with a punch-and-suck behavior that removes leaf chlorophyll, causing white to silver patches and streaks, which were observed on all infected plants. The plant samples were collected and subjected to ELISA test using IYSV polyanteriserum. The results revealed that about 90 % of the collected samples with symptoms were positive. For further confirmation, the ELISA positive samples were subjected to PCR amplification using nuclear coat protein specific primers. The PCR results were in agreement with the results obtained by ELISA. Thrip tabaci adults were reared on the infected plant and biological transfer was performed onto new healthy plants. After 15 days to 4 weeks post inoculation, symptoms were observed on the plant. Biologically infected plant samples were collected at different times after thrips-inoculation and the extracted RNA was subjected to Real Time PCR using the coat protein gene primers. The results showed that the expression of the coat protein fluctuated but reached its peak on day five (264 %). Differential display technique was performed on the newly infected plant tissues to identify changes in gene expression in leek elicited by IYSV that causes a symptomatic phenotype. Both up- and down- regulated genes were observed in infected plants conjugated with the healthy ones. Sequence analysis of the up-regulated genes was performed and the encoding sequence analysis showed that the obtained genes include: MFS family protein, Pathogenesis- related protein, Mitogen-activated protein kinase, N-acetylserotonin O-methyltransferase-like protein, Serine/threonine-protein kinase, and Putative Retrosat2 Ty3-Gypsy\_retroelement. On the other hand, only one down-regulated gene was identified, alpha- tubulin suppressor-like protein. Most of the identified genes are suppress defensin genes (innate/adaptive). It can be concluded that viral infection is capable of inducing a huge number of genes which are important in the plant immune system.

**Keywords:** Allium porrum; Iris yellow spot virus; iysv; Thrips; Defense system; Up-Regulated; Down-regulated genes.

### 523. Pollen Grains as an Additional food for Asian Lady Beetle, *Harmonia Axyridis* Pallas (Coleoptera: Coccinellidae)

Samy M. Sayed and S. A. El-Arnaouty

*Life Science Journal*, 10: 1755-1759 (2013) IF: 0.165

The multicolored Asian lady beetle, *Harmonia axyridis* (Pallas) (Coleoptera: Coccinellidae) has been considered a good candidate for biological control of many insect pests. The non-prey foods as pollen are used by coccinellids to increase survival when prey is scarce, reduce mortality during diapause, fuel migration, and enhance reproductive capacity. We assessed the biological performance of this predator when reared on three different crop pollens (corn, clover, or pulverized bee pollen) as dietary supplements in addition to *Ephestia kuehniella* eggs. Results showed that the duration of pre-imaginal stages was significantly differed among all tested diets. Adult female weights were heavier than males in all treatments. Moreover, pollen type as additive food affect the adult weight and female longevity of *H. axyridis*. Number of egg batches/female were 46.3, 47.2, 22.5 and 34.9; the mean number of eggs/female were 829.5, 1033, 475.5 and 899;

hatchability were 86.85, 48.82, 62.84 and 64.61% when fed on clover pollen with *Ephestia* eggs, corn pollen with *Ephestia* eggs, pulverized bee pollen with *Ephestia* eggs and *Ephestia* eggs only, respectively. It can be concluded that a mixture of clover pollen with *Ephestia* eggs is the best suitable diet for rearing of *H. axyridis*.

**Keywords:** Biological control; Coccinellidae; *Harmonia axyridis*; Pollen; *Ephestia kuehniella*; Additional food.

### 524. Impact of Spinosad and Nucleopolyhedrovirus Alone and in Combination against the Cotton Leaf Worm *Spodoptera Littoralis* under Laboratory

Alexandra Magdalina Ahmed El Helaly

*Applied Science Reports*, 2: 17-21 (2013)

The toxicity of the two biorational insecticides, Spinosad and NPVs, against neonates of *Spodoptera littoralis* (Bosidival) (Lepidoptera: Noctuidae) was tested under laboratory conditions in order to determine the competitive efficacy. The ability of Spinosad to protect the SpLiNPV from Ultra Violet effects under synthetic laboratory conditions was determined, and some biological aspects of both biorational insecticides and their mixture were studied. In order to determine whether or not there is a synergetic effect when both of these biorational pesticides are added together, six different Spinosad concentrations (1, 2, 5, 10, 15 and 30 ppm) alone and mixed with a sub-lethal concentration of SpLiNPV ( $1 \times 10^3$ ) were investigated. When the Ultra Violet effect was determined, the LC<sub>90</sub> of NPVs mixed with LC<sub>10</sub> of Spinosad, in order to investigate the ability of Spinosad in prolonging the virus activity. Sample: Department of Entomology (Virology Unit) faculty of Agriculture, Cairo university, between July 2012 and May 2013. The percent of mortality increased; it was 11.66, 19.33, 33.33, 55.00, 71.66 and 85.00 % compared with 11.66, 13.33, 15.00, 26.66, 36.66 and 63.33 % in Spinosad alone and 20.11% in NPVs treatment. It gave almost complete protection after 30 minutes of exposure to artificial ultraviolet light and gave 47 % death percentage 5 hours post-application in comparison to 2.8 % death percentage for NPVs alone treatment. The larval duration was affected with Spinosad only; pupal period and adult longevity were not affected by all tested treatments. The number of eggs laid per female and percent of hatchability were affected in Spinosad and Spinosad NPVs in combination treatments compared with that of control. These findings indicate that the biorational insecticides Spinosad and NPVs can be used in combination, thus giving promising results against the cotton leaf worm. These results suggest that Spinosad and NPVs represent an important choice to be used in integrated pest management where *S. littoralis* is a major pest.

**Keywords:** *Spodoptera littoralis* spinosad; NPVs combination biological aspects.

### 525. Promising Additives to Protect the Activity of Baculovirus Biocontrol Agent under Field-Sunlight Conditions in Egypt

Alexandra El-Helaly, Magda Khatlab, Said El-Salamouny, Mohammed El-Sheikh and Salah Elnagar

*Journal of Life Sciences*, 7 (5): 495-500 (2013)

-Baculoviruses are effective biocontrol agents except of their short persistence under sunlight conditions. Four promising additives containing different groups of antioxidants were tested on cotton plant foliage. *Spodoptera littoralis* test insect and its nucleopolyhedrovirus (SpliNPV) are the standard material used in the investigation. Results are based on leaf-bioassays, to test Original Activity Remaining (OAR) and Lethal Infectivity Time to 50% (LIT<sub>50</sub>) of tested population of the virus after exposure to natural sunlight. The results showed that cacao additive at 10%, sustained 50% of virus activity for five days post application (113.11 hours) and three days and a half (83.33 hours) at 5% concentration. The virus alone treatment sustained 50% of its activity for only 24.07 hours. The obtained results suggested the possibility of prolonging the virus activity on plant foliage under field applications.

**Keywords:** Antioxidants; Baculovirus activity; Field-biocontrol application; *Spodoptera littoralis* NPV; Virus protection.

#### Dept. of Food Science and Technology

##### 526. Effect of Storage on Antioxidant Activity of Freeze-Dried Potato Peels

Amir Al-Weshahy, Mohammad El-Nokety, Mahmud Bakhete and Venket Rao

*Food Research International*, 50 (2): 507-512 (2013) IF: 3.005

A study was undertaken with the objective of evaluating the storage stability of the polyphenols and the antioxidant activity in the peel from two varieties of potatoes, Penta and Marcy, grown in Ontario, Canada. Samples were stored at -20, 4 and 25 °C for 0, 2, 4 and 8 weeks. Peel from Penta variety contained higher levels of total polyphenolic compounds, 2.4 mg/g of peel d.w. compare to Marcy, 1.14 mg/g of peel d.w. Chlorogenic and caffeic acids were the major polyphenolic compounds present in both varieties. Levels of polyphenolic compounds in the peel were influenced by storage temperature with maximum loss observed at 25 °C. Storage time caused a decline in the levels of polyphenolic compounds up to 4 weeks at all temperatures followed by a significant increase at the end of week 8. There was a parallel increase in the antioxidant activity of the peel samples during storage and until the end of 8 weeks of storage. At all temperatures of storage, there was a significant relationship ( $r = 0.43$ ,  $P \leq 0.05$ ) between the amount of polyphenolic compound in the peel samples and their antioxidant capacity. Results suggest potato peel as a valuable source of polyphenolic compounds requiring proper storage condition to maintain their antioxidant properties.

**Keywords:** Antioxidant; Polyphenolic compounds; Potato peel; Storage.

##### 527. Antioxidant and Antimicrobial Activities of Marjoram (*Origanum Majorana* L.) Essential Oil

A.Z.M. Badee, R.K. Moawad, M.M. ElNoketi and M.M. Gouda

*Journal of Applied Sciences Research*, 9 (2): 1193-1201 (2013)

Marjoram essential oil (MEO) was analyzed by gas chromatography coupled with mass spectrometry (GC/MS), the analysis revealed that, the major components were  $\gamma$ -terpinene (23.20%),  $\alpha$ -terpinene (19.71%) and terpinen-4-ol (12.64%), followed by  $\alpha$ -terpinolene (6.76%), sabinene hydrate (6.56%), p-

cymene (5.81%),  $\alpha$ -phellandrene (5.43%) and Limonene (5.40%), they constituted 85.51% of total essential oil, indicating that Egyptian marjoram oil belonged to terpinen-4-ol /sabinene-hydrate chemotype. GC/MS studies also indicated that, the oil was dominated by monoterpene-hydrocarbons (75.79%), followed by oxygenated-monoterpenes (21.50%) and Sesquiterpene-hydrocarbons (2.34%). Results of total phenolic content (TPC) revealed that MEO is a rich source of polyphenols which are known natural antioxidants. MEO also exhibited strong antioxidant activities as shown by the consistently high values of DPPH free radical-scavenging inhibition (83.6 %) and  $\beta$ -carotene / linoleic acid system inhibition (76.2 %), at 400  $\mu$ g / mL oil concentration. Antioxidant effectiveness was further confirmed on the essential oil using automatic determination of the oxidative stability for sunflower oil (Rancimat). MEO was found to be very effective in stabilizing sunflower oil in comparison with BHT, the stability of the oil was increased with the increasing in essential oil concentration. On the basis of the results obtained, marjoram essential oil could be used as a potential source of natural antioxidant with possible applications in food systems. In antimicrobial investigation with the agar disc diffusion assay, all the microorganisms tested were susceptible to the action of marjoram essential oil, with a range of inhibition zone diameter values from 13 to 34 mm/sample. *Candida albicans* was the most sensitive strain tested to the MEO with the strongest inhibition zone (34 mm). While, *Aspergillus flavus* was the most resistance strain tested, with the lowest inhibition zone (13 mm). Minimum inhibitory concentrations (MIC) for *Candida albicans* was determined as 32  $\mu$ L/ mL MEO, in comparison to 98  $\mu$ L/mL with commercial Amphotericin B (antifungal agent). According to the results, the studied essential oil potentially might be used as a natural preservative ingredient in food industry.

**Keywords:** Marjoram; Natural preservatives; DPPH;  $\beta$ -carotene; Phenolic compound; GC/MS.

##### 528. Chemical Composition, Antioxidant and Antimicrobial Activities of Partially Deterpenated Mandarin (*Citrus Reticulate*) Essential Oil

A.Z.M. Badee, Shahinaz A. Helmy and Rushdy M.A.

*International Journal of Academic Research*, 5 (2): 117-125 (2013)

The main chemical component of mandarin peels oil, determined by using GC and GC/MS, were d-limonene and  $\gamma$ -terpinene, which represented 65.75 and 23.07% respectively of total content. Partially deterpenation of mandarin oil was carried out by different adsorbent ratio, (1:7.5 and 1:15) oil to silica gel (DM1 and DM2, respectively). Regarding the deterpenated mandarin oil, (DM1 1:7.5), oil adsorbent ratio it was noticed that reduced monoterpene hydrocarbon from 95.42% to 80.41% and consequently increased total oxygenated component from 2.34% to 14.25%. On the other hand, (DM2, 1:15), oil adsorbent ratio reduced monoterpene hydrocarbons content to 49.35% and increased total oxygenated components content to 18.88%. The free radical scavenging activity of mandarin oil and its partially deterpenated oils at various concentrations (ranged from 50 to 200  $\mu$ g/mL), compared with ascorbic acid was determined. Mandarin oil at 200  $\mu$ g/mL exhibited ability to reduce the concentrations of DPPH free radical to DPPH-H reaching 65.97 % of DPPH scavenging effect. In the partially deterpenated mandarin oils, antioxidant activity increased by decreasing

monoterpenes content as it increased to 71.42% in DM2 oil versus 66.55% scavenging activity for DM1. The antimicrobial activities of mandarin oil and its partially deterpenated oils were evaluated by using the disc diffusion method against five bacteria strains, three mold strains and one yeast strain at concentration (10 µL/disc), compared with ampicilline (an antibiotic, as positive control, at 10 µg/disc). Results proved that the deterpenated mandarin essential oils exhibited antifungal activity against all tested strains (*Aspergillus niger* NRRL 2322, *Aspergillus flavus* spp. and *Aspergillus parasiticus* spp.) with superior activity of DM2 deterpenated ones, meanwhile, no inhibition activity was noticed for mandarin oil. Also, DM2 oil exhibited strongest effectiveness towards Gram-negative bacteria strains (*Escherichia coli* ATCC 6933, *Escherichia coli* ATCC 3515 and *Pseudomonas aeruginosa* ATCC 9027), with no significant difference compared with ampicillin (at  $p = 0.05$ ), followed by DM1, then the original oil. On the other hand, a moderate antimicrobial activity was recorded for all tested oils against Gram-positive bacteria strains (*Bacillus subtilis* ATCC 3321 and *Staphylococcus aureus* ATCC 20231) with non significances among all tested oils and also, comparing with the potency of ampicillin as positive control.

**Keywords:** Mandarin peel oil; Deterpenation; Antioxidant; Antimicrobial.

### 529. Effect of Some Treatments and Different Drying Methods on the Quality and Shelf-Life of Whole Bolti Fish

A.Z.M. Badee, A.T. El-Akel, E.A. Moghazy and Abass I. Shereen

*International Journal of Academic Research*, 5: 56-64 (2013)

Drying fish is the cheapest and simplest preservation method. The main problem of salt- dried fish during manufacturing and storage is lipid oxidation leading to inferior quality and shelf- life. Therefore bolti fish were salted in a saturated sodium chloride solution (contains 0.5% ascorbic acid) for 48 hr at 4°C, then, drained and left for 10 minutes. The samples were divided into three group: Oven dried, sun- dried, and solar dried, then the product were coated by forming a film of Arabic gum or Sodium alginate, products were stored for 6 months at room temperature (25-35°C), Samples were then analyzed periodically (every 2 months) during storage period. The results indicated that during storage at room temperature for 6 month, The moisture content of all samples decreased continuously as the time of storage increased till 6 month. It could be observed that the loss of moisture content were: 0.53, 0.65, 0.72, 0.53, 0.47, 0.57, 0.57, 0.72, and 0.6%, for SDF, SDFG, SDFA, ODF, ODFG, ODFA, SODF, SODFG and SODFA respectively after storage for 6 months. Total protein content of dried fish samples was slightly decreased during storage 1.46, 1.66, 1.91, 2.6, 1.88, 1.56, 1.16, 1.29, and 1.62% for SDF, SDFG, SDFA, ODF, ODFG, ODFA, SODF, SODFG and SODFA respectively at the end of storage peiode, Fat was decreased together. It was noticed that the decreasing percents of fat content after 6 months of storage was 0.22, 0.63, 0.78, 0.48, 0.55, 0.58, 0.74, 0.75, and 0.7% for SDF, SDFG, SDFA, ODF, ODFG, ODFA, SODF, SODFG and SODFA. The decrease of fat content of dried fish samples during storage might be attributed to lipid oxidation occurred during storage. During storage period, it could be noticed that there was gradually increase in TBA, TVN values for all dried fish samples (TBA: 0.26 to 1.62), (TVN: 56.08 to 159.6) this may be attributed

to high enzyme activity and high microbial load during storage. The results also indicated that the best dried methods was Oven drying then Solar drying and finally Sun drying. Coating with Arabic gum was better than coating with Sodium alginate, as detected from sensory evaluation.

**Keywords:** Drying; Bolti fish; Salting; Quality; Coating; Arabic gum; Sodium alginate.

### 530. Improving the Quality and Shelf-Life of Refrigerated Chicken Meat By Marjoram Essential Oil

A.Z.M. Badee, R.K. Moawad, M.M. ElNoketi and M.M. Gouda

*Journal of Applied Sciences Research*, 9 (11): 5718-5729 (2013)

Nowadays consumers are demanding more natural foods; the present study was designed to investigate the effect of marjoram essential oil (MEO) dipping treatments (based Nano-emulsion technique) on the quality and shelf-life of raw chicken drumsticks during refrigerated storage for 12 days. Identification of chemical constituents and phenolic compounds responsible for antioxidant and antimicrobial activities were also investigated in marjoram extracts using GC/MS and HPLC analytical systems. The results indicated that significant ( $p < 0.05$ ) incremental pattern was observed in TVB-N, TBARS and pH values in all chicken samples during subsequent cold storage by different rates. The lowest significant ( $p < 0.05$ ) incremental rate was recorded in samples soaked in 0.2% stabilized MEO. The results also reveal that both dipping treatments (T1 and T2) significantly reduced the microbial load of aerobic plate counts (APC), psychrotrophic counts (PTC) and Enterobacteriaceae counts (EBC) just after dipping and throughout the storage period in comparison with the control. However, samples dipped in MEO at 0.2% showed the lowest incremental pattern in bacterial counts at any time of the refrigerated storage. A small but statistically significant ( $P < 0.05$ ) reduction in the color parameters  $L^*$ ,  $a^*$  and  $b^*$  values was recorded throughout the storage, indicates increased graying over storage days particularly in control samples. MEO dipping significantly reduced color loss in chicken drumsticks. Finally, there was also a significant ( $p < 0.05$ ) enhancement in sensory attributes and shelf-life stability of chicken drumsticks due marjoram oil dipping, the untreated drumsticks would have a refrigerated shelf life between 6 and 7 days while after natural active dipping, the shelf life extended to 9 days in T1-drumstick samples and 12 days in T2-samples. The major identified components by GC/MS were  $\alpha$ -terpinene,  $\alpha$ -terpinene and terpinen-4-ol, followed by  $\alpha$ -terpinolene, sabinene hydrate,  $p$ -cymene,  $\alpha$ -phellandrene and limonene. While HPLC results indicated that catchin, cinnamic, gallic, caffeic, chlorogenic, vanillic, ferulic, and cumaric acids were positively identified in the present study. Among the positive effects of these compounds on chicken meat characteristics are retarding lipid oxidation, color loss, off-odor formation and microbial growth occurring during refrigerated storage and may offer a promising choice in food safety and preservation.

**Keywords:** Nano-emulsion; Lamiaceae; Natural preservatives; Marjoram oils; Phenolic compounds; Quality attributes.

### 531. Utilization of Some Essential Oils to Extend the Shelf -Life of Coated Semi Fried Nile Perch Fish Fillets During Cold Storage

Badee, A.Z.M., El-Akel, A.T. and Thuraya A. Abuhlela

*Journal of Applied Sciences Research*, 9 (6): 3508-3519 (2013)

This research was performed to evaluate the antioxidant and antimicrobial effects of marjoram (*Marjorana hortensis*), mint (*Mentha piprita*) and thyme (*Thymus capitatus*) essential oils as natural preservatives to extend the shelf - life of coated semi fried Nile perch ( *Lates niloticus*) fish fillets. Skinless Nile perch fish fillets were treated with two ratios; 0.5 (T<sub>1</sub>) and 1.0 (T<sub>2</sub>) ml of marjoram essential oil per 100g fish fillets, 1.5 (T<sub>3</sub>) and 2.0 (T<sub>4</sub>) ml of mint essential oil per 100g fish fillets and with 0.5 (T<sub>5</sub>) and 1.0 (T<sub>6</sub>) ml of thyme essential oil per 100g fish fillets. The treated fish fillets with tested essential oils and untreated one (control sample) were coated with dough mixture (wheat flour, cold water, whole egg, sodium chloride, cumin powder and xanthan gum) and fried at 170±5°C for 1 mint. The coated semi fried fillets were packed in polyethylene bags and after that stored at 4±1°C for 16 days. The physico-chemical quality criteria; total volatile basic-nitrogen (TVB-N) content, trimethylamine-nitrogen (TMA-N) content, thiobarbituric acid (TBA) value, acid value and the pH value, microbiological quality indices; the total viable bacteria (TVB), psychrotrophic bacteria, pseudomonas spp. bacteria and yeasts and molds counts, and sensory analysis were used to evaluate the preservative effect of tested essential oils during storage at 4±1°C for 16 days. The present results showed that there was a significant (P≤0.05) increase in TVB-N, TMA-N, TBA and acid values in different ratios depending on the ratio and the kind of tested essential oil itself. The lowest significant incremental rate was recorded in samples (T<sub>2</sub>). All treatments, except (T<sub>3</sub>), gave significantly (P≤0.05) reduction in the TVB-N values and psychrotrophic, and pseudomonas spp. bacteria counts immediately after treatment as compared with control treatment. The marjoram, mint and thyme essential oils in both ratios were able significantly to reduce the yeast and mold counts immediately at zero time. The increase in all tested microbiological quality criteria continued during the cold storage in all treatments which was lower than control sample. The obtained results also showed that there was a significant (P=0.05) enhancement in sensory quality attributes of fish fillets' samples treated with marjoram, mint and thyme essential oils at both tested ratios. In general, the tested essential oils' treatments caused a significant (P≤0.05) extending of the shelf-life, as well as enhancement the physico-chemical, microbiological and sensory quality attributes for coated semi fried Nile perch fish fillets during cold storage. In addition, fish samples treated with 1.0 ml marjoram essential oil (T<sub>2</sub>) followed by samples treated with 1.0 ml thyme essential oil (T<sub>6</sub>) per 100 g fish fillets attained the highest scores for sensory quality attributes and exhibited the better acceptability than the control and the other treated fish samples. Therefore, the present findings recommended that the essential oils of marjoram, mint and thyme should be utilized for extending the shelf-life and enhancing quality attributes of coated semi fried fish fillets during cold storage.

**Keywords:** Essential oils; Shelf-life; Semi fried fish; Quality criteria; Cold storage.

### Dept. of Genetics

### 532. Ly49Q Positively Regulates Type I Ifn Production By Plasmacytoid Dendritic Cells in An Immunoreceptor Tyrosine-Based Inhibitory Motif-Dependent Manner

Mir Munir A. Rahim, Lee-Hwa Tai, Angela D. Troke, Ahmad Bakur Mahmoud, Elias Abou-Samra, Justin G. Roy, Amelia Mottashed, Nicholas Ault, Chloe Corbeil, Marie-Line Goulet, Haggag S. Zein, Melisa Hamilton-Valensky, Gerald Krystal, William G. Kerr, Noriko Toyama-Sorimachi and Andrew P. Makrigiannis

*The Journal of Immunology*, 190: 3994-4004 (2013) IF: 5.52

Plasmacytoid dendritic cells (pDC) are the major producers of type I IFN during the initial immune response to viral infection. Ly49Q, a C-type lectin-like receptor specific for MHC-I, possesses a cytoplasmic ITIM and is highly expressed on murine pDC. Using Ly49Q-deficient mice, we show that, regardless of strain background, this receptor is required for maximum IFN- $\alpha$  production by pDC. Furthermore, Ly49Q expression on pDC, but not myeloid dendritic cells, is necessary for optimal IL-12 secretion, MHC-II expression, activation of CD4<sup>+</sup> T cell proliferation, and nuclear translocation of the master IFN- $\alpha$  regulator IFN regulatory factor 7 in response to TLR9 agonists. In contrast, the absence of Ly49Q did not affect plasmacytoid dendritic cell-triggering receptor expressed on myeloid cells expression or pDC viability. Genetic complementation revealed that IFN- $\alpha$  production by pDC is dependent on an intact tyrosine residue in the Ly49Q cytoplasmic ITIM. However, pharmacological inhibitors and phosphatase-deficient mice indicate that Src homology 2 domain-containing phosphatase 1 (SHP)-1, SHP-2, and SHIP phosphatase activity is dispensable for this function. Finally, we observed that Ly49Q itself is downregulated on pDC in response to CpG exposure in an ITIM-independent manner. In conclusion, Ly49Q enhances TLR9-mediated signaling events, leading to IFN regulatory factor 7 nuclear translocation and expression of IFN-I genes in an ITIM-dependent manner that can proceed without the involvement of SHP-1, SHP-2, and SHIP.

**Keywords:** Plasmacytoid dendritic cells; IFN- $\alpha$ ; Ly49q; Nk cell.

### Dept. of Genetics

### 533. Optimized Tetramer Analysis Reveals Ly49 Promiscuity for Mhc Ligands

Emily McFall, Megan M. Tu, Nuha Al-Khattabi, Lee-Hwa Tai, Aaron S. St.-Laurent, Velina Tzankova, Clayton W. Hall, Simon Belanger, Angela D. Troke and Andrew Wight, Ahmad Bakur Mahmoud, Haggag S. Zein, Mir Munir A. Rahim, James R. Carlyle and Andrew P. Makrigiannis

*The Journal of Immunology*, 191: 5722-5729 (2013) IF: 5.52

Murine Ly49 receptors, which are expressed mainly on NK and NKT cells, interact with MHC class I (MHC-I) molecules with varying specificity. Differing reports of Ly49/MHC binding affinities may be affected by multiple factors, including cis versus trans competition and species origin of the MHC-I L chain ( $\beta$ 2-microglobulin).

To determine the contribution of each of these factors, Ly49G, Ly49I, Ly49O, Ly49V, and Ly49Q receptors from the 129 mouse strain were expressed individually on human 293T cells or the mouse cell lines MHC-I-deficient C1498, H-2b-expressing MC57G, and H-2k-expressing L929. The capacity to bind to H-2Db- and H-2Kb-soluble MHC-I tetramers containing either human or murine  $\beta$ 2-microglobulin L chains was tested for all five Ly49 receptors in all four cell lines. We found that most of these five inhibitory Ly49 receptors show binding for one or both self-MHC-I molecules in soluble tetramer binding assays when three conditions are fulfilled: 1) lack of competing cis interactions, 2) tetramer L chain is of mouse origin, and 3) Ly49 is expressed in mouse and not human cell lines. Furthermore, Ly49Q, the single known MHC-I receptor on plasmacytoid dendritic cells, was shown to bind H-2Db in addition to H-2Kb when the above conditions were met, suggesting that Ly49Q functions as a pan-MHC-Ia receptor on plasmacytoid dendritic cells. In this study, we have optimized the parameters for soluble tetramer binding analyses to enhance future Ly49 ligand identification and to better evaluate specific contributions by different Ly49/MHC-I pairs to NK cell education and function.

**Keywords:** Plasmacytoid dendritic cells; Nk cell education and function; Nk and Nkt cells.

#### 534. Genetic Analysis of Health-Related Secondary Metabolites in A Brassica Rapa Recombinant Inbred Line Population

Hedayat Bagheri, Mohamed El-Soda, Hye Kyong Kim, Steffi Fritsche, Christian Jung and Mark G. M. Aarts.

*International Journal of Molecular Sciences*, 14: 15561-15577 (2013) IF: 2.464

The genetic basis of the wide variation for nutritional traits in Brassica rapa is largely unknown. A new Recombinant Inbred Line (RIL) population was profiled using High Performance Liquid Chromatography (HPLC) and Nuclear Magnetic Resonance (NMR) analysis to detect quantitative trait loci (QTLs) controlling seed tocopherol and seedling metabolite concentrations.

RIL population parent L58 had a higher level of glucosinolates and phenylpropanoids, whereas levels of sucrose, glucose and glutamate were higher in the other RIL population parent, R-o-18. QTL related to seed tocopherol ( $\alpha$ -,  $\beta$ -,  $\gamma$ -,  $\delta$ -,  $\alpha$ - $\gamma$ - and total tocopherol) concentrations were detected on chromosomes A3, A6, A9 and A10, explaining 11%–35% of the respective variation. The locus on A3 co-locates with the BrVTE1 gene, encoding tocopherol cyclase.

NMR spectroscopy identified the presence of organic/amino acid, sugar/glucosinolate and aromatic compounds in seedlings. QTL positions were obtained for most of the identified compounds. Compared to previous studies, novel loci were found for glucosinolate concentrations. This work can be used to design markers for marker-assisted selection of nutritional compounds in B. rapa.

**Keywords:** Brassica rapa; Secondary metabolites; Nutritional value; Quantitative trait.

#### 535. A Multidisciplinary Approach for Dissecting Qtl Controlling High Yield and Drought Tolerance-Related Traits in Durum Wheat

Ayman A. Diab, Mohamed A. M. Atia, Ebtissam H. A. Hussein, Hashem A. Hussein and Sami S. Adawy

*Int. J. of Agricultural Science and Research*, 3: 99-116 (2013)

Durum wheat (*Triticum turgidum* ssp. durum) is an economically and nutritionally important cereal crop in the Mediterranean region and its production is largely influenced by environmental stresses, such as drought, salinity, heat and nutrient deficiency. The objective of this study was to dissect quantitative trait loci (QTL) controlling grain yield, yield components and drought tolerance in durum. A molecular genetic linkage map for F2 durum mapping population derived from an intraspecific cross between Baniswif-1 x Sohag-2 was constructed using 114 DNA markers (9 SSRs, 14 SCoTs, 90 AFLPs and 1 RAPDs) distributed over the 14 linkage groups and spanning 2040.9 cM of the durum wheat genome. The size of linkage groups varied greatly from 6.8cM for LG11 to 317.5cM for LG4 with an average length of 145.8cM. Based on the used anchor SSR markers, only eight linkage groups were assigned to chromosomes, where LG1, LG3, LG5, LG6, LG7, LG9, LG13 and LG14 were assigned to chromosomes 1B, 3B, 5B, 6A, 6B, 7A, 3A and 2B, respectively. Single point analysis was used to identify genomic regions controlling eleven morpho-physiological traits related to grain yield, yield components and drought tolerance. A total of 74 QTL were identified for the eleven traits on all linkage groups except (LG10 and LG11). These included 3 QTL for root length (RL), 11 QTL for plant height (PH), 7 QTL for spike length (SL), 3 QTL for number of branches/plant (NBP), 3 QTL for number of spike/plant (NSP), 8 QTL for number of spikelets /spike (NSS), 15 QTL for number of kernel/spike (NKS), 10 QTL for thousand-kernel weight (TKW), 4 QTL for fresh weight (FW), 5 QTL for dry weight (DW) and 5 QTL for total amino acids (TAA). This work represents the first genetic linkage map for durum wheat population derived from an intraspecific cross between Baniswif-1' and Sohag-2' showing chromosomal regions associated with 11 morpho-physiological traits related to grain yield, yield components and drought tolerance in durum wheat.

**Keywords:** D QTL; Durum; Drought; Yield; Molecular markers; Scot; Ssr; Aflp.

#### Dept. of Horticulture Pomology

#### 536. Histological Indicators of Dwarfism of Some Olive Cultivars

El Said S. Hegazi, Ayman A. Hegazi and Abdou M. Abd Allatif

*World Applied Sciences Journal*, 28(6): 835-841(2013)

The current study was conducted during 2011 season on eleven olive cultivars namely "Picual", "Manzanillo", "Teffahi", "Aggezi", "Chemlali", "Dolce", "Koroneiki", "Frantoio", "Coratina", "Arbequina" and "Cairo7". Stem anatomy conducted to examine the relation between internal structure and plant vigours. Measurements on stem cross section showed that vigour cultivars had higher xylem and low phloem percentage and high number of the large vessels. The stem anatomy indicated that Cairo7 cv. had the highest dwarfing potential.

**Keywords:** Olive; Anatomy; Xylem; Phloem; Dwarfism.



**Dept. of Plant Pathology****537. Protocol Suggested for Management of Cantaloupe Downy Mildew.**

Abada, K.A. and Kh. E. Eid

*Journal of Applied Sciences Research*, 9(11): 5633-5642 (2013)

The inhibitory effect of the fungicides Acrobat copper, Previcure-N and Unilax, the inducer resistance chemicals (IRC)s bion, chitosan, salicylic acid and zinc sulphate and the bioagents *Bacillus polymyxa*, *B. subtilis* and *Pseudomonas fluorescens* on sporangial germination of fungus like *Pseudoperonospora cubensis*, the causal of cantaloupe downy mildew was tested in vitro. The role of the tested fungicides, IRCs and bioagents on management of cantaloupe downy mildew was evaluated under greenhouse conditions. In addition, the alternation between the sprayed tested fungicide Unilax, IRC chitosan and bioagent *P.fluorescens* on management of the disease under field conditions was investigated. The inhibitory effect of the tested fungicides, IRCs and bioagents on sporangial germination of *P. cubensis* revealed that they caused significant reduction to the germinated sporangia. The tested fungicides were the most efficient ones followed by the bioagents then IRCs. Disease management showed the same trend of in vitro experiment when they sprayed on artificially inoculated cantaloupe plants with the sporangia of the causal fungus like under greenhouse conditions. Under field conditions, spraying cantaloupe plants with the tested fungicide Unilax still the most efficient trial for management the disease during 2012 and 2013 growing seasons compared with spraying any of IRC (chitosan) and the bioagent (*P. flurescens*) alone. However, spraying the tested fungicide in alternation with the tested IRC and the bioagent ranked the second efficiency of disease management. Meanwhile, spraying the tested fungicide in alternation with any of the tested IRC and bioagent was of moderate efficiency.

**Keywords:** Bacterial bioagents; Cantaloupe; Chemical control; Downy mildew; Fungicides; Inducer resistance chemicals.

**538. Effect of Combination Between Bioagents and Solarization on Management of Crown-And Stem-Rot of Egyptian Clover**

Effat Abdel-Mageed Zaher, Khairy Abdel-Maksoud Abada and Marwa Abedl-Lateef Zyton.

*Journal of Plant Sciences*, 1(3): 43-50 (2013)

Fourteen isolates of *Trichoderma* sp. and eight isolates of *Bacillus* sp., isolated from a field has severe infection by stem and crown-rot of Egyptian clover plants were screened for their efficacy against the fungus *Sclerotinia sclerotiorum* Lib. de Bary, the causal of crown and stem-rot of Egyptian clover, in vitro and in vivo. In general, *Bacillus* spp. were more efficient in reducing the radial growth of *S.sclerotiorum* than *Trichoderma* spp and the opposite was found in case of sclerotial germination. In addition, the isolates of *B.thuringiensis* and *T.harzianum* showed maximum percentages of radial growth inhibition and sclerotial viability. Meanwhile, isolates of *B. pumilus* and *T.viride* resulted in the lowest percentages of radial growth inhibition and sclerotial viability. The tested bioagents, i.e. *B.thuringiensis*-1 and *T.harzianum*-3 as well as soil solarization resulted in significant reduction to the severity of clover crown and stem-rot with significant increase to the green forage yield compared with

control treatment. In addition, *T.harzianum*-3 was more efficient than *B.thuringiensis*-1 and solarization, when each of them was applied alone. Moreover, the combination among *B.thuringiensis*-1 + *T.harzianum*-3 + solarization was the most efficient in this regard, which no apparent infection by crown and stem-rot was detected and the highest green forage yield was obtained. However, the combination between solarization and any of the tested bioagents was of intermediate effect in this regard.

**Keywords:** Egyptian clover, *Bacillus* sp., Biological control; *Sclerotinia sclerotiorum*; *Trichoderma* sp.; Viability.

**Dept. of Soil Sciences****539. Assessment of Optimum Land Use and Water Requirements for Agricultural Purpose in Some Soils South Paris Oasis, Western Desert, Egypt**

Wael Ahmed Mohamed Abdel Kawy and Kh. M. Darwish

*Arabian Journal of Geoscience*, 1: 1-10(2013) IF: 0.74

The current work is aimed to realizing land suitability and water use efficiency and determining the optimum land use system. The main aims were to identify the physiographic features and calculate the crop water requirements for specific crops. The study area was observed through a soil survey inventory in Paris Oasis, Western Desert, Egypt. Ten soil profiles plus a number of auger observations and mini pits were selected to represent the different mapping units. A fieldwork and morphological description were carried out, and soil samples were collected for demonstrating the physical and chemical soil properties. Based on satellite data that can integrate with GIS utility, field work, and laboratory analysis, the physiographic map was generated. The study found that the main land type units are plateaus, hills, dunes, and depression floor. Concerning the second aim, the main land qualities of different mapping units were rated and matched to obtain the current and potential land suitability using automated land evaluation system. This research concluded that the best crops adapted with the soil conditions and could be feasible for economic use are clover, wheat, beans, sugar beet, onions, maize, sunflower, tomato, potato, groundnut, pea, lentil, barley, sesame, and carrots. Crop water requirements were determined in variable rate according to the actual plant requirements using the aid of FAO-Cropwat model. Irrigation schedule and consumptive use of suitable crops were calculated and adopted. The crop water requirements for each selected crop were determined as follow: 828.0, 596.7, 410.3, 679.95, 409.52, 791.60, 712.2, 902.93, 456.55, 529.95, 231.4, 217.95, 303.93, 502.65, and 274.35 mm, respectively.

**Keywords:** Consumptive use; Darb El-arbean area; Geographic information system; Optimum land use.

**Dept. of Vegetable Crops****540. Effect of Foliar Nutrition on Post-Harvest of Onion Seed under Sandy Soil and Saline Irrigation Water Conditions**

Shehata, S. A., Hashem, M. Y., Mahmoud, G. I., Abd El-Gawad, K. F., El-Ramady, H. R. Alshaal, T. A., Domokos-Szabolcsy, E., Elhawwat, N., Prokisch, J. and Fári, M.

*Int. J. of Horticulture*, 19 (1-2 ) 85-92, 19: 29-92 (2013)

Foliar application has been determined to be an effective nutrients delivery strategy in vegetable and fruits. The enhancement of vegetable and fruit yields affected by foliar nutrients application has been recognized in previously conducted studies with perennial tree crops. The efficiency of foliar nutrition is dependent on soil, climate, fertilizer and the amount of nitrogen used. There is no sufficient information concerning cooperation of foliar nutrition with all nutrients form as well as the rates of these nutrients fertilization in vegetable and fruit crops. Two successive winter seasons of 2008/2009 and 2009/2010 were conducted under sandy soil conditions to study the effect of spraying with 12 commercial compounds on inflorescences diameter, flower stalk length, number of seed stem /plant, weight of 1000 seed, germination percentage, seed yield, moisture content, catalase, peroxidase activity and malondialdehyde content of onion seeds. The plants sprayed with union Zn, union Mn, union feer, shams k, elga 600, boron, and amino x had the highest vegetative growth parameter, germination percent and enzyme activity. The plants sprayed with union Zn, union feer, shams K, magnesium, caboron, hummer and amino X had the highest seed yield ha-1. The seeds were stored for one year to study the effect of different commercial compounds and storage temperatures on germination, moisture content and change in antioxidant enzymes activities of onion seeds during the storage period. Storage at cold temperature showed higher germination percent, moisture content and lower malondialdehyde content than storage at room temperature. The treatment with union Zn, union feer, union Mn, boron, elga 600, caboron, amica, hummer and amino x had the highest germination percent.

**Keywords:** Onion; Pre-harvest; Post-harvest; Foliar application; Seeds production; Sandy soil.

#### **541. Effect of hot water Dips and Modified Atmosphere Packaging on Extend the Shelf Life of Bell Pepper Fruits**

Said A. Shehata; M.I.A. Ibrahim; Mohamed M. El-Mogy, and Karima F. Abd El- Gawad

*Wulfenia Journal*, Vol 20(3): 315-328 (2013)

This study was carried out on sweet pepper fruits (El-Usr 3 hybrid) obtained from private farm, at Ismailia Governorate during 2007/2008 and 2008/2009 seasons to evaluate the effect of hot water dipping (HWD) at 50 °C for 3 min and 55 °C for 1 min, modified atmosphere packaging (sealed with polyethylene and polypropylene bags) and combination between them on quality changes in sweet pepper fruits during storage at 8 °C plus 95% RH. In general, sweet pepper fruits treated with hot water led to slightly increasing in weight loss percentage as compared to untreated fruits (control), while those dipped in hot water plus packaging had the lowest weight loss percentage during storage. Pepper fruits stored in polypropylene bags were perceived the higher intensities of freshness, firmness and yellowness as compared with those in polyethylene bags. No decay was observed in sweet pepper fruits treated with hot water at 50 °C for 3 min or 55 °C for 1 min plus packaging in polypropylene bags during storage. Furthermore, it is also reduced weight loss, maintained fruit firmness and retarded the loss of ascorbic acid and carotenoids and gave fruits with excellent to good appearance without any visible injury for 28 days of storage at 8 °C.

**Keywords:** Bell pepper; Hot water treatment; Map; Polyethylene; Polypropylene; Storage.

#### **542. Effects of Foliar Nutrition on Onion Seed Storage under Modified Atmosphere Packages**

LShehata, S. A., Hashem, M. Y., Mahmoud, G. L., Abd Et-Gawad, K. F., El-Ramady, H. R. Abhatd, T. A., Domoko.s-Szabolesy, E., Elhawaw, N., Prokisch, J. and Fin, M.

*International Journal of Horticulture*, 19(1-2): 93-100 (2013)

Modified atmosphere packaging (MAP) and controlled atmosphere storage techniques to reduce the oxygen around the food are largely used for the preservation of fresh produce. There have been great technological advances in this area of preservation, particularly as it refers to improving the quality and shelf-stability of highly perishable food products, such as produce. Two successive winter seasons of 2008/2009 and 2009/2010 were conducted under sandy soil conditions to study the effect of spraying with 12 commercial compounds on onion seeds storage under modified atmosphere packages. Germination percent of seeds decreased in 5°C than storage in room temperature. Germination percent of seeds was gradually decreased with increasing the storage period. Packaging treatments had a significant effect on germination percent of seeds. All the packaging treatments had the higher germination percent than the paper package (control). The highest germination percent after 12 months of storage was recorded for the treatment with non perforated polypropylene in room temperature and polyethylene and non perforated polypropylene in 5°C. Catalase activity decreased with the prolongation of storage period. The non perforated polypropylene package had the highest catalase activity. The treatment with non perforated polypropylene had the highest catalase activity after 12 months of storage in both room and 5°C temperatures. Peroxidase activity of seeds was gradually decreased with increasing the storage period. The highest peroxidase activity after 12 months of storage was recorded in non perforated polypropylene in both storage temperatures.

**Keywords:** Onion; Pre-harvest; Post-harvest; Foliar application; Seeds production; Modified atmosphere packages.

#### **Faculty of Veterinary Medicine**

##### *Dept. of Biochemistry*

#### **543. Adverse Effect of Mobile Phone on Tp53, Brcal Genes and DNA Fragmentation in Albino Rat Liver**

Gouda E.M., Galal M.K. and Abdalaziz S.A.

*International Journal of Genomics and Proteomics*, 4: 84-88 (2013)

Although mobile phones among daily indispensable wireless accessories a big concern about their emitted electromagnetic radiation (EMR) hazard. The present study investigated the possible damage induced by their EMR strength and duration on mammalian genome, using male Albino rats as an animal model. Animals were exposed to mobile phone emitted radiation of 1800 MHz frequency for a period of 2 hours. Exposure was performed either continuously or intermittent manners for 3 different exposure periods. The possible mutation in BRCA1 and TP53 tumor suppressor genes were studied, and the degree of genomic DNA fragmentation was followed. The obtained results revealed that longer period (six weeks) of continuous EMR exposure induced mutation in both studied genes with relative increase in

DNA fragmentation when compared with intermittent exposure. The study warrants the public against excessive exposure to mobile phone-induced EMR. Minimization of such exposure has to safeguard against genetic DNA fragmentation with possible consequent mutation and cancer formation.

**Keywords:** Emr; Mobile phone; BRCA1; TP53.

#### 544. Genetic Variants and Allele Frequencies of Kappa Casein in Egyptian Cattle and Buffalo Using Pcr-Rflp

Eman M. Gouda, Mona Kh. Galal and Samy A. Abdelaziz

*Journal of Agricultural Science, 5(2): 197-203 (2013)*

Kappa casein (K-Ca) genetic variations affected quality and composition of the milk. Several variants of Kappa casein (K-Ca) gene locus IV have been reported with special interest for the 'B' allele for its relation to the milk protein and fat yields. Genotyping and allelic frequencies of K-Ca among Native Egyptian breeds of cattle and buffalo were the aim of the present study. PCR amplification of DNA isolated from 300 blood samples collected from Holstein and Baladi cattle and buffalo were performed followed by restriction fragment length polymorphism using Hind-III restriction endonuclease (PCR-RFLP). Detection of 'AA' and 'AB' genotypes in cattle breeds, 'BB' and 'AB' in buffalo and two alleles 'A' and 'B' in the studied breeds. Molecular selection for animals carrying the 'B' allele could impact breeding programs for dairy production in native cattle and buffalo breeds in Egypt.

**Keywords:** Kappa casein; Polymorphism; Cattle' buffalo pcr-Rflp.

#### Dept. of Clinical Pathology

#### 545. Clinicopathological and Immunological Effects of Multistrain Probiotic on Broiler Chicken Vaccinated Against Avian Influenza Virus

Abeer Ahmed Abd el-baky

*Global Veterinaria, 10(5): 534-541 (2013)*

Avian influenza virus considered one of the most important avian viruses causing economic losses in poultry industry. In February 2006, highly pathogenic avian influenza (HPAI) virus was firstly recognized in Egypt and since this time the disease had become enzootic in poultry throughout much of the country. In the present work, a total of 160 one day old commercial (Cobb) broiler chicks were used for studying clinicopathological and immunological effects associated with the use of multistrain probiotic (Protexin®) on vaccinated chicks against avian influenza virus. To evaluate probiotic immunological effect, geometric mean haemagglutination inhibition antibody (GM-HI) titers of chicken against avian influenza virus (AIV) H5N2 was carried. Hematological and serum biochemical parameters were carried also, to evaluate its clinicopathological effects. Immunological and clinicopathological results revealed, the used multistrain probiotic (Protexin®) has immunostimulatory, hepatostimulatory and hepatoprotective effects on vaccinated chicks against avian influenza virus H5N2.

**Keywords:** Clinical pathology; Immunology; Avian influenza virus; Probiotic.

#### 546. Clinicopathological Effect of Camellia Sinensis Extract on Streptozotocin-Induced Diabetes in Rats

Abeer Ahmed Abd el-baky

*World Journal of Medical Sciences, 8(3): 205-211(2013)*

Diabetes Mellitus presents a major challenge to healthcare systems around the world. One of the outcomes of diabetes is oxidative stress that is caused by the effect of hyperglycemia. Recent studies indicate that, oxidative agents in diabetes result in many complications such as cardiovascular disease, nephropathy, retinopathy and neuropathy. The present experimental study was carried out on 40 Sprague-Dawley Albino rats (weighing about 180±10 g) which were divided randomly into 4 groups. Diabetes was induced by a single intra-peritoneal injection of Streptozotocin (STZ, 60 mg/kg). The experimental groups received alcohol extract of Camellia sinensis (green tea) leaves (200 mg/kg) for a period of 4 weeks. Blood samples were collected for studying clinicopathological changes (hematological parameters, blood glucose level, lipid profile and some antioxidant enzymes activity) associated with the use of green tea extract on STZ-induced diabetic rats. Results revealed that, oral administration of green tea extract improved the stress picture and caused a significant decrease in serum glucose and total cholesterol levels in diabetic rats treated with green tea extract when compared to levels of diabetic control group. No significant changes were observed in hematological parameters, total triglycerides, LDL-c and HDL-c levels in non diabetic rats treated with green tea extract. It appears that, green tea extract had both antihyperglycemic and hypocholesterolemic effect and increased the activity of antioxidant enzymes on STZ-induced diabetic rats. Further studies are needed to determine its protective effects on the other diabetes complications.

**Keywords:** Clinical hematology; Clinical biochemistry; Diabetes mellitus; Camellia sinensis (green tea).

#### 547. Clinicopathological Studies on Endosulfan-Induced Oxidative Stress and the Protective Role of Vitamin E

Khaled Mohamed Ahmed Mahran

*Global Veterinaria, 11: 258-265 (2013)*

Endosulfan, an organochlorine acaricide and insecticide, has been used in agriculture on food and non-food crops for several years. The present study aimed to evaluate the clinicopathological changes associated with the oxidative stress induced by endosulfan in male rats and to evaluate the possible protective effect of vitamin E. The present experimental study was carried out on 40 albino rats (150-200 g) which were divided randomly into 4 groups; control group, endosulfan treated-group (2 mg/kg b.wt./day), vitamin E treated group (200 mg/kg b.wt. twice a week) and endosulfan with vitamin E treated-group. Blood samples were weekly collected for studying changes in clinical hematology and serum biochemistry. At the end of experiment, antioxidant enzymes activities [superoxide dismutase (SOD), glutathione peroxidase (GPX) and Catalase (CAT)] in RBCs hemolysate and tissue homogenates (heart, liver, kidney and spleen) were studied. Results revealed that, oral administration of endosulfan induced microcytic hypochromic anemia, thrombocytopenia, leukocytosis with lymphocytosis, significant hypoproteinemia, hypoalbuminemia with decreased A/G ratio,

increased activities of ALT and ALP, total hypercholesterolemia, hypertriglyceridemia and increased BUN and creatinine concentrations. Moreover, endosulfan induced decreased activities of antioxidant enzymes (SOD, GPX and CAT) in hemolysates and tissue homogenates. The present study concluded that oral administration of vitamin E improved the adverse effects of oxidative stress induced by endosulfan.

**Keywords:** Clinical hematology; Clinical biochemistry; Oxidative stress; Antioxidant enzymes; Endosulfan; Vitamin E; Rats.

#### *Dept. of Cytology and Histology*

##### **548. Histological and Immunohistochemical Studies of the Effect of Vitamin C and Nigella Sativa on the Palate of Albino Mice's Offspring After Cadmium Exposure**

Shaymaa Hussein. Mohamed El-Sakhawy. Abdel-Aleem El-Saba, Abd Rabou M.I, Hany Sherif and Abdel Razik, Hashim

*Life Science Journal*, 10(1): 2766-2772 (2013) IF: 0.165

Performance of the current study utilized a well elicited CD-1 albino mouse. 50 females divided into 5 groups, 10 females in each group separated from males for one month, all groups were get the drug doses twice a week for one month before gestation and during pregnancy until delivery. For breeding purposes each 2 females were mated with 1 male from 5 pm. until 9 am. at the following day. Female mice were classified into five groups. Group I (control group, female animals were injected intramuscularly with 0.5 ml of sterile normal saline); group II (dams were injected i.m. with 5 mg/kg body weight of cadmium chloride (Cd Cl<sub>2</sub>) dissolved in 0.5 ml of sterile normal saline); group III; (treated with Cd Cl<sub>2</sub> as in group II, plus i.m. injection of 10 mg/ kg body weight of vitamin C. group IV(was injected i.m. with Cd Cl<sub>2</sub> as in group II and given 50 mg/kg body weight of Nigella sativa orally) and group V(animals were administrated cadmium and vitamin C as in group III and Nigella sativa as same as in group IV). After delivery, heads of pups were decapitated. The heads were fixed in Bouin's fixative and prepared routinely for paraffin sectioning and staining for histological and immunohistochemical investigations. Morphological and histological observations showed that 44.77% of cadmium treated pups affected with cleft palate, 13.51% of them with secondary palatal cleft. All control group animals were normally developed, as well as the pups of the remaining groups which treated with vitamin C and / or Nigella sativa with cadmium. Immunohistochemical examination of transforming growth factor alpha revealed that, control pups expressed a strong immune reaction in the primary palatal region in the palatine epithelium, while it was moderately positive in the underlying mesenchymal tissue cells. The reaction was strongly expressed in the endothelium of the blood capillaries and in the ossifying centers of the secondary palatal region. Cadmium treated mice (group II) revealed negative immune TGF- $\alpha$  reaction. Cadmium and vitamin C treated animals expressed moderate TGF- $\alpha$  reaction in the palatine epithelium and faint reaction in the underlying connective tissue cells, endothelium of the blood capillaries and in the ossifying centers. Animals treated with cadmium and Nigella sativa expressed the same immune reaction as in group III. Cadmium, vitamin C and Nigella sativa treated pups

expressed strong immune reaction of TGF- $\alpha$  similar to that of control group.

**Keywords:** Cadmium; Palate; Vitamin C; Nigella Sativa; Tgf- $\alpha$ .

#### *Dept. of Fish Diseases and Management*

##### **549. The Role of Spirulina Platensis (Arthrospira Platensis) in Growth and Immunity of Nile Tilapia (Oreochromis Niloticus) and Its Resistance To Bacterial Infection**

Mai D. Ibrahim, Mohamed F. Mohamed and Marwa A. Ibrahim

*Journal of Agricultural Science*, 5(6): 109-117 (2013)

The current study was designed to optimize the dietary levels of Spirulina platensis in Oreochromis niloticus; this was tested via graded levels. Six isonitrogenous and isocaloric rations containing graded levels of dried spirulina 0, 5, 7.5, 10, 15 and 20 g/kg diet were fed separately to six equal groups of O. niloticus fingerlings for 3 months. Growth performance, non-specific immune parameters, tissue reactions and resistance of tilapias post challenge infection with Pseudomonas fluorescens were estimated monthly. There were significant increase in growth performance parameters and survival rates in spirulina-supplemented groups at concentration level of 10 g/kg for 2 months. Significant increases in hematocrit, nitroblue tetrazolium and lysozyme activity were observed in most of the supplemented groups. Bacterial challenge infections resulted in significantly lower mortality rate in all Spirulina groups with remarkable increase in protection of fish received 10 g/kg. In sum, it advisable to incorporate 10 g/kg diet of spirulina for 2 months for maximum growth performance, immunity and disease resistance in O. niloticus.

**Keywords:** Spirulina platensis; Growth performance; Hematocrit; Nitroblue tetrazolium; Lysozyme activity; Challenge infection.

#### *Dept. of Food Hygiene and Control*

##### **550. Sources of Escherichia Coli Deposited on Beef During Breaking of Carcasses Carrying Few E. Coli At Two Packing Plants**

Mohamed K. Youssef, Madhu Badoni, Xianqin Yang and Colin O. Gill

*Food Control*, 31: 166-171(2013) IF: 2.738

Microbiological samples were obtained from the hands of workers, personal equipment and conveyor belts, in the carcass breaking facility of a beef packing plant where chilled carcasses carry coliforms and Escherichia coli at numbers < 1 cfu/10,000 cm<sup>2</sup>. Before work started, steel mesh gloves carried coliform and E. coli at numbers of 4 and 3 log cfu/25 items, respectively, while their numbers on conveyor belts were >2 and <2 log cfu/2500 cm<sup>2</sup>, respectively. After a period of work the numbers of both coliforms and E. coli on steel mesh gloves and conveyor belts were reduced by about 1 log unit, but the numbers on cotton gloves worn under steel mesh gloves were 5 and >4 log cfu/25 items, respectively. The findings indicate that the proximate source of most coliforms and E. coli that contaminate cuts and trimmings are, respectively, cotton gloves and conveyors. Microbiological samples were similarly obtained at a second plant where drying of carcass surfaces during chilling gave carcasses



with coliforms and *E. coli* at numbers about 1 cfu/1000 cm<sup>2</sup>. Before work started, steel mesh gloves were free of coliforms and *E. coli*; and the uniform wearing of rubber gloves over cotton ones precluded contamination of cotton gloves. The conveyor belt carried coliforms and *E. coli* at numbers about 1 cfu/cm<sup>2</sup> and >1 cfu/100 cm<sup>2</sup>, respectively, before work started; and at numbers < 1 cfu/cm<sup>2</sup> and about 1 cfu/100 cm<sup>2</sup>, respectively, after a period of work. The findings indicate that at the second plant both cuts and trimmings are contaminated with coliforms and *E. coli* from the conveyor.

**Keywords:** Beef; Carcas Breaking; Cuts; Trimmings; Sources of Contamination.

### 551. Survival of Acid-Adapted *Escherichia Coli* O157:H7 and Not-Adapted *E. Coli* on Beef Treated With 2% or 5% Lactic Acid

Mohamed Kamel Hussein Youssef M.K. Youssef, X. Yang, M. Badoni and C.O. Gill

*Food Control*, 34: 13-18 (2013) IF: 2.738

Decontamination of beef by spraying with solutions of lactic acid is common practice in North America and is to be permitted in the EU. Validation of each such treatment is necessary for HACCP purposes. The utility of validation by reference to reduction in numbers of *Escherichia coli* naturally present on beef is questioned. This is because reductions of *E. coli* generally might be greater than reductions of the main target organism, *E. coli* O157:H7, which can be more acid tolerant. To investigate the effects of lactic acid sprays on the two types of *E. coli* on beef surfaces, slices of beef with cut muscle, fat or membrane surfaces were prepared. The surfaces were inoculated with a five strain cocktail of acid-adapted *E. coli* O157:H7 or with a not-acid-adapted strain of *E. coli* at number of 5, 1 or 1 log cfu/cm<sup>2</sup>. Inoculated slices were not treated or were sprayed with water or 2% or 5% lactic acid at 0.5 ml/cm<sup>2</sup>. For each slice of lactic acid-treated meat the numbers of *E. coli* or *E. coli* O157:H7 recovered on agars that allowed resuscitation of injured cells or did not allow resuscitation were similar. The differences in the log mean numbers (log A) and in the log total numbers (N) of bacteria recovered from slices that were not treated or treated with acid were calculated. Differences in log A and N for bacteria recovered from slices treated with water or acid were calculated also. Means of the differences indicated that each acid treatment gave similar reductions in the numbers of *E. coli* or *E. coli* O157:H7. However, reductions were somewhat greater with 5% than with 2% lactic acid. The findings suggest that the *E. coli* or *E. coli* O157:H7 that survived acid treatments of meat surfaces were protected from exposure to injurious concentrations of undissociated acid. Consequently, strains of *E. coli* that are or are not relatively tolerant of acid conditions will be inactivated to similar extents by solutions of lactic acid applied to beef surface.

**Keywords:** *Escherichia coli* O157; Acid adaptation; Lactic acid; Beef cuts; Decontamination.

### 552. Inactivation Kinetics of *Bacillus Coagulans* Spores under Ohmic and Conventional Heating

Romel Somavat, Hussein M.H. Mohamed, Sudhir K. Sastry.

*Lwt -Food Science and Technology*, 54: 194-198 (2013) IF: 2.546

*Bacillus coagulans* spores are commonly involved in the spoilage of food of pH between 4 and 4.5. Recent studies on ohmic heating have indicated the presence of an additional nonthermal effect of electricity on the bacterial spores of *Geobacillus stearothermophilus* and *Bacillus subtilis*. We investigated the kinetics of inactivation of *B. coagulans* spores (ATCC 8038) in fresh tomato juice under ohmic heating at frequencies of 10 kHz and 60 Hz, and compared it with conventional heating using a specially designed experimental setup that assured identical temperature histories for all treatments. Ohmic heating at 60 Hz showed significantly lower D-values at 95, 100 and 105 C compared to conventional heating. While 10 kHz also showed a similar trend of higher inactivation compared to conventional heating, the difference was significant only at 105 C. Both ohmic treatments also showed higher inactivation than conventional heating during the come-up time. In conclusion, ohmic heating resulted in accelerated inactivation of *B. coagulans* spores compared to conventional treatment.

**Keywords:** Ohmic Heating *Bacillus Coagulans* Inactivation Kinetics

### 553. Mathematical Modeling and Microbiological Verification of Ohmic Heating of A Solid-Liquid Mixture in A Continuous Flow Ohmic Heater System With Electric Field Perpendicular To Flow

Pitiya Kamonpatana, Hussein M.H. Mohamed, Mykola Shynkaryk, Brian Heskitt, Ahmed E. Yousef and Sudhir K. Sastry

*Journal of Food Engineering*, 118: 312-325 (2013) IF: 2.276

To ensure sterility of a solid-liquid mixture processed in continuous-flow ohmic systems, the slowest heating solid particle needs to receive sufficient heat treatment at the outlet of the holding section. We describe herein, the development of a mathematical model for solid-liquid mixtures in a commercial ohmic heater with electric field oriented perpendicular to the flow. The fastest moving particle velocity was identified using over 299 particles and a radio-frequency identification technique, and used as an input to the model for the worst-case heating scenario.

Thermal verification was conducted by comparing predicted and measured fluid temperatures at heater and hold tube outlets; the model showed good agreement between calculated and experimental fluid temperatures ( $P > 0.05$ ) with a maximum error of 0.4 C.

The model predicted a hold tube length of 15.85 m at 134.0 C process temperature to achieve a target lethal effect at the cold spot of the slowest-heating particle. Using this length of hold tube, microbiological tests were conducted using at least 299 chicken/alginate particles inoculated with *Clostridium sporogenes* spores per run. These tests showed the absence of viable microorganisms at the target treatment and positive growth when temperatures were below target, thereby verifying model predictions.

**Keywords:** Ohmic heating; Aseptic process; Modeling; Simulation Solid-Liquid Mixture; Microbiological verification; Residence Time; Spores; *Clostridium sporogenes*; Alginate.



#### 554. Mathematical Modeling and Microbiological Verification of Ohmic Heating of A Multicomponent Mixture of Particles in A Continuous Flow Ohmic Heater System With Electric Field Parallel To Flow

Pitiya Kamonpatana, Hussein M. H. Mohamed, Mykola Shynkaryk, Brian Heskitt, Ahmed E. Yousef and Sudhir K. Sastry

*Journal of Food Science*, 78: E1721-E1734 (2013) IF: 1.775

To accomplish continuous flow ohmic heating of a low-acid food product, sufficient heat treatment needs to be delivered to the slowest-heating particle at the outlet of the holding section. This research was aimed at developing mathematical models for sterilization of a multicomponent food in a pilot-scale ohmic heater with electric-field-oriented parallel to the flow and validating microbial inactivation by inoculated particle methods. The model involved 2 sets of simulations, one for determination of fluid temperatures, and a second for evaluating the worst-case scenario. A residence time distribution study was conducted using radio frequency identification methodology to determine the residence time of the fastest-moving particle from a sample of at least 300 particles. Thermal verification of the mathematical model showed good agreement between calculated and experimental fluid temperatures ( $P > 0.05$ ) at heater and holding tube exits, with a maximum error of  $0.6^{\circ}\text{C}$ . To achieve a specified target lethal effect at the cold spot of the slowest-heating particle, the length of holding tube required was predicted to be 22 m for a  $139.6^{\circ}\text{C}$  process temperature with volumetric flow rate of  $1.0 \times 10^{-4} \text{ m}^3/\text{s}$  and 0.05 m in diameter. To verify the model, a microbiological validation test was conducted using at least 299 chicken-alginate particles inoculated with *Clostridium sporogenes* spores per run. The inoculated pack study indicated the absence of viable microorganisms at the target treatment and its presence for a subtarget treatment, thereby verifying model predictions.

**Keywords:** *Clostridium sporogenes*; Mathematical model; Multicomponent mixture; Ohmic Heating; Verification.

#### 555. Microbiological Quality Evaluation of Raw Goat's Milk in Egypt

Saad Mf, Nagah M. Hafiz and Salwa A. Aly

*International Journal of Biology, Pharmacy and Allied Sciences*, 2(10): 1837-1848 (2013)

Microbiological quality of fresh goat's milk collected from ten flocks in Cairo and Giza Governorates were evaluated, as a measure of food safety. Milk samples were analyzed for Total Mesophilic Count (TMC), Total Psychotrophic Count (TPC), Total Lipolytic Count (TLC), Total Staphylococci Count (TSC), Total Coagulase Positive Staphylococci (CPS) & Coagulase Negative Staphylococci (CNS) Count, Total Yeast & Mold Count (TYMC) and Coliforms Count (CC). The obtained results were in mean values of (8.6 & 9.7), (4.5 & 5.0), (3.6 & 5.2), (7.7 & 8.9), (7.2 & 8.2), (7.5 & 7.4), (5.4 & 5.2) log CFU/ml. and (7.3 & 7.5) log MPN/ml. respectively in the two Governorates. Somatic Cell Count were found (5.88 & 6.14) cells log/ml respectively in the two governorates. Milk samples were also analyzed for the presence of selected foodborne pathogens such as *E. coli* and *Klebsiella pneumoniae*. Results revealed the presence of microbial contaminants which indicates bad milk quality and requires

immediate attention as it can cause serious public health risk to consumers.

**Keywords:** Prevalence; Raw Goat's Milk; Pathogens; Safety; Quality; Somatic cell count.

#### Dept. of Medicine and Infecous Diseases

#### 556. Epidemiological Studies on Johne'S Disease in Ruminants and Crohn'S Disease in Humans in Egypt

Amr Abdel Aziz Abdel Kadder El-Sayed A. Fawzy, A. Prince, A.A. Hassan, A. Fayed, M. Zschöck, M. Naga, M. Omarg, M. Salem, A. El-Sayed

*International Journal of Veterinary Science and Medicine*, 1: 79-86 (2013) IF: 2

The correlation between Johne's disease (JD) and Crohn's disease (CD) in Egypt was investigated. A total of 371 human and 435 animal sera were collected from the same Egyptian governorates that had a known history of paratuberculosis infection and were subjected to screening for paratuberculosis using ELISA to assess the human/animal risk at a single time point. Five CD patients and five JD clinically infected dairy cattle were also included. Out of 435 animal serum samples, 196 (45.2%) were MAP-ELISA positive. Twenty three (6.1%) out of 371 human serum samples were MAP-ELISA positive, while 37 (9.9%) were positive for anti-*Saccharomyces cerevisiae* antibodies (ASCA) ELISAs. There was a very poor agreement between human MAP and ASCA ELISAs (0.036 by kappa statistics). The prevalence of MAP antibodies among humans is clearly lower than in animals. In conclusion there is an increase in Johne's disease incidence in animals and a very weak relationship between MAP and Crohn's disease in humans in Egypt.

**Keywords:** Asca; Crohn'S Disease; Egypt; Johne's disease; *Mycobacterium avium* paratuberculosis; Epidemiology.

#### 557. Genotyping of Mycobacterium Avium Field Isolates Based on Repetitive Elements

A. El-Sayed, S. Natur, Nadra-Elwgoud M.I. Abdou, M. Salem, A. Hassan and M. Zschöck

*International Journal of Veterinary Science and Medicine*, 1: 36-42 (2013) IF: 2

The economic and zoonotic importance of infections caused by *Mycobacterium avium* complex (MAC) strains in human, animals and birds are increasing. At present, few data are available about the genetic diversity of field isolates of *M. avium* subsp. *hominissuis* (MAH) and subspecies *avium* (MAA). The close relationship between human and swine isolates indicates a possible zoonotic role for such strains. In the present work 73 *M. avium* field strains isolated from feces and lymph nodes of diseased/slaughtered animals in Hesse State, Germany were investigated. Forty eight primers were used for the confirmation, differentiation and finally the genotyping of the isolates based on the presence of polymorphism of different repetitive loci. These include the Large Sequence Polymorphism (LSP), the *Mycobacterial* Interspersed Repetitive Units (MIRU) and Variable Number Tandem Repeats (VNTR). The genotyping of MAA ( $n = 27$ ) and MAH ( $n = 16$ ) isolates revealed 33 different genotypes (18 MAA, 14 MAH and 1 shared profile). The

described methods show great potential for epidemiological mapping of *M. avium* subspecies.

**Keywords:** Lspa; *Mycobacterium avium* subsp; Hominissuis; MAH; MIRU; VNTR; Germany

### 558. Molecular Characterization of *Mycobacterium Avium* Subsp. Paratuberculosis Field Isolates Recovered from Dairy Cattle in Germany

Mohamed Salem, Saleh Natur, Amr A. El-Sayed, Abdulwahed Hassan, Georg Baljer and Michael Zschöck

*International Journal of Veterinary Science and Medicine*, 1: 30-35 (2013) IF: 2

In the present work a total of 143 *Mycobacterium avium* subsp. paratuberculosis (Map) field isolates recovered from faeces of dairy cattle in Hessen State, Germany were investigated. Different Short Sequence Repeats (SSR), *Mycobacterial Interspersed Repetitive Units* (MIRU) and *Variable Number Tandem Repeats* (VNTR) were applied to classify these cattle-group field isolates into subgroups.

When combining the results obtained from SSR sequencing together with the data obtained from other genotyping PCR techniques applied in the current study, 78 different Map profiles were detected.

One profile dominates over the investigated field isolates. This profile was detected in 24 isolates (16.8%) with 11 G (SSR); amplicon size of 280 bp, 300 bp, 200 bp, 200 bp, 210 bp, 350 bp, 210 bp, 300 bp and 300 bp for the primer MIRU 2, MIRU 3, X3, Primer 3, Primer 7, Primer 25, Primer 47, 292 and VNTR 1658, respectively. One profile was represented by eight isolates. Two profiles were represented by six members each. The remaining isolates were subdivided into smaller groups (2 profiles each 4 isolates, 3 profiles each 3 isolates, 13 profiles as 2 isolates each and finally 56 profiles were represented by a single strain for each profile).

**Keywords:** S *Mycobacterium Avium* Subsp. Paratuberculosis; VNTR; SSR; John's disease; Dairy cattle; Germany.

### 559. *Mycobacterium Avium* Subspecies Paratuberculosis: An Insidious Problem for the Ruminant Industry

Mohamed Salem, Carsten Heydel, Amr El-Sayed, Samia A. Ahmed, Michael Zschöck and George Baljer

*Trop Anim Health Prod.*, 45: 351-366 (2013) IF: 1.09

*Mycobacterium avium* subspecies paratuberculosis is considered as one of the most serious problems affecting the world's ruminant industry due to its significant impact on the global economy and the controversial issue that it may be pathogenic for humans.

*M. avium* subspecies paratuberculosis is the causative agent of Johne's disease in animals and might be implicated in cases of human Crohn's disease. We provide an insight into *M. avium* subspecies paratuberculosis from some bacteriological, clinical, and molecular epidemiological perspectives.

**Keywords:** *Mycobacterium avium*; Subspecies paratuberculosis; Johne's disease; Crohn's disease.

### 560. Isolation and Identification of Main Mastitis Pathogens in Mexico

H. Castañeda Vázquez, S. Jäger, W. Wolter, M. Zschöck, M.A. Castañeda Vazquez and A. El-Sayed

*Arquivo Brasileiro De Medicina Veterinária E Zootecnia*, 65 (2): 377-382 (2013) IF: 0.269

The present work is a large epidemiological study aiming to detect the prevalence of subclinical mastitis and to investigate the major udder pathogens in Jalisco State, western Mexico. For this purpose, 2205 dairy cows, representing 33 Mexican dairy herds, were involved. Of 2205 cows, 752 mastitic animals were diagnosed and only 2,979 milk samples could be obtained for further investigation. All 2979 milk samples were subjected to California Mastitis Test (CMT) to differentiate clinical cases from subclinical ones where 1996 samples (67 %) reacted positively. Of these, 1087 samples (54.5%) came from cows suffering from clinical cases of mastitis. Bacteriological identification of the causative agents revealed the presence of a major group of pathogens including the Coagulase negative staphylococci (CNS), *S. aureus*, *S. agalactiae*, *Corynebacterium* spp. and Coliform bacteria which were detected in 464 (15.6%), 175 (5.9%), 200 (6.8%), 417 (14%) and 123 (4.1%) of the 2927 investigated quarters, 295 (15.4%), 118 (15.7%), 111 (14.8%), 227 (30.2%) and 109 (14.5%) of the 752 examined cows and in 33 (100%), 22 (66.7%), 19 (57.6%), 30 (90.1%) and 27 (81.8%) of the 33 herds involved, respectively. Other pathogens could be detected in the investigated milk samples such as *S. dysgalactiae* (0.4%), *S. uberis* (0.37%), *Bacillus* spp. (1%), *Nocardia* spp. (0.6%) and *Candida* spp. (0.1%). Meanwhile, others were present in a negligible ratio; including the *Aerococcus viridans*, and *Enterococcus* spp., *Lactococcus lactis*, *S. bovis*.

**Keywords:** Bovine Mastitis; *Corynebact* Spp; Mexico; *S. aureus*; *S. agalactiae*.

### 561. Alteration in Clinical, Hemobiochemical and Oxidative Stress Parameters in Egyptian Cattle Infected With Foot and Mouth Disease (FMD)

Mousa S. A. and Galal M. KH.

*Journal of Animal Science Advances*, 3(9): 485-491 (2013)

The current study was carried out to study alteration in clinical, hemobiochemical and oxidative stress parameters in native cattle infected with foot and mouth disease (FMD). For this purpose twenty native cattle were used, divided into two equal groups: 10 apparently healthy cattle (control group), 10 cattle with FMD. All cattle were exposed to complete physical clinical examination, blood samples were taken. Hematological analysis revealed significant increase in MCV and MCH ( $p \leq 0.001$ ); PCV ( $p \leq 0.01$ ); while significant decrease in RBCs ( $p \leq 0.001$ ) was ( $p \leq 0.001$ ) in serum level of calcium, total protein and globulin; while significant increase in serum phosphorus ( $p \leq 0.05$ ) and glucose levels ( $p \leq 0.001$ ) were observed. Nitric oxide (NO), Malondialdehyde (MDA) and DNA fragmentation percentage were significantly increased ( $p \leq 0.001$ ) in diseased cattle. However significant reduction in total antioxidant capacity ( $p \leq 0.001$ ) and albumin as biomarker for antioxidant status were detected. The highest levels of MDA and NO indicate the occurrence of oxidative stress and lipid peroxidation. In conclusions cattle affected with FMDV experienced strong

oxidative stress. So antioxidant drugs recommended during treatment of viral diseases as FMD.

**Keywords:** Clinical; Hemobiochemical; Oxidative stress; Cattle; FMD; Egypt.

### 562. Epidemiology, Diagnosis and Therapy of Theileria Equi Infection in Giza, Egypt

Fayez A. Salib, Raouf R.Youssef, Laila G. Rizk and Samer F. Said

*Veterinary World*, 6 (2): 76-82 (2013)

**Aim:** To study the prevalence of Theileria equi among horses in different age groups, both sexes, months and seasons of the year, and regions of Giza governorate. Studying the changes in the blood picture, blood chemistries, liver enzymes associated with T.equi infections in horses. Evaluating IFA and CFT at different dilutions in the serodiagnosis of T.equi infections in horses. Evaluating four anti-Theileria medication regimens (diminazine aceturate, imidocarb 7%, buparvaquone and a combination of imidocarb 7% and buparvaquone) in treatment of T.equi infections in horses.

**Materials and Methods:** Total of 149 horses were examined by clinical signs and blood smears. Forty whole blood samples from T.equi infected horses were examined to measure haemoglobin, total RBCs count and PCV. Forty serum samples from T.equi infected horses were examined to measure total bilirubin, direct bilirubin, ALT and AST enzymes. Serum samples from T.equi infected (40) and non infected (14) horses were tested by indirect fluorescent antibody test (IFA) and complement fixation test (CFT) at different dilutions. Four groups of T.equi infected horses (A,B,C,D), each group was represented by 10 horses and was separately treated with diminazine aceturate, imidocarb 7%, buparvaquone and a combination of imidocarb 7% and buparvaquone respectively.

**Results:** the prevalence of T.equi was 41.61% in totally examined horses. The prevalence was higher in males than females. The highest prevalence was among age group ranged from 5-10 years as (22.81%). The highest prevalence was in July and was recorded as (25.81%) and the disease was more prevalent in summer than winter. The highest prevalence was recorded in Nazlet-alsamman as (51.61%). Equine theileriosis was clinically characterized by fever, haemoglobinuria, oedema, anaemia and icterus. The best dilution for IFA was 1/160 where sensitivity, specificity and accuracy were the highest for this test as (98%), (92.86%) and (97.44%) respectively. The best dilution for CFT was 1/32 where sensitivity, specificity and accuracy were collectively the best as (90%), (92.86%) and (90.74%) respectively.

**Conclusion:** It was concluded that T.equi is prevalent among horses in Giza governorate, its prevalence is varied according to the age, sex of horses, months, seasons and regions. T.equi infections in horses are accompanied with changes in blood pictures, blood chemistries and liver enzymes. Both IFA and CFT could be used for the serodiagnosis of T.equi. The used four anti-Theileria medication regimens have the same ability to eradicate T.equi from the infected horses.

**Keywords:** Diagnosis; Egypt; Epidemiology, Giza; Theileria Equi; Therapy.

### 563. Fading Puppy Syndrome Associated With Toxocara Canis Infection

Fayez Awadalla Salib Awadalla

*Journal of Advanced Veterinary Research*, 3: 93-97 (2013)

Aim of this work was studying the role of Toxocara canis infection in fading puppy syndrome and evaluating its treatment. Twelve German shepherd puppies suffered from fading puppy syndrome and their dam were presented. The dead puppies (N.=8) were necropsied. On the other hand, living puppies (N.=4) and their dam were examined both clinically and parasitologically. The collected worms from necropsied puppies were parasitologically identified as Toxocara canis and their counts ranged from 48 to 75 per puppy. The live cases were treated by Flubendazole. The parasitological examinations of stool of live puppies and dam revealed eggs identified as Toxocara canis eggs and their counts ranged from 50 to 350 eggs per gram stool. Post-treatment counts of Toxocara canis worms in stool of live puppies and their dam were ranged from 13 to 79 worms per animal. The results of treatment proved the efficacy of Flubendazole for eradication of Toxocara canis. Toxocara canis considers one of the causes of fading puppy syndrome and could be cured by Flubendazole.

**Keywords:** Toxocara canis; Death; Puppy; Diagnosis; Treatment.

### 564. Hepatic Pseudo-Fasciola Infection in German Shepherd Dogs

Fayez A. Salib, Haithem A. Farghali and Nadra-Elwgoud M. I. Abdou

*Journal of Advanced Veterinary Research*, 3: 83-85 (2013)

Fasciola gigantica is liver parasite of herbivorous animals and man. It cause great economic losses in livestock animals. Tracing the literature, few reports about Fasciola gigantica infection in dogs were recorded. In this study, five German Shepherd dogs were routinely examined before vaccination by stool analysis, it revealed presence of Fasciola eggs that were counted. Our investigation depend upon counting Fasciola eggs in dogs stool daily, history of food, measuring liver enzymes and bilirubin and examining dogs liver, gall bladders and bile ducts by ultrasonography.

The results confirmed that it is Fasciola gigantica pseudo-infection where stool eggs count declined daily with stopping feeding on the Fasciola infected bovine liver and the Fasciola eggs completely disappear from stool at the 4th day. The liver enzymes and bilirubin are within the normal range. The ultrasound images of the liver, gall bladders and bile ducts of the five dogs were normal. It is concluded that a pseudo-infection with Fasciola gigantica could be happened in dogs that may confuse the Vets.

**Keywords:** Pseudo, Fasciola; Infection; Hepatic, Dogs

### 565. Monensin Toxicosis in Camels Reared in Egypt: Updating Clinical and Clinicopathological Investigations

Mousa S. A. and El-Hamamsy H. T.

*Journal of Animal Science Advances*, 3 (10): (2013)

An acute and sub acute onset of illness were reported in a camel ranch in Egypt after accidental feeding a claimed newly imported broiler finisher concentrate containing ionophore monensin sodium with concentration (100mg/kg feed). So this work was carried out to study the alterations in clinical and clinicopathological pictures in victim camels with acute illness (6) and sub acute illness (9). Clinical observations were recorded and blood and urine samples were taken from all victim camels for clinicopathological analysis. Victim camels showed signs of acute heart failure with significant increase in respiratory rate, heart rate, muscular tremors, staggering and falling with lateral recumbancy in acute cases while sub acute cases showed signs of congestive heart failure, S.C edema in the area extended from the prepuce toward umbilicus and varying degree of myoglobinuria. Clinicopathological picture showed significant elevations in PCV, AST, CPK and LDH ( $p \leq 0.001$ ), hypocalcaemia, and hyperphosphatemia i.e disturbance in Ca: P ratio. Urinalysis revealed severe myoglobinuria with chocolate brown discoloration of urine in acute toxicosis and red brown discoloration in sub acute cases. We can concluded that acute and sub acute monensin toxicosis in camels characterized by signs of heart failure, elevation in serum muscle enzymes, hemoconcentration and myoglobinuria.

**Keywords:** Monensin; Toxicity; Camels; Clinical; Clinic-Pathological; Egypt.

### 566. Sero-Prevalence of Avian Influenza in Animals and Human in Egypt

A. El-Sayed, A. Prince, A. Fawzy, Nadra-Elwgoud, M.I. Abdou, L. Omar, A. Fayed and M. Salem

*Pakistan Journal of Biological Sciences*, 16: 524-529 (2013)

In opposite to most countries, avian influenza virus H5N1 became endemic in Egypt. Since, its first emerge in 2006 in Egypt, the virus could infect different species of birds and animals and even human. Beside the great economic losses to the local poultry industry in Egypt, the virus infected 166 confirmed human cases, 59 cases ended fatally. In the present study, the persistence of the avian influenza in the Egyptian environment was studied. For this purpose, serum samples were collected from human, cattle, buffaloes, sheep, goat, horses, donkeys, swine, sewage rats, stray dogs and stray cats. The sera were collected from Cairo and the surrounding governorates to be examined for the presence of anti-H5N1 antibodies by Haemagglutination Inhibition Test (HI) and ELISA test. Clear differences in the seroprevalence were noticed among different species and also between the results obtained by both techniques indicating the difference in test accuracy. The present data indicate wide spread of the H5N1 virus in the Egyptian environment.

**Keywords:** Avian influenza; Egypt; ELISA; Equine; H5N1; Hi Test.

### 567. Seroprevalence of Caprine Arthritis Encephalitis Virus among Three Different Goat Breeds

Diea Gamal Aboelhassan

*Int. J. of Biology Pharmacy and Allied Science*, 2 (11): 2058-2064 (2013)

Seroprevalence of caprine arthritis-encephalitis virus (CAEV) in Qassim Region, Saudi Arabia, was determined for the first time in

three different breeds of goats at different age groups using competitive ELISA kit (cELISA). The overall seroprevalence was 10.75 % (86/800), with seropositivity 19.33% (58 /300) in Saanen goats, 8.00 % (16/200) in Damascus goats and 4.00 % (12/300) in Aardi goats. Seroprevalence was significantly different ( $P < 0.05$ ) between the three goat breeds. Also, age group over 25 months (17.93 %) showed significantly higher seroprevalence ( $P < 0.05$ ) than those of 15 – 24 months old (5.73 %) in all goat breeds. Bucks had a significantly higher ( $P < 0.05$ ) frequency of infection 25.76 % than does (9.40 %).

**Keywords:** Caprine Arthritis–Encephalitis Virus; Seroprevalence; Saanen Goats; Damascus goats; Aardi goats; Competitive elisa, Monoclonal antibodies

### Dept. of Microbiology

### 568. Antimicrobial Resistance and Virulence-Associated Genes of Salmonella Enterica Subsp. Enterica Serotypes Muenster, Florian, Omuna and Noya Strains Isolated From Clinically Diarrheic Humans in Egypt

Kamelia M. Osman, Sherif H. Marouf and Nayerah Alatfeehy

*Microbial Drug Resistance*, 19 (5): 370-377 (2013) IF: 2.364

Four serotypes recovered from clinically diarrheic human faecal samples (Salmonella Muenster, Salmonella Florian, Salmonella Omuna and Salmonella Noya) were investigated for the presence of 11 virulence genes (*invA*, *avrA*, *ssaQ*, *mgtC*, *siiD*, *sopB*, *gipA*, *sodC1*, *sopE1*, *spvC*, and *bcfC*) and their association with antibiotic resistance. The 4 Salmonella serotypes lacked virulence genes *gipA* and *spvC*. Resistance to 7 of the 14 antimicrobials was detected. The frequency of resistance, to lincomycin and streptomycin (100% of the Salmonella Muenster [2/5], Salmonella Florian [1/5], Salmonella Omuna [1/5], and Salmonella Noya [1/5] isolates), chloramphenicol (100% of the Salmonella Muenster [2/5] and Salmonella Florian [1/5] isolates) and trimethoprim-sulfamethoxazole (100% of the Salmonella Florian [1/5] and Salmonella Omuna [1/5] isolates) was an outstanding feature. With the rest of the antibiotics, the four Salmonella serotypes exhibited a great diversity in their resistance patterns. Overall, the four Salmonella serotypes were resistant to more than one antimicrobial. The antimicrobials to which the Salmonella Muenster, Salmonella Florian, and Salmonella Omuna isolates were resistant, contributed to five different antimicrobial resistance profiles. The virulence associated genes *invA*, *ssaQ*, *siiD*, *sopB*, and *bcfC* genes were 100% associated with certain antimicrobial resistance phenotypes (streptomycin and lincosamide) not recorded previously, and secondly, the presence of *invA*, *avrA*, *ssaQ*, *mgtC*, *siiD*, *sopB*, and *bcfC* was associated with resistance to chloramphenicol. The results of this study will help in understanding the spread of virulence genotypes and antibiotic resistance in Salmonella in the region of study.

**Keywords:** Salmonella Omuna

### 569. Salmonella Enterica Isolated From Pigeon (Columba Livia) in Egypt

Osman K. M., Mehrez M., Erfan A.M., Nayerah A.

*Foodborne Pathog Dis.*, 10 (5): 481-483 (2013) IF: 2.283

Understanding the association between human salmonellosis cases and animal sources is an important epidemiological factor needed to successfully control the spread of the infection within communities. To determine the extent to which pigeons might harbor this pathogen and pose a risk to the human population in Egypt, we screened pigeons in Cairo for the presence of *Salmonella* relevant to public health and antimicrobial susceptibility testing. The isolated serotypes recovered from pigeon fecal samples were the following: *Salmonella* serotype Typhimurium, Braenderup, and Lomita. All strains were multiresistant. Our success in the isolation of *Salmonella* ser. Typhimurium, Braenderup, and Lomita has important implications because they are a significant cause of food poisoning and enteric fever in humans.

**Keywords:** *Salmonella*.

#### **570. The Distribution of Escherichia Coli Serovars, Virulence Genes, Gene Association and Combinations and Virulence Genes Encoding Serotypes in Pathogenic E. coli Recovered From Diarrhoeic Calves, Sheep and Goat.**

Osman KM, Mustafa AM, Elhariri M, Abdelhamed GS.

*Transbound Emerg Dis*, 60 (1): 69-78 (2013) IF: 2.096

Ruminants, especially cattle, have been implicated as a principal reservoir of one of the enterovirulent *Escherichia coli* pathotypes. The detection of the virulence genes in diarrhoeic calves and small ruminants has not been studied in Egypt. To determine the occurrence, serotypes and the virulence gene markers, stx1, stx2, hlyA, FliC(h7), stb, F41, K99, sta, F17, LT-I, LT-II and eae, rectal swabs were taken from diarrhoeic calves, sheep and goats and subjected to bacterial culture and PCR. The *E. coli* prevalence rate in the diarrhoeic animals was 63.6% in calves, 27.3% in goat and 9.1% in sheep. The 102 *E. coli* strains isolated from the calves, goat and sheep were 100% haemolytic non-verotoxigenic and fitted into the Eagg group. The isolates belonged to seven O serogroups (O25, O78, O86, O119, O158, O164 and O157). The eae gene was detected in six of the strains isolated from the calves. The 102 bovine, ovine and caprine *E. coli* strains isolated in this study were negative for stx1, stx2, F41, LT-I and FliC(h7) genes. The highest gene combinations were found to occur in the form of 24/102 isolates (23.5%) that carried the F17 gene predominantly associated with eaeA, hlyA, K99 and Stb genes in the calves, while the hlyA, K99 and Sta were the only genes found to be in conjunction in both calves and goats (6/102; 5.9% each). Our data show that in Egypt, large and small ruminants could be a potential source of infection in humans.

**Keywords:** Ruminants

#### **571. Emerging of Coagulase Negative Staphylococci As A Cause of Mastitis in Dairy Animals: An Environmental Hazard**

Jakeen K. El-Jakee, Noha E. Aref, Alaa Gomaa, Mahmoud D. El-Hariri, Hussein M. Galal, Sherif A. Omar, Ahmed Samir  
*International Journal of Veterinary Science and Medicine*, 1: 74-78 (2013) IF: 2

In Egypt, knowledge about the coagulase negative staphylococci (CNS) involved in mastitis in animals is limited. CNS have emerged

to be pathogens causing intramammary infections in Egyptian dairy herds. Therefore, the current study was conducted to investigate the occurrence of CNS in dairy ruminants (cattle, buffaloes, sheep and goats). A total of 884 quarter milk samples were investigated to study the prevalence of CNS among mastitic and subclinically mastitic cows, buffalo-cows, ewes and does in Egypt. Identification of the isolates was achieved using API staph test and polymerase chain reaction (PCR). CNS were isolated from the examined subclinical mastitic cattle, buffaloes, sheep and goats with percentages of 16.6%, 59.4%, 50% and 55.6%, respectively. *Staphylococcus xylosum*, *Staphylococcus cohnii*, *Staphylococcus haemolyticus*, *Staphylococcus hominis*, *Staphylococcus saprophyticus*, *Staphylococcus chromogenes*, *Staphylococcus lentus*, *Staphylococcus lugdunensis* and *Staphylococcus simulans* were identified as CNS that recovered from the examined milk samples. The CNS as mastitis-causing agents could not be neglected as they can cause substantial economic losses.

**Keywords:** Dairy ruminants; Mastitis; CNS; Egypt.

#### **572. A Simple Technique for Long-Term Preservation of Leptospires**

Ahmed Samir and Momtaz O. Wasfy

*Journal of Basic Microbiology*, 53: 299-301 (2013) IF: 1.198

The viability of six serovars of *Leptospira* spp. was studied after long storage at 70 °C. The bacteria were either preserved in Ellinghausen–McCullough–Johnson–Harris (EMJH) liquid growth medium or in sheep blood added as a cryoprotectant. The viability of the strains was observed on a monthly basis by dark-ground microscopy over a period of 20 months at 70 °C. Addition of sheep blood was not significantly advantageous, since leptospires that were stored in EMJH showed a slight increase in number after recovery. The results suggest a very simple and useful technique for long-term preservation of such *Leptospira*.

**Keywords:** Long-term; Preservation; *Leptospira*.

#### **573. Antibiotic Resistance of Clostridium Perfringens Isolates From Broiler Chickens in Egypt**

K.M. Osman and M. Elhariri

*Rev. Sci. Tech. Off. Int. Epiz.*, 32 (3): 841-850 (2013) IF: 0.69

The use of antibiotic feed additives in broiler chickens results in a high prevalence of resistance among their enteric bacteria, with a consequent emergence of antibiotic resistance in zoonotic enteropathogens. Despite growing concerns about the emergence of antibiotic-resistant strains, which show varying prevalences in different geographic regions, little work has been done to investigate this issue in the Middle East. This study provides insight into one of the world's most common and financially crippling poultry diseases, necrotic enteritis caused by *Clostridium perfringens*. The study was designed to determine the prevalence of antibiotic resistance in *C. perfringens* isolates from clinical cases of necrotic enteritis in broiler chickens in Egypt. A total of 125 isolates were obtained from broiler flocks in 35 chicken coops on 17 farms and were tested using the disc diffusion method. All 125 isolates were resistant to gentamicin, streptomycin, oxolinic acid, lincomycin, erythromycin and spiramycin. The prevalence of resistance to other antibiotics was also high: rifampicin (34%), chloramphenicol (46%),



spectinomycin (50%), tylosin-fosfomycin (52%), ciprofloxacin (58%), norfloxacin (67%), oxytetracycline (71%), flumequine (78%), enrofloxacin (82%), neomycin (93%), colistin (94%), pefloxacin (94%), doxycycline (98%) and trimethoprim-sulfamethoxazole (98%). It is recommended that *C. perfringens* infections in Egypt should be treated with antibiotics for which resistant isolates are rare at present; namely, amoxicillin, ampicillin, cephradine, fosfomycin and florfenicol.

**Keywords:** Antibiotic resistance; Broiler chickens; *Clostridium perfringens*; Egypt; Middle East; Necrotic enteritis.

#### 574. Protective Efficacy of Salmonella Local Strains Representing Groups B, C, D and E in A Prepared Polyvalent Formalin Inactivated Oil Adjuvant Vaccine in Layers

Mona I. El-Enbaawy, Zakia A.M. Ahmed, M.A. Sadek and H.M. Ibrahim

*International Journal of Microbiological Research*, 4 (3): 288-295 (2013)

Salmonellosis is one of the most important bacterial diseases affecting poultry. Its importance is derived from the loss in productivity in affected birds and the hazard it causes for public health. Vaccination is the best mean for controlling salmonellosis in birds. In the present study, the immunizing and protective efficacy of local strains (*S. Typhimurium*, *S. Infantis*, *S. Enteritidis* and *S. Meleagridis*) and imported ones (*S. Typhimurium* and *S. Enteritidis*) in a prepared polyvalent and bivalent formalin inactivated oil adjuvant vaccines had been studied. A total of 150, six-weeks old SPF Lohman layer chickens were divided into 3 groups; 50 chickens each. The 1 group was vaccinated with the polyvalent locally prepared vaccine, the 2 group was vaccinated with the imported bivalent vaccine and the 3 group was kept unvaccinated as a control group. The three groups were challenged with virulent *S. Typhimurium*, *S. Infantis*, *S. Enteritidis* and *S. Meleagridis* strains (10 CFU/ml of each) 1 ml orally, 3 weeks post boosting of the vaccines. The degree of protection was assessed according to the severity of the clinical signs, the mortality and fecal shedding of the challenged organisms. Blood samples were collected weekly and humoral immune response was measured against *Salmonella* strains using micro-agglutination test (MAT) and ELISA. In Conclusion: the locally prepared polyvalent vaccine induced higher protection rates in challenge test with reduced fecal shedding and higher antibody response compared with the imported bivalent one.

**Keywords:** *Salmonella typhimurium*; *Salmonella infantis*; *Salmonella enteritidis*; *Salmonella meleagridis*; Vaccines; Layers.

#### 575. Antibiotic Resistance Patterns of S. Agalactiae Isolated From Mastitic Cows and Ewes in Egypt

J. El-Jakee, H.S. Hableel, M. Kandil, O.F. Hassan, Eman A. Khairy and S.A. Marouf

*Global Veterinaria*, 10 (3): 264-270 (2013)

Streptococcal mastitis causes great economic losses in dairy industries all over the world. For humans, *S. agalactiae* is responsible for persistent disease in adults and neonates. The present study investigated the prevalence of streptococci in mastitic cows and ewes as well as, the antibiotic resistance

patterns of *Streptococcus agalactiae* isolates. A total of 570 milk samples collected from cow (n=300) and ewes (n=270) were examined. *Streptococcus* species were isolated from cows (55 %) and ewes (50.4%). *S. agalactiae*, *S. dysgalactiae*, *S. uberis*, *S. pyogenes* and *S. pneumoniae* were isolated from the examined cow samples with incidence of 19.3, 17, 15.3, 2.7 and 0.7% respectively. Also, *S. agalactiae*, *S. dysgalactiae*, *S. uberis*, *S. pyogenes* and *S. pneumoniae* were isolated from the examined ewes with incidence of 20.4, 15.9, 10.4, 2.6 and 1.1% respectively. The objective of this work was to characterize *S. agalactiae* isolated from mastitic cows and ewes by RAPD and antibiotic sensitivity test to detect the diversity of the isolates. *S. agalactiae* isolated from dairy cows and ewes was sensitive to ampicillin, penicillin and cefotaxime. Resistant to vancomycin, chloramphenicol, tetracycline and clindamycin was recorded among the examined *S. agalactiae* isolated from cows and ewes. The data indicated the existence of different RAPD patterns among the multidrug resistant *S. agalactiae* isolates.

**Keywords:** Mastitis Ewes Cows; *Streptococci* Antibiotics; RAPD-PCR.

#### 576. Characterization of Clostridium Perfringens Isolated From Poultry

J. El-Jakee, Nagwa S. Ata, Mona A. El Shabrawy, Azza S.M. Abu Elnaga, Riham H. Hedia, N.M. Shawky and H.M. Shawky

*Global Veterinaria*, 11 (1): 88-94 (2013)

*Clostridium perfringens* organisms have an economic concern in poultry production. The goal of this study was to characterize *C. perfringens* isolated from poultry farms. Intestinal and liver samples were collected from apparently healthy and diarrheic chickens (n≤120), ducks (n≤90) and turkeys (n≤90) aged 1-10 days old. *C. perfringens* was isolated from 33.3, 33.3 & 42.2% of apparently healthy chickens, ducks and turkeys respectively and 75, 66.7 & 62.2% from diarrheic chickens, ducks and turkeys respectively. Toxigenic isolates were typed using dermonecrotic test and PCR. Out of the 157 isolates 107 (68.2%) produced toxins. Toxigenic *C. perfringens* isolates collected from chickens were type A (53.8%) and type D (15.4%). While turkeys isolates were belonged to type A (38.3%), type D (19.1%) and type C (10.6%). The majority of toxigenic ducks isolates were type A (48.9%) followed by type C (17.8%). Diversity of 16 *C. perfringens* isolates were investigated using random amplified polymorphic DNA (RAPD). Also a trial was done to describe the *C. perfringens* toxins by SDS-PAGE. The results illustrated the diversity of *C. perfringens* isolates and the prevalence of these pathogens in poultry production sites.

**Keywords:** Sheep Blood Agar Egg Yolk Agar Cooked Meat Media Dna Fingerprint Nagler's Test

#### 577. Prozone effect and False Negative Leptospirosis Microscopic Agglutination Test in Experimental Immunized Mice

Rehab Elhelw, Mahmoud Hatem, Mona El-Enbaawy and Ahmed Elsanousi

*Global Veterinaria*, 11 (5): 534-540 (2013)

Leptospirosis is a world-wide bacterial disease affecting many mammals, including man and has been considered to be the

zoonosis with widest geographical distribution in the world. MAT and ELISA are the most serological tests used for seroprevalences of susceptible infected mammalian populations world-wide. The detection of positive leptospirosis clinical cases depending on isolation of leptospira, which is affected by the technical difficulties in isolating leptospire from carrier animals or from clinical/pathological material. So, the serological detection of positive cases of leptospira is the most laboratory investigations method for leptospira infection. In this study, Mice experimentally immunized with a three different antigenic preparations (boiled, sonicated, successive frozen and thawed), pathogenic strain of *Leptospira interrogans* serovar Canicola evoked the production of high antibody titer in the immunized mice. All the examined sera collected from 45- tested mice produced positive result with ELISA test. In microscopic agglutination test [MAT], the most of serum samples with high IgM produced false negative results [Prozone Effect], which it was more for 1:50, 1:100 and 1:200 sample dilutions. This phenomenon was correlated with increased antibody titres in the acute and convalescence phases post-infection.

**Keywords:** Leptospira; Prozone effect; Experimental immunization; Mice; ELISA; MAT.

#### 578. Rapid Method for Detection of *Staphylococcus Aureus* Enterotoxins in Food

J. El-Jakee, S.A. Marouf, Nagwa S. Ata, Eman H. Abdel-Rahman, Sherein I, El-Moez, A.A. Samy and Walaa E. El-Sayed

*Global Veterinaria*, 11 (3): 335-341 (2013)

Food-borne bacteria have the most concern in public health and food safety. *S. aureus* food poisoning is one of the most economically important food-borne pathogen worldwide. In the present study a total of 250 food samples (milk samples n=50, white soft cheese samples n=50, yoghurt samples n=50, meat and meat products n=50 and chicken products n=50) were investigated bacteriologically to detect the occurrence of enterotoxigenic *S. aureus* among the examined food samples. Out of 250 examined food samples, 127 isolates were identified as *Staphylococcus* species (50.8%). 32 *S. aureus* isolates were identified from the examined samples with an incidence of 12.8%.

The highest isolation rate was observed in raw milk samples (56%) followed by yoghurt samples (22%), chicken products (6%), white soft cheese samples and pasteurized milk samples (4% each) then meat and meat products samples (2%). Using PCR, out of 32 *S. aureus* isolated from the examined food samples 10 isolates could produce enterotoxins. Protein profile analysis of 8 enterotoxigenic *S. aureus* strains were analyzed by Sodium Dodecyl Sulphate PolyAcrylamide Gel Electrophoresis (SDS-PAGE).

All enterotoxigenic isolates had a band at 26 to 29 kDa. Direct detection of *S. aureus* enterotoxins were investigated among 6 samples (3 raw milk samples, 2 yoghurt samples and one chicken product sample) using mPCR. It could be concluded that *S. aureus* producing enterotoxins present in the food samples.

**Keywords:** Food PCR; SDS-PAGE S; *Aureus Staphylococci* Enterotoxins (Ses).

#### Dept. of Obstetrics, Reproduction and Artificial Insemination

#### 579. Critical Role of Hyaluronidase-2 during Preimplantation Embryo Development.

Waleed F.A. Marei, Mazdak Salavati and Ali A. Fouladi-Nashta

*Molecular Human Reproduction*, 19(9): 590-599 (2013)

IF: 4.524

Biological functions of hyaluronan (HA) depend on its molecular size. Small size HAs are known to regulate cell proliferation; however, the expression of HA synthases (HASs) and hyaluronidase-2 (HYAL2) and their role during early embryo development have not been previously identified. In this paper, we have shown by immunostaining that HA is produced by bovine in vitro-produced embryos at all stages of early development to blastocyst. Addition of HA-synthesis inhibitor (4-methylumbelliferone; 4MU) to in vitro embryo culture inhibited blastocyst formation. HASs HAS2 and HAS3 mRNA were expressed at all stages of embryo development; however, relative mRNA expression of HAS2 was significantly reduced as the embryos develop to the blastocyst stage. HAS1 was detected during 2- and 4-cell stages but was barely detectable in subsequent stages. HYAL2 mRNA expression was detected in oviducts at the early luteal phase but was only detected in the embryos at morula and blastocyst stages (Day 6 and 7 post-fertilization). Addition of HYAL2 to embryo culture media at Day 2 post-fertilization increased phosphorylated mitogen-activated protein kinases (MAPK1 and 3) in the embryos and improved development to the blastocyst stage and increased embryo cell numbers. Addition of an anti-CD44 antibody or a MAPK inhibitor (U0126) abrogated the positive effects of HYAL2 on blastocyst rates. In conclusion, we demonstrate that the expression of different HAS genes and HYAL2 in bovine embryos varies according to the stage of development and that the supplementation of HYAL2 in vitro mimics oviductal conditions and is shown to improve the blastocyst rate and embryo quality, an effect which requires CD44 activity and MAPK signalling.

**Keywords:** CD44; HYAL2; IVF Media, Mapk, Blastocyst

#### 580. L-Carnitine Supplementation During Vitrification of Mouse Oocytes at the Germinal Vesicle Stage Improves Preimplantation Development Following Maturation and Fertilization in Vitro

Adel R. Moawad, Seang Lin Tan, Baozeng Xu, Hai Ying Chen and Teruko Taketo

*Biology of Reproduction*, 88: 1-8 (2013) IF: 4.027

Oocyte cryopreservation is important for assisted reproductive technologies (ART). Although cryopreservation of metaphase II (MII) oocytes has been successfully used, MII oocytes are vulnerable to the damage inflicted by the freezing procedure. Cryopreservation of germinal vesicle stage oocytes (GV-oocytes) is an alternative choice; however, blastocyst development from GV-oocytes is limited largely due to the need for in vitro maturation (IVM). Herein, we evaluated the effects of L-carnitine (LC) supplementation during vitrification and thawing of mouse GV-oocytes, IVM, and embryo culture on preimplantation development after in vitro fertilization (IVF). We first compared

the rate of embryonic development from the oocytes that had been collected at the GV stage from three mouse strains, (B6.DBA)F1, (B6.C3H)F1, and B6, and processed for IVM and IVF, as well as that from the oocytes matured in vivo, i.e. ovulated (IVO). Our results demonstrated that the rate of blastocyst development was the highest in the (B6.DBA)F1 strain and the lowest in the B6 strain.

We then supplemented the IVM medium with 0.6 mg/ml LC. The rate of blastocyst development improved in the B6 but not in the (B6.DBA)F1 strain. Vitricification of GV-oocytes in the basic medium alone reduced the rate of blastocyst development in both of those mouse strains. LC supplementation to the IVM medium alone did not change the percentage of blastocyst development. However, LC supplementation to both vitricification and IVM mediasignificantly improved blastocyst development to the levelscomparable with those obtained from vitricified/thawed IVOocytes in both of the (B6.DBA)F1 and B6 strains. We conclude that LC supplementation during vitricification is particularly efficient in improving the preimplantation development from the GV-oocytes that otherwise have lower developmental competence in culture.

**Keywords:** B6 Mouse Strain, Blastocyst, GV Oocytes; IVF; IVM; L-Carnitine, Vitricification

### 581. Regulation of the Hyaluronan System in Ovine Endometrium By Ovarian Steroids

Kabir A Raheem, Waleed F Marei, Karen Mifsud, Muhammad Khalid, D Claire Wathes and Ali A Fouladi-Nashta  
*Reproduction*, 145(5): 491-504 (2013) IF: 3.555

In this study, we investigated steroid regulation of the hyaluronan (HA) system in ovine endometrium including HA synthases (HAS), hyaluronidases, and HA receptor-CD44 using 30 adult Welsh Mountain ewes. Eight ewes were kept intact and synchronized to estrous (day 0). Intact ewes were killed on day 9 (luteal phase; LUT; n=5) and day 16 (follicular phase; FOL; n=3). The remaining ewes (n=22) were ovariectomized and then treated (i.m.) with vehicle (n=6) or progesterone (n=8) for 10 days, or estrogen and progesterone for 3 days followed by 7 days of progesterone alone (n=8). Estradiol and progesterone concentrations in plasma correlated with the stage of estrous or steroid treatment. Our results showed trends ( $P<0.1$ ) and statistically significant effects ( $P<0.05$ , by t-test) indicating that LUT had lower HAS1 and HAS2 and higher HAS3 and CD44 mRNA expression compared with FOL.

This was reflected in immunostaining of the corresponding HAS proteins. Similarly, in ovariectomized ewes, progesterone decreased HAS1 and HAS2 and increased HAS3 and CD44, whereas estradiol tended to increase HAS2 and decrease CD44. Sometimes, HAS mRNA expression did not follow the same trend observed in the intact animals or the protein expression. HA and its associated genes and receptors were regulated by the steroids.

In conclusion, these results show that the level of HA production and the molecular weight of HA in the endometrium are regulated by ovarian steroids through differential expression of different HAS both at the gene and at the protein levels.

**Keywords:** Hyaluronan; Progesterone; Has; Hyal2; Cd44; Ovine endometrium; Ovariectomy.

### 582. Production of Good-Quality Blastocyst Embryos Following Ivf of Ovine Oocytes Vitricified at the Germinal Vesicle Stage Using A Cryoloop

Adel R. Moawad, Jie Zhu, Inchul Choi, Dasari Amarnath, Wenchao ChenA and Keith H. S. Campbell

*Reproduction, Fertility and Development*, 25: 1204-1215(2013) IF: 2.583

The cryopreservation of immature oocytes at the germinal vesicle (GV) stage would create an easily accessible, non-seasonal source of female gametes for research and reproduction. The present study investigated the ability of ovine oocytes vitricified at the GV stage using a cryoloop to be subsequently matured, fertilised and cultured in vitro to blastocyst-stage embryos. Selected cumulus-oocyte complexes obtained from mature ewes at the time of death were randomly divided into vitricified, toxicity and control groups. Following vitricification and warming, viable oocytes were matured in vitro for 24 h. Matured oocytes were either evaluated for nuclear maturation, spindle and chromosome configuration or fertilised and cultured in vitro for 7 days. No significant differences were observed in the frequencies of IVM (oocytes at the MII stage), oocytes with normal spindle and chromatin configuration and fertilised oocytes among the three groups. Cleavage at 24 and 48 h post insemination was significantly decreased ( $P,0.01$ ) in vitricified oocytes. No significant differences were observed in the proportion of blastocyst development between vitricified and control groups (29.4% v. 45.1%, respectively). No significant differences were observed in total cell numbers, the number of apoptotic nuclei or the proportion of diploid embryos among the three groups. In conclusion, we report for the first time that ovine oocytes vitricified at the GV stage using a cryoloop have the ability to be matured, fertilised and subsequently developed in vitro to produce good-quality blastocyst embryos at frequencies comparable to those obtained using fresh oocytes.

**Keywords:** Oocyte, Vitricification.

### 583. Protective Effects of Antioxidants on Linoleic Acid-Treated Bovine Oocytes During Maturation and Subsequent Embryo Development.

Wael A. Khalil, Waleed F.A. Marei, Muhammad Khalid

*Theriogenology*, 80: 161-168 (2013) IF: 2.082

Linoleic acid (LA; n-6, 18:2) is the most abundant polyunsaturated fatty acid in the ovarian follicular fluid and is known to inhibit oocyte maturation and its subsequent development. In the present study, we investigated how its effects on cumulus cell expansion, oocyte nuclear maturation, and blastocyst development are altered by supplementation of the media with vitamin E (VE; 100  $\mu$ M) and glutathione peroxidase (GPx; 1  $\mu$ M) either alone or in combination, and whether it has any effect on the mRNA expression of GPx1, GPx4, or superoxide dismutase (SOD2) in the bovine cumulus oocyte complexes (COCs). LA supplementation of the culture media significantly ( $P\leq 0.05$ ) reduced the percentage of COCs exhibiting full cumulus cell expansion and the percentage of oocytes reaching metaphase II stage, and lowered the blastocyst rate compared with controls. And these inhibitory effects were associated with a reduction in the relative mRNA expression of GPx1 and SOD2 but not of GPx4 compared with controls.

However, VE and GPx, both alone and in combination, completely abrogated the inhibitory effects of LA on nuclear maturation of oocytes and blastocyst rate but failed to do so for cumulus cell expansion. In conclusion, these data suggest that the detrimental effects of LA on oocyte developmental competence are mediated, at least in part, by a reduction in GPx1 and SOD2 mRNA expression. Moreover, VE and GPx may provide protection to most of the inhibitory effects of LA

**Keywords:** Linoleic acid; Antioxidants; Oocyte development.

#### **584. Effect of Cytochalasin B Pretreatment on Developmental Potential of Ovine Oocytes Vitrified at the Germinal Vesicle Stage**

Adel R. Moawad, Jie Zhu, Inchul Choi, Dasari Amarnathan and Keith H.S. Campbell

*Cryoletters*, 34: 634-644 (2013) IF: 0.837

Oocyte cryopreservation remains a challenge in most mammalian species because of their sensitivities to chilling injuries. Relaxation of the cytoskeleton during vitrification may improve post-thaw viability and pre-implantation embryo development. The aim of this study was to investigate the effect of cytochalasin B (CB) pre-treatment before vitrification on viability, frequencies of in vitro fertilisation (IVF) and subsequent development of ovine cumulus-oocyte complexes (COCs) vitrified at the germinal vesicle (GV) stage using cryoloop. COCs obtained at slaughter were randomly divided into two groups and incubated with or without 7.5 µg/mL CB for 60 min. Oocytes from each group were then vitrified using a cryoloop or used as toxicity and controls. Oocytes were then matured, fertilised, and cultured in vitro for 7 days. Viability following vitrification and warming, fertilisation events following IVF and subsequent preimplantation embryo development were evaluated. No significant differences were observed in survival rates between CB treated and non-treated oocytes in both vitrified and toxicity groups. Frequencies of fertilisation were increased in CB-vitrified group (oocytes pre-treated with CB before vitrification) than those vitrified without CB pre-treatment (57.0% vs 40.7%). Cleavage was significantly lower ( $P < 0.05$ ) in vitrified and CB-vitrified oocytes at both 24 hpi (12.5% vs 9.1%) and 48 hpi (25.0% vs 16.2%) than in other groups. Based on the numbers of cleaved oocytes, (48 hpi), 16.1% and 18.8% of the cleaved embryos developed to blastocysts in both vitrified and CB-vitrified groups. These values did not differ significantly from those obtained in CB-control group (37.8%). No significant differences were observed in mean cell numbers per blastocyst between all groups. In conclusion, pre-treatment of ovine GV oocytes with cytochalasin B as cytoskeleton stabilizer before vitrification increased frequencies of in vitro fertilisation and subsequently resulted in production of good quality late stage pre-implantation embryos following IVF.

**Keywords:** Oocyte, Vitrification, Ovine

#### **585. Follicular Fluid Composition in Relation To Follicular Size in Pregnant and Non-Pregnant Dromedary Camels (Camelus Dromedaries)**

K.H. El-Shahat, A.M. Abo-El Maaty and A.R. Moawad

*Animal Reproduction*, 10: 16-23 (2013)

The aim of this study was to evaluate the effects of the reproductive status of female dromedary camels (pregnant vs. non-pregnant) on the chemical composition, hormonal profile and antioxidant capacity of follicular fluid collected from different sized ovarian follicles during the breeding season. One hundred ovaries were collected at slaughterhouse from fifty female dromedary camels. The ovaries were collected in pairs from each animal and allocated into two groups according to the reproductive status of the females; 25 pairs were obtained from pregnant females and 25 pairs were obtained from non-pregnant animals. The follicles on each ovary were categorized according to their diameter into three categories; small (1-3 mm), medium (4-9 mm) and large (10-20 mm). Follicular fluid (FF) aspirated from each follicle category from each pair of ovaries was analyzed. The results showed that the average number of follicles per ovary was greater ( $P < 0.05$ ) in the ovaries obtained from non-pregnant females compared to those collected from pregnant ones ( $6.4 \pm 1.2$  vs.  $3.6 \pm 0.9$ , respectively). Progesterone concentrations were significantly higher in the follicular fluid collected from all follicle categories in pregnant animals than those obtained from non-pregnant animals. Glucose concentrations were higher ( $P < 0.05$ ) in the follicular fluid collected from large follicles in the non-pregnant group ( $64.9 \pm 6.1$  mg/dl) than those obtained from the same follicle category in the pregnant ovaries ( $45.4 \pm 4.0$  mg/dl). Concentrations of malondialdehyde (MDA) were higher ( $P < 0.05$ ) in the FF collected from small, medium and large follicles in pregnant ovaries than non-pregnant ones. In conclusion, these data indicate that FF composition differs according to the reproductive status of the female. In pregnant camels, the presence of the corpus luteum on the ovaries could play an important role not only in the process of follicle growth and development, but also in the concentrations of biochemical metabolites and hormonal profiles in the FF of dromedary camels

**Keywords:** Camel, Corpus Luteum, Follicular Fluid, Ovary, Follicular Size; Pregnancy.

#### **Dept. of Medicine Parasitology**

#### **586. Genetic Characterization of Viable Toxoplasma Gondii Isolates from Stray Dogs from Giza, Egypt**

A.M. El Behairy, S. Choudhary, L.R. Ferreira, O.C.H. Kwok, M. Hilali, C. Su and J.P. Dubey

*Veterinary Parasitology*, 193 (1-3): 25-29 (2013) IF: 2.381

Stray dogs are considered as sentinels in the epidemiology of *Toxoplasma gondii* because they are carnivores and eat variety of foods, including garbage. In the present study, tissues and sera of 51 stray dogs (*Canis familiaris*) from Giza, Egypt were examined for *T. gondii* infection. Sera were examined for antibodies to *T. gondii* by the modified agglutination test (MAT); 50 of 51 (98%) were seropositive with titers of 20 in four, 40 in four, 80 in one, 100 in eight, 200 in 17, 400 in 11, 800 or higher in five. Hearts of 43 seropositive dogs were bioassayed in mice. Viable *T. gondii* was isolated from 22 dogs; these isolates were designated TgDogEg1 to TgDogEg22. DNA isolated from cell culture derived tachyzoites of 22 isolates was genotyped using 10 PCR-restriction fragment length polymorphism markers (SAG1, SAG2, SAG3, BTUB, GRA6, c22-8, c29-2, L358, PK1, and Apico). The results revealed three genotypes and one mixed infection. The three genotypes are ToxoDB PCR-RFLP #2 (type III, four isolates), #3 (type II variant, 11 isolates), #20 (six isolates), 1 mixed infection. These results revealed the dominance of clonal



type II, III and ToxoDB #20 lineages of *T. gondii* in stray dogs from Giza, Egypt.

**Keywords:** *Toxoplasma Gondii*; Dog (*Canis Familiaris*); Egypt; Prevalence; Genotype.

### 587. Experimental Transmission of *Sarcocystis Muris* (Apicomplexa: Sarcocystidae) Sporocysts From A Naturally Infected Cat (*Felis Catus*) to Immunocompetent and Immunocompromised Mice

Y. M. Al-Kappany, S. A. Abu-Elwafa, M. Hilali, B. M. Rosenthal, D. B. Dunams and J. P. Dubey

*Journal of Parasitology*, 99(6): 997-1001(2013) IF: 1.321

Cats serve as definitive hosts for zoonotic *Toxoplasma gondii*, a protozoan that threatens human reproductive health, but they also excrete sporocysts of related protozoan that pose no known human health risk. Here we provide the first definitive evidence for natural infection with the enzootic parasite *Sarcocystis muris*, one such enzootic parasite. Sporulated *Sarcocystis* sp. Sporocysts were found in rectal contents of an adult feral cat (*Felis catus*) in Giza, Egypt. After these sporocysts were orally inoculated into 2 Swiss Webster mice, sarcocysts were found to have developed in skeletal muscles 114 days later. As observed through transmission electron microscopy, the cyst wall corresponded to Type 1, and the parasitophorous vacuolar membrane had tiny outpocketing of blebs (<200 nm thick) that were not invaginated into the interior of the cyst; these structures were identical to the sarcocyst wall described for a Costa Rican isolate of *S. muris* that has served as an experimental model for nearly 4 decades. Two parasite-free cats fed sarcocyst-infected muscles developed patent infections; fully sporulated sporocysts (10–11 × 7.0 µm) were found in the lamina propria of small intestines of cats killed 6 and 7 days postinoculation (PI). Interferon gamma gene knockout (KO) mice were orally inoculated with sporocysts from experimentally infected cats, and their tissues were examined histologically; sarcocysts were found in 5 KO mice killed 87, 115, 196, 196, 196 days PI, but no stages were seen in 5 KO mice 10, 14, 14, 18, and 39 days PI. Bradyzoites were released from intramuscular sarcocysts of a KO mouse killed 115 days PI and orally inoculated into 5 KO mice. No stage of *Sarcocystis* was found in any organ (including intestinal lamina propria) of KO mice killed 4, 8, 81, 190, and 190 days PI, confirming that the definitive host is required to complete the life cycle even in the case of immunodeficient mice. This is the first confirmation of *S. muris* infection in a naturally infected cat anywhere.

**Keywords:** Experimental transmission; *Sarcocystis muris*.

### 588. Serological Survey of Dogs From Egypt for Antibodies to Leishmania Species

Alexa C. Rosypal, Sha'nae S. Bowman, Samuel A. Epps, A. M. El Behairy, M. Hilali, and J. P. Dubey

*J. Parasitol.*, 99 (1): 170–171 (2013) IF: 1.321

Leishmaniasis is an insect-transmitted parasitic disease with a worldwide distribution. *Leishmania* spp. infections cause a broad spectrum of clinical signs, ranging from skin lesions to fatal visceral disease. Dogs are a major reservoir host for visceral leishmaniasis in humans. While the disease is endemic in the Middle East and North Africa, little is known concerning canine *Leishmania* spp. infections in Egypt. Accordingly, blood samples

were collected from 50 stray dogs in Giza, Egypt. Canine sera were tested for antibodies to visceralizing *Leishmania* spp. by commercial immunochromatographic strip assays based on recombinant antigen K39. Antibodies to *Leishmania* spp. were found in 5 of 50 (10%) of dogs tested from Egypt. Results from this study indicate that stray dogs are exposed to visceralizing *Leishmania* species in Egypt.

### 589. A Contribution in Ectoparasitic Infection and Its Control in Cultured *Oreochromis Niloticus* in Egypt

Marzouk M. S. M, Mahdy O. A1, El-Khatib N. R. and Yousef N.S. I

*American J. of Research Communication*, 1(12): 326-338 (2013)

A total of 420 *Oreochromis niloticus* live fish specimens were collected from some farms fishes, (Central Lab for Aquaculture Research (CLAR) Abbassa, Sharkia and private fishes from Kalubia & Giza governorates), at different seasons. Inspected fishes were recovered infection with 4 genera of protozoan including; (*Trichodina heterodontata*, *Trichodina mutabilis*), *Chilodonella hexasticha*, *Myxobolus ellipsoids* and *Epistylis* spp.) with infection rates of 42.7%, 17.9%, 8.8% and 31.2%, respectively. Infection with *Cichlidogyrus halli* (monogenea), encysted metacercariae (digenetic larvae) and *Lamproglana monodi* (crustacea) were recorded in the examined with rates of 22.7%, 12.4% and 17.6%, respectively. Moreover, mixed infection with *Trichodina*, *Epistylis* and encysted metacercariae (EMC) were detected with rate of 3.6% in the examined fishes. The main clinical signs of infected fish were slimy dark skin with signs of asphyxia, detached scales with frayed fins with presence of hemorrhagic lesions on the skin, fins, and gills with congested gills. Treatment trials on *O. niloticus* fishes with mixed natural infected *Trichodina*, *Epistylis* and EMC by using three products were used; 1<sup>st</sup> Chemical treatment with Peroxygen compound®, surfactant organic acids and buffer systems; the 2<sup>nd</sup> natural product Humate® (humic, ulmic and fulvic acids) and the 3<sup>rd</sup> Probiotic product as (*Bacillus thuringiensis* kurstak). The experimental treatment result revealed that Peroxygen® compounds at concentration (2ppm/40 min. & 5ppm/20min.) and at concentration (1000ppm/30 min. & 1500 ppm /15min.) were sufficient completely eradicates *Trichodina* spp. & *Epistylis* but did not affect on EMC in different doses. However, the natural product as Humate® was proved to be the most effective product at concentration 3ppm/ 30 min. to eradicate *Trichodina*, *Epistylis* and at the same concentration for 60 min. was to be killing EMC infection. Hematological parameters of infected fish showed increase significant in RBCs & hemoglobin ( $P \leq 0.005$ )  $2.2 \pm 0.03 \times 10^6/\mu l^6$  and ( $P \leq 0.001$ )  $6.7 \pm 0.01 g/dl$ .

**Keywords:** *O. niloticus*; External parasites, Clinical signs; Treatment; Peroxygen® compounds; Humate®; Probiotic product; Hematological parameters.

### 590. An Investigation into Marine Ciliates with Establishment of a New Genus, *Phyllopharyngean Americana* Nov. Gen., Nov. Spec.

Magdy M. Fahmy, Nisreen Ezz El-Din M., Khaled M. El-Dakhly, Mona Khattab and Tokuma Yanai

*Asian Journal of Animal and Veterinary Advances*, 8 (4): 663-669 (2013)



Marine fish contain a large diversity of parasitic ciliates. Among those, cyrtophorids constitute large populations and many species of these ciliates have not been yet identified. Therefore, morphology and infraciliature of a new marine cyrtophorid ciliate, *Phyllopharyngean americana* g. nov. sp. nov., which was isolated from the skin and gills of striped bass and the gills of white perch fish collected from the Chesapeake bay, Maryland, USA. Fish were collected and ciliates were isolated and examined using the protargol silver impregnation technique. The ciliate was characterized by burrowing motion of the live specimens, reniform shape and measured 30.2x22.9 (18-41x14-30)  $\mu$ m in vivo. The right side was ciliated and convex, while the left one was almost straight. There were 10 ridges on the dorsal surface and nine to eleven right ventral somatic kineties curved anteriorly. Two ovoid macronuclei and a single micronucleus were present. Two contractile vacuole pores detected between the second and the third right kineties and short transverse fibers deriving from the left kineties towards the middle of the body were present. Morphogenetic observations revealed cystic and precystic stages in the infected fish. It is concluded that, these data provide an evidence for the taxonomic placement of *Phyllopharyngean americana* as a new genus (nov. g.) and new species (nov. sp.) in the Cyrtophorida.

**Keywords:** *Phyllopharyngean americana*; Marine ciliates.

#### Dept. of Pathology

##### 591. Nutritional Impact of Cauliflower and Broccoli against Development of Early Vascular Lesions Induced by Animal Fat Diet (Biochemical and Immunohistochemical Studies)

Amany, A. Salem, Faten. F. Mohammed and Samiha, A. Alloush  
*Life Science Journal*, 10(4): 2496-2509 (2013) IF: 0.165

This study was performed to evaluate the nutritional effect of cauliflower and broccoli against development vascular histological alterations and related changes in biochemical parameters induced by feeding of rats on animal fat diet. The 24 adult male rats (105 $\pm$ 5g) were randomly divided into 4 groups, negative control, animal fat diet (positive control), animal fat diet supplemented either with 5% fiber of cauliflower or broccoli for third and fourth group respectively. Estimation of serum glucose, lipid profile, liver and kidney function were performed and histopathological and immunohistochemical studies on blood vessels, liver and kidney were carried out. Results revealed that cauliflower improves the lipid profile than broccoli. Both plants significantly lowering of serum total lipid, total cholesterol, HDL-C, LDL-C and VLDL-C compared with positive control, improvement of liver and kidney function were achieved in the cauliflower and broccoli supplemented dietary groups. Histopathological examination showed alleviation of vascular histopathological alterations that were observed in animal fat diet fed group including focal intimal thickening and vacuolation of tunica media with strong positive expression of vascular endothelial growth factor (VEGF) in smooth muscle cells comprising vascular tunica media these alterations were markedly ameliorated in cauliflower then broccoli group. Conclusion: ameliorative effect of cauliflower and broccoli against development of changes in lipid profile and vascular pathology were attributed in partly to lowering the serum level of total lipid, total cholesterol, HDL-C, LDL-C and VLDL-C and decrease the

expression of VEGF in smooth muscle cells of blood vessel wall.

**Keywords:** Broccoli; Cauliflower; Fiber; Lipid profile; Vascular histopathology; Vascular endothelial growth factor expression (VEGF).

##### 592. Antiviral Competence of Broad-Spectrum Antiinfective Drug Artesunate against Bovine Herpesvirus-1

Mohamed K. EL- Bayoumy, Khaled A. Abdelrahman, Sherein S.A. Elgayed, Ahmad M. Allam and Samira S. Taha

*International Journal of Basic and Applied Virology* 2(2): 6-13 (2013)

An in-vitro and in-vivo evaluation of the antiviral activity of Artesunate (ART) as a natural antiviral agent against Bovine Herpes Virus-1 (BoHV-1) and compared its activity in-vitro against Ribavirin. In-vitro evaluation was done on the MDBK cell culture system. Artesunate was able to reduce the release of the virus which was obvious in dropping of the titer of the released virus from cell culture system. Regarding Ribavirin, it showed an antiviral activity on the BoHV-1 but with lower response than that of Artesunate. In-vivo evaluation, three groups of rabbits were used as a laboratory animal's model. The clinical signs of the rabbits and histopathological examination were done on lungs collected from rabbits which were treated with Artesunate, showed a noticeable antiviral activity response against BoHV-1, while those infected with BoHV-1 without Artesunate treatment showed pneumonia and bad general health condition. However, molecular detection by the gel-based PCR was able to detect BoHV-1 in the lung tissues of both groups.

**Keywords:** Bovine Respiratory Disease (Brd) Cattle Mortality Bronchopneumonia Infectious Bovine Rhinotracheitis Infectious Pustular Vulvovaginitis

##### 593. New Methods for the Control of Lesser Grain Borer, *Rhyzopertha Dominica*

Hussein A. Kaoud, Sherein Saeid, Ahmed R. EL-dahshan, Ahmed M. El-Behary

*International Journal of Engineering and Innovative Technology (IJEIT)*, 3: 285-289 (2013) IF: 1.9

The aim of this work was evaluation of the efficacy of entomopathogenic fungi and new natural superoxide water (Envirolyte-Egypt) to control the lesser grain borer, *Rhyzopertha dominica* (Coleoptera: Bostrichidae). For this purpose: (1) isolated *Trichoderma album* was evaluated [Individual solutions of 0 (untreated control, water only), 10, 102, 103, 104 and 107 spores .ml<sup>-1</sup> of the strain of fungus /100 g corn grains and poultry ration were used]. (2) Fogging solutions of 0 (untreated control, water only), 1:100 and 1:250 of Envirolyte-Egypt /100 g corn grains and poultry ration were used. *Trichoderma album* caused 20 % mortality within 7 days post spraying at the lowest concentration and 100% mortality at the highest concentration of the spores at 7 days post spraying. *Trichoderma album* proved to be fatal against the lesser grain borer, *Rhyzopertha dominica*. Envirolyte - Egypt caused 40% mortality within 7 days post spraying at the lowest concentration and 80% mortality at the highest concentration. Envirolyte-Egypt has potential effect on *Rhyzopertha dominica*.

**Keywords:** Index-biological control; Entomopathogenic fungi; Envirolite-Egypt; Rhyzopertha dominica.

#### Dept. of Pharmacology

##### 594. Matrix enhancement effect: A blessing or a curse for gas chromatography?—A review

Md. Musfiqur Rahman, A.M. Abd El-Aty, Jae-Han Shim

*Analytica Chimica Acta*, 801: 14-21 (2013) IF: 4.387

The matrix enhancement effect in gas chromatography (GC) has been a problem for the last decade and results in unexpected high recovery. Most efforts, including the use of different types of injectors/matrix simplification procedures, and further clean-up associated with removing this effect has focused on equalizing the response of the standard in the solvent and matrix. However, after eliminating the matrix enhancement effect, the sensitivity of GC remained unchanged. But, GC sensitivity can be increased by utilizing this matrix effect originating from a matrix-matched standard. Very few studies have highlighted utilizing the matrix effect but have rather advocated eliminating it. Analyte protectants (3-ethoxy-1,2-propanediol, gulonolactone and sorbitol) have been introduced as an alternative for GC–mass spectroscopy (GC–MS) (not examined for other GC detectors), as they equalize the response without removing the matrix effect, and, hence, increase sensitivity. Versatile applications of analyte protectants are not observed in practice. The European guidelines recommend the use of matrix-matched standard calibration for residue measurements. As a result, numerous applications are available for matrix-matched standards that compensate for the matrix effect. Moreover, the matrices (among them pepper leaf matrix) act as a protectant for thermolabile analytes in some cases. A lower detection limit should be achieved to comply with the maximum residue limits. Therefore, the matrix enhancement effect, which is considered a problem, can play an important role in lowering the detection limit by increasing the transfer of analyte from the injection port to the detector.

**Keywords:** Gas Chromatography; Matrix Effect; Sensitivity; Analyte Protectants; Signal Enhancement; Thermal Protection

##### 595. Cellular Influx, Efflux, and Anabolism of 3-Carboranyl Thymidine Analogs: Potential Boron Delivery Agents for Neutron Capture Therapy

Elena Sjuvarsson, Vijaya L. Damaraju, Delores Mowles, Michael B. Sawyer, Rohit Tiwari, Hitesh K. Agarwal, Ahmed Khalil, Sherifa Hasabelnaby, Ayman Goudah, Robin J. Nakkula, Rolf F. Barth, Carol E. Cass, Staffan Eriksson and Werner Tjarks

*The Journal of Pharmacology and Experimental Therapeutics*, 347: 388-397 (2013) IF: 3.891

3-[5-{2-(2,3-Dihydroxyprop-1-yl)-o-carboran-1-yl} pentan-1-yl] thymidine (N5-2OH) is a first generation 3-carboranyl thymidine analog (3CTA) that has been intensively studied as a boron-10 ( $^{10}\text{B}$ ) delivery agent for neutron capture therapy (NCT). N5-2OH is an excellent substrate of thymidine kinase 1 and its favorable biodistribution profile in rodents led to successful preclinical NCT of rats bearing intracerebral RG2 glioma. The present study explored cellular influx and efflux mechanisms of N5-2OH, as well as its intracellular anabolism beyond the monophosphate level. N5-2OH entered cultured human CCRF-CEM cells via

passive diffusion, whereas the multidrug resistance-associated protein 4 appeared to be a major mediator of N5-2OH monophosphate efflux. N5-2OH was effectively monophosphorylated in cultured murine L929 [thymidine kinase 1 ( $\text{TK1}^+$ )] cells whereas formation of N5-2OH monophosphate was markedly lower in L929 ( $\text{TK1}^-$ ) cell variants. Further metabolism to the di- and triphosphate forms was not observed in any of the cell lines. Regardless of monophosphorylation, parental N5-2OH was the major intracellular component in both  $\text{TK1}^+$  and  $\text{TK1}^-$  cells. Phosphate transfer experiments with enzyme preparations showed that N5-2OH monophosphate, as well as the monophosphate of a second 3-carboranyl thymidine analog [3-[5-(o-carboran-1-yl)pentan-1-yl]thymidine (N5)], were not substrates of thymidine monophosphate kinase. Surprisingly, N5-diphosphate was phosphorylated by nucleoside diphosphate kinase although N5-triphosphate apparently was not a substrate of DNA polymerase. Our results provide valuable information on the cellular metabolism and pharmacokinetic profile of 3-carboranyl thymidine analogs.

**Keywords:** Cellular Influx; Efflux; Anabolism; 3-Carboranyl Thymidine Analogs; Neutron Capture Therapy

##### 596. Feasibility and Application of An Hplc/Uvd To Determine Dinotefuran and Its Shorter Wavelength Metabolites Residues in Melon With Tandem Mass Confirmation

Md. Musfiqur Rahman, Jong-Hyoun Park, A.M. Abd El-Aty, Jeong-Heui Choi, Angel Yang, Ki Hun Park, Md. Nashir Uddin Al Mahmud, Geon-Jae Im, Jae-Han Shim

*Food Chemistry*, 136: 1038-1046 (2013) IF: 3.334

A new analytical method was developed for dinotefuran and its metabolites, MNG, UF, and DN, in melon using high-performance liquid chromatography (HPLC) coupled with an ultraviolet detector (UVD). Due to shorter wavelength, lower sensitivity to UV detection, and high water miscibility of some metabolites, QuEChERS acetate-buffered version was modified for extraction and purification. Mobile phases with different ion pairing or ionisation agents were tested in different reverse phase columns, and ammonium bicarbonate buffer was found as the best choice to increase the sensitivity of target analytes to the UV detector. After failure of dispersive SPE clean-up with primary secondary amine, different solid phase extraction cartridges (SPE) were used to check the protecting capability of analytes against matrix interference. Finally, samples were extracted with a simple and rapid method using acetonitrile and salts, and purified through C18SPE. The method was validated at two spiking levels (three replicates for each) in the matrix. Good recoveries were observed for all of the analytes and ranged between 70.6% and 93.5%, with relative standard deviations of less than 10%. Calibration curves were linear over the calibration ranges for all the analytes with  $r^2 \geq 0.998$ . Limits of detection ranged from 0.02 to 0.05  $\text{mg kg}^{-1}$ , whereas limits of quantitation ranged from 0.06 to 0.16  $\text{mg kg}^{-1}$  for dinotefuran and its metabolites. The method was successfully applied to real samples, where dinotefuran and UF residues were found in the field-incurred melon samples. Residues were confirmed via LC–tandem mass spectrometry (LC–MS/MS) in positive-ion electrospray ionisation ( $\text{ESI}^+$ ) mode.

**Keywords:** Dinotefuran; Metabolites; Hplc–Uvd; Matrix Interaction; Spe Clean-Up.

### 597. Quantifying fenobucarb residue levels in beef muscles using liquid chromatography–tandem mass Spectrometry and Quechers Sample Preparation

Ki Hun Park, Jeong-Heui Choi, A.M. Abd El-Aty, Md. Musfiquir Rahman, Jin Jang, Ah-Young Ko, Ki Sung Kwon, Hee Ra Park, Hyung Soo Kim, Jae-Han Shim

*Food Chemistry*, 138: 2306-2311 (2013) IF: 3.334

This paper describes a comparison of the properties of the three versions of the QuEChERS method (quick, easy, cheap, effective, rugged and safe) – the original (unbuffered), acetate-buffered, and citrate-buffered methods – for the determination of fenobucarb residues in beef muscles via liquid chromatography–electrospray ionisation tandem mass spectrometry (LC–ESI+–MS/MS). The recovery results were good for all the versions; however, the acetate-buffered version gave higher and more consistent recoveries for fenobucarb than the other versions. Performance characteristics, such as linearity, accuracy, and precision were determined. Matrix-matched standard calibration was used for quantification, obtaining recoveries in the range of 83.7–93.4% with relative standard deviations of <5%, at two spiking levels: 10 and 40 µg/kg. The limits of detection (LOD) and quantification (LOQ) were estimated to be 1.5 and 5 µg/kg, respectively. Finally, the method was applied to the analysis of 15 market samples, and no residues were found over the limit of quantification. The method developed was found able to determine the analyte with satisfactory intensity and accuracy.

**Keywords:** Beef Muscles; Carbamate; Fenobucarb; Lc–Ms/Ms; Residue analysis.

### 598. Simple Multiresidue Extraction Method for the Determination of Fungicides and Plant Growth Regulator in Bean Sprouts Using Low Temperature Partitioning and Tandem Mass Spectrometry

Soon-Kil Cho, A.M. Abd El-Aty, Ki Hun Park, Jong-Hyounk Park, M.E. Assayed, Yang-Mo Jeong, Young-Seok Park and Jae-Han Shim

*Food Chemistry*, 136: 1414-1420 (2013) IF: 3.334

A simple multiresidue analytical method is developed for the simultaneous determination of carbendazim (CB), thiabendazole (TB), and 6-benzyl aminopurine (6-BA) in bean sprouts. The samples were extracted with acetonitrile followed by partitioning at -80 °C for 5–10 min. A YMC C8 column was used to separate the analytes before being qualitatively and quantitatively determined by liquid chromatography–electrospray ionization tandem mass spectrometry (LC–ESI–MS/MS) in positive ion mode using multiple reaction monitoring (MRM). The matrix-matched calibration curves showed good linearity in the range 0.01–1.0 mg/kg with correlation coefficients in excess of 0.998. The mean recoveries were in the range of 80.4–96.3% at 0.1 and 0.5 spiked levels, and the relative standard deviations (RSDs) were in the range of 0.5–7.6%. The limits of quantifications (LOQ) were in the range of 0.005–0.01 mg/kg. The method was successfully applied to 90 samples (among which 45 were organic) collected from a commercial bean sprout production house throughout the city. Except for 6-BA, the rest of the analytes had values lower than their LOQs. In sum, carbendazim, thiabendazole, and 6-BA were extracted in a single step, and no

steps for clean-up or concentration of the extracts were needed. The current method can be used for sensitive and accurate determination and confirmation of residues in bean sprout samples.

**Keywords:** Bean sprouts; Plant growth regulator; Fungicides; Multiresidue analysis; Tandem mass spectrometry.

### 599. Analysis of Kresoxim-Methyl and Its Thermolabile Metabolites in Korean Plum: An Application of Pepper Leaf Matrix as a Protectant for GC Amenable Metabolites

Md. Musfiquir Rahman, Jong-Hyounk Park, A. M. Abd El-Aty, Jeong-Heui Choi, Soon-Kil Cho, Angel Yang, Ki Hun Park and Jae-Han Shim

*Journal of Separation Science*, 36: 203-211 (2013) IF: 2.591

A new method was developed for kresoxim-methyl (parent compound) and its two thermolabile metabolites, BF 490-2 and BF 490-9, in Korean plum, introducing pepper leaf matrix as a natural analyte protectant for GC-amenable metabolites using a GC-electron capture detector. Samples were extracted with a simple and rapid method using a mixture of ethyl acetate–n-hexane (1:1) and salts, and purified via SPE. Due to the elution gap between parent compound and metabolites in the SPE cartridge and matrix interference, kresoxim-methyl was isolated separately from its metabolites. An optimized amount of pepper leaf matrix (0.25 g/mL) was added to the metabolites prior to each injection. Calibration curves were linear over the concentration ranges with coefficient of determination ( $r^2$ ) ≥ 0.999. The method was validated in triplicate at two fortification levels, giving recoveries ranging between 74.3 and 101.4%, and RSDs less than 5%. The LOD and LOQ were 0.015 and 0.05 mg/kg, respectively. The method was successfully applied to real samples where kresoxim-methyl residues were detected in field-incurred plum samples. Residues were confirmed using GC–MS.

**Keywords:** Gc-Electron capture detector; Korean Plum; Kresoxim-methyl; Leaf Matrix; Thermolabile metabolites.

### 600. Application of Hollow-Fiber-Assisted Liquid-Phase Microextraction to Identify Avermectins in Stream Water Using Ms/Ms

Jong-Hyounk Park, A. M. Abd El-Aty, Md. Musfiquir Rahman, Jeong-Heui Choi and Jae-Han Shim

*Journal of Separation Science*, 36: 2946-2951 (2013) IF: 2.591

In this study, a hollow-fiber-assisted liquid-phase microextraction (HF-LPME) technique coupled with LC–MS/MS is described to detect avermectins (abamectin, ivermectin, moxidectin, and doramectin) in stream water. An Accurel polypropylene membrane was used as the hollow fiber, and dihexyl ether was used as the extraction solvent. The optimal extraction conditions for HF-LPME were 4 cm fiber length, 45 min extraction time, 200rpm, and 1 min desorption time with methanol as the desorption solvent. The linear range was 0.15–100 ng/mL ( $r^2$  = 0.994–0.998), and the LOD and LOQ were 0.15 and 0.5 ng/mL, respectively. Recovery rates were determined at 1, 5, and 10 ng/mL, and the results were in the range of 80.1 to 93.7%. The intraday and interday repeatability ranged from 2.8 to 8.0% and from 6.1 to 13.3%, respectively. The HF-LPME method

developed was applied to detect avermectins in stream water samples collected from 14 different sites near livestock farms located in Honam area, Republic of Korea; however, none of the samples contained avermectin residues. HF-LPME combined with a LC-MS/MS method was successfully applied for an environmentally friendly identification of avermectins in water samples. HF-LPME represents an attractive approach for conventional liquid-liquid extraction.

**Keywords:** Avermectins; Hollow-Fiber-Assisted Liquid-Phase Microextraction; Liquid Chromatography-Tandem Mass Spectrometry; Stream Water; Veterinary Medicines

#### 601. Development of an Extraction Method for the Determination of Avermectins in Soil Using Supercritical CO<sub>2</sub> Modified with ethanol and liquid chromatography-Tandem mass spectrometry

Jong-Hyounk Park, Jeong-Heui Choi, A. M. Abd El-Aty, Joon-Seong Park, Bo Mi Kim, Tae-Woong Na, Ki Hun Park, Angel Yang, Md. Musfiquir Rahman and Jae-Han Shim

*Journal of Separation Science*, 36: 148-155 (2013) IF: 2.591

The aim of the present study was to develop a multiresidue analytical method for determination of avermectins (abamectin, ivermectin, moxidectin, and doramectin) in soil samples using supercritical fluid extraction and LC-MS/MS. The optimal extraction conditions for supercritical fluid extraction were 80°C for temperature, 300 kg/cm<sup>2</sup> for pressure, 40 min as an extraction time, and 30% of a modifier ratio. The linearity of the calibration curves was excellent and yielded the correlation coefficients ( $r^2 = 0.998-0.999$ , at a range of 1.5–500 ng/g). Soil samples were fortified with known quantities of the analytes at three different concentration levels (5, 10, and 50 ng/g) and the recoveries were in the range of 82.5–96.2% with relative standard deviation values ranging between 2.1 and 7.9%. The limits of detections and limits of quantitations were 1.5 and 5 ng/g, respectively. The developed method was successfully applied to analyze avermectin residues in soil samples collected from 13 sites in the Honam area, Republic of Korea. In sum, a combination of supercritical fluid extraction and LC-MS/MS has been proven to be highly efficient as an environmentally friendly technique for the simultaneous determination of avermectins in soil samples.

**Keywords:** Avermectins; Soil; Supercritical fluid extraction; Tandem Ms/Ms.

#### 602. A Quenchers-Based Extraction Method for the Residual Analysis of Pyraclofos and Tebufenpyrad in Perilla Leaves Using Gas Chromatography: Application to Dissipation Pattern

M. N. U. Al Mahmud, Musfiquir Rahman, Tae-Woong Na, Jong-Hyounk Park, Angel Yang, Ki Hun Park, A. M. Abd El-Aty, Nilufar Nahar and Jae-Han Shim

*Biomedical Chromatography*, 27: 156-163 (2013) IF: 1.945

The objective of this work was to establish a simple extraction method for the residual analysis of pyraclofos and tebufenpyrad in Perilla leaves. A QuEChERS (quick, easy, cheap, effective, rugged and safe) method was used for extraction using ethyl acetate as an extraction solvent, and cleanup was carried out using dispersive solid-phase extraction technique. The samples were

analyzed using gas chromatography with nitrogen phosphorous detector and confirmed by gas chromatography-mass spectrometry. The linearity was excellent ( $r^2=1.0$ ) in matrix-matched calibration for both pesticides. The recoveries at two fortification levels were 80.76–95.38% with relative standard deviation lower than 5%. The limits of detection and limits of quantification were 0.01 and 0.033 mg/kg for both pesticides, respectively. The results revealed that the dissipation pattern of pyraclofos and tebufenpyrad followed first-order kinetics. The pyraclofos and tebufenpyrad residues declined to a level below the maximum residue limits within 14 day between the last application and harvesting. We suggest that pyraclofos and tebufenpyrad could be used efficiently on perilla leaves under the recommended dosage conditions.

**Keywords:** Quenchers; Pyraclofos; Tebufenpyrad; Perilla leaves; Gas chromatography; Mass spectrometry; Dissipation pattern

#### 603. Analysis of Imidacloprid and Pyrimethanil in shallot (*Allium ascalonicum*) grown under greenhouse conditions using tandem mass spectrometry: establishment of pre-harvest residue limits

Jong-Hyounk Park, Joon-Seong Park, A. M. Abd El-Aty, Md. Musfiquir Rahman, Tae-Woong Naa and Jae-Han Shim

*Biomedical Chromatography*, 27: 451-457 (2013) IF: 1.945

In this study, the original Quick, Easy, Cheap, Effective, Rugged and Safe method was used for the extraction of imidacloprid and pyrimethanil followed by a rapid clean-up through dispersive solid-phase extraction technique with primary secondary amine sorbent and magnesium sulfate in shallot. Residues were analyzed using LC-tandem mass spectrometry in positive-ion electrospray ionization mode. The limits of detection and quantification were estimated to be 0.006 and 0.02mg/kg, respectively. The samples were fortified at two different concentration levels (0.2 and 1.0mg/kg), and the recoveries ranged between 79.7 and 83.9% with relative standard deviation values < 6%. The method was successfully applied for the establishment of the pre-harvest residue limits (PHRL). The rate of disappearance of imidacloprid and pyrimethanil on shallot was described with first-order kinetics (imidacloprid,  $y^2=0.9670$ ; pyrimethanil,  $y^2= 0.9841$ ), with half-lives of 2.87 and 2.08 days, respectively. Based on the dissipation patterns of the pesticide residues, the PHRL was recommended at 7.86mg/kg for 14days (PHRL<sub>14</sub>) and 1.98mg/kg for 7days (PHRL<sub>7</sub>) before harvest for imidacloprid, and 21.64 mg/kg for days (PHRL<sub>7</sub>) and 9.28mg/kg for 4 days (PHRL<sub>4</sub>) before harvest for pyrimethanil in shallot.

**Keywords:** Imidacloprid; Pyrimethanil; Lc-Ms/Ms; Pre-harvest Residue limit; Half-life; Decline pattern.

#### 604. Determination of Alachlor Residues in Pepper and Pepper Leaf Using Gas Chromatography and Confirmed Via Mass Spectrometry with Matrix Protection

Md. Musfiquir Rahman, Hiron Moy Sharma, Jong-Hyounk Park, A. M. Abd El-Aty, Jeong-Heui Choi, Nilufar Nahar and Jae-Han Shim

*Biomedical Chromatography*, 27: 924-930 (2013) IF: 1.945

Alachlor residues were determined in pepper and pepper leaf, after 49 days of manufacturer-recommended single- and double-

dose application to the soil and plant. The samples were extracted with acetonitrile, partitioned with n-hexane, and purified through solid-phase extraction, and finally detected with a gas chromatography–microelectron capture detector. The linearity of the analytical response across the studied range of concentrations (0.05–4.0 µg/mL) was excellent, obtaining coefficients of determination ( $r^2$ ) of 0.999. Recovery studies were carried out on spiked pepper and pepper leaf samples, at two concentrations levels (0.2 and 1.0 mg/kg), with three replicates performed at each level. Mean recoveries of 73.1–109.0% with relative standard deviations of 1.3–2.3% were obtained. The method was successfully applied to field samples, and alachlor residue was found in pepper (0.02 mg/kg) and pepper leaf (0.03 mg/kg), at levels lower than the maximum residue limits (0.2 mg/kg) set by the Korea Food and Drug Administration. The field-detected residues were further confirmed with gas chromatography–mass spectrometry with the help of pepper leaf matrix protection.

**Keywords:** Alachlor; Gas chromatography; Matrix protection; Pepper and Pepper leaf.

#### 605. Isolation of Volatiles from Nigella Sativa Seeds Using Microwave-Assisted Extraction: Effect of Whole Extracts on Canine and Murine CYP1A

Xue Liu, Jong-Hyoun Park, A. M. Abd El-Aty, M. E. Assayed, Minoru Shimodae and Jae-Han Shim

*Biomedical Chromatography*, 27: 938-945 (2013) IF: 1.945

The volatile components of *Nigella sativa* seeds were isolated using microwave-assisted extraction (MAE) and identified using gas chromatography. Further investigations were carried out to demonstrate the effects of whole extracts on canine (dog) and murine (rat) cytochrome P450 1A (CYP1A). The optimal extraction conditions of MAE were as follows: 25 mL of water, medium level of microwave oven power and 10 min of extraction time. A total of 32 compounds were identified under the conditions using GC-FID and GC-MS. Thymoquinone (38.23%), p-cymene (28.61%), 4-isopropyl-9-methoxy-1-methyl-1-cyclohexene (5.74%), longifolene (5.33%),  $\alpha$ -thujene (3.88) and carvacol (2.31%) were the main compounds emitted from *N. sativa* seeds. Various extracts including pure compounds, essential oil, nonpolar partition, relatively high-polar/nonpolar partition, and polar partition extracts effectively inhibited the reaction of ethoxyresorufin O-de-ethylation, which is specified for CYP1A activity both in dog and rat. This *in vitro* data should be heeded as a signal of possible *in vivo* interactions. The use of human liver preparations would considerably strengthen the practical impact of the data generated from this study.

**Keywords:** *Nigella sativa*; Volatile compounds; Microwave-Assisted extraction; Ethoxyresorufin O-De-Ethylation; Cytochrome P450 1A; Dog and Rat.

#### 606. Single-Step Modified Quechers for Determination of Chlorothalonil in Shallot (*Allium Ascalonicum*) Using Gc-Mecd and Confirmation Via Mass Spectrometry

Md. Musfiqur Rahman, Jong-Hyoun Park, A. M. Abd El-Aty Jeong-Heui Choi, Hey Ree Bae, Angel Yang, Ki Hun Park and Jae-Han Shim

*Biomedical Chromatography*, 27: 416-421 (2013) IF: 1.945

A single extraction method was developed for chlorothalonil in shallot using gas chromatography with an electron capture detector (GC- $\mu$ ECD). Samples were extracted with single-step modified quick, easy, cheap, effective, rugged, and safe (QuEChERS) method using ethyl acetate as an extraction solvent. Significant matrix effects were observed, and the calibration curve was constructed from the matrix. The linearity of the analytical response across the studied range of concentrations (0.01–1.00 mg/L) was excellent, obtaining a correlation coefficient ( $r^2$ ) of 0.996. Recovery studies were carried out on spiked shallot blank samples, at two concentration levels (0.4 and 2.0 mg/kg) with three replicates performed at each level. Mean recoveries of 97.2–104.9% with RSDs of 1.3–2.7% were obtained. The method is demonstrated to be suitable for the determination of chlorothalonil in shallot. The dissipation rates of chlorothalonil were described using first-order kinetics, and its half-life was 2.8 days. Based on the dissipation pattern of the pesticide residues, the pre-harvest residue limit (PHRL) was also calculated. Residues were confirmed via mass spectrometry.

**Keywords:** Quechers; Chlorothalonil; Shallot; Gc-Mecd.

#### 607. Pharmacokinetics and distribution of ceftazidime to milk after Intravenous and intramuscular administration to lactating female dromedary camels (*Camelus dromedarius*)

Ayman M. Goudahand and Sherifa M. Hasabelnaby

*Journal of the American Veterinary Medical Association*, 243: 424-429 (2013) IF: 1.72

**Objective**—To determine the plasma disposition kinetics, absolute bioavailability, and milk concentrations of ceftazidime in healthy lactating female dromedary camels (*Camelus dromedarius*) following IV and IM administration of a single dose of 10 mg/kg (4.5 mg/lb). **Design**—Prospective crossover study. **Animals**—8 healthy adult lactating female dromedary camels. **Procedures**—Camels received ceftazidime (10 mg/kg) IV and IM in a crossover study design with a 15-day washout period between treatments. Plasma and milk samples were collected at predetermined times for 48 hours after drug administration and analyzed by use of high-performance liquid chromatography. **Results**—A 2-compartment open model best represented the plasma concentration-versus-time data after IV and IM administration of ceftazidime to camels. Plasma ceftazidime concentrations decreased biexponentially after IV administration with mean distribution and elimination half-lives of 0.3 hours and 2.85 hours, respectively. After IM administration, the mean maximum plasma concentration of ceftazidime was 32.43 µg/mL (1.21 hours after administration), mean elimination half-life was 3.20 hours, mean residence time was 4.84 hours, and mean systemic bioavailability was 93.72%. Distribution of ceftazidime from plasma to milk was rapid and extensive as indicated by the ratio of the area under the milk concentration-versus-time curve to the area under the plasma concentration-versus-time curve and the ratio of the maximum milk concentration to the maximum plasma concentration of ceftazidime after IV and IM administration. **Conclusions and Clinical Relevance**—Results suggested that ceftazidime may be a useful treatment for female camels with mastitis caused by susceptible microorganisms.

**Keywords:** Pharmacokinetics; Distribution; Ceftazidime; Milk; *Camelus dromedarius*.



**608. Dissipation Pattern and Pre-Harvest Residue Limit of Abamectin in Perilla Leaves**

Md. Musfiqur Rahman, Tae Woong Na & A. M. Abd El-Aty, Jong-Hyouk Park & M. N. U. Al Mahmud, Angel Yang, Ki Hun Park and Jae-Han Shim

*Environmental Monitoring and Assessment*, 185: 9461-9469 (2013) IF: 1.592

The pre-harvest residue limit (PHRL) of abamectin (abamectin B1a and B1b) in *Perilla frutescens* leaves grown under greenhouse conditions were investigated using high-performance liquid chromatography with a fluorescence detector. Samples were extracted with acetonitrile. The extract was purified through a solid phase extraction procedure. Then the purified extract was derivatized with trifluoroacetic anhydride and N-methylimidazole to form a strong stable fluorescent derivative of abamectin. Finally, derivatized abamectins were conveyed to the detector via an Atlantis C18 column, with water and methanol as a mobile phase. Calibration curves were linear over the calibration ranges with coefficients of determinants  $r^2 = 0.999$ . The limits of detection and quantification were 0.0033 and 0.01 mg kg<sup>-1</sup> for abamectin B1a and B1b, respectively. Recovery was assessed in a control matrix at two different fortification concentrations, with three replicates for each concentration. Good recoveries were obtained for the target analytes and ranged from 82.11 to 93.03 %, with relative standard deviations of less than 8 %. The rate of disappearance of total abamectin on perilla leaves for recommended and double the recommended doses was described as first-order kinetics with a half-life of 0.7 days. Using the PHRL curve, we could predict the residue level of total abamectin to be 0.92 mg kg<sup>-1</sup> at 7 days before harvest or 0.26 mg kg<sup>-1</sup> at 4 days before harvest, which would be below the provisional MRL designed by the Korea Food and Drug Administration.

**Keywords:** Abamectin; Perilla Leaves; Dissipation Pattern; Pre-Harvest Residue Limit

**609. Effect of Chronic Lead Intoxication on the Distribution and Elimination of Amoxicillin in Goats**

Ahmed M. Soliman, Ehab A. Abu-Basha, Salah A. H. Youssef, Aziza M. Amer, Patricia A. Murphy, Catherine C. Hauck, Ronette Gehring, Walter H. Hsu

*Journal of Veterinary Science*, 14 (4): 395-403 (2013) IF: 0.926

A study of amoxicillin pharmacokinetics was conducted in healthy goats and goats with chronic lead intoxication. The intoxicated goats had increased serum concentrations of liver enzymes (alanine aminotransferase and  $\gamma$ -glutamyl transferase), blood urea nitrogen, and reactivated d-aminolevulinic acid dehydratase compared to the controls. Following intravenous amoxicillin (10 mg/kg bw) in control and lead-intoxicated goats, elimination half-lives were 4.14 and 1.26 h, respectively. The volumes of distribution based on the terminal phase were 1.19 and 0.38 L/kg, respectively, and those at steady-state were 0.54 and 0.18 L/kg, respectively. After intramuscular (IM) amoxicillin (10 mg/kg bw) in lead-intoxicated goats and control animals, the absorption, distribution, and elimination of the drug were more rapid in lead-intoxicated goats than the controls. Peak serum concentrations of 21.89 and 12.19  $\mu$ g/mL were achieved at 1 h and 2 h, respectively, in lead-intoxicated and control goats. Amoxicillin bioavailability in the lead-intoxicated goats

decreased 20% compared to the controls. After amoxicillin, more of the drug was excreted in the urine from lead-intoxicated goats than the controls. Our results suggested that lead intoxication in goats increases the rate of amoxicillin absorption after IM administration and distribution and elimination. Thus, lead intoxication may impair the therapeutic effectiveness of amoxicillin.

**Keywords:** Amoxicillin; Bioavailability; Disposition; Lead intoxication; Pharmacokinetics.

**610. Antiobesity, Antioxidant and Antidiabetic Activities of Red Ginseng Plant Extract in Obese Diabetic Rats**

Mostafa Abbas Shalaby and Ashraf Abd-Elkhalik Hamouda

*Journal of Intercultural Ethnopharmacology*, 2 (3): 165-172 (2013)

**Aim:** This study aimed to investigate the effects of red ginseng extract (RGE) on adiposity index, some serum biochemical parameters and tissue antioxidant activity in obese diabetic rats.

**Methods:** Five groups of male Sprague-Dawley rats were used. Group (1) was negative control and the other 4 groups were fed on high fat-diet for 6 weeks to induce obesity. The obese rats were then rendered diabetic by intraperitoneal injection of alloxan for 5 days. Group (2) was kept obese diabetic (positive control) and the other 3 groups were orally given RGE at 100, 200 and 400 mg /kg /day, respectively, for 4 weeks. Blood samples were collected for biochemical analyses and kidneys were taken to assay of activities of antioxidant enzymes.

**Results:** oral dosage of RGE to obese diabetic rats significantly ( $P < 0.05$ ) reduced adiposity index; decreased serum levels of aspartate aminotransferase (AST), alanine aminotransferase (ALT), gamma- glutamyl transpeptidase (GGT) enzymes, total cholesterol (TC), triglycerides (TG), and low density lipoproteins (LDL-c) and improved atherogenic index. Blood glucose and leptin hormone decreased, but insulin increased by administration of RGE. It increased activities of superoxide dismutase (SOD), glutathione peroxidase (GPx) and catalase (CAT) antioxidant enzymes in kidneys tissues.

**Conclusion:** Red ginseng extract produces antiobesity, antioxidant, and antidiabetic activities in obese diabetic rats. The study suggests that red ginseng plant may be beneficial for the treatment of patients who suffer from obesity associated with diabetes.

**Keywords:** Red ginseng, obesity; Diabetes; Biochemistry; Hormones; Antioxidant.

**611. Assessment of Toxicity of Chlorpyrifos Insecticide on Fetuses and Suckling Pups of Rats**

Mostafa A. Shalaby, K. Abo-ElSooud and A.A. Hamoda

*Insight Ecology*, 2 (1): 1-7 (2013)

**Background:** The female reproductive toxicity and teratogenic risk of organophosphates had been a global concern because of the wide spread use of these compounds. Chlorpyrifos is a broad-spectrum organophosphate insecticide used extensively in agriculture and for residential pest control throughout the world.

**Material and Methods:** The developmental toxicity of chlorpyrifos on fetuses and suckling pups of rats was assessed.

Pregnant rats were divided into 5 groups (n=10); one was used as a control (received vehicle) and two groups were given orally chlorpyrifos at 5 and 10 mg kg<sup>-1</sup> b. wt. (Corresponding to 1/20 and 1/10 of LD50) from the day 6th through the 15th day of gestation. The other groups were given the same doses from the 15th day of gestation through the day 21st after delivery (weaning age). Rats were euthanized using ether anaesthetic, uteri were dissected out and fetuses were subjected to morphological, visceral and skeletal examinations.

**Results:** It was found that chlorpyrifos caused embryotoxic and teratogenic effects with growth retardation of fetuses. The observed visceral malformations included microcephaly, dilated cerebral ventricles and hypoplasia of the heart and lungs. The skeletal abnormalities were incomplete ossification of skull bones and absence of the last rib. Chlorpyrifos significantly decreased the viability, gestation and weaning indexes of fetuses. Deaths of all sulking pups were reported before the end of weaning age.

**Conclusion:** exposure to chlorpyrifos during pregnancy and lactation periods should be prohibited to avoid its teratogenic action and its lethal effect on suckling pups.

**Keywords:** Insecticides; Chlorpyrifos; Teratogenicity; Suckling pups.

#### 612. Nephroprotective Effects of Some Essential Oils against Nanobacteria- Induced Infection in Mice

K. Abo-EL-Sooud, M. M. Hashem, Mona M. E.Eleiwa and A. Q. Gab-Allaha

*Nano Science and Nano Technology: An Indian Journal Nsntaij*, 8 (2): 46-52 (2013)

The purpose of this study was to evaluate the nephroprotective effects of nine essential oils against nanobacteria-isolated from human kidney stones in Swiss mice. We found evidence of their inflammatory infiltration and accumulation in the renal tubules indicating that the kidney is a preferred site for mineralization by nanobacteria. Among all tested essential oils, dill, almond, cinnamon, sesame and olive were found to possess highly nephro-protective effect against nanobacteria-induced infection in mice.

They prevented the nanobacterial-nephro-toxicity as evidenced by a significantly reduced ( $p \leq 0.01$ ) level of serum urea and creatinine. Moreover, the nephroprotective effects of the prior oils were confirmed by a reduced intensity of renal cellular damage, as evidenced by histological findings.

Although, rocket, mint, clove and lettuce oils had no renal protective effect as the biochemical and pathological findings were significantly altered. The oils-treated sub-cultures from kidneys were negative for nanobacterial growth from dill, almond, cinnamon, sesame and olive treatments while the growth were positive for the rest of the tested oils.

In conclusion, nanobacteria may be involved in the pathogenesis of nephrolithiasis and dill, almond, cinnamon, sesame and olive oils have a protective role against nanobacteria-induced nephrotoxicity in mice.

**Keywords:** Nanobacteria; Essential Oils; Kidneys; Urolithiasis.

#### 613. Synthesis, Characterization and Evaluation of the Anticancer and Antimicrobial Activities of Some Novel Banzazole and Benzazine Derivatives

Samar Mohamed Mouneir Hafez El Yamany Wesam. S.Shehab, Naglaa. Z.H.Eleiwa and Samar.M.Mouneir

*Journal of Advances in Chemistry*, 3 (3): 252-263 (2013)

The present study was designed to synthesize and develop new useful lead compounds (some novel benzazole and benzazine derivatives) of simple structure, exhibiting optimal in vitro anticancer and antimicrobial potency. Phenylenediamine derivative 1 was condensed with dithiocarboxylic acid derivatives 2 and produced benzimidazole derivative 4. The benzotriazepines 8 and 10 were formed by the reaction of 1 with dicarbonyl derivatives followed by intermolecular coupling reaction. The synthesis of benzotriazine 12, benzotriazole 14, 17, benzimidazole 16 and benzothiadiazine 19 from compound 1 was also described. The Synthesized Compounds were characterized by Spectral Studies like IR, <sup>1</sup>H – NMR and Analysis Spectra. The title compounds were screened for their possible In vitro anticancer and antimicrobial activities. Among the synthesized compounds, some have shown promisingly remarkable activities against different cancer cell lines (MCF-7 human breast cancer cells, HepG2 human hepatocarcinoma cells and PC3 human prostate cancer cells) and moderate to high antibacterial and antifungal activities. The obtained results showed that the most active compounds could be useful as a template for future design, modification and investigation to produce more active analogs.

**Keywords:** Keywords: diamine; Benzotriazepine; Benzotriazole; Benzimidazole; Benzothiadiazine; Anticancer and antimicrobial activities.

#### Dept. of Poultry Diseases

#### 614. A Flagellated Motile Salmonella Gallinarum Mutant (SG Fla<sup>+</sup>) Elicits A Pro-Inflammatory Response From Avian Epithelial Cells and Macrophages and Is Less Virulent To Chickens

Oliveiro Caetano de Freitas Neto, Ahmed Setta, Ariel Imre, Agnes Bukovinski, Altaeb Elazomi, Pete Kaiser, Angelo Berchieri Junior, Paul Barrow and Michael Jones

*Veterinary Microbiology*, 165: 425-433 (2013) IF: 3.127

Salmonella enterica subspecies enterica serovar Gallinarum biovar Gallinarum (SG) is a non-flagellated bacterium which causes fowl typhoid, a systemic disease associated with high mortality in birds. It has been suggested that the absence of flagella in SG is advantageous in the early stages of systemic infection through absence of TLR-5 activation. In order to investigate this hypothesis in more detail a flagellated and motile SG mutant (SG Fla<sup>+</sup>) was constructed. The presence of flagella increased invasiveness for chicken kidney cells (CKC) while its presence did not alter survival in HD11 macrophages. SG Fla<sup>+</sup> induced higher levels of CXCL2, IL-6 and iNOS mRNA expression in CKC than the SG parent strain. The expression of genes responsible for immune response mediators in infected HD11 macrophages were not related to the presence of flagella. Mortality rates were lower in birds challenged with SG Fla<sup>+</sup> when compared with the SG parent. SG Fla<sup>+</sup> was recovered from caecal

contents which showed pathological changes suggestive of inflammation and suggested increased colonization ability.

**Keywords:** Cytokines; Innate Immunity; Flagella; Macrophages; Epithelial Cells; Salmonella gallinarum; Chickens.

### 615. Evaluation of the Efficacy of Feed Additives to Counteract the Toxic Effects of Aflatoxicosis in Broiler Chickens

Wafaa Abd El-Ghany Abd El-Ghany

*International Journal Animal and Veterinary Advances*, 5 (5): 171-182 (2013)

This work was designed to evaluate the efficacy of certain feed additives containing hydrated sodium calcium aluminosilicate (HSCAS) as well as a phytobiotic (turmeric powder) either singly or in combination to counteract the adverse toxic effects of aflatoxin B1 in broiler chickens. Five hundred, day-old broiler chicks were randomly divided into 5 equal groups (1-5) of 100 birds assigned to 2 replicates of 50 each. Birds of group (1) were fed on plain ration containing neither aflatoxin B1 nor treatment (blank control negative), while birds in groups 2, 3, 4 and 5 were fed on ration contaminated with aflatoxin B1 at concentration of 2.5 ppm of ration from day old till the end of the experiment (5 weeks). Chickens in group (2) were given ration contaminated with aflatoxin B1 only (control positive). Group (3) was treated with concomitant HSCAS at a concentration of 0.5%, while group (4) was fed on ration containing turmeric powder in a dose of 80 mg/kg of the ration. Chickens in group (5) were given ration containing HSCAS and turmeric powder at the recommended doses. All groups were kept under observation from day old till 5 weeks of age. Clinical signs, mortalities, gross lesions as well as zootechnical performance parameters were observed; moreover, organs body weights ratio, humoral immune response to Newcastle disease (ND) and serum biochemical variables were undertaken taken as criteria for evaluation. The results cleared that treatment of aflatoxicated birds either with HSCAS or turmeric powder even their combination induced protection from the development of signs and lesions and significant ( $P<0.05$ ) improvement of performance when compared with un-treated control group. In addition, both HSCAS and turmeric powder treatment succeeded in inducing significant ( $P<0.05$ ) amelioration of the measured organs body weights ratio, humoral immune response to ND and biochemical parameters in aflatoxicated chickens. It could be concluded that addition of HSCAS and or turmeric powder can be considered an integrated approach for the control of aflatoxicosis in broiler chickens.

**Keywords:** Aflatoxicosis; Hydrated Sodium Calcium Aluminosilicate; Poultry; Turmeric Powder

### 616. The Effect of A Combination of $\beta$ (1-3) D-Glucan and Propionibacterium Granulosum on Productive Performance and Immune Modulation of Immunocompromised and Non Immunocompromised Broiler Chickens

M. H. H. Awaad, A. M. Atta, M. A. Elmenawey, H. B. Gharib, Wafaa A. Abd El-Ghany and A. A. Nada

*Veterinary World*, 6: 31-38 (2013)

**Aim:** The effect of a specific combination of a soluble  $\beta$  (1-3) D-Glucan and Propionibacterium granulosum (Betamune) was investigated on productive performance, immune response and immune dysfunction caused by cyclophosphamide (CP) in broiler chickens.

**Materials and Methods:** Three hundred and sixty one-day-old broiler chicks were randomly allocated into four groups for 5 weeks. Betamune supplementation of 0.25 ml / L drinking water (presence or absence) for the first 7 days of age and CP (presence or absence) subcutaneous inoculation with 4 mg / chick for the first 3 days of life was done.

**Results:** Treatment of broiler chicks with Betamune improved productive performance variables as compared with the blank control birds, where there were 10 points less in cumulative feed conversion ratio and significant increase ( $P<0.05$ ) in final body weight, both intestinal length and diameter, and European production efficiency factor (EPEF). It also modulated the immune response, where there was non-significant improve in haemagglutination inhibition (HI) antibody titers against Newcastle disease (ND) virus vaccine and significant increase ( $P<0.05$ ) in phagocytic % and phagocytic index. The lesion score after ND challenge reached only 70 in  $\beta$  (1-3) D-Glucan group as compared with 80 in blank control group. The histomorphological examination of Betamune treated chickens at 5 weeks of age revealed lymphoid hyperplasia in bursal follicles, lymphoid cells of cortical portion of thymus glands and lymphoid cells in the white pulps of spleen. CP did affect bird's weight and suppressed immune system. Treatment CP suppressed birds with Betamune significantly increased ( $P<0.05$ ) final body weight, dressing weight %, giblets weight %, intestinal diameter, improved FCR (28 points less than untreated group), decreased cumulative mortality and improved EPEF. Betamune counter attacked immune dysfunction caused by CP, where there was significant increase in HI antibody titer against ND vaccine, no significant increase in phagocytic % and phagocytic index and improve in the lesion score after ND challenge (99 as compared to 133). Betamune supplementation reduced microscopic lesion scores associated with CP immune dysfunction.

**Conclusion:** It could be concluded that administration of a specific combination of soluble  $\beta$ 1.3, D-Glucan and Propionibacterium granulosum (Betamune ) to broiler chickens improved chicken zootechnical performance response variables, had a potent immunomodulatory effect (potentiated immune response), evoked their immune response and enhanced their vaccination effectiveness.

**Keywords:** Chickens; Cyclophosphamides; Propionibacterium Granulosum,  $\beta$ (1-3); D-Glucan.

### Dept. of Surgery Anesthesiology and Radiology

### 617. Regenerative Potential Following Revascularization of Immature Permanent Teeth with Necrotic Pulp

H. Tawfik, A. M. Abu-Seida, A. A. Hashem and M. M. Nagy

*International Endodontic Journal*, 46: 910-922 (2013) IF: 2.051

**Aim:** To assess the regenerative potential of immature teeth with necrotic pulps following revascularization procedure in dogs.

**Methodology:** Necrotic pulps and periapical pathosis were created by infecting 108 immature teeth, with 216 root canals in nine mongrel dogs. Teeth were divided into three equal groups

according to the evaluation period each group was further subdivided into six subgroups according to the treatment protocol including MTA apical plug revascularization protocol revascularization enhanced with injectable scaffold, MTA over empty canal. All root canals were disinfected with a triple antibiotic paste prior to revascularization with the exception of control subgroups. After disinfection, the root length, thickness and apical diameter were measured from radiographs. Histological evaluation was used to assess the inflammatory reaction, soft and hard tissue formation.

**Results:** In the absence of revascularization, the length and thickness of the root canals did not change over time. The injectable scaffold and growth factor was no more effective than a revascularization procedure to promote tooth development following root canal revascularization. The tissues formed in the root canals resembled periodontal tissues.

**Conclusion:** The revascularization procedure allowed the continued development of roots in teeth with necrotic pulps.

**Keywords:** Immature teeth; Necrotic pulp; Regeneration; Revascularization.

#### 618. Cutaneous Adenocarcinoma in a Desert Tortoise (*Gopherus Agassizii*)

Ashraf Abu-Seida and Sherein Saeid

*International Journal of Veterinary Science and Medicine*, 1: 48-50 (2013) IF: 2

This report describes the clinical and histopathological findings of a rare case of cutaneous adenocarcinoma in a 40-year-old desert tortoise. Surgical excision of the neoplasm improved the general health condition and locomotion of the tortoise although recurrence of the neoplasm had been recorded 1 year post-surgery.

**Keywords:** Adenocarcinoma; Desert tortoise; *Gopherus agassizii*.

#### 619. Clinical and Ultrasonographic Characteristics of Salivary Mucoceles in 13 Dogs

Faisal A. Torad and Elham A. Hassan

*Veterinary Radiology and Ultrasound*, 54 (3): 293-298 (2013) IF: 1.414

Salivary mucocele is one of the causes of submandibular swelling in dogs and is due to a collection of mucoid saliva that has leaked from a damaged salivary gland. The purpose of this case series report was to describe the clinical and ultrasonographic characteristics of confirmed salivary mucoceles in 13 dogs admitted to the Faculty of Veterinary Medicine at Cairo University. The final diagnosis of salivary mucocele was based on aspirate cytology for all dogs and additional surgical excision for seven dogs. For dogs admitted from 2 weeks to 1 month from the onset of clinical signs, the cervical mucocele appeared as a round echogenic structure with a large volume of central anechoic content. The wall was a clearly identified hyperechoic structure surrounding the gland. For dogs admitted between 1 to 2 months from the onset of clinical signs, the volume of anechoic material appeared less than that seen in the acute cases. The overall appearance of the salivary mucocele was heterogeneous. For dogs admitted after 2 months from the onset of clinical signs, the salivary mucocele appeared grainy or mottled, with a heterogeneous appearance and a further decrease in anechoic

content. For one dog that presented after 3 months from the onset of clinical signs, the salivary mucocele was hard on palpation and appeared hyperechoic with distal acoustic shadowing. Findings from this study indicated that ultrasonographic characteristics of salivary mucoceles in dogs vary depending on the chronological stage of the disease.

**Keywords:** Dog; Mucocele; Salivary gland; Ultrasound.

#### 620. The Effect of Different Formulations of Calcium Hydroxide on Healing of Intentionally Induced Periapical Lesions in Dogs

Ashraf Mohamed Abdel Rahman Abu-Seida

*Pakistan Veterinary Journal*, 33 (1): 48-52 (2013) IF: 1.365

The aim of the present work is to study the effect of different formulations of Ca(OH)<sub>2</sub> on healing of induced periapical lesions in dog. A total of 96 teeth with intentionally induced periapical lesions were classified according to the observation period into three groups; I, II and III (2 dogs each). Each group was subdivided into four subgroups (8 teeth each) namely; A, B, C and D which were dressed with Ca(OH)<sub>2</sub> with saline, Ca(OH)<sub>2</sub> with chlorhexidine, Ca(OH)<sub>2</sub> with iodoform and control respectively. Histopathological findings showed that the apical and periapical repair were better in subgroup A than in other subgroups in all groups. Total inflammatory cell count was significantly different between the four subgroups in group I. In both groups II and III, there was no significant difference between subgroups B and C. In conclusion, the use of saline as a vehicle for Ca(OH)<sub>2</sub> has a favorable action on periapical tissue healing in endodontically treated dogs.

**Keywords:** Calcium hydroxide; Chlorhexidine; Dogs; Iodoform; Periapical tissue; Saline.

#### Dept. of Veterinary Hygiene and Management

#### 621. Copper Intoxication in Tropical Freshwater Prawn, *Macrobrachium Rosenbergii*

Hussein Abd El-Hay ElSayed Kaoud

*International Journal of Engineering and Innovative Technology*, 3: 220-227 (2013)

The aim of this study was to investigate LC<sub>50</sub> and toxic effect of Cu<sup>2+</sup> on some defense functions of tropical freshwater prawn, *Macrobrachium rosenbergii* [including total hemocyte count (THC), hyaline cell count (HCC), and phagocytic activity] as well as survivability of the prawn. The experiments were conducted to determine LC<sub>50</sub> and the toxic effect of copper sulphate (Cu<sup>2+</sup>) on THC, HCC, phagocytic activity % and survival % for 24, 48, 72 and 96 hr exposure. The 24, 48, 72 and 96 hr LC<sub>50</sub> (nominal calculation) were 0.60, 0.55, 0.45 and 0.35 mg L<sup>-1</sup>, respectively. Survival of prawns exposed to more than 0.20 mg L<sup>-1</sup> of Cu<sup>2+</sup> was significantly (P < 0.05), reduced and resulted in great reduction in THC, HT, phagocytic activity %, and histopathological alterations in gills (hyper mucus, congestion, swelling, edema, hyperplasia, haemolymph cell infiltration as well as thickened and enlarged gill chambers & lamellar sinuses), hepatopancreas (dissolving of the hepatocytes, haemolysis, haemocytic infiltration in the interstitial sinuses, thickening and ruptures of the basal laminae) and skeletal muscles (degeneration in muscles

with infiltration and aggregations of hemocytes between them and focal areas of necrosis). Caution should be exercised against water source contamination and exposure to fertilizer and industrial pollution.

**Keywords:** Copper; *Macrobrachium rosenbergii*; Immunity; Toxicity.

## 622. Effect of Disinfectants on Highly Pathogenic Avian Influenza Virus (H5N1) in Lab and Poultry Farms

Hussein Abd ElHay ElSayed Kaoud

*International Journal of Engineering Science and Innovative Technology*, 2: 144-149 (2013)

This study was carried out in 6 layer houses at Giza province, during 2010-2011 outbreaks of high pathogenic avian influenza (HPAI) diagnosed in Egypt. The present investigation was undertaken to evaluate the virucidal activity of different disinfectants against avian influenza virus (AIV) under laboratory and field conditions. Anigen Rapid AIV Ag Test Kit was used for detection of AIV from environment and embryonated chicken's eggs (ECE). Five disinfectants were evaluated for their effectiveness against AIV contaminated premises (in vitro and vivo). They were an organic acid (Longlife 250 S), a peroxygen compound (Virkon-S)-, Glutaldehyde (Aldekol) and (TH4) - (a combination of four quaternary ammonium compounds and glutaraldehydes) and innovative Envirolite-Egypt (It contains various mixed oxidants predominantly hypochlorous acid and sodium hypochlorite). Envirolite-Egypt (1/250) and Virkon S 1% were the most effective disinfectants in killing AIV. Despite the good results obtained with Aldekol 0.5%, Longlife 250 S 0.5% and TH4 0.5% in laboratory test after 10 min, but the effect of both disinfectants on AIV infected premises was failed.

**Keywords:** Highly Pathogenic; Avian Influenza; Virucidal Activity; Disinfectants; Field Study.

## 623. Effect of Disinfectants on the Recovery, Titer and Viral RNA of Highly Pathogenic Avian Influenza Virus (H5N1)

Hussein A. Kaoud and Salah Yosseif

*International Journal of Engineering and Innovative Technology (Ijeit)*, 3: 307-311 (2013)

The present investigation was undertaken to evaluate the virucidal activity of five disinfectants; a peroxygen compound (Virkon-S), Glutaldehyde (Aldekol), an organic acid (Longlife 250 S), an innovative Disinfectant-lyte (It contains various mixed oxidants predominantly hypochlorous acid and sodium hypochlorite) and TH4 (a combination of four quaternary ammonium compounds and glutaraldehydes) against avian influenza virus (AIV) under laboratory conditions. Disinfectant-Lyte 1/250 (Envirolite-Egypt) was the most effective disinfectant in killing AIV, showed complete reduction in hemagglutinating (HA) activity) and damage of the nucleic acid (RNA) and viral protein. We report that; disinfectants are inactivating AIV by different methods. The study, however, points out that, we have to know how much damage must be done to the virus before virus infection is prevented.

**Keywords:** Disinfectant; Hemagglutinating activity; Titer; Avian influenza virus; Polymerase chain reaction.

## 624. Effect of Gingko Biloba, Dry Peppermint and Vitamin C As Anti-Stress on Broiler Welfare During Summer Heat Stress

K.G. El Iraqi, E.M. Abdelgawad, H.M. Ibrahim and A.E. El Sawe

*Global Veterinaria*, 10 (7): 770-778 (2013)

This study was conducted to evaluate the effects of anti-stress herbs (Gingko Biloba and Dry Peppermint) and vitamin C as feed additives, on behavioral parameters, productive performance, Histopathology and Hematology of broiler chickens during the summer heat stress. A total of 300 one day-old chicks of Cobb species were the subject of this study, chicks were divided into 5 dietary treatments, each consisting of 2 replication (n=10). First treatment (Control group) the chicks were fed on commercial basal diet, second group (T1), fed on the same diet enriched with 0.2 % dry peppermint, third group (T2) fed on the same diet enriched with 0.06 % Gingko biloba (GB), fourth group (T3) fed on the same diet enriched with 0.2 % dry peppermint plus 0.06% Gingko biloba (GB) and fifth group (T4) fed on the same diet supplemented with 0.05% Vitamin C. During 5 weeks experimental period, the behavioural measurements as frequency of feeding, drinking, comfort behaviour; including leg and wing stretch, preening, ground scratch, body shaking and resting behaviour were observed and recorded. Broiler performance including feed intake and body weight gain, final body weight, feed conversion ratio, dressing percentage, mortality rate, internal organs weight (gizzard, liver, heart, spleen and bursa). Hematological and Immunity parameters including antibodies titer for infectious bronchitis, Newcastle and Infectious Bursal were measured also Total erythrocyte count, Total leukocyte count, lymphocyte percentage, Hemoglobin concentration and packed cell volume. Histopathology section for bursa, spleen small and large intestine were examined. Significant differences were observed between different herbal treatments and vitamin C in ingestive behavior, comfort behaviour, feed intake, final body weight, food conversion ratio, dressing weight, dressing percentage, mortality rate, Internal organs weight and immunity. It can be concluded that Broiler welfare, productive performance and immune response of broilers against Newcastle disease, Infectious Bursal disease and Infectious Bronchitis improved through supplying broiler with Anti-stress plants like dry peppermint, Gingko Biloba as management practices during summer.

**Keywords:** Broiler; Heat stress; Herbal; Behavior.

## 625. Effects of Acute Sub-Lethal Dose of Tramadol on $\alpha_2$ -Adrenergic Receptors and Liver Histopathology in Rat

Hussein A. Kaoud, M.H. Hellal, Farag M. Malhat, Sherein Saeid, Ibtesam A. Elmawella and Ashour H. Khali

*Global Journal of Current Research*, 1(2): 70-76 (2013)

Tramadol is an atypical opioid with monoamine re-uptake inhibition properties. The aims of the current study were 1) to investigate the effects of acute oral tramadol administration (sub-lethal dose) on the binding of [ $^3$ H] RX 821002, a selective  $\alpha_2$ -



adrenergic receptor ligand, in the rat brain,<sup>2</sup>) and its pathological effect on liver of rat. The results revealed that; Tramadol (single dose), at 3 hr after dosing, induced a significant decrease in the  $\alpha_2$ -adrenergic receptors in all brain regions studied (hippocampus; cerebral cortex; thalamus). Liver histopathology revealed that: Leucocytic sinusoidal permeation, congested blood vessels in the portal tract, degeneration of some hepatocytes and vacuolation of hepatocytes.

**Keywords:** Tramadol;  $\alpha_2$ -Adrenergic receptors; Liver histopathology.

#### **626. Efficacy of Composting Poultry Mortality and Farms Wastes with Mixed Respiratory Infection Viruses H5N1 and H9N2 in Egypt**

Zakia A.M. Ahmed, H.A. Hussein, M.A. Rohaim and H.A. Abdel Rahman

*Global Veterinaria*, 11(5): 640-648 (2013)

Proper hygienic disposing of dead poultry with respiratory infection and their wastes is imperative from socioeconomic concept. Composting is one of disposing methods and represents a major goal for control and combating this infection. Collected fresh dead birds as well their litter and wastes from broiler farms high mortalities associated mixed respiratory symptoms were subjected to composting process. The avian influenza viruses (H5N1 & H9N2) were isolated and characterized phenotypically and genotypically from trachea prior subjecting to composting. Compost mix was kept in environmentally controlled composter from 1-28 days (end experiment). Monitoring thermal profile of the composting process was recorded. Failure of re-isolation and characterization of AIV (H5N1 & H9N2) in current work on days 15 confirmed the efficacy of composting poultry farms mortality and wastes with special concern to the current isolated classical AIV H5N1 and H9N2. Secured Composting potentiated microclimatic determinants for both virus strains (heat and dryness) with failure of re-characterization from field dead birds and their wastes. Composting suggested being a reliable, environmentally safe way to dispose poultry mortality and wastes infected with mixed respiratory infection viruses H5N1 and H9N2.

**Keywords:** Composting Dispose; Mixed Infection; H5N1; H9N2 Characterization.

#### **627. Efficacy of Composting Poultry Mortality and Farms Wastes With Mixed Respiratory Infection Viruses H9n2 and Ndv in Egypt**

Zakia A.M. Ahmed, H.A. Hussein and M.A. Rohaim

*Global Veterinaria*, 11 (2): 177-185 (2013)

Composting poultry mortality and farm wastes infected with mixed respiratory infection viruses one of major goals for control and combating this infection. To achieve fair level of biosecurity protocol in poultry farms infected with virus induced mortality, proper hygienic disposing is imperative from socioeconomic and health risk concept. Collected fresh dead birds, their litter and wastes from commercial flocks with high mortalities associated with mixed respiratory symptoms were subjected to composting process. Molecular characterization of avian influenza virus (H9N2) and Newcastle disease virus (H9N2 & NDV) were

recorded from cecal tonsils and trachea respectively of morbid and dead chickens before subjecting to composting.

Characterization was done by Reverse Transcriptase Polymerase Chain Reaction (RT-PCR) using specific primers targeting the matrix (M) gene, H9 gene of AIVs and fusion (F) gene of NDV were used. The (HA) hemagglutinin glycoprotein gene of H9N2 isolates were partially amplified by RT-PCR, directly sequenced.

The nucleotide and amino acid sequence analysis of the hemagglutinin gene of the characterized Egyptian viruses showed the highest similarity with one group of recent Israeli circulating strains. The Phylogenetic analysis for HA gene of H9 AIV showed the placement of the Egyptian viruses within the same lineage of H9N2 viruses that circulated in the region from 2006 especially with recent Israeli strains of G1 lineage (group B).

Failure of re-characterization of AIV (H9N2) and NDV in the current work on day 15<sup>th</sup> of composting treatment confirmed the efficacy of composting poultry farm mortalities and wastes. Composting in closed vessel (newly designed closed composter) achieved proper secure microbial activity that inactivated H9N2 AIV and NDV viruses via increased temperature and decreased moisture content of composting poultry mortality and farms wastes with no isolation and characterization of these viruses. The product suggested to be used for agronomic activities.

**Keywords:** Composting mixed infection; NDV; H9N2 AIV.

#### **628. Efficacy of Silver Nanoparticles and Activated Electro-Chemical Water as Poultry Disinfectants Against Salmonella Enteritidis**

Hussein A. Kaoud and Salah Youssef

*Global Journal of Scientific Researches*, 1(1): 8-13 (2013)

Salmonellae are commonly found in the environment and there are many instances throughout the grow-out phase in which birds can come into contact with Salmonella and other pathogens. Laboratory trial and other two separate field trials were conducted to evaluate the efficacy of various disinfectants on the isolated Salmonella enteritidis when applied to poultry house floors, as well as an innovative trial also, carried out to evaluate the efficacy of same disinfectants when they contained Ag nanoparticles. The results revealed that (1).

The following disinfectants without Ag nanoparticles: white wash, phenique, formalin, iodophors and Envirolyte-Anolyte (1/1000) for disinfection of floor plots significantly impacted Salmonella populations ( $P < 0.05$ ) (2; 3; 3; 3; 5 log<sub>10</sub> reduction, respectively) but unfortunately, failed to kill all the populations. While, Envirolyte-Anolyte (1/500) significantly reduced the population of *S. enteritidis* with a complete reduction of the population. (2) White wash and iodophores containing Ag nanoparticles showed highly significant ( $P < 0.05$ ) reduction of Salmonella populations in floor after disinfection process (5; 4 log<sub>10</sub> reduction, respectively). Interestingly, Salmonella populations completely destroyed when exposed to phenique and formalin containing Ag nanoparticles in field trial. This may be due to the ubiquitous nature of Ag nanoparticles, which are able to enhance the disinfectant power.

**Keywords:** Salmonella, Ag Nanoparticles; Envirolyte-Anolyte, Disinfectants.

### 629. Efficacy of Some Aquaculture Disinfectants Enhanced By Silver

Hussein A. Kaoud, Sayed N. Abou Elgheit, Eman Ismael and Salah Yosseif

*The Journal of Veterinary Science, 114: 227-234 (2013)*

In this study, three aquaculture disinfectants were evaluated alone and when enhanced by silver nanoparticles as well as a novel disinfectant (Envirolyte-Anolyte) for their efficacy against three common species of aquatic bacteria, *F. enterococci*, *Ps. Putida* and *Flavobacterium columnare*. The results revealed that, Envirolyte-Anolyte (1\500) and other disinfectants containing Ag nanoparticles (Virkon-S, 1% and Glutaraldehyde, 2%) were very effective against *Fecal enterococci*, *Ps. Putida* and *Flavobacterium columnare*, killing all bacteria within 1 min (*Fecal enterococci*, *Ps. Putida*) and 5 min (*Flavobacterium columnare*) of contact time, respectively. Formalin containing Ag nanoparticles was effective after 5 min of contact time against *Fecal enterococci*, *Ps. Putida* and *Flavobacterium columnare*.

**Keywords:** *F. Enterococci*; *Ps. Putida* and *Flavobacterium Column.*

### 630. In Vitro Evaluation the Disinfectant Efficacy of Silver Nanoparticles and Envirolite-Anolyte for the Control of Flavobacterium columnare

Hussein A. Kaoud, Sherein Saeid and AbouElgheit

*Global Journal of Current Research, 1: 10-15 (2013)*

An experiment was performed to evaluate the in vitro efficacy of silver nanoparticles (Ag NP) and Envirolite-Anolyte (Env-1/1000) against *Flavobacterium columnare*. *F. columnare* was isolated from naturally infected Tilapia fish (*Oreochromis niloticus*). In vitro, *F. columnare* treated with Ag NP at 0.1 mg/L for 1 h exhibited a 90% reduction in colony-forming units (CFU). While; Env required half an h at 1/1000 to reduce 80 % of colony-forming units (CFU). The results suggest that Ag NPs and Env are beneficial for reducing *F. columnare* load in the water column and possibly on fish. Further research is warranted to investigate the value of Ag NPs and Env as a therapeutic agent for fish with a columnare infection and as a treatment to prevent further spread of columnare in a fish population

**Keywords:** Envirolite-Anolyte; Nanoparticles; *F. Columnare*; *Oreochromis niloticus*; Disinfection.

### 631. Innovative method for the Treatment of mastitis in Dairy Animals

Hussein A. Kaoud and Salah Yosseif

*The Journal of Veterinary Science, 114: 240-244 (2013)*

The study was conducted in a herd consists of 800 buffaloes, in which 120 out of 160 clinically mastitic animals were selected to carry out the field study and to apply a novel strategy to control microbial infections in animal production. The mastitic buffaloes were having mixed infection with *E. coli*, *Staphylococcus aureus* and *Streptococcus agalactiae*. When applying 6 lines of treatment, the diseased animals were classified into 6 groups (20 each). The first group received local treatment by intramammary infusion of ceftiofur hydrochloride; the second one received systemic

treatment of both enrofloxacin and carprofen; the third one received a combination of both local (ceftiofur) and systemic treatment (enrofloxacin and carprofen). The fourth group received local treatment by intramammary infusion with 1\500 Envirolite-Anolyte (2 mg of active chlorine). The fifth group received local treatment by intramammary infusion with AgNPs suspension. The sixth group received both local treatments with 1\500 Envirolite-Anolyte (2 mg of active chlorine) and systemic treatment (enrofloxacin and carprofen). The cure rate was 60 % for the first group, 80 % for the second and third group. The fourth and fifth group both were 60 %, while 100% in the sixth group.

**Keywords:** Mastitis; Innovation; Superoxide Water; Silver

### 632. Innovative Method for the Treatment of Skin Infections in Dogs

Hussein A. Kaoud and Salah Yosseif

*The Journal of Veterinary Science, 114: 235-239 (2013)*

some of these affections tolerate the antibiotic treatments. This study was carried out on police service dogs at different regions and some clinics in Egypt. 30 affected dogs (10 suffering of MRSA, 10 of *Trichophyton mentagrophytes* & *verrucosum* and 10 of *Microsporum canis*) were selected to carry out the field study to identify new antimicrobial agents. Results revealed that, Envirolite-Anolyte (strong degree of ionization, and when oxidation) and Silver nanoparticles (AgNPs) were induced high curing rate of skin affection in dogs.

**Keywords:** Skin Affections; Dogs; New antimicrobial agents.

### 633. Removal of Ammonia Gas Emission From Broiler Litter

Hussein AbdElHay ElSayed Kaoud

*Global Journal of Scientific Researches, 1(2): 42-47 (2013)*

Microbial mineralization of urea and uric acid in poultry litter results in the production of ammonia, which can lead to decreased poultry performance, malodorous emissions, and loss of poultry litter value as a fertilizer. The experiment was conducted to test the validity of novel amendments to reduce the presence of these ammonia producing microbes and reduce ammonia emissions from poultry houses. The experiment was consisted of 4 treatments x 2 replication, each 150 broiler chicks of both sexes per pen (treatment A: 2% Sodium perborate, treatment B: 2% TiO<sub>2</sub> Photocatalyst and treatment D: 2% TiO<sub>2</sub> + 0.25 % Paraformaldehyde granules). The results revealed that: 1) Sodium perborate treatment reduced the total bacterial population by 2 log within 2 wk and ammonia concentrations were 20,15,18,15,20,25,25 and 20 mg/m<sup>3</sup> at 7,14,20,25,30,35,40 and 45 days of the cycle period, respectively 2) TiO<sub>2</sub> Photocatalyst of the poultry litter resulted in >2 log decreases in total fungal concentrations, and bacterial decreasing by >3 logs within the first 2 to 3 wk of the litter treatment as well as delayed mineralization events for both uric acid and urea (ammonia concentrations were 15 and 25 mg/m<sup>3</sup> at 40 and 45 days, respectively). 3) Ammonia concentrations in TiO<sub>2</sub> + Paraformaldehyde granules treated group were significantly (P< 0.05) lower than in the control and other treated groups. Ammonia concentrations were 10 mg/m<sup>3</sup> up to 35 days and slightly increased to 15 mg/m<sup>3</sup> up to 45 days of the cycle period.

**Keywords:** Gas; Broiler litter; Emission.

**634. The Bioremediation Potential of Spirulina Platensis and Lemna Gibba L in Grass Carp, Ctenopharyngodon idella Exposed to Cadmium Toxicity**

Hussein A. Kaoud, Sayed N. Abou Elgheit, Ahmed R. Eldahshan and Sherein Saeid

*The Journal of Veterinary Science, 114: 218-226 (2013)*

The effect of cadmium (Cd) toxicity, its impact on histopathological changes, the median lethal concentration (LC50-96 h) and the bioremediation effect of Lemna gibba L and dried Spirulina platensis to grass carp, Ctenopharyngodon idella, were investigated through semi-static acute toxicity test developed with cadmium chloride (CdCl<sub>2</sub>).

This study indicated that: 1) Cd poisoning caused structural damage in the fish organs, 2) Lemna gibba L weed was effective in removing Cd from water and reducing its bioaccumulation in liver and muscular tissues of fish, 3) Addition of dried Spirulina platensis reduced significantly ( $P < 0.05$ ) the Cd level uptake as compared to fish exposed to Cd alone and 4) Addition of Lemna gibba L weed and dried Spirulina platensis were remediated the toxic effect of Cd and provided protection against the degenerative action of Cd in grass carp, Ctenopharyngodon idella. Spirulina platensis was effective in removing Hg from water and reducing Hg bioaccumulation in liver and muscular tissues of fish, as well as remediated the toxic effect of Hg and provided protection against the degenerative action of Hg in Nile tilapia, Oreochromis Niloticus.

**Keywords:** Bioremediation; Cadmium; Ctenopharyngodon Idella.

**635. Trichoderma Album and Envirolite-Egypt: New Innovated Methods for the Control of Toxigenic Aspergillus Flavus in the Field of Corn Plant and Stored-Grains**

Hussein A. Kaoud Mohey M. Mekawy and Salah Yosseif

*International Journal of Engineering and Innovative Technology, 3: 104-109 (2013)*

The aim of this work was to apply recent ways for the control of toxigenic Aspergillus flavus and aflatoxin contamination in the field and stored-grains of corn. The phytopathogenic fungi (T. album) and Envirolite (electrochemically activated water) were applied to contaminated soil and stored-corn grains with toxigenic strain of A.flavus as trials to test their capability of destroying the toxigenic A.flavus.

For this purpose, 1) Maize plots were used for planting and growing in the contaminated soil with toxigenic A. flavus without any treatment and other plots were treated with spore-culture of T. album, 2) Envirolite-Egypt diluted solutions (1/100 and 1/250). The results indicated that T. album (1.5x10<sup>5</sup> spores.ml<sup>-1</sup> sterile saline solutions) and Envirolite-Egypt (at concentration of 1/100) were completely destroyed the toxigenic A. flavus of maize plant in field and in contaminated stored-corn grains.

**Keywords:** Biocontrol; Phytopathogenic Fungi; Toxigenic

**Dept. of Zoonoses**

**636. Characterization of Clostridium Perfringens Enterotoxin in Food Animals and Human**

Nahed, H. Ghoneim, Waffaa W.M. Reda, Samah F. Darwish and Dalia A. Hamza

*Global Veterinaria, 10 (2): 171-175 (2013)*

Enterotoxin (CPE) - producing C. perfringens type A is considered one of the most common causes of food poisonings encoded by C. perfringens enterotoxin gene (cpe). C. perfringens is widely dispersed, but enterotoxin gene carrying (cpe-positive) isolates are rarely found in nature. So, the aim of this work was to study the occurrence and characterization of C. perfringens enterotoxin. A total of 296 rectal swabs collected from different species of food animals and 60 stool samples from human were examined in this study. The results revealed high occurrence of C. perfringens in all examined samples. Cpe-positive C. perfringens were confirmed in 3.1% of the C. perfringens isolates from animals and 3% from human. Cpe positive isolates were represented by type A, C and E. Enterotoxin was produced only from cpe-positive C. perfringens isolates of type A and C.

**Keywords:** Clostridium perfringens; Enterotoxin; Food animals; Man.

**637. Methicillin-Resistant Staphylococci in Mastitic Animals in Egypt**

Sohad M. Dorgham, Dalia A. Hamza, Eman A. Khairy and Riham H. Hedia

*Global Veterinaria, 11 (6): 714-720 (2013)*

Twenty six staphylococci strains were isolated from 40 milk samples with aprevalence 11(16) 68.75% and 15(24) 62.5 % of clinical and sub-clinical mastitis cases respectively. The samples were collected from (cows, buffaloes and goats). All the isolates were fully identified phenotypically to coagulase positive and negative staphylococci. Antibiotic sensitivity test was carried out by using (10) antibiotic disks (Oxoid) in vitro against (26) staphylococci strains. Resistance against pencillinG, oxacillin, ceftiofene, erythromycin, gentamycin, tetracycline and amikacin showed with an incidence 97.00%, resistance against ciprofloxacin with an incidence 92%. sulph/trimetho and amoxy/flucloxacillin with an incidence 94. %. According to PCR results on (10) staphylococci strains, all of them carried 16SrRNA at 228bp. Three strains carried nuc gene at 279bp and (5) strains carried mecA gene at 147bp.

**Keywords:** Mrsa; Coagulase positive; Coagulase negative staphylococci and PCR.

**638. The Potential Role of Animals in the Epidemiology of Avian Influenza Virus H<sub>5</sub> N<sub>1</sub> and Its Public Health Implications**

Nahed H. Ghoneim, Khaled A. Abdel-Moein and Hala M. Zaher

*Avian Influenza H5n1 Animals Epidemiology, 11 (5): 609-613 (2013)*

In the last few years, Avian influenza virus H5N1 (AIV H5N1) was known to infect several mammalian species. Much remains

unknown about the role of animals in the epidemiology of the virus. The current study was carried out to investigate the possible role of animals in the epidemiology of AIV H5N1. For this purpose, nasal and pharyngeal swabs as well as blood samples were obtained from 30 stray dogs, 39 stray cats, 42 donkeys and 50 rats. All animals were collected from villages heavily concentrated with poultry farms. Nasal and pharyngeal swabs were examined for the presence of AIV H5N1 genome by real-time reverse transcriptase polymerase chain reaction whereas blood samples were tested by competitive enzyme linked immunosorbent assay for the presence of AIV H5 antibodies. Of the examined animals only dogs and cats showed seropositive results with high seroprevalence 50% and 56.4% for dogs and cats respectively while none of donkeys and rats was seroreactors. On the other hand, viral RNA of AIV H5N1 was not detected in both pharyngeal and nasal swabs from all examined animals. Therefore, Dogs and cats seems to be important mammalian reservoirs for AIV H5N1 and may have a potential role in the epidemiology of the virus with great public health burden.

**Keywords:** Avian influenza H5n1 animals epidemiology.

## National Institute of Laser Enhanced Sciences

*Dept. of Laser Applications in Metrology, Photochemistry and Agriculture (LAMP)*

### 639. Biological Application of Laser Induced Breakdown Spectroscopy Technique for Determination of Trace Elements in Hair

Elshaimaa M. Emara, Hisham Imam, Mouyed A. Hassan and Salah H. Elnaby

*Talanta*, 117: 176-183 (2013) IF: 3.498

Analysis of trace elements in mammalian hair has the potential to reveal retrospective information about an individual's nutritional status and exposure. As trace elements are incorporated into the hair during the growth process, longitudinal segments of the hair may reflect the body burden during growth. Using LIBS technique, Na, K, Ca, Mg, Si, Fe, Pb and Zn were detected in a single strand of horse hair. The results obtained through LIBS technique on hair samples were compared with the traditional technique (AAS) on digested acidified solution of the same samples. The effects of the experimental parameters on the emission lines were studied and the local thermodynamic equilibrium (LTE) in produced plasma was investigated. The transient plasma condition was verified at specific time region (1500–2000ns) in the plasma evolution corresponding to its dynamic expanding characteristic. The relative mass concentrations of Fe and Zn were calculated by setting the concentration of C as the calibration. The information obtained from the trace elements' spectra of horse hair in this study substantiates the potential of hair as a biomarker.

**Keywords:** Hair; Libs; Trace elements.

### 640. LIBS analysis of artificial calcified tissues matrices

M.A. Kasem, J.J. Gonzalez, R. E. Russo and M. A. Harith

*Talanta*, 108: 53-58 (2013) IF: 3.498

In most laser-based analytical methods, the reproducibility of quantitative measurements strongly depends on maintaining uniform and stable experimental conditions. For LIBS analysis this means that for accurate estimation of elemental concentration, using the calibration curves obtained from reference samples, the plasma parameters have to be kept as constant as possible. In addition, calcified tissues such as bone are normally less “tough” in their texture than many samples, especially metals. Thus, the ablation process could change the sample morphological features rapidly, and result in poor reproducibility statistics. In the present work, three artificial reference sample sets have been fabricated. These samples represent three different calcium based matrices, CaCO<sub>3</sub> matrix, bone ash matrix and Ca hydroxyapatite matrix. A comparative study of UV (266nm) and IR (1064nm) LIBS for these three sets of samples has been performed under similar experimental conditions for the two systems (laser energy, spot size, repetition rate, irradiance, etc.) to examine the wavelength effect. The analytical results demonstrated that UV-LIBS has improved reproducibility, precision, stable plasma conditions, better linear fitting, and the reduction of matrix effects. Bone ash could be used as a suitable standard reference material for calcified tissue calibration using LIBS with a 266 nm excitation wavelength.

**Keywords:** UV-LIBS; Calibration; Stark broadening; Bone ash; Hydroxyapatite.

### 641. Qualitative evaluation of maternal milk and commercial infant Formulas Via libs

Z. Abdel-Salam, J. Al Sharnoubi and M. A. Harith

*Talanta*, 115: 422-426 (2013) IF: 3.498

This study focuses on the use of laser-induced breakdown spectroscopy (LIBS) for the evaluation of the nutrients in maternal milk and some commercially available infant formulas. The results of such evaluation are vital for adequate and healthy feeding for babies during lactation period. Laser-induced breakdown spectroscopy offers special advantages in comparison to the other conventional analytical techniques. Specifically, LIBS is a straightforward technique that can be used in situ to provide qualitative analytical information in few minutes for the samples under investigation without preparation processes. The samples studied in the current work were maternal milk samples collected during the first 3 months of lactation (not colostrum milk) and samples from six different types of commercially available infant formulas. The samples' elemental composition has been compared with respect to the relative abundance of the elements of nutrition importance, namely Mg, Ca, Na, and Fe using their spectral emission lines in the relevant LIBS spectra. In addition, CN and C<sub>2</sub> molecular emission bands in the same spectra have been studied as indicators of proteins content in the samples. The obtained analytical results demonstrate the higher elemental contents of the maternal milk compared with the commercial formulas samples. Similar results have been obtained as for the proteins content. It has been also shown that calcium and proteins have similar relative concentration trends in the studied samples. This work demonstrates the feasibility of adopting LIBS as a fast, safe, less costly technique evaluating qualitatively the nutrients content of both maternal and commercial milk samples.

**Keywords:** Infant milk formulas; LIBS; Maternal milk; Proteins; Trace elements.

#### 642. Production of Aerosols by Optical Catapulting: Imaging, Performance Parameters and Laser-Induced Plasma Sampling Rate

M. Abdelhamid, F.J. Fortes, A. Fernández-Bravo, M. A. Harith and J.J. Laserna

*Spectrochimica Acta Part B*, 89: 1-6 (2013) IF: 3.141

Optical catapulting (OC) is a sampling and manipulation method that has been extensively studied in applications ranging from single cells in heterogeneous tissue samples to analysis of explosive residues in human fingerprints. Specifically, analysis of the catapulted material by means of laser-induced breakdown spectroscopy (LIBS) offers a promising approach for the inspection of solid particulate matter. In this work, we focus our attention on the experimental parameters to be optimized for a proper aerosol generation while increasing the particle density in the focal region sampled by LIBS. For this purpose we use shadowgraphy visualization as a diagnostic tool. Shadowgraphic images were acquired for studying the evolution and dynamics of solid aerosols produced by OC. Aluminum silicate particles (0.2–8  $\mu\text{m}$ ) were ejected from the substrate using a Q-switched Nd:YAG laser at 1064 nm, while time-resolved images recorded the propagation of the generated aerosol. For LIBS analysis and shadowgraphy visualization, a Q-switched Nd:YAG laser at 1064 nm and 532 nm was employed, respectively. Several parameters such as the time delay between pulses and the effect of laser fluence on the aerosol production have been also investigated. After optimization, the particle density in the sampling focal volume increases while improving the aerosol sampling rate till ca. 90%.

**Keywords:** Optical catapulting; Laser-induced breakdown spectroscopy; Shadowgraphy; Solid Aerosol.

#### 643. Structural and Nanomechanical Properties of InN Films Grown on Si (100) By Femtosecond Pulsed Laser Deposition

M. A. Hafez, M. A. Mamun, A. A. Elmustafa and H. E. Elsayed-Ali

*Journal of Physics D: Applied Physics*, 46: 175301-175309 (2013) IF: 2.528

The structural and nanomechanical properties of InN films grown on Si(100) using femtosecond pulsed laser deposition were studied for different growth conditions. Atomic nitrogen was generated by either thermal cracking or laser-induced breakdown (LIB) of ammonia. Optical emission spectroscopy was conducted on the laser plasma and used to observe atomic nitrogen formation. An indium buffer layer was initially grown on the Si substrate at low temperature. The surface structure and morphology were investigated by in situ reflection high-energy electron diffraction, ex situ atomic force microscopy and x-ray diffraction (XRD). The results show that the initial buffer indium layers were terminated with the  $(2 \times 1)$  structure and had a smooth surface. With increased coverage, the growth mode developed from two-dimensional layers to three-dimensional islands. At room temperature (RT), formation of submicrometre islands resulted in mixed crystal structure of In and InN. As the substrate temperature was increased to 250–350 °C, the crystal structure was found to be dominated by fewer In and more InN, with only InN formed at 350 °C. The XRD patterns show that the

grown InN films have wurtzite crystal structure. The film hardness near the surface was observed to increase from less than 1 GPa, characteristic of In for the sample grown at RT using the thermal cracker, to a hardness of 11 GPa at 30 nm from surface, characteristic of InN for samples grown at 350 °C by LIB. The hardness at deep indents reaches the hardness of the Si substrate of ~12 GPa.

**Keywords:** Thin film structure and morphology; Laser deposition; Femtosecond laser; Structure of clean surfaces; Nanomechanical properties.

#### 644. Synthesis and Antimicrobial Evaluation of Some Novel Bis- $\alpha,\beta$ -Unsaturated Ketones, Nicotinonitrile, 1,2-Dihydropyridine-3-Carbonitrile, Fused Thieno[2,3-*b*]Pyridine and Pyrazolo[3,4-*b*]Pyridine Derivatives

Farag Mohamed A. Altalbawy

*International Journal of Molecular Sciences*, 14 (2): 2967-2979 (2013) IF: 2.464

The title compounds were prepared by reaction of 1,1'-(5-methyl-1-phenyl-1*H*-pyrazole-3,4-diyl)diethanone (**1**) with different aromatic aldehydes **2a–c**, namely Furfural (**2a**), 4-chlorobenzaldehyde (**2b**) and 4-methoxybenzaldehyde (**2c**) to yield the corresponding  $\alpha,\beta$ -unsaturated ketones **3a–c**. Compound **3** was reacted with malononitrile, 2-cyanoacetamide or 2-cyanothioacetamide yielded the corresponding bis[2-amino-6-(aryl)nicotinonitrile] **4a–c**, bis[6-(2-aryl)-2-oxo-1,2-dihydropyridine-3-carbonitrile] **5a–c** or bis[6-(2-aryl)-2-thioxo-1,2-dihydropyridine-3-carbonitrile] **6a,b**, respectively. The reaction of compound **6a** with each of 2-chloro-*N*-(4-bromophenyl) acetamide (**7a**), chloroacetamide (**7b**) in ethanolic sodium ethoxide solution at room temperature to give the corresponding 4,4'-(5-methyl-1-phenyl-1*H*-pyrazole-3,4-diyl)bis-6-(2-furyl)thieno[2,3-*b*]pyridine-2-carboxamide derivatives **9a,b**. While compound **6a** reacted with hydrazine hydrate yielded the 4,4'-(5-methyl-1-phenyl-1*H*-pyrazole-3,4-diyl)bis[6-(2-furyl)-1*H*-pyrazolo[3,4-*b*]pyridin-3-amine] **11**. The structures of the products were elucidated based on their spectral properties, elemental analyses and, wherever possible, by alternate synthesis. Antimicrobial evaluation of the products was carried out.

**Keywords:** Heterocycles;  $\alpha,\beta$ -unsaturated ketones; Pyrazoles; Antimicrobial activity.

#### 645. Fluorescent Sensor for Bacterial Recognition

Rehab Amin, Souad A. Elfeky

*Spectrochimica Acta - Part A: Molecular and Biomolecular Spectroscopy*, 108: 338-341 (2013) IF: 1.977

Boronic acid-based fluorescent sensor is one of the non-enzymatic methods used for the recognition of saccharides. Since bacterial membrane has polysaccharides with diol groups, boronic acids probe could be applied for rapid bacterial recognition. *Escherichia coli* (XL-1 blue) were recognized by applying (3-(5-(dimethylamino) naphthalene-1-sulfonamido) phenyl) boronic acid (DNSBA) as a sensor and the fluorescence recorded by fluorometer micro-plate reader. Results showed that, fluorescence records of DNSBA increase in a dose dependent manner upon increasing the bacterial cell numbers. Moreover, the increase in



the number of bacterial cells induces a shift in the spectra due to the formation of the anionic form of boronic acid complex. Therefore, DNSBA is an efficient sensor for monitoring bacterial cells.

**Keywords:** Boronic acid; Sensor; Bacterial detection; Fluorescence.

#### 646. Effect of SPIO Nanoparticle Concentrations on Temperature Changes for Hyperthermia via MRI

Alsayed A. M. Elsherbini and Ahmed El-Shahawy

*Journal of Nanomaterials*, 1-6 (2013) IF: 1.547

Magnetic nanoparticles (MNPs) are being developed for a wide range of biomedical applications. In particular, hyperthermia involves heating the MNPs through exposure to an alternating magnetic field (AMF). These materials offer the potential for selectively by heating cancer tissue locally and at the cellular level. This may be a successful method if there are enough particles in a tumor possessing sufficiently high specific absorption rate (SAR) to deposit heat quickly while minimizing thermal damage to surrounding tissue. The current research aim is to study the influence of super paramagnetic iron oxides  $\text{Fe}_3\text{O}_4$  (SPIO) NPs concentration on the total heat energy dose and the rate of temperature change in AMF to induce hyperthermia in Ehrlich carcinoma cells implanted in female mice. The results demonstrated a linearly increasing trend between these two factors.

**Keywords:** Magnetic nanoparticles (MNPs); Hyperthermia; Ehrlich carcinoma.

#### 647. In-depth Micro-spectrochemical Analysis of Archaeological Egyptian Pottery Shards

A. Khedr and M.A. Harith

*Applied Physics A*, 113: 835-842 (2013) IF: 1.545

Old Egyptian pottery samples have been in-depth microchemically analyzed using laser induced breakdown spectroscopy (LIBS), energy dispersive X-ray (EDX), and X-ray diffraction (XRD) techniques. Samples from two different ancient Islamic eras, Mamluk (1250–1517 AD), Fatimid (969–1169 AD) in addition to samples from the Roman period (30 BC–395 AD) were investigated. LIBS provided the analytical data necessary to study in micrometric steps the depth profiling of various elements in each sample.

Common elements such as silicon, calcium, and aluminum relevant to the originally manufactured and processed clay, showed up in all the investigated samples. EDX and XRD techniques that have been used in the present work provided important chemical insight about the structure of the samples.

The obtained analytical results demonstrated the possibility of using LIBS technique in performing in situ spectrochemical analysis of archaeological pottery. This leads to fast in-depth spatial characterization of the samples in the micron range with nearly invisible surface destructive effects. There is no doubt that this can help in restoration and conservation of such precious objects.

**Keywords:** Depth; Laser; Archaeological; Pottery.

#### 648. Characterisation of Lustre Compositions from Egypt by LIBS and IBA

Amal AbdelFattah Omar Khedr

H. Sadek, A. Khedr, M. Simileanu and R. Radvan

*Digest Journal of Nanomaterials and Biostructures*, 8 (4): 1357-1363 (2013) IF: 1.092

Ion Beam Analysis (IBA) and Laser Induced Breakdown Spectroscopy (LIBS) are particularly useful tools for analysis of artworks, systematic characterisation of lustre were performed using IBA and LIBS. Spatially resolved elements distribution obtained by area scans in addition to spot analysis provided detailed information about the glaze and lustre nano particles, the analytical results and the context of the lustre were used to extract information about the lustre technology. This work reports the analysis of ceramic samples decorated with lustre, these sherds were collected from Al-Fustat site, the samples refers to Fatimid period in Egypt. The study aims to understand the technology of lustre in Egypt through non-destructive techniques via the two different methods.

**Keywords:** IBA; PIXE;  $\mu$ -PIXE; LIBS; Glaze; Lustre and Al-Fustat.

#### 649. Spectrophotometric Determination of Acidity Constant of 1-Methyl-4-[4'-Aminostyryl] Quinolinium Iodide in Aqueous Buffer and Micellar Solutions in the Ground and Excited States

Farag M.A. Altalbawy and El-Sayed A.M. Al-Sherbini

*Asian Journal of Chemistry*, 25: 6181-6185 (2013) IF: 0.253

Electronic absorption and excitation spectra of 1-methyl-4-[4'-amino styryl] quinolinium iodide ( $\text{Q-NH}_2$ ) were measured in aqueous buffer and micellar solutions. The acid dissociation constants in ground and excited states,  $\text{pK}$  and  $\text{pK}^*$ , were determined spectrophotometrically and amount for the aqueous solution to 3.24 and 1.19, respectively and the  $\text{pK}$  and  $\text{pK}^*$  for the ( $\text{Q-NH}_2$ ) in sodium dodecyl sulphate are 3.72 and -1.95. The results indicated that the  $\text{pK}$ s of the micellar solution is higher than that of the aqueous solution due to the concentration of protons at the micellar interface which suppress the protonation in the ground state. This reflects the large difference between the excited and the ground state dissociation constants of the micellar solution. The mechanism of the studied reactions is discussed.

**Keywords:** 1-Methyl-4-[4'-Amino Styryl] quinolinium iodide; Acidity constant; Spectrophotometric; Surfactant.

#### 650. A Study on the Effect of Different Light Treatment on Some Morphological, Physiological Parameters and Menthol Content of Mentha Piperita

Mohamed S. Khater, Taher A. Salah El-Din, Ahmed Elzatahry, Shaimaa Z. Sallam and Tarek Youssef

*Life Science Journal*, 10 (4): 2092-2098 (2013) IF: 0.165

The present study was conducted to assess the effects of Ultraviolet-A (UV-A) 367nm, and White light (W) and ultraviolet+white light (UV-A+W) in addition to control plants in presence of sun light (untreated) on menthol content, some

morphological and physiological parameters of *Mentha piperita*. Growth parameters, photosynthetic pigments, total phenol, total indoles, total amino acids, menthol content and DNA were measured. The results showed that a significant increase in height of plants in presence of UV-A irradiation group, as well as increase in total indoles, total amino acids, Whereas UV- A group and UV-A +W group showed a significant decrease in total phenol, leaf area, chlorophyll content, carotenoids concentration and also decreased in menthol content compared to W group and control group respectively.

**Keywords:** *Mentha piperita*; Light treatment; Ultraviolet; Chlorophyll content; Menthol content.

### 651. Study of the Effects of Silver Nanoparticles Exposure on the Ovary of Rats

M. Amr El-Nouri, Osama Mahmoud Azmy, Awatif Omar I. Elshal, Ayah Mohamed H. Ragab and El-Sayed Abdel-Majjed Elsherbini

*Life Science Journal*, 10 (2): 1887-1894 (2013) IF: 0.165

**Purpose:** The aim of the work is to investigate the effects of silver nanoparticles exposure on the ovary of adult rats.

**Material and Methods:** 36 adult Wister albino rats were used in this experiment. They were divided into six groups of (2 control and 4 experimental), 6 rats each. The first and second group was the control groups where physiological saline was given for 2 and 4 weeks, respectively. The third and fourth groups received low (30 mg/kg) and high dose (300 mg/kg) of silver nanoparticles orally once per day for two weeks, respectively. The fifth and sixth groups received low (30 mg/kg) and high dose (300 mg/kg) of silver nanoparticles orally once per day for four weeks, respectively. The samples were obtained after sacrificing of the rats and were prepared to be examined by light microscopy (after staining with Haematoxylin and Eosin stain, Masson's trichrome stain and Immunohistochemistry for Caspase 3).

**Results:** All experimental groups showed congestion and haemorrhage that increase as dose and duration increase. Mononuclear cell infiltrations were observed indicating the presence of inflammation. Also, there were excess of collagen deposition in all groups. Immunohistochemical studies showed that there were increased immunoreponse to Caspase 3 with the increase of the dose and duration which revealed the increase of cell apoptosis in the specimens.

**Conclusion:** Silver nanoparticles showed evidences of congestion, bleeding, fibrosis and apoptosis in cells of the ovary in all examined doses and durations.

**Keywords:** Silver nanoparticles; Ovary; Apoptosis.

### 652. Studying the Role of the Physical Processes Dependence on Gas Pressure in the Breakdown of Molecular Oxygen by 1064 Nm Laser Radiation

Laila Gaabour, Maha M. Badahdah and Yosr E E-D Gamal

*Life Science Journal*, 10 (4): 2548-2556 (2013) IF: 0.165

This work presents an investigation of the experimental measurements that carried out to study the breakdown threshold dependence on gas pressure in the breakdown of molecular oxygen by a Nd: YAG laser source operating at wavelengths 1064 nm with a pulse duration of 5.5 ns over a gas pressure range

varies between 190- 3000 torr. The study is devoted to find out the role played by the physical processes in determining the threshold intensity of molecular oxygen breakdown as a function of gas pressure.

In doing so a previously developed electron cascade model is modified and applied. The modification assigned the inclusion of an electron diffusion term to account for electron losses out of the focal volume on the experimentally tested low pressure regime. Besides, the model takes into account most of the physical processes which might take place during the interaction between the laser beam and the oxygen molecules.

The result of computations showed reasonable agreement between the calculated threshold intensities and the experimentally measured ones over the tested gas pressure range. This proves the validity of the model. In addition the study of the performed of the electron energy distribution function, EEDF, and its correlated parameters viz, temporal evolution of: electron density, excitation rate, ionization rate and electron mean energy as well as the variation of the EEDF during the laser pulse verified the exact correlation between gas pressure and the physical process responsible for the production and loss of electrons or their energy during the breakdown phase.

**Keywords:** Oxygen breakdown; Plasma density; Plasma production by laser; Electric breakdown; Optical focusing; Plasma diagnostics; Laser –produced plasma; Oxygen.

### 653. Effect of Foliar Spraying Using Ascorbic Acid, Sodium Bicarbonate and Iron (III) Chloride on *Mentha Piperita* Under Different Lights Exposure

Tahar A. Salah, Mohamed S. Khater, Shaimaa Z. Sallam and Tareq Youssef

*European Journal of Scientific Research*, 116 (3): 365-378 (2013)

The present work aimed to address the effects those might be taken place to the chemical constitution of *Mentha piperita* due to foliar spraying of 10 ppm ascorbic acid, iron (III) chloride and sodium bicarbonate combined with exposure to different light irradiation, ultra violet –A (UV-A), White light (W), Mixed light ( UV-A+W) and control (C). Rhizomes of *Mentha piperita* L. were transplanted in 16cm plastic pots (12 pots for each treatment) in a controlled chamber.

The experimental results in general revealed that, the tested concentrations of ascorbic acid, iron (III) chloride and sodium bicarbonatesignificantly deceased the content of chlorophyll a, chlorophyll b, and total amino acids, total phenols and total sugars. While the carotenoids significantly increased.

The major effects were observed with the combination between UV- A and the tested materials especially ascorbic acid. That can be correlated to that ascorbic acid has absorption band in UV region which increase the effect of the UV-A more than the use of ultra violet alone. Also the lower rates of chlorophyll synthesis may be attributed to reducing gene expression encoding chlorophyll binding proteins or break down of structural integrity of chloroplasts and also decreasing total amino acids and total phenols respectively.

**Keywords:** Ascorbic acid; *Mentha piperita*; UV-A effect; Iron (III) chloride; Sodium bicarbonate; Foliar spraying.

### 654. Energy Levels, Transition Probabilities, Collision Strength, and Reduced Population Calculations for High Gain Predictions in Neon-Like Krypton

Wessameldin Salaheldin Abdelaziz

*Journal of Russian Laser Research*, 34 (5): 488-495 (2013)

We calculate the atomic structure, energy levels, oscillator strengths, transition probabilities, and collision strengths for Kr XXVII. The data refer to the 157 fine-structure levels belonging to the configurations  $(1s^2) 2s^2 2p^6, 2s^2 2p^5 3l, 2s^1 2p^6 3l, 2s^2 2p^5 4l, 2s^1 2p^6 4l, 2s^2 2p^5 5l$ , and  $2s^1 2p^6 5l$ , where  $l = s, p, d, f$ , and the calculations are performed using the fully relativistic atomic structure program FAC. We use the obtained data to calculate the level populations and gain coefficients employing the MATLAB R2012a computer program for solving simultaneously the coupled rate equations. Finally, we determine the 157 fine-structure population levels and gain coefficients for those transitions with a positive inversion factor and plot the electron density in wide range from  $10^{19}$  to  $10^{23}$ .

**Keywords:** Structure; Energy levels; Oscillator strengths; Transition probabilities, Neon-like krypton.

### 655. Gain Coefficient Calculation for Short Wave Laser Emission from Sodium Like Co

Wessameldin S. Abdelaziz, Mai E. Ahmed, Mohamed Atta Khedr and Tharwat M. El-Sherbini

*Optics and Photonics Journal*, 3: 369-378 (2013)

Level structure, oscillator strengths, transition probabilities and radiative life times are evaluated for  $1s^2 2s^2 2p^6 3l, 4l, 5l$  ( $l = 0, 1, 2, 3, 4$ ) states in sodium like  $Co^{16+}$ . The calculations are carried out using COWAN code. The calculations made were compared with other results in literature where a good agreement is found. We also report on some unpublished energy values and oscillator strengths. Our results are used in the calculation of reduced population of 21 fine structure levels over a wide range of electron density values ( $10e^{18}$  to  $10e^{20}$ ) at various electron plasma temperature. For those transitions with positive population inversion factor, the gain coefficients are evaluated and plotted against the electron density.

**Keywords:** Level structure; Oscillator strengths; Transition probabilities and Radiative life times; Sodium like  $Co^{16+}$ .

### 656. Numerical Study of the Threshold Intensity Dependence on Wavelength in Laser Spark Ignition of Molecular Hydrogen Combustion

Kholoud A. Hamam, Galila Abdellatif and Yosr E. E.-D. Gamal

*Journal of Modern Physics*, 4: 311-320 (2013)

A numerical investigation of laser wavelength dependence on the threshold intensity of spark ignition in molecular hydrogen over a wide pressure range is presented. A modified electron cascade model (Gamal et al., 1993) is applied under the experimental conditions that carried out by Phuoc (2000) to determine the threshold intensity dependence on gas pressure for spark ignition in hydrogen combustion using two laser wavelengths namely; 1064 nm and 532 nm. The model involves the solution of the time dependent Boltzmann equation for the electron energy

distribution function (EEDF) and a set of rate equations that describe the change of the formed excited molecules population. The model takes into account most of the physical processes that expected to occur in the interaction region. The results showed good agreement between the calculated thresholds for spark ignition and those measured ones for both wavelengths, where the threshold intensities corresponding to the short wavelength (532 nm) are found to be higher than those calculated for the longer one (1064 nm). This result indicates the depletion of the high density of low energy electrons generated through multi-photon ionization at the short wavelength via electron diffusion and vibrational excitation. The study of the EEDF and its parameters (viz, the temporal evolution of: the electron density, ionization rate electron mean energy,) revealed the important role played by each physical process to the spark ignition as a function of both laser wavelength and gas pressure. More over the study of the time variation of the EEDF explains the characteristics of the ignited spark at the two wavelengths for the tested pressure values.

**Keywords:** Laser wavelength; Hydrogen gas; Threshold intensity; Electron energy distribution function; Combustion; Spark ignition.

### 657. Quality Assurance System of Air Pollution Monitoring Network

Mai Ezzeldin Ahmed and Wessameldin Salaheldin Abdelaziz

*International Journal of Environmental Monitoring and Analysis*, 1(4): 133-138 (2013)

Perform a quality assurance system such as applying calibration systems ensures the data will meet defined standards quality with a standard level of confidence. The work represents the way of using the standards to represent the highest level in the traceable chain of calibrations in the environmental monitoring network. The calibration of the Air Quality Monitoring to keep the performance at the confident level 95%; through determining and documenting the deviation of the indication of a measuring instrument from the true value.

**Keywords:** Environmental monitoring; Air pollutants; Calibration; Reference standards; Gas cylinders.

### Dept. of Laser Sciences and Interactions (LSI)

### 658. Quantum Effects in Electron Beam Pumped GaAs

M. E. Yahia, I. M. Azzouz and W. M. Moslem

*Applied Physics Letters*, 103: (2013) IF: 3.794

Propagation of waves in nano-sized GaAs semiconductor induced by electron beam are investigated. A dispersion relation is derived by using quantum hydrodynamics equations including the electrons and holes quantum recoil effects, exchange-correlation potentials, and degenerate pressures. It is found that the propagating modes are unstable and strongly depend on the electron beam parameters, as well as the quantum recoil effects and degenerate pressures. The instability region shrinks with the increase of the semiconductor number density. The instability arises because of the energetic electron beam produces electron-hole pairs, which do not keep in phase with the electrostatic potential arising from the pair plasma.

**Keywords:** Nano semiconductor; Quantum optics.

### 659. Stimulated Emission from ZnO Thin Films with High Optical Gain and Low Loss

A.-S. Gadallah, K. Nomenyo, C. Couteau, D. J. Rogers and G. Léronde

*Applied Physics Letters*, 102: (2013) IF: 3.794

Stimulated surface- and edge-emissions were investigated for ZnO thin films grown epitaxially by pulsed laser deposition. The lasing threshold was  $0.32 \text{ MW/cm}^2$  for surface pumping and  $0.5 \text{ MW/cm}^2$  for edge pumping, which is significantly lower than thresholds observed previously. A modified variable stripe length method was used to measure the gain, which was  $1369 \text{ cm}^{-1}$  for the N-band emission. Losses were measured using the shifting excitation spot method and values of  $6.2 \text{ cm}^{-1}$  and  $6.3 \text{ cm}^{-1}$  were found for the N-band and P-band, respectively. The measured gain and loss were the highest and lowest (respectively) ever reported for ZnO films.

**Keywords:** Stimulated emission; ZnO thin films; Gain; Loss.

### 660. Effect of Silver Nps Plasmon on Optical Properties of Fluorescein Dye

Alaa EL-din E.A. Ragab, A. Gadallah, Mona B. Mohamed and I.M. Azzouz.

*Optics and Laser Technology*, 52: 109-112 (2013) IF: 1.365

In this work we studied the effect of silver nanoparticles "AgNPs" on the optical properties of fluorescein dye. Fluorescein dye solutions have been mixed with different concentrations of colloidal AgNPs. Absorption and fluorescence enhancement of fluorescein dye molecules was detected in the presence of AgNPs. Fluorescence enhancement of the dye molecules was observed with a maximal enhancement factor of about 3-fold. Enhancement of the rate of radiative transition was also detected. The enhancement mechanisms are attributed to a modification of the local density of electromagnetic modes in the vicinity of AgNPs at energies resonant with surface Plasmon. The ability of fluorophore-metal mixture to actively enhance the dye's luminescence could lead to new opportunities for technological development of light emitting and photonic devices. It also may have applications in the fields of bio-technology and medical diagnostics as new class of fluorescence based sensing.

**Keywords:** Fluorescein dye; Ag NPs plasmon; Fluorescence.

### 661. High Gain Predictions for Ni-Like Ta Ions

Wessameldin S. Abdelaziz, A. A. Farrag, H. M. Hamed and Mai E. Ahmed

*Chinese Physics Letters*, 30 (11): (2013) IF: 0.811

Atomic structure data and effective collision strengths for  $1s^2 2s^2 2p^6 3s^2 3p^6 3d^{10}$  and 54 fine-structure levels are contained in the configurations  $1s^2 2s^2 2p^6 3s^2 3p^6 3d^9 4l$  ( $l = s, p, d, f$ ) for the nickel-like Ta ion. These data are used in the determination of the reduced population for the 55 fine structure levels over a wide range of electron densities (from  $10e^{21}$  to  $10e^{23}$ ) and at various electron plasma temperatures. The gain coefficients for those transitions with a positive population inversion factor are determined and plotted against the electron density.

**Keywords:** X-Ray laser; Reduced population; Plasma.

### Dept. of Medical Applications of Lasers (MAL)

### 662. Fluorescence-Guided Laparoscopic Cholecystectomy: A New Technique for Visualization of Biliarysystem by Using Fluorescein

Amr A. Mohsen, Mahmoud S. Elbasiouny and Yasser Sherif Fawzy

*Surgical Innovation*, 20 (2): 105-108 (2013) IF: 1.537

**Background:** Safe cholecystectomy requires confident identification of extrahepatic biliary anatomy. This is the first report of the use of fluorescein and ultraviolet light to improve visualization of biliary topography during laparoscopic cholecystectomy.

**Methods:** Five patients who had symptomatic gallstones underwent laparoscopic cholecystectomy with intraoperative intravenous fluorescein injection. Ultraviolet A from an LED light source was used to induce fluorescence of bile. It was delivered by a device that was designed and built by the authors.

**Results:** Within 4 to 5 minutes the bile ducts were shining with green fluorescence and were easily differentiated from the surrounding tissues. In all cases, identification of the extrahepatic biliary anatomy by the fluorescence technique preceded its identification with conventional white light. Fluorescence remained for the whole duration of operation that extended for 42 to 77 minutes.

**Conclusions:** At laparoscopic cholecystectomy, intravenous fluorescein injection and ultraviolet a excitation induce bile ducts to fluoresce. The technique allows better and earlier real-time visualization of biliary anatomy than conventional white light. The technique is simple and inexpensive. It serves as an additional tool that would improve safety of laparoscopic cholecystectomy

**Keywords:** Fluorescence; Cholecystectomy; Fluorescein; Ultraviolet; LED.

### 663. Comparative Study in the Management of Allergic Rhinitis in Children Using LED Phototherapy and Laser Acupuncture

Yousry Moustafa, Ahmed Nazmi Kassab, Jehan el Sharnoubi and Hala Yehia

*International Journal of Pediatric Otorhinolaryngology*, 77(5): 658-665 (2013) IF: 1.35

**Objective:** The objective of this study was to compare the outcomes of LED phototherapy and laseracupuncture treatment on allergic rhinitis in children.

**Methods:** 40 patients with perennial allergic rhinitis were divided randomly into two groups. Patient's ages ranged from 7 to 18 years. One group was subjected to LED phototherapy and the other group was managed by laser acupuncture .The patients were followed-up for 1 year.

**Results:** There was a significant improvement in the severity score symptoms in both groups throughout by the end of the follow up period.

**Conclusion:** This led to the conclusion that both techniques are equally safe, reliable, non invasive and successful.

**Keywords:** Allergic rhinitis in children; LED; Laser acupuncture.

CAIRO UNIVERSITY

Publication  
in  
Book & Chapters



## Publication in Book/ Chapter

### Faculty of Science

#### Dept. of Astronomy and Meteorology

##### 664. Solar Forcings on Nile and Earthquakes

Saad Mohammed Al-Shehri, Ismail Sabbah, Shahinaz Moustafa Yousef and Magdy Y. Amin

*The Smithsonian/NASA Astrophysics Data System, PP. 330-336 (2013)*

Nile and earthquake periodicities are examined in the light of solar and geomagnetic periodicities in order to uncover the role of the sun in initiating such terrestrial phenomena. The Nile periodicities under considerations covers the period 622-1420 AD. 1749- 1800 and 1870-1945 and are taken from an earlier paper by Yousef and El-Rae (1995). It is found that 11 yr and 21 yr solar periodicities affected the White Nile originating from the Equatorial plateau. On the other hand the Blue Nile arising mainly from Lake Tana in Ethiopia was affected mostly by the 3.3 yr, 2.9 yr, 2.7 yr, and the 2.52 yr periodicities. Such short periodicities are also present in cosmic rays. This is fairly true as during weak solar cycles series at the bottom of the 80-120 year Solar Wolf-Gleissberg Cycles, the level of the second to last of the weak cycles rise and fall coherently with full solar cycles with a correlation coefficient of about 0.9. Rain over Ethiopia is affected by the Monsoon precipitation which is related to the quasi biennial oscillations QBO of the equatorial zonal wind between the easterlies and the westerlies in the tropical stratosphere with a mean period of 29 months. We propose that the QBO are stimulated by the 2.52-2.48yr solar periodicities. The 2.52 and 2.48 yr periodicity is strong in odd solar cycles 21 and 23. Generally speaking, it looks that different solar periodicities are space-time dependent and that they affect different regimes of terrestrial responses. In the case of earthquakes, we think that they are related to geomagnetic storms initiated by solar stimuli. Several solar periodicities are found in earthquakes. We postulate that electric currents in the ring current and in the ionosphere induce surface as well as deep electric currents in the magma thus produce motion and disturbances of the plates and the magma leading to earthquakes and volcanoes.

**Keywords:** Cosmic Rays; Nile; Sun; Earthquakes.

#### Dept. of Biophysics

##### 665. Recording Brain Electrical Activity from Conscious Animal

Haitham Sharaf Eldin Mohammed

*Book Published By Lambert Academic Publishing, (2013)*

The application of techniques which allow the investigator to examine nerve cells activity during behavioral changes in conscious animal is a corner stone in modern electrophysiology. Recording and analysis of spontaneous and evoked brain activity from conscious animal gives a great insight into how the brain works. Ultimately, the advancement in modern technology will encourage the brain scientists to use this technology to explore the mysterious areas of the brain functions

**Keywords:** Brain; Electrical activity; Conscious animal.

##### 666. Detection of Breast Cancer Lumps Using Scattered X-Ray Profiles: A Monte Carlo Simulation Study

Wael M. Elshemey

*Theory and Applications of Monte Carlo Simulations, (2013)*

The difference in the position of the main scattering peak of adipose and soft tissue has been utilized by many authors for the purpose of differentiating between healthy and malignant excised breast tissue samples. Evans et al 1991 [3] measured the x-ray scattering profiles of nineteen samples of healthy and diseased human breast tissues. They reported that while large differences were found in the shapes of scattered photon distributions between adipose and fibroglandular tissues, only small differences existed between carcinomas and fibroglandular tissue. Kidane et al 1999 [2] measured the diffraction patterns of one hundred excised breast tissue samples. They found that breast tissue types could be characterized on the basis of the shape of scattered spectrum (from 1.0 to 1.8nm<sup>-1</sup>) and the relative intensities of the adipose and fat free peaks at 1.1 and 1.6nm<sup>-1</sup> respectively. Poletti et al 2002a [4] found that the scattered photon distribution of healthy and cancerous breast tissues were considerably different. They also found differences in the scattered photon distributions of human breast tissue & breast equivalent materials. They pointed out that the scattered photon distribution of adipose tissue was similar to corresponding commercial breast-equivalent materials and that of glandular tissue was equivalent to water.

Using x-ray from a synchrotron, Ryan and Farquharson 2004 [5] showed the well documented differences between the scattering profiles of adipose and diseased (malignant) tissue while Castro et al 2004 [6] measured scattering distributions at six different sites in breast tissue sample and showed that the fat content decreased as the tumor infiltrated the tissue.

**Keywords:** Breast cancer; Lumps; X-ray scattering.

#### Dept. of Chemistry

##### 667. La, Nd and Er Complexes of Schiff Bases Derived From Benzopyran-4-One: Synthesis and Characterization

Nora Saeed Morsy Abdel-Kader

*Book Published By Lap Lambert Academic Publishing, (2013)*

Schiff bases have played an important role in the development of coordination chemistry. The growing importance of the Schiff bases in modern coordination chemistry is attributable to recent observations about their antibacterial and antifungal properties. Lanthanide coordination compounds are the subject of intense research efforts owing to their unique structures and their potential applications. Accordingly, this book contains preparation and characterization of a series of Schiff bases derived from the condensation of benzopyran-4-one derivatives with aliphatic diamines (ethylenediamine and trimethylenediamine), aromatic diamines (o-phenylenediamine and p-phenylene-diamine) and 2-aminopyridine and their antimicrobial activities were screened. The mode of chelation of La (III), Nd(III), Er(III) with these Schiff bases was elucidated by different techniques. The luminescence properties of the prepared Schiff bases and their complexes with Nd(III) and Er(III) ions are

also discussed. The book is a valuable study to inorganic chemists those research coordination compounds as well as those looking for a novel approach in drug development.

**Keywords:** Lanthanides; Thermal analysis; Ir; Fluorescence; Schiff bases; <sup>1</sup>H-Nmr; Benzopyran-4-one; Antimicrobial activity.

### 668. Coordination Chemistry of Polyvinyl Alcohol

Wafaa Mahmoud Hosny

*Book Published By Lap Lambert Academic Publishing, (2013)*

Poly (vinyl alcohol) (PVA;  $[-CH_2-CHOH-]_n$ ) is the world's largest volume synthetic polymer produced for its excellent chemical resistance and physical properties and complete biodegradability, which has led to broad practical applications. PVA is a semi-crystalline polymer whose crystalline index depends on the synthetic process and the physical aging (Pichard, 1970 and Brunelli et al., 1998). PVA is a water-soluble polyhydroxy polymer, one of the few linear, non-halogenated aliphatic polymers. PVA has a two dimensional hydrogen-bonded network sheet structure. The physical and chemical properties of PVA depend to a great extent on its method of preparation. Poly(vinyl alcohol) could be considered as a good host material due to good thermo-stability, chemical resistance and film forming ability. PVA is an important material in view of its large scale applications. It is used in surgical devices, sutures, hybrid islet transplantation, implantation, blend membrane and in synthetic cartilage in reconstructive joint surgery (Garrel, et al., 1991; Kim, et al., 1992; Sexena, et al., 1999; Peppas, et al., 1977). Copper has been used as a biocide for centuries (Dollwet and Sorenson, 2001). In ancient Egypt (2000 BC), copper was used to sterilize water and wounds. The ancient Greeks in the time of Hippocrates (400 BC) prescribed copper for pulmonary diseases and for purifying drinking water. Gangajal, "Holy water", given to Hindu devotees to drink as a blessed offering, is stored in copper utensils as it keeps the water sparkling clean. During the Roman Empire, copper cooking utensils were used to prevent the spread of disease.

**Keywords:** Polyvinyl alcohol (Pva).

### 669. Synthesis and Sensing Applications of Nano-Structured Conducting Polymers and Conducting Polymers-Based Nanocomposites

Ahmed Galal Helmy Abdo

*Nanosensors: Materials and Technologies, International Frequency Sensor Association Publishing, (2013)*

This chapter presents the synthesis and sensing applications of nanostructured conducting polymers and conducting polymers-based nanocomposites. Because their chemical and physical properties may be tailored over a wide range of characteristics, the use of conducting polymers (CPs) is finding a permanent place in sophisticated electronic measuring devices such as sensors. Better selectivity and rapid measurements have been achieved by replacing classical sensor materials with CPs involving nanotechnology. Nanomaterials of CPs are found to have superior performance relative to conventional materials due to their much larger exposed surface area. In addition, Polymer-based nanocomposites, which incorporate advantages of both nanoparticles and polymers, have received increasing attention in both academia and industry. They present outstanding mechanical

properties and compatibility owing to their polymer matrix, the unique physical and chemical properties caused by the unusually large surface area to volume ratios and high interfacial reactivity of the nanofillers. The composites provide an effective approach to overcome the bottleneck problems of nanoparticles in practice such as separation and reuse. Thus, polymers used in sensor devices either participate in sensing mechanisms or immobilize the component responsible for sensing the analyte. This chapter summarizes the preparation methods and sensing applications of CPs nanomaterials and polymer-based nanocomposites. Challenges and future directions are also discussed.

**Keywords:** Conducting polymers; Nano-structures; Nano-composites; Nanosensors; Nanofillers; chemically modified electrodes.

### 670. Chapter 1: Polymer Grafting: A Versatile Means to Modify the Polysaccharides

Magdy Sabaa Wadid

*Polysaccharide Based Graft Copolymers, Springer, (2013)*

The polysaccharides are the most abundant natural organic materials, and polysaccharide-based graft copolymers are of great importance and widely used in the various fields. Natural polysaccharides have received more attention due to their advantages over the synthetic polymers such as non-toxic, biodegradable and low cost. Modification of polysaccharides through graft copolymerisation improves the properties of natural polysaccharides. Grafting is known to improve the characteristic properties of the backbones. Such properties include water repellency, thermal stability, flame resistance, dye ability and resistance towards acid-base attack and abrasion. Graft copolymers play an important role as reinforcing agents in the preparation of green composites. These graft copolymers on subjecting both for composting and soil burial biodegradation studies are found to be biodegradable in nature. Polysaccharides and their graft copolymers find extensive applications in diversified fields. Applications of modified polysaccharides include drug delivery devices, controlled release of fungicides, selective water absorption from oil-water emulsions and purification of water. Methods for the modification of various polysaccharides through graft copolymerisation technique have been reported in this chapter.

**Keywords:** Chitosan- copolymerization.

### Dept. of Entomology

### 671. Insecticides Synergists: Concepts, Significance, and Future

El-Sayed Hassan Shaurub

*Book Published By Lap Lambert Academic Publishing, (2013)*

In the current book we presented the nature, mode of action, role in resistance management, natural occurrence, and significance in research of insecticide synergists. The mode of action of the majority of synergists is to block the metabolic systems that would otherwise break down insecticide molecules. They interfere with the detoxification of insecticides through their action on polysubstrate monooxygenases and other enzyme systems. The role of synergists in resistance management is related directly to an enzyme inhibiting action, restoring the

susceptibility of insects to the chemical, which would otherwise require higher levels of the toxicant for their control. For this reason synergists are considered straightforward tools for overcoming metabolic resistance, and can also delay the manifestation of resistance. However, the full potential of these compounds may not have been realized in resistance management. The contributions of synergists as research tools and as control agents are quite different, and at times these approaches are conflicting. As research tools, they can help define the potential toxicity of a compound, and they can aid in determining the particular mechanisms of insecticide resistance encountered. Moreover, they also can be used in understanding the effects of other xenobiotics in nontarget organisms. The search for and the need of new molecules capable of synergizing existing or new pesticides has reactivated the identification and characterization of secondary plant compounds possessing such activity. Plants do possess and utilize synergists to overcome the damage produced by phytophages. This has to be exploited in integrated pest management programs (IPM). Hopefully, it will lead to a new perspective on the nature and significance of synergism. As control agents, synergists can potentially render resistant populations susceptible and/ or prevent the development of resistance. This book also shows that synergists can be less active on predators than on pests, and the implications to IPM are discussed. A number of practical usage problems remain, however, and these represent major hurdles to widespread application. To overcome these hurdles, synergists will have to be viewed in a broader sense than previously, and integrated into a complex array of interactions between the insect and its environment.

**Keywords:** Insecticide resistance; Metabolic inhibitors; Synergists.

#### Dept. of Geophysics

### 672. Geophysical Study of Farafra Oasis Area, Western Desert, Egypt

Ahmed Mohsen Hassan Metwally

Book Published By Lap Lambert Academic Publishing, (2013)

This book represents an integrated geophysical study for the farafra area, Western desert, Egypt including a general review for the different geological data and studies carried out over this area, followed by the petrophysical analysis for Ammonite-1 well which is the nearest well for this area, then the interpretation of the allowed seismic reflection data by picking of four different sequence boundaries and tying them with the well data, finally we used the aeromagnetic and gravity data to determine the depth to basement and detect the different basin locations.

**Keywords:** Seismic; Gravity; Magnetic; Seismic; Petrophysics.

#### Dept. of Mathematics

### 673. Boundary Integrals in Plane Elasticity with Mixed Boundary Conditions

Hosni Abdulsalam

Book Published By Lambert Academic Publishing, (2013)

The objective of this book is to present a low cost, efficient semi-analytical scheme to solve the static, plane problems of elasticity

in stresses for homogeneous, isotropic media occupying a long cylinder with simply connected normal cross-section and subjected to mixed boundary conditions on the lateral surface. The method relies on the use of boundary integrals and provides approximate solutions. Besides test problems, the cases of the circular and elliptical boundaries are considered. The boundary singularity of the solution is put in evidence. It is hoped that the material contained in this book will benefit to researchers involved in research work in the fields of plane linear elasticity with mixed boundary conditions and partial differential equations relating to the biharmonic equation.

**Keywords:** Plane elasticity; Isotropic medium; Mixed boundary conditions; Boundary integral method collocation method.

### 674. Molecular Dynamics Simulations of the DNA Interaction with Metallic Nanoparticles and TiO<sub>2</sub> Surfaces

Nasser Hassan Sweilam

Kholmirzo T. Kholmurodov (Edts)

*Models in Bioscience and Materials Research: Molecular Dynamics and Related Techniques*, NOVA Publishers, ch (12) (2013)

The understanding of the mechanism of DNA interactions and binding with metallic nanoparticles (NPs) and surfaces represents a great interest in today medicine applications due to diagnostic and treatment of oncology diseases. Recent experimental and simulation studies involve the DNA interaction with highly localized proton beams or metallic NPs (such as Ag, Au, etc.), aimed on targeted cancer therapy through the injection of metal micro- or nanoparticles into the tumor tissue with consequent local microwave or laser heating. The effects of mutational structure changes in DNA and protein structures could result in destroying of native chemical (hydrogen) bonds or, on the contrary, creating of new bonds that do not normally exist there. The cause of such changes might be the alteration of one or several nucleotides (in DNA) or the substitution of specific amino acid residues (in proteins), that can brought to the essential structural destabilization or unfolding. At the atomic or molecular level, the replacement of one nucleotide by another (in DNA double-helices) or replacement of one amino acid residue by another (in proteins) cause essential modifications of the olecular force fields of the environment that break locally important hydrogen bonds underlying the structural stability of the biological molecules. In this work, the molecular dynamics (MD) simulations were performed on four DNA models and the flexibilities of the purine and pyrimidine nucleotides during the interaction process with the metallic NPs and TiO<sub>2</sub> surface were clarified.

### 675. Frequent Statement and De-Reference Elimination for Distributed Programs

Mohamed Abdelmoneim Mahmoud Mohamed El-Zawawy

*Computational Science and Its Applications – Iccsa 2013*, Springer-Verlag Berlin, Heidelberg Platz 3, D-14197 Berlin, Germany, (2013)

This paper introduces a new approach for the analysis of frequent statement and de-reference elimination for distributed programs run on parallel machines equipped with hierarchical memories.

The address space of the language studied in the paper is globally partitioned. This language allows programmers to define data layout and threads which can write to and read from other thread memories. Simply structured type systems are the tools of the techniques presented in this paper which presents three type systems. The first type system defines for program points of a given distributed program sets of calculated (ready) statements and memory accesses. The second type system uses an enriched version of types of the first type system and determines which of the specified statements and memory accesses are used later in the program. The third type system uses the information gather so far to eliminate unnecessary statement computations and memory accesses (the analysis of frequent statement and de-reference elimination). Two advantages of our work over related work are the following. The hierarchical style of concurrent parallel computers is similar to the memory model used in this paper. In our approach, each analysis result is assigned a type derivation (serves as a correctness proof).

**Keywords:** Ready Statement and memory access analysis; Semi-expectation analysis; Frequent statement and de-reference elimination analysis; Certified code; Distributed programs; Semantics of programming languages; Operational semantics; Type systems.

#### Dept. of Physics

##### 676. New Neutral Heavy Particles at the LHC's CMS by Monte Carlo Simulation

Hesham M. M. Mansour and Nady Bakhet

*Book Description, 100 Pages (2013)*

In this book, we simulated B-L model at Large Hadron Collider by using Monte Carlo simulation software. B-L model is one of many scenarios proposed to add an extension of the Standard Model of particle physics. These scenarios or models try to find a solution for many problems where the Standard Model can not solve it like dark matter, neutrino oscillation. B-L model predicts the existence of three new particles at the LHC. They are new neutral massive gauge boson, three heavy neutrinos (Right-Handed) and new heavy Higgs boson which is different from than Higgs of SM. We simulated these new particles at the LHC using Monte Carlo simulation programs and predict that the three particles may be found at the LHC particular new neutral massive gauge boson  $Z'$  and it has a mass in the range 1TeV to 1.5TeV. Also the particle Higgs-Like which was discovered in 2012 at the LHC may be the Higgs of B-L model of this book and is not of the SM. Finally we predict the existence three heavy neutrinos which are different from the light neutrino of the Standard Model.

**Keywords:** B-L Model; New particles; Beyond the standard model; Monte Carlo simulation.

##### 677. New Neutral Heavy Particles at the Lhc's Cms by Montecarlo Simulation

Hesham Mohamed Mohamed Mansour

*Book Published By Lap Lambert Academic Publishing Gmbh & Co., Saarbrücken, Germany., (2013)*

In this book, we simulated B-L model at Large Hadron Collider by using Monte Carlo simulation software. B-L model is one of many scenarios proposed to add an extension of the Standard

Model of particle physics. These scenarios or models try to find a solution for many problems where the Standard Model can not solve it like dark matter, neutrino oscillation. B-L model predicts the existence of three new particles at the LHC. They are new neutral massive gauge boson, three heavy neutrinos (Right-Handed) and new heavy Higgs boson which is different from than Higgs of SM. We simulated these new particles at the LHC using Monte Carlo simulation programs and predict that the three particles may be found at the LHC particular new neutral massive gauge boson  $Z'$  and it has a mass in the range 1TeV to 1.5TeV. Also the particle Higgs-Like which was discovered in 2012 at the LHC may be the Higgs of B-L model of this book and is not of the SM. Finally we predict the existence three heavy neutrinos which are different from the light neutrino of the Standard Model.

**Keywords:** B-L Model; New Particles; Beyond the standard model; Monte Carlo simulation.

##### 678. Analysis of Reactivity Induced Accidents in Power Reactors [Paperback]

Hesham Mohamed Mohamed Mansour

*Book Published By Lap Lambert Academic Publishing Gmbh and Co., Saarbrücken, Germany, (2013)*

The purpose of studying the point kinetics equations, which are solved numerically using the stiffness confinement method (SCM). The difficulty in the numerical solution of these equations is due to the stiffness of the system arising from the difference order of magnitude between the prompt and delayed neutron lifetimes. Numerical examples of applying this method to a variety of problems confirm that the step size of time increment can be greatly increased and the computing time much saved as compared to other conventional methods. The solution is applied to the kinetics equations in the presence of different types of reactivities, and is compared with different methods. The present work is a consistent comparison of the performances of the numerical method applied to the point reactor kinetics equations for different transient's methods. In this work, the SCM is used for large time steps. Click to open expanded view with the greatest accuracy for developing. This method is, also used to analyze reactivity induced accidents in two different types of reactors. The first is a thermal reactor (HTR-M) fueled by uranium-235 and the second is a fast reactor (PRISM) fueled by plutonium-239. Product D.

**Keywords:** Reactivity induced accidents; Kinetics equations; Reactors safety.

#### Dept. of Zoology

##### 679. Myxosporidiosis and Microsporidiosis of Fish: Some Parasitic Species of Myxosporidia and Microsporidia Infecting Marine Fish of the Red Sea

Fathy Abdel-Ghaffar

*Book Published By Lap Lambert Academic Publishing, (2013)*

Parasitological research today focused on studying protozoan parasites infecting fish especially myxosporidian and microsporidian parasites which cause adverse effects on the fish health causing high losses in fish production. Also the presence of Heavy infections with muscle-invading species destroy the texture of the fish flesh making it unmarketable. Morphological

description of these parasites help in the exact determination of their taxonomy which may aid with the molecular tools in the development of anti substances against these parasites. The present book described some of these parasites including two myxosporidian and three microsporidian species infecting flesh of four of the most economically important marine fishes of the Red Sea in Egypt. The study described the different developmental stages of these parasites which undergoes its maturation within fish flesh until its progressive development into the infective spores which are the most dangerous and infective part of the cycle.

**Keywords:** Microsporidia; Myxosporidia; Red Sea; Light; Ultrastructural study.

#### **680. Marine Parasites Part I: Studies on Some Monogenean Parasites Infecting Economically Important Marine Fish of the Red Sea**

Kareem Saied Morsy Said

*Book Published By Lap Lambert Academic Publishing, (2013)*

Fish are well known to act as direct or indirect carriers of different zoonotic pathogens including parasites, viruses, bacteria and fungi. Parasitic infection is one of the most important problems facing fish breeding and production at commercial scales. So the most important reason for studying fish parasites is to study the relationships of these parasites to fishes, animals and man and also to understand some human health problems. The name "monogenea" means born once, and refers to the simple life cycle. In heavy infections, they can kill captive fish and occasionally wild ones. Gill worms have a distinct attachment organ on their posterior end called a haptor (or opisthaptor) with hardened anchors or specialized clamps to pierce the epithelium and hold on to the host, sclerotized marginal hooks often surround the haptor, and bars, disks, scales or spines may occur on or near the haptor, the head sometimes has eye spots and specialized holdfast organs, many monogenean parasites of big game fish have large suckers or numerous clamps adapted for holding on to these fast moving animals.

**Keywords:** Fish; Monogenea; Haptor; Hooks.

#### **681. Helminthosis in Fish: Helminthes of the Economically Important Fish of the Red Sea and Their Role as Biological Indicators of Pollution**

Kareem Saied Morsy Said

*Book Published by Lap Lambert Academic Publishing, (2013)*

Helminthosis is the disease caused by the presence of helminth parasites within or outside the gastrointestinal tract of an individual. All species of animals can be infected with helminth parasites. The infection usually is more severe in the very young and the very old or immuno compromised individuals. Some adult animals can thrive fairly well while infected with some helminth parasites without showing obvious clinical signs while the vast majority suffer reduced productivity under heavy worm burdens. It appears some breeds of animals are more resistant to certain helminth parasites than others. Helminthosis has been a long time standing problem against breeding of fish hosts leading to economic losses that may reach billions of dollars.

**Keywords:** Helminthosis; Pollution; Red Sea.

#### **682. Marine Parasites Part II: Studies on Some Helminth Parasites Infecting Economically Important Marine Fish of the Red Sea**

Abdel Rahman Mohamed El Sayed Bashtar

*Book Published By Lap Lambert Academic Publishing, (2013)*

Fish are well known to act as direct or indirect carriers of different zoonotic pathogens including parasites, viruses, bacteria and fungi. Parasitic infection is one of the most important problems facing fish breeding and production at commercial scales. So the most important reason for studying fish parasites is to study the relationships of these parasites to fishes, animals and man and also to understand some human health problems. Helminthosis is the disease caused by the presence of helminth parasites within or outside the gastrointestinal tract of an individual. All species of animals can be infected with helminth parasites. The infection usually is more severe in the very young and the very old or immunocompromised individuals. Some adult animals can thrive fairly well while infected with some helminth parasites without showing obvious clinical signs while the vast majority suffer reduced productivity under heavy worm burdens. It appears that some breeds of animals are more resistant to certain helminth parasites than others. Helminthosis has been a long time standing problem against breeding of fish hosts leading to economic losses that may reach billions of dollars.

**Keywords:** Helminthosis; Marine fish; Red Sea; Lighe; Electron microscopy.

#### **683. Uses of Invertebrate Animals to Detect Water Pollution**

Salwa Abdel Hamid Hamdi Abdel Salam

*Lambert Academic Publishing, PP. 1-144 (2013)*

The excessive use of pesticides in agriculture has sparked the interest of scientists in investigating the harmful effects of these compounds. The present study evaluates the pesticides Atrazine and Roundup (glyphosate) on biochemical and molecular aspects of *Biomphalaria alexandrina* snails. The results showed that LC10 of these two pesticides caused considerable reduction in survival rates and egg production of treated snails. Additionally, Atrazine proved to be more toxic to *B. alexandrina* snails than Roundup. In treated snails, glucose concentration (GL) in the hemolymph as well as lactate (LT) and free amino acid (FAA) in soft tissues of treated snails increased while glycogen (GN), pyruvate (PV), total protein (TP), nucleic acids (DNA and RNA) levels in snail's tissues decreased. The activities of glycogen phosphorylase (GP), superoxide dismutase (SOD), catalase (CAT) and glutathione reductase (GR), succinic dehydrogenase (SDH), acetylcholinesterase (AChE), lactic dehydrogenase (LDH) and phosphatases (ACP and ALP) enzymes in homogenate of snail's tissues were reduced in response to the treatment with the two pesticides while lipid peroxide (LP) and transaminases (GOT and GPT) activity increased ( $P < 0.001$ ). The changes in the number, position and intensity of DNA bands induced by pesticides may be attributed to the fact that pesticide can induce genotoxicity through DNA damage. It was concluded that the pollution of the aquatic environment by Atrazine and Roundup pesticides, would adversely affect the metabolism of the *B. alexandrina* snails, and have adverse effects on its reproduction.



**Keywords:** Invertebrate animals; Biomphalaria alexandrina; Atrazin and roundup pesticides; Water pollution.

#### 684. Snail Control

Salwa Abdel Hamid Hamdi Abdel Salam

*Book Published By Lap Lambert Academic Publisher, (2013)*

The present work evaluates the molluscicidal activities of certain plant extracts (water suspension, Cold water, Boiled water, methanol, ethanol, acetone and chloroform extract). The data obtained from preliminary screening tests conducted on 10 plant species belonging to 10 different families, revealed in a descending order.

The higher potency of Agave celsii, Ammi visnaga and Chenopodium ambrosioides). Also, It was found that, the exposure of B. alexandrina to such plant extracts had led to a significant reduction in the survival rate and in the growth rate as well as in the infectivity of Schistosoma mansoni miracidia. The results obtained also revealed that the glucose concentration showed a significant increase in haemolymph, on the other hand soft tissue glycogen and protein contents were significantly decreased. The activity level of Hexokinase, pyruvatekinase and lactate dehydrogenase was also significantly reduced in response to treatment. The results obtained also showed that adenosine triphosphatase (ATPase) activity of the tissue of the snails was significantly increased in response to the tested extracts.

The effect of low concentrations of different synthetic and natural mollusciciding agents may introduce to fresh water environment on reproduction and biochemical aspects of Biomphalaria alexandrina was studied. Different mollusciciding agents (copper sulphate, Bayluscide, Uccmaluscide, Agave franzosinii, Agave filifera & Agave attenuate) inhibited egg production, induced marked increased the percent of abnormal laid eggs and induced marked reduction in their hatchability. The maximal reductions in egg hatchability resulted with Bayluscide (0.0%) and Uccmaluscide (18%), A. filifera (21%) and A. attenuate (15%). All the antimolluscal material caused a successful killing effect against miracidia and cercariae of Schistosoma mansoni. CuSo<sub>4</sub>, Bayluscide and Uccmaluscide killed 40% of the exposed miracidia and 50% of cercariae after an hour exposure.

The plants sublethal concentration killed 100% of cercariae and miracidia after 6 hours exposure. Water leaving behavior among the exposed snails was noticed especially during the first three weeks, showing maximal percentage (60%) after one week of exposure to Bayluscide. A general decrease in the activity of alkaline phosphatase (ALP) especially with Bayluscide (48.4%) and in acetylcholine esterase activity in the haemolymph especially on applying plant molluscicide A. filifera (50.8%) was noticed. Transaminases showed marked elevations in activities during the 1st three weeks, then began to drop (ASAT: 61.5%, with Bayluscide & ALAT: 50.8% with Uccmaluscide). The results reflect the effect of the metabolic disorders on life, egg laying, egg hatchability, hepatic cells damages, lack of smooth transmission at nerve junction, loss of muscular coordination and convulsions, then snails' death.

**Keywords:** Snail control; Molluscicid; Synthetic and of plant origin.

#### 685. Developing Capacities for Teaching Responsible Science in the MENA Region: Refashioning Scientific Dialogue

Mona Mostafa Mohamed Elsayed Amin

*National Research Council of the National Academies (2013)*

A wave of discoveries in the life sciences, supported by new enabling technologies and drawing on many fields beyond biology, is yielding great social and economic benefits and promises continuing gains in the future. Inspired by this vision, governments across the globe, as well as regional and international organizations, are launching strategies and making investments to apply these advances to address challenges related to food, energy, economic development, the environment, animal and plant health, and human well-being.

One of the exciting aspects of this "Century of Biology" is the diffusion of research capacity and infrastructure to many parts of the world, creating an increasingly global life sciences research enterprise.

Along with these hopes and achievements, however, have come concerns about the implications of such rapid advances. Concerns include uneasiness about how an increased understanding of basic life processes, and the resulting potential to manipulate and control them, may result in unintended impacts on the environment or human well-being, or the risk of deliberate misuse of knowledge, tools, and techniques from the life sciences to cause harm.

How the scientific community responds to these concerns can be considered part of the broader relationship between science and society. Beyond its fundamental quest for greater knowledge and understanding, science is conducted in a social context. Science depends on public support, including but not limited to the substantial funding that enables research to take place. Ensuring that scientific research is carried out responsibly is essential to maintaining the relationship between science and society.

**Keywords:** Responsible Conduct Of Research, Mena Region.

#### 686. Effect of Acrylamide on Male and Female Albino Rats

Sohair Ramadan Fahmy Ramadan

*Book Published By Lap: Lambert Academic Publishing, (2013)*

Acrylamide (ACR) is neurotoxic to experimental animals and humans. The literature on its neurotoxic effect in the mature animals is huge, but the effect of acrylamide on the immature is relatively less understood. The present study was carried out to investigate the hematological, biochemical, neurological and histopathological effects of acrylamide (15 mg/kg b.wt.) in immature and mature male and female rats as well as mature male and female rats at (50 mg/kg b. wt.). As could be shown histopathological alteration in the structures of treated liver, kidney, brain, testis and ovary which resulted following ACR administration. In conclusion, the present study showed that, acrylamide induced hematological, biochemical, neurological and histopathological disorders in the immature and mature male and female rats. So, we recommended that it must be eat a balanced diet, rich in fruits and vegetables and avoid fast or junk foods.

**Keywords:** Acrylamide; Hematological; Biochemical; Histopathological.

### 687. Parasitic Diseases - Schistosomiasis

Rashika Ahmed Fathi El Ridi

*Book Published By Intech, (2013)*

Reports on schistosomiasis epidemiology and clinical features in Africa and Brazil, and development of novel drugs that affect the worm tegument, and vaccine based on excretory-secretory products and Type 2 cytokines.

**Keywords:** Schistosoma; Epidemiology; Vaccine; Cytokines.

## Faculty of Agriculture

### Dept. of Agricultural Biochemistry Section

### 688. Soybean - Pest Resistance

Hany El-Shemy

*Book Published By Intech, Under Cc by 3.0 License, (2013)*

Legumes are important for the diet of a significant part of the world's population; they are a good source of protein, carbohydrates, minerals and vitamins. The importance of soybean lies in the overall agriculture and trade and in its contribution to food supply. Soybean contains the highest protein content and has no cholesterol in comparison with conventional legume and animal food sources. Furthermore, soybean is a cheap source of food, and at the same time medicinal due to its genistein, photochemical, isoflavones content. Soybean has been found to be extremely helpful in the fight against heart disease, cancer and diabetes, among others. Soybean protein and calories are presently being used to prevent body wasting often associated with HIV. The importance of soybean nutrition intervention is amplified where medications are unavailable. Its economic potential inherent in a wide range of industrial uses can be harnessed to the benefit of smallholder soybean producers.

**Keywords:** Agricultural; Biological sciences.

### 689. Drug Discovery

Hany El-Shemy

*Book Published By Intech, Chapters Published January 23, 2013 under Cc By 3.0 License, (2013)*

Natural products are a constant source of potentially active compounds for the treatment of various disorders. The Middle East and tropical regions are believed to have the richest supplies of natural products in the world. Plant derived secondary metabolites have been used by humans to treat acute infections, health disorders and chronic illness for tens of thousands of years. Only during the last 100 years have natural products been largely replaced by synthetic drugs. Estimates of 200 000 natural products in plant species have been revised upward as mass spectrometry techniques have developed. For developing countries the identification and use of endogenous medicinal plants as cures against cancers has become attractive. Books on drug discovery will play vital role in the new era of disease treatment using natural products.

**Keywords:** Pharmacology; Toxicology; Pharmaceutical science.

### 690. Soybean - Bio-Active Compounds

Hany El-Shemy

*Book Published By Intech, Chapters Published February 20, 2013 under Cc By 3.0 License, (2013)*

Legumes are important for the diet of a significant part of the world's population; they are a good source of protein, carbohydrates, minerals and vitamins. The "importance of soybean" lies in the overall agriculture and trade and in its contribution to food supply. Soybean contains the highest protein content and has no cholesterol in comparison with conventional legume and animal food sources. Furthermore, soybean is a cheap source of food, and at the same time medicinal due to its genistein, photochemical, isoflavones content. Soybean has been found to be extremely helpful in the fight against heart disease, cancer and diabetes, among others. Soybean protein and calories are presently being used to prevent body wasting often associated with HIV. The importance of soybean nutrition intervention is amplified where medications are unavailable. Its economic potential inherent in a wide range of industrial uses can be harnessed to the benefit of smallholder soybean producers.

**Keywords:** Agricultural; Biological sciences.

### 691. Radical Scavenging Activity of Algal Species

Emad Ahmed Shalaby

*Book Published By Lambert Academic Publisher, (2013)*

There is emerging interest in the use of naturally occurring antioxidants for the preservation of foods and in the management of a number of pathophysiological conditions, most of which involve free radical damage. The implication of oxidative and nitrosative stress in the etiology and progression of several acute and chronic clinical disorders has led to the suggestion that antioxidants can have health benefits as prophylactic agents.

Epidemiological studies have consistently shown an inverse association between consumption of vegetables and fruits and the risk of cardiovascular diseases and certain forms of cancer.

Although the protective effects have been primarily attributed to the well-known antioxidants, such as Vitamin C, Vitamin E and -carotene, plant phenolics may also play a significant role.

Moreover, restrictions over the use of synthetic antioxidants BHA and BHT in food further strengthen the concept of using naturally occurring compounds as antioxidants.

**Keywords:** Antioxidant activity; Algae; Mode of action

### 692. Anticancer Activity of Natural Compounds and Alternative Trials (Back To Nature)

Ahmed Mahmoud Mostafa Aboul-enein

*Book Published By Lap Lambert Academic Publishing, (2013)*

From more than 50 years, the mortality rates for cancer did not significantly improve. Cancer synthetic chemoprevention involves pharmacologic intervention chemicals to prevent, inhibit or reverse carcinogenesis or prevent the development of invasive cancer. However, several side effects are appeared by these chemotherapeutic drugs. Therefore, we did several attempts as spotlight on cancer therapeutics "back to nature" to avoid these effects by using natural anticancer. In this book, various Egyptian

medicinal plants, traditional herbs, spices, vegetables, fruits, and aquatic organisms from desert areas, coastal areas, and traditional market were studied. Their extracts and active principles were implemented and tested for antioxidant and anticancer activities. (Most of the experimental work was funded through STDF-Egypt project ID 312)

**Keywords:** Anticancer; Natural compounds; Alternative trials.

### 693. Natural Products as Biomaterials Cancer Therapy and Prevention

Ahmed Mahmoud Mostafa Aboul-enein

*Establishment of Integrative Research Base By Humanities and Sciences on Valorization of Useful Plants For Regional Development in North Africa, Alliance for Research on North Africa, University of Tsukuba, (2013)*

Cancer is undoubtedly one of our most serious human health problems with there being high mortality rates worldwide of more than seven million death per year. plants have played a significant role in the treatment of cancer and infectious diseases for the last four decades. Natural products have been rediscovered as important tools for drug development despite advances in combinatorial chemistry. herbal, or botanical, medicines, recorded in developing countries with ancient civilizations, such as Egypt, India and China provide an abundant pharmacopoeia of products that have been prescribed for many disease over many centuries. the natural products underlying traditional medicines. May active anticancer compounds isolated from natural plant extracts have been recognized.

**Keywords:** Anticancer; Natural compounds; Alternative trials.

### 694. Biofuel: Sources, Extraction and Determination

Emad Ahmed Shalaby

*Liquid, Gaseous and Solid Biofuels-Conversion Techniques, Intech Publisher, (2013)*

Biofuel is a type of fuel whose energy is derived from biological carbon fixation. Biofuels include fuels derived from biomass conversion (Figure 1, JICA, Okinawa, Japan), as well as solid biomass, liquid fuels and various biogases. Although fossil fuels have their origin in ancient carbon fixation, they are not considered biofuels by the generally accepted definition because they contain carbon that has been "out" of the carbon cycle for a very long time. Biofuels are gaining increased public and scientific attention, driven by factors such as oil price hikes, the need for increased energy security, concern over greenhouse gas emissions from fossil fuels, and support from government subsidies. Biofuel is considered carbon neutral, as the biomass absorbs roughly the same amount of carbon dioxide during growth, as when burnt.

**Keywords:** Biofuel; Biodiesel; Sources; Extraction; Determination.

### Dept. of Agricultural Microbiology

### 695. Biofertilizers for Organic Farming

Nabil Abraham Hegazi

*Book Published By Lap Lambert Academic Publishing, (2013)*

Organic farming and good agricultural practices (G.A.P) intrigues the concern of both consumers and producers of agricultural commodities. Principally, such practices are based on the concept of rationalizing agrochemical inputs and maximizing biological activities in the plant-soil system. Bio-preparates (Biofertilizers and Bio-pesticides) of various rhizobacteria are potential candidates supporting plant nutrition and health. Their applications are extensively experimented for prospective future marketing and practicing. The book with its 7 chapters is providing strong experimental evidences on the value add of using agro-industrial effluents (Bakers' yeast, starch, sugar and olive oil industries) and plant juices as accessible/economic substrates for biomass production and formulation of bio-preparates of rhizobacteria. The presented results of pot and field trials strongly emphasize the importance of bio-preparates as a potential practice for organic farming of field and vegetable crops under the impoverished conditions of semi-arid deserts. The book is an important resource for experts, researchers and students of agriculture, biotechnology, organic farming and environment.

**Keywords:** Bio-Preparates; Bio-Fertilizers; Bio-Pesticides; Inoculants; Rhizospheric Microorganisms; Rhizobacteria; Associative Diazotrophs; Rhizobium; Bakers' Yeast; Alpechin; Starch And Sugar Industries; Pero-Dextrin; Organic Agriculture; Good Agricultural Practices (Gap); North Sinai; Semi-Arid Deserts; Plant Juices.

### 696. The River Nile of Egypt

Nabil Abraham Hegazi

*Book Published By Lap Lambert Academic Publishing, (2013)*

"I never polluted the river Nile water": So supposedly swore every ancient Egyptian, in front of the gods, during the moral judgment of the dead. Were Egyptians able to respect their oath along the years? Modern history witnessed that the Nile was as much the primary source of fresh water as the major receptor of wastewater and drainage of different activities. Cities along the banks are the meeting points of all types of industrial activities, posing pollution stress on the river. The first chapter of the book presents a historic glance on the bond between Nile and the ancient Egyptian civilization. The remaining chapters provide scientific evidences on the impact of discharging agro-industrial effluents on the physico-chemical and microbiological quality of the river water around Cairo. Presented as well is the potential of in-situ bio-remediation activities exerted by the dominant Nile water microflora on the expense of discharged organic effluents. The forecasted future water deficit strongly recommends better management of water resources, including pre-treatment of such agro-industrial effluents for microbial biomass and bio-preparates production prior to discharge.

**Keywords:** Egypt; The River Nile; Cairo City; Water pollution; Water quality of River Nile; Microbiological analysis of River Nile water; Agro-industrial effluents; Sugar industry; Glucose and Starch industry; Bio-remediation; Nile microflora.

**Dept. of Vegetable Crops**

**697. Foliar Nutrition and Post-Harvest of Vegetable Crops**

Said Abdalla Shehata

*Contemporary Environmental Readings (Volume 2): Towards Sustainability For Agriculture, Lap Lambert Academic Publishing, (2013)*

Most people recognize that soil plays a significant role in food production, but fewer are aware of the role of soils in food security from a health perspective. Many of the elements that are required for human health come from the soil through either plant or animal products consumed by humans. Some essential elements may also be acquired directly through the voluntary and/or involuntary consumption of soil. There are also a number of ways that soils can have a detrimental effect on human health. Heavy metals in soil can be taken up by plants and passed on to those who consume them.

Ingestion or inhalation of soil particles can expose humans to heavy metals, organic chemicals, and pathogens, and airborne dust can cause direct health problems through irritation of the respiratory passages. Despite the obvious connections between soils and human health, there has not been a great amount of research done in this area when compared to many other fields of scientific and medical study. More research in this area is essential to protect and enhance human health.

In order to create conditions conducive to sustainable crop production, involving optimum utilization of all sources of plant nutrients with minimum environmental pollution, it is necessary to reorient agricultural producers to use those types of fertilization that are environmentally safe and appropriate which can also satisfy all crop nutrient requirements. This gives particular importance to foliar nutrition as this model poses the lowest risk of soil and groundwater contamination with undesirable mineral elements. The fertilization type used can substantially alter and disturb the growth and development of a fruit tree if fertilizers are applied incorrectly, regardless of the adequately predefined fruit tree nutrient requirements.

It could be concluded that this review will be focused on the integrated nutrient management to enhance plant nutrition, restore degraded soils, and describe the impact of foliar application on increasing agronomic production and advancing global food security. The relationship between integrated plant nutrition and postharvest of crops will be also addressed.

**Keywords:** Plant nutrient management; Sustainable agriculture; Postharvest management; Foliar nutrition.

**698. Organic Farming in Egypt**

Said Abdalla Shehata

*Contemporary Environmental Readings Volume 3: Egyptian Agriculture: Present and Future, Lap Lambert Academic Publishing, (2013)*

Organic farming refers to agricultural production systems used to produce food and fiber. Organic farming management relies on developing biological diversity in the field to disrupt habitat for pest organisms, and the purposeful maintenance and replenishment of soil fertility. Organic farmers are not allowed to use synthetic pesticides or fertilizers. All kinds of agricultural

products are produced organically, including produce vegetable crops, grains, meat, dairy, eggs, flowers, and processed food products. Some of the essential characteristics of organic systems include: design and implementation of an "organic system plan" that describes the practices used in producing crops and livestock products; a detailed recordkeeping system that tracks all products from the field to point of sale; and maintenance of buffer zones to prevent inadvertent contamination by synthetic farm chemicals from adjacent conventional fields.

**Keywords:** Organic farming; Sustainable; System produces healthy; Livestock; Crops; Damaging.

**699. Sprout Production and Storage of Some Legume Seeds**

Said Abdalla Shehata

*Sprout Production and Storage of Some Legume Seeds, Lap Lambert Academic Publishing, (2013)*

The experiments were conducted in the Physiology Lab in the Exportation Competition Project of some Vegetables, Faculty of Agriculture, Cairo University, Giza from 2009 to 2011.

The effect of sprouting media, seedling density and growth duration on character and yield of faba bean, pea and cowpea as well as storage and microbial load of faba bean and pea sprouts were studied. In faba bean sprout production, using rice straw, 50 % seeding density and 7 days duration were ideal for production. In pea sprout production, using kitchen paper, 75 % seeding density and 9 days duration were ideal for production.

In cowpea sprout production, using rice straw, 50 % seeding density and 6 days growth duration were ideal for production. During faba bean sprouting, fiber, ash, K, aspartic, threonine, serine, glycine, valine, isoleucine, leucine, phenylalanine, histidine, linoleic acid, linolenic acid, antioxidant and total phenol were increased. Sprouting of pea caused increase in fiber, protein, lipid and ash, K, vitamin A and E, aspartic, histidine and glutamic acid, linoleic acid, linolenic acid and antioxidant on a dry weight basis as compared with dry seeds. Cowpea sprout showed increase in fiber, ash, K, Ca, vitamin A, and E, aspartic, threonine, valine, isoleucine, phenylalanine, arginine, Linoleic acid, linolenic acid and antioxidant. Pea and faba bean sprouts stored in black punnets covered with cling significantly exhibited lower weight loss percentage, higher visual quality, lower off odor, lower off flavor and lighter color (higher lightness value) as compared to those stored in strawberry punnets.

The interaction among package type, storage and shelf life period on off flavor of pea sprouts showed that the most suitable conditions for lowest sprout off flavor was storing pea sprout at 0 °C for 4 days in black punnets covered with stretch or at 0 °C for 2 days plus 2 days at 10 °C in strawberry, while it was storing faba bean sprouts at 0 °C for 6 days plus 1 day at 10 °C in black punnets covered with stretch or at 0 °C for 2 days plus 2 days at 10 °C in strawberry punnets.

Salmonella, Shigella, Staphylococcus and Faecal coliform were not detected on pea and faba bean sprouts during storage.

**Keywords:** Germination; Sprouts; Storage; Nutritional value; Legumes.

## Faculty of Veterinary Medicine

### Dept. of Veterinary Hygiene and Managment

#### 700. Diseases of Fish and Crustaceans

Hussein AbdElHay ElSayed Kaoud

Book Published By Discovery Publishing House Pvt.Ltd. (2013)

Aquaculture literature describes a large number of infectious and noninfectious diseases caused by various pathogenic agents. Pathogens are always present in the environment. The main concern, therefore, is of introducing new disease organisms or causing environmental deterioration that can result in increased populations and virulence of indigenous pathogens, and disease outbreaks in wild stocks as a result of waste discharges from aquaculture farms, or the introduction or transplantation of culture stocks. Distinction has to be made between indigenous opportunistic pathogens that can cause disease only when the host's resistance is lowered or when unusual circumstances favour its growth and development, and obligate disease-causing organisms that cannot survive in nature unless susceptible or carrier hosts are present.

Fishes, as with other animals, are subjected to a wide spectrum of diseases. Such diseases require a somewhat different approach to solving the problem than terrestrial animals. Fishes are in an entirely different environment.

The pathogenic agents described in the culture systems are usually present in wild fish populations. However, in natural environments, they rarely cause mortality due to the lack of the stressful conditions that usually occur in the culture facilities.

It is important to point out that diseases classically considered as typical of fresh water aquaculture, such as furunculosis (*Aeromonas salmonicida*), bacterial kidney disease (BKD) (*Renibacterium salmoninarum*) and some types of streptococcosis, are today important problems also in marine culture. Clinical signs (external and internal) caused by each pathogen are dependent on the host species, fish age and stage of the disease (acute, cronic, subclinic carrier). In addition, in some cases, there is no correlation between external and internal signs. In fact, systemic diseases (i.e., pasteurellosis, piscirickettsiosis) with high mortality rates cause internal signs in the affected fish but they often present a healthy external appearance. On the contrary, other diseases with relatively lower mortality rates (i.e., flexibacteriosis, bwinter ulcer syndrome, some streptococcosis) cause significant external lesions, including ulcers, necrosis, exophthalmia which make fish unmarketable.

Diagnosis is a label given for a medical condition or disease identified by its signs, symptoms, and from the results of various diagnostic procedures. The term "diagnostic criteria" designates the combination of signs, symptoms, and test results that allows the clinician to ascertain the diagnosis of the respective disease. Proper diagnosis leads to accurate therapies and avoid indiscriminate use of chemotherapeutics.

The periodical careful ensuring that adequate drainage and disinfection of tanks and raceways is carried out are hygienic and indispensable prophylactic measures and preventing the infection due to parasites and similar biological factors which give rise to disease problems in cultivated waters.

The cure of certain fish disease is therapeutically possible therapy in general, as much in aquarium fish rearing as in fish farming, is of secondary importance to prophylaxis and hygiene. Diagnosis, prophylaxis and disease prevention and aquaculture hygiene has become subject offered by veterinarians.

The present book includes: Epidemiology of Fish Diseases; Interactions of pH, Carbon Dioxide, Alkalinity; The Immune System; Diseases of fish; Diseases of shrimp, prawn, crayfish and crabs; Diagnosis of fish diseases ; Disinfection of aquaculture; Prevention and Therapy of Fish Diseases; Recent articles; Therapy and drugs administered in feed and Laboratory Practices.

**Keywords:** Pathogens; Fish and crustaceans; Epidemiology; Diagnosis; Therapy.

#### 701. Aquatic Biodiversity and Pollution

Hussein AbdElHay ElSayed Kaoud

Book Published By Discovery Publishing House Pvt.Ltd. (2013)

Seasonal dynamic of microbial and physico-chemical characteristic of *Claris Gariepinus* hatchery system, Effect of copper intoxication on survival and immune response in tropical freshwater prawn, *Macrobrachium rosenbergii*; Ecological services of freshwater biodiversity that maintain water quality and health ecosystem; Histopathological alterations and bioaccumulation of heavy metals in *Oreochromis niloticus* fish; Zooplankton composition in fresh water bodies; Effect of exposure to mercury on health in tropical *Macrobrachium rosenbergii*; Structure and functions of aquatic ecosystem and its biodiversity; Toxic effect of mercury exposure in Nile tilapia (*Oreochromis*); wetlands- A fragile ecosystem: its prospectus, conservation and management strategies and action plan in Indian scenario.

The present book mainly deals with aquatic biodiversity, conservation, aquaculture and environmental pollution. The book will be of beneficial for both present and future colleagues, who teach, study and working in the field of environment, ecology, aquatic ecosystem, environmental threats, fisheries and aquaculture.

**Keywords:** Pollution; Conservation; Aquaculture; Environmental Threats.

#### 702. Biodiversity of Aquatic Ecosystem

Hussein AbdElHay ElSayed Kaoud

Book Published by Discovery Publishing House Pvt.Ltd. (2013)

However, the effects of pollution are dangerous especially for all the living inhabitants of the seas and oceans. These consequences are diverse. Primary critical violations in the functioning of living organisms under the influence of pollutants occur at the level of biological effects: after changing the chemical composition of the cells are broken processes of respiration, growth and reproduction of organisms, may mutate and carcinogenesis; violated the motion and orientation in the marine environment. Morphological changes are often manifested in the form of various pathologies of internal organs: changes in size, development of abnormal forms. Particularly often, these phenomena are recorded in case of chronic pollution. All this affects the state of individual populations, their relationships. Thus, there are environmental consequences of pollution. An important indicator of disturbances of ecosystems is a change in the number of higher taxa - fish. Changes significantly the photosynthetic action in general. Increases the biomass of microorganisms, phytoplankton and zooplankton. This is characteristic of the eutrophication of marine waters; they were especially significant in the inland seas, seas



closed. In the Caspian Sea, Black Sea, Baltic Sea over the past 10 - 20 years, microbial biomass increased almost 10 times. In the Sea of Japan scourge became "red tides", a consequence of eutrophication, in which rapidly developing microscopic algae, and then disappears oxygen in the water, killing aquatic animals and formed a huge mass of decaying residues of toxic, not only sea but also the atmosphere. Pollution of the oceans leads to a gradual reduction of primary biological production. Scientists estimate that it declined to the present time to 10%. Accordingly, the annual growth rate is reduced and other sea creatures.

**Keywords:** Disturbances of ecosystems; Biomass; Pollution of the oceans.

## National Institute of Laser Enhanced Sciences

*Dept. of Laser Applications in Metrology, Photochemistry and Agriculture (LAMP)*

### **703. Laser and Radiofrequency Induced Hyperthermia Treatment via Gold-Coated Magnetic Nanocomposites**

El-sayed Abdel-Majied Al-Sherbini

*Hyperthermia, Intech, (2013)*

There is renewed interest in magnetic and plasmonic photo-thermal hyperthermia, as a cancer treatment method. In the current study, super paramagnetic iron oxides nanoparticles, gold nanospheres and gold-iron oxide core shell nanoparticles were prepared and characterized for inducing hyperthermia to treat subcutaneous Ehrlich carcinoma implanted in female Swiss albino mice through three treatment techniques (Magnetic, Optical and Magneto-Optical) resonance hyperthermia. The maximum temperatures achieved in the tumors were  $45\pm 2.0^{\circ}\text{C}$ ,  $50\pm 1.5^{\circ}\text{C}$ ,  $58\pm 2.0^{\circ}\text{C}$ , respectively. The results revealed that, all mice treated by the first two techniques, the tumors were still as the same as before the treatments, as well as the rate of tumors growth were very slow if compared with the control mice. In contrast more than 50% of the mice treated with the third revealed a complete disappearance of the tumor. So, this simple, non-invasive method shows great promise as a treatment technique for clinical setting.

### **704. Analysis of corroded metallic heritage artifacts using laser induced breakdown spectroscopy (LIBS)**

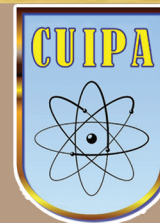
Mohamed Abdel-Harith Mohamed

*Corrosion and Conservation of Cultural Heritage Metallic Artefacts, Woodhead Publisher (2013)*

In the present chapter laser induced breakdown spectroscopy (LIBS) is introduced as a powerful spectrochemical analytical technique that can be exploited to characterize corroded artifacts. Scientific and technological aspects of LIBS are briefly presented. LIBS does not need sample preparation, it is nondestructive and it can be used for in situ measurements. Examples of LIBS applications that can help archeologists in conservation and restoration of metallic artifacts are given. We demonstrated the use of LIBS in analysis of corroded metal threads, depth profiling of copper based decorative artifact, analysis of corroded Punic coins, and LIBS and XRF analysis of Roman silver denarii.



Cairo University



# **(2) Engineering Sciences Sector**

2-1 1 Faculty of Engineering

2-2 2 Faculty of Computers and Information

2-3 Institute of Statistical Studies and Research

CAIRO UNIVERSITY

Publication  
in  
Journals



## Faculty of Engineering

### Dept. of Aeronautical and Aerospace Engineering

#### 705. A Low-dimensional Approach to Closed-loop Control of a Mach 0.6 Jet

Kerwin R. Low, Zachary P. Berger, Stanislav Kostka, Basman ElHadidi, Sivaram Gogineni and Mark N. Glauser

*Experiments in Fluids*, 54: 1-17 (2013) IF: 1.572

Simultaneous time-resolved measurements of the near-field hydrodynamic pressure field, 2-component streamwise velocity field, and far-field acoustics are taken for an un-heated, axisymmetric Mach 0.6 jet in co-flow. Synthetic jet actuators placed around the periphery of the nozzle lip provide localized perturbations to the shear layer. The goal of this study was to develop an understanding of how the acoustic nature of the jet responds to unsteady shear layer excitation, and subsequently how this can be used to reduce the far-field noise. Review of the cross-correlations between the most energetic low-order spatial Fourier modes of the pressure and the far-field region reveals that mode 0 has a strong correlation and mode 1 has a weak correlation with the far-field. These modes are emulated with the synthetic jet array and used as drivers of the developing shear layer. In open loop forcing configurations, there is energy transfer among spatial scales, enhanced mixing, a reconfiguration of the low-dimensional spatial structure, and an increase in the overall sound pressure level (OASPL). In the closed loop configuration, changes to these quantities are more subtle but there is a reduction in the overall fluctuating sound pressure level OASPL<sub>r</sub> by 1.35 dB. It is argued that this reduction is correlated with the closed loop control feeding back the dynamical low-order information measured in the largest noise producing region.

**Keywords:** Closed loop control; Jet flow.

#### 706. Comparison of Coarse Grid Lattice Boltzmann and Navier Stokes for Real Time Flow Simulations in Rooms

Basman Elhadidi and H. Ezzat Khalifa

*Building Simulation*, 6: 183-194 (2013) IF: 0.649

Coarse grid lattice Boltzmann models (LBM) and computational fluid dynamics (CFD) are compared in building simulations. Three simulations are used to assess the different numerical models: (I) a 2D isothermal flow case, (II) a 3D isothermal flow case and (III) a 2D non-isothermal flow case. Both models predicted the correct flow patterns and temperature field and could be used for real time (RT), near real time (NRT) and faster than real time (FRT) simulations without loss of accuracy on multi-core processors. The results indicate that the coarse grid CFD is both faster and more time accurate than the LBM for unsteady simulations.

**Keywords:** Coarse grid CFD; Fast fluid dynamics; Lattice Boltzmann methods.

#### 707. Aerodynamic Resuspension of Particles Due to a Falling Flat Disk

Basman Elhadidi and H. Ezzat Khalifa

*Particulate Science and Technology*, 31: 35-44 (2013) IF: 0.435

In this article, computational fluid dynamics (CFD) is used to compute the unsteady, compressible flow caused by a flat falling circular disk. CFD results are coupled with a particle trajectory model to determine particle trajectories for different particle sizes and examine which particles are trapped or ejected from the closing gap. CFD results show that the normalized radial velocity profiles are self similar for different Reynolds numbers based on the gap height, and that flow compressibility results in a density increase toward the center of the disk for decreasing gap height. To efficiently couple CFD results with the particle trajectory model, a regression model representing both the velocity field and density variation inside the gap is developed and coupled with a particle detachment model. Particle trajectories are shown to be sensitive to the flow compressibility and must be taken into account. The escaped and trapped particle distribution is computed for a thin mono-layer of Arizona Test Dust under the disk. The simulations show that higher impact velocities tend to cause more of the heavier and larger particles to be trapped under the disk because they are catapulted from the floor and are quickly driven down again by the descending disk.

**Keywords:** CFD; Detachment; falling disk; resuspension.

### Dept. of Architectural Engineering

#### 708. Assessment and Review of Infill Designs' Guidelines for Residential Urban Conservation Areas

Sahar Imam

*International Journal for Housing Science*, 37 (3): 137-149 (2013)

Building in traditional existing context has always presented a serious challenge, raising critical questions on how new designs should interact with the context. Some theories are claiming that interaction is achieved by relating the new buildings to older buildings' aesthetics and replicating the old style. Other theories are declaring that a new design should respond to its own period of time since architecture always represents its time. Old historical contexts are characterized by high level of mixed uses, and residential use is the highest. Therefore the cooperation and agreement of local community seems to be essential in each infill design case, in order to understand local communities' culture and needs, and thus aesthetics dilemma becomes a problem to be related to community not just keep it exclusive to designers and theorists. The current paper critically studies the guidelines and design criteria commonly applied to infill design in urban conservation areas by specialized control agencies and centers. It intends to assess the relation between these guidelines and laypersons' response and preferences especially that many actors are involved in infill issues related to special historical contexts starting from local communities, control agencies, intellectuals to professionals and designers. Most of the guidelines' lists focus on the formal aesthetics of the environments and its physical qualities, especially visual and spatial qualities. The paper critically reviews the necessity of focusing on the content of the environment form and the way lay persons see it and relate to it, by having a comprehensive design brief specific to the site of infill, the brief has common key physical and formal guidelines to preserve area character and ways to include local community in design decisions in order to relate to community preferences, values and needs. The paper stresses the idea that including the community in the design brief helps the infill project to be deeply

related to the context and the local community, thus increasing its chances of success. The paper deploys an Egyptian infill experience carried out by Agha Khan Trust of Culture (AKTC) in Al Darb Al Ahmar – Aslam neighborhood- a historical residential area in Islamic Cairo, assessing the processes followed by AKTC to include the community in the infill design process, and whether the results succeeded in meeting community preferences, values and needs.

**Keywords:** Historical contexts; Infill design; Design guidelines; Formal aesthetics; Symbolic aesthetics.

#### Dept. of Chemical Engineering

### 709. Newtonian Viscosity Behavior of Dilute Solutions of Polymerized Whey Proteins. Would Viscosity Measurements Reveal More Detailed Molecular Properties?

Ahmed S. Eissa

*Food Hydrocolloids*, 30: 200-205 (2013) IF: 3.494

Dilute solution Newtonian viscosity of whey protein polymers at different temperatures has not been assessed in literature. In this work, a thermally-treated whey protein solution at 8% w/w and pH 6.8 was prepared. Dilute solution viscometry was investigated at different temperatures from 30 °C to 65 °C. Intrinsic viscosity and voluminosity data indicate slight shrinkage in molecular size upon temperature increase. The temperature dependence of viscosities was expressed by the Arrhenius–Frenkel–Eyring equation and the thermodynamic parameters of viscous flow of polymer solutions were calculated. Results show a positive entropy change of viscous flow, indicating ordered structures. Chromatographic separation results prove that although disulphide bonds form the polymer backbone chain, both hydrophobic associations and hydrogen bonding still play a role in molecular structuring, even at very low protein concentrations. The calculated shape factor indicates spherical polymer molecules over the entire investigated temperature range.

**Keywords:** Whey proteins; Dilute solution viscometry; Thermodynamics.

### 710. Free Radical Grafting Kinetics of Acrylamide Onto a Blend of Starch/Chitosan/Alginate

Sorour M, El-Sayed M, El Moneem NA, Talaat H, Shaalan H and El Marsafy S.

*Carbohydrate Polymers*, 98: 460-464 (2013) IF: 3.479

Grafting of monomer onto polymer backbone is one of the effective and accessible methods for the chemical modification of polysaccharides. Grafting of acrylamide (AAM) onto polysaccharides blend (PsB) composed of starch, chitosan and alginate has been carried out using potassium persulfate (KPS) as an initiator. The kinetics of the grafting polymerization also has been studied. The grafting parameters have been evaluated by changing the initial concentrations of AAM from 8 to 16 g, PsB from 6 to 14 g and KPS from 0.2 to 1 g. Evidence of grafting has been obtained from FTIR, XRD and TGA. The kinetics of the grafting polymerization also has been studied. The grafting rate equation of the produced hydrogel (PsB-g-AAM) hydrogel has been expressed by:  $R_g = k[AAM][PsB](0.5)[KPS](0.5)$ . The

grafting rate is a first order dependence to [AAM] initial concentration and square root to [PsB] and [KPS] initial concentrations in the used concentrations range.

**Keywords:** Acrylamide; Graft polymerization; Kinetics; Starch.

### 711. Semi-Empirical Correlation for Binary Interaction Parameters of the Peng–Robinson Equation of State With the Van Der Waals Mixing Rules for the Prediction of High-pressure Vapor–liquid Equilibrium

Seif-Eddeen K. Fateen, Menna M. Khalil and Ahmed O. Elnabawy

*Journal of Advanced Research*, 4: 137-145 (2013) IF: 3

Peng–Robinson equation of state is widely used with the classical van der Waals mixing rules to predict vapor liquid equilibria for systems containing hydrocarbons and related compounds. This model requires good values of the binary interaction parameter  $k_{ij}$ . In this work, we developed a semi-empirical correlation for  $k_{ij}$  partly based on the Huron–Vidal mixing rules. We obtained values for the adjustable parameters of the developed formula for over 60 binary systems and over 10 categories of components. The predictions of the new equation system were slightly better than the constant- $k_{ij}$  model in most cases, except for 10 systems whose predictions were considerably improved with the new correlation.

**Keywords:** Peng–Robinson equation of state; Vapor–liquid equilibrium; Mixing rules; Binary interaction parameters.

### 712. Synthesis and Characterization of Laminated Si/SiC Composites

Salma M. Naga, Sayed H. Kenawy, Mohamed Awaad, Hamada S. Abd El-Wahab, Peter Greil and Magdi F. Abadir

*Journal of Advanced Research*, 4: 75-82 (2013) IF: 3

Laminated Si/SiC ceramics were synthesized from porous preforms of biogenous carbon impregnated with Si slurry at a temperature of 1500 °C for 2 h. Due to the capillarity infiltration with Si, both intrinsic micro- and macrostructure in the carbon preform were retained within the final ceramics. The SEM micrographs indicate that the final material exhibits a distinguished laminar structure with successive Si/SiC layers. The produced composites show weight gain of 5% after heat treatment in air at 1300 °C for 50 h. The produced bodies could be used as high temperature gas filters as indicated from the permeability results.

**Keywords:** Laminates; Si/SiC composites; Microstructure; permeability; Oxidation resistance.

### 713. Rapid Synthesis of Titania–silica Nanoparticles Photocatalyst by a Modified Sol–gel Method for Cyanide Degradation and Heavy Metals Removal

Farid A. Harraz, Omar E. Abdel-Salam, Ahlam A. Mostafa, Reda M. Mohamed and M. Hanafy

*Journal of Alloys and Compounds*, 551: 1-7 (2013) IF: 2.39



Titania-silica ( $\text{TiO}_2\text{-SiO}_2$ ) photocatalyst was prepared by a modified sol-gel technique. Titania sol was firstly synthesized by acid hydrolysis of a  $\text{TiCl}_4$  precursor instead of titanium alkoxides. The titania sol was further modified with  $\text{SiO}_2$  to obtain a modified catalyst. The as-prepared  $\text{TiO}_2\text{-SiO}_2$  catalyst demonstrated a remarkable photocatalytic activity toward degradation of cyanide and heavy metals removal ( $\text{Cr(III)}$ ,  $\text{Co(II)}$  and  $\text{Pb(II)}$ ). The influence of the preparation parameters; the reaction time, the calcination temperature and time, the  $[\text{H}^+]/[\text{Ti}]$  ratio, the pH value and the acid concentration on the structural and chemical properties of the catalyst was investigated in details. The catalytic performance was found to depend essentially on the catalyst and target concentrations and the reaction time. The as-synthesized catalyst was characterized by a variety of techniques including surface area measurement, X-ray diffraction analysis (XRD), scanning electron microscopy (SEM) transmission electron microscopy (TEM) and ultraviolet-visible (UV-vis) spectroscopy measurements. Results of the synthesis and characterization of  $\text{TiO}_2\text{-SiO}_2$  catalyst and its photocatalytic performance are presented and thoroughly discussed.

**Keywords:** Titania- silica; Modified sol- gel; TEM; Photocatalysis.

#### 714. Assessment of Capabilities and Limitations of Stochastic Global Optimization Methods for Modeling Mean Activity Coefficients of Ionic Liquids

A. Bonilla-Petriciolet, S.E.K. Fateen, G.P. Rangaiah

*Fluid Phase Equilibria*, 340: 15-26 (2013) IF: 2.379

In this paper, we have studied and analyzed the capabilities and limitations of seven stochastic global optimization methods to model mean activity coefficients of ammonium aqueous electrolytes using the electrolyte NRTL model. These stochastic methods are: simulated annealing (SA), genetic algorithm (GA), differential evolution (DE), particle swarm optimization (PSO), DE with tabu list (DETL), harmony search (HS) and bare bones PSO (BBPSO). Convergence characteristics and performances of these optimization methods have been tested and compared using different stopping conditions. Overall, our results indicate that SA, DETL and BBPSO offer better performance and promising convergence characteristics for solving parameter estimation problems involved in the modeling of thermodynamic properties of ionic liquids (ILs).

**Keywords:** Parameter estimation; Ionic liquids; Stochastic optimization methods; Global optimization.

#### 715. Cuckoo Search: A New Nature-Inspired Optimization Method for Phase Equilibrium Calculations

V. Bhargavaa, S.E.K. Fateenb and A. Bonilla-Petriciolet

*Fluid Phase Equilibria*, 337: 191-200 (2013) IF: 2.379

In this study, Cuckoo Search is introduced for performing phase equilibrium and stability calculations for the first time. Cuckoo Search is a population-based method that mimics the reproduction strategy of cuckoos. This meta-heuristics have been successfully used for solving some engineering design and optimization problems with promising results. However, this emerging optimization method has not been applied in chemical

engineering problems including thermodynamic calculations. This study reports the application of Cuckoo Search and its modified version for phase equilibrium and stability calculations in both reactive and non-reactive systems. Performance of this nature-inspired optimization method has been analyzed using several phase stability, phase equilibrium and reactive phase equilibrium problems. Results show that Cuckoo Search offers a reliable performance for solving these thermodynamic calculations and is better than other meta-heuristics previously applied in phase equilibrium modeling.

**Keywords:** Phase equilibrium; Phase stability analysis; Chemical equilibrium; Cuckoo search; Stochastic global optimization.

#### 716. Mechanism and Kinetics of the Non-Isothermal Degradation of Ethylenepropylene Diene Monomer (EPDM)

Ehab Fouad Abadir

*Journal of Thermal Analysis and Calorimetry*, 114: 1409-1413 (2013) IF: 1.982

The thermal degradation behaviour of ethylene-propylene-diene (EPDM) elastomer, was examined under non-isothermal conditions at different heating rates (5, 7, 10 and 12 °C/min) using thermogravimetric analysis. Kinetic parameters of degradation were evaluated using the Flynn-Wall-Ozawa isoconversional method, as well as the integral method of Coats and Redfern. A comparison between the two methods showed that the degradation of EPDM follows the Avrami-Erfeev two dimensional nucleation model. The thermodynamic parameters were also calculated and the effect of the heating rate on each was deduced.

**Keywords:** EPDM elastomer; Kinetics; Degradation; Activation energy; Thermodynamic parameters.

#### 717. Green Synthesis of Antibacterial Chitosan Films Loaded With Silver Nanoparticles

Neama A. Reiad, Omar E. Abdel Salam, Ehab F. Abadir and Farid A. Harraz

*Chinese Journal of Polymer Science*, 31(7): 984-993 (2013) IF: 1.27

An eco-friendly chemical reduction method was successfully used for the preparation of chitosan (CTS) composite films loaded with silver nanoparticles (AgNPs) by self assembly method using poly(ethylene glycol) as both reducing and stabilizing agent. UV-Vis spectra of the prepared chitosan loaded silver nanoparticles (CTSLAg) films reveal that full reduction of silver ions to silver nanoparticles takes place at 90 °C. The effect of reaction conditions on the silver nanoparticles formation was investigated using UV-Vis spectrophotometer. The morphology of the films was tested by scanning electron microscopy (SEM). The DSC curves showed that the CTSLAg film had a favorable compatibility and heat stability. AgNPs were confirmed by XRD and UV-Vis spectroscopy. The TEM findings revealed that the silver nanoparticles synthesized were spherical in shape with uniform dispersal, and by increasing CTS:PEG ratio larger silver nanoparticles could be obtained. The results of antibacterial study

reveal that the prepared nanocomposite films exhibited potential inhibition.

**Keywords:** Chitosan; Silver nanoparticles; Antibacterial activity.

#### **718. Characterization of Hydrogel Synthesized from Natural Polysaccharides Blend Grafted Acrylamide Using Microwave (MW) and Ultraviolet (UV) Techniques**

Mohamed Sorour, Marwa El-Sayed, Nabil Abd El Moneem, Hala A. Talaat, Hayam Shalaan and Sahar El Marsafy

*Starch - Stärke*, 65: 172-178 (2013) IF: 1.22

Grafting is a powerful method for producing substantial modification in the polysaccharide polymer properties thereby enlarging the range of its utilization. The aim of this work is to identify the appropriate conditions for grafting a candidate synthetic monomer (acrylamide) onto a blend of polysaccharides (PsB) comprising of starch, chitosan, and alginate. Grafting process was carried out in the presence of a low concentration of potassium persulfate initiator and methylenebisacrylamide crosslinker using microwave (MW) or ultraviolet (UV) irradiation techniques. Different Am/PsB weight ratios (0.6–0.96) has been performed. The produced hydrogel was characterized using Fourier transform infrared (FTIR) spectroscopy and scanning electron microscope (SEM) as well as nitrogen percent (%N). This study is focusing on comparing hydrogel samples in terms of grafting percentage (%G), grafting efficiency (%GE) and %add-on. UV graft PsB (PsB-g-Am) gave the highest %G (157.8%), %GE (84%), %add-on (61.95%) and %N (8.79%). Swelling water ratio (SWR) for the grafted samples in distilled water (DW) and different pH solutions (3–13) has been studied. UV grafted hydrogel gave a maximum SWR of 39 g/g. Am/PsB weight ratio and irradiation source had a direct effect on SWR of the produced hydrogel.

**Keywords:** Acrylamide; Grafting; Hydrogel; Polysaccharides; Swelling.

#### **719. Process and Financial Considerations Pertinent to Hydrogel Manufacture**

Mohamed H. Sorour, Marwa M. El Sayed, Nabil M. Abd El Moneem, Hala A. Talaat, Hayam F. Shaalan and Sahar M. El Marsafy

*Starch/ Stärke*, 1-8 (2013) IF: 1.22

Hydrogels are hydrophilic networks of crosslinked synthetic polymers or grafted natural polymers. The latter type involves grafting of a monomer onto a natural polymer using initiator and crosslinker. The present paper comprises of hydrogel manufacturing processes for starch grafted acrylamide (St-g-Am) using three different grafting techniques (conventional, microwave (MW), and ultraviolet (UV) irradiation). The prepared hydrogel has been characterized using XRD, FTIR, TGA, and SEM. Grafting indicators are compared on the basis of reported typical international and national studies. Moreover, economics and environmental aspects are addressed using the investigated manufacturing procedures. Recommendations for clean technology applications pertinent to hydrogel manufacture are included.

**Keywords:** Financial; Grafting; Microwave; Starch; Ultraviolet.

#### **720. Characterization of Used and Fresh Hydraulic Oils of Heavy Machinery Plants. Simple Treatment Methodology and Characterization of Treated Oil**

A. S. Eissa, N. I. Mohammed, R. I. Abd-Allah and S. T. El-Sheltawy

*Petroleum Science and Technology*, 31: 625-632 (2013) IF: 0.3

Fresh and used hydraulic oil samples were characterized. Density, kinematic viscosity, pour point, flash point, rust prevention, total acid number, oxidation stability, thermal stability, foam characteristics, foaming tendency, water content, and particle count were assessed for both fresh and used oil samples. Results show that water content has considerably affected most of the oil properties. The used oil sample failed the appearance, thermal stability, oxidation stability, foaming tendency, water content, and particle count. Simple treatment methodology was adopted, involving settling, dry-air bubbling, and vacuum filtration. Treated oil sample passed the tests of appearance, water content, particle count, and thermal stability.

**Keywords:** Characterization; Hydraulic oil; Recycled oil; Treatment; Used.

#### **721. Removal of Urea from Industrial Wastewater Using Electrochemical Decomposition**

Mahmoud H. Mahmoud, Omar E. Abdel-Salam, Nabil M. Abdel-Monem, Ahmed F. Nassar and Mohamed A. El-Halwany

*Life Science Journal*, 10 (3): 2048-2055 (2013) IF: 0.165

In this study, experiments were carried out using a bench-scale electrochemical cell incorporating flow-by porous graphite electrodes for decomposition of urea. The effect of anodic current density, influent feed flow rate, sodium chloride concentration, and urea concentration, on basic process indices, the removal rate of urea, current efficiency, and energy consumptions, were investigated. The experimental results showed that, the removal rates of urea increased with increasing the current density; at the same time, the energy power consumption increased, and the current efficiency decreased. At initial urea concentration of 2500 ppm, maximum current efficiency is 82, maximum removal rate is 0.78 g/h, and minimum energy consumption is 11 kWh/kg.

**Keywords:** Urea; Flow-by; Graphite; Porous; Decomposition.

#### **722. Effect of Silica Content on the Acid Resistance of Enamels**

Sh. K. Amin, M.M. Ahmed, El S.K. El-Sayed and M.F. Abadir

*Advances in Natural and Applied Sciences*, 7(3): 300-306 (2013)

Acid resistant enamels are used in the chemical industry in the lining of reactors subjected to aggressive chemicals. An acid resistant enamel recipe is presented, where the silica content in mill addition is varied from 0 to 35 %. The effect of this addition on the crazing and the mechanical adherence of the enamel to steel were investigated. It was found that while the crazing resistance was not affected, the adherence decreased with an increase in silica content, although still being in the acceptable range even at a 35 % silica level. Steel enameled sheets, with different silica content, were then tested for acid corrosion for time periods reaching 250 hours at 60 oC by subjecting them to

solutions of 20 % HCl, 98 % H<sub>2</sub>SO<sub>4</sub>, 85 % H<sub>3</sub>PO<sub>4</sub>, and 90 % ClCH<sub>2</sub>COOH (monochloroacetic acid). It was found that, in all cases, a mill addition of 30 – 35 % silica showed an excellent performance. These results were then compared by subjecting low carbon steel, 316 stainless steel and Hastelloy–C sheets to the same chemical solutions, under the same conditions. The results were comparable to those of Hastelloy–C, with the obvious economic advantages of using enameled steel over this expensive alloy. The kinetics of acid attack was disclosed showing a marked decrease in the rate of reaction with increased silica in mill addition.

**Keywords:** Enamels; Silica; Corrosion; Acids.

### 723. Oxidation of Urea in Human Urine Using Flow-by Porous Graphite Electrode

Nabil M. Abdel-Monem, Omar E. Abdel-Salam, Ahmed F. Nassar and Mahmoud H. Mahmoud

*International Journal of Scientific and Engineering Research*, 4 (12): 1715-1723 (2013)

In this study, experiments were carried out using a bench-scale electrochemical cell incorporating flow-by porous graphite electrodes for oxidation of human urine was collected from a mosque during baths on urea were analyzed and found that the concentration ranges of urea between 50 to 100 ppm.

The effect of anodic current density, and influent feed flow rate, on basic process indices, the removal rate of urea, and current efficiency, and energy consumptions, were investigated.

The experimental results showed that, the removal rates of urea increased with increasing the current density; at the same time, the energy power consumption increased, and the current efficiency decreased. At human urine concentration of 100 ppm, the maximum current efficiency is 27, the maximum removal rate is 0.33 g/h, and minimum energy consumption is 196 kWh/kg.

**Keywords:** Urea; Flow-by; Graphite; Porous; Decomposition.

#### Dept. of Computer Engineering

### 724. A Ga-Based Approach for Epipolar Geometry Estimation

Nehal Khaled, Elsayed E. Hemayed and Magda B. Fayek

*International Journal of Pattern Recognition and Artificial Intelligence*, 27(8): 1355014-1-1355014-19 (2013) IF: 0.562

In this paper, a genetic algorithm (GA)-based approach to estimate the fundamental matrix is presented. The aim of the proposed GA-based algorithm is to reduce the effect of noise and outliers in the corresponding points which affect the accuracy of the estimated fundamental matrix. Although in the proposed approach the GA is allowed to select the significant among all detected points, on the average half of the matched points have been determined to give optimum estimation of the fundamental matrix. Experiments with synthetic and real data show that the proposed approach is accurate especially in the presence of a high percentage of outliers.

The proposed GA can always obtain good results in both high and low detailed images. Even for low detailed images which have a small number of matched points available to estimate the fundamental matrix, the proposed GA outperformed other methods.

**Keywords:** Camera calibration; Genetic algorithm; Epipolar geometry; Computer vision.

### 725. A Class of Almost-optimal Size-independent Parallel Prefix Circuits

Hatem Mahmoud El-Boghdadi

*Journal of Parallel and Distributed Computing*, 73: 888-894 (2013)

Prefix computation is one of the fundamental problems that can be used in many applications such as fast adders. Most proposed parallel prefix circuits assume that the circuit is of the same width as the input size. In this paper, we present a class of parallel prefix circuits that perform well when the input size,  $n$ , is more than the width of the circuit,  $m$ . That is, the proposed circuit is almost optimal in speed when  $n > m$ . Specifically, we derive a lower bound for the depth of the circuit, and prove that the circuit requires one time step more than the optimal number of time steps needed to generate its first output. We also show that the size of the circuit is optimal within one. The input is divided into subsets, each of width  $m - 1$ , and presented to the circuit in subsequent time steps. The circuit is compared with functionally similar circuits of (Lin, 1999 [9]; Lin and Hung, 2009 [12]) to show its outperforming speed. When  $n > m$ , the circuit is shown to be faster than the family of waist-size optimal circuits with waist 1 (WSO-1) of the same width and fan-out.

**Keywords:** Depth-size optimal; Prefix operations; Parallel algorithms; Problem-size independent.

#### Dept. of Electric Power and Machines

### 726. A Noniterative Optimized Algorithm for Shunt Active Power Filter Under Distorted and Unbalanced Supply Voltages

Parag Kanjiya, Vinod Khadkikar and Hatem H. Zeineldin

*Ieee Transactions on Industrial Electronics*, 60 (12): 5376-5390 (2013) IF: 5.165

In this paper, a single-step noniterative optimized algorithm for a three-phase four-wire shunt active power filter under distorted and unbalanced supply conditions is proposed. The main objective of the proposed algorithm is to optimally determine the conductance factors to maximize the supply-side power factor subject to predefined source current total harmonic distortion (THD) limits and average power balance constraint. Unlike previous methods, the proposed algorithm is simple and fast as it does not incorporate complex iterative optimization-techniques (such as Newton–Raphson and sequential quadratic programming), hence making it more effective under dynamic load conditions. Moreover, separate limits on odd and even THDs have been considered. A mathematical expression for determining the optimal conductance factors is derived using the Lagrangian formulation. The effectiveness of the proposed single-step noniterative optimized algorithm is evaluated through comparison with an iterative optimization-based control algorithm and then validated using a real-time hardware-in-the-loop experimental system. The real-time experimental results demonstrate that the proposed method is capable of providing load compensation

under steady-state and dynamic load conditions, thus making it more effective for practical applications.

**Keywords:** Active power filter (APF); Harmonic compensation; Optimized control; Power quality; Unity power factor (UPF).

### 727. A Parameterization Approach for Enhancing PV Model Accuracy

Yousef A. Mahmoud, Weidong Xiao and Hatem H. Zeineldin

*Transactions on Industrial Electronics*, 60 (12): 5708-5716 (2013) IF: 5.165

Reliable and accurate photovoltaic (PV) models are essential for simulation of PV power systems. A solar cell is typically represented by a single diode equivalent circuit. The circuit parameters need to be estimated accurately to get an accurate model. However, one circuit parameter was assumed because of the limited information provided by commercial manufacturing datasheets, and thus the model accuracy is affected. This paper proposes a parameterization approach for PV models to improve modeling accuracy and reduce implementation complexity. It develops a method to accurately estimate circuit parameters, and thus improving the overall accuracy, relying only on the points - provided by all commercial modules datasheet. The proposed modeling approach results in two simplified models demonstrating the advantage of fast simulation.

The effectiveness of the modeling approach is thoroughly evaluated by comparing the simulation results with experimental data of solar modules made of mono-crystalline, multi-crystalline, and thin film.

**Keywords:** Equivalent circuit; Modeling; Parameterization; Photovoltaic (PV); Solar cell.

### 728. Efficient Modeling of Vector Hysteresis Using a Novel Hopfield Neural Network Implementation of Stoner–wohlfarth-like Operators

Amr Amin Adly and Salwa K. Abd-El-Hafiz

*Journal of Advanced Research*, 4: 403-409 (2013) IF: 3

Incorporation of hysteresis models in electromagnetic analysis approaches is indispensable to accurate field computation in complex magnetic media. Throughout those computations, vector nature and computational efficiency of such models become especially crucial when sophisticated geometries requiring massive sub-region discretization are involved. Recently, an efficient vector Preisach-type hysteresis model constructed from only two scalar models having orthogonally coupled elementary operators has been proposed.

This paper presents a novel Hopfield neural network approach for the implementation of Stoner–Wohlfarth-like operators that could lead to a significant enhancement in the computational efficiency of the aforementioned model. Advantages of this approach stem from the non-rectangular nature of these operators that substantially minimizes the number of operators needed to achieve an accurate vector hysteresis model. Details of the proposed approach, its identification and experimental testing are presented in the paper.

**Keywords:** Hopfield neural networks; Stoner–wohlfarth-like; Operators; Vector hysteresis.

### 729. Optimal Allocation of HTS-FCL for Power System Security and Stability Enhancement

Surour Alaraifi, M. S. El Moursi and H. H. Zeineldin

*IEEE Transactions on Power Systems*, 28 (4): 4701-4711 (2013) IF: 2.921

This paper presents a new problem formulation for allocation of high-temperature superconducting fault current limiter (HTS-FCL) in power systems for security and stability enhancement. A dynamic current-dependent model HHTS-FCL is developed using PSCAD/ETMDC. The proposed formulation includes three functions related to security, voltage stability, and rotor angle stability which represent key features of deploying the HTS-FCL. The three functions were combined into a multi-objective function, and the problem is formulated as a mixed-integer nonlinear programming (MINLP) problem and optimal FCL locations are determined using particle swarm optimization. The optimal FCL locations for the New-England 39-bus system are determined, and the system transient performance is validated using MATLAB and PSCAD. The simulation results demonstrate the effectiveness of proposed approach for achieving optimal performance of HTS-FCL in power system in terms of security and system stability.

**Keywords:** Angular stability; High-temperature superconducting Fault current limiter (HTS-FCL); Multimachine system; Particle swarm optimization (PSO); Voltage recovery.

### 730. Vector Magnetic Hysteresis Modeling of Stress Annealed Galfenol

Amr Amin Adly, D. Davino, A. Giustiniani and C. Visone

*J. of Applied Physics*, 113: 17A931-1-17A931-3 (2013) IF: 2.21

In the past years, utilization of magnetostrictive materials has been increasing in different applications including actuation, sensing, and energy harvesting. Special interest has been recently directed to galfenol (iron-gallium alloy). This paper experimentally investigates the vector hysteresis properties of stress-annealed galfenol as well as to test the capability of recently proposed models to mimic those properties. Details of the measurements, model identification, and experimental testing of the model accuracy are reported in the paper.

**Keywords:** Magnetic materials; Ferromagnetism; Magnetic hysteresis.

### 731. Effect of Electromagnetic Field of Overhead Transmission Lines on the Metallic Gas Pipe-lines

Ossama E. Gouda, Adel Z. El Dein, Mostafa A.H. El-Gabalawy

*Electric Power Systems Research* 103 129-136 (2013) IF: 1.694

This paper presents a study of the overhead transmission lines (OHTLs) electromagnetic fields effects on the metallic gas pipelines. The inductive and conductive voltages between the overhead transmission line and metallic gas pipelines, in normal operation and under phase to ground fault condition of the overhead transmission lines, are calculated. ATP software is used to simulate the OHTL under faulty condition. MATLAB program is used to calculate the induced voltages taking into account the effects of various parameters, such as: separation distance

between the OHTL and the metallic gas pipelines, case of transmission line (phase to ground fault condition or normal operating condition), the screening factor and the soil resistivity on the magnitude of the induced voltage along the length of the metallic gas pipeline. The method used to calculate the induced voltage by inductive is based on the well known method "distributed source analysis". Case study, to measure the induced voltage on the metallic gas pipelines from OHTL under normal operating condition, is presented. The comparison between the measured and calculated results shows a good agreement between them.

**Keywords:** AC corrosion; Conductive coupling; Inductive coupling; OHTL; Pipeline.

### 732. Optimal Allocation of Distributed Energy Resources Through Simulation-Based Optimization

Ahmed Saif, V. Ravikumar Pandi, H.H. Zeineldin and Scott Kennedy

*Electric Power Systems Research*, 104: 1-8 (2013) IF: 1.694

In this study, a new two-layer simulation-based optimization (SBO) approach is proposed to determine the optimal allocation and capacity of distributed energy resources (DER) in a power distribution system with an imperfect grid connection. In the first layer, a dynamic optimal power flow (DOPF) routine is embedded in a simulation algorithm that is run for each system configuration based on a set of operational rules to calculate the cost and reliability level of the system over one year. In the second layer, a particle swarm optimization (PSO) algorithm uses the outputs of the first layer to optimize the location and capacity of wind turbines, PV panels, and grid-scale batteries, in order to minimize cost while meeting reliability requirements. The proposed approach is tested on a 16-bus U.K. generic distribution system (GDS) under different grid availability conditions, and the results are reported. The merits and limitations of the proposed approach are discussed, and the differences between it and rule-free constrained optimization approaches are highlighted.

**Keywords:** Distributed energy resources; Dynamic optimal Power flow; Hybrid power systems; Particle swarm optimization; Simulation-based optimization.

### 733. Optimal Penetration Levels for Inverter-Based Distributed Generation Considering Harmonic Limits

V. Ravikumar Pandi, H.H. Zeineldin, Weidong Xiao and Ahmed F. Zobaa

*Electric Power Systems Research*, 97: 68-75 (2013) IF: 1.694

The installation of inverter-based distributed generation (DG) has been increasing rapidly in recent years, and specifically, photovoltaic power systems. Such increased penetration will result in increased harmonics which could exceed the IEEE 519 allowable harmonic distortion levels. In this paper, the maximum DG penetration level is determined taking into consideration the IEEE 519 allowable voltage harmonic limits. The proposed study is formulated as a mixed integer non-linear programming (MINLP) problem where harmonics are determined using the decoupled harmonic power flow approach. The maximum DG penetration level based on optimal DG size and location is determined using particle swarm optimization (PSO) algorithm.

The proposed formulation is tested on 18-bus and 33-bus radial distribution systems considering ten load and DG scenarios. The results show that by decentralizing the DG capacity, higher penetration levels could be achieved. The limiting effect of preinstalled DG at a certain bus on the overall DG penetration is also analyzed.

**Keywords:** Distributed power generation; Photovoltaic systems; Power system harmonics; Harmonic flow; Particle swarm optimization.

### 734. Data Mining Approach to Fault Detection for Isolated Inverter-Based Microgrids

Erik Casagrande, Wei Lee Woon, Hatem Hussein Zeineldin and Nadim H. Kan'an

*IET Generation, Transmission and Distribution*, 7 (7): 745-754 (2013) IF: 1.414

This study investigates the problem of fault protection in a microgrid containing inverter-based distributed generators (IBDGs). Owing to the low magnitude of short circuit currents generated by IBDGs, traditional protection techniques which rely on current (fuses and overcurrent relays) may fail to protect such networks. This study addresses the problem of finding suitable features derived from local electrical measurements that can be used by statistical classifiers to better discriminate fault events from normal network events. Given a series of simple electrical features, a study of feature selection and data mining techniques is conducted in the context of fault detection in isolated microgrids with IBDGs. Two statistical classifiers are compared and implemented in this framework: Naive Bayes and decision trees. The proposed approach is tested on a facility scale microgrid consisting of three IBDGs.

**Keywords:** Inverter based DG; Microgrid.

### 735. Simple Control Strategy for Inverter-Based Distributed Generator to Enhance Microgrid Stability in the Presence of Induction Motor Loads

Ali Hassan Kasem Alaboudy, Hatem Hussein Zeineldin and Jim Kirtley

*IET Generation, Transmission and Distribution*, 7 (10): 1155-1162 (2013) IF: 1.414

Owing to the increasing penetration of decentralised generation, stable islanded microgrid operation is essential. Fault provoked islanding conditions may lead to unstable microgrid operation, particularly when direct connected induction motor (IM) loads are included. This study proposes a control strategy for inverter-based DG to support microgrid stability.

A transient control mode (TCM), based on droop design and flow management of current components is proposed to enable the microgrid to withstand transient faults and resume stable islanded operation. The microgrid model, which includes a mix of synchronous generation, inverter-based DG and IM loads, has been simulated in Matlab. Results show that inverter control schemes supported with TCM can withstand longer fault durations. Inverter current control scheme equipped with TCM gives better stability performance for the microgrid with IM loads.

**Keywords:** Inverter based DG; Microgrid.



### 736. Turn-to-Earth Fault Modelling of Power Transformer Based on Symmetrical Components

Osama E. Gouda, Adel Zein El Dein and Ibrahim Moukhtar

*IET Generation, Transmission and Distribution*, 7 (7): 709-716 (2013) IF: 1.414

In this paper, a new approach to simulate transformer turn to earth fault, by using symmetrical components approach, has been presented. In the suggested novel modeling technique, the transformer turn to earth fault is simulated as a new healthy transformer with new short circuit (SC) impedance. This SC impedance is considered as the SC impedance of the transformer with the fraction part of the transformer winding through which the turn to earth fault occurs. The SC impedance of the reminder part of the transformer winding is added to the transmission line impedance or load impedance as external impedance. Hence, by using this suggested modelling technique, the system of turn to earth fault transformer is represented with a new system of a new healthy transformer, and the turn to earth fault is represented as an external line to ground fault.

The values of the turn to earth fault current from this novel modelling technique (using the symmetrical components approach) were compared with those obtained by Electromagnetic Transient Program/Alternative Transient Program (EMTP/ ATP). Finally, a suggestion method to estimate general information about the SC impedance of a three-phase three-winding transformer at different percentages of turn to earth fault is discussed.

**Keywords:** Transformer; ATP; Turn to earth fault; symmetrical components.

### 737. Improving the Performance of the Egyptian Second Testing Nuclear Research Reactor Using Interval Type-2 Fuzzy Logic Controller Tuned By Modified Biogeography-Based Optimization

M. M. Sayed, M. S. Saad, H. M. Emara and E. E. Abou El-Zahab

*Nuclear Engineering and Design*, 262: 294-305 (2013) IF: 0.805

Power stabilization is a critical issue in nuclear reactors. The conventional proportional derivative (PD) controller is currently used in the Egyptian second testing research reactor (ETRR-2). In this paper, we propose a modified biogeography-based optimization (MBBO) algorithm to design the interval type-2 fuzzy logic controller (IT2FLC) to improve the performance of the Egyptian second testing research reactor (ETRR-2). Biogeography-based optimization (BBO) is a novel evolutionary algorithm that is based on the mathematical models of biogeography.

Biogeography is the study of the geographical distribution of biological organisms. In the BBO model, problem solutions are represented as islands, and the sharing of features between solutions is represented as immigration and emigration between the islands.

A modified version of the BBO is applied to design the IT2FLC to get the optimal parameters of the membership functions of the controller. We test the optimal IT2FLC obtained by modified biogeography-based optimization (MBBO) using the integral square error (ISE) and is compared with the currently used PD controller.

**Keywords:** A modified version of the bbo was proposed; A novel method for interval type-2 flc design tuned by mbbo was Proposed; the performance of the etrr-2 was improved by using it2flc tuned by mbbo.

### 738. A Bivariate Chance Constraint of Wind Sources for Multi-objective Dispatching

Mostafa Elshahed, Hussein Zeineldin and Magdy Elmarsfawy

*Smart Grid and Renewable Energy*, 4: 325-332 (2013)

The economic emission dispatch (EED) problem minimizes two competing objective functions, fuel cost and emission, while satisfying several equality and inequality constraints. Since the availability of wind power (WP) is highly dependent on the weather conditions, the inclusion of a significant amount of WP into EED will result in additional constraints to accommodate the intermittent nature of the output. In this paper, a new correlated bivariate Weibull probability distribution model is proposed to analytically remove the assumption that the total WP is characterized by a single random variable. This probability distribution is used as chance constraint. The inclusion of the probability distribution of stochastic WP in the EED problem is defined as the here-and-now strategy. Non-dominated sorting genetic algorithm built in MATLAB is used to handle the EED problem as a multi-objective optimization problem. A 69-bus ten-unit test system with non-smooth cost function is used to test the effectiveness of the proposed model.

**Keywords:** Correlated weibull distribution; Economic emission dispatch; Stochastic programming; Wind power.

### 739. A Multi-objective Genetic Algorithm Based Pid Controller for Load Frequency Control of Power Systems

M. A. Tammam, Magdy A. S. Aboelela, M. A. Moustafa and A. E. A. Seif

*International Journal of Emerging Technology and Advanced Engineering*, 3 (12): 463-467 (2013)

This paper studies control of load frequency in single area power system with PID controller. In this study, PID parameters are improved using the multiobjective genetic algorithm technique. The proposed controller compared with a conventional PID controllers tuned by Ziegler-Nicholas technique, Particle Swarm Optimization (PSO). The effectiveness of the anticipated scheme is confirmed through the comparison of steady state response characteristics. For this study, MATLABSimulink software is used.

**Keywords:** Load frequency control; Single area Power system; PID controller; Multi-objective genetic algorithm.

### 740. A Protection Coordination Index for Evaluating Distributed Generation Impacts on Protection for Meshed Distribution Systems

H. H. Zeineldin, Yasser Abdel-Rady I. Mohamed, Vinod Khadkikar and V. Ravikumar Pandi

*IEEE Transactions on Smart Grid*, 4 (3): 1523-1532 (2013)

Depending on the capacity, type and location, distributed generation (DG) can have an impact on protection coordination of directional over-current relays for looped distribution systems. In this paper, a new index is proposed, "protection coordination index" (PCI), which can serve as an effective measure when planning the protection of meshed distribution systems with DG. A two-phase non-linear programming (NLP) optimization problem is proposed to determine the PCI by optimally calculating variations in the maximum DG penetration level with changes in the protection coordination time interval. Furthermore, the influence of connecting a DG at a certain location on the system PCIs is examined. The presented analysis is tested on the distribution section of the IEEE 14-bus and IEEE 30-bus systems. The PCI can serve as an efficient index for distribution system planners: (i) to determine the best DG candidate locations for utility owned DG and (ii) to evaluate the impact of a customer owned DG, considering distribution system protection.

**Keywords:** Distributed generation; Faults; Optimization; Protection coordination.

#### 741. Assessing Partial Discharge on Composite Insulators Under Desert Pollution Conditions

Mohammed El-Shahat and Hussein Anis

*International Journal of Emerging Technology and Advanced Engineering*, 3 (7): 492-499 (2013)

Transmission lines located in the Sinai desert are subjected to desert climate, one of whose features, especially in the spring, is sand storms. Line insulators are thus exposed to sand contamination, which may produce streamer discharges in the air surrounding insulator surface. Such discharges may lead to flashover. This paper examines the electric field and potential distributions on sand-polluted composite insulators. These insulators are nominated to replace ceramic insulators on transmission lines in Sinai. A case study is presented using an ABB-designed composite insulator, where the insulator surface electric field is investigated under dry sand-pollution conditions and with different sand grain sizes. The latter were provided by a previous study of the Sinai desert. Finite element techniques are used to simulate the insulator and seek electric field distribution on the polluted insulator model and around it.

This study helps in partially assessing and thus justifying- the use of these insulators in those critical areas.

**Keywords:** Composite insulators; Desert pollution; Partial discharge; Ansys software; Sinai.

#### 742. Direct Torque Control of a Three-level Inverter Fed Induction Motor, Analysis and Simulation

Sherif Wael Abd El-Aziz Al-Dosokey, Sherif Ahmed Zaid and Mahmoud Abd El-Hakeem

*Journal of Electrical Engineering*, 13 (4): 37-44 (2013)

This paper investigates the direct torque control (DTC) of a three-phase induction motor (IM) using a three-level neutral-point lamped (NPC) inverter. Most papers related to DTC concentrate on two-level inverters.

Three-level inverters solve the problem of voltage and power limitations of two-level inverters. A simulation model is implemented to compare the performance of DTC based on two- and three-level operation. The comparison includes speed

performance, torque and flux ripples, voltage and current harmonics...etc. Also a simple balancing scheme is introduced to solve the problem of neutral-point (NP) voltage deviation in the three-level NPC inverter. Simulation results are provided to confirm the advantages of using the three-level NPC inverter.

**Keywords:** Direct torque control; Three-level neutral-point Clamped (NPC) Inverter

#### 743. Dynamic Analysis of A New Connection for Dual Voltage Operation of Single Phase Capacitor Run Motor

Hanafy Hassan Hanafy

*Journal of Electrical Engineering (Jee)*, 13: 230-237 (2013)

This paper presents the dynamic analysis of a new connection of Single-Phase Capacitor Run Motor (SPCRM) for dual voltage operation. A program simulating the dynamic behavior of the new connection in the stationary d-q reference frame gives sufficient results. The analysis is carried out under the no-load and load conditions. Experimental measurements are carried out for comparison and verification of simulating results. The agreement of experimental and computational results approves the dynamic model of the new connection.

**Keywords:** Single phase induction motor; Capacitor run motor; Dynamic analysis; Dual voltage.

#### 744. Force Computation and Analysis of Single-phase Capacitor-start Induction Motors Using Finite Element Method at Broken Bars Conditions

Hanafy H. Hanafy, Tamer M. Abdo and Amr A. Adly

*International Review of Electrical Engineering (IREE)*, 8 (5): 1427-1436 (2013)

This paper studies the effects of broken bars faults on the single-phase capacitor-start induction motor. A transient model for the motor is used in this study that depends on self and mutual inductance calculations based on accurate finite element method (FEM). The rotor broken bars faults are studied thoroughly including their effects on the rotor bar currents distribution, the rotor bar frequency content, the electromagnetic forces exerted on the rotor bars, the motor speed and motor torque. The electromagnetic tangential and radial forces affecting the rotor bars were calculated using finite element method (FEM). It was found that the non-uniform distribution of the rotor bar currents will lead to non-uniform radial forces affecting the bars. This will increase the mechanical stresses on the rotor shaft which may lead to eccentricity.

**Keywords:** Broken rotor bars; Capacitor-start motors; Finite element method (FEM); Single-phase induction motors.

#### 745. Hardware Implementation of Mtpa for Spmsm-Dsp Based

sherif ahmed Zaid farag

*Journal of Electrical Engineering*, 13/1: 100-105 (2013)

In this paper, the maximum torque per ampere (MTPA) using vector control (VC) has been implemented on a surface permanent

magnet synchronous motor (SPMSM). A complete hardware setup based on the digital signal processor (DSP) has been constructed to verify the MTPA concept. Texas F28335 DSP will be used for executing the control algorithm and MATLAB Target Support Package has been used to write the code. A serial communication will be used for sending the desired value of the speed and to collect the readings via the DSP. In addition to executing the TPA concept, the DSP has been used to act as a data acquisition to collect those data that don't need high scan rate.

**Keywords:** SPMSM; MTPA; Dsp; MATLAB.

#### 746. Hybrid Modeling and Control of a Power Plant Using State Flow Technique With Application

Marwa M. Abdulmoneim, Magdy A. S. Aboelela and Hassen T. Dorrah

*International Journal of Emerging Technology and Advanced Engineering*, 3 (5): 24-30 (2013)

This paper presents a hierarchical hybrid system modeling and simulation framework using the bond graph. Bond graphs are a domain-independent graphical description of dynamic behavior of physical systems. This means that systems from different domains (electrical, mechanical, hydraulic, thermodynamic, and material) are described in the same way. The basis is that bond graphs are based on energy and energy exchange. "Modeling and simulation of thermal Power generation Station for power control" will be presented by using hybrid bond graph approach. This work includes the structure and components of the thermal electrical power generation stations and the importance of hybrid bond graph to model and control complex hybrid system, controlling of steam generator will be presented by using State flow controller.

**Keywords:** Hybrid system; Bond graph; Word bond graph; Hydraulic system.

#### 747. Rotor Broken Bar Diagnosis in Asd Using Instantaneous Power Spectrum and Mean Absolute Difference Approach—a Combined Technique

Hanafy Hassan Hanafy, A. M. Hussien and E. A. El-Zahab

*Journal of Electrical Engineering (Jee)*, 13: 69-75 (2013)

Rotor broken bars is a common fault in squirrel cage induction motors. Rotor failures due to that fault, now account for a moderate percentage of total induction motor failures. This paper will deal with detection of broken rotor bar of an induction motor which is supplied from adjustable speed drive (ASD) equipped with AC reactor and sine-wave shaping filter on the output side. The experimental results show that the instantaneous power spectrum (IPS) analysis method is only effective when the motor is supplied from sinusoidal supply, in contrast for the demonstrated ASD. So the instantaneous power spectrums of the healthy rotor case and the broken bar rotor cases is processed with mean absolute difference (MAD) algorithm to investigate the dissimilarity between them. The results show that this combined technique is highly effective in diagnosis of broken rotor bar fault in case of ASD.

**Keywords:** Fault diagnosis; Induction motor; Rotor broken bars; Instantaneous power spectrum; Mean absolute difference.

#### 748. Statistic and Parallel Testing Procedure for Evaluating Maximum Power Point Tracking Algorithms of Photovoltaic Power Systems

Weidong Xiao, H. H. Zeineldin and Peng Zhang

*IEEE Journal of Photovoltaics*, 3 (3): 1062-1069 (2013)

Maximum power point tracking (MPPT) methods are essential for photovoltaic (PV) systems to take full advantage of the available solar energy. Over the past few years, an increasing number of new MPPT methods have been proposed in the literature, and they show better capability of capturing the maximum power point. The testing and evaluation procedure of any new MPPT method is a crucial step for assessing its robustness and performance. PV panel manufacturers always specify power output tolerances, ranging from  $\pm 2\%$  to  $\pm 5\%$ . Thus, nonideal factors might dominate the subsystem output and defeat any performance comparison attempt and might lead to inaccurate results. This paper highlights the main shortcomings of previous MPPT testing procedures and proposes a comprehensive testing approach using paired difference tests to evaluate the performance of MPPT. The dual channel bench system demonstrates a systematic framework to deal with the nonideal factors associated with PV manufacturing, quantify experimental data, and correctly illustrate the performance improvement of MPPT. The case study shows that the 1% improvement of MPPT could be easily overshadowed by the nonideal factors shown previously. The proposed test setup and analysis method provide the effective solution for evaluating the MPPT performance.

**Keywords:** Control; Maximum power point tracking (MPPT); Paired different test; Photovoltaic (PV) power systems.

#### 749. Steady State Performance of A Proposed Connection for Dual Voltage Operation of Permanent Capacitor Motor

Hanafy Hassan Hanafy

*Int. J. Power and Energy Conversion*, 4 (4): 293-303 (2013)

The purpose of this paper is to evaluate the steady state performance of a proposed connection of permanent capacitor motor (PCM) for dual voltage operation. The performance of the proposed connection is compared with the performance of the normal motor connection. The proposed connection has been tested using a dynamometer to experimentally verify the results of the theory and simulation results. Good agreement between the simulated and the experimental results has been obtained.

**Keywords:** Single phase induction motor; Capacitor motor; Dual voltage.

#### 750. The Investigations and 2-D Computations of Electromagnetic Fields and forces Distribution of Squirrel Cage Induction Motor With Broken End Rings

H. H. Hanafy Tamer M. Abdo and Amr A. Adly

*Journal of Electrical Engineering (JEE)*, 13: 80-87 (2013)

In this paper an ABC transient model of the three phase induction motor is developed that depends on self and mutual inductance

calculations based on accurate 2D finite element analysis (FEA). This model can represent both healthy and faulty motor conditions. The rotor broken end rings faults are studied thoroughly including their effects on the motor speed, motor torque, rotor bars and end ring currents distribution. Flux distribution and the forces exerted on the rotor bar are also studied. Broken end rings causes non-uniform distribution of the rotor bar currents which will lead to fluctuations in the motor torque and speed. Also it results in non-uniform radial forces affecting the bars which will increase the mechanical stresses on the rotor shaft and bearings.

**Keywords:** Induction motor; Finite element analysis; Broken end rings.

#### Dept. of Electronics and Communication Engineering

##### 751. Two Integrator Loop Quadrature Oscillators: A Review

Ahmed M. Soliman

*Journal of Advanced Research*, 4: 1-11 (2013) IF: 3.0

A review of the two integrator loop oscillator circuits providing two quadrature sinusoidal output voltages is given. All the circuits considered employ the minimum number of capacitors namely two except one circuit which uses three capacitors. The circuits considered are classified to four different classes. The first class includes floating capacitors and floating resistors and the active building blocks realizing these circuits are the Op Amp or the OTRA. The second class employs grounded capacitors and includes floating resistors and the active building blocks realizing these circuits are the DCVC or the unity gain cells or the CFOA. The third class employs grounded capacitors and grounded resistors and the active building blocks realizing these circuits are the CCII. The fourth class employs grounded capacitors and no resistors and the active building blocks realizing these circuits are the TA. Transformation methods showing the generation of different classes from each other is given in details and this is one of the main objectives of this paper.

**Keywords:** Two integrator loop oscillators; Op amp; Operational transresistance amplifier; Unity gain cells; Current conveyor; Current feedback operational amplifier.

##### 752. A Feedback- soft Sensing-based Access Scheme for Cognitive Radio Networks

Ahmed M. Arafa, Karim G. Seddik, Ahmed K. Sultan, Tamer ElBatt and Amr A. El-Sherif

*IEEE Transactions on Wireless Communications*, 12 (7): 3226-3237 (2013) IF: 2.418

In this paper, we examine a cognitive spectrum access scheme in which secondary users exploit the primary feedback information. We consider an overlay secondary network employing a random access scheme in which secondary users access the channel by certain access probabilities that are functions of the spectrum sensing metric. In setting our problem, we assume that secondary users can eavesdrop on the primary link's feedback. We study the cognitive radio network from a queuing theory point of view. Access probabilities are determined by solving a secondary throughput maximization problem subject

to a constraint on the primary queues' stability. First, we formulate our problem which is found to be non-convex. Yet, we solve it efficiently by exploiting the structure of the secondary throughput equation. Our scheme yields improved results in, both, the secondary user throughput and the primary user packet delay as compared to the scheme where no feedback information is exploited. In addition, it comes very close to the optimal genie-aided scheme in which secondary users act upon the presumed perfect knowledge of the primary users' activity.

**Keywords:** ARQ feedback; Cognitive radio; Markov chains; Soft sensing.

##### 753. Cross-layer Minimum-delay Scheduling and Maximum-throughput Resource Allocation for Multiuser Cognitive Networks

Ghada Saleh, Amr El-Keyi and Mohammed Nafie

*IEEE Transactions on Mobile Computing*, 12 (4): 761-773 (2013) IF: 2.395

A cognitive network is considered that consists of a base station (BS) communicating with multiple primary and secondary users. Each secondary user can access only one of the orthogonal primary channels. A model is considered in which the primary users can tolerate a certain average delay. A special case is also considered in which the primary users do not suffer from any delay. A novel cross-layer scheme is proposed in which the BS performs successive interference cancellation and thus a secondary user can coexist with an active primary user without adversely affecting its transmission. A scheduling algorithm is proposed that minimizes the average packet delay of the secondary user under constraints on the average power transmitted by the secondary user and the average packet delay of the primary user. A resource allocation algorithm is also proposed to assign the secondary users' channels such that the total throughput of the network is maximized. Our results indicate that the network throughput increases significantly by increasing the number of transmitted packets of the secondary users and/or by allowing a small delay for the primary user packets.

**Keywords:** Cognitive radio; Multiple access; Cross-layer design; Delay minimization; Resource allocation.

##### 754. Dual and Wide-band Inductively-loaded Dipole-based Antennas for WLAN/UMTS Applications

Mohamed A. Othman, Tamer M. Abuelfadl and Amr M. E. Safwat

*Ieee Transactions on Antennas and Propagation*, 61: 1430-1435 (2013) IF: 2.332

Electrically-small antennas can be designed using inductively-loaded dipoles. A simplified design procedure is carried out, using circuit models and EM simulations, to implement efficient dual and wide-band antennas with omni-directional radiation patterns. Measured performance agrees with simulations, and the proposed designs are employed for the UMTS 1.8/1.9/2.1/2.6-GHz and WLAN 2.4/3.6-GHz frequencies. A USB dongle antenna is prototyped to cover these frequency bands with impedance bandwidth reflection coefficient better than -10 dB.

**Keywords:** Electrically-Small antennas; WLAN antennas; Z-antennas; Metamaterial-inspired antennas.

### 755. Design, Implementation and Characterization of Practical Distributed Cognitive Radio Networks

Ahmed Khattab, Dmitri Perkins and Magdy A. Bayoumi

*IEEE Transactions on Communications*, 61 (10): 4139-4150 (2013) IF: 1.75

Opportunistic Spectrum Access (OSA) in distributed cognitive radio networks (CRNs) has been well studied in the literature from a theoretical perspective. However, such theoretically-optimized distributed OSA approaches are challenged by several practical implementation issues. In this paper, we design a custom cross-layer framework that enables the: (i) clean-slate implementation of a wide variety of OSA mechanisms; (ii) experimental evaluation of the individual practical OSA components of the Rate-Adaptive Probabilistic (RAP) framework; and (iii) detailed comparison of the performance of such a practical OSA approach against theoretical OSA approaches developed for fully-capable CRNs. Our evaluation reveals the multi-fold goodput improvement and remarkable fairness characteristics of the practical RAP OSA approach compared to the OSA approaches that overlook the OSA and CR practical limitations. However, the superior performance of practical OSA comes at the expense of more outages to the primary licensed networks but within the permissible bounds. Another key finding is that the wide family of existing theoretically-optimized OSA protocols can benefit from the gains available to the individual components of the practical RAP approach, namely, the random spectrum sensing and the probabilistic non-greedy access.

**Keywords:** Cognitive radio; Radio spectrum management; Ad hoc networks; Design for experiments; Performance evaluation.

### 756. On the Scheduling, Multiplexing and Diversity Trade-Off in MIMO Ad Hoc Networks: A Unified Framework

Tamer Abde Mottalib ElBatt

*Ad Hoc Networks*, 11: 639-653 (2013) IF: 1.456

In this paper we study the fundamental scheduling, multiplexing and diversity trade-off in MIMO ad hoc networks. In particular, we propose a unified framework for the scheduling-multiplexing and scheduling-diversity sub-problems that constitutes a major step towards solving the overall problem. The two sub-problems are motivated by a fundamental trade-off between scheduling full multiplexing (diversity) gain non-interfering links and scheduling interfering links using lower multiplexing (diversity) gain in conjunction with interference nulling. First, we cast each sub-problem as a cross-layer optimization problem that jointly decides the scheduling and MIMO stream allocation, subject to signal-to-interference- and-noise-ratio (SINR) constraints. Second, we characterize the problem as non-convex integer programming which is quite challenging to solve. Hence, we shift our focus to characterize the optimal for the simple case of two links. The main result of this paper is that the two fundamentally different sub-problems give rise to structurally similar SINR-based decision rules which constitute the basis for a resource allocation algorithm with linear complexity in the number of links, namely Iterative MIMO Link Scheduling (IMLS), that solves the two sub-problems and achieves significant gains for any number of links. Numerical results exhibit more than twofold/quadratic

improvement over scheduling non-interfering links with full multiplexing/diversity gain, for plausible scenarios. IMLS and its variants reveal an important throughput-fairness trade-off which is an interesting topic for future research.

**Keywords:** Ad hoc networks; Cross-layer optimization; MIMO Scheduling; Spatial multiplexing; Diversity; Convexity.

### 757. Dual-band Low-profile Stripline-FED Z-antenna

Mohamed A. Othman, Tamer M. Abuelfadl and Amr M. E. Safwat

*Microwave and Optical Technology Letters*, 55 (2): 286-290 (2013) IF: 0.585

This letter proposes a new interpretation for the Z-antenna. It describes the Z-antenna as an asymmetrically-fed bent and meandered inductively-loaded dipole antenna. This explanation provides a simple methodology to design a dual-band stripline-fed Z-based antenna that operates at 1.8 and 2.45 GHz. Measurements and EM simulations validate the proposed theory.

**Keywords:** Electrically small antennas; Metamaterial-inspired antennas; Planar monopole antennas; Z-Antenna.

### 758. An Ultra Low Power QPSK Receiver Based on Super-Regenerative Oscillator With A Novel Digital Phase Detection Technique

G.H. Ibrahim, A. Hafez and A.H. Khalil

*International Journal of Electronics and Communications (Aeü)*, 67: 967-974 (2013) IF: 0.551

An original proposal of using SRO-based receiver to demodulate QPSK signals is presented. The receiver is composed of an LNA and a super-regenerative oscillator (SRO), both combined in a single stacked configuration for current reuse. The demodulation of received RF signal is performed via a novel digital circuit capable of detecting phase information embedded in the SRO output. The receiver is able to demodulate incoming signal without the need of an LO, PLL or an ADC. The complete receiver was designed using a 0.13  $\mu\text{m}$  technology and pre-layout simulation confirms proper and efficient operation, where the designed receiver operating in the 402–405 MHz MICS band shows 135  $\mu\text{W}$  power consumption, while being able to properly detect and extract sent information of a -80 dBm, 2 Mbps signal.

**Keywords:** Super-regenerative Low power; QPSK; Phase detection; Receiver.

### 759. Improved Synchronization, Channel Estimation, and Simplified LDPC Decoding for the Physical Layer of the DVB-T2 Receiver

Doaa H. Sayed, Maha Elsabrouty and Ahmed F. Shalash

*Eurasip Journal on Wireless Communications and Networking*, 60: 1-16 (2013) IF: 0.540

The newly developed 2nd generation standard for digital video broadcasting (DVB-T2) emerges as a significant upgrade over its first generation predecessor DVB-T. The DVB-T2 standard



targets an increased system throughput by at least 30% over the DVB-T. This article introduces algorithms in the signal processing chain to improve the mobile operation for DVB-T2. The proposed modified synchronization blocks, along with the improved channel estimation, show significant improvement compared to the results reported in the DVB-T2 implementation guide. In addition, state-of-the-art low-complexity algorithms in the bit processing chain, particularly in the LDPC decoder, are used to provide robustness and support throughput increase, while reducing the implementation complexity. The integrated system is simulated including implementation effects. The simulation results confirm the enhanced performance of the developed integrated model and provide better results compared to those reported in literature.

**Keywords:** DVB; OFDM; Integrated receiver, LDPC.

### 760. Joint Power and Rate Scheduling for Cognitive Multi-access Networks With Imperfect Sensing

Ghada Saleh, Amr El-Keyi and Mohammed Nafie

*Eurasip Journal on Wireless Communications and Networking*, 198 (2013) IF: 0.540

A cognitive multi-access network in which a primary user and a secondary user transmit to a common receiver is considered. The secondary user senses the channel at the beginning of each time slot to determine whether the primary user is active or idle. The sensing is not perfect; hence, the secondary user can miss the detection of an active primary user or erroneously declare an idle primary user as active. The secondary user can vary its transmission rate and power from a time slot to the other. A joint rate and power scheduling algorithm is proposed that minimizes the probability of packet loss of the secondary user under a maximum probability of collision constraint at the primary user and a constraint on the average power transmitted by the secondary user. The case in which no retransmissions are allowed and the cases in which one or both users retransmit the collided packets are also considered. The problem is posed as a linear optimization problem that can be solved efficiently.

**Keywords:** Cognitive radio; Multiple access; Cross-layer design; Delay minimization; Loss minimization; Imperfect sensing; Power control.

### 761. Error Analysis and Detection Procedures for Probabilistic Public Key Cryptography (NTRU)

Naglaa F. Saady, Ahmed F. Shalash and Abdel-karim S.O. Hassan

*Wulfenia*, 20 (12): 97-113 (2013) IF: 0.467

The emergence of new applications and the increase of reliance on networks to offer new services is pushing forward the need for improved security paradigms. To that end, NTRU public key cryptosystem was introduced. In this paper, fault detection scheme is introduced to improve the security and reliability of the NTRU in realistic environments. As the NTRU will be working in real networks, which have their own set of transient errors, handling such errors in analyzing the NTRU performance becomes a must. A single transient error occurring during the NTRU encryption or decryption process will likely result in a large number of errors in the encrypted/decrypted data. Such faults must be detected before sending and encrypting the

information to avoid the transmission and use of erroneous data. Fault detection is important not only to protect the encryption/decryption process from random faults, but it will also protect the decryption operation from an attacker who may maliciously inject faults in order to find the secret key. We first describe the effects that faults may have on NTRU security while operating over a network by analyzing the propagation of such faults to the outputs. We then present fault detection scheme by using an error detecting code, using one parity bit. We will add the parity bits to the polynomials and disable the device output when any of these parity checks are violated. This fault detection scheme has more than 99% fault detection coverage in the encryption process and in the first part in the decryption process. In the second part in the decryption process, it has more than 67 % fault detection coverage. We can increase this ratio by adjusting the choices of the parameters of the NTRU network security system.

**Keywords:** NTRU encryption cryptography.

### 762. Adaptive Bit Loading and Puncturing Using Long Single Codewords in OFDM Systems

Mai Abdelhakim, Mohammed Nafie, Ahmed Shalash and Ayman Elezabi

*Wireless Personal Communications*, 71: 1557-1576 (2013) IF: 0.428

Adaptive puncturing over single codewords offers a new dimension in the family of adaptive coding and modulation techniques for communication systems. In the context of orthogonal frequency-division multiplexing systems, adaptive puncturing provides variable transmission rates across tiles within a single code-word (SCW). This contrasts with the more common multiple code-words (MCWs) structure, where variable rates are obtained using multiple codewords each is uniformly punctured. In this paper, an adaptive puncturing, interleaving, and bit loading schemes are proposed and an extensive performance evaluation is provided for both convolutional and turbo codes. The adaptively punctured SCW structure is compared to the MCWs, as well as to the per-frame adaptation. The comparisons are made using various adaptive loading methods for both constant and variable bit rate wireless applications. The SCW structure provides significantly improved goodput compared to the other two schemes, particularly for turbo-coded transmission. An analytical approximation for the goodput is obtained for both the SCW and the MCWs structures in the case of convolutional codes. The tile size effect is also investigated and it is shown that the SCW offers flexibility over the MCWs structure, since the tile size does not impose any restriction on the codeword length.

**Keywords:** Adaptive Puncturing; Adaptive Modulation and Coding (AMC); Single Codeword (SCW); Multiple Codewords (MCWs); Mutual Information Effective SNR Mapping (MIESM).

### 763. Outage Probability Analysis of Cooperative Diversity Networks Over Weibull and Weibull-Lognormal Channels

Abdelrahman H. Gaber, Mahmoud H. Ismail and Hebat-Allah M. Mourad

*Wireless Personal Communications*, 70: 695-708 (2013) IF: 0.428

This paper presents the analysis of outage probability for a cooperative diversity wireless network using amplify-and-forward relays over independent non-identical distributed Weibull and Weibull-lognormal fading channels for single as well as multiple relays. To reach that end, a closed-form expression for the moment-generating function of the total signal-to-noise-ratio (SNR) at the destination is derived in terms of the tabulated Meijer's G-function. Since it is hard to determine the exact probability distribution function of the SNR, a tight lower bound approximation is proposed. Simulation results are presented that show that the outage probability lower bound tends to be tight at high SNR values thus verifying the analytical results. The results also show the potential gain of relaying on the outage probability.

**Keywords:** Outage probability; Cooperative diversity; Amplify-and-Forward; Weibull fading; Weibull-lognormal fading.

#### 764. Outage Probability Analysis of Selection and Switch-and-Stay Combining Diversity Receivers Over the $\alpha$ - $\mu$ Fading Channel With Co-channel Interference

Mahmoud H. Ismail and Refaat Mohamed

*Wireless Personal Communications*, 71: 2181-2195 (2013)

IF: 0.428

In this paper, we evaluate the performance of two dual-branch diversity techniques operating over the  $\alpha$ - $\mu$  fading channel in presence of a dominant co-channel interferer with a minimum desired signal power constraint. These two diversity schemes are selection combining and switch-and-stay combining. We derive expressions for the outage probability in both cases, which are very simple to calculate numerically using the commercially available mathematical packages. The obtained expressions are valid for integer values of the parameter  $\mu$  and, in many special cases, they reduce to either a closed form or to expressions with finite-limit integrals that can also be easily evaluated. Also, our expressions reduce to previously published well-known results for the Rayleigh as well as the Weibull fading channels as special cases. We present a set of numerical results which show the effect of fading severity of both the desired signal and the interferer on the performance.

**Keywords:** Diversity receivers;  $\alpha$ - $\mu$  fading; Co-Channel interference; Selection combining; Switch-and-stay combining.

#### 765. A Note on the Transformation of Grounded Inductors to Floating Inductors Using of a and Fccii

Ahmed Mohamed Soliman

*Journal of Circuits, Systems, and Computers*, 22: 1-3 (2013)

IF: 0.238

Recently this author published a paper<sup>1</sup> discussing the transformation of grounded inductors to floating inductors using operational floating amplifier (OFA) or floating current conveyor (FCCII). The author classified the paper as a partially review paper as stated in the abstract and in the introduction of Ref. 1. The author states in the abstract that: It is well known that a floating inductor circuit is realized from a grounded inductor circuit by replacing the operational amplifier by a floating operational transconductance amplifier. This idea is extended to transform current conveyor grounded inductors to floating

inductors by replacing the current conveyor by the recently introduced floating current conveyor.

**Keywords:** Operational floating amplifier; Floating current conveyors; Grounded inductors; Floating inductors.

#### 766. Generation of Third-order Quadrature Oscillator Circuits Using Nam Expansion

Ahmed Mohamed Soliman

*Journal of Circuits, Systems, and Computers*, 22: 1-13 (2013)

IF: 0.238

A systematic synthesis procedure for generating third-order grounded passive element quadrature oscillators is given. The synthesis procedure is based on using nodal admittance matrix (NAM) expansion applied to the Y matrix of a recently reported three Op Amp third-order oscillator circuit. Four new circuits using current conveyors (CCII) are reported. In addition four more new circuits using inverting current conveyors (ICCI) are also given. Many more quadrature third-order oscillator circuits using combinations of CCII and ICCI can be obtained. Simulation results demonstrating the practicality of one of the generated circuits are included.

**Keywords:** Third-order oscillators; Current conveyors.

#### 767. Closed-form Capacity Expressions For The $\alpha$ - $\mu$ Fading Channel With SC Diversity Under Different Adaptive Transmission Strategies

Refaat Mohamed, Mahmoud H. Ismail, Fatma Newagy and Heba M. Mourad

*Frequenz*, 67 (3-4): 127-137 (2013) IF: 0.168

Stemming from the fact that the  $\alpha$ - $\mu$  fading distribution is one of the very general fading models used in the literature to describe the small scale fading phenomenon, in this paper, closed-form expressions for the Shannon capacity of the  $\alpha$ - $\mu$  fading channel operating under four main adaptive transmission strategies are derived assuming integer values for  $\mu$ . These expressions are derived for the case of no diversity as well as for selection combining diversity with independent and identically distributed branches. The obtained expressions reduce to those previously derived in the literature for the Weibull as well as the Rayleigh fading cases, which are both special cases of the  $\alpha$ - $\mu$  channel. Numerical results are presented for the capacity under the four adaptive transmission strategies and the effect of the fading parameter as well as the number of diversity branches is studied.

**Keywords:** SC (selection combiner); OPRA (optimum power and rate adaption); ORA (optimum rate adaption); CIFR (channel inversion with fixed rate); TIFR (truncated channel inversion with fixed rate).

#### 768. Fast and Accurate Algorithm for Core Point Detection in Fingerprint Images

G. A. Bahgat, A.H. Khalil, N. S. Abdel Kader and S. Mashali

*Egyptian Informatics Journal*, 14: 15-25 (2013)

The core point is used to align between the fingerprints in the fingerprint authentication systems faster than the conventional

techniques. To speed up the processing for the real time applications, it is more convenient to implement the image processing algorithms using embedded modules that can be used in the portable systems. To do this, the algorithm should be characterized by a simple design for easier and more feasible implementation on the embedded modules. The proposed work, in this paper, presents a mask that locates the core point simply from the ridge orientation map. The introduced algorithm detects the core point at the end of the discontinuous line appearing in the orientation map presented by a gray-scale. A property is presented and supported with a mathematical proof to verify that the singular regions are located at the end of this discontinuous line. The experimental results, on the public FVC2002 and FVC2004 databases, show that the proposed mask exhibits an average increase in the correct core point detection per fingerprint by 17.35%, with a reduction in the false detection by 51.23%, compared to a fast edge-map based method. Moreover, the execution time is reduced by an average factor of 1.8

**Keywords:** Fingerprint core point detection; Singular point; Fingerprint segmentation; Ridge orientation; Orientation smoothing.

#### *Dept. of Engineering Mathematics and Physics*

#### **769. On the Reported Experimental Evidence for the Quasi-fermi Level Split In Quantum-dot Intermediate-band Solar Cells**

Ahmed A. Abouelsaood, Moustafa Y. Ghannam and Jef Poortmans

*Progress In Photovoltaics, 21: 209-216 (2013) IF: 7.712*

The reported experimental evidence for the quasi-Fermi level split in quantum-dot intermediate-band solar cells is carefully examined. It is shown that the separation of the quasi-Fermi level of the intermediate band from that of the conduction band is not consistent with the experimental results of the quantum efficiency and the luminescence intensity of the InAs/GaAs cells. The fact that the electroluminescence spectrum is too wide, extending much further than we expect on the basis of the measured quantum efficiency in the direction of increasing photon energies, indicates that the temperature of the optically active regions of the cell during the electroluminescence measurements is considerably higher than room temperature. The best agreement with the experimental results is achieved with a temperature of about 525K. This temperature rise is probably a result of the heating effect of the relatively high forward current used in the luminescence experiments. It is argued that the lack of a quasi-Fermi level split in this case is associated with the absence of a gap in the emission/absorption spectrum of sub-bandgap photons.

**Keywords:** Intermediate band; Solar cell; Quantum dot.

#### **770. A Low-cost Screening Method for the Detection of the Carotid Artery Diseases**

Doaa Mohammad Shawky Farag Seddik

*Knowledge-Based Systems, 52: 236-245 (2013) IF: 4.104*

Carotid artery diseases are defined as the narrowing or the blockage of the carotid arteries. These two conditions are called carotid artery stenosis or occlusion respectively. Stenosis and occlusion are usually caused by cholesterol deposits and fatty

substances which are called plaque. In addition, they represent significant causes of strokes. Thus, they should be a part of regular physical examinations. An important and preliminary diagnosis is to listen to the arteries in the neck using a stethoscope or a Doppler ultrasound (US) device. However, it is sometimes very difficult for a non-professional physician to differentiate between a normal and an abnormal sound due to blood flow blockage. This paper presents a low-cost efficient method that can be used in the automatic screening of carotid artery diseases, especially in areas with high population. Doppler US signals are preprocessed for noise elimination. Then, some features for normal, stenosis and occlusion signals are extracted from the frequency domain of these signals using their spectrograms. A multi-layer feed forward neural-network (MLFFNN) and a k-nearest neighbor (KNN) classifiers were used to automatically diagnose the input signals. The approach is applied to 72 samples divided into three equal sets which represent the three main classes to be identified, i.e., normal, stenosis and occlusion patterns. We used in the training phase 75% of each set and the rest was used in the test phase. Experimental results show the simplicity and efficiency of the presented approach for automatic diagnosis of carotid artery diseases. The maximum obtained classification accuracies are 91.67%, 100%, and 95.89% for the normal, stenosis and occlusion patterns respectively when the MLFFNN classifier is used. In comparison with similar approaches, the proposed approach is less complex, hence runs faster which suggests its suitability as an efficient screening method for the detection of carotid artery diseases.

**Keywords:** Automatic diagnosis; Carotid artery diseases; Doppler signal classification; Artificial neural networks; K-nearest neighbor?

#### **771. Boundary Conditions for Hyperbolic Systems of Partial Differentials Equations**

Amr G. Guaily and Marcelo Epstein

*Journal of Advanced Research, 4: 321-329 (2013) IF: 3*

An easy-to-apply algorithm is proposed to determine the correct set(s) of boundary conditions for hyperbolic systems of partial differential equations. The proposed approach is based on the idea of the incoming/outgoing characteristics and is validated by considering two problems. The first one is the well-known Euler system of equations in gas dynamics and it proved to yield set(s) of boundary conditions consistent with the literature. The second test case corresponds to the system of equations governing the flow of viscoelastic liquids.

**Keywords:** Hyperbolic systems; Boundary conditions; Characteristics; Euler equations; Viscoelastic liquids.

#### **772. Multiproperty Empirical Isotropic Interatomic Potentials for CH<sub>4</sub>-inert Gas Mixtures**

Mohamed Sayed Abdel Kader

*Journal of Advanced Research, 4: 501-508 (2013) IF: 3*

An approximate empirical isotropic interatomic potentials for CH<sub>4</sub>-inert gas mixtures are developed by simultaneously fitting the Exponential-Spline-Morse-Spline-van der Waals (ESMSV) potential form to viscosity, thermal conductivity, thermal diffusion factors, diffusion coefficient, interaction second pressure virial coefficient and scattering cross-section data.

Quantum mechanical lineshapes of collision-induced absorption (CIA) at different temperatures for CH<sub>4</sub>-He and at T = 87 K for CH<sub>4</sub>-Ar are computed using theoretical values for overlap, octopole and hexadecapole mechanisms and interaction potential as input. Also, the quantum mechanical lineshapes of collision-induced light scattering (CILS) for the mixtures CH<sub>4</sub>-Ar and CH<sub>4</sub>-Xe at room temperature are calculated. The spectra of scattering consist essentially of an intense, purely translational component which includes scattering due to free pairs and bound dimers, and the other is due to the induced rotational scattering. These spectra have been interpreted by means of pair-polarizability terms, which arise from a long-range dipole-induced-dipole (DID) with small dispersion corrections and a short-range interaction mechanism involving higher-order dipole-quadrupole A and dipole-octopole E multipole polarizabilities. Good agreement between computed and experimental lineshapes of both absorption and scattering is obtained when the models of potential, interaction-induced dipole and polarizability components are used.

**Keywords:** Intermolecular potential; Absorption; Scattering; CH<sub>4</sub>-inert gases.

### 773. On Some Generalized Discrete Logistic Maps

Ahmed G. Radwan

*Journal of Advanced Research*, 4: 163-171 (2013) IF: 3

Recently, conventional logistic maps have been used in different vital applications like modeling and security. However, unfortunately the conventional logistic maps can tolerate only one changeable parameter.

In this paper, three different generalized logistic maps are introduced with arbitrary powers which can be reduced to the conventional logistic map. The added parameter (arbitrary power) increases the degree of freedom of each map and gives us a versatile response that can fit many applications. Therefore, the conventional logistic map is considered only a special case from each proposed map. This new parameter increases the flexibility of the system, and illustrates the performance of the conventional system within any required neighborhood. Many cases will be illustrated showing the effect of the arbitrary power and the equation parameter on the number of equilibrium points, their locations, stability conditions, and bifurcation diagrams up to the chaotic behavior.

**Keywords:** Logistic map; Bifurcation diagram; Stability; Generalized 1D map; Arbitrary power; Chaos.

### 774. On the Oscillation of Higher Order Dynamic Equations

Said R. Grace

*Journal of Advanced Research*, 4: 201-204 (2013) IF: 3

We present some new criteria for the oscillation of even order dynamic equation

$$(a(t)(x^{\Delta n-1}(t))^{\alpha})^{\Delta} + q(t)(x(t))^{\alpha} = 0,$$

on time scale  $T$ , where  $\alpha$  is the ratio of positive odd integers  $a$  and  $q$  is a real valued positive rd-continuous functions defined on  $T$ .

**Keywords:** Oscillation; Higher order; Dynamic equations.

### 775. Vibration Analysis of Structural Elements Using Differential Quadrature Method

Mohamed Nassar, Mohamed S. Matbully and Ola Ragb

*Journal of Advanced Research*, 4: 93-102 (2013) IF: 3

The method of differential quadrature is employed to analyze the free vibration of a cracked cantilever beam resting on elastic foundation. The beam is made of a functionally graded material and rests on a Winkler-Pasternak foundation. The crack action is simulated by a line spring model. Also, the differential quadrature method with a geometric mapping is applied to study the free vibration of irregular plates. The obtained results agreed with the previous studies in the literature. Further, a parametric study is introduced to investigate the effects of geometric and elastic characteristics of the problem on the natural frequencies.

**Keywords:** Vibration; Differential quadrature; Crack; Irregular boundaries.

### 776. Generalized Analysis of Symmetric and Asymmetric Memristive Two-Gate Relaxation Oscillators

Mohamed E. Fouda, Moustafa A. Khatib, Ahmed G. Mosad and Ahmed G. Radwan

*IEEE Transactions on Circuits and Systems*, 60 (10): 2701-2708 (2013) IF: 2.24

Memristive oscillators are a novel topic in nonlinear circuit theory, where the behavior of the reactive elements is emulated by the memristor. This paper presents symmetric and asymmetric memristive two-gate relaxation oscillators. First, the analysis of the two series memristors is introduced to study the effect of changing their polarities, as well as the mobility factor to be used in the two-gate relaxation oscillator instead of the RC circuit. The generalized analysis for the proposed memristive two-gate oscillator is introduced, where the generalized expressions for the oscillation frequency and conditions for oscillation are derived then four special cases for different mismatching of the memristors are introduced; showing a perfect matching with the PSPICE simulations. Finally, the discussion and comparison are proposed to discuss the four special cases and MATLAB simulations are also provided to study the effect of the memristance and the mobility ratio between the memristors on the oscillation frequency.

**Keywords:** "Asymmetric oscillator; Circuit analysis; Circuit theory, Mathematical analysis; Memristive circuit; Oscillators; Reactance-less oscillator; Relaxation oscillator.

### 777. Modeling Light Absorption by Bound Electrons in Self-assembled Quantum Dots

Tarek A. Ameen, Yasser M. El-Batawy and A. A. Abouelsaood

*Journal of Applied Physics*, 113: (2013) IF: 2.21

A theoretical model of the absorption coefficient of quantum dot devices is presented. Both of bound to bound absorption and bound to continuum absorption are taken into consideration in this model which is based on the effective mass theory and the nonequilibrium Greens function formalism. The results of the model have been compared with a published experimental work

and a good agreement is obtained. The effects of the dot dimensions and electron filling on the bound to continuum absorption coefficient are also investigated. In general, increasing the dot filling increases the absorption and decreasing the dots dimensions will increase the absorption and move the absorption peak towards longer wavelengths.

**Keywords:** Quantum dots; Absorption coefficient; Bound states; Excited states; Self assembly; Effective mass; Photodetectors; Lead; Wave functions; Ground states.

### 778. Polarization Dependence of Absorption by Bound Electrons in Self-assembled Quantum Dots

Tarek A. Ameen and Yasser M. El-Batawy

*Journal of Applied Physics*, 113: (2013) IF: 2.21

In this paper, the effects of the incident light polarization on the bound to continuum linear absorption coefficient of quantum dot devices have been investigated.

The study is based on the effective mass theory and the Non Equilibrium Green's Function formalism. for the bound to continuum component of the absorption coefficient, both of in-plane and perpendicular polarization effects are studied for different sizes of conical quantum dots. Generally, decreasing the dot's dimensions results in an increase of the in-plane polarized light absorption and in moving the absorption peak towards longer wavelengths.

On the other hand, decreasing the dot's dimensions results in a decrease of the perpendicularly polarized light absorption coefficient and in moving the absorption peak towards longer wavelengths.

**Keywords:** Quantum dots; Absorption coefficient; Polarization; Bound states; Effective mass; Photodetectors; Lead; Wave functions; Ground states.

### 779. Dipole-octopole Polarizability of Sulfur Hexafluoride from Isotropic and Anisotropic Light Scattering Experiments

M.S.A. El-Kader and T. Bancewicz

*Chemical Physics Letters*, 571: 16-22 (2013) IF: 2.145

The higher order dipole-octopole polarizability  $E$  of sulfur hexafluoride has been determined from isotropic and anisotropic collision-induced light scattering (CILS) experiments of pure SF<sub>6</sub> gas and from anisotropic light scattering of its mixture with inert gases. The CILS spectra are analyzed by using the new updated and different intermolecular potentials. Our final estimates for this property is  $|E| = 96.405 \pm 12.045$  a.u. which is in excellent agreement with the ab initio theoretical value.

**Keywords:** The higher order dipole-octopole polarizability.

### 780. Theoretical Study of Metal-insulator-metal Tunneling Diode Figures of Merit

Islam E. Hashem, Nadia H. Rafat and Ezzeldin A. Soliman

*IEEE Journal of Quantum Electronics*, 49 (1): 72-79 (2013) IF: 1.83

The performance of metal-insulator-metal (MIM) diodes is investigated. In this paper, we derive an analytical model that uses the Transfer Matrix Method based on the Airy Functions (AF-TMM) for the tunneling transmission probability through any number of insulating layers.

The fast-computing AF-TMM simulator results show a complete matching with the numerical Non-Equilibrium Green's Function and a reasonable matching with previously published experimental results. This study shows the effect of the work function difference and insulator thickness on MIM diode performance. The advantage of using two insulator layers on enhancing the diode responsivity, resistance, and nonlinearity is also investigated.

**Keywords:** Airy function; Metal-insulator-metal (MIM) diode; Rectenna; Tunneling current.

### 781. Effectiveness of Porosity on Transient Generalized Couette Flow With Hall Effect and Variable Properties Under Exponential Decaying Pressure Gradient

M. A. M. Abdeen, H. A. Attia, W. Abbas and W. Abd El-Meged

*Indian Journal of Physics*, 87 (8): 767-775 (2013) IF: 1.785

The transient generalized Couette flow with heat transfer through a porous medium between two infinite parallel porous plates is studied considering the Hall effect and temperature dependent physical properties. The upper plate is moving with a uniform velocity while the lower plate is kept stationary. An exponential decaying pressure gradient is imposed in the axial direction and an external uniform magnetic field as well as a uniform suction and injection are applied perpendicular to the horizontal plates. A numerical solution for the governing non-linear coupled set of equations of motion and the energy equation including the viscous and Joule dissipations is adopted. The effect of the porosity of the medium, the Hall current and the temperature dependent viscosity and thermal conductivity on both the velocity and temperature distributions is investigated.

**Keywords:** Couette flow; Variable properties; Hydromagnetics; Hall effect; Porous medium; Heat transfer; Numerical solution.

### 782. Domain-limited Solution of the Wave Equation in Riemannian Coordinates

Adel Khalil, Mohamed Hesham and Mohamed El-Beltagy

*Geophysics*, 78 (1): T21-T27 (2013) IF: 1.723

We propose to solve the two-way time domain acoustic wave equation in a generalized Riemannian coordinate system via finite-differences. The coordinate system is defined in such a way that one of its independent variables conforms to the primary wavefront, for example, using a ray coordinate system with the traveltime being one of the coordinates. At each finite-difference time-step, the solution domain is limited to a narrow corridor around the primary wavefront, leading to an increase in the computational performance. A new finite-difference scheme is introduced to stabilize the solution and facilitate its implementation. This new scheme is a blend of the simple explicit and the stable implicit schemes. As a proof of concept, the proposed method is compared to the classical explicit finite-difference scheme performed in Cartesian coordinates on two



synthetic velocity models with varying complexities. At a reduced cost, the proposed method produces similar results to the classical one; however, some amplitude differences arise due to various implementation issues. The most direct application for the proposed method is the source side of reverse time migration.

**Keywords:** Acoustic; Finite difference; Wave propagation; Wave equation; Rtm.

### 783. Snap-through Buckling of a Shallow Arch Resting on a Two-parameter Elastic Foundation

Adel Abdelgawad, Ahmed Anwar and Mohamed Nassar

*Applied Mathematical Modelling*, 37: 7953-7963 (2013)

IF: 1.706

In this paper, we study the static and dynamic snap-through of a shallow arch resting on a two-parameter elastic foundation under a point load moving at a constant speed. The deformation of the arch is expressed in Fourier series. We extend the previous works when the arch resting on a certain model of two-parameter elastic foundation. Each model of foundation has a different definition for the second foundation parameter, where the model is discussed in this paper is Pasternak model. for quasi-static analysis, it is noted that the first four modes in the expansion are sufficient to predict the response of the arch. Similarly, when the point load moves with a significant speed, we integrate the equation of motion numerically using the first modes in the expansion.

**Keywords:** Two-parameter foundation; Shallow arch; Moving point load; Snap-through buckling.

### 784. Statistical Analysis of the Stochastic Solution Processes of 1-D Stochastic Navier–Stokes Equation Using WHEP Technique

Magdy A. El-Tawil and AbdelHafeez A. El-Shekhpy

*Applied Mathematical Modelling*, 37: 5756-5773 (2013)

IF: 1.706

In this paper, the one dimensional Navier–Stokes equation under stochastic excitation is analysed using WHEP technique. The Wiener Hermite expansion properties are used together with the perturbation technique (WHEP) to obtain an approximate formula for the ensemble average, variance and higher statistical moments of the solution process. Some case studies are considered to illustrate the method of analysis.

**Keywords:** Stochastic differential equations; Perturbation method HPM; WHEP technique; Wiener–hermite expansion (WHE); Stochastic white noise process.

### 785. Thermophysical Properties and Collision-induced Light Scattering as a Probe for Gaseous Helium Interatomic Potentials

M.S.A. El-Kader

*Molecular Physics*, 111 (2): 307-320 (2013) IF: 1.67

Isotropic and anisotropic collision-induced light scattering spectra of helium gas at room temperature 294.5K and at 99.6K with the second pressure virial coefficients, second acoustic virial

coefficients, viscosity and thermal conductivity have been used for deriving the empirical models of the pair-polarizability trace and anisotropy and the interaction potential. Theoretical zeroth and second moments of the binary spectra using various models for the pair-polarizabilities and interatomic potential are compared with the experimental values performed by Le Duff's group.

In addition, third pressure virial coefficients, isotopic thermal factors, self diffusion coefficients, second virial dielectric constants and second Kerr coefficients calculated for these models are compared with experimental ones. The results show that these models are the most accurate models reported to date for this system.

**Keywords:** Collision-induced light scattering spectra; Potential; Helium.

### 786. Shakedown Analysis of 90-degree Mitred Pipe Bends

Ahmed G. Korba, Mohammad M. Megahed, Hany F. Abdalla and Mohamed M. Nassar

*European Journal of Mechanics A/Solids*, 40: 158-165 (2013)

IF: 1.592

The behaviours of smooth 90-degree pipe bends under cyclic loading have received substantial attention in recent years where shakedown and ratchetting domains have been determined. However, such data are considerably lacking for mitred pipe bends. In the current research, the lower bound shakedown limit loads of 90-degree mitred pipe bends are determined via a simplified direct non-cyclic numerical technique recently developed by Abdalla et al. (2007) The analysed mitred pipe bends are subjected to the combined effect of steady internal pressures and cyclic in-plane or out-of-plane bending moments. Both in-plane closing and opening bending moment cases are considered.

The shakedown boundaries of three mitred pipe bend geometries with one, two, and three welded joints are determined and compared with the shakedown boundary of a smooth 90-degree pipe bend. All analysed bends have diameter to thickness ratio of 25 and bend radius of 1.5 times the pipe mean diameter. The results indicate that the shakedown boundaries of mitred bends have reduced domains compared with the smooth pipe bend of similar geometrical parameters. Shakedown domains of mitred bends increase in size as the number of welded joints increase until it approaches the shakedown boundary of the smooth pipe bend simulating a mitred bend with infinite number of welded joints. The percentage of the area under shakedown domain for the mitred pipe bends to that of the smooth pipe bend ranges from 20% for the single mitred pipe bend to 75% for the 3-weld mitred bend.

Results also revealed that reducing the number of mitred welded joints, dominates reversed plasticity response at the expense of ratchetting response. Out-of-plane bending generally showed larger shakedown domain than the in-plane bending shakedown domain. Additionally, the shakedown domains for in-plane closing and opening moments are quite similar.

**Keywords:** Mitred pipe bend; Shakedown; Ratchetting; Reversed plasticity; Limit load; Smooth pipe bend.

### 787. Enlarged Omnidirectional Photonic Gap in One Dimensional Ternary Plasma Photonic Crystals That Contain Metamaterials

Sahar A. El-Naggara

*European Physical Journal D*, 67: - (2013) IF: 1.513

In contrast to most of the previous work that has been devoted to the enlargement of omnidirectional band gap (OBG) originating from Bragg scattering, we address the enlargement of zero-effective phase (zero-?) gap arising in one dimensional photonic crystals (IDPCs) that contain alternating single negative materials. In this article, we propose a new structure termed ternary plasma PCs (TPPCs) by introducing a thin un-magnetized plasma layer between the two single negative materials in each period. The influences of plasma thickness, plasma frequency and collision frequency on the gap width are discussed. Numerical results show that TPPCs structure has wider OBG than that of the corresponding binary PCs. Moreover, the gap width can be continually enlarged by tuning the plasma layer parameters. The proposed structure promises to improve filters, switches and other devices in the microwave range.

**Keywords:** Omnidirectional photonic band gap; Plasma photonic crystals; Single negative materials.

### 788. Oscillation of Integro-dynamic Equations on Time Scales

Said R. Grace, John R. Graef and Ağacık Zafer

*Applied Mathematics Letters*, 26: 383-386 (2013) IF: 1.501

In this paper, the authors initiate the study of oscillation theory for integro-dynamic equations on time-scales. They present some new sufficient conditions guaranteeing that the oscillatory character of the forcing term is inherited by the solutions.

**Keywords:** Integro-dynamic equations; Oscillation; Time scales; Volterra equations.

### 789. Three-dimensional Identification of Crack Location in Conducting Slabs Using Wavelets

S. K. Abd-El-Hafiz and A. A. Adly

*IEEE Transactions on Magnetics*, 49 (7): 3472-3475 (2013) IF: 1.422

Different nondestructive crack inspection approaches have been previously proposed for a wide range of industrial applications. Among those approaches, field measurement resulting from impressed current crack perturbation has been suggested. In this paper, semi-orthogonal compactly supported spline wavelets are used to efficiently identify the 3D spatial location of embedded cracks in conducting slabs of finite thicknesses. Within the proposed approach a couple of oppositely arranged field sensor pairs are employed on top and bottom of the conducting slab under consideration. Details of the crack detection methodologies and simulations are given in the paper.

**Keywords:** Fredholm integral equation; Inverse problem; Nondestructive testing; Spline wavelets.

### 790. A Simple Model of Double-loop Hysteresis Behavior in Memristive Elements

A. S. Elwakil, M. E. Fouda and A. G. Radwan

*IEEE Transactions on Circuits and Systems II: Express Briefs*, 60 (8): 487-491 (2013) IF: 1.327

This brief investigates the double-loop hysteresis behavior in memristive elements. Here, we propose a very simple dimensionless equation to model the double-loop behavior and then show how physical voltage- and current-controlled memristor models can be derived. Furthermore, we introduce the incremental/ decremental positive/negative memristance/ transmemristance and present circuit emulators which are capable of emulating these devices. Experimental results are given.

**Keywords:** Memristive elements; Memristor; Memristor circuits.

### 791. A Mixed Breadth-Depth First Strategy for the Branch and Bound Tree of Euclidean $K$ -center Problems

Hatem A. Fayed and Amir F. Atiya

*Computational Optimization and Applications*, 54 (3): 675-703 (2013) IF: 1.278

The  $k$ -center problem arises in many applications such as facility location and data clustering. Typically, it is solved using a branch and bound tree traversed using the depth first strategy. The reason is its linear space requirement compared to the exponential space requirement of the breadth first strategy. Although the depth first strategy gains useful information fast by reaching some leaves early and therefore assists in pruning the tree, it may lead to exploring too many subtrees before reaching the optimal solution, resulting in a large search cost. To speed up the arrival to the optimal solution, a mixed breadth-depth traversing strategy is proposed. The main idea is to cycle through the nodes of the same level and recursively explore along their first promising paths until reaching their leaf nodes (solutions). Thus many solutions with diverse structures are obtained and a good upper bound of the optimal solution can be achieved by selecting the minimum among them. In addition, we employ inexpensive lower and upper bounds of the enclosing balls, and this often relieves us from calling the computationally expensive exact minimum enclosing ball algorithm. Experimental work shows that the proposed strategy is significantly faster than the naked branch and bound approach, especially as the number of centers and/or the required accuracy increases.

**Keywords:**  $K$ -Center; Minimum enclosing ball; Branch and bound; Breadth first; Depth first.

### 792. Modeling of Field Effect Transistor Channel as a Nonlinear Transmission Line for Terahertz Detection

Nihal Y. Ibrahim, Nadia H. Rafat and Salah E. A. Elnahwy

*Journal of Infrared, Millimeter, and Terahertz Waves*, 34: 606-616 (2013) IF: 1.12

This paper revisits the theory of operation of field effect transistor in the extremely high frequency scale, where the analysis has

gone beyond the conventional cutoff frequency of the transistor. In this range, which is typically the terahertz (THz) and subterahertz range, the transistor blocks the high frequency signal and generates a rectified signal related to the input high frequency signal. An analytical model is derived for the channel of the FET in the linear mode of operation in non-resonant THz detection conditions. A transmission line distributed circuit model is applied. This is, from the authors' point of view, the suitable model for high frequency non-quasi static operation and the characteristic parameters of this model are derived from the differential equation governing the electron gas in the channel. A comparison is presented for the calculated photoresponse with previously published experimental one showing good agreement away from the threshold potential. Finally, the effects of coupling between the present model and the external input circuit have been taken into account including the loading effects of the antenna and a discussion is given for the effect on frequency selectivity of the FET.

**Keywords:** Terahertz; High electron mobility transistor; Detector; Model; Nonlinear transmission line.

### 793. Amplitude Modulation and Synchronization of Fractional-order Memristor-based Chua's Circuit

A. G. Radwan, K. Moaddy and I. Hashim

*Abstract and Applied Analysis*, (2013) IF: 1.102

This paper presents a general synchronization technique and an amplitude modulation of chaotic generators. Conventional synchronization and antisynchronization are considered a very narrow subset from the proposed technique where the scale between the output response and the input response can be controlled via control functions and this scale may be either constant (positive, negative) or time dependent. The concept of the proposed technique is based on the nonlinear control theory and Lyapunov stability theory.

The nonlinear controller is designed to ensure the stability and convergence of the proposed synchronization scheme. This technique is applied on the synchronization of two identical fractional-order Chua's circuit systems with memristor. Different examples are studied numerically with different system parameters, different orders, and with five alternative cases where the scaling functions are chosen to be positive/negative and constant/dynamic which covers all possible cases from conventional synchronization to the amplitude modulation cases to validate the proposed concept.

**Keywords:** Modulation; Synchronization; Fractional-order; Memristor; Chua's circuit.

### 794. On the Integral Solution of the One-dimensional Bratu Problem

Adel Abde kader Mohsen

*Journal of Computational and Applied Mathematics*, 251: 61-66 (2013) IF: 0.989

A brief survey of the properties and different treatments of the one-dimensional (1D) planar Bratu problem is presented. The treatment using Green's function is considered. Different iterative treatments of the resulting nonlinear system of equations are discussed. Starting the solution with simple sinusoidal function

having appropriate amplitude is recommended. Then the resulting system is solved using a nonlinear conjugate-gradient (NL-CG) method. The importance of the proper choice of the starting function as well as the stopping criterion of the iterative solution are stressed.

**Keywords:** Bratu's problem; Green's functions; Integral equations; Nonlinear conjugate; gradient; Rod buckling problem; Troesch problem.

### 795. Optimization of Fractional-order RLC Filters

Ahmed G. Radwan and M. E. Fouda

*Circuits, Systems, and Signal Processing*, 32: 2097-2118 (2013) IF: 0.982

This paper introduces some generalized fundamentals for fractional-order  $RL_\beta C_\alpha$  circuits as well as a gradient-based optimization technique in the frequency domain.

One of the main advantages of the fractional-order design is that it increases the flexibility and degrees of freedom by means of the fractional parameters, which provide new fundamentals and can be used for better interpretation or best fit matching with experimental results. An analysis of the real and imaginary components, the magnitude and phase responses, and the sensitivity must be performed to obtain an optimal design. Also new fundamentals, which do not exist in conventional RLC circuits, are introduced. Using the gradient-based optimization technique with the extra degrees of freedom, several inverse problems in filter design are introduced. The concepts introduced in this paper have been verified by analytical, numerical, and PSpice simulations with different examples, showing a perfect matching.

**Keywords:** Fractional calculus; Fractional filters; Optimization; RCL circuit; Sensitivity analysis; Fractional-order elements.

### 796. Limiting Behavior of MHD Flow Over a Porous Rotating Disk With Hall Currents

Tarek M.A. El-Mistikawy and Faiza M.N. El-Fayez

*Zeitschrift Für Angewandte Mathematik Und Mechanik*, 93 (9): 706-712 (2013) IF: 0.948

An electrically conducting fluid is driven by a rotating disk, in the presence of a magnetic field that is strong enough to produce significant Hall currents. The disk is porous, allowing mass transfer through suction or injection. The limiting behavior of the flow is studied, as the magnetic field strength grows indefinitely. The flow variables are properly scaled, and uniformly valid asymptotic expansions of the velocity components are obtained through parameter straining. The leading order approximations show sinusoidal behavior that is decaying exponentially, as we move away from the disk surface.

The two-term expansions of the radial and azimuthal surface shear stress components, as well as the far field inflow speed, compare well with the corresponding finite difference solutions; even at moderate magnetic fields.

**Keywords:** MHD flow; Rotating disk; Hall current; Suction and injection; Limiting behavior.

### 797. Fully Digital Jerk-based Chaotic Oscillators for High Throughput Pseudo-random Number Generators UP to 8.77 Gbits/S

A. S. Mansingka, M. Affan Zidan, M. L. Barakat, A. G. Radwan and K. N. Salama

*Microelectronics Journal*, 44: 744-752 (2013) IF: 0.912

This paper introduces fully digital implementations of four different systems in the 3rd order jerk-equation based chaotic family using the Euler approximation. The digitization approach enables controllable chaotic systems that reliably provide sinusoidal or chaotic output based on a selection input. New systems are introduced, derived using logical and arithmetic operations between two system implementations of different bus widths, with up to 100× higher maximum Lyapunov exponent than the original jerk-equation based chaotic systems. The resulting chaotic output is shown to pass the NIST SP. 800-22 statistical test suite for pseudo-random number generators without post-processing by only eliminating the statistically defective bits. The systems are designed in Verilog HDL and experimentally verified on a Xilinx Virtex 4 FPGA for a maximum throughput of 15.59 Gbits/s for the native chaotic output and 8.77 Gbits/s for the resulting pseudo-random number generators.

**Keywords:** Chaos; Random number generator; Lyapunov exponent, NIST, Field programmable gate array.

### 798. Improved Memristor-based Relaxation Oscillator

A. G. Mosad, M. E. Fouda, M. A. Khatib, K. N. Salama and A. G. Radwan

*Microelectronics Journal*, 44: 814-820 (2013) IF: 0.912

This paper presents an improved memristor-based relaxation oscillator which offers higher frequency and wider tuning range than the existing reactance-less oscillators. It also has the capability of operating on two positive supplies or alternatively a positive and negative supply. Furthermore, it has the advantage that it can be fully integrated on-chip providing an area-efficient solution. On the other hand, The oscillation concept is discussed then a complete mathematical analysis of the proposed oscillator is introduced. Furthermore, the power consumption of the new relaxation circuit is discussed and validated by the PSPICE circuit simulations showing an excellent agreement. MATLAB results are also introduced to demonstrate the resistance range and the corresponding frequency range which can be obtained from the proposed relaxation oscillator.

**Keywords:** Memristor; Reactance-less oscillator; Relaxation oscillator; Memristive circuits.

### 799. Properties of Defect Modes in one-dimensional Photonic Crystals That Contain Single Negative Materials

Sahar A. ELNaggar

*Optical Engineering*, 52 (2): (2013) IF: 0.88

We examine the properties of the defect modes arising in the zero-effective phase (zero- $\phi$ ) gap when a dielectric defect layer is

introduced in a one-dimensional photonic crystal containing single negative materials. We show that the defect modes inside the zero- $\phi$  gap can be as sensitive to the incidence angle as those inside the Bragg gap. In addition, adjusting the properties of the dielectric defect layer can control the frequencies and the number of defect modes. We present a brief design of a polarization-independent spatial filter based on those defects. The proposed spatial filter can work at dual carrier frequencies with low-pass and wide-pass characteristics. Our results can help improve the performance of microwave devices independent of the source wave polarization.

**Keywords:** Defect mode; Zero-effective Phase gap; Single negative materials; Spatial filter.

### 800. Approximate Solutions of Nonlinear Partial Differential Equations By Modified $q$ -Homotopy Analysis Method

Shaheed N. Huseen and Said R. Grace

*Journal of Applied Mathematics*, (2013) IF: 0.834

A modified  $q$ -homotopy analysis method ( $mq$ -HAM) was proposed for solving  $n$ th-order nonlinear differential equations. This method improves the convergence of the series solution in the  $n$ -HAM which was proposed in (see Hassan and El-Tawil 2011, 2012). The proposed method provides an approximate solution by rewriting the  $n$ th-order nonlinear differential equation in the form of  $n$  first-order differential equations. The solution of these  $n$  differential equations is obtained as a power series solution. This scheme is tested on two nonlinear exactly solvable differential equations. The results demonstrate the reliability and efficiency of the algorithm developed.

**Keywords:**  $n$ -Homotopy analysis

### 801. Stochastic 2D Incompressible Navier-stokes Solver Using the Vorticity-stream Function Formulation

Mohamed A. El-Beltagy and Mohamed I. Wafa

*Journal of Applied Mathematics*, (2013) IF: 834

A two-dimensional stochastic solver for the incompressible Navier-Stokes equations is developed. The vorticity-stream function formulation is considered. The polynomial chaos expansion was integrated with an unstructured node-centered finite-volume solver. A second-order upwind scheme is used in the convection term for numerical stability and higher-order discretization.

The resulting sparse linear system is solved efficiently by a direct parallel solver. The mean and variance simulations of the cavity flow are done for random variation of the viscosity and the lid velocity. The solver was tested and compared with the Monte-Carlo simulations and with previous research works. The developed solver is proved to be efficient in simulating the stochastic two-dimensional incompressible flows.

**Keywords:** Polynomial chaos expansion; Unstructured grids; Incompressible navier-stokes; Upwind finite-volume; Vorticity-streamfunction; Cavity flow.

### 802. Generalized Hardware Post-processing Technique for Chaos-based Pseudorandom Number Generators

Mohamed L. Barakat, Abhinav S. Mansingka, Ahmed G. Radwan and Khaled N. Salama

*Etri Journal*, 35 (3): 448-458 (2013) IF: 0.742

This paper presents a generalized post-processing technique for enhancing the pseudorandomness of digital chaotic oscillators through a nonlinear XOR-based operation with rotation and feedback. The technique allows full utilization of the chaotic output as pseudorandom number generators and improves throughput without a significant area penalty. Digital design of a third-order chaotic system with maximum function nonlinearity is presented with verified chaotic dynamics. The proposed post-processing technique eliminates statistical degradation in all output bits, thus maximizing throughput compared to other processing techniques. Furthermore, the technique is applied to several fully digital chaotic oscillators with performance surpassing previously reported systems in the literature. The enhancement in the randomness is further examined in a simple image encryption application resulting in a better security performance. The system is verified through experiment on a Xilinx Virtex 4 FPGA with throughput up to 15.44 Gbit/s and logic utilization less than 0.84% for 32-bit implementations.

**Keywords:** Chaos; Pseudorandom number generator; Post-processing; FPGA.

### 803. Oscillatory Behavior of Higher-order Neutral Type Dynamic Equations

Said R. Grace, Raziye Mert and A Gacik Zafer

*Electronic Journal of Qualitative Theory of Differential Equations*, 29: 1-15 (2013) IF: 0.74

The oscillation behavior of solutions for higher-order delay dynamic equations of neutral type is investigated by making use of comparison with second-order dynamic equations. The method can be utilized to study other types of higher-order equations on time scales as well.

**Keywords:** Oscillation; Neutral; Time scale; Higher-order; Comparison.

### 804. On the Oscillation of $\pi$ th Order Dynamic Equations on Time-scales

Said Grace

*Mediterranean Journal of Mathematics*, 10: 147-156 (2013) IF: 0.641

We present some new criteria for the oscillation of even order dynamic equation

$$(a(t)(x^{\Delta n-1}(t))^{\alpha})^{\Delta} + q(t)(x^{\sigma}(t))^{\lambda} = 0$$

on an unbounded above time scale  $T$ , where  $\alpha$  and  $\lambda$  are the ratios of positive odd integers,  $a$  and  $q$  is a real valued positive rd-continuous functions defined on  $T$

**Keywords:** Oscillation;  $n$ th order; Dynamic equation; Time-scale.

### 805. Effect of Periodically Varying Cross Section on Beam'S Behavior

Mostafa A. M. Abdeen, W. Abbas and S. M. Bichir

*Wulfenia Journal*, 20 (10): 169-179 (2013) IF: 0.467

Analytical solution for beams with variable cross section is very complicated where the bending differential equation will be a fourth order linear differential equation with variable coefficients. Generally the cross section of any structural member does not vary in an arbitrary manner. Commonly, the depth of the beams varies linearly or parabolically. In the present paper analytical solutions for the deflection and its slope of two types of beams with variable cross section are obtained. The depth varies periodically with odd number in a triangular shape in the first beam and in a parabolic shape in the second beam. The depth is expanded by using Fourier series as an even function and by using the perturbation technique. An excellent agreement is obtained between the present general analytical solution and a previous one for which the depth varies in a single triangular shape along the beam length.

**Keywords:** Beams; Periodic shape; Fourier series; Perturbation technique.

### 806. On the Effectiveness of Variation of Physical Variables on Steady Flow Between Parallel Plates With Heat Transfer in A Porous Medium

Hazem Ali Attia and Mostafa A. M. Abdeen

*Journal of Theoretical and Applied Mechanics*, 51 (1): 53-61 (2013) IF: 0.452

The effect of variation of physical variables on a steady flow through a porous medium with heat transfer between parallel plates is examined. The viscosity and the thermal conductivity are assumed to be temperature dependent. A constant pressure gradient is applied in the axial direction and the two plates are kept at two constant but different temperatures, while the viscous dissipation is considered in the energy equation. A numerical solution for the governing non-linear coupled equations of motion and the energy equation is determined. The effect of porosity of the medium, the variable viscosity, and the variable thermal conductivity on both the velocity and temperature distributions is reported.

**Keywords:** Variable properties; Porous medium; Heat transfer; Parallel plates; Steady state.

### 807. Oscillation Criteria for Fourth-order Functional Differential Equations

Said R. Grace, Martin Bohner and Ailian Liu

*Mathematica Slovaca Mathematica Slovaca*, 63: 1303-1320 (2013) IF: 0.394

Some new criteria for the oscillation of all solutions of certain fourth-order functional differential equations are established.

**Keywords:** Functional differential equation; Oscillation; Boundedness; Fourth-order equation.



### 808. Analysis of Simply Supported Thin FGM Rectangular Plate Resting on Fluid Layer

Mostafa A. M. Abdeen and S. M. Bichir

*Arabian Journal for Science and Engineering*, 38: 3267-3273 (2013) IF: 0.385

The deflection response of initially stressed functionally graded material rectangular plates subjected to distributed impulsive lateral loads and resting on a fluid layer is obtained. In the current work, material properties are chosen to be graded in the thickness direction according to a simple power law distribution. The developed artificial neural network (ANN) model uses some output results obtained using differential quadrature method.

The effects of material variation, initial stress, and fluid reaction on the plate deflection are obtained. Application of ANN method to the current problem showed that ANN technique, with less effort and time, is very efficiently capable of simulating and predicting the plate deflection and the effect of different parameters.

**Keywords:** Artificial neural network ; Functionally graded material rectangular plate; Fluid layer foundation; Numerical simulation.

### 809. Steady MHD Flow of a Dusty Incompressible Non-newtonian Oldroyd 8-Constant Fluid in a Circular Pipe

Hazem Ali Attia and Mostafa A. M. Abdeen

*Arabian Journal for Science and Engineering*, 38: 3153-3160 (2013) IF: 0.385

The steady magneto-hydrodynamic flow of a dusty incompressible electrically conducting and non-Newtonian Oldroyd 8-constant fluid through a circular pipe is examined considering the Hall effect. A constant pressure gradient is imposed in the axial direction of the pipe while an external uniform magnetic field is applied in the perpendicular direction. A numerical solution for the governing nonlinear momentum equations is obtained using the method of finite differences. The effect of the Hall current, the non-Newtonian fluid characteristics and the particle-phase viscosity on the velocity, the volumetric flow rates, and the skin friction coefficients of both the fluid and the particle phases is investigated.

**Keywords:** Magneto-hydrodynamic flow; Non-newtonian fluid; Circular pipe flow; Hall effect; Numerical solution.

### 810. Transient Generalized Couette Flow of Viscoelastic Fluid Through a Porous Medium With Variable Viscosity and Pressure Gradient

Hazem Ali Attia, Mostafa A. M. Abdeen and Waleed Abd El-Meged

*Arabian Journal for Science and Engineering*, 38: 3451-3458 (2013) IF: 0.385

The transient generalized Couette flow through a porous medium of a non-Newtonian viscoelastic fluid between two parallel porous plates is studied with heat transfer. A uniform suction from above and injection from below are applied perpendicular to the plates which are maintained at two fixed, but different,

temperatures while the viscosity of the fluid is assumed to vary exponentially with temperature. The fluid is driven by a uniform horizontal exponential decaying pressure gradient. The coupled set of equations of motion and the energy equation is solved numerically using finite differences. The influence of the different physical parameters of the model on the velocity and temperature fields is investigated and presented.

**Keywords:** Transient generalized couette flow; Viscoelastic fluid; Porous medium; Heat transfer.

### 811. Active Electromagnetic Suspension System Design Using Hybrid Neural-swarm Optimization

A. A. Adly and S. K. Abd-El-Hafiz

*International Journal of Applied Electromagnetics and Mechanics*, 43: 85-91 (2013) IF: 0.384

Recently, utilization of electromagnetic suspension systems has been on the rise as a result of novel space and automotive-related industrial applications. This paper presents an efficient iterative hybrid neural-swarm optimization methodology for electromagnetic suspension system design involving nonlinear magnetic media. Within this approach, 2D field computations are carried out using the integral equation approach in an automated mechanism through continuous Hopfield neural network (HNN) implementation.

Optimal dimensions of the system are identified through the minimization of an error function of some target performance using the particle swarm optimization (PSO) evolutionary approach. Details of the approach and sample design examples are given in the paper.

**Keywords:** Design optimization; Electromagnetic suspension; Hopfield neural network; Particle swarm optimization.

### 812. Effect of Ion Slip on the Time-varying Hartmann Flow of a Non-newtonian Viscoelastic Fluid With Heat Transfer

H. A. Attia and M. A. M. Abdeen

*Journal of Applied Mechanics and Technical Physics*, 54 (2): 268-276 (2013) IF: 0.253

Ion slip in a time-varying Hartmann flow of a conducting incompressible non-Newtonian viscoelastic fluid between two parallel horizontal insulating porous plates is studied with allowance for heat transfer. A uniform and constant pressure gradient is applied in the axial direction. An external uniform magnetic field and uniform suction and injection through the surface of the plates are applied in the normal direction. The two plates are maintained at different but constant temperatures; the Joule and viscous dissipations are taken into consideration. Numerical solutions for the governing momentum and energy equations are obtained with the use of finite differences, and the effect of various physical parameters on both the velocity and temperature fields is discussed.

**Keywords:** MHD flow; Heat transfer; Non-newtonian; Viscoelastic; Electrically conducting fluids; Hall current; Ion slip; Porous plates.

### 813. Proposed Conditions to Select Best Technique for $0\nu\beta\beta$ Decay Mode of $^{128,130}\text{Te}$

M. H. Sidky

*Life Science Journal*, 10 (4): 3509-3515 (2013) IF: 0.165

This work presents new distributions of three nuclear parameters versus the strength of the particle-particle interaction  $g_{pp}$  for the  $0\nu\beta\beta$  decay mode of  $^{128,130}\text{Te}$ . These parameters are: (1)  $RM0$  which is the ratio between the nuclear matrix elements of  $^{128,130}\text{Te}$ . (2)  $DR0$  which is the ratio between the total  $\beta\beta$ -decay rates of  $^{128,130}\text{Te}$ . (3) neutrino mass  $m_\nu$ .

This is carried out by using pn-QRPA, pn-RQRPA, full-RQRPA and SQRPA techniques with small and large basis of Hilbert space. Conditions are proposed to select the best technique. It is found that pn-QRPA and SQRPA techniques should not be applied to the  $0\nu\beta\beta$  decay mode of  $^{128,130}\text{Te}$ . The other techniques are accepted to operate the  $0\nu\beta\beta$  decay mode of  $^{128,130}\text{Te}$  with small basis of Hilbert space as follows: pnRQRPA and full-RQRPA techniques may be used within  $0.8 \leq g_{pp} = 0.85, 0.85 \leq g_{pp} = 0.9$  respectively. These ranges are determined such that the distributions of  $RM0$ ,  $DR0$ ,  $m_\nu$  which belong to the accepted techniques verify the criterion  $RM0 \approx 1$  and agree with the available experimental limits  $3.41 \times 10^{-4} \leq DR0 \leq 3.85 \times 10^{-4}$ ,  $0.21 \text{ eV} \leq m_\nu \leq 0.27 \text{ eV}$ .

**Keywords:** Neutrino mass; Pn-RQRPA technique; Hilbert space; Strength of the Particle- particle interaction.

### 814. Selection Rules of Nuclear Parameters for Neutrinoless Double Beta Decay

M. H. Sidky

*Life Science Journal*, 10(4): 3516-3521 (2013) IF: 0.165

Theoretical and experimental nuclear data are collected from different sources to establish selection rules for the probability of the neutrino less double beta decay and neutrino mass. In this work the proposed selection rules have been applied to five double beta decay emitters by using different alterations of the QRPA model within the available range of the strength of the particle- particle interaction  $0.8 \leq g_{pp} \leq 1.2$ . It is found that acceptable results have been obtained with the emitters  $^{100}\text{Mo}$ ,  $^{130}\text{Te}$  by using full-RQRPA, pn-RQRPA techniques with small basis of Hilbert space. New value for neutrino mass  $m_\nu \pm \delta m_\nu = 0.262 \pm 0.009 \text{ eV}$  is determined. Such value agrees with the available experimental determinations and improves the relative uncertainty  $\delta m_\nu / m_\nu$  from 12.5% to 3.43%.

**Keywords:** Phase space factor; Nuclear matrix element; Probability of  $0\nu\beta\beta$  decay mode; Pn-QRPA technique.

### 815. A Theoretical Study of Light Absorption in Self Assembled Quantum Dots

Tarek A. Ameen, Yasser M. El-Batawy and A. A. Abouelsaood

*Optics and Photonics Journal*, 3: 243-247 (2013)

Self assembled quantum dots have shown a great promise as a leading candidate for infrared detection at room temperature. In this paper, a theoretical model of the absorption coefficient of

quantum dot devices is presented. Both of bound to bound absorption and bound to continuum absorption are taken into consideration in this model. This model is based on the effective mass theory and the Non Equilibrium Greens Function (NEGF) formalism. NEGF formalism is used to calculate the bound to continuum absorption coefficient. The results of the model have been compared with a published experimental work and a good agreement is obtained. Based on the presented model, the bound to bound absorption coefficient component is compared to the bound to continuum absorption coefficient component. In addition, the effects of the dot dimensions and electron filling on the bound to continuum absorption coefficient are also investigated. In general, increasing the dot filling increases the absorption and decreasing the dots dimensions will increase the absorption and move the absorption peak towards longer wavelengths.

**Keywords:** Absorption coefficients; Non equilibrium greens function; Self assembled quantum dots.

### 816. Asymptotic Behavior of Non-oscillatory Solutions of Second Order Integro-dynamic Equations on Time Scales

Said R Grace, Mohamed A El-Beltagy and Sarah A Deif

*Applied and Computational Mathematics*, 2 (4): (2013)

In this paper, we investigate some new criteria on the asymptotic behavior of non-oscillatory solutions of second order integro-dynamic equations on time-scales. We also provide some numerical examples to illustrate the relevance of the obtained results.

**Keywords:** Asymptotic behavior; Non-oscillatory; Integro-dynamic equations; Time scales.

### 817. Development of Calcium Phosphate Ceramics of Controlled Ca/P Ratio as a Bone Substitute

Mana Mostafa Awad, Medhat Abdelmonem El-Messierly and Mohamed Bahgat El Kholy

*Journal of Materials Science and Engineering*, 3(7): 467-474 (2013)

In this paper, a study was carried out to produce calciumphosphate ceramics whose composition comes close to that of natural dry bone. Dicalcium phosphate dehydrated ( $\text{CaHPO}_4 \cdot 2\text{H}_2\text{O}$ ) and calcium carbonate ( $\text{CaCO}_3$ ) were mixed at different proportions so that three batches of ceramics whose Ca/P ratio are 1.5, 1.7 and 1.9 are obtained. These ratios lie in close vicinity to the reported data for dry cortical bone (Ca/P = 1.67). Sintering was carried out at temperatures ranging from 1,100 °C to 1,350 °C. The variation in batch composition as well as in sintering temperature has proved to play a decisive role in determining the end product characteristics. Parameters such as bulk density, porosity, firing shrinkage, modulus of mechanical rupture, mineralogical and textural features behavior, were studied to assess their matching with those of human cortical bone.

**Keywords:** Bone ceramic substitute; Ca/P ratio; Mechanical properties.

### 818. Evaluation of EMF Power Absorption in Human Eye Tissue

Mona A, El Naggar and M. A. El Messieri

*Int. Journal of Advanced Research*, 1 (7): 658-665 (2013)

A deterministic mathematical method is adopted to evaluate the electromagnetic power absorbed by human eye tissue. Specific absorption rate (SAR) is calculated for a multilayer human eye mathematical model. The effect of electric field strengths ranging from 1V/m to 1kV/m is investigated for wide frequency spectra. Mathematical simulation, using recently reported frequency dependent electrical properties, is applied for three different models. The models investigate the exposure and absorption level of the eye lens. The frequency dependence of the SAR and the irradiance is illustrated for different electric field strengths. The present work investigates the microwave and low frequency range(100Hz-1GHz) effect on different eye tissue. Results are compared with recent international safety standards.

**Keywords:** Electromagnetic absorption; Irradiance-electric Permittivity-human eye; Specific absorption rate; Safety standards.

### 819. Finite Element Analysis of Tidal Currents Over the Red Sea

Samir Abohadima and Ahmed Rakha

*Hydrology Science Publishing Group*, 1(2): 12-17 (2013)

Hydrodynamic models represent the core of any simulation for water quality, siltation, and morphology studies. In this study a finite element model was setup for the Red Sea to predict the tidal currents and tidal water level variations. The boundary for the model is located at the Straits of Bab-al-Mandeb. The model was simulated using two dimensional depth averaged model with an element size varying from 15 km to less than 1 km. The model was shown to provide good results for the water level variations at many stations in the Red Sea.

**Keywords:** Finite element; Red Sea; Unstructured grid; Tidal currents; Tides.

### 820. Fractional Order Butterworth Filter: Active and Passive Realizations

A. Soltan Ali, A. G. Radwan and Ahmed M. Soliman

*IEEE Journal on Emerging and Selected Topics in Circuits and Systems*, 3 (3): 346-354 (2013)

This paper presents a general procedure to obtain Butterworth filter specifications in the fractional-order domain where an infinite number of relationships could be obtained due to the extra independent fractional-order parameters which increase the filter degrees-of-freedom. The necessary and sufficient condition for achieving fractional-order Butterworth filter with a specific cutoff frequency is derived as a function of the orders in addition to the transfer function parameters. The effect of equal-orders on the filter bandwidth is discussed showing how the integer-order case is considered as a special case from the proposed procedure. Several passive and active filters are studied to validate the concept such as Kerwin-Huelsman-Newcomb and Sallen-Key filters through numerical and Advanced Design System (ADS)

simulations. Moreover, these circuits are tested experimentally using discrete components to model the fractional order capacitor showing great matching with the numerical and circuit simulations.

**Keywords:** Butterworth filter; Fractance; Fractional-order Circuit; Fractional-order filter; Kerwin-huelsman-newcomb (KHN) filter; Sallen-key filter; Stability analysis.

### 821. Fuzzy Inference System and Neuro-fuzzy Systems for Analog Fault Diagnosis

Mohamed El-Gama and Samah El-Tantawy

*Electrical Engineering Research*, 1 (4): 116-125 (2013)

A Fuzzy Inference System (FIS) is built to model and classify faults in analog circuits. The measurements that characterize the circuit under test (CUT) behavior are selected using feature extraction and dimensionality reduction techniques. These measurements are utilized to construct a rule based system that relates measurements (symptoms) to different faults (causes). In addition, hybrid neuro-fuzzy systems are also constructed and trained to isolate the CUT faults. The integration of FIS and neural networks in these systems combines the remarkable pattern recognition capabilities of neural networks with the ability of fuzzy logic to incorporate and interpret linguistic knowledge. As a result, a superior diagnosis performance is obtained even if the CUT has overlapping faults. A benchmark circuit is tested to demonstrate the high classification performance of the proposed procedure.

**Keywords:** Analog circuits; Fault diagnosis; Fuzzy inference system; Neural network; Neuro; Fuzzy system.

### 822. Measurement Fractional Order Sallen-key Filters

Ahmed Soltan, Ahmed G. Radwan and Ahmed M. Soliman

*International Journal of Electrical, Electronic Science and Engineering*, 7 (12): 1-5 (2013)

This work aims to generalize the integer order Sallen Key filters into the fractional-order domain. The analysis in the case of two different fractional-order elements introduced where the general transfer function becomes four terms which is unusual in the conventional case. In addition, the effect of the transfer function parameters on the filter poles and hence the stability is introduced and closed forms for the filter critical frequencies are driven. Finally, different examples for the fractional order Sallen-Key filter design are presented with circuit simulations using ADS where a great matching between the numerical and simulation results is obtained.

**Keywords:** Analog filter; Low-pass filter; Fractance; Sallen-key; Stability.

### 823. Modular Analysis of Sequential Solution Methods for Almost Block Diagonal Systems of Equations

Tarek M. A. El-Mistikawy

*Advances in Numerical Analysis*, (2013)

Almost block diagonal linear systems of equations can be exemplified by two modules. This makes it possible to construct

all sequential forms of band and/or block elimination methods. It also allows easy assessment of the methods on the basis of their operation counts, storage needs, and admissibility of partial pivoting. The outcome of the analysis and implementation is to discover new methods that outperform a well-known method, a modification of which is, therefore, advocated.

**Keywords:** Modular analysis; Almost block diagonal; Operation counts; Storage needs; Pivoting.

#### 824. Nonsteady Flow of A Power-Law Fluid in A Porous Medium Between Parallel Plates With Heat Transfer, Suction, and Injection

Hazem Ali Attia, Mostafa A. M. Abdeen and Alaa El-Din Abdin

*Journal of Engineering Physics and Thermophysics*, 86 (3): 677-682 (2013)

The time-varying flow of a viscous incompressible non-Newtonian power-law fluid through a porous medium between two parallel horizontal porous plates under the action of a constant pressure gradient with consideration for heat transfer is studied. Uniform suction and injection through the surfaces of the plates take place where the two plates are kept at different, but constant temperatures, and the Joule and viscous dissipation terms are considered in the energy equation.

Numerical solutions for the governing nonlinear momentum and energy equations are obtained using finite differences.

The effect of the medium porosity, the parameter describing the non-Newtonian behavior, and the velocity of suction and injection on both the velocity and temperature distributions, as well as on the dissipation terms, is investigated.

**Keywords:** Parallel plates flow; Heat transfer; Non-newtonian fluid; Porous medium; Numerical solution.

#### 825. On the Application of Mean Square Calculus for Solving Random Differential Equations

Magdy. A. El-Tawil and Ahlam H. Tolba

*Electronic Journal of Mathematical Analysis and Applications*, 1 (2): 202-211 (2013)

In this paper, the random Finite Difference Methods are used in solving random differential initial value problems of first order. The random Finite Difference method is presented and the conditions for the mean square convergence are established. Numerical examples show that random Finite Difference method gives good results. The some statistical properties of the numerical solutions are computed through numerical case studies.

**Keywords:** Random finite; Numerical examples.

#### 826. On the Effectiveness of Porosity on Steady Flow of a Viscoelastic Fluid Over A Stretching Sheet With Heat and Mass Transfer

Hazem Ali Attia and Mostafa A. M. Abdeen

*Kragujevac Journal of Science*, 35: 5-10 (2013)

The steady flow through a porous medium of a non-Newtonian viscoelastic Walter's liquid-B model fluid flow over a stretching sheet is studied with heat and mass transfer. Two different

conditions for the temperature at the surface are considered. Analytical solution for the governing equations of momentum, mass and heat transfer are given. The influence of various physical parameters as the porosity parameter, non-Newtonian fluid characteristics on the flow, heat and mass transfer are examined.

**Keywords:** Fluid flow; Heat transfer; Mass transfer; Non-newtonian viscoelastic; Stretching sheet; Exact solution; Porous medium.

#### 827. On the Fractional-Order Memristor Model

M. E. Fouda and A. G. Radwan

*Journal of Fractional Calculus and Applications*, 4: 1-7 (2013)

Fractional order calculus is the general expansion of linear integer-order calculus and is considered as one of the novel topics for modelling dynamical systems in different applications. In this paper, the generalized state equation of the nonlinear two-terminal element which is called memristor is discussed in the fractional-order sense. The effect of the added fractional-order parameter on the memristor characteristics and output behavior are introduced.

The fractional order resistance of the memristor in general for any applied voltage is derived. The generalized formulas and numerical analysis of the step response of the memristor including the instantaneous resistance, startup time and saturation time are studied which will be reduced to the conventional memristor response as  $\alpha=1$ .

**Keywords:** Fractional-order; Memristor; Modeling.

#### 828. On the Oscillatory Behavior of Volterra Integral Equations on Time-scales

Said R. Grace, John R. Graef, Saroj Panigrahi and Ercan Tunc

*Panamerican Mathematical Journal*, 23 (2): 35-41 (2013)

The authors establish some new criteria for the oscillation of the Volterra integral equation on a time-scale

$$x(t) = e(t) - \int_0^t k(t, s) f(s, x(s)) \Delta s, \text{ for } t \geq 0.$$

They apply a technique that allows them to employ Gronwall's inequality instead of a Bihari inequality. The results obtained extend some existing results in the literature.

**Keywords:** Volterra equations; Oscillation; Time scale.

#### 829. Oscillation Criteria for $N^{\text{th}}$ Order Nonlinear Dynamic Equations on Time-scales

Said R. Grace, Sandra Pinelas and Ravi P. Agarwal

*Journal of the Indian Math. Soc.*, 80 (1-2): 79-85 (2013)

Some new criteria for the oscillation of  $n^{\text{th}}$  order nonlinear dynamic equation

$$x^{\Delta^n}(t) + q(t)x^{\Delta}(\sigma(t)) = 0$$

are established.

**Keywords:** Oscillation; Nonoscillation; Dynamic equations; Higher or- der.

### 830. Parametric Control on Fractional-order Response for Lü Chaotic System

K Moaddy, A. G. Radwan, K. N. Salama, S. Momani and I. Hashim

*Journal of Physics: Conference Series*, 423: (2013)

This paper discusses the influence of the fractional order parameter on conventional chaotic systems. These fractional-order parameters increase the system degree of freedom allowing it to enter new domains and thus it can be used as a control for such dynamical systems. This paper investigates the behaviour of the equally-fractional-order Lü chaotic system when changing the fractional-order parameter and determines the fractional-order ranges for chaotic behaviour. Five different parameter values and six fractional-order cases are discussed through this paper. Unlike the conventional parameters, as the fractional-order increases the system response begins with stability, passing by chaotic behaviour then reaches periodic response. As the system parameter  $\alpha$  increases, a shift in the fractional order is required to maintain chaotic response. Therefore, the range of chaotic response can be expanded or minimized by controlling the fractional-order parameter. The non-standard finite difference method is used to solve the fractional-order Lü chaotic system numerically to validate these responses.

**Keywords:** Control; Fractional order; Chaos; Lü chaotic system.

### 831. Resonance and Quality Factor of the $RL_\alpha C_\alpha$ Fractional Circuit

Ahmed Gomaa Ahmed Radwan

*IEEE Journal on Emerging and Selected Topics in Circuits and Systems*, 3: 377-385 (2013)

This paper introduces the general fundamentals of the fractional order  $RL_\alpha C_\alpha$  circuit, where  $\alpha$  is the order of the elements. The generalized complex impedance of the  $RL_\alpha C_\alpha$  circuit can be purely real, imaginary, or short circuit. The stability analyses where two regions have been classified are introduced with many numerical examples. General maps for transient and frequency responses are investigated showing the damping parameters for each case. The resonance, 3 dB frequencies, bandwidth, and quality factor for all possible cases have been investigated with detailed analytical formulas. Numerical and PSpice simulations are provided using different examples to validate these concepts.

**Keywords:** Bandwidth; Damping ratios; Distortion; Fractional calculus; Fractional-order filter; Quality factor; Resonance; Stability analysis;  $RL_\alpha C_\alpha$  circuit.

### 832. Stability Behavior and Free Vibration of Tapered Columns With Elastic End Restraints Using the DQM Method

Mohamed Taha and Mohamed Hassan

*Ain Shams Engineering Journal*, 4: 515-521 (2013)

The stability behavior and free vibration of axially loaded tapered columns with rotational and/or translational end restraints are studied using the differential quadrature method (DQM). The governing differential equations are derived and transformed into a homogeneous system of algebraic equations using the DQM

technique. The boundary conditions are discretized and substituted into the governing differential equations, then the problem is transformed into a two parameter eigenvalue problem, namely the critical load and the natural frequency. The solution of the eigenvalue problem yields the critical load for the static case ( $\omega = 0$ ) and yields the natural frequencies for the dynamic case with a prescribed value of axial load ( $P_0 < P_{cr}$ ). The obtained solutions were verified against those obtained from FEM and found in close agreement.

**Keywords:** Tapered column; End restraints; Differential quadrature; Critical load; Natural frequencies.

### 833. Stability of Flow Through A Porous Medium of A Viscoelastic Fluid Above A Stretching Plate

Hazem Ali Attia and Mostafa A. M. Abdeen

*Kragujevac Journal of Science*, 35: 11-14 (2013)

The effect of the porosity of the medium on the stability characteristics of a viscoelastic fluid flow over a stretching plate is investigated. A three-dimensional linear stability analysis is performed by means of the Method of Weighted Residuals for disturbances of the Taylor-Gortler type. It is found that the porosity of the medium exerts a stabilizing influence on the flow.

**Keywords:** Porous medium; Stability characteristics; Viscoelastic fluid flow; Stretching plate.

### 834. Static And Dynamic Behavior of Tapered Beams on Two-parameter Foundation

Mohamed Taha Hassan and Mohamed Nassar

*International Journal of Research and Reviews in Applied Sciences*, 14: 176-187 (2013)

The static and dynamic behaviors of tapered beams resting on two-parameter foundations are studied using the differential quadrature method (DQM). The governing differential equations are derived and discretized; then the appropriate boundary conditions are discretized and substituted into the governing differential equations yielding a system of homogeneous algebraic equations. The equivalent two-parameter eigenvalue problem is obtained and solved for critical loads in the static case ( $\omega = 0$ ) and natural frequencies in the dynamic case with a prescribed value of the axial load ( $P_0 < P_{cr}$ ). The obtained solutions are found compatible with those obtained from other techniques. A parametric study is performed to investigate the significance of different parameters.

**Keywords:** Tapered beams; Two-parameter foundation; Differential quadrature; Critical load; Natural frequencies

### 835. The Optimal q-Homotopy Analysis Method (Oq-HAM)

Shaheed N. Huseen, Said R. Grace and Magdy A. El-Tawil

*International Journal of Computers and Technology*, 11 (8): 2859-2866 (2013)

In this paper, an optimal q-homotopy analysis method (Oq-HAM) is proposed. We present some examples to show the reliability and efficiency of the method. It is compared with the one-step



optimal homotopy analysis method. The results reveal that the Oq-HAM has more accuracy to determine the convergence-control parameter than the one-step optimal HAM.

**Keywords:** Optimal q-homotopy analysis method; Convergence-control parameter.

### 836. Wavelet-scalogram Based Study of Non-periodicity in Speech Signals as a Complementary Measure of Chaotic Content

Mohamed Hesham Farouk El-Sayed

*International Journal of Speech Technology*, 16 (3): 353-361 (2013)

In recent studies, the chaotic behavior of a signal is confirmed using scalogram analysis of continuous-wavelet transform. Chaotic component of a speech signal can be verified through scalogram analysis, since, it investigates the periodicity content of a signal.

The periodicity analysis helps in proving that a signal is not periodic, which is an essential condition on chaotic activity. In this work, a scale-index based on scalogram-analysis is calculated for a set of recordings of Arabic vowels. Also, Largest-Lyapunov Exponents (LLE) are computed for these recordings. The obtained measures are, then, compared. The comparison proves the efficacy of scale index for confirming chaotic behavior even for highly-periodic waveforms which is the case in speech vowels. Additionally, it is noted that both LLE and scale-index exhibit classification ability for Arabic vowels.

**Keywords:** Chaos in speech signals; Scale-index; Largest lyapunov exponent (LLE); Continuous-wavelet analysis; Wavelet scalogram.

#### Dept. of Mechanical Design and Production

### 837. A Self-tuning Resonator for Vibration Energy Harvesting

Noha A. Aboulfotouh, Mustafa H. Arafa and Said M. Megahed

*Sensors and Actuators A: Physical*, a201: 328-334 (2013)  
IF: 1.841

This work is concerned with developing a vibration-based energy harvester with a tunable natural frequency. The harvester is designed to automatically adjust its own natural frequency to match that of the imposed base excitation. The proposed device consists of a cantilever beam carrying a tip mass in the form of a magnet which is placed in close proximity to another magnet with opposite polarity that can move axially thereby adjusting the beam's natural frequency by mechanical straining. The system is designed to autonomously adjust the gap between the two magnets so as to achieve a harvester whose natural frequency matches that of the excitation. As such, the movable magnet is mounted on a motordriven tray that undergoes linear motion and adjusts its position in accordance with the frequency of the support motion. The base motion frequency is detected by an electromagnetic means, wherein another magnet, fixed to the base, moves past a stationary coil generating an electric signal. The signal is conditioned through a microprocessor to detect its frequency and is then used to determine the

favorable gap between the tuning magnets to achieve resonance from a lookup table. Based on the findings of this work, the natural frequency of the harvester is successfully tuned from 4.7 Hz to 9.0 Hz generating voltage peracceleration from 6.3 V/m/s<sup>2</sup> to 1.1 V/m/s<sup>2</sup>, respectively

**Keywords:** Vibration energy harvesting; Self-tunable harvester; Permanent magnets.

### 838. Modeling and Experimental Verification of Multi-Modal Vibration Energy Harvesting from Plate Structures

Mohamed M. R. El-Hebeary, Mustafa H. Arafa and Said M. Megahed

*Sensors and Actuators A: Physical*, a193: 35-47 (2013)  
IF: 1.841

The focus of the present work is on the design of plate structures for vibration energy harvesting from two or more modes of vibration. The work is motivated by the quest to design resonators that respond to variable frequency sources of base excitation. The geometry of two-dimensional structures, such as Vshaped and open delta-shaped plates, is explored to obtain closely spaced harvestable vibration modes to scavenge energy across a broader bandwidth. To this end, an electromagnetic energy harvester in the form of a base excited plate is proposed. The plate carries tip magnets that oscillate past stationary coils to generate power from the lower modes of vibration. The plate dynamic behavior is governed by its geometry and placement of the magnets on its tip. An effort is made to optimize the system configuration so as to control the spacing between the resonance frequencies while efficiently harvesting energy from all modes. Plates possessing three natural frequencies in the range from 8 to 19 Hz are developed, and findings of the present work are verified numerically and experimentally

**Keywords:** Vibration energy harvesting; Plates; Multi-modal.

### 839. Wear Characterization of Carbon Nanotubes Reinforced Polymer Gears

Yousef, S.; Khattab, A.; Zaki, M. and Osman, T.A.

*Nanotechnology, IEEE Transactions on*, 12 (4): 616-620 (2013)  
IF: 1.4

In last decade, polymeric gears have found wide applications in industrial fields. This is due to their advantages likenoise reduction, self-lubricating features, weight reduction, cost savings as well as lower tribological characteristics in term of friction and wear. The main objective of this paper is to study the wear behavior of spur gears that makes polymer blended by carbon nanotubes (CNTs) (acetal). This was made by using appropriate adhesive oil (Paraffin) during injection moulding practice to produce thick flanges with diameter 134 mm and thickness 29 mm. The CNTs were produced by a fully automatic system using arc discharge technique multielectrodes. The synthesizing CNT/acetal flanges contain 1% CNTs by weight. The flanges were machined using CNC milling machine to produce spur gears. The dispersion of CNTs in polymer were examined by scanning electron microscope. The experiments were performed at

a running speed of 1420 r/min and at torques of 13 and 16 N·m. In addition, the mechanical properties of CNT/acetal have been tested. The results showed that the wear resistances of the CNTs/acetal spur gears increased with the addition of CNT. The strength, Young's modulus and stiffness also increased while the hardness was not affected by the addition of CNT.

**Keywords:** Carbon Nanotubes (Cnts), Reinforced Polymer Gears And Wear.

#### 840. Effects of Increasing Electrodes on Cnts Yield Synthesized by Using Arc-discharge Technique

Samy Yousef, A. Khattab, T. A. Osman and M. Zaki

*Journal of Nanomaterials*, (2013) IF: 1.547

A new design of fully automatic system was built up to produce multiwalled carbon nanotube (MWCNT) using arc discharge technique in deionized water and extra pure graphite multiple electrodes (99.9% pure). The goal of the experimental research is to determine the yield of CNT in two different cases: (a) single plasma electrodes and (b) multiplasma electrodes, particularly 10 electrodes. The experiments were performed at constant parameters (75 A, 238V). The obtained CNT was examined by scanning electron microscope (SEM), transmission electron microscope (HRTEM), X-ray diffraction (XRD), and thermogravimetric analysis (TGA). The results showed that the produced CNT is of type MWCNT, with a diameter of 5 nm, when using multiplasma electrodes and 13 nm when using single plasma electrodes. The yield of MWCNT was found to be 320% higher in case of comparing multielectrodes to that of single plasma electrodes. Under the experimental test conditions, a yield of 0.6 g/hr soot containing 40% by mass nanotube was obtained in case of single plasma electrodes and above 60% in case of multiplasma electrodes.

**Keywords:** Carbon nanotubes (CNTS); Arc-discharge technique.

#### 841. A Dynamic Programming Approach for Minimizing the Number of Drawing Stages and Heat Treatments in Cylindrical Shell Multistage Deep Drawing

Tamer F. Abdelmaguid, Ragab K. Abdel-Magied, Mostafa Shazly and Abdalla S. Wifi

*Computers and Industrial Engineering*, 66: 525-532 (2013)  
IF: 1.516

Deep drawing is an important sheet metal forming process that appears in many industrial fields. It involves pressing a blank sheet against a hollow cavity that takes the form of the desired product. Due to limitations related to the properties of the blank sheet material, several drawing stages may be needed before the required shape and dimensions of the final product can be obtained. Heat treatment may also be needed during the process in order to restore the formability of the material so that failure is avoided. In this paper, the problem of minimizing the number of drawing stages and heat treatments needed for the multistage deep drawing of cylindrical shells is addressed. This problem is directly related to minimizing manufacturing costs and lead time. It is required to determine the post-drawing shell diameters along with whether heat treatment is to be conducted after each drawing stage such that the aforementioned objectives are

achieved and failure is avoided. Conventional computer-aided process planning (CAPP) rules are used to define the search space for a dynamic programming (DP) approach in which both the post-drawing shell diameter and material condition are used to define the states in the problem. By discretizing the range of feasible shell diameters starting from the initial blank diameter down to the final shell diameter, the feasible transitions from state to another is represented by a directed graph, based upon which the DP functional equation is easily defined. The DP generates a set of feasible optimized process plans that are then verified by carrying out finite element analysis in which the deformation severity and the resulting strains and thickness variations are investigated. Two case studies are presented to demonstrate the effectiveness of the developed approach. The results suggest that the proposed approach is a valuable, reliable and quick computer aided process planning approach to this complicated problem.

**Keywords:** Dynamic programming; Deep drawing; Number of drawing stages; CAPP; Finite elements.

#### 842. Simplified Mathematical Modeling of Implant Limit Stress and Maximum HAZ Hardness

A. Fotouh, M. El-Shennawy and R. El-Hebeary

*Welding Journal*, 92: 336-s -346-s (2013) IF: 1

Hydrogen-induced cracking (HIC) susceptibility in the heat-affected zone (HAZ) was investigated and modeled using implant static tensile limit stress ( $\sigma_{imp}$ ) and maximum hardness of the HAZ ( $HV_{10MAX}$ ). C-Mn and high-strength low-alloy (HSLA) steels were used as base metals with a carbon equivalent (CE) ranging from 0.38 to 0.48% and 0.52 to 0.69%, respectively. The shielded metal arc welding (SMAW) and gas metal arc welding (GMAW) processes with  $CO_2$  shielding gas were used. The diffusible hydrogen (H) content was varied taking the values between 2 and 40 mL/100 g.  $\sigma_{imp}$  and  $HV_{10MAX}$  were the two measures used to evaluate the weldment susceptibility to HIC. Using Pearson's product-moment coefficient ( $P_{pm}$ ) and the developed analysis of HIC susceptibility, two simplified models were developed using simple mechanistic models, linear and logarithmic, to simulate  $\sigma_{imp}$  and  $HV_{10MAX}$ .  $\sigma_{imp}$  was modeled as a function of  $HV_{10MAX}$  and H, while  $HV_{10MAX}$  was modeled as a function of CE and  $t_{800/500}$ . The two new simplified models were capable of accurately simulating both  $\sigma_{imp}$  and  $HV_{10MAX}$ . The newly developed models form a simplified tool that can be used to assess HIC susceptibility in steel weldments.

**Keywords:** Modeling; Hydrogen-induced cracking (hic); Implant Test; Implant Static Tensile Limit; Stress; Maximum heat-Affected zone (haz) hardness; Shielded metal arc Welding (SMAW); Gas metal arc welding (GMAW).

#### 843. A Continuum Based Three-dimensional Modeling of Wind Turbine Blades

Ahmed H. Bayoumy Ayman A. Nada and Said M. Megahed

*Journal of Computational and Nonlinear Dynamics*, 8/3: 031004-1- 031004-14 (2013) IF: 0.927

Accurate modeling of large wind turbine blades is an extremely challenging problem. This is due to their tremendous geometric complexity and the turbulent and unpredictable conditions in which they operate. In this paper, a continuum based three

dimensional finite element model of an elastic wind turbine blade is derived using the absolute nodal coordinates formulation (ANCF). This formulation is very suitable for modeling of large deformation, large-rotation structures like wind turbine blades. An efficient model of six thin plate elements is proposed for such blades with non-uniform, and twisted nature. Furthermore, a mapping procedure to construct the ANCF model of NACA (National Advisory Committee for Aeronautics) wind turbine blades airfoils is established to mesh the geometry of a real turbine blade. The complex shape of such blades is approximated using an absolute nodal coordinate thin plate element, to take the blades tapering and twist into account. Three numerical examples are presented to show the transient response of the wind turbine blades due to gravitational/aerodynamics forces. The simulation results are compared with those obtained using ANSYS code with a good agreement

**Keywords:** ANCF; Wind turbine blade; Thin plate element.

#### 844. Effect of Die Design Parameters on Thinning of Sheet Metal in the Deep Drawing Process

H. Zein, M. El-Sherbiny, M. Abd-Rabou and M. El Shazly

*American Journal of Mechanical Engineering*, 1 (2): 20-29 (2013)

Prediction of the forming results, determination of the thickness distribution and the thinning of the sheet metal blank will decrease the production cost through saving material and production time. In this paper, A Finite Element (FE) model is developed for the 3-D numerical simulation of deep drawing process (Parametric Analysis) by using ABAQUS/EXPLICIT FEA program with the proper material properties (anisotropic material) and simplified boundary conditions.

The FE results are compared with experimental results for validation. The developed model can predict the thickness distribution and thinning of the blank with the die design parameters (geometrical and physical parameters). Furthermore, with numerical simulation, working parameters can be optimized without expensive shop trials.

**Keywords:** Finite element; Parametric analysis; Geometrical parameters; Thickness distribution; Thinning.

#### 845. Influence of Nano Grease Composite on Rheological Behaviour

Alaa Mohamed, A. Khattab, T.A. Osman and M. Zaki

*International Journal of Engineering Research and Applications*, 3 (6): 1126-1131 (2013)

The aim of this work is to study the rheological behaviors of carbon nanotubes (CNTs) as an additive on lithium grease at different concentrations. The results indicated that the optimum concentrations of the CNTs was 2 %. These experimental investigations were evaluated with a HAAKE Rheovisco RV20, Penetrometer and Measurement of the dropping point.

The results indicated that the shear stress and apparent viscosity increase with the increase of CNTs concentration, penetration and consistency not effect of base grease, and the dropping point increasing about 25%. The microstructure of CNTs and lithium grease was examined by high resolution transmission electron

microscope (HRTEM) and transmission electron microscope (TEM).

**Keywords:** Carbon nanotubes; Rheological behavior; Lithium grease; Microstructure.

#### 846. Optimal Kinematic Synthesis of 4-Bar Planar Crank-Rocker Mechanisms for A Specific Stroke and Time Ratio

Galal A. Hassaan, Mohammed A. Al-Gamil And Maha M. Lashin

*International Journal of Mechanical and Production Engineering Research and Deelpment*, 3 (2): 87-98 (2013)

Optimal synthesis of mechanisms is a successful approach for mechanism design to satisfy all the desired characteristics of the designed mechanism. The 4-bar crank-rocker mechanism has wide industrial applications and its synthesis is of increasing importance. The optimal design problem in this case is a constrained multi-dimensional problem. Powell optimization technique is used to minimize a special objective function combining the mechanism stroke and time ratio. 3 functional constraint functions are used to perform a successful optimization process leading to satisfying the requirements of a successful operation of the mechanism. The mechanism kinematical functions are derived in a dimensionless form. The results are tabulated for an easy reference to them without any calculations.

Power law models are fitted to the optimization results. It was possible to obtain a mechanism stroke between 20 and 55 degrees and a time ratio between 1.05 and 1.204 for a transmission angle in the range 45 to 135 degrees. A comparison is conducted between the optimal design results using the tabulated normalized dimensions and the optimal values using the proposed power law models.

**Keywords:** Planar 4-Bar Mechanism; Optimal mechanism synthesis; Specific stroke; Time ratio.

#### 847. Optimization of Hypoid Gear Using Genetic Algorithm

Alaa Mohamed, A. Khattab, T.A. Osmana and Mostafa. Shazly

*International Journal of Engineering Research and Applications*, 3 (6): 1132-1138 (2013)

Genetic algorithm (GA) is a Non-Traditional method is useful and applicable for optimization of mechanical component design. The GA is an efficient search method which is inspired from a natural genetic selection process to explore a given search space. In this work, GA is applied to minimize the volume of hypoid gear with respect to a specified set of constraints. Module, face width and number of teeth of hypoid are used as design variables and the bending stress, contact stress and a geometric limit on the face width are set as constraints. The results showed that the optimal procedure reduced the volume of a gear designed according to ANSI/AGMA 2003-B97 to 54% of its original volume. Further analysis was performed to study the effect of the design variables and the input parameters of the objective function.

**Keywords:** Genetic algorithms; Hypoid gears; Volume optimization.

**848. Rheological Behavior of Carbon Nanotubes as an Additive on Lithium Grease**

Alaa Mohamed, Aly Ahmed Khattab, Tarek Abdel Sadek Osman and Mostafa Zaki

*Journal of Nanotechnology*, (2013)

The rheological behaviors of carbon nanotubes (CNTs) as an additive on lithium grease at different concentrations were examined under various settings of shear rate, shear stress and apparent viscosity. The results indicated that the optimum content of the CNTs was 2 %. These experimental investigations were evaluated with a Brookfield programmable Rheometer DV-III ULTRA. The results indicated that the shear stress and apparent viscosity increase with the increase of CNTs concentration. The microstructure of CNTs and lithium grease was examined by high resolution transmission electron microscope (HRTEM) and scanning electron microscope (SEM). The results indicated that the microscopic structure of the lithium grease presents a more regular and homogeneous network structure, with long fibers, which confirms the rheological stability.

**Keywords:** Carbon nanotubes; Rheological behavior; Lithium grease; Microstructure.

**849. The Effect of Fiber Orientation and Laminar Stacking Sequences on the Torsional Natural Frequencies of Laminated Composite Beams**

Mohammed Fahmy Aly, Galal.A.Hassan and Ibrahim Goda

*International Journal of Research in Engineering and Technology*, 2 (12): 209-218 (2013)

The composite materials are well known by their excellent combination of high structural stiffness and low weight. The main feature of these anisotropic materials is their ability to be tailored for specific applications by optimizing design parameters such as stacking sequence, ply orientation and performance targets. Finding free torsional vibrations characteristics of laminated composite beams is one of the bases for designing and modeling of industrial products.

With these requirements, this work considers the free torsional vibrations for laminated composite beams of doubly symmetrical cross sections. The torsional vibrations of the laminated beams are analyzed analytically based on the classical lamination theory, and accounts for the coupling of flexural and torsional modes due to fiber orientation of the laminated beams are neglected. Also, the torsional vibrations of the laminated beams analyzed by shear deformation theory in which the shear deformation effects are considered. Numerical analysis has been carried out using finite element method (FEM). The finite element software package ANSYS 10.0 is used to perform the numerical analyses using an eight-node layered shell element to describe the torsional vibration of the laminated beams. Numerical results, obtained by the ANSYS 10.0, classical lamination theory, and shear deformation theory are presented to highlight the effects of fibers orientation and layers stacking sequence on torsional frequencies of the beams.

**Keywords:** Composite materials; Laminated composite beams; Torsional vibrations; Shear deformation; Finite element analysis.

**850. Tuning of A Lag-lead Compensator Used With A First Order Plus An Integrator Process**

Galal A. Hassaan, Mohammed A. Al-Gamil and Maha M. Lashin

*International Journal of Mechanical and Production Engineering Research and Development*, 3 (5): 41-48 (2013)

Lag-lead compensators are well known in automatic control engineering. They have 4 parameters to be adjusted (tuned) for proper operation. The frequency response of the control system or the root locus plot are traditionally used to tune the compensator in a lengthy procedure. A first order with an integrator process in a unity feedback loop of 67.3 % maximum overshoot and 12 seconds settling time is controlled using a lag-lead compensator (through simulation). The lag-lead compensator is tuned by minimizing the sum of absolute error of the control system using MATLAB. Four functional constraints are used to control the performance of the lag-lead compensated control system. The result was reducing the process oscillation to 2.438 % overshoot and an 0.648 seconds settling time. The performance of the lag-lead compensated system with the present tuning approach is compared with the classical tuning using the root locus technique. The comparison showed that the present tuning technique is superior.

**Keywords:** Compensator; Root locus; Overshoot; Frequency response; Settling time and matlab.

**851. Tuning of A PIDF Controller Used With A Highly Oscillating Second Order Process**

Galal A. Hassaan, Mohammed A. Al-Gamil and Maha M. Lashin

*International Journal of Emerging Technology and Advanced Engineering*, 3 (3): 943-945 (2013)

High oscillation in industrial processes is something undesired and controller tuning has to solve this problem. PDF and PIDF are controller modes which are expected to overcome this problem. This research work has proven that the PIDF is the genuine solution for the high level process oscillation. A second order process of 85.45 % maximum overshoot and 8 seconds settling time is controlled using a PIDF controller (through simulation). The controller is tuned by minimizing the sum of absolute error of the control system using MATLAB. A functional constraint is imposed on the maximum percentage overshoot. The result was cancelling completely the process oscillation with a zero overshoot and a 0.62 seconds settling time. The performance of the PIDF controller is compared with the classical PID controller with the same process.

**Keywords:** PDF controller; PIDF controller; Overshoot; Maximum overshoot; Gain; Settling time.

**Dept. of Mining, Petroleum and Metallurgy****852. Failure Analysis and Flexural Behavior of High Chromium White Cast Iron and AISI4140 Steel Bimetal Beams**

H.E.M. Sallam, Kh. Abd El-Aziz, H. Abd El-Raouf and E.M. Elbanna

*Materials and Design*, 52: 974-980 (2013) IF: 2.913

Failure analysis and flexural behavior of high-Cr white cast iron (HCWCI) and AISI4140 Steel bimetal beams in the as-cast condition under 3PB test were experimentally and numerically investigated. The bimetal beams of HCWCI as a wear resistant part and AISI4140 Steel as a ductile part were fabricated using a new method. In this method, the two parts of bimetal castings are joined mechanically together by dovetail joint and/or connector pins. The experimental results showed that the flexural strengths of the bimetal beams were excellent and ranged from 650 to 790 MPa. The bimetal beam with sufficient connector pins exhibited the highest flexural strength compared with the other bimetal casting specimens. The numerical results of the bimetal beams are in agreement with the experimental results. The failure of the bimetal beams occurred in three stages. In the first stage, a sliding crack (mode II) initiated at the interface between the wear resistant and ductile parts at the mid-span of specimens. In the second stage, mode I crack initiated in the wear resistant part at the mid span and propagated toward the point of loading. In the last stage, a third main crack initiated and propagated in the ductile part.

**Keywords:** Failure analysis; White cast iron; Bimetal.

### 853. Bacterially Induced Phosphate-dolomite Separation Using Amphoteric Collector

A.M. Elmahdy, S.E. El-Mofty, M.A. Abdel-Khalek, N.A. Abdel-Khalek and A.A. El-Midany

*Separation and Purification Technology*, 102: 94-102 (2013)  
IF: 2.894

The phosphate-dolomite separation has a limited separation selectivity using conventional flotation. The utilization of bacteria alone or in presence of collector offers a good solution in terms of increasing the separation selectivity. In this study, the bioflotation was tested using two bacterial strains (*Corynebacterium diphtheriae-intermedius*, CDI, or *Pseudomonas Aeruginosa*, PA) in the presence of amphoteric collector. Statistical design of experiments (DOE) was used to screen, optimize, and study the factors mutual interactions. The screening design indicated that the bacteria concentration, bacteria conditioning time, and collector dosage are the most significant parameters. In addition, full factorial design indicated that the presence of bacteria improves the separation selectivity. Moreover, it was found that the PA performs better than CDI in presence of collector in terms of lowering the MgO% and increasing P<sub>2</sub>O<sub>5</sub>%. A concentrate containing 0.69% MgO and ~30.8 % P<sub>2</sub>O<sub>5</sub> with a recovery of ~ 80% can be obtained at 11.4x10<sup>7</sup> cells, 20 minutes and 4.0 Kg/t for pH, PA concentration, PA conditioning time, and collector dosage, respectively.

**Keywords:** Dolomite; Phosphate; Statistical design; Bacteria; bioflotation.

### 854. Adsorption of *Paenibacillus Polymyxa* and Its Impact on Coal Cleaning

M. A. Abdel-Khalek and A. A. El-Midany

*Fuel Processing Technology*, 113: 52-56 (2013) IF: 2.816

The adsorption of micro-organisms and bacteria on minerals surfaces depends mainly on the type of the bacteria used as well as the nature of the studied mineral surface. Such adsorption could

change the surface properties of the mineral surface and leads to control its surface for increasing its separation selectivity from associated impurities or enhance/retard the adhesion with other substances. Therefore, in the current study, adsorption of *Paenibacillus polymyxa* (P.*polymyxa*) on coal was studied. Several methods were used such as: zeta potential, adsorption isotherms, adsorption kinetics and Fourier Transform InfraRed (FTIR). The main goal is to determine the difference in surface behaviour of coal particles before and after the treatment with P.*polymyxa* bacteria. The results showed that electrostatic interactions are insignificant in P.*polymyxa* adsorption on coal particles. The results suggest that the adsorption of bacteria on the coal particles is mainly physical and it depends on electrostatic forces, hydrogen bonding as well as the hydrophobic forces between the bacteria wall and the organic matter in the coal and coal hydrophobicity.

**Keywords:** Adsorption; Bacteria; Coal; *Paenibacillus polymyxa*; Separation; Ash; Sulfur.

### 855. Why Relatively Coarse Calcareous Phosphate Particles Are Better in a Static-bed Calciner?

A.A. El-Midany, F.A. Abd El-Aleem and T.F. Al-Fariss

*Powder Technology*, 237: 180-185 (2013) IF: 2.024

The calcination process is a direct and clean process for calcareous phosphate ore upgrading. In this study, calcination experiments of Al-Jalamid calcareous phosphate ore were conducted. Different size fractions were used to evaluate their performance while heating in a static-bed furnace at different calcination time and temperature. The results showed that the calcined product of coarse particles gives a higher P<sub>2</sub>O<sub>5</sub>%. A Phosphate concentrate with a grade as high as 34% P<sub>2</sub>O<sub>5</sub> was obtained. Although the larger particle size is higher in grade, the finer particles showed a higher conversion. This behaviour was correlated to the change in bed-structure in terms of the particle specific surface area and bed permeability due to the exposure to high temperatures. The fast fall in both particle surface area and bed permeability in the case of fine particles leads to capture of the generated CO<sub>2</sub>, as a calcination product, inside the individual particle or the entire bed. Once CO<sub>2</sub>, gas forms an appreciable pressure gradient, it starts to find its way through either the available voids in the coarse particle bed or by forming cracks that appears only in fine particle bed.

**Keywords:** Calcareous phosphate; Upgrading; Calcination; Bed permeability; Sintering.

### 856. Microstructure and Wear Behavior of Solidification Sonoprocessed B390 Hypereutectic Al-Si Alloy

Waleed Khalifa, Shima El-Hadad and Yoshiki Tsunekawa

*Metallurgical and Materials Transactions A*, 44A: 5817-5824 (2013) IF: 1.627

The hypereutectic Al-Si alloys constitute an important family of alloys because of their excellent wear resistance and low thermal expansion. However, the optimal microstructure and hence the optimal service performance of these alloys cannot be achieved by the conventional melt treatments used in industry today, because of the chemical incompatibility between the primary-Si



refiners and the eutectic-Si modifiers used in microstructure control.

The current study aimed at using ultrasonic vibrations to improve the microstructure and the properties of these alloys. The results of the current study showed that for the B390 Al-Si alloy (i) the ultrasonic treatment has potential refining effect on the primary Si and Fe intermetallic phases, (ii) the primary Si particles become finer as the pouring temperature decreases from 1033 K (760 °C) to 938 K (665 °C), (iii) pouring and ultrasonic treatment at temperatures below the start of primary Si precipitation result in the coexistence of large and fine Si particles in microstructure, (iv) phosphorous additions of 50 ppm did not show any substantial effect in the ultrasonically treated ingots, (v) ultrasonic-treated samples have uniform hardness over the surface while the untreated samples show large scattering (high standard deviation) in hardness levels and (vi) ultrasonic-treated samples showed better wear resistance in the absence of phosphorous.

**Keywords:** Al-Si; Solidification; Ultrasonic; Hypereutectic; Wear; Primary Si.

### 857. Application of Bacillus Subtilis for Reducing Ash and Sulfur in Coal

M. A. Abdel-Khalek and A. A. El-Midany

*Environmental Earth Sciences*, 70: 753-760 (2013) IF: 1.445

The replacement of coal with other energy sources is due to the presence of harmful impurities such as sulfur can lead to emission of harmful and corrosive gases such as H<sub>2</sub>S and SO<sub>2</sub>. These gases can affect the human health due to its toxicity. Also, the mineral matter (ash) can cause several types of respiratory system diseases due to the presence of heavy metals and formation of hazardous compounds while burning of coal. In order to avoid the production of such emissions, the researcher all over the world were looking for a methodology that can eliminate or reduce these impurities from coal. Therefore, the current study aims at decreasing the sulfur and ash content in Egyptian coal (Maghara coal), using bioflotation technique. The effect of *Bacillus subtilis* (*B. subtilis*) on the removal/reduction of sulfur and ash was investigated.

The affinity of the *B. subtilis* to coal surface was characterized using zeta-potential, adsorption tests and FTIR. The bioflotation results showed that, at optimum conditions, a clean coal contains 0.92% total sulfur and 1.95% ash with yield exceeds 72 % was obtained from the starting coal containing 3.3% sulfur and 6.65% ash.

**Keywords:** Bacteria; Coal; Bioseparation; Bioflotation; De-ashing; Desulfurization.

### 858. Concentration of A Sudanese Low-grade Iron Ore

Ahmed A.S. Seifelnassr, Eltahir M. Moslim and Abdel-Zaher M. Abouzeid

*International Journal of Mineral Processing*, 122: 59-62 (2013) IF: 1.378

The iron ore deposit of the Northern State of Sudan, at Wadi Halfa, is a huge deposit, but is low in grade. It assays 36% Fe and 48% silica. The present study is an attempt to investigate the amenability of this newly discovered ore for upgrading. Based on the appreciable differences in specific gravity and magnetic

susceptibility between the desired iron minerals and the gangue minerals, it was suggested that gravity separation and/ or magnetic separation may be useful to concentrate this type of low-grade ore. As a result of the fine dissemination of the iron minerals and the most abundant gangue mineral, quartz, the optimum degree of grind is around 150 µm. Using two-stage separation, roughing and cleaning, it was possible to obtain a high grade concentrate assaying about 64% Fe at a recovery of 72%.

**Keywords:** Beneficiation of wadi halfa iron ore; Concentration of a low-grade iron ore; Magnetic separation; Gravity concentration; Combined gravity magnetic beneficiation.

### 859. Coal – Mycobacterium Phlei Interaction and Its Effect on Coal Cleaning

Mohamed A. Abdel-Khalek and Ayman A. El-Midany

*Tenside Surfactant and Detergents*, 50: 414-419 (2013) IF: 0.981

The adsorption of micro-organisms and bacteria can be used in separation of valuable minerals from their gangue minerals. The coal is one of the important sources of energy. Most of the coal deposits are low rank coals that contain sulfur compounds and mineral matters which release harmful and toxic gases while burning of coal.

In the current study, the interaction of *Mycobacterium phlei* (*M.phlei*) with coal was characterized with several techniques such as zeta potential, adsorption kinetics, adsorption isotherms and Fourier Transform InfraRed (FTIR). In addition, the *M.phlei* was tested for sulfur and ash removal from coal. The results of surface characterization indicated that the optimum pH was 2-4 where the *M.phlei* is physically adsorbed to coal particles due to slight electrostatic interactions as well as the hydrophobic interaction. The *M.phlei* increases the coal separation selectivity from its associated impurities and reduces the total sulfur and ash to 0.99 and 2.1%, respectively.

**Keywords:** Adsorption; Bacteria; Coal; M.Phlei; Bioflotation.

### 860. Flexural Strength and toughness of Austenitic Stainless Steel Reinforced High-cr White Cast Iron Composite

H.E.M. Sallam, Kh. Abd El-Aziz, H. Abd El-Raouf and E.M. Elbanna

*Journal of Materials Engineering and Performance*, 22: 3769-3777 (2013) IF: 0.915

Flexural behavior of high-Cr white cast iron (WCI) reinforced with different shapes, i.e., I- and T-sections, and volume fractions of austenitic stainless steel (310 SS) were examined under three-point bending test. The dimensions of casted beams used for bending test were (5031003500 mm<sup>3</sup>). Carbon and alloying elements diffusion enhanced the metallurgical bond across the interface of casted beams.

Carbon diffusion from high-Cr WCI into 310 SS resulted in the formation of Cr-carbides in 310 SS near the interface and Ni diffusion from 310 SS into high-Cr WCI led to the formation of austenite within a network of M<sub>7</sub>C<sub>3</sub> eutectic carbides in high-Cr WCI near the interface. Inserting 310 SS plates into high-Cr WCI beams resulted in a significant improvement in their toughness. All specimens of this metal matrix composite failed in a ductile

mode with higher plastic deformation prior to failure. The high-Cr WCI specimen reinforced with I-section of 310 SS revealed higher toughness compared to that with T-section at the same volume fraction.

The presence of the upper flange increased the reinforcement efficiency for delaying the crack growth.

**Keywords:** Flexural strength; Flexural toughness; High-cr white cast iron; Metal matrix composites.

### 861. Column Vs. Mechanical Flotation for alcaeous Phosphate Fines Upgrading

T. F. Al-Fariss, K. A. El-Nagdy, F. A. Abd El-Aleem and A. A. El-Midany

*Particulate Science and Technology*, 31: 488-493 (2013)  
IF: 0.435

Froth flotation, either conventional or column, has been studied for phosphate upgrading. In this study, a reverse flotation scheme using either mechanical or column flotation was applied for the beneficiation of Al-Jalamid Saudi phosphate ores. It is classified as a sedimentary phosphate with calcite as main impurity (calcareous type). The effects of different operating parameters were evaluated for both conventional and column flotation. A mixture of Oleic acid and kerosene is used as a collector, sulfuric acid as pH regulator and sodium sulfate as phosphate depressant. The results of this study revealed that both conventional and column flotation technology can be adopted for this type of ore. A high grade concentrate of 35%  $P_2O_5$  can be achieved at a high recovery of 95%. Comparing the results of the both techniques indicates the superiority of column at fine sizes. However, the mechanical cells are more suitable at high solid liquid ratios because of good particle dispersion and good mixing in the mechanical cells.

**Keywords:** Calcareous phosphate; Flotation; Column flotation; Mechanical flotation; Carbonate removal.

### 862. Dolomite-apatite Separation by Amphoteric Collector in Presence of Bacteria

Elmahdy Ahmed, El-Mofty Salah, Abdel-Khalek Mohamed, Abdel-Khalek Nagui and El-Midany Ayman

*Journal of Central South University*, 20: 1645-1652 (2013)  
IF: 0.434

Bioflotation represents one of the growing trends to enhance the selectivity of conventional flotation processes. It utilizes the micro-organisms to replace or to interact with the chemical reagents to increase the gap between surface properties of similar minerals and to enhance the separation selectivity. In this work, dolomite-phosphate separation was investigated using amphoteric collector (dodecyl-N-carboxyethyl-N-hydroxyethyl-imidazoline) in presence of bacteria. Two types of bacteria, *Corynebacterium diptheriae*-intermedius (CDI), and *Pseudomonas aeruginosa* (PA), were used. The collector-bacteria interaction was characterized by Fourier transform infra-red (FTIR), frothing height and Zeta potential. The results show that the collector-bacteria interaction improves the flotation selectivity. Although, the PA positively affects the separation results, the CDI cannot lower the MgO to less than 1%. A

phosphate content of 0.7% MgO and 31.77%  $P_2O_5$  with a recovery of 68% at pH 11, 3.0 kg/t amphoteric collector,  $4 \times 10^7$  cells of PA is obtained.

**Keywords:** Dolomite; Phosphate; Amphoteric collector; Bacteria; Bio-flotation; Carbonate minerals.

### 863. Development of a New Simulator “Matrod” for the Design of Sucker Rod Pumping Systems

M. Abu El Ela And A. Hamdy

*Oil Gas European Magazine*, 39: 193-197 (2013) IF: 0.417

Rod pumping continues to be the most widely used means for artificial lift of oil wells. Because of the wide use, the methods for design and analysis of rod pumping systems are being refined and improved continually. In this article, a computer program “MATROD” is described, which has been developed using MATLAB R2010a to simulate the API RP 11L design method for sucker rod pumping systems. MATROD can perform a complete design for sucker rod pumping systems. It can identify a number of rod designations for a wide range of the pumping conditions. MATROD can design hundreds of sucker rod pumping system alternatives for a given set of conditions. It arranges the output in a table and figures formats so that it can be easily manipulated for the optimization process. Decision making of the selection between the alternatives depends on the available equipment and the required pump displacement. In order to verify MATROD, its results were compared with the output of an existing simulator “PUMPMAX” using previously published data. It was found that MATROD is accurate enough to provide meaningful data. The absolute average errors between the results of the two simulators for the calculated peak polished rod load, polished rod torque, polished rod horse power and pumping displacements are 1.94%, 3.06%, 2.25% and 2.56%, respectively. Such work is an original contribution to develop a tool for solving the conceptual design problems and design of alternative sucker rod pumping systems.

**Keywords:** Rod pumping; Design of sucker rod Pumping; Artificial lift of oil Wells.

### 864. CO<sub>2</sub> Use Could Boost Egypt’S Western Desert Oil Recovery

Mahmoud Abu El Ela, Helmy Sayyoub and El Sayed El-Tayeb

*Oil and Gas Journal*, 111: 96-101 (2013) IF: 0.201

The main objective of this study was to develop a strategy that maximizes use of CO<sub>2</sub> emissions from the Egyptian Western Desert. The study evaluates ways to capture these emissions for enhanced oil recovery (EOR) and assesses the applicability of CO<sub>2</sub> injection in candidate fields. The first activity in this project was to screen 37 reservoirs to identify those most suitable for CO<sub>2</sub> injection. The screening was carried out with specialized software (EOR Graphical User Interface-EORgui). Results of the screening indicated five reservoirs as candidates. These lie in three Badr El-Din Petroleum Co. (Bapetco) oil fields: the Abu Roash G formation in Badr El Din (BED) 3C9 field, the Abu Roash C formation in BED 3-6/3-11 field, and Abu Roash C, Kharita, and Bahariya formations in BED 1 field. The results indicate 76.2 billion std. cu ft (bscf) of CO<sub>2</sub> to be required for injection. Injection of CO<sub>2</sub> is expected to increase the

incremental oil recovery by 7.62 million stock-tank bbl (stb), or 10% of the original oil in place. The study clarifies that the main sources of CO<sub>2</sub> in the Western Desert are gas processing plants. Currently, 51.2 MMscfd of CO<sub>2</sub>-rich gas (about 70% CO<sub>2</sub>) can be recovered as byproduct from four main gas processing plants: Obayed, El Salam, Tarek, and El Qasr. The CO<sub>2</sub>-rich gas streams can be gathered from the four plants to a central point in the El Salam area, then transported via 130-mile, 16-in. pipeline to Abu Sennan field to be stored in order to fulfill the EOR project's needs. This project can contribute to the improvement of Egyptian security of supply by increasing oil production and assisting in the reduction of greenhouse emissions.

**Keywords:** Enhanced oil recovery "EOR"; Eor projects; Eor screening criteria.

### 865. Egypt's Tut Field a Candidate for CO<sub>2</sub> Miscible Flooding

Mahmoud Abu El Ela

*Oil and Gas Journal*, 111: 74-80 (2013) IF: 0.201

Tut field has proved to be feasible for the application of enhanced oil recovery technology. The field is on the Khalda concession in the north part of Egypt's Western Desert and is under waterflood. Discovered in 1986, the field currently has 50 oil producing wells and 11 water injection wells. A recent investigation on the applicability of using EOR method in Tut field was conducted. Preliminary screening was carried out to select the most suitable method for the Alam El Bueib-3D (AEB-3D) formation; one of the field's producing zones. The incremental production for potentially applicable EOR techniques to AEB-3D was quantified. The analysis of the screening results is based on successful EOR field application worldwide. Results indicate CO<sub>2</sub> miscible flooding to be the most appropriate and promising EOR method for the AEB-3D. The study also showed that CO<sub>2</sub> can be an attractive injection fluid because of (1) the availability of CO<sub>2</sub> and (2) miscibility could be achieved under current reservoir conditions. Using water alternating gas (WAG) process with a WAG ratio of 0.5, incremental production of 1.44 million stock-tank bbl (stb) or a 10.8% recovery factor could be achieved. The study's results encourage Khalda Petroleum Co. to investigate implementing CO<sub>2</sub> injection in other formations and fields on KPC's concession. It is expected that application of such technology will yield incremental oil recovery of about 30 million stb assuming a 10% additional recovery factor.

**Keywords:** CO<sub>2</sub> miscible flooding; Eor; Case study of tut field.

### 866. Eor Via CO<sub>2</sub> Flood Requires Careful Transportation Assessment

Mahmoud Abu El Ela

*Oil and Gas Journal*, 111: 112-117 (2013) IF: 0.201

Enhanced oil recovery via miscible flooding with CO<sub>2</sub> is an increasingly viable substitute globally for water flooding, but each case requires careful project design and cost estimation of the CO<sub>2</sub> transport system supplying the field. This article uses Egypt's Tut field as an example of how to determine the weight of particular design and cost variables. A previous study indicated that the CO<sub>2</sub> miscible flooding seems to be the most appropriate and promising EOR methods for AEB-3D formation in Tut field. The current study shows that CO<sub>2</sub> can be attractive injection fluid

because its availability as a byproduct in Salam gas plant (One of Khalda gas plants in the Western Desert). The study designs the required surface facilities for a 5mmscf/d CO<sub>2</sub> injection pilot project. It includes a conceptual design for five stages compression station that will compress the gas and transfer it through 4" pipeline of 5 km from Salam gas plant to the injector at Tut field. The EOR method selection requires a life cycle analysis of the capital and operating expenditure (CAPEX/OPEX) trade-offs together with the required technical skills to prepare the project for the implementation phases. Therefore, CAPEX and OPEX of the pilot project are estimated. The study indicates that the CO<sub>2</sub> injection pilot project is commercially attractive and achievable. The total CAPEX and OPEX of the pilot project are estimated \$ 27.5 million and \$ 2.2 million, respectively; which can be earned in two years of pilot production. The total project duration is estimated 12-16 months.

**Keywords:** CO<sub>2</sub> miscible flooding; Enhanced oil recovery "EOR"; Cost estimate of CO<sub>2</sub> miscible flooding project.

### 867. Statistical Interactions in Phosphate Rock Calcination

T.F. Al-Fariss, F.A. Abd El-Aleem and A. A. El-Midany

*Mp Materials Testing*, 55: 221-227 (2013) IF: 0.184

Most of the marine phosphate deposits are calcareous phosphates. Calcination process is one of the famous processes used for upgrading sedimentary calcareous phosphate ore. In this study, evaluation of the calcination process performance in terms of its operating parameters was carried out. The effect of operating parameters and their significance on calcination of calcite as a main phosphate ore impurity was studied using statistical design of experiments. A statistical model was developed to correlate the studied parameters with the phosphate grade in the calcined product. The studied parameters were temperature, time, and particle size. The analysis of the design results showed that the temperature is the most significant parameter. The higher the temperature is the higher the calcite conversion to calcium oxide and release of carbon dioxide. In addition, the particle size plays a significant role in contact area between particles as well as the voids among them that help to release the CO<sub>2</sub> faster. Moreover, a phosphate concentrate, suitable for phosphoric acid production, containing ~32 % P<sub>2</sub>O<sub>5</sub> can be achieved at optimum values of studied parameters, i. e., at a temperature of 850 °C, after a calcination time of 40 minutes and with a particle size of 0.074 mm, respectively. Furthermore, quenching and slacking of calcined products increased the grade by 2–3 % to reach 34 % to 35 % P<sub>2</sub>O<sub>5</sub> in the final concentrate.

### 868. Complete and Cost-effective Approach for Diagnosing formation Damage and Performing Successful Stimulation Operations

Mahmoud Abu El Ela

*Journal of Petroleum Science Research (Jpsr)*, 2 (2): 65-74 (2013)

This paper presents and describes a comprehensive and cost effective approach to diagnose and treat the formation damage problems. The proposed approach consists of systematic steps: recognition of the immediate problem; data collection, analysis

and integration; identification of the source of the formation damage problem; assessment of the formation damage; identification of the proposed treatment techniques; evaluation of all options; selection of the best stimulation technique; stimulation process design, implementation of the plan; and evaluation and analysis of the results. Application of such approach in an oil producing well (case study from the Gulf of Suez area) of an international joint venture company in Egypt achieved oil production rate of 560 bbl/day after complete mud losses during the drilling operations. Such study is an original contribution to the knowledge of diagnosing and solving formation damage problems.

**Keywords:** Formation damage; Stimulation operations.

### 869. Corrosive Wear Characteristics of Bronze Friction Resisting Composites

Kh. A. Ragab, R. Abdel-Karim, M. Bournane, S. Farag and S. M. El-Raghy and H. A. Ahmed

*Tribology- Materials, Surfaces & Interfaces*, 7 (1): 52-59 (2013)

Three groups of bronze based composites with different amounts of slide additive (graphite) and friction additives (SiC and SiO<sub>2</sub>) were prepared by powder metallurgy technique. The corrosive wear behaviours of the resulting composites in electrochemical aqueous solutions, namely, acidic rain, neutral rain and wastewater, were comparatively investigated. The corrosive wear mechanisms of the bronze composites were discussed based on examination of the worn surface morphologies of the composite block materials by means of scanning electron microscopy equipped with an energy dispersion spectrometry. The determination of corrosive wear rates was carried out by means of a combination of electrochemical and gravimetric techniques. Increasing both slide and friction additives improved the corrosion resistance of these bronze composites. Samples with 1.5% graphite, 3%SiO<sub>2</sub> and 3%SiC had the highest corrosive wear resistance in neutralised as well as in acid rain due to the high amount of antifriction and slide additives, in addition to low porosity.

**Keywords:** Bronzes; Composites; Wear.

### 870. Effect of Quenching Temperature on the Mechanical Properties of Cast Ti-6Al-4V Alloy

Reham Reda, Adel A. Nofal, Abdel-Hamid and A. Hussein

*Journal of Metallurgical Engineering*, 2 (1): 48-54 (2013)

Ti-6Al-4V alloy is a workhorse of titanium industry; it accounts for about 60 percent of the total titanium alloy production. The high cost of titanium makes net shape manufacturing routes very attractive.

Casting is a near net shape manufacturing route that offers significant cost advantages over forgings or complicated machined parts. However, the disadvantage of the as-cast titanium alloys, like other cast metals, is that the heat treatment remains only a limited option for improvement of their properties.

The objective of this work was to study the effect of water quenching on mechanical properties of cast Ti-6Al-4V alloy. Tensile, hardness and Charpy impact toughness tests were performed.

The results showed that the final properties of cast Ti-6Al-4V alloy are highly dependent on the quenching temperature.

**Keywords:** Heat treatment; Cast ti-6Al-4V alloy; Tensile properties; Hardness; Impact toughness; Fracture surface.

### 871. Effect of Single and Duplex Stage Heat Treatment on the Microstructure and Mechanical Properties of Cast Ti-6Al-4V Alloy

Reham Reda, Adel Nofal and Abdel-Hamid Hussein

*Metallography, Microstructure, and Analysis*, 2: 388-393 (2013)

The effect of single and duplex stage heat treatment on the microstructure and mechanical properties of cast Ti-6Al-4V alloy was studied.

The single stage heat treatment (SSHT) involved solution annealing at 935 °C for 10 min followed by water quenching, while the duplex stage heat treatment (DSHT) involved solution annealing at 935 °C for 10 min, furnace cooling to 600 and 700 °C, followed by isothermal holding for 30 min and subsequent waterquenching. The properties characterization was conducted using microstructure investigation along with tensile, hardness, and Charpy impact tests.

The impact fracture surfaces were observed using Scanning Electron Microscope. After SSHT, an increase in the tensile strength and hardness at the expense of the tensile elongation and impact toughness was recorded as compared with the as-cast alloy.

This is attributed to the formation of a brittle α0 martensite phase in the microstructure after quenching from 935 °C. On the other hand, DSHT enhances the percent elongation and impact toughness over the as-cast alloy and SSHT. The formation of α0 martensite-free microstructure as well as controlling the composition of the different microstructural constituents during DSHT optimizes the mechanical properties.

**Keywords:** Single/duplex stage heat treatment; Cast ti-6Al-4V Alloy; Microstructure; Tensile strength; Tensile Elongation; hardness; Impact toughness; Fracture surface.

### 872. Influence of Heat Input and Post-Weld Heat Treatment on Boiler Steel P91 (9Cr-1Mo-V-Nb) Weld Joints

#### Part 1 – Microstructure

M. Abd El-Rahman Abd El-Salam, I. El-Mahallawi and M. R. El-Koussy

*International Heat Treatment and Surface Engineering*, 7(1): 23-31 (2013)

Steel P91 is known for its excellent high temperature properties. The achievement of optimum weld metal properties for steel P91 within the course of its extensive applications in power plants has however often caused concern. In the present work, three thick pipes of P91 steel were welded using three different levels of heat inputs within the range of 1.15–3.5 kJ mm<sup>-1</sup>. A circumferentially multipass butt welded P91 steel pipe, typically used for high temperature applications in power plants was selected for this investigation. The achievements of optimum weld metal properties, which are closely linked to microstructure, are known to cause concern in such weldments. Two types of heat treatments were employed, subcritical post-weld heat treatment

and normalising/tempering treatment. The microstructure was evaluated by optical, scanning electron microscope, X-ray diffraction and magnetic permeability. The results have shown a great influence of heat input and heat treatment on the microstructure. Martensite and ferrite were the main structures obtained. Bainite and  $\delta$ -ferrite have been observed in the weld metal, heat affected zone and weld metal for all heat input/treatment conditions. The volume fraction of bainite and  $\delta$ -ferrite increased with increase in heat input till a critical value slightly lower than  $1.15 \text{ kJ mm}^{-1}$ ; then decreased with the increase in heat input. The normalising/tempering treatment resulted in a decrease in the volume fraction of  $\delta$ -ferrite and bainite compared to the subcritical post-weld treatment which is conventionally used. This explains the enhancement in the toughness and creep properties of the steel presented in the second paper.1

**Keywords:** Microstructures;  $\delta$ -Ferrite; Modified 9Cr–1Mo Steel; Welding; Heat treatments; Heat Input.

### 873. Influence of Heat Input and Post-weld Heat Treatment on Boiler Steel P91 (9Cr–1Mo–V–Nb) Weld Joints

#### Part 2 – Mechanical Properties

M. Abd El-Rahman Abd El-Salam, I. El-Mahallawi and M. R. El-Koussy

*International Heat Treatment And Surface Engineering*, 7(1): 32-37 (2013)

Three thick pipes of modified 9Cr–1Mo steel were welded using three different levels of heat inputs: low heat input  $1.1 \text{ kJ mm}^{-1}$ , medium heat input  $2.3 \text{ kJ mm}^{-1}$  and high heat input  $3.16 \text{ kJ mm}^{-1}$ . Two types of heat treatments were employed, namely subcritical post-weld heat treatment and normalising/tempering treatment. The influence of heat input and post-weld heat treatment on the microstructure of boiler steel P91 weld joints has been investigated in the previous paper. In the present work hardness, tensile, impact toughness and stress rupture properties were evaluated. Our results show a great influence of heat input and heat treatment on mechanical properties. The best combination of properties was obtained in low to medium range of heat input, between 1 and  $2.8 \text{ kJ mm}^{-1}$  for both treatments and a 90% increase in time to rupture was observed for normalising/tempering treatment compared to subcritical post-weld treatment.

**Keywords:** Mechanical Properties ;  $\delta$ -Ferrite ; Modified 9Cr–1Mo Steel ; Welding ; Heat Treatments ; Heat Input ; Stress Rupture

### 874. Influence of Nanodispersions on Properties and Microstructure Features of Cast and T6 Heat-Treated Al Si Hypoeutectic Alloys

El Mahallawi, H. Abdelkader, L. Shehata, A. Amer and J. Mayer, A. Schwedt

*Solid State Phenomena*, (192 - 193): 76-82 (2013)

Cast light metal alloys have retained their importance and unique characteristics as first candidates when the cost-function relationship is considered. Hypoeutectic aluminum silicon alloys such as A356 exhibit several specific and interesting properties that qualify them to be used in many automotive and aeronautical

applications. Evidence of significant enhancement in strength in the properties of Al-Si cast alloys by incorporating nano-particles has been recently presented. The present study aims to develop nano-dispersed Al-Si alloys with suitable casting methods that assure the dispersion of the nano-particles. In this work a number of cast samples of A356 were prepared by rheo-casting in a specially designed and built furnace unit allowing for the addition of the nanoparticles into the molten Al-Si alloy in the semi-solid state with mechanical stirring. The microstructural features and the mechanical properties of the cast and T6 heat treated samples were investigated. The results obtained in this work showed enhancement in the mechanical strength of the nano-dispersed alloys, accompanied by significant increase in the elongation percentage, supported by evidence of refined dendrite arm length, and inter-lamellar spacing.

**Keywords:** Aluminium silicon hypoeutectic alloys; Strength; T6; Grain refinement; Sem microanalysis.

### 875. Microseismic Imaging of Hydraulically Induced-fractures in Gas Reservoirs: a Case Study in Barnett Shale Gas Reservoir, Texas, Usa

Abdulaziz M. Abdulaziz

*Open Journal of Geology*, 3: 361-369 (2013)

Microseismic technology has been proven to be a practical approach for in-situ monitoring of fracture growth during hydraulic fracture stimulations. Microseismic monitoring has rapidly evolved in acquisition methodology, data processing, and in this paper, we evaluate the progression of this technology with emphasis on their applications in Barnett shale gas reservoir. Microseismic data analysis indicates a direct proportion between microseismic moment magnitude and depth, yet no relation between microseismic activity and either injection rate or injection volume has been observed. However, large microseismic magnitudes have been recorded where hydraulic fracturing stimulation approaches a fault and therefore the geologic framework should be integrated in such programs. In addition, the geometry of fracture growth resulted by proppant interactions with naturally fractured formations follows unpredictable fashion due to redirecting the injection fluids along flow paths associated with the pre-existing fault network in the reservoir. While microseismic imaging is incredibly useful in revealing the fracture geometry and the way the fracture evolves, recently several concerns have been raised regarding the capability of microseismic data to provide the fracture dimensional parameters and the fracture mechanism that could provide detailed information for reservoir characterization.

**Keywords:** Microseismic imaging; Barnett shale; Fracture monitoring; Unconventional reservoirs stimulations.

### 876. Neuro-fuzzy Inference System for Modeling Equilibrium Ratio for Heptanes-Plus Fraction

Abbas Mohamed Al-Khudafi, Eissa M. El-M Shokir, Khaled Ahmad Abdel-Fattah and Abdulrageeb Kadi

*International Journal of Innovation and Applied Studies*, 4: 334-342 (2013)

Equilibrium constant has many applications in solving problems in reservoir engineering and petroleum processing. Various



correlations are available for estimating K- values for heptanes plus fractions. These correlations can be classified into simple and complicated. However these correlations are not able to predict K values adequately for a wide range of conditions. They lose validity in specific range of pressure and temperature and exhibit some error. In this work neuro-fuzzy modeling techniques (ANFIS) is developed to predict K- values for heavy fractions. A large collection of K- values data points (more than 1340 data points) were extracted from experimental 570 PVT reports using the principal of material balance are used in developing the neuro-fuzzy model. 80% of the data points were used to train ANFIS model and 20% of data sets were used to validate, and test the model. Statistical analysis (average absolute percent error, correlation coefficient, standard deviation, maximum error, minimum error, etc.) is used for comparison the proposed model with empirical correlations. Graphical tools have also been utilized for the sake of comparison the performance of the new model and experimental data. Results showed that the new hybrid neural fuzzy model outperforms some available empirical correlations.

**Keywords:** Heptanes plus; Neuro-fuzzy model; K-Values; Empirical correlations; Equilibrium ratio.

### 877. Exploitation of Bacterial Activities in Mineral Industry and Environmental Preservation: an Overview

Ahmed A. S. Seifelnassr and Abdel-Zaher M. Abouzeid

*Journal of Mining, 2013: (2013)*

Since the identification and characterization of iron and sulfur oxidizing bacteria in the 1940s, a rapid progress is being made in minerals engineering based on biological activities. Microorganisms can play a beneficial role in all facets of minerals processing, from mining to waste disposal and management. Some of the applications, such as biologically assisted leaching of copper sulfide ores, uranium ores, and biooxidation of refractory sulfide gold ores, are now established on the scale of commercial processes. A variety of other bioleaching opportunities exist for nickel, cobalt, cadmium, and zinc sulfide leaching. Recently, other uses of microorganisms are potentially possible. These include the bioleaching of nonsulfide ores, bioflotation, and bioflocculation of minerals, and bioremediation of toxic chemicals discharged from mineral engineering operations. These activities acquire considerable opportunities for further research and development in these areas. This paper is an attempt to provide a critical summary on the most important efforts in the area of bacterial activities in the mineral and mining industry.

**Keywords:** Exploitation; Bacterial activities; Mineral industry.

### Dept. of Public Works

### 878. Long-Term Starvation and Subsequent Recovery of Nitrifiers in Aerated Submerged Fixed-Bed Biofilm Reactors

Abdelsalam Elawwad, Hendrik Sandner, Uwe Kappelmeyer and Heinz Koeser

*Environmental Technology, 34 (8): 945-959 (2013) IF: 1.606*

The effectiveness of three operational strategies for maintaining nitrifiers in bench-scale, aerated, submerged fixed-bed biofilm reactors (SFBBRs) during long-term starvation at 20°C were evaluated.

The operational strategies were characterized by the resulting oxidation-reduction potential (ORP) in the SFBBRs. The activity rates of the nitrifiers were measured and the activity decay was expressed by half-life times. It was found that anoxic and alternating anoxic/aerobic conditions were the best ways to preserve ammonia-oxidizing bacteria (AOB) during long starvation periods and resulted in half-life times of up to 34 and 28 days, respectively. Extended anaerobic conditions caused the half-life for AOB to decrease to 21 days. In comparison, the activity decay of nitrite-oxidizing bacteria (NOB) tended to be slightly faster.

The activity of AOB biofilms that were kept for 97 days under anoxic conditions could be completely recovered in less than one week, while over 4 weeks was needed for AOB kept under anaerobic conditions. NOB were more sensitive to starvation and required longer recovery periods than AOB. For complete recovery, NOB needed approximately 7 weeks, regardless of the starvation conditions applied. Using the fluorescence in situ hybridization (FISH) technique, *Nitrospira* was detected as the dominant NOB genus. Among the AOB, the terminal restriction fragment length polymorphism (TRFLP) technique showed that during starvation and recovery periods, the relative frequency of species shifted to *Nitrosomonas europaea/eutropha*, regardless of the starvation condition. The consequences of these findings for the operation of SFBBRs under low-load and starvation conditions are discussed.

**Keywords:** Biofilm; Nitrification; Starvation; Recovery; TRFLP.

### 879. Static and Cyclic Behavior of North Coast Calcareous Sand in Egypt

Manal Salem, Hussein Elmallouk and Shehab Agaiby

*Soil Dynamics and Earthquake Engineering, 55 83-91 (2013)*

*IF: 1.276*

This research studies the behavior of calcareous sand located in the North Coast of Egypt, Dabaa area, under static and cyclic loading. The study is performed through a series of monotonic and cyclic undrained triaxial tests conducted on two relative densities and different effective confining pressures. The cyclic tests were carried out at different cyclic stress ratios. Failure under cyclic loading was found to be governed by the gradual development of excess pore water pressure until liquefaction is reached, rather than cumulative development of axial strain (cyclic mobility).

The cyclic strength of the tested sand is compared with other calcareous and siliceous sands reported in the literature. The test results indicate that loose Dabaa calcareous sand has higher cyclic strength compared to other siliceous sands, probably due to the existence of different shapes of calcareous sand particles within the tested soil. Relationship between cyclic resistance ratio, effective confining pressure, and relative density was developed for the tested sand.

**Keywords:** Calcareous sand; Static loading; Cyclic loading; Triaxial; Liquefaction.

### 880. Evaluation of SPT Energy for Donut and Safety Hammers Using CPT Measurements in Egypt

Rami M. El-Sherbiny and Manal A. Salem

*Ain Shams Engineering Journal*, 4: 701-708 (2013)

Standard Penetration Test (SPT) blow counts require correction prior to utilization in soil characterization and determination of properties and behavior. Among the most important corrections is the energy correction required to adjust the blow counts to 60% energy efficiency. However, there are no published data supporting commonly used value in Egypt. This paper presents an evaluation of the energy efficiency of the Donut and Safety hammers commonly used in Egypt and the associated energy correction factor. The energy efficiency is estimated by comparing N-values from the SPT to back-calculated N<sub>60</sub> values from the Cone Penetration Test (CPT) using well established correlations. Results indicate that the energy efficiency of the Donut hammer based on current practice in Egypt is approximately 50%. Thus, the back-calculated energy correction factor is approximately 0.82. For the Safety hammer, results indicate that the energy efficiency is approximately 60%, and the energy correction factor is approximately 1.0.

**Keywords:** SPT; CPT; Hammer efficiency; Energy correction.

### 881. Upgrading of the Existing Wastewater Treatment Plants in Egypt Using Discfilter

Khaled Zaher Abdalla and Adel Fayed Gaid

*Civil and Environmental Research*, 3 (13): 131-136 (2013)

Wastewater can be used after treatment. Using of the treated wastewater depends on the quality of the final effluent. Implementation of new wastewater treatment plants is very expensive; hence, upgrading of existing wastewater treatment plants can be considered as a suitable alternative. In this study, upgrading of wastewater treatment plant in Kom Hamada was evaluated by adding discfilter to improve the quality of the final effluent. TSS, BOD<sub>5</sub>, COD, and helminth eggs were obtained for the influent and effluent over a period of four months. The average removal efficiencies of TSS, BOD<sub>5</sub>, and COD were found to be 79.98 %, 28.17 %, and 30.4 % respectively. The helminth eggs were totally removed. The effluent obtained after using discfilter was suitable for irrigation according to the Egyptian regulations for reuse of treated wastewater.

**Keywords:** Discfilter; Helminth eggs; Tertiary treatment; Wastewater treatment.

### Dept. of Structural Engineering

### 882. Multiobjective Optimization Algorithm for Sewer Network Rehabilitation

Mohamed Marzouk and Magdy Omar

*Structure and Infrastructure Engineering*, 1-9 (2013) IF: 2.805

Understanding of deterioration mechanisms in sewers helps asset managers in developing prediction models for estimating whether or not sewer collapse is likely. Effective utilization of deterioration prediction models along with the development and use of life cycle maintenance cost analysis contribute to reducing operation and

aintenance costs in sewer systems. This paper presents a model for life-cycle maintenance planning of deteriorating sewer network as a multiobjective optimization problem that treats the sewer network condition and service life as well as life-cycle maintenance cost (LCMC) as separate objective functions. The developed model utilizes Markov chain model for the prediction of the deterioration of the network. A multi-objective genetic algorithm is used to automatically locate an appropriate maintenance scenario that exhibits an optimized tradeoff among conflicting objectives.

Monte Carlo simulation is used to account for LCMC uncertainties. The optimization algorithm provides an improved opportunity for asset managers to actively select near-optimum maintenance scenario that balances life-cycle maintenance cost, condition, and service life of deteriorating sewer network. A case study is used to demonstrate the practical features of developed methodology.

**Keywords:** Life cycle cost analysis; Markov chain model; Optimization; Rehabilitation; Sewer deterioration models.

### 883. Feasibility Study of Industrial Projects Using Simos Procedure

Mohamed Marzouk, Omar Amer and Moheeb El-Said

*Journal of Civil Engineering and Management*, 19 (1): 59-68 (2013) IF: 2.016

Feasibility study is conducted in a stage prior to design, procurement and construction stages in order to determine the viability of project undertaken by an investor. This helps investors to decide whether to proceed with the project or not. Multi-Criteria Decision Making (MCDM) process can be utilized in the feasibility study stage to avoid wrong decisions might cause undesired losses.

In industrial projects, wrong decisions might lead to bankruptcy of crucial economic entities. Private investors might have good initiative and the capital to establish economically successful projects but they might either select the inappropriate type of industry that might turn the investment to a failure or might not include some important/crucial considerations into account.

This paper presents a key-list of gathered factors that are considered the important factors and affect the selection of industrial projects. Importance, relative importance and weights of these factors are determined using Simos' procedure.

The key-list has been applied on five case-studies of industrial projects and a Weighted-Sum Model (WSM) has been selected as a MCDM technique in order to acquire their final preferences, rank them and consequently come-up with the most preferred/suitable alternative to be constructed. Then, a sensitivity analysis has been performed to determine the most critical criterion of the key-list. Additionally, several scenarios have been processed to verify that the most important criterion of the key-list does not necessarily be the most critical criterion. Moreover, the sensitivity analysis also determines the most critical measure of performance assembled from the five case-studies.

**Keywords:** Multi-criteria decision making; Feasibility study; Simos; Procedure; Weighted-sum model; Sensitivity analysis; Ranking techniques; Industrial projects.

#### 884. Planning of Tunneling Projects Using Computer Simulation and Fuzzy Decision Making

Moatassem Abdallah and Mohamed Marzouk

*Journal of Civil Engineering and Management*, 19 (4): 591-607 (2013) IF: 2.016

Tunnel construction is one of the important infrastructure projects, which is vital for enhancing the transportation networks, specially in congested cities.

Tunnel projects are characterized by long durations, large budgets, complexities, repetitive construction tasks, risks, and uncertainties. Several construction techniques have been developed in the tunnel construction industry to improve the constructability of tunnels and decrease the impact on surrounding structures. This paper presents a framework for planning tunnel construction using computer simulation. The proposed tool aids contractors in estimating the required time and cost for construction. Five tunnel construction techniques have been considered in the development of this tool with different ground supporting techniques. The proposed framework consists of three modules: (1) tunnel analyzer module, (2) simulation module, and (3) decision support module, and is capable of selecting the best construction technique using fuzzy group decision-making method based on time, cost and other selection criteria that could be defined during the decision-making phase. This decision method ranks alternatives based on a group of experts and a predefined set of criteria. Numerical examples are introduced to illustrate the capabilities of the proposed framework.

**Keywords:** Planning; Tunnel construction techniques; Computer simulation; Cost and scheduling; Fuzzy decision-making.

#### 885. Modeling Safety Considerations and Space Limitations in Piling Operations Using Agent Based Simulation

Mohamed Marzouk and Hossam Ali

*Expert Systems With Applications*, 40(12): 4848-4857 (2013) IF: 1.854

Site space availability is an aspect resource that must be taken into consideration when estimating the duration of construction operations. Site space availability has significant effect in meeting target schedule. This paper proposes a model for estimating the productivity of bored piles, taking into consideration safety requirements and space availability. Executing bored piles requires special equipment resources that require space to work and to move. The cost of equipment that is used in bored pile operations ranges from 25% to 30 % of the total cost. Therefore, it is deemed important to decide on the exact number of required equipment in piling operations. The proposed model utilizes Agent Based Simulation (ABS) to estimate bored pile productivity depending on the available resources (rig and crane equipment). The model captures the probabilities of equipment breakdowns based on equipment historical data. It also animates movements of equipment taking into consideration safety requirements. A case study is presented to demonstrate the practical features of the proposed ABS model.

**Keywords:** Agent based simulation; Piling operations; Safety considerations; Space limitations.

#### 886. A Coupled BEM-stiffness Matrix Approach for Analysis of Shear Deformable Plates on Elastic Half Space

Ahmed Mostafa Shaaban and Youssef F. Rashed

*Engineering Analysis With Boundary Elements*, 37(4): 699-707 (2013) IF: 1.596

In this paper, a new direct Boundary Element Method (BEM) is presented to solve plates on elastic half space (EHS). The considered BEM is based on the formulation of Vander Weeën for the shear deformable plate bending theory of Reissner. The considered EHS is the infinite EHS of Boussinesq–Mindlin or the finite EHS (with rigid end layer) of Steinbrenner. The multi-layered EHS is also considered. In the present formulation, the soil stiffness matrix is computed. Hence, this stiffness matrix is directly incorporated inside the developed BEM. Several numerical examples are considered and results are compared against previously published analytical and numerical methods to validate the present formulation.

**Keywords:** Boundary element method; Elastic half space; Plates; Stiffness matrix; Reissner plates.

#### 887. A Hybrid Model for Selecting Location of Mobile Cranes in Bridge Construction Projects

Mohamed Marzouk and Mohamed Hisham

*Baltic Journal of Road and Bridge Engineering*, 8 (3): 184-189 (2013) IF: 1.478

Mobile cranes are considered one of main equipment in bridge construction projects. Choosing the best locations for mobile cranes in bridge construction sites is an important task that must be done efficiently.

This paper presents a hybrid model that integrates Genetic Algorithms and Bridge Information Modeling to choose the best locations of mobile cranes in bridges construction sites, taking into account different constraints related to: safety, clearance, existing site conditions, construction schedule, and duration of erecting structural members. The proposed model is novel since it explores more features of Bridge Information Modeling such as decision making including location of mobile cranes and less boom maneuvers.

**Keywords:** Genetic algorithms (GAs); Building information modeling (BrIM); 3D Modeling; Construction equipment.

#### 888. Damping Identification Procedure for Linear Systems: Mixed Numerical-Experimental Approach

Hazem Hossam El-Anwar, Mohammed Hassanien Serror and Hesham Sobhy Sayed

*Earthquakes and Structures*, 4 (2): 203-217 (2013) IF: 1.381

In recent decades, it has been realized that increasing the lateral stiffness of structure subjected to lateral loads is not the only parameter enhancing safety or reducing damage. Factors such as ductility and damping govern the structural response due to lateral loads. Despite the significant contribution of damping in resisting lateral loads, especially at resonance, there is no accurate mathematical representation for it. The main objective of this study is to develop a damping identification procedure for linear

systems based on a mixed numerical-experimental approach, assuming viscous damping. The proposed procedure has been applied to a laboratory experiment associated with a numerical model, where a hollow rectangular steel cantilever column, having three lumped masses, has been fixed on a shaking table subjected to different exciting waves. The modal damping ratio has been identified; in addition, the effect of adding filling material to the hollow specimen has been studied in relation to damping enhancement. The results have revealed that the numerically computed response based on the identified damping is in a good fitting with the measured response. Moreover, the filling material has a significant effect in increasing the modal damping

**Keywords:** Damping identification; Linear system; Shaking table; Steel tube; Filling material.

### 889. A Methodology for Constitutive Relationships Estimation for SWNT Reinforced Composites

Ahmed M. Hussein and Youssef F. Rashed

*Engineering Computations International Journal for Computer-Aided Engineering and Software*, 30 (3): 409 -447 (2013)

IF: 1.214

**Purpose:** This paper computationally estimates the constitutive relationships of composite materials reinforced by single walled carbon nanotubes (SWNT). **Design/methodology/approach:** A multiscale analysis is considered. At the nanoscale level, molecular dynamics (MD) are used to predict the stiffness for an equivalent beam. A BEM solver for the elasticity problems is extended to allow the presence of inclusions and hence is used to model a RVE for the composite matrix with the equivalent nanotube beams. A genetic algorithm (GA) is developed to generate an initial population of anisotropic materials based on FEM. The GA evolves the population of properties of anisotropic materials till a material is found whose mechanical response is the same as that of the nanocomposite. **Findings:** The overall process is suitable for the constitutive relationships estimation according to the verification process outlined. **Research limitations/implications:** The present work is limited to 2D linear problems. However, extending it to 3D non-linear applications is straight forward.

**Practical implications:** The present technique could be used to estimate properties of NCT composites, hence practical applications such as aeroplane structures or turbine blades could be analysed using commercial finite element software. The present methodology could be used to estimate non-mechanical properties such as the thermal and electric properties.

**Originality/value:** The present computational technique has never been presented in the literature.

**Keywords:** Anisotropic; Boundary element; Composite materials; Matrix composite; Mechanical property.

### 890. Analytical Study for Deformability of Laminated Sheet Metal With Full Interfacial Bond

Mohammed Hassanien Serror and Junya Inoue

*Journal of Engineering Mechanics*, 139 (1): 94-103 (2013)

IF: 1.116

While a freestanding high-strength sheet metal subject to tension will rupture at a small strain, it is anticipated that lamination with

a ductile sheet metal will retard this instability to an extent that depends on the relative thickness, relative stiffness, and hardening exponent of the ductile sheet. This paper presents an analytical study for the deformability of such a laminate under tensile load within the context of necking instability. Laminates of high-strength sheet metal and ductile low-strength sheet metal are studied assuming (1) the sheets are fully bonded and (2) the metals obey the power-law material model. The effect of the hardening exponent, volume fraction, and relative stiffness of the ductile component has been studied. The stability of both uniform and nonuniform deformations has been investigated. The results have shown retardation of the high-strength layer instability by lamination with the ductile layer. The laminate exhibits marked enhancement in the strength-ductility combination, which is essential in metal-forming applications.

**Keywords:** Sheet metal laminate; Necking instability; Deformability; Power-law model.

### 891. A Variational Boundary Element formulation for Shear-deformable Plate Bending Problems

Taha H. A. Naga and Youssef F. Rashed

*Journal of Applied Mechanics*, 80 (5): (2013) IF: 1.041

This paper presents the derivation of a new boundary element formulation for plate bending problems. The Reissner's plate bending theory is employed. Unlike the conventional direct or indirect formulations, the proposed integral equation is based on minimizing the relevant energy functional. In doing so, variational methods are used.

A collocation based series, similar to the one used in the indirect discrete boundary element method (BEM), is used to remove domain integrals.

Hence, a fully boundary integral equation is formulated. The main advantage of the proposed formulation is production of a symmetric stiffness matrix similar to that obtained in the finite element method. Numerical examples are presented to demonstrate the accuracy and the validity of the proposed formulation.

**Keywords:** Boundary element method; Variational formulation; Shear-deformable plates; Stiffness matrix.

### 892. Selecting Sustainable Building Materials Using System Dynamics and Ant Colony Optimization

Mohamed Marzouk, Manal Abdelhamid and Mohamed Elsheikh

*Journal of Environmental Engineering and Landscape Management*, 21(4): 237-247 (2013) IF: 1.041

Selecting environmentally preferable building materials is one way to reduce the negative environmental impacts associated with the built environment. This paper proposes a framework that incorporates environmental and economic constraints while maximizing the number of credits reached under the Leadership in Energy and Environmental Design (LEED) rating system. The framework helps decision makers with the appropriate selection of conventional and green building materials. It consists of two modules: System Dynamics module and Ant Colony Optimization module. The paper describes the developments made in these two modules, where the selection of building materials is carried out based on LEED credits and costs. The proposed framework provides more credits when using

environmentally friendly materials. A case study of residential building is presented to demonstrate the main features of proposed framework.

**Keywords:** Materials selection; Environmental sustainability; Green building materials; LEED; System dynamics; Ant colony optimization.

### 893. Predicting Construction Materials Prices Using Fuzzy Logic and Neural Networks

Mohamed Marzouk and Ahmed Amin

*Journal of Construction Engineering and Management*, 139 (9): 1190-1198 (2013) IF: 0.876

Changes in construction materials' prices have a great impact on the cost of construction projects. Such changes in prices occur randomly at different rates over time. There is no clear relationship that can be used to provide accurate calculations of materials' prices. One of the biggest problems that face the construction contracts is unbalanced rights and obligations between owners and contractors (the two parties of construction contracts).

It is necessary to have a system that is capable to estimate the size and amount of the change in materials' prices at reasonable accuracy. There is also a need to predict the change in building materials' prices (either increase or decrease) during the execution phase of the project as well as during the preparation of tenders. Thus, determination of the appropriate lead time to order needed building materials to execute various activities could be done. This research presents a system that utilizes fuzzy logic to identify construction materials that are most sensitive to the change in prices.

The research proposes a methodology for identification of construction materials that are most sensitive to the change in prices to be used in modifying the contract price with an attempt to predict the amount of future change in materials prices using neural networks technique. to achieve this objective, the research classifies construction cost items into four different components (building materials, equipment, labor, and administrative expenses) which represent the basic cost elements of any cost item.

The system is based on the study of the changes in materials' prices that occurred in Egyptian market from 2000 to 2010. It also provides the impact on the prices of cost items in the priced bill of quantities (BOQ) which is determined by the change in prices of cost items' materials and their share percent on forming the cost item. Getting to identify materials' share in the bill of quantities' items has a great influence on the price of the cost item and the priority in ordering these materials according to their impact on item's price.

The developed system aids construction contractors in studying bids during tendering stage and procurement planning during project's execution. It can also be used by owners' representatives to estimate the expected total cost of upcoming projects. The system data is obtained from the Central Agency for Public Mobilization and Statistics in Egypt through published periodicals. A numerical example is presented to demonstrate the use of the proposed system.

**Keywords:** Cost estimating; Construction materials prices; Fuzzy logic; Neural networks; Quantitative methods.

### 894. Evaluating Codes Criteria for Regular Seismic Behavior of Continuous Concrete Box Girder bridges With Unequal Height Piers

J. E. B. Guirguis and S. S. F. Mehanny

*Asce Journal of Bridge Engineering*, 18(6): 486-498 (2013) IF: 0.793

The seismic design and response prediction of irregular bridges supported on piers of unequal heights—a commonly adopted solution when crossing steep-sided valleys—represent a particularly challenging problem that is yet to be effectively addressed by seismic design code provisions worldwide. From a force-based design perspective, shorter piers are subjected to increased ductility demand, and consequently damage tends to localize in these relatively stiff piers at increasing seismic hazard levels. This paper presents an investigation of the seismic response of a few schemes of a three-span case-study continuous bridge (commonly encountered in practice), featuring two unequal piers with relative heights of 0.5, 0.64, 0.75, and 0.86, respectively. Static pushover and time history (under incrementally scaled-up actual records) nonlinear inelastic analyses are performed using OpenSees to check the validity of Eurocode 8 (EC8) and recently proposed AASHTO-LRFD provisions for regular seismic behavior of ductile bridges dimensioned per a force-based design procedure. It has been demonstrated that satisfying the EC8 regularity condition does not necessarily result in a near-simultaneous failure of unequal piers at the extreme hazard level, especially for a low ratio between pier heights ( $\leq 0.5$ ).

It has been further concluded that regularity criteria in both provisions fall short of providing the absolute regular seismic behavior of the bridge under investigation. Finally, a new design criterion is introduced (and verified) herein and is promoted for bridges with unequal height piers but with the same cross-section dimensions as may be typically dictated by some compelling aesthetical and practical considerations. However, it is worth mentioning that pier behavior (and, hence, failure) is assumed to be governed by flexure, and no shear failure and buckling are considered.

**Keywords:** EC8; AASHTO-LRFD; Regular seismic behavior; Ductile bridges; Unequal height Piers.

### 895. Computer-aided Assessment of Progressive Collapse of Reinforced Concrete Structures According to GSA Code

Huda Helmy, Hamed Salem and Sherif Mourad

*Journal of Performance of Constructed Facilities*, 27 (5): 529-539 (2013) IF: 0.571

A building is subjected to progressive collapse when a primary vertical structural element fails resulting in failure of adjoining structural elements which, in their turn, cause further structural failure leading eventually to partial or total collapse of the structure. The failure of a primary vertical support might occur due to extreme loadings such as a bomb explosion in a terrorist attack, a car colliding with supports in parking garage, an accidental explosion of explosive materials and severe earthquake. Different design codes address the progressive collapse of structures due to the sudden loss of a main vertical



support such as the General Services Administration (GSA) and the Unified Facilities Criteria (UFC). Alternative Path Method (APM) is the main analysis method for evaluating the hazard of progressive collapse in the two codes. The (APM) requires that the structure be capable of bridging over a missing structural element, with the resulting extent of damage being localized. In the current study, a progressive collapse assessment according to the GSA code is carried out for a typical ten-story reinforced concrete framed structure. The structure is designed according to the building code requirements for structural concrete (ACI 318-08). Fully nonlinear dynamic analysis for the structure is carried out using the Applied Element Method (AEM). According to the GSA code, a primary vertical structural element is removed and the collapse area is investigated. The investigated cases include the removal of a corner column, an edge column, an edge shear wall, internal columns, internal shear wall and a corner shear wall. The numerical analysis showed that for an economic design, the analysis should consider slabs and can't be simplified into a 2D or 3D frame analysis. Neglecting the slabs in the progressive collapse analysis is a very conservative approach which may lead to uneconomic design. Reinforced concrete structures designed according to the ACI 318-08 met the GSA limits and were found to have a low potential for progressive collapse.

**Keywords:** Progressive collapse; ELS; AEM; Slabs; Collapsed area; Rotation limits.

### 896. Quantifying Weather Impact on formwork Shuttering and Removal Operation Using System Dynamics

Mohamed Marzouk and Ahmed Hamdy

*KSCE Journal of Civil Engineering*, 17(4): 620-626 (2013)  
IF: 0.383

Weather condition is a significant factor that influences the activities of construction projects. This paper presents a framework that forecasts the losses on productivity due to the impact of weather conditions. The framework consists of three components; historical records database, analytical fuzzy model, and system dynamic model. The productivity of formwork shuttering and removal is directly impacted by two weather aspects; level of rain and temperature degree. The loss in productivity is modeled via analytical fuzzy model and system dynamic model. The proposed framework incorporates historical weather records, expert experiences, and fuzzy-set techniques in productivity losses forecasting. It provides more realistic forecast for productivity losses considering the impact of rain and temperature rises. Construction contractors benefit from the framework by assigning appropriate crew size for formwork shuttering and removal to meet project requirements with respect to total duration of project execution. A numerical example is presented to demonstrate the use of the proposed framework.

**Keywords:** System dynamics; Weather conduction; Fuzzy modeling; Formwork shuttering; Removal.

### 897. Highlights of the Design and Construction of a 12 Km Elevated APM Bridge Project in Saudi Arabia

Essam Ayoub, Charles Malek and Gamal Helmy

*Structural Concrete*, 14 (3): 250-259 (2013) IF: 0.289

The automated people mover (APM) bridge project constructed at Princess Nora University (PNU) in Saudi Arabia and inaugurated in May 2012 is a major project with many challenges in design and construction due to its strict time-frame compared with the big scale of the project. Therefore, the design had to be such that it ensured simplicity, time-savings, lowest costs, aesthetics and the high quality required for bridge project elements. For aesthetic reasons, a box section was chosen for all the APM bridge sections for the bridge project, including straight, bifurcation and curved parts. This paper highlights the efficiency of the precast concrete techniques used in the design and construction of big projects such as this elevated APM bridge project at PNU in Saudi Arabia.

**Keywords:** Precast construction; Bridges; Prestressing; Stress analysis; Unsymmetrical beam; Box girder; Curved structure.

### 898. A Simulation Based Decision tool for Transportation of Ready Mixed Concrete

Mohamed Marzouk and Ahmed Younes

*International Journal of Architecture, Engineering and Construction*, 2 (4): 234-245 (2013)

This paper presents a simulation tool which is applied to ready mixed concrete operations to analyze the utilization and assignment of production and transportation resources. In the developed simulation model, concrete pouring activities are classified into seven main types according to the type of pouring machine and the degree of difficulty of poured structure element. Productivity-unit cost charts are generated to aid in decision making process by processing different generated outputs, including productivity rates, resources' utilization, unit cost of poured concrete, and system performance measurements. The productivity unit cost charts are used to determine production time, production cost, and resources combinations for a specified distance from a plant. Whereas, the unit cost contours' charts are used to determine the range of best alternative solutions to minimize production time and cost of the available plant resources, according to the transportation distance. A numerical example is presented to demonstrate the developed model and illustrate its essential features. The output results are compared against site orders and the sensitivity analysis tables.

**Keywords:** Ready mixed concrete; Discrete event simulation; Productivity-unit cost charts; Decision index technique; Sensitivity analysis.

### 899. Alternate Path Method Analysis of RC Structures Using Applied Element Method

Islam Hafez, Ahmed Khalil and Sherif Mourad

*International Journal of Protective Structures*, 4 (1): 45-64 (2013)

Recent research using the Applied Element Method (AEM) shows that the method is efficient in modeling progressive collapse analysis of structures. Recent research on progressive collapse design of structures based on the UFC code shows it can be used in optimizing the design for structures for which the alternate path method is required. This paper demonstrates the efficiency of the use of AEM in progressive collapse analysis of reinforced concrete structures by comparison to results of published experimental tests. A case study based on a typical seven-story

reinforced concrete frame commercial building is used to demonstrate the advantages of using the alternate path method in progressive collapse design of concrete structures even for the cases where the code permits the use of the tie force method. The contribution of infill walls in resisting progressive collapse is also studied.

**Keywords:** Progressive collapse analysis; Applied element method; Alternate load path; Design optimization; Unified facilities criteria; Reinforced concrete structures; Infill walls.

### 900. Factors Influencing Sub-contractors Selection in Construction Projects

Mohamed M. Marzouk Ahmed A. El Kherbawy and Mostafa Khalifa

*Housing and Building National Research Center (HBRC) Journal, 9 (2): 150-158 (2013)*

Selection of best sub-contractor is a vital process in construction projects. There are many factors that must be taken into consideration when selecting sub-contractors. Improper selection of sub-contractors might lead to many problems during work progress. These include bad quality of work, and delay in project duration. This process is controlled by many factors. Forty six factors are collected from previous studies that influence sub-contractor selection. This paper identifies the most important factors that influence the selection of sub-contractors. A questionnaire was distributed to experts in the construction domain to determine the importance of factors that are taken into consideration by the main contractor to select the most suitable sub-contractor. A survey was carried out which was conducted with twenty nine experts in construction field to determine the score of each factor. Statistical analysis is carried out on the feedback of the respondents of the survey. By using SPSS software, the frequency of the results of the questionnaire was determined. Examples of crosstabs between some of the most important factors are presented to provide comparison between two factors. The mean score of each factor and calculating the p-value by using SPSS software, the significance of each factor used in the questionnaire is determined. Any factor that has a p-value less than 0.05 is considered a significant one.

**Keywords:** Sub-contractors selection; Construction management; Questionnaire surveys.

### 901. Measuring Sensitivity of Procurement Decisions Using Superiority and Inferiority Ranking

Mohamed Marzouk, Noha El Shinnawy, Osama Moselhi and Moheeb El-Said

*International Journal of Information Technology and Decision Making, 12(3): 395-423 (2013)*

Wrong decisions or inappropriate selection of equipment may lead to increase in cost and reduction in efficiency and effectiveness. Selecting right equipment has always been a key factor in the success of the process it is used for. In this study, Analytical Hierarchy Process (AHP) and the Superiority and Inferiority Ranking (SIR) methods are utilized for evaluation of most suitable offer for procurement of equipment installed inside a facility. to achieve this target, a methodological framework of a series of interviews are conducted, then two questionnaire surveys

are developed for identifying the important factors affecting the selection process of equipment and determining their relative importance. A solution of the problem is then designed in a model using AHP and SIR methods in addition to using the Simple Additive Weighting (SAW) and Technique for Order Preference by Similarity to the Ideal Solution (TOPSIS) procedures to generate the superiority and inferiority flows. The model is generic and flexible and is used for the application of the MCDM methods in the procurement process. The model also offers an efficient and convenient tool that aids its users to act in an orderly and methodical thinking, and guides them in making logical and robust decisions. A case study is presented to demonstrate the use of the developed model and sensitivity analysis is carried out to measure the robustness of the model in different scenarios.

**Keywords:** Multiple criteria decision making; Procurement; Facility-fitted equipment; Analytical hierarchy Process; Superiority and Inferiority ranking method; Sensitivity analysis.

### Dept. of Bioengineering & medical System

### 902. Noninvasive Detection of Lipids in Atherosclerotic Plaque Using Ultrasound Thermal Strain Imaging in Vivo Animal Study

Ahmed M. Mahmoud, Debaditya Dutta, Linda Lavery, Douglas N. Stephens, Flordeliza S. Villanueva and Kang Kim

*Journal of the American College of Cardiology, 62 (19): 1804-1809 (2013) IF: 14.086*

**Objectives:** This study sought to examine the feasibility of in vivo detection of lipids in atherosclerotic plaque (AP) by ultrasound (US) thermal (or temporal) strain imaging (TSI).

**Background:** Intraplaque lipid content is thought to contribute to plaque stability. Lipid exhibits a distinctive physical characteristic of temperature-dependent US speed compared with water-bearing tissues. As tissue temperature changes, US radiofrequency (RF) echoes shift in time of flight, which produces an apparent strain (thermal or temporal strain [TS]).

**Methods:** US heating-imaging pulse sequences and transducers were designed and integrated into commercial US scanners for US-TSI of arterial segments. US-RF data were collected while gradually increasing tissue temperature. Phase-sensitive speckle tracking was applied to reconstruct TS maps coregistered to B-scans. Segments from injured atherosclerotic and uninjured nonatherosclerotic common femoral arteries (CFA) in cholesterol-fed New Zealand rabbits, and segments from control normal diet-fed rabbits (N =14) were scanned in vivo at different time points up to 12 weeks.

**Results:** Lipid-rich atherosclerotic lesions exhibited distinct positive TS ( $+0.19 \pm 0.08\%$ ) compared with that in nonatherosclerotic ( $-0.10 \pm 0.13\%$ ) and control ( $-0.09 \pm 0.09\%$ ) segments ( $p < 0.001$ ). US-TSI enabled serial monitoring of lipids during atherosclerosis development. The coregistered set of morphological and compositional information of US-TSI showed good agreement with histology.

**Conclusions:** US-TSI successfully detected and longitudinally monitored lipid progression in atherosclerotic CFA. US-TSI of relatively superficial arteries may be a modality that could be integrated into a commercial US system for noninvasive lipid detection in AP.

**Keywords:** Ultrasound; Thermal strain imaging; Atherosclerosis.

### 903. Segmentation of Choroidal Neovascularization in Fundus Fluorescein Angiograms

Walid M. Abdelmoula, Syed M. Shah and Ahmed S. Fahmy

*IEEE Transactions on Biomedical Engineering*, 60 (5): 1439-1445 (2013) IF: 2.348

Choroidal neovascularization (CNV) is a common manifestation of age-related macular degeneration (AMD). It is characterized by the growth of abnormal blood vessels in the choroidal layer causing blurring and deterioration of the vision. In late stages, these abnormal vessels can rupture the retinal layers causing complete loss of vision at the affected regions. Determining the CNV size and type in fluorescein angiograms is required for proper treatment and prognosis of the disease. Computer-aided methods for CNV segmentation is needed not only to reduce the burden of manual segmentation but also to reduce inter- and intraobserver variability. In this paper, we present a framework for segmenting CNV lesions based on parametric modeling of the intensity variation in fundus fluorescein angiograms. First, a novel model is proposed to describe the temporal intensity variation at each pixel in image sequences acquired by fluorescein angiography. The set of model parameters at each pixel are used to segment the image into regions of homogeneous parameters. Preliminary results on datasets from 21 patients with Wet-AMD show the potential of the method to segment CNV lesions in close agreement with the manual segmentation.

**Keywords:** Choroidal neovascularization; Fluorescein angiograms; Modeling; Segmentation; Temporal intensity variation.

### 904. High-Resolution Vascular Tissue Characterization in Mice Using 55 MHz Ultrasound Hybrid Imaging

Ahmed M. Mahmoud, Cesar Sandoval, Bunyen Teng, Jorgen B. Schnermann, Karen H. Martin, S. Jamal Mustafa and Osama M. Mukdadi

*Ultrasonics*, 53: 727-738 (2013) IF: 2.028

Ultrasound and Duplex ultrasonography in particular are routinely used to diagnose cardiovascular disease (CVD), which is the leading cause of morbidity and mortality worldwide. However, these techniques may not be able to characterize vascular tissue compositional changes due to CVD.

This work describes an ultrasound-based hybrid imaging technique that can be used for vascular tissue characterization and the diagnosis of atherosclerosis. Ultrasound radiofrequency (RF) data were acquired and processed in time, frequency, and wavelet domains to extract six parameters including time integrated backscatter ( $T_{IB}$ ), time variance ( $T_{var}$ ), time entropy ( $T_E$ ), frequency integrated backscatter ( $F_{IB}$ ), wavelet root mean square value ( $W_{rms}$ ), and wavelet integrated backscatter ( $W_{IB}$ ). Each parameter was used to reconstruct an image co-registered to morphological B-scan.

The combined set of hybrid images were used to characterize vascular tissue in vitro and in vivo using three mouse models including control (C57BL/6), and atherosclerotic apolipoprotein E-knockout (APOE-KO) and APOE/A1 adenosine receptor double knockout (DKO) mice. The technique was tested using high-frequency ultrasound including single-element (center frequency = 55 MHz) and commercial array (center frequency =

40 MHz) systems providing superior spatial resolutions of 24  $\mu$ m and 40  $\mu$ m, respectively. Atherosclerotic vascular lesions in the APOE-KO mouse exhibited the highest values (contrast) of  $-10.11 \pm 1.92$  dB,  $-12.13 \pm 2.13$  dB,  $-7.54 \pm 1.45$  dB,  $-5.10 \pm 1.06$  dB,  $-5.25 \pm 0.94$  dB, and  $-10.23 \pm 2.12$  dB in  $T_{IB}$ ,  $T_{var}$ ,  $T_E$ ,  $F_{IB}$ ,  $W_{rms}$ ,  $W_{IB}$  hybrid images ( $n = 10$ ,  $p < 0.05$ ), respectively. Control segments of normal vascular tissue showed the lowest values of  $-20.20 \pm 2.71$  dB,  $-22.54 \pm 4.54$  dB,  $-14.94 \pm 2.05$  dB,  $-9.64 \pm 1.34$  dB,  $-10.20 \pm 1.27$  dB, and  $-19.36 \pm 3.24$  dB in same hybrid images ( $n = 6$ ,  $p < 0.05$ ). Results from both histology and optical images showed good agreement with ultrasound findings within a maximum error of 3.6% in lesion estimation. This study demonstrated the feasibility of a high-resolution hybrid imaging technique to diagnose atherosclerosis and characterize plaque components in mouse. In the future, it can be easily implemented on commercial ultrasound systems and eventually translated into clinics as a screening tool for atherosclerosis and the assessment of vulnerable plaques.

**Keywords:** High resolution ultrasound; Tissue characterization; Atherosclerosis; Signal; Image processing.

### 905. A Pilot Study to Assess the Effectiveness of Orthotic Insoles on the Reduction of Plantar Soft Tissue Strain

Musab Ibrahim, Rana El Hilaly, Mona Taher and Ahmed Morsy

*Clinical Biomechanics*, 28: 68-72 (2013) IF: 1.869

**Background:** Plantar ulcers pose a frequent serious complication in the neuropathic foot. Previous studies suggested that ulcer initiation occurs within the plantar soft tissue rather than on the plantar surface. This study investigated the effectiveness of different shaped silicone insoles on the reduction of both plantar soft tissue strain and ressure. The authors have found no previous experimental studies on the effectiveness of insole shape on reducing plantar soft tissue strain during standing.

**Methods:** A custom molded silicone insole which allowed passage of ultrasound to the plantar surface of the foot was prototyped for this study. Soft tissue strain was computed from soft tissue thickness measured using ultrasound in five conditions: unloaded, barefoot, wearing a prefabricated silicone insole, wearing the custom molded silicone insole alone then with a metatarsal pad. Plantar pressure was measured for the same conditions.

**Findings:** The custom molded insole was found to significantly reduce soft tissue strain and plantar pressure relative to both the barefoot condition and the prefabricated insole under the second and third metatarsal heads. The metatarsal pad was found to significantly reduce soft tissue strain but not significantly affect plantar pressure.

**Interpretation:** A custom molded silicone insole can effectively reduce both soft tissue strain and plantar pressure and is thus preferable to a prefabricated insole. It is suggested that quantifying the reduction of soft tissue strain is an essential design requirement for orthotic insoles since plantar pressure may not be a sufficient indicator of the effectiveness of an insole in preventing ulcer initiation.

**Keywords:** Plantar soft tissue strain; Custom molded insole; Plantar ulceration; Ultrasound.

### 906. The Estimation of the instantaneous Amplitudes of Sum of Sinusoids With Unknown Frequency and Phases: the Martingale Approach

A. Abutaleb

*Signal Processing*, 93: 811-817 (2013) IF: 1.851

The martingale optimality principle is used to estimate the positive time-varying amplitudes that appear in the sum of sinusoids models. A closed form expression is obtained for the estimates of the time-varying amplitudes. These estimates are then embedded into the observation equation and nonlinear optimization methods are used to find the unknown frequencies. Given are examples and comparisons to existing methods.

**Keywords:** Ito calculus; Martingales; Time-varying parameters; Time-series analysis; Estimation.

### 907. Flexible Integration of High-Imaging-Resolution and High-Power Arrays for Ultrasound-Induced Thermal Strain Imaging (US-TSI)

Douglas N. Stephens, Ahmed M. Mahmoud, Xuan Ding, Steven Lucero, Debaditya Dutta, Francois T. H. Yu, Xucai Chen and Kang Kim

*IEEE Transactions on Ultrasonics, Ferroelectrics, and Frequency Control*, 60 (12): 2645-2656 (2013) IF: 1.822

Ultrasound-induced thermal strain imaging (USTSI) for carotid artery plaque detection requires both high imaging resolution ( $<100\ \mu\text{m}$ ) and sufficient US-induced heating to elevate the tissue temperature ( $\sim 1^\circ\text{C}$  to  $3^\circ\text{C}$  within 1 to 3 cardiac cycles) to produce a noticeable change in sound speed in the targeted tissues. Because the optimization of both imaging and heating in a monolithic array design is particularly expensive and inflexible, a new integrated approach is presented which utilizes independent ultrasound arrays to meet the requirements for this particular application. This work demonstrates a new approach in dual-array construction. A 3-D printed manifold was built to support both a high-resolution 20 MHz commercial imaging array and 6 custom heating elements operating in the 3.5 to 4 MHz range. for the application of US-TSI in carotid plaque characterization, the tissue target site is 20 to 30 mm deep, with a typical target volume of 2 mm (elevation)  $\times$  8 mm (azimuthal)  $\times$  5 mm (depth). The custom heating array performance was fully characterized for two design variants (flat and spherical apertures), and can easily deliver 30 W of total acoustic power to produce intensities greater than  $15\ \text{W}/\text{cm}^2$  in the tissue target region.

**Keywords:** Thermal strain imaging; Ultrasound dual-array construction; High imaging resolution.

### 908. Motion Artifact Reduction in Ultrasound Based Thermal Strain Imaging of Atherosclerotic Plaques Using Time-series Analysis

Debaditya Dutta, Ahmed M. Mahmoud, Steven A. Leers and Kang Kim

*IEEE Transactions on Ultrasonics, Ferroelectrics, and Frequency Control*, 60 (8): 1660-1668 (2013) IF: 1.822

Large lipid pools in vulnerable plaques, in principle, can be detected using ultrasound-based thermal strain imaging (US-TSI).

One practical challenge for in vivo cardiovascular application of US-TSI is that the thermal strain is masked by the mechanical strain caused by cardiac pulsation. Electrocardiography (ECG) gating is a widely adopted method for cardiac motion compensation, but it is often susceptible to electrical and physiological noise. In this paper, we present an alternative time-series analysis approach to separate thermal strain from the mechanical strain without using ECG. The performance and feasibility of the time-series analysis technique was tested via numerical simulation as well as in vitro water tank experiments, using a vessel-mimicking phantom and an excised human atherosclerotic artery, for which the cardiac pulsation is simulated by a pulsatile pump.

**Keywords:** Thermal strain; Time series analysis.

### 909. Myocardium Segmentation in Strain-Encoded (SENC) Magnetic Resonance Images Using Graph-Cuts

Ahmed O. Al-Agamy, Nael F. Osman and Ahmed S. Fahmy

*Int Image Processing*, 7 (5): 415-422 (2013) IF: 0.895

Evaluation of cardiac functions using Strain Encoded (SENC) magnetic resonance (MR) imaging is a powerful tool for imaging the deformation of left and right ventricles. However, automated analysis of SENC images is hindered due to the low signal-to-noise ratio SENC images. In this work, the authors propose a method to segment the left and right ventricles myocardium simultaneously in SENC-MR short-axis images. In addition, myocardium seed points are automatically selected using skeletonisation algorithm and used as hard constraints for the graph-cut optimization algorithm. The method is based on a modified formulation of the graph-cuts energy term. In the new formulation, a signal probabilistic model is used, rather than the image histogram, to capture the characteristics of the blood and tissue signals and include it in the cost function of the graph-cuts algorithm. The method is applied to SENC datasets for 11 human subjects (five normal and six patients with known myocardial wall motion abnormality). The segmentation results of the proposed method are compared with those resulting from both manual segmentation and the conventional histogram-based graph-cuts segmentation algorithm. The results show that the proposed method outperforms the histogram-based graph-cuts algorithm especially to segment the thin structure of the right ventricle.

**Keywords:** Cardiology; Optimisation; Medical image processing; Probability; Image segmentation; MRI.

### 910. Clutter Rejection for Doppler Ultrasound Based on Blind Source Separation

Sulieman M. S. Zobly and Yasser M. Kadah

*Journal of Medical Imaging and Health Informatics*, 3 (2): 1-8 (2013) IF: 0.642

Doppler ultrasound is widely used diagnostic tool for measuring and detecting blood flow. to get a Doppler ultrasound spectrum image with a good quality, the clutter signals generated from stationary and slowly moving tissue must be removed completely. Without enough clutter rejection, low velocity blood flow cannot

be measured, and estimates of higher velocities will have a large bias.

In most cases it is very difficult to achieve a complete suppression without affecting the Doppler signal. Usually finite impulse response FIR, infinite impulse response IIR and polynomial regression PR filters were used for cluttering. In this paper we proposed a new method for clutter rejection in Doppler ultrasound to subtract all the clutter so as to achieve more accurate flow estimation. We proposed a new clutter rejection based on blind source separation using principal component analysis (PCA) and independent component analysis (ICA) methods.

The proposed clutter was implanted to reduce the clutter originated from moving structure and backscattered flow, beside FIR, IIR and PR. The proposed clutter rejection method presentation is quantified in simulated FR Doppler data beside real Doppler data (heart data). The result shows that the proposed method gives better clutter rejection over other present types of clutters.

**Keywords:** Blood flow; Clutter rejection filter; Doppler ultrasound signal; Independent component analysis; Principal component analysis; Spectrum.

#### 911. A Hybrid Feature Selection Approach of Ensemble Multiple Filter Methods and Wrapper Method for Improving the Classification Accuracy of Microarray Data Set

Ahmed Sofi Abutaleb, Ahmed Hassan, Osama Abdo Mohamed and Amr Hassan

*International Journal of Computer Science and Information Technology and Security*, 3 (2): 185-190 (2013)

Classification is one of the important tasks in bioinformatics. This can be obviously seen in cancer classification which is recently addressed by many researchers specially after emerging of microarrays.

This technology opens the way for computer researchers to classify cancer samples without any previous biological knowledge. Microarrays data is facing a critical challenge because of the nature of high-dimensional and small sample size this problem forces scientists to design gene selection techniques as a preceding step to the implemented classifier. Feature selection is the assignment of selecting a small subset from original features that can perform maximum classification accuracy. This subset of features has some very important benefits such as; it reduces computational complexity of learning algorithms, improves accuracy and save time. In this paper we propose a hybrid feature selection techniques that performed in two phases.

In the first phase we use ensemble filter method to ranking all genes and select top genes. This phase helps in improving the classification performance by removing redundant and unimportant features. In the second phase we used SVM-RFE (Recursive Feature Elimination) is a wrapper method. We evaluated our technique on three data sets of gene expression profiles; the Leukemia, the Lung and the Breast cancer; using six classifiers, which are Naïve Bayes (NB), Random Forest (RF), Decision Trees (C4.5), Support Vector Machines (SVM), K-Nearest Neighbor (KNN) and Logistic Regression (LR) and show the potentiality of the proposed method with the advantage of improving the classification performance.

**Keywords:** Feature selection; Filter; Wrapper; SVM-RFE (recursive feature elimination); SVM (support vector machines), RF (random forest); NB (naïve bayes); C4.5 (decision trees); KNN (k-nearest neighbor); Microarrays; Logistic regression (LR); AUC (area under receiver operating characteristic curve); Bioinformatics; Classification; Data mining; Gene selection.

#### 912. Hybridizing Filters and Wrapper Approaches for Improving the Classification Accuracy of Microarray Dataset

Ahmed Soufi Abou-Taleb, Ahmed Ahmed Mohamed, Osama Abdo Mohamed and Amr Hassan Abdelhalim

*International Journal of Soft Computing and Engineering (IJSCE)*, 3 (3): 155-159 (2013)

Feature selection aims at finding the most relevant features of a problem domain. However, identification of useful features from hundreds or even thousands of related features is a nontrivial task. This paper is aimed at identifying a small set of genes, to improving computational speed and prediction accuracy; hence we have proposed a three-stage of gene selection algorithm for microarray data.

The proposed approach combines information gain (IG), Significance Analysis for Microarrays (SAM), mRMR (Minimum Redundancy Maximum Relevance) and Support Vector Machine Recursive Feature Elimination (SVM-RFE). In the first stage, intersection part of feature sets is identified by applying the (SAM-IG). While, the second minimizes the redundancy with the help of mRMR method, which facilitates the selection of effectual gene subset from intersection part that recommended from the first stage. In the third stage, (SVM-RFE) is applied to choose the most discriminating genes. We evaluated our technique on AML and ALL (leukemia) dataset using Support Vector Machines (SVM- RBF) classifier, and show the potentiality of the proposed method with the advantage of improving the classification performance.

**Keywords:** Feature selection; Filters; Wrappers; Support vector machine; Microarray.

#### Faculty of Computers and Information Dept. of Information Technology (IT)

#### 913. A Physical-layer Location Privacy-preserving Scheme for Mobile Public Hotspots in NEMO-based VANETs

Sanaa Mohamed Taha and Xuemin Shen

*IEEE Transactions on Intelligent Transportation System*, 14 (4): 1665-1680 (2013) IF: 3.064

A network mobility (NEMO)-based vehicular ad hoc network (VANET) is a new approach to integrate the NEMO protocol with VANETs. This integration supports communications between roadside units (RSUs) and vehicles and provides Internet access through public hotspots located inside public transportation systems, such as buses, trains, and shuttles. Passengers inside these public transportation systems enjoy full Internet access by using different mobile network nodes (MNNs), such as cell phones and personal digital assistants. However, due to the open



nature of wireless network environments, physical-layer attackers can easily localize the MNNs by measuring their received signal strength (RSS) through positioning schemes such as the triangulation scheme. In this paper, we modify obfuscation, i.e., concealment, and power variability ideas and propose a new physical-layer location privacy scheme, i.e., the fake point-cluster-based scheme, to prevent attackers from localizing users inside NEMO-based VANET hotspots. The proposed scheme involves fake-point- and cluster-based subschemes, and its goal is to confuse the attackers by increasing the estimation errors of their RSSs measurements and, hence, preserving MNNs' location privacy.

Using correctness, accuracy, and certainty metrics, we show that the fake point-cluster-based scheme achieves higher MNN's location privacy when the number of network grid points in the hotspot decreases. In addition, our extensive simulations show that the fake point-cluster-based scheme achieves 23% and 37% decreases in the average sender's power and the MNN-AP route path length, respectively, compared with the fake-point subscheme.

**Keywords:** Network mobility (NEMO); Based vanet; Nemo security; Physical-layer location privacy; Physical-layer.

#### 914. A Multi-hop Authentication Proxy Mobile IP Scheme for Asymmetric VANETs

Sanaa Mohamed Taha, Cespedes, S. and Xuemin Shen

*IEEE Transactions on Vehicular Technology*, 62 (7): 3271-3286 (2013) IF: 2.063

Vehicular communications networks are envisioned for the access to drive-thru Internet and IP-based infotainment applications. These services are supported by roadside access routers (ARs) that connect vehicular ad hoc networks (VANETs) to external IP networks. However, VANETs suffer from asymmetric links due to variable transmission ranges caused by mobility, obstacles, and dissimilar transmission power, which make it difficult to maintain the bidirectional connections and to provide the IP mobility required by most IP applications. Moreover, vehicular mobility results in short-lived connections to the AR, affecting the availability of IP services in VANETs. In this paper, we study the secure and timely handover of IP services in an asymmetric VANET and propose a multihop-authenticated Proxy Mobile IP (MA-PMIP) scheme. MA-PMIP provides an enhanced IP mobility scheme over infrastructure-to-vehicle-to-vehicle (I2V2V) communications that uses location and road traffic information. The MA-PMIP also reacts, depending on the bidirectionality of links, to improve availability of IP services. Moreover, our scheme ensures that the handover signaling is authenticated when V2V paths are employed to reach the infrastructure so that possible attacks are mitigated without affecting the performance of the ongoing sessions. Both analysis and extensive simulations in OMNeT++ are conducted, and the results demonstrate that the MA-PMIP improves service availability and provides secure seamless access to IP applications in asymmetric VANETs.

**Keywords:** Asymmetric links; Infrastructure-to-Vehicle-To Vehicle (I2V2V); Ip Mobility; Multihop Networks; Mutual Authentication Proxy Mobile Ip (PMIP); Vehicular Ad Hoc Network.

#### 915. Extraction and Application of Deformation-Based Feature in Medical Images

Kai Xiao, A. Lei Liang, Hai Bing Guan and Aboul El Hassanien

*Neurocomputing*, 120: 177-184 (2013) IF: 1.811

One of the most challenging issues that hinder the development of accurate medical image segmentation system is the insufficiency of features which are relevant to actual anatomical meaning from the images. Although deformation of normal structures caused by compression from abnormal structures has usually been considered as undesired or even a problem to be tackled in medical image segmentation tasks, it is actually relevant to the correlation between normal and pathological structures. With the objective of investigating the feasibility of extracting and applying deformation-based features of such type, we propose an approach to estimate feature from the correlation between brain lateral ventricular (LaV) deformation and tumor and apply the extracted feature for computerized magnetic resonance (MR) image tumor segmentation. Experimental results on feature extraction show the relevancy between LaV deformation and location of tumor; comparative experiments on tumor segmentation suggest that, in most cases, tumor segmentation accuracy improves when the extracted feature is applied

**Keywords:** Feature extraction; Deformation; Pattern recognition; Segmentation; Medical image; MRI.

#### 916. Computational Intelligence Techniques in Bioinformatics

Aboul Ella Hassanien, Eiman Tamah Al-Shammari and Neveen I. Ghali,

*Computational Biology and Chem.*, 47: 37-47 (2013) IF: 1.793

Computational intelligence (CI) is a well-established paradigm with current systems having many of the characteristics of biological computers and capable of performing a variety of tasks that are difficult to do using conventional techniques. It is a methodology involving adaptive mechanisms and/or an ability to learn that facilitate intelligent behavior in complex and changing environments, such that the system is perceived to possess one or more attributes of reason, such as generalization, discovery, association and abstraction. The objective of this article is to present to the CI and bioinformatics research communities some of the state-of-the-art in CI applications to bioinformatics and motivate research in new trend-setting directions. In this article, we present an overview of the CI techniques in bioinformatics. We will show how CI techniques including neural networks, restricted Boltzmann machine, deep belief network, fuzzy logic, rough sets, evolutionary algorithms (EA), genetic algorithms (GA), swarm intelligence, artificial immune systems and support vector machines, could be successfully employed to tackle various problems such as gene expression clustering and classification, protein sequence classification, gene selection, DNA fragment assembly, multiple sequence alignment, and protein function prediction and its structure. We discuss some representative methods to provide inspiring examples to illustrate how CI can be utilized to address these problems and how bioinformatics data can be characterized by CI. Challenges to be addressed and future directions of research are also presented and an extensive bibliography is included.

**Keywords:** Bioinformatics; Computational intelligence.

### 917. Fuzzy and Hard Clustering Analysis for Thyroid Disease

Ahmad Taher Azar, Shaimaa Ahmed El-Said and Aboul Ella Hassanien

*Computer Methods and Programs in Biomedicine*, 111(1): 1-16 (2013) IF: 1.555

Thyroid hormones produced by the thyroid gland help regulation of the body's metabolism. A variety of methods have been proposed in the literature for thyroid disease classification. As far as we know, clustering techniques have not been used in thyroid diseases data set so far.

This paper proposes a comparison between hard and fuzzy clustering algorithms for thyroid diseases data set in order to find the optimal number of clusters. Different scalar validity measures are used in comparing the performances of the proposed clustering systems. To demonstrate the performance of each algorithm, the feature values that represent thyroid disease are used as input for the system. Several runs are carried out and recorded with a different number of clusters being specified for each run (between 2 and 11), so as to establish the optimum number of clusters. To find the optimal number of clusters, the so-called elbow criterion is applied. The experimental results revealed that for all algorithms, the elbow was located at  $c = 3$ . The clustering results for all algorithms are then visualized by the Sammon mapping method to find a low-dimensional (normally 2D or 3D) representation of a set of points distributed in a high dimensional pattern space. At the end of this study, some recommendations are formulated to improve determining the actual number of clusters present in the data set.

**Keywords:** Thyroid disease; K-means clustering; K-medoids clustering; Fuzzy C-means; Gustafson-kessel algorithm; Gath-Geva algorithm.

### 918. Adaptive K-means Clustering Algorithm for MR Breast Image Segmentation

Hossam M. Moftah, Ahmad Taher Azar, Eiman Tamah Al-Shammari, Neveen I. Ghali, Aboul Ella Hassanien and Mahmoud Shoman

*Neural Computing and Application*, (2013) IF: 1.168

Image segmentation is vital for meaningful analysis and interpretation of the medical images. The most popular method for clustering is k-means clustering. This article presents a new approach intended to provide more reliable magnetic resonance (MR) breast image segmentation that is based on adaptation to identify target objects through an optimization methodology that maintains the optimum result during iterations. The proposed approach improves and enhances the effectiveness and efficiency of the traditional k-means clustering algorithm. The performance of the presented approach was evaluated using various tests and different MR breast images. The experimental results demonstrate that the overall accuracy provided by the proposed adaptive k-means approach is superior to the standard k-means clustering technique.

**Keywords:** K-means clustering; Image segmentation; Magnetic resonance (MR) image; Breast cancer; Adaptive segmentation.

### 919. ALPP: Anonymous and Location Privacy Preserving Scheme for Mobile IPv6 Heterogeneous Networks

Sanaa Mohamed Ahmed Taha

*Security and Communication Networks*, 6: - (2013) IF: 0.311

The integration of mobile IPv6 heterogeneous networks enhances networking performance; however, it also breaks mobile node's anonymity and location privacy. In this paper, we propose an anonymous and location privacy preserving scheme (ALPP) that consists of two complementary sub-schemes: anonymous home binding update (AHBU) and anonymous return routability (ARR). In addition, anonymous mutual authentication and key establishment schemes have been proposed to work in conjunction with ALPP to authenticate a mobile node to its foreign gateway and create a shared key between them. ALPP adds anonymity and location privacy services to mobile IPv6 signaling to achieve mobile senders and receivers privacy. Unlike existing schemes, ALPP alleviates the trade-off between the networking performance and the achieved privacy level. Combining onion routing and anonymizer in ALPP scheme increases the achieved location privacy level where no entity in the network except the mobile node itself can identify this node's location. Using entropy model, we show that ALPP achieves higher degree of anonymity than that achieved by the mix-based scheme. AHBU and ARR sub-schemes require less computation overheads and thwart both internal and external adversaries. Simulation results demonstrate that our schemes have low control-packets routing delays and are suitable for the seamless handover.

**Keywords:** Anonymity; Location Privacy; Mobile IPv6 Security; Heterogeneous Networking Privacy; Next Generation Networks

### 920. A Blind 3D Watermarking Approach for 3D Mesh Using Clustering Based Methods

Mona M. Soliman, Aboul Ella Hassanien and Hoda M. Onsi

*International Journal of Computer Vision and Image Processing*, 3 (2): 43 -53 (2013)

Blind and robust watermarking of 3D mesh aims to embed message into a 3D mesh model such that the mesh is not visually distorted from the original model. An essential condition is that the message should be securely extracted even after the mesh model was processed. This paper explores use of artificial intelligence techniques to build blind and robust 3D-watermarking approach. It is based on clustering 3D vertices into appropriate or inappropriate candidates for watermark insertion using K-means clustering and Self Organization Map (SOM) clustering algorithms. The watermark insertion was performed only on set of selected vertices come out from clustering technique. These vertices are used as candidates for watermark carriers that will hold watermark bits stream. Through the simulations, the authors prove that the proposed approach is robust against various kinds of geometrical attacks such as mesh smoothing, noise addition and mesh cropping.

**Keywords:** 3D Mesh model; Artificial intelligence techniques; Self organization map (SOM); Three-dimensional (3D); Watermarking.

### 921. A Pso-Inspired Multi-Robot Map Exploration Algorithm Using Frontier-Based Strategy

Yi Zhou, Kai Xiao, Yiheng Wang, Alei Liang and Aboul Ella Hassanien

*International Journal of System Dynamics Applications*, 2 (2): 1-13 (2013)

Map exploration is a fundamental problem in mobile robots. This paper presents a distributed algorithm that coordinates a team of autonomous mobile robots to explore an unknown environment. The proposed strategy is based on frontiers which are the regions on the boundary between open and unexplored space. With this strategy, robots are guided to move constantly to the nearest frontier to reduce the size of unknown region. Based on the Particle Swarm Optimization (PSO) model incorporated in the algorithm, robots are navigated towards remote frontier after exploring the local area. The exploration completes when there is no frontier cell in the environment. The experiments implemented on both simulated and real robot scenarios show that the proposed algorithm is capable of completing the exploration task. Compared to the conventional method of randomly selecting frontier, the proposed algorithm proves its efficiency by the decreased 60% exploration time at least. Additional experimental results show the decreased coverage time when the number of robots increases, which further suggests the validity, efficiency and scalability.

**Keywords:** Autonomous mobile robots; Frontier; Map Exploration; Multi-robot; Particle swarm optimization (PSO).

### 922. An Improvement of Chaos-based Hash Function in Cryptanalysis Approach: an Experience with Chaotic Neural Networks and Semi-collision Attack

Aboul Ella Otify Hassanien

*Memetic Computing*, 5: 179-185 (2013)

In this paper, the chaos-based hash function is analyzed, then an improved version of chaos-based hash function is presented and discussed using chaotic neural networks. It is based on the piecewise linear chaotic map that is used as a transfer function in the input and output of the neural network layer. The security of the improved hash function is also discussed and a novel type of collision resistant hash function called semi-collision attack is proposed, which is based on the collision percentage between the two hash values. In the proposed attack particle swarm optimization algorithm is used to define the fitness function parameters. Finally, numerical and simulation results provides strong collision resistance and high performance efficiency.

**Keywords:** Chaos theory; Cryptanalysis.

### 923. Employment of Neural Network and Rough Set in Meta-learning

Mostafa A. Salama, Aboul Ella Hassanien and Kenneth Revett

*Memetic Computing*, 5(4): 165-177 (2013)

The selection of the optimal ensembles of classifiers in multiple-classifier selection technique is un-decidable in many cases and it is potentially subjected to a trial-and-error search. This paper

introduces a quantitative meta-learning approach based on neural network and rough set theory in the selection of the best predictive model. This approach depends directly on the characteristic, meta-features of the input data sets. The employed meta-features are the degree of discreteness and the distribution of the features in the input data set, the fuzziness of these features related to the target class labels and finally the correlation and covariance between the different features. The experimental work that consider these criteria are applied on twenty nine data sets using different classification techniques including support vector machine, decision tables and Bayesian believe model. The measures of these criteria and the best result classification technique are used to build a meta data set. The role of the neural network is to perform a black-box prediction of the optimal, best fitting, classification technique. The role of the rough set theory is the generation of the decision rules that controls this prediction approach. Finally, formal concept analysis is applied for the visualization of the generated rules.

**Keywords:** Rough sets; Meta-learning; Decision rules; Feature selection.

### 924. Fuzzy Clustering With Multi-Resolution Bilateral Filtering for Medical Image Segmentation

Kai Xiao, Jianli Li, Shuangjiu Xiao, Haibing Guan and Fang Fang and Aboul Ella Hassanien

*Int. Journal of Fuzzy System Applications*, 3 (4): 47-59 (2013)

Although fuzzy c-means (FCM) algorithm and some of its variants have been extensively widely used in unsupervised medical image segmentation applications in recent years, they more or less suffer from either noise sensitivity or loss of details, which always is a key point to medical image processing. This paper presents a novel FCM variation method that is suitable for medical image segmentation. The proposed method, typically by incorporating multi-resolution bilateral filter which is combined with wavelet thresholding, provides the following advantages: (1) it is less sensitive to both high- and low-frequency noise and removes spurious blobs and noisy spots, (2) it yields more homogeneous clustering regions, and (3) it preserves detail, thus significantly improving clustering performance. By the use of synthetic and multiple-feature magnetic resonance (MR) image data, the experimental results and quantitative analyses suggest that, compared to other fuzzy clustering algorithms, the proposed method further enhances the robustness to noisy images and capacity of detail preservation.

**Keywords:** Bilateral filtering; Fuzzy C-means (FCM); Medical image segmentation; Multi-resolution; Wavelet.

### 925. Hybrid Dual-tree Wavelet Transform and Adaptive Threshold for Image Denoising.

Hala S. Own, Neveen I. Ghali and Aboul Ella Hassanien

*International Journal of Imaging and Robotic*, 9 (1): 17-25 (2013)

The paper presents an improvement of image denoising algorithm based on adaptive threshold using Dual-tree complex wavelet transform (DT-CWT) and multiresolution local contrast entropy (MLCE). The proposed adaptive threshold enables the denoising technique to be adaptive to unknown smoothness of the noisy images. To evaluate the performance of presented algorithm, we

present simulation results that shows the performance of the proposed image denoising algorithm, and a comparative analysis with other popular denoising algorithms such as VisuShrink, Wiener2 and our previous work based on DWT.

**Keywords:** Image denoising; Wavelet transform.

## 926. Hybrid System Based on Rough Sets and Genetic Algorithms for Medical Data Classifications

Hanaa Ismail Elshazly, Ahmad Taher Azar, Aboul Ella Otify Hassanien and Abeer Mohamed Elkorany

*Int. Journal of Fuzzy System Applications*, 3 (4): 31-46 (2013)

Computational intelligence provides the biomedical domain by a significant support. The application of machine learning techniques in medical applications have been evolved from the physician needs. Screening, medical images, pattern classification, prognosis are some examples of health care support systems. Typically medical data has its own characteristics such as huge size and features, continuous and real attributes that refer to patients' investigations. Therefore, discretization and feature selection process are considered a key issue in improving the extracted knowledge from patients' investigations records. In this paper, a hybrid system that integrates Rough Set (RS) and Genetic Algorithm (GA) is presented for the efficient classification of medical data sets of different sizes and dimensionalities. Genetic Algorithm is applied with the aim of reducing the dimension of medical datasets and RS decision rules were used for efficient classification. Furthermore, the proposed system applies the Entropy Gain Information (EI) for discretization process. Four biomedical data sets are tested by the proposed system (EI-GA-RS), and the highest score was obtained through three different datasets. Other different hybrid techniques shared the proposed technique the highest accuracy but the proposed system preserves its place as one of the highest results systems four three different sets. EI as discretization technique also is a common part for the best results in the mentioned datasets while RS as an evaluator realized the best results in three different data sets.

**Keywords:** Biomedical classification; Data mining; Discretization; Entropy gain information (EI), Feature selection (FS); Genetic algorithm (GA); Machine learning (ML), Rough set (RS).

## 927. Image Color Transfer Approach By Analogy With Taylor Expansion

Hongbo Liu, Ye Ji and Aboul Ella Hassanien

*Int. J. of System Dynamics Applications*, 2 (2): 43 -54 (2013)

The Taylor expansion has shown in many fields to be an extremely powerful tool. In this paper, the authors investigated image features and their relationships by analogy with Taylor expansion. The kind of expansion could be helpful for analyzing image feature and engraftment, such as transferring color between images. By analogy with Taylor expansion, the image color transfer algorithm is designed by the first and second-order information. The luminance histogram represents the first-order information of image, and the co-occurrence matrix represents the second-order information of image. Some results illustrate the proposed algorithm is effective. In this study, each polynomial in the Taylor analogy expansion of images is considered as one of

image features which help in re-understanding images and its features. By using the proposed technique, the features of image, such as color, texture, dimension, time series, would be not isolated but mutual relational based on image expansion.

**Keywords:** Co-occurrence matrix; Image color transfer; Image feature analysis; Luminance histogram; Taylor expansion.

## 928. Searching DNS for Malicious Domain Registration: Identification Through Hybrid Cuckoo Search Metaphor and Object-Oriented Implementation

Manash Sarkar and Soumya Banerjee and Aboul Ella Hassanien

*International Journal of Reasoning-Based Intelligent Systems*, 5 (4): 280-289 (2013)

Several new domains are being registered everyday due to the rapid enhancement of web users. Out of those domains, substantial number of domains become harmful and may initiate malicious activities on the web. It is very difficult to segregate these types of domain to protect our system from different types of attack. The system becomes more vulnerable due to the malicious propagation of domains. It is too complex to identify the exact classification of malicious domain. Contemporary trend of adaptive and learning methodologies could assist to learn such pattern of ill defined domain activities. Hence, intelligent methodologies can be better suitable to support unsupervised classification of domain. Thus metaheuristics-based searching support algorithm called cuckoo search (CS) could be applied for this purpose. Finally, an insight of object oriented engineering to implement the proposed model has been initiated and elaborated future extension of the model has also been discussed.

**Keywords:** Cuckoo search; Metaheuristics; Optimisation; Malicious domain registration; Fuzzy logic.

## 929. Secure Multicast Routing Protocols in Mobile Ad-hoc Networks

Haitham S.Hamza, Ahmed Abdel Moamen and Iman A. Saroit

*International Journal of Communication Systems*, (2013)

A mobile ad-hoc network (MANET) is a collection of autonomous nodes that communicate with each other by forming a multi-hop radio network. Routing protocols in MANETs define how routes between source and destination nodes are established and maintained. Multicast routing provides a bandwidth-efficient means for supporting group-oriented applications. The increasing demand for such applications coupled with the inherent characteristics of MANETs (e.g., lack of infrastructure and node mobility) have made secure multicast routing a crucial yet challenging issue. Recently, several multicast routing protocols (MRP) have been proposed in MANETs. Depending on whether security is built-in or added, MRP can be classified into two types: secure and security-enhanced routing protocols, respectively. This paper presents a survey on secure and security-enhanced MRP along with their security techniques and the types of attacks they can confront. A detailed comparison for the capability of the various routing protocols against some known attacks is also presented and analyzed.

**Keywords:** Mobile ad-hoc Network (MANET); Multicast routing protocols (MRP); Multicast routing protocols (MRP); Security techniques; multicast routing attacks.

## Institute of Statistical Studies and Research

### Dept. of Operational Research

#### 930. A Hybrid Particle Swarm Algorithm With Artificial Immune Learning for Solving the Fixed Charge Transportation Problem

Mahmoud M. El-Sherbiny and Rashid M. Alhamali

*Computers and Industrial Engineering*, 64: 610-620 (2013) 1 F: 1.516

Fixed Charge Transportation Problem (FCTP) is an NP-hard problem with many applications in both traditional and modern industrial situations. This paper introduces a Hybrid Particle Swarm algorithm with artificial Immune Learning (HPSIL) for solving fixed FCTPs. In HPSIL algorithm a flexible particle (chromosome) structure, decoding procedure and allocation procedure are used instead of a Prüfer number and a spanning tree that used with genetic algorithms. The proposed allocation procedure guarantees finding a feasible solution for each generated particle. The HPSIL algorithm can be used for solving both balanced and unbalanced FCTPs without introducing dummy supplier or dummy demand. With regard to solution quality, the HPSIL algorithm can be considered as a viable alternative for solving FCTPs in addition to the recent algorithms.

**Keywords:** Fixed charge transportation; Convergence; particle swarm; genetic algorithm; artificial immune system.

#### 931. HRCTL: A Specification Logic for Hierarchical Hybrid Automata

Ammar Mohammed

*International Journal of Advanced Studies in Computer Science and Engineering (IJASCSE)*, 2 (2): 14-23 (2013)

his paper proposes HRCTL a specification logic of hierarchical hybrid automata that extends the temporal logic CTL in order to specify quantitative and qualitative properties of hybrid systems. in contrast to others proposed quantitative logics, HRCTL is interpreted over the run hierarchical hybrid automata. additionally, it can be used to specify both state and event based requirements of the models under considerations.

**Keywords:** Temporal logics; Hybrid automata.

#### 932. A Developed Multi-Criteria Decision Making Model to Rank Different Scenarios of Electrical Power Generation in Egypt

Hamed M. Elsayed, Hesham A. Hefny and Hisham F. Aly

*International Journal of Computer Applications*, 84 (3): 6-14 (2013)

Multi-criteria decision support systems are used in various fields of human activities. Every alternative multi-criteria decision making problem can be represented by a set of properties or constraints. The properties may be qualitative & quantitative. There are different unit, as well as there are different optimization techniques to measure these properties. In this paper a developed fuzzy ANP model is proposed. This model helps decision makers

to rank different scenarios of electrical power generation in Egypt. After that a comparison is made between the proposed model and the other ANP techniques.

**Keywords:** Fuzzy; Analytic network process; Gaussian function; decision-Making.

#### 933. An Extension of Fuzzy Decision Maps for Multi-Criteria Decision-Making

Basem Mohamed Elomda, Hesham Ahmed Hefny and Hesham Ahmed Hassan

*Egyptian Informatics Journal*, 14: 147-155 (2013)

This paper presents a new extension to Fuzzy Decision Maps (FDMs) by allowing use of fuzzy linguistic values to represent relative importance among criteria in the preference matrix as well as representing relative influence among criteria for computing the steady-state matrix in the stage of Fuzzy Cognitive Map (FCM). The proposed model is called the Linguistic Fuzzy Decision Networks (LFDNs). The proposed LFDN provides considerable flexibility to decision makers when solving real world Multi-Criteria Decision-Making (MCDM) problems. The performance of the proposed LFDN model is compared with the original FDM using a previously published case study. The result of comparison ensures the ability to draw the same decisions with a more realistic decision environment.

**Keywords:** Multi-Criteria Decision; making (Mcdm); Analytic Network Process( Anp); Analytical Hierarchical Process( Ahp); Fuzzy Cognitive Maps (Fcm); Fuzzy Decision Maps (Fdm).

#### 934. Attacks on Anonymization-Based Privacy-Preserving: A Survey for Data Mining and Data Publishing

Abou-el-ela Abdou Hussien, Nermin Hamza and Hesham A. Hefny

*Journal of Information Security*, 4: 101-112 (2013)

Data mining is the extraction of vast interesting patterns or knowledge from huge amount of data. The initial idea of privacy-preserving data mining PPDM was to extend traditional data mining techniques to work with the data modified to mask sensitive information. The key issues were how to modify the data and how to recover the data mining result from the modified data. Privacy-preserving data mining considers the problem of running data mining algorithms on confidential data that is not supposed to be revealed even to the party running the algorithm. In contrast, privacy-preserving data publishing (PPDP) may not necessarily be tied to a specific data mining task, and the data mining task may be unknown at the time of data publishing. PPDP studies how to transform raw data into a version that is immunized against privacy attacks but that still supports effective data mining tasks. Privacy-preserving for both data mining (PPDM) and data publishing (PPDP) has become increasingly popular because it allows sharing of privacy sensitive data for analysis purposes. One well studied approach is the k-anonymity model [1] which in turn led to other models such as confidence bounding, l-diversity, t-closeness, (a,k)-anonymity, etc. In particular, all known mechanisms try to minimize information loss and such an attempt provides a loophole for attacks. The aim of this paper is to present a survey for most of the common



attacks techniques for anonymization-based PPDM & PPDP and explain their effects on Data Privacy.

**Keywords:** Privacy; K-Anonymity; Data Mining; Privacy-Preserving Data Publishing; Privacy-Preserving Data Mining

### 935. Forecasting of Egypt Wheat Imports Using Multivariate Fuzzy Time Series Model Based on Fuzzy Clustering

Ashraf K. Abd-Elaal, Hesham A. Hefny and Ashraf H. Abd-Elwahab

*IAENG Inte. J. of Computer Science*, 40 (4): 230-237 (2013)

This paper presents Multivariate-Factors fuzzy time series model for improving forecasting accuracy. The proposed model is based on fuzzy clustering and it employs eight main procedures to build the multivariate-factors model. The model is evaluated by studying the Egypt Wheat imports as a forecasting problem. Forecasting Egypt wheat imports depend on three factors: population size, wheat area, and wheat production. This forecasting problem is considered to be a good benchmark for comparing different forecasting techniques since it exhibits highly nonlinearities over a long period of time and it provides important economical indicators needed for national future planning. Experimental results show that the proposed model provides higher forecasting accuracy than ARIMA model, Regression model and neural network model. Therefore, the proposed model can lead to satisfactory high performance for fuzzy time series.

**Keywords:** ARIMS; Egypt wheat imports; Fuzzy clustering; Multivariate-factors fuzzy time series.

### 936. Fuzzy Multi-criteria Decision Making Model for Different Scenarios of Electrical Power Generation in Egypt

Hesham A. Hefny, Hamed M. Elsayed and Hisham F. Aly

*Egyptian Informatics Journal*, 14: 125-133 (2013)

In the analytic network process (ANP) a hierarchy or network is created to represent a decision and establishes a matrix containing the pair wise comparison judgments for the elements linked under a parent element. A priority vector of relative weights for these elements is derived. Then all the priority vectors are appropriately weighted and summed to obtain the overall priorities for the alternatives of a decision. In this paper we will develop an efficient fuzzy ANP model which helps decision makers to choose among the alternatives for the Egyptian scenarios of electrical power generation

**Keywords:** Fuzzy; Analytic network process; Gaussian function; Decision-making.

### 937. Maintaining the Search Engine Freshness Using Mobile Agent

Marwa Badawi, Ammar Mohamed, Ahmed Hussein and Mervat Gheith

*Egyptian Informatics Journal*, 14: 27-36 (2013)

Search engines must keep an up-to-date image to all Web pages and other web resources hosted in web servers in their index and

data repositories, to provide better and accurate results to its clients. The crawlers of these search engines have to retrieve the pages continuously to keep the index up-to-date. It is reported in the literature that 40% of the current Internet traffic and bandwidth consumption is due to these crawlers. So we are interested in detecting the significant changes in web pages which reflect effectively in search engine's index and minimize the network load. In this paper, we suggest a document index based change detection technique and distributed indexing using mobile agents. The experimental results have shown that the proposed system can considerably reduce the network traffic and the computational load on the search engine side and keep its index up-to-date with significant changes

**Keywords:** Search engine; Mobile crawling; distributed Indexing; web page change detection.

### 938. Near Optimal Solution for the Step Fixed Charge Transportation Problem

Khalid M. Altassan, Mahmoud M. El-Sherbiny and Bokkasam Sasidhar

*Applied Mathematics and Information Sciences*, 7 (21): 661-669 (2013)

Step Fixed-charge transportation problem (SFCTP) is considered to be one of the versions of Fixed-charge transportation problem (FCTP) where the fixed cost is incurred for every route that is used in the solution. This is considered to be an NP-hard problem since the cost structure causes the value of the objective function to behave like a step function. In this paper three formulae are proposed to construct intermediate coefficient matrix as a base for finding an initial solution for SFCTP. The proposed formulae overcome the drawbacks of one of the earlier proposed formulae, which fails to address the cases when load units become equal to or greater than the minimum of the supplies and demand for particular route. In addition, the achieved initial solution for the SFCTP is considered to be the best as compared to the initial solution achieved by the earlier proposed formula in the literature. In order to confirm the superiority of the proposed formula, forty problems with different sizes have been solved to evaluate and demonstrate the performance of the proposed formula and to compare their performance with the earlier proposed formula.

**Keywords:** Fixed charge transportation; Step fixed charge Transportation; Heuristic algorithm.

### 939. On Uncertain Granular Numbers

Assem A. Alsaway and Hesham A. Hefny

*International Journal of Computer Applications*, 62: 20-27 (2013)

When a quantity is measured, the outcome depends on several factors like the measuring system, the measurement procedure, the skill of the operator, the environment, and other effects. In case of inexact quantity the outcome may also depend on the uncertainty representation. Recently inexact numbers got a lot of attention from many researchers in different fields. In this paper, we have tried to give an overview for the different representations of the inexact granular numbers. The objective of this overview is providing a certain insight into the essence of granular data representation being regarded as a framework of representing and manipulation of inexact information, and

introduce a new representation of granular uncertain number to be as step in formulate a general form for all uncertain numbers.

**Keywords:** Granular computing; Soft computing; Uncertainty.

#### 940. A Rule of Thumb for Testing Symmetry About An Unknown Median Against A Long Right Tail

Amitava Mukherjee, A. M. Abd-Elfattah and Barendra Pukait

*Journal of Statistical Computation and Simulation*, 84: 1-18 (2013)

A rule of thumb for testing symmetry of an unknown univariate continuous distribution against the alternative of a long right tail is proposed. Our proposed test is based on the concept of exceedance statistic and is ad hoc in nature. Exact performances of the proposed rule are investigated in detail. Some results from an asymptotic point of view are also provided. We compare our proposed test with several classical tests which are practically applicable and are known to be exact or nearly distribution free. We see that the proposed rule is better than most of the existing tests for symmetry and can be applied with ease. An illustration with real data is provided.

**Keywords:** Adaptive test; Distribution free; Long right tail; Monte-carlo study; Positively skewed; Power; Test of symmetry.

#### 941. A New Bivariate Distribution With Generalized Gompertz Marginals

E. A. El-Sherpieny, S. A. Ibrahim and R. E. Bedar

*Asian Journal of Applied Sciences*, 1 (4): 141-150 (2013)

In this paper, we introduce a new bivariate generalized Gompertz distribution, it is of Marshall-Olkin type. Some properties of the distribution are studied, as bivariate moment generating function, marginal moment generating function and conditional distribution. Parameters estimators using the maximum likelihood method are obtained. A numerical illustration is used to obtain maximum likelihood estimators (MLEs) and we study the behavior of the estimators numerically

**Keywords:** Generalized gompertz distribution; Maximum likelihood estimators; Moment estimators; Fisher information matrix. Gamma Duplication

#### 942. A New Bivariate Distribution With Gompertz Marginals

El-Sherpieny E. A, Ibrahim S.A and Bedar. R.E

*International Journal of Basic and Applied Sciences*, 2: 346-355 (2013)

In this paper, we propose a new bivariate distribution with the Gompertz marginals. Some properties of this new bivariate distribution have been investigated. Several properties of this distribution have been discussed. Parameters estimation using moments and maximum likelihood methods are obtained. A numerical illustration experiments have been performed to see the behavior of the MLEs. One data set has been analyzed for illustrative purpose.

**Keywords:** Bivariate model; Gompertz distribution function; Maximum Likelihood estimators; Moment estimators; Fisher Information Matrix.

#### 943. A New Generalization of Quadratic Hazard Rate Distribution

Ibrahim Elbatal and Nadeem Shafique Butt

*Pakistan Journal of Statistics and Operation Research*, 9 (4): 343-361 (2013)

For the first time, a five-parameter distribution, called the kumaraswamy quadratic hazard rate distribution is defined and studied. The new distribution contains as special models some well-known distributions discussed in lifetime literature, such as the Linear failure rate, Exponential and Rayleigh distributions, among several others. We obtain the moments, moment generating and quantile functions. We discuss the method of maximum likelihood to estimate the model parameters and determine the observed information matrix. A real data sets illustrate the importance and flexibility of the proposed models

**Keywords:** Quadratic hazard rate distribution; Order statistics; Maximum likelihood estimation; Reliability function.

#### 944. A New Generalized Lindley Distribution

Ibrahim Elbatal, Faton Merovci and M. Elgarhy

*Mathematical Theory and Modeling*, 3 (13): 30-47 (2013)

In this paper, we present a new class of distributions called New Generalized Lindley Distribution(NGLD). This class of distributions contains several distributions such as gamma, exponential and Lindley as special cases. The hazard function, reverse hazard function, moments and moment generating function and inequality measures are obtained. Moreover, we discuss the maximum likelihood estimation of this distribution. The usefulness of the new model is illustrated by means of two real data sets. We hope that the new distribution proposed here will serve as an alternative model to other models available in the literature for modelling positive real data in many areas.

**Keywords:** Generalized lindley distribution; Gamma Distribution; Maximum likelihood estimation; Moment Generating function.

#### 945. A Simple Representation of the Weighted Non-Central Chi-square Distribution

Elsayed A. Elsherpieny, Sahar A. Ibrahim and Yassmen, Y. Abdelall

*International Journal of Innovative Research in Science, Engineering and Technology*, 2 (9): 4977-4986 (2013)

In this paper we consider the probability density function (pdf) of the weighted non-central chi-square distribution with  $\nu$  degrees of freedom. This pdf presented in the literature as an infinite sum. Herein, we present an alternative simple expression to this pdf which may be useful in the future studies. The results of Kettani (2006) and Andras and Baricz (2008) can be obtained as a special case from ours.

**Keywords:** Weighted non-central chi-square distribution; Modified Bessel function; Modified Struve function; Hoppe's formula.

#### 946. A Unified Approach for Mixtures from Two Certain Families of Distributions

Ali A. A. Rahman

*Applied Mathematical Sciences*, 7 (29): 1419 -1428 (2013)

A mixture from two distribution families is characterized via a differential equation as well as a recurrence relation between three consecutive conditional moments of some function  $h^k(X)$ ,  $k = 1, 2, 3, \dots$  given  $X > y$ . Some well-known results follow as special cases from our results.

**Keywords:** Characterization; Mixture of distributions; Burr, Pareto, Beta, Weibull, Exponential and 1st type Pearsonian distributions.

#### 947. A Unified Approach of Some Characterization Results

Ali A. A. Rahman

*Journal of Statistics and Mathematics*, 4 (1): 141-146 (2013)

This paper considers the problem of identifying some probability distributions using the concepts of right and left truncated moments of some function of the  $k$ th order statistic. Furthermore, it investigates the necessary and sufficient conditions to characterize distributions by the equation as well as. Some well-known results follow from our results as special cases.

**Keywords:** Characterization; Truncated moments; Exponentiated Weibull; Inverse Weibull; Exponentiated Pareto; Burr; Power; Uniform; Ferguson distributions.

#### 948. Characterizations of a Mixture of Two Exponential Families

Ali Ahmed Abdel-Rahman

*Applied Mathematical Sciences*, 7 (78): 3861-3872 (2013)

A mixture from two exponential families is identified using a differential equation, a recurrence relation between conditional moments and conditional variance. New characterizations to other different mixtures are deduced. Some well-known results follow as special cases from our results.

**Keywords:** Characterization; Mixture of distributions; Burr; Pareto; Beta; Weibull; Exponential and 1st type Pearsonian distributions.

#### 949. Discriminating Between Weibull and Log-Logistic Distributions

Elsayed A. Elsherpieny, Sahar A. N. Ibrahim and Noha U. M. M. Radwan

*International Journal of Innovative Research in Science, Engineering and Technology*, 2: 3358-3371 (2013)

Weibull and log-logistic distributions are two popular distributions for analyzing lifetime data. In this paper it is

assumed that the data are coming either from Weibull or log-logistic distributions. The maximized likelihood ratio test to discriminate between the two distributions is used. The asymptotic distributions of the logarithm of the ratio of the maximized likelihood are obtained. These asymptotic results are used to estimate the probability of correct selection and the minimum sample size needed to discriminate between the two distributions. Two real data life are analyzed to see how the proposed method works in practice.

**Keywords:** Asymptotic distribution; Weibull distribution; Log-logistic distribution; Maximized likelihood ratio statistic; Probability of correct selection.

#### 950. Maximum Likelihood and Bayes Estimators of the Unknown Parameters for Exponentiated Exponential Distribution Using Ranked Set Sampling

Amal Soliman Hassan

*International Journal of Engineering Research and Applications*, 3 (1): 720-725 (2013)

Estimation of the shape and scale parameters of exponentiated exponential distribution is considered based on simple random sample and ranked set sample. Bayesian method of estimation under squared error loss function and maximum likelihood method will be used. Comparison between estimators is made through simulation via their absolute relative biases, mean square errors, and efficiencies. Comparison study revealed that the Bayes estimator is better than maximum likelihood estimator under both sampling schemes. The results show that the estimators based on ranked set sample are more efficient than that from simple random sample at the same sample size.

**Keywords:** Bayes; Estimation; Ranked set sampling; Simple random sample; Exponentiated exponential distribution.

#### 951. Moment Generating Function of the Unbalanced Non-central Chi-square Distribution

El-Sayed, A. Elsherpieny; Sahar A. Ibrahim and Yassmen Y. Abdelall

*Int. J. of Engineering and Applied Sciences*, 4 (3): 24-30 (2013)

In this paper, a general form of the cumulative distribution function and a moment generating function of the unbalanced (weighted) non-central chi-square distribution with  $\nu$  degrees of freedom are obtained. Graub's result of moments (2009) can be obtained easily from the given moment generating function.

**Keywords:** Weighted non-central chi-Square distribution; Capability indices; Moment generating function.

#### 952. On Characterizing Some Mixtures of Probability Distributions

Ali A. A. Rahman

*Journal of Applied Mathematics and Bioinformatics*, 3 (3): 153-172 (2013)

The concept of recurrence relations is used to characterize mixtures of two exponential families, two 1<sup>st</sup> type Ouyang's

distributions and two 2<sup>nd</sup> type Ouyang's distributions. Our results are used to deduce conclusions concerning some mixtures of some well known distributions like Burr, Pareto, Power Weibull, 1<sup>st</sup> type Pearsonian and Ferguson's distributions. Furthermore, some characterizations related to some recently distributions like, mixtures of two exponentiated Weibull, exponentiated Pareto and generalized exponential distributions are derived from our results. In addition, some well-known results follow from our results as special cases.

**Keywords:** Mixtures of distributions; Truncated moments; Failure rate; Reversed failure rate; Recurrence relations; Exponentiated burr; Exponentiated weibull; Generalized exponential; Ouyang's distributions; Ferguson's distributions.

### 953. On the Computation of Weighted Non-central Chi-square Distribution Function

El-Sayed, A. Elsherpieny, Sahar, A. Ibrahim and Yassmen Y. Abdelall

*Journal of Applied Sciences Research*, 9 (8): 4507-4516 (2013)

Generally the cumulative distribution function is very important in calculating the power function of some statistical tests. The cumulative distribution function of weighted non-central chi-square distribution involves an integral which is difficult to obtain. In this paper we present two formulas for the cumulative distribution function of the weighted non-central chi-square distribution which are easy to handle in computation. The first one for any degrees of freedom, while the second is appropriate for only odd degrees of freedom. A numerical illustration is given. Ashour and Abdel-Samad (1990) results can be obtained as a special case of our results.

**Keywords:** Weighted non-central chi-square distribution, Gamma supplication.

### 954. on the Estimation of $P(Y < X < Z)$ for Weibull Distribution in the Presence of $k$ Outliers

Amal S. Hassan, Elsayed, A. Elsherpieny and Rania M. Shalaby

*International Journal of Engineering Research and Applications*, 3 (6): 1728-1734 (2013)

This paper deals with the estimation problem of reliability  $R = P(Y < X < Z)$ , where  $X$ ,  $Y$  and  $Z$  are independently Weibull distribution with common known shape parameter but with different scale parameters, in presence of  $k$  outliers in strength  $X$ . The moment, maximum likelihood and mixture estimators of  $R$  are derived. An extensive computer simulation is used to compare the performance of the proposed estimators using MathCAD (14). Simulation study showed that the mixture estimators are better and easier than the maximum likelihood and moment estimators.

**Keywords:** Maximum likelihood estimator; Mixture estimator; Moment estimator; Outliers; Weibull distribution.

### 955. On the Optimal Design of Failure Step-Stress Partially Accelerated Life Tests for Exponentiated Inverted Weibull With Censoring

Amal Soliman Hassan

*Australian J. of Basic and Applied Sciences*, 7 (1): 97-104 (2013)

This article deals with the optimal designing of failure step-stress partially accelerated life tests with two stress levels under type-I censoring. The lifetime of the test items is assumed to follow exponentiated inverted Weibull distribution. The point and interval estimates of the model parameters are obtained. Based on type I censoring, optimum test plans for failure step stress partially accelerated test are also developed through the D-optimality criterion. Such method minimizes the generalized asymptotic variance of the maximum likelihood estimators for the model parameters. Some numerical illustrations are provided to illustrate the proposed procedure.

**Keywords:** Partially accelerated life test; Failure step stress test; Exponentiated Inverted Weibull Distribution; Type i censoring; Maximum likelihood method; Optimal design; D-optimality.

### 956. On the Transmuted Fréchet Distribution

M. R. Mahmoud and R. M. Mandouh

*Journal of Applied Sciences Research*, 9 (10): 5553-5561 (2013)

New parameters can be introduced to expand families of distributions for added flexibility or to construct covariate models and this could be done in various ways. In this paper, we will use the quadratic rank transmutation map (QRTM) in order to generate a flexible family of probability distribution taking Fréchet distribution as the base distribution. The new distribution is called the transmuted Fréchet distribution. Some properties of this distribution are studied. Also, Parameter estimation using maximum likelihood and Bayesian methods are discussed.

**Keywords:** Fréchet distribution, Quadratic rank transmutation Map; Moment generating function; Maximum likelihood Estimation and bayesian estimation.

### 957. On the Transmuted Additive Weibull Distribution

Ibrahim Elbatal and Gokarna Aryal

*Austrian Journal of Statistics*, 42 (2): 117-132 (2013)

In this article a continuous distribution, the so-called transmuted additive Weibull distribution, that extends the additive Weibull distribution and some other distributions is proposed and studied. We will use the quadratic rank transmutation map proposed by Shaw and Buckley (2009) in order to generate the transmuted additive Weibull distribution. Various structural properties of the new distribution including explicit expressions for the moments, random number generation and order statistics are derived. Maximum likelihood estimation of the unknown parameters of the new model for complete sample is also discussed. It will be shown that the analytical results are applicable to model real world data.

**Keywords:** Additive weibull distribution; Order statistics; Transmutation map; Maximum likelihood estimation; Reliability Function.

### 958. Parameters Estimation of Generalized Extreme Value Distribution Under Progressive Type II Censored

El Sherpieny, E. A., Assar, S. M. and Amer. N. M.

*Asian Journal of Applied Sciences*, 1(2): 68-72 (2013)

In this paper, the estimation for the three unknown parameters of the generalized extreme value distribution under progressive type-II censored will be considered. The corresponding asymptotic variance covariance matrix for the parameters and also asymptotic confidence intervals for the parameters are obtained. Finally, A numerical illustration will be carried out. Some literatures may be considered as special cases from our results.

**Keywords:** Generalized extreme value distribution; Progressive censoring; Variance- covariance matrix.

### 959. Preservation of Classes of Discrete Distributions Under Reliability Operations

I. Elbatal and M. Ahsanullah

*Journal of Statistical Theory and Applications*, 12 (1): 1-10 (2013)

In this paper we consider some widely utilized classes of discrete distributions and aim to provide a systematic overview about their preservation under convolution. This paper will serve as a detailed reference for the study and applications of the preservation of the discrete NBU(2), NBUC classes of discrete distributions

**Keywords:** Discrete ageing classes; NBUC; NBUC; NBU (2); Convolution.

### 960. Shannon Entropy for the Generalized Feller-Pareto (GFP) Family and Order Statistics of GFP Subfamilies

Mahmoud Riad Mahmoud and Amani S. Abd El Ghafour

*Applied Mathematical Sciences*, 7 (65): 3247-3253 (2013)

In this paper, we derive the exact analytical expressions of entropy for the Generalized Feller-Pareto (GFP) and order statistics of GFP subfamilies. The GFP family traces its roots back to Zandonatii 2001 as mentioned in Kiefer and Kotz [2]. But it is defined and investigated by Paranaíba et al. [4] under different name which is called Beta Burr XII (BBXII) distribution. The GFP family is a very general distribution which includes some known distributions such as FP and beta Weibull distributions. Also, The GFP family includes some new distributions such as beta-Lomax and generalized Burr XII distributions. These distributions are applied in reliability, medicine, actuarial science, and economics.

**Keywords:** Entropy; Generalized feller-Pareto; Beta burr xii; Generalized Burr Xii; Beta lomax; Order statistics.

### 961. Statistical Properties of Kumaraswamy Quasi Lindley Distribution

I.Elbatat and M. Elgarhy

*International Journal of Mathematics Trends and Technology*, 4 (10): 237-246 (2013)

In this paper, we present a new class of distributions called kumaraswamy Quasi Lindley Distribution. This class of distributions contains several distributions such as kumaraswamy Lindley distribution, Quasi Lindley, and kumaraswamy gamma distribution as special cases. The hazard function, moments and

moment generating function are presented. Moreover, we discuss the maximum likelihood estimation of this distribution.

**Keywords:** Kumaraswamy quasi lindley distribution; Maximum likelihood estimation; Moment generating function.

### 962. The Kumaraswamy Exponentiated Pareto Distribution

I. Elbatal

*Economic Quality Control*, 28 (1): 1-8 (2013)

Modeling and analysis of lifetimes is an important aspect of statistical work in a wide variety of scientific and technological fields. for the first time, the called Kumaraswamy Exponentiated Pareto distribution, is introduced. Some structural properties of the proposed distribution are studied including explicit expressions for the moments and generating function. An explicit expression for Rényi entropy is obtained. The method of maximum likelihood is used for estimating the model parameters

**Keywords:** Hazard function; Moment and generating functions; Maximum likelihood estimation.

### 963. Transmuted Generalized Linear Exponential Distribution

Elbatal, I.; Diab, L. S. and Abdul Alim, N. A.

*International Journal of Computer Applications*, 83: 29-37 (2013)

The linear exponential distribution is a very well-known distribution for modeling lifetime data in reliability and medical studies. We introduce in this paper a new four-parameter generalized version of the transmuted generalized linear exponential distribution. We provide a comprehensive account of the mathematical properties of the new distributions. In particular, A closed-form expressions for the density, cumulative distribution, quantile and median of the distribution is given. Also, the  $r$ -th order moment and moment generating function are derived. The maximum likelihood estimation of the unknown parameters is discussed. Real data are used to determine whether the TGLED is better than other well-known distributions in modeling lifetime data or not.

**Keywords:** Transmuted generalized linear exponential Distribution; Quantile and median; Maximum likelihood Estimation; Moments

### 964. Transmuted Modified Inverse Weibull Distribution: A Generalization of the Modified Inverse Weibull Probability Distribution

I. Elbatal

*International Journal of Mathematical Archive*, 4 (8): 117-129 (2013)

A functional composition of the cumulative distribution function of one probability distribution with the inverse cumulative distribution function of another is called the transmutation map. In this article, we will use the quadratic rank transmutation map (QRTM) in order to generate a flexible family of probability distributions taking modified inverse weibull distribution as the base value distribution by introducing a new parameter that would



offer more distributional flexibility. It will be shown that the analytical results are applicable to model real world data.

**Keywords:** Modified inverse weibull distribution; Order statistics; Transmutation map; Maximum likelihood estimation; Reliability function.

#### **965. Transmuted Quasi Lindley Distribution: A Generalization of the Quasi Lindley Distribution**

I. Elbatal and M. Elgarhy

*International Journal of Pure and Applied Sciences and Technology*, 18 (2): 59-70 (2013)

The Lindley distribution is one of the important for studying stress--strength reliability modeling. Besides, some researchers have proposed new classes of distributions based on modifications of the quasi Lindley distribution. In this paper, a new generalized version of this distribution which is called the transmuted quasi Lindley (TQL) distribution is introduced. A comprehensive mathematical treatment of the TL distribution is provided. We derive the  $r$ th moment and moment generating function this distribution. Moreover, we discuss the least squares, weighted least squares and the maximum likelihood estimation of this distribution.

**Keywords:** Quasi lindley distribution; Hazard function; Moments; Maximum likelihood estimation.

#### **966. Real Parameter Optimization by an Effective Differential Evolution Algorithm**

Ali Wagdy Mohamed, Hegazy Zaher Sabry and Tareq Abd-Elaziz

*Egyptian Informatics Journal*, 14: 37-53 (2013)

This paper introduces an Effective Differential Evolution (EDE) algorithm for solving real parameter optimization problems over continuous domain. The proposed algorithm proposes a new mutation rule based on the best and the worst individuals among the entire population of a particular generation. The mutation rule is combined with the basic mutation strategy through a linear decreasing probability rule. The proposed mutation rule is shown to promote local search capability of the basic DE and to make it faster. Furthermore, a random mutation scheme and a modified Breeder Genetic Algorithm (BGA) mutation scheme are merged to avoid stagnation and/or premature convergence. Additionally, the scaling factor and crossover of DE are introduced as uniform random numbers to enrich the search behavior and to enhance the diversity of the population. The effectiveness and benefits of the proposed modifications used in EDE has been experimentally investigated. Numerical experiments on a set of bound-constrained problems have shown that the new approach is efficient, effective and robust. The comparison results between the EDE and several classical differential evolution methods and state-of-the-art parameter adaptive differential evolution variants indicate that the proposed EDE algorithm is competitive with, and in some cases superior to, other algorithms in terms of final solution quality, efficiency, convergence rate, and robustness.

**Keywords:** Differential evolution; Best--worst mutation; Global optimization; Modified BGA mutation.

CAIRO UNIVERSITY

Publication  
in  
Book & Chapters

## Publication in Book/ Chapter

### Faculty of Engineering

#### Dept. of Aeronautics and Aerospace Engineering

##### **967. Finite Element Analysis for Satellite Structures, Application to Their Design, Manufacture and Testing**

Mohamed Nader Mohamed Abuelfoutouh

*Springer - Verlag, (2013)*

This book is about finite element analysis of spacecraft structures. I tried to reflect the importance of numerical simulation not only in design stages but also in manufacturing simulation and testing. This book covers a wide range of applications using finite element method. This includes linear and nonlinear analysis, which makes this book very useful for many engineers in different areas and not only in spacecraft structures design.

#### Dept. of Architectural Engineering

##### **968. Shaping Development In Limited Resources Settings - Notes on the Egyptian Context**

Nasamat Mohamed Amin Abdel-Kader

*Lambert Academic Publishing, (2013)*

In Egypt the gap between the declared “Development” objectives and adopted strategies and policies to achieve it, invariably proved hard to bridge, breach and compromise. The present work brings together selected parts of the authors’ research endeavor in “Development” and beyond, during the past two decades, most of which was presented and published at International journals, conferences and symposia. Three overlapping objectives are behind the conception and form of this work, namely: 1- To critically present certain aspects and features of the development experience in Egypt - an interesting and challenging “Developing” setting - during the past three decades, emphasizing Community Design and Development, and Housing. 2- To prove that the gap separating theory and practice, can be bridged and compromised. 3- To allow access to scattered research polemics and discourses, to all interested in urban and community development, in developing settings (Egypt included), and to represent it to delineate and highlight facets of an integrated approach to community design and development, and housing in “Developing” contexts.

##### **969. Sustainability, Energy and Architecture Case Studies in Realizing Green Buildings**

Mohsen Mohamed Abo-Elnaga

*Elsevier, Chapter 6 - Sustainable Building for a Green and an Efficient Built Environment: New and Existing Case Studies in Dubai, (2013)*

This chapter describes and argues about the way that sustainable buildings (new and retrofitted) can contribute to increase the efficiency of the sustainable built environment with the intent of cutting carbon emissions. It also presents an overview on how do sustainability regulations and laws contribute to carbon emission

reduction with emphasis on those developed in Europe, Australia and Dubai—United Arab Emirates. The goals of this chapter are to discuss and showcase Dubai's sustainable buildings (new and existing) and to present the energy-efficiency principles exploited in them, and their performance. This chapter contains case studies, which represent three new buildings and three refurbished buildings. It presents an impartial assessment and evaluation of the cutting-edge green buildings. It also portrays Dubai's first carbon-neutral warehouse and the first Leadership in Energy and Environmental Design-certified existing office building in the Middle East. They are legendary green buildings in the context of Dubai as well as of the region. Additionally, this chapter discusses some of the energy-efficiency features and water-recycling elements in the highest skyscraper in the world, Burj Khalifa, in an effort to address encountered challenges of climate change, particularly carbon emissions.

#### Dept. of Electronics and Communication Engineering

##### **970. Synthesis of Generalized Impedance Converter and Inverter Circuits Using NAM Expansion**

Ahmed Mohamed Soliman

*Springer - Verlag, (2013)*

The generalized impedance converter (GIC) is an active two port network in which the input impedance is equal to the load impedance times a conversion function of the complex frequency variable .

There are two types of the GIC, the first is the voltage generalized impedance converter (VGIC) and the second is the current generalized impedance converter (CGIC). In this chapter the nodal admittance matrix (NAM) expansion is used to generate all possible VGIC and CGIC circuits. The realizations of two types of the generalized impedance inverter (GII) circuits using NAM expansion are also given.

##### **971. Generation of Grounded Capacitors Minimum Component Oscillators**

Ahmed Mohamed Soliman

*Springer - Verlag, (2013)*

The oscillators considered in this chapter uses the minimum number of passive elements namely two capacitors and two resistors. The generated oscillators employ two grounded capacitors and all reported circuits except two have the advantage of their ability to absorb parasitic resistance and parasitic capacitance elements effects. Four classes of oscillators are generated in this chapter, the class I oscillator circuits include three nodes, the classes II and III oscillator circuits include four nodes and the class IV oscillator circuits include five nodes.

##### **972. Cognitive Radio Networks From Theory to Practice**

Ahmed Khattab Fathi Khattab

*Springer - Verlag, (2013)*

Cognitive Radio Networks (CRNs) are the key enabling technology for realizing Opportunistic Spectrum Access (OSA) to

alleviate the severe spectrum underutilization and provide a solution for the wireless spectrum scarcity. OSA refers to the communications paradigm in which the communicating parties dynamically exploit the spectrum bands that are not utilized by the primary wireless services licensed to operate over such bands. CRNs are foreseen as the future of wireless communication technologies that provide wireless connectivity for emerging services. In this chapter, we introduce the basics of OSA and CRNs and define the scope and the objectives of the book.

### 97\*. Particle Filters for Object Tracking: Enhanced Algorithm and Efficient Implementations

Serag Eldin Elsayed Habib

*Lambert Academic Publishing, (2013)*

Particle filters are advanced for building robust object trackers capable of operation under difficult tracking conditions. An Excitation Particle Filter (EPF) is introduced in this book for object tracking. A new likelihood model is proposed. It depends on multiple likelihood functions: position likelihood; gray level intensity likelihood and similarity likelihood. Also, we modify the PF as a robust estimator to overcome the well-known sample impoverishment problem of the PF. The proposed enhanced PF (EPF) is implemented in software and evaluated. Simulation results demonstrated the superior performance of the proposed tracker in terms of accuracy, robustness and occlusion over classical tracking algorithms. Three efficient novel hardware architectures of the Sample Important Resample Filter (SIRF) and the EPF are introduced and implemented on FPGA platform. These architectures feature speed improvement, efficient memory utilization, and/or hardware resource saving.

### Dept. of Engineering Mathematics and Physics

### 97\*. Bifurcation Behaviour and Control on Chaotic Convection of Nanofluids with Fractional-Orders

Ahmed Gomaa Ahmed Radwan

*World Scientific and Engineering Academy and Society, (2013)*

In this paper, we study the effect of the fractional -order chaotic behaviour of nanofluids on in a fluid layer heated from below. Adams-Bashforth-Moulton predictor corrector method was adopted to solve the fractional nonlinear system. The synchronization based on the active control theory and Lyapunov stability theory and the effective chaotic range of the fractional-order chaotic system for variation of the single control parameter have been determined. The transition to chaos occurs by a subcritical Hopf bifurcation in this fractional-order system. The results show that inhibition of chaotic convection with fractional-order can be observed when using nanofluids. Numerical simulations are provided to illustrate the effectiveness of the synchronization results derived in this paper.

### 97\*. Surrogate-Based Circuit Design Centering

Abdel-Karim Shabaan Omar Hassan

*Springer - Verlag, (2013)*

Circuit design centering is one of the most important problems concerning the optimal design of circuits. Circuit design centering seeks nominal values of designable circuit parameters that maximize the probability of satisfying the design specifications (yield function). Design centering can be performed geometrically by finding the center of the feasible region (region in the designable parameter space where the design specifications are satisfied), or by maximizing the yield function explicitly. For all cases, the high expense of circuit simulations required obstructs the design centering process, especially for microwave circuits. To overcome this, computationally cheap surrogate-based models (e.g., space mapping, response surfaces, kriging, and neural networks) can be used for approximating the response functions or the yield function itself. In this chapter the design centering problem is formulated as an optimization problem, and the estimation of the yield function through several sampling techniques is explained. The difficulties facing the design centering process, especially for microwave circuits, are discussed, and the role of surrogate-based models in overcoming these difficulties is demonstrated. Special interest is devoted to space mapping surrogates and microwave circuit design centering. Some of the important surrogate-based circuit design centering approaches are reviewed with an overview of their theoretical bases. Tutorial and practical circuit examples are given to show the effectiveness of these approaches.

### 97\*. Homotopy WHEP Algorithm, Solving Stochastic Differential Equations

Magdy A. El-Tawil

*Springer - Verlag, (2013)*

The WHEP algorithm showed a great efficiency in computing some statistical moments of the solution process for many perturbed stochastic differential equations. This technique has been greatly extended by the use of homotopy perturbation to yield what is called Homotopy WHEP in which the homotopy technique replaces the ordinary perturbation method which enables the application of the technique on non-perturbed problems. In this paper, the algorithm is applied on some nonlinear stochastic differential equations.

### Dept. of Mining, Petroleum and Metallurgy

### 97\*. Modern Surface Engineering Treatments

Randa Abdel-Karim

*Intech, (2013)*

Nanocoatings are one of the most important topics within the range of nanotechnology. Through nanoscale engineering of surfaces and layers, a vast range of functionalities and new physical effects can be achieved.

### 97\*. Recycling of Metal Products : Influence of heat input and post-weld heat treatment on boiler steel p91 (9cr-1m0-v-Nb) weld joints

Iman Salah Eldin El-Mahallawi

*Reuse of Materials and Byproducts in Construction, Chapter 3, (2013)*

The cities of today are the mines of tomorrow” is a vision that was foreseen in 1969 by Jacobs. In the twenty first century, the sustainability issue has gained wide acceptance and a wider concept of sustainability has been developed to accommodate recycling of the engineering parts in a comprehensive life-cycle approach from cradle to grave. This chapter discusses recycling of metallic components, namely; steel and aluminum in the construction industry. The chapter aims to provide the readers from various backgrounds with the necessary knowledge to understand the production and properties of steel and aluminum. Through the chapter, from section to section the reader will end up building knowledge regarding the nature of steel and aluminum used within the construction industry, with regard to processing, production and manufacturing routes that affect recycling. The quality of the products made from recycled metals, and the risk elements in the recycling industry are also discussed.

#### **Dept. of Systems and Biomedical Engineering**

##### **٩٧٩. Molecular Classification of Cancer by Gene Expression Monitoring**

Yasser Mostafa Ibrahim Kadah

*Lambert Academic Publishing, (2013)*

Gene expression is critical for tumor initiation and progression. However, we lack a comprehensive understanding of all genes that are aberrantly expressed in human cancer. Recently, microarrays have been used to obtain global views of human cancer gene expression and identify genetic markers that might be important for diagnosis and therapy. The initial sequencing of the human genome, coupled with technological advances, now make it possible to embrace the genetic complexity of common human cancers in global fashion. Tools are currently available, or are being developed, for the identification of all changes that take place in cancer at the DNA, RNA, and protein levels. In particular, the use of microarrays for the comprehensive analysis of RNA expression in human tumor samples holds much promise.

#### **Faculty of Computers and Information**

##### **Dept. of Information Technology**

##### **٩٨٠. Secure IP Mobility Management for Vanet**

Sanaa Mohamed Ahmed Taha

*Springer - Verlag, (2013)*

Nowadays, academic and industry are concerning about supporting vehicular networks with seamless communications, by which mobile nodes (MNs), i.e., vehicles, are allowed to roam through different RoadSide Units (RSUs) while keeping their active IP sessions [1]. Achieving such communications is required to support IP-based applications, such as video streaming and infotainment. Mobility management protocols, such as Mobile IPv6 (MIPv6) and the Network Mobility (NEMO) protocols, are envisioned to implement seamless communications in mobile networks, including Vehicular Ad Hoc Networks (VANETs).

##### **Dept. of Operation Research and Decision Support**

##### **98١. TOPSIS Algorithms for Multiple Objectives Decision Making: Large Scale Programming Approach**

Tarek Hanafi Mohamed AbouElEnien

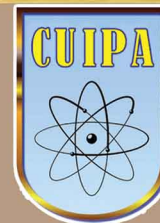
*Lambert Academic Publishing, (2013)*

This book consists of five chapters. Chapter (1) presents a literature review on the theory, softwares and applications of multiple criteria decision making problems. In chapter (2), we extend TOPSIS (Technique for Order Preference by Similarity Ideal Solution) for solving Large Scale Multiple Objective Decision Making (LSMODM) problems. In Chapter (3), we extend TOPSIS for solving LSMODM problems with fuzzy parameters in the right hand side of the independent constraints. In chapter (4), we extend TOPSIS for solving Interactive Large Scale Multiple Objective Programming problems with fuzzy parameters in the objective functions and the right hand side of the independent constraints. Chapter (5) focuses on the solution of a Large Scale Integer Linear Multiple Objective Decision Making with chance constraints (CHLSILMODM) of a special type through the TOPSIS approach.





Cairo University



# **(3) Medical Sciences Sector**

**3-1 Faculty of Medicine**

**3-2 Faculty of Oral & Dental Medicine**

**3-3 Faculty of Pharmacy**

**3-4 National Cancer Institute**

**3-5 Faculty of Physical Therapy**

**3-6 Faculty of Nursing**

CAIRO UNIVERSITY

Publication  
in  
Journals

## Faculty of Medicine

### Dept. of Anatomy

#### 982. Thyroid Hormone Dysfunctions Affect the Structure of Rat Thoracic Aorta: A Histological and Morphometric Study

S.M. Zaki and M.F. Youssef

*Folia Morphologica*, 72(4): 333-339 (2013) IF: 0.469

**Background:** There are limited data about the influence of hypothyroidism and hyperthyroidism on the connective tissue component and smooth muscle cells of the thoracic aorta. The aim was to study the histological changes of the wall of the thoracic aorta in the hypothyroid and hyperthyroid rats. Morphometric measurements were also done.

**Materials and Methods:** Thirty adult rats were used. They were divided into control, hyperthyroid, and hypothyroid groups. Each group consisted of 10 rats. The animals were sacrificed at the end of 8 weeks and the descending aorta was excised. Sections were stained with haematoxylin and eosin, orcein and Masson's trichrome stains. The morphometric measurement included: number of smooth muscle cell nuclei, number of the elastic lamellae, thickness of the tunica media, elastic fibre optic density, and relative collagen area.

**Results:** Atheromatous plaques had been observed in the hyperthyroid group. Thinning and rupture of the elastic lamellae had been observed in the hypothyroid group; these were accompanied with intimal ulceration and aortic dissection. The average number of smooth muscle cell nuclei in the hyperthyroid group had doubled and tripled compared to their fellows in the control and hypothyroid groups, respectively. The thickness of the tunica media increased in the hyperthyroid and hypothyroid groups by 75% and 35%. In addition, the relative collagen area increased in the previously mentioned groups by 142% and 120%, respectively. On the other hand, the mean elastic fibre optic density decreased in both groups by 30%.

**Conclusions:** Structure wall affections of the intima and media of the descending aorta were associated with the thyroid hormone dysfunctions. These changes were more severe in the hypothyroid group.

**Keywords:** Hyperthyroidism; Hypothyroidism; Descending Aorta.

### Dept. of Andrology and Sexology

#### 983. Erectile Dysfunction

Rany Mohamed Mahmoud Shamloul and Hussein Ghanem

*The Lancet*, 381:153-165 (2013) IF:39.06

Erectile dysfunction is a common clinical entity that affects mainly men older than 40 years. In addition to the classical causes of erectile dysfunction, such as diabetes mellitus and hypertension, several common lifestyle factors, such as obesity, limited or an absence of physical exercise, and lower urinary tract symptoms, have been linked to the development of erectile dysfunction. Substantial steps have been taken in the study of the association between erectile dysfunction and cardiovascular disease. Erectile dysfunction is a strong predictor for coronary artery disease, and cardiovascular assessment of a non-cardiac patient presenting with erectile dysfunction is now recommended

Substantial advances have occurred in the understanding of the pathophysiology of erectile dysfunction that ultimately led to the development of successful oral therapies, namely the phosphodiesterase type 5 inhibitors. However, oral phosphodiesterase type 5 inhibitors have limitations, and present research is thus investigating cutting-edge therapeutic strategies including gene and cell-based technologies with the aim of discovering a cure for erectile dysfunction.

#### 984. Drug Addiction and Sexual Dysfunction

Adham Zaazaa, Anthony J. Bella and Rany Shamloul

*Endocrinology and Metabolism Clinics of North America*, 42: 585-592 (2013) IF:3.792

Even though alcohol is prevalent in many societies with many myths surrounding its sexual-enhancing effects, current scientific research cannot provide a solid conclusion on its effect on sexual function. The same concept applies to tobacco smoking; however, most of the current knowledge tends to support the notion that it, indeed, can negatively affect sexual function. Cannabinoid receptors in the human cavernous report the nonrelaxing effects of marijuana. Heroin exerts a depletion effect on plasma levels of free testosterone and raises testosterone-binding globulin levels, irrespective of age, amount of heroin intake per day, and period of contact with the drug with no effect on the pituitary gonadotropins. Initially, the use of cocaine may enhance the sexual functioning of men, but prolonged use may diminish sexual desire and performance and may contribute to difficulty in achieving orgasm.

**Keywords:** Drug addiction; Sexual dysfunction; Heroin; Cocaine.

#### 985. Androgen Receptor Expression Relationship with Semen Variables in Infertile Men with Varicocele

Adel A. Zalata, Naglaa Mokhtar, Abd El-Naser Badawy, Gamal Othman, Moheiddin Alghobary and Taymour Mostafa

*J. Urology*, 189 (6): 2243-2247 (2013) IF: 3.696

**Purpose:** Androgen receptor, a member of the nuclear receptor superfamily, has important roles in male reproductive function. It is required for sexual differentiation, pubertal development, spermatogenesis regulation, meiosis completion and spermatocyte transition to haploid round spermatids. We assessed the association of androgen receptor expression and semen variables in infertile men with varicocele.

**Materials and Methods:** A total of 299 men were grouped into healthy, fertile controls, infertile men without varicocele and men with infertility associated with varicocele. A history was obtained, clinical examination and semen analysis were done and reproductive hormones were estimated. Androgen receptor expression and the acrosome reaction were determined in recovered spermatozoa.

**Results:** Androgen receptor expression was significantly decreased in infertile men with varicocele more than in infertile men without varicocele compared to fertile controls. Androgen receptor correlated positively with sperm count, motility, normal forms, velocity, linear velocity, acrosome reaction and  $\alpha$ -glucosidase. It correlated negatively with serum follicle-stimulating hormone and estradiol. Multiple stepwise regression analysis of androgen receptor expression revealed that the sperm

acrosome reaction and linearity index were the most affected independent variables.

**Conclusions:** Androgen receptor expression was significantly decreased in infertile men with varicocele more than in infertile men without varicocele compared to fertile men. Androgen receptor expression correlated positively with sperm count, motility, normal forms, velocity, linear velocity and acrosome reaction.

**Keywords:** Testis; Infertility; Male; Spermatozoa; Varicocele; Receptors; Androgen.

### 986. Position Paper: Management of Men Complaining of a Small Penis Despite an Actually Normal Size

Hussein Mohamed Hafez Ghanem, Sidney Glina, Pierre Assalian and Jacques Buvat

*The Journal of Sexual Medicine, 10 (1): 294-303 (2013) IF:3.513*

**Introduction:** with the worldwide increase in penile augmentation procedures and claims of devices designed to elongate the penis, it becomes crucial to study the scientific basis of such procedures or devices, as well as the management of a complaint of a small penis in men with a normal penile size.

**Aim:** The aim of this work is to study the scientific basis of opting to penile augmentation procedures and to develop guidelines based on the best available evidence for the management of men complaining of a small penis despite an actually normal size.

**Methods:** We reviewed the literature and evaluated the evidence about what the normal penile size is, what patients complaining of a small penis usually suffer from, benefits vs. complications of surgery, penile stretching or traction devices, and outcome with patient education and counseling. Repeated presentation and detailed discussions within the Standard Committee of the International Society for Sexual Medicine were performed.

**Main Outcome Measure:** Recommendations are based on the evaluation of evidence-based medical literature, widespread standards committee discussion, public presentation, and debate.

**Results:** We propose a practical approach for evaluating and counseling patients complaining of a small-sized penis.

**Conclusions:** Based on the current status of science, penile lengthening procedure surgery is still considered experimental and should only be limited to special circumstances within research or university institutions with supervising ethics committees.

**Keywords:** Small penis; Dysmorphophobia; Body dysmorphic Disorder; Penile augmentation.

### 987. Sop Conservative (Medical and Mechanical) Treatment of Erectile Dysfunction

Hartmut Porst, Arthur Burnett, Gerald Brock, Hussein Ghanem, Giuliano, Sidney Glina, Wayne Hellstrom, Antonio Martin-Morales and Andrea Salonia

*Journal of Sexual Medicine, 10 (1): 130-171 (2013) IF: 3.513*

**Introduction:** Erectile dysfunction (ED) is the most frequently treated male sexual dysfunction worldwide. ED is a chronic condition that exerts a negative impact on male self-esteem and

nearly all life domains including interpersonal, family, and business relationships.

**Aim:** The aim of this study is to provide an updated overview on currently used and available conservative treatment options for ED with a special focus on their efficacy, tolerability, safety, merits, and limitations including the role of combination therapies for monotherapy failures.

**Methods:** The methods used were PubMed and MEDLINE searches using the following keywords: ED, phosphodiesterase type 5 (PDE5) inhibitors, oral drug therapy, intracavernosal injection therapy, transurethral therapy, topical therapy, and vacuum-erection therapy/constriction devices. Additionally, expert opinions by the authors of this article are included.

**Results:** Level 1 evidence exists that changes in sedentary lifestyle with weight loss and optimal treatment of concomitant diseases/risk factors (e.g., diabetes, hypertension, and dyslipidemia) can either improve ED or add to the efficacy of ED-specific therapies, e.g., PDE5 inhibitors. Level 1 evidence also exists that treatment of hypogonadism with total testosterone < 300 ng/dL (10.4 nmol/L) can either improve ED or add to the efficacy of PDE5 inhibitors. There is level 1 evidence regarding the efficacy and safety of the following monotherapies in a spectrum-wide range of ED populations: PDE5 inhibitors, intracavernosal injection therapy with prostaglandin E1 (PGE1, synonymous alprostadil) or vasoactive intestinal peptide (VIP)/phenolamine, and transurethral PGE1 therapy. There is level 2 evidence regarding the efficacy and safety of the following ED treatments: vacuum-erection therapy in a wide range of ED populations, oral L-arginine (3–5 g), topical PGE1 in special ED populations, intracavernosal injection therapy with papaverine/phenolamine (bimix), or papaverine/phenolamine/PGE1 (trimix) combination mixtures. There is level 3 evidence regarding the efficacy and safety of oral yohimbine in nonorganic ED. There is level 3 evidence that combination therapies of PDE5 inhibitors + either transurethral or intracavernosal injection therapy generate better efficacy rates than either monotherapy alone. There is level 4 evidence showing enhanced efficacy with the combination of vacuum-erection therapy + either PDE5 inhibitor or transurethral PGE1 or intracavernosal injection therapy. There is level 5 evidence (expert opinion) that combination therapy of PDE5 inhibitors + L-arginine or daily dosing of tadalafil + short-acting PDE5 inhibitors pro re nata may rescue PDE5 inhibitor monotherapy failures. There is level 5 evidence (expert opinion) that adding either PDE5 inhibitors or transurethral PGE1 may improve outcome of penile prosthetic surgery regarding soft (cold) glans syndrome. There is level 5 evidence (expert opinion) that the combination of PDE5 inhibitors and dapoxetine is effective and safe in patients suffering.

**Keywords:** Erectile dysfunction; Oral drug treatment; Phosphodiesterase inhibitors; Intracavernous self-injection therapy; Transurethral alprostadil therapy; Combination therapies; Vacuum device therapy.

### 988. Sop: Corpus Cavernosum Assessment (Cavernosography/Cavernosometry)

Hussein Mohamed Hafez Ghanem and Hussein Ghanem

*The Journal of Sexual Medicine, 10 (1): 111-114 (2013) IF:3.513*

**Introduction:** There is no universal gold standard diagnostic test to differentiate psychogenic from organic erectile dysfunction



(ED). Cavernosography/ cavernosometry has been used to evaluate veno- occlusive dysfunction (VOD) in men with a proposed organic ED.

**Aim:** To develop evidence-based guidelines for the performance and interpretation of cavernosography cavernosometry.

**Methods:** Review the methodology behind cavernosography cavernosometry and evaluate the evidence that supports its use and interpretation of results.

**Main Outcome Measure:** Expert opinion based on review of the literature, extensive internal committee discussion, public presentation, and debate.

**Results:** The detailed technique of cavernosography cavernosometry is described An evidence ased perspective to the use and in terpretation of cavernosometry is presented.

**Conclusion:** The positive predictive value of cavernosometry still needs further assessment. It is unknown how many potent men would test positive for VOD (false positive).

**Keywords:** Cavernosometry; Cavernosography; Corpus cavernosum assessment; Venogenic; Erectile dysfunction.

### 989. Sop: Physical Examination and Laboratory Testing for Men with Erectile Dysfunction

Hussein Mohamed Hafez Ghanem, Andrea Salonia and Antonio Martin-Morales

*The Journal of Sexual Medicine, 10 (1): 108-110 (2013) IF:3.513*

**Introduction:** Physical examination and laboratory evaluation of men with erectile dysfunction (ED) are opportunities to identify potentially life-threatening etiologies and comorbid conditions.

**Aim:** To review genital anatomy, identify any physical abnormalities, assess for comorbid conditions, and reveal significant risk factors for ED.

**Methods:** Expert opinion was based on evidence- based medical literature and consensus discussions between members of this International Society for Sexual Medicine (ISSM) standards committee.

**Results:** For men with ED, a general examination including blood pressure and pulse measurements and a focused genital exam are advised. Fasting blood sugar, serum total testosterone, prolactin levels, and a lipid profile may reveal significant comorbid conditions.

**Conclusions:** Though physical examination and laboratory evaluation of most men with ED may not reveal the exact diagnosis, these opportunities to identify critical comorbid conditions should not be missed.

**Keywords:** Erectile dysfunction; Diagnosis; Physical examination; Laboratory tests.

### 990. The Global Online Sexuality Survey (GOSS): the United States of America in 2011 Chapter III- Premature Ejaculation Among English-Speaking Male Internet Users

Osama Shaeer

*Journal of Sexual Medicine, 10 (7): 1882-1888 (2013) IF:3.513*

**Introduction:** The Global Online Sexuality Survey (GOSS) is a world-wide epidemiologic study of sexuality and sexual disorders. in 2010, the first report of GOSS came from the Middle East.

**Aim:** This report studies the prevalence rate of premature ejaculation (PE) in USA as of 2011-2012 and evaluates risk factors for PE. Main Outcome Measures Prevalence of PE as per the International Society of Sexual Medicine's (ISSM) definition.

**Methods:** GOSS was randomly deployed to English-speaking male web surfers in USA via paid advertising on Facebook®, comprising 146 questions.

**Results:** 1133 participants reported on sexual function with a mean age was 52.38 years  $\pm$  14.5. As per the ISSM definition of PE, the prevalence rate of premature ejaculation in USA as of 2011 was 6.3%. This is in contrast to 49.6% as per the Premature Ejaculation Diagnostic Tool (PEDT), 77.6% as per unfiltered subjective reports and 14.4% as per subjective reporting on more consistent basis. 56.3% of the latter reported life-long PE. 63.2% could be classified as having natural variable PE. ED is a possible predisposing factor for acquired PE, while Genital size concerns may predispose to life-long PE. Age, irregular coitus, circumcision and the practice of masturbation did not pose a risk for PE, among other risk factors. Oral treatment for PE was more frequently used and reported to be more effective than local anesthetics, particularly in those with life-long PE.

**Conclusion:** Applying the ISSM definition, prevalence of PE is far less than diagnosed by other methods; 6.3% among internet users in USA as of the year 2011. PEDT measures both lifelong and acquired PE, in addition to 35% men with premature-like ejaculatory dysfunction, making it inaccurate for isolating life-long and acquired PE cases.

**Keywords:** USA; Prevalence; Premature Ejaculation; ISSM; Definition; PEDT.

### 991. The Global Online Sexuality Survey: Public Perception of Female Genital Cutting Among Internet Users in the Middle East

Osama Shaeer and Eman Shaeer

*Journal of Sexual Medicine, 10: 2904-2911 (2013) IF:3.513*

**Introduction:** Female genital cutting (FGC) is a ritual involving cutting part or all of the female external genitalia, performed primarily in Africa. Understanding the motivation behind FGC whether religious or otherwise is important for formulating the anti-FGC messages in prevention and awareness campaigns.

**Aim:** Investigation of opinion over FGC, the root motive/s behind it, in addition to the current prevalence of FGC among Internet users in the Middle East. Main Outcome Measures Prevalence of and public opinion on FGC among Internet users.

**Methods:** The Global Online Sexuality Survey (GOSS) was undertaken in the Middle East via paid advertising on Facebook®, comprising 146 questions.

**Results:** 31.6% of 992 participants experienced FGC at an average age of 9.6  $\pm$  3.5 years, mostly in Egypt (50.2%). FGC was more prevalent among Muslims (36.9%) than Christians (18.8%), more in rural areas (78.7%) than urban (47.4%), and was performed primarily by doctors (54.7%) and nurses (9.5%). Whether or not it is necessary for female chastity, FGC was reported as highly necessary (22.5%), necessary (21.6%), more so among males, more among those with rural origin, with no difference as per educational level. Religious opinion among Muslims was: 55.4% anti-FGC and 44.6% pro-FGC. Only 3.7% saw it as a mandate of Islam.

**Conclusion:** An important motivation driving FGC seems to be males seeking female chastity rather than religion, especially with



FGC not being an Islamic mandate, not to undermine the importance of religion among other motives. School and university education were void of an effective anti-FGC message, which should be addressed. There is a shift towards doctors and nurses for performing FGC, which is both a threat and an opportunity. We propose that the primary message against FGC should be delivered by medical and paramedical personnel who can deliver a balanced and confidential message.

**Keywords:** Female genital cutting; Female genital mutilation; Prevalence; Islam; Middle East; Egypt.

### 992. Effect of Chronic Low-Dose Tadalafil on Penile Cavernous Tissues in Diabetic Rats

Mohamed E. Mostafa, Amira M. Senbel and Taymour Mostafa

*Urology, 81(6): 1253-1259 (2013) IF:2.424*

**Objective:** To assess the effect of chronic low-dose administration of tadalafil (Td) on penile cavernous tissue in induced diabetic rats.

**Methods:** The study investigated 48 adult male albino rats, comprising a control group, sham controls, streptozotocin-induced diabetic rats, and induced diabetic rats that received Td low-dose daily (0.09 mg/ 200 g weight) for 2 months. The rats were euthanized 1 day after the last dose. Cavernous tissues were subjected to histologic, immunohistochemical, morphometric studies, and measurement of intracavernosal pressure and mean arterial pressure in anesthetized rats.

**Results:** Diabetic rats demonstrated dilated cavernous spaces, smooth muscles with heterochromatic nuclei, degenerated mitochondria, vacuolated cytoplasm, and negative smooth muscle immunoreactivity. Nerve fibers demonstrated a thick myelin sheath and intra-axonal edema, where blood capillaries exhibited thick basement membrane. Diabetic rats on Td showed improved cavernous organization with significant morphometric increases in the area percentage of smooth muscles and elastic tissue and a significant decrease of fibrous tissue. The Td-treated group showed enhanced erectile function (intracavernosal pressure/mean arterial pressure) at 0.3, 0.5, 1, 3, and 5 Hz compared with diabetic group values at the respective frequencies ( $P < .05$ ) that approached control values.

**Conclusion:** Chronic low-dose administration of Td in diabetic rats is associated with substantial improvement of the structure of penile cavernous tissue, with increased smooth muscles and elastic tissue, decreased fibrous tissue, and functional enhancement of the erectile function. This raises the idea that the change in penile architecture with Td treatment improves erectile function beyond its half-life and its direct pharmacologic action on phosphodiesterase type 5.

**Keywords:** Erectile dysfunction; PDE-5 Inhibitors; Tadalafil; Penis; Erection.

### 993. Seminal Soluble Fas Relationship with Oxidative Stress in Infertile Men with Varicocele

Gamil A. Tawadrous, Amal A. Aziz and Taymour Mostafa

*Urology, 82 (4): 820-823 (2013) IF: 2.424*

**Objective:** To assess seminal plasma soluble Fas (sFas) relationship with oxidative stress and varicocele (Vx) grade in infertile men.

**Methods:** In all, 230 men were prospectively investigated: fertile men without Vx, fertile men with Vx, infertile men without Vx, and infertile men with Vx. In their semen, seminal oxidant (malondialdehyde [MDA]), antioxidants (ascorbic acid, glutathione peroxidase [GPx], catalase [CAT], and superoxide dismutase [SOD]), and seminal sFas were assessed.

**Results:** Either fertile or infertile men with Vx demonstrated significantly higher seminal oxidants (MDA) and significantly lower seminal antioxidants (SOD, GPx, CAT, and ascorbic acid), sFas compared with fertile or infertile men without Vx. Infertile men with or without Vx had significantly higher seminal MDA and significantly lower seminal antioxidants, sFas compared with fertile men with or without Vx. Men with Vx grade III had significantly higher seminal MDA and significantly lower antioxidants, sFas compared with Vx grade II and I, respectively. Seminal sFas demonstrated significant positive correlation with sperm count, sperm motility, sperm normal forms, seminal ascorbic acid, SOD, GPx, and CAT and significant negative correlation with seminal MDA.

**Conclusion:** Down regulation of seminal sFas in Vx associated men is related to increased oxidative stress and is correlated with Vx grade.

**Keywords:** Male infertility; Semen; Smoking; Sfas.

### 994. Tumor Necrosis Factor- $\alpha$ Gene Polymorphism Relationship to Seminal Variables in Infertile Men

Adel Zalata, Amany Atwa, Abd El-Naser Badawy, Amal Aziz, Rizk El-Baz, Samir Elhanbly and Taymour Mostafa

*Urology, 81 (5): 962-929 (2013) IF: 2.424*

**Objective:** To assess the tumor necrosis factor (TNF)- $\alpha$  gene polymorphism relationship with seminal variables in fertile men (N) and those with as the nozoospermia (A), as the noteratozoospermia (AT), and oligoasthenoteratozoospermia (OAT).

**Materials and Methods:** A total of 50 infertile men without a female factor who were attending a fertility clinic and 48 fertile men were randomly screened for semen analysis, analysis of the TNF- $\alpha$  promoter region for polymorphism, seminal caspase-9, acrosin activity,  $\alpha$ -glucosidase, and reproductive hormones.

**Results:** The TNF- $\alpha$  GG genotype was present in 83.9%, 72.7%, 66.7%, and 59.5%, the TNF- $\alpha$  AA genotype in 3.2%, 6.8%, 10.4%, and 11.9%, and TNF- $\alpha$  AG genotype in 12.9%, 20.5%, 22.9%, and 28.6% in the N, A, AT, OAT groups, respectively. The occurrence of A allele was significantly greater among infertile patients than among fertile controls (21.6% vs 9.7%; odds ratio 0.388, 95% confidence interval 0.2 to 0.75,  $P = .005$ ). Men with the TNF- $\alpha$  AA genotype demonstrated a significant decrease in the sperm count, sperm motility, normal sperm morphology, acrosin activity, and seminal  $\alpha$ -glucosidase and a significant increase in seminal caspase-9 compared with those with the TNF- $\alpha$  GG genotype.

**Conclusion:** This single nucleotide polymorphism in the TNF- $\alpha$  (-308) gene was associated with significantly increased seminal caspase-9 and a significantly decreased sperm count; sperm motility; normal sperm morphology; acrosin activity and seminal  $\alpha$ -glucosidase.

**Keywords:** Male infertility; Semen; TNF alpha; Polymorphism.

### 995. A 6-Month, Prospective, Observational Study of Pde5 Inhibitor Treatment Persistence and Adherence in Middle Eastern and North African Men with Erectile Dysfunction

Amr El-Meliegy, Danny Rabah, Kutaiba Al-Mitwalli, Taymour Mostafa, Tarek Hussein, Mohamed Istarabadi and Yao LeSirel Gurbuzi

*Current Medical Research and Opinion*, 29 (6): 707-717 (2013)  
IF:2.263

**Background:** Erectile dysfunction (ED) negatively impacts quality of life. Phosphodiesterase type 5 inhibitors (PDE5Is) are effective in treating ED; however, rates of discontinuation remain high.

**Objectives:** To assess on-demand PDE5I treatment persistence and adherence through 6 months in Middle Eastern and North African (MENA) men with ED in a prospective, non-interventional, observational trial.

**Research Design and Methods:** Enrolled men were  $\geq 18$  years old from Saudi Arabia, Egypt, and the United Arab Emirates, PDE5I naïve, and sexually active. PDE5Is were selected per routine clinical practice. Persistence was defined as use of  $\geq 1$  dose during the prior 4 weeks, adherence as compliance with dosing instructions during the most recent dose. Logistic regression models were used to identify factors associated with persistence and adherence.

**Main Outcome Measures:** Persistence and Adherence Questionnaire; Partner Relationship Questionnaire; Self-Esteem and Relationship Questionnaire; International Index of Erectile Function (IIEF); Erectile Dysfunction Inventory of Treatment Satisfaction.

**Results:** Patients' (n = 493) mean age was 49.8 years, mean BMI was 29.3, and the majority (n = 354, 71.8%) were from Saudi Arabia. Tadalafil was the most prescribed PDE5I (69.6%), versus sildenafil (15.4%), or vardenafil (15.0%). Patients' mean IIEF-Erectile Function scores improved from moderate to mild and Erection Hardness Scores (SD) improved from 1.8 (1.0) at baseline to 3.5 (0.7) at 6 months. At 6 months, 64.9% of patients were treatment persistent (tadalafil, 68.8%, sildenafil, 65.8%, and vardenafil, 45.9%) and 59.6% were adherent. Factors significantly predictive (p < 0.05) of persistence at 6 months included age, employment status, and ED severity. Factors significantly predictive of adherence were age, employment status, and duration of ED. Interpretation of differences between drugs was limited by substantial differences in prescription rates between countries.

**Conclusions:** At 6 months, 64.9% of men were treatment persistent. In this study, age, employment status, ED severity, and duration of ED were associated with persistence and adherence.

**Keywords:** Adherence; Erectile dysfunction; PDE5 Inhibitors; Persistence; Sildenafil; Tadalafil; Vardenafil.

### 996. Cavernous Antioxidant Effect of Green Tea, Epigallocatechin-3-Gallate with/ without Sildenafil Citrate Intake in Aged Diabetic Rats

T. Mostafa, D. Sabry, A. M. Abdelaal, I. Mostafa and M. Taymour

*Andrologia*, 45 (4): 272-277 (2013) IF:1.748

This study aimed to assess the cavernous antioxidant effect of green tea (GT), epigallocatechin-3-gallate (EGCG) with/without sildenafil citrate intake in aged diabetic rats. One hundred and four aged male white albino rats were divided into controls that received ordinary chow, streptozotocin (STZ)-induced aged diabetic rats, STZ-induced diabetic rats on infused green tea, induced diabetic rats on epigallocatechin-3-gallate and STZ-induced diabetic rats on sildenafil citrate added to EGCG. After 8 weeks, dissected cavernous tissues were assessed for gene expression of eNOS, cavernous malondialdehyde (MDA), glutathione peroxidase (GPx), cyclic guanosine monophosphate (cGMP), and serum testosterone (T). STZ-induced diabetic rats on GT demonstrated significant increase in cavernous eNOS, cGMP, GPx and significant decrease in cavernous MDA compared with diabetic rats. Diabetic rats on EGCG demonstrated significant increase in cavernous eNOS, cGMP, GPx and significant decrease in cavernous MDA compared with diabetic rats or diabetic rats on GT. Diabetic rats on EGCG added to sildenafil showed significant increase in cavernous eNOS, cGMP and significant decrease in cavernous MDA compared with other groups. Serum T demonstrated nonsignificant difference between the investigated groups. It is concluded that GT and EGCG have significant cavernous antioxidant effects that are increased if sildenafil is added.

**Keywords:** Diabetes; Epigallocatechin-3-gallate; Green tea; Oxidative stress; Sildenafil; Testosterone.

### 997. Sperm DNA and RNA Abnormalities in Fertile and Oligoasthenoteratozoospermic Smokers

I. Selit, M. Basha, A. Maraee, S. H. El-Naby, N. Nazeef, R. El-Mehrath and Taymour Mostafa

*Andrologia*, 45 (1): 35-39 (2013) IF:1.748

This study aimed to assess sperm DNA and RNA abnormalities in fertile and oligoasthenoteratozoospermic (OAT) smokers. In all, 140 subjects were included and classified into fertile nonsmokers, fertile smokers, OAT nonsmokers and OAT smokers. They were subjected to history taking, clinical examination, semen analysis, assessment of sperm DNA and RNA abnormalities. The results showed that an increased percentage of abnormal sperm DNA and RNA was demonstrated in fertile smokers compared with fertile nonsmokers and in OAT smokers compared with OAT nonsmokers. Increased percentage of severe, moderate sperm DNA and RNA damage was demonstrated in fertile heavy smokers compared with fertile light smokers and in OAT heavy smokers compared with OAT light smokers. It is concluded that smoking has a negative impact on sperm DNA and RNA abnormalities that is accentuated in heavy smokers compared with light smokers.

**Keywords:** Male infertility; RNA; Semen; Smoking; Sperm DNA.

### 998. Addressing the Barriers to Optimal Management of Penile Fracture

Rany Mohamed Mahmoud Shamloul and Anthony J. Bella

*Canadian Urological Association Journal*, 7:258-259 (2013)  
IF:1.657

Immediate surgical repair is the standard of care and is superior to non-operative management for penile fracture. Nason and

colleagues add supportive evidence to conclusions based on more than a dozen series: prompt repair of the corpora is associated with far fewer complications following penile injury, most notably erectile dysfunction and penile deformity, and there is little to no role for delaying intervention or observation in these cases.

**Keywords:** Penile; Fracture.

### 999. A Study of the Possible Effects of Repeated Intracorporeal Self-Injection of Vasoactive Drugs in Patients With Elevated End Diastolic Velocity During Pharmacopenile Duplex Ultrasonography

Ashraf Hasan Fayez, Yasser El-Khayat, Hosam Hosny, Shady Zaki and Rany Shamloul

*Central European Journal of Urology*, 66: 210-214 (2013)

**Introduction:** The aim of the work is to evaluate the effect of repeated intracavernosal self-injection of vasoactive drugs in patients with elevated End Diastolic Velocity ( $>5$  cm/sec) during pharmacopenile duplex ultrasonography (PPDU).

**Methods:** Duplex evaluation was performed to the patients on self-injection therapy for comparison of end diastolic velocity and resistive index before and after completing the eight doses of IC self-injection.

**Results:** After the 8 trials of home therapy, 21 (52.5%) patients showed improvement in the duplex parameters regarding the end diastolic velocity, ten of them showed improvement in the EDV to the level of  $<5$  cm/sec. The effect of different factors that may contribute to the improvement in EDV to  $<5$  cm/sec are shown in the table 2. Age was the only predictive factor for successful response to home therapy intracavernous injection (ICI). Improvement in erectile response was assessed before and after the course of the therapy. Erection response to ICI during penile duplex improved in only six patients (E4 & E4-5)) to the point that it was sufficient for satisfactory sexual performance, 3 of them (7.5%) regained spontaneous erection and stopped using ICI (Table 3). The IIEF score was  $10.6 \pm 2.8$  before the home therapy and it became  $14 \pm 3.9$  one month after completing the treatment course (P value  $<0.001$ ).

**Conclusions:** Early rehabilitation of the patients with venous leakage ED using ICI may help to regain normal erection and avoid unnecessary penile prosthesis surgeries.

**Keywords:** erectile dysfunction; venous leakage; intracavernosal injection.

### 1000. Cell Phone Usage and Erectile Function

Badereddin Mohamad Al-Ali, Johanna Patzak, Katja Fischereder, Karl Pummer and Rany Shamloul

*Central European Journal of Urology*, 1: 75-77 (2013)

**Introduction:** The objective of this pilot study was to report our experience concerning the effects of cellphone usage on erectile function (EF) in men. **Material and Methods:** We recruited 20 consecutive men complaining of erectile dysfunction (ED) for at least six months (Group A), and another group of 10 healthy men with no complaints of ED (Group B). Anamnesis, basic laboratory investigations, and clinical examinations were performed. All men completed the German version of the Sexual Health Inventory for Men (SHIM) for evaluation of the International Index of Erectile Function (IIEF), as well as another questionnaire

designed by our clinicians that assessed cell phone usage habits.

**Results:** There was no significant difference between both groups regarding age, weight, height, and total testosterone (Table 1). The SHIM scores of Group A were significantly lower than that of Group B,  $11.2 \pm 5$  and  $24.2 \pm 2.3$ , respectively. Total time spent talking on the cell phone per week was not significantly higher in Group A over B,  $17.6 \pm 11.1$  vs.  $12.5 \pm 7$  hours. Men with ED were found to carry their 'switched on' cell phones for a significantly longer time than those without ED,  $4.4 \pm 3.6$  vs.  $1.8 \pm 1$  hours per day.

**Conclusions:** We found a potential correlation with cell phone usage and a negative impact on EF. Further large-scale studies confirming our initial data and exploring the mechanisms involved in this phenomenon are recommended.

**Keywords:** Testosterone; Erectile dysfunction.

### 1001. Clinical and Laboratory Profiles of A Large Cohort of Patients with Different Grades of Varicocele

Badereddin Mohamad Al-Ali, Rany Shamloul, Martin Pichler, Herbert Augustin and Karl Pummer

*Central European Journal of Urology*, 2: 71-74 (2013)

**Objective:** In this retrospective study we attempted to report our own data on the different clinical parameters in association with the presence and severity of varicocele in a large group of Austrian men. **Methods:** The records of 1,111 consecutive patients with clinical varicocele from 1993 to 2010 were evaluated. The presence, grade, and side of any varicocele were recorded. Semen samples, serum FSH, LH, and testosterone levels, and testicular volume were assessed.

**Results:** The mean age was  $28.8 (\pm 7.3)$  years. Three hundred seventeen (28.5%) patients presented with grade I varicocele, 427 (38.4%) with grade II varicocele, and 367 (33%) with grade III varicocele. Correlation between different grades of varicocele and semen quality indicated an over-representation of oligospermia and asthenoteratozoospermia in the group of grade III varicocele ( $p < 0.05$ ), whereas other parameters of semen quality showed no significant difference between the three groups. Serum testosterone levels and BMI were significantly associated ( $p < 0.05$ ) with the grade of varicocele, but no association was found with the other parameters analyzed.

**Conclusions:** Our analysis showed a significant relationship between the grade of varicocele and semen analysis. Moreover, higher testosterone levels and lower body mass index were associated with the higher grade of varicocele and decreased semen quality. More prospective studies are recommended.

**Keywords:** Body mass index; Varicocele; Follicle stimulating hormone (FSH); Luteinizing hormone (LH); Testosterone (T).

### 1002. Correlation Between Seminal Lead and Cadmium and Seminal Parameters in Idiopathic Oligoasthenozoospermic Males

Emad A. Taha, Sohair K. Sayed, Nagwa M Ghandour, Ali M. Mahran, Medhat A. Saleh, Magdy M. Amin and Rany Shamloul

*Central European Journal of Urology*, 1: 84-92 (2013)

**Introduction:** The Exact causes of the decline in semen quality are not yet known, environmental factors have been considered to

play an important role. Lead (Pb) and Cadmium (Cd) are two of the well-known reproductive toxicants to which humans are exposed occupationally and environmentally and can lead to negative effects on the testicular functions. The aim of this study was to evaluate lead and cadmium levels in seminal plasma of men with idiopathic oligoasthenozoospermia in comparison to fertile healthy controls and to correlate these levels with conventional semen parameters, sperm hypo-osmotic swelling (HOS) percentage, sperm DNA fragmentation percentage, and semen reactive oxygen species (ROS) levels.

**Material and Methods:** Thirty infertile male patients with idiopathic oligo and/or asthenozoospermia and thirty healthy fertile men, which was the control group, were included in the study. Lead and cadmium levels in seminal plasma, semen parameters, sperm HOS, sperm DNA fragmentation percentage and semen ROS assay were measured in all subjects.

**Results:** There was a significant increase in seminal lead and cadmium levels among infertile males in comparison to controls. There were significant negative correlations between seminal lead and cadmium levels on one hand and certain semen parameters especially progressive sperm motility and vitality (HOS). Importantly, significant positive correlations were noted between seminal lead and cadmium levels on one hand and sperm DNA fragmentation percentage and semen ROS level in infertile men and controls on the other hand.

**Conclusions:** Thus, men with idiopathic male infertility had higher levels of lead and cadmium in their semen which correlated with impairment of sperm motility and vitality percentages and more importantly with higher sperm DNA fragmentation% and semen ROS level.

**Keywords:** Azoospermia; Lead; Cadmium.

### 1003. Effect of Neonatal Administration of Estrogen, Antiestrogen, and Testosterone on the Histological Picture and Estrogen Receptor Pattern of the Adult Rat Prostate

Mohamed D.M. El-Shafei, Mohamed E.A. Mostafa and Taymour Mostafa

*Human Andrology*, 3: 1-5 (2013)

**Background:** Normal sexual development and functioning of the male reproductive organs are primarily controlled by androgens. However, estrogen also plays a role in the normal development, although this is not well defined.

**Aim:** The aim of this study was to assess the effect of neonatal administration of estrogen (E), antiestrogen (AE), and testosterone (T) on the histological picture and estrogen receptor (ER) pattern of the adult rat prostate.

**Materials and Methods:** In all, 40 male albino rats at the age of 2 days were divided into four equal groups: untreated controls, rats that received E, those that received AE, and those that received T orally for 5 days starting from the second day. All rats were euthanized at the age of 6 weeks, after which specimens from the ventral lobe of the prostate were obtained.

**Main Outcome Measures:** Histopathological and immune histochemical analysis of the investigated sections.

**Results:** In the E-treated rats, the diameter of the prostatic acini was reduced with increased fibromuscular stroma and epithelial hyperplasia. AE-treated or T-treated rats showed no histological changes compared with controls.

The prostate of E-treated rats exhibited strong immunoreactivity against the ER compared with that of AE-treated or T-treated rats. The mean area percentage of ER immunoreactivity showed a significant increase in E-treated rats compared with the controls, AE-treated rats, and T-treated rats.

**Conclusion:** The prostate, despite being an androgen-dependant gland, on exposure to E early in life could undergo structural disturbances that might lead to the development of prostatic disorders later.

**Keywords:** Antiestrogen; Development; Estrogen; Prostate; Testosterone.

### 1004. Psychotropics and Sexual Dysfunctions

Anthony J. Bella and Rany Shamloul

*Central European Journal of Urology*, 66: 466-471 (2013)

**Introduction:** Sexual dysfunction (SD) is common in patients taking antipsychotics, and is the most bothersome symptom and adverse drug effect compromising treatment compliance. Mechanisms involved in psychotropics – induced SD are either largely unknown or poorly understood. The aim of this review is to present an updated analysis of SD associated with the use of psychotropic drugs in psychiatric patients.

**Results:** Contemporary evidence from available studies demonstrates that SD rates are drug-related rather than drug-class specific, and that these rates vary widely. Mechanisms involved in psychotropics: induced SD are either largely unknown or poorly understood. Our understanding of psychotropics – induced SD is limited by the inability to differentiate whether these effects are really drug – induced or due to different inclusion criteria.

**Conclusions:** Rigorous research, basic and clinical, is needed to understand the exact incidence, severity and mechanisms involved in the development of SD induced by various psychotropic treatment regimens.

**Keywords:** Psychotropics; Sexual dysfunction.

### 1005. Seminal Osteopontin Relationship with Semen Variables in Infertile Men with Varicocele

Shawki El-Haggag, Laila Rashed, Neveen Y. Saleh, Mai Taymour and Taymour Mostafa

*Urology*, 3: 90-93 (2013)

**Purpose:** To assess seminal plasma osteopontin (OPN) relationship with semen variables in infertile and infertile men with varicocele (Vx). Patients and methods: A total of 88 men were investigated, who were divided into the following groups: healthy fertile men without Vx, healthy fertile men with Vx, oligoasthenozoospermic (OAT) infertile men without Vx, and OAT infertile men with Vx.

They were subjected to assessment of history, clinical examination, semen analysis, and assessment of seminal OPN, malondialdehyde (MDA), and glutathione peroxidase (GPx). Results: Infertile men associated with Vx showed a significant increase in seminal OPN and MDA, and a significant decrease in seminal GPx compared with infertile men without Vx and fertile men with or without Vx.

Infertile men without Vx showed a significant increase in seminal OPN and MDA, and a significant decrease in seminal GPx compared with fertile men with or without Vx. Fertile men with Vx showed a significant increase in seminal OPN and MDA,

and a significant decrease in seminal GPx compared with fertile men without Vx. Seminal OPN showed a significant positive correlation with seminal MDA, significant negative correlations with sperm count, sperm motility, sperm normal forms, seminal GPx, and a nonsignificant correlation with age.

**Conclusion:** Seminal OPN is significantly increased in infertile OAT men associated with Vx. Seminal OPN showed a positive correlation with seminal MDA and sperm abnormal forms and a significant negative correlation with sperm count, sperm motility, and seminal GPx.

**Keywords:** Male infertility; Osteopontin; Oxidative stress; Semen; Varicocele.

### 1006. The Effect of Radiofrequency Waves Produced by Cell Phones on the Semen Quality of Infertile Men

Shaer, Kamal Z.; Elkhiat, Yasser I. and Algashaa, Khadeeja A.

*Human Andrology*, (2013)

**Purpose:** The aim of this study was to determine the effect of radiofrequency electromagnetic waves emitted from cell phones on the semen quality of infertile men and also to determine whether these could aggravate their infertility problem.

**Patients and methods:** This pilot study was carried out on 316 infertile men divided into four groups according to the duration of their daily cell phone use: group I, control group of non-cell-phone users; group II who used cell phones for 1 h/day or less; group III who used cell phones for 1–2 h/day; and group IV who used cell phones for more than 2 h/day. The duration of infertility for the cell phone users was  $1.7 \pm 0.7$  years, and they had been users since  $5.7 \pm 1.9$  years. The patients were subjected to medical taking, history of cell phone use (period of cell phone use, frequency and duration of use per day, mode of use, and model of the cell phone), clinical examination, and conventional semen analysis according to WHO 2010 criteria. A stained smear was prepared from semen samples of all patients for sperm morphological analysis.

**Results:** There was no statistically significant difference as regards the sperm count between the groups. However, as regards the total sperm count and progressive motility, there was a statistically significant difference between the control group and all cell phone user groups.

As regards the occurrence of abnormal forms, the control group showed a statistically significant difference on comparison with the less than 1 h/day cell phone use group and a highly significant difference on comparison with the more than 2 h/day cell phone use group.

There were no statistically significant differences in terms of semen parameters between those who kept their cell phones in belt holders and those who kept them in their trouser pockets and between Bluetooth users and nonusers. Moreover, no statistically significant differences were found in terms of semen parameters between those who used original brands and those who used imitations.

**Conclusion:** Prolonged daily use of cell phones has negative effects on the semen quality, especially sperm motility, progressive motility, and morphology. The mode of cell phone use and the cell phone model do not add to the problem. Infertile men may be more vulnerable to this negative effect.

### Dept. of Anesthesiology

### 1007. A Novel Mutation of the Ornithine Transcarbamylase Gene Leading to Fatal Hyperammonemia in a Liver Transplant Recipient

A. Mukhtar, H. Dabbous, R. El Sayed, F. Aboulfetouh, M. Bahaa, A. Abdelaal, M. Fathy and M. El-Meteini

*American Journal of Transplantation*, 13: 1084-1087 (2013)  
IF: 6.192

Ornithine transcarbamylase (OTC) deficiency (OTCD) is an X-linked urea cycle disorder. Being an X-linked disease, the onset and severity of the disease may vary among female carriers. Some of them start to develop the disease early in life, whereas others remain asymptomatic throughout their lives.

Our patient was a 42-year-old man who developed severe hyperammonemia and fatal brain edema after receiving a right lobe graft from an asymptomatic female living donor with unrecognized OTCD. The donor developed hyperammonemia and disturbed level of consciousness that was managed successfully by hemodialysis. Molecular testing of the OTC gene in the donor revealed a heterozygous nonsense mutation (c.429T > A) in exon 5.

**Keywords:** Living donor liver transplant; Ornithine transcarbamylase deficiency.

### 1008. The Effect of Magnesium Sulphate Infusion on the Incidence and Severity of Emergence Agitation in Children Undergoing Adenotonsillectomy Using Sevoflurane Anaesthesia

M. Abdulatif, A. Ahmed and A. Mukhtar S. Badawy

*Anaesthesia*, 68 (10): 1045-1052 (2013) IF: 3.486

This randomised, controlled, double-blind study investigated the effects of intra-operative magnesium sulphate administration on the incidence of emergence agitation in children undergoing adenotonsillectomy using sevoflurane anaesthesia. Seventy children were randomly allocated to receive a 30 mg.kg<sup>-1</sup> bolus of intravenous magnesium sulphate after induction of anaesthesia followed by a continuous infusion of 10 mg.kg<sup>-1</sup>.h<sup>-1</sup> or an equal volume of saline 0.9%.

All children received titrated sevoflurane anaesthesia adjusted to maintain haemodynamic stability. The Pediatric Anesthesia Emergence Delirium scale and the Children's Hospital of Eastern Ontario Score were used for the assessment of postoperative emergence agitation and pain, respectively. Emergence agitation was more common in the control group than in the magnesium group (23 (72%) and 12 (36%), respectively ( $p = 0.004$ )), with a relative risk of 0.51 (95% CI 0.31–0.84), an absolute risk reduction of 0.35 (95% CI 0.10–0.54), and number needed to treat of 3 (95% CI 2–9). Postoperative pain scores were comparable in the two groups. Magnesium sulphate reduces the incidence and severity of emergence agitation in children undergoing adenotonsillectomy using sevoflurane anaesthesia and is not associated with increased postoperative side-effects or delayed recovery.



### 1009. A Comparative Study Between Amiodarone and Magnesium Sulfate as Antiarrhythmic Agents for Prophylaxis Against Atrial Fibrillation Following Lobectomy

Mohamed A. Khalil, Ahmed E. Al-Agaty, Wael G. Ali and Mohsen S. Abdel Azeem

*Journal of Anesthesia*, 27 (1): 56-61 (2013) IF: 0.867

**Purpose:** Atrial fibrillations are common after thoracic surgery. Amiodarone and magnesium sulfate have been used for the management of atrial fibrillation following cardiac and non-cardiac surgery. However, to our knowledge, comparisons of both drugs with each other and with a control group in relation to the prevention of AF following lung surgery have not been performed. Our primary aim in this study was to prospectively evaluate the prophylactic effects of magnesium sulfate and amiodarone used separately and compare them with a control group analyzed retrospectively during and following lobectomy surgeries.

**Patients and Methods:** The prophylactic value of amiodarone (group A; 219 patients) administered as an intravenous infusion (15 mg/kg for 48 h postoperatively) after a loading dose (5 mg/kg) was compared with magnesium sulfate (group M; 219 patients) administered intravenously as a loading dose (80 mg/kg magnesium sulfate over 30 min preoperatively) and then as an intravenous infusion (8 mg/kg/h for 48 h) in 438 patients undergoing lobectomy. These two groups were compared with a control group of 219 patients who were analyzed retrospectively.

**Results:** The results showed significantly lower incidences of AF in groups A and M when compared with group C ( $P < 0.05$ ). There was no significant difference between the amiodarone and magnesium sulfate groups. However, the incidence of postoperative AF was lower in the amiodarone group, where only 21 (10 %) patients developed AF in comparison to 27 (12.5 %) patients in the magnesium sulfate group. Group C showed a higher incidence, 44 (20.5 %) patients, when compared with both groups. In addition, there were significant differences between the three groups concerning intensive care unit (ICU) and total hospital stays ( $P < 0.05$ ).

**Conclusion:** Our study showed that during the intra- and postoperative periods, both amiodarone and magnesium sulfate are effective at preventing the incidence of atrial fibrillation following lung resection surgery in comparison to the control group.

**Keywords:** Magnesium sulfate; Amiodarone; Atrial fibrillation; Lobectomy.

### 1010. Levosimendan is Superior to Dobutamine as an Inodilator in the Treatment of Pulmonary Hypertension for Children Undergoing Cardiac Surgery

Abdelhay A. Ebade, Mohamed A. Khalil and Ahmed K. Mohamed

*Journal of Anesthesia*, 27 (3): 334-339 (2013) IF: 0.867

**Purpose:** To compare the effectiveness of levosimendan and dobutamine in reducing pulmonary artery pressure (PAP) and increasing cardiac output for children undergoing cardiac surgery. Patients and methods: The study included 50 patients with high systolic pulmonary artery pressure (PAP) undergoing surgical

repair of cardiac septal defects. Patients were randomly allocated to two equal groups: group L received levosimendan and group D received dobutamine. PAP was measured preoperatively, by use of transthoracic echocardiography (baseline), intraoperatively, directly, by use of a 22-gauge catheter inserted in the pulmonary artery, and postoperatively, by use of transesophageal echocardiography (TEE). Cardiac index (CI) was recorded by use of a transesophageal 4-MHz Doppler probe.

**Results:** Both drugs significantly reduced PAP compared with the level at the time of induction of anesthesia. Mean PAP measurement before chest closure, 1 and 20 h after ICU admission were significantly lower for patients who received levosimendan ( $32.7 \pm 4.1$ ,  $25.8 \pm 2.8$ ,  $19.8 \pm 2$  mmHg, respectively) than for those who received dobutamine ( $37.6 \pm 2.75$ ,  $32.8 \pm 2.36$ ,  $26.5 \pm 2.2$  mmHg, respectively). Both drugs significantly improved CI compared with its level at the time of induction of anesthesia. Mean CI measurements 5 min after weaning from cardiopulmonary bypass (CPB) until 20 h after ICU admission were significantly higher for patients who received levosimendan than for those who received dobutamine ( $3.55 \pm 0.35$ ,  $3.8 \pm 0.36$ ,  $3.81 \pm 0.34$ , respectively, in group L vs.  $3.4 \pm 0.36$ ,  $3.6 \pm 0.33$ ,  $3.66 \pm 0.29$ , respectively, in group D).

**Conclusion:** Levosimendan is better than dobutamine for treatment of pulmonary hypertension of children undergoing cardiac surgery.

**Keywords:** Levosimendan; Dobutamine; Congenital cardiac septal defects; Pulmonary hypertension.

### 1011. Smoking as a Risk Factor for Intraoperative Hypoxemia During one Lung Ventilation

Mohamed A. Khalil

*Journal of Anesthesia*, 27 (4): 550-556 (2013) IF: 0.867

**Background:** Smoking is associated with many intra and postoperative events, especially respiratory complications. Hypoxemia and airway damage are found to a greater extent in pre-existing respiratory pathology among smokers. One lung ventilation (OLV) carries a 4–10 % risk of development of hypoxia.

**Aim:** The purpose of this study was to predict the incidence of hypoxemia for smokers during OLV for patients undergoing video-assisted thoracoscopic surgery (VATS).

**Patients and Methods:** Sixty patients undergoing VATS using OLV by double lumen tube were included in this pilot cross-sectional study. These patients were divided into 2 groups, group S which included 30 heavy smoker patients (smoking more than 20 cigarettes per day for more than 20 years) and group NS which included 30 non-smoker patients. Intra and postoperative arterial oxygen tension ( $PaO_2$ ), arterial carbon dioxide tension ( $PaCO_2$ ), and intraoperative peak airway pressure were compared between the 2 groups.

**Results:**  $PaO_2$  was significantly higher in the non-smoker group than in the smoker group, both at the start and end of OLV. It was  $173 \pm 68$  mmHg for NS compared with  $74 \pm 10.8$  mmHg for S at the start of OLV; at the end of OLV it was  $410 \pm 78$  mmHg for the former and  $360 \pm 72$  mmHg for the latter ( $P < 0.05$ ).

**Conclusion:** From this study it can be concluded that for heavy smoker patients there was a significant reduction in arterial oxygen tension ( $PaO_2$ ) in comparison with non-smokers. However, hypoxemia reported for both groups was comparable.

**Keywords:** Smoking; one-lung ventilation; Video assisted thoracoscopic surgery (VATS); Hypoxemia.

### 1012. Syrian Revolution: A Field Hospital Under Attack

Ahmed Hasanin, Ahmed Mukhtar, Ali Mokhtar and Ahmed Radwan

*American Journal of Disaster Medicine*, 8: 259-65 (2013)

**Background:** Syrian revolution that began on March 15, 2011 represents not only a political crisis but also a humanitarian one where many relief attempts for saving civil injured were tried.

**Methods:** A secret field hospital organized by the medical rab union was set in Al- Bab town in the district of Aleppo. Egyptian volunteer physicians were the operating team who reached Syria through the Turkish border. Medical supplies were delivered from Turkey and medical equipments were taken from the government hospital which was not running at that time. Many Syrian volunteers helped in running this field hospital most of them were non-medical personnel who were trained to help in some medical purposes.

**Results:** Total number of cases referred to the hospital was 75. Surgical intervention was needed for 28 patients. Most common procedures needed were vascular procedures (32 percent), orthopedic procedures (32 percent), and abdominal exploration (25 percent). Median injury severity score (ISS) for admitted patients were 21 with interquartile range (14-21). Two patients died intraoperatively due to massive bleeding.

**Conclusion:** Setting up a field hospital in such an area with unsafe conditions needs good communication with medical and relief organizations in the site of crisis, selection of a location as near as possible to the Turkish border, developing a convenient triaging plan, and training nonmedical volunteers to do simple tasks.

**Keywords:** Syrian revolution; Field hospital; Anesthesia.

### 1013. The Impact of Dexmedetomidine Infusion in Sparing Morphine Consumption in Off-Pump Coronary Artery Bypass Grafting

Mohamed A. Khalil and Mohsen S. Abdel Azeem

*Seminars in Cardiothoracic and Vascular Anesthesia*, 17 (1): 66-71 (2013)

**Purpose:** Recovery from off-pump coronary artery bypass (OPCAB) has been reported to be more advantageous than conventional coronary artery bypass grafting with regard to both hospital and intensive care unit length of stay. Dexmedetomidine is a selective  $\alpha_2$  agonist that has been used successfully as an adjunct to narcotics in adult and pediatric cardiac surgery. The aim of this study was to assess the effect of dexmedetomidine on the recovery, total narcotic consumption, and total hospital and intensive care unit length of stay in patients undergoing OPCAB.

**Methods:** The recovery, hospital and intensive care unit length of stay, as well as total morphine consumption of patients receiving dexmedetomidine infusion ( $0.5 \mu\text{g}/\text{kg}/\text{h}$ ; dexmedetomidine group), after induction of general anesthesia, were compared with those receiving placebo (saline group).

**Results:** The duration of intubation of patients in the dexmedetomidine group was significantly shorter than in the control group ( $289 \pm 44$  minutes in the dexmedetomidine group vs  $530 \pm 119$  minutes in the control group). The total hospital and intensive care unit length of stay were significantly shorter in the dexmedetomidine group ( $P < .05$ ). Also, total fentanyl and morphine consumptions were lower in the

dexmedetomidine group than in the control group ( $P < .05$ ).

**Conclusion:** Our study showed that dexmedetomidine might be an effective adjuvant in reducing both total hospital and intensive care unit length of stay in patients undergoing OPCAB. Dexmedetomidine might play a role in reducing total morphine and fentanyl consumption in OPCAB.

**Keywords:** Dexmedetomidine; Off-pump coronary artery bypass; Morphine; Coronary artery bypass grafting.

### Dept. of Cardiology

### 1014. Giant Congenital Left Atrial Appendage Aneurysm

Mohamed Hassan, Karim Said, Ismail El-Hamamsy, Sherin Abdelsalam, Ahmed Afifi, Hatem Hosny and Magdi Yacoub

*J. of the American College of Cardiology*, 61(4): (2013) IF: 14.086

A 10-year-old girl presented with a 2-month history of atrial fibrillation. Chest x-ray film showed marked cardiomegaly (A). Transthoracic echocardiography showed a giant (13 × 10 cm) saccular aneurysm, related to and communicating with the left atrium (LA) through a 3.5-cm neck with dense spontaneous echo contrast and a large (5.5 × 7.3 cm) thrombus (B, Online Videos 1, 2, and 3). Left ventricular (LV) function was markedly impaired, with anterior wall akinesia. Coronary angiography revealed displacement and compression of the left anterior descending (LAD) coronary artery due to a mass effect from the aneurysm (C, arrows). Diagnosis of a giant LA appendage aneurysm was made intraoperatively (D). The aneurysm was resected and the aneurismal neck (E, arrows; asterisk indicates thrombus) was closed with an autologous pericardial patch (F). The post-operative course was uneventful, and the patient regained sinus rhythm, with improvement of global and regional LV function.

### 1015. HACEK Infective Endocarditis: Characteristics and Outcomes From A Large, Multi-National Cohort

Stephen T. Chambers mail, David Murdoch, Arthur Morris, David Holland, Paul Pappas, Manel Almela, Nuria Fernández-Hidalgo, Benito Almirante, Emilio Bouza, Davide Forno, Ana del Rio, Margaret M. Hannan and John Harkness

*Plos One*, 8 (5): e63181-e63181 (2013) IF: 3.73

The HACEK organisms (Haemophilus species, Aggregatibacter species, Cardiobacterium hominis, Eikenella corrodens, and Kingella species) are rare causes of infective endocarditis (IE). The objective of this study is to describe the clinical characteristics and outcomes of patients with HACEK endocarditis (HE) in a large multi-national cohort. Patients hospitalized with definite or possible infective endocarditis by the International Collaboration on Endocarditis Prospective Cohort Study in 64 hospitals from 28 countries were included and characteristics of HE patients compared with IE due to other pathogens. Of 5591 patients enrolled, 77 (1.4%) had HE. HE was associated with a younger age (47 vs. 61 years;  $p < 0.001$ ), a higher prevalence of immunologic/vascular manifestations (32% vs. 20%;  $p < 0.008$ ) and stroke (25% vs. 17%  $p = 0.05$ ) but a lower prevalence of congestive heart failure (15% vs. 30%;  $p = 0.004$ ), death in-hospital (4% vs. 18%;  $p = 0.001$ ) or after 1 year follow-up (6% vs. 20%;  $p = 0.01$ ) than IE due to other pathogens ( $n = 5514$ ). On multivariable analysis, stroke was associated with

mitral valve vegetations (OR 3.60; CI 1.34–9.65;  $p < 0.01$ ) and younger age (OR 0.62; CI 0.49–0.90;  $p < 0.01$ ). The overall outcome of HE was excellent with the in-hospital mortality (4%) significantly better than for non-HE (18%;  $p < 0.001$ ). Prosthetic valve endocarditis was more common in HE (35%) than non-HE (24%). The outcome of prosthetic valve and native valve HE was excellent whether treated medically or with surgery. Current treatment is very successful for the management of both native valve prosthetic valve HE but further studies are needed to determine why HE has a predilection for younger people and to cause stroke. The small number of patients and observational design limit inferences on treatment strategies. Self selection of study sites limits epidemiological inferences.

**Keywords:** Endocarditis; Hacek.

### 1016. Coronary Artery Ectasia Diagnosed Using Multidetector Computed Tomography: Morphology and Relation to Coronary Artery Calcification

Azza Farrag, Amr El Faramawy, Mohammed Ali Salem, Rabab Abdel Wahab and Soliman Ghareeb

*Int. J. of Cardiovascular Imaging*, 29: 427-433 (2013) IF: 2.648

Coronary artery ectasia (CAE) is usually considered a variant of coronary artery atherosclerosis; however, a definite link has not yet been confirmed. As not all patients with CAE are symptomatic, the real incidence is unknown. The aim of this study was to evaluate the prevalence of CAE and its clinical and angiographic characteristics as well as its relation to coronary artery calcification and any associated vascular abnormality by using multidetector computed tomography (MDCT). We prospectively enrolled 2,600 patients (mean age  $55 \pm 10$  years) who were scheduled for computed tomography coronary angiography (CTCA). CTCA was performed using 64-MDCT with dedicated software for calcium measurement. CAE was defined as an arterial segment with a diameter of 1.5 times the diameter of the adjacent normal segment. The presence of  $\geq 70\%$  diameter stenosis of any major epicardial vessel was considered an obstructive lesion. CAE was encountered in 192 (7.4 %) patients and showed gender predominance in men (88 %). Patients with CAE were more hypertensive but less diabetic. Left anterior descending artery was the most commonly affected vessel. Only 16 % of CAE patients had no atherosclerotic lesion. Coronary artery calcium score (CACS) and prevalence of ascending aorta aneurysm were shown to be significantly higher in CAE patients compared to patients having no ectasia. A significant negative correlation was noted between CACS and Markis classification. CTCA is a feasible technique to identify and evaluate morphology of CAE. The link between CACS and CAE may favor the consideration that ectasia is an advanced form of atherosclerosis.

**Keywords:** Coronary ectasia; Calcium score; Computed tomography.

### 1017. The Association Between Extracoronary Calcification and Coronary Artery Disease in Patients with Type 2 Diabetes Mellitus

Azza Farrag, Sameh Bakhom, Mohammed Ali Salem, Amr El-Faramawy and Emmanuel Gergis

*Heart and Vessels*, 28: 12-18 (2013) IF: 2.126

Cardiovascular complications are the major cause of diabetes-associated morbidity and mortality. However, not all patients with diabetes are at increased risk for cardiovascular disease (CVD). Coronary artery calcification was found to be a powerful predictor of coronary artery disease (CAD). The presence of extracoronary cardiac calcification as a useful predictor of CAD is not yet established, especially in type 2 diabetes mellitus (T2DM). The aim of this study was to evaluate the relation between extracoronary calcification and extent of CAD in a group of T2DM patients who were scheduled for computed tomographic coronary angiography (CTCA). We prospectively studied 380 patients (151 had T2DM) under the age of 60 years who were scheduled for CTCA because of suspected CAD. Severity of CAD was assessed by Gensini score. Coronary artery calcium score (CACS) as well as calcium score in the aortic valve, mitral annulus, ascending aorta, and descending aorta were measured by a 256-row multidetector computed tomography scanner with dedicated software for calcium calculation. Patients with known CAD were excluded. Diabetic and nondiabetic patients had comparable age and gender distribution. However, the diabetic group had higher Gensini score, CACS, and extracoronary calcium score (ECCS). Logistic regression analyses identified male gender and ECCS as significant predictors for the presence of CAD in diabetic patients. Age, smoking, and ECCS were the significant predictors of CAD in nondiabetic patients. Type 2 diabetic patients had increased coronary and extracoronary calcification. ECCS was found to be a significant predictor of CAD in diabetic and nondiabetic patients only when CACS was not taken into account.

**Keywords:** Extracoronary calcification; Coronary artery disease; Diabetes.

### 1018. In-Hospital and 1-Year Mortality in Patients Undergoing Early Surgery For Prosthetic Valve Endocarditis

Tahaniyat Lalani, Vivian H. Chu, Lawrence P. Park, Enrico Cecchi, G. Ralph Corey, Emanuele Durante-Mangoni, Vance G. Fowler Jr, David Gordon, Paolo Grossi, Margaret Hannan, Bruno Hoen, Patricia Muoz, Hussien Rizk, Souha S. Kanj, Christine Selton-Suty Daniel J. Sexton, Denis Spelman, Veronica Ravasio, Marie Françoise Tripodi and Andrew Wang

*Jama Internal Medicine*, 173(16): 1495-1504 (2013)

**Importance** There are limited prospective, controlled data evaluating survival in patients receiving early surgery vs medical therapy for prosthetic valve endocarditis (PVE). **Objective** To determine the in-hospital and 1-year mortality in patients with PVE who undergo valve replacement during index hospitalization compared with patients who receive medical therapy alone, after controlling for survival and treatment selection bias. **Design, Setting, and Participants** Participants were enrolled between June 2000 and December 2006 in the International Collaboration on Endocarditis—Prospective Cohort Study (ICE-PCS), a prospective, multinational, observational cohort of patients with infective endocarditis. Patients hospitalized with definite right- or left-sided PVE were included in the analysis. We evaluated the effect of treatment assignment on mortality, after adjusting for biases using a Cox proportional hazards model that included inverse probability of treatment weighting and surgery as a time-dependent covariate. The cohort was stratified by probability (propensity) for surgery, and outcomes were compared between the treatment groups

within each stratum. Interventions Valve replacement during index hospitalization (early surgery) vs medical therapy. Main Outcomes and Measures In-hospital and 1-year mortality. Results of the 1025 patients with PVE, 490 patients (47.8%) underwent early surgery and 535 individuals (52.2%) received medical therapy alone. Compared with medical therapy, early surgery was associated with lower in-hospital mortality in the unadjusted analysis and after controlling for treatment selection bias (in-hospital mortality: hazard ratio [HR], 0.44 [95% CI, 0.38-0.52] and lower 1-year mortality: HR, 0.57 [95% CI, 0.49-0.67]). The lower mortality associated with surgery did not persist after adjustment for survivor bias (in-hospital).

**Mortality:** HR, 0.90 [95% CI, 0.76-1.07] and 1-year mortality: HR, 1.04 [95% CI, 0.89-1.23]. Subgroup analysis indicated a lower in-hospital mortality with early surgery in the highest surgical propensity quintile (21.2% vs 37.5%;  $P = .03$ ). At 1-year follow-up, the reduced mortality with surgery was observed in the fourth (24.8% vs 42.9%;  $P = .007$ ) and fifth (27.9% vs 50.0%;  $P = .007$ ) quintiles of surgical propensity. Conclusions and Relevance Prosthetic valve endocarditis remains associated with a high 1-year mortality rate. After adjustment for differences in clinical characteristics and survival bias, early valve replacement was not associated with lower mortality compared with medical therapy in the overall cohort. Further studies are needed to define the effect and timing of surgery in patients with PVE who have indications for surgery.

**Keywords:** Endocarditis; Mortality; Prosthetic valve endocarditis; Surgery.

#### Dept. of Clinical and Chemical Pathology

##### 1019. Incidence and Pathogen Distribution of Healthcare-Associated Infections in Pilot Hospitals in Egypt

Isaac See, Fernanda C. Lessa, Omar Abo ElAta, Soad Hafez, Karim Samy, Amani El-Kholy, Mervat Gaber El Anani, Ghada Ismail, Amr Kandeel, Ramy Galal, Katherine Ellingson and Maha Talaat

*Infection Control and Hospital Epidemiology*, 34(12): 1281-1288 (2013) IF: 4.02

**Objective:** To report type and rates of healthcare-associated infections (HAIs) as well as pathogen distribution and antimicrobial resistance patterns from a pilot HAI surveillance system in Egypt.

**Methods:** Prospective surveillance was conducted from April 2011 through March 2012 in 46 intensive care units (ICUs) in Egypt. Definitions were adapted from the Centers for Disease Control and Prevention's National Healthcare Safety Network. Trained healthcare workers identified HAIs and recorded data on clinical symptoms and up to 4 pathogens. A convenience sample of clinical isolates was tested for antimicrobial resistance at a central reference laboratory. Multidrug resistance was defined by international consensus criteria.

**Results:** ICUs from 11 hospitals collected 90,515 patient-days of surveillance data. of 472 HAIs identified, 47% were pneumonia, 22% were bloodstream infections, and 15% were urinary tract infections; case fatality among HAI case patients was 43%. The highest rate of device-associated infections was reported for ventilator-associated pneumonia (pooled mean rate, 7.47 cases per 1,000 ventilator-days).

The most common pathogens reported were *Acinetobacter* species (21.8%) and *Klebsiella* species (18.4%). All *Acinetobacter* isolates tested (31/31) were multidrug resistant, and 71% (17/24) of *Klebsiella pneumoniae* isolates were extended-spectrum  $\beta$ -lactamase producers.

**Conclusions:** Infection control priorities in Egypt should include preventing pneumonia and preventing infections due to antimicrobial-resistant pathogens

**Keywords:** Healthcare; Associated; Infection; Hospital; Infection; Nosocomial infections.

##### 1020. Interleukin-12B Gene Polymorphism Frequencies in Egyptians and Sex-Related Susceptibility to Hepatitis C Infection

Samar Samir Youssef, Asmaa Mostafa Abd el Aal, Amal Soliman Nasr, Taher el Zanaty and Sameh Mohamed Seif

*Journal of Interferon and Cytokine Research*, 33: 415-419 (2013) IF: 3.297

Hepatitis C virus (HCV) infection is a major health problem worldwide. Egypt is the country with the highest HCV infection epidemic in the world. Interleukin (IL)-12 is a cytokine that has been shown to have a potent role as an antiviral cytokine. IL-12 is a heterodimer of the polypeptides p35 and p40. IL-12 B, the gene encoding IL-12 p40, is polymorphic, and a functional single-nucleotide polymorphism (SNP) of the 3'-untranslated region at position rs3212227 was associated with apparent resistance to CV. The genotype distribution of this polymorphism differs by race. This study is sought to identify the genotype distribution of the IL-12 SNP rs3212227 polymorphism in Egyptians and to assess its role in susceptibility to chronic HCV infection alone or in a sex-dependent way. The study included 238 subjects: 100 healthy controls and 138 patients with HCV infection. The IL-12 SNP rs3212227 was genotyped by the polymerase chain reaction-restriction fragment length polymorphism method (PCR-RFLP). Results showed a genotype frequency of 46%, 39%, and 15% for AA, AC, and CC IL-12 genotypes, respectively. No significant result ( $P = 0.5$ ) was shown in the differential distribution of the IL-12 SNP genotypes between controls and patients with HCV infection. Nonetheless, this difference in the IL-12 genotype distribution was significant (0.005) when it was stratified according to sex; moreover, the C allele distribution in men and women differed with a statistically high significance ( $P = 0.0001$ ) in controls versus HCV patients. In conclusion, the IL-12 SNP rs3212227 polymorphism confers a susceptibility to HCV infection in a sex-dependent way in Egyptians.

**Keywords:** Interleukin 12 B; Polymorphisms; Hcv.

##### 1021. Immunotherapy by Autologous Dendritic Cell Vaccine in Patients with advanced HCC

Mervat El Ansary, Sherif Mogawer, Samah Abd Elhamid, Sahr Alwakil, Fatma Aboelkasem, Hatem El Sabaawy and Olfat Abdelhalim

*J. Cancer Res Clin Oncol*, 139: 39-48 (2013) IF: 2.914

**Background:** Dendritic cells (DCs) could be used as potential cellular adjuvant for the production of specific tumor vaccines. Objectives Our study was aimed to evaluate the safety and efficacy of autologous pulsed DC vaccine in advanced



hepatocellular carcinoma (HCC) patients in comparison with supportive treatment.

**Methods:** Thirty patients with advanced HCC not suitable for radical or loco-regional therapies were enrolled. Patients were divided into 2 groups, group I consisted of 15 patients received I.D vaccination with mature autologous DCs pulsed ex vivo with a liver tumor cell line lysate. Group II (control group, no. 15) received supportive treatment. One hundred and 4 ml of venous blood were obtained from each patient to generate DCs. DCs were identified by CD80, CD83, CD86 and HLA-DR expressions using flow cytometry. Follow up at 3, and 6 months post injection by clinical, radiological and laboratory assessment was done.

**Results:** Improvement in overall survival was observed. Partial radiological response was obtained in 2 patients (13.3 %), stable course in 9 patients (60 %) and 4 patients (26.7 %) showed progressive disease (died at 4 months post-injection). Both CD8 T cells and serum interferon gamma were elevated after DCs injection. **Conclusion:** Autologous DC vaccination in advanced HCC patients is safe and well tolerate.

**Keywords:** DCS; HCC; Adjuvant immunotherapy.

### 1022. Mesenchymal Stem Cell Transfusion for Desensitization of Positive Lymphocyte Cross-Match Before Kidney Transplantation: Outcome of 3 Cases

G. Saadi, F. Fadel, M. El Ansary and S. Abd El-Hamid

*Cell Prolif*, 46: 121-126 (2013) IF: 2.265

**Objectives:** Donor specific antibodies (DSA) and a positive cross-match are contraindications for kidney transplantation. Trials of allograft transplantation across the HLA barrier have employed desensitization strategies, including the use of plasmapheresis, intravenous immunoglobulins, anti-B-cell monoclonal antibodies and splenectomy, associated with high intensity immunosuppressive regimens. Our case 1 report suffered from repeatedly positive lymphocyte cross match after 1st renal transplantation. Graft nephrectomy could not correct the state of sensitization. Splenectomy was done in a trial to get rid of the antibody producing clone. Furthermore plasmapheresis with low dose IVIG could not as well revert the state of sensitization for the patient.

**Material and Methods:** About 50 millions donor specific MSCs were injected to the patient.

**Results:** MSCs transfusion proved to be the only procedure which could achieve successful desensitization before performing the second transplantation owing to their immunosuppressive properties.

**Conclusion:** This case indicates that DS-MSCs is a potential option for anti- HLA desensitization. in cases 2 and 3 IV DS-MSCs transfusion was selected from the start as a successful line of treatment for pre renal transplantation desensitization to save other unnecessary lines of treatment that were tried in case 1.

**Keywords:** Mesenchymal; Stem cell; Desensitization; Renal transplantation.

### 1023. Trail Mrna Expression in Peripheral Blood Mononuclear Cells of Egyptian Sle Patients

Safaa Mostafa El-Karaksy, Naglaa Mohamed Kholoussi, Rasha Mohamad Hosny Shahin, Mona Mohsen Abou El-Ghar and Rasha El-Sayed Gheith

*Gene*, 527: 211-214 (2013) IF: 2.196

Although the definite etiopathogenesis of systemic lupus erythematosus (SLE) remains unclear, many different mechanisms may contribute to its pathogenesis. Tumor-necrosis factor-related apoptosis-inducing ligand (TRAIL) is a member of the tumor necrosis factor (TNF) family with pro- apoptotic activity. The accumulation of apoptotic cell debris has been hypothesized to induce the autoimmune inflammation in SLE, and TRAIL may trigger this programmed cell death. We investigated TRAIL mRNA expression levels in peripheral blood mononuclear cells (PBMCs) from 60 SLE patients and 40 controls using quantitative real-time reverse transcription polymerase chain reaction (RT-PCR), and we studied the association between the results and clinical and laboratory parameters of the patients. Expression levels of TRAIL mRNAs in SLE patients were significantly higher than in controls ( $p < 0.001$ ). A statistically significant association was detected between TRAIL mRNA expression and SLE activity ( $p = 0.001$ ).

**Keywords:** Systemic lupus erythematosus; Tumor-Necrosis Factor-Related apoptosis inducing ligand (TRAIL); Real-time reverse transcription; Polymerase chain reaction.

### 1024. Validation of A Proposed Warfarin Dosing Algorithm Based on the Genetic Make- Up of Egyptian Patients

Sherif M. M. Ekladios, Marianne Samir M. Issa, Sahar Abd El-Atty Sharaf and Hazem S. Abou-Youssef

*Molecular Diagnosis and Therapy*, 17: 381-390 (2013) IF: 1.692

**Background:** Warfarin is the most frequently prescribed oral anticoagulant worldwide. Due to its narrow therapeutic index and inter-patient variability in dose requirement, this drug has been considered an ideal target for personalised medicine. Several warfarin dosing algorithms have been proposed to tailor the warfarin dosage in the European, Asian and African-American populations. However, minimal interest was directed towards Middle East countries. The factors affecting warfarin dose requirement could be different in patients from different geographical and ethnic groups, limiting the value of published dosing algorithms.

**Objective:** The first objective of this study was to examine the contribution of genetic and nongenetic factors on the variability of warfarin dose requirements in the Egyptian population using an easy, cost-effective and rapid analysis of vitamin K epoxide reductase complex subunit 1 (VKORC1) and cytochrome P450 (CYP) 2C9 single nucleotide polymorphism (SNP) genotyping of patients. A second objective was to develop and validate an algorithm for warfarin dose prediction that is tailored to Egyptian

**Patients Methods:** Eighty- four patients, 41 males and 43 females, with a median (25th–75th percentiles) age of 39 (31–48) years were recruited in this study. Fifty patients whose international normalised ratio (INR) was in the range of 2–3 were allocated to a study cohort. SYBR Green-based multiplex allele-specific real-time PCR was used for genotyping of YP2C9 (1075A>C) and VKORC1 (1173C>T) polymorphisms. Linear regression analysis, including the variables age, gender, CYP2C9 and VKORC1 SNP genotypes, was run to derive the best model for estimating the warfarin dose that achieves an INR of 2–3. The new warfarin dosing algorithm was examined in a second cohort of patients ( $n = 34$ ) to check its validity. The predicted dose requirements for a subgroup of our patients were calculated



according to Gage and International Warfarin Pharmacogenetics Consortium (IWPC) algorithms available at.

**Results:** In the study cohort, warfarin dose/week in VKORC1 TT subjects was statistically significantly lower than in VKORC1 CC/CT subjects ( $p = 0.032$ ), while there was no statistically significant difference in warfarin dose/week between CYP2C9\*1\*1 and \*1\*3 ( $p = 0.925$ ). A multivariate stepwise linear regression analysis revealed that age and VKORC1 had independent and significant contributions to the overall variability in warfarin dose with a  $p$ -value = 0.013 and 0.042, respectively. Maintenance dose (mg/week) =  $65.226 - 0.422 \times (\text{age}) - 9.474 \times (\text{VKORC1})$ . The estimated regression equation was able to account for 20.5 % of the overall variability in warfarin maintenance dose. A significant positive correlation, with sufficient strength, was observed between the predicted warfarin dose and the actual prescribed dose ( $r = 0.453$ ,  $p = 0.001$ ). In the validation cohort, after application of the dosing algorithm, correlation between predicted and actual dose was statistically significant ( $p = 0.023$ ). The equation was particularly successful among patients with a dose  $\approx 35$  mg/ week. The correlation coefficient between the actual and predicted doses for IWPC and Gage were 0.304 and 0.276, respectively. When compared with our algorithm ( $r = 0.279$ ), the difference was non-significant:  $p = 0.903$  and 0.990, respectively.

**Conclusion:** VKORC1 (1173C >T) contributes to the warfarin dose variability. Patients' age and genetic variants of VKORC1 account for nearly 20.5 % of the variability in warfarin dose required to achieve an INR of 2–3. The success of a prediction equation based on these variables was proved in a different cohort: the predicted dose correlated significantly with the maintenance dose and the equation was more successful among patients with a dose  $\approx 35$  mg/week. The results of the warfarin algorithm we developed were comparable with those of the IWPC and Gage algorithms with the advantage of using one SNP (VKORC1 1173C>T) only. This represents an economic advantage in our community. Replication of this study in a larger cohort of patients is necessary before translation of this knowledge into clinical guidelines for warfarin prescription.

**Keywords:** Warfarin; Vkorc1; Cyp 2C 9.

#### 1025. Excision Repair Cross-Complementing Group 2/Xeroderma Pigmentousm Complementation Group D (Ercc2/ Xpd) Genetic Variations and Susceptibility to Diffuse Large B Cell Lymphoma in Egypt

Mennat Allah Kamal El-Din, Mervat Mamdooh Khorshied, Zainab Ali El-Saadany, Marwa Ahmed El-Banna and Ola M. Reda Khorshid

*International Journal of Hematology- Springer*, 98: 681-686 (2013) IF: 1.681

Diffuse large B-cell lymphoma (DLBCL) is a genetically heterogeneous neoplasm. Although several genetic and environmental factors have been postulated, no obvious risk factors have been emerged for DLBCL in the general population. DNA repair systems are responsible for maintaining the integrity of the genome and protecting it against genetic alterations that can lead to malignant transformation.

The current study aimed at investigating the possible role of ERCC2/XPD Arg156Arg, Asp312Asn and Lys751Gln genetic polymorphisms as risk factors for DLBCL in Egypt. The study included 81 DLBCL patients and 100 healthy controls. Genotyping of the studied genetic polymorphisms was performed

by polymerase chain reaction – restriction fragment length polymorphism technique.

Our results revealed that there was no statistical difference encountered in the distribution of Asp312Asn and Lys751Gln polymorphic genotypes between DLBCL cases and controls, thus it could not be considered as molecular risk factors for DLBCL in Egyptians.

However, Arg156Arg polymorphism at exon- 6 conferred two fold increased risk of DLBCL (OR 2.034, 95 % CI 1.015 – 4.35,  $p = 0.43$ ), and the risk increased when co-inherited with Lys751Gln at exon-23 (OR 3.304, 95 % CI 1.113 – 9.812,  $p = 0.038$ ). In conclusion, ERCC2/XPD Arg156Arg polymorphism might be considered as a genetic risk factor for DLBCL in Egyptians, whether alone or conjoined with Lys751Gln.

**Keywords:** Ercc2/ Xpd; Arg156arg; Asp312asn; Lys751gln; Nhl; Dlbcl; Egypt.

#### 1026. Monoclonal Gammopathy Among Patients with Chronic Hepatitis C Virus Infection

Nehad M. Tawfik, Manal El Deeb and Aml S. Nasr

*The American Journal of the Medical Sciences*, 345: 366-368 (2013) IF: 1.334

**Background:** An association between monoclonal gammopathies and chronic liver diseases has been previously reported. Hence the objective of this study was to determine the prevalence of monoclonal gammopathies in patients with chronic hepatitis C virus (HCV) infection in Egypt.

**Methods:** This is a prospective study of 200 HCV-positive and 100 HCV-negative patients with chronic liver diseases recruited consecutively at the Kasr El Aini Hospital Departments of Internal Medicine and Hematology, Cairo University. Clinical data were gathered, serum protein electrophoresis was performed and immune electrophoresis was carried out for the detection of monoclonal component. Histological examination of bone marrow was performed in patients with monoclonal gammopathy.

**Results:** A monoclonal band was detected in 2% of the HCV-positive patients and in 0% of the HCV-negative patients ( $P = 0.05$ ).

**Conclusions:** In this study, 4 cases of monoclonal gammopathy of undetermined significance were observed in the HCV-positive group, whereas none was observed in the HCV-negative group, which supports prior observations that HCV infection is associated with an excess risk for monoclonal gammopathy of undetermined significance.

**Keywords:** Monoclonal gammopathy; HCV; Non-HCV.

#### 1027. Cannabinoid Cb2 Receptor Gene (Cnr2) Polymorphism is Associated with Chronic Childhood Immune Thrombocytopenia in Egypt

Heba Mahmoud Gouda and Nermin R. Mohamed Kamel

*Blood Coagulation and Fibrinolysis*, 24: 247-251 (2013) IF: 1.248

Immune thrombocytopenia (ITP) is a heterogeneous autoimmune disorder characterized by thrombocytopenia with or without mucocutaneous bleeding manifestations. ITP patients have significant defects in immune self-tolerance: autoreactive T-lymphocyte clones are capable of directly damaging platelets and

possibly megakaryocytes and are likely to proliferate under the influence of Th lymphocytes. The CB2 receptor is thought to be the principal cannabinoid receptor that mediates immune modulation by endocannabinoid. The later has shown a complex range of immunomodulatory effects, primarily suppressive effects on leukocytes and immune functions, including modulation of Th cell development, chemotaxis and cytokine secretion. In this study, we investigated the association between cannabinoid CB2 receptor gene (CNR2) Q63R polymorphism and the susceptibility to childhood ITP in Egyptian population. CNR2 genotyping in ITP patients revealed that 41% of patients had the QR(AA/GG) heterotype and 49% had the RR(AA/AA) homotype. There was a significantly higher frequency of homomutant genotype (RR) in ITP patients than in controls, which conferred more than two-fold increased risk of ITP among Egyptian children [odds ratio (OR) 2.352, 95% confidence interval (CI) 1.313–4.215]. There was a significant statistical difference in the distribution of CNR2 Q63R genotypes between chronic ITP patients group and the control groups. The homomutant genotype carried nearly three-fold increased risk for chronic ITP (OR 2.701, 95% CI 1.462–5.009). In conclusion, CNR2 Q63R polymorphism may represent a novel genetic risk factor in the pathophysiology of chronicity development of ITP in Egyptian children.

**Keywords:** Cannabinoid 2; Chronic immune thrombocytopenia; CNR2; gene polymorphism; Immune thrombocytopenia; Restriction fragment length polymorphism.

### 1028. P2Y12 Receptor Gene Polymorphism and Antiplatelet Effect of Clopidogrel in Patients with Coronary Artery Disease After Coronary Stenting

Samah Mohamed Abd Elhamid Saleh, Naguib Zoheir, Samah Abd Elhamid, Nelly Abulata, Mehry El. Sobky, Doaa Khafagy and Amr Mostafa

*Blood Coagul Fibrinolysis*, 24 (5): 525-531 (2013) IF: 1.248

**Background** Platelets had a central role in the pathophysiology of thrombosis. Adenosine diphosphate (ADP) plays a pivotal role as an agonist of platelet activation. Genetic polymorphisms of the P2Y12 ADP receptor might influence the activation of this receptor by ADP or the response of patients to platelet inhibitors.

**Patients and Method:** The present study was conducted on a total number of 80 participants, 40 patients were diagnosed with acute coronary syndrome and 40 sex and aged-matched healthy volunteers were included as controls. Platelet aggregation was assessed (before and 1 week after clopidogrel administration) and genotyping of the T744C genetic polymorphism of P2Y12 receptor gene was carried out using restriction fragment length polymorphism polymerase chain reaction (PCR-RFLP).

**Method Results:** Platelet aggregation of the patients had a range of 54–183% before clopidogrel administration and had a range of 4–113% after its administration. Genotyping of the candidate gene revealed that 72.5% of the patients had a wild allele (TT), whereas 27.5% had a C allele (heterozygous CT, homozygous CC). On the contrary, 97.5% of controls had a wild allele (TT), whereas 2.5% had a C allele (heterozygous CT, homozygous CC).

**Conclusion:** Our study elicited an association between the T744C polymorphism of the P2Y12 ADP receptor gene and platelet reactivity. Carrying C allele at this position is associated with an increased platelet activation response to ADP.

**Keywords:** P2Y12; Receptor; Clopidogrel; Cad.

### 1029. HLA Alloimmunization Inegyptian Aplastic Anemia Patients Receiving Exclusively Leukoreduced Blood Components

Nermeen Ahmed Eldesoukey

*Transfusion and Apheresis Science*, 48 (2): 213-218 (2013)

IF: 1.225

**Background:** The aim of the work was to detect the presence of anti-human leukocyte anti-gens (anti-HLAs) class I and II antibodies in sera of multitransfused aplastic anemia pediatric patients using two different techniques. The effect of the implemented transfusion practice on the frequency of these antibodies was studied as well as their effect on the patient's clinical condition.

**Methods:** Flow cytometry panel reactive antibodies (FlowPRA) for HLA class I and II were determined and compared to the results obtained by Complement-dependent cytotoxicity (CDC) assay.

**Results:** Over the past 3 years, 20 aplastic anemia patients received leukoreduced blood components, 5/20 patients received leukoreduced products exclusively throughout their disease (group 1), 15/20 patients had received non-leukoreduced components previously (group 2). None of the patients in group 1 was FlowPRA positive. Six patients from group 2 (40%) were FlowPRA positive, only four out of these six patients showed positive CDC test. Positive and negative predictive values of CDC were 44.4 and 81.4% respectively, with 65% accuracy. Platelet refractoriness was encountered in 13/20 patients; only 3 out of these 13 patients (23%) were FlowPRA positive (38±18%). One refractory patient died from intra-cranial hemorrhage. His FlowPRA was 65.7% and CDC assay failed to detect it.

**Conclusion:** Leukoreduction of blood components minimizes the incidence of HLA alloimmunization. Further investigations for other immune causes of platelet refractoriness are recommended. FCM is a simple and reliable technique for detection of anti-HLA antibodies, while CDC assay lacks sensitivity and specificity.

**Keywords:** HLA alloimmunization; Leukoreduction; Refractoriness; Single donor platelets.

### 1030. Intrafamilial Transmission of Hepatitis C Infection in Egyptian Multitransfused Thalassemia Patients

Fadwa Said, Amal El Beshlawy, Mona Hamdy, Mona El Raziky, Mai Sherif, Ahmed Abdel kader and Lamis Ragab

*Journal of Tropical Pediatrics*, (2013) IF: 1.006

**Objective:** Detecting the current prevalence of hepatitis C virus (HCV) among Egyptian multitransfused thalassemic patients and evaluating the risk of its transmission within their family members.

**Methods:** Multitransfused Egyptian thalassemia patients (n = 137) were tested for HCV infection. Household contacts of positive members were compared with household contacts of HCV-negative patients.

Antibodies to HCV were detected by enzyme immunoassay. Antibody-positive cases were retested for viral load using reverse transcriptase polymerase chain reaction. HCV genotyping was performed on positive samples of the patients and the positive household contacts.

**Results:** In all, 34.4% of patients (n = 47) were positive for HCV antibodies and RNA. The study of 24 families of HCV-positive patients showed 14 affected family members (19.2%). In 27 families of HCV-negative patients, four family members were affected (4.9%). HCV genotyping of seven families was similar in both patients and their family members.

**Conclusion:** Our results support the role of intrafamilial transmission in the spread of HCV.

**Keywords:** Egypt hepatitis C intrafamilial multitransfused thalassemia.

### 1031. B- Cell Activating Factor Promoter Polymorphisms in Egyptian Patients with Systemic Lupus Erythematosus

Rania A. Zayed, Hala F. Sheba, Mennat Allah K. Abo Elazaem, Zainab A. Elsaadany, Lobna O. Elmessery, Jelan A. Mahmoud, Dalia R. Abdel Rahman and Faten R. Abdou

*Annals of Clinical and Laboratory Science*, 43 (3): 111-116 (2013) IF: 0.879

**Background:** Systemic lupus erythematosus (SLE) is a heterogenous autoimmune disease involving most immune cells. Studies have revealed a number of cytokine pathways that play important roles in the disease process. Among these are B- cell activating factor (BAFF), which regulates B-cell maturation, survival, and function.

**Objective:** To study the association between BAFF promoter polymorphism and systemic lupus erythematosus (SLE).

**Methods:** Single nucleotide polymorphisms in the BAFF promoter region; -2841 (T>C), -2701 (T>A), -871 (C>T) were investigated by PCR-RFLP genotyping in fifty Egyptian SLE patients and thirty normal controls.

**Results:** The frequency of mutant alleles of both -871C >T and -2701 T>A was higher among SLE patients than controls (p-value <0.001 and 0.000 respectively). There was a highly significant relationship between -871 C>T polymorphism and SLE (P<0.001), with the sensitivity and the specificity of the test being 100 %, and 70%, respectively. Patients expressing the -2701 T>A allele were seven times more prone to SLE than those with the T/T wild genotype (sensitivity of the test = 78%, specificity = 66.7%, odds ratio = 7.09, C.I at 95% = 2.29-22.64).

**Conclusion:** Polymorphisms in the regulatory region of the BAFF gene do contribute to the susceptibility to SLE in Egyptian patients, which indicates BAFF as a potential therapeutic target.

**Keywords:** SLE; BAFF; Polymorphism; 871 C>T; 2841 T>C; 2701 T>A.

### 1032. Chromogenic Cica-β Testing for Detection of Extended-Spectrum and Ampc β-Lactamases Among Cefoxitin-Resistant Isolates

Mona A. Wassef and Eiman Mohammed Abdul Rahman

*Lab Medicine*, 44 (1): 18-21 (2013) IF: 0.229

**Objective:** To evaluate the Cica-β test for rapid detection of extended-spectrum β- lactamases (ESBLs) in Gram- Negative bacteria.

**Methods:** Forty strains of *Pseudomonas* spp, *Klebsiella* spp, *Escherichia coli* and *Enterobacter* spp that produce previously characterized β- lactamases were retested using the Cica-β test.

This test measures hydrolysis of the chromogenic oxyimino-cephalosporin HMRZ- 86 with and without specific inhibitors of extended- spectrum and Amp C β- lactamases. The results were scored according to color changes from yellow to red.

**Results:** A total of 33.3% of extended-spectrum producers and 66.7% of AmpC β-lactamase producers were correctly identified by the Cica-β test. **Conclusion:** The Cica- β test is not likely to be useful in routine screening for extended-spectrum β-lactamase because it is very expensive and performs poorly in this context.

**Keywords:** Cica β- Test; Esbl; Amp C β-Lactamase.

### 1033. Study of Cytotoxic T Lymphocyte Antigen 4 Gene Polymorphism A49g in Egyptian Children with Idiopathic

Somaya Elgawhary, Shahira Zayed, Hanan Alwakeel, Abeer Abdelrazik and Rania Ismail

*Life Science Journal*, 10: 3242-3246 (2013) IF: 0.165

**Objective:** The cytotoxic T lymphocyte associated antigen-4 (CTLA-4) is transiently expressed on activated T lymphocytes to antagonize the activating signals resulting in T cell inhibition and prevention of the its clonal expansion. CTLA-4 A49G polymorphism was studied in different autoimmune disorders as it has been suggested that the presence of G allele reduce the expression and the inhibitory function of the CTLA-4 protein and this may predispose to autoimmunity.

**Subjects and Methods:** in this study, we evaluated the frequency of CTLA-4 A49G polymorphism in 30 Egyptian children patients with immune thrombocytopenic purpura (ITP), and 40 healthy individuals using polymerase chain reaction (PCR) – restriction fragment length polymorphism (RFLP) technique.

**Results:** Allele frequencies and genotype distributions were similar in both ITP patients compared to healthy individuals.

**Conclusion:** Our results suggest that CTLA-4 A49G polymorphism does not contribute to the pathogenesis of immune thrombocytopenic purpura.

**Keywords:** Cytotoxic T lymphocyte antigen; 4 (Ctla-4); A49g Polymorphism; Idiopathic thrombocytopenic.

### 1034. Association of C46T Genetic Polymorphism of Coagulation Factor XII with Deep Venous Thrombosis: A Cohort Study on Egyptian Patients

Naguib M. Zoheir, Mona S. Hamdy, Mervat M. Khorshied, Nelly N. Abulata, Mehry El Sobky, Amr M. Saleh and Hussein M. Khairy

*Comparative Clinical Pathology- Springer*, 22: 203-207 (2013)

Deep vein thrombosis (DVT) is a common multifactorial disease, with serious short- and long-term complications, and a potential fatal outcome. Many genes are involved in determining the interindividual variation in traits that define the onset and progression of disease, as well as the response to treatment. Several association studies have designed the relationship between factor XII C46T polymorphism and the risk of arterial and venous thrombosis. Some studies reported that FXII gene polymorphism is not associated with venous thrombosis, whereas other studies found an increased risk of venous thrombosis in carriers of a FXII-T variant. We constructed an age–gender–ethnic– matched case–control study including 52 DVT patients

and 100 healthy volunteers. C46T polymorphism of the coagulation factor XII was carried out using allelic discrimination assay by real-time polymerase chain reaction for patients and controls, while plasma factor XII activity was detected by one-step clotting assay. FXII C46T genotyping in DVT patients revealed that 34.6% were heterozygous harboring the FXII-CT heterotype and 3.85% were homozygous; FXII-TT homotype, with no statistically significant difference in the distribution of the mutant genotypes between DVT patients and the control group. FXII activity was significantly reduced in DVT patients harboring the mutant genotypes. In the present study, FXII C46T gene polymorphism was not associated with increased risk of deep venous thrombosis.

**Keywords:** Deep venous thrombosis; Factor Xii C46T genetic polymorphism; Factor XII activity.

### 1035. Clinical Implication of Nucleophosmin Gene Mutation and Flt-3 Internal Tandem Duplication in A Cohort of Egyptian Aml Patients

Mervat M. Khorshied, Wael A. Said and Hebat Allah M. Shaaban  
*Comparative Clinical Pathology- Springer, 22: 497-506 (2013)*

Nucleophosmin (NPM) gene mutations are the most frequent genetic abnormality in adult AML. NPM gene mutation (NPM1) leads to aberrant localization of the NPM protein into the cytoplasm. As NPM1 mutation is frequently associated with FMS-like tyrosine kinase 3—internal tandem duplication (FLT3-ITD) that appears to abrogate its favorable prognostic effect. This study aimed at detecting the frequency of NPM1 exon-12 gene mutation and FLT3-ITD in 62 de novo AML patients by reverse-transcriptase polymerase chain reaction and immunocytochemical staining. Twenty age- and sex-matched healthy volunteers were included in the current study as a control group. NPM1 mutation was detected in 30/62 (48.3%) of cases, while 27/62 (43.5%) of cases were FLT3-ITD-positive.

All the control subjects were negative for the studied genetic mutations. Immunostaining for NPM revealed cytoplasmic positivity (NPMc+) in 32/62 (51.6%) of case. NPM1 mutation was significantly higher in patients with normal karyotype, FAB-M4 subtype, low expression of CD34 and favorable response to induction therapy. FLT3-ITD was higher among female patients and was associated with poor response to induction therapy. Patients harboring both mutations showed unfavorable response as the presence of FLT3-ITD abolished the favorable effect of NPM1. In conclusion, all AML cases should be screened prior to therapy for both mutations as two important prognostic markers that can be valuable in predicting the response to therapy, in addition to their role in monitoring minimal residual disease and early detection of relapse. Furthermore, they represent potential therapeutic targets.

**Keywords:** Nucleophosmin; FLT3; ITD; AML; RT-PCR; Immunohistochemical staining.

### 1036. Influence of Interleukine-1 Beta and Interleukine-1 Receptor Antagonist Genes Polymorphism on Rheumatoid Arthritis

T.M. Gaafar, F.S. Bayoumi, W.M. El-Senousy, H.A. Raafat, M.M. Sherif and B.G. Morcos

*World Applied Sciences Journal, 27 (5): 574-584 (2013)*

Rheumatoid arthritis (RA) is a systemic autoimmune disease with different factors contributing to the etiology and pathogenesis. IL-1 has been implicated in RA and the ability of IL-1 to drive inflammation and joint erosion and to inhibit tissue repair processes has been clearly established in in vitro systems and animal models. IL-1 receptor antagonist (IL-1Ra) prevents the interaction between IL-1 and its cell-surface receptors, thus acting as a naturally occurring inhibitor. The aim of this study is to assess the role of IL-1 and IL-1Ra gene polymorphism in RA disease susceptibility and severity.

The study was conducted on 50 adult RA patients and 10 controls. Results indicated that IL-1 (+3953) gene polymorphism is related to RA severity, but plays no role in RA susceptibility. It was also shown that IL-1Ra gene polymorphism (IL1RN2) plays no role in RA susceptibility or severity. Therefore the presence of allele 2 of IL-1 gene in RA might be considered as a prognostic factor for RA.

**Keywords:** Rheumatoid; Arthritis; Cytokines systemic; Autoimmune disease; RFLP.

### 1037. Mannose-Binding Lectin (Mbl2) Gene Polymorphism in Sickle Cell Anemia: An Egyptian Study

Mervat Mamdooh Ahmed Khorshied

*Comparative Clinical Pathology- Springer, 22: 387-394 (2013)*

Sickle cell disease (SCD) is an inherited disorder of sickle hemoglobin affecting millions of people worldwide. The current study aimed at detecting the prevalence of MBL2 exon-1 (codons 52, 54, and 57) and promoter region (-221, X/Y) genetic polymorphisms in Egyptian children with SCD to clear out its possible role as a genetic risk factor for susceptibility to vaso-occlusive crisis (VOC) and/or infections. Genotyping of exon-1 and the promoter region was done by polymerase chain reaction for 50 SCD patients and 50 healthy controls.

The frequency of MBL2 promoter polymorphism was 32% for the heteromutant genotype, Y/X and 8% for the homomutant genotype, and X/X with no statistical difference in the distribution of the mutant genotypes between SCD patients and controls. MBL2 exon-1 gene mutation in SCD patients was 18% for the heteromutant genotype A/O and 32% for the homomutant genotype O/O.

The O/O genotype was significantly higher in SCD patients. Mutation at codon 57 of exon-1 (C allele) was significantly higher in SCD Patients. The frequency of intermediate MBL2 expressers was significantly higher in the control group, while the frequency of low MBL2 expressers was higher among the patients.

The distribution of MBL2 expressers did not differ between SCD patients with or without recurrent attacks of VOC. There was no association between MBL2 exon-1 or promoter region (-221 Y/X) genetic polymorphisms and the susceptibility to neither VOC nor infections in Egyptian children with SCD.

**Keywords:** Mbl2; Genetic Polymorphism; Sickle Cell Anemia. Egypt.



### 1038. Prevalence of Factor V Leiden (G1619a) and Prothrombin Gene (G20210a) Mutation in Egyptian Children with Sickle Cell Disease

Mona Salah El-Din Hamdy, Heba Mahmoud Gouda, Iman Abdel-Mohsen Shaheen, Mervat M. Khorshied and Rania Hosny Tomerak

*Comparative Clinical Pathology*, 22: 679-702 (2013)

Patients with sickle cell disease (SCD) show activation of the blood coagulation. The purpose of the current study was to detect the prevalence of factor V Leiden (G1691A) and prothrombin gene (G20210A) mutations in a group of Egyptian children with SCD, and to clear out their possible role as genetic risk factors for vaso-occlusive crises (VOC) in SCD. The current study included fifty Egyptian SCD children and fifty age and sex matched healthy children as a control group. Genotyping was performed by polymerase chain reaction restriction fragment length polymorphism technique. Heterozygous factor V Leiden was significantly higher in the SCD patients (30 %) compared to controls (16 %), while there was no statistical difference between the two groups regarding heterozygous prothrombin gene (G20210A) mutation. Factor V Leiden conferred increased risk of VOC in SCD patients (OR01.7, 95 %CI0 1.01–3.43). Screening for factor V Leiden in SCD patients is recommended to verify patients at higher risk of VOC.

**Keywords:** Sickle cell disease; Factor V Leiden; Prothrombin gene (G20210a) Mutation; Vaso; Occlusion crises.

#### Dept. of Clinical Oncology and Nuclear Medicine

### 1039. Estimation of Intracranial Failure Risk Following Hippocampal-Sparing Whole Brain Radiotherapy

Saskia Harth, Yasser Abo-Madyan, Lei Zheng, Kerstin Siebenlist, Carsten Herskind, Frederik Wenz and Frank A. Giordano

*Radiotherapy and Oncology*, 109: 152-158 (2013) IF: 4.52

**Purpose:** To Estimate the risk of undertreatment in hippocampal-sparing whole brain radiotherapy (HS-WBRT).

**Methods:** Eight hundred and fifty six metastases were contoured together with the hippocampi in cranial MRIs of 100 patients. For each metastasis, the distance to the closest hippocampus was calculated. Treatment plans for 10 patients were calculated and linear dose profiles were established. For SCLC and NSCLC, dose-response curves were created based on data from studies on prophylactic cranial irradiation, allowing estimating the risk for intracranial failure.

**Results:** Only 0.4% of metastases were located inside a hippocampus in 3% of all patients. SCLC showed a relatively high rate of hippocampal metastasis (18.2% of all SCLC patients) and HS-WBRT in a commonly applied fractionation scheme would increase the risk for brain relapse by 4% compared to conventional WBRT. NSCLC showed a lower rate of brain metastasis in the hippocampi (2.8%) and HS-WBRT would account for a slightly increased absolute risk of 0.2%.

**Conclusions:** Prophylactic or therapeutic HS-WBRT is expected to be associated with a low risk of undertreatment. For SCLC, it bears a minimally elevated risk of failure compared to standard WBRT. In NSCLC, HS-WBRT is most likely not associated with a clinically relevant increase in risk of failure.

**Keywords:** Brain metastasis; Hippocampal-sparing whole brain radiotherapy; Whole brain radiotherapy; Prophylactic cranial irradiation.

### 1040. Phase II Study of Single Agent Oral Vinorelbine as First-Line Treatment in Patients with Her-2 Negative Metastatic Breast Cancer

Maged Mansour and Cynthia Mourad

*Cancer Chemotherapy Pharmacology*, 72 (2): 429-435 (2013) IF: 2.795

**Purpose:** Previous studies indicated that oral chemotherapy is convenient and preferred by many patients. We hereby report the efficacy and safety of oral vinorelbine as first-line chemotherapy for metastatic breast cancer (MBC). **Methods:** Thirty-one patients with HER-2 negative MBC were enrolled between January 2007 and December 2010 in a prospective phase II trial. Patients were treated every 3 weeks with oral vinorelbine 60 mg/m<sup>2</sup> Days 1 and 8 for the 1st cycle and thereafter 80 mg/m<sup>2</sup> Days 1 and 8 every 3 weeks. Treatment was administered until disease progression or unexpected adverse event or patient refusal to continue. Primary endpoint was objective response rate (ORR); secondary endpoints were time-to-progression (TTP), overall survival (OS) and safety. Follow-up results until October 2012 are reported.

**Results:** Median age was 42 years (range 33–75). 26 (84 %) patients had 2 or more metastatic sites. A median of 6 cycles were administered (range 2–20).

ORR was achieved in 9 (29 %) patients including 1 complete and 8 partial responses. 12 (39 %) patients had stable disease, resulting in a disease control rate of 68 %. Median TTP was 5.2 months [95 % CI 2.8–7.5]. Median OS was 16 months [95 % CI 11.3–20.7]. 3 (10 %) patients developed

Grade 3 – 4 neutropenia. No events of febrile neutropenia, cardiac, renal toxicities or alopecia were recorded. Grade 3 thrombocytopenia and nausea-vomiting were reported in 2 (6 %) and 5 (16 %) patients, respectively.

**Conclusion Results:** show a good efficacy and tolerance profile of oral vinorelbine as first-line chemotherapy for HER-2 negative MBC patients.

**Keywords:** Oral chemotherapy; Oral vinorelbine; Single agent advanced breast cancer.

### 1041. Tc-99 M Diethylenetriamine-Pentaacetic Acid (Dtpa): is it Reliable for Assessment of Methotrexate-Induced Cumulative Effect on Renal Filtration in Rheumatoid Arthritis Patients

Amr Amin, Dina Effat, Nabila Goher and Basma Ramadan

*Rheumatology International Clinical and Experimental Investigations*, 33: 3059-3063 (2013) IF: 2.214

Methotrexate (MTX) is commonly employed as the initial DMARD used for the treatment of rheumatoid arthritis (RA). We aimed to contribute to the safety profile of MTX by assessing its cumulative effect on renal filtration. A total of 52 RA adult female patients with normal baseline serum creatinine and GFR at the initial diagnosis of the disease were included. Group 1 (G1) included 30 patients (mean age 40.4 ± 4.4 years) on MTX and NSAIDs, while 22 RA patients (mean age 38.5 ± 8.2 years) who received NSAIDs only served as control group (G2). Renal



function was assessed by GFR measurement using technetium diethylenetriamine-pentaacetic acid (Tc-99 m DTPA) at a point of the study time corresponding to disease duration. twenty-one out of thirty (70 %) in G1 showed reduced GFR compared to 6/22 (27.3 %) in G2 ( $P = 0.007$ ), with  $3.3 \pm 0.5$  % annual reduction in GFR. Reduced GFR in G1 showed significant negative correlation with age ( $r = -0.396$ ,  $P = 0.005$ ), MTX cumulative dose ( $r = -0.263$ ,  $P = 0.049$ ), MTX-intake duration ( $r = -0.293$ ,  $P = 0.031$ ) and NSAIDs-intake duration ( $r = -0.344$ ,  $P = 0.014$ ). Low-dose MTX has a slow cumulative effect on renal filtration manifested by GFR reduction overtime that could be monitored by Tc-99m DTPA.

**Keywords:** Rheumatoid arthritis; GFR. Gates; Method. MTX.

#### 1042. Dose-Escalated Salvage Radiotherapy After Radical Prostatectomy in High Risk Prostate Cancer Patients Without Hormone Therapy: Outcome, Prognostic Factors and Late Toxicity

Mohamed Shelan, Yasser Abo-Madyan, Grit Welzel, Christian Bolenz, Julia Kosakowski, Nadim Behnam, Frederik Wenz and Frank Lohr

*Radiation Oncology*, 8: (2013) IF: 2.107

**Purpose:** Evaluation of dose escalated salvage radiotherapy (SRT) in patients after radical prostatectomy (RP) who had never received antihormonal therapy. to investigate prognostic factors of the outcome of SRT and to analyze which patient subsets benefit most from dose escalation.

**Materials and Methods:** Between 2002 and 2008, 76 patients were treated in three different dose-groups: an earlier cohort treated with 66 Gy irrespective of pre-RT-characteristics and two later cohorts treated with 70 Gy or 75 Gy depending on pre-RT-characteristics. Biochemical-relapse-free-survival (bRFS), clinical-relapse-free-survival (cRFS) and late toxicity were evaluated.

**Results:** Four-year bRFS and cRFS were 62.5% and 85%. Gleason score <8, positive surgical resection margin (PSRM) and low PSA.

**Keywords:** Radical prostatectomy; Salvage radiotherapy; Dose escalation

#### 1043. Prevalence of Preclinical Renal Dysfunction in Obese Egyptian Patients with Primary Knee Osteoarthritis, Preliminary Data

Amr Amin Hania S. Zayed, Gehan Younis and Reem Bader

*The Egyptian Rheumatologist*, 35: 239-244 (2013) IF: 2

**Aim of the work:** Obesity and the related metabolic syndrome cluster of cardiovascular risk factors have been associated with chronic kidney disease (CKD). Patients with knee osteoarthritis (OA) are frequently obese and due to the combined effects of obesity and the chronic use of non-steroidal anti-inflammatory drugs (NSAIDs); they may represent a high risk group for renal dysfunction. We aimed to detect preclinical renal involvement in obese patients with knee OA. Patients and methods: Forty patients with knee OA and a body mass index (BMI)  $\geq 30$  (mean age  $43.5 \pm 3.7$  years) not on chronic NSAID use and forty age and sex matched non-obese controls were enrolled in this study. For all subjects anthropometric measures were taken. Laboratory

assessment included fasting blood sugar, serum triglycerides, high density lipoprotein cholesterol (HDL), serum uric acid, urea, creatinine and microalbuminuria assay. For patients with knee OA, knee radiographs were done and the disease severity was assessed according to Kellgren–Lawrence (K–L) scale. Tc-99 m DTPA was used for the measurement of the glomerular filtration rate (GFR) and the results were classified into normal and CKD according to Kidney–dialysis outcomes and quality initiative stages.

**Keywords:** Preclinical renal dysfunction; Obesity; Tc-99 M Dtpa; Knee osteoarthritis; GFR.

#### 1044. Influence of Early (F+ 0) Intravenous Furosemide Injection on the Split Renal Function Using 99mTc-Dtpa Renography

Ahmed A. Kandeel, Salwa A. Elhossainy and Nahla D. Elsayed

*Nuclear Medicine Communications*, 34 (4): 354-358 (2013) IF: 1.379

In busy nuclear medicine departments, the F + 0 protocol for diuretic renography is routinely used to shorten the acquisition time. The aim of this study was to evaluate the influence of the F+ 0 protocol on the split renal function (SRF) during a dynamic renal scan using technetium-99m diethylene triamine pentaacetic acid (99mTc-DTPA) compared with that using the standard technetium 99 m dimercaptosuccinic acid (99mTc-DMSA). A total of 102 patients referred for a dynamic renal scan for varied etiologies were divided into two groups: the F+ 0 group, comprising 53 patients who were injected with furosemide just before 99mTc-DTPA injection, and the F+ 10 group, comprising 49 patients who were injected with the diuretic at the 10th minute after radiotracer injection. All patients were also subjected to a static cortical 99mTc-DMSA scan with geometric quantification of SRF. A highly significant statistical difference ( $P < 0.001$ ) was obtained on comparing the mean value of the difference in SRF calculated using DTPA and DMSA between the F + 0 and F+ 10 groups, being  $5.0 \pm 2.6$  and  $1.5 \pm 0.6$ %, respectively. All 49 patients in the F + 10 group had a difference in split function of 5% or less, whereas 17/53 patients representing 32.1% of the F+ 0 group had a difference in SRF of greater than 5%. Early (F+ 0) furosemide injection before administration of 99mTc-DTPA has a significant influence on the estimation of SRF of the diseased kidney (either obstructed or functionally impaired) when compared with furosemide injection after standard 99mTc-DMSA administration. Care should be taken during interpretation of the scan findings when accurate split function is required.

**Keywords:** 99 MTC–dmsa; 99MTC-Dtpa; Diuretic renography; F + 0 Protocols.

#### 1045. Patients with End-Stage Renal Disease: Optimal Diagnostic and Prognostic Performance of Myocardial Gated-Spect, Initial Results

Amr Amin, Gehan Younis, Mohamed El-Khatib and Ismail Ali

*Nuclear Medicine Communications*, 34: 314-321 (2013) IF: 1.379

**Purpose:** We investigated the role of Tc-99m sestamibi myocardial perfusion gated single photon emission computed tomography (GSPECT) in identifying those patients with end-

stage renal disease (ESRD) in whom optimal diagnosis of coronary artery disease and prediction of cardiac events (CEs) could be achieved.

**Methods:** This was a prospective study that included 41 asymptomatic ESRD patients who had been undergoing hemodialysis for 12 months or less (22 men and 19 women) with restricted selection criteria (asymptomatic traditional risk). Tc-99m sestamibi GSPECT was carried out for all patients, whereas coronary angiography (Cath) was carried out only for abnormal GSPECT patients, with a 2-year follow-up for CEs. Twenty individuals matched for age, sex, and BMI formed the control group.

**Results:** Of the 41 ESRD patients, 13 showed abnormal GSPECT [11/13 with myocardial perfusion defects and left ventricular dysfunction in concordance with Cath and 2/13 with only left ventricular dysfunction (i.e. stunning)] compared with 1/20 in the control group. None of the patients with negative results experienced CEs (negative predictive value 100%); these patients had a 2-year CE-free survival rate of 100% compared with 46% for patients with positive results on GSPECT ( $P < 0.0001$ ; seven GSPECT-positive patients developed CEs during their follow-up). Patients with positive results were more frequently male ( $P < 0.001$ ), were significantly older ( $P = 0.01$ ), and had highly sensitive C-reactive protein levels ( $P = 0.002$ ). Abnormal GSPECT was the only independent predictor of CEs (95% confidence interval, 7.1–46.7; hazard ratio, 46.1;  $P < 0.001$ ).

**Conclusion:** GSPECT exhibited optimum performance for coronary artery disease detection and risk stratification in asymptomatic ESRD patients during their first year of regular hemodialysis who were selected according to our modification of the traditional risk category. This may help in selecting suitable candidates for Cath, revascularization, and future renal transplantation.

**Keywords:** Coronary artery disease; End-stage renal disease; Gated single photon emission computed tomography; Modified traditional risk; TC-99M sestamibi.

#### 1046. Stunning Phenomenon After A Radioactive Iodine-131 Diagnostic Whole-Body Scan: Is It Really A Point of Clinical Consideration

Amr Amin, Mahasen Amin and Ahmed Badwey

*Nuclear Medicine Communications*, 34: 771-776 (2013)  
IF: 1.379

**Purpose:** Stunning of thyroid remnants after diagnostic scanning (Dx-WBS) using radioactive iodine-131 ( $^{131}\text{I}$ ) may limit the efficacy of  $^{131}\text{I}$  therapy. We aimed to evaluate this assumption in a prospectively designed study.

**Methods:** Forty patients who underwent thyroidectomy for differentiated thyroid carcinoma were studied and divided into two identical groups: G1 and G2. In the G1 group, no Dx-WBS was performed and the ablation dose was given directly on the basis of the risk stratification; in the G2 group, Dx-WBS was performed with 185 MBq (5 mCi) of  $^{131}\text{I}$ , and ablation was given for a mean number of  $11 \pm 1.1$  days; stunning was found on a semiquantitative basis in all patients. At a mean of  $6.5 \pm 0.3$  months, the ablation success rate (ASR) was evaluated on the basis of Dx-WBS, thyroglobulin levels, and neck sonography. Complete ASR was considered when no  $^{131}\text{I}$  uptake could be seen in the neck or elsewhere, thyroglobulin was less than 2 ng/ml, and neck sonography was negative for any disease-related abnormalities.

**Results:** G1 and G2 groups were completely identical as no significant differences were found between their different characteristics, including the mean ablative dose. ASR was 81.7 and 78.3% in G1 and G2 groups, respectively ( $P = 0.6$ ). Multivariate Cox regression analysis showed the mean ablation dose to be the most influential factor in ASR (odds ratio 1.045; 95% confidence interval 0.936–1.1189;  $P = 0.01$ ).

**Conclusion:** Our data suggest that stunning had no influence on ASR and is not a point of clinical consideration with respect to this aspect.

**Keywords:** Radioactive iodine;  $^{131}\text{I}$  Diagnostic dose; Radioactive iodine;  $^{131}\text{I}$  Treatment; Stunning effect; Well-differentiated thyroid carcinoma.

#### 1047. Chemotherapy Management of Malignant Pleural Mesothelioma: A Phase II Study Comparing Two Popular Chemotherapy Regimens

E. E. Habib and E. S. Fahmy

*Clinical and Translational Oncology*, 15: 965-968 (2013)  
IF: 1.276

**Purpose:** The aim of this prospective, phase II clinical study is to evaluate the activity of gemcitabine and cisplatin in comparison to pemetrexed and carboplatin in patients with malignant pleural mesothelioma. Patients and methods The patients were recruited from May 2008 to May 2011. One group included 21 cases who received cisplatin and gemcitabine. The other group included 19 cases who received pemetrexed and carboplatin.

**Results:** Response is superior in the pemetrexed group ( $p = 0.041$ ). The median follow-up was 18 months (range 6–30 months). Cumulative survival at 1.5 years was 57.8 % for the pemetrexed carboplatin group. For the gemcitabine cisplatin group, the cumulative survival proportion at 1.5 years was 41 % ( $p = 0.0599$ ).

**Conclusions:** Pemetrexed plus carboplatin are a step forward in the treatment of mesothelioma, the prognosis for these patients remains poor. Cheaper combinations as gemcitabine and cisplatin may be considered sufficient to treat cases with advanced mesothelioma.

**Keywords:** Mesothelioma; Chemotherapy; Gemcitabine; Pemetrexed.

#### 1048. Survival of Mesothelioma in A Palliative Medical Care Unit in Egypt

Noha Y Ibrahim, Enas Abou-Elela and Dalia Darwish

*Asian Pacific Journal of Cancer Prevention*, 14: 739-742 (2013)  
IF: 1.271

**Background:** This study was to evaluate the survival of patients with pleural and intraperitoneal malignant mesothelioma and to investigate the efficacy of chemotherapy (CT) as well as radiotherapy (RTH) and surgery compared to best supportive care (BSC).

**Materials and Methods:** Forty patients with malignant mesothelioma (38 with pleural and 2 with intraperitoneal) were enrolled. Twenty seven patients underwent (CT) chemotherapy of which 2 also received (RTH) and surgery was only for biopsy in 15/40. Combination chemotherapy included cisplatin-gemcitabine, cisplatin-avelbline and cisplatin (or carboplatin)

with premetrexed. Thirteen patients received only best supportive care.

**Results:** A total of 12 (30%) patients were male, and 28 (70%) female. Median age was 54.0 years and the male/female ratio was 1/2.33 ( $P=0.210$ ). Residential exposure played a major role in two regions, Helwan and Shoubra, in 20% and 15%, respectively. Overall mean survival time was  $13.9 \pm 2.29$  months. That for patients who had received best supportive care was  $7.57 \pm 1.85$  months, for chemotherapy was  $16.5 \pm 3.20$  months, and multimodality treatment regimen  $27 \pm 21.0$  months ( $P=0.028$ ). Kaplan-Meier survival did not significantly vary for sex, residence and the pathological types epithelial, mixed and sarcomatous. The median survival for performance status and treatment modalities was significant ( $P=0.001$  and  $0.028$ ). Best supportive care using opioids with a mean dose of 147.1 mg (range 0-1680) of morphine sulphate produced good subjective response and reasonable quality of life but did not affect survival.

**Conclusions:** We conclude that CT prolongs survival compared to BSC in patients with malignant mesothelioma. Moreover, using escalating doses of opioids provides good pain relief and subjective responses.

**Keywords:** Mesothelioma; Survival; Quality of life; Best supportive care; Chemotherapy; Radiotherapy.

#### 1049. Pattern of Cancer Deaths in A Saudi Tertiary Care Hospital

Abdullah S. Al-Zahrani, Amr T. El-Kashif and Samy A. Alsirafy

*American Journal of Hospice and Palliative Medicine*, 30: 21-24 (2013) IF: 1.233

The medical records of deceased patients were reviewed to describe the pattern of cancer deaths in a newly established Saudi tertiary care hospital. During eleven months, 87 patients died of cancer. The majority (80 patients, 92%) died of incurable cancer; among which 53% did not receive any systemic anti-cancer therapy (SAT) and 43% received SAT with palliative intent. Younger age ( $< 65$  years), relatively chemosensitive tumours and initial presentation in a potentially curable stage were associated with higher prevalence of palliative SAT administration ( $p = 0.009, 0.019$  and  $0.001$ , respectively). The last palliative SAT was administered during the last two months of life in 66% and during the last two weeks in 14%. During the last admission, 54% of patients were admitted through emergency room, 50% stayed  $>14$  days and 14% died in intensive care unit or emergency room. The results demonstrate that palliative care is a realistic treatment for the majority of patients in our setting and that a significant proportion of these patients receive aggressive care at the end-of-life. There is a need to establish an integrative palliative care program to improve the quality-of-life of dying cancer patients in our region and to minimize the aggressiveness of end-of-life care.

**Keywords:** Cancer deaths; Palliative care; End-of-life care; Quality indicators; Palliative chemotherapy; Saudi arabia.

#### 1050. Prediction of in-Hospital Mortality of Patients with Advanced Cancer Using the Chuang Prognostic Score

Abdullah S. Al-Zahrani, Amr T. El-Kashif, Amrallah A. Mohammad, Shereef Elsamany and Samy A. Alsirafy

*American Journal of Hospice and Palliative Medicine*, 30: 707-711 (2013) IF: 1.233

The prediction of in-hospital mortality may help in improving end-of-life care for patients dying of cancer. The Chuang Prognostic Score (CPS) was developed to predict survival of terminally ill patients with cancer. The CPS was assessed in 61 hospitalized adult patients with advanced cancer. Using a CPS cutoff point of 6, in-hospital mortality was predicted with 71% positive predictive value, 91% negative predictive value, 75% sensitivity, 89% specificity, and 85% overall accuracy. The patients were divided according to the CPS score into 3 groups (Group 1:  $CPS < 3.5$ , Group 2:  $CPS 3.5-6$ , and Group 3:  $CPS > 6$ ) with a median survival of not reached, 118 days, and 16 days, respectively ( $P < .001$ ). The CPS may be useful in predicting in-hospital mortality of hospitalized patients with advanced cancer.

**Keywords:** Advanced cancer; Palliative care; In-hospital mortality; Prognosis; Chuang prognostic score.

#### 1051. Prevalence of Methicillin-Resistant Staphylococcus Aureus Colonization and Infection in Hospitalized Palliative Care Patients with Cancer

Hafez M. Ghanem Ahmad M. Abou-Alia and Samy A. Alsirafy

*American Journal of Hospice and Palliative Medicine*, 30: 377-379 (2013) IF: 1.233

Little is known about the pattern of methicillin-resistant Staphylococcus aureus (MRSA) colonization and infection in hospitalized palliative care (PC) patients. We reviewed 854 admissions for 289 patients with advanced cancer managed by a PC service in a tertiary care hospital. The MRSA screening was performed at least once in 228 (79%) patients, and 21 (9%) of them were MRSA positive.

Other cultures were done in 251 (86.8%) patients, and 8 (3%) patients were MRSA positive. The total number of MRSA positive admissions was 28 (3%), with a median admission duration of 8 days. A substantial proportion of hospitalized PC patients with cancer are MRSA positive. Research is required to study the impact of infection control measures on the quality of PC delivered to MRSA-positive terminally ill patients in hospitals.

**Keywords:** Methicillin-resistant staphylococcus aureus; Infection control; Hospital-based palliative care; Advanced cancer; Prevalence; Quality of life.

#### 1052. Does Fluid Restriction Affect the Image Quality of Skeletal Scintigraphy

Amr Amin, Mahasen Amin and Ayah Nawwar

*Iranian J. Nuclear Medicine*, 21: 77-80 (2013)

**Introduction:** in Islamic countries in the month of Holy Ramadan many Muslims based on their religious Legislation refuse fluid intake during the fasting time though instructed to drink after injection of Tc-99m Methylene-diphosphonates [Tc-99m MDP] used for skeletal scintigraphy. We aimed to establish whether fluid restriction in Tc-99m MDP skeletal scintigraphy has an impact on its quality.

**Methods:** One hundred forty-four patients referred for skeletal scintigraphy were studied. Group 1 was well hydrated while group 2 was instructed not to drink till imaging. Image quality

was assessed using quantitative measures where by the end of imaging, equal regions of interest (ROI) were drawn over the femoral diaphysis, and the contralateral adductor area. The total number of counts from the bone [B] ROI and soft tissue [ST] ROI was expressed as a ratio [B:ST ratio], and a mean value for each group was established. The image quality was also assessed without knowledge of individual's water intake by a semiquantitative score.

**Results:** No statistically significant difference was found between the B:ST ratio means [P=0.46] and the semiquantitative scores [P=0.42] in both groups.

**Conclusion:** Fluid restriction had no impact on the image quality in Tc-99m MDP skeletal scintigraphy though a higher radiation dose to the urinary bladder wall is anticipated.

**Keywords:** Skeletal scintigraphy; Fluid restriction; Tc-99M MDP; Image quality; Bone to soft tissue ratio.

### 1053. Involved Nodal Radiotherapy vs. Involved Field Radiotherapy After Chemotherapy in the Treatment of Early Stage Hodgkin'S Lymphoma

Hamdy M. Zwam, Emad E. Habib and Mustafa E. AL-Daly

*Journal of Cancer Therapy*, 4: 271-279 (2013)

**Aim of work:** This study is a prospective randomized trial aiming to investigate whether radiotherapy volume can be reduced without loss of efficacy from involved field radiotherapy (IFRT) to involved node radiotherapy (INRT) after four cycles of ABVD chemotherapy in the treatment of early stage Hodgkin's lymphoma.

**Patients and Methods:** Between September 2009 and January 2012, all patients with newly diagnosed early-stage favorable and unfavorable Hodgkin's lymphoma attending to the Clinical Oncology department of Cairo University, faculty of medicine were enrolled into this study after a written consent was obtained from those cases enrolled. Patients were assigned to receive (ABVD) for four cycles followed by randomization for radiotherapy into two arms one arm of 30 Gy INRT +/- 6 Gy to residual disease or another arm of 30 Gy IFRT +/- 6 Gy to residual disease.

**Results:** 35 patients were enrolled in this study: 16 patients in the INRT arm and 19 patients in the IFRT arm. The median observation time was 25 months. The overall survival for all eligible patients was 97% and freedom from treatment failure was 85.7%. Survival rates at the end of the study revealed no differences between INRT and IFRT arms. Also, in terms of complete remission post radiotherapy (14 versus 15), relapse (1 versus 4), and death (0 versus 1) respectively the outcome was similar in both arms.

As regard acute and sub-acute toxicities no significant difference could be detected between both arms except that IFRT arm was associated with a higher incidence of radiation pneumonitis (4 versus 1 patient).

**Conclusion:** Radio-therapy volume size reduction from IFRT to INRT after ABVD chemotherapy for four cycles produces similar results and less toxicity in patients with early-stage Hodgkin's lymphoma especially in patients with mediastinal disease.

**Keywords:** Hodgkin'S lymphoma; Nodal radiotherapy; Field radiotherapy.

### 1054. Short Term Prognostic Utility of Tc-99M DMSA Renal Imaging in Sepsis Induced Acute Renal Failure; Provisional Data

Amr Amin, Hatem Nasr, Gehan Younis and Hatem Gamal

*International Journal of Clinical Medicine*, 4: 543-547 (2013)

**Background:** Sound prognostic data in sepsis induced acute renal failure (SARF) are lacking especially on the short term outcome [STO] in the intensive care unit [ICU]. We addressed the use of Tc-99m DMSA [2,3-dimercaptosuccinic acid] renal cortical imaging as a prognostic tool in SARF.

**Methods:** Forty patients with acute renal failure due to sepsis [age range 15- 74 years; median 44.5] were subjected for full history taking complete physical examination, routine ICU monitoring, routine laboratory investigations, APACHE II [Acute Physiology and Chronic Health Evaluation] and SOFA [Sequential Organ Failure Assessment] together with Tc-99m DMSA cortical renal scintigraphy. Patients' death in the ICU or discharge was considered as the end point of the study representing the so-called short term outcome [STO].

**Results:** 25% mortality rate [10/40] was found along the admission period in the ICU. All non-survivors were abnormal with DMSA imaging [NPV & PPV 100% & 66.7% respectively]. Abnormal DMSA cases showed significant positive associations with serum creatinine at admission [r = 0.5; P 0.02]; admission duration [r = 0.4; P 0.002]; APACHE II score [r = 0.5; P 0.004] and STO [r = 0.4; P 0.03]. Statistically significant difference was elicited between subjects with normal and abnormal DMSA regarding the same parameters.

**Conclusion:** This preliminary data could raise Tc-99m DMSA renal imaging as a prognostic tool in SARF that could allow influential interference to prohibit dramatic outcomes as mortality.

**Keywords:** Acute renal failure; Tc-99M DMSA; Sepsis induced acute renal failure.

### 1055. Significance of Popliteal Lymph Nodes Visualization During Radionuclide Lymphoscintigraphy for Lower Limb Lymphedema

Ahmed Abdel-Samie Kandeel, Jehan Ahmed Younes and Ahmed Mohamed Zaher

*Indian Journal of Nuclear Medicine*, 28: 6-9 (2013)

**Purpose:** To examine the frequency and significance of visualization of popliteal nodes during lymphoscintigraphy for the investigation of lower extremity swelling.

**Materials and Methods:** Technetium-99m-labeled nanocolloid was injected subcutaneously in the first web spaces of both feet of 90 patients (24 males, 66 females; age range, 4-70 years) who had clinical evidence of lower limb lymphedema and were referred for routine lymphoscintigraphy; imaging was performed 5, and 90 minutes after injection without any vigorous exercise between the injection and imaging.

**Results:** According to the scan findings, patients were divided into two groups; group I included 63 patients without popliteal nodes visualization on scanning, and group II included 27 patients with positive popliteal nodes uptake. None of patients with primary lymphedema (N = 22) due to agenesis or hypoplasia showed popliteal node uptake, whereas, patients with secondary



lymphedema (N = 68) had either severe (N = 23) or partial (N = 45) lymphatic obstruction. A high positive association of popliteal node uptake with the severity of lymphatic obstruction was noted. Popliteal nodes were visualized in 26 of 57 patients with dermal back flow (46%), and in only 1 of 33 patients without dermal back flow (3%). There was a strong association between skin rerouting and popliteal node visualization ( $P < 0.01$ ). Skin changes were detected in 24 patients (38%) with positive popliteal node uptake.

**Conclusion:** Popliteal lymph nodes uptake during lymphoscintigraphy for clinical lymphedema of the lower limb indicates lymph rerouting through the deep system and raises a diagnosis of higher severity and longer duration of lymphatic dysfunction.

**Keywords:** Lower limb edema; Lymphoscintigraphy; Popliteal lymph node.

#### 1056. The Use of Opioids at the end-of-Life and the Survival of Egyptian Palliative Care Patients with Advanced Cancer

Samy A. Alsirafy, Khaled M. Galal, Enas N. Abou-Elela, Noha Y. Ibrahim, Dina E. Farag and Ahmed M. Hammad

*Annals of Palliative Medicine*, 2: 173-177 (2013)

**Background and Aim:** One of the barriers to cancer pain control and palliative care (PC) development is the misconception that the use of opioids may hasten death. This concern is exaggerated when higher doses of opioids are used at the end-of-life. The aim of this study was to investigate the relationship between survival and the dose of opioids used at the end-of-life of patients with advanced cancer in an Egyptian PC setting.

**Methods:** Retrospective review of the medical records of 123 patients with advanced cancer managed in an Egyptian cancer center-based palliative medicine unit (PMU). Patients were classified according to the last prescribed regular opioid dose expressed in milligrams of oral morphine equivalent (OME) per day (mg OME/24 h) into three groups: no opioid or low-dose group ( $<120$  mg OME/24 h), intermediate-dose group ( $120-300$  mg OME/24 h) and high-dose group ( $\geq 300$  mg OME/24 h). Survival was calculated from the date of first referral to the PMU to death.

**Results:** The median age of patients was 53 years, breast cancer was the most common diagnosis (18%) and the majority (68%) died at home. Opioids were prescribed for pain control in 94% of patients and were prescribed on regular basis in 89%. The mean last prescribed opioid dose for the whole group of patients was  $167 (\pm 170)$  mg OME/24 h and it was highest among patients with pleural mesothelioma [ $245 (\pm 258)$  mg OME/24 h]. The last prescription included no opioids or low-dose opioids in 57 (46%) patients, intermediate-dose in 42 (34%) and high-dose in 24 (20%). The estimated median survival was 45 days for the no opioid/low-dose group, 75 days for the intermediate-dose group and 153 days for the high-dose group ( $P=0.031$ ).

**Conclusions:** The results suggest that the dose of opioids has no detrimental impact on the survival of patients with advanced cancer in an Egyptian PC setting. Further research is needed to overcome barriers to cancer pain control especially in settings with inadequate cancer pain control.

**Keywords:** Cancer pain control; Opioids; Survival; Palliative care (PC); Egypt.

#### 1057. Role of CYP2C9, VKORC1 and Calumenin Genotypes in Monitoring Warfarin Therapy: an Egyptian Study

Naguib Zohir, Reham Afifi, Asmaa Ahmed, Zinab Aly, Mehry Elsobekey, Heba Kareem and Rehab Helmy

*Macedonian Journal of Medical Sciences*, 6: 414-420 (2013)

**Background:** Oral anticoagulant therapy is conditioned by environmental and genetic factors. Objectives: To verify the effect of the calumenin, cytochrome P-450 variants and VKORC1 genetic polymorphisms on the response to warfarin therapy and warfarin dose adjustment. Patients and

**Methods:** We selected fifty warfarin treated patients with dose adjusted at INR value between 2 and 3. PCR-RFLP is used for of calumenin gene polymorphism. Insitu Hybridization was used for identification of VKORC1 promoter and CYP2C9 variants polymorphisms.

**Results:** The warfarin dose in the patients with Calumenin and CYP2C9 genetic polymorphism was lower than the wild type gene. The warfarin dose in the patients with VKORC1 variants was statistically lower compared to that of the wild-type. The presence of combined CYP2C9 genetic variants and VKORC1 polymorphism was associated with lower warfarin dose than that the wild types.

**Conclusion:** Calumenin (CALU) might be a new genetic factor involved in the pharmacogenetics of anticoagulant therapy. Introduction

**Keywords:** VKORC1; CALU; CYP2C9; PCR; RFLP.

#### Dept. of Dermatology

#### 1058. Assessment of Interleukin-17 and Vitamin D Serum Levels in Psoriatic Patients

Hesham Abd El-Moaty Zaher, Mohamed Hussein Medhat El-Komy, Rehab Aly Hegazy, Heba Amr Mohamed El Khashab and Hanaa Hamdy Ahmed

*Journal of the American Academy of Dermatology*, 69: 840-842 (2013) IF: 4.906

Psoriasis is considered a prototypic T helper (Th) 17-mediated disease with a putative role played by vitamin D deficiency in its pathogenesis. 1,2 Several reports have verified the existence of interplay between Th17 and vitamin D3; however, whether such a relationship exists in the context of psoriasis has not been verified, the investigation of which is the aim of this current work. Forty-eight histopathologically proven psoriatic patients and 40 age-, sex-, skin phototype-, and socioeconomic-matched controls were included. Presence of any criteria that might affect serum vitamin D or interleukin (IL)-17 levels in a subject deemed that subject ineligible for inclusion. Topical applications, apart from emollients, and systemic treatments were stopped for a minimum of 4 weeks before inclusion. Each patient was subjected to history taking and clinical examination to document the Psoriasis Area and Severity Index. Serum levelsof IL-17, 25-hydroxy vitamin D, and parathyroid hormone (PTH) were measured by enzyme-linked immunosorbent assay.

**Keywords:** Psoriasis; Th17; Vitamin D.



### 1059. Scleromyxedema: A Novel Therapeutic Approach

Mohammad Aly Abdel-Qader El Darouti

*Journal of the American Academy of Dermatology*, 69: 1062-1066 (2013) IF: 4.906

Scleromyxedema (SM) is a rare chronic disabling disease with an unclear pathogenesis. Currently there is no consensus on the treatment for SM. Numerous therapeutic strategies have been tried, including systemic steroids, melphalan, retinoids, thalidomide, intravenous immunoglobulins, interferon alpha, photochemotherapy, and autologous stem cell transplant, with variable results. To treat SM the following events should be targeted: (1) abnormal serum paraprotein, (2) increased fibroblastic proliferation, (3) increased mucopolysaccharide, and (4) collagen production.

**Keywords:** Scleromyxedema; Systemic steroids; Melphalan.

### 1060. Autoimmune Reactivity Against Precursor form of Desmoglein 1 in Healthy Tunisians in the Area of Endemic Pemphigus Foliaceus

Amina Toumi, Marwah Adly Saleh, Jun Yamagami, Olfa Abida, Maryem Kallel, Abderrahmen Masmoudi, Soudes Makni, Hamida Turki, Takahisa Hachiya, Keiko Kuroda, John R. Stanley, Hatem Masmoudi and Masayuki Amagai

*Journal of Dermatologic Science*, 70: 19-25 (2013) IF: 3.52

**Background:** Desmoglein 1 (Dsg1), the pemphigus foliaceus (PF) antigen, is produced as a precursor (preDsg1) and is transported to the cell surface as the mature form (matDsg1). Recent studies show that B cells from North American individuals without pemphigus can potentially produce anti-preDsg1 IgG antibodies, but ELISA screening of large numbers of normal people in North America and Japan hardly ever shows circulating antibodies against preDsg1 or matDsg1. In contrast, in Tunisia, where PF is endemic, anti-Dsg1 IgGs are frequently detected in healthy individuals.

**Objective:** To characterize these anti-Dsg1 antibodies from normal individuals in Tunisia.

**Methods:** Sera from 16 healthy individuals and 9 PF patients in the endemic PF area in Tunisia, and sera from Japanese non-endemic PF patients were analyzed by immunoprecipitation-immunoblotting using recombinant proteins of preDsg1, matDsg1, and domain-swapped Dsg1/Dsg2 molecules.

**Results:** Sera from normal Tunisian individuals reacted to preDsg1 alone (8/16) or more strongly to preDsg1 than to matDsg1 (7/16), while those from all Tunisian PF patients and Japanese non-endemic PF patients reacted similarly to preDsg1 and matDsg1, or preferentially to matDsg1. The epitopes recognized by anti-Dsg1 IgGs from normal Tunisian individuals were more frequently found in the C-terminal extracellular domains (EC3 to EC5), while those in Tunisian endemic PF patients were more widely distributed throughout the extracellular domains, suggesting IgGs against EC1 and EC2 developed during disease progression.

**Conclusions:** These findings indicate that IgG autoantibodies against Dsg1 are mostly raised against preDsg1 and/or C-terminal domains of Dsg1 in healthy Tunisians in the endemic area of PF.

**Keywords:** Pemphigus foliaceus; Desmoglein 1; Precursor; Autoantibody.

### 1061. Serum Ferritin and Vitamin D in Female Hair Loss: Do They Play A Role

H. Rasheed, D. Mahgoub, R. Hegazy, M. Elkomy, R. Abdel Hay, M.A. Hamid and E. Hamdy

*Skin Pharmacology and Physiology*, 26: 101-107 (2013) IF: 2.885

**Aim:** Evaluation of serum ferritin and vitamin D levels in females with chronic telogen effluvium (TE) or female pattern hair loss (FPHL), in order to validate their role in these common hair loss diseases.

**Methods:** Eighty females (18 to 45 years old) with hair loss, in the form of TE or FPHL, and 40 age-matched females with no hair loss were included in the study. Diagnosis was based upon clinical examination as well as trichogram and dermoscopy. Serum ferritin and vitamin D-2 levels were determined for each participant.

**Results:** Serum ferritin levels in the TE (14.7  $\pm$  22.1  $\mu$ g/l) and FPHL (23.9  $\pm$  38.5  $\mu$ g/l) candidates were significantly lower than in controls (43.5  $\pm$  20.4  $\mu$ g/l). Serum vitamin D-2 levels in females with TE (28.8  $\pm$  10.5 nmol/l) and FPHL (29.1  $\pm$  8.5 nmol/l) were significantly lower than in controls (118.2  $\pm$  68.1 nmol/l;  $p < 0.001$ ). These levels decreased with increased disease severity. Serum ferritin cut-off values for TE and FPHL were 27.5 and 29.4  $\mu$ g/l, respectively, and those for vitamin D were 40.9 and 67.9 nmol/l.

**Conclusion:** Low serum ferritin and vitamin D2 are associated with hair loss in females with TE and FPHL. Screening to establish these levels in cases of hair loss and supplementing with them when they are deficient may be beneficial in the treatment of disease.

**Keywords:** Female Pattern Hair Loss; Serum Iron; Serum Vitamin D; Telogen Effluvium.

### 1062. The Antioxidant Role of Paraoxonase 1 and Vitamin E in Three Autoimmune Diseases

S. Ramadan, A. Tawdy, R. Abdel Hay and L. Rashed D. Tawfik

*Skin Pharmacology and Physiology*, 26: 2-7 (2013) IF: 2.885

**Purpose of The Study:** To investigate the role of paraoxonase 1 (PON1) and vitamin E in the pathogenesis of some autoimmune diseases, and to correlate their levels with the disease activity.

**Procedures:** This randomized case control study was performed on 60 subjects: 45 patients [suffering from psoriasis, vitiligo and alopecia areata (AA) 15 patients each group] and 15 healthy Controls. Venous blood and tissue biopsy were collected from each subject to estimate the levels of vitamin E and PON1.

**Results:** All patients showed significantly lower levels of both PON1 and vitamin E in tissue and serum than the controls ( $p < 0.001$ ). **Conclusion:** An association between oxidative stress and pathogenesis of these autoimmune diseases is identified. Attenuation of oxidative stress might be a relevant therapeutic approach and it would be useful to recommend additional drugs with antioxidant effects in the treatment of these conditions.

**Keywords:** Paraoxonase; Vitamin E; Psoriasis; Vitiligo; Alopecia areata.

### 1063. Osteopontin and Adiponectin: How Far are They Related in the Complexity of Psoriasis?

D. Kadry, R. A. Hegazy and L. Rashed

*Archives of Dermatological Research*, 305: 939-944 (2013) IF: 2.708

Increasing attention has been drawn towards the involvement of both osteopontin (OPN) and adiponectin in psoriasis. The relationship between them has been studied before in the context of essential hypertension. To our knowledge, whether a relation between them exists in cases of psoriasis and the metabolic status in such patients have not been investigated. We aimed to verify their possible roles and relations in psoriasis and its metabolic associations. 35 patients with psoriasis vulgaris and 35 controls were included. Patients were clinically assessed by PASI and investigated for the presence of metabolic syndrome (MetS) and/or its components. Plasma levels of OPN and adiponectin were measured using ELISA. On comparing psoriatics to controls, patients showed significantly elevated levels of OPN ( $90.474 \pm 21.22$  vs  $34.709 \pm 13.95$  ng/mL) and significantly depressed levels of adiponectin ( $4,586 \pm 1.187$  vs  $5,905 \pm 1.374$  ng/mL), ( $p < 0.001$ ). Strong negative correlation between plasma OPN and adiponectin was detected in patients ( $r = -0.912$ ,  $p < 0.001$ ), but not in controls. OPN elevation was related to diabetes mellitus, insulin resistance, and MetS. Adiponectin depression was related to body mass index, and MetS. This study demonstrates for the first time a significant correlation between OPN and adiponectin in psoriasis, hypothesized to be mostly attributed to the inflammatory milieu of psoriasis and MetS as well as the enhanced renin-angiotensin-aldosterone system previously documented in psoriasis. Adjuvant therapies aiming at modulating levels of OPN and adiponectin are speculated to add benefit in psoriasis treatment and protecting against its metabolic risks.

**Keywords:** Adiponectin; Metabolic syndrome; Osteopontin; Psoriasis.

### 1064. Estimation of Tissue Osteopontin Levels Before and After Different Traditional Therapeutic Modalities in Psoriatic Patients

N.H. El-Eishi, D. Kadry, R.A. Hegazy and L. Rashed

*Journal of the European Academy of Dermatology and Venereology*, 27: 351-355 (2013) IF: 2.694

**Background:** Several lines of evidences support a major role for Th1 cells in psoriasis. Treatment of psoriasis with cyclosporine, methotrexate and psoralen plus ultraviolet A (PUVA) is associated with clinical improvement and decrease in epidermal hyperplasia. Osteopontin (OPN) exerts a T-helper type 1 (Th1) cytokine function, regulating inflammatory cell accumulation and function. Objective to detect the effects of methotrexate, cyclosporine and PUVA on OPN expression in psoriatic plaques, and whether these changes correlate with clinical response.

**Methods:** For three groups of psoriatic patients (each including 12 patients), the Psoriasis Area Severity Index (PASI) and levels of lesional skin OPN were determined using enzyme-linked immunosorbent assays before and after treatment with methotrexate, cyclosporine or PUVA. Skin biopsies from 20 healthy volunteers served as control for OPN levels in normal skin.

**Results:** Baseline lesional skin of psoriatic patients showed a statistically significant elevation of OPN levels in comparison to controls. Three months after therapy, the three therapeutic modalities were associated with a significant decrease in the mean levels of PASI and tissue OPN, with the PUVA group showing the highest level of reduction in OPN levels and cyclosporine group showing the highest level of reduction in PASI.

**Conclusion:** Our study points to the possible role played by OPN in the pathogenesis of psoriasis and in reflecting disease severity. These standard therapeutic modalities used in the current study were associated with a significant decrease in PASI and OPN levels.

They constitute highly effective therapeutic modalities for psoriasis, which might exert their anti-psoriatic activity partially through altering the expression of OPN.

**Keywords:** Psoriasis; Osteopontin; Therapy.

### 1065. PTPN22 Gene Polymorphism in Egyptian Alopecia Areata Patients and Its Impact on Response to Diphencyprone Immunotherapy

Bakr Mohamed El-Zawahry, Omar Ahmed Azzam, Nagla Sameh Zaki, Heba Mohamed Abdel-Raheem, Dalia Ahmed Bassiouny and Mervat Mamdooh Khorshied

*Gene*, 523: 147-151 (2013) IF: 2.196

PTPN22 1858C > T gene polymorphism has been associated with several autoimmune disorders including alopecia areata. The aim of the current study was to investigate the effect of the inherited genetic polymorphism 1858C > T of PTPN22 gene on the predisposition to severe forms of alopecia areata and its effect on the response to DPC treatment. To achieve our aim, PTPN22 1858C > T genotyping was performed by PCR-based restricted fragment length polymorphism (PCR-RFLP) analysis.

The study included 103 Egyptian patients with extensive alopecia areata treated by DPC. Hundred healthy age and sex matched blood donors were included in the current study as a control group.

Results of genotyping showed that PTPN22 CT and TT mutant genotypes were significantly higher in AA patients compared to controls and conferred increase risk of AA (OR = 2.601, 95% CI = 1.081–6.255). Statistical comparison between AA patients with wild and mutant genotypes revealed that the duration of the illness was significantly longer in those harboring the mutant genotypes.

Moreover, the association of other autoimmune diseases as atopy and diabetes mellitus was higher in patients with mutant genotypes. Furthermore, PTPN22 1858C > T genetic polymorphism did not affect the patients' response to DPC immunotherapy.

**Keywords:** PTPN22; 1858C > T; Polymorphisms.

### 1066. A 15-Patient Pilot Trial of Lipolysis of the Hips and Thighs Using A Phosphatidylcholine and Deoxycholate Formulation

Nahla S. Hunter, Amira M. El Tawdy, Rehab A. Hegazy, Slwan. I. El Samanoudy and Khaled El-Kaffas

*Dermatologic Surgery*, 39: 5: 791-794 (2013) IF: 1.866

Despite the widespread usage of injection lipolysis, only a few studies have addressed its safety. The primary objective of this

pilot study was to verify the safety profile of this popular technique.

**Keywords:** Lipolysis; Liver function; Cholines.

**1067. Anti-Type VII Collagen Autoantibodies, Detected by Enzyme- Linked Immunosorbent Assay, Fluctuate in Parallel with Clinical Severity in Patients with Epidermolysis Bullosa Acquisita**

Yoshihiro Ito, Hiroko Kasai, Tetsuya Yoshida, Marwah A. Saleh, Masayuki Amagai and Jun Yamagami

*Journal of Dermatology*, 40: 864-868 (2013) IF: 1.765

Epidermolysis bullosa acquisita (EBA) is an autoimmune subepidermal blistering disease caused by autoantibodies against type VII collagen. An enzyme-linked immunosorbent assay (ELISA) is currently available to detect autoantibodies in EBA. There have been reports suggesting generically that ELISA indices reflect EBA disease severity; however, there is, as yet, no conclusion as to whether ELISA indices fluctuate with disease activity over time in each EBA patient.

This study aimed to investigate whether ELISA titers fluctuate with EBA disease activity and to validate the clinical significance of checking ELISA values in EBA by monitoring type VII collagen ELISA titers and disease severity, evaluated in terms of numbers of blisters and erosions as a clinical score, over time in three Japanese patients with EBA. All three cases in this study, which were treated successfully, showed titers of anti-type VII collagen autoantibodies detected by ELISA that fluctuated in parallel with disease activity. Especially in case 1, we could determine that the expanding erosions were not due to flare-ups of EBA because the ELISA indices stayed low, although new lesions continued to appear. In fact, control of infection and nutrition helped the lesions to become epithelialized. In conclusion, we found that repeated ELISA measurements are useful in monitoring disease activity and making decisions in EBA treatment plans.

**Keywords:** Autoantibody; Clinical severity; Enzyme-linked immunosorbent assay; Epidermolysis bullosa acquisita; Type VII collagen.

**1068. Impact of Vitiligo on the Health-Related Quality of Life of 104 Adult Patients, Using Dermatology Life Quality Index and Stress Score: First Egyptian Report**

Marwa Mohamed and Rehab A. Hegazy

*European Journal of Dermatology*, 23(5): 733-734 (2013) IF: 1.756

Despite the large number of vitiligo patients in our rapidly expanding population, no studies are available addressing the health-related quality of life (QOL) of vitiligo patients in our community. The current study verified the health-related QOL in vitiligo patients in our country, with its peculiar settings, using both the Dermatology life quality index (DLQI) and the stress score (SS).

**Keywords:** Vitiligo; Quality of life; Stress score.

**1069. Interleukin 17, Interleukin 22 and Foxp3 Expression in Tissue and Serum of Non-Segmental Vitiligo: A Case- Controlled Study on Eighty-Four Patients**

Mostafa Abou Elela, Rehab A. Hegazy, Marwa Mohamed Fawzy, Lalia A. Rashed and Hoda Rasheed

*European Journal of Dermatology*, 23 (3): 350-355 (2013) IF: 1.756

**Background:** Skewing of responses towards T helper (Th) 17 and away from T regulatory cells (T-regs) has been suggested to be partially involved in autoimmune diseases like vitiligo. Aims: Clarify the possible role and relationship between Th17 and T-regs in vitiligo by measuring tissue, systemic levels of interleukin (IL)-17, IL-22 and Foxp3.

**Patients and Methods:** 84 non-segmental vitiligo patients and 80 controls were included. Vitiligo Area Scoring Index, Vitiligo Disease Activity and stress score were determined. Skin biopsies underwent immunohistochemical staining for IL-17, IL-22 and Foxp3 and their systemic levels were determined by ELISA and quantitative real time PCR.

**Results:** Mean area % of +ve immunostaining and serum levels of IL-17 ( $34.12 \pm 5.12$ ,  $23.62 \pm 8.17$  pg/mL) and IL-22 ( $48.63 \pm 19.23$ ,  $43.53 \pm 11.95$  pg/mL) were significantly higher in patients compared to controls ( $15.33 \pm 4.19$ ,  $12.83 \pm 3.29$  pg/mL) ( $13.44 \pm 3.82$ ,  $9.92 \pm 4.7$  pg/mL) ( $P < 0.001$ ). Mean area % of +ve immunostaining and peripheral blood levels of Foxp3 were significantly lower in patients ( $2.67 \pm 0.54$ ,  $0.574 \pm 0.32$ ) compared to controls ( $7.12 \pm 0.18$ ,  $1.48 \pm 0.49$ ) ( $P < 0.001$ ). In patients, a positive correlation between IL-17 and IL-22 was detected ( $r = 0.671$ ,  $P < 0.001$ ), each showing negative correlation with Foxp3 ( $r = -0.548$ ,  $P < 0.001$ ), ( $r = -0.382$ ,  $P < 0.001$ ). VASI, VIDA and stress score correlated positively with IL-17, IL-22 and negatively with Foxp3.

**Conclusion:** Th17 and T-regs are intertwined in the complexity of vitiligo giving hope of treatment through adjuvant therapies controlling the delicate balance between them.

**Keywords:** Vitiligo; Th-17; IL-17; IL-22; Foxp3; T-regs.

**1070. Propranolol and Infantile Hemangiomas: Different Routes of Administration, A Randomized Clinical Trial**

Hesham Zaher, Hoda Rasheed, Samia Esmat, Ranya A. Hegazy, Heba I. Gawdat, Rehab A. Hegazy, Mohamed El-Komy and Dalia M. Abdelhalim

*European Journal of Dermatology*, 23: 646-652 (2013) IF: 1.756

Oral propranolol has become the treatment of choice of infantile hemangiomas (IH)s. However, the safety of systemic propranolol is questioned. Topical therapy with 1% propranolol has been reported to be safe and effective. Intralesional (IL) administration may possibly allow safe delivery of higher drug dosages. Aim: To assess the efficacy and safety of two locally administered routes of propranolol (topical and IL), in comparison with its systemic oral use in the treatment of IHs.

**Patients and Methods:** 45 patients with IHs were randomly divided into 3 groups, A, B and C ( $n = 15$  in each), receiving oral propranolol, 2 mg/kg/day, topical propranolol 1% ointment twice daily, IL propranolol, 1 mg of propranolol hydrochloride in 1 ml

of injection once weekly, respectively. Follow up was done for 6 months after treatment was stopped.

**Results:** Excellent response was achieved in 9 patients in group A (60%), 3 in group B (20%) and 2 in group C (13.3%), (P value: 0.04). As regards safety, all 3 modalities proved safe with no major side effects apart from 1 patient in group A and 3 in group C who dropped out due to pain or inconvenience of therapy.

**Conclusions:** Further work is needed to establish clear guidelines and reach best formulations. Nevertheless, in properly selected patients with IHs, we recommend the usage of oral propranolol. Topically administered propranolol could be considered in patients at risk of potential side effects from oral administration. As IL application did not offer any more benefits, it could not be recommended.

**Keywords:** Infantile hemangioma; Propranolol; Oral; Topical; Intralesional; Side effects.

### 1071. Mycophenolate Mofetil: A Novel Immunosuppressant in the Treatment of Dystrophic Epidermolysis Bullosa, A Randomized Controlled Trial

Mohammad Aly Abdel-Qader El Darouti, Mohammad A. El-Darouti, Marwa M. Fawzy, Iman M. Amin, Rania M. Abdel Hay, Rehab A. Hegazy and Dalia M. Abdel Halim

*Journal of Dermatological Treatment*, 24: 422-426 (2013)  
IF: 1.504

**Background:** No effective treatment has been found for epidermolysis bullosa dystrophica (EBD).

**Objective:** To evaluate the efficacy and safety mycophenolate mofetil (MMF) in treating EBD.

**Methods:** This randomized controlled double-blinded study included 35 patients with severe generalized EBD. Patients were randomly divided into two groups: group I (18 patients) received cyclosporine therapy (5 mg/kg/day) and group II (17 patients) received MMF therapy (500-1500 mg/day). Clinical assessment was made weekly for 3 months from the start of the treatment. Patients were assessed by measuring the extent of the disease, the % of improvement, assessing the number of new blister formation and the time of complete healing of new blisters. Side effects were recorded when detected.

**Results:** The % of improvement in the disease extent was statistically significantly higher ( $p = 0.009$ ) in group I (mean  $\pm$  SD: 59.21  $\pm$  22.676) than in group II (mean  $\pm$  SD: 44.03  $\pm$  25.71). As regards the number of new blisters and the rate of healing of blisters, there was no statistically significant difference between both groups ( $p = 0.693$  and  $0.404$ , respectively). No serious side effects were reported.

**Conclusion:** MMF seems to be a good therapeutic option for the long-term treatment of EBD, it can be a good alternative for patients who cannot tolerate cyclosporine.

**Keywords:** Cyclosporine; Epidermolysis bullosa dystrophica; Mycophenolate mofetil.

### 1072. Ear, Nose and Throat Involvement in Egyptian Patients with Pemphigus Vulgaris: A Step Towards A Better Management

Marwa Mohamed Fawzy, Rehab A. Hegazy and Ahmed F. Abdel Fattah

*Int. Journal of Dermatology*, 52 (10): 1268-1273 (2013) IF: 1.342

**Background:** The frequency of ear, nose, and throat (ENT) involvement in pemphigus vulgaris (PV) is not clear; thereby, the importance of setting routine ENT examination for patients with PV could not be deduced.

**Objective:** Determine the prevalence of ENT involvement in patients with PV in Egypt; to modify the routine protocol and achieve a step towards better management.

**Patients and Methods:** Thirty-four patients with PV were included. Patients were asked about ENT symptomatology and evaluated for ENT manifestations.

**Results:** Twenty-five patients complained from ENT symptoms (74%). The pharyngeal/ laryngeal-related symptoms were the most common. Eighty-two percent of patients had positive endoscopic findings. The most common were pharyngeal/laryngeal (76.5%). In total, the positive endoscopic findings superseded the positive symptomatic.

**findings:** More severe involvement was documented in non-smoking patients ( $P < 0.05$ ).

**Conclusion:** Full ENT examination as a routine for all patients with PV could be of great value, as it would lead to more accurate diagnosis, therefore improved management.

**Keywords:** Pemphigus vulgaris; Ent; Examination; Management.

### 1073. Broadband Ultraviolet A vs Psoralen Ultraviolet A in the Treatment of Vitiligo: A Randomized Controlled Trial

M. El Mofty, M. Bosseila, H. M. Mashaly, H. Gawdat and H. Makaly

*Journal of Clinical and Experimental Dermatology*, 38: 830-835 (2013) IF: 1.329

**Background:** Psoralen ultraviolet A (PUVA) and narrowband (NB)-UVB have been shown to be efficacious in the treatment of vitiligo. With large and repeated doses, UVA may lead to immediate skin darkening and to delayed tanning. Our previous experience with broadband (BB)-UVA in vitiligo showed encouraging results.

**Aim:** To test the efficacy of BB-UVA in vitiligo and to evaluate if it could provide an alternative treatment for this condition.

**Methods:** This prospective, randomized, controlled, comparative clinical trial enrolled 45 patients with vitiligo, who were randomly divided into three groups, with group A receiving UVA 15 J/cm<sup>2</sup>/session, group B receiving UVA 10 J/cm<sup>2</sup>/ session, and group C receiving PUVA. The patients received three sessions/week for months, with 60 sessions in total.

**Results:** At the mid-point of treatment, clinical response was significantly higher in patients receiving PUVA than in the other two groups. At the end of the study, clinical response was comparable for groups A and C (UVA 15 J/cm<sup>2</sup> and PUVA, respectively), and both were significantly higher than the group receiving UVA 10 J/cm<sup>2</sup>. Patients in the PUVA group responded mainly with perifollicular pigmentation, whereas those receiving UVA responded mainly with lesional tanning.

**Conclusions:** BB-UVA at a dose of 15 J/cm<sup>2</sup>/session gives results for vitiligo that are comparable to PUVA, suggesting it might be useful when oral psoralens are contraindicated.

**Keywords:** Vitiligo; BB- UVA; PUVA; Efficacy.

#### 1074. Amide 1 Expression in Psoriasis and Lichen Planus Using Synchrotron Infrared Microspectroscopy

Ahmed EL Bedewi, Randa Yousef, Dalia Abdel Halim, Rehab Hegazy, William Willis, Lisa M. Miller and Medhat EL Mofty

*International Journal of Peptide Research and Therapeutics*, 19: 203-207 (2013) IF: 1.28

Psoriasis vulgaris and, Lichen planus are cutaneous inflammatory conditions that usually exhibit distinctive morphology. Ten psoriasis vulgaris and, ten Lichen planus patients (mean age, 45 +/- A 10.27 years) with confirmed histopathological diagnoses were analyzed. in the current study synchrotron infrared (IR) microspectroscopy was used to differentiate between these two conditions based on their lymphocytic proteins analyses. It was found that beta-sheets protein structure, known to represent cell apoptosis, were expressed significantly in Lichen planus conditions than that of the psoriasis vulgaris when analyzed against the established normal control groups of five patients of comparable age and, genders ( $P = 0.001$ ,  $0.03$  respectively). Also, the amide 1 protein type within the epidermis of Lichen planus were expressed in significant proportions as compared to psoriasis vulgaris ( $P < 0.001$ ). on the contrary, the amide 1 protein structural types were found clustered in psoriasis vulgaris in different IR spectra than that in Lichen planus as observed in a number of patients during this study. These observations indicated that the concentration of amide 1 protein in psoriasis vulgaris varies to that of Lichen planus. in conclusion, both psoriasis vulgaris and, Lichen planus have different types of epidermal and, dermal protein structures and, this information can be of clinical diagnostic and therapeutic use for these cutaneous inflammatory conditions in near future.

**Keywords:** Psoriasis; Lichen planus; Amide 1; Fourier; Transform infra red micro; Spectroscopy (FT-IRM) Fourier; Transform infra red (FT-IR).

#### 1075. Biochemical Changes Observed After PUVA Versus PUVA Plus Methotrexate Therapy in Mycosis Fungoides Using Synchrotron Infrared Microspectroscopy

Rehab Aly Abdel Salam Hegazy, Ahmed E. L. Bedewi, Randa Youssef, Dalia M. Abdel Halim, Rehab A. Hegazy, William Willis, Lisa M. Miller, Safinaz S. Sayed and Medhat E. L. Mofty

*International Journal of Peptide Research and Therapeutics*, 19: 209-215 (2013) IF: 1.28

Mycosis fungoides (MF) is the most common type of cutaneous T cell lymphoma in which the distinction between early stage MF and other inflammatory dermatosis remains difficult. Twenty patients of early stage MF and nine patients with psoriasis and lichen planus were included in this study. Ten MF patients were treated with psoralen plus UVA (PUVA) and the other 10 MF patients were treated with PUVA plus methotrexate (MTX) until complete clinical remission. Synchrotron infrared microspectroscopy (SIRM) found that MF lesions were biochemically different compared to inflammatory diseases. After treating MF with either therapeutic modality, the lymphocytic count decreased significantly in both the epidermis and dermis ( $P < 0.001$ ) but no biochemical changes were observed in the

remaining lymphocytes after treatment, indicating the disease process was slowed by treatment but not eradicated. in conclusion SIRM is a promising method for distinguishing MF from other inflammatory diseases such as psoriasis and lichen planus. A significant reduction in lymphocyte count indicated that PUVA therapy is an effective treatment for early stage MF, and MTX could be reserved for more advanced cases that are not PUVA responsive. However, SIRM evidence of persistent disease suggests that maintenance therapy is recommended after clinical remission.

**Keywords:** Mycosis fungoides; Cutaneous lymphoma; PUVA; methotrexate; Synchrotron; FTIR.

#### 1076. Clinical Study of Nail Changes in Vitiligo

Tag Anbar, Rania Abdel Hay, Amal T Abdel-Rahman, Noha H. Moftah and Mohamed A Al-Khayyat

*Journal of Cosmetic Dermatology*, 12: 67-72 (2013) IF: 0.871

Both vitiligo and alopecia areata (AA) are associated together, associated with other autoimmune diseases, and autoimmunity is one of the important theories in their etiology. Nail changes are a known association with AA, thus we hypothesized that nail changes can be found in vitiligo patients. on revising the literature, only two types of nail changes were described in association with vitiligo. Our aim was to study the frequency and types of nail changes among vitiligo patients in comparison with normal healthy volunteers. This multi-centric study was carried on 91 patients with vitiligo, as well as 91 normal healthy control subjects who were age- and sex-matched. Nails were examined for changes in nail plates as regards striations, texture, curvature, dystrophy, and pigmentation. The presence or absence of the thumb lunula was also reported. Nail changes were observed in 62 patients (68.1%) and 46 (50.5%) control subjects with a statistically significant difference ( $P=0.016$ ). Longitudinal ridging and absent lunula were significantly higher in patients than in the controls ( $P=0.001$  and  $0.037$ , respectively). Other reported nail abnormalities in the current study included punctate leukonychia, pitting, flag sign, and Terry's nails. Awareness of this association will widen the clinician's perspective to carefully examine the nail changes in vitiligo patients and conversely examine patients with nail changes for vitiligo.

**Keywords:** Vitiligo; Nails; Alopecia areata.

#### 1077. Non-Ablative 1540 Fractional Laser: How far Could it Help Injection Lipolysis and Dermal Fillers in Lower-Face Rejuvenation A Randomized Controlled Trial

Tahra Lehta, Yehia ElGarem, Rehab Hegazy Rania M. Abdel Hay and Dalia Halim

*J. of Cosmetic and Laser Therapy*, 15: 13-20 (2013) IF: 0.857

**Background:** Rejuvenation of the lower face can be challenging and no single modality can accomplish all its complex events. **Patients and methods:** This 18-month study included 24 female patients with a primary complaint of lower-face aging signs. They were randomly allocated to either Group A, who received injection lipolysis and hyaluronic acid dermal filler, or Group B who in addition received non-ablative 1540 fractional laser. The improvement evaluation score used was the global aesthetic



improvement scale (GAIS). Patient's satisfaction level was also recorded. Both were repeated at Months 6, 13 and 18.

**Results:** At all evaluations, laser group showed higher degree of improvement. Interestingly, at short-term evaluation (6 month), there was no significant difference between both groups ( $P > 0.05$ ). However, the laser group improvement in comparison to the other group became significant in the long-term evaluations (13 and 18 months) ( $P < 0.05$ ).

**Conclusion:** This study further documents the importance of combination therapy in facial rejuvenation, offering a treatment protocol combining injection lipolysis and hyaluronic acid as an effective, safe, short-term therapeutic option in lower-face rejuvenation. The addition of 1540 non-ablative fractional laser to the protocol offers a higher efficacy with longer-term effects and no adverse events.

**Keywords:** Dermal filler; Injection lipolysis; Lower; Face rejuvenation; Non ablative laser.

#### Dept. of Diagnostic Radiology

#### 1078. Variability in Brain Treatment During Mummification of Royal Egyptians Dated to the 18<sup>th</sup>–20<sup>th</sup> Dynasties: MDCT Findings Correlated with the Archaeologic Literature

Sahar Nasr Saleem and Zahi Hawass

*American Journal of Roentgenology (AJR)*, 200 (4): 336-344 (2013) IF: 2.897

**Objective:** The objective of our study was to use MDCT to study brain treatment and removal (excerebration) as part of mummification of royal Egyptian mummies dated to the 18th to early 20th Dynasties and to correlate the imaging findings with the archaeological literature.

**Materials and Methods:** As part of an MDCT study of the Royal Ancient Egyptian Mummies Project, we analyzed CT images of the heads of 12 mummies dated to circa 1493–1156 BC (18th to early 20th Dynasties). We reconstructed and analyzed CT images for the presence of cranial defects, brain remnants, intracranial embalming materials, and nasal packs. We compared the CT findings of mummies dated to the 18th Dynasty with those dated to the 19th to early 20th Dynasties.

**Results:** The Akhenaten mummy was excluded because of extensive postmortem skull fractures. CT showed that no brain treatment was offered to three mummies (Thutmose I, II, and III) who dated to the early 18th Dynasty and was offered to the eight mummies who dated later. The route of excerebration was transnasal in eight mummies; an additional suspected route was via a parietal defect. CT showed variable appearances of the intracranial contents. There were larger volumes of cranial packs and more variability in the appearances of the cranial packs in the royal mummies dated to the 19th to 20th Dynasties than in those dated to the 18th Dynasty.

**Conclusion:** MDCT shows variations in brain treatment during mummification of royal Egyptian mummies (18th–20th Dynasties). This study sets a template for future CT studies of the heads of ancient Egyptian mummies and focuses on the key elements of cranial mummification in this ancient era.

**Keywords:** Brain; CT; Egypt; Mummification; Mummy; Royal Egyptians.

#### 1079. Feasibility of Targeting Atherosclerotic Plaques By High-Intensity-Focused Ultrasound: an In Vivo Study

Islam A. Shehata, John R. Ballard, Andrew J. Casper, Dalong Liu, Mitchell Troutman and Emad S. Ebbini

*Journal of Vascular and Interventional Radiology*, 24: 1880-1887 (2013) IF: 2.002

**Purpose:** To investigate the feasibility and acute safety of targeting atherosclerotic plaques by high-intensity-focused ultrasound (US) in vivo through a noninvasive extracorporeal approach.

**Materials and Methods:** Four swine were included in this prospective study, three of which were familial hypercholesterolemic swine. The procedure was done under general anesthesia. After US identification of atherosclerotic plaques within the femoral arteries, plaques were targeted by high-intensity focused US with an integrated dual-mode US array system. Different ablation protocols were used to meet the study objectives, and animals were then euthanized at different time points. Targeted arterial segments were stained by hematoxylin and eosin for histopathologic examination. Numeric values are presented as means  $\pm$  standard deviation.

**Results:** All swine tolerated the procedure well, with no arterial dissection, perforation, or rupture. Discrete lesions were detected in the first two swine, measuring  $0.54 \text{ mm} \pm 0.10$  and  $0.25 \text{ mm} \pm 0.03$  in cross-sectional dimensions in the first and  $0.50 \text{ mm} \pm 0.12$  and  $0.24 \text{ mm} \pm 0.15$  in the second. Confluent ablation zones were identified in the last two swine, measuring  $6.92 \text{ mm}$  and  $0.93 \text{ mm}$  in the third and  $2.97 \text{ mm}$  and  $2.52 \text{ mm}$  in the fourth. Lesions showed necrotic cores and peripheral reactive inflammatory infiltration. The endothelium overlying targeted arterial segments remained intact.

**Conclusions:** The results demonstrate the feasibility and acute safety of targeting atherosclerotic plaques by high-intensity-focused US in vivo. Further long-term studies are needed to assess how induction of these lesions can modify the progression of atherosclerotic plaques.

**Keywords:** High intensity focused ultrasound (Hifu); Atherosclerosis; Dual-mode ultrasound arrays (Dmuas).

#### 1080. High Intensity Focused Ultrasound (HIFU): Call for Careful Patient Selection!

Islam Ahmed Shehata

*Abdominal Imaging*, 38: 419-420 (2013) IF: 1.905

High intensity focused ultrasound (HIFU) is a noninvasive technology for ablation of body tumors among other applications [1]. Unfortunately, this non-invasive nature may have given a false thought that HIFU is the magic stick to treat any tumor anywhere.

While we share the impression that HIFU is exciting and unique in many ways, we still think that it has its limitation; as any other medical modality. As such, we believe that careful patient selection and sufficient understanding of the nature of HIFU therapy are essential considerations for a successful and safe treatment. A valuable article published by Jung et al. [2] touched upon the complications related to HIFU therapy for hepatic and pancreatic tumors.

The study enrolled 114 patients and reported serious complications like skin burns, hepatic and abdominal abscesses, fistulas, and rib fractures. We think that the incidence of such complications should have been more clearly linked to the treatment circumstances of every single case, particularly size of the treated tumors. It is known that the lengthy nature of HIFU ablation is one of its main limitations [1]; thus, every single attempt should be made to shorten the treatment time. Treating large tumors (>3 cm) would result in increased treatment time and complications rate. The mean diameter of treated hepatic tumors in this study ranged from 3 to 3.5 cm with some tumors reaching up to 11 cm. For pancreatic tumors, the mean diameter was 3.7 cm. Average sonication time for primary and secondary hepatic tumors was 72 and 119 min, respectively. We think that some of the complications reported in this study can be avoided if the selection is narrowed to smaller tumors (≤3 cm). Skin burns, for example, can be avoided by appropriate skin preparation [1] and balancing the waiting time between sonications in view of the sonication time. Edema of the Subcutaneous tissue overlying the path of the HIFU beam is frequently encountered and usually resolves spontaneously [2, 3], thus should not be considered a serious complication. However, development of skin burns is unacceptable and can be avoided by allowing sufficient time for skin cooling between sonications. Therefore, attempts to shorten the lengthy HIFU procedures should be directed toward selecting smaller tumors rather than reducing the cooling time.

#### 1081. Fetal Magnetic Resonance Imaging (MRI): A Tool for a Better Understanding of Normal and Abnormal Brain Development

Sahar Nasr Saleem

*Journal of Child Neurology*, 28 (7): 890-908 (2013) IF: 1.385

Knowledge of the anatomy of the developing fetal brain is essential to detect abnormalities and understand their pathogenesis. Capability of magnetic resonance imaging (MRI) to visualize the brain in utero and to differentiate between its various tissues makes fetal MRI a potential diagnostic and research tool for the developing brain. This article provides an approach to understand the normal and abnormal brain development through schematic interpretation of fetal brain MR images. MRI is a potential screening tool in the second trimester of pregnancies in fetuses at risk for brain anomalies and helps in describing new brain syndromes with in utero presentation. Accurate interpretation of fetal MRI can provide valuable information that helps genetic counseling, facilitates management decisions, and guides therapy. Fetal MRI can help in better understanding the pathogenesis of fetal brain malformations and can support research that could lead to disease-specific interventions.

**Keywords:** Anomaly; Syndrome; Genetic; Malformation; Fetal; MRI.

*Dept. of Ear Nose and Throat*

#### 1082. Circumferential Tracheal Resection with Primary Anastomosis for Post-Intubation Tracheal Stenosis: Study of 24 Cases

Hesham Negm, Mohamed Mosleh and Hesham Fathy

*European Archives of Oto-Rhino-Laryngology*, 270 (10): 2709-2717 (2013) IF: 1.458

The objective of this study is to evaluate the results of circumferential tracheal and cricotracheal resection with primary anastomosis for the treatment of post-intubation tracheal and cricotracheal stenosis. This is a retrospective analytical study. A total number of 24 patients were included in this study. The relevant preoperative, operative and postoperative records were collected and analyzed. Twenty patients were finally symptom-free reflecting an anastomosis success rate of 83.3 %. Variable grades of anastomotic restenosis occurred in 11 (45.8 %) patients, three patients were symptom-free and eight had airway obstructive symptoms. Four out of the eight patients with symptomatic restenosis were symptom-free with endoscopic dilatation while the remaining four patients required a permanent airway appliance (T-tube, tracheostomy) for the relief of airway obstruction and this group was considered as anastomotic failure. Cricoid involvement, associated cricoid resection and the type of anastomosis were the variables that had statistical impact on the occurrence of restenosis ( $P = 0.017, 0.017, 0.05$ ; respectively). Tracheal resection with primary anastomosis is a safe effective treatment method for post-intubation tracheal stenosis in carefully selected patients. Restenosis does not always mean failure of the procedure since it may be successfully managed with endoscopic dilatation.

**Keywords:** Tracheal; Stenosis; Tracheal; Resection post; Intubation stenosis.

#### 1083. Cytokeratin Immunohistochemically Detected Nodal Micrometastases in N0 Laryngeal Cancer: Impact on the Overall Occult Metastases

Hesham Negm, Mohamed Mosleh, Hesham Fathy, Amal Hareedy and Ahmad Elbattawy

*European Archives of Oto-Rhino-Laryngology*, 270(3): 1085-1092 (2013) IF: 1.458

The objective of this study is to evaluate the incidence of occult nodal micrometastases in N0 laryngeal squamous cell carcinoma using cytokeratin immunohistochemical analysis (CKIHA) and its influence on the overall occult metastatic rate. This is a prospective cohort study. A total number of 30 patients with N0 stage laryngeal cancer underwent 46 selective neck dissections for elective treatment of the neck. Nodes found to be negative using routine histopathological examination were evaluated for the presence of micrometastasis using CKIHA. The occult micrometastasis rate for all cases was 26.7 % which significantly increased the overall occult metastasis rate to 50 % ( $P = 0.014$ ). The micrometastasis rate was 30.8, 25 and 20 % for glottic, supraglottic and transglottic tumors, respectively, which increased the overall occult metastasis rate to 53.8, 50 and 40 % but without statistical impact. The micrometastasis rate was 35.7 and 23.1 % in T3 and T4 tumors, respectively, and this increased the overall occult metastasis rate to 50 and 61.5 % with statistical influence in T3 tumors ( $P = 0.046$ ). Micrometastasis upstaged the neck in 7 (23.3 %) patients with statistical impact on the PN stage ( $P = 0.007$ ). The overall occult nodal metastasis rate in N0 laryngeal cancer is underestimated. Nodal micrometastasis may be missed during routine histopathological examination and can be detected using CKIHA.

**Keywords:** Nodal micrometastasis occult metastasis; Laryngeal cancer; Immunohistochemistry.

### 1084. Recurrent Acute Otitis Media in Infants: Analysis of Risk Factors

Mohamed Salah, Mosaad Abdel-Aziz, Ahmed Al-Farok and Azzam Jebrini

*International Journal of Pediatric Otorhinolaryngology*, 77: 1665-1669 (2013) IF: 1.35

**Objective:** Recurrence acute otitis media (RAOM) may cause a considerable morbidity and a great parental concern. The aim of this study was to analyze the risk factors that are likely to be responsible for RAOM in infants, and their impact on treatment failure.

**Methods:** A retrospective study on 340 infants with RAOM was conducted. Data were collected from hospital charts. A 10 days course of amoxicillin/clavulanate was used for treatment of recurrence, while surgical management in the form of adenoidectomy and/or myringotomy was reserved for patients with persistent disease. We analyzed various risk factors that may affect the prognosis of RAOM, including: age, prematurity, upper respiratory tract infections (URTI), duration of breastfeeding, use of pacifiers, parental smoking, seasonality, the presence of siblings (family size), gender, adenoid hypertrophy, allergy, and craniofacial abnormalities.

**Results:** Use of pacifiers, short duration of breastfeeding, older infantile age, winter season, URTI and presence of adenoid hypertrophy were identified as risk factors for RAOM. Treatment failure may be due to adenoid hypertrophy, short duration of breastfeeding and it is more common in older age infants. We did not find a significant association between RAOM and gender, prematurity, exposure to passive smoking, the presence of siblings, allergy, craniofacial abnormalities.

**Conclusions:** Factors that may cause recurrence of the disease in infant population are use of pacifiers, short duration of breastfeeding, older infantile age, winter season, upper respiratory tract infections and adenoid hypertrophy. Also, treatment failure may be caused by adenoid hypertrophy and short duration of breastfeeding. Good understanding of these factors may help to decrease the recurrence rate and to improve the treatment of the disease.

**Keywords:** Acute; Otitis media adenoid breastfeeding; Allergy upper respiratory; Infection infantile infection.

### 1085. Speech Outcome After Early Repair of Cleft Soft Palate Using Furlow Technique

Mosaad Mosaad Abdel-Aziz

*International Journal of Pediatric Otorhinolaryngology*, 77: 85-88 (2013) IF: 1.35

**Objective:** The earlier closure of palatal cleft is the better the speech outcome and the less compensatory articulation errors, however dissection on the hard palate may interfere with facial growth. In Furlow palatoplasty, dissection on the hard palate is not needed and surgery is usually limited to the soft palate, so the technique has no deleterious effect on the facial growth. The aim of this study was to assess the efficacy of Furlow palatoplasty technique on the speech of young infants with cleft soft palate.

**Methods:** Twenty-one infants with cleft soft palate were included in this study, their ages ranged from 3 to 6 months. Their clefts were repaired using Furlow technique. The patients were followed up for at least 4 years; at the end of the follow up period

they were subjected to flexible nasopharyngoscopy to assess the velopharyngeal closure and speech analysis using auditory perceptual assessment.

**Results:** Eighteen cases (85.7%) showed complete velopharyngeal closure, 1 case (4.8%) showed borderline competence, and 2 cases (9.5%) showed borderline incompetence. Normal resonance has been attained in 18 patients (85.7%), and mild hypernasality in 3 patients (14.3%), no patients demonstrated nasal emission of air. Speech therapy was beneficial for cases with residual hypernasality; no cases needed secondary corrective surgery.

**Conclusion:** Furlow palatoplasty at a younger age has favorable speech outcome with no detectable morbidity.

**Keywords:** Furlow palatoplasty; Z-Plasty; Cleft palate; Speech.

### 1086. Double J Stent of Frontal Sinus Outflow Tract in Revision Frontal Sinus Surgery

Mansour H A.

*J. Laryngol Otol.*, 127(1): 43-47 (2013) IF: 0.681

**Objective:** Frontal sinus surgery continues to challenge even the most experienced endoscopic sinus surgeon. Revision frontal sinus surgery is even more challenging. The use of stents in frontal sinus surgery has long been described, as an attempt to decrease the incidence of synechiae and stenosis.

**Method:** This study included five patients who had previously undergone functional endoscopic sinus surgery but suffered recurrence of frontal sinusitis. Two had bilateral disease. Double J stents were used after endoscopic frontal sinusotomy. The stents were left in place for six months.

**Results:** Four of the 5 patients (6 out of 7 sinuses) had a patent frontal outflow tract after 10 to 36 months' follow up.

**Conclusion:** Double J stents can be used as frontal sinus stents. They are well tolerated by patients, easily applied, and self-retaining with no need for sutures. The length of the stent can be altered according to the patient's anatomy and pathology.

**Keywords:** Frontal sinus; Sinusitis; Stents.

### Dept. of Endemic

### 1087. How to Optimize HCV Therapy in Genotype 4 Patients

Gamal Esmat, Mohamed El Kassas, Mohamed Hassany, Mohamed Esmat Gamil and Maisa El Raziky

*Liver International*, 33: 41-45 (2013) IF: 3.87

HCV is a worldwide disease with an estimated prevalence by WHO of 3%. Hepatitis C virus 4 is prevalent in Africa and the Middle East, especially Egypt. The treatment of HCV4 is affected by many factors, related to the virus itself (genotype, pretreatment viral load and prevalent quasispecies), to the host (genetic factors, age, ethnicity and liver histology), to the presence of comorbidities (obesity, insulin resistance and co-infections) and to the therapeutic drugs (type, dose and duration). Optimizing treatment is the goal of daily practice to obtain the best results for the patient.

**Keywords:** Genotype 4; Hepatitis C virus; Treatment predictors.

### 1088. Serum Autoantibodies Positivity Prevalence in Patients with Chronic HCV and Impact on Pegylated Interferon and Ribavirin Treatment Response

Marwa Khairy, Maissa El-Raziky, Wafaa El-Akel, Mohamed S. Abdelbary, Hany Khatib, Badawy El-Kholy, Gamal Esmat and Mahassen Mabrouk

*Liver International*, 33: 1504-1509 (2013) IF: 3.87

**Background and Aims:** Prevalence of serum autoantibodies in chronic hepatitis C (HCV) patients is higher than that in the general population. Interferon may induce autoimmune manifestations in patients treated with peg- interferon and ribavirin. Effect of autoantibody seropositivity and treatment response are limited and controversial. to detect the prevalence of serum autoantibodies in patients with chronic HCV and impact on histopathology and treatment response.

**Methods:** Retrospective study including 3673 Egyptian chronic HCV naïve patients enrolled in the Egyptian national programme for HCV treatment with pegylated interferon and ribavirin in the years 2007–2010. Antinuclear antibody (ANA) was determined by ELISA considered positive with a titre =1:40 by indirect immunofluorescence. ANA-positive patients pre treatment workup including serum aminotransferases, thyroid profile and liver biopsy, follow-up during treatment and sustained virological response (SVR) were assessed compared to ANA negative patients.

**Results:** Serum ANA was positive in 1.6% of the studied patients. There were no statistically significant differences concerning the demographic, biochemical and histopathological data in ANA positive and negative patients. SVR was comparable between ANA-positive and ANA negative patients (67.8% and 61.3% respectively). Follow-up treatment; ANA-positive patients' did not experience statistically significant haematological complications, flare-up of serum transaminases, thyroid dysfunction. No systemic autoimmune disorders developed during follow-up.

**Conclusions:** ANA positivity is not a factor in chronic HCV disease progression and does not affect the treatment response. Pegylated interferon and ribavirin therapy is safe and effective in autoantibodies-positive chronic HCV patients with no need for further follow-up or worry during the treatment in absence of systemic autoimmune disorders.

**Keywords:** ALT; ANA; AST; HCV; Histological activity; Treatment response.

### 1089. Transluminal Retroperitoneal Endoscopic Necrosectomy with the Use of Hydrogen Peroxide and Without External Irrigation: a Novel Approach for the Treatment of Walled-Off Pancreatic Necrosis

Mohamed Abdelhafez, Mayada Elnegouly, M. S. Hasab Allah, Mostafa Elshazli, Hany M. S. Mikhail and Ayman Yosry

*Surgical Endoscopy*, 27(10): : 3911-3920 (2013) IF: 3.427

**Background:** Transluminal retroperitoneal endoscopic Necrosectomy (TREN) is an attractive NOTES technique alternative to surgery for treatment of walled-off pancreatic necrosis (WOPN). The main limitations to this technique are the need for repeated sessions, prolonged external irrigation, and EUS availability. in our study, we introduced new modifications,

including the use of hydrogen peroxide, and abandoning the use of EUS and external irrigation.

**Methods:** This is a retrospective study of outcome of consecutive patients who underwent TREN for WOPN between April 2011 and August 2012. The technique included (1) non-EUS-guided transluminal drainage, and (2) direct endoscopic debridement using hydrogen peroxide and different accessories. No external irrigation was used.

**Results:** Ten patients were included. Initial clinical and technical success was achieved in all patients. Complete radiological success and long-term clinical efficacy was achieved in nine patients (1 patient had an inaccessible left paracolic gutter collection and died 62 days after endotherapy). Mean number of sessions was 1.4 (range 1-2). Complications included bleeding, which was self-limited in three patients and endoscopically controlled in one. All patients avoided surgery, and no recurrence was reported during median follow-up of 289 (range 133-429) days.

**Conclusions:** TREN is a safe and effective treatment for WOPN and could be performed safely without EUS guidance in selected cases. Hydrogen peroxide played a major role in reduction of number of sessions and timing. External irrigation of WOPN is not necessary, if adequate debridement could be achieved.

**Keywords:** Endoscopic necrosectomy; Walled; Off pancreatic necrosis; Notes; Debridement; Hydrogen peroxide; Acute pancreatitis.

### 1090. The State of Hepatitis B and C in the Mediterranean and Balkan Countries: Report from A Summit Conference

Gamal Esmat

*Journal of Viral Hepatitis*, 20 (S2): 1-20 (2013) IF: 3.082

**Summary:** The burden of disease due to chronic viral hepatitis constitutes a global threat. in many Balkan and Mediterranean countries, the disease burden due to viral hepatitis remains largely unrecognized, including in high-risk groups and migrants, because of a lack of reliable epidemiological data, suggesting the need for better and targeted surveillance for public health gains. in many countries, the burden of chronic liver disease due to hepatitis B and C is increasing due to ageing of unvaccinated populations and migration, and a probable increase in drug injecting. Targeted vaccination strategies for hepatitis B virus (HBV) among risk groups and harm reduction interventions at adequate scale and coverage for injecting drug users are needed. Transmission of HBV and hepatitis C virus (HCV) in healthcare settings and a higher prevalence of HBV and HCV among recipients of blood and blood products in the Balkan and North African countries highlight the need to implement and monitor universal precautions in these settings and use voluntary, nonremunerated, repeat donors. Progress in drug discovery has improved outcomes of treatment for both HBV and HCV, although access is limited by the high costs of these drugs and resources available for health care. Egypt, with the highest burden of hepatitis C in the world, provides treatment through its National Control Strategy. Addressing the burden of viral hepatitis in the Balkan and Mediterranean regions will require national commitments in the form of strategic plans, financial and human resources, normative guidance and technical support from regional agencies and research.

**Keywords:** Balkan region; Mediterranean; Hepatitis B; Hepatitis C; Hepatocellular carcinoma; Northern africa; Surveillance.

### 1091. Towards Realistic Estimates of HCV Incidence in Egypt

R. Breban, W. Doss, G. Esmat, M. Elsayed, M. Hellard, P. Ayscue, M. Albert, A. Fontanet and M. K. Mohamed

*Journal of Viral Hepatitis*, 20 (4): 294-296 (2013) IF: 3.082

Accurate incidence estimates are essential for quantifying hepatitis C virus (HCV) epidemic dynamics and monitoring the effectiveness of public health programmes, as well as for predicting future burden of disease and planning patient care. In Egypt, the country with the largest HCV epidemic worldwide, two modelling studies have estimated age-specific incidence rates that, applied to the age pyramid, would correspond to more than 500 000 Egyptians getting infected annually. This is in contrast to figures of the Egyptian Ministry of Health and Population that estimates new infections to be approximately 100 000 per year. We performed new analyses of nationwide data to examine the modelling assumptions that led to these estimates. Thus, we found that the key assumption of these models of a stationary epidemic is invalid. We propose an alternate approach to estimating incidence based on analysing cohort data; we find that the number of annual new infections is <150 000.

**Keywords:** hepatitis C; Nationwide incidence; Age-stratified prevalence.

### 1092. Hepatic and Intestinal Schistosomiasis: Review

Tamer Elbaz and Gamal Esmat

*Journal of Advanced Research*, 4: 445-452 (2013) IF: 3.00

Schistosomiasis is an endemic disease in Egypt caused by the trematode *Schistosoma* which has different species. Hepatic schistosomiasis represents the best known form of chronic disease with a wide range of clinical manifestations.

The pathogenesis of schistosomiasis is related to the host cellular immune response. This leads to granuloma formation and neo angiogenesis with subsequent periportal fibrosis manifested as portal hypertension, splenomegaly and esophageal varices. Intestinal schistosomiasis is another well identified form of chronic schistosomal affection. Egg deposition and granuloma formation eventually leads to acute then chronic schistosomal colitis and is commonly associated with polyp formation. It frequently presents as abdominal pain, diarrhea, tenesmus and anal pain.

Definite diagnosis of schistosomiasis disease depends on microscopy and egg identification. Marked progress regarding serologic diagnosis occurred with development of recent PCR techniques that can confirm schistosomal affection at any stage. Many antischistosomal drugs have been described for treatment, praziquantel being the most safe and efficient drug. Still ongoing studies try to develop effective vaccines with identification of many target antigens. Preventive programs are highly needed to control the disease morbidity and to break the cycle of transmission.

**Keywords:** Hepatic schistosomiasis; Portal hypertension; Intestinal schistosomiasis; Praziquantel.

### 1093. Human Schistosomiasis: Clinical Perspective: Review

Rashad S. Barsoum, Gamal Esmat and Tamer El-Baz

*Journal of Advanced Research*, 4: 433-444 (2013) IF: 3.00

The clinical manifestations of schistosomiasis pass by acute, sub acute and chronic stages that mirror the immune response to infection. The later includes in succession innate, TH1 and TH2 adaptive stages, with an ultimate establishment of concomitant immunity. Some patients may also develop late complications, or suffer the sequelae of co-infection with other parasites, bacteria or viruses.

Acute manifestations are species-independent; occur during the early stages of invasion and migration, where infection-naivety and the host's racial and genetic setting play a major role. Sub acute manifestations occur after maturity of the parasite and settlement in target organs.

They are related to the formation of granulomata around eggs or dead worms, primarily in the lower urinary tract with *Schistosoma haematobium*, and the colon and rectum with *Schistosoma mansoni*, *Schistosoma japonicum*, *Schistosoma intercalatum* and *Schistosoma mekongi* infection. Secondary manifestations during this stage may occur in the kidneys, liver, lungs or other ectopic sites.

Chronic morbidity is attributed to the healing of granulomata by fibrosis and calcification at the sites of oval entrapment, deposition of schistosomal antigen-antibody complexes in the renal glomeruli or the development of secondary amyloidosis. Malignancy may complicate the chronic lesions in the urinary bladder or colon. Co-infection with salmonella or hepatitis viruses B or C may confound the clinical picture of schistosomiasis, while the latter may have a negative impact on the course of other co-infections as malaria, leishmaniasis and HIV. Prevention of schistosomiasis is basically geared around education and periodic mass treatment, an effective vaccine being still experimental. Praziquantel is the drug of choice in the treatment of active infection by any species, with a cure rate of 80%. Other antischistosomal drugs include metrifonate for *S. haematobium*, oxamniquine for *S. mansoni* and Artemether and, possibly, Mirazid for both. Surgical treatment may be needed for fibrotic lesions

**Keywords:** Hepatointestinal schistosomiasis; Urinary schistosomiasis; Neuroschistosomiasis; Schistosomal coinfection; Treatment schistosomiasis.

### 1094. Coinfection with Hepatitis C Virus and Schistosomiasis: Fibrosis and Treatment Response

Aisha Mahmoud Abdelaziz Elsharkawy

*World J. Gastroenterol*, 19: 2691-2696 (2013) IF: 2.547

**Aim:** To assess whether schistosomiasis coinfection with chronic hepatitis C virus (HCV) influences hepatic fibrosis and pegylated-interferon/ribavirin (PEG-IFN/RIB) therapy response.

**Methods:** This study was designed as a retrospective analysis of 3596 chronic HCV patients enrolled in the Egyptian National Program for HCV treatment with PEG-IFN/RIB. All patients underwent liver biopsy and anti-schistosomal antibodies testing prior to HCV treatment. The serology results were used to categorize the patients into group A (positive schistosomal serology) or group B (negative schistosomal serology). Patients in



group A were given oral antischistosomal treatment (praziquantel, single dose) at four weeks prior to PEG-IFN/RIB. All patients received a 48-wk course of PEG-IFN (PEG-IFNa2a or PEG-IFNa2b)/RIB therapy. Clinical and laboratory follow-up examinations were carried out for 24 wk after cessation of therapy (to week 72). Correlations of positive schistosomal serology with fibrosis and treatment response were assessed by multiple regression analysis.

**Results:** Schistosomal antibody was positive in 27.3% of patients (15.9% females and 84.1%).

#### 1095. CXCL 10 Antagonism and Plasma Sdppiv Correlate with Increasing Liver Disease in Chronic HCV Genotype 4 Infected Patients

Dina Ragab, Melissa Laird Darragh Duffy, Armanda Casrouge Rasha Mamdouh, Amal Abass, Dina El. Shenawy, Abdelhadi M. Shebl, Wagdi F. Elkashef, Khaled R. Zalata, Mostafa Kamal, Gamal Esmat, Philippe Bonnard, Arnaud Fontanet, Mona Rafik and Matthew L. Albert

*Cytokine*, 63(2): 105-112 (2013) IF: 2.518

Egypt has the highest prevalence of hepatitis C virus infection worldwide. CXCL10 is a potent chemoattractant that directs effector lymphocytes to sites of inflammation. It has been reported that plasma CXCL10 is processed by dipeptidylpeptidase IV (DPPIV) thus leading to the generation of an antagonist form. Using Luminex-based immunoassays we determined the concentration of different forms of CXCL10 (total, agonist, and antagonist). We also evaluated plasma soluble DPPIV (sDPPIV) concentration and plasma dipeptidylpeptidase (DPP) activity. Using flow cytometry and immunohistochemistry, we analyzed the distribution of lymphocyte subsets. Plasma CXCL10 was elevated in chronic HCV patients, however the agonist form was undetectable. Increased sDPPIV concentration and DPP activity supported the NH2-truncation of CXCL10. Finally, we demonstrated an increased frequency of CXCR3+ cells in the peripheral blood, and low numbers of CXCR3+ cells within the lobular regions of the liver. These findings generalize the observation of chemokine antagonism as a mechanism of immune modulation in chronic HCV patients and may help guide the use of new therapeutic immune modulators.

**Keywords:** Chronic HCVg 4; CXCL10; IP10; DPPIV; Chemokine antagonism.

#### 1096. Dynamic Interplay Between CXCL Levels in Chronic Hepatitis C Patients Treated by Interferon

Abdel-Rahman N. Zekri, Abeer A. Bahnassy, Waleed S. Mohamed, Hanaa M. Alam EL-Din, Hend I. Shousha, Naglaa Zayed, Dina H. Eldahshan and Ashraf Omar Abdel-Aziz

*Virology Journal*, 10 (218): (2013) IF: 2.092

**Background:** Combined pegylated interferon- $\alpha$  and ribavirin therapy has sustained virological response (SVR) rates of 54% to 61%. Pretreatment predictors of SVR to interferon therapy have not been fully investigated yet. The current study assesses a group of chemokines that may predict treatment response in Egyptian patients with chronic HCV infection.

**Patients and Methods:** CXCL5, CXCL9, CXCL11, CXCL12, CXCL 13, CXCL 16 chemokines and E-Cadherin were assayed in

57 chronic HCV patients' sera using quantitative ELISA plate method. All studied patients were scheduled for combined pegylated interferon alpha and ribavirin therapy (32 patients received pegylated interferon a 2b, and 25 patients received pegylated interferon a 2a). Quantitative hepatitis C virus RNA was done by real time RT-PCR and HCV genotyping by INNOLIPAIL. **Results:** There was no significant difference ( $p > 0.05$ ) in baseline HCV RNA levels between responders and non-responders to interferon. A statistically significant difference in CXCL13 ( $p = 0.017$ ) and E-Cadherin levels ( $P = 0.041$ ) was reported between responders and nonresponders at week 12. Significant correlations were found between changes in the CXCL13 levels and CXCL9, CXCL16, E-cadherin levels as well as between changes in E-cadherin levels and both CXCL16 and ALT levels that were maintained during follow up. Also, significant changes have been found in the serum levels of CXCL5, CXCL13, and CXCL16 with time (before pegylated interferon a 2 a and a 2 b therapy, and at weeks 12 and 24) with no significant difference in relation to interferon type and response to treatment. **Conclusion:** Serum levels of CXCL13 and E-Cadherin could be used as surrogate markers to predict response of combined PEG IFN- $\alpha$ /RBV therapy, especially at week 12. However, an extended study including larger number of patients is needed for validation of these findings.

**Keywords:** HCV; IFN; Chemokine'S; E-cadherin.

#### 1097. Adipokines and Insulin Resistance, Predictors of response to therapy in Egyptian patients with chronic hepatitis C virus genotype 4

Yasmin Saad, Amal Ahmed, Doa'a A. Saleh and Wahid Doss

*European Journal of Gastroenterology and Hepatology*, 25: 920-925 (2013) IF: 1.915

**Background** Hepatitis C virus (HCV) infection has major health impact worldwide and is a significant cause of chronic liver disease. in Egypt, HCV is highly endemic (up to 15% of the population); 91% of the patients are infected with genotype 4. Searching for new predictors of response to therapy is mandatory to decrease the cost and the adverse effects of current therapy.

**Aim:** The aim of this study was to clarify the usefulness of serum leptin, adiponectin, and insulin resistance (IR) as predictors of response to treatment in hepatitis C virus genotype 4 (HCVG4).

**Methods:** One hundred patients with chronic HCVG4 who were candidates for treatment with pegylated interferon  $\alpha$  and ribavirin were included in the study. Age, sex, and BMI were determined, and quantitative HCV PCR, assessment of serum leptin, adiponectin, IR, and pretreatment liver profile, and liver biopsy were performed.

**Results:** The male to female ratio was 68/32; the mean age of the patients was  $40.9 \pm 7.8$  years and BMI was  $28.3 \pm 10$  kg/m<sup>2</sup>. Sustained virological response (SVR) was achieved by 56% of the patients. on performing logistic regression, BMI [odds ratio (OR) 6.5;  $P = 0.004$ ], serum leptin (OR 27.8;  $P < 0.001$ ), aspartate aminotransferase (OR 1.06;  $P < 0.001$ ), IR (OR 1.15;  $P < 0.001$ ), histological activity index (OR 1.77;  $P = 0.006$ ), and fibrosis (OR 2.93;  $P = 0.001$ ) were found to be independent negative predictors of SVR, whereas serum adiponectin (OR 0.74;  $P < 0.001$ ) was found to be an independent positive predictor of SVR. Pretreatment adiponectin (cutoff 13.75; sensitivity 92.86%; specificity 86.86%) shows area under the curve of 0.879 (95% confidence interval 0.802–0.956;  $P < 0.001$ ) and insignificant area

under the curve for leptin or IR. **Conclusion:** BMI, pretreatment high leptin levels, and IR are negative predictors for SVR and pretreatment low adiponectin levels are an independent positive predictor for SVR in HCVG4.

**Keywords:** Adiponectin; Hepatitis C Virus Genotype 4; Insulin resistance.

### 1098. Hypertonic Saline-Enhanced Radiofrequency Versus Chemoembolization Sequential Radiofrequency in the Treatment of Large Hepatocellular Carcinoma

El-Kady, Nabeel M., Esmat Gamal, Mahmoud, Ekram H.; Darweesh, Samar K, Mahmoud, Sherif H. Elagawy and Waleed A.

*European Journal of Gastroenterology and Hepatology*, 25(5): 628-633 (2013) IF: 1.915

**Background and Study Aim:** Large hepatocellular carcinoma (HCC) appears to be a major obstacle for radiofrequency ablation (RFA); therefore, attempts to increase the volume of coagulation by injecting hypertonic saline before and/or during RFA have been made. Transarterial chemoembolization (TACE) combines the effect of targeted chemotherapy with ischemic necrosis and eliminates heat loss if combined with RFA. Our aim was to compare the efficacy of hypertonic saline-enhanced RFA versus TACE sequential RFA in the treatment of medium and large nodular HCC.

**Patients And Methods:** This prospective study was carried out on 40 patients with 40 HCCs between 2008 and 2010 in the Tropical Medicine and Hepatology Department, Faculty of Medicine, Cairo University. They were divided into two groups (20 patients each): the first group received hypertonic saline-enhanced RFA (RFA+HS) and the second group underwent transarterial chemoembolization, followed by RFA (TACE+RFA).

**Results:** Triphasic computed tomography 1 month after the procedure showed that 17 (85%) patients in each group achieved complete ablation, whereas three (15%) in each group achieved partial ablation. In the RFA+HS group, 12/13 (92%) of medium HCC and 5/7 (71%) of large HCC were successfully ablated. In the TACE+RFA group, 8/8 (100%) medium HCC and 9/12 (75%) of large lesions were successfully ablated. The relation between success rate and lesion diameter was statistically significant only in RFA+HS group. After 6 months, 73.7% of patients in the RFA+HS group and 83.3% of patients in the TACE+RFA group showed maintained ablation ( $P=0.86$ ).

**Conclusion:** RFA+HS and TACE+RFA are safe and equally effective treatments for medium to large HCC.

**Keywords:** Carcinoma; Hepatocellular; Pathology; Combined Modality therapy.

### 1099. New Genetic Markers for Diagnosis of Hepatitis C Related Hepatocellular Carcinoma in Egyptian Patients

Yasmin Saad, Magdy El-Serafy, Mona S Eldin, Zeinab Abdellatif, Hany Khatib, Tamer Elbaz and Hasan Elgarem

*Journal of Gastrointestinal and Liver Disease*, 22: 419-425 (2013) IF: 1.855

**Background and Aim:** Early detection of hepatocellular carcinoma (HCC) enhances effective and curative management. New genetic markers with distinct diagnostic ability are required. Aim: determine the expression of GPC3, PEG10, SERPINI1, MK and QP-C in the peripheral blood of HCC patients.

**Methods:** 74 HCV patients were recruited and divided into three groups; chronic hepatitis (I), liver cirrhosis (II) and HCC (III). Demographics, laboratory and imaging data were collected. Child score and metastatic work up were completed. The expression of the candidate genes in the peripheral blood was performed by qRT-PCR assay.

**Results:** Groups were gender matched, age in group I was significantly lower than in groups II and III (37.7 vs 50.4 and 55.6,  $p$  value  $<0.005$ ). CHILD score; group II and III A/B/C = (7/5/6) and (20/6/3). AFP was significantly higher in group III than I and II (204 vs 3.9 and 6.9,  $p < 0.01$ ). In HCC group 69% of the lesions were  $< 5$  cm, and had 1-2 nodules; 14% had metastases. GPC3, PEG10, SERPINI1 and MK mRNA were significantly higher in the HCC group compared to the other groups while QP-C mRNA was higher in chronic hepatitis C group compared to other groups. Gene expression values in HCC patients were independent of the tumor size, AFP levels or extrahepatic metastasis. Combined measurement of the candidate gene markers showed 100% sensitivity and 33% specificity, 48% PPV and 100% NPV.

**Conclusion:** GPC3, PEG10, SERPINI1 and MK are genetic markers that can represent a useful tool for detection of HCC.

**Keywords:** GPC3; PEG10; SERPINI1; MK; QP-C; Hepatocellular carcinoma; Gene markers.

### 1100. Liver Fibrosis in Young Egyptian Beta-Thalassemia Major Patients: Relation to Hepatitis C Virus and Compliance with Chelation

Gamal Esmat

*Annals of Hepatology*, 12 (5): 774-781 (2013) IF: 1.671

**Background:** The main causes of liver fibrosis in transfusion-dependent thalassemia major are hepatitis C virus (HCV) infection and hepatic iron overload. The study aimed to assess liver fibrosis in Egyptian adolescents and young adult poly-transfused beta thalassemia patients infected with HCV using liver FibroScan in relation to iron overload and Liver iron concentration (LIC).

**Material and Methods:** Fifty-one regularly transfused beta thalassemia patients above 12 years old were subjected to measurement of serum alanine transaminase (ALT), serum ferritin (SF), HCV (antibody and RNA), LIC assessed by hepatic R2\* and transient elastography (TE) (FibroScan). FibroTest and liver biopsy were done to 25 patients.

**Results:** Eighty two% of studied thalassemia patients were HCV antibody positive; 21(49%) of them were viremic (HCV RNA positive); median LIC was 12 mg/gm dry weight. There were strong positive correlation between the degree of liver stiffness and Ishak fibrosis score assessed in liver biopsy specimens ( $P = 0.002$ ) and between FibroScan and FibroTest results ( $P < 0.001$ ). Patients with HCV viremia showed significantly higher ALT, glutamyl transpeptidase (GGT), SF, LIC and increased liver stiffness compared to patients with no viremia ( $P = 0.0001$ , 0.001, 0.012, 0.006 and 0.001) respectively. Liver cirrhosis (TE values  $> 12.5$  kPa) was encountered in 23.5% and variable degrees of liver fibrosis (TE values  $> 6-12.5$  kPa) in 35% of studied thalassemic patients.

**Conclusion:** Young beta thalassemia patients with active hepatitis C infection may have hepatic cirrhosis or fibrosis at young age when accompanied with hepatic siderosis. Non invasive Liver FibroScan and Fibro-Test were reliable methods to assess liver fibrosis in young thalassemic-patients.

**Keywords:** Adolescent; Algorithms; Apolipoprotein A-I/blood; Bilirubin blood; Biological markers; Blood; Biopsy; Large-core needle.

### 1101. Hepatitis C Genotype 4 with Normal Transaminases: Correlation With Fibrosis and Response to Treatment, a Cohort Egyptian Study of 4277 Patients

Mahasen Abdel-Rahman, Yasmin Saad, Maissa El-Raziky, Naglaa Zayed, Wafaa El-Akel, Mohamed Said, Mohamed El-Beshlawy and Gamal Esmat

*Clinics and Research in Hepatology and Gastroenterology*, 37: 479-484 (2013) IF: 1.348

**Background and objective:** Chronic hepatitis C virus (HCV) patients with persistently normal transaminases represent a subgroup of patients with mild, slowly progressive disease, natural history, and optimal management of these patients needs to be investigated in Egypt. Our aim is to assess the severity of hepatic fibrosis and response to therapy in a cohort of Egyptian HCV patients with normal transaminases.

**Patients and Methods:** Retrospective demographics, laboratory, histological features and treatment outcome of patients included in the national program for the control of viral hepatitis in Egypt since 2007 were collected. Combined pegylated IFN/ribavirin therapy was given for patients with fibrosis stage=F1 and elevated transaminases while those with normal transaminase; therapy was initiated only in patients with fibrosis stage=F2.

**Results:** Normal ALT and AST were detected in 1308/4277 (30.6%) and 1662/4277 (38.9%) c patients, respectively, while both enzymes were normal in 943 patients (22%). Multivariate regression analysis showed that lower AFP and higher platelets count (compared with elevated transaminases group) were significantly correlated with normal transaminases ( $P < 0.01$ ), however, HCV-RNA levels did not show such significance. The number of patients with HAI score=A1 was significantly lower in normal than elevated transaminases (36.5% vs 40.9%, respectively,  $P < 0.01$ ) and patients with fibrosis=F2 was significantly lower in normal than elevated transaminases (36.4%) and (43%), respectively ( $P < 0.01$ ). There was no significant correlation between baseline transaminases levels and response to treatment. **Conclusion:** Normal transaminases are frequently encountered in chronic HCV Egyptian patients (22%). They show low AFP level, mild degree of activity and stage of fibrosis with no correlation with response to therapy

**Keywords:** HCV; Fibrosis; Response to therapy.

### 1102. The Assessment of Data Mining for the Prediction of Therapeutic Outcome in 3719 Egyptian Patients with Chronic Hepatitis C

Naglaa Zayed, Abu Bakr Awad, Wafaa El-Akel, Wahid Doss, Tahany Awad, Amr Radwan and Mahasen Mabrouk

*Clinics and Research in Hepatology and Gastroenterology*, 37(3): 254-261 (2013) IF: 1.3

**Introduction:** Decision-tree analysis; a core component of data mining analysis can build predictive models for the therapeutic outcome to antiviral therapy in chronic hepatitis C virus (HCV) patients. **AIM:** To develop a prediction model for the end virological response (ETR) to pegylated interferon PEG-IFN plus ribavirin (RBV) therapy in chronic HCV patients using routine clinical, laboratory, and histopathological data.

**Patients and Methods:** Retrospective initial data (19 attributes) from 3719 Egyptian patients with chronic HCV presumably genotype-4 was assigned to model building using the J48 decision tree-inducing algorithm (Weka implementation of C4.5). All patients received PEG-IFN plus RBV at Cairo-Fatemia Hospital, Cairo, Egypt in the context of the national treatment program. Factors predictive of ETR were explored and patients were classified into seven subgroups according to the different rates of ETR. The universality of the decision-tree model was subjected to a 10-fold cross-internal validation in addition to external validation using an independent dataset collected of 200 chronic HCV patients. **Results:** At week 48, overall ETR was 54% according to intention to treat protocol. The decision-tree model included AFP level ( $<8.08$  ng/ml) which was associated with high probability of ETR (73%) followed by stages of fibrosis and Hb levels according to the patients' gender followed by the age of patients. **Conclusion:** In a decision-tree model for the prediction for antiviral therapy in chronic HCV patients, AFP level was the initial split variable at a cutoff of 8.08 ng/ml. This model could represent a potential tool to identify patients' likelihood of response among difficult-to-treat presumably genotype-4 chronic HCV patients and could support clinical decisions regarding the proper selection of patients for therapy without imposing any additional costs.

### 1103. Disease Progression from Chronic Hepatitis C to Cirrhosis and Hepatocellular Carcinoma is Associated with Increasing DNA Promoter Methylation

Abd El-Rahman Nabawy Zekri, Auhood Abdel-Monem Nassar, Mahmoud Nour El-Din El-Rouby, Hend Ibrahim Shousha, Ahmed Barakat Barakat, Eman Desouky El-Desouky, Naglaa Ali Zayed, Ola Sayed Ahmed, Amira Salah El-Din Youssef, Ahmed Omar Kaseb, Ashraf O. Abd El-Aziz and Abeer Ahmed Bahnassy

*Asian Pacific Journal of Cancer Prevention*, 14: (2013) IF:1.271

**Background:** Changes in DNA methylation patterns are believed to be early events in hepatocarcinogenesis. A better understanding of methylation states and how they correlate with disease progression will aid in finding potential strategies for early detection of HCC. The aim of our study was to analyze the methylation frequency of tumor suppressor genes, P14, P15, and P73, and a mismatch repair gene (O6MGMT) in HCV related chronic liver disease and HCC to identify candidate epigenetic biomarkers for HCC prediction.

**Materials and Methods:** 516 Egyptian patients with HCV-related liver disease were recruited from Kasr Alaini multidisciplinary HCC clinic from April 2010 to January 2012. Subjects were divided into 4 different clinically defined groups – HCC group (n=208), liver cirrhosis group (n=108), chronic hepatitis C group (n=100), and control group (n=100) – to analyze the methylation status of the target genes in patient plasma using EpiTect Methyl qPCR Array technology. Methylation was considered to be hypermethylated if  $>10\%$  and/or intermediately methylated if  $>60\%$ .

**Results:** In our series, a significant difference in the hypermethylation status of all studied genes was noted within the different stages of chronic liver disease and ultimately HCC. Hypermethylation of the P14 gene was detected in 100/208 (48.1%), 52/108 (48.1%), 16/100 (16%) and 8/100 (8%) among HCC, liver cirrhosis, chronic hepatitis and control groups, respectively, with a statistically significant difference between the studied groups (p-value 0.008). We also detected P15 hypermethylation in 92/208 (44.2%), 36/108 (33.3%), 20/100 (20%) and 4/100 (4%), respectively (p-value 0.006). In addition, hypermethylation of P73 was detected in 136/208 (65.4%), 72/108 (66.7%), 32/100 (32%) and 4/100 (4%) (p-value <0.001). Also, we detected O6MGMT hypermethylation in 84/208 (40.4%), 60/108 (55.3%), 20/100 (20%) and 4/100 (4%), respectively (p value <0.001).

**Conclusions:** The epigenetic changes observed in this study indicate that HCC tumors exhibit specific DNA methylation signatures with potential clinical applications in diagnosis and prognosis. In addition, methylation frequency could be used to monitor whether a patient with chronic hepatitis C is likely to progress to liver cirrhosis or even HCC. We can conclude that methylation processes are not just early events in hepatocarcinogenesis but accumulate with progression to cancer.

**Keywords:** HCV; Cirrhosis; Hepatocellular carcinoma; Tumor Suppressor gene methylation; Progression.

#### 1104. The Effect of Peginterferon Alpha-2A Vs. Peginterferon Alpha-2B in Treatment of Naive Chronic HCV Genotype-4 Patients: A Single Centre Egyptian Study

Maissa El Raziky, Waleed Fouad Fathalah, Wafaa Ahmed El-Akel, Ahmed Salama, Gamal Esmat, Mahassen Mabrouk, Rabab Mamoun Salama and Hany Mahmoud Khatab

*Hepatitis Monthly*, 13(5): 1-8 (2013) IF: 1.245

**Background :** Egypt has one of the highest (16-8%) prevalence rates of HCV infection in the world. Approximately 90% of Egyptian HCV isolates belong to a single subtype (4a), which responds less successfully to interferon therapy than other subtypes. Studies comparing the efficacy and safety of PEGIFN alfa-2a and PEGIFN alfa-2b in treatment-naive HCV-infected patients have shown conflicting results.

**Objectives :** Assessing the effects of Peginterferon alpha-2a versus Peginterferon alpha-2b on the sustained virological response in naive chronic HCV genotype-4 Egyptian patients.

**Patients and Methods:** This retrospective study cohort consists of 3718 chronic HCV patients admitted to a large, Egyptian medical center. 1985 patients had been treated with PEG-IFN alfa-2a plus RBV and 1733 patients with PEG-IFN alfa-2b plus RBV between years 2007-2011. Efficacy outcomes were sustained virologic response (SVR) and treatment discontinuation rates due to serious adverse effects.

**Results :** The ETR & SVR in patients treated with PEGIFN alfa-2a was 64.1% and 59.6% as compared to treatment with PEGIFN alfa-2b where these parameters were 58.2% and 53.9% respectively ( $P < 0.05$ ). Treatment discontinuation rates, were similar in the two types of PEGIFN [0.66 (0.37-1.16);  $P = 0.15$ ]. Significant dose reduction was evident with peginterferon alfa-2b (35.3%) than peginterferon alpha-2a (27.3 %) ( $P < 0.01$ ). Patients with lower base line AFP and ALT were most likely to achieve SVR using INF alpha 2-a.

**Conclusions :** Peginterferon alpha-2a has a higher efficacy regarding ETR and SVR as compared to Peginterferon alfa-2b in treatment of naive chronic HCV genotype-4 patients.

**Keywords:** Chronic hepatitis C; Peginterferon- alpha- 2A; Peginterferon- alpha- 2B.

#### 1105. Differentiation of Benign and Malignant Omental Thickening: the Efficacy of Morphologic Ultrasonographic Features and Doppler Flow Parameters

Maha S Hasab Allah, Dalia A Omran and Naglaa A Zayed

*Annals of Gastroenterology and Hepatology*, 4(1): 18-27 (2013)

**Objectives:** To study prospectively the ability of high-frequency transabdominal ultrasound (5-8 MHz) and Doppler examination to differentiate benign and malignant omental involvement in patients with ascites of unclear origin. The diagnostic value of ultrasound-guided omental biopsy was also evaluated.

**Keywords:** Omentum; High-frequency ultrasound; Color doppler ultrasound; Benign and malignant omental masses.

#### 1106. Fibroscan of Chronic HCV Patients Coinfected with Schistosomiasis

Gamal Esmat, Aisha Elsharkawy, Wafaa El Akel, Ahmed Fouad, Kareem Helal, Mostafa Kamal Mohamed, Dina Attia, Hany Khattab, Wahid Doss and Sameh Labib

*Arab Journal of Gastroenterology*, 14: 109-112 (2013)

**Background and Study Aims:** Both hepatitis C virus (HCV) and schistosomiasis are highly endemic in Egypt and coinfection is frequently encountered. Such coinfection is responsible for leading to a more severe liver disease. Hence, the aim of the study was to assess the fibroscan in chronic HCV patients coinfecting with *Schistosoma*. **Patients and Methods:** This study included 231 chronic HCV patients. Routine pre-treatment work-up was done including anti-schistosomal antibodies. Liver stiffness measurements using fibroscan and reference needle-liver biopsy were done. Patients were categorised into two groups: HCV patients with positive schistosomal serology and HCV patients with negative schistosomal serology.

**Results:** Anti-schistosomal antibody was positive in 29% of the studied population. Positive schistosomal serology status was significantly associated with the disagreement between the results of liver biopsy (Metavir) and the fibroscan results (p value=0.02), which was more obvious in F2 and F3 fibrosis stages. The sensitivity of fibroscan for the detection of the F2 stage decreased from 64% among negative schistosomal serology patients to 30.8% among positive schistosomal serology patients, and for the F3 stage it decreased from 43.8% to 21.4%, respectively. Multivariate logistic regression showed that fibrosis stages (F0-F1 and F4) were the most independent factors that were associated with the agreement between fibroscan and liver biopsy (odds ratio (OR) 3.4, 7.12 and p value <0.001, <0.001, respectively).

**Conclusion:** Although the sensitivity of fibroscan for the detection of fibrosis stages (F2 and F3) was impaired in patients with positive schistosomal serology, fibrosis stages (F0-F1 and F4) were the most independent factors associated with the agreement between fibroscan and liver biopsy.

**Keywords:** Fibroscan; HCV; Liver stiffness; Schistosomiasis.

### 1107. Lack of Estrogen Receptors Expression in Malignant and Pre-Malignant Colorectal Lesions in Egyptian Patients

Mohamed Said, Marwa Khairy, Aly El-Hendawy, Osama A. Khalf, Mohamed S. Abdelbary, Yasmin Saad and Ayman Yosry  
*Open Journal of Gastroenterology*, 3: 155-163 (2013)

**Background:** incidence of Colorectal cancer (CRC) is increasing globally. In Egypt, CRC ranks the sixth most common cancer in males and the fifth in females.

**Aim:** To assess the expression of estrogen receptors (alpha and beta) in pre-malignant (adenomatous polyps and IBD), malignant colorectal lesions and normal colonic mucosa in group of Egyptian patients.

**Methods:** This prospective study was done on 45 patients presenting with colonic symptoms, patients were divided into four groups; 15 CRC patients, 10 patients with adenomatous polyps, 10 IBD patients and 10 patients in the control group. Patients subjected to: Stool analysis, FOBT, CBC, CEA, Abdominal ultrasound & colonoscopy and biopsy (number = 80), Pathological, immunohistochemistry and RT-PCR quantification of ERα and ERβ were done.

**Results:** Mean age: 39.2 (12- 73), gender: M/F: 28/17. Bleeding per rectum was the commonest presentation; 29/45 (64.4%). CEA was significantly elevated in the CRC group compared with other studied groups (1692 mg/L vs. 4.0, 4.0 and 4.4 mg/L). Ultrasonography of the studied patients showed that metastatic CRC: 3/15 (20%); Colonic wall thickening: 5/15 (33.3%), 1/10 showed colonic polypoidal lesions in adenomatous polyps groups, in IBD group: 4/10 (40%) showed colonic and ileocecal thickening. All the studied patients showed negative results for estrogen receptors (alpha and beta) by the use of immunohistochemistry staining and RT-PCR technique.

**Conclusion:** Role of estrogen receptors in the colonic mucosa, precancerous and colorectal cancer is doubtful, contradictory results with some literature data could be due to racial and genetic difference in the studied population.

**Keywords:** Colorectal cancer; Premalignant lesions; Estrogen receptors.

### 1108. Liver Stiffness Measurement by Fibroscan Predicts the Presence and Size of Esophageal Varices in Egyptian Patients with HCV Related Liver Cirrhosis

Yasmin Saad, Mohamed Said, Mohamed O. Idris, Ayman Rabee and Zakaria Salama

*Journal of Clinical and Diagnostic Research*, 7: 2253-2257 (2013)

**Background and Aim:** Liver stiffness measured by transient elastography correlates with Hepatic vein pressure gradient, liver Stiffness value of 21 kpa predicts significant portal hypertension. Aim is to predict esophageal varices presence by fibroscan and possible grading by degree of liver stiffness in HCV related cirrhotic

**Patients Material and Methods :** Thirty two HCV related cirrhotic patients were recruited, age > 18 years, BMI < 35, no history of: upper GI bleeding, hepatocellular carcinoma, abdominal collaterals ascites. Patients underwent clinical

examination, laboratory investigations, abdominal ultrasonography, upper endoscopy and fibroscan. They divided into (Group I = no varices, Group II = small varices (Grade 1 & 2), Group III = large varices (Grade 3 & 4).

**Results:** Age is higher in Group III than I & II (55±6.6 vs 49.5±4.7 & 48.9±4.7, p-value 0.04) respectively, Groups were gender & BMI matched, fibroscan values in Group I vs II & III were 27 Vs 49.4, p value 0.01, cutoff 29.7 Kpa (sensitivity 95% & specificity 67%) while its value in Group II vs III were 38.4 vs 60.4, p value 0.002, cutoff 38.2 Kpa (sensitivity 100% & specificity 77.3%). Platelet count, splenic size, platelet count/splenic size in Group I vs II & III were 107.166 vs 72.900, 13.8 vs 15.4, 803.6 vs 478, p value 0.01, 0.008, 0.005, cutoff 80.000, 14.5, 545, sensitivity & specificity (85%&75%, 75%&75%, 85%&84%) respectively. on multivariate analysis fibroscan (OR 1.113; p=0.005) & platelet count/splenic size (OR 0.995; p=0.012) were positive predictors of esophageal varices presence.

**Conclusion:** Fibroscan is a good non-invasive method to predict esophageal varices presence & possible grading with high sensitivity

**Keywords:** Fibroscan; Esophageal varices; Grading; Non-invasive methods.

### 1109. Management of Hepatocellular Carcinoma: Updated Review

Tamer Elbaz, Mohamed El Kassas and Gamal Esmat

*Journal of Cancer Therapy*, 4: 536-545 (2013) IF: 0.21

Hepatocellular carcinoma (HCC) represents one of the most challenging potentially curable tumors with high incidence, prevalence and mortality rates. For proper assessment, prognosis estimation and treatment decisions, at least seven important guidelines and staging systems were designated. Proper treatment needs the interaction of multidisciplinary HCC clinic to choose the most appropriate line of treatment. The different modalities of management include resection (surgery or transplantation), local ablation, chemoembolization, radioembolization and molecular targeted therapies with a wide range of investigational drugs that developed after the FDA approved sorafenib. Downstaging and bridging are two important strategies to manage HCC patients who will undergo liver transplantation to improve their postoperative survival. Finally, survival and prognosis depends on several prognostic factors that are either patient related or tumor related. In our study, we aim to provide an updated comprehensive review of the different aspects of liver cancer management starting from staging systems to the different applied treatment modalities.

**Keywords:** Hepatocellular carcinoma; Staging; Molecular targeted therapies.

### 1110. Occult Hepatitis B Virus Infection Among Egyptian Blood Donors

Zeinab N Said, Manal H El Sayed, Iman I Salama, Enas K Aboel-Magd, Magda H Mahmoud, Maged El Setouhy, Faten Mouftah, Manal B Azzab, Heidi Goubbran, Amal Bassili and Gamal E Esmat

*World J. Hepatol.* 5(2): 64-73 (2013)



**AIM:** To identify blood donors with occult hepatitis B virus (HBV) infection (OBI) to promote safe blood donation.

**Methods:** Descriptive cross sectional study was conducted on 3167 blood donors negative for hepatitis B surface antigen (HBsAg), hepatitis C antibody (HCV Ab) and human immunodeficiency virus Ab.

They were subjected to the detection of alanine aminotransferase (ALT) and aspartate transaminase (AST) and screening for anti-HBV core antibodies (total) by two different techniques; [Monoliza antibodies to hepatitis B core (Anti-HBc) Plus-Bio-Rad] and (ARC-HBc total-ABBOT). Positive samples were subjected to quantitative detection of antibodies to hepatitis B surface (anti-HBs) (ETI-AB-AUK-3, Dia Sorin-Italy). Serum anti-HBs titers > 10 IU/L was considered positive. Quantitative HBV DNA by real time polymerase chain reaction (PCR) (QIAGEN-Germany) with 3.8 IU/mL detection limit was estimated for blood units with negative serum anti-HBs and also for 32 whose anti-HBs serum titers were > 1000 IU/L. Also, 265 recipients were included, 34 of whom were followed up for 3-6 mo. Recipients were investigated for ALT and AST, HBV **Serological Markers:** HBsAg (ETI-MAK-4, Dia Sorin-Italy), anti-HBc, quantitative detection of anti-HBs and HBV-DNA.

**Results:** 525/3167 (16.6%) of blood units were positive for total anti-HBc, 64% of those were anti-HBs positive. Confirmation by ARCHITECT anti-HBc assay were carried out for 498/525 anti-HBc positive samples, where 451 (90.6%) confirmed positive. Reactivity for anti-HBc was considered confirmed only if two positive results were obtained for each sample, giving an overall prevalence of 451/3167 (14.2%) for total anti-HBc. HBV DNA was quantified by real time PCR in 52/303 (17.2%) of anti-HBc positive blood donors (viral load range: 5 to  $3.5 \times 10^5$  IU/mL) with a median of 200 IU/mL (mean:  $1.8 \times 10^4 \pm 5.1 \times 10^4$  IU/mL). Anti-HBc was the only marker in 68.6% of donors. Univariate and multivariate logistic analysis for identifying risk factors associated with anti-HBc and HBV-DNA positivity among blood donors showed that age above thirty and marriage were the most significant risk factors for prediction of anti-HBc positivity with AOR 1.8 (1.4-2.4) and 1.4 (1.0-1.9) respectively. Other risk factors as gender, history of blood transfusion, diabetes mellitus, frequent injections, tattooing, previous surgery, hospitalization, Bilharziasis or positive family history of HBV or HCV infections were not found to be associated with positive anti-HBc antibodies.

Among anti-HBc positive blood donors, age below thirty was the most significant risk factor for prediction of HBV-DNA positivity with AOR 3.8 (1.8-7.9). According to HBV-DNA concentration, positive samples were divided in two groups; group one with HBV-DNA = 200 IU/mL (n = 27) and group two with HBV-DNA < 200 IU/mL (n = 26).

No significant difference was detected between both groups as regards mean age, gender, liver enzymes or HBV markers. Serological profiles of all followed up blood recipients showed that, all were negative for the studied HBV markers. Also, HBV DNA was not detected among studied recipients, none developed post-transfusion hepatitis (PTH) and the clinical outcome was good.

**Conclusion:** OBI is prevalent among blood donors. Nucleic acid amplification/ HBV anti core screening should be considered for high risk recipients to eliminate risk of unsafe blood donation.

**Keywords:** Blood donors; Nucleic acid.

### 1111. Pattern of Recurrent Hepatitis C in Deceased Vs Living Donor Liver Transplantation: an Egyptian Experience

Dalia Omran, Eiman A Hussein and Mohamad Nagib

*Euroasian Journal of Hepato-Gastroenterolog*, 3(2): 111-116 (2013)

**Introduction:** Hepatitis C virus (HCV) is the leading cause for liver transplantation (LT) and viral recurrence.

**Objective:** Whether HCV recurrence occurs earlier and severer for living donor liver transplantation (LDLT) than for deceased donor liver transplantation (DDLT).

**Design:** We evaluated preoperative and postoperative clinical, laboratory, and histological outcomes of 180 patients with LT (65 DDLT and 115 LDLT) since 1998 till 2006. Patients diagnosed for recurrence histologically were treated by combination therapy of pegylated interferon (IFN) and ribavirin (RBV).

**Results:** The LDLT group was significantly younger. CTP score was insignificant, while MELD score was higher in LDLT than DDLT. The mean preoperative (p = 0.012) and postoperative HCV-RNA (p = 0.027) count was significantly lower in DDLT group than LDLT group. At onset of recurrence, laboratory parameters were not significantly different between two groups. Histologically, 59.57 and 41.89% patients with DDLT and LDLT, respectively, diagnosed to have recurrence (p > 0.05). Fibrosis and activity scores were significantly higher in the LDLT group (p <= 0.01) compared to DDLT group. The response to treatment was higher in DDLT group.

**Conclusion:** HCV recurrence rates and severity of reinfection remain comparable for living and deceased organs. However, LDLT significantly increase the risk and severity of HCV recurrence than DDLT.

**Keywords:** Living donor liver transplantation, Deceased donor liver transplantation, HCV recurrence, Interferon therapy.

### 1112. Predictors of Complete Early Virological Response to Pegylated Interferon and Ribavirin in Egyptian Patients with Chronic Hepatitis C Genotype-4

Gamal Esmat, Maissa El S. El Raziky, Rabab M. Salama, Wafaa A. El Akel, Waleed F. Fathalah and Dina I. Attia

*Advanced Infectious Disease*, 3: 78-83 (2013)

We aim to determine the baseline factors associated with partial and cEVR by analyzing the data of 1861 Egyptian patients treated for 12 weeks with a course of Peg-IFN plus RBV. Base line data of 1861 Egyptian patients with chronic hepatitis C coming at Cairo-Fatemic Hospital for HCV treatment were studied including full clinical, Ultrasonographic examination, laboratory evaluation and liver biopsy. The most significant variables in relation to complete early virological response were low Hb level (<13 gm/dl) with p < 0.01, the stage of fibrosis p value < 0.05 and the grades of inflammation p value < 0.05 were associated with less achievement of cEVR. We conclude that identifying the most significant predictors of response such as Hb, stage of fibrosis F, at baseline before initiating treatment is mandatory to predict which patient will be more expected to achieve a cEVR and thus reducing the side-effects and healthcare costs associated with interferon therapies.

**Keywords:** Predictors of response; cEVR; HCV treatment; Peg ifn/ribavirin.

### 1113. Prospective Study Evaluating the Value of Subjective Global Assessment and National Risk Score 2002 for Post- Operative Risk Detection in Living Related Donor Liver Transplant Recipien

A. Abd Elrehim, O. Fekry, M. Abd Elaziz, W. Fathalah, M. Abd Elbary and T. Darwish

*Open Journal of Gastroenterology, 3: 119-127 (2013)*

**Background:** Chronic liver disease may be associated with protein energy malnutrition. Those malnourished patients undergoing liver transplantation suffer great morbidities and even mortalities. Estimating the degree of malnutrition in patients with end stage liver disease is a difficult job, Subjective Global Assessment (SGA) and Nutritional Risk Score-2002 (NRS-2002) are among many tools that can give an overview for the nutritional status of the patients.

**Aim:** To detect the efficacy and the predictive validity of SGA and NRS 2002 for post-operative risk detection for liver transplant patients.

**Patients and Methods:** 30 recipients of end stage liver disease had undergone a nutritional assessment by SGA score & NRS-2002 score, to be compared with the parameters of outcome of post-operative liver transplantation (ALT, AST, INR, Bilirubin, time spent in ICU, hospital infective episodes & number of antibiotic courses).

**Results:** Patients declared as malnourished by SGA and NRS-2002 had higher post operative ALT & AST value, more prolonged INR, spent more time at ICU and hospital, suffered from more infective episodes and had more antibiotic courses in a significant statistical manner.

**Conclusion:** SGA and NRS-2002 could be useful, simple and dependable tools to be used for risk detection of post-operative morbidities after liver transplantation.

**Keywords:** Malnutrition; Subjective global assessment; National risk assessment-2002; Chronic liver disease; Liver transplantation.

### 1114. Response and Seroconversion Rates Among HBeAg-Positive Chronic HBV Egyptian Patients Treated with Peginterferon Alpha 2a (Pegasys), A Single-Centre Experience

Sahar Maklad, Gamal Esmat, Wahid Doss, Alaa Abou-Zeid and Sameh Seif El-Din

*Arab J. Gastroenterol, 14 (2): 73-77 (2013)*

**Background and Study Aims:** We aimed to evaluate the therapeutic efficacy of pegylated interferon alpha-2a 180µg as a treatment for hepatitis B 'e' antigen (HBeAg)-positive genotype D chronic hepatitis B patients

**Patients and Methods:** Thirty patients attending the outpatient clinic at the National Hepatology and Tropical Medicine Research Institute were treated with peg.interferon alpha-2a (180µg) weekly for a period of 48 weeks. Pre-enrolment assessment was performed through biochemical, serological and quantitative HBV DNA testing. Liver biopsy was performed in all patients. Evaluation was done at weeks 12, 24 and 48 of treatment by liver

enzymes, complete blood count (CBC), HBeAg/HBeAb and quantitative HBV DNA testing.

**Results:** At the end of 48 weeks of treatment only three cases (10%) of the study population showed HBeAg seroconversion and an undetectable HBV DNA level. None of responders exhibited hepatitis B surface antigen (HbsAg) loss. There were five (16.7%) primary non-responders, four (13.3%) relapsers, four (13.3%) cases flared at week 12, and 14 (46.6%) cases who were non-responders. No specific predictors of response could be identified among patients.

**Conclusion:** One year of peg. interferon alpha-2a 180µg weekly led to HBeAg seroconversion and an undetectable HBV DNA level in 10% of cases. Considering the privilege of a finite duration of treatment, tailoring of treatment and proper patient selection is of great importance in considering this therapy as a first line of treatment among HBeAg-positive chronic HBV Egyptian patients.

**Keywords:** HBV; Hbeag positive; Peginterferon Alpha-2a; Genotype D; Egypt.

### 1115. Risk Factors for Developing Hepatocellular Carcinoma in Egypt

Ashraf Omar, Ghassan K. Abou-Alfa, Ahmed Khairy and Heba Omar

*Chinese Clinical Oncology, 2(4): 1-9 (2013)*

Hepatocellular carcinoma (HCC) is a common disorder worldwide and ranks 2nd and 6th most common cancer among men and women in Egypt. HCC has a rising incidence in Egypt mostly due to high prevalence of viral hepatitis and its complications. Proper management requires the interaction of multidisciplinary HCC clinic to choose the most appropriate plan. The different modalities of treatment include resection (surgery or transplantation), local ablation, chemoembolization, radioembolization and molecular targeted therapies. This paper summarizes both the environmental and host related risk factors of HCC in Egypt including well-established risk factors such as hepatitis virus infection, aflatoxin, as well as possible risk factors.

**Keywords:** Hepatocellular carcinoma (HCC); Egypt; Risk factors; Epidemiology.

### 1116. Role of Fibroscan and Apri in Detection of Liver Fibrosis: A Systematic Review and Meta-Analysis

Ayman Yosry Abd El Rihim, Rabab Fouad Omar, Waleed Fathalah, Inas El Attar, Hanan Abdel Hafez and Wesam Ibrahim

*Arab Journal of Gastroenterology, 14: 44-50 (2013)*

**Background and study aims:** Fibroscan and APRI are promising noninvasive alternatives to liver biopsy for detecting hepatic fibrosis. However, their overall test performance in various settings remains questionable. The aim of our study was to perform a systematic review and meta-analysis of diagnostic accuracy studies comparing fibroscan and APRI with liver biopsy for hepatic fibrosis.

**Patients and methods:** Electronic and manual bibliographic searches to identify potential studies were performed. Selection of studies was based on reported accuracy of fibroscan and APRI compared with liver biopsy. Data extraction was performed

independently by two reviewers. Meta-analysis combined the sensitivities, specificities, and likelihood ratios of individual studies. Extent and reasons for heterogeneity were assessed. **Results:** 23 studies for fibroscan and 20 studies for APRI in full publication were identified. For patients with stage IV fibrosis (cirrhosis), the pooled estimates for sensitivity of fibroscan were 83.4% (95% confidence interval [CI], 71.7–95.0%) and specificity 92.4% (95% CI, 85.6–99.2%). For patients with stage IV fibrosis (cirrhosis), the pooled estimates for sensitivity of APRI at cutoff point of 1.5 were 66.5% (95% CI, 25.0–100%) and specificity 71.7% (95% CI, 35.0–100%). Diagnostic threshold bias was identified as an important cause of heterogeneity for pooled results in both patient groups. **Conclusions:** Fibroscan and APRI appear to be clinically useful tests for detecting cirrhosis however not useful tools in early stages of fibrosis.

**Keywords:** Fibroscan; Apri; Metaanalysis; Liver biopsy.

### 1117. Safety of Blood Transfusion: an Egyptian Study

Dalia Omran, Eiman A Hussein and Mohamad Nagib

*J. Infect. Dis. Ther., 2 (1): 1-4 (2013)*

**Introduction:** Blood safety presents a serious challenge in Egypt, having the highest prevalence of hepatitis C virus (HCV).

**Objectives:** To evaluate the effectiveness of blood donor recruitment strategies, the seroprevalence of positive infectious markers among volunteer donors (VD) and family replacement donors (RD) at a University Hospital Blood Bank was studied.

**Keywords:** Blood transfusion; Safety; Screening; infections.

### 1118. Towards an Easier Pleurodesis: Ultrasound-Guided Iodopovidone Sclerotherapy in Cirrhotic Patients with Hepatic Hydrothorax

Ahmed M. Abdelhafeez, Mohammed W. Zakaria, Waleed F. Fathalah and Dalia Omran

*Open Journal of Gastroenterology, 3: 195-201 (2013)*

**Background and Aim:** Hepatic hydrothorax is one of the complications encountered in end stage liver disease. Pleural drainage carries the risk of massive protein and electrolyte depletion as well as the risk of bleeding and hepatic encephalopathy. Pleurodesis following pleural aspiration decreases the chance of pleural effusion recurrence, and has been a widely used long-standing method of controlling recurrent pleural effusions. The aim of this study is to evaluate the effect of pleurodesis using ultrasound-guided iodopovidone sclerotherapy in hepatic hydrothorax.

**Patients and Methods:** This prospective study included 56 patients with clinical, laboratory and radiological evidence of liver cirrhosis and symptomatic right sided hepatic hydrothorax. All patients were subjected to repeated thoracentesis. Ten ml of lidocaine 2% were injected in the pleural space followed by 20 ml of iodopovidone. The follow-up was done after 3 months.

**Results:** The sclerotherapy procedure was successful in 40 out of 56 cases (71.4%), and the success rate was 66.7% in massive effusion and reached 80% in moderate effusion. Twenty eight patients (50%) had to repeat the procedure for a second time, sixteen of which (28.6%) failed despite the second trial and twelve cases (21.4%) showed no fluid reaccumulation.

**Conclusion:** Ultrasound-guided iodopovidone sclerotherapy is

an effective approach for a successful pleurodesis in hepatic hydrothorax.

**Keywords:** Pleurodesis; Ultrasound; Iodopovidone; Effusion.

### Dept. of Histology

### 1119. Experimental Study on the Effect of Intravenous Stem Cell Therapy on Intestinal Ischemia Reperfusion Induced Myocardial Injury

Maha Baligh Zickri and Azza Embaby

*Int J Stem Cells, 6(2): 121-128 (2013)*

The myocyte death that follows intestinal ischemia reperfusion (I/R) injury is a major factor contributing to high mortality and morbidity in ischemic heart disease. The purpose of stem cell (SC) therapy for myocardial infarction is to improve clinical outcomes. The present study aimed at investigating the possible therapeutic effect of intravenous human cord blood mesenchymal stem cells (HCBMSCs) on intestinal ischemia reperfusion induced cardiac muscle injury in albino rat.

**Keywords:** Mesenchymal stem cells; Ischemia reperfusion; Cord blood; Cardiac injury.

### 1120. Histological Experimental Study on the Effect of Stem Cell Therapy on Adriamycin Induced Chemobrain

Maha Baligh Zickri, Dalia Hussein Abd El Aziz and Hala Gabr Metwally

*Int. J. Stem. Cells., 6 (2): 104-112 (2013)*

**Background and Objectives:** Negative consequences of chemotherapy on brain function were suggested and were addressed in animal models as the clinical phenomenon of chemobrain. It was postulated that adriamycin (ADR) induce changes in behaviour and in brain morphology. Human umbilical cord mesenchymal stem cells (HUCMSCs) could be induced to differentiate into neuron-like cells. The present study aimed at investigating the possible therapeutic effect of HUCMSC therapy on adriamycin induced chemobrain in rat. **Methods and Results:** Twenty five female albino rats were divided into control group, ADR group where rats were given single intraperitoneal (IP) injection of 5 mg/kg ADR. The rats were sacrificed two and four weeks following confirmation of brain damage. In stem cell therapy group, rats were injected with HUCMSCs following confirmation of brain damage and sacrificed two and four weeks after therapy. Brain sections were exposed to histological, histochemical, immunohistochemical and morphometric studies. In ADR group, multiple shrunken neurons exhibiting dark nuclei and surrounded by vacuoles were seen. In response to SC therapy, multiple normal pyramidal nerve cells were noted. The area of shrunken nerve cells exhibiting dark nuclei, Prussian blue and CD105 positive cells were significantly different in ADR group in comparison to SC therapy group. **Conclusions:** ADR induced progressive duration dependant cerebral degenerative changes. These changes were ameliorated following cord blood human mesenchymal stem cell therapy. A reciprocal relation was recorded between the extent of regeneration and the existence of undifferentiated mesenchymal stem cells.

**Keywords:** Adriamycin; Chemobrain; Cord blood; Mesenchymal stem cells.

### 1121. Relation Between Endogenous Stem Cells and Green Tea Extract in Overconsumption and Amiodarone Induced Thyroid Damage in Rat

Maha Baligh Zickri and Azza Embaby

*Int. J. Stem. Cells.*, 6 (2): 113-120 (2013)

dysfunction. Green tea extract (GTE) supplementation would attenuate oxidative stress and activate progenitor cells. However, the potential toxicity of GTE on various organs when administered at high doses has not been completely investigated. The present study aimed at investigating the possible relation between endogenous stem cells and GTE in overconsumption and AM induced thyroid damage in albino rat.

**Methods and Results:** Twenty four male albino rats were divided into control group, GTE group (rats given 50 mg/kg), Overconsumption group (rats given 1,000 mg/kg GTE), AM group (rats given 30 mg/kg) and combined AM, GTE therapy group. AM and GTE were administered orally 5 days/week for 8 weeks. Serological tests were performed. Thyroid sections were exposed to histological, immunohistochemical and morphometric studies. In overconsumption group, multiple distorted follicles with cellular debris in the lumen and multiple follicles devoid of colloid were found. In AM group, multiple follicles exhibiting crescent of colloid and few follicles devoid of colloid were detected. In combined therapy group, multiple follicles were filled with colloid. Significant decrease in area of colloid and significant increase in the area% of collagen were recorded in overconsumption and AM groups. Area% of CD 105 +ve cells denoted significant increase in combined therapy group. Serological tests were confirmative.

**Conclusions:** Endogenous SCs activation was proved in AM and GTE combined therapy group with regression of AM induced morphological, morphometric and serological changes. However, overconsumption of GTE recruited endogenous SCs suppression.

**Keywords:** Amiodarone, Green Tea Extract, Mesenchymal Stem Cells, Thyroid

#### Dept. of Internal Medicine

### 1122. Short-Term Evaluation of Autologous Transplantation of Bone Marrow-Derived Mesenchymal Stem Cells in Patients with Cirrhosis: Egyptian Study

Mona A. Amin, Dina Sabry, Laila A. Rashed, Wael M. Aref, Mohamed Ahmed el-Ghobary, Marwa Salah Farhan, Hany Ahmed Fouad and Youssef Abdel-Aziz Youssef

*Clinical Transplantation*, 27: 607-612 (2013) IF: 1.634

**Background:** Stem cell-based therapy has received attention as a possible alternative to organ transplantation. The aim of this study was to assess the safety and efficacy of autologous transplantation of bone marrow (BM) – derived stromal cells in post-HCV liver cirrhosis

**Patients Methodology:** 10 × 10<sup>6</sup> of isolated human bone marrow (HBM)-stromal cells in 10 mL normal saline were injected in the spleen of 20 patients with end-stage liver cirrhosis guided by the

ultrasonography, and then patients were followed up on monthly basis for six months.

**Results:** A statistically significant decrease was detected in the total bilirubin, aspartate transaminase (AST), alanine transaminase (ALT) (p-value < 0.01), prothrombin time (PT), and international normalized ratio (INR) levels (p-value < 0.05), while a statistically significant increase in the albumin and PC (p-value < 0.05) after follow-up.

**Conclusion:** This study suggested the safety, feasibility, and efficacy of the intrasplenic injection of autologous BM stromal cells in improving liver function in Egyptian patients with cirrhosis.

**Keywords:** Egypt; Human; Intrasplenic injection; Liver cirrhosis patients; Mesenchymal stem cells.

### 1123. The Burden of Anti-Hcv Genotype-4 Positivity in Renal Transplant Recipients 8 Years Follow-Up

Soliman A.R., Fathy A., Khashab S. and Shaheen N.

*Int. Urology Nephrology*, 45: 1453-1461 (2013) IF: 1.325

Whether renal transplant recipients with anti-HCV antibodies positivity and normal liver function tests within the first year after transplantation have different morbidity and mortality and graft failure compared to anti-HCV-negative recipients remains controversial. In this retrospective study, on 411 renal transplant recipients, we analyzed grafts morbidity, survival, and liver function tests over a period of 8 years. Patients were stratified according to their anti-HCV antibody status 1 year after transplantation into anti-HCV-positive and HCV-negative patients. The presence of normal liver function tests was mandatory at inclusion. All patients received the same immunosuppressive protocol consisting of cyclosporine A, mycophenolate mofetil and steroids. One year after transplantation, 137 patients were anti-HCV negative (33 %) while the rest 274 (67 %) were positive. At 5 years of follow-up, the study population consisted of 205 patients (71 patients, 35 % with anti-HCV negativity, and 134, 65 % with positivity). At the end of the study, only 144 patients were followed up (43 patients, 30 % with negative anti-HCV and 101 patients, 70 %, with positivity). We found that graft survival was not different between both groups. Moreover, serum creatinine showed a trend to be lower in HCV-positive patients compared to negative group although difference was not statistically significant. The number of graft loss was not different between both groups. Moreover, there was no difference between both groups as regards prevalence of acute rejection, diabetes mellitus, hypertension, CMV disease and proteinuria. We can conclude that anti-HCV positivity for 8 years in patients with normal liver function tests at 1 year does not impact graft morbidity and patient survival.

**Keywords:** Hepatitis C; Renal transplantation; Prognosis.

### 1124. Diabetes Mellitus as Predictor of Patient and Graft Survival After Kidney Transplantation

Maamoun H. A., Soliman A. R., Fathy A., Elkhatib M. and Shaheen N.

*Transplantation Proceedings*, 45: 3245-3248 (2013) IF: 0.952

**Background:** In this study, we used a single-center database to examine the risks of renal transplantation in patients with diabetes



mellitus (DM). We aimed to compare 1-year outcomes of survival and morbidity after renal transplantation among recipients with and without DM.

**Methods:** We reviewed retrospectively 1211 adult patients who underwent renal transplantation from January 2001 to December 2010. The patients were divided into 2 groups: Those with (33%) and those without (67%) pretransplant diabetes. Unpaired Student's t tests and (2) tests were used to compare outcomes between diabetic and nondiabetic renal transplant recipients. We analyzed survival, renal function, development of proteinuria, rejection, and infection (requiring hospitalization).

**Results:** Patients with diabetes were older, had a greater body mass index (mean, 29.5 vs 25.3 kg/m<sup>2</sup>;  $P < .05$ ), and had lower creatinine clearance ( $44.2 \pm 11.4$  vs  $56.0 \pm 18.2$ ;  $P = .01$ ). Forty-one patients died in hospital (3.4%;  $P =$  nonsignificant). Furthermore, survival rates were similar between these 2 groups. However, we found a trend toward decreased survival for those with DM at 1 year (80.4% vs 88.7%;  $P = .20$ ). Mean follow-up time was 3.2 years. Infection rate within 6 months was greater among those with DM (19% vs 5%; odds ratio, 6.25). Freedom from rejection at 3 years was similar (75.2% vs 76.8%;  $P = .57$ ). Multivariate analysis showed increased baseline creatinine level as a significant risk factor for survival. Body mass index  $>30$  kg/m<sup>2</sup> was a significant risk factor for survival among patients with DM.

**Conclusion:** We found an increased risk of serious infections in patients with DM, particularly within the first 6 months. However, our data suggest that diabetes is not associated with worse 1-year survival or higher morbidity in renal transplant patients, as long as good blood glucose control is maintained.

**Keywords:** Diabetes; Renal transplantation; Graft survival.

#### 1125. Comparison of Abbreviated Modification of Diet in Renal Disease Formula (aMDRD) and the Cockcroft-Gault Adjusted for Body Surface (aCG) Equations in Stable Renal Transplant Patients and Living Kidney Donors

Soliman A. R., Fathy A., Khashab S. and Shaheen N.

*Renal Failure*, 35: 94-97 (2013) IF: 0.941

The performance of abbreviated modification of diet in renal disease formula (aMDRD) and the Cockcroft-Gault adjusted for body surface (aCG) equations as compared with measured 125I-iothalamate glomerular filtration rate was analyzed in patients with stable renal transplantation (RTx) and in potential living kidney donors (LKD). One hundred and thirty-one patients had RTx and 150 were LKD. The paired t-test showed that the estimated glomerular filtration rate (GFR) values through the aMDRD and the corrected CG equations were significantly different from each other ( $p < 0.01$ ). There were significant differences between GFRs estimated using aCG and aMDRD equations ( $p < 0.001$ ) in both groups (RTx and LKD) of different ages. The Pearson correlation coefficient between aCG and aMDRD equations was good (0.77,  $p < 0.01$ ), but the kappa coefficient was 0.39, indicating a low agreement between the two formulae. In RTx patients with GFR  $<60$  mL/min/1.73 m<sup>2</sup>, the aMDRD equation performed better than the aCG formula with respect to bias (-0.6 vs. 3.0 mL/min/1.73 m<sup>2</sup>, respectively) and accuracy within 30% (72% vs. 56%, respectively) and 50% (91% vs. 73%, respectively). Similar results are reported for 48 diabetic RTx patients. In the LKD, the aMDRD equation significantly

underestimated the measured GFR when compared with the aCG formula, with a bias of -8.0 versus 2.2 mL/min/1.73 m<sup>2</sup>, respectively ( $p < 0.05$ ). We can conclude that the Cockcroft and MDRD equations cannot be used interchangeably in clinical transplantation practice and in order to adjust drug doses.

**Keywords:** Renal insufficiency; Chronic; Drug therapy; Surgery.

#### 1126. HLA DRB1 Alleles and Hepatitis C Virus Infection in Chronic Kidney Disease Patients

Shaheen N. M., Soliman A. R., El-Khashab S. O. and Hanna M. O.

*Renal Failure*, 35: 386-390 (2013) IF: 0.941

T cell responses against HCV are regulated by the host's human leukocyte antigen (HLA) alleles, which thus are ideal candidate genes to investigate for associations with HCV susceptibility. We aimed to identify associations of HLA DRB1\* alleles with HCV infection in a high risk of exposure population, chronic kidney disease (CKD) patients on dialysis, and to study any possible relationships with allele zygosity. The study population comprised 110 HCV infected and 143 HCV uninfected CKD patients undergoing regular hemodialysis. HLA DRB1\* alleles were determined using polymerase chain reaction followed by hybridization with sequence-specific oligonucleotide probes. We found a significant negative association between HLA DRB1\*03 and HCV infection, but the association did not retain significance after adjustment for multiple comparisons. HLA DRB1\*03 was found at reduced frequency in HCV antibody positive compared to HCV antibody negative CKD patients on regular dialysis (corrected  $p$  was not significant). No significant association between HCV infection and HLA DRB1\* zygosity was observed. Our results suggest that there is minimal evidence for a significant role of a particular HLA DRB1\* allele or allele zygosity in the susceptibility or protection to HCV in high-risk hemodialysis patients with similar exposure to infection.

**Keywords:** Hepatitis C; Complications; Genetics.

#### 1127. Sirolimus Conversion May Suppress Viral Replication in Hepatitis C Virus-Positive Renal Transplant Candidates

Soliman A. R., Fathy A., Khashab S., Shaheen N. and Soliman M. A.

*Experimental and Clinical Transplantation*, 11: 408-411 (2013) IF: 0.588

**Objectives:** Hepatitis C virus in renal transplant recipients is an independent risk factor for sickness and death. It has been shown that one might limit hepatitis C virus progression in liver transplant recipients with sirolimus-based immunosuppression. The mammalian target of rapamycin is an influential molecule for the anti-hepatitis C virus action of interferon. We report our experience with sirolimus conversion in hepatitis C virus-positive patients with chronic allograft nephropathy regarding hepatic and hematologic effects that might affect its future use.

**Materials and Methods:** Twenty-five patients who had received renal transplants with anti-hepatitis C virus-positive and normal liver function were enrolled. Ten patients had allograft dysfunction because of cyclosporine nephrotoxicity. Sirolimus was initiated at 2 mg/d and adjusted to 6 to 8 ng/mL. Cyclosporine was gradually tapered and then stopped; 15 patients



were used as a control group. Sirolimus-related hepatitis was defined as a rise in liver transferases or alkaline phosphatase or bilirubin over twice the upper limit of normal. Viral replication was defined as elevated liver enzymes and increasing viral load and/or biopsy-proven hepatitis C virus active hepatitis.

**Results:** After conversion, there was a reduction of hemoglobin and hematocrit. In 1 patient, the immunosuppressive regimen was changed back to cyclosporine owing to anemia and hepatotoxicity leading to prompt return of hematocrit and liver enzymes to their original values. One of 10 antihepatitis C virus-positive patients (10.0%) developed sirolimus-associated hepatotoxicity, compared with 2 patients in the control group (13%). Sirolimus patients showed a significant decrease in the HCV PCR levels from 700 000 to 400 000 IU/mL;  $P < .001$ , compared to 680 000 to 660 000 IU/mL in cyclosporine patients;  $P = NS$ , with comparable levels of transaminases.

**Conclusions:** Our data suggest that sirolimus has the potential to suppress viral replication in hepatitis C virus-positive renal transplant candidates.

**Keywords:** Sirolimus; Renal transplant; Hepatitis C.

### 1128. Sitagliptin Might Be A Favorable Antiobesity Drug for New Onset Diabetes After A Renal Transplant

Soliman AR, Fathy A, Khashab S, Shaheen N and Soliman MA  
*Experimental and Clinical Transplantation*, 11: 494-498 (2013)  
IF: 0.588

**Objectives:** The aim of this study was to evaluate the effectiveness of sitagliptin, alone or in combination with metformin, in kidney transplant patients with newly diagnosed new-onset diabetes mellitus after transplant who had inadequate glycemic control, compared with a group of patients receiving insulin glargine with special emphasis on weight gain.

**Materials and Methods:** Newly diagnosed renal transplant patients with new-onset diabetes mellitus after a transplant was defined by a blood glucose = 11.1 mmol/L after an oral glucose tolerance test were examined. They were treated with standard immunosuppression composed of triple therapy with tacrolimus or cyclosporine, mycophenolate mofetil or azathioprine, and prednisone. They had stable graft function for more than 6 months after the transplant.

**Results:** Patients with new-onset diabetes mellitus after transplant ( $n=28$ ) whose glycemia was not controlled adequately with oral hypoglycemic agents (either alone or in combination) received oral sitagliptin 100 mg once daily in addition to existing therapy for 12 weeks. Patients who received insulin glargine as add-on therapy ( $n=17$ ) served as the control group. Data analyses included glycated hemoglobin, fasting plasma glucose, lipid profile, body weight, and the occurrence of hypoglycemia. We found significant reductions in glycated hemoglobin and fasting plasma glucose values after 12 weeks of additional sitagliptin therapy that were comparable to those with insulin glargine. While the addition of sitagliptin resulted in a small weight loss (0.4 kg), the addition of insulin glargine resulted in a weight gain (0.8 kg). The overall incidence of adverse experiences was low and generally mild in both groups.

**Conclusions:** In a group of renal transplant recipients with new-onset diabetes mellitus after a transplant in whom glycemia was not controlled adequately by oral hypoglycemic agents, the addition of sitagliptin helped to achieve glycemic control similar to insulin glargine but with a marginal weight advantage.

### 1129. Red Cell Distribution Width as A Marker of Inflammation in Type 2 Diabetes Mellitus

Heba Sherif, Nagwa Ramadan, Mona Radwan, Enas Hamdy and Rabab Reda

*Life Science Journal*, 10 (4): 32-39 (2013) IF: 0.165

**Background:** Red cell distribution width (RDW) is considered a prognostic marker which may reflect an underlying inflammatory process. This marker can be used as a predictor for macrovascular and microvascular complications of diabetes mellitus.

**Aim of the study :** was to investigate the relation between RDW and vascular complications in patients with type 2 diabetes and its relation to other inflammatory marker high sensitivity C-reactive protein (hs-CRP). **Subjects and methods:** This study is a cross-sectional study of 75 subjects with type 2 diabetes mellitus and 15 healthy controls. All subjects underwent thorough history, clinical examination and investigations including measurement of hs-CRP and calculation of RDW.

**Results:** In the present study RDW was found to be elevated in diabetic patients with macrovascular complications ( $15.251 \pm 1.77$ ) as compared to those without macrovascular complications with statistically significant difference ( $p = 0.04$ ). Also RDW was found to be elevated in diabetic patients with microvascular complications but this was not statistically significant ( $p = 0.87$ ). Hs-CRP was elevated in diabetic patients with macro- and microvascular complications ( $3.12 \pm 4.06$ ) with statistically significant difference as compared to control group ( $p = 0.02$ ). There was significant positive correlation between hs-CRP and HbA1c. Also positive correlations were found between RDW and hs-CRP.

**Conclusion:** High levels of RDW are associated with increased risk of macrovascular complications in type 2 diabetes mellitus. [Heba Sherif, Nagwa Ramadan, Mona Radwan, Enas Hamdy and Rabab Reda.

**Keywords:** Red cell distribution width; Inflammation; Type 2 diabetes mellitus.

### 1130. Significance of Urinary Monocyte Chemoattractant Protein-1 In Early Detection of Nephropathy in Type 2 Diabetic Patients

Mona I. Nabih, Ahmed El-Mazny, Nadia A. Mohamed and Amal R. El-Shehaby

*Life Science Journal*, 10 (1): 3030-3039 (2013) IF: 0.165

**Objective:** Monocyte Chemoattractant Protein-1 (MCP-1) is the strongest known monocytes chemotactic factor and has been implicated in the development and progression of diabetic nephropathy. So, measuring urinary MCP-1 would be of great significance in the diagnosis and intervention of diabetic nephropathy.

This study aimed at determining the levels of urinary MCP-1 (uMCP-1) at different stages of diabetic nephropathy and to study its correlation with other clinical and laboratory parameters in Egyptian type 2 diabetic subjects.

**Materials and methods:** A total of 45 type 2 diabetic subjects were classified into three groups based on their urinary albumin excretion and were compared with non-diabetic controls (Group IV) ( $n=15$ ).

The groups of diabetic subjects were Group I (normoalbuminuria) ( $n=15$ ), Group II (microalbuminuria) ( $n=15$ ) and Group III

(macroalbuminuria) (n=15). The four groups were age and sex matched. Medical history, clinical examination, anthropometric and biochemical details were recorded for all the subjects. Urinary MCP-1 levels were measured by using solid phase ELISA method.

**Results:** The mean level of uMCP-1 in patients with type 2 diabetes was significantly higher than in control subjects ( $p<0.0001$ ) and the mean level of uMCP-1 in the normoalbuminuric group was significantly higher than in the controls ( $p<0.0001$ ). Compared with the normoalbuminuric group, the mean levels of uMCP-1 in the microalbuminuric and macroalbuminuric groups were significantly higher ( $p<0.0001$ ). Also, the mean level of uMCP-1 in the macroalbuminuric group was significantly higher than that in the microalbuminuric group ( $P<0.0001$ ).

The levels of uMCP-1 were positively correlated with the levels of albuminuria in all diabetics ( $p<0.0001$ ) and in the macroalbuminuric group ( $p<0.05$ ). The levels of uMCP-1 were significantly negatively correlated with eGFR in the microalbuminuric group ( $p<0.05$ ).

The levels of uMCP-1 correlated positively with HbA1C in all diabetics ( $r=0.6$ ,  $p<0.0001$ ) and in the macroalbuminuric group ( $r=0.6$ ,  $p<0.05$ ) and correlated positively with serum total cholesterol ( $r=0.7$ ,  $p<0.0001$ ) and LDL-C in diabetic patients ( $r=0.7$ ,  $p<0.0001$ ).

**Conclusion:** Our study demonstrated that urinary MCP-1 levels increased gradually in type 2 diabetic subjects with increased albuminuria. It is significantly associated with the same risk factors of diabetic nephropathy.

**Keywords:** Diabetes mellitus; Diabetic nephropathy; Cytokines; Monocyte chemoattractant protein.

### 1131. Activated Protein C Resistance in Behcet's Disease

Hoda Abdel Badaee, Amr Edrees, Sherif Amin and Maher El Amirand Gaafar Ragab

*Thrombosis Journal*, 11: (2013)

Behcet's disease is a chronic multi-system disorder of unknown etiology with protean manifestations. Venous thromboembolism is more common than arterial thrombosis, with deep vein thrombosis being the most frequent. Endothelial dysfunction resulting from vascular inflammation is considered to be an important factor of thrombosis, although the endothelial injury itself cannot completely explain the hypercoagulable state of the disease because other vasculitis syndromes do not increase the risk of thrombosis.

The aim of this study is to evaluate the prevalence of activated protein C resistance (APC-R) in Egyptian patients with Behcet's disease. Also, to detect hyperhomocysteinemia in selected cases (with vascular complications) to assess their relationship with thromboembolic complications.

The APC resistance ratio mean in the group of patients with vascular involvement was  $2.6 \pm 0.8$  which was less than the group with no vascular involvement  $2.8 \pm 0.6$ , with non-significant P-value (0.5). There was more incidence of ocular lesions in the group of patients with high homocysteine level than the group of patients with normal homocysteine level with significant P-value (0.08).

**Keywords:** Activated protein C; Anticoagulant; Behcet's disease.

### 1132. Azathioprine Increases Cyclosporine-Induced Hyperuricemia in Renal Transplant Recipients

Hoda Abdel Hamid Maamoun, Dawlat Belal, Sahir Elkhatab and Amin Roshdy Soliman

*Journal of Nephrology and Renal Transplantation*, 5: 34-39 (2013)

**Background:** Hyperuricemia is a common side-effect of cyclosporine A (CsA) treatment in renal transplant recipients. While it is well established that the calcineurin inhibitors (CNI) whether cyclosporine A or tacrolimus can induce hyperuricemia in transplant population.

The present study was designed to compare the effects of azathioprine and mycophenolate mofetil (MMF) on CsA-induced hyperuricemia in post-renal transplant recipients. This study was also aimed to assess the prevalence of hyperuricemia and gout in renal transplant patients and to correlate hyperuricemia to patient variables such as cyclosporine level, dyslipidemia, diabetes mellitus and renal impairment.

**Methods:** Sixty renal transplant recipients on a stable dose of CsA. They were randomized in a double-blind, parallel-group manner to receive either azathioprine (group A, n = 37) or MMF (group B, n = 23) for 2 years. The primary outcome measure was the change from baseline in serum uric acid concentrations measured every 6 months. Secondary analyses of efficacy were based on changes in renal function and cyclosporine level, lipid pattern and blood glucose levels.

**Results:** Hyperuricemic patients represents 65% of all patients (n=39), while normouricemic were 35% (n=21). There was statistically significant increase in the prevalence of hyperuricemia in post-transplant renal recipients.

Group A had a higher trough level of cyclosporine compared to group B with statistically significant difference between both groups in both intervals.

There was a significant positive correlation between CsA trough level and post transplant uric acid level with no correlation with other variables. Azathioprine significantly increased serum uric acid levels at 2 years while MMF showed non significant effect although serum creatinine was not different between both groups at the end of the study.

**Conclusions:** MMF could be more appropriate than azathioprine for CsA-induced hyperuricemia in renal transplant recipients.

**Keywords:** Azathioprine; Uric acid; Cyclosporine; Renal transplant.

### 1133. Comparative Diagnostic Study of Biomarkers Using Fibromax™ and Pathology for Prediction of Liver Steatosis in Patients with Chronic Hepatitis C Virus Infection: an Egyptian Study

Ahmad Fouad, Dina Sabry, Rasha Ahmed, Manal Kamal, Sayed Abd Allah, Samar Marzouk, Mona Amin, Rokaya Abd El Aziz, Ahmad El Badri, Hany Khattab and Dina Helmy

*International Journal of General Medicine*, 6: 127-134 (2013)

**Background:** Steatosis is common in patients with hepatitis C virus (HCV) infection and may be a major determinant of progression of liver injury. This study evaluated FibroMax™ for noninvasive diagnosis of steatosis in patients with chronic HCV.

**Methods:** This cross-sectional study included 44 patients naïve to treatment who were referred to our hepatology clinic for

assessment of fitness for antiviral therapy. Chronic HCV infection was diagnosed by viral markers. Investigations included assessment of abdominal ultrasonography, liver biopsy, calculation of body mass index, and biomarker parameters in serum using FibroMax.

**Results:** Histopathology of liver biopsies showed steatosis in 30 of 44 (68%) patients. FibroMax results were positively correlated with viral load by quantitative polymerase chain reaction and histopathological findings. Body mass index was significantly higher in steatotic patients ( $P = 0.003$ ) and was significantly associated with the results on FibroMax ( $P = 0.005$ ).

**Conclusion:** FibroMax was correlated with histopathology and body mass index in patients with HCV. Abdominal ultrasonography could not be used as a single tool to diagnose steatosis with HCV. Steatosis is correlated with viral load, which suggests a direct viral effect. We recommend FibroMax assessment in a larger number of patients to assess its applicability in patients with HCV and steatosis.

**Keywords:** Steatosis; Hepatitis C virus; Histopathology; Fibromax™.

#### 1134. Distance from Treatment Facility and Risk of Death From Cardiovascular and Infectious Causes in Renal Transplant Patients

A. R. Soliman, A. Fathy, M. Elkhatab, M. A. Soliman and N. Shaheen

*Indian Journal Nephrology*, 23: 98-102 (2013) IF: 0.42

We investigated whether patients receiving RTx who live farther from their attending nephrologist are more likely to die than those who live closer.

A random sample of 167 patients who undergone RTx between 1996 and 2004 was examined. We calculated the distance between each patient's residence and the practice location of their attending nephrologist. We used Cox proportional hazards models to examine the adjusted relation between distance and clinical outcomes (death from all causes, rejection episodes, infectious causes, and cardiovascular complications) over a follow-up period of upto 6 years. During the follow-up period (median:3.3, range:1.0-6.5 years), 22% of patients died. Compared with patients who lived within 50 km of their nephrologist, the adjusted hazard ratio of death was 1.04 among those who lived 50.1-150 km away, 1.16 for those who lived 150.1-300 km away, and 1.19 for those who lived more than 300 km ( $P$  for trend  $<0.001$ ). The risk of death from infectious causes increased with greater distance from the attending nephrologist ( $P$  for trend  $<0.001$ ).

The risk of developing acute rejection episodes did not increase with distance from the attending nephrologist ( $P$  for trend = 0.2). The risk of death from cardiovascular causes increased with distance from the attending nephrologist ( $P$  for trend  $<0.05$ ). Compared with patients who lived within 50 km of their nephrologist, the adjusted hazard ratio of death among those who lived  $>300$  km away was 1.75 for infectious causes and 1.39 for cardiovascular causes. We conclude that mortality and morbidity associated with RTx was greater among patients who lived farther from their attending nephrologist, as compared with those who lived closer.

**Keywords:** Cardiovascular; Infection; Renal transplant.

#### 1135. The Prevalence of Helicobacter Pylori Infection in Diabetic Patients and its Relation to the Presence of Gastrointestinal Tract Complications

Osama Mohamady, Nagwa Ramadan and Heba Arnaout

*International Journal of Academic Research*, 5(4): 201-209 (2013)

**Background:** It's well known that diabetic patients are more prone to infection. In these patients, chronic infections are frequent and severe due to impairment of their immune system. The relationship between H. pylori infection and diabetes mellitus have shown in some studies but the relationships remain controversial. Aim of The study: was to determine the prevalence of Helicobacter pylori infection (H. pylori) among diabetic patients (type 1 and type 2 diabetes mellitus) and the relation of H. pylori infection to gastrointestinal (GI) complications in diabetics. **Subjects and Methods:** the study included 100 subjects were divided into 2 groups. Group I 50 patients with diabetes mellitus and have dyspeptic symptoms, group II 50 non-diabetic with dyspeptic symptoms. This is a case and control study comparison of diabetic and non-diabetic groups. The study was conducted at Police Hospital Cairo during the period from (January-December 2012).

**Methods:** H. pylori were assessed by H. pylori stool antigen (HpSag) test among diabetic and non-diabetic group.

**Results:** a positive cases for H. pylori infection by (HpSag) test was 61.1% in type 1 diabetic patients and 65.6% in type 2 diabetic patients compared to 50% of the non-diabetic group ( $p$  0.36) non significant (N.S). The prevalence of gastrointestinal symptoms in H. pylori positive diabetic patients as regarding dyspepsia (62.5%), early satiety (56.25%), heart burn (62.5%), bloating (25%), diarrhea (15.63%), constipation (25%), nausea (43.75%), vomiting (9.38%) and abdominal pain (53.13%), but by comparison with negative diabetic group these was statistically insignificant. Glycosylated Hb (HBA1c) was higher among positive cases, but yet not significant, ( $p$  0.07). Also, FBS ( $p$  0.08) and PPBS ( $p$  0.1) were not significant. The Presence of H. pylori not associated with increase duration of diabetes. The mean age of diabetic patients positive for H. pylori was  $48.750 \pm 11.09$  years compared to  $40.167 \pm 12.76$  years in diabetic patients negative for H. pylori infection ( $p$  0.017) significant (s). Age and BMI was higher among those positive for H. pylori in studied cases. **Conclusion:** The study reported no significant association between H. pylori infection and the prevalence of diabetes, but there is a borderline increased risk for H. pylori infection in diabetic among participants with a BMI greater than 25 kg/m<sup>2</sup>.

**Keywords:** H. Pylori; Diabetes mellitus; Gastrointestinal tract (GIT) complications.

#### Dept. of Medical Biochemistry and Molecular Biology

#### 1136. Human Leukocyte Antigen Class II Alleles (DQB1 and DRB1) as Predictors for Response to Interferon Therapy in HCV Genotype 4

Olfat Shaker, Heba Bassiony, Maissa El Raziky, Samer S. El-Kamary, Gamal Esmat, Akmal M. El-Ghor and Mona M. Mohamed

*Mediators of Inflammation*, 392746: 1-8 (2013) IF: 3.882

Human leukocyte antigens class II play an important role in immune response against HCV. We investigated whether HLA class II alleles influence susceptibility to HCV infection and response to interferon therapy. HLA-DRB1 and-DQB1 loci were genotyped using PCR-SSO Luminex technology. According to our regimen, 41 (66%) of patients achieved sustained virological response to combined treatment of IFN and ribavirin. Frequencies of DQB1 \* 0313 allele and DRB1 \* 04- DRB1 \* 11, DQB1 \* 0204- DQB1 \* 0313, DQB1 \* 0309- DQB1 \* 0313, and DQB1\*0313-DQB1\*0319 haplotypes were significantly more frequent in nonresponders than in responders. In contrast, DQB1\* 02, DQB1 \* 06, DRB1 \* 13, and DRB1 \* 15 alleles were significantly more frequent in responders than in nonresponders. Similarly, DRB1\* 1301, DRB1 \* 1361, and DRB1 \* 1369 alleles and DRB1 \* 1301-DRB1\*1328, DRB1\*1301-DRB1 \* 1361, DRB1 \* 1301-DRB1\*1369, DRB1\*1328-DRB1\*1361, and DRB1\*1328- DRB1\*1369 haplotypes were significantly found only in responders. Some alleles and linkages showed significantly different distributions between patient and healthy groups. These alleles may be used as predictors for response to treatment or to susceptibility to HCV infection in the Egyptian population.

### 1137. Liver Fibrosis Staging Through A Stepwise Analysis of Non-Invasive Markers (Fibrosteps) in Patients with Chronic Hepatitis C Infection

Samer S. El-Kamary, Mona M. Mohamed, Maissa El-Raziky, Michelle D. Shardell, Olfat G. Shaker, Wafaa A. ElAkel and Gamal Esmat

*Liver International*, 33(7): 982-990 (2013) IF: 3.87

**Background:** Non-invasive fibrosis markers can distinguish between liver fibrosis stages in lieu of liver biopsy or imaging elastography.

**Aims:** To develop a sensitive, non-invasive, freely-available algorithm that differentiates between individual liver fibrosis stages in chronic hepatitis C virus (HCV) patients.

**Methods:** Chronic HCV patients (n = 355) at Cairo University Hospital, Egypt, with liver biopsy to determine fibrosis stage (METAVIR), were tested for preselected fibrosis markers. A novel multistage stepwise fibrosis classification algorithm (FibroSteps) was developed using random forest analysis for biomarker selection, and logistic regression for modelling. FibroSteps predicted fibrosis stage using four steps: Step 1 distinguished no (F0)/mild fibrosis(F1) vs. moderate(F2)/severe fibrosis(F3)/cirrhosis(F4); Step 2a distinguished F0 vs. F1; Step 2b distinguished F2 vs. F3/F4; and Step 3 distinguished F3 vs. F4. FibroSteps was developed using a randomly selected training set (n = 234) and evaluated using the remaining patients (n = 118) as a validation set.

**Results:** Hyaluronic Acid; TGF- $\beta$ 1;  $\alpha$ 2 macroglobulin; MMP-2; Apolipoprotein A1; Urea; MMP-1;  $\alpha$ 1. etoprotein:haptoglobin, RBCs, haemoglobin and TIMP-1 were selected into the models, which had areas under the receiver operating curve (AUC) of 0.973, 0.923 (Step 1); 0.943, 0.872 (Step 2a); 0.916, 0.883 (Step 2b) and 0.944, 0.946 (Step 3), in the training and validation sets respectively. The final classification had accuracies of 94.9% (95% CI:91.3–97.4%) and 89.8% (95% CI:82.9–94.6%) for the training and validation sets respectively.

**Conclusions:** FibroSteps, a freely available, non-invasive liver fibrosis classification, is accurate and can assist clinicians in making prognostic and therapeutic decisions. The statistical code

for FibroSteps using R software is provided in the supplementary materials.

**Keywords:** Chronic hepatitis; Fibrosis markers; Hepatitis C virus; Liver fibrosis; Logistic regression.

### 1138. TGF- $\beta$ 1 Pathway as Biological Marker of Bladder Carcinoma Schistosomal and Non-Schistosomal

Olfat Shaker, Olfat Hammam, Mohamed Wishahi and Mamdouh Roshdi

*Urologic Oncology: Seminars and Original Investigations*, 31 (3): 372-378 (2013) IF: 3.647

**Objectives:** Study TGF- $\beta$ 1 pathway in bladder carcinoma. Design and methods: Eighty-one patients were enrolled: 16 chronic cystitis and 60 malignant bladder lesions; 15 schistosomal squamous cell carcinoma (SQCC), 45 transitional cell carcinoma (TCC). Five healthy individuals served as controls. mTGF- $\beta$ 1, protein, and its receptor expression in urine and bladder tissue were measured using in situ hybridization and immunohistochemical techniques, respectively.

**Results:** Overexpression of TGF-mRNA in invasive TCC group was compared with superficial TCC, high grade TCC was compared with low grade, and SQCC was compared with TCC. TGF- $\beta$ 1 protein and its receptor I (TGF-R1) were overexpressed in urine samples in malignant group compared with chronic cystitis and in SQCC group compared with TCC group. TGF- $\beta$ 1 protein and its receptor were significantly increased in schistosomal malignant group compared with non-schistosomal group.

**Conclusion:** Expression of TGF- $\beta$ 1 and TGF- $\beta$ R1 could be used as biological markers of bladder carcinoma. © 2013 Elsevier Inc. All rights reserved.

**Keywords:** TGF- $\beta$ 1; TGF-  $\beta$  R1; mRNA; Cancer bladder; TCC; SqCC; Schistosomiasis.

### 1139. Dendritic Cell Co-Stimulatory and Co-Inhibitory Markers in Chronic HCV: an Egyptian Study

Hanan Fouad, Maissa Saeed El Raziky, Rasha Ahmed Abdel Aziz, Dina Sabry, Ghada Mahmoud Abdel Aziz, Manal Ewais and Ahmed Reda Sayed

*World Journal of Gastroenterology*, 19: 7711-7718 (2013) IF: 2.547

**Aim:** To assess co-stimulatory and co-inhibitory markers of dendritic cells (DCs) in hepatitis C virus (HCV) infected subjects with and without uremia.

**Methods:** Three subject groups were included in the study, group 1: involved 50 control subjects, group 2 involved 50 patients with chronic HCV infection and group 3 involved 50 HCV uremic subjects undergoing hemodialysis. CD83, CD86 and CD40 as co-stimulatory markers and PD-L1 as a co-inhibitory marker were assessed in peripheral blood mononuclear cells by realtime polymerase chain reaction (PCR). Interleukin-10 (IL-10) and hyaluronic acid (HA) levels were also assessed. All findings were correlated with disease activity, viral load and fibrogenesis.

**Results:** There was a significant decrease in costimulatory markers; CD83, CD86 and CD40 in groups 2 and 3 vs the control group. Co-stimulatory markers were significantly higher in group

3 vs group 2. There was a significant elevation in PD-L1 in both HCV groups vs the control group. PD-L1 was significantly lower in group 3 vs group 2. There was a significant elevation in IL-10 and HA levels in groups 2 and 3, where IL-10 was higher in group 3 and HA was lower in group 3 vs group 2. HA level was significantly correlated with disease activity and fibrosis grade in group 2. IL-10 was significantly correlated with fibrosis grade in group 2. There were significant negative correlations between co-stimulatory markers and viral load in groups 2 and 3, except CD83 in dialysis patients. There was a significant positive correlation between PD-L1 and viral load in both HCV groups.

**Conclusion:** A significant decrease in DC co-stimulatory markers and a significant increase in a DC coinhibitory marker were observed in HCV subjects and to a lesser extent in dialysis patients.

**Keywords:** Hepatitis C Virus; Uremia; Hemodialysis; Dendritic cells; CD83; CD86, CD40; PD-L1; Interleukin-10; Hyaluronic acid.

#### 1140. Vaspin Gene in Rat Adipose Tissue: Relation to Obesity-Induced Insulin Resistance

Olfat G. Shaker and Nermin Abdel Hamid Sadik

*Molecular and Cellular Biochemistry*, 373: 229-239 (2013)  
IF: 2.329

Visceral adipose fat has been claimed to be the link between obesity and insulin resistance through the released adipokines. This study aimed to assess the expression of vaspin as one of the recent adipokines in rats abdominal subcutaneous and visceral fat in diet-induced obese (DIO) and in DIO performing 3 weeks swimming exercise (DIO EXE) compared to control and control exercise (C EXE) groups.

Vaspin mRNA and protein expression assessed using RT-PCR and Western blotting analysis revealed vaspin expression in DIO and DIO EXE but not in controls groups. in DIO group, visceral vaspin expression was higher than in that of subcutaneous fat and was positively correlated with body weight. Upregulation of visceral vaspin expression in DIO was concomitant with the development of insulin resistance (increase in fasting serum insulin and HOMA-IR) and rise in serum leptin level.

Unchanged visceral vaspin mRNA in DIO EXE rats, with significant improvements of insulin resistance parameters and serum leptin compared to DIO group was found. in conclusion, increased visceral vaspin expression in obesity was associated with insulin resistance.

Further investigations into the molecular links between vaspin and obesity may unravel innovative therapeutic strategies in people affected by obesity-linked insulin resistance, metabolic syndrome, and type 2 diabetes.

**Keywords:** Vaspin; Insulin resistance; Obesity; Rat; RT-PCR; Western blot.

#### 1141. Impact of Single Nucleotide Polymorphism in Tumor Necrosis Factor-A Gene 308G/A in Egyptian Asthmatic Children and Wheezing Infants

Olfat G. Shaker, Nermin Abdel Hamid Sadik and Nehal Abd El-Hamid

*Human Immunology*, 74: 796-802 (2013) IF: 2.298

Bronchial asthma is a common disease with multiple determinants that include genetic variation. Although tumor necrosis factor alpha (TNF-a) is a major pro-inflammatory cytokine, the functions of genetic polymorphisms in this cytokine has not been thoroughly examined in the context of asthma pathology. Therefore, we aimed to investigate whether single nucleotide polymorphism (SNP) in TNFa is associated with asthma and wheezing and whether the association is related to the severity of the disease and other epidemiological factors. Frequencies of TNF-a-308G/A polymorphism were compared in 100 asthmatic children, 100 wheezy infants and 100 age and gender matched controls. Genotype frequencies for TNF-a-308G/A were significantly higher in asthmatic children (60%) and wheezy infants (68%) than the control group (30%). Higher serum levels of TNF-a were observed in genotypes G/A and G/G of asthmatic children and wheezy infants than in controls. No association was found between the G/A polymorphism and the severity of the disease, the total eosinophil count and IgE levels in both groups. We can conclude that genetic variation in TNF-a-308G/A may contribute to childhood asthma and wheezing. These findings could be helpful for future early intervention studies which may have a potential impact on family counseling and management.

**Keywords:** Bronchial asthma; TNF; Polymorphism.

#### 1142. Single Nucleotide Polymorphisms of IL-10 and IL- 28B As Predictors to the Response of Interferon Therapy in HCV Genotype 4 Infected Children

Olfat G. Shaker, Yasser H. Nassar, Zeinab A. Nour and Mona El Raziky

*J. Pediatr Gastroenterol Nutr.*, 57(2): 155-160 (2013) IF: 2.196

**Background and Aims:** Single- nucleotide polymorphisms (SNPs) in the IL-10 gene (1082 [rs1800896], 819 [rs3021097], and 592 [rs1800872]) and the IL-28B gene (rs12979860) in adults were shown to be associated with hepatitis C virus (HCV) clearance. The present study aimed to investigate the possible association of SNPs of IL- 10 and IL-28B in predicting the treatment response of HCV genotype 4 in pediatric patients.

**Patients and Methods:** A restriction fragment length polymer phismpolymerase chain reaction and real-time polymerase chain reaction techniques were used to genotype 34 pediatric patients with HCV genotype 4 for IL-10 and IL-28B SNPs, respectively. Patients received pegylated interferon-a/ribavirin for 48 weeks subdivided according to their response to treatment into responders and nonresponders; also, 20 healthy individuals served as controls.

**Results:** A significant difference ( $P < 0.005$ ) was observed in SNP of IL-28B rs12979860 frequencies between responders and nonresponders. in responders, CC genotype had greater frequency than CT and TT genotypes (60%, 30%, 10%), respectively, with C allele in its homozygous (CC) genotype more likely to respond to treatment than in its homozygous (TT) genotypes. SNPs of IL-10 at 819 (rs3021097) showed significant differences in their genotype frequencies between responders and nonresponders to therapy, and TT genotype had greater frequency in responders than CT and CC (55%, 20%, 25%), respectively. Genotypes with T allele (CT/TT) showed higher rates of response than those with noT allele (CC).

**Conclusions:** SNPs of the IL-28B gene at (rs12979860) CC genotype as well as the IL-10 gene SNPs at 819 (rs3021097)/TT genotype can be used for predicting response to treatment before



patients are prescribed the expensive pegylated interferon- $\alpha$ /ribavirin therapy.

**Keywords:** Hepatitis C Virus; Interleukin 28-B; Interleukin-10; Pediatrics.

### 1143. Is There A Correlation Between HPV and Urinary Bladder Carcinoma

Olfat Gamil Shaker, Olfat A. Hammam and Mohamed M. Wishahi

*Biomedicine and Pharmacotherapy*, 67 (3): 183-191 (2013)  
IF: 2.068

**Aims:** To detect human papilloma virus (HPV) infection, p21 oncogene, DNA content of urothelial cells in different bladder lesions with and without schistosomiasis and to correlate them with histopathological grade and stage.

**Methods:** Eighty-five patients were enrolled: 25 chronic cystitis and 60 malignant bladder lesions; 15 schistosomal squamous cell carcinoma (SQCC), 45 urothelial carcinoma (transitional cell carcinoma TCC) schistosomal and non-schistosomal. Ten healthy individuals served as controls. Genotyping of HPV 6/11 and 16/18 were done using in situ hybridization and p21 protein expression by Immunohistochemical technique in formalin-fixed, paraffin-embedded tissues. DNA content of urothelial cells were stained with felugen stains and measured using Automated Image analysis System.

**Results:** HPV DNA 6/11 and 16/18 expression was increased from cases of schistosomal cystitis with dysplasia to TCC with schistosomiasis compared to TCC and SQCC. The expression increased with statistical significance in invasive TCC and high-grade compared with superficial and low grade. Overexpression of p21 in invasive TCC group was compared with superficial TCC, high-grade TCC was compared low grade and TCC was compared with SQCC. Almost all cases of TCC associated with schistosomiasis exhibit aneuploid histogram compared to SQCC and all invasive TCC exhibited aneuploid histograms.

**Conclusions:** Both HPV infection and p21 gene abnormalities may contribute to bilharzial bladder carcinogenesis. DNA image cytometric features may predict stage progression in TCC. Expression of p21, DNA HPV 6/11 and 16/18 may be used as biological markers of bladder carcinoma.

**Keywords:** Human papilloma Virus; in situ hybridization; Bladder carcinoma; p21; IHC.

### 1144. The Effect of a Novel Curcumin Derivative on Pancreatic Islet Regeneration in Experimental Type-1 Diabetes in Rats (Long Term Study)

Ismail Mohamed T. Abdel Aziz, Mohamed F. El-Asmar, Ameen M. Rezq, Soheir M. Mahfouz, Mohamed A. Wassef, Hanan H. Fouad, Hanan H. Ahmed and Fatma M. Taha

*Diabetology and Metabolic Syndrome*, 5: 75- (2013) IF: 1.924

**Background:** Several studies highlight curcumin's benefit as a hypoglycemic agent, however; a limited number of reports present the importance of curcumin in improvement of pancreatic islets in diabetes. The aim of the present study is to evaluate the antidiabetic effect of a novel curcumin derivative and its effect on pancreatic islet regeneration in type I diabetes-induced by STZ.

**Materials and Methods:** Rats were divided into diabetic rats and

diabetic rats treated orally with the novel curcumin derivative (NCD) for 40 days. Fasting blood samples were withdrawn periodically from all rats to estimate plasma glucose, insulin and C-peptide for 10 months. Histopathology was performed to allow the assessment of pancreatic islet morphology. Insulin and CD105 were detected immunohistochemically.

**Results:** in diabetic rats, the plasma glucose, insulin and C-peptide levels remained within the diabetic range for about 4 months, after which a gradual decrease in glucose and increase in insulin and C-peptide was observed, which reached almost normal levels after 10 months. NCD treated diabetic rats showed significantly lowered plasma glucose and increased plasma insulin and C-peptide levels. This was followed by a further significant decrease in plasma glucose and increase in plasma insulin and C-peptide after two months from oral administration of the NCD. The plasma insulin and C-peptide continued to increase for ten months reaching levels significantly higher than the basal level. Histopathological examination of diabetic rat pancreas revealed absence of islets of Langerhans, minimal adipose tissue infiltration and localized lymphocytic infiltrates. However, after 6 months of induction of diabetes, rat pancreas showed the appearance of small well formed islets and positive insulin cells but no CD105 positive cells. NCD treated rats showed the appearance of primitive cell collections, large insulin positive cells and CD105 positive cells in the adipose tissue infiltrating the pancreatic tissues. This was followed by the gradual appearance of insulin positive cells in the islets while, CD 105 positive cells remained in the adipose tissue. After 5 and 10 months from the onset of diabetes, rat pancreas showed, well developed larger sized islets with disappearance of primitive cell collections and CD 105 positive cells. Also, insulin positive islets of variable size with disappearance of insulin positive cells in adipose tissue were detected.

**Conclusion:** The NCD possesses antidiabetic actions and enhanced pancreatic islets regeneration.

**Keywords:** Curcumin derivative; Type I diabetes; Pancreatic islet regeneration; Insulin secretion.

### 1145. Heme Oxygenase Effect on Mesenchymal Stem Cells Action on Experimental Alzheimer'S Disease

M.T. Abdel Aziz, H.M. Atta, H. Samer, H.H. Ahmed, L.A. Rashed, D. Sabry, E.R. Abdel Raouf and M.A. ALKaffas

*Experimental and Clinical Science*, 12: 778-792 (2013) IF: 1.923

**Objective:** The objective is to evaluate the effect of heme oxygenase-1 (HO-1) enzyme inducer and inhibitor on Mesenchymal Stem Cells (MSCs) in Alzheimer disease.

**Materials and Methods:** 70 female albino rats were divided equally into 7 groups as follows: group 1: healthy control; group 2: Aluminium chloride induced Alzheimer disease; group 3: induced Alzheimer rats that received intravenous injection of MSCs; group 4: induced Alzheimer rats that received MSCs and HO inducer cobalt protoporphyrin; group 5: induced Alzheimer rats that received MSCs and HO inhibitor zinc protoporphyrin; group 6: induced Alzheimer rats that received HO inducer; group 7: induced Alzheimer rats that received HO inhibitor. Brain tissue was collected for HO-1, seladin-1 gene expression by real time polymerase chain reaction, heme oxygenase activity, cholesterol estimation and histopathological examination.

**Results:** MSCs decreased the plaque lesions, heme oxygenase induction with stem cells also decreased plaque lesions however there was hemorrhage in the brain. Both heme oxygenase inducer

alone or with stem cells increased seladin-1 expression and decreased cholesterol level.

**Conclusion:** MSCs alone or with HO-1 induction exert a therapeutic effect against the brain lesion in Alzheimer's disease possibly through decreasing the brain cholesterol level and increasing seladin-1 gene expression.

**Keywords:** Alzheimer's disease; Stem cell; Heme oxygenase.

#### 1146. Antiangiogenic Effect of Methotrexate and PUVA on Psoriasis

Olfat G. Shaker, Mongy Khairallah, Hoda M. Rasheed, Mona R. Abdel-Halim, Ola M. Abuzeid, Amira M. ElTawdi, Heba H. El Hadidi and Ali Ashmaui

*Cell Biochemistry and Biophysics*, 67: 735-742 (2013) IF: 1.912

Vascular endothelial growth factor (VEGF) is important factor for angiogenesis in psoriasis. Methotrexate and psoralen and ultraviolet light A (PUVA) mainly target the T cell-mediated immunopathology of psoriasis. Our work aimed at estimating VEGF mRNA in psoriatic patients and investigating whether the standard therapeutic modalities (methotrexate and PUVA) exert their antiangiogenic activity through altering VEGF levels. Twenty-four chronic plaque psoriasis patients were enrolled. Patients were divided into two groups (12 patients each); group A received intramuscular methotrexate and group B was treated by PUVA three times/week in a PUVA1000 cabin for 10 weeks each. Twelve healthy volunteers served as controls. A skin biopsy was taken from lesional skin before and after treatment for RT-PCR detection of VEGF mRNA. Capillary perfusion scanning using LASER Doppler perfusion imaging was performed on the same psoriatic plaque before and after treatment and was also done for the controls. Following both methotrexate and PUVA, a significant reduction in the amount of VEGF mRNA ( $P < 0.001$  and  $P = 0.002$ , respectively) and capillary perfusion ( $P = 0.002$ ) occurred. These reductions were significantly higher in the methotrexate group ( $P < 0.001$  and  $P = 0.001$ , respectively) than in the PUVA group. The percentage of clinical improvement in the examined psoriatic plaque was significantly positively correlated with the percentage of reduction in the amount of VEGF mRNA ( $r = 0.850$ ,  $P < 0.001$ ) and the percentage of reduction in the capillary perfusion ( $r = 0.684$ ,  $P < 0.001$ ). Both modalities may exert an antiangiogenic effect. Methotrexate appears to have possibly a more potent antiangiogenic effect than PUVA.

**Keywords:** Psoriasis; Angiogenesis; VEGF; Capillary perfusion; Methotrexate; PUVA.

#### 1147. Osteopontin Gene Polymorphisms as Predictors for the Efficacy of Interferon Therapy in Chronic Hepatitis C Egyptian Patients with Genotype 4

Olfat Shaker, Amal El-Shehaby, Salwa Fayez, Amr Zahra, Samar Marzouk and Maissa El Raziky

*Cell Biochemistry and Function*, 31(7): 620-625 (2013) IF: 1.854

This study aimed to determine the relationship between osteopontin gene polymorphisms and its protein level and the efficacy of interferon-based therapies in Hepatitis C virus (HCV) patients. Hundreds HCV patients genotype 4, treated with pegylated interferon alfa-2b plus ribavirin and 60 healthy subjects were enrolled. All individuals were subjected to clinical and

laboratory parameters, including hepatitis markers and HCV quantitation by real-time polymerase chain reaction. Single nucleotide polymorphisms (SNPs) of osteopontin (OPN) gene (nucleotide 155, 443 and 1748) were analysed by direct sequencing in addition to estimation of serum level of OPN. SNP at 443 (C/C versus C/T, T/T) was found to represent predictors for treatment response by univariate logistic regression analysis. OPN serum level was independent predictors for treatment response by both univariate and multivariate logistic regression analysis. SNP at nucleotide 443 and serum OPN protein levels could be used as useful markers to predict the efficacy of treatment.

**Keywords:** Hepatitis C; Osteopontin; Polymorphism.

#### 1148. Pathogenesis of Preeclampsia: Implications of Apoptotic Markers and Oxidative Stress

O.G. Shaker and N.A.H. Sadik

*Human and Experimental Toxicology*, 32(11): 1170-1178 (2013) IF: 1.453

This study aimed to investigate the implication of some apoptotic and lipid peroxidation markers in preeclampsia (PE). A total of 25 women with PE and 25 age- and parity-matched normal pregnant women were enrolled in this study. The malondialdehyde (MDA) level, caspase-9 activity and the percentage of DNA fragmentation were significantly higher in placental tissue of PE than in control women. The serum level of MDA was significantly elevated in women with PE having delivery by cesarean section (CS) than in women with PE having vaginal delivery. In vitro study demonstrated that the addition of 0.5 mM Fe<sup>2+</sup> and 0.1 mM ascorbate caused increase in the production of MDA level in placental tissue with PE than normal placentas, and vitamin E (100 mM) caused lower inhibition of in vitro lipid peroxidation in placental tissue with PE when compared with normal tissue. The activity of caspase-9 and percentage of DNA fragmentation were associated with the severity of the PE and both could differentiate between PE and control women with 88% and 100% sensitivity and 96% and 100% specificity, respectively. The activities of caspase-8 and/or-9 were positively correlated with the maternal age but only caspase-8 was negatively correlated with neonatal birth weight and placental weight. In conclusion, the elevations of MDA, caspase-9 activity and the percentage of DNA fragmentation in the placentas of women with PE implicate the involvement of lipid peroxidation and apoptosis in PE. The placenta represents a considerable source of the elevated circulating MDA in PE.

**Keywords:** Preeclampsia; Apoptosis; Lipid peroxidation; MDA; Caspases DNA fragmentation.

#### 1149. Transforming Growth Factor Beta 1 and Monocyte Chemoattractant Protein-1 as Prognostic Markers of Diabetic Nephropathy

O.G. Shaker and N.A.H. Sadik

*Human and Experimental Toxicology*, 32(10): 1089-1096 (2013) IF: 1.453

We aimed to find the relationship between serum transforming growth factor beta 1 (TGF- $\beta$ 1) and urinary monocyte chemoattractant protein-1 (MCP-1) throughout the course of diabetic

nephropathy (DN) and to assess the relationship between both levels and other parameters of renal injury such as albumin/creatinine ratio and estimated glomerular filtration rate (eGFR). Serum TGF- $\beta$ 1, urinary MCP-1, eGFR, and glycosylated hemoglobin (HbA1c) were measured in 60 patients with type II diabetes mellitus with different degrees of nephropathy (20 patients with normoalbuminuria, 20 patients with microalbuminuria, and 20 patients with macroalbuminuria) and compared with 20 matched healthy control subjects. Both the levels of serum TGF- $\beta$ 1 and urinary MCP-1 were significantly higher in patients with micro- and macroalbuminuria ( $137.8 \pm 69.5$  and  $329.25 \pm 41.46$  ng/dl, respectively, for TGF- $\beta$ 1 and  $167.41 \pm 50.23$  and  $630.87 \pm 318.10$  ng/g creatinine, respectively, for MCP-1) compared with normoalbuminuric patients and healthy controls ( $33.25 \pm 17.5$  and  $29.64 \pm 10.57$  ng/dl, respectively, for TGF- $\beta$ 1 and  $63.85 \pm 21.15$  and  $61.50 \pm 24.81$  ng/g creatinine, respectively, for MCP-1;  $p < 0.001$ ). There was a positive significant correlation between the levels of serum TGF- $\beta$ 1 and those of urinary MCP-1 ( $r = 0.73$ ,  $p < 0.001$ ). Also, serum TGF- $\beta$ 1 and urinary MCP-1 correlated positively with HbA1c ( $r = 0.49$  and  $0.55$ , respectively,  $p < 0.05$  for both) and inversely with eGFR ( $r = -0.69$  and  $-0.60$ , respectively,  $p < 0.001$  for both). We can conclude that serum TGF- $\beta$ 1 and urinary MCP-1 can be used as the markers for detection of progression of DN. Antagonizing TGF- $\beta$ 1 and MCP-1 might be helpful in attenuating the progression of nephropathy in diabetic patients.

**Keywords:** Diabetic nephropathy; TGF- $\beta$ 1; MCP-1.

#### 1150. An Insight Into the Pathogenesis of Oral Lichen Planus: a Genomic and Proteomic Case Control Study

Fat'heya M. Zahran, Safia A. Al-Attas, Olfat G. Shaker and Mona H.A. Hassan

*Australian Journal of Basic and Applied Sciences*, 7(8): 480-487 (2013)

Oral lichen planus (OLP) is a refractory mucosal disease. Its pathogenesis is thought to involve immunologic and genetic alterations. As previous literature pointed out to the significance of interferon-gamma (INF- $\gamma$ ) gene polymorphisms in the pathogenesis of OLP, the present study was performed on a total of 60 OLP patients and 20 unrelated individuals not suffering from any mucosal lesions, to test the role of one of the polymorphisms previously identified among some populations and investigate its link to increased INF- $\gamma$  production and disease severity.

INF- $\gamma$  polymorphism at position 5644 (A/T) was identified using Sequence Specific Primers-Polymerase Chain Reaction (SSP-PCR). Also, whole unstimulated saliva samples were collected from all the included individuals in order to determine INF- $\gamma$  level in saliva utilizing the ELISA technique.

The results revealed no statistically significant difference in T allele distribution among different types of OLP, neither when all patients were considered as a whole nor when they were considered as separate groups. However, there was highly significant increase in the frequency of TT genotype among OLP patients compared to controls. Conversely, there was an increase in AT genotype in controls. Patients carrying TT homozygous genotype were found to have about 9 times more risk of developing OLP, while those with AT heterozygous genotype had low risk of developing the disease. When cases with reticular

pattern were considered alone, the risk was found to increase to 12. The results also showed that the control group had the lowest level of salivary INF- $\gamma$ , whereas all types of OLP showed highly significant increase in its level. The highest values were registered by the atrophic and erosive groups. When genotypes were considered, TT individuals registered significantly increased salivary INF- $\gamma$  levels than other genotypes. It seems that the tested INF- $\gamma$  gene polymorphism contributes to the predisposition to OLP where the genetic variation affects the gene expression and may contribute to the disease chronicity.

**Keywords:** Oral lichen planus; Interferon- $\gamma$ ; Interferon- $\gamma$  gene; Salivary cytokines; Gene polymorphism; Genetics.

#### 1151. Correlation and Multiple Regression Analyses of Pituitary Growth Hormone and Hepatic Activities in Hepatitis C Infection and Interferon Response

Emad F. Eskander, Ahmed A. Abd-Rabou, Shaymaa M. M. Yahya, Ashraf El Sherbini, Mervat S. Mohamed and Olfat G. Shaker

*Indian Journal of Clinical Biochemistry*, 28 (4): 348-357 (2013)

The prevalence of hepatitis C virus (HCV) infection varies across the world, with the highest percent of infections reported in Middle East, increasingly in Egypt. The current study aimed at examining the bio-statistical correlation and multiple regression analyses of pituitary growth hormone (GH) and liver activities among HCV genotype-4 patients treated with PEG-IFN- $\alpha$  plus RBV therapy. Herein, the current study was conducted on 100 HCV genotype-4 infected patients and 50 healthy controls. Patients received PEG-IFN- $\alpha$ /RBV for 24 weeks. Host RNA was isolated from patients' sera for HCV genotyping and viral load determination. Moreover, the enzymatic activities of the liver, AFP, GH, PT, and CBC were performed in all volunteers. The present study resulted that the activities of the hepatic enzymes among HCV genotype-4 patients correlated together significantly. While, human GH showed a significant positive regression with pre-treatment ALT concentration in responders. Furthermore, multiple regression analysis for GH showed a significant positive correlation with pre-treatment ALT in HCV genotype-4 infected patients. We concluded that there were a putative significant relation between GH and pre-treatment ALT activity in HCV infection and response to IFN-based therapy.

**Keywords:** Hepatitis C; Interferon pituitary; Growth hormone liver enzymes.

#### 1152. Effect of Mesenchymal Stem Cells on Anti-Thy1,1 Induced Kidney Injury in Albino Rats

Saber Sakr, Laila Rashed, Waheba Zarouk and Rania El-Shamy

*Asian Pacific Journal of Tropical Biomedicine*, 3: 174-181 (2013)

**Objective:** To evaluate the effect of mesenchymal stem cells (MSCs) in rats with anti-Thy1,1 nephritis.

**Methods:** Female albino rats were divided into three groups, control group, anti-Thy1,1 group and treatment with i.v. MSCs group. MSCs were derived from bone marrow of male albino rats, Y-chromosome gene was detected by polymerase chain reaction in the kidney. Serum urea and creatinine were estimated for all groups. Kidney of all studied groups was examined histologically

and histochemically (total carbohydrates and total proteins). DNA fragmentation and expression of  $\alpha$ -SMA were detected.

**Results:** Kidney of animals injected with anti-Thy1, 1 showed inflammatory leucocytic infiltration, hypertrophied glomeruli, tubular necrosis and congestion in the renal blood vessels. The kidney tissue also showed reduction of carbohydrates and total proteins together with increase in apoptosis and in expression of  $\alpha$ -SMA. Moreover, the levels of urea and creatinine were elevated. Treating animals with MSCs revealed that kidney tissue displayed an improvement in the histological and histochemical changes. Apoptosis and  $\alpha$ -SMA expression were decreased, and the levels of urea and creatinine decreased.

**Conclusions:** The obtained results demonstrated the potential of MSCs to ameliorate the structure and function of the kidney.

**Keywords:** Anti-Thy1; 1, Nephritis; Mesenchymal stem cells;  $\alpha$ -SMA; Apoptosis.

### 1153. Evaluation of the Potentials of Autologous Blood Injection for Healing in Diabetic Foot Ulcers; Three Study Cases

Mohammed Al azrak, Taher Ismail and Olfat Shaker

*Journal of the American College of Clinical Wound Specialists, 4: 45-50 (2013)*

Healing is a complex multifactorial process, hence it is not easy to be studied accurately. In this paper we tried to demonstrate the potentials of application of autologous blood by injection into the raw areas and ulcers of three diabetic patients using their blood as an alternative to synthesized and cultured stem cells or growth factors. It was found that a natural easily obtained blood can be used to enrich the media of the wound. Also it was applicable in relation to its cost-effectiveness as well as availability. The healing process was accelerated in the injected side more than the non-injected one.

**Keywords:** Autologous blood; Blood injection; Healing; Diabetic ulcers.

### 1154. Hepatic Fibrosis and Serum Alpha-Fetoprotein (AFP) As Predictors of Response to HCV Treatment and Factors Associated with Serum AFP Normalisation After Treatment

Maissa El Raziky, Dina Attia, Wafaa El akel, Olfat Shaker, Hany Khatab, Shaimaa Abdo Aisha Elsharkawy and Gamal Esmat

*Arab Journal of Gastroenterology, 14: 94-98 (2013)*

**Background and Study Aim:** Elevated levels of alpha-fetoprotein (AFP) can be seen in patients with chronic hepatitis C (CHC) and liver cirrhosis without hepatocellular carcinoma and were negatively associated with treatment response. However, factors associated with its changes are not identified. We aimed in this study to verify a cut-off value for AFP as a predictor of response to standard of care (SOC) antiviral therapy in Egyptian chronic hepatitis C virus (HCV)-infected patients and identify factors associated with its changes post treatment.

**Patients and methods:** A total of 175 chronic non-cirrhotic HCV-infected patients were evaluated for baseline serum AFP and liver biopsy were classified according to Ishak scoring system of hepatic fibrosis.

All patients were scheduled to receive SOC antiviral therapy for 48 weeks and had been followed up to week 72. Reassessment of AFP and repeated liver biopsy at week 72 were feasible only in 79 patients.

**Results:** High baseline AFP levels were observed in non-respondents (non-sustained virological respondents (non-SVRs)) ( $P < 0.01$ ); the AFP level decreased in all patients post treatment ( $P = 0.01$ ), especially in the SVRs ( $P < 0.01$ ). In multivariate analysis, hepatic fibrosis was a predictor of response to treatment ( $P = 0.02$ ), while body mass index (BMI) (25–30 kg m<sup>2</sup>), hepatic activity (A2), hepatic fibrosis stage (F2–F4) and fibrosis improvement were predictors of AFP difference ( $P = 0.007, 0.01, 0.012, <0.001, 0.030$ , and  $0.018$ ), respectively. The diagnostic performance to predict the HCV treatment response was best by adding both AFP and hepatic fibrosis stage factors; the best cut-off value for AFP was 3.57 ng dl<sup>-1</sup> with 50% sensitivity and 68% specificity with area under the curve (AUC) of 0.55 and for hepatic fibrosis stage was 3, with a sensitivity of 88%, a specificity of 30% with an AUC of 0.58.

**Conclusion:** In chronic HCV-infected patients, serum AFP below 3.57 ng dl<sup>-1</sup> and hepatic fibrosis stage 3 are expected to have good response to treatment; BMI (25–30 kg m<sup>2</sup>), A2, fibrosis  $>2$  and fibrosis improvement predict AFP change post treatment.

**Keywords:** Chronic hepatitis C Virus; Hepatic fibrosis; Alpha-fetoprotein.

### 1155. Hepcidin Levels in Egyptian Patients with Chronic Hepatitis C and The Effect of Anti-Viral Therapy

Hanan A. Marzouk, Naglaa A. Zayed, Mahmoud Al-Ansary, Mohamed S. Abdelbary Shereen S. Hunter, Wael Safwat, Moustafa Abdel-Moneim and Olfat Shaker

*World Applied Sciences Journal, 22 (8): 1140-1145 (2013)*

Disruption of hepatic production of the iron regulatory hormone-hepcidin has been postulated as a possible mechanism causing iron overload in chronic hepatitis C. This study aimed at assessing the hepcidin level in CHC patients & its relation to interferon therapy.

Serum iron indices and hepcidin/ferritin ratio were assessed in CHC patients (n=30) and healthy volunteers (n=20), before and after 24 weeks of pegylated (PEG)-IFN and ribavirin therapy. Results revealed that baseline serum hepcidin, iron and hepcidin/ferritin ratio were significantly lower in CHC patients than in controls ( $p=0.0194, 0.000$  and  $0.0037$  respectively) with significant correlation between and baseline serum hepcidin and ferritin ( $r=0.605$ ;  $p=0.000$ ). Following 24 weeks of PEG-IFN/ribavirin therapy, hepcidin levels significantly increased to be higher than that of the control group ( $p=0.0386$ ) whereas iron and hepcidin/ferritin ratio increased, but their levels were still significantly lower compared to the control group ( $p=0.039$  and  $0.0051$  respectively) and this was not related to the virological response. On the other hand, both baseline and follow up ferritin levels were significantly higher in CHC patients than the control group ( $p$ -value  $0.0003$  and  $0.0007$ ). In conclusion, serum hepcidin and hepcidin/ferritin ratio were significantly lower in CHC patients than HCV-negative controls. Following antiviral therapy, both hepcidin and hepcidin/ferritin ratio were elevated irrespective of the virologic response.

**Keywords:** Hepcidin; Ferritin ratio; Ferritin; Iron; Virologic response; Interferon.



### 1156. HIV Prevalence Among HCV Egyptian Infected Patients and Its Impact on the Result of HCV Treatment

Rabab Fouad, Olfat Shaker, Hanan Abdel Hafez, Rabab Salama, Mayssa El Raziky, Samar Marzouk, Wafaa El Akel, Marwa Abdel Ghany and Gamal Esmat

*Advances in Infectious Diseases*, 3: 71-77 (2013)

**Background and Aim of the Study:** HCV infection is the most common co-infection in HIV patients so we aimed to determine the prevalence of HIV infection in chronic HCV patients and its impact on chronic HCV patients treatment response.

**Patients and Methods:** A retrospective study performed on 1852 chronic HCV patients subjected to anti HCV treatment with alpha 2a, alpha 2b or standard interferon and Ribavirin and tested and confirmed for HIV co infection by ELISA twice. Upon HIV testing, two groups were generated, Group 1:1840 HCV patients, positive for HCV RNA, and Group 2:12 HIV positive patients and positive also for HCV. Informed consents were obtained from patients. Proper hematological biochemical investigations and other causes of hepatitis rather than HCV were carried out and excluded.

**Results:** The prevalence of HIV among HCV infected Egyptian patients was 0.64%. We found a male gender predominance; the hematological and biochemical parameters were similar in both groups with mild elevations in liver enzymes in group II. High rates of failure to treatment (77.8%) with lower SVR (22.2%) were in group II compared to group I (59.9%) as SVR was 22.1% in group II vs. 34.1% in group I, however with no statistical significance.

**Conclusion:** Despite the lower prevalence of HIV in Egyptian patients with HCV infection, it still affects their response to treatment. Therefore; we must screen HIV in all HCV patients and recommend its test to routine investigations before starting HCV therapy.

**Keywords:** HCV; HIV; Co-Infection; Response; IFN/ ribavirin.

### 1157. New Approach of Bone Marrow-Derived Mesenchymal Stem Cells and Human Amniotic Epithelial Cells Applications in Accelerating Wound Healing of Irradiated Albino Rats

Samah S. Mehanni, Noha F. Ibrahim, Alyaa R. Hassan and Laila A. Rashed.

*International Journal of Stem Cells*, 6(1) : 45-54 (2013)

**Background and Objectives:** Irradiated wound healing is a highly complex and dynamic process. The latest technology making a huge difference in this process is stem cell therapy. The goal of this study was to evaluate the use of bone marrow-derived mesenchymal stem cells (BM-MSCs) or human amniotic epithelial cells (HAECs) in the healing of irradiated wounds.

**Methods and Results:** Forty five male albino rats were subjected to whole body 6 gray gamma radiations. One day post irradiation, full-thickness incisional wound was created in the tibial skin. The rats were randomly equally divided into three groups. The incisions of the first group (*gp I*) were injected intra-dermally with saline before stitching and those of both the second (*gp II*) and the third groups (*gp III*) were intradermally injected with BM-MSCs and HAECs before stitching respectively. Animals

were sacrificed after the third, seventh and fourteenth days postoperative. The healing process was assessed histopathologically. CXCL-5, SDF-1 and Transforming growth factor-beta 1 (TGF- $\beta$ 1) expression were also detected in biopsies from all wounds. Expression of TGF- $\beta$ 1 in *gp I* was more than the other groups leading to severe inflammation, deficient healed dermis and delayed reepithelialization. SDF-1 expression was high in *gp II* while CXCL-5 expression was high in *gp III* causing accelerated wound healing. BM-MSCs showed a great effect on the quality of the dermis, while superiority of the epithelium and its appendages were achieved in HAECs group.

**Conclusions:** Using BM-MSCs and HAECs could be used safely in case of irradiated wounds.

**Keywords:** Wound healing; BM-MSCs; HAECs.

### 1158. Pivka-Ii as Early Diagnostic Marker for Hepato Cellular Carcinoma: an Egyptian Study

Olfat Shaker, Amal A. Mohamed, Hosam El Sayed, Ahmed Ebrahim, Eman Mohamed and Mohamed A. Atallah

*International Journal of Advanced Research*, 1( 9): 135-141 (2013)

Hepatocellular carcinoma (HCC) is one of the most aggressive cancers worldwide. In Egypt, the disease is detected in an advanced stage at which no treatment may be effective including surgery. Among Egyptians, viral hepatitis is the most common risk factor for HCC. Early detection of the disease is thus an important goal allowing the patient to be treated before the enlargement of the tumor or its metastasis to distant organs. Serum tumor markers may be useful in predicting the tumor at early stages. The current work aimed to determine the level of prothrombin induced by vitamin K absence-II (PIVKA-II) and Interleukin – 8 (IL-8 ) in sera of patients suffering from HCC & cirrhosis and comparing which one is more sensitive and specific for early diagnosis of HCC. The current study was carried out on 150 individuals within three groups; Normal control, Cirrhosis and HCC groups. Complete examination was carried out for each individual to confirm diagnosis. Individuals' sera were subjected to quantitative determination of alpha-fetoprotein (AFP), TNF, PIVKA-II, IL-8 and other biochemical parameters. PIVKA-II was proved to be superior to AFP, TNF and IL-8 for early detection of HCC patients being highly sensitive and specific. Using the best cut-off value of AFP (6.5), showed a sensitivity of (88 %) and specificity of (60 %) and IL-8 cut-off value ( 128.5 ), showed a sensitivity of (96 %) and specificity of (99% ), While cut-off value of PIVKA-II (9.45 ) showed (100%) sensitivity and specificity (99% ).

**Keywords:** HCC; Prothrombin Induced By Vitamin K Absence-II; Interleukin-8.

### 1159. Potential Role of Bone Marrow Derived Mesenchymal Stem Cells with or Without Injectable Calcium Phosphate Composite in Management of Osteoporosis in Rat Model

Hanaa H. Ahmed, El-Sayed M. El-Sayed Mahdy, Wafaa Gh. Shousha, Laila A. Rashed and Sara M. Abdo

*International Journal of Pharmacy and Pharmaceutical Sciences*, 5: 494-504 (2013)



**Objective:** The purpose of the present study was to evaluate the possible therapeutic role of bone marrow mesenchymal stem cells (BM-MSCs) alone or in combination with injectable calcium phosphate composite in management of osteoporosis in ovariectomized rats.

**Methods:** The MSCs were harvested from femoral bone marrow of male rats, as sex mismatched, to track the MSCs fate and to ensure their homing to the injured females' femurs. The isolated BM-MSCs proved their MSCs identity via their morphological appearance, multilineage potential and the positive expression for CD29, CD44 as well as CD106 and negative expression for CD14, CD34 and CD45. A total number of seventy adult female albino rats were used in the present study. The rats were classified as follows: group 1 was the gonad intact control, group 2 served as untreated ovariectomized (OVX) rats, while the groups from the third to seventh were OVX rats treated with, BM-MSCs, BM-MSCs with injectable bone substitute (IBS), IBS, calcitonin and calcitonin with IBS respectively. Core binding factor alpha-1 (Cbfa-1 or Runx-2) and nuclear factor kappa B (NF- $\beta$ ) gene expression levels in femur bones were detected using real time PCR. Serum osteoprotegerin (OPG) and monocyte chemoattractant protein-1 (MCP-1) were estimated using ELISA technique.

**Results:** The positive expression of Y-chromosome (sry) gene detected in the BM-MSCs treated groups indicated that the systemically delivered single dose of undifferentiated MSCs was able to home at the females' femur bones.

The expression level of Runx-2 showed down-regulation while that of NF- $\beta$  showed up-regulation in femur bones of OVX group. Additionally, serum OPG level was significantly reduced while serum level of MCP-1 was significantly elevated in OVX group as compared to gonad intact control group.

The MSCs injection with or without the biphasic calcium phosphate hydroxy-propyl-methyl-cellulose (HMPC) composite produced significant up-regulation of Runx-2 gene expression associated with significant down-regulation of NF- $\beta$  gene expression levels in femur bones. Moreover, this type of treatments produced significant increase in serum OPG level associated with significant decrease in serum MCP-1 level when compared with the untreated OVX group.

**Conclusion:** These results demonstrate the usefulness of MSCs in management of osteoporosis. Additionally, the current study spots light on a novel approach of utilizing injectable biphasic calcium phosphate composite with undifferentiated BM-MSCs as a therapeutic application for osteoporosis

**Keywords:** Osteoporosis; Ovariectomized rats; Bone marrow mesenchymal stem cells; Calcium phosphate composite.

#### 1160. Protective Effects of Pomegranate Seed Extract on Streptozotocin-Induced $\beta$ -Cell Damage in Rats : Inhibition of Pancreatic Nuclear Factor Kappa Beta, Transforming Growth Factor Beta and Matrix Metalloproteinase-2 Genes Expression

Olfat G. Shaker and Doaa A. Sourour

*International Journal of Advanced Research*, 1(10): 88-102 (2013)

**Aim of the Work:** This study evaluated the possible protective effect of pomegranate seed extract (PSE) on streptozotocin (STZ)-induced  $\beta$ -cell dysfunction in rats and its probable mechanism of action by analyzing nuclear factor kappa beta (NF-

$\beta$ ), transforming growth factor beta (TGF- $\beta$ ) and matrix metalloproteinase (MMP)-2 genes expression in the pancreas.

**Materials and Methods:** Diabetes was induced in rats by single intraperitoneal injection of STZ (50 mg/kg body weight). Rats were divided into three groups (10 each): group I: control; group II: diabetic rats and group III: diabetic rats treated with PSE (300 mg/kg/day) administered orally for 4 weeks. Pancreatic NF- $\beta$ , TGF- $\beta$  and MMP-2 expressions were determined by RT-PCR. Reduced glutathione (GSH), was also measured in the pancreas. Immunohistochemical (IHC) staining of insulin was done on pancreatic sections.

**Results:** Pancreatic expression of NF- $\beta$ , TGF- $\beta$  and MMP-2 genes were significantly decreased with significant increase in pancreatic GSH content in pomegranate treated diabetic rats compared to non-treated diabetic rats.

A significant increase in the mean area percent of insulin in pomegranate treated diabetic rats compared to non-treated diabetic rats by IHC.

**Conclusion:** PSE treatment prevented STZ-induced pancreatic  $\beta$ -cell damage and protects  $\beta$ -cells from apoptosis and destruction in diabetes mellitus induced in rats which may be related to its antioxidant effect and to the significant decrease of TGF- $\beta$  and MMP-2 genes expression in the pancreas via suppression of pancreatic NF- $\beta$  gene expression.

Thus PSE could be used as a dietary supplement in patients with diabetes mellitus.

**Keywords:** Pomegranate seed extract; Diabetes; Nf- $\beta$ ; TGF- $\beta$ ; MMP-2.

#### 1161. Role of Cell Membrane Fatty Acids in Insulin Sensitivity in Diabetic Rats Treated with Flaxseed Oil

Zakaria El-Khayat, Dina Abo El-Matty, Wafaa Rasheed, Jihan Hussein, Olfat Shaker and Jakleen Raafat

*International Journal of Pharmacy and Pharmaceutical Sciences*, 5 ( 2): 146-151 (2013)

**Introduction:** The cell functions involved in the action of insulin receptor binding enzyme and transporter activities are controlled by membrane properties, and the amount of dietary fat as well as the nature of fatty acids regulates various steps in the biosynthesis of membrane phospholipids.

**Objective:** To investigate the effect of flaxseed oil on improving erythrocyte membrane components and insulin sensitivity in diabetic rats.

**Methods:** Thirty two adult male albino rats were used in this study and classified into four groups control, flaxseed oil, diabetic and treated groups. Fasting blood glucose and plasma insulin were estimated. Total lipids in the red blood cells membrane were extracted with chloroform/ methanol method. Erythrocyte membrane total lipids, total cholesterol and triglycerides were determined. Fatty acids and phospholipids fractions were measured by HPLC.

**Results:** Flaxseed oil administration effectively improved cell membrane components.

**Conclusion:** Flaxseed oil has an important role in enhancing insulin sensitivity and decreasing blood glucose in diabetic rats.

**Keywords:** Cell membrane; Diabetes; Insulin; Fatty acids; Flaxseed oil.

### 1162. Some Biomarkers in Carbon Monoxide-Induced Cardiotoxicity

Manal M. Ismail, Hoda El-Ghamry, Olfat G. Shaker, Marwa M. Fawzi and Samah F. Ibrahim

*Journal of Environmental and Analytical Toxicology*, 3 (4): 1-7 (2013)

**Background:** Myocardial injury is a frequent consequence of carbon monoxide (CO) poisoning. Oxidative stress affection seems to be a relevant mechanism in the patho-physiology of patients with acute CO poisoning.

**Methodology:** Cardiovascular system examination and Electrocardiography (ECG) were performed for fifty CO intoxicated patients admitted to Poison Control Center, Ain Shams university Hospital for whom some oxidative stress indices have been investigated through the assessment of plasma level of malondialdehyde (MDA), superoxide dismutase (SOD) and nitric oxide (NO). Both cardiac enzymes; troponin I and beta natriuretic peptide (BNP) have been also assessed in addition to carboxyhemoglobin (COHb) levels. The investigated parameters were compared with those of 40 non-smoker healthy controls (comparable in terms of age and gender).

**Results:** ECG changes were present in 96% of patients, whereas only 4% had a normal ECG. In intoxicated patients, a statistical significant increase in plasma level of COHb level, MDA, NO, troponin I, and BNP peptide was reported compared to control individuals, while SOD enzyme was significantly decreased. BNP showed a significant positive correlation with COHb level and a negative correlation with SOD, while SOD showed a significant negative correlation with COHb level.

**Conclusions:** and recommendations: Myocardial injury occurs frequently in patients hospitalized for CO poisoning. The oxidative stress indices are significantly affected after acute CO poisoning. We suggested that such affection could be partially mediated by CO. Patients admitted to the hospital with CO poisoning should have a baseline ECG and serial cardiac biomarkers.

**Keywords:** Carbon monoxide; Cardiotoxicity; Oxidative stress.

#### Dept. of Medical BioChemistry

### 1163. Signaling Mechanisms of a Water Soluble Curcumin Derivative in Experimental Type 1 Diabetes with Cardiomyopathy

Mohamed Talaat Abdel Aziz, Ibrahim Naguib El Ibrashy, Dimitri P. Mikhailidis, Ameen Mahmoud Rezaq, Mohamed Abdel Aziz Wassef, Hanan Hassan Fouad, Hanan Hosni Ahmed, Dina A. Sabry, Heba Mohamed Shawky and Rania Elsayed Hussein

*Diabetology and Metabolic Syndrome*, 5: 1-13 (2013) IF: 1.924

**Background:** Curcumin exhibits anti-diabetic activities, induces heme-oxygenase-1 (HO-1) and is an inhibitor of transcriptional co-activator p300.

A novel water soluble curcumin derivative (NCD) has been developed to overcome low in vivo bioavailability of curcumin. We evaluated the effect of the NCD on signaling mechanisms involved in cardiomyocyte hypertrophy and studied whether its action is mediated via inducible HO-1.

**Materials and Methods:** Rats were divided into controls, controls receiving NCD, diabetic, diabetic receiving NCD,

diabetic receiving pure curcumin, diabetic receiving HO inhibitor, zinc protoporphyrin IX (ZnPP IX) and diabetic receiving NCD and ZnPP IX. NCD and curcumin were given orally. After 45 days, cardiac physiologic parameters, plasma glucose, insulin, glycated hemoglobin (GHb), HO-1 gene expression and HO activity in pancreas and cardiac tissues were assessed. Gene expression of p300, atrial natriuretic peptide (ANP) and myocyte enhancer factor 2 (MEF2A and MEF2C) were studied.

**Results:** NCD and curcumin decreased plasma glucose, GHb and increased insulin levels significantly in diabetic rats. This action may be partially mediated by induction of HO-1 gene. HO-1 gene expression and HO activity were significantly increased in diabetic heart and pancreas.

Diabetes upregulated the expression of ANP, MEF2A, MEF2C and p300. NCD and curcumin prevented diabetes-induced upregulation of these parameters and improved left ventricular function. The effect of the NCD was better than the same dose of curcumin.

**Keywords:** Curcumin; Diabetes type I; Heme-oxygenase-I; Diabetic cardiomyopathy; P300.

#### Dept. of Medical Microbiology and Immunology

### 1164. Resistant Virulent Candida Species Colonizing Preterm Neonates and in Vitro Promising Prospect of Chlorhexidine Gluconate

Iman E. Wali, Rasha H. Bassyouni, Eman Ahmed El-Seidi, Amira Edris, Abdel-Rahman Ahmed Abdel-Razek, Amina Abdel-Salam and Reem Fouad

*African Journal of Microbiology Research*, 7: 3421-3428 (2013)

The present study aimed to investigate the potential virulence factors and antifungal resistance of 31 *Candida albicans* and 21 non-*albicans* *Candida* isolates colonizing preterm neonates. The study also compared the susceptibility results with the in vitro activity of chlorhexidine in the eradication of *Candida* colonization.

*Candida albicans* produced significantly more phospholipase and coagulase than non-*albicans* *Candida*, whereas proteinase production was higher in non-*albicans* *Candida*. Biofilm production was demonstrated in *Candida albicans* and non-*albicans* *Candida* ( $P = 0.214$ ). None of the planktonic growth of *Candida* isolates were resistant to either fluconazole or amphotericin B, whereas 40% and 84% *Candida* isolates grown as biofilm became resistant to fluconazole and amphotericin B, respectively.

Both coagulase and phospholipase production strongly correlated with the resistance of sessile *Candida* isolates to amphotericin B ( $P < 0.001$ ). Whereas both proteinase and phospholipase correlated with the resistance of in vitro *Candida* biofilms to fluconazole ( $P < 0.05$  and  $P = 0.001$ ; respectively). Chlorhexidine was comparable to fluconazole towards planktonic and sessile grown *Candida* isolates. In conclusion, the study demonstrated an association between certain virulence factors and the development of biofilm drug resistance and highlighted the value of chlorhexidine as a promising prospect in the eradication of *Candida* colonization.

**Keywords:** Antifungal susceptibility; Biofilm resistance; *Candida* colonization; Chlorhexidine; Preterm neonates; Virulence factors.

**Dept. of Medical Oncology**

**1165. Effect of Mesenchymal Stem Cells and A Novel Curcumin Derivative on Notch1 Signaling in Hepatoma Cell Line**

Mohamed Talaat Abdel Aziz, Hussien Mostafa Khaled, Ali El Hindawi, Nagwa Kamal Roshdy, Laila A. Rashed, Dina Sabry, Amira A. Hassouna, Fatma Taha and Walaa Ibrahim Ali

*Biomed Research International*, (2013)

This study was conducted to evaluate the effect of mesenchymal stem cells (MSCs) and a novel curcumin derivative (NCD) on HepG2 cells (hepatoma cell line) and to investigate their effect on Notch1 signaling pathway target genes. HepG2 cells were divided into HepG2 control group, HepG2 cells treated with MSC conditioned medium (MSCs CM), HepG2 cells treated with a NCD, HepG2 cells treated with MSCs CM and NCD, and HepG2 cells treated with MSCs CM (CM of MSCs pretreated with a NCD). Expression of Notch1, Hes1, VEGF, and cyclin D1 was assessed by real-time, reverse transcription-polymerase chain reaction (RT-PCR) in HepG2 cells. In addition, HepG2 proliferation assay was performed in all groups. Notch1 and its target genes (Hes1 and cyclin D1) were downregulated in all treated groups with more suppressive effect in the groups treated with both MSCs and NCD. Also, treated HepG2 cells showed significant decrease in cell proliferation rate. These data suggest that modulation of Notch1 signaling pathway by MSCs and/or NCD can be considered as a therapeutic target in HCC.

**Dept. of Microbiology**

**1166. Co-Existence of Aminoglycoside Modifying Enzymes (AMEs) Genes and Meca Gene Among Nosocomial Isolates of Staphylococcus Aureus in Surgical Intensive Care Units in Kasr Al-Ainy Hospitals, Cairo University**

Ashraf E. Sorour, Basma A. El-Awady and Mukhtar AM

*The International Arabic Journal of Antimicrobial Agents*, 3 (4): 1-8 (2013):

**Background:** In Staphylococcus aureus aminoglycosides and methicillin resistances are closely associated. We aimed at detection of the prevalence of methicillin and aminoglycosides resistances in S. aureus isolated from surgical ICUs in Kasr Al-Ainy hospitals, the association of mecA gene and aminoglycoside modifying enzymes (AMEs) genes among these isolates and the accuracy of cefoxitin disc diffusion method in relation to PCR. 150 clinical samples were collected. Cultivation and identification of isolates were done by the standard microbiological techniques. All S. aureus isolates were tested for methicillin and aminoglycosides resistance by disc diffusion method and for presence of mecA gene and AMEs genes by multiplex-PCR. 48 S. aureus were isolated (32%) with a high prevalence of mecA gene (89.58%) and AME genes (60.42%) and co-existence of mecA gene and one or more of AME genes in 60%. mecA gene was detected in 87% of cefoxitin resistant isolates and aac(6)-Ie+aph(2'') was the most predominant AME genes.

**Keywords:** S. Aureus; MecA gene; Aminoglycoside modifying enzymes genes; PCR.

**Dept. of NeuroSurgery**

**1167. Value of 3- Dimensional High – Resolution Magnetic Resonance Imaging in Detecting the Offending Vessel in Hemifacial Spasm: Comparison with Intraoperative High Definition Endoscopic Visualization**

Ehab El Refaee, Soenke Langner, Joerg Baldauf, Marc Matthes, Michael Kirsch and Henry W.S. Schroeder

*Neurosurgery*, 73: 58-67 (2013) IF: 2.532

**Background:** High- resolution 3- dimensional (3-D) magnetic resonance imaging (MRI) is widely used to predict the neurovascular anatomy within the cerebellopontine angle. **Objective:** To assess the value of 3-D steady-state free precession imaging (SSFP) and time-of-flight magnetic resonance angiography (TOF MRA) in detecting the offending vessels in hemifacial spasm in comparison to intraoperative endoscopic visualization.

**Methods:** 42 patients underwent endoscope- assisted microvascular decompression (MVD). All available preoperative 3-D SSFP and TOF MRA images were checked. Intra- operative videos were captured by a high-definition endoscopic camera attached to endoscopes while exploring the area of facial nerve root exit zone (REZ). Evaluation of the 3-D images was performed by 2 independent groups of observers and compared with the operative findings. **RESULTS:** Three- D MRI had an average positive predictive value (PPV) of 89.1% in differentiating between simple and complex compression. Mean accuracy of the images in detection of the offending vessels was 83.3% and 77% according to the first and second groups of observers, respectively. Averaged inter-observer agreement between the 2 groups of observers was substantial, with an averaged Kappa coefficient (K) of 0.56. in the simple compression group, mean accuracy was 97% and 89.4% according to the first and second groups of observers, respectively. Averaged K for agreement was substantial (K = 0.65).

**Conclusion:** According to endoscopic visualization, 3-D SSFP and TOF MRA images are accurate in detecting the offending vessels in simple compression of the facial nerve, and in predicting presence of a complex compression with variable sensitivity in identifying all offending vessels.

**Keywords:** Hemifacial spasm; Endoscope assisted; Microvascular decompression; High resolution MRI.

**1168. Endoscopic Cyst Fenestration in the Treatment of Uniloculated Hydrocephalus in Children.**

Nasser M. F. El-Ghandour

*J. Neurosurg Pediatr.*, 11(4): 402-409 (2013) IF: 1.628

The treatment of uniloculated hydrocephalus is a difficult problem in pediatric neurosurgery. Definitive treatment is surgical, yet the approach remains controversial. This study evaluates the role of endoscopic cyst fenestration (ECF) in the management of this disease.

**Methods:** Thirty-one pediatric patients with uniloculated hydrocephalus who underwent endoscopic surgery, performed by the author, between May 1999 and December 2010 constitute the patient group for this study. The patients included 17 boys and 14

girls, with ages ranging from 5 months to 5 years (mean 22.9 months). Patients with multiloculated hydrocephalus were not included. The patients' charts were reviewed for demographic data, radiological findings, information regarding morbidity, improvement of hydrocephalus, incidence of recurrence, shunt dependency, and the need for shunt revision.

**Results:** Neuroepithelial cysts were the most common cause (17 cases), followed by postoperative gliosis due to previous shunt infection (9 cases), intraventricular hemorrhage (3 cases), and meningitis (2 cases). Multiplanar MRI was reliable in making the diagnosis and is indicated if CT shows disproportionate hydrocephalus. Surgical treatment included ECF (31 cases), endoscopic revision of malfunctioning preexisting shunts (9 cases), endoscopic third ventriculostomy (4 cases), and placement of a new shunt (3 cases). Endoscopic cyst fenestration was easily performed in all the cases, with devascularization of the cyst wall by coagulation to prevent recurrence. Improvement of hydrocephalus was observed in 26 cases (83.9%). Among the group of patients without prior shunts (22 cases), 3 patients (13.6%) required repeat ECF and 3 patients (13.6%) required placement of a shunt (new shunt placement). In the 9 patients with preexisting shunts, endoscopy reduced the mean rate of shunt revision from 2.7 revisions per year before fenestration to 0.25 per year after fenestration. Four of these 9 patients had multiple shunts, which could be converted to a single shunt; however, repeat ECF was necessary in all 9 patients. With a mean follow-up duration of 4.3 years, none of the patients with a prior shunt was able to become shunt-independent, whereas 86.4% of patients without a prior shunt were able to avoid shunt placement. Endoscopic complications were reversible (unilateral subdural effusion in 5 cases, minor arterial bleeding in 2 cases, CSF leakage in 1 case), and there was no death (0%).

**Conclusions:** Endoscopic cyst fenestration is recommended in the treatment of uniloculated hydrocephalus because it is effective, simple, minimally invasive, and associated with low morbidity and mortality rates. The fact that all previously shunt-treated patients needed repeat ECF and that none of these patients was able to become shunt-independent makes it clear that uniloculated hydrocephalus due to postoperative gliosis induced by previous shunt infection carries the worst prognosis

**Keywords:** Endoscopy; Fenestration; Uniloculated Hydrocephalus.

### 1169. Endoscopic Treatment of Quadrigeminal Arachnoid Cysts in Children

Nasser M. F. El-Ghandour

*J. Neurosurg-Pediatr*, 12(5): 521-528 (2013) IF: 1.628

**Object:** Quadrigeminal arachnoid cysts (QACs) are rare, comprising approximately 5%-10% of all intracranial arachnoid cysts. The management of these cysts is challenging, and their optimal surgical treatment is controversial. This study evaluates the role of endoscopy in the treatment of QACs in children, focusing on some factors or technical aspects that might influence the outcome.

**Methods:** Eighteen children with symptomatic QACs were the subject of this study. The group included 10 boys and 8 girls, with a mean age of 2.5 years. All patients had hydrocephalus. Surgical treatment included ventriculocystostomy (14 cases), endoscopic third ventriculostomy (14 cases), ventriculocystocisternostomy (2 cases), cystocisternostomy (2 cases), and removal of preexisting malfunctioning cystoperitoneal shunt (4 cases).

**Results:** Significant clinical improvement occurred in 15 cases (83.3%). Postoperative MRI showed a reduction in the cyst size in 14 cases (77.8%), whereas in the remaining 4 cases (22.2%) the cyst size was unchanged. A postoperative decrease in ventricular size was encountered in 16 cases (88.9%). Minor intraoperative bleeding occurred in 1 case (5.6%), which stopped spontaneously without any postoperative sequelae. Postoperative subdural hygroma occurred in 3 cases (16.7%) and required a subduroperitoneal shunt in 2 cases. During follow-up (mean 45.8 months), a repeat endoscopic procedure was performed in 7 patients (all 4 patients with a prior shunt and 3 patients without a prior shunt), and new shunt placement was required in 5 patients (all 4 patients with a prior shunt and 1 patient without a prior shunt). Thus, none of the patients with a prior shunt was able to become shunt independent, whereas 92.9% of patients without a prior shunt were able to avoid shunt placement.

**Conclusions:** Arachnoid cysts of the quadrigeminal cistern and the associated hydrocephalus can be effectively treated by endoscopy. The procedure is simple, minimally invasive, and associated with low morbidity and mortality rates. The fact that all patients who previously received shunts required a repeat endoscopic procedure and that none of these patients was able to become shunt independent makes it clear that endoscopic treatment should be considered the first choice in the management of patients with arachnoid cysts in the quadrigeminal cistern.

**Keywords:** Quadrigeminal Arachnoid cyst; Endoscopy technique; Endoscopic third ventriculostomy; Ventriculocystectomy; Ventriculocystocisternostomy; Cystocisternostomy.

### 1170. The Benefits of Navigated Intraoperative Ultrasonography During Resection of Fourth Ventricular Tumors in Children

Mohamed A. El Beltagy and Mostafa M. E. Atteya

*Child's Nervous System*, 29 (7): 1079-1088 (2013) IF: 1.241

**Background:** Safe and radical excision of pediatric fourth ventricular tumors is by far the best line of management. Pediatric fourth ventricular tumor surgery is a challenge for neurosurgeons. The aim of the study is to present the authors' experience and to evaluate the possible benefits of neuro-navigated intraoperative ultrasonography (NIOUS) during the surgery of fourth ventricular tumors in children.

**Methods:** Nonrandomized clinical trial study was conducted on 60 children with fourth ventricular tumors who were treated at Children's Cancer Hospital-Egypt. Mean age was 5.2 ( $\pm 2.6$ ) years. Thirty cases were operated upon utilizing the conventional microneurosurgical techniques. Another 30 cases were operated upon utilizing the NIOUS technique.

**Results:** Total tumor excision was achieved in 29 cases (96.7 %) of NIOUS group versus 24 cases (80 %) in the conventional group. Mean operative time NIOUS group was 150 min [standard deviation (SD)= $\pm 18.28$ ] versus 140.6 min (SD= $\pm 18.6$ ) in the conventional group (p value= $\pm 0.055$ ). The mean operative blood loss was 67.5 ml (SD= $\pm 17$ ) in NIOUS group versus 71 ml (SD= $\pm 15.4$ ) in the conventional group. Postoperative cerebellar mutism occurred in one case (3.3 %) of NIOUS group versus in six cases (20 %) of the conventional group.

**Keywords:** Nious.

### 1171. Is it Safe to Sacrifice the superior hypophyseal Artery in Aneurysm Clipping? A Report of Two Cases

Ehab Ahmed El Refaee, Jörg Baldauf Valentin Balau, Christian Rosenstenge and Henry Schroeder

*Central European Neurosurgery Journal of Neurological Surgery- A, 74: 255-260 (2013)*

Clipping of paraclinoid internal carotid artery aneurysms related to the superior hypophyseal artery (SHA) carries risk of occlusion of this artery when originating distal to the neck of the aneurysm. Sometimes it is inevitable to sacrifice the artery to achieve total aneurysm occlusion. Otherwise a residual aneurysm would remain, which may lead to aneurysm regrowth and subsequent rupture. However, consequences of SHA sacrifice are rarely reported in the literature. In the two presented cases, the SHA was found originating distal to the neck and within the wall of the aneurysm, making the optimal clipping of the aneurysm at the neck unfeasible without trapping of the SHA. Intraoperative indocyanine green (ICG) angiography revealed a retrograde blood flow in the SHA distal to the clip in both patients, indicating some collateral circulation. No endocrinologic deficits were encountered after surgery. The vision was not affected in one patient. In the other patient, bilateral visual field defects occurred, which improved partially in the follow-up 2 months after surgery. The consequences of SHA occlusion are difficult to predict. A large variety of anatomical variations of the vascular anatomy exists. Intraoperative ICG angiography may help to estimate collateral blood flow but is not able to predict visual decline. Although no conclusions cannot be drawn from two patients, it seems that in case of multiplicity of superior hypophyseal complex, sacrifice of one even larger branch is safe. However, visual sequelae have to be taken into consideration when a single SHA has to be sacrificed for total aneurysm clipping.

**Keywords:** Superior hypophyseal; Artery aneurysm; Superior hypophyseal; Artery Sacrifice; Aneurysm clipping; Collateral blood.

### Dept. of Obstetrics and Gynecology

### 1172. Embryo Culture Media and IVF/ICSI Success Rates: A Systematic Review

E. Mantikou, M.A.F.M. Youssef, M. Van Wely, F. Van der Veen, H.G. Al-Inany, S. Repping and S. Mastenbroek

*Human Reproduction Update, 19 (3): 210-220 (2013) IF: 8.847*

**Background:** The media that are used to culture human preimplantation embryos are considered to be an important factor for the success rates of IVF/ICSI. Here, we present a systematic review of randomized controlled trials (RCTs) on the effect of culture media on IVF/ICSI success rates. **Methods:** RCTs published between January 1985 and July 2012 were eligible for inclusion. The primary outcome was live birth. Secondary outcomes were health of babies born, ongoing pregnancies, clinical pregnancies, miscarriages, multiple pregnancies, implantation rate, cryopreservation rate, embryo quality and fertilization rate. For those media that were evaluated in more than one comparison, an unconventional meta-analysis was performed by pooling the data of the media they were compared to.

**Results:** Twenty-two RCTs were included that evaluated 31 different comparisons. Conventional meta-analysis was not possible for any of the outcomes as nearly all trials compared different culture media. Only four trials reported on live birth, and one of them reported a significant difference. Nine trials reported on ongoing and/or clinical pregnancy rates, of which four showed a significant difference. Pooling the data did not reveal a superior culture medium.

**Conclusions:** It is yet unknown what culture medium leads to the best success rates in IVF/ICSI. Given the potential importance of culture media for treatment outcome, rigorously designed RCTs are needed for currently available, as well as newly introduced culture media.

**Keywords:** Culture medium; IVF; ICSI; Live birth; Randomized Controlled trial; Meta; Analysis.

### 1173. Levonorgestrel-Releasing Intrauterine Device (LNG-IUD) for Symptomatic Endometriosis Following Surgery

Ahmed M. Abou-Setta, Brett Houston, Hesham G Al-Inany and Cindy Farquhar

*Cochrane Database Syst Rev., 13: 1-36 (2013) IF: 5.785*

**Background:** Various options exist for treating endometriosis, including surgical, medical, such as ovarian suppression, or a combination of these strategies. Surgical treatment of endometriosis aims to remove visible areas of endometriosis. The aim of medical therapy is to inhibit growth of endometriotic implants by induction of a hypo-estrogenic state. Treatment with a hormone-releasing intrauterine device, using levonorgestrel (LNG-IUD), has also been suggested. **OBJECTIVES:** To determine whether postoperative LNG-IUD insertion in women with endometriosis improves pain and reduces recurrence of symptoms compared with no postoperative treatment, postoperative insertion of a placebo, or postoperative therapy. **Search Methods:** The following databases were searched from inception to June 2012: Cochrane Menstrual Disorders and Subfertility Group Specialised Register of controlled trials, Cochrane Central Register of Controlled Trials (CENTRAL), MEDLINE, PsycINFO, CINAHL, and the World Health Organization (WHO) International Clinical Trials Registry Platform. EMBASE was searched from 2010 to June 2012. The citation lists of relevant publications, review articles, abstracts of scientific meetings, and included studies were also searched.

**Selection Criteria:** Trials were included if they compared women undergoing surgical treatment for endometriosis with uterine preservation and then randomised within three months to LNG-IUD insertion versus no postoperative treatment, placebo (inert IUD), or other treatment. Diagnostic laparoscopy alone was not considered suitable treatment.

**Data Collection and Analysis:** Two review authors independently selected studies for inclusion and extracted data to allow for an intention-to-treat analysis. For dichotomous data, the risk ratio (RR) and 95% confidence interval (CI) were calculated using the Mantel-Haenszel random-effects method. For continuous data, the mean difference (MD) and 95% CI were calculated using the inverse variance random-effects method.

**Main Results:** Three randomised controlled trials were included. In two trials, there was a statistically significant reduction in the recurrence of painful periods in the LNG-IUD group compared with expectant management (RR 0.22, 95% CI 0.08 to 0.60, 95



women,  $I(2) = 0\%$ , moderate strength of evidence). The proportion of women who were satisfied with their treatment was also higher in the LNG-IUD group but did not reach statistical significance (RR 1.21, 95% CI 0.80 to 1.82, 95 women,  $I(2) = 0\%$ ).

The number of women reporting a change in menstruation was significantly higher in the LNG-IUD group (RR 37.80, 95% CI 5.40 to 264.60, 95 women,  $I(2) = 0\%$ ) but the number of women not completing the allocated treatment did not differ between groups (RR 0.66, 95% CI 0.08 to 5.25,  $I(2) = 43\%$ ). In one trial, women receiving LNG-IUD noted lower pain scores compared with women receiving gonadotrophin-releasing hormone agonists (MD-0.16, 95% CI -2.02 to 1.70, 40 women) but this did not reach statistical significance. **AUTHORS'**

**Conclusions:** There is limited but consistent evidence showing that postoperative LNG-IUD use reduces the recurrence of painful periods in women with endometriosis. Further well-designed RCTs are needed to confirm these findings.

**Keywords:** Endometriosis; Levenorgestrel; Pain.

#### 1174. Three-Dimensional Power Doppler Study of Endometrial and Subendometrial Microvascularization in Women with Intrauterine Device-Induced Menorrhagia

Akmal El-Mazny, Nermeen Abou-Salem and Hossam ElShenoufy

*Fertility and Sterility*, 99 (7): 1912-1915 (2013) IF: 4.174

**Objective:** To evaluate endometrial and subendometrial microvascularization, using three-dimensional (3D) power Doppler ultrasound, in women with intrauterine device (IUD)-induced menorrhagia; and whether those potential findings could predict the risk of bleeding before IUD insertion.

**Design:** Prospective clinical trial.

**Setting:** University teaching hospital.

**Patient(S):** One hundred twenty women, who requested the insertion of a copper IUD for contraception.

**Intervention(S):** Endometrial thickness and volume, uterine artery pulsatility index and resistance index, and endometrial and subendometrial 3D power Doppler vascularization index, flow index, and vascularization flow index were measured twice: immediately before and 3 months after IUD insertion.

**Main Outcome Measure(S):** Doppler indices before and after IUD insertion.

**Result(S):** Before IUD insertion, no significant difference was detected in the clinical characteristics, endometrial thickness and volume, and Doppler indices between women who had IUD-induced menorrhagia ( $n = 47$ ) and those without menorrhagia ( $n = 73$ ). However, after IUD insertion, there was a significant increase in the endometrial and subendometrial vascularization index, flow index, and vascularization flow index in women with menorrhagia, whereas other parameters remained not significantly different between the two groups.

**Conclusion(S):** Endometrial and subendometrial microvascularization increases in women with IUD-induced menorrhagia; however, this finding has no predictive value before IUD insertion.

**Keywords:** 3D Power doppler; Endometrial and subendometrial Vascularity; Intrauterine device; Menorrhagia.

#### 1175. Comfort, Ease of Use and Practicality of the Pen Injector for Follitropin $\alpha$ for Assisted Reproduction: an Observational Post-Marketing Study in Egypt

Mohamed Yehia, Waleed El-Khayat, Ashraf Kortam, Aly Hossam Mowafy, Amr A. Aziz Khalifa, Azza Awad and Sherif Khattab

*Current Medical Research and Opinion*, 29: 1429-1434 (2013) IF: 2.263

**Objective:** We evaluated the ease of use of a pen injector for follitropin  $\alpha$  (recombinant human follicle-stimulating hormone [r-hFSH]) during assisted reproduction technologies (ARTs) in Egypt.

**Methods:** One hundred women undergoing ART completed a questionnaire in a non-interventional, observational study. The primary endpoint was patients' rating of the comfort associated with the injector. The main limitations of the study were the design and lack of knowledge regarding any impact of failure of ART on perceptions of treatment for a minority of patients.

**Results:** Patients rated the follitropin  $\alpha$  pen injector as 'very comfortable' (61%), 'comfortable' (29%), or 'somewhat comfortable' (10%). Understanding instructions and using it were 'very easy' or 'easy' for 97–99%; 94% reported 'no' or 'minimal' difficulty with injections, 83% were 'very confident' about altering doses, 77% reported no interference with normal daily activities and 94% reported 'no' or 'minimal' stress using the device. Women with previous experience of ART rated the device as more practical than their previous injection system. Overall, 96% were 'very satisfied' or 'satisfied' with the device and 99% would recommend its use to others. Pregnancy rates were consistent with previous clinical experience. Injection site reactions occurred in 10% (all of mild severity except one moderate event).

**Conclusions:** Positive perceptions of the follitropin  $\alpha$  pen injector identify this device as suitable for use for Middle Eastern women undergoing ART.

**Keywords:** Assisted reproduction Technologies; Follitropin  $\alpha$ ; Patient-reported outcomes; Recombinant human follicle; Stimulating hormone.

#### 1176. Doppler Study of Uterine Hemodynamics in Women with Unexplained Infertility

Akmal El-Mazny, Nermeen Abou-Salem and Hossam ElShenoufy

*European Journal of Obstetrics and Gynecology and Reproductive Biology*, 171(1): 84-87 (2013) IF: 1.843

**Objective:** To evaluate uterine artery blood flow using pulsed Doppler, and endometrial and sub endometrial microvascularization using three-dimensional (3D) power Doppler, in women with unexplained infertility.

**Study Design:** In a prospective clinical trial at a university teaching hospital, 40 women with unexplained infertility were compared to 40 fertile parous controls. In the mid-luteal (peri-implantation) phase, the endometrial thickness and volume, uterine artery pulsatility index (PI) and resistance index (RI), endometrial and subendometrial 3D power Doppler vascularization index (VI), flow index (FI), and vascularization

flow index (VFI), and serum estradiol and progesterone levels were measured in both groups.

**Results:** The uterine artery PI ( $P = 0.003$ ) and RI ( $P = 0.007$ ) were significantly increased and the endometrial VI ( $P = 0.029$ ), FI ( $P = 0.031$ ), and VFI ( $P = 0.001$ ) and subendometrial VI ( $P = 0.032$ ), FI ( $P = 0.040$ ), and VFI ( $P = 0.005$ ) were significantly decreased in the unexplained infertility group. The endometrial thickness and volume and serum estradiol and progesterone levels, however, were not significantly different between the two groups.

**Conclusion:** Peri-implantation endometrial perfusion is impaired in women with unexplained infertility: Doppler study of uterine hemodynamics should therefore be considered in infertility work up.

**Keywords:** 3D Ultrasonography; Doppler; Endometrial perfusion.

### 1177. Role of Fetal Echocardiography in the Evaluation of Structure and Function of Fetal Heart in Diabetic Pregnancies

Usama M. Fouda, Mohamed M. Abou ElKassem, Shamel M. Hefny, Ragai M. Fouda and Ahmed T. Hashem

*J. Matern Fetal Neonatal Med.*, 26 (6): 571-575 (2013) IF: 1.518

**Objective:** To detect the structural and functional changes of fetal hearts in diabetic pregnancies by using Doppler echocardiography.

**Methods:** This prospective study included 119 pregnant women divided into three groups. Group 1 included 47 pregnant patients with pre-existing diabetes mellitus (DM), group 2 included 40 patients with gestational diabetes and group 3 included 32 non-diabetic pregnant women. M-mode echocardiography was used to measure the thickness of the fetal ventricular walls and interventricular septum. The mitral and tricuspid early (E) and late (A) diastolic velocities and the ventricular shortening fraction were measured.

**Results:** HbA1c % was significantly lower in gestational diabetes group compared with the pre-existing diabetes group. The interventricular septum was significantly thicker in the pre-existing diabetes group compared with other groups. Tricuspid and mitral E/A ratios were significantly lower in the pre-existing diabetes group compared with gestational diabetes and control groups. Moreover, there were no significant differences in the tricuspid and mitral E/A ratios between gestational diabetes group and the control group. The right and left ventricular shortening fractions were similar in the three groups.

**Conclusion:** Fetuses of women with well-controlled gestational diabetes lack the diastolic dysfunction that is present in fetuses of women with pre-existing diabetes.

**Keywords:** Gestational diabetes; Diabetes mellitus; Fetal echocardiography; Cardiomyopathy; Diastolic dysfunction.

### 1178. Three Decades After Gjönnæss's Laparoscopic Ovarian Drilling for Treatment of PCOS; What Do We Know? an Evidence-Based Approach

Hatem Abu Hashim, Hesham Al-Inany Michel De Vos and Herman Tournaye

*Arch Gynecol Obstet.*, 288: 409-422. (2013) IF: 1.33

**Background:** The introduction of laparoscopic ovarian drilling (LOD) by Gjönnæss in 1984 as a substitute for ovarian wedge resection created opportunities for extensive research given its worldwide application for ovulation induction in women with polycystic ovary syndrome (PCOS).

**Purpose:** To critically evaluate and summarize the current body of literature regarding the role of LOD for the management of PCOS entailing its different preoperative, operative and postoperative aspects. In addition, long-term efficacy, cost-effectiveness, patient preference and health-related quality of life issues will be evaluated together with other available alternatives of ovulation induction treatments.

**Methods:** A PubMed search was conducted looking for the different trials, reviews and various guidelines relating to the role of LOD in the management of PCOS.

**Results:** LOD whether unilateral or bilateral is a beneficial second-line treatment in infertile women with clomiphene citrate (CC)-resistant PCOS. It is as effective as gonadotrophin treatment but without the risk of multiple pregnancy or ovarian hyperstimulation and does not require intensive monitoring. Increased responsiveness of the ovary to CC especially in patients who remain anovulatory following LOD is another advantage. Recent evidence suggests that relatively novel oral methods of ovulation induction, e.g. CC plus metformin, CC plus tamoxifen, rosiglitazone plus CC and aromatase inhibitors represent a successful alternative to LOD in CC-resistant PCOS. Meanwhile current evidence does not support LOD as a first-line approach in PCOS-related anovulation or before IVF.

**Conclusion:** LOD is currently recommended as a successful and economical second-line treatment for ovulation induction in women with CC-resistant PCOS.

**Keywords:** Laparoscopic surgery; Polycystic ovary syndrome; Laparoscopic Ovarian drilling; Laparoscopic ovarian diathermy.

### 1179. Anti-Müllerian Hormone and Antral Follicle Count For Prediction of Ovarian Stimulation Response in Polycystic Ovary Syndrome

Akmal Nabil El-Mazny and Nermeen Abou-Salem

*Gynecological Endocrinology*, 29(9): 826-829 (2013) IF: 1.303

**Objective:** To evaluate the ability of a combination of multiple ovarian reserve markers to predict ovarian stimulation response in polycystic ovary syndrome (PCOS).

**Methods:** On cycle Day 3 of 75 infertile patients with PCOS, serum follicle stimulating hormone (FSH), luteinizing hormone (LH), and anti-Müllerian hormone (AMH) were measured, and antral follicle count (AFC) and ovarian volume (OV) were evaluated by transvaginal sonography (TVS). All patients underwent the same mild ovarian stimulation protocol using clomiphene citrate and highly purified FSH. Ovulation was monitored by TVS and confirmed by midluteal serum progesterone level.

**Results:** AMH, AFC, and "ovulation index" [OI, serum AMH (ng/ml)  $\times$  bilateral AFC] were significantly lower in the ovulatory group ( $n = 57$ , 76%) compared with the anovulatory group, whereas LH, FSH, LH/FSH ratio, and OV were not significantly different. Using receiver-operating characteristic curve analysis, the OI at a cutoff value of "85" had a sensitivity of 73.7% and a specificity of 72.2% in the prediction of ovulation, with an area under the curve of 0.733. Patients with OI  $< 85$  had significantly higher ovulation rate ( $p < 0.001$ ).

**Conclusion:** The OI, combining both AMH and AFC, is a potentially useful predictor of the outcome of ovarian stimulation in PCOS.

**Keywords:** Anti- müllerian hormone; Antral follicle count; Ovarian reserve; Ovulation index; Polycystic ovary syndrome.

### 1180. Endothelial Nitric Oxide Synthase (eNOS) (Glu298Asp) and Urotensin II (UTS2S89N) Gene Polymorphisms in Preeclampsia: Prediction and Correlation with Severity in Egyptian Females

Walid S. El-Sherbiny, Ahmed S. Nasr and Aml Soliman

*Hypertension in Pregnancy*, 32(3): 292-303 (2013) IF: 0.928

**Background:** Preeclampsia is a leading cause of maternal and fetal/ neonatal morbidity and mortality. Early prediction of preeclampsia can minimize maternal and fetal complications. Gene polymorphisms are promising markers for early prediction of preeclampsia.

**Aim of work:** To assess the value of endothelial nitric oxide synthase (eNOS) (Glu298Asp) and urotensin II (UTS2 S89N) gene polymorphisms for early prediction of preeclampsia.

**Methods:** The preeclamptic group consisted of 53 pregnant who developed preeclampsia (35 mild and 18 severe), while the control group consisted of 65 age-matched pregnant females who completed uncomplicated pregnancies. eNOS and urotensin II gene polymorphisms were tested using polymerase chain reaction– restriction fragment length polymorphism (PCR–RFLP).

**Results:** Concerning the eNOS gene polymorphism, there were highly significant differences between the two groups regarding the GG genotype as well as the G and T allele frequency (p50.001) and a statistically significant differences regarding the GT, TT genotypes (p ¼ 0.002, 0.0276, respectively). Concerning the urotensin II gene polymorphisms, there were highly significant differences regarding the SS, SN genotypes as well as the S and N allele frequency (p50.001), statistically significant differences regarding the NN genotype (p ¼ 0.063).

**Conclusion:** Women having mutation in any of the two studied genes are at risk to develop mild preeclampsia, and those having mutations in both genes are at risk to develop severe preeclampsia, while the females with normal pregnancy are protected by the higher percentage of expression of the normal (wild alleles) of both genes.

**Keywords:** eNOS; Gene polymorphisms; Preeclampsia; Urotensin II.

### 1181. A Randomised Controlled Trial of Sublingual Misoprostol and Intramuscular Oxytocin for Prevention of Postpartum Haemorrhage

A. Al-Sawaf, A. El-Mazny and A. Shohayeb

*Journal of Obstetrics and Gynaecology*, 33(3): 277-279 (2013) IF: 0.546

This study aims to evaluate the efficacy and side-effects of 200 µg sublingual misoprostol vs 5 IU i.m. oxytocin, administered immediately following cord clamping in normal non-augmented vaginal delivery, in prevention of postpartum haemorrhage (PPH).

A total of 104 women were randomised into three groups: misoprostol group (28 patients); oxytocin group (37 patients) and control group (39 patients). Misoprostol and oxytocin significantly minimised the blood loss during the third stage of labour and reduced the need for additional treatments for PPH as compared with the control group.

Oxytocin was more effective than misoprostol in minimising blood loss and the need for additional uterotonic treatments. However, a significant decrease in systolic and diastolic blood pressure, associated with tachycardia was observed in the oxytocin group. In conclusion, sublingual misoprostol appears to be less effective than i.m. oxytocin in the prevention of PPH; however, it has the potential advantages of being easily used, cost-effective and stable at room temperature. Therefore, sublingual misoprostol is still a feasible drug for routine management of third stage, especially in areas with limited medical facilities.

**Keywords:** Misoprostol; Oxytocin; Postpartum haemorrhage; Vaginal delivery.

### 1182. Role of Middle Cerebral Artery, Umbilical Artery Resistance Indices and Middle Cerebral Artery to Umbilical Artery Resistance Index Ratio in Predicting Unfavorable Perinatal Outcomes of Normotensive and Hypertensive Diabetic Pregnancies

Usama M. Fouda, Mohamed M. Abou ElKassem, Shamel M. Hefny and Ahmed T. Hashem

*Life Science Journal*, 10 (3): 2371-2377 (2013) IF: 0.165

**Objective:** To evaluate the role of middle cerebral artery (MCA), umbilical artery (UA) resistance indices (RI) and middle cerebral artery/ umbilical artery resistance index ratio (MCA/UA RI) in predicting unfavorable perinatal outcomes in pregnancies complicated with diabetes mellitus.

**Methods:** This prospective study included 96 women divided into 4 groups. Group 1 included 23 pregnant patients with preexisting diabetes, group 2 included 22 patients with gestational diabetes, group 3 included 24 diabetic pregnancies associated with hypertension and group 4 was a control group which included 27 patients with uncomplicated pregnancies. The umbilical artery and middle cerebral artery resistance indices were measured weekly starting from the 34th till the 38th week of pregnancy.

**Results:** Abnormal UA RI (= 95th centile) had 78.57% sensitivity in detecting adverse perinatal outcomes in group 3 compared with 16.67 % and 0% sensitivity in group 1 and group 2 respectively. Abnormal MCA RI (= 5th centile) had 50% sensitivity in detecting adverse perinatal outcomes in group 3 compared with 0% sensitivity in groups 1 and 2. Abnormal MCA/UA RI (< 1) had 71.43 % sensitivity in detecting adverse perinatal outcomes in group 3 compared with 0 % sensitivity in groups 1 and 2.

**Conclusion:** The abnormal UA RI, MCA RI and MCA/UA RI may be useful parameters in predicting adverse perinatal outcomes in diabetic pregnancies associated with hypertension. On the other hand, there were weak correlations between abnormal UA RI, MCA RI, MCA/UA RI and adverse perinatal outcomes of diabetic pregnancies not associated with hypertension.

Therefore the results of the UA RI, MCA RI and MCA/UA RI should be interpreted with caution in the management of diabetic pregnancies, especially those not associated with hypertension, as

adverse perinatal outcomes frequently occur in patients with normal Doppler indices. [Usama M. Fouda, Mohamed M. Abou ElKassem, Shamel M. Hefny and Ahmed T. Hashem. Role of middle cerebral artery, umbilical artery resistance indices and middle cerebral artery to umbilical artery resistance index ratio in predicting unfavorable perinatal outcomes of normotensive and hypertensive diabetic pregnancies.

**Keywords:** Diabetes mellitus; Hypertension; Doppler ultrasound; Resistance index; Pregnancy.

### 1183. Is Evidence Based Medicine (EBM) Applicable in Our Real Life

Mohamed A. F. M. Youssef

*Middle East Fertility Society Journal, 18: 217-219 (2013)*

Applying evidence based medicine (EBM) in our daily practice and health settings is a great challenge for residents due to the lack of time and experience. The following case scenario is an example of real life application of EBM.

**Keywords:** EBM; Clinical scenarios.

### 1184. Obstructed Hemivagina and Ipsilateral Renal Anomaly Syndrome with Uterus Didelphys (OHVIRA)

Mohamed A. F. M. Youssef

*Middle East Fertility Society Journal, 18: 58-63 (2013)*

To report a case of obstructed hemivagina and ipsilateral renal anomaly (OHVIRA syndrome) with uterus didelphys that has been diagnosed successfully with ultrasound and managed with a single stage vaginoplasty.

**Keywords:** Ohvira, Uterus didelphys; Obstructed hemivagina; Vaginal septum excision Ultrasound; MRI

### 1185. Primary Anterior Vaginal Wall Pure Ammonium Acid Urate Stone. Case Report

Sherif M. Khattab and Mohamed Abdel Fattah Mahmoud Youssef

*Middle East Fertility Society Journal, 18: 120-122 (2013)*

Vaginal stones are extremely rare and are classified as primary and secondary. A 45-year-old female presented with an unexplained dyspareunia and vaginal discomfort for 2 years unresponsive to traditional treatment. Vaginal examination revealed no prolapse or vaginal fistula. Digital examination revealed multiple small rounded firm to hard or tender masses varying in size from 0.5 to 1.5 cm anterior to the vagina. Patient was treated with mid line anterior vaginal wall incision with the extraction of eight smooth surfaced stones with uneventful postoperative course. Stone analysis revealed that they were composed of pure ammonium acid urate (AU). We recommend that for any patient with unexplained dyspareunia or vaginal discomfort that has proved to be unresponsive to traditional treatment, the possibility of anterior vaginal wall stones should be kept in mind.

**Keywords:** Vaginal stone; Dyspareunia; Acid urate.

### 1186. Three-Dimensional Ultrasonography Using the Vocal Technique for Estimation of Reference Range Between 7 and 11 Weeks Embryonic Volume

Hassan Mostafa Gaafar, Ghada Abdel Fattah Abdel Moety and Waleed El-Khayat

*Middle East Fertility Society Journal, 18: 115-119 (2013)*

**Objective:** Accurate estimation of gestational age (GA) is the basis of vital decisions in pregnancy and hence its importance in obstetric management. This study tries estimating a reference range of 3D embryonic volume using the VOCAL technique for pregnancies between 7 and 11 weeks.

**Materials and Methods:** This cross-sectional study included 62 singleton normal uneventful pregnancies. All women were essentially sure of the date of last menstrual period. All women were submitted to 3D ultrasonographic examination with VOCAL technique to determine the embryonic volume. In addition the crown-rump length was measured.

Regression analysis was performed to predict the gestational age from the fetal volume.

**Results:** There was a strong positive correlation between embryonic volume and menstrual age, gestational age and crown-rump length ( $r=0.919, 0.938$  and  $0.941$ , respectively). Power regression model produced  $R^2$  value of  $0.838$  with a regression equation ( $y=52.22+6.5x$ ).

**Conclusion:** This study demonstrated that embryonic/fetal volume is a good predictor of gestational age with a power regression equation ( $y=52.22+6.5x$ ) for the period from 7 to 10 weeks+6 days. We suggest using the embryo volume as an early evidence of growth restriction in high risk pregnancy.

**Keywords:** Vocal; Embryonic volume; Three-dimensional Ultrasonography.

### Dept. of Ophthalmology

### 1187. ICL Versus Veriflex Phakic IOL for Treatment of Moderately High Myopia: Randomized Paired-Eye Comparison.

Ahmed Awadein and Ahmed E. Habib

*Journal of Refractive Surgery, 29: 445-452 (2013) IF: 2.474*

**Purpose:** To compare the objective and subjective outcome of implantable collamer lenses (ICLs; Staar Surgical, Monrovia, CA) versus Veriflex lenses (AMO, Santa Ana, CA) for the correction of moderately high myopia.

**Methods:** A prospective randomized comparative eye study was performed on 24 patients with bilateral myopia that ranged from -6 to -14.5 diopters (D). One eye was implanted with an ICL and the other eye was implanted with a Veriflex phakic intraocular lens (PIOL). Uncorrected distance visual acuity (UDVA), corrected distance visual acuity (CDVA), higher-order aberrations (HOAs), contrast sensitivity, patient satisfaction, central endothelial cell count, and PIOL centration were determined 6 months after surgery.

**Results:** The logMAR UDVA and CDVA improved significantly in both groups ( $P < .001$ ). There was no statistically significant difference in postoperative logMAR UDVA ( $P = .41$ ) or logMAR CDVA ( $P = .36$ ) between the two groups. Postoperative deviation from target refraction was  $-0.06 \pm 0.41$  D in the ICL group and  $-0.07 \pm 0.49$  D in the Veriflex group ( $P = .15$ ). The difference in

both induced and absolute postoperative HOAs between groups was not statistically significant. The area under the log contrast sensitivity function increased significantly in both groups postoperatively. The difference in patient satisfaction between both PIOLs was not statistically significant. A higher but statistically insignificant central endothelial cell count loss occurred in the Veriflex group ( $P = .11$ ).

**Conclusion:** Both ICL and Veriflex PIOLs have equally satisfactory objective and subjective visual outcomes after surgery.

**Keywords:** Phakic IOL; Implantable collamer lens; Veriflex.

### 1188. Effect of Cryopreserved Amniotic Membrane on the Development of Adhesions and Fibrosis After Extraocular Muscle Surgery in Rabbits

Rehab R. Kassem, Mostafa M. Khodeir, Mostafa Salem, Mohammed A. Abdel-Hamid, Randa M. Abdel-Moneim El-Mofty, Ahmed M. Kamal and Hala M. Elhilali

*Acta Ophthalmologica*, 91(2): 140-148 (2013) IF: 2.345

**Purpose:** To histopathologically evaluate the effect of cryopreserved human amniotic membrane (AM) transplant on preventing the development of postoperative adhesions after extraocular muscle surgery.

**Methods:** Ten albino rabbits were used. The superior rectus muscles were bilaterally resected. In right eyes, the muscle was wrapped with cryopreserved human AM (group AM). In left eyes, the muscle was not wrapped with AM and served as a control group (group C). The rabbits were killed, and the eyes were enucleated 6 weeks after surgery to perform histopathological examination.

**Results:** On histopathological examination, the AM was present in eight eyes, surrounded by periamniotic inflammation, with no adhesions detected between rectus muscle and sclera, conjunctiva and Tenon's capsule in the segment where the AM was present, but detected elsewhere. Adhesions were detected in the other two eyes of group AM, in which the AM was absent, and in all group C eyes. When comparing eye pairs of each rabbit, AM eyes showed significantly less adhesions between the muscle and sclera ( $p = 0.009$ ) and between the muscle and Tenon's capsule and conjunctiva ( $p = 0.008$ ), in the region of AM application, and significantly more foreign body inflammation ( $p = 0.031$ ), than C eyes. The differences between AM and C eye pairs, in terms of conjunctival inflammation and vascularity and muscle fibrosis, were insignificant ( $p > 0.05$ ).

**Conclusions:** Cryopreserved AM is effective in reducing postoperative extraocular muscle adhesions. Its application is, therefore, recommended during strabismus reoperations.

**Keywords:** Adhesions; Cryopreserved amniotic membrane; Extraocular muscles; Fibrosis; Strabismus reoperation.

### 1189. Polypropylene Vs Silicone Ahmed Valve with Adjunctive Mitomycin C in Paediatric Age Group: A Prospective Controlled Study

Y. Elsayed and A. Awadein

*Eye (London)*, 27: 728-734 (2013) IF: 1.818

**Purpose:** To compare the results of silicone and polypropylene Ahmed glaucoma valves (AGV) implanted during the first 10 years of life.

**Methods:** A prospective study was performed on 50 eyes of 33 patients with paediatric glaucoma. Eyes were matched to either polypropylene or silicone AGV. In eyes with bilateral glaucoma, one eye was implanted with polypropylene and the other eye was implanted with silicone AGV.

**Results:** Fifty eyes of 33 children were reviewed. Twenty five eyes received a polypropylene valve, and 25 eyes received a silicone valve. Eyes implanted with silicone valves achieved a significantly lower intraocular pressure (IOP) compared with the polypropylene group at 6 months, 1 year, and 2 years postoperatively. The average survival time was significantly longer ( $P = 0.001$  by the log-rank test) for the silicone group than for the polypropylene group and the cumulative probability of survival by the log-rank test at the end of the second year was 80% (SE:8.0, 95% confidence interval (CI):64-96%) in the silicone group and 56% (SE:9.8, 95% CI:40-90%) in the polypropylene group. The difference in the number of postoperative interventions and complications between both groups was statistically insignificant.

**Conclusion:** Silicone AGVs can achieve better IOP control, and longer survival with less antiglaucoma drops compared with polypropylene valves in children younger than 10 years.

**Keywords:** Paediatric glaucoma; Ahmed valves; Buphthalmos; silicone; Polypropylene.

### 1190. Pattern of Uveitis in an Egyptian Population with Multiple Sclerosis: a Hospital-Based Study

Ahmed M. Karara, Tamer A. Macky and Mai H. Sharawy

*Ophthalmic Research*, 49: 25-29 (2013) IF: 1.562

**Purpose:** To investigate the prevalence and pattern of uveitis in patients with multiple sclerosis (MS).

**Patients and Methods:** This is a cross-sectional, observational, descriptive clinical study of patients with MS who had complete ophthalmological examination. Data collected comprised demographics of the patients and complete ocular examination findings. Exclusion criteria were history of ocular surgery, trauma or diagnosis of any other ocular pathology.

**Results:** Seventy-five patients with a mean age of 32.64 years (ranging from 16 to 50) diagnosed with MS of the relapsing-remitting type were included in this study. There were 34 males and 41 females, a ratio of 5:6. The mean duration of the MS disease was 5.6 years. Eight eyes of 7 patients with a mean age of 20 years had intermediate uveitis, of which 5 were males. Out of the 7 patients, 5 had exacerbated MS, and 2 were in remission; 4 had relative afferent papillary defect. In the 8 eyes with uveitis, 6 had a best spectacle-corrected visual acuity (BSCVA) of 1, 1 had a BSCVA of 0.5 and 1 had a BSCVA of 0.25.

**Conclusion:** Uveitis occurs in about 10% of patients with MS affecting younger males with exacerbated disease. Most inflammations of the uveitic MS patients were in the form of intermediate uveitis that was controlled with medication with no visual threatening complications.

**Keywords:** Uveitis intermediate uveitis; Pars planitis; Multiple sclerosis.



### 1191. Lateral Rectus Recession With/Without Transposition in V-Pattern Exotropia Without Inferior Oblique Overaction

Ahmed Awadein

*Canadian Journal of Ophthalmology*, 48: 500-505 (2013)  
IF: 1.145

**Objective:** To compare bilateral lateral rectus (BLR) recession with BLR recession combined with half-tendon upward transposition in the management of patients with V-pattern exotropia (XT; 15-20 prism diopters [PD] greater XT in upgaze than downgaze) with no or minimal inferior oblique overaction.

**Design:** Retrospective, observational, cohort study.

**Participants:** Twenty-nine patients had BLR recession (Group A). Twenty-one patients had BLR recession combined with half-tendon upward transposition (Group B).

**Methods:** A retrospective study was performed on patients with V-pattern XT with no or minimal inferior oblique overaction. Ductions, versions, pattern strabismus, stereoacuity, and degree of fundus torsion were analyzed in all patients before and after surgery. Patients were included in the study only if they achieved a minimum follow-up of 6 months.

**Results:** Normalization of V pattern ( $<5^\circ$ ) was achieved in 14% in Group A and 64% in Group B ( $p < 0.001$ ). Mean reduction in V pattern after surgery was  $7 \pm 6$  in Group A and  $13 \pm 4$  in Group B ( $p < 0.001$ ). No change in fundus intorsion occurred in Group A, whereas fundus extorsion occurred in 8 patients (44%) in Group B. Orthophoria within  $8^\circ$  in the primary position was achieved in 79% in Group A and 82% in Group B ( $p = 1.00$ ). There was no statistically significant difference in the postoperative stereoacuity in both groups ( $p = 0.67$ ).

**Conclusions:** BLR with half-tendon upward transposition is much more effective than BLR recession alone in correcting V pattern.

**Keywords:** V-Pattern exotropia; Lateral; Rectus recession; Upward transposition.

### 1192. The Effect of Glycemic Control on Visual and Anatomic Outcomes in Response to Therapy for Diabetic Macular Edema.

Tamer A. Macky and Mohamed M. Mahgoub

*European Journal of Ophthalmology*, 23: 94-100 (2013)  
IF: 0.912

**Purpose:** To evaluate the effect of glycemic control on response to therapy of diabetic clinically significant macular edema (CSME).

**Methods:** Patients with CSME had their glycosylated hemoglobin (HbA1c) measured at baseline and 6 months. Central foveal thickness (CFT) and best-corrected visual acuity (BCVA) in logMAR were measured at baseline, 3 months, and 6 months. Therapy included laser and intravitreal bevacizumab. HbA1c was graded as G1  $<7\%$ , G2 7%–7.9%, G3 8%–8.9%, G4  $>9\%$ .

**Results:** Fifty-two eyes were included with mean logMAR BCVA and CFT as follows: baseline 0.75 and  $423 \pm 106 \mu\text{m}$ ; 3 months 0.47 and  $293 \pm 69 \mu\text{m}$ ; and 6 months 0.48 and  $324 \pm 76 \mu\text{m}$ . Mean HbA1c was 8.13% and 7.43% at baseline and 6 months, respectively. There was no statistically significant difference between baseline and 6 months HbA1c groups and logMAR

BCVAs and CFTs at baseline, 3 months, and 6 months. However, there were positive correlations between baseline HbA1c levels and each of baseline logMAR BCVA ( $p=0.024$ ), baseline CFT ( $p<0.001$ ), and 6-month logMAR BCVA ( $p=0.007$ ). Improved HbA1c by 6 months did not show any correlation with logMAR BCVA and CFT at 6 months.

**Conclusions:** Lower HbA1c appeared to be correlated with better visual acuity and lower CFT values at baseline, and also correlated with significantly better vision and nonsignificantly thinner CFT with therapy at 6 months.

**Keywords:** Diabetic macular edema; Glycemic control; HbA1c.

### 1193. A Computerized Version of the Lancaster Red-Green Test.

Ahmed Awadein

*Journal of the American Association for Pediatric Ophthalmology and Strabismus*, 17: 197-202 (2013) IF: 0.731

**Purpose:** To compare results from a computerized version of the Lancaster red-green test with those of the conventional test.

**Methods:** Consecutive adult patients with noncomitant strabismus were tested with the conventional Lancaster red-green test and with a computerized version of the same. The computerized test was administered by means of a 40-inch monitor at a working distance of 50 cm or a projector and screen at a working distance of 1 meter. Agreement between the measured horizontal, vertical, and torsional deviations in the conventional test and both computerized versions was evaluated with the mountain plot, Bland-Altman plot, and Deming regression analysis models.

**Results:** A total of 82 patients were tested. Agreement of measured horizontal deviation in the conventional test was better with the projector version of the test (limits of agreement: right eye,  $-4.6^\circ$  to  $3.4^\circ$ ; left eye,  $-4.9^\circ$  to  $3.5^\circ$ ) than the monitor version (limits of agreement: right eye,  $-10^\circ$  to  $4.2^\circ$ ; left eye,  $-8.9^\circ$  to  $4.1^\circ$ ). The measured vertical and torsional deviation in the conventional test showed good agreement with both versions of the computerized test (limits of agreement  $<5^\circ$  for vertical measurements and  $<3^\circ$  for torsional measurements). Agreement was similar for right and left eyes.

**Conclusions:** The vertical and torsional deviations measured with both computerized versions of the test were in good agreement with those obtained with the conventional test. For measured horizontal deviations, the projector version had better agreement than the monitor version.

**Keywords:** Lancaster red; Green; Dissociated tests; Hess screen.

### 1194. Inferior Oblique Myectomy for Upshoots Mimicking Inferior Oblique Overaction in Duane Retraction Syndrome.

Ahmed Awadein

*Journal of the American Association for Pediatric Ophthalmology and Strabismus*, 17: 253-258 (2013) IF: 0.731

**Purpose:** To evaluate the results of inferior oblique myectomy in selected patients with Duane retraction syndrome with upshoot on adduction.

**Methods:** This was a prospective, interventional study of consecutive patients with types 1, 2, or 3 Duane syndrome with

isolated upshoot in adduction operated on from January 2007 to December 2011. Patients underwent inferior oblique myectomy on the side of the upshooting eye. Only patients with gradual elevation of the eye in adduction in a pattern similar to inferior oblique overaction or patients with hypertropia in the primary position were included. All patients were followed for at least 6 months. Ductions, versions, degree of upshoot, degree of fundus torsion, and pattern of strabismus were analyzed in all patients before and after surgery.

**Results:** A total of 11 patients were included in the study. Mean patient age at time of surgery was  $6.4 \pm 5.2$  years (range, 3-22 years). Two patients had bilateral inferior oblique myectomy and 4 had simultaneous bilateral medial rectus muscle recession to correct horizontal misalignment. Mean duration of follow-up was 8.6 months (range, 6-36 months). Of the 11 patients, 10 (91%) had complete disappearance of the upshoot at last follow-up. None of the patients developed inferior oblique underaction postoperatively. There was a statistically significant improvement of V pattern after surgery ( $P < 0.01$ ). Mean vertical misalignment in primary position was 5( ) before surgery and 1( ) after ( $P = 0.02$ ). Most patients had no significant fundus torsion before or after surgery.

**Conclusions:** Inferior oblique muscle weakening can improve upshoot in selected patients with Duane retraction syndrome without inducing inferior oblique muscle underaction.

**Keywords:** Duane syndrome; Upshoots; Inferior oblique Myectomy.

### 1195. Management of Large V-Pattern Exotropia with Minimal or no Inferior Oblique Overaction

Ahmed Awadein and Heba M. Fouad

*Journal of the American Association for Pediatric Ophthalmology and Strabismus*, 17: 588-593 (2013) IF: 0.731

**Purpose:** To compare the outcomes of patients with large V-pattern exotropia and minimal inferior overaction who underwent bilateral lateral rectus recession combined with full-tendon-width upward transposition of the lateral rectus muscles or bilateral inferior oblique myectomy.

**Methods:** The medical records of consecutive patients with V-pattern exotropia (at least 20( ) greater in upgaze than in downgaze) with minimal inferior oblique overaction who underwent either of the above procedures and who had at least 6 months' follow-up were retrospectively reviewed. Pre- and postoperative ductions, versions, pattern strabismus, stereoacuity and fundus torsion were analyzed. Success was defined as esophoria  $< 8( )$  / tropia  $= 5( )$  to exophoria/tropia  $= 8( )$  in primary gaze.

**Results:** A successful outcome was achieved in 9 patients (56%) in the transposition group and 13 (72%) in the myectomy group ( $P = 0.48$ ). Reduction of V pattern to  $< 10( )$  was achieved in 7 cases (44%) in the transposition group and 14 (78%) in the myectomy group ( $P = 0.04$ ), with mean reductions of  $16( ) \pm 5( )$  and  $25( ) \pm 5( )$ , respectively ( $P = 0.03$ ). In the myectomy group, 4 patients (22%) had overcorrection with consecutive A patterns of  $2( )$ - $6( )$ .

**Conclusions:** In patients with a V pattern exotropia and minimal inferior oblique over action, bilateral lateral rectus recessions plus bilateral inferior oblique myectomy can successfully eliminate the V pattern but the surgery may occasionally result in

**Keywords:** V-Pattern exotropia; Lateral rectus recession; Upward Transposition; Inferior oblique myectomy.

### 1196. Comparison of Different Intraocular Pressure Measurement Techniques in Normal Eyes, Post Surface and Post Lamellar Refractive Surgery

Shireen M. A. Shousha, Mahmoud A. H. Abo Steit, Mohamed H. M. Hosny, Wael A. Ewais and Ahmad M. M. Shalaby

*Clinical Ophthalmology*, 7 : 71-79 (2013)

**Background:** The purpose of this study was to determine the accuracy of intraocular pressure (IOP) measurement after laser in situ keratomileusis (LASIK) or epithelial laser in situ keratomileusis (Epi)-LASIK using Goldmann applanation tonometry, air puff tonometry, ocular response analyzer corneal compensated IOP (ORA IOPcc) and Pentacam corrected IOP.

**Methods:** A prospective comparative clinical study was conducted between February and September 2011 on 30 eyes divided into four groups, i.e. 20 corneas of 10 patients before LASIK (group A), 20 corneas of the same patients 2 months postoperatively (group B), 10 corneas of five patients before Epi-LASIK (group C), and 10 corneas of the same patients 2 months postoperatively (group D). Patient age ranged from 20 to 50 years. IOP was measured using Goldmann applanation and air puff tonometry, ORA corneal compensation, and Pentacam correction (which also measured central corneal thickness).

**Results:** Significant positive linear correlations were found between IOP values measured by Goldmann applanation tonometry and other techniques, and with preoperative pachymetry in group A. The correlation between preoperative Pentacam-corrected and preoperative ORA corneal-compensated IOP was strongest for Goldmann applanation tonometry ( $r = 0.97$  and  $r = 0.858$  respectively,  $P, 0.001$ ). Compared with preoperative values, postoperative IOP measured by the four methods were significantly lower. The difference was statistically significant when IOP was measured using Goldmann applanation and air puff tonometry compared with the ORA and Pentacam methods ( $P, 0.001$  for LASIK patients and  $P = 0.017$  for Epi-LASIK patients). Nonsignificant correlations were found between the degree of lowering of postoperative IOP and postoperative pachymetry in groups B and D.

**Conclusion:** Refractive surgery causes significant lowering of IOP as measured using Goldmann applanation tonometry, air puff tonometry, ORA compensation, and Pentacam correction. LASIK has a greater effect than Epi-LASIK on IOP measurement error following refractive surgery.

**Keywords:** Intraocular pressure measurement; Refractive surgery; Corneal biomechanics; Corneal thickness.

### 1197. Retinopathy and Dyslipidemia in Type II Diabetes Mellitus in Egyptian Patients

Hala El-Mofty, Mohamad A. Abdel Hakim, Hala Ali Gamal El Din, Ossama Khalaf Allah and Pierre Samir Mosaad

*J. Clin. Exp. Ophthalmol*, 4 (1): 1-3 (2013)

**Purpose:** Dyslipidemia potentially contributes to microvascular disease, and this is in addition to its known effects on macrovascular disease. The aim of this study was to detect the relation between apolipoprotein B (apo B) and diabetic retinopathy (DR).

**Methods:** This is a cross sectional study conducted on 168 patients with types II diabetes mellitus. The primary outcome measures were to assess the grade of diabetic retinopathy and

serum level of apo B. The Secondary outcome measures were to assess the patients' best corrected visual acuity.

**Results:** There was a significant increase in apo B in subjects with retinopathy as compared to those without retinopathy ( $p < 0.001$ ). Correlating apo B levels to the grade of retinopathy was statistically significant ( $r = 0.432$ ;  $p < 0.001$ ). Also a statistically significant relation was found between apo B and diabetic maculopathy ( $p = 0.003$ ).

**Conclusion:** There was a statistically significant increase in apo B in subjects with retinopathy as compared to those without retinopathy, and a fair correlation between apo B levels and grade of DR. Furthermore a statistically significant relation was found between the apo B level and the presence of maculopathy.

**Keywords:** Type 1 diabetes mellitus; Diabetic retinopathy; Apolipoprotein B; Diabetic maculopathy; Dyslipidemia.

#### Dept. of Orthopaedic

### 1198. Unreamed Intramedullary Nailing in Distal Tibial Fractures

Khaled Hamed Salem

*International Orthopaedics*, 37: 2009-2015 (2013) IF: 2.319

**Purpose:** Unreamed nailing has gained acceptance in the treatment of diaphyseal long bone fractures, especially in cases with polytrauma or high-energy injuries. Its application in distal tibial fractures, however, remains controversial.

**Methods:** in this study, 101 distal tibial fractures treated using closed unreamed nailing were reviewed after a mean follow-up of 32 months. There were 59 type A and 42 type B fractures. The most common fracture pattern was the A1 spiral fracture ( $n = 40$ ) followed by the B2 wedge fracture ( $n = 18$ ). Intra-articular extension was encountered in 14 cases. One-fourth of the patients ( $n = 24$ ) had open injuries. Forty-seven patients had additional injuries, and nearly one-third of them were polytraumatized.

**Results:** Union occurred after a mean time of 23.9 (range, 11-134) weeks. There were 13 cases of delayed union and seven non-unions; all healed eventually with additional surgery in only six fractures. Malunion was seen in 12 cases (five valgus, two varus and five external torsion), ten of which were associated with unplate fibular fractures. Three fractures (two open) were treated for deep infection. The most common complication seen was fatigue failure of the locking screws (27 cases).

**Conclusions:** Unreamed nailing of distal tibial fractures is associated with a rather high rate of bone healing complications and locking screw failure. The decision for its use in the notoriously challenging fractures of this segment should be critically considered.

**Keywords:** Unreamed nailing; Distal tibial fractures; Fracture healing; Malunion.

### 1199. Cervical Microendoscopic Discectomy and Fusion: Does it Affect the Postoperative Course and the Complication Rate a Blinded Randomized Controlled Trial

Hesham Magdi Soliman

*Spine Journal*, 38: 2064-2070 (2013) IF: 2.159

**Study Design:** A blinded randomized controlled trial.

**Objective:** The purpose of this study was to evaluate the cervical microendoscopic discectomy and fusion.

**Summary of Background Data:** Minimally invasive treatment of spinal disorders allows surgeons to have direct access to the pathology with a reduced surgical morbidity, which is reflected over the improved postoperative course. Minimally invasive techniques for cervical discectomy including the posterior microendoscopic discectomy and the percutaneous endoscopic discectomy have a high success rate but are limited by the narrow range of indications. Lately, preliminary reports about cervical microendoscopic discectomy and fusion (CMEDF) showed high success rates without restrictions in the indications.

**Methods:** Seventy consecutive patients were randomly assigned in 2 equal groups, the first operated by the "gold standard" anterior cervical discectomy and fusion and the second by CMEDF. Blinding included the patient—until dressing removal, the evaluating physician, and the radiologist throughout the entire study.

The mean follow-up period was 28 months and outcome has been assessed using the Japanese Orthopaedic Association score, Odom criteria and the visual analogue scale. In addition, the operative time, complication rate, hospitalization, and the postoperative analgesic doses were recorded.

**Results:** The functional outcome of the CMEDF at the final follow-up was 91% good to excellent. Results in the open group were very similar. Meanwhile, CMEDF demonstrated improved cosmesis, reduced laryngopharyngeal complication rate, postoperative analgesics, and hospital stay.

**Conclusion:** The results of the CMEDF are very promising. However, a much larger patient series from multicenter studies is still required for drawing up a final conclusion. Level of Evidence.

**Keywords:** Cervical microendoscopic discectomy and fusion; Cervical endoscopic discectomy; Minimally invasive spine surgery; Cervical disc; Radiculopathy.

### 1200. Next Generation of Growth-Sparing Techniques

Behrooz A. Akbarnia, Kenneth Cheung, Hilali Noordeen, Hazem Elsebaie, Muharrem Yazici, Zaher Dannawi and Nima Kabirian

*Spine*, 38(8): 665-670 (2013) IF: 2.159

**Study Design.** Prospective nonrandomized study. **Objective.** to report the preliminary results of magnetically controlled growing rod (MCGR) technique in children with progressive early-onset scoliosis.

**Summary of Background:** Data. The growing rod (GR) technique is a viable alternative for treatment of early-onset scoliosis. High complication rate is attributed to frequent surgical lengthening. The safety and efficacy of MCGR were recently reported in a porcine model.

**Methods:** Multicenter study of clinical and radiographical data of patients who underwent MCGR surgery and at least 3 distractions. Distractions were performed in clinic without anesthesia/analgesics. T1–T12 and T1–S1 heights and the distraction distance inside the actuator were measured after lengthening.

**Results:** Fourteen patients (7 girls, 7 boys) with a mean age of 8 years, 10 months (3 yr, 6 mo to 12 yr, 7 mo) had 14 index surgical procedures. Of the 14, 5 had single-rod (SR) surgery and 9 had dual-rod (DR) surgery, with overall 68 distractions. Diagnoses were idiopathic ( $N = 5$ ), neuromuscular ( $N = 4$ ),

congenital (N = 2), syndromic (N = 2), and neurofibromatosis (N = 1). Mean follow-up was 10 months (5.8–18.2). The Cobb angle changed from 60 ° to 34 ° after initial surgery and 31 ° at latest follow-up. During distraction period, T1–T12 height increased by 7.6 mm for SR (1.09 mm/mo). Growth-sparing techniques for treatment of progressive early-onset scoliosis (EOS) have evolved significantly during the past few decades.

Originally, it was Paul Harrington, the developer of Harrington instrumentation, in 1962 who recommended distraction instrumentation without fusion for children less than 10 years of age to allow continuous spinal growth. Moe et al [2] popularized instrumentation without fusion and included periodic construct lengthening to achieve both deformity correction and spinal growth using hooks and single distraction rod.

The dual growing rod (GR) technique was introduced to provide stability, more predictable outcomes, and fewer complications than previous techniques [3, 4]. During the past 5 years, other techniques have also been introduced as growth-friendly procedures. Skaggs et al [6] have proposed a classification of the major growth-friendly techniques into 3 main categories: “distraction-based” (e.g., GR, vertical expandable prosthetic titanium rib, and remote control), “tension-based” (e.g., staple and tether), and “guided-growth” (e.g., Luque and Shilla). GR is currently the most commonly used distraction-based technique, which has the advantage of correcting spinal deformity, allowing normal growth, and may even have a potential for growth stimulation beyond the normal growth rate. [4]. However, the technique requires frequent surgical procedures for lengthening to allow adequate spinal growth and to maintain scoliosis curve correction. Frequent surgical procedures.

**Keywords:** Early; Onset scoliosis; Magnetic rod; Growing rod; MCGR.

### 1201. Computer-Assisted Fluoroscopic Navigation of Percutaneous Spinal Interventions.

Jörg A. K. Ohnsorge, Khaled H. Salem, Andreas Ladenburger, Uwe M. Maus and Markus Weißkopf

*European Spine Journal*, 22: 642–647 (2013) IF: 2.133

**Purpose:** Percutaneous spine procedures may occasionally be difficult and subject to complications. Navigation using a dynamic reference base (DRB) may ease the procedure. Yet, besides other shortcomings, its fixation demands additional incisions and thereby defies the percutaneous character of the procedure.

**Methods:** A new concept of atraumatic referencing was invented including a special epiDRB. The accuracy of navigated needle placement in soft tissue and bone was experimentally scrutinized. Axial and pin-point deviations from the planned trajectory were investigated with a CT-based 3D computer system. Clinical evaluation in a series of ten patients was also done.

**Results:** The new epiDRB proved convenient and reliable. Its fixation to the skin with adhesive foil provided a stable reference for navigation that improves the workflow of percutaneous interventions, reduces radiation exposure and helps avoid complications.

**Conclusions:** Percutaneous spine interventions can be safely and accurately navigated using epiDRB with minimal trauma or radiation exposure and without additional skin incisions.

**Keywords:** Spine navigation; Computer assisted surgery; DRB; epiDRB.

### 1202. Irrigation Endoscopic Discectomy: A Novel Percutaneous Approach for Lumbar Disc Prolapse

Hesham Magdi Soliman

*European Spine Journal*, 22: 1037–1044 (2013) IF: 2.133

**Purpose:** The purpose of this study is to present a new endoscopic procedure, aiming to achieve the success rate equivalent to microsurgical discectomy, while addressing the drawbacks and limitations of other percutaneous techniques.

**Methods:** A series of 43 patients with uncontained lumbar disc herniation underwent surgery with irrigation endoscopic discectomy (IED).

The endoscope and instruments are placed directly over the surface of the lamina through two posterior skin portals 5 mm each without any muscle retraction or dilatation. Pump irrigation is used for the opening of a potential working space. The rest of the procedure is performed endoscopically like the standard microsurgical discectomy.

**Results:** Outcome according to modified Macnab criteria was excellent in 78 %, good in 17 %, and poor in 5 % of patients. VAS for leg pain dropped from 78 preoperatively to 7, and the Oswestry Low-Back Pain Disability Questionnaire dropped from 76 to 19. The mean time for postoperative ambulation was 4 h, hospital stay was 8 h, and for return to work was 7 days.

**Conclusions:** Preliminary clinical experience with IED shows it to be as effective as microsurgical discectomy, and in comparison to other percutaneous procedures addressing noncontained herniations, a reduction in the cost, technical difficulty and surgical invasiveness has been demonstrated.

**Keywords:** Irrigation endoscopic discectomy; Endoscopic discectomy; Minimally invasive spine surgery; Lumbar discectomy; Percutaneous discectomy.

### 1203. Perforator-Based Radial Forearm Fascial Flap for Management of Recurrent Carpal Tunnel Syndrome

Mostafa Mahmoud, Sherif El Shafie, Erin E. Coppola and John C. Elfar

*Journal of Hand Surgery*, 38: 2151–2158 (2013) IF: 1.733

**Purpose:** To study the benefit of using the perforator-based radial forearm fascial flap for patients with recurrent carpal tunnel syndrome.

**Methods:** We used a perforator-based radial forearm fascial flap in 8 patients to cover the median nerve. All of the patients had undergone an index carpal tunnel release, and 3 of them had undergone at least 1 revision surgery to further decompress the median nerve.

**Results:** At average of 20 months (range, 6–30 mo) after the forearm fascial flap, all patients reported symptomatic improvement with complete resolution of nighttime symptoms. No patient reported worsening of symptoms; however, some subjective paresthesias persisted in 3 of the 8 patients. Objective assessment revealed complete resolution of a Tinel sign in 5 of 8 patients and noteworthy improvement in the remaining 3 patients. Average 2-point discrimination was 10.0 mm before surgery and 5.4 mm after surgery, average grip strength improved from 13.5 kg to 21.0 kg, and average tip pinch strength improved from 4.1 kg to 7.0 kg.

**Conclusions:** The perforator-based radial forearm fascial flap may prove useful in the setting of recurrent carpal tunnel syndrome after surgical decompression. Level of evidence Therapeutic IV.

**Keywords:** Carpal tunnel; Perforator flap; Radial artery.

#### 1204. New Flap for Widening of the Web Space and Correction of Palmar Contracture in Complex Clasped Thumb

Mostafa Mahmoud, Hisham Abdel-Ghani and John C. Elfar

*Journal of Hand Surgery, 38A: 2251-2256 (2013) IF: 1.733*

In our experience, previous flaps designed for correction of the skin deficiency in complex clasped thumb do not sufficiently address the palmar contracture of the deformity. Moreover, the index finger flap, previously described by Ezaki and Oishi, provides insufficient skin at its apex with the possibility of incomplete correction and the frequent need of a thenar release incision.

This article describes a flap designed for widening of the narrow thumb-index web space and release of the palmar thumb contracture in cases of congenital clasped thumb. This flap provides sufficient correction of the palmar contracture and at the same time provides adequate width and depth of the thumb-index web space.

**Keywords:** Clasped thumb; Index finger flap; Palmar flap; Palmar contracture.

#### 1205. Avascular Necrosis After Chemotherapy for Haematological Malignancy in Childhood

K. H. Salem, A-K. Brockert, R. Mertens and W. Drescher

*Bone and Joint Journal, 95-B(12): 1708-1713 (2013)*

Avascular necrosis (AVN) is a serious complication of high-dose chemotherapy for haematological malignancy in childhood. In order to describe its incidence and main risk factors and to evaluate the current treatment options, we reviewed 105 children with a mean age of 8.25 years (1 to 17.8) who had acute lymphoblastic or acute myeloid leukaemia, or a non-Hodgkin's lymphoma. Overall, eight children (7.6%) developed AVN after a mean of 16.8 months (8 to 49). There were four boys and four girls with a mean age of 14.4 years (9.8 to 16.8) and a total of 18 involved sites, 12 of which were in the femoral head. All these children were aged > nine years ( $p < 0.001$ ). All had received steroid treatment with a mean cumulative dose of prednisone of 5967 mg (4425 to 9599) compared with a mean of 3943 mg (0 to 18 585) for patients without AVN ( $p = 0.005$ ). No difference existed between genders and no thrombophilic disorders were identified.

Their initial treatment included 11 core decompressions and two bipolar hip replacements. Later, two salvage osteotomies were done and three patients (four hips) eventually needed a total joint replacement. We conclude that AVN mostly affects the weight-bearing epiphyses. Its risk increases with age and higher steroid doses. These high-risk patients may benefit from early screening for AVN.

**Keywords:** Avascular necrosis; Chemotherapy; Childhood lymphomas; Core decompression; Leukaemias; Steroids.

#### 1206. Early Results of A Remotely-Operated Magnetic Growth Rod in Early-Onset Scoliosis

Z. Dannawi, F. Altaf, N. S. Harshavardhana, H. El Sebaie and H. Noordeen

*Spine, 95 (1): 75-81 (2013)*

Conventional growing rods are the most commonly used distraction-based devices in the treatment of progressive early-onset scoliosis. This technique requires repeated lengthenings with the patient anaesthetised in the operating theatre. We describe the outcomes and complications of using a non-invasive magnetically controlled growing rod (MCGR) in children with early-onset scoliosis. Lengthening is performed on an outpatient basis using an external remote control with the patient awake. Between November 2009 and March 2011, 34 children with a mean age of eight years (5 to 12) underwent treatment. The mean length of follow-up was 15 months (12 to 18). In total, 22 children were treated with dual rod constructs and 12 with a single rod. The mean number of distractions per patient was 4.8 (3 to 6). The mean pre-operative Cobb angle was  $69^\circ$  ( $46^\circ$  to  $108^\circ$ ); this was corrected to a mean  $47^\circ$  ( $28^\circ$  to  $91^\circ$ ) post-operatively. The mean Cobb angle at final review was  $41^\circ$  ( $27^\circ$  to  $86^\circ$ ). The mean pre-operative distance from T1 to S1 was 304 mm (243 to 380) and increased to 335 mm (253 to 400) in the immediate postoperative period. At final review the mean distance from T1 to S1 had increased to 348 mm (260 to 420). Two patients developed a superficial wound infection and a further two patients in the single rod group developed a loss of distraction. In the dual rod group, one patient had pullout of a hook and one developed prominent metalwork. Two patients had a rod breakage; one patient in the single rod group and one patient in the dual rod group. Our early results show that the MCGR is safe and effective in the treatment of progressive early-onset scoliosis with the avoidance of repeated surgical lengthenings.

**Keywords:** Magnetic; Growth rod; Early; Onset scoliosis.

#### Dept. of Parasitology

#### 1207. Molecular Characterization of Cutaneous Leishmaniasis in Al-Madinah Al-Munawarah Province, Western Saudi Arabia

Hesham A. El-Beshbishy, Khalil H. Al-Ali and Ayman A. El-Badry

*International Journal of Infectious Diseases, 17: 334-338 (2013) IF: 2.357*

**Background:** Leishmaniasis is a parasitic disease affecting a large number of people worldwide. In this study we carried out the molecular characterization of cutaneous leishmaniasis (CL) in Al-Madinah Al-Munawarah Province, Saudi Arabia, confirming *Leishmania major* and *Leishmania tropica* as the prevalent species using molecular techniques.

**Methods:** One hundred and five patients with suspected CL were identified from four different localities in Al-Madinah Al-Munawarah Province and Al-Miqat Hospital, Al-Madinah, Saudi Arabia. Thirty-four of the 105 patients were selected at random for molecular investigation.

**Results:** Characterization of CL species by internal transcribed spacer 1 (ITS1) PCR-restriction fragment length polymorphism (RFLP) and kinetoplast DNA (kDNA) PCR established *L. major*



and *L. tropica* as the causative organisms. kDNA PCR had a sensitivity of 90.7%, whereas ITS1 PCR had a sensitivity of 70.1%, thus facilitating the diagnosis and species identification. Parasite culture alone detected 39.2% and smear alone 55.3% of the positive samples. With the exception of kDNA PCR, all other assays were 100% specific.

**Conclusions:** This study provides the first findings for the comprehensive molecular characterization of CL in Saudi Arabia.

**Keywords:** Molecular characterization; Cutaneous leishmaniasis; Al-Madinah Al-munawarah.

### 1208. Molecular Characterization of Leishmania Infection in Sand Flies from Al-Madinah Al-Munawarah Province, Western Saudi Arabia

Ayman Abdel-Moamen El-Badry

*Experimental Parasitology*, 134 (2): 211-215 (2013) IF: 2.154

Cutaneous leishmaniasis (CL) is caused by various species of the genus *Leishmania*. The disease is considered a major health problem in different areas of Saudi Arabia including Al-madinah Al-munawarah province. We aimed to identify *Leishmania* species isolated from sand fly vectors by molecular analysis. Sand fly sampling was carried out from May 2010 to October 2010 in province of Al-madinah Al-munawarah from four different localities. Female sand flies collected were subjected to DNA extraction followed by molecular analysis using the semi-nested PCR and conventional PCR protocols, respectively, against minicircle kDNA and ribosomal internal transcribed spacer 1 (ITS1-rDNA). The PCR positive specimens against ITS1-rDNA locus were digested for further confirmation of species identification.

A total of 2910 sand flies were collected. *Phlebotomus papatasi* accounted for 93.8% (1673 males and 1057 females), however, the number of *Phlebotomus sergenti* was only 180 (109 males and 71 females). Sixty-two out of 250 (23.7%) female *P. papatasi* tested for *Leishmania* parasite were positive for *Leishmania major* using the semi-nested PCR method against kDNA. All of the 62 positive specimens produced a band size 650 bp. A 31% of female *P. sergenti* were positive against kDNA of *Leishmania tropica* and produced a 720 bp band. These positive *P. sergenti* for *L. tropica* DNA produced ITS1-PCR-RFLP profile showed two bands of ~200 bp and 57 bp which are specific for *L. tropica*, confirming the presence of *L. tropica* in *P. sergenti*. However, the ITS1-PCR-RFLP profile showed two bands of ~203 bp and 132 bp which are specific for *L. major* in *P. papatasi*. We concluded that, the semi-nested PCR method against kDNA and the ITS1-PCR-RFLP analysis are useful tools for molecular identification of both *L. major* and *L. tropica*. A multicenter study is necessary in order to evaluate the extent of the disease and functional analysis of new *Leishmania* genes.

**Keywords:** Molecular characterization; *Leishmania*; Sand flies; Al-Madinah Al-munawarah.

### 1209. Therapeutic Potential of Myrrh and Ivermectin Against Experimental Trichinella Spiralis Infection in Mice

Maha M. A. Basyoni and Abdel-Aleem A. El-Sabaa

*Korean J Parasitol* 51 (3): 297-304 (2013) IF: 0.881

Trichinosis is a parasitic zoonosis caused by the nematode *Trichinella spiralis*. Anthelmintics are used to eliminate intestinal adults as well as tissue-migrating and encysted larvae.

This study aimed to investigate the effects of ivermectin and myrrh obtained from the aloe-gum resin of *Commiphora molmol* on experimental trichinosis. Ninety albino mice were orally infected with 300 *T. spiralis* larvae. Drugs were tested against adult worms at day 0 and day 5 and against encysted larvae on day 15 and day 35 post-infection (PI). Mature worms and encysted larvae were counted in addition to histopathological examination of muscle specimens.

Serum aspartate aminotransferase (AST), alanine aminotransferase (ALT), total protein, albumin, globulin, urea, and creatinine values were estimated. Significant reductions in mean worm numbers were detected in ivermectin treated mice at day 0 and day 5 PI achieving efficacies of 98.5% and 80.0%, while efficacies of myrrh in treated mice were 80.7% and 51.5%, respectively.

At days 15 and 35 post-infection, ivermectin induced significant reduction in encysted larval counts achieving efficacies of 76.5% and 54.0%, respectively, while myrrh efficacies were 76.6% and 35.0%, respectively. AST, ALT, urea, and creatinine levels were reduced, while total proteins were increased in response to both treatments compared to their values in the infected non-treated mice. Ivermectin use for controlling *T. spiralis* could be continued. Myrrh was effective and could be a promising drug against the Egyptian strains of *T. spiralis* with results nearly comparable to ivermectin.

**Keywords:** *Trichinella spiralis*; Ivermectin; Myrrh; Mouse.

### 1210. Potential Use of Biomphalaria Alexandrina Snail Antigens for Serodiagnosis of Schistosomiasis Mansoni by Immunoblot Analysis

Maha M. A. Basyoni and Azza Abd EL-Wahab

*Iranian J. Parasitol*, 8 (1): 65-72 (2013) IF: 0.326

**Background:** The aim of this study was to evaluate the possible use of *Biomphalaria alexandrina* snail antigens in diagnosis of schistosomiasis *mansoni* using enzyme linked immunoelectrotransfere blot (EITB).

**Methods:** *S. mansoni* adult worm crude antigens (AWA), feet and visceral humps of *B. alexandrina* and *Bulinus truncatus* were used. Hyperimmune mice sera (HIS) versus each antigen were prepared for diagnosis of *S. mansoni* using western blot (WB).

**Results:** Snail foot antigens were more specific in antibodies detection than visceral hump antigens. Three of five polypeptides of *B. alexandrina* foot antigen identified by *S. mansoni* HIS showed specific positive reactivity. These polypeptides were at MW of 31/32 and 43 kDa. While, only one of the six polypeptides of *B. alexandrina* hepatopancrease antigen identified by *S. mansoni* HIS, at a MW of 43 kDa was specific. Similarly, 2 polypeptides at MW of 44 and 55 kDa were specific in detection of anti-*S. haematobium* antibodies. However, the antigenically active polypeptide of *B. truncatus* hepatopancrease antigen had no specific reactivity towards anti-*S. haematobium* antibodies.

**Conclusion:** *B. alexandrina* foot antigens were the most specific of the tested snail antigens in diagnosis of schistosomiasis *mansoni*.

**Keywords:** Schistosomiasis *mansoni*; Snail antigens; EITB.

### 1211. Cytotoxic Activity of Methanolic Extract of *Mentha Longifolia* and *Ocimum Basilicum* Against Human Breast Cancer

Khalil H.Al-Ali, Hesham A. El-Beshbishy, Ayman A-El-Badry and Moussa Alkhalaf

*Pakistan Journal of Biological Sciences*, 16: 1744-1750 (2013)

Labiatae family is represented in Saudi Arabia. The aim of the present study was to go insight to investigate the anticancer activity and antioxidative potentials of methanolic extracts of *Mentha longifolia* L. (ML) and *Ocimum basilicum* L. (OB) that grown in Madina province, western region, Saudi Arabia. OB exhibited the greater phenolic contents as mg gallic acid equivalent/g weight (mg GAE/g) for a value of  $105 \pm 5.5$  mg GAE/g. on the other hand, ML produced  $29 \pm 3.12$  mg GAE/g. The standard antioxidant vitamin E used in this experiment elicited a value of total phenolic contents equal  $22 \pm 2.2$  mg GAE/g. The percentage scavenging activity of against diphenylpicrylhydrazyl (DPPH.) was 850 and 160% for OB and ML extracts, respectively. Vitamin E elicited% scavenging activity of against DPPH. equal to 198%. Brine shrimp cytotoxic assay clearly indicated the cytotoxic effects of either ML or OB extract. The brine shrimp survival is inversely proportional to the concentration of either ML or OB extract used with LD50 191.23 and 235.50 ppm, respectively. Toxic effects on brine shrimps indicated the anticancer potential of ML or OB extract. The ML or OB extract was unable to produce pbluescript (pBS) plasmid DNA damage, while the plasmid DNA treated with EcoRI produced a single band as a result of DNA damage. Also, both ML and OB extract exhibited marked cytotoxic activity against MCF-7 cells at various concentrations (20, 40, 80, 160 and 320  $\mu$ g mL<sup>-1</sup>). The 160 and 320  $\mu$ g mL<sup>-1</sup> showed more cytotoxic effect against MCF-7 cells. Based on results achieved, we can concluded that, OB and ML extracts have the potency to act as powerful antioxidants and protect against DNA damage and have cytotoxic activity against MCF-7 cell line.

**Keywords:** Cytotoxic activity; *Mentha longifolia*; *Ocimum basilicum*; Breast cancer.

### Dept. of Pathology

### 1212. E-Education for Medical Students Using Wsi in Egypt

Essam Ayad

*Diagnostic Pathology*, 8 (suppl 1): 1-5 (2013) IF: 1.85

**Background:** Classic education of pathology for Medical students in emerging countries with limited resources faces many obstacles because of equipment cost and small laboratories which are not suitable for the large number of the students. Digital Pathology may provide ideal solutions.

**Methods:** We scanned the whole set of the slides used for teaching practical pathology sessions for third year medical students using the Whole Slide Image [WSI] technique. We upload all this digital material on the computer network in the pathology department or the Grand Student Library in the Faculty of Medicine, Cairo University. A group of our medical students viewed digital pathology slides either in the pathology department or the library using the computer network or their iPad tablet device. They were allowed to view it at home through connecting

the server at the Grand Student Library in the Faculty of Medicine, Cairo University. We reported student experience with virtual slides on a local network and a remote image server. Furthermore we compared the results of the digital exam with the classic exam [using glass slides & microscope].

**Results:** The quality of images of the scanned slides was very good. Comparing the different ways for viewing the slides, we found the best method was using the computer network in the computer lab in the pathology or in the Grand Student Library, it was evidently faster and preferred by the participants in this study, followed by using the iPad tablet device in the library then viewing it at home through accessing the server at the Grand Student Library. The grades of the students using the virtual slides beside the glass slides were much higher than those using the glass slides & microscope only.

**Conclusions:** Using the WSI Virtual slides for Medical Students learning can be the best solution for equipment and technical obstacles and could enhance student learning in emerging countries with limited resources.

**Keywords:** Digital pathology; Virtual slide; Wsi; Medical education; E-education; Egypt.

### 1213. Immunohistochemical Expression of C-Kit in Fibroepithelial Tumors of Breast

Rasha A. Hammad, Mohamed F. Darweesh, Walid M. Sharaf Reham S.E. Esmail, Abdel Razik Farrag and Menar M. Ayoub

*World Journal of Medical Sciences*, 8 ( 3): 170-176 (2013)

Fibroadenomas are the most common breast tumors. Phyllodes tumors are a fibroepithelial tumor composed of an epithelial and a cellular stromal component.

They may be considered benign, borderline, or malignant depending on histologic features. CD117, also called KIT or C-kit receptor, is a proto-oncogene that its expression or mutations can lead to cancer. C-kit shows stromal expression in malignant phyllodes tumors. The present study included thirty fibroepithelial breast tumor cases.

This work aimed to study the expression of C-kit in fibroepithelial tumors of the breast and its relation with their clinicopathological parameters. According to our results, there was a progressive increase in C-kit expression from benign to malignant tumors, all cases of fibroadenomas were negative for C-kit [except for one case showed weak staining (score 1)].

All cases of phyllodes tumor showed positive staining with variable degrees of intensity. The difference in results of the immunostaining between fibroadenomas and phyllodes tumors were statistically significant ( $P=0.001$ ). Within the phyllodes tumor cases score1 immunostaining was seen in 80 % of the benign cases, only one benign phyllodes tumor case showed moderate staining score 2. The malignant cases showed moderate immunostaining (score 2) in 40 % of the cases and strong staining (score 3) pattern in 60 % of the malignant cases. The borderline cases showed score 2 in 60 % of cases and score 3 in 40 % of these cases. in conclusion, the notable increase in C-kit expression in the mammary fibroepithelial tumors provides strong evidence that C-kit receptor mediated tyrosine kinase involvement in the pathogenesis of phyllodes tumors and the therapeutic agent, tyrosine inhibitor (Glivec) may be a potentially useful drug for management or preventing their recurrence.

**Keywords:** Fibroepithelial; Tumors; Breast Cd 117.

### 1214. Immunohistochemical Expression of Cyclin D1 in Egyptian Patients with Prostatic Carcinoma

Ilia Anis, Hala Naguib Hosni, Mohammed F. Darweesh and Marwa Abd El Rahman

*World Journal of Medical Sciences, 8 (4): 306-313 (2013)*

Prostatic carcinoma is a common and growing public health problem. Cyclin D1 is a cell regulatory protein, which is believed to play an important role in both tumorigenesis and grading of many cancers. The role of Cyclin D1 as a prognostic factor in cancer prostate is controversial. The present study was done on a total of forty cases of prostatic carcinoma removed by radical prostatectomy. Immunohistochemical expression of Cyclin D1 was evaluated in all cases. Correlation between the intensity of Cyclin D1 expression and patient's age, serum PSA level, PIN, Gleason grades, Gleason scores and stages of prostatic carcinoma was evaluated. All cases (100%) revealed foci (>10 % of cancer cells) with positive nuclear staining for Cyclin D1 with different grades of intensity ranging from moderate to strong, while positive Cyclin D1 expression was observed in the nuclei of PIN of 30 cases with grades of intensity ranging from weak to strong. No significant correlation was found between the intensity of Cyclin D1 expression and patient's age, PIN, Gleason grades, Gleason scores or stages of prostatic carcinoma, while a significant correlation between intensity of expression of Cyclin D1 and preoperative serum PSA level was observed. Cyclin D1 expression might affect PSA expression, which is considered an important tumor marker. Cyclin D1 plays an important role in the pathogenesis and evolution of prostate cancer rather than the prognosis, thus Cyclin D1 is not a reliable prognostic factor in cancer prostate.

**Keywords:** Immunohistochemical cyclin D1; Egyptian prostatic carcinoma.

#### Dept. of Pediatrics

### 1215. ANKS6 is A Central Component of A Nephronophthisis Module Linking NEK8 to INVS and NPHP3

Sylvia Hoff, Jan Halbritter, Daniel Epting, Valeska Frank, Thanh-Minh T Nguyen, Jeroen van Reeuwijk, Christopher Boehlke, Christoph Schell, Takayuki Yasunaga, Martin Helmstädter, Miriam Mergen, Emilie Filhol, Karsten Boldt, Nicola Horn, Marius Ueffing, Edgar A Otto, Tobias Eisenberger, Mariet W Elting, Joanna A E van Wijk, Detlef Bockenhauer, Neil J Sebire, Søren Rittig, Mogens Vyberg, Troels Ring, Martin Pohl, Lars Pape, Thomas J Neuhaus, Neveen A Soliman Elshakhs, Sarah J Koon, Peter C Harris, Florian Grahmmer, Tobias B Huber, E Wolfgang Kuehn, Albrecht Kramer-Zucker, Hanno J Bolz, Ronald Roepman, Sophie Saunier, Gerd Walz, Friedhelm Hildebrandt, Carsten Bergmann and Soeren S Lienkamp

*Nature Genetics, 45: 951-956 (2013) IF: 35.209*

Nephronophthisis is an autosomal recessive cystic kidney disease that leads to renal failure in childhood or adolescence. Most NPHP gene products form molecular networks. Here we identify ANKS6 as a new NPHP family member that connects NEK8 (NPHP9) to INVS (NPHP2) and NPHP3. We show that ANKS6 localizes to the proximal cilium and confirm its role in renal development through knockdown experiments in zebrafish and

*Xenopus laevis*. We also identify six families with ANKS6 mutations affected by nephronophthisis, including severe cardiovascular abnormalities, liver fibrosis and situs inversus. The oxygen sensor HIF1AN hydroxylates ANKS6 and INVS and alters the composition of the ANKS6-INVS-NPHP3 module. Knockdown of Hif1an in *Xenopus* results in a phenotype that resembles loss of other NPHP proteins. Network analyses uncovered additional putative NPHP proteins and placed ANKS6 at the center of this NPHP module, explaining the overlapping disease manifestation caused by mutation in ANKS6, NEK8, INVS or NPHP3.

**Keywords:** Nephronophthisis; Nephrocystin; Molecular genetics; ANKS6; Ciliopathy; Phenotype.

### 1216. AMPD2 Regulates GTP Synthesis and is Mutated in A Potentially Treatable Neurodegenerative Brainstem Disorder

Naiara Akizu, Vincent Cantagrel, Jana Schroth, Na Cai, Keith Vaux, Douglas McCloskey, Robert K. Naviaux, Jeremy Van Vleet, Ali G. Fenstermaker, Jennifer L. Silhavy, Judith S. Scheliga, Keiko Toyama, Hiroko Morisaki, Fatma M. Sonmez, Figen Celep, Azza Oraby, Maha S. Zaki, Raidah Al-Baradie, Eissa A. Faqeh, Mohammed A.M. Saleh, Emily Spencer, Rasim Ozgur Rosti, Eric Scott, Elizabeth Nickerson, Stacey Gabriel, Takayuki Morisaki, Edward W. Holmes and Joseph G. Gleeson

*Cell, 154/3: 505-517 (2013) IF: 31.975*

Purine biosynthesis and metabolism, conserved in all living organisms, is essential for cellular energy homeostasis and nucleic acid synthesis. The de novo synthesis of purine precursors is under tight negative feedback regulation mediated by adenosine and guanine nucleotides. We describe a distinct early-onset neurodegenerative condition resulting from mutations in the adenosine monophosphate deaminase 2 gene (AMPD2). Patients have characteristic brain imaging features of pontocerebellar hypoplasia (PCH) due to loss of brainstem and cerebellar parenchyma. We found that AMPD2 plays an evolutionary conserved role in the maintenance of cellular guanine nucleotide pools by regulating the feedback inhibition of adenosine derivatives on de novo purine synthesis. AMPD2 deficiency results in defective GTP-dependent initiation of protein translation, which can be rescued by administration of purine precursors. These data suggest AMPD2-related PCH as a potentially treatable early-onset neurodegenerative disease.

**Keywords:** GTP synthesis; AMPD2; Neurodegenerative Brainstem disorder.

### 1217. ARHGDI3 Mutations Cause Nephrotic Syndrome Via Defective Rho GTPase Signaling

Heon Yung Gee, Pawaree Saisawat, Shazia Ashraf, Toby W. Hurd, Virginia Vega-Warner, Humphrey Fang, Bodo B. Beck, Olivier Gribouval, Weibin Zhou, Katrina A. Diaz, Sivakumar Natarajan, Roger C. Wiggins, Svjetlana Lovric, Gil Chernin, Dominik S. Schoeb, Bugsu Ovunc, Yaacov Frishberg, Neveen A. Soliman, Hanan M. Fathy et al.

*Journal of Clinical Investigation, 123: 3243-3253 (2013) IF: 12.812*

Nephrotic syndrome (NS) is divided into steroid-sensitive (SSNS) and-resistant (SRNS) variants. SRNS causes end-stage kidney disease, which cannot be cured. While the disease mechanisms of NS are not well understood, genetic mapping studies suggest a multitude of unknown single-gene causes. We combined homozygosity mapping with whole-exome resequencing and identified an ARHGDIA mutation that causes SRNS. We demonstrated that ARHGDIA is in a complex with RHO GTPases and is prominently expressed in podocytes of rat glomeruli. ARHGDIA mutations (R120X and G173V) from individuals with SRNS abrogated interaction with RHO GTPases and increased active GTP-bound RAC1 and CDC42, but not RHOA, indicating that RAC1 and CDC42 are more relevant to the pathogenesis of this SRNS variant than RHOA. Moreover, the mutations enhanced migration of cultured human podocytes; however, enhanced migration was reversed by treatment with RAC1 inhibitors.

The nephrotic phenotype was recapitulated in arhgdia-deficient zebrafish. RAC1 inhibitors were partially effective in ameliorating arhgdia-associated defects. These findings identify a single-gene cause of NS and reveal that RHO GTPase signaling is a pathogenic mediator of SRNS.

**Keywords:** Nephrotic syndrome; Arhgdia mutation; Zebrafish; Genetics.

#### 1218. International Survey Of T2\* Cardiovascular Magnetic Resonance In B-Thalassemia Major

Amal Mohamed Ibrahim El Beshlawy

*Haematologica*, 98(9): 1368-1374 (2013) IF: 5.935

Accumulation of myocardial iron is the cause of heart failure and early death in most transfused thalassemia major patients. T2\* cardiovascular magnetic resonance provides calibrated, reproducible measurements of myocardial iron.

However, there are few data regarding myocardial iron loading and its relation to outcome across the world. A survey is reported of 3,095 patients in 27 worldwide centers using T2\* cardiovascular magnetic resonance.

Data on baseline T2\* and numbers of patients with symptoms of heart failure at first scan (defined as symptoms and signs of heart failure with objective evidence of left ventricular dysfunction) were requested together with more detailed information about patients who subsequently developed heart failure or died. At first scan, 20.6% had severe myocardial iron ( $T2^* \leq 10$ ms), 22.8% had moderate myocardial iron ( $T2^* 10$ -20ms) and 56.6% of patients had no iron loading ( $T2^* > 20$ ms). There was significant geographical variation in myocardial iron loading (24.8-52.6%;  $P < 0.001$ ). At first scan, 85 (2.9%) of 2,915 patients were reported to have heart failure (81.2% had  $T2^* < 10$ ms; 98.8% had  $T2^* < 20$ ms).

During follow up, 108 (3.8%) of 2,830 patients developed new heart failure. Of these, T2\* at first scan had been less than 10ms in 96.3% and less than 20ms in 100%.

There were 35 (1.1%) cardiac deaths. Of these patients, myocardial T2\* at first scan had been less than 10ms in 85.7% and less than 20ms in 97.1%. Therefore, in this worldwide cohort of thalassemia major patients, over 43% had moderate/severe myocardial iron loading with significant geographical differences, and myocardial T2\* values less than 10ms were strongly associated with heart failure and death.

#### 1219. Identification of 99 Novel Mutations in A Worldwide Cohort of 1,056 Patients with A Nephronophthisis-Related Ciliopathy

Jan Halbritter, Jonathan D. Porath, Katrina A. Diaz, Daniela A. Braun, Stefan Kohl, Moumita Chaki, Susan J. Allen, Neveen A. Soliman, Friedhelm Hildebrandt and Edgar A. Otto

*Human Genetics*, 132: 865-884 (2013) IF: 4.633

Nephronophthisis-related ciliopathies (NPHP – RC) are autosomal-recessive cystic kidney diseases. More than 13 genes are implicated in its pathogenesis to date, accounting for only 40 % of all cases. High-throughput mutation screenings of large patient cohorts represent a powerful tool for diagnostics and identification of novel NPHP genes. We here performed a new high-throughput mutation analysis method to study 13 established NPHP genes (NPHP1-NPHP13) in a worldwide cohort of 1,056 patients diagnosed with NPHP-RC. We first applied multiplexed PCR-based amplification using Fluidigm Access-Array™ technology followed by barcoding and next-generation resequencing on an Illumina platform. As a result, we established the molecular diagnosis in 127/1,056 independent individuals (12.0 %) and identified a single heterozygous truncating mutation in an additional 31 individuals (2.9 %). Altogether, we detected 159 different mutations in 11 out of 13 different NPHP genes, 99 of which were novel. Phenotypically most remarkable were two patients with truncating mutations in INVS/NPHP2 who did not present as infants and did not exhibit extrarenal manifestations. In addition, we present the first case of Caroli disease due to mutations in WDR19/NPHP13 and the second case ever with a recessive mutation in GLIS2/NPHP7. This study represents the most comprehensive mutation analysis in NPHP-RC patients, identifying the largest number of novel mutations in a single study worldwide.

**Keywords:** Nephronophthisis; Ciliopathy; High throughput mutation; Genetics.

#### 1220. Phase I, Open-Label, Single-Dose Study to Evaluate the Pharmacokinetics and Safety of Telbivudine in Children and Adolescents With Chronic Hepatitis B (Team)

Mortada Hassan Fakhri El-Shabrawi

*Antimicrobial Agents And Chemotherapy (AAC)*, 57: 4128-4133 (2013) IF: 4.565

Telbivudine is a nucleoside analogue that has been approved for the treatment of chronic hepatitis B virus (HBV) infection in adults at 600 mg/day. We conducted a phase I, open-label, first-in-pediatrics study to investigate the safety and pharmacokinetics of a single dose of telbivudine in HBV-infected children and adolescents. Eligible patients were enrolled sequentially from older to younger groups, with evaluation of safety and available pharmacokinetic data after each stratum. Adolescent patients (>12 to 18 years) received a single dose of 600 mg telbivudine as an oral solution, while children aged 2 to 12 years received a single dose of 15 or 25 mg/kg of body weight up to a maximum of 600 mg. Telbivudine was well tolerated; all adverse events were mild, and none occurred in more than one patient. The plasma telbivudine concentration-versus-time profiles in adolescents given 600 mg were similar to the mean profile of healthy adults



receiving the same oral dose. Children aged 2 to <6 and 6 to 12 years receiving a single 15-mg/kg dose showed similar plasma exposures. To predict the steady-state exposure, plasma concentration- versus-time profiles for patients aged 2 to 12 years (15 mg/kg) and >12 to 18 years (600 mg) were fitted to a two-compartment 1st-order, microconstant, lag time, 1st-order elimination pharmacokinetic (PK) model. This analysis predicted the following dosages to mimic exposures in healthy adults receiving 600 mg/day: 20 mg/kg/day for children 2 to 12 years and 600 mg/day for adolescents. Studies are ongoing to evaluate the efficacy of the recommended dose in pediatric patients. (This study has been registered at ClinicalTrials.gov under registration no. NCT00907894.)

**Keywords:** Telbivudine; HBV.

### 1221. A Dose-Escalation Phase Iia Study of 2,2-Dimethylbutyrate (HQB-1001), an Oral Fetal Globin Inducer, in Sickle Cell Disease

Abdullah Kutlar, Marvin E. Reid, Adlette Inati, Ali T. Taher, Miguel R. Abboud, Amal El-Beshlawy, George R. Buchanan, Hedy Smith, Kenneth I. Ataga, Susan P. Perrine and Richard G. Ghalie

*American Journal of Hematology*, 255-260 (2013) IF: 4.138

2, 2- dimethylbutyrate (HQB-1001), an orally-bioavailable promoter-targeted fetal globin gene-inducing agent, was evaluated in an open-label, randomized dose-escalation study in 52 subjects with hemoglobin SS or S/b 0 thalassemia. HQB-1001 was administered daily for 26 weeks at 30 mg/kg (n515), 40 mg/kg (n518) and 50 mg/kg (n519), either alone (n521) or with hydroxyurea (n531). The most common drug-related adverse events were usually mild or moderate and reversible. Gastritis was graded as severe in three subjects at 40 mg/kg and was considered the dose-limiting toxicity. Subsequently all subjects were switched to the maximum tolerated dose of 30 mg/kg. Due to early discontinuations for blood transfusions, adverse events or non-compliance, only 25 subjects (48%) completed the study. Drug plasma concentrations were sustained above targeted levels at 30 mg/kg. Increases in fetal hemoglobin (Hb F) were observed in 42 subjects (80%), and 12 (23%) had increases4%. The mean increase in Hb F was 2% [95% confidence interval (CI), 0.8–3.2%] in 21 subjects receiving HQB-1001 alone and 2.7% (95% CI, 1.7–3.8%) in 31 subjects receiving HQB-1001 plus hydroxyurea. Total hemoglobin increased by a mean of 0.65 g/dL (95% CI, 0.5–1.0 g/dL), and 13 subjects (25%) had increases1 g/dL. Future studies are warranted to evaluate the therapeutic potential of HQB-1001in sickle cell disease. *Am. J. Hematol.* 88:E255–E260, 2013.VC 2013 Wiley Periodicals, Inc.

**Keywords:** 2,2-Dimethylbutyrate; Fetal Globin Inducer; Sickle Cell Disease.

### 1222. Modifiable Diarrhoea Risk Factors in Egyptian Children Aged <5 Years

Mortada Hassan Fakhri El-Shabrawi, A. M. Mansour, H. El Mohammady, M. El Shabrawi, S. Y. Shabaan, M. Abou Zekri, M. Nassar, M. E. Salem, M. Mostafa, M. S. Riddle, J.D. Klena, I.A. Abdel Messih, S. Levin and S. Y. N. Young

*Epidemiology and Infection*, 141: 2547-2559 (2013) IF: 2.867

**Summary:** By conducting a case-control study in two university hospitals, we explored the association between modifiable risk behaviours and diarrhoea. Children aged <5 years attending outpatient clinics for diarrhoea were matched by age and sex with controls. Data were collected on family demographics, socioeconomic indicators, and risk behaviour practices. Two rectal swabs and a stool specimen were collected from cases and controls. Samples were cultured for bacterial pathogens using standard techniques and tested by ELISA to detect rotavirus and *Cryptosporidium* spp. Four hundred cases and controls were enrolled between 2007 and 2009. The strongest independent risk factors for diarrhoea were: presence of another household member with diarrhoea [matched odds ratio (mOR) 4.9, 95% CI 2.8-8.4] in the week preceding the survey, introduction to a new kind of food (mOR 3, 95% CI 1.7-5.4), and the child being cared for outside home (mOR 2.6, 95% CI 1.3-5.2). While these risk factors are not identifiable, in some age groups more easily modifiable risk factors were identified including: having no soap for handwashing (mOR 6.3, 95% CI 1.2-33.9) for children aged 7-12 months, and pacifier use (mOR 1.9, 95% CI 1.0-3.5) in children aged 0-6 months. In total, the findings of this study suggest that community-based interventions to improve practices related to sanitation and hygiene, handwashing and food could be utilized to reduce the burden of diarrhoea in Egyptian children aged <5 years.

**Keywords:** Diarrhoea.

### 1223. Efficacy and Safety of Deferasirox at Low and High Iron Burdens: Results from the EPIC Magnetic Resonance Imaging Substudy

J. B. Porter, M. S. Elalfy, A. T. Taher, Y. Aydinok, L. L. Chan, S.-H. Lee, P. Sutcharitchan, D. Habr, N. Martin and A. El-Beshlawy

*Annals of Hematology*, 92:211-219 (2013) IF: 2.866

The effect of deferasirox dosing tailored for iron burden and iron loading based on liver iron concentration (LIC) was assessed over 1 year in less versus more heavily iron-overloaded patients in a substudy of the Evaluation of Patients' Iron Chelation with Exjade®. Deferasirox starting dose was 10–30 mg/kg/day, depending on blood transfusion frequency, with recommended dose adjustments every 3 months. Therapeutic goals were LIC maintenance or reduction in patients with baseline LIC <7 or =7 mg Fe/g dry weight (dw), respectively. Changes in LIC (R2-magnetic resonance imaging) and serum ferritin after 1 year were assessed. Adverse events (AEs) and laboratory parameters were monitored throughout. Of 374 patients, 71 and 303 had baseline LIC <7 and =7 mg Fe/g dw, respectively; mean deferasirox doses were 20.7 and 27.1 mg/kg/day (overall average time to dose increase, 24 weeks). At 1 year, mean LIC and median serum ferritin levels were maintained in the low-iron cohort (-0.02±2.4 mg Fe/g dw, -57 ng/mL; P0not significant) and significantly decreased in the high-iron cohort (-6.1±9.1 mg Fe/g dw, -830 ng/mL; P<0.0001). Drug-related gastrointestinal AEs, mostly mild to moderate, were more frequently reported in the <7 versus =7 mg Fe/g dw cohort (39.4 versus 20.8 %; P00.001) and were not confounded by diagnosis, dosing, ethnicity, or hepatitis B and/or C history. Reported serum creatinine increases did not increase in low- versus high-iron cohort patients. Deferasirox doses of 20 mg/kg/day maintained LIC <7 mg Fe/g dw and doses of 30 mg/kg/day were required for net iron reduction in the high-iron cohort, with clinically manageable safety profiles. The higher



incidence of gastrointestinal AEs at lower iron burdens requires further investigation.

**Keywords:** Iron overload; Iron chelation Therapy; Deferasirox; Liver iron concentration.

#### 1224. Neonatal Hyperbilirubinemia and Rhesus Disease of the Newborn: Incidence and Impairment Estimates for 2010 at Regional and Global Levels

Vinod K. Bhutani, Alvin Zipursky, Hannah Blencowe, Rajesh Khanna, Michael Sgro, Finn Ebbesen, Jennifer Bell, Rintaro Mori, Tina M. Slusher, Nahed Fahmy, Vinod K. Paul, Lizhong Du, Angela A. Okolo, Maria-Fernanda de Almeida, Bolajoko O. Olusanya, Praveen Kumar, Simon Cousens and Joy E. Lawn

*Pediatric Research*, 74: 86-100 (2013) IF: 2.673

**Background:** Rhesus (Rh) disease and extreme hyperbilirubinemia (EHB) result in neonatal mortality and long term neurodevelopmental impairment, yet there are no estimates of their burden.

**Methods:** Systematic reviews and meta-analyses were undertaken of national prevalence, mortality, and kernicterus due to Rh disease and EHB. We applied a compartmental model to estimate neonatal survivors and impairment cases for 2010.

**Results:** Twenty-four million (18% of 134 million live births = 32 wk gestational age from 184 countries; uncertainty range: 23–26 million) were at risk for neonatal hyperbilirubinemia-related adverse outcomes. Of these, 480,700 (0.36%) had either Rh disease (373,300; uncertainty range: 271,800–477,500) or developed EHB from other causes (107,400; uncertainty range: 57,000–131,000), with a 24% risk for death (114,100; uncertainty range: 59,700 – 172,000), 13% for kernicterus (75,400), and 11% for stillbirths. Three-quarters of mortality occurred in sub-Saharan Africa and South Asia. Kernicterus with Rh disease ranged from 38, 28, 28, and 25/ 100,000 live births for Eastern Europe/Central Asian, sub-Saharan African, South Asian, and Latin American regions, respectively. More than 83% of survivors with kernicterus had one or more impairments.

**Conclusion:** Failure to prevent Rh sensitization and manage neonatal hyperbilirubinemia results in 114,100 avoidable neonatal deaths and many children grow up with disabilities. Proven solutions remain underused, especially in low-income countries.

**Keywords:** Neonatal hyperbilirubinemia; Rhesus disease.

#### 1225. Burden of Pediatric Hepatitis C

Mortada Hassan El-Shabrawi and Naglaa Mohamed Kamal Alanani

*World J. of Gastroenterology*, 19: 7880-7888 (2013) IF: 2.547

Hepatitis C virus (HCV) is a major health burden infecting 170-210 million people worldwide. Additional 3-4 millions are newly-infected annually. Prevalence of pediatric infection varies from 0.05%-0.36% in the United States and Europe; up to 1.8%-5.8% in some developing countries. The highest prevalence occurs in Egypt, sub-Saharan Africa, Amazon basin and Mongolia. HCV has been present in some populations for several centuries, notably genotypes 1 and 2 in West Africa. Parenteral anti-schistosomiasis therapy practiced in the 1960s until the early 1980s had spread HCV infection throughout Egypt. Parenteral acquisition of HCV remains a major route for infection among

Egyptian children. Insufficient screening of transfusions, unsterilized injection equipment and re-used needles and syringes continue to be major routes of HCV transmission in developing countries, whereas vertical transmission and adolescent high-risk behaviors (e.g., injection drug abuse) are the major routes in developed countries.

The risk of vertical transmission from an infected mother to her unborn/newborn infant is approximately 5%. Early stages of HCV infection in children do not lead to marked impairment in the quality of life nor to cognitive, behavioral or emotional dysfunction; however, caregiver stress and family system strain may occur. HCV slowly progresses to serious complications as cirrhosis (1%-2%) and hepatocellular carcinoma (HCC) especially in the presence of risk factors as hemolytic anemias, obesity, treated malignancy, and concomitant human immune deficiency and/or hepatitis B virus co-infection. HCV vaccine remains elusive to date. Understanding the immune mechanisms in patients who successfully cleared the infection is essential for vaccine development.

The pediatric standard of care treatment consists of pegylated interferon- $\alpha$  2a or b plus ribavirin for 24-48 wk. The new oral direct acting antivirals, approved for adults, need further evaluation in children. Sustained virologic response varies depending on the viral load, genotype, duration of infection, degree of aminotransferase elevation, adiposity and single nucleotide polymorphisms of interleukin (IL)-28B locus. The goals of treatment in individual patients are virus eradication, prevention of cirrhosis and HCC, and removing stigmatization; meanwhile the overall goal is decreasing the global burden of HCV. IL-28B polymorphisms have been also associated with spontaneous clearance of vertically acquired HCV infection.

The worldwide economic burden of HCV for children, families and countries is estimated to be hundreds of millions of US dollars per year.

The United States, alone, is estimated to spend 199-336 million dollars in screening, monitoring and treatment during one decade. The emotional burden of having an HCV infected child in a family is more difficult to estimate.

**Keywords:** Hepatitis C Virus; Burden; Genotypes; Cost; Pediatrics.

#### 1226. Stenting the Arterial Duct in Neonates and Infants with Congenital Heart Disease and Duct-Dependent Pulmonary Blood Flow: A Multicenter Experience of an Evolving Therapy Over 18 Years

Floris E.A. Udink ten Cate, Narayanswami Sreeram, Hala Hamza Hala Agha, Eric Rosenthal and Shakeel A. Qureshi

*Catheterization and Cardiovascular Interventions*, 82(3): 233-243 (2013) IF: 2.514

**Objectives:** The primary aim of this multi-institutional study was to describe our 18-year experience of ductal stenting (DS) in infants with a duct-dependent pulmonary circulation. The secondary aim sought to identify a subgroup of patients who may benefit the most using this evolving technique.

**Background:** No study has examined the extraordinary evolution of this promising therapy over the last two decades.

**Methods:** Between 1991 and 2009, 65 neonates and infants (39 male, 60%) underwent cardiac catheterization for DS in 3 participating centres. Patients were divided according to whether

DS was attempted between 1991–2000 (Group 1, n = 20) or between 2001–2009 (Group 2, n = 45).

**Results:** DS was successful in 52/65 (80%) patients. DS outcome was associated with ductal morphology and cardiac diagnosis. DS failed more often in patients with univentricular physiology and tortuous duct morphology ( $p < 0.001$ ). Most patients undergoing DS in Group 2 had pulmonary atresia with intact ventricular septum (PAIVS) ( $p < 0.001$ ). DS was successful in 94% of these patients.

Groups differed significantly in diameter and length of first implanted stent ( $p < 0.001$ ), implanting additional stent ( $p < 0.001$ ), and occurrence of complications ( $p = 0.033$ ). Freedom from re-intervention for the 52 patients was 92.3%. No procedure-related mortality occurred.

**Conclusions:** The technical aspects and clinical application of percutaneous DS has changed in the last two decades. DS has become a practical and safe therapy in a subgroup of neonates with ductal-dependent pulmonary blood flow. © 2013 Wiley Periodicals, Inc.

**Keywords:** Arterial duct; Stenting; Congenital heart disease; Tortuous duct; Cardiac catheterization; Intervention.

### 1227. Serial Echocardiographic Left Ventricular Ejection Fraction Measurements: A Tool for Detecting Thalassemia Major Patients at Risk of Cardiac Death

Aurelio Maggio, Angela Vitrano, Giuseppina Calvaruso, Rita Barone, Paolo Rigano Luigi Mancuso Liana Cuccia, Marcello Capra, Lorella Pitrolo, Luciano Prossomariti, Aldo Filosa, Vincenzo Caruso, Calogera Gerardi, Saveria Campisi, Paolo Cianciulli Androulla Eleftheriou, Michel Angastiniotis, Hala Hamza, Paul Telfer, John Malcolm Walker, Arintaya Phrommintikul and Nipon Chattipakorn

*Blood Cells, Molecules, and Diseases*, 50 (4): 241-246 (2013) IF: 2.259

Cardiac damage remains a major cause of mortality among patients with thalassemia major. The detection of a lower cardiac magnetic resonance T2 (CMR-T2) signal has been suggested as a powerful predictor of the subsequent development of heart failure. However, the lack of worldwide availability of CMR-T2 facilities prevents its widespread use for follow-up evaluations of cardiac function in thalassemia major patients, warranting the need to assess the utility of other possible procedures. In this setting, the determination of left ventricular ejection fraction (LVEF) offers an accurate and reproducible method for heart function evaluation. These findings suggest a reduction in LVEF = 7%, over time, determined by 2-D echocardiography, may be considered a strong predictive tool for the detection of thalassemia major patients with increased risk of cardiac death. The reduction of LVEF = 7% had higher (84.76%) predictive value. Finally, Kaplan–Meier survival curves of thalassemia major patients with LVEF = 7% showed a statistically significant decreased probability of survival for heart disease ( $p = 0.0022$ ). However, because of limitations related to the study design, such findings should be confirmed in a large long-term prospective clinical trial.

**Keywords:** Thalassemia major; Left ventricular ejection fraction (LVEF); Chelation; Echocardiography; Cardiac magnetic resonance; T2.

### 1228. Association Between PM<sub>10</sub> Exposure and Sleep of Egyptian School Children

Maha K. Abou-Khadra

*Sleep and Breathing*, 17: 653-657 (2013) IF: 2.256

**Purpose:** This study aims to investigate the potential association between exposure to particulate matter with an aerodynamic diameter  $< 10 \mu\text{m}$  (PM<sub>10</sub>) and sleep disturbances among Egyptian school children.

**Methods:** In this cross-sectional study, parents of school children from four elementary schools in areas with different PM<sub>10</sub> exposures filled out the Sleep Disturbance Scale for Children questionnaire in Arabic. Air pollution data were obtained from the Egyptian Environmental Affairs Agency.

**Results:** The sample consisted of 276 children, 121 (44 %) of them were boys with a mean age of  $9.26 \pm 1.96$  years. Disorders of initiating and maintaining sleep (DIMS), disorders of excessive somnolence, and the total score were reported in the clinical range (T score  $> 70$ ) in 19.9, 24.3, and 24.3 % of the sample, respectively. A generalized additive model with adjustment for potential confounding factors was used to examine the association between PM<sub>10</sub> exposure and sleep disturbances. There were statistically significant associations between PM<sub>10</sub> exposure and DIMS and sleep hyperhidrosis ( $P < 0.05$ ).

**Conclusions:** Air pollution exposure has a negative impact on children's sleep with significant association between exposure to PM<sub>10</sub> and sleep disturbances.

**Keywords:** Air pollution; Sleep problems.

### 1229. Parent-Reported Sleep Problems, Symptom Ratings, and Serum Ferritin Levels in Children with Attention-Deficit/Hyperactivity Disorder: A Case Control Study

Maha K Abou-Khadra, Omnia R. Amin, Olfat G. Shaker and Thanaa M. Rabah

*Bmc Pediatrics*, 13: 217-222 (2013) IF: 1.982

**Background:** Sleep problems are common among children with attention-deficit/hyperactivity disorder (ADHD). Serum ferritin levels have been associated with the severity of symptoms and sleep disturbances among children with ADHD. This study was conducted to investigate parent-reported sleep problems in a sample of Egyptian children with ADHD and to examine the relationship between their sleep, symptom-ratings, and low serum ferritin levels.

**Methods:** Parents of 41 ADHD children, aged 6 to 12 years, filled out the Children's Sleep Habits Questionnaire (CSHQ) and Conners' Parent Rating Scale-Revised: Long Version (CPRS-R:L) in Arabic. Serum ferritin levels were determined with an enzyme-linked immunosorbent assay. The parents of the 62 controls filled out the CSHQ.

**Results:** The ADHD group showed significantly higher scores in CSHQ subscales and total score. Children with serum ferritin levels  $< 30 \text{ ng/mL}$  had more disturbed sleep. There were significant negative correlations between sleep duration subscale, total score of CSHQ, and serum ferritin levels. There were no significant differences in hyperactivity, cognitive problems/inattention, oppositional, or ADHD index subscale scores between children with serum ferritin levels  $< 30 \text{ ng/mL}$  and those with serum ferritin levels  $\geq 30 \text{ ng/mL}$ .

**Conclusions:** Sleep problems are common, and this study suggests an association between low serum ferritin levels and sleep disturbances.

**Keywords:** Adhd; Ferritin levels; Sleep.

### 1230. Revised Recommendations for the Management of Gaucher Disease in Children

Paige Kaplan, Hagit Baris, Linda De Meirleir, Maja Di Rocco, Amal El-Beshlawy, Martina Huemer, Ana Maria Martins, Ioana Nascu, Marianne Rohrbach, Lynne Steinbach and Ian J. Cohen

*Eur J Pediatr*, 172: 447-458 (2013) IF: 1.907

Gaucher disease is an inherited pan-ethnic disorder that commonly begins in childhood and is caused by deficient activity of the lysosomal enzyme glucocerebrosidase. Two major phenotypes are recognized: non-neuropathic (type 1) and neuropathic (types 2 and 3). Symptomatic children are severely affected and manifest growth retardation, delayed puberty, early-onset osteopenia, significant splenomegaly, hepatomegaly, thrombocytopenia, anemia, severe bone pain, acute bone crises, and fractures. Symptomatic children with types 1 or 3 should receive enzyme replacement therapy, which will prevent debilitating and often irreversible disease progression and allow those with non-neuropathic disease to lead normal healthy lives. Children should be monitored every 6 months (physical exam including growth, spleen and liver volume, neurologic exam, hematologic indices) and have one to two yearly skeletal assessments (bone density and imaging, preferably with magnetic resonance, of lumbar vertebrae and lower limbs), with specialized cardiovascular monitoring for some type 3 patients. Response to treatment will determine the frequency of monitoring and optimal dose of enzyme replacement. Treatment of children with type 2 (most severe) neuropathic Gaucher disease is supportive. Pre-symptomatic children, usually with type 1 Gaucher, increasingly are being detected because of affected siblings and screening in high-prevalence communities. In this group, annual examinations (including bone density) are recommended. However, monitoring of asymptomatic children with affected siblings should be guided by the age and severity of manifestations in the first affected sibling. Treatment is necessary only if signs and symptoms develop.

**Conclusion:** Early detection and treatment of symptomatic types 1 and 3 Gaucher disease with regular monitoring will optimize outcome. Pre-symptomatic children require regular monitoring. Genetic counseling is important.

**Keywords:** Gaucher disease type 1; Gaucher disease type 2; Gaucher disease type 3; Glucocerebrosidase. Glucocerebrosidase; Enzyme replacement Therapy; Genetic counseling; Monitoring; Disease Management; Treatment recommendations.

### 1231. Study of Primary IGF-1 Deficiency in Egyptian Children with Idiopathic Short Stature

Ghada M. Anwar, Wafaa A. Kandeel, Iman A. Mandour and Ayat N. Kamal

*Hormone Research in Pediatrics*, 79 (5): 277-282 (2013)

IF: 1.553

**Background:** Primary insulin-like growth factor-1 (IGF-1) deficiency (IGFD) is defined by low levels of IGF-1 without

growth hormone (GH) deficiency and absence of secondary causes. The aim of this study was to evaluate IGF-1 in Egyptian children with idiopathic short stature (ISS) and describe patients with IGFD.

**Methods:** This cross-sectional study included 50 children with ISS following up at the Diabetes Endocrine and Metabolism Pediatric Unit at Cairo University Pediatric Hospital. Children were included based on the following criteria: (1) short stature with current height standard deviation score (SDS)  $\leq -2.5$ ; (2) age between 2 and 9 years in boys and 2 and 8 years in girls, and (3) prepubertal status.

Exclusion criteria were: (1) identified cause of short stature and (2) pubertal children. IGF-1-deficient children were defined as children without GH deficiency and with IGF-1 levels below the 2.5th percentile.

**Results:** Among 50 children with ISS, 14 (28%) patients had low IGF-1 levels, consistent with the diagnosis of primary IGFD. When compared with non-IGFD children, IGFD children had lower birth weight SDS (-1.8 vs. -0.7 SDS,  $p < 0.0001$ ) and lower height SDS (-4.2 vs. -3.1 SDS,  $p < 0.05$ ) and more delayed bone age (2.6 vs. 1.6 years,  $p = 0.001$ ).

**Conclusion:** Primary IGF-1 deficiency is found in 28% of children with ISS.

**Keywords:** Idiopathic short stature; Insulin like growth factor; 1. Prepubertal; Egyptian children; Primary IGF-1 Deficiency.

### 1232. Cryptorchidism in Egyptian Neonates

Mostafa Zakaria, Sherif Azab, Mohamed El baz, Lubna Fawaz and Amro Bahagat

*Journal of Pediatric Urology*, 9: 815-819 (2013) IF: 1.368

Cryptorchidism is one of the most common genital malformations in newborn males, but its etiology remains largely unknown. The observation of geographical variability in the prevalence of cryptorchidism suggests a role for environmental factors. The aim of this study was to determine the prevalence of this condition among Egyptian neonates.

**Methods:** The initial study population comprised 1000 neonates recruited from El Galaa maternity teaching hospital. To determine the risk factors for cryptorchidism in Egypt, 40 healthy full term infants were selected randomly during the same time period as a control group.

**Results:** Twenty-nine cases of cryptorchidism per 1000 newborn males were detected, i.e. a frequency of 2.9%; 10 (34.5%) had bilateral cryptorchidism while 19 (65.5%) had a unilateral lesion. Other congenital anomalies were detected in 5 (17.2%) of the cryptorchid newborns.

Five factors were significantly associated with higher risk of cryptorchidism: gestational age of 37 weeks or less, birth weight equal to or less than 2.75 kg, cesarean delivery, steroid therapy and twin pregnancy. Using logistic regression, birth weight = 2.75 kg was the only independent factor predicting cryptorchidism, with an odds ratio of 10.3 and 95% confidence interval of 2.9–36.4.

**Conclusion:** These results highlight low birth weight as the cardinal risk factor for cryptorchidism. A larger scale multicentric study is needed to clearly identify all the risk factors for cryptorchidism in Egyptian neonates.

**Keywords:** Cryptorchidism; Low birth weight; Genital malformations; Testicular malignancy.



### 1233. Association Between Sleep and Behavioural Problems Among Children with Enuresis

Maha K. Abou-Khadra, Omnia R Amin and Dalia Ahmed

*J. of Paediatrics and Child Health*, 49: 160-166 (2013) IF: 1.254

**Aim:** This study was conducted to describe sleep problems in a sample of children with enuresis and to investigate the association between sleep and behavioural problems.

**Methods:** In this cross-sectional study, 100 children with enuresis were recruited from paediatric enuresis clinic. The children's sleep problems and behaviours were assessed by the Children's Sleep Habits Questionnaire and Child Behaviour checklist.

**Results:** The most frequently reported sleep problems were in daytime sleepiness, bedtime resistance and sleep anxiety subscales. Children with T-scores  $\geq 60$  in internalising, externalising and total behavioural problems had higher scores on daytime sleepiness subscale and total score than children with T-scores  $< 60$ . Multivariate logistic regression analysis revealed that daytime sleepiness subscale was significantly related to behavioural disturbances.

**Conclusions:** Sleep problems are common among this sample of children with enuresis, and the presence of sleep disturbance such as daytime sleepiness could explain the association between enuresis and disturbed daytime behaviour.

**Keywords:** Behavioural problem; Enuresis; Sleep problem.

### 1234. Assessment of Coagulation and Fibrinolysis in Children with Chronic Liver Disease

Mohsen R El-Sayed, Hanaa El-Karaksy, Mona El-Raziky, Manal El-Hawary, Nehal El Koofy, Heba Helmy and Mona Fahmy

*Blood Coagul Fibrinolysis*, 24 (2): 113-117 (2013) IF: 1.248

We aimed at assessing the coagulation profile and detecting early evidence of fibrinolysis in pediatric patients with chronic liver disease. Seventy-six patients (40 boys) with a mean age of  $9.8 \pm 3.4$  years suffering from chronic liver disease were enrolled in this study. They were followed up in the Pediatric Hepatology Unit, Cairo University Children's Hospital. Thirty healthy children were included as controls. Patients were classified etiologically into four groups: chronic viral hepatitis, autoimmune hepatitis, miscellaneous and cryptogenic groups. Investigations to detect coagulopathy were done for all patients and controls: prothrombin time (PT), activated partial thromboplastin time, fibrinogen, fibrinogen degradation products, and D-dimer and complete blood count. Liver functions were done for all patient groups. A significantly lower platelet count, prolonged prothrombin time, with prolonged aPTT time was detected in all patients compared with controls ( $P < 0.001$ ). The fibrinogen level showed no significant difference between patients and controls. D-dimer level was significantly higher in the miscellaneous and cryptogenic groups when compared to other patient groups and control group ( $P < 0.001$ ). Significantly higher D-dimer levels were detected in patients with liver cirrhosis of child class A and B compared with noncirrhotic and control groups ( $P < 0.001$ ). D-dimer correlated positively with PT ( $r = 0.290$ ,  $P = 0.003$ ), and negatively with platelet count ( $r = -0.324$ ,  $P = 0.001$ ) and prothrombin concentration ( $r = -0.270$ ,  $P = 0.018$ ). Fibrinolytic activity, as evidenced by high D-dimer, was detected in pediatric patients with chronic liver disease particularly if cirrhotic.

**Keywords:** Antifibrinolysis; Chronic liver disease; D-Dimer; Fibrinolysis; Haemostasis.

### 1235. Commentary on: the Optimal Dose of Ribavirin for Chronic Hepatitis C: from Literature Evidence to Clinical Practice

Mortada El-Shabrawi and Mona Isa

*Hepatitis Monthly*, 13: 7867-7869 (2013) IF: 1.245

We enjoyed reading the excellent article by Abenavoli and colleagues on the clinical role of Ribavirin (RBV), and particularly the selection and maintenance of the optimal RBV dosing strategy that are required to achieve sustained viral suppression in patients with chronic hepatitis C (CHC) infection. They concluded that contemporary therapy for CHC infection is to deliver doses of both RBV and pegylated interferon-alpha (PEG-IFN) that confer optimal antiviral efficacy for a sufficient time to minimize viral relapse. At the same time, it is important to minimize the impact of side effects that might erode the effectiveness of therapy due to dose reductions below the level of therapeutic efficacy, or because the patient is unable to complete an optimal treatment course (1). The early diagnosis and treatment of CHC infection is still a great worldwide healthcare problem.

**Keywords:** Ribavirin; Hepatitis C; Chronic; Interferons.

### 1236. Behavioral Changes in Egyptian Children with Nephrotic Syndrome

Emad E Ghobrial, Sameh S Fahmey, Maha E Ahmed and Osama E Botrous

*Iranian Journal of Kidney Diseases*, 7 (2): 108-116 (2013) IF: 0.94

**Introduction:** Chronic illnesses, including nephrotic syndrome (NS), are associated with psychosocial stress. Our study aimed to assess psychological problems in children with NS.

**Materials and Methods:** Sixty children with NS were assessed at the Children Hospital, in Cairo for behavioral changes. They responded to the Arabic version of the Strength and Difficulties Questionnaire. The results were compared between those with steroid-sensitive NS (SSNS), steroid-dependent NS (SDNS), and steroid-resistant NS (SRNS). Results. Three groups of patients with SSNS, SDNS, and SRNS, each consisting of 20 children aged between 4 and 16 years, were included. The SRNS group was significantly different from the other two groups regarding age at the onset of disease, total serum protein, serum albumin, serum calcium, and estimated glomerular filtration rate (lowest in the SRNS group) as well as 24-hour urine protein, blood urea nitrogen, and serum total cholesterol (highest in the SRNS group). In the SRNS group, the scores for emotional symptoms, peer relationship problems, and the total score were higher and the prosocial score was lower than the other groups, but with no statistical significance.

**Conclusions:** Emotional symptoms, conduct problems, peer relationship problems, hyperactivity, and the overall poor behavior scores might be more likely to be seen in children with SRNS group than other NS treatment status. We recommend that attention to behavioral problems of children with NS should be given early in the course of disease.

**Keywords:** Behavioral symptoms; Nephrotic syndrome; Child.

### 1237. Oxidative Stress in Egyptian Hemodialysis Children

Emad E. Ghobrial, Nermine N. Mahfouz, Gihan A. Fathy, Amany A. Elwakkad and Heba M.R. Sebail

*Iranian J. of Kidney Diseases*, 7 (6): 485-491 (2013) IF: 0.94

**Introduction:** Nitric oxide (NO) is one of the endothelium-dependent relaxing factors released by the vascular endothelium. It is decreased in chronic kidney disease. It was found that higher levels of circulating proinflammatory cytokines such as interleukin-1beta (IL-1beta), tumor necrosis factor-alpha (TNF-alpha), IL-6, and IL-13 are associated with mortality. The aim of our study was to evaluate the disturbance in NO in chronic kidney failure and its relationship with hypertension and inflammatory and nutritional parameters, as indirect indexes of uremic oxidative stress.

**Materials And Methods:** This study included 31 children consisting of 23 children, aged from 4 to 18 years old, with ESRD, on regular hemodialysis, and 8 children admitted to hospital for other diseases (control group). Predialysis blood samples were tested for IL-1beta, TNF-alpha, and NO, and were compared with the control group.

**Results:** Serum levels of TNF-alpha and IL-1beta were significantly higher in children on hemodialysis as compared to the control group (TNF-alpha, 104.54 +/- 17.31 pg/mL versus 48.19 +/- 6.28 pg/mL, P = .005; IL-1beta, 5.35 +/- 0.75 pg/mL versus 2.13 +/- 0.61 pg/mL, P = .02; respectively). However, the levels of NO, albeit higher in this group had no significant difference with the controls. **Conclusions:** The levels of cytokines are high in pediatric patients on hemodialysis, which reflects a state of oxidative stress.

**Keywords:** Hemodialysis; Child; Oxidative stress; Cytokines.

### 1238. Assessment of Immune Function in Down Syndrome Patients

Ekram Abdel-Salam, Iman Abdel-Meguid and Soheir Korraa

*The Egyptian Journal of Medical Human Genetics*, 14: 307-310 (2013)

In Down syndrome (DS), trisomy 21 leads to overexpression of gene coding for specific enzymes. This overexpression translates directly into biochemical aberrations that affect multiple interacting metabolic pathways which culminates in cellular dysfunction and contributes to the unique pathogenesis of DS. The aim of this study is to evaluate parameters of immune response in terms of cytokines [tumor necrosis factor-alpha (TNF-alpha) and interleukin-2 (IL-2)] together with the quantitative expression of cystathionine beta synthase (CBS), whose transsulfuration pathway generates cysteine and hydrogen sulfide (H<sub>2</sub>S). H<sub>2</sub>S is known to boost host defense at physiological concentrations and to display cytotoxic activity at higher concentrations. Calcineurin activity (CAN) was also measured as its dysregulation has been shown to cause immune suppression. Subjects were 60 DS patients vs. 30 age and socioeconomic matching healthy controls. In their blood, the cytokines:TNF-alpha and IL-2, together with CBS and its by product H<sub>2</sub>S as well as CAN activity, were measured. Results showed that CBSmRNA relative expression (0.56±.06 vs. 0.32 ±.02), plasma H<sub>2</sub>S (72 ±8.5 vs. 50.8 ±4.1) and TNF-alpha (8.11 ±.01 vs. 3.6±0.9) were significantly higher among DS patients compared to controls, while CAN (0.27 ±0.1 vs. 0.45

±0.2 units), was significantly decreased in blood of DS patients compared to controls. IL-2 (36.4 ±2.6 vs. 37.4 ±0.9) showed no significant difference between DS patients and controls. Accordingly it can be concluded that excessive synthesis of multiple gene products derived from overexpression of the genes present on chromosome 21 may be the cause for decreased immunity in DS patients compared to controls.

**Keywords:** Down syndrome; Cystathionine beta synthase (CBS); H<sub>2</sub>S; Calcineurin activity (CAN); Tumor necrosis factor-alpha (TNF-alpha); Interleukin-2 (IL-2).

### 1239. Can the Score for Neonatal Acute Physiology II (SNAPII) Predict Morbidity and Mortality in Neonates with Sepsis?

Nahed Fahmy Helal, Nashwa Mamdouh Samra, Eman Abdel Ghany Abdel Ghany and Ebtehal Adel Said

*Journal of Neonatal Biology*, 2: (2013)

**Objective:** We investigated whether Score for Neonatal Acute Physiology II (SNAP II) score can predict mortality and or Organ Dysfunction (OD) in neonatal sepsis.

**Methods:** Eighty Egyptian newborns hospitalized for neonatal sepsis were investigated through a multicenter observational prospective study to determine whether SNAP II applied in the 1st 12 hours of admission would predict mortality and or OD.

**Results:** The median SNAP II was significantly higher in babies who died or developed OD versus those who survived and improved (P=0.003 and P=0.001 respectively). Individual parameters of the SNAP II didn't contribute equally to the risk of death, low mean arterial blood pressure and lowest blood pH were significantly associated with OD and death (P=0.002). ROC curves for the SNAP II score = 40 showed moderate predictive accuracy and 90.4% and 88.9% sensitivity for OD and death, respectively. **Conclusion:** SNAP II score can predict mortality and OD in neonatal sepsis.

**Keywords:** SNAP II; Neonate; Sepsis; Organ dysfunction; Mortality.

### 1240. Current Management Options for Tyrosinemia

Mortada Hassan El-Shabrawi and Naglaa Mohamed Kamal

*Orphan Drugs: Research and Reviews*, 3: 1-9 (2013)

Hypertyrosinemia is observed in three inherited disorders of tyrosine metabolism. Hereditary Tyrosinemia Type I (HTT-I), or hepatorenal tyrosinemia, is an autosomal recessive disorder caused by mutation in the fumarylacetoacetate hydrolase (FAH) gene. HTT-I is associated with severe involvement of the liver, kidneys, and central nervous system, and is due to toxic accumulation of metabolites of tyrosine, such as succinylacetone. HTT-I is the inborn error with the highest incidence of progression to hepatocellular carcinoma. Elevated succinylacetone, in dried filter paper blood samples, or in plasma or urine, is pathognomonic and diagnostic for HTT-I and is the most reliable neonatal screening method. Liver transplantation is the definitive management, but the need for this is markedly decreased by the combined dietary and drug management. A diet low in tyrosine and phenylalanine, plus nitisinone (2-[2-nitro-4-trifluoromethylbenzoyl]-1,3-cyclohexanedione) (NCTB) are considered the gold standard management options. Carnitine and



1,25-OH-vitamin D are adjuvant therapy. Strict follow up with succinylacetone level for monitoring of treatment should be done. Abdominal ultrasonography and abdominal computerized tomography scan or magnetic resonance imaging should also be done for surveillance of the possible development of hepatocellular carcinoma.

**Keywords:** Tyrosinemia; Management; NTBC; Hepatocellular Carcinoma.

### 1241. Markers of Neural Degeneration and Regeneration in Down Syndrome Patients

Iman Ehsan Abdel-Meguid Ekram Abdel-Salam, Doaa M Abdel Latif, Soheir Korraa and Amal Ismaiel

*The Egyptian J. of Medical Human Genetics*, 14: 49-53 (2013)

On the trisomy Down syndrome Critical Region (DSCR1) is located the APP gene, which accelerates amyloid peptide protein (APP) expression leading to cerebral accumulation of APP-derived amyloid-beta peptides (Ab) and age-dependent cognitive sequelae. Also DSCR1 attenuates endothelial cell proliferation and angiogenesis required for tissue repair. The aim of the present work is to determine markers of neural degeneration and regeneration in the blood of young and adolescent Down syndrome (DS) patients as well as controls. Markers of regeneration were measured in terms of circulating mononuclear cells expressing Nestin and CD34, while markers of degeneration were measured in terms of plasma Ab42 and advanced glycation end products receptors (RAGES). Results showed a significant increase in plasma Ab42 ( $20 \pm 5.1$  vs.  $11.9 \pm 3.4$ ) and RAGES leucocytes mRNA relative expression ( $1.9 \pm 0.2$  vs.  $1.1 \pm 0.6$ ) in adolescent DS patients compared to young DS. Both parameters were also significantly increased in DS compared to controls: Ab42 ( $15.4 \pm 5.9$  vs.  $12.3 \pm 4.5$ ); RAGES ( $1.4 \pm 0.5$  vs.  $0.7 \pm 0.2$ ). Nestin ( $5.2 \pm 1.4$  vs.  $6.3 \pm 0.6$ ) and CD34 ( $52 \pm 2.5$  vs.  $53 \pm 4.7$ ) were non-significantly lower in adolescent DS patients compared to young DS, but significantly lower in DS patients compared to controls: Nestin ( $6.3 \pm 1.5$  vs.  $9 \pm 4.4$ ); CD34 ( $54 \pm 3.4$  vs.  $60 \pm 4.8$ ). The significant decrease in the number of mononuclear cells bearing Nestin and CD34 markers accompanied by a significant increase in Ab42 and RAGES indicate that degeneration in DS is an ongoing process, which is not counterbalanced by the regenerative mechanism.

**Keywords:** Markers of neural degeneration; Regeneration in down syndrome patients.

### 1242. Pattern of Rheumatic Fever in Egyptian Children Younger Than 5 Years

Hala Salah El Din Mahmoud Hamza L. A. Ibrahim, A. M. Fattouh, H. S. Hamza and W. A. Attia

*British Journal of Medicine and Medical Research*, 3(4): 1893-1899 (2013)

**Aims:** Acute rheumatic fever (ARF) is common between 5-15 years, uncommon with different presentation 25 in children below 5 years. The aim of this study is to assess the frequency and characterize the pattern of 26 presentation of rheumatic fever (RF) in Egyptian children younger than 5 years.

**Study Design:** Retrospective study. Place and Duration of the Study: Pediatric department, cardiology division, Cairo University Children's Hospital, 5 years follow up.

**Methodology:** We retrospectively reviewed the pre-completed data of 766 patients following up in the rheumatic fever clinic. Those with incomplete medical records were excluded. We compared between children younger than 5 years and those who are 5 years or older as regards their demographic data, clinical presentations, laboratory findings and echocardiographic findings. **Results:** We enrolled 667 patients; 17 of them (2.5%) were younger than 5 years (mean age  $3.82 \pm$  SD 0.393 years). The group of patients younger than 5 years old; included 10 females (58.8%) and 7 males (41.2%). Positive family history was encountered in 6 patients (37.7%). The most common presentations of the younger age group of patients were arthritis in 12 patients (70.5%), followed by carditis in 5 patients (29.4%), chorea in 3 patients (17.6%), and skin manifestations in 2 patients in the form of erythema marginatum (11.7%). Subclinical carditis was more common in younger children than the older group, with more severe valve affection. None of the patients in the younger age group had recurrence of the RF during a period of 5 years follow up while recurrences were encountered in 16 patients (2.5%) of the older age group.

**Conclusion:** ARF can occur in children younger than 5 years. The possibility of rheumatic fever should be adequately investigated in those young children presenting with arthritis, chorea, or skin rash especially in developing countries like Egypt. Echocardiography is an essential tool to diagnose cases with subclinical carditis.

**Keywords:** Rheumatic fever; Pattern; Children; <5 Years.

### 1243. Prevalence of Hepatitis B Virus Infection Among Egyptian Pregnant Women- A Single Center Study

Mortada El-Shabrawi, Mohamed Farouk Mohamed, Mona Salah El Din Hamdi, Mohamed Ehab, Shaimaa Shaaban Khamiss and Hanaa El-Karaksy

*Int. J. of Tropical Disease and Health*, 3: 157-168 (2013)

**Background:** Hepatitis B virus (HBV) infection still has a relatively high incidence and prevalence worldwide. In the post-vaccination era in developing countries, perinatal vertical transmission remains the most common mode of transmission. Prevention of mother-to-child transmission requires screening for HBV surface antigen (HBsAg) in pregnant women to identify which newborns that must be immunized.

**Aim:** This study aimed to evaluate the prevalence of HBV infection among pregnant mothers who were attending outpatient clinic of the Obstetric Department, and Social and Preventive Medicine Center at Cairo University Hospital Campus, for routine antenatal care.

**Methods:** A cross sectional study included 2,000 pregnant women. A rapid screening test for HBV "One Step HBsAg Rapid Test" was done for all women and all HBsAg-positive cases were confirmed by ELISA for HBsAg. A structured questionnaire for risk factors for HBV acquisition was filled for every pregnant mother positive for HBsAg and a control group of HBsAg negative mothers.

**Results:** Out of 2,000 pregnant women, 35 (1.75%) were positive by the rapid test, out of whom 32/35 cases (91.43%) were confirmed to be positive by the confirmatory test representing 1.6% of the study population. Family history of HBV, previous intravenous (IV) injections, medical clinic attendance, hospital admission, and surgeries were the risk factors for acquiring HBV infection (P-value=0.001, 0.003, 0.002, 0.000, and 0.011, respectively).

**Conclusion:** HBV infection is prevalent among pregnant mothers attending our outpatient services. Therefore we recommend screening for HBV in all Egyptian pregnant mothers to prevent neonatal infection by immunoprophylaxis.

**Keywords:** Prevalence; Epidemiology; Egypt; Hepatitis B; Perinatal infection; Pregnancy.

#### 1244. Telomerase Activity and Apoptosis Genes as Parameters of Lymphocyte Aging in Down Syndrome Patients

Ekram Abdel-Salam, Iman Abdel-Meguid and Soheir Korraa

*The Egyptian J. of Medical Human Genetics*, 14 (2): 171-176 (2013)

It is hypothesized that Down syndrome (DS) patients are associated with abnormalities of the immune system. Accordingly, this study was conducted to measure replicative aging and apoptosis in lymphocytes, which play an important role in the immune system, before and after being biostimulated with He:Ne laser. Replicative aging was measured in terms of telomerase activity, and ETS-2 gene relative expression. Apoptosis was measured in terms of DNA fragmentation and apoptosis genes (Fas, FasL and Bax) and antiapoptotic Bcl-2 protein. Results showed that Telomerase activity, ETS-2 mRNA expression, plasma DNA fragmentation, Fas and FasL were significantly higher among DS patients compared to controls: Telomerase activity ( $1.5 \pm 0.5$  vs.  $0.9 \pm 0.4$ ,  $p < 0.001$ ); ETS2 mRNA expression ( $0.6 \pm 0.1$  vs.  $0.43 \pm 0.04$ ,  $p < 0.0001$ ); plasma DNA fragmentation ( $0.45\% \pm 0.12$  vs.  $0.2\% \pm 0.1$ ,  $p < 0.0001$ ); Fas protein ( $5.3 \pm 1.2$  vs.  $2.3 \pm 0.2$ ,  $p < 0.0001$ ); FasL mRNA relative expression ( $0.37 \pm 0.05$  vs.  $0.24 \pm 0.01$ ,  $p < 0.001$ ); Bax mRNA relative expression ( $0.9 \pm 0.1$  vs.  $0.5 \pm 0.1$ ,  $p < 0.00001$ ). Bcl-2 protein was significantly low in DS patients compared to controls ( $8.6 \pm 1.3$  vs.  $10 \pm 2.1$ ,  $p < 0.01$ ). He:Ne laser biostimulation applied to evaluate lymphocytes' response significantly increased the former parameters in DS patients compared to their level before irradiation, except for Bcl-2, which was significantly decreased. In conclusion: increased telomerase activity associated with increased activity and overexpression of ETS-2 on chromosome 21 in DS patients may contribute to the increased rate of early senescence in circulating lymphocytes, which consequently contributes to the abnormalities of the immune system observed in DS. Increased apoptosis is due to increased oxidative stress, which induces an increase in the apoptotic genes Bax, Fas and FasL accompanied by a decrease in the antiapoptotic gene Bcl-2.

**Keywords:** Down syndrome; Bax; Bcl-2; ETS-2 gene; Fas; FasL; Telomerase.

#### Dept. of Pharmacology.

#### 1245. Telmisartan, an AT1 Receptor Blocker and A PPAR Gamma Activator, Alleviates Liver Fibrosis Induced Experimentally By Schistosoma Mansoni Infection

Yasmeen M. Attia, Essam F. Elalkamy, Olfat A. Hammam, Soheir S. Mahmoud and Aiman S. El-Khatib

*Parasites and Vectors*, 6: 199-211 (2013) IF: 3.246

**Background:** Hepatic schistosomiasis is considered to be one of the most prevalent forms of chronic liver disease in the world due to its complication of liver fibrosis. The demonstration of the pro-fibrogenic role of angiotensin (Ang) II in chronic liver disease brought up the idea that anti-Ang II agents may be effective in improving hepatic fibrosis by either blocking Ang II type 1 (AT1) receptors or inhibiting the angiotensin converting enzyme. Peroxisome proliferator-activated receptors gamma (PPAR  $\gamma$ ) activation has been also shown to inhibit hepatic stellate cell activation and progression of fibrosis. The present study has aimed at testing the anti-fibrogenic effects of telmisartan; an AT1 receptor blocker and a PPAR partial agonist, alone or combined with praziquantel (PZQ) on *Schistosoma mansoni*-induced liver fibrosis in mice.

**Methods:** To achieve the aim of the study, two sets of experiments were performed in which telmisartan was initiated at the 5th (set 1) and the 10th (set 2) weeks post infection to assess drug efficacy in both acute and chronic stages of liver fibrosis, respectively. *Schistosoma mansoni*-infected mice were randomly divided into the following four groups: infected-control (I), telmisartan – treated (II), PZQ- treated (III), and telmisartan+ PZQ-treated (IV). In addition, a normal non-infected group was used for comparison. Parasitological (hepatomesenteric worm load and oogram pattern), histopathological, morphometric, immunohistochemical (hepatic expressions of matrix metalloproteinase-2; MMP-2 and tissue inhibitor of metalloproteinase-2; TIMP-2), and biochemical (serum transforming growth factor beta 1; TGF- $\beta$ 1 and liver function tests) studies were performed.

**Results:** Telmisartan failed to improve the parasitological parameters, while it significantly ( $P < 0.05$ ) decreased the mean granuloma diameter, area of fibrosis, and serum TGF- $\beta$ 1. Additionally, telmisartan increased MMP-2 and decreased TIMP-2 hepatic expression. Combined treatment failed to show any additive properties, yet it did not affect the anti-schistosomal activity of PZQ.

**Conclusions:** These results suggest potential anti-fibrotic effects of telmisartan, an AT1 receptor blocker and a PPAR partial agonist, in acute and chronic stages of *Schistosoma mansoni*-induced liver fibrosis in mice.

**Keywords:** Hepatic fibrosis; *Schistosoma mansoni*; Telmisartan; MMP-2; TIMP-2; TGF- $\beta$ 1.

#### 1246. Comparison Between The Effect of Glibenclamide and Captopril on Experimentally Induced Diabetic Nephropathy in Rats

Daad H. Akbar, Magda M. Hagra, Hanan A. Amin and Omayma A. Khorshid

*Journal of the Renin-Angiotensin-Aldosterone System*, 14 (2): 103–115 (2013) IF: 2.286

**Hypothesis:** This study aimed to elucidate the role of glibenclamide in the prevention of diabetic nephropathy and to compare it with a reference drug captopril in rats.

**Materials and methods:** There were two main groups of rats. Control group (I) was subdivided into four subgroups which received distilled water, vehicle of streptozotocin, glibenclamide or captopril. The streptozotocin-diabetic Group (II) was subdivided into three subgroups: untreated, glibenclamide or captopril treated. Measurement of arterial blood pressure, serum glucose and creatinine levels, 24 h urinary protein and

albumin/creatinine ratio, kidney weight and its histological examination were done after 1, 2, 4, 8, 12 and 16 weeks of treatment.

**Results:** In treated diabetic rats captopril reduced blood pressure significantly, while no significant change in the mean arterial blood pressure or blood glucose level was recorded with glibenclamide treatment. Glibenclamide and captopril-treated diabetic rats showed significant decrease in serum creatinine level, urine volume, urinary protein excretion, albumin:creatinine ratio and kidney:body weight ratio compared with the diabetic non-treated group.

Histological examination of diabetic kidneys treated with either glibenclamide or captopril showed reduced glomerular hypertrophy, glomerulosclerosis, tubular degeneration and interstitial fibrosis compared with untreated diabetic rats.

**Conclusion:** Glibenclamide attenuated some biochemical and histological changes produced by diabetic nephropathy, despite persistent hyperglycemia and hypertension.

**Keywords:** Diabetic nephropathy; Glibenclamide; Captopril; Streptozotocin; Mesangial matrix index; Albumin–creatinine ratio.

#### 1247. Febuxostat Improves the Local and Remote Organ Changes Induced by Intestinal Ischemia/Reperfusion in Rats

Amani Nabil Shafik

*Digestive Diseases and Sciences*, 58 (3): 650-659 (2013)

IF: 2.26

**Background:** Xanthine oxidase has been implicated in the pathogenesis of a wide spectrum of diseases, and is thought to be the most important source of oxygen-free radicals and cell damage during re-oxygenation of hypoxic tissues.

**Aims:** The present study was undertaken to demonstrate whether febuxostat is superior to allopurinol in prevention of the local and remote harmful effects of small intestinal ischemia/reperfusion injury in rats.

**Methods:** Intestinal ischemia was induced by superior mesenteric artery ligation. The rats were assigned to five groups: the sham control; the intestinal ischemia/reperfusion; the allopurinol; and the febuxostat 5 and 10 mg/kg pretreated ischemia/reperfusion groups. Treatment was administered from 7 days before ischemia induction. After the reperfusion, the serum and tissues were obtained for biochemical, pharmacological, and histological studies.

**Results:** Intestinal reperfusion led to an elevation in the serum levels of alanine aminotransferase, aspartate aminotransferase, tumor necrosis factor- $\alpha$ , malondialdehyde, and xanthine oxidase as well as intestinal myeloperoxidase, malondialdehyde, and xanthine oxidase/xanthine dehydrogenase activity. Furthermore, the ischemia/reperfusion induced a reduction in the contractile responsiveness to acetylcholine. These changes were significantly regulated by the pretreatment with febuxostat compared to allopurinol. The degree of pathological impairment in the intestinal mucosa, liver, and lung tissues was lighter in the pretreated groups.

**Conclusions:** Febuxostat may offer advantages over allopurinol in lessening local intestinal injury as well as remote hepatic and lung injuries induced by small intestinal ischemia/reperfusion.

**Keywords:** Allopurinol; Febuxostat; Intestine ischemia; Reperfusion liver injury; Lung injury.

#### 1248. Do MDR1 and SLCO1B1 Polymorphisms Influence The Therapeutic Response to Atorvastatin? A Study on A Cohort of Egyptian Patients with Hypercholesterolemia

Mona F. Shabana, Amal A. Mishriki, Marianne Samir M. Issac and Sameh W. G. Bakhoun

*Molecular Diagnosis and Therapy*, 17: 299-309 (2013)

IF: 1.692

**Background:** Statins are among the most prescribed drugs worldwide to reduce the risk of cardiovascular events. Interindividual variability in drug response is a major clinical problem and is of concern during drug development. Statins, such as atorvastatin, are taken orally and access to their site of action in the liver is greatly facilitated by both intestinal and hepatic transporters.

**Objective:** To examine the impact of polymorphisms of the multidrug resistance 1 (MDR1) and solute carrier organic anion transporter 1B1 (SLCO1B1) genes on the therapeutic response to atorvastatin as well as the presence of gender–gene interaction.

**Methods:** Serum lipid levels were determined at baseline and 4 weeks following 40 mg/day atorvastatin treatment in 50 Egyptian hypercholesterolemic patients (27 males and 23 females). Identification of MDR1 C3435T and SLCO1B1 A388G gene polymorphisms was performed using a polymerase chain reaction–restriction fragment length polymorphism (PCR-RFLP) method.

**Results:** Treatment with atorvastatin resulted in a mean reduction of total cholesterol (TC), low density lipoprotein cholesterol (LDL-C), and triglyceride (TG) of 8.7 %, 9.2 %, and 4.1 %, respectively, and a mean increase of high density lipoprotein cholesterol (HDL-C) of 1 %. Baseline and post-treatment HDL-C levels were statistically significantly higher in the MDR1 TT homozygotes when compared with the CC wild type.

The percentage change in TC, LDL-C, TG, and HDL-C did not show any statistically significant difference when compared among the different MDR1 C3435T or SLCO1B1 A388G genotypes.

The SLCO1B1 GG homozygotes showed a decrease in TG, whereas there was an increase in TG following atorvastatin treatment in AA and AG carriers in females; however, males did not show any statistically significant difference. There was no statistically significant association between either the coronary artery disease (CAD) risk factors (family history of CAD, hypertension, diabetes mellitus, smoking) or concomitant medications with the percentage change in different lipid parameters.

**Conclusion:** MDR1 C3435T was associated with baseline and post-treatment HDL-C variation. SLCO1B1 A388G showed gender-related effects on TG change following atorvastatin treatment. None of the comorbidities or the concomitant medications influenced the percentage change of lipid parameters following atorvastatin treatment.

The results of this study may lead to an improved understanding of the genetic determinants of lipid response to atorvastatin treatment.

**Keywords:** Atorvastatin; Polymorphisms; MDR1; SLCO1B1; Hypercholesterolemia; Egyptian patients.

**Dept. of Physiology**

**1249. Effects of Obesity and Estradiol on  $\text{Na}^+/\text{K}^+$ -ATPase and their Relevance to Cardiovascular Diseases**

Milan Obradovic, Predrag Bjelogrić, Manfredi Rizzo, Niki Katsiki, Mohamed Haidara, Alan J. Stewart, Aleksandra Jovanovic and Esma R. Isenovic

*Journal of Endocrinology*, 218(3): R13-R23 (2013) IF: 4.058

Obesity is associated with aberrant sodium/ potassium- ATPase ( $\text{Na}^+/\text{K}^+$ -ATPase) activity, apparently linked to hyperglycemic hyperinsulinemia, which may repress or inactivate the enzyme. The reduction of  $\text{Na}^+/\text{K}^+$ -ATPase activity in cardiac tissue induces myocyte death and cardiac dysfunction, leading to the development of myocardial dilation in animal models; this has also been documented in patients with heart failure (HF). During several pathological situations (cardiac insufficiency and HF) and in experimental models (obesity), the heart becomes more sensitive to the effect of cardiac glycosides, due to a decrease in  $\text{Na}^+/\text{K}^+$ -ATPase levels. The primary female sex steroid estradiol has long been recognized to be important in a wide variety of physiological processes. Numerous studies, including ours, have shown that estradiol is one of the major factors controlling the activity and expression of  $\text{Na}^+/\text{K}^+$ -ATPase in the cardiovascular (CV) system. However, the effects of estradiol on  $\text{Na}^+/\text{K}^+$ -ATPase in both normal and pathological conditions, such as obesity, remain unclear. Increasing our understanding of the molecular mechanisms by which estradiol mediates its effects on  $\text{Na}^+/\text{K}^+$ -ATPase function may help to develop new strategies for the treatment of CV diseases. Herein, we discuss the latest data from animal and clinical studies that have examined how pathophysiological conditions such as obesity and the action of estradiol regulate  $\text{Na}^+/\text{K}^+$ -ATPase activity.

**1250. Cardioprotective Modulation of Cardiac Adiponectin and Adiponectin Receptors by Omega-3 in the High-Fat Fed Rats**

Sandra M. Younan, Leila A. Rashed and Osama M. Abd El Aziz

*Chinese Journal of Physiology*, 56(2): 65-76 (2013) IF: 0.748

Obesity is an important risk factor for heart disease. This study investigated the effects of omega- 3 (-3) on reversal of high fat (HF) diet-induced changes in the expression of the cardiac adiponectin and adiponectin receptors R1 and R2. Male rats were fed low-fat (LF; 10% energy from fat) or HF (45% energy from fat) for 16 weeks, LF--3 or a HF--3 (LF or HF for 16 weeks supplemented by-3 as 36 g/kg diet for the last 6 weeks, respectively) and a HF diet for 10 weeks to demonstrate HF effect before-3 administration. HF diet induced obesity, glucose intolerance, increased heart end systolic and diastolic volumes, decreased serum adiponectin, reduced expression of cardiac and adipose tissue adiponectin and adipo R1 & R2 with elevated serum tumour necrosis factor- $\alpha$  (TNF- $\alpha$ ) compared to the LF diet. on the other hand, the HF--3 group compared with the HF group had improved glucose tolerance (area under the glucose curve  $837.14 \pm 45.7$  versus  $1158.5 \pm 69.8$ ) and insulin resistance with a significant increase in serum adiponectin ( $4.22 \pm 0.39$  versus  $2.82 \pm 0.69$  ng/ml) and a significant decrease in serum TNF- $\alpha$  ( $129.84 \pm 13.63$  versus  $209.8 \pm 16.42$  pg/ml) and triglycerides

independent of obesity. Also the data showed significant increases in the expression of cardiac and adipose tissue adiponectin and adiponectin R1 and adipose tissue adipo R2 as well as cardiac pAMP kinase with improvement in end-systolic and-diastolic volumes. These parameters were also improved compared to initial values in HF-10-week group. in conclusion, dietary-3 supplementation has a beneficial effect on fat-induced cardiac dysfunction and insulin resistance partly through increasing adiponectin and adiponectin receptors expression in heart and adipose tissue.

**Keywords:** Adiponectin; Cardiac adiponectin receptors; Omega-3-; High fat diet.

**1251. Effect of GLP-1 on After Experimental Ischemic Reperfusion Injury in Rats**

Hany El Sebaee, Maged Haroum, Rehab Ahmed Mohammed and Ahmed Soliman

*Life Sci. J.*, 10 (1): 4326-3437 (2013) IF: 0.165

Glucagon-like peptide-1 (GLP-1) is an incretin hormone secreted by L-cells of small intestine in response to nutrient ingestion. Although the major physiological function of GLP-1 appears to be in relation to glycaemic control, there is growing evidence to suggest that it may also play an important role in the cardiovascular system. GLP-1 receptors (GLP-1Rs) are expressed in the heart and vasculature of both rodents and humans, and recent studies have demonstrated that GLP-1R agonists have wide-ranging cardiovascular actions, such as modulation of heart rate, blood pressure, vascular tone and myocardial contractility. in this study the cardiac effect of native GLP-1 after experimental induction of ischemia was studied. Fifty rats were used in this study. Their weight ranged from 200-250 grams. Rats were anesthetized and the hearts were excised. The hearts were mounted on a Langendorff perfusion system and a retrograde perfusion was started within 3min of the heart excision. After 30 min of stabilization, the following groups were defined:(1) Control group (group1a):consists of 10 rats, no ischemia, the flow was continuous for 2 hours. (Sham operation). in the other groups the flow was turned off for 35 min to elicit global ischemia and reperfusion was continues for 120min. (2) Control group (group1b):consists of 10 rats, no pharmacological agents were added during the first 15min of reperfusion. (3) DPP4 inhibitor group (group2):consists of 10 rats, sitagliptin 20mg/l was added during the first 15min of reperfusion. (4) GLP-1group (group3):consists of 10 rats, GLP-1 (0.3nM/l) + sitagliptin 20mg/l were added during the first 15min of reperfusion. (5) GLP-1 high dose group (group4):consists of 10 rats, GLP-1(10.3nM) + sitagliptin 20mg/l were added during the first 15min of reperfusion. The following parameters were measured at the end of stabilization period (reading1) and at the end of reperfusion (reading2) 1- Heart rate/ min. 2-Left ventricular developed pressure/mmHg =left ventricular systolic-diastolic pressure. 3- Rate pressure product/mmHg/min =HR  $\times$  LVDP and 4-Maximum rate of pressure rise P/ T/mmHg/sec. Histopathological studies of sections from the 5 studied groups were performed using Hematoxylin and Eosin

**Keywords:** GLP-1; Sitagliptin; Mycaardial infarction; Reperfusion injury.



## 1252. The Effect of Human Bone Marrow Mesenchymal Stem Cells on Diabetic Heart Failure Rats

Hany E. El Said, Hala M Gabr and Rasha I Ammar

*Life Sci. J.*, 10 (1): 3413-3425 (2013) IF: 0.165

**Aim:** The purpose of this study was to investigate the effect of bone marrow mesenchymal stem cells (MSCs) on cardiovascular complications of type 1 diabetes mellitus (DM) in rats associated with heart failure.

**Material and Methods:** BM-MSCs were derived from the human bone marrow. The MSCs were characterized morphologically and by RT-PCR for CD29 expression. They were then infused into rat tail vein which were they were made diabetic by IP injection of streptozotocin (STZ) and also we induce heart failure through injection of adramycin. The rats were divided into control, diabetic(D), and diabetic and heart failure(D\_HF) plus MSC groups where D-HF rats injected with human bone marrow derived stem cells(BM-MSC). Serum glucose, insulin, and fibrinogen were estimated in all groups. Physiological cardiovascular functions: Systolic and diastolic blood pressure, echocardiography were assessed. Homing of BM-MSCs in cardiac tissue and histological examination were done at the end of the experiment.

**Results:** Diabetic rats which received MSCs showed significantly lower serum glucose and increased serum insulin levels compared with the D- HF group. Improvement of cardiovascular performance was also observed in the D-HF group compared with the D group. Homing of stem cells was detected in cardiac tissues of the BM-MSC group.

**Conclusions:** Human bone marrow harbors cells that have the capacity to differentiate into functional insulin-producing cells capable of controlling blood glucose level in diabetic rats.

Furthermore, MSC transplantation can improve cardiac function in diabetic rats associated with heart failure.

**Keywords:** Human bone marrow; Derived mesenchymal; Stem cells; Diabetes; Streptozotocin; Heart failure; Adramycin; Rats.

## 1253. A Histological and Functional Study on Hippocampal Formation of Normal and Diabetic Rats

Shaimaa N. Amin, Sandra M. Younan, Mira F. Youssef, Laila A. Rashed and Ibrahim Mohamady

*F1000 Research*, 2: 1-22 (2013)

**Background:** The hippocampus is a key brain area for many forms of learning and memory and is particularly sensitive to changes in glucose homeostasis.

**Aim of the work:** To investigate in experimentally induced type 1 and 2 diabetes mellitus in rat model the effect of diabetes mellitus on cognitive functions and related markers of hippocampal synaptic plasticity, and the possible impact of blocking N-methyl-D-aspartic acid (NMDA) receptors by memantine.

**Materials and Methods:** Seven rat groups were included: non-diabetic control and non-diabetic receiving memantine; type-1 diabetic groups- untreated, treated with insulin alone and treated with insulin and memantine; and type 2 diabetic groups- untreated and memantine treated. Cognitive functions were assessed by the Morris Water Maze and passive avoidance test. Biochemical

analysis was done for serum glucose, serum insulin and insulin resistance. Routine histological examination was done, together with immunohistochemistry for detection of the hippocampal learning and memory plasticity marker, namely activity regulated cytoskeletal-associated protein (Arc), and the astrocytes reactivity marker, namely glial fibrillary acidic protein (GFAP).

**Results:** Both type 1 and 2 untreated diabetic groups showed significantly impaired cognitive performance compared to the non-diabetic group. Treating the type 1 diabetic group with insulin alone significantly improved cognitive performance, but significantly decreased GFAP and Arc compared to the untreated type 1 group. In addition, the type 2 diabetic groups showed a significant decrease in hippocampus GFAP and Arc compared to the non-diabetic groups. Blocking NMDA receptors by memantine significantly increased cognitive performance, GFAP and Arc in the type 1 insulin-memantine group compared to the type 1-insulin group and significantly increased Arc in the type 2-memantine group compared to the untreated type 2 diabetic group. The non-diabetic group receiving memantine was, however, significantly adversely affected.

**Conclusion:** Cognitive functions are impaired in both types of diabetes mellitus and can be improved by blockage of NMDA receptors which may spark a future therapeutic role for these receptors in diabetes-associated cognitive dysfunction.

**Keywords:** Diabetes; Cognitive functions; Hippocampus.

## Dept. of Physiology of the Nervous System - Nerve Disease

### 1254. Botulinum Toxin-Type A: Could it Be an Effective Treatment Option in Intractable Trigeminal Neuralgia

Hatem S. Shehata, Mohamed S. El-Tamawy, Nevin M. Shalaby and Gihan Ramzy

*The Journal of Headache and Pain*, 14 (1): 92-97 (2013)  
IF: 2.779

**Background:** Botulinum toxin type A (BTX-A) has been reported to have analgesic effects independent of its action on muscle tone, mostly by acting on neurogenic inflammatory mediators and controlling the neurotransmitter release of sensory and autonomic nerve terminals that are involved in many chronic painful conditions as chronic intractable trigeminal neuralgia (TN). The aim of our work was evaluating the efficacy, safety, and tolerability of BTX-A for the treatment of intractable idiopathic TN.

**Methods:** This was a randomized, single-blinded, placebo-control study carried out on 20 Egyptian patients with intractable TN. Patients received a one-time subcutaneous administration of BTX-A using "follow the pain" method. The primary efficacy measure was reduction in pain severity on the 10-cm VAS score as well as in paroxysms frequency from the baseline to week 12 (endpoint last observation carried forward [LOCF]). Secondary efficacy measures included QoL assessment and number of acute medications received from baseline to the endpoint.

**Results:** Pain reduction at the 12-week endpoint was significant in BTX-A group ( $p < 0.0001$ ); VAS scores at endpoint LOCF relative to baseline for BTX-A group showed a decrease of 6.5 compared with a decrease of 0.3 for placebo, also there was a significant decrease in the number of acute medications and an increase in QoL functioning scale.



**Conclusion:** These results indicate that BTX-A has a direct analgesic effect in patients with TN and can represent a therapeutic option for intractable cases.

**Keywords:** Botulinum toxin; Intractable; Trigeminal; Neuralgia.

### 1255. Thrombolysis in the Developing World: is there A Role for Streptokinase

Ken Butcher, Ashfaq Shuaib, Jeffrey Saver, Geoffrey Donnan, Stephen M. Davis, Bo Norrving, K. S. Lawrence Wong, Foad Abd-Allah, Rohit Bhatia and Adnan Khan

*International Journal of Stroke*, 8 (7): 560-565 (2013) IF: 2.748

Intravenous thrombolysis with tissue plasminogen activator is the only proven acute therapy for ischemic stroke. This therapy has not been translated into clinical practice in the developing world primarily due to economic constraints. Streptokinase, a lower cost alternative thrombolytic agent, is widely available in developing countries where it is utilized to treat patients with acute coronary syndromes. Although this drug has previously been found to be ineffective in ischemic stroke, the lack of benefit may have been related to a number of factors related to trial design rather than the drug itself. Specific features of prior trial designs that may have adversely affected outcomes include a prolonged treatment window, inclusion of patients with established infarction on computed tomography scan, failure to treat excessive arterial pressures, a fixed dose of streptokinase, and concomitant use of antithrombotic medications. Given the lack of therapeutic alternatives in developing countries, a new trial of streptokinase in acute stroke, utilizing stricter inclusion criteria similar to those in more recent thrombolytic studies, appears warranted.

**Keywords:** Acute stroke therapy; Clinical trial; Cost factors; Developing countries; Ischemic stroke; Thrombolysis.

### 1256. The Impact of Vascular Risk Factors Multiplicity on Severity of Carotid Atherosclerosis—A Retrospective Analysis of 1969 Egyptian Subjects

Essam Baligh, Foad Abd-Allah, Reham Mohammed Shamloul, Ehab Shaker, Hani Shebly and Mohamed Abdel-Ghany

*World Journal of Cardiovascular Diseases*, 3 (6) : 414-418 (2013)

**Background and Purpose:** Carotid atherosclerosis has been recognized as a major cause of stroke. The current study aimed to describe the effect of multiplicity rather than the type of vascular risk factors on severity of carotid atherosclerosis among a large sample of Egyptian population.

**Methods:** We analyzed the data of 1969 Egyptian subjects, who proved to have extra cranial carotid atherosclerotic disease by duplex scanning at the vascular laboratories of Cairo University Hospitals. Demographic, clinical data and causes of referral were recorded and correlated with ultrasound findings. Atherosclerotic indices, namely IMT, plaque number and percentage of stenosis were used for evaluation of severity of carotid atherosclerosis. Furthermore, subjects were classified according to multiplicity of major atherosclerotic risk factors and multivariate regression analysis was performed to detect independent predictors of significant carotid disease.

**Results:** Out of 1969 subjects with proved signs of extracranial carotid atherosclerosis by duplex ultrasonographic scan, 225

(11.4%) showed hemodynamic significant stenosis ( $\geq 50\%$ ). Multiplicity of risk factors beyond the age of 50 years was the strongest predictor of significant stenosis.

**Conclusion:** Age more than 50 years and multiplicity rather than the type of risk factors were the strongest predictors of significant carotid atherosclerotic disease (CAD).

**Keywords:** Carotid; Atherosclerosis; Risk factors; Duplex; Carotid stenosis.

### Dept. of Psychology

### 1257. Adapting and Evaluating A Social Cognitive Remediation Program for Schizophrenia in Arabic

Sherif M. Gohar, Emad Hamdi, Lamis A. El Ray, William P. Horan and Michael F. Green

*Schizophrenia Research*, 148: 12-17 (2013) IF: 4.59

Although growing evidence supports the efficacy of social cognitive training interventions for schizophrenia, nearly all studies to date have been conducted in Westernized countries. In the current study, we translated and adapted an existing social cognitive skills training (SCST) program into Arabic and conducted a preliminary efficacy evaluation in schizophrenia outpatients in Egypt. Twenty-two patients were randomized to 16 sessions of group-based SCST and 20 were randomized to a format- and time-matched illness management training control condition. Pre- and post-intervention assessments included a primary social cognition outcome measure that assessed four branches of emotional intelligence and a battery of neurocognitive tests.

The SCST group demonstrated significant treatment effects on total emotional intelligence scores ( $F=24.31$ ,  $p<.001$ ), as well as the sub-areas of Identifying Emotions ( $F=11.77$ ,  $p<.001$ ) and Managing Emotions ( $F=23.27$ ,  $p<.001$ ), compared with those in the control condition. There were no treatment benefits for neurocognition for either condition, and both interventions were well-tolerated by patients. These initial results demonstrate the feasibility of implementing social cognitive interventions in different cultural settings with relatively minor modifications. The findings are encouraging regarding further efforts to maximize the benefits of social cognitive interventions internationally.

**Keywords:** Schizophrenia; Social cognition; Psychosocial treatment; Arabic; Culture; Remediation.

### 1258. Lifetime Prevalence of Alcohol and Substance Use in Egypt: A Community Survey

Emad Hamdi, MRCPsych, Tarek Gawad, Aref Khoweiled, Albert Edward Sidrak, Dalal Amer, Rania Mamdouh, Heba Fathi and Nasser Loza FRCPsych

*Substance Abuse*, 34: 97-104 (2013) IF: 1.245

**Objective:** The aim of this study was to determine the prevalence of substance use and addiction in Egypt and study its sociodemographic correlates.

**Method:** A total of 44,000 subjects were interviewed from 8 governorates by stratified sampling. A questionnaire derived from the Addiction Severity Index (ASI) was individually administered.

**Results:** The lifetime prevalence of any substance use varies between 7.25% and 14.5%. One-month prevalence varies between

5.4% and 11.5% when adjusted to different population parameters.

A total of 4832 subjects were identified as using illicit substances at least once in their life (9.6%), including 1329 experimental and social use (3.3%), 1860 regular use (4.64%), and 629 substance dependence (1.6%).

The prevalence of substance use in males is 13.2% and 1.1% in females. Prevalence increases significantly in males of Bedouin origin, in seaside governorates, with lesser levels of education, and in certain occupations. The 15–19 age group showed the highest onset of substance use. Cannabis is the drug mostly misused in Egypt; alcohol is a distant second.

**Conclusions:** The prevalence of substance use is lower than Western countries and higher compared with a 1996 survey. The true population prevalence is probably higher due to underreporting. The demographic pattern reflects availability and accessibility to drugs.

**Keywords:** Abuse; Community survey dependence; Prevalence; Substance misuse.

### 1259. Euthanasia and Physician-Assisted Suicide: Historical and Religious Perspective in the Middle East

Mona Y. Rakhawy, George Tadros, Farooq Khan and Ahmed Mahmoud El Houssini

*International Psychiatry, 10: 20-21 (2013)*

**Conclusions:** The Middle East has a unique position in history. People from the region have collectively developed their cultures through years of interaction with different eras of history, cultures and religions. There are sizeable minorities in the USA, Australia, the UK and mainland Europe who emigrated from or have links with the Middle East. Also, there are millions of Muslims who currently live in Western countries. Therefore, it is essential for doctors practising in those countries to understand the historical, spiritual and cultural perspective of those who have their cultural roots in the Middle East. We also need to understand who the physician is, the relationship between professional and patient, and the impact of societal structures on that relationship. Only if professionals understand the cultural and religious needs of diverse groups of our patients can we offer them appropriate suggestions and advise on end-of-life decisions.

**Keywords:** Middle East; Historical; Spiritual; Cultural Perspective; Religions

### 1260. Psychosocial and Sexual Aspects of Female Circumcision

S. Abdel-Azim

*African Journal of Urology, 19 no 3: 141-142 (2013)*

Sexual behavior is a result of interaction of biology and psychology. Sexual excitement of the female can be triggered by stimulation of erotogenic areas; part of which is the clitoris. Female circumcision is done to minimize sexual desire and to preserve virginity. This procedure can lead to psychological trauma to the child; with anxiety, panic attacks and sense of humiliation. Cultural traditions and social pressures can affect as well the unexcised girl. Female circumcision can reduce female

sexual response, and may lead to anorgasmia and even frigidity. This procedure is now prohibited by law in Egypt.

**Keywords:** Psychosocial; Sexual; Aspects; Female circumcision.

### Dept. of Public Health

#### 1261. Hepatitis C Virus-Specific Cell-Mediated Immune Responses in Children Born to Mothers Infected with Hepatitis C Virus

Samer S. El-Kamary, Mohamed Hashem, Doaa A. Saleh, Sayed F. Abdelwahab, Maha Sobhy, Fatma M. Shebl, Michelle D. Shardell, Thomas Strickl and Mohamed Tarek Shata

*The Journal of Pediatrics, 162: 148-154 (2013) IF: 4.035*

**Objective to Investigate:** The association between hepatitis C virus (HCV)-specific cell-mediated immunity (CMI) responses and viral clearance in children born to mothers infected with HCV. Study design A cross-sectional study of children from a mother-infant cohort in Egypt were enrolled to detect CMI responses to recombinant core and nonstructural HCV antigens (nonstructural segments NS3, NS4a/ b, and NS5 of the HCV genome) using an interferon-gamma enzyme-linked immunospot assay. Children born to mothers with chronic HCV were enrolled into 3 groups: transiently viremic (n = 5), aviremic (n = 36), and positive control (n = 6), which consisted of 1 child with chronic HCV from this cohort and another 5 children with chronic HCV from a companion study. Children without HCV born to mothers without HCV (n = 27) served as a negative control group. Wilcoxon rank sum test was used to compare the magnitude of CMI responses between groups.

**Results:** None of the 6 control children who were positive for HCV responded to any HCV antigen, and 4 (80%) of 5 children with transient viremia responded to at least one HCV antigen, compared with 5 (14%) of 36 and 3 (11%) of 27 children in the aviremic and negative control groups, respectively. Children with transient viremia elicited stronger responses than did negative controls (P = .005), positive controls (P = .011), or children without HCV viremia (P = .012), particularly to nonstructural antigens.

**Conclusions:** HCV-specific CMI responses were significantly higher in magnitude and frequency among transiently infected children compared with those persistently infected. This suggests CMI responses may be associated with past viral clearance and can identify children at high risk of infection, who can be targeted for health education, screening, and follow-up.

**Keywords:** Anti-HCV; CMI; Elispot; HCV; IFN-G; Ns3/Ns4; Ns5; PBMC; SFC.

#### 1262. Community Medicine Education Reform Throughout 2006/2013: Needs for Reactivating the Reform

Ghada Wahby Mohamed, Wahby G. and Eman Taher

*International Journal of Academic Research in Progressive Education and Development, 2-i4: 65-77 (2013)*

Throughout the period 2007-2013, Cairo University- Faculty of Medicine-Community Medicine Department (CU-FOM-CMD) devoted efforts to capitalize on the successful EDUCATION reform model implemented in 2006/2007.

**Objectives:** were to explore the medical students' and staff perspectives towards CU-CMEC in two academic years 2006/2007 and 2011/2012. The study was a health system (evaluation) design. Data were quantitative from a 523 students of year 2011/2012 and qualitative from community medicine department (CMD) staff members.

**Results:** The reported satisfaction by the 2012 versus 2007 students was as follows: general satisfaction was 52% versus 69% ( $p=0.00$ ), satisfaction from generic skills was reported by 61% versus 83%, from technical skills was reported by 54% versus 64%, and from creative activities was reported by 41% versus 59%. CMD staff members affirmed that, the reform persisted for seven years due to continuous role of the critical mass of staff members.

**Conclusion:** focusing on students' autonomy, learning-service and hands-on training, could boost the CMER and respond to the changing students' expectation and community needs over time.

**Keywords:** Education reform; Community medicine course; Health system research; Critical mass.

#### Dept. of Rheumatology

### 1263. Anti-Annexin V Antibodies in Primary Fibromyalgia Syndrome: Relation to Associated Sjögren'S Syndrome

Tamer A. Gheita, Rehab W. El Sisi, Hala A. Raafat and Hossam M. Khalil

*Journal of Clinical Immunology*, 33: 311-312 (2013) IF: 3.382

Fibromyalgia syndrome (FMS) is a complex disorder that affects up to 5 % of the general population worldwide, more frequently in women. Sjögren's syndrome (SS), the second most common autoimmune rheumatic disease results from immune lymphocytes that infiltrate the lacrimal and salivary glands. The distinction between FMS patients and primary SS remains difficult. Damages to the lacrimal and salivary glands and development of SS may accompany various autoimmune diseases. Apoptosis (programmed cell death) plays a fundamental role in the pathogenesis of SS. Annexins are a group of highly conserved proteins which exert several regulatory functions on cell biology and are involved in numerous cell processes including apoptosis. The aim of this study was to measure the level of serum Anti-Annexin V antibodies in FMS patients diagnosed according to the American College of Rheumatology criteria and to study their significance in relation to associated SS diagnosed according to the revised version of classification criteria.

**Keywords:** Anti-annexin V antibodies; Primary fibromyalgia syndrome; Sjögren'S syndrome.

### 1264. Elevated Serum Resistin in Juvenile Idiopathicarthritis: Relation to Categories and Disease Activity

Gheita Tamer A. Gheita, Iman I. El-Gazzar, Reem I. El Shazly, Abeer M. Nour El-Din, Enas Abdel-Rasheed and Rasha H. Bassyouni

*Journal of Clinical Immunology*, 33: 297-301 (2013) IF: 3.382

**Background:** Juvenile Idiopathic Arthritis (JIA) is one of the more common chronic diseases of childhood that often persists

into adulthood and can result in significant longterm morbidity, including physical disability. The aim of the present study was to assess the serum level of resistin in JIA patients and compare its levels according to the categories, clinical manifestations and disease activity.

**Methods:** Sixty-eight JIA patients and 33 age and sex matched control children were included in the present study. All patients included in this study were subjected to full history taking, clinical examination. Juvenile arthritis disease activity score in 27 joints (JADAS-27) was calculated and Childhood Health Assessment Questionnaire (CHAQ) was used to measure the functional status. Serum resistin levels were measured by enzyme-linked immunosorbent assay (ELISA).

**Results:** The mean serum resistin was significantly higher in the JIA patients ( $4.01 \pm 2.46$  ng/ml) compared to the control ( $2.08 \pm 1.23$  ng/ml) ( $p < 0.001$ ) especially those with systemic onset. Its level was significantly higher in those receiving steroids and those with a positive antinuclear antibody. Resistin significantly correlated with the JADAS27 ( $r=0.26$ ,  $p=0.035$ ) and CHAQ ( $r=0.4$ ,  $p=0.001$ ). The JIA patients were 50 females and 18 males; however, the level of resistin was insignificantly different according to the gender although there was a tendency to be higher in females.

**Conclusion:** Our results reinforce the proposition of an important role for resistin in JIA and may be considered an interesting biomarker for disease activity especially those with systemic onset.

**Keywords:** Childhood HAQ; JADAS27; Juvenile idiopathic Arthritis; Resistin; Categories.

### 1265. Soluble Levels of Osteopontin in Patients with Behcet's Disease: Association with Disease Activity and Vascular Involvement

Iman H. Bassyouni, Mohammed M. El-Wakd and Rasha H. Bassyouni

*J. Clin Immunol* 3: 361-367 (2013) IF: 3.382

**Aim:** Osteopontin (OPN) is a multifunctional molecule highly expressed in chronic inflammatory and autoimmune diseases. We aimed to assess the plasma OPN levels in Behcet's disease (BD) patients and identify potential associations between these levels with disease activity, severity and clinical manifestations with special emphasis on vascular affection.

**Methods:** We studied 55 BD patients and 31 age- and gender-matched healthy controls. Demographic, clinical and serological data were prospectively assessed. Activity and severity of BD were assessed using clinical scores and laboratory parameters. Plasma OPN levels were measured using enzyme-linked immunosorbent assay (ELISA).

**Results:** Plasma OPN levels were significantly higher in patients with BD compared to healthy controls ( $p < 0.000$ ). The means for plasma OPN levels in active and inactive BD patients were significantly higher than that for the normal controls (with  $p < 0.000$  and  $p=0.002$  respectively). The mean OPN levels significantly associated with the BD clinical severity score from mild to severe ( $p=0.011$ ). BD patients with vascular involvement had significant elevation of plasma OPN levels than those without ( $P=0.03$ ). OPN levels positively correlated with severity score, IL6, hsCRP, ESR, leucocytes count and neutrophil count.

**Conclusion:** Plasma OPN levels were higher in BD patients than in healthy controls and were found to be associated with disease

activity, severity and vascular involvement. to confirm our results we propose that larger scale, multicentre studies with longer evaluation periods are needed.

**Keywords:** Behcet's disease; Disease severity; Osteopontin; vasculitis.

### 1266. Anti-Cyclic Citrullinated Peptide (Anti-CCP) Antibody in Juvenile Idiopathic Arthritis (JIA): Correlations with Disease Activity and Severity of Joint Damage (A Multicenter Trial)

Aziza Omar, Ihab Abo-Elyoun, Hanan Hussein, Mohammad Nabih, Hoda Atwa, Suzan Gadeand and Yasser Emad

*Joint. Bone. Spine., 80 (1): 38-43 (2013) IF: 2.748*

**Objectives:** To determine the presence of anti-CCP antibodies in children with JIA and to correlate its levels with Juvenile Arthritis Disease Activity Score (JADAS) and Sharp/Van der Heijde Score.

**Methods:** The study population comprised 54 cases, with 29 patients (53.7%) who had polyarticular onset, 19 (35.2%) had pauciarticular onset and six (11.1%) had systemic onset JIA. All patients were subjected to complete clinical examination, assessment of disease activity by JADAS-27 (ESR), and radiological damage by Sharp/Van der Heijde Score. Laboratory investigations included a complete blood count, ESR first hour, ANA, IgM Rheumatoid factor (RF) and serum anti-CCP2, and were used for further correlations.

**Results:** RF was positive in 14 (25.9%) patients and anti-CCP antibodies were positive in 13 (24.1%) patients, 12 of whom had polyarticular onset.

There were significant differences between groups relative to RF ( $F=8.577$ ,  $P=0.001$ ) and anti-CCP antibodies ( $F=4.845$ ,  $P=0.012$ ) being higher in JIA patients with polyarticular onset compared to other subsets of JIA patients.

The mean total of the Sharp/Van der Heijde Score was significantly higher among polyarticular-JIA patients with positive anti-CCP antibodies compared to those negative for anti-CCP antibodies ( $P=0.05$ ). Anti-CCP positively correlated with CRP ( $r=0.521$ ,  $P<0.001$ ) and Sharp/Van der Heijde Score ( $r=0.457$ ,  $P<0.001$ ).

**Conclusion:** Anti-CCP antibodies were prevalent among JIA patients with polyarticular patterns compared to other disease patterns. Anti-CCP positively and significantly correlated with Sharp's score and CRP levels. Given that anti-CCP may be influential in the choice of the best therapeutic strategy in JIA with polyarticular pattern of onset.

**Keywords:** Anti-cyclic Citrullinated peptide Antibodies (anti-CCP); Juvenile idiopathic arthritis (JIA); Juvenile arthritis disease activity score (JADAS); Sharp/van der heijde radiological score.

### 1267. Axial Involvement with Facet Joint Arthropathy and Bony Ankylosis in A Case of Camptodactyly, Arthropathy, Coxa Vara, Pericarditis (CACP) Syndrome

Yasser Emada, Yasser Ragab, Maher Khalifa, Iman Bassyouni, Nashwa El-Shaarawy and Johannes J. Rasker

*Joint. Bone. Spine., 80 (5): 520-522 (2013) IF: 2.748*

Familial arthropathy associated with congenital camptodactyly has been previously recognized as a definite clinical entity in the literature. The clinical spectrum of this disease seems to be variable. The typical features of congenital camptodactyly, arthropathy, coxa vara and pericarditis (CACP syndrome) appear to be a more frequent presentation in children from the Middle East and North Africa. Musculoskeletal presentation of this rare familial form of arthropathy is unique and heterogeneous. In all previous reports, non-inflammatory pattern of arthropathy involving the peripheral joints with typical coxa vara deformity were described, and in a few cases spine abnormalities, including kyphosis, lordosis, or scoliosis. We describe the first case of axial involvement in a typical case of CACP syndrome with facet joint arthropathy and ankylosis at L5/S1 levels.

**Keywords:** Axial joints affection; Camptodactyly; Arthropathy; Coxa vara; Pericarditis (CACP) Syndrome; Facet joint ankylosis; Facet joint arthropathy.

### 1268. Suboptimal Management of Rheumatoid Arthritis in the Middle East and Africa: Could the EULAR Recommendations Be the Start of a Solution

Bassel El Zorkany, Humaid A. AlWahshi, Mohamed Hammoudeh, Samar Al Emadi, Romela Benitha, Adel Al Awadhi, Elyes Bouajina, Ahmed Laatar, Samir El Badawy, Marzooq Al Badi, Mustafa Al-Maini, Jamal Al Saleh, Ramiz Alswailem, Mahmood Moosa Tar Mahomed Ally, Wafaa Batha, Hachemi Djoudi, Ayman El Garf, Khaled El Hadidi, Mohamed El Marzouqi, Musa Hadidi, Ajesh Basantharan Maharaj, Abdel Fattah Masri, Ayman Mofti & Ibrahim Nahar, Clive Allan Pettipher, Catherine Elizabeth Spargo and Paul Emery

*Clinical Rheumatology, 32(2): 151-159 (2013) IF: 2.037*

Although the prevalence of RA in the Middle East and Africa is comparable with that in other parts of the world, evidence indicates that its management in this region is suboptimal for a variety of reasons, including misconceptions and misunderstandings about the disease's prevalence and severity in the region, compounded by the lack of local epidemiological and health-economic data around the disease; the perception that RA is a low priority compared with other more prevalent conditions; delayed diagnosis, referral and treatment; and a lack of a region-specific, evidence-based management approach. In the absence of such an approach, the EULAR treatment recommendations may provide a useful starting point for the creation of guidelines to suit local circumstances. However, although agreement with the EULAR recommendations is high, many barriers prevent their implementation in clinical practice, including lack of timely referral to rheumatologists; suboptimal use of synthetic DMARDs; poor access to biologics; lack of awareness of the burden of RA among healthcare professionals, patients and payers; and lack of appropriate staffing levels. To optimise the management of RA in the Middle East and Africa, will require a multi-pronged approach from a diverse group of stakeholders-including local, national and regional societies, such as the African League of Associations in Rheumatology and International League of Associations for Rheumatology, and service providers-to collect data on the epidemiology and burden of the disease; to increase awareness of RA and its burden among healthcare professionals, payers and patients through various educational programmes; to encourage early referral and optimise use of DMARDs by promoting the EULAR treatment

recommendations; to encourage the development of locally applicable guidelines based on the EULAR treatment recommendations; and to facilitate access to drugs and the healthcare professionals who can prescribe and monitor them.

**Keywords:** Rheumatoid arthritis; Middle east; Management.

### 1269. Clinical Significance of Serum Interleukin-6 and -174 G/C Promoter Polymorphism in Rheumatoid Arthritis Patients

Wafaa Gaber, Ghada S. Azkalany, Tamer A. Gheita, Abeer Mohey and Randa Sabry

*The Egyptian Rheumatologist*, 35: 107-113 (2013) IF: 2

**Aim of the work:** To evaluate the clinical significance of serum levels of interleukin-6 (IL-6) and 174 G/C promoter polymorphism in Rheumatoid arthritis (RA) patients.

**Patients and Methods:** We studied 37 RA patients and 10 age and gender matched healthy controls. Demographic, clinical and serological data were prospectively evaluated. Disease activity score (DAS28) and Health Assessment Questionnaire (HAQ) were assessed. Serum IL-6 level was measured and promoter (174G/C) genotyped.

**Results:** Serum IL-6 levels were significantly higher in RA patients compared to control ( $p=0.04$ ), especially those with CC promoter polymorphism. Twenty-four patients had GG IL-6 (174 G/C) gene promoter polymorphism, 11 were GC and 2 CC. Nine controls were GG and 1 GC. In patients with more advanced polymorphism (174 CC) there was a significantly increased functional impairment (HAQ score) ( $p=0.029$ ) and platelet count ( $p=0.049$ ). In those with GG genotype, there was a significant correlation between IL-6 and Morning stiffness duration ( $r=0.44, p=0.03$ ), while those with GC genotype had a significant negative correlation of the IL-6 level with the parameters of disease activity and the DAS28 ( $r=0.69, p=0.019$ ). None of the studied parameters would predict the IL-6 promoter polymorphism.

**Conclusion:** Serum IL-6 levels and 174 G/C promoter polymorphism were higher in RA patients than in healthy controls. The inverse relation of IL-6 with the DAS28 in those with an increased IL-6 promoter polymorphism may confirm its increased involvement in the pathogenesis of RA and in the increased disease activity which may point to the need for considering of anti-IL-6 agents in their management plan.

**Keywords:** IL-6; (-174 G/C) promoter polymorphism; Rheumatoid arthritis.

### 1270. Clinical Significance of Soluble-Triggering Receptor Expressed on Myeloid Cells-1 (Strem-1) in Patients with Rheumatoid Arthritis

Samah A. El Bakry, Iman H. Bassyouni, Reem El-Shazly and Amany A. Abou-El Alla

*The Egyptian Rheumatologist*, 35: 95-100 (2013) IF: 2

**Aim of the Work:** To assess serum concentrations of triggering receptor expressed on myeloid cells-1 (sTREM-1) in rheumatoid arthritis (RA) patients, and correlate them with the main clinical, serological, radiological features and functional capacity of RA patients.

**Patients and Methods:** Sera from 61 RA patients, and 30 healthy controls were assayed for sTREM-1 by Enzyme Linked Immunosorbant Assay. RA disease activity was assessed using 28-joint disease activity score (DAS-28). Assessment of patient's functional capacity was done using modified health assessment questionnaire (mHAQ). Standardized X-rays were done to all RA participants and evaluated according to Larsen score.

**Results:** Serum levels of sTREM-1 were significantly higher in RA patients vs healthy controls ( $57.61 \pm 28.87$  and  $43.72 \pm 10.64$  ng/ml;  $p=0.027$ ). These levels were higher in patients with severe disease activity ( $68.27 \pm 36.14$  ng/ml) than those with mild and moderate disease activity ( $43.50 \pm 6.49$  ng/ml and  $47.52 \pm 12.26$  ng/ml, respectively;  $p=0.008$ ). On the contrary, no significant difference was found in levels of sTREM-1 in patients with extra-articular involvement or positive RF than those without. Levels of sTREM-1 showed a highly significant positive correlation with DAS-28 ( $P=0.001$ ), ESR ( $P=0.02$ ) and mHAQ ( $p=0.003$ ). There were no significant correlations between sTREM-1 level with age, disease duration, morning stiffness, nor radiological narrowing and erosion scores.

**Conclusion:** Levels of sTREM-1 were elevated in RA patients and correlated significantly with clinical and laboratory markers of disease activity as well as functional disability (as determined by mHAQ). To confirm our results we propose that larger scale, multicenter studies with longerevaluation periods are needed.

**Keywords:** Triggering receptor expressed on myeloid cells-1; Rheumatoid arthritis; Disease activity.

### 1271. Could Women with Systemic Lupus Erythematosus (SLE) Have Successful Pregnancy outcomes? Prospective Observational Study

A. Mokbel, A. M. Geilan and S. Abo Elgheit

*The Egyptian Rheumatologist*, 35: 133-139 (2013) IF: 2

**Aim of the Work:** The aim of this study was to determine the frequencies and predictors of maternal and fetal pregnancy outcomes in women with systemic lupus erythematosus (SLE).

**Patients and Methods:** Data of 37 pregnancies of 34 patients with systemic lupus erythematosus were collected prospectively from patients at Rheumatology and Rehabilitation department of Cairo University Hospitals from 2007 to 2009. Univariate analysis and logistic regression analysis were used.

**Results:** There were five spontaneous miscarriages, and 32 pregnancies resulting in live births. There were 20 full term babies and 12 preterm babies. Eight fetuses were born with intrauterine growth retardation (IUGR) and seven babies were born with low birth weight (LBW). Six babies were incubated at NICU (premature) with four neonatal deaths. Among 37 pregnancies, 32 women (86.5%) were in clinical remission before pregnancy; only five patients (13.5%) were active. There were 21/32 episodes of SLE flare up (65.6%) during pregnancy and eight postpartum flare up (21.6%). Eight women (21.6%) developed preeclampsia during pregnancy. Planned pregnancy and SLEDAI at the beginning of pregnancy were significantly associated with fetal loss at univariate analysis. However, there were no significant predictors of fetal loss at binary logistic regression analysis. There was no maternal mortality reported. Renal lupus disease was found to be a predictor of pre-eclampsia occurrence in univariate analysis ( $P=0.04$ ).

**Conclusion:** In general, pregnancies can be successful in most women with SLE with a favorable fetal outcome. SLE tends to



flare during pregnancy. Flares are maximal during the second trimester.

**Keywords:** Systemic lupus erythematosus; Pregnancy; Preeclampsia; Prematurity; Lupus flare.

### 1272. Does Anti-DNA Positivity Increase the Incidence of Secondary Antiphospholipid Syndrome in Lupus Patients?

Sherif M. Gamal, Samar Fawzy and Ibrahim Siam

*The Egyptian Rheumatologist*, 35 (3): 141-144 (2013) IF: 2

**Aim of the work:** To detect the incidence of secondary antiphospholipid syndrome (APS) among Systemic lupus erythematosus (SLE) patients with positive anti-DNA antibodies.

**Patients and Methods:** We studied 342 SLE patients; Group I: anti-DNA positive SLE patients (n = 208) and Group II: anti-DNA negative SLE patients (n = 134), with a female to male ratio of 9.39:1 and a mean age of  $27.49 \pm 7.94$  years and disease duration of  $5.74 \pm 3.97$  years. Full history taking, thorough clinical examination, laboratory and relevant radiological investigations were performed. Disease activity was assessed using systemic lupus erythematosus disease activity index (SLEDAI). Anti-dsDNA tests were carried out by indirect Immunofluorescence (IF) technique. Anti cardiolipin antibodies (IgG and IgM) and Anti- $\beta_2$  glycoprotein-I antibody of IgG and/or IgM isotype were detected by ELISA.

**Results:** The clinical manifestations, disease activity and laboratory investigations of the SLE patients varied according to the anti-DNA antibodies. Thirty-six patients (17.3%) had secondary APS in those with positive anti-DNA antibodies while only 16 (11.9%) had secondary APS in those with negative anti-DNA antibodies, with no significant differences between both groups.

**Conclusion:** Apparent higher incidence of secondary APS was detected in anti-DNA positive SLE patients. The non significant differences between both groups may suggest that anti-DNA positivity cannot be considered as the only predictor of secondary APS and further studies may be needed to detect other factors which may increase the incidence of APS in SLE patients.

**Keywords:** SLE; APS; Anti-DNA positivity.

### 1273. Evaluation of Left Ventricular Myocardial Function in Egyptian Patients with Systemic Lupus Erythematosus: Tissue Doppler Study and its Relation to Disease Activity

Nashwa T. Allam, Hanan E.A. Darweesh, Nehal Hamadallah and Zeinab A. Ashour

*The Egyptian Rheumatologist*, 35: 217-223 (2013) IF: 2

**Background:** Systemic lupus erythematosus (SLE) is associated with high cardiovascular morbidity and mortality. It is frequently underestimated by routine imaging techniques. Aim of the work was to determine if new echocardiographic imaging modalities like tissue Doppler, can detect abnormalities in left ventricular function in asymptomatic SLE patients. Patients and methods: Fifty SLE patients were attending the rheumatology department of the Kasr El Aini hospital. All patients were subjected to cardiac, musculoskeletal examination, routine laboratory investigations. Twenty healthy age matched subjects

were taken as controls. Ultrasound examination by two dimensional echocardiography and color tissue Doppler were performed on the patients and control to obtain the cardiac chamber diameters, systolic and diastolic myocardial velocities.

**Keywords:** Systemic lupus erythematosus; 2 Dimensional and tissue; Doppler echocardiography; Systemic lupus erythematosus disease activity index.

### 1274. Frequency and Causes of Discontinuation of Methotrexate in A Cohort of Egyptian Patients

Bassel K. El-Zorkany, Sherif M. Gamal and Sherine A. El-Mofty

*The Egyptian Rheumatologist*, 35 (2): 53-57 (2013) IF: 2

**Aim of the work:** To evaluate frequency and causes of discontinuation of methotrexate (MTX) in a group of Egyptian patients and to identify factors that may increase the incidence of its discontinuation.

**Patients and methods:** One hundred and fifty seven rheumatoid arthritis (RA) patients with disease duration of at least one year, using or were using methotrexate, were included in this study. All patients were subjected to full history taking including the cause of discontinuation of methotrexate, full detailed clinical examination, laboratory assessment, X-ray hands and assessment of disease activity score (28 joints) (DAS 28) for all RA patients. Patients were divided into two groups according to the current status of MTX use, to identify factors which may increase the incidence of MTX discontinuation.

**Results:** Forty six (29.3%) of the patients stopped MTX due to different causes, hepatic and gastrointestinal side effects were the most common causes of discontinuation, representing together 69.5% of causes of discontinuation. We found significant statistical difference between the two groups regarding disease duration, erythrocyte sedimentation rate (ESR), corticosteroid and non steroidal-anti-inflammatory drug (NSAID) use.

**Conclusion:** MTX is a safe and effective drug for RA patients and usually well tolerated, however the use of NSAIDs and corticosteroid may be associated with increased risk of discontinuation of methotrexate especially in patients with long standing disease.

**Keywords:** Rheumatoid arthritis; Methotrexate; Egyptian; Causes of discontinuation.

### 1275. Frequency of Disease Subsets and Patterns of Organ Involvement Among Egyptian Patients with Systemic Sclerosis-A Retrospective Study

Geilan Abdel Moneim, Hanan E. A. Darweesh, Mervat Ismael and Shymaa Raafat

*The Egyptian Rheumatologist*, 35: 145-149 (2013) IF: 2

**Aim of the work:** To determine the prevalence and disease characteristics of Systemic Sclerosis among Egyptian patients presented to Rheumatology departments in Cairo University & Bani Swief University.

**Patients & methods:** This is a retrospective study that included 75 patients with systemic sclerosis diagnosed according to the American college of rheumatology criteria. Their ages ranged between 17 and 70 years, all patients data were collected by medical records review.

**Results:** Out of the studied 75 patients, 14 (18.7%) were males and 61 (81.3%) were females with a ratio of 1:4.3. Fourteen patients (18.7%) had diffuse cutaneous systemic sclerosis and 61/75 (81.3%) had limited cutaneous systemic sclerosis. The commonest initial presenting manifestation in all patients was Raynaud's phenomenon in 58/75 patients (77.3%), followed by arthritis in 9/75 patients (12%) & skin tightness in 7/75 patients (9.3%). Interstitial lung disease was significantly more frequent within the diffuse compared to the limited subtype (78.6%, 47.5%, respectively  $P = 0.042$ ). Secondary pulmonary hypertension was significantly more common among the patients with dcSSc compared to the limited subtype (35.7%, 6.6%, respectively  $P = 0.009$ ). No significant difference was observed between males and females in the disease pattern.

**Keywords:** Systemic sclerosis (SSC); Diffuse cutaneous systemic sclerosis (DCSSC); limited cutaneous systemic sclerosis (LCSSC).

### 1276. Liposynovitis Prepatellaris in A Child (Hoffa'S Syndrome): Lessons from MRI

Yasser Emad and Yasser Ragab

*The Egyptian Rheumatologist*, 35, (3): 181-183 (2013) IF: 2

**Background:** Liposynovitis prepatellaris (Hoffa's syndrome) is a rare condition in children and rarely discussed in the literature. Hoffa's syndrome can lead to an obscure anterior knee pain resulting from impingement and inflammation of the infrapatellar fat pad.

**Aim of the work:** The aim of this case report is to increase awareness among rheumatologists about this condition among children to avoid erroneous diagnosis of juvenile idiopathic arthritis (JIA) and unnecessary treatment with disease-modifying antirheumatic drugs (DMARDs). Case report in this report we presented a 12 year-old child with this condition who presented with chronic pain and intermittent swelling involving his right knee. The patient was wrongly diagnosed as a case of JIA and wrongly treated with DMARDs for three years duration. The report will shed light on the characteristic MRI features of this condition and the value to order MRI in such atypical presentation.

**Conclusion:** Hoffa's syndrome can present with chronic arthropathy in children that can mimic mono-articular JIA presentation and eventually unnecessary treatment with DMARDs. MRI is generally very helpful from the diagnostic point of view, it clearly depicts Hoffa's infrapatellar fat pad entrapment and its findings may suggest Hoffa's syndrome.

**Keywords:** Hoffa'S syndrome; Knee injuries; Liposynovitis; Prepatellaris; Juvenile idiopathic arthritis (JIA).

### 1277. Post Chlamydial Reactive Arthritis in A Case of Vogt-Koyanagi-Harada Syndrome (VKH) with Negative HLA-B27: an Association Or Just Coincidence

Y. Emad, Y. Ragab and Johannes J. Rasker

*The Egyptian Rheumatologist*, 35, (4): 249-251 (2013) IF: 2

**Background:** Vogt-Koyanagi-Harada (VKH) syndrome is a multisystem disorder characterized by granulomatous panuveitis with exudative retinal detachments that is often associated with neurologic and cutaneous manifestations.

**Aim of the work:** The aim of this case report is to describe a rare case with Vogt-Koyanagi-Harada syndrome that developed an explosive form of reactive arthritis shortly after attack of Chlamydial urethritis. An association between Vogt-Koyanagi-Harada and ulcerative colitis was previously described in several case reports. The case is described in detail and the literature was reviewed. Case report in this report we described a male patient with long standing Vogt-Koyanagi-Harada syndrome, who developed aggressive reactive arthritis two weeks after an attack of Chlamydial urethritis. Clinically the patient presented with bilateral sacroiliitis, peripheral arthritis, and wide spread enthesitis. The patient had positive family history of scleroderma in his first degree relative and HLA-B27 testing was negative. **Conclusion:** in this report we theoretically proposed a possible relationship between VKH and Seronegative spondyloarthropathy group of disorders.

**Keywords:** Vogt-koyanagi-harada (VKH); Post chlamydial reactive arthritis; Ulcerative colitis; Seronegative spondyloarthropathy (SPA).

### 1278. Preclinical Coronary Endothelial Dysfunction in Egyptian Behçet'S Disease Patients; Tc-99m Sestamibi Pharmacological Gated-SPECT, is it A Useful Screening Tool?

Amr M. Amin and Zeinab O. Nawito

*The Egyptian Rheumatologist*, 35: 159-166 (2013) IF: 2

**Introduction:** Behçet's disease (BD) is an idiopathic multisystem disorder. Cardiac involvement [cardio-BD] occurs in 7–60% of BD patients. Technetium 99m-Methoxyisobutyl isonitrile (Tc-99m sestamibi) is a myocardial perfusion imaging agent that is used for evaluation of the coronary flow.

**Aim of the work:** To evaluate the usefulness of Dipyridamole pharmacological stress test in conjunction with Tc-99m sestamibi cardiac gated single photon emission computed tomography (GSPECT) to investigate the prevalence of subclinical coronary endothelial dysfunction [SCED] in asymptomatic Egyptian BD patients; also to assess possibly associated clinical predictive variables.

**Patients and Methods:** Twenty-five BD patients without overt cardiac involvement and fifteen healthy controls matched for age, BMI and sex were included. Database included full history, clinical examination, relevant laboratory tests, and Tc-99m sestamibi myocardial GSPECT with coronary angiography [CAG] in GSPECT positive cases. Disease activity was assessed using Behçet's Disease Current Activity Form (BDCAF).

**Results:** SCED detected by reduced flow or left ventricular dysfunction (LVD) or both was found in 13/25 [52%] of BD-patients [12 males and 1 female] vs. 1/15 [6.7%] of controls [ $P < 0.0001$ ] with normal CAG. Subjects with positive GSPECT had significantly older age [ $P = 0.01$ ] and longer disease duration ( $P = 0.02$ ) and were more frequently males ( $P < 0.0001$ ) than those with negative GSPECT. No statistically significant differences between cases with negative and positive GSPECT were found regarding other clinical or laboratory parameters.

**Conclusion:** Tc-99m sestamibi GSPECT could be a useful screening tool for detection of SCED in BD patients, so early prophylactic measures and therapy modifications could be considered.

**Keywords:** Behçet'S disease; Subclinical vascular endothelial dysfunction; Cardio-Behçet; Gated-SPECT.

### 1279. Serum Level of APRIL/ BLYS in Behçet'S Disease Patients: Clinical Significance in Uveitis and Disease Activity

Tamer A. Gheita, Hala Raafat, Hossam Khalil and Hani Hussein

*Modern Rheumatology*, 23: 542-546 (2013) IF: 1.716

**Objective:** The aim of the study reported here was to assess the serum concentration of B-cell activating factors, B lymphocyte stimulators (BLYS), and a proliferation inducing ligand (APRIL) in Behçet disease (BD) patients in order to evaluate their role and study their relation to uveitis subtype and disease activity.

**Methods:** The study included 58 consecutively recruited BD patients with a mean age of  $35.54 \pm 8.85$  years and disease duration of  $8.33 \pm 5.84$  years and 30 age- and sexmatched controls. Disease activity was assessed using the BD current activity form score. Patients were subclassified according to the presence and type of uveitis. Serum BLYS and APRIL were measured by enzyme-linked immunosorbent assay. Results Recurrent uveitis was present in 42 (72.41 %) patients, of whom 19 had the anterior form, 13 had the posterior form, and ten had a combined anterior with posterior form; 16 had no eye involvement. Serum APRIL ( $60.29 \pm 57.99$  ng/ml) and BLYS ( $2.31 \pm 1.97$  ng/ml) levels were significantly higher in the BD patients than in the controls ( $4.14 \pm 4.31$  and  $0.49 \pm 0.39$  ng/ml, respectively;  $P < 0.0001$ ). The levels were clearly higher in those with combined uveitis. The BLYS level significantly correlated with disease activity.

**Conclusions:** The overexpression of BLYS and APRIL in BD patients supports the notion of a critical role for B cell activation factors in BD, particularly in terms of uveitis and disease activity. This provides an interesting prospect for the use of anti-BLYS/APRIL antibodies against future therapeutic targets.

**Keywords:** Behçet'S disease; Uveitis; APRIL; BLYS.

### 1280. Systemic Sclerosis: an Ultrasonographic Study of Skin and Subcutaneous Tissue in Relation to Clinical Findings.

Manal Mohamed Sedky, Samar Mohamed Fawzy, Noha Abd El Baki, Nermine H. El Eishi and Abo El Magd Mohamed El Bohy

*Skin Res Technol.*, 19 (1): 78-84 (2013) IF: 1.409

**Background:** Skin thickening and tightness are characteristic manifestations of systemic sclerosis (SSc) and the only major diagnostic criterion. The aim of this study is to compare the results of high frequency ultrasound of skin and subcutaneous tissue (SC) in SSc patients and healthy control subjects and also to correlate our patients' US findings with the severity score and with different clinical parameters.

**Keywords:** Systemic sclerosis; Skin score; Severity score; Ultrasound; Skin thickness; Subcutaneous fat thickness.

### 1281. Resistin in Inflammatory and Degenerative Rheumatologic Diseases. Relationship Between Resistin and Rheumatoid Arthritis Disease Progression

S.M.H. Fadda, M. Gamal, N.Y. Elsaid and A.M. Mohy  
*Zeitschrift Für Rheumatologie*, 72 (6): 594-600 (2013) IF: 0.45

**Aims of The Study:** To assess and compare resistin levels in the serum and synovial fluid of patients with rheumatoid arthritis (RA; an inflammatory rheumatologic disease) and osteoarthritis (OA; a degenerative rheumatologic disease) and to study the relationship between resistin levels and prognostic factors of RA disease progression.

**Patients and Methods :** This study included a total of 50 patients: 25 with RA and 25 with OA. Full case history was documented for all patients and all underwent a thorough clinical examination and laboratory testing. Body mass index (BMI) values were also calculated. Radiographs were made of OA patients' knees and RA patients' hands. Disease Activity Score 28 (DAS28) was calculated for RA patients. Serum and synovial fluid samples were obtained from the effused knees of all patients and tested for resistin level.

**Results:** Serum resistin levels were higher in RA patients than in those with OA ( $p < 0.01$ ). Synovial fluid resistin levels were also higher in RA than OA patients ( $p < 0.001$ ). While serum resistin levels correlated with Larsen score and total leukocyte count (TLC), synovial fluid resistin levels correlated with rheumatoid factor (RF) and anti-citrullinated protein antibody (ACPA) levels in addition to Larsen score and TLC.

**Conclusion:** Resistin levels were found to be higher in the serum and synovial fluid of RA patients than in those with OA. This may suggest a role for resistin in inflammatory rheumatologic diseases. The observed statistically significant correlation between synovial fluid resistin levels and RF, ACPA and Larsen score may suggest that high synovial fluid resistin levels can be considered a poor prognostic factor for RA progression. However, further studies employing a larger cohort of patients are needed to confirm the relevance of resistin as a prognostic marker in RA patients.

**Keywords:** Osteoarthritis; Adipokines; Serum; Synovial fluid; Rheumatoid factor.

### 1282. Infliximab Induced Remission in A Case of Severe Crohns Enteropathic Arthropathy with Pyoderma Gangrenosum

Tamer A.G., Heba A.G. and Sanaa A.K.

*African Journal of Rheumatology*, 1: 8-12 (2013)

**Background:** The indications for anti-TNF therapy for inflammatory bowel diseases (IBD) have increased to include demonstrable mucosal healing, improvement in quality of life, and treatment of extraintestinal manifestations including arthritis, sacroiliitis and pyoderma gangrenosum (PG). Case report: A male smoker, 27 years old, with enteropathic arthropathy on top of Crohns disease (CD) had a disease duration of 2.25 years. He had severe Crohns disease activity index (CDAI = 473) and a poor health status as assessed by the IBD questionnaire (IBDQ) of 39. He had oligoarthritis and bilateral sacroiliitis. There was limited chest expansion and lumbar spine mobility. The patient had PG on the dorsum of the right foot and mild bilateral uveitis. He was receiving sulphasalazine 2000 mg/day and low dose corticosteroids 10 mg/day and was then given cyclosporine for a month and the steroid dose elevated (60 mg/day) but with partial improvement.

Cyclosporine was stopped and the patient remarkably improved after receiving, in addition to the corticosteroids, IV induction regimen of infliximab 5mg/kg at 0,2 and 6 weeks. A remission occurred (CDAI 98.5) with fading of arthritis, notable decrease in

the size and severity of the PG lesion and a significant disappearance of the back stiffness with an increase in the chest expansion and lumbar spine mobility. The IBDQ significantly improved to be 159.

**Conclusion:** Anti-TNF such as infliximab could be considered as a promising option for treatment of severe CD patients and for those with PG.

**Keywords:** Crohns disease; Infliximab; Pyoderma gangrenosum.

### 1283. TNF- $\alpha$ -308 Promoter G/A and PTPN22 (1858 C/T) Genes Polymorphisms in Egyptian Patients with Systemic Lupus Erythematosus

Mona M.fathy, Manal.M Kamal, Fatma El-Mougny, Tamer Gheita and Asmaa Kamel

*Comparative Clinical Pathology*, 22: 947-954 (2013)

Tumor necrosis factor alpha (TNF- $\alpha$ ) promoter gene polymorphism at position 308 and that of the protein tyrosine phosphatase nonreceptor type 22 (PTPN22) at position 1858 C/T have been inconsistently implicated as genetic risk factors for systemic lupus erythematosus (SLE) in some populations. We investigated the possible association of these polymorphisms with SLE susceptibility, and whether serum TNF- $\alpha$  level is related to different genotypes and disease activity in Egyptian SLE patients. TNF- $\alpha$ -308 G/ A and PTPN22 C1858T polymorphisms were determined by PCR-restriction fragment length polymorphism analysis in 40 SLE patients and 40 unrelated healthy controls. Serum TNF- $\alpha$  level was measured by ELISA

**Method.** The median serum TNF- $\alpha$  was significantly higher in SLE patients than in controls ( $P < 0.001$ ). A significant positive correlation was detected between serum TNF- $\alpha$  and SLE activity index ( $r = 0.723$ ,  $P < 0.001$ ). There was no significant difference in TNF- $\alpha$ -308 G/A genotypes or allele frequency between SLE cases and controls ( $P = 0.108$  and  $P = 0.133$ , respectively). Diabetes was the only clinical feature in SLE patients that showed significant higher frequency with GA genotype than with GG genotype ( $P = 0.001$ ). Risk estimation for the TNF- $\alpha$ -308 genotypes was of no significant (odds ratio 02.429; 95 % CI 00.8 – 7.2;  $P = 0.108$ ). Concerning PTPN22 1858 C/T, there was no significant difference in PTPN22 C/T genotypes or allele frequency between SLE cases and controls ( $P = 0.152$  and  $P = 0.155$ , respectively). TNF- $\alpha$ -308 G/A and PTPN22 (1858 C/T) polymorphisms do not exhibit a significant influence on the susceptibility of SLE in Egyptian patients. However, serum TNF- $\alpha$  level could be a sensitive marker of SLE disease activity.

**Keywords:** Systemic Lupus Erythematosus; TNF- $\alpha$ -308 G/A; Polymorphism; PTPN22 1858 C/T polymorphism.

#### Dept. of Surgery

### 1284. Eradication of Keloids: Surgical Excision Followed by A Single Injection of Intralesional 5-Fluorouracil and Botulinum Toxin

Adel Michel Wilson

*Canadian Journal of Plastic Surgery*, 21: 87-91 (2013) IF: 0.206

**Background:** Keloids may complicate wound healing secondary to trauma, inflammation or surgical incision. Although various treatment modalities have been used with variable degrees of

success, overall recurrence rates have remained unacceptably high.

**Methods:** The present study involved 80 patients with keloids of at least one-years' duration. Following total surgical excision of the keloid, a single dose of 5-fluorouracil was injected into the edges of the healing wound on postoperative day 9 together with botulinum toxin. The concentration of 5-fluorouracil used was 50 mg/mL and approximately 0.4 mL was infiltrated per cm of wound tissue, with the total dose  $< 500$  mg. The concentration of botulinum toxin was 50 IU/mL with the total dose  $< 140$  IU.

**Results:** Patients were followed-up for 17 to 24 months and a recurrence rate of 3.75% was found, which was significantly lower than in previously reported studies using other therapeutic modalities.

**Conclusion:** The author recommends that this treatment be routinely applied to all keloids because it is significantly more effective than those described by other authors.

**Keywords:** 5-Fluorouracil; Botulinum toxin; Keloids; Scars; wound healing.

### 1285. Pulsating Suprasternal Lump: A Diagnostic and Management Dilemma

Ahmed Sayed, Alaa Farok, Hosam El-Sayed and Said A. Soliman

*Methodist Debaquey Cardiovasc Journal*, 9: 233-234 (2013)

We report a 70- year- old female who complained of shortness of breath and a pulsating suprasternal lump. CT scan showed innominate artery dilatation. in addition, operative exposure showed tortuous arteries and a common origin of the left common carotid and innominate arteries. Surgical correction by innominate artery division and reimplantation at the ascending aorta was performed, and the patient's symptoms completely disappeared after the procedure.

**Keywords:** Pulsating suprasternal lump; Innominate artery; Trachea compression.

#### Dept. of Urology

### 1286. Effect of Size and Site on the Outcome of Extracorporeal Shock Wave Lithotripsy of Proximal Urinary Stones in Children

Enmar I. Habib, Hany A. Morsi, Mohammed S. ElSheemy, Waseem Aboulela and Mohamed A. Eissa

*J. Pediatr Urol.*, 9 (3): 323-327 (2013) IF: 1.368

**Objective:** To determine the effect of location and size of stones on the outcome of extracorporeal shock wave lithotripsy (ESWL) in children.

**Patients and Methods:** In 2008-2010, 150 children (median age 6.6 years) with radio-opaque ureteric and renal stones measuring  $\geq 4$  cm were treated. Exclusion criteria were coagulation disorders, pyelonephritis, distal obstruction, non-functioning kidney and hypertension. ESWL was performed under general anesthesia. Follow up period was 5-22 months. RESULTS: 186 stones were treated: 76 calyceal, 92 pelvic and 18 proximal ureteral. Mean stone size was 1.3 cm. A total of 312 sessions were performed (mean per stone = 1.67 sessions). The mean number of shock waves per session was 2423.68. Overall stone-free rate was 89.24%. Having a calyceal location did not significantly affect the



stone-free rate ( $p = 0.133$ ). The failure rate was significantly higher (66.7%) in stones  $>3$  cm in size ( $p < 0.001$ ). Complications were encountered in 18 patients; 2 underwent auxillary ureteroscopy and 4 retrolithotomy for treatment of steinstrasse. **Conclusion:** ESWL is a safe and effective method for treatment of stones up to 2 cm in children. Rate of auxillary procedures increases in stones  $>2$  cm in size. About 80% of failures were associated with stone size  $>1.35$  cm while 52.3% of completely cleared stones were associated with size  $<1.35$  cm.

**Keywords:** Eswl; Pediatric; Stone.

### 1287. Renal Pelvis Reduction During Dismembered Pyeloplasty: is it Necessary

Hany A. Morsi, Khaled Mursi, Ahmed Y. Abdelaziz, Mohammed S. ElSheemy, Mohamed Salah and Mohamed A. Eissa

*Journal of Pediatric Urology*, 9: (2013) IF: 1.368

**Objective:** To compare treatment results in patients who underwent pyeloplasty with and without pelvic reduction for ureteropelvic junction obstruction (UPJO).

**Methods:** This randomized prospective study involved 40 patients, all diagnosed with unilateral UPJO; 20 each were randomly selected to undergo open dismembered pyeloplasty with pelvic reduction (group A) or pelvis-sparing pyeloplasty (group B). Patients were evaluated with ultrasound and DPTA renography scans 6 months postoperatively. Mean follow-up was 9 months.

**Results:** The mean age in group B was  $5.71 \pm 6.36$  years; in group A it was  $4.81 \pm 6.78$  years. There was a decrease in mean anteroposterior renal pelvic diameter (from  $49.9$  to  $26.35 \pm 0.949$  mm in A and  $50.9$  to  $30.8 \pm 1.556$  mm in B) with improvement of split renal function (from  $39 \pm 22.47\%$  to  $42.4 \pm 22.13\%$  in A and  $34.92 \pm 16.79\%$  to  $38.8 \pm 19.66\%$  in B), glomerular filtration rate (from  $37.25 \pm 15.33$  to  $41.7 \pm 19.34$  ml/min in A and  $31.3 \pm 18.50$  to  $38.1 \pm 23.23$  ml/min in B) and draining curves on the 6-month scans, but without any significant difference between groups ( $p > 0.05$ ). Two cases in group A and three in group B needed redo pyeloplasty, but without any significant difference in failure rate.

**Conclusion:** Excision of the pelvis is not necessary in dismembered pyeloplasty procedures. We had similar surgical outcomes for patients with or without pelvis reduction.

**Keywords:** Pyeloplasty; Renal pelvis; Reduction.

### 1288. Renal Recoverability in Infants with Obstructive Calcular Anuria: is it Better than in Older Children

Mohammed Said ElSheemy Ali Sameh Kotb, Mohammed S. ElSheemy, Hany A. Morsi, Tamir Zakaria, Mohamed Salah and Mohamed A. Eissa

*J. Pediatr Urol.*, 9(6 Pt B): 1178-1182 (2013) IF: 1.368

**Objective:** Urolithiasis in infants can cause considerable morbidity. The literature regarding calcular anuria in this age group is very defective. Our aim was to evaluate impact of intervention on renal recoverability in these infants.

**Patients and Methods:** A series of 24 patients presenting with obstructive calcular anuria were included in this study. Mean age was  $16.5 \pm 6.2$  months. They were treated either by initial urinary diversion or definitive endoscopic (ureteroscopy or JJ stenting

with medical alkalization) or open surgical (ureterolithotomy or pyelolithotomy) treatment.

**Results:** Mean serum creatinine was  $5.8 \pm 2.6$  mg/dl. Initial peritoneal dialysis and/or urinary diversion was needed in 11 patients (45.8%). Open surgical treatment was applied in 5 (20.8%), endoscopic treatment was applied in 15 (62.5%), while combined treatment was applied in 4 (16.6%) patients. All patients had normal serum creatinine on discharge. Three (12.5%) had residual stones which were cleared by 2ry ureteroscopic intervention at 6 months. The overall complication rate in this study was 12.5% in the form of postoperative leakage (1) and postoperative fever (2). No mortality or development of chronic renal failure was reported at 6 months follow up. in comparison with these results, a previous study carried out in our centre on an older age group had a higher complication rate (28%) with higher mortalities and lower renal function recoverability rate (94%). **Conclusions:** Appropriate and timely medical and surgical management of calcular anuria will mostly lead to full recovery of renal functions. in comparison with older children, renal prognosis in those less than 2 years seems more favorable.

**Keywords:** Anuria; Calculi; Infants; Obstructive nephropathy; Renal recoverability.

### 1289. Semi-Rigid Ureteroscopy for Ureteric and Renal Pelvic Calculi: Predictive Factors for Complications and Success

Khaled Mursi, Mohammed S. Elsheemy, Hany A. Morsi, Abdel-Karim Ali Ghaleb and Omar M. Abdel-Razzak

*Arab Journal of Urology*, 11 (2): 136-141 (2013)

**Objective:** To analyse and compare the effect of stone site and size, method of lithotripsy, and level of experience on the results and complications of semi-rigid ureteroscopy for ureteric and renal pelvic stones. Patients and methods Between April 2010 and May 2011, 90 patients underwent 95 ureteroscopies, using 7.5- and 9-F semi-rigid ureteroscopes, with or without pneumatic or laser lithotripsy. The peri-operative findings were analysed and compared.

**Results:** The mean (SD) longest diameter of the stones was 11.8 (4.5) mm. Laser lithotripsy was used in 32 cases and pneumatic lithotripsy in 26. There were complications in 35 procedures in the form of colicky pain (2%), haematuria (1%), stone migration (7%), equipment failure (5%), access failure (8%), mucosal injury (7%), fever (2%) and extravasation (3%). The calculi were successfully retrieved in 75 patients (83%). The success rate was 95%, 77%, 85%, and 53% in the lower, middle, upper ureter and renal pelvis, respectively.

**Conclusions:** Upper ureteric stones can be managed safely with the semi-rigid ureteroscope. Renal pelvic stones are associated with a lower success rate, and thus they were not a primary indication for ureteroscopic intervention. The secondary ureteroscopic management of renal pelvic stones improved the results of subsequent alkalisation or shock-wave lithotripsy if they could not be eradicated completely. The failure rate was significantly small in lower ureteric stones and stones of  $<10$  mm. Less experience, a stone size of  $>15$  mm and patients 2 years old were associated with more complications or a lower success rate. There was no significant difference in the success or complication rate between laser and pneumatic lithotripsy.

**Keywords:** Laser; Lithotripsy; Pneumatic; Ureteroscopy; Urinary tract stones.



## Faculty of Oral Dental Medicine

### Dept. of Endodontics

#### 1290. Computed Tomographic Evaluation of Canal Shape Instrumented by Different Kinematics Rotary Nickel-Titanium Systems

Abeer M. Marzouk and Angie G. Ghoneim

*J. Endod. (JOE), 39 (7): 906-909 (2013) IF: 2.929*

**Introduction:** This study evaluated the effects of 2 different kinematics rotary nickel-titanium (NiTi) systems, Twisted File (TF), a continuous rotation full-sequence system, and WaveOne (WO), a reciprocating single-file system, on transportation, curvature, and volumetric changes of curved root canals by using cone-beam computed tomography.

**Methods:** Forty mesiobuccal canals of mandibular molars with angle of curvature ranging from 25°-35° were divided according to the NiTi rotary system used in canal preparation into 2 groups of 20 samples each, TF group and WO group. Canals were scanned by using an i-CAT cone-beam computed tomography scanner before and after instrumentation to evaluate canal transportation at coronal, middle, and apical thirds, canal curvature, and volumetric changes. The significance level was set at  $P \leq .05$ .

**Results:** TF system recorded significantly lower mean of canal transportation than WO group at all canal thirds (apical  $P = .034$ , middle  $P = .003$ , and coronal  $P = .012$ ). In both groups the apical third recorded the significantly least amount of transportation ( $P < .05$ ). There was no significant difference between the 2 groups in canal curvature and volumetric changes after instrumentation ( $P > .05$ ).

**Conclusion:** Both TF and WO NiTi systems can be safely used to the full working length, resulting in satisfactory preservation of the original canal shape.

**Keywords:** Canal transportation; Computed tomography; Root canal volume; Twisted file; Waveone file.

#### 1291. Expression Levels of Matrix Metalloproteinase-9 and Gram-Negative Bacteria in Symptomatic and Asymptomatic Periapical Lesions

Geraldine Mohamed Ahmed, Alaa A. El-Baz, Ahmed Abdel Rahman Hashem and Abeer K. Shalaan

*Journal of Endodontics, 39 (4): 444-448 (2013) IF: 2.929*

**Introduction:** The aim of this study was to test the hypothesis that the expression of matrix metalloproteinase (MMP)-9 is significantly elevated in patients with symptomatic apical periodontitis and to correlate this with the detected amount of gram-negative bacteria.

**Methods:** Twenty-six patients with periapical lesions involving at least 2 teeth were included in this study. The patients were divided into 2 groups: the symptomatic (SYM) group included 13 patients expressing pain with periapical lesions, and the asymptomatic (ASYM) group included 13 patients expressing no pain. Root canal treatment was performed followed by endodontic surgery and periapical lesion collection. Periapical lesions were serially cut into 4- $\mu$  sections. Some sections were processed for histologic examination using hematoxylin-eosin stain. Other sections were processed for immunohistochemical examination.

for MMP-9, the area fraction of the positive cells was measured, and the percentage of the MMP-9-immunopositive area to the total area of the microscopic field was calculated. For gram-negative stain cells, the number of cells showing the pink-red color was counted per microscopic field. The Student's *t* test was used to compare the SYM and ASYM groups. The Pearson correlation coefficient was used to determine a significant correlation between the number of cells and the MMP-9 level. The significance level was set at  $P = .05$ .

**Results:** The SYM group showed a statistically significantly higher mean number of gram-negative cells ( $P = .001$ ) and MMP-9 area percent ( $P < .001$ ) than the ASYM group. There was a statistically significant positive ( $r = .927$ ) correlation between the number of gram-negative cells and the MMP-9 area percent ( $P < .001$ ).

**Conclusions:** There is good evidence to suspect a significant role of gram-negative bacteria and MMP-9 in symptomatic periapical lesions.

**Keywords:** Gram-negative bacteria; Matrix metalloproteinase-9; Matrix metalloproteinases; Periapical lesions; Symptomatic.

### Dept. of Operative Dentistry

#### 1292. Bond Durability of Adhesives Containing Modified-Monomer with/ without-Fluoride After Aging in Artificial Saliva and Under Intrapulpal Pressure Simulation

Enas Hussein Mobarak, Heba El Deeb and Heba Al Sherbiney

*Operative Dentistry, 38: 48-56(2013) IF: 1.4*

**Objective:** To evaluate the dentin bond strength durability of adhesives containing modified-monomer with/without-fluoride after storage in artificial saliva and under intrapulpal pressure simulation (IPPS).

**Materials and Methods:** The occlusal enamel of 48 freshly extracted teeth was trimmed to expose midcoronal dentin. Roots were sectioned to expose the pulp chamber and to connect the specimens to the pulpal-pressure assembly. Specimens were assigned into four groups ( $n=12$ ) according to adhesive system utilized: a two-step etch-and-rinse adhesive system (SB, Adper Single Bond 2, 3M ESPE), a two-step self-etch adhesive system (CSE, Clearfil SE Bond, Kuraray Medical Inc), and two single-step self-etch adhesives with the same modified monomer (bis-acrylamide)-one with fluoride (AOF, AdheSE One F, Ivoclar-Vivadent) and the other without (AO, AdheSE One, Ivoclar-Vivadent). Bonding was carried out while the specimens were subjected to 15-mm Hg IPPS. Resin composite (Valux Plus, 3M ESPE) buildups were made. After curing, specimens were aged in artificial saliva and under 20-mm Hg IPPS at 37°C in a specially constructed incubator either for 24 hours or six months prior to testing. Bonded specimens ( $n=6$ /group) were sectioned into sticks ( $n=24$ /group) with a cross section of  $0.9 \pm 0.01 \text{ mm}^2$  and subjected to microtensile bond strength ( $\mu$ TBS) testing using a universal testing machine. Data were statistically analyzed using two-way analysis of variance (ANOVA) with repeated measures, one-way ANOVA tests, and a *t*-test ( $p < 0.05$ ). Failure modes were determined using a scanning electron microscope.

**Results:** The  $\mu$ TBS values of SB and CSE fell significantly after six-month storage in artificial saliva and under IPPS, yet these values remained significantly higher than those for the other two adhesives with modified monomers. There was no significant

difference in the bond strength values between fluoride-containing and fluoride-free self-etch adhesive systems (AOF and AO) after 24 hours or six months. Modes of failure were mainly adhesive and mixed.

**Conclusion:** Based on the results of this study, 1) Fluoride addition did not affect dentin bond durability; and 2) despite the fact that the single-step adhesive system with modified monomer showed stability, bond strengths associated with these systems remained lower than those of multistep adhesive systems.

**Keywords:** Bond durability; Adhesives; Modified-monomer; Fluoride; Aging; Artificial saliva; Intrapulpal pressure simulation.

### 1293. Bond Durability of Self-Etch Adhesive to Ethanol-Based Chlorhexidine Pretreated Dentin After Storage in Artificial Saliva and Under Intrapulpal Pressure Simulation

Enas Hussein Mobarak, Amr A. Ali, Heba A. El Deeb and Omar Badran

*Operative Dentistry*, 38: 439-446 (2013) IF: 1.4

**Objective:** To evaluate the bond strength durability of a single-step self-etch adhesive to dentin pretreated with either ethanol-based chlorhexidine (ECHX) or water-based chlorhexidine (WCHX) after storage in artificial saliva and under intrapulpal pressure simulation (IPPS).

**Methods:** The occlusal enamel of 30 freshly extracted premolars was trimmed to expose midcoronal dentin. Roots were sectioned to expose the pulp chamber. Specimens were distributed over three groups (n=10) according to the dentin pretreatment used. In the first group, Adper Easy One (3M ESPE) was applied to the dentin surfaces according to the manufacturer's instructions (control group). In the second group, dentin was pretreated before bonding with 1 mL of 2% CHX diacetate dissolved in 100% ethanol (ECHX). The third group received the same pretreatment; however, CHX was dissolved in distilled water (WCHX). Pretreatment and bonding were carried out while the specimens were subjected to IPPS. Resin composite (Valux Plus, 3MESPE) buildups were made. After curing, specimens were stored in artificial saliva and under IPPS at 37°C in a specially constructed incubator (n=5/group) either for 24 hours or six months prior to testing. Thereafter, bonded specimens were sectioned into sticks with a cross section of  $0.9 \pm 0.01 \text{ mm}^2$  and subjected to microtensile bond strength ( $\mu\text{TBS}$ ) testing (n=25/subgroup) using a universal testing machine. Data were statistically analyzed using two-way analysis of variance (ANOVA) with repeated measures, one-way ANOVA, and Bonferroni post hoc tests (p=0.05). Failure modes were determined using a scanning electron microscope.

**Results:** After 24 hours of storage, control and WCHX groups revealed significantly higher  $\mu\text{TBS}$  than the ECHX group. After six-month storage in artificial saliva and IPPS, only the WCHX group maintained its  $\mu\text{TBS}$  value. The predominant mode of failure was the mixed type, except for the ECHX group, which was mostly adhesive.

**Conclusion:** Pretreatment of the dentin with ECHX had a negative effect on bonding of the tested single-step self-etch adhesive; however, WCHX showed bond stability under IPPS.

**Keywords:** Bond durability; Adhesives; Ethanol-based; Chlorhexidine; Storage; Artificial saliva, Intrapulpal pressure simulation.

### 1294. Effect of Using Silorane-Based Resin Composite for Restoring Conservative Cavities on the Changes in Cuspal Deflection

Enas Hussein Mobarak, Nermine M. Shabayek and Fayez M. Hassan

*Operative Dentistry*, 38: 1-8 (2013) IF: 1.4

**Objective:** To investigate the effect of using two resin-composite materials for restoring conservative mesio-occluso-distal (MOD) cavities on the changes (incremental and cumulative) in cuspal deflection.

**Methods:** Forty extracted sound human maxillary second premolars were subjected to standardized MOD cavity preparation and then divided into two groups (n=20). The first group of teeth was restored with Filtek Z250 (3M ESPE, St Paul, MN, USA), and Filtek P90 (3M ESPE, St Paul, MN, USA) was used in the second group. Incremental cuspal deflection was calculated by measuring the intercusp distance between the indexed cusp tips before the restoration and at five-minute intervals up to 30 minutes using a stereomicroscope connected to a digital camera. Cumulative cuspal deflection for both materials was also calculated.

**Results:** Comparing the incremental cuspal deflection of the tested groups at each time interval, it was found that there was no significant difference immediately after curing and at five, 15, 20, and 25 minutes. However, a significant difference was recorded at 10 and 30 minutes. For the cumulative cuspal deflection, Filtek P90 showed significantly lower deflection values than Filtek Z250 only after five minutes.

**Conclusion:** Incremental cuspal deflections of both materials over the tested intervals were almost comparable. However, after five minutes of curing, silorane-based resin composite surpassed the methacrylate-based resin composite in controlling the cumulative cuspal deflection.

**Keywords:** Silorane-based Resin composite; Conservative cavities; Cuspal deflection.

### 1295. Interfacial Nanoleakage and Bonding of Self-Adhesive Systems Cured with A Modified-Layering Technique To Dentin of Weakened Roots

Enas Hussein Mobarak and Reham Seyam

*Operative Dentistry*, 38: E154-165(2013) IF: 1.4

**Objective:** The purpose of the study was to evaluate the nanoleakage and bond strength of different self adhesive systems cured with a modified-layering technique (MLT) to dentin of weakened roots.

**Methods:** Twenty-one maxillary incisors were decoronated and then root canals were instrumented and obturated with the cold lateral compaction technique. Weakened roots were simulated by flaring root canals until only 1 mm dentin thickness remained. Teeth were distributed into three groups. The canals were backfilled with Vertise Flow (VF group), a self-adhering system, following a modified-layering technique using two light-transmitting posts, sizes 6 and 3. DT Light Post size 2 was cemented using the same material. Remaining roots were prepared and cured in the same way as the VF group. However, in the TS/MF group, Clearfil Tri-S Bond (TS) adhesive and Clearfil Majesty Flow (MF) composite were used, while in the ED/PF group, ED primer II (ED)/Panavia F2.0 (PF) were used. After one

week of storage, each root was sectioned to obtain six slices (two slices from each root third: coronal, middle and apical) of  $0.9 \pm 0.1$  mm thickness. Interfacial nanoleakage expression was analyzed using a field emission scanning electron microscope (FEG-SEM), and the micro push-out bond strength ( $\mu$ POBS) was measured at different root regions. Modes of failure were also determined using SEM. Data were statistically analyzed using two-way analysis of variance with repeated measures and Tukey post hoc test ( $p=0.05$ ).

**Results:** with MLT, all adhesive systems showed nanoleakage. For  $\mu$ POBS, there was a statistically significant effect for adhesive systems ( $p<0.001$ ) but not for root region ( $p<0.64$ ) or for their interaction ( $p=0.99$ ). Tukey post hoc test revealed that the bond strength of the VF group was significantly higher than the TS/MF and ED/PF groups for all root regions.

**Conclusion:** All of the tested self-adhesive systems cured using MLT had slight nanoleakage and were not sensitive to root regional differences. Self-adhering systems had higher bond strength than self-etch adhesives.

**Keywords:** Interfacial nanoleakage; Bonding; Adhesive system; Modified-layering technique; Dentin; Weakened roots.

### 1296. Two-Year Interfacial Bond Durability and Nanoleakage of Repaired Silorane-Based Resin Composite

Enas Hussein Mobarak and Heba El-Deeb

*Operative Dentistry, 38: 408-418(2013) IF: 1.4*

**Objectives:** To investigate the effect of silane primer application, intermediate adhesive agent/repair composite, and storage period on the interfacial microtensile bond strength ( $\mu$ TBS) of repaired silorane-based resin composite compared with unrepaired composites and on the nanoleakage.

**Methods:** Forty-eight 1-month-old substrate specimens from Filtek P90 were roughened, etched, and distributed over two groups ( $n=24$ ) based on receiving silane (Clearfil Ceramic Primer) or not. Then, half of the specimens ( $n=12$ ) were repaired with P90 System Adhesive/Filtek P90 and the other half with Adper Scotchbond Multipurpose adhesive/Filtek Z250 resin composite. Within each repair category, repaired specimens were stored in artificial saliva at  $37^\circ\text{C}$  for either 24 hours ( $n=6$ ) or two years before being serially sectioned into sticks ( $0.6 \pm 0.01$  mm<sup>2</sup>). From each specimen, two sticks were prepared for nanoleakage determination and four sticks were used for  $\mu$ TBS testing. Additional unrepaired specimens from each composite ( $n=12$ ) were made to determine the cohesive strength at 24 hours and two years. Mean  $\mu$ TBS were calculated and statistically analyzed. Modes of failure were also determined.

**Results:** General linear model analysis revealed no significant effect for the silane priming, intermediate adhesive agent/repair composite, and storage period or for their interactions on the  $\mu$ TBS values of the repaired specimens. There was no significant difference between the cohesive strength of Filtek P90 and Filtek Z250; both were significantly higher than all repaired categories. At 24 hours, nanoleakage was not detected when silorane-based composite was repaired with the same material. However, after two years, all repair categories showed nanoleakage.

**Conclusion:** Silane application has no effect on  $\mu$ TBS and nanoleakage. Durability of the interfacial bond of repaired silorane-based resin composite appeared successful regardless of the chemistry of the intermediate adhesive agent/composite used

for repair. However, nanoleakage was detected early when a different repair intermediate adhesive agent/composite was used.

**Keywords:** Bond durability; Nanoleakage; Repair; Silorane-based; Resin composite.

### Dept. of Oral and Maxillofacial Surgery

### 1297. Soft-Tissue Profile Changes Associated with Anterior Maxillary Osteotomy for Severe Maxillary Protrusion

Emad Tawfik M. M. Daif

*The Journal of Craniofacial Surgery, 24: 80-83 (2013) IF: 1.6*

**Objectives:** The aim of this study was to evaluate the soft-tissue profile changes after correction of severe maxillary protrusion with anterior maxillary osteotomy via a cephalometric analysis.

**Patients and Methods:** Using Wunderer technique, anterior maxillary osteotomies were performed in 14 patients (12 females and 2 males) having severe maxillary protrusion. Standardized lateral digital cephalograms, true size, were taken before the treatment and 12 months after removal of the fixation means. The soft-tissue profile changes resulting from anterior maxillary osteotomy were evaluated by comparing the preoperative and postoperative cephalometric analyses. A statistical analysis was performed using paired  $t$  test. The differences were considered significant at  $P < 0.05$ .

**Results:** The labial prominence showed reductions of 31% and 20% for the upper and lower lips, respectively. An increase in the nasolabial angle (16%) was noted subsequent to anterior maxillary osteotomies. Also, the facial convexity angle was increased (7%) postoperatively. The interlabial gap and the upper-lip curvature obviously decreased (56% and 60%, respectively) after surgery. The curvature of the lower lip, labiomental fold, showed a decrease of 17% after surgery, causing flatness to the lower face. The postoperative changes in the soft-tissue cephalometric measurements were statistically significant except for the lower-lip curvature and prominence as well as the lower-face height.

**Conclusions:** Anterior maxillary osteotomy is a highly recommended treatment modality for patients with severe maxillary protrusion. The technique is simple with minimal postoperative complications, and the soft-tissue profile changes after surgery are predictable.

**Keywords:** Profile changes; Anterior maxillary osteotomy; Maxillary protrusion.

### 1298. Botulinum Toxin Injection for Management of Temporomandibular Joint Clicking

Aala Shoukry Emara, M. I. Faramawey, M. A. Hassaan and M. M. Hakam

*Int. J. Oral; Maxillofacial Surgery, 42: 759-764 (2013) IF: 1.521*

The aim of the present study was to investigate the effect of botulinum toxin type A (BTX-A) injection in the lateral pterygoid (LP) muscle on temporomandibular joint (TMJ) clicking. The study enrolled seven patients with a total of 11 joints; all patients were stage I or II of Wilke's staging for internal derangement. BTX-A was injected in the ipsilateral LP muscle with electromyogram (EMG) guidance and the subjects were assessed for 4 months. Maximum inter-incisal opening, range of lateral

movement, and the presence of a click were recorded throughout the follow-up period, and magnetic resonance imaging (MRI) was ordered at the end of the 4 months. The results showed that the decrease in inter-incisal opening and side to side movement immediately postoperative was statistically significant, while the difference by the end of the follow-up period was insignificant. MRI showed a marked improvement in disc position postoperatively. It may be concluded that BTX injection in the LP muscle leads to the disappearance of joint clicking clinically and a significant improvement in disc position as shown on MRI.

**Keywords:** Temporomandibular joint; Click; BOTOX; MRI.

### 1299. Effect of A Multiporous Beta-Tricalcium Phosphate on Bone Density Around Dental Implants Inserted Into Fresh Extraction Sockets

Emad Tawfik Daif

*Journal of Oral Implantology*, 39: 339-344 (2013) IF: 1.5

The aim of this study was to assess, via multi-slice helical computerized tomography (CT), the influence of the pure-phase multiporous beta-tricalcium phosphate (beta-TCP) on bone density around dental implants inserted into fresh extraction sockets. Twenty-eight patients (18 women and 10 men), indicated for extraction of their lower premolars and insertion of immediate dental implants, were included in this study. They were randomly divided into two equal groups (14 patients each). Group A received immediate dental implants without any filling material around the implants, while in group B, a pure-phase multiporous beta-TCP was gently packed into the bone gaps around the implants. Three and 6 months after loading the implants, a CT, sagittal and coronal, was made to measure the bone density around the implants. The results of the current study have shown that the mean values of the bone density measurements around the implants in group A were 1150  $\pm$  6205 (range, 645–1460) at 3 months and 1245  $\pm$  165 (range, 884–1650) at 6 months after loading the implants. In group B, the mean values of the bone density measurements around the implants were 1280  $\pm$  320 (range, 876–1790) and 1490  $\pm$  358 (range, 1061–1965) at 3 and 6 months after loading the implants, respectively. The statistical analysis of the collected data showed a significant increase in the bone density measurements from 3 to 6 months only in group B ( $P$  .05). Also, the difference between group A and B in the bone density measurements around the implants was statistically significant ( $P$  .05) at only 6 months after loading. On the basis of the results presented in this study, it may be possible to mention that the pure-phase multiporous beta-TCP may enhance the bone density when inserted into the bone gaps around immediate dental implants.

**Keywords:** Immediate implants; Beta-tricalcium Phosphate; Bone density.

### 1300. Effect of Autologous Platelet-Rich Plasma on Bone Regeneration in Mandibular Fractures

Emad Tawfik Daif

*Journal of Dental Traumatology*, 29: 399-403, (2013) IF: 1.5

**Objectives:** The aim of this study was to assess the effect of autologous platelet-rich plasma (PRP) on bone regeneration in

mandibular fractures via a cone beam computed tomography (CBCT). Patients and

**Methods:** Twenty-four patients having parasymphseal fractures participated in this study. They were randomly divided into two equal groups. Group A was treated by two titanium miniplates and screws plus local application of activated PRP along the fracture line, whereas group B was treated by the same bone plates and screws without application of PRP. The patients were recalled at 1 week, 3 and 6 months after surgery for clinical assessment and measuring the bone density via CBCT at a region of interest (ROI) including the fracture line.

**Results:** The mean values of the bone density measurements, in both groups, were higher at 3 and 6 months than 1 week after surgery. At 1 week after surgery, the values were 542  $\pm$  93 HU and 515  $\pm$  81 HU in group A and B, respectively. In group A, the mean value of bone density measurements was 728  $\pm$  58 HU (range 620–796 HU) at 3 months after surgery and it was 1024  $\pm$  188 HU (range 825–1490 HU) 6 months later. While in group B, the mean values of the bone density measurements at the ROI were 600  $\pm$  78 HU (range 520–790 HU) and 756  $\pm$  53 HU (range 710–890 HU) at 3 and 6 months after surgery, respectively. The increase in the bone density measurements at 3 and 6 months after surgery was statistically significant only in group A ( $P$  = 0.0002 and  $P$  = 0.0001, respectively).

**Conclusions:** It can be concluded that direct application of the PRP along the fracture lines may enhance the bone regeneration in mandibular fractures.

**Keywords:** Platelet-rich plasma; Bone regeneration; Mandibular fracture.

### 1301. Prognostic Evaluation of Preserving Palatal Mucosa After Resection of Maxillary Myxoma: 10 Years' Follow-Up

Emad Tawfik Daif

*The Journal of Craniofacial Surgery*, 24: 361-365 (2013) IF: 1.6

**Objectives:** This study was carried out to assess the clinical and radiological outcomes of preserving palatal mucosa after resection of odontogenic maxillary myxomas.

**Study Design:** Fifteen patients (9 females and 6 males) with odontogenic maxillary myxomas participated in this study. Their ages ranged between 22 and 40 years. They were diagnosed as having myxomas by clinical and computed tomographic examinations as well as by performing biopsies on them. All lesions were treated by maxillary resection with preserving palatal mucosa. After surgery, the resultant surgical defects were followed up for 10 years.

**Results:** No clinical or radiological evidence of recurrence was observed after 20 years' follow-up. The healing process was rapidly progressing without any serious complications. However, 6 patients complained of sore areas in their palatal mucosa because of the acrylic stents. They were successfully treated with mouthwash, anti-inflammatory drugs, and relief of the acrylic stents. After surgery, numbness of the upper lip was observed in all cases; however, it improved gradually in 5 patients over a period of 2 years. Computed tomographic scan of the surgical sites has shown incomplete filling of the resultant surgical defects. Constantly, there was empty space beneath the orbital floor in all computed tomographic images.

**Conclusions:** Maxillary resection with preserving palatal mucosa is a recommended treatment modality for odontogenic maxillary

myxomas as it minimizes the unpleasant sequelae after surgery without recurrence. However, this technique should be restricted only to the cases having intact palatal bone.

**Keywords:** Maxillary myxoma; Odontogenic tumors; Odontogenic myxoma.

#### Dept. of Oral Pathology

##### 1302. Assessment of the Effect of Low-Energy Diode Laser Irradiation on Gamma Irradiated Rats' Mandibles

Dalia Hussein El-rouby, Eman M.F. El-Maghraby and Ali M. Saafan

*Archives of Oral Biology*, 58: 796-805 (2013) IF: 1.549

**Objective:** The purpose of the present study was to evaluate the biostimulative and regenerative effects of low intensity laser irradiation (LILT) (applied before or after initiation of radiotherapy) on gamma irradiated rats' jaw bones.

**Methods:** Forty eight male Albino rats were equally divided into two groups: group 1, in which the left side of the mandible was subjected to three successive sessions of laser (LILT) prior to whole body gamma radiation (2 Gy/3 fractions/week) and group 2, received whole body gamma radiation (2 Gy/3 fractions/week) prior to three successive sessions of laser applied to left side. The right side of both groups was used as gamma irradiated non-lased control group. Each group was then subdivided into four equal subgroups (a, b, c, d) according to the time of scarification (3, 7, 14, 21 days respectively). Specimens were subjected to histological, histomorphometric and scanning electron microscopic examinations.

**Results:** Thin irregular bone trabeculae and widened marrow spaces were identified in the control group. The lased sides of groups 1 and 2 demonstrated regular, thick and continuous bone trabeculae. Ultrastructurally, collagen fibres of the control group appeared irregularly arranged and more spaced compared to groups 1 and 2. Normal-sized osteocytic lacunae were seen in the lased groups, as compared to the wide lacunar spaces noted in the control group. Histomorphometric analysis showed a significant increase in the area of bone trabeculae, as well as the width of compact bone, for the lased groups.

**Conclusions:** LILT seemed to attenuate the radiation-related damage in alveolar bones.

**Keywords:** Laser therapy; Low-level; Bone and bones; Radiotherapy; Osteoradionecrosis.

##### 1303. Assessment of the Role of Cone Beam Computed Sialography in Diagnosing Salivary Gland Lesions

Naglaa Abdel-Wahed, Maha E. Amer and Noha Saleh M. Abo-Taleb

*Imaging Science in Dentistry*, 43: 17-23 (2013)

**Purpose:** The purpose of this study was to assess cone-beam computed (CBCT) sialography imaging in the detection of different changes associated with lesions of salivary glands.

**Materials and Methods:** This study consisted of 8 cases with signs and symptoms from salivary gland lesions. Conventional sialography using digital panoramic and lateral oblique

radiographs and CBCT sialography were performed for each subject. The radiographs were evaluated by 3 radiologists independently of each other. The results were compared between conventional sialography and CBCT sialography in the evaluation of various lesions associated with the salivary glands.

**Results:** There was an agreement between the radiologists in interpreting the lesions that affected salivary glands with both techniques. The detection of the presence of stones or filling defects, stenosis, ductal evagination, dilatation, and space occupying lesions was 83% for conventional sialography compared with CBCT sialography. CBCT sialography was superior to conventional sialography in revealing stones, stenosis, and strictures, especially in the second and third order branches. **Conclusion:** It would be advisable to perform CBCT sialography in cases of obstructive salivary gland diseases for better demonstration of the ductal system of the gland.

**Keywords:** Cone-beam computed tomography; Salivary glands; Sialography.

#### Dept. of Prosthetic Dentistry

##### 1304. The Effect of Varying Implant Position in Immediately Loaded Implant-Supported Mandibular Overdentures

Mohammed A. Shaarawy and Ehab M. Aboelross

*J. Oral Implantol.*, 39(3): 345-354(2013) IF: 1.148

This study was carried out to evaluate the effect of varying implant position in immediately loaded implant-supported mandibular overdentures on peri-implant bone density, muscle activity, and patient satisfaction. Fourteen completely edentulous patients were selected for the study. After complete denture construction, patients were divided into 2 equal groups. Four dental implants were installed bilaterally in the interforaminal region in the first group, while in the second group, 4 dental implants were inserted bilaterally: 2 in the interforaminal region and 2 in the first molar area. Immediately after suturing, telescopic abutments were screwed to the implants, and the retaining caps were picked up into the fitting surface of the lower denture, which was delivered to the patient. Patients were recalled for radiographic bone density evaluation just after denture delivery and then at 3, 6, and 12 months thereafter. Muscle activities of masseter and temporalis muscles as well as patient satisfaction were also evaluated. The results of the study showed a high success rate approximating 98.2% of the immediately loaded implants. The electromyographic (EMG) records of both muscles in group 1 were significantly higher during chewing hard food after 3 months compared with group 2 ( $P < .05$ ). Bone density changes were comparable in the 2 groups except at the end of the follow-up period, when group 2 showed a significant increase in peri-implant bone density values of the posteriorly placed implants compared with group 1 ( $P < .05$ ). From the results of this study, it may be concluded that wide distribution of immediately loaded implants used for supporting mandibular overdentures through posterior placement beyond the interforaminal area results in a favorable response in terms of increased peri-implant bone density as well as decreased EMG activity of masseter and temporalis muscles.

**Keywords:** Dental implant position; Implant supported overdenture; Immediate loading; Telescopic copings; Bone density.



## Faculty of Pharmacy

### Dep. Of Analytical chemistry

#### 1305. Coupled Solid Phase Extraction and Microparticle-Based Stability and Purity-Indicating Immunosensor for the Determination of Recombinant Human Myelin Basic Protein in Transgenic Milk

Medhat Ahmed Abdelhamid Al-Ghobashy, Martin A.K. Williams, Götz Laible and David R.K. Harding

*Talanta*, 109: 7-12 (2013) IF: 3.498

An optical immunosensor was developed and validated on the surface of microparticles for the determination of a biopharmaceutical protein. The recombinant human myelin basic protein (rhMBP) was produced in milk of transgenic cows as a His-tagged fusion protein. Previous work indicated exclusive association of rhMBP with milk casein micelles that hindered direct determination of the protein in milk. In this work, a solid phase extraction using a cation exchange matrix was developed in order to liberate rhMBP from casein micelles. A sandwich-type immunoassay was then used for in-process monitoring of the full-length protein in the presence of major milk proteins. The assay was successfully employed for detection of ultra-traces of rhMBP ( $\text{LOD}=6.04 \text{ ng mL}^{-1} \approx 0.3 \text{ nmol L}^{-1}$ ) and for quantitative determination over a wide concentration range ( $10.00\text{--}10,000.00 \text{ ng mL}^{-1}$ ). The assay was able also to detect the rhMBP in the presence of its human counterpart that lacks the His-tag. The high sensitivity along with the ability of the assay to determine the full length protein enabled monitoring of the stability of rhMBP. The testing protocol is particularly useful for intrinsically unstructured proteins that are extremely sensitive to proteolysis and lack a traceable enzymatic activity. This immunosensor provides a specific, ultrasensitive high throughput tool for in-process monitoring in biopharmaceutical industry.

**Keywords:** Biopharmaceuticals; Optical immunosensors; Bio-Plex; Myelin basic protein; Solid phase extraction.

#### 1306. Simultaneous Determination of Olanzapine and Fluoxetine Hydrochloride in Capsules by Spectrophotometry, TLC-Spectrodensitometry and HPLC

Mahmoud Abdallah El-Tantawy Abdallah, Nagiba Y. Hassan, Nariman A. Elragehy and Mohamed Abdelkawy

*Journal of Advanced Research*, 4: 173-180 (2013) IF: 3

This paper describes sensitive, accurate and precise spectrophotometric, TLC- spectrodensitometric and high performance liquid chromatographic (HPLC) methods for simultaneous determination of olanzapine and fluoxetine HCl. Two spectrophotometric methods were developed, namely; first derivative ( $D^1$ ) and derivative ratio ( $DD^1$ ) methods. The TLC method employed aluminum TLC plates precoated with silica gel GF<sub>254</sub> as the stationary phase and methanol: toluene: ammonia (7:3:0.1, by volume) as the mobile phase, where the chromatogram was scanned at 235 nm. The developed HPLC method used a reversed phase C18 column with isocratic elution. The mobile phase composed of phosphate buffer pH 4.0:acetonitrile: triethylamine (53:47:0.03, by volume) at flow rate

of  $1.0 \text{ mL min}^{-1}$ . Quantitation was achieved with UV detection at 235 nm. The methods were validated according to the International Conference on Harmonization (ICH) guidelines. The selectivity of the proposed methods was tested using laboratory-prepared mixtures. The developed methods were successfully applied for the determination of olanzapine and fluoxetine HCl in bulk powder and combined capsule dosage form.

**Keywords:** Spectrophotometry; TLC-spectrodensitometry; HPLC; Olanzapine; Fluoxetine HCL.

#### 1307. Spectrophotometric and TLC-Densitometric Methods for the Simultaneous Determination of Ezetimibe and Atorvastatin Calcium

Medhat Ahmed Abdelhamid Al-Ghobashy, Yehia Z. Baghdady, Abdel-Aziz E. Abdel-Aleem and Soheir A. Weshahy

*Journal of Advanced Research*, 4 (1): 51-59 (2013) IF: 3

Three sensitive methods were developed for simultaneous determination of Ezetimibe (EZB) and Atorvastatin calcium (ATVC) in binary mixtures. First derivative ( $D^1$ ) spectrophotometry was employed for simultaneous determination of EZB (223.8 nm) and ATVC (233.0 nm) with a mean percentage recovery of  $100.23 \pm 1.62$  and  $99.58 \pm 0.84$ , respectively. Linearity ranges were  $10.00\text{--}30.00 \mu\text{g mL}^{-1}$  and  $10.00\text{--}35.00 \mu\text{g mL}^{-1}$ , respectively. Isosbestic point (IS) spectrophotometry, in conjunction with second derivative ( $D^2$ ) spectrophotometry was employed for analysis of the same mixture. Total concentration was determined at IS, 224.6 nm and 238.6 nm over a concentration range of  $10.00\text{--}35.00 \mu\text{g mL}^{-1}$  and  $5.00\text{--}30.00 \mu\text{g mL}^{-1}$ , respectively. ATVC concentration was determined using D2 at 313.0 nm ( $10.00\text{--}35.00 \mu\text{g mL}^{-1}$ ) with a mean recovery percentage of  $99.72 \pm 1.36$ , while EZB was determined mathematically at 224.6 nm ( $99.75 \pm 1.43$ ) and 238.6 nm ( $99.80 \pm 0.95$ ). TLC-densitometry was employed for the determination of the same mixture;  $0.10\text{--}0.60 \mu\text{g band}^{-1}$  for both drugs. Separation was carried out on silica gel plates using diethyl ether-ethyl acetate (7:3 v/v). EZB and ATVC were resolved with  $R_f$  values of 0.78 and 0.13. Determination was carried out at 254.0 nm with a mean percentage recovery of  $99.77 \pm 1.30$  and  $99.86 \pm 0.97$ , respectively. Methods were validated according to ICH guidelines and successfully applied for analysis of bulk powder and pharmaceutical formulations. Results were statistically compared to a reported method and no significant difference was noticed regarding accuracy and precision.

**Keywords:** Ezetimibe; Atorvastatin calcium; Derivative spectrophotometry; Isosbestic spectrophotometry; Spectrophotometry.

#### 1308. Comparative ANNs with Different Input Layers and GA-PLS Study for Simultaneous Spectrofluorimetric Determination of Melatonin and Pyridoxine HCL in the Presence of Melatonin'S Main Impurity

Hany Wagih Darwish, Mohamed I. Attia, Ali S. Abdelhameed Amer M. Alanazi and Ahmed H. Bakheit

*Molecules*, 18: 974-996 (2013) IF: 2.428

Melatonin (MLT) has many health implications, therefore it is important to develop specific analytical methods for the

determination of MLT in the presence of its main impurity, *N*-[2-[1-({3-[2-(acetylamino) ethyl] - 5-methoxy-1*H*-indol-2-yl} methyl)- 5-methoxy- 1*H*-indol-3-yl ] ethyl] acetaamide (DMLT) and pyridoxine HCl (PNH) as aco-formulated drug.

This work describes simple, sensitive, and reliable four multivariate calibration methods, namely artificial neural network preceded by genetic algorithm (GA-ANN), principal component analysis (PCA-ANN) and wavelet transform procedures (WT-ANN) as well as partial least squares preceded by genetic algorithm (GA-PLS) for the spectrofluorimetric determination of MLT and PNH in the presence of DMLT.

Analytical performance of the proposed methods was statistically validated with respect to linearity, accuracy, precision and specificity.

The proposed methods were successfully applied for the assay of MLT in laboratory prepared mixtures containing up to 15% of DMLT and in commercial MLT tablets with recoveries of no less than 99.00%. No interference was observed from common pharmaceutical additives and the results compared favorably with those obtained by a reference method.

**Keywords:** Melatonin; Pyridoxine HCL; Spectrofluorimetry; Multivariate calibration methods; Pharmaceutical tablets.

### 1309. Determination of Insecticides Malathion and Lambda-Cyhalothrin Residues in Zucchini by Gas Chromatography

Hany Hunter Monir Bebawi, Hayam M. Lofty and Abd El-Aziz A. Abd El-Aleem

*Bulletin of Faculty of Pharmacy, Cairo University, 51: 255-260 (2013)*

A sensitive gas chromatographic method has been developed for the determination of malathion and lambda-cyhalothrin (k-cyhalothrin) insecticide residues in zucchini. The developed method consists of extraction with acetone, purification and partitioning with methylene chloride, column chromatographic clean up, and finally capillary gas chromatographic determination of the insecticides.

The recoveries of method were greater than 90% and limit of determination was 0.001 ppm for both insecticides. The method was applied to determine residues and the rate of disappearance of malathion and  $\lambda$ -cyhalothrin from fruits of zucchini (open field treatment, 50 cc of Malason/Cormandel 57% EC (emulsifiable concentrate) for 100 L of water, 20 cc of LAMBDA SUPER FOG 5% liquid for 100 L of water).

The insecticide incorporated into the plants decreased rapidly with a half-life time around 0.77 day (18.5h) for malathion and 4 days for  $\lambda$ -cyhalothrin. It is not recommended to use zucchini before 12 h of malathion application. For  $\lambda$ -cyhalothrin, the preharvest interval is 5 days. Four market samples were chosen from different regions from A.R.E. and all of them showed no residues of malathion or  $\lambda$ -cyhalothrin.

**Keywords:** Malathion;  $\lambda$ -Cyhalothrin; Gas chromatography; Residues; Zucchini.

### 1310. Determination of Ofloxacin and Dexamethasone in Dexaflox Eye Drops Through Different Ratio Spectra Manipulating Methods

Marianne Nebsen Morcos Iskander, Ghada M. Elsayed, M. AbdelKawy and S.Z. ELkhateeb

*Bulletin of The Faculty of Pharmacy Cairo University, 51: 175-184 (2013) IF: 2*

Different sensitive and selective spectrophotometric methods for the determination of ofloxacin and dexamethasone in their binary mixture were presented. Ofloxacin was determined simply by zero order at its  $\lambda_{\max}$  293.4 nm in a linear range of 1.5–12  $\mu\text{g mL}^{-1}$  with mean percentage recovery of  $100.07 \pm 0.66\%$  without any interference of dexamethasone even in low or high concentrations. Dexamethasone was determined by first derivative of ratio spectra  $^1\text{DD}$  at 266.5 nm, ratio subtraction and mean centering at 243 nm with methods in a linear range of 2.5–27.5  $\mu\text{g mL}^{-1}$  with mean percentage recoveries of  $100.09 \pm 0.70\%$ ,  $100.00 \pm 0.72\%$  and  $99.92 \pm 0.62\%$ , respectively. These methods were applied to the analysis of pharmaceutical dosage form and bulk powder where good recoveries were obtained. The proposed methods were validated according to USP guidelines.

**Keywords:** Ofloxacin; Dexamethasone; Derivative ratio; Ratio subtraction; Mean centering.

### 1311. Novel Stability Indicating Methods for the Determination of Certain Synthetic Estrogen Level Modifiers

Hanan Abd El-Monem Ahmed Merey, Maha M. Galal, Maissa Y. Salem and Ezzat M. Abdel-Moety

*Bulletin of Faculty of Pharmacy Cairo University, 51: 69-79 (2013) IF: 1.7*

Tamoxifen citrate (TC) and raloxifene hydrochloride (RH) are two selective estrogen receptor modifiers. TC is usually used in the treatment of breast cancer while RH is used in the treatment of osteoporosis. Two stability indicating methods, namely, first derivative of ratio spectra ( $^1\text{DD}$ ) and TLC-densitometric method are used for the determination of TC in the presence of its photodegradants and RH in the presence of its oxidative degradants. For the first derivative of ratio spectra method, TC was quantitatively measured at 263 nm and 298.2 nm in a concentration range of 10–60  $\mu\text{g/mL}$  while RH was determined at 267.6 nm in a concentration range of 2–18  $\mu\text{g/mL}$ . In the spectro-densitometric method, TC was separated from its photodegradants using a developing system consisting of acetonitrile: 33% ammonia solution (10: 0.1, v/v) in a concentration range of 6–20  $\mu\text{g/band}$  while RH was separated from its oxidative degradants using ethyl acetate: methanol: 33% ammonia solution (7: 3: 0.1, by volume) as a developing system in a concentration range of 3–11  $\mu\text{g/band}$ . The two methods were successfully applied for the stability indicating the determination of the two drugs in a pure powdered form and a pharmaceutical dosage form and showing good recoveries. Statistical comparison between the results obtained by applying the proposed methods and the official method or the reported method for TC and RH, respectively was done and no significant difference was found at  $p=0.05$ .

**Keywords:** First derivative of ratio spectra; Spectrophotometry; Raloxifene; Tamoxifen; Spectro-densitometry; Stability indicating method; Synthetic estrogen level modifiers.

### 1312. Spectrophotometric; Chemometric and Chromatographic Determination of Naphazoline Hydrochloride and Chlorpheniramine Maleate in the Presence of Naphazoline Hydrochloride Alkaline Degradation Product

Maha Abdel-Monem Aboseri Hegazy, Nour El-Deen Sayed and Mohammed Abdelkawy

*Bulletin of Faculty of Pharmacy, Cairo University, 51: 57-68 (2013)*

Four accurate and sensitive methods were developed and validated for determination of naphazoline hydrochloride (NAP) and chlorpheniramine maleate (CLO) in the presence of naphazoline hydrochloride alkaline degradation product (NAP Deg). The first method is a spectrophotometric one where NAP was determined by the fourth derivative ( $D^4$ ) spectrophotometric method by measuring the peak amplitude at 302 nm, while CLO was determined by the second derivative of the ratio spectra ( $DD^2$ ) spectrophotometric method at 276.4 nm. The second method is a chemometric-assisted spectrophotometric method in which partial least squares (PLS-1) and partial component regression (PCR) were used for the determination of NAP, CLO and NAP Deg using the information contained in their absorption spectra of ternary mixture. The third method is a TLC-densitometric one where NAP, CLO and NAP Deg were separated using HPTLC silica gel F254 plates using ethyl acetate:methanol:ammonia: (8:2:0.5, by volume) as the developing system followed by densitometric measurement at 245 nm. The fourth method is HPLC method where NAP, CLO and NAP Deg were separated using ODS  $C_{18}$  column and a mobile phase consisting of 0.1M  $KH_2PO_4$  (pH=7) : methanol (55:45 v/v) delivered at 1.5 mL  $min^{-1}$  followed by UV detection at 265 nm. The proposed methods have been successfully applied to the analysis of NAP and CLO in pharmaceutical formulations without interference from the dosage form additives and the results were statistically compared with a reported method.

**Keywords:** Naphazoline hydrochloride; Chlorpheniramine maleate; Spectrophotometry; Chemometrics; Spectrodensitometry; HPLC.

### 1313. Three Different Methods for Determination of Binary Mixture of Amlodipine and Atorvastatin Using Dual Wavelength Spectrophotometry

Said Abd El-Monem Hassan, Hany W. Darwish, Maissa Y. Salem and Badr A. El-Zeany

*Spectrochimica Acta Part A: Molecular; Biomolecular Spectroscopy, 104: 70-76 (2013) IF: 2*

Three simple, specific, accurate and precise spectrophotometric methods depending on the proper selection of two wavelengths are developed for the simultaneous determination of Amlodipine besylate (AML) and Atorvastatin calcium (ATV) in tablet dosage forms. The first method is the new Ratio Difference method, the second method is the Bivariate method and the third one is the Absorbance Ratio method. The calibration curve is linear over the concentration range of 4–40 and 8–32  $\mu g/mL$  for AML and ATV, respectively. These methods are tested by analyzing synthetic mixtures of the above drugs and they are applied to commercial pharmaceutical preparation of the subjected drugs. Methods are

validated according to the ICH guidelines and accuracy, precision, repeatability and robustness are found to be within the acceptable limit. The mathematical explanation of the procedures is illustrated.

**Keywords:** Spectrophotometry; Absorbance ratio; Bivariate; Ratio difference; Atorvastatin; Amlodipine.

### 1314. Comparative Study between Derivative Spectrophotometry and Multivariate Calibration as Analytical Tools Applied for the Simultaneous Quantitation of Amlodipine, Valsartan and Hydrochlorothiazide

Said Abd El-Monem Hassan, Hany W. Darwish, Maissa Y. Salem and Badr A. El-Zeany

*Spectrochimica Acta Part A: Molecular and Biomolecular Spectroscopy, 113: 215-223 (2013) IF: 2*

Four simple, accurate and specific methods were developed and validated for the simultaneous estimation of Amlodipine (AML), Valsartan (VAL) and Hydrochlorothiazide (HCT) in commercial tablets. The derivative spectrophotometric methods include Derivative Ratio Zero Crossing (DRZC) and Double Divisor Ratio Spectra-Derivative Spectrophotometry (DDRS-DS) methods, while the multivariate calibrations used are Principal Component Regression (PCR) and Partial Least Squares (PLSs). The proposed methods were applied successfully in the determination of the drugs in laboratory-prepared mixtures and in commercial pharmaceutical preparations. The validity of the proposed methods was assessed using the standard addition technique. The linearity of the proposed methods is investigated in the range of 2–32, 4–44 and 2–20  $\mu g/mL$  for AML, VAL and HCT, respectively.

**Keywords:** PLS; PCR; Double divisor; Amlodipine; Valsartan; Hydrochlorothiazide.

### 1315. Development and Validation of New Spectrophotometric Ratio H-Point Standard Addition Method and Application to Gastrointestinal Acting Drugs Mixtures

Ali Mohamed Abd-Eltawab M. Yehia

*Spectrochimica Acta Part A: Molecular and Biomolecular Spectroscopy, 109: 193-200 (2013) IF: 1.977*

New, simple, specific, accurate and precise spectrophotometric technique utilizing ratio spectra is developed for simultaneous determination of two different binary mixtures. The developed ratio H-point standard addition method (RHPSAM) was managed successfully to resolve the spectral overlap in itopride hydrochloride (ITO) and pantoprazole sodium (PAN) binary mixture, as well as, mosapride citrate (MOS) and PAN binary mixture. The theoretical background and advantages of the newly proposed method are presented. The calibration curves are linear over the concentration range of 5–60  $\mu g/mL$ , 5–40  $\mu g/mL$  and 4–24  $\mu g/mL$  for ITO, MOS and PAN, respectively. Specificity of the method was investigated and relative standard deviations were less than 1.5. The accuracy, precision and repeatability were also investigated for the proposed method according to ICH guidelines.

**Keywords:** Ratio H-point standard addition method; Binary mixtures; Itopride hydrochloride; Pantoprazole sodium; Mosapride citrate.

### 1316. Simultaneous Determination of Some Cholesterol-Lowering Drugs in Their Binary Mixture by Novel Spectrophotometric Methods

Maha Abdel-Monem A. Hegazy and Hayam Mahmoud Lotfy

*Spectrochimica Acta Part A: Molecular and Biomolecular Spectroscopy*, 113: 107-114 (2013) IF: 1.977

Four simple, specific, accurate and precise spectrophotometric methods manipulating ratio spectra were developed and validated for simultaneous determination of simvastatin (SM) and ezetimibe (EZ) namely; extended ratio subtraction (EXRSM), simultaneous ratio subtraction (SRSM), ratio difference (RDSDM) and absorption factor (AFM). The proposed spectrophotometric procedures do not require any preliminary separation step. The accuracy, precision and linearity ranges of the proposed methods were determined, and the methods were validated and the specificity was assessed by analyzing synthetic mixtures containing the cited drugs. The four methods were applied for the determination of the cited drugs in tablets and the obtained results were statistically compared with each other and with those of a reported HPLC method. The comparison showed that there is no significant difference between the proposed methods and the reported method regarding both accuracy and precision.

**Keywords:** Simvastatin; Ezetimibe; Extended ratio subtraction; Simultaneous ratio subtraction; Ratio difference and absorption factor.

### 1317. Studying the Compatibility of a Metoclopramide- HCL-Paracetamol Mixture Via IHCMC and Establishing A Validated RP-HPLC Method for its Determination in Tablets

Nagiba Yehia Mohamed Hassan, Amira M. Hegazy, Raimar Loebenberg, Fadia H. Metwally and Mohammad Abdel-Kawy

*Analytical Methods*, 5: 3714-3720 (2013) IF: 1.855

Currently metoclopramide hydrochloride (MCP-HCl) and paracetamol (PCM) are co-formulated together in a tablet form which is widely used in relief of painful migraine. The purpose of this work was to investigate the physicochemical compatibility of this co-mixture in the solid form and in different media as well. A highly selective and sensitive RP-HPLC method was established to quantify MCP-HCl and PCM in the presence of their degradation products. Chromatographic separation was achieved on a C-8 column using phosphate buffer, acetonitrile and methanol (40: 15: 10, v/v/v, pH 3) as a mobile phase at a flow rate of 0.5 mL min<sup>-1</sup> with UV detection at 220 nm. Isothermal Heat-Conduction Micro-Calorimetry (IHCMC) was used to investigate heat-flow caused by physico-chemical incompatibility. The method was linear within concentration ranges such as 20–80 mg mL<sup>-1</sup> and 10–70 mg mL<sup>-1</sup> for MCP-HCl and PCM, respectively. The LOD and LOQ of the method for determination of MCP-HCl and PCM were 0.501, 0.101, 1.67 and 3.39, respectively. Other analytical validation parameters such as accuracy, precision, selectivity and applicability of the method were evaluated using an external standard addition technique. The

tablets containing MCP-HCl and PCM in the concentration ratio of 1 : 100 were analyzed by the method successfully via two concentration levels. Thermal analysis of solid mixtures of the drugs showed compatibility over short and long terms in contrast with their aqueous mixtures. So it is not recommended that this drug mixture be formulated in a liquid form.

**Keywords:** Compatibility; Metoclopramide; IHCMC; RP-HPLC.

### 1318. Multivariate Versus Classical Univariate Calibration Methods for Spectrofluorimetric Data: Application to Simultaneous Determination of Olmesartan Medoxamil and Amlodipine Besylate in Their Combined Dosage form

Hany Wagih Darwish and Ahmed H. Backeet

*Journal of Fluorescence*, 23: 79-91 (2013) IF: 1.789

Olmesartan medoxamil (OLM, an angiotensin II receptor blocker) and amlodipine besylate (AML, a dihydropyridine calcium channel blocker), are co-formulated in a single-dose combination for the treatment of hypertensive patients whose blood pressure is not adequately controlled on either component monotherapy. In this work, four multivariate and two univariate calibration methods were applied for simultaneous spectrofluorimetric determination of OLM and AML in their combined pharmaceutical tablets in all ratios approved by FDA. The four multivariate methods are partial least squares (PLS), genetic algorithm PLS (GAPLS), principal component ANN (PC-ANN) and GA-ANN. The two proposed univariate calibration methods are, direct spectrofluorimetric method for OLM and isoabsorptivity method for determination of total concentration of OLM and AML and hence AML by subtraction. The results showed the superiority of multivariate calibration method over univariate ones for the analysis of the binary mixture. The optimum assay conditions were established and the proposed multivariate calibration methods were successfully applied for the assay of the two drugs in validation set and combined pharmaceutical tablets with excellent recoveries. No interference was observed from common pharmaceutical additives. The results were favorably compared with those obtained by a reference spectrophotometric method.

**Keywords:** Olmesartan medoxamil; Amlodipine besylate; Spectrofluorimetry; Multivariate calibration methods; Pharmaceutical tablets.

### 1319. Determination of Sumatriptan and Zolmitriptan in Presence of Their Corresponding Degradation Products by HPTLC Methods

Mamdouh Reda Rezk Yousef, Hayam M. Lotfy, Adel M. Michael and Mostafa A. Shehata

*Chromatographia*, 76: 187-194 (2013) IF: 1.437

Accurate, sensitive, and precise high performance thin layer chromatographic (HPTLC) methods were developed and validated for the determination of sumatriptan and zolmitriptan in presence of their degradation products. Sumatriptan was separated from its degradation products and analyzed on TLC silica gel 60 F254 plates using chloroform–ethyl acetate–methanol–ammonia (4:3: 3:0.1, v/v) as a developing system followed by densitometric measurement of the bands at 228 nm. Zolmitriptan was determined using chloroform–ethyl acetate–methanol–ammonia



(3:3:3:1, v/v) as a developing system followed by densitometric measurement at 222 nm. The methods were validated over a range of 0.5–4 lg/spot for sumatriptan and 0.5–3 lg/spot for zolmitriptan. The proposed methods were successfully applied for the determination of the studied drugs in bulk powder and in their pharmaceutical formulations.

**Keywords:** HPTLC; Sumatriptan; Zolmitriptan; Pharmaceutical formulation.

### 1320. Stability-Indicating HPLC and RP-TLC Determination of Cefpirome Sulfate with Kinetic Study

Mohamed Refaat Elsayed Elghobashy, Lories I. Bebawy, Samah S. Abbas and Rafeek F. Shokry

*Chromatographia*, 76: 1141-1151 (2013) IF: 1.437

Two sensitive and selective stability-indicating methods were developed for the determination of the antibiotic cefpirome sulfate in bulk powder, pharmaceutical formulation and in presence of its acid, alkaline, photo- and oxidative degradation products. Method A was based on HPLC separation of cefpirome sulfate in the presence of its degradation products on a reversed phase column C18, 250 × 4.6 mm, 5-µm particle size and mobile phase consisting of 0.1 M disodium hydrogenphosphate dihydrate pH 3.9 adjusted with phosphoric acid–acetonitrile (85:15, v/v). Quantitation was achieved with UV detection at 270 nm.

The linear calibration curve was in the range 5.0–50.0 lg mL<sup>-1</sup>. Method B was based on reversed phase TLC separation of the cited drug in the presence of its degradation products followed by densitometric measurement of the intact drug at 270 nm. These separation was carried out using disodium hydrogenphosphate dihydrate 2.0 g % w/v, at pH 3.5 adjusted with phosphoric acid–acetone (15:10, v/v) as a developing system. The calibration curve was in the range of 1.0–10.0 lg/spot. The HPLC method was used to study the kinetic of cefpirome sulfate acid degradation. The results obtained were statistically analyzed and compared with those obtained by applying the official Japanese method.

**Keywords:** Cefpirome sulfate; Stability study; HPLC; RP-TLC; Kinetic study.

### 1321. Application of Smart Spectrophotometric Methods and Artificial Neural Network for the Simultaneous Quantitation of Olmesartan Medoxamil, Amlodipine Besylate and Hydrochlorothiazide in their Combined Pharmaceutical Dosage form

Hany Wagih Darwish

*Chemistry Central Journal*, 7: (2013) IF: 1.31

**Background:** New, simple and specific spectrophotometric methods and artificial neural network (ANN) were developed and validated in accordance with ICH guidelines for the simultaneous estimation of Olmesartan (OLM) Amlodipine (AML), and Hydrochlorothiazide (HCT) in commercial tablets.

**Results:** For spectrophotometric

**Methods:** First, Amlodipine (AML) was determined by direct spectrophotometry at 359 nm and by application of the ratio subtraction, the AML spectrum was removed from the mixture spectra. Then Hydrochlorothiazide (HCT) was determined directly

at 315 nm without interference from Olmesartan medoxamil (OLM) which could be determined using the isoabsorptive method. The calibration curve is linear over the concentration range of 5–40, 2.5–40 and 2–40 µg mL<sup>-1</sup> for AML, OLM and HCT, respectively. ANN (as a multivariate calibration method) was also applied for the simultaneous determination of the three analytes in their combined pharmaceutical dosage form using spectral region from 230–340 nm.

**Conclusions:** The proposed methods were successfully applied for the assay of the three analytes in laboratory prepared mixtures and combined pharmaceutical tablets with excellent recoveries. No interference was observed from common pharmaceutical additives. The results were favorably compared with those obtained by a reference spectrophotometric method. The methods are validated according to the ICH guidelines and accuracy, precision and repeatability are found to be within the acceptable limit.

**Keywords:** Olmesartan medoxamil; Amlodipine besylate; Hydrochlorothiazide; Spectrophotometry; Artificial neural network.

### 1322. Simultaneous Determination of Sitagliptin and Metformin in their Pharmaceutical Formulation

Mamdouh Reda Rezk Yousef

*Journal of Aoac International*, 96: 301-306 (2013) IF: 1.23

Two simple, accurate, and rapid methods were developed for simultaneous determination of sitagliptin phosphate and metformin hydrochloride in their pharmaceutical formulation. The first is a TLC method coupled with densitometry. The second is an HPLC method using a C18 column. The selectivity of the proposed methods was checked using laboratory-prepared mixtures. The proposed methods were successfully applied to the analysis of sitagliptin phosphate and metformin hydrochloride in bulk form and in their pharmaceutical formulation without interference from other additives.

**Keywords:** Sitagliptin; Metformin; TLC; HPLC.

### 1323. Ion Selective Phosphotungstate and β-Cyclodextrin Based Membrane Electrodes for Stability-Indicating Determination of Midodrine Hydrochloride

Eman Saad Hassan Elzanfaly, Hala E. Zaazaa and Hanan A. Mery

*Acta Chim. Slov.*, 60 (2): 256-262 (2013) IF: 1.135

This paper reports the construction and evaluation of two ion selective electrodes for the determination of midodrine hydrochloride (MD) by direct potentiometry in pure drug substance and in tablet formulations. Precipitation based technique was used for fabrication of the first membrane sensor (sensor 1) using phosphotungstate (PT) and dioctylphthalate (DOP) as cation exchanger and solvent mediator, respectively. β-cyclodextrin (β-CD)-based technique with PT as a fixed anionic site in PVC matrix was used for fabrication of the second membrane sensor (sensor 2). The proposed sensors showed fast, stable Nernstian responses of 54 and 56 mV/decade for sensors 1 and 2, respectively, across a relatively wide MD concentration range (1 × 10<sup>-4</sup> to 1 × 10<sup>-1</sup> mol/L and 5 × 10<sup>-5</sup> to 1 × 10<sup>-1</sup> mol/L for sensor 1 and 2, respectively) in the pH range of 5–7. Sensor 1 and sensor



2 can be used for three and two weeks, respectively without any measurable change in sensitivity. The suggested electrodes succeeded to determine intact MD in the presence of up to 10% of its degradation product and displayed good selectivity in presence of common inorganic and organic species.

**Keywords:** Ion-selective electrodes; Phosphotungstate;  $\beta$ -cyclodextrin; Midodrine hydro-chloride; Deglymidodrine; Determination; Tablets.

#### 1324. Application of Pcr and Pls Methods for the Simultaneous Determination of Candesartan Cilexetil and Hydrochlorothiazide in their Pharmaceutical Preparations

Hany Wagih Darwish, Wedad A. Al-Onazi, Nawal A. Al-Arfaj and Amina M. Al-Brashy

*Digest Journal of Nanomaterials and Biostructures*, 8: 1253-1262 (2013) IF: 1.092

Candesartan cilexetil (CND, an angiotensin II receptor blocker), and hydrochlorothiazide (HCT, a diuretic of the class of benzothiadiazines) are co-formulated in a single-dose combination for the treatment of hypertensive patients whose blood pressure is not adequately controlled on either component monotherapy. In this work, two multivariate calibration methods were applied for simultaneous spectrophotometric determination of CND and HCT in their combined pharmaceutical tablets. The multivariate methods are principal component regression (PCR) and partial least squares (PLS). Both methods are useful in spectral analysis because of the simultaneous inclusion of many spectral wavelengths instead of the single wavelength used in derivative spectrophotometry. The optimum assay conditions were established and the proposed methods were successfully applied for the assay of the two drugs in an independent validation set and combined pharmaceutical tablets with excellent recoveries. No interference was observed from common pharmaceutical additives. The results were favorably compared with those obtained by a reference HPLC method.

**Keywords:** Candesartan cilexetil; Hydrochlorothiazide; Spectrophotometry; Multivariate calibration methods; Pharmaceutical tablets.

#### 1325. Three Multivariate Calibration Methods for Simultaneous Spectrophotometric Determination of Olmesartan Medoxamil, Amlodipine Besylate and Hydrochlorothiazide in Their Combined Dosage Form

Hany Wagih Darwish, Ahmed H. Bakheit and Mohamed I. Attia

*Digest Journal of Nanomaterials and Biostructures*, 8: 323-333 (2013) IF: 1.092

Olmesartan medoxamil (OLM, an angiotensin II receptor blocker) amlodipine besylate (AML, a dihydropyridine calcium channel blocker) and hydrochlorothiazide (HCT, a diuretic of the class of benzothiadiazines) are co-formulated in a single-dose combination for the treatment of hypertensive patients whose blood pressure is not adequately controlled on either component monotherapy. In this work, three multivariate calibration methods were applied for simultaneous spectrophotometric determination of OLM, AML

and HCT in their combined pharmaceutical tablets. The multivariate methods are classical least squares (CLS), principal component regression (PCR) and partial least squares (PLS). The results showed the superiority of PLS over CLS and PCR for the analysis of the ternary mixture. The optimum assay conditions were established and the proposed methods were successfully applied for the assay of the three drugs in an independent validation set and combined pharmaceutical tablets with excellent recoveries. No interference was observed from common pharmaceutical additives. The results were favorably compared with those obtained by a reference spectrophotometric method.

**Keywords:** Olmesartan medoxamil; Amlodipine besylate; Hydrochlorothiazide spectrophotometry; Multivariate calibration methods; Pharmaceutical tablets.

#### 1326. Bivariate Versus Multivariate Smart Spectrophotometric Calibration Methods for the Simultaneous Determination of A Quaternary Mixture of Mosapride, Pantoprazole and Their Degradation Products

Ali Mohamed Abd-Eltawab Mohamed Yehia, M. A. Hegazy and A. A. Moustafa

*Die Pharmazie*, 68: 317-326 (2013) IF: 0.96

The ability of bivariate and multivariate spectrophotometric methods was demonstrated in the resolution of a quaternary mixture of mosapride, pantoprazole and their degradation products. The bivariate calibrations include bivariate spectrophotometric method (BSM) and H-point standard addition method (HPSAM), which were able to determine the two drugs, simultaneously, but not in the presence of their degradation products, the results showed that simultaneous determinations could be performed in the concentration ranges of 5.0–50.0 g/ml for mosapride and 10.0 – 40.0 g/ml for pantoprazole by bivariate spectrophotometric method and in the concentration ranges of 5.0–45.0 g/ml for both drugs by H-point standard addition method. Moreover, the applied multivariate calibration methods were able for the determination of mosapride, pantoprazole and their degradation products using concentration residuals augmented classical least squares (CRACLS) and partial least squares (PLS). The proposed multivariate methods were applied to 17 synthetic samples in the concentration ranges of 3.0–12.0 g/ml mosapride, 8.0–32.0 g/ml pantoprazole, 1.5–6.0 g/ml mosapride degradation products and 2.0–8.0 g/ml pantoprazole degradation products. The proposed bivariate and multivariate calibration methods were successfully applied to the determination of mosapride and pantoprazole in their pharmaceutical preparations.

**Keywords:** Bivariate calibration; Multivariate calibration; Mosapride; Pantoprazole.

#### 1327. Chromatographic Methods for the Simultaneous determination of Metoprolol Tartrate and Hydrochlorothiazide in the Presence of Hydrochlorothiazide Degradation Product

Nesrin Khamis Ramadan Selim, Heba M. Mohamed and Azza A. Mostafa

*Journal of Planar Chromatography*, 26: 510-516 (2013) IF: 0.96

Metoprolol tartrate (MT) (Figure1) is a selective adrenergic antagonist that is devoid of intrinsic sympathomimetic activity [1]. It is used in the management of hypertension, angina pectoris, cardiac arrhythmia and myocardial infarction [2]. Hydrochlorothiazide (HZ) (Figure 1) is a thiazide diuretic that is used in the treatment of hypertension either alone or with other antihypertensives. It is also used to treat edema associated with heart failure, with renal and hepatic disorders, and with acute glomerulonephritis [1, 2]. MT and HZ are co-formulated together in commercial tablets for their antihypertensive effect.

**Keywords:** Metoprolol tartrate; Hydrochlorothiazide; HPLC; TLC.

### 1328. A Comparative Study of Validated Spectrophotometric and TLC- Spectrodensitometric Methods for the Determination of Sodium Cromoglicate and Fluorometholone in Ophthalmic Solution

Hayam Mahmoud Lotfy Ibrahim, Sarah S. Saleh, Nagiba Y. Hassan and Samia M. Elgizawy

*Saudi Pharmaceutical Journal*, 21: 411-421 (2013)  
IF: 0.954

The determination of sodium cromoglicate (SCG) and fluorometholone (FLU) in ophthalmic solution was developed by simple sensitive and precise methods. Three spectrophotometric methods were applied: absorptivity factor (a-Factor method), absorption factor (AFM) and mean centering of ratio spectra (MCR). The linearity ranges of SCG were found to be (2.5–35 lg/mL) for (a-Factor method) and (MCR) while for (AFM), it was found to be (7.5–50 lg/mL). The linearity ranges of FLU were found to be (4–16 lg/mL) for (a-Factor method) and (AFM); while for (MCR), it was found to be (2–16 lg/mL).

The mean percentage recoveries/ RSD for SCG were found to be 100.31/0.90, 100.23/0.57 and 100.43/1.21; while for FLU, they were found to be 100.11/0.56, 99.97/0.35 and 99.94/ 0.88 using (a-Factor method), (AFM) and (MCR), respectively. A TLC-spectrodensitometric method was developed by separation of SCG and FLU on silica gel 60F<sub>254</sub> using chloroform: methanol: toluene: triethylamine in the ratio of (5:2:4:1 v/v/v/v) as developing system followed by spectrodensitometric measurement of the bands at 241 nm.

The linearity ranges and the mean percentage recoveries/ RSD were found to be (0.4–4.4 lg/band), 100.24/1.44 and (0.2–1.6 lg/band), 99.95/1.50 for SCG and FLU, respectively. A comparative study was conducted between the proposed methods to discuss the advantage of each method.

The suggested methods were validated in compliance with the ICH guidelines and were successfully applied for the determination of SCG and FLU in their laboratory prepared mixtures and commercial ophthalmic solution in the presence of benzalkonium chloride as a preservative. These methods could be an alternative to different HPLC techniques in quality control laboratories lacking the required facilities for those expensive techniques.

**Keywords:** Absorptivity factor; Absorption factor; Mean centering; TLC – spectrodensitometric; Sodium cromoglicate; Fluorometholone.

### 1329. Simultaneous Determination of Naphazoline Hydrochloride, Chlorpheniramine Maleate and Methylene Blue in their Ternary Mixture

Maha Abdel-Monem Aboseri Hegazy, Nouruddin Wageih Ali, Mohamad Abdelkawy and Rehab Magdy Abdelfatah

*Pakistan Journal of Pharmaceutical Sciences*, 26 (3): 641-648 (2013) IF: 0.947

Validated spectrophotometric and chemometric methods were developed for determination of Naphazoline Hydrochloride (NAP) Chlorpheniramine maleate (CLO) and Methylene blue (MB) in their ternary mixture.

Method A was a spectrophotometric method, where NAP and MB were determined using second derivative (D<sup>2</sup>) spectrophotometric method using the peak amplitudes at 299 nm and 337 nm for NAP and MB respectively, while CLO was determined using second derivative ratio (DD<sup>2</sup>) spectrophotometric method using the peak amplitude at 276.6 nm.

Method B used the chemometric techniques; principal component regression (PCR) and partial least squares (PLS) for determination of NAP, CLO and MB using the information contained in the absorption spectra of their ternary mixture solutions.

The proposed methods have been successfully applied for the analysis of NAP, CLO and MB in their pharmaceutical formulation and the obtained results were statistically compared with the reported methods.

**Keywords:** Naphazoline hydrochloride; Chlorpheniramine maleate; Methylene blue; Derivative spectrophotometry; Chemometrics.

### 1330. Chromatographic Methods for Simultaneous Determination of Diiodohydroxyquinoline and Metronidazole in their Binary Mixture

Mohammed Abdelkawy, Nouruddin Wageih Ali and Mohammed Gamal

*Pakistan Journal of Pharmaceutical Sciences*, 26 (5): (2013)  
IF: 0.947

Two chromatographic methods were developed for analysis of diiodohydroxyquinoline (DIHQ) and metronidazole (MTN). In the first method, diiodohydroxyquinoline and metronidazole were separated on TLC silica gel 60F<sub>254</sub> plate using chloroform: acetone: glacial acetic acid (7.5: 2.5: 0.1, by volume) as mobile phase. The obtained bands were then scanned at 254 nm. The second method is a RP-HPLC method in which diiodohydroxyquinoline and metronidazole were separated on a reversed-phase C18 column using water : methanol (60 :40, V/V, PH=3.6) as mobile phase at a flow rate of 0.7 mL.min<sup>-1</sup> and UV detection at 220 nm. The mentioned methods were successfully used for determination of diiodohydroxyquinoline and metronidazole in pure form and in their pharmaceutical formulation.

**Keywords:** TLC-Spectrodensitometry, RP-HPLC; Diiodohydroxyquinoline and Metronidazole.

### 1331. Validated Chromatographic Methods for Determination of Perindopril and Amlodipine in Pharmaceutical Formulation in the Presence of their Degradation Products

Hebat Allah Mohammed Essam El-Din, Hala E. Zaazaa, Samah S. Abbas and Mohammed G. El-Bardicy

*Journal of Chromatographic Science*, 51: 533-543 (2013)  
IF: 0.794

Two specific, sensitive, and precise stability-indicating chromatographic methods have been developed, optimized and validated for determination of perindopril arginin (PER) and amlodipine besylate (AML) in their mixtures and in the presence of their degradation products. The first method was based on thin-layer chromatography (TLC) combined with densitometric determination of the separated bands. Adequate separation was achieved using silica gel 60 F254 TLC plates and ethyl acetate – methanol – toluene – ammonia solution, 33% (6.5:2.1:0.5 by volume), as a developing system. The second method was based on high-performance liquid chromatography, by which the proposed components were separated on a reversed-phase C18 analytical column using a mobile phase consisting of phosphate buffer (pH 2.5, 0.01 M) – acetonitrile – tetrahydrofuran (60:40:0.1% by volume) with ultraviolet detection at 218 nm. Different parameters affecting the suggested methods were optimized for maximum separation of the cited components. System suitability parameters of the two developed methods were also tested. The suggested methods were validated in compliance with the ICH guidelines and were successfully applied for the quantification of PER and AML in their commercial tablets. Both methods were also statistically compared to each other and to reference methods with no significant differences in performance.

**Keywords:** Amlodipine; Perindopril; Stability indicating Methods; HPLC.

### 1332. A Rapid, Sensitive and Environmentally Friendly on-Line Solid Phase Extraction Using Protein-coated $\mu$ -Bondapak Cyanide Silica Pre-Column for Chromatographic Determination of Paracetamol in Human Serum

Hala Zaazaa, Samy Emara, Tsutomu Masujima, Ghada Hadad, Maha Kamal and Mohamed Abdel Kawi

*Journal of Liquid Chromatography and Related Technologies*, 36: 1297-1311 (2013) IF: 0.56

A simple, rapid and sensitive green high-performance liquid chromatographic (HPLC) method with automated pre-column extraction has been developed and evaluated for analysis of paracetamol (PC) in human serum. The method is performed by direct injection of serum samples onto a homemade protein-coated  $\mu$ -Bondapak CN silica precolumn, where PC is pre-concentrated and retained while proteins and very polar components are washed to waste using phosphate buffer saline, pH 7.4. The trapped drug is then back-flushed from the pre-column by column-switching followed by separation on a Thermo Scientific Hypersil ODS analytical column with an environmentally friendly mobile phase consisting of ethanol and phosphate buffer (0.01M, pH 3.5) in the ratio of 5:95 (v/v).

Detection is performed at 254 nm. The chromatographic procedure yields precise results and is able to run one sample in only 6 min. The calibration curve is linear over the concentration range of 10–10000 ng mL<sup>-1</sup> PC. The applicability of the method is successfully evaluated by monitoring the concentration of PC in human serum after an oral administration of 500 mg.

**Keywords:** Column; Switching; HPLC; Paracetamol; Protein-coated pre-column.

### 1333. Simultaneous Determination of Pramocaine HCL and Hydrocortisone Acetate in Pharmaceutical Dosage form

Hanan Abd El-Monem A. Merey, Mohammed A. Mohammed, Fahima A. Morsy and Maissa Y. Salem

*Journal of Liquid Chromatography and Related Technologies*, 36(19): 2774-2784 (2013) IF: 0.953

Two sensitive and selective methods were developed and validated for simultaneous determination of pramocaine HCl and hydrocortisone acetate in pharmaceutical dosage form. The first method is a spectrodensitometric method where pramocaine HCl and hydrocortisone acetate were separated using toluene: methanol: chloroform: 10% NH<sub>3</sub> [(5:3:6:0.1, by volume) as the developing system followed by densitometric measurement at 290 nm] and 250 nm for pramocaine HCl and Hydrocortisone acetate, respectively. The second method is a high performance liquid chromatographic method for separation and determination of both drugs using reversed phase C<sub>18</sub> column and mobile phase consisting of distilled water: acetonitrile: triethylamine (530:470:0.1, by volume); pH was adjusted to 3 by o-phosphoric acid. The proposed methods were successfully applied for the analysis of pramocaine HCl and hydrocortisone acetate in laboratory prepared mixtures and in pharmaceutical dosage form and the results obtained were assessed by applying the standard addition technique. Statistical comparison between the results obtained by applying the proposed methods and official method for the cited drugs was done and no significant difference was found at p=0.05.

**Keywords:** Hydrocortisone acetate; Pramocaine HCL; Pramoxine HCL; Reversed phase high performance liquid chromatography; Spectrodensitometry.

### 1334. Stability-Indicating High Performance Liquid Chromatographic Determination of Fluconazole in the Presence of its Oxidative Degradation Product- Kinetic and Stress Study

Hany Hunter Monir Bebawi, Hayam Mahmoud Lotfy and Abdel-Aziz Al-Byoumy Abdel-Aleem

*Journal of Liquid Chromatography and Related Technologies*, 36: 1013-1029 (2013) IF: 0.565

A simple, specific, accurate, and stability-indicating high performance liquid chromatographic method (HPLC) has been established for analysis of fluconazole (FLZ) in the presence of its degradation products generated in the stress degradation study. FLZ was subjected to stress conditions of acid, alkali, and neutral hydrolysis, oxidation, photolysis, and thermal decomposition. Extensive degradation was found to occur in oxidative medium under thermal stress. Successful separation of

drug from degradation products was achieved on a C-18 column using phosphoric acid 0.5% v/v: acetonitrile (80:20% v/v) as the mobile phase. The flow rate was  $1.5 \text{ mL min}^{-1}$  and the detector was set at 261 nm.

The retention times of FLZ and its main oxidative degradation product were found to be 5.389 min and 2.729 min, respectively. Linearity was established for fluconazole in the range of 0.5–50  $\mu\text{g mL}^{-1}$ . The percentage recovery of fluconazole was found to be 99.910.74. Because the method effectively separates fluconazole from its oxidative degradation products, it can be used as stability-indicating method.

The proposed method was also used to study the kinetics of fluconazole oxidative degradation that was found to follow a zero-order reaction. The  $t_{1/2}$  was 21.66 min while  $k$  (reaction rate constant) was  $2.91 \times 10^{-8} \text{ mole/min}$ .

**Keywords:** Fluconazole; HPLC; Kinetic study; Oxidation; Stability indicating method.

### 1335. Comparative Study of New Spectrophotometric Methods; an Application on Pharmaceutical Binary Mixture of Ciprofloxacin Hydrochloride and Hydrocortisone

Hayam Mahmoud Lotfy Ibrahim, Nagibay. Hassan, Samia M. Elgizawy and Sarah S. Saleh

*The Chilean Chemical Society*, 58 (3): 1651-1657 (2013)  
IF: 0.65

Simple, specific, accurate and precise spectrophotometric methods were developed and validated for simultaneous estimation of Ciprofloxacin hydrochloride (CIP) and Hydrocortisone (HYD) in their pure form and pharmaceutical dosage form.

Two new spectrophotometric methods were applied: extended ratio subtraction (EXRSM) and ratio difference (RDSM) methods. The results were compared to three well-established.

**Methods:** Mean centering of ratio spectramethod (MCR), Isoabsorptive point spectrophotometric method (IsoM) and Absorbance ratio method (ARM).

The linearity range for the spectrophotometric methods was found to be (2-14  $\mu\text{g/mL}$ ) and (1-14  $\mu\text{g/mL}$ ) for CIP and HYD respectively.

The selectivity of the developed methods was investigated by analyzing laboratory prepared mixtures of the two drugs and their combined dosage form.

The results obtained from the proposed methods were statistically compared using one-way analysis of variance (ANOVA) where no significant difference was observed between the new (EXRSM and RDSM) and the well-established methods which prove their validity for the analysis of this binary mixture.

The methods were validated as per ICH guidelines regarding accuracy, precision, repeatability and robustness; which were found to be within the acceptable limits.

The new methods were simple, sensitive and don't need a special program, so they could be easily applied as alternative methods to LC methods in quality control laboratories lacking the required facilities for those techniques.

**Keywords:** Ciprofloxacin; Hydrocortisone; Extended ratio subtraction; Ratio difference; Mean centering; Isoabsorptive point.

### 1336. Application of Classical Least Squares, Principal Component Regression and Partial Least Squares Methods for Simultaneous Spectrophotometric Determination of Rutin and Ascorbic Acid in their Combined Dosage Form

Hany Wagih Darwish, Ahmed H. Bakheit, Ali S. Abdelhameed and Ramzi A. Mothana

*Life Science Journal-Acta Zhengzhou University Overseas Edition*, 10: 1680-1686 (2013) IF: 0.165

This presented paper deals with application of three multivariate calibration methods for simultaneous spectrophotometric determination of two active substances in combined pharmaceutical formulation composed of rutin (RU) and ascorbic acid (AA). The multivariate methods are classical least squares (CLS), principal component regression (PCR) and partial least squares (PLS). The results showed the high performance of three methods for the analysis of the binary mixture. The optimum assay conditions were established and the proposed methods were successfully applied for the assay of the two drugs in an independent validation set and combined pharmaceutical tablets with excellent recoveries. No interference was observed from common pharmaceutical additives.

**Keywords:** Rutin; Ascorbic acid; Spectrophotometry; Multivariate calibration methods; Pharmaceutical tablets.

### 1337. A Comparative Study of Spectrophotometric Methods Versus Chemometric Methods; an Application on A Pharmaceutical Binary Mixture of Ofloxacin and Dexamethasone

Hayam Mahmoud Lotfy Ibrahim, Nagiba Y. Hassan, Samia M. Elgizawy and Sarah S. Saleh

*International Research Journal of Pure and Applied Chemistry*, 3 (2): 90-110 (2013)

**Aim:** To conduct a comparative study between the smart novel ratio difference spectrophotometric method (RDSM) versus four spectrophotometric.

**Methods:** first derivative spectrophotometry ( $D^1$ ), first derivative of the ratio spectra ( $^1DD$ ), isoabsorptive point (Aiso), ratio subtraction (RS), and two chemometric techniques based on principal component regression (PCR) and partial least-squares (PLS-1) for the determination of a binary mixture of Ofloxacin (OFX) and Dexamethasone (DXM).

**Study Design:** The results obtained from the proposed methods were statistically compared to the reported HPLC method using student's t-test, F-test and One way ANOVA.

**Methodology:** (OFX) was determined by the application of direct spectrophotometry, by measuring its zero-order ( $D_0$ ) absorption spectra at its  $\lambda_{\text{max}} = 296.6 \text{ nm}$ . (DXM) was determined by ( $D^1$ ) at 227.1 nm. By applying ( $^1DD$ ), (DXM) was determined at 237.3. The total concentration of both (OFX + DXM) was determined at their isoabsorptive point  $\lambda_{\text{iso}} = 238.3 \text{ nm}$ , then the concentration of (DXM) in mixtures were calculated by subtraction. (DXM) was determined using the (RS) method at its  $\lambda_{\text{max}} = 239 \text{ nm}$ . (DXM) was determined using (RDSM) by measuring amplitude difference at two selected wavelengths (248.4 and 290 nm). A concentration of  $10 \mu\text{g mL}^{-1}$  of OFX was used as a advisor. The

linearity range was found to be (1-10  $\mu\text{g.mL}^{-1}$ ) and (2-14  $\mu\text{g.mL}^{-1}$ ) for OFX and DXM respectively.

**Results:** The recovery percentage for OFX was found to be  $100.07 \pm 0.65$  and for DXM was found to be  $100.41 \pm 0.84$ ,  $100.15 \pm 0.97$ ,  $100.14 \pm 0.91$ ,  $100.54 \pm 0.75$  and  $100.11 \pm 0.66$  for the five methods, respectively.

**Conclusion:** The novel method showed advantages over the other proposed methods regarding simplicity, minimal data manipulation and maximum reproducibility and robustness; which enabled the analysis of binary mixtures with overlapped spectra for routine quality control testing with quite satisfactory and in lower cost.

**Keywords:** Ofloxacin; Dexamethasone; Ratio difference; Isoabsorptive point; Ratio subtraction; Chemometric.

### 1338. A Selective Sensor for Determination of Sitagliptin Phosphate in Pharmaceutical Formulation

Safa'a M. Riad, Mamdouh R. Rezk, Ghada Y. Mahmoud and Abdel-Aziz El Bayoumi Abdel Aleem

*Analytical and Bioanalytical Electrochemistry*, 5: 416-425 (2013)

A selective electrode was developed for determination of sitagliptin using precipitation based technique with ammonium reineckate as anionic exchanger in polyvinylchloride matrix. Linear responses of  $1 \times 10^{-5}$  to  $1 \times 10^{-2}$  M with slope of 40.9 mV/decade within pH 4-7. The percentage recovery for determination of sitagliptin by the proposed sitagliptin selective electrode was  $100.06 \pm 1.15$ . Determination of sitagliptin in its pharmaceutical formulation by the proposed electrode revealed its applicability for its determination. The proposed method was compared with a reported one. No significant difference for both accuracy and precision was observed. The electrode exhibits good selectivity for sitagliptin with respect to a large number of inorganic, organic cations, sugars and amino acids. The proposed electrode offers the advantages of simplicity, accuracy and applicability to turbid and colored samples. The fabricated sensor was validated according to the International Conference on Harmonization (ICH) guidelines and successfully applied for the determination of the studied drug in pure form and pharmaceutical formulation without any interference.

**Keywords:** Ammonium reineckate; Sitagliptin; Potentiometry; Poly vinyl chloride.

### 1339. A Validated Stability- Indicating Method for the Determination of Sumatriptan and Kinetic Study of the Degradation

Mamdouh Reda R. Yousef, Hayam M. Lotfy, Adel M. Michael, Ayman O.S.El-Kadi and Mostafa A.Shehata

*Analytical Chemistry an Indian Journal*, 12 (4): 127-132 (2013)

A simple, specific, accurate and stability-indicating liquid chromatographic method has been developed for determination of sumatriptan in the presence of its alkaline degradation product and in pharmaceutical formulation. The analysis was carried out on Grace C18 (2.1 x 250 mm with 5  $\mu\text{m}$  particle size) column with a mobile phase consisting of water (contains 0.1 % triethylamine, adjust pH to 6.5 by phosphoric acid): acetonitrile in the ratio (6 : 4, v/v). The detection was accomplished fluorometrically setting the excitation wavelength at 225 nm and

emission wavelength at 350 nm. The retention time was 4.1 min. and 5.2 min. for sumatriptan and its alkaline degradation, respectively, at flow rate 0.2  $\text{mL min}^{-1}$ . The developed and validated method was successfully applied to the analysis of pharmaceutical formulation. The calibration curve was linear over the range 50-800  $\text{ng mL}^{-1}$ . The LOD and LOQ values were found to be 16.6 and 50  $\text{ng mL}^{-1}$ , respectively. Statistical analysis of the results has been carried out revealing high accuracy and good precision. A kinetic study of the degradation reaction was done and proved to follow first order kinetics.

**Keywords:** Sumatriptan; Stability indicating; HPLC; Kinetic study.

### 1340. A Validated Stability Indicating RP-LC Method for Determination of Moxifloxacin in Bulk Powder and in Pharmaceutical Formulations

Mamdouh Reda R. Yousef and Iman A. Abdel-Karim

*Analytical Chemistry an Indian Journal, Acaij*, 12 (12): 461-466 (2013)

A simple stability indicating HPLC method was developed and validated for determination of moxifloxacin hydrochloride in the presence of its induced degradation products. The drug was subjected to stress stability studies including acidic, alkaline and oxidative stress conditions, and the stressed samples were analyzed by the proposed method. The developed method utilized Symmetry C<sub>18</sub> column (250 x 4.6 mm, 5  $\mu\text{m}$ ) in an isocratic separation mode. The mobile phase consisted of methanol: 0.2 % triethylamine (pH 2.5 with orthophosphoric acid), (35: 65, v/v) at a flow rate 1.5  $\text{mL/min}$  with UV-detection at 290 nm. The proposed method was validated according to the International Conference on Harmonization (ICH) guidelines. The method was applied for determination of moxifloxacin hydrochloride in pure powder and in its pharmaceutical formulations.

**Keywords:** Assay; Moxifloxacin; RP-HPLC; Stability; Validation.

### 1341. Application and Validation of Two Smart Spectrophotometric and A HP-TLC Densitometric Methods for Determination of Metoclopramide Hydrochloride/ Paracetamol in Raw Material and in Pharmaceuticals

Nagiba Yehia M. Hassan, Amira M. Hegazy, Fadia H. Metwally and Mohammad Abdel-Kawy

*International Journal of Pharmacy*, 3 (3): 470-481 (2013)

Currently the anti-emetic drug metoclopramide hydrochloride (MCP-HCl) is co-formulated with paracetamol (PCM). Three simple, economic and fast methods for determination of both drugs, simultaneously and without previous separation were developed. In first method (A) a third derivative spectrophotometric method was developed. The peaks amplitudes of third derivative spectra of MCP- HCl and PCM were measured at 334.5 and 299 nm, respectively. In second method (B), a ratio subtraction spectrophotometric method was developed. The peak amplitude of first derivative spectrum of MCP-HCl was measured at 321 nm at which PCM spectrum gives zero crossing point whereas the peak amplitude of ratio subtraction spectrum of PCM was measured at 292 nm. Both spectrophotometric methods were



linear within concentration range of MCP- HCl; 12-60  $\mu\text{g/mL}$  and PCM; 35-165  $\mu\text{g/mL}$  with high correlation coefficients. In third method (C), HP-TLC method was developed. The mobile phase composed of methanol, chloroform and conc. ammonia solution (10: 2: 0.15) gave typical chromatogram for MCP-HCl and PCM at  $R_f$ s  $0.21 \pm 0.02$  &  $0.59 \pm 0.02$ , respectively and the UV scanning was carried out at 270 nm. The method was linear within range of MCP- HCl; 6-18  $\mu\text{g/mL}$  and PCM; 5-50  $\mu\text{g/mL}$  giving high correlation coefficients. Complete validation process of the established methods was performed according to ICH guidelines and USP requirements and gave relative standard deviation values for all the key validation parameters less than 2%.

**Keywords:** Metoclopramide-hydrochloride; Paracetamol; Spectrophotometry; HP-TLC densitometry; Validation.

### 1342. Application of Membrane Selective Electrodes for the Determination of Azelastine Hydrochloride in the Presence of its Alkaline Degradant in Eye Drops and plasma

Mohamed Refaat Elsayed Elghobashy, Osama Mohamed Badran, Maissa Yacoub Salem and Khadiga Mohamed Kelani

*Analytical; Bioanalytical Electrochemistry*, 5: 325-340 (2013)

Azelastine Hydrochloride (AZT) was described by using the ion association complex between these drugs with either sodium tetraphenyl-borate (TPB) or ammonium reineckate (RNC) counter ions. The performance characteristics of the sensors were evaluated according to IUPAC recommendations, reveal a fast, stable and linear response over the concentration range  $10^{-5}$ -  $10^{-2}$  M for AZT. The sensors are used for determination of AZT in eye drops and plasma. The developed method was found to be simple, accurate and precise when compared with the Manufacturer method.

**Keywords:** Azelastine hydrochloride; Ion selective electrode; PVC membranes ammonium Reineckate; Sodium tetraphenyl-borate.

### 1343. Application of Three Novel Spectrophotometric Methods Manipulating Ratio Spectra for Resolving A Pharmaceutical Mixture of Chlorphenoxamine Hydrochloride and Caffeine

Amr Mohamed M. Badawey, Ayman M. Mohsen, Hayam M. Lotfy, Hesham Salem and Sonia Z. Elkhateeb

*International Journal of Pharmacy and Pharmaceutical Sciences*, 5 (s1): 478-487 (2013)

Three spectrophotometric methods are presented for the determination of a binary mixture of Chlorphenoxamine hydrochloride (CPX) and Caffeine (CAF) in laboratory prepared mixture and pharmaceutical dosage form without prior separation. Method (I) is an extended ratio subtraction method (EXRSM) coupled with ratio subtraction method (RSM), which depends on subtraction of the plateau values from the ratio spectrum. Method (II) is a ratio difference spectrophotometric method (RDSM), which depends on the difference in value between two different wavelengths of the ratio spectrum. Method (III) is a mean centering of ratio spectra (MCR). Mathematical explanation of the three methods is illustrated. Calibration curves of the three

methods are linear over the concentration ranges of 4-24  $\mu\text{g mL}^{-1}$  and 2-24  $\mu\text{g mL}^{-1}$  for CPX and CAF, respectively. The three methods proved to be simple, specific, accurate and precise. Solvent used is double distilled water. The three methods are validated as per the ICH guidelines where accuracy, precision, repeatability and robustness are found to be within the acceptable limits.

**Keywords:** Chlorphenoxamine HCL; Caffeine; Extended ratio subtraction method; Ratio subtraction method; Mean centering ratio spectra; Mean centering; Ratio difference; Ratio spectra.

### 1344. Chromatographic Determination of Sitagliptin and Simvastatin in their Pharmaceutical Formulation

Mamdouh Reda R. Yousef and Sherif A. Abdel-Gawad

*Analytical Chemistry an Indian Journal, Acaij*, 12 (7): 243-247 (2013)

Two methods namely, coupled TLC densitometry and high performance liquid chromatography, were used to determine sitagliptin and simvastatin simultaneously in their pharmaceutical dosage form. A TLC separation with densitometric detection of both drugs was achieved using benzene:n-butanol: triethylamine (9:2:0.5, by volumes) as a developing solvent. Furthermore, a high performance liquid chromatographic procedure with ultraviolet detection at 220 nm was developed for the separation and determination of the studied drugs using a  $C_{18}$  column. The mobile phase was composed of water: methanol: acetonitrile (1: 2: 2, by volumes). The final pH was adjusted to  $4.6 \pm 0.1$  with *O*-phosphoric acid. The proposed methods were successfully applied for the determination of the studied drugs in pure forms, their mixtures and in pharmaceutical formulation containing them.

**Keywords:** Sitagliptin; Simvastatin; TLC; HPLC.

### 1345. Conductometric Determination of Torasemide in Bulk Drug, in Formulations and in Plasma

Safaa Mohamed Riad Mohany

*Analytical and Bioanalytical Electrochemistry*, 5: 99-108 (2013)

Two simple and sensitive conductometric procedures were investigated for the determination of torasemide (TOS) using potassium tetraphenyl borate (K TPB) and ammonium reineckate (Amm. RNC) were described. Optimized conditions in cluding temperature solvent and reagent concentration were studied. The suggested methods were used for conductometric determination of (TOS) in its pharmaceutical preparations. Precision, measured as relative standard deviation was less than 1% and accuracy was 99.76%. The obtained results were comparable with data using the reported method. The proposed procedures were successfully adapted for the determination of (TOS) in plasma. For comparison, some interference was also determined by the conductometric titrations. At equimolar concentration levels, some molecules of similar structure interfere with the original drug. A reduction in interferent concentration by a factor of 10 negated the interference.

**Keywords:** Torasemide; Conductometry; Potassium tetraphenyl borate and ammonium reineckate.

### 1346. Determination of Gemfibrozil and Fenofibrate in Pharmaceuticals in Presence of their Degradation Products

Samah Sayed Abbas, Zeinab A Elsherif, Mai H. Abdelwahab and Soher El-Weshahy

*International Journal of Pharmacy and Pharmaceutical Sciences*, 5: 886-896 (2013)

The developed study portrays stability indicating methods for the determination of gemfibrozil and fenofibrate in pharmaceuticals. Three methods were presented for the determination of gemfibrozil in presence of its acid degradation products. The first method was based on HPLC separation of gemfibrozil from its degradation products on a reversed phase ODS column and UV detection at 276 nm. The second method was based on TLC separation followed by densitometric measurement of the spots. The third method was based on measuring the native fluorescence of the cited drug at  $\lambda_{em}$ . 405 nm upon excitation at  $\lambda_{ex}$ . 300nm. The three proposed methods were successfully applied to the determination of gemfibrozil in the range of 4-20  $\mu\text{g mL}^{-1}$ , 4-20  $\mu\text{g/spot}$  and 0.1-1.1  $\mu\text{g mL}^{-1}$  for the HPLC, TLC and spectrofluorimetric methods, respectively. Two methods were presented for the determination of fenofibrate in presence of its acidic and basic degradation products. The first method was based on TLC separation of the drug from its degradation products, followed by densitometric measurement of the spots at 286 nm. The second method was based on measuring the peak amplitude of the first derivative curve at 248.4 nm for the drug in presence of its acid degradates and at 250.8 nm in the presence of its basic degradate. The two proposed methods were applied to the determination of fenofibrate in the range of 1-9  $\mu\text{g/spot}$  and 2-12  $\mu\text{g mL}^{-1}$  for the TLC and the spectrophotometric methods, respectively. Commercial tablets and Laboratory prepared mixtures for both drugs in different proportions were assayed using the developed methods; also the fluorimetric method was applied to spiked human plasma. The analytical results were quite good in all cases. The main degradation products were subjected to IR and Mass spectrometry to confirm their structures and scheme for their formation.

**Keywords:** Gemfibrozil; Fenofibrate; Degradation products; HPLC; TLC densitometric measurement; Spectrofluorimetric measurement; First derivative.

### 1347. Development and Validation of A Simple RP-HPLC Method for Simultaneous Estimation of Ezetimibe and Atorvastatin Calcium in Pharmaceutical Dosage form and Spiked Human Plasma

Medhat Ahmed A. Al-Ghobashy, Yehia Z. Baghdady, Abdel-Aziz E. Abdel-Aleem and Soheir A. Weshahy

*International Journal of Advanced Research*, 1(6): 302-12 (2013)

A simple, sensitive, and specific method was developed for simultaneous determination of ezetimibe (EZB) and atorvastatin calcium (ATVC) by high performance liquid chromatography without previous separation. Satisfactory resolution was achieved using a RP-C18 chromatographic column, Kromasil RP-18 column (250 mm x 4.6 mm i.d) and a mobile phase consisting of acetonitrile: water (6: 4, v/v) at a flow rate 0.7 mL/min and the

wavelength detection was 260.0 nm. The retention time for EZB and ATVC was  $7.47 \pm 0.02$  and  $4.67 \pm 0.02$  min; respectively. The described method was linear over a range of 10-100  $\mu\text{g/mL}$  for EZB and 5-100  $\mu\text{g/mL}$  for ATVC. The mean percent recoveries were  $99.87 \pm 0.769$  and  $100.04 \pm 0.480$  for EZB and ATVC, respectively. Method was validated according to ICH guidelines and successfully applied for analysis of bulk powder, pharmaceutical formulations and spiked human plasma.

**Keywords:** Ezetimibe; Atorvastatin calcium; Reverse phase high performance liquid chromatography; Pharmaceutical preparation; Plasma.

### 1348. Development and Validation of Novel Stability Indicating Methods for Estimation of Amylocaine Hydrochloride in Bulk and Dosage form

Hanan Abd El-Monem A. Meray, Fahima A. Morsy, Mohammed A. Mohammed and Maissa Y. Salem

*Analytical Chemistry an Indian Journal*, 12 (3): 103-110 (2013)

Three sensitive and selective methods were developed and validated as stability indicating methods for the determination of amylocaine HCl in presence of its degradation product. The first method is based on the use of derivative ratio spectrophotometry (<sup>1</sup>DD) for the determination of amylocaine HCl in presence of its degradation product and of methyl and propyl parabens by measurement of the peak amplitudes of the first derivative of ratio spectra at 234 and 247 nm using the spectrum of 20  $\mu\text{g}$  of total parabens as a divisor. The second method is a spectro-densitometric method for the determination of amylocaine HCl after separation from its degradation product and additives of pharmaceutical dosage form using toluene: Methanol: chloroform: 10%  $\text{NH}_3$  (5:3:6:0.1 v/v) followed by detection at 234 nm. The third method is an isocratic high performance liquid chromatographic method (HPLC) on a reversed phase  $\text{C}_{18}$  column using mobile phase consisting of distilled water: acetonitrile: triethylamine (530: 470: 0.1 v/v) and the pH was adjusted to 3 by o-phosphoric acid. The proposed methods were successfully applied for the analysis of amylocaine HCl in laboratory prepared mixtures and in pharmaceutical dosage form and the results obtained were assessed by applying the standard addition technique. Statistical comparison between the results obtained by applying the proposed methods and manufacturer's method for amylocaine HCl in its pure powder form was done and no significant difference was found at  $p = 0.05$ .

**Keywords:** Derivative ratio spectrophotometry; Spectro-densitometry; High performance liquid chromatography; Amylocaine HCL; Benzoic acid.

### 1349. Development and Validation of Spectrophotometric, Chemometric and High Pressure Liquid Chromatographic Methods for the Determination of Cefepime Hydrochloride in the Presence of its Acid and Alkaline Degradation Products

Shereen Ahmed Hassan Boltia, Laila Abdel-Fattah, Soheir A. Weshahy, Nagib Y. Hassan and Nadia M. Mostafa

*International Journal of Analytical and Bioanalytical Chemistry*, 3: 86-96 (2013)

In this study, stability-indicating methods for the determination of cefepime hydrochloride (CPM) were conducted by the application of spectrophotometry, chemometry and high-performance liquid chromatography (HPLC). Five different, accurate, sensitive and reproducible methods were applied for the simultaneous analysis of cefepime hydrochloride (CPM) in the presence of its acid and alkaline degradation products in their laboratory prepared mixtures and pharmaceutical preparations. The first method is based on derivative spectrophotometry. First derivative spectrophotometry was applied where CPM was determined at 279 and 312 nm in the presence of its alkaline degradation product and also second derivative spectrophotometry was applied where CPM was determined at 236 nm in the presence of its acid degradation product. The second method is based on the first derivative of ratio spectrophotometry (<sup>1</sup>DD) of CPM at 258 and 286 nm in the presence of its acid degradation product and at 251 and 285 nm in the presence of its alkaline degradation product. The third method is based on ratio subtraction spectrophotometry where the drug is determined at 236 nm in laboratory prepared mixtures of CPM with its acid or alkaline degradation product. The fourth method is the application of multivariate calibration models, namely, Principle Component Regression (PCR) and Partial Least Squares (PLS). The four proposed spectrophotometric methods permit the determination of CPM in the range of 3.0-30.0 µg/ml. The fifth method is an isocratic reversed-phase HPLC procedure, a Zorbax C<sub>18</sub> column was used to separate CPM from its acid and alkaline degradation products using acetonitrile: water (20:80, v/v) as a mobile phase and detection at 254 nm. The suggested procedures were successfully applied for the analysis of CPM in bulk powder and in pharmaceutical preparations. The results obtained by the proposed methods were statistically comparable with those obtained by the official method. All the proposed methods were validated according to the International Conference on Harmonization (ICH) guidelines.

**Keywords:** Cefepime hydrochloride; Stability indicating method; Degradation; High-performance liquid chromatography.

### 1350. Development of Stability-Indicating Methods for Determination of Sulpiride in Presence of its Degradation Products in Bulk and Dosage Forms

Amal Mahmoud Abo Al Alamein, Maha Farouk, Lobna Abd El Aziz, Amal Mahmoud and Ekram Hany

*Analytical Chemistry, an Indian Journal, Acaij, 13 (3): 107-117 (2013)*

Simple, accurate, sensitive, and precise UV spectrophotometric and chemometric methods were developed for determination of Sulpiride (SLP) in presence of its degradation products. Two spectrophotometric methods were developed, namely, double divisor ratio spectra (DDRD) and ratio subtraction (RS); the linearity range was 20-200 µg.ml<sup>-1</sup> for both spectro- photometric methods, with mean percentage recoveries of 99.51 – 0.24 and 99.73 – 0.32 for the double divisor ratio spectra and ratio subtraction method respectively. The developed chemometric-assisted spectrophotometric methods were the principle component regression (PCR) and partial least squares (PLS) methods.

The linearity range was also 20-100 µg.ml<sup>-1</sup> for both methods while the mean percentage recoveries were found to be 99.63 ±0.22 and 99.60 ±0.26 for the PCR and PLS methods

respectively. The developed methods were successfully applied for determination of SLP in bulk powder, laboratory-prepared mixtures and in dosage form. The results obtained were compared to the reported spectrophotometric method; there was no significant difference between the proposed methods and the reported method.

**Keywords:** Sulpiride; Double divisor ratio spectra; Ratio subtraction; Chemometrics; Dosage form; Stability study.

### 1351. Different Stability-Indicating Techniques for the Determination of Triclabendazole

Nesrin Khamis Ramadan Selim, Afaf O. Mohamed, Sara E.Shawky and Maissa Y.Salem

*Analytical Chemistry an Indian Journal, 12: 428-438 (2013)*

Three simple, accurate and sensitive methods were developed for the determination of triclabendazole (TCZ) in presence of its degradation product. Method (A) was depending on third derivative spectrophotometry 3D, then measuring the peak amplitude at 266 nm. Method (B) was a TLC method, using silica gel 60 F<sub>254</sub> plates; the optimized mobile phase was ethyl acetate/ methanol/ ammonium hydroxide (8:1:0.2 by volume). The spots were scanned densitometrically at 300 nm. Method (C) was an HPLC method, performed on C18 column using acetonitrile/ 0.05M potassium dihydrogen phosphate (60:40 v/v), the pH was adjusted to 3.5±0.2 with ortho-phosphoric acid as a mobile phase with a flow rate of 1.5 ml/min. Detection was performed at 300 nm. Linearity ranges were 5- 40 µg/ml for method (A), 0.5- 5 µg/band for method (B) and 0.5- 5 µg/ml for method (C), the mean percentage recoveries were 100.0 ± 1.0%, 100.5 ± 1.2% and 99.8 ± 1.1% for methods (A), (B) and (C) respectively. The proposed methods were found to be specific for triclabendazole in presence of up to 70% of its degradation product for method (A) and 90% of its degradation product for methods (B) and (C). Statistical comparison between the results obtained by these methods and the manufacturer's method was done, and no significance difference was obtained.

**Keywords:** Triclabendazole; Degradation; Spectrophotometry; HPLC; TLC.

### 1352. Different Stability-Indicating Methods for the Determination of quetiapine Fumarate

Nesrin Khamis Ramadan Selim, Afaf O. Mohamed, Roaida M. Fouad and Azza A. Moustafa

*Analytical Chemistry an Indian Journal, 12: 246-276 (2013)*

Five accurate, precise and sensitive methods were developed for the determination of Quetiapine fumarate (QF) in presence of its degradation product. Method (A) was based on second derivative spectrophotometry <sup>2</sup>D, then measuring the amplitude at 266 nm. Method (B) was depended on measuring the peak amplitudes of the first derivative of the ratio spectra <sup>1</sup>DD at 244, 285 and 344 nm. Method (C) was based on the separation of the drug from its oxidized degradation product followed by densitometric measurement of the intact drug band at 302 nm.

The separation was carried out on Fluka TLC plates of silica gel 60 F<sub>254</sub> using ethyl acetate/ methanol/ 10% ammonium hydroxide (8.5:1:0.5 by volume) as a mobile phase. Method (D) was high performance liquid chromatographic one, separation by HPLC was achieved using an Eclipse XDB C18RP-column and

methanol/ water in a ratio of 80:20 (v/v) as a mobile phase. The flow rate was 1ml/min. Method (E) was based on the reaction of QF with P-Chloranilic acid (PCA) in presence of its degradation product. Linearities were obtained in concentration range 10- 60 µg/ml in case of methods (A) and (B). While in case of methods (C) and (D), linearities were obtained in concentration range of 4- 20 µg/ml and 1-20 µg/ml respectively. While in method (E), the linearity was achieved in the range of 40-400 µg/ml. In method (A), the mean percentage recovery was  $99.9 \pm 0.6\%$ . In method (B) the mean percentage recoveries were  $99.9 \pm 0.4\%$ ,  $99.2 \pm 0.8\%$  and  $99.4 \pm 0.8\%$  at 244, 285 and 344 nm respectively. Method (C) showed percentage mean recovery of  $99.9 \pm 0.7\%$ , while in methods (D) and (E) were  $99.8 \pm 0.7\%$  and  $99.9 \pm 0.4\%$  respectively.

The degradation product was obtained in oxidative stress condition, separated, and identified by IR and MS spectral analysis from which the degradation product was confirmed, and the degradation pathway was suggested. The five methods were found to be specific for QF in presence of different concentration % of its degradation product. The proposed methods were validated according to ICH guidelines Q2(R1). The five proposed methods were successfully applied for the determination of QF in Seroquel tablets. Statistical comparison between the results obtained by these methods and that obtained by the manufacturer method for the determination of the drug was done, and it was found that there was no significant differences between them.

**Keywords:** Stability indicating method; Derivative ratio; HPLC; TLC; Quetiapine fumarate; Second derivative; P-chloranilic acid; Degradation product.

### 1353. Electrochemical Determination of Ciprofloxacin Hydrochloride in Pharmaceutical Formulation, Aquatic Environment and in Fish Tissues

Mamdouh Reda Rezk Yousef, Safaa M. Riad, Fatma I. Khatib and Hoda M. Marzouk

*International Journal of Biological and Pharmaceutical Research* 4 (6): 390-396 (2013)

Two ciprofloxacin hydrochloride (CPX) selective electrodes were developed using dioctyl phthalate (DOP) as a plasticizer in a polymeric matrix of polyvinyl chloride (PVC). Sensor I was fabricated using tetrakis(4-chlorophenyl)borate (TpClPB) as an anionic exchanger without incorporation of an ionophore. Sensor II was developed using 2-hydroxy propyl  $\beta$ -cyclodextrin as an ionophore. Linear responses of CPX within a concentration range of  $10^{-5}$ - $10^{-2}$  M, with slopes of  $51.7 \pm 0.31$  and  $48.7 \pm 0.40$  mV/decade over pH range of 4-7 were obtained using sensors I and II, respectively. The selectivity coefficients of the developed sensors indicated excellent selectivity for CPX. The proposed method displayed useful analytical characteristics for determination of ciprofloxacin hydrochloride in pharmaceutical formulation, fish water and fish tissues with average recoveries of  $100.91 \pm 0.47$ ,  $96.42 \pm 1.34$  and  $86.46 \pm 1.28$ , respectively for sensor I and  $101.2 \pm 0.37$ ,  $97.26 \pm 1.56$  and  $86.67 \pm 1.70$ , respectively for sensor II.

**Keywords:** Aquatic environment; Ciprofloxacin hydrochloride; Fish tissues; Potentiometry; PVC.

### 1354. Establishment and Validation of Two Smart UV-Spectrophotometric and A Novel Spectrodensitometric Methods for Simultaneous Determination of Metoclopramide Hydrochloride/Pyridoxine Binary Mixture in Raw Material and in Syrup

Nagiba Yehia Mohamed Hassan, Amira M. Hegazy, Fadia H. Metwally and Mohammad Abdel-Kawy

*International Journal of Pharmacy*, 3 (3): 490-500 (2013)

Currently the anti-emetic drug metoclopramide hydrochloride (MCP-HCl) is co-formulated with pyridoxine (VB6). Three simple, economic and fast spectroscopic methods for determination of both drugs, simultaneously and without previous separation were developed. The first method is a ratio derivative spectrophotometry. The peaks amplitudes of first derivative spectra of MCP-HCl and VB6 were measured at 318.5 nm and 327.5 nm, respectively. The second one is an isosbestic point spectrophotometry. The peaks amplitudes of MCP-HCl and VB6 spectra were measured at 321.5 and 299.5 nm, respectively. The third method is spectrodensitometry. The mobile phase was composed of benzene, methanol, glacial acetic acid, and acetone (10: 8: 0.5: 0.5; by volume). It gave typical chromatogram for MCP-HCl and VB6 at  $R_s$   $0.2 \pm 0.02$  &  $0.51 \pm 0.01$ , respectively and the UV scanning was carried out at 245 nm. Complete validation processes of the established methods were performed according to ICH guidelines and USP requirements. All methods were linear within wide concentrations ranges with high correlation coefficients. The proposed methods showed high accuracy, precision and selectivity results. Relative standard deviation values for all the key parameters were less than 2.00%.

**Keywords:** Metoclopramide-hydrochloride; Pyridoxine; Spectroscopy; Assay; Validation.

### 1355. High Throughput Quantitative Bioanalytical LC/MS/MS Determination of Gemifloxacin in Human Urine

Hany Wagih Darwish, Adnan A. Kadi, Rihab F. Angawi, Mohamed W. Attwa and Ali Saber Abdelhameed

*Journal of Chemistry*, (2013)

A highly specific, sensitive, and rapid method, to quantify gemifloxacin in human urine using HPLC coupled to the triple quadrupole mass spectrometer system, was developed and validated. Gemifloxacin and ofloxacin (internal standard) were rapidly extracted from urine samples without any tedious pretreatment procedure. Urine samples were filtered through a Millex-GP, 0.22 µm syringe filter. Optimal chromatographic separation of the analytes was achieved on Zorbax SB-C<sub>18</sub> (30mm × 2mm i.d., 3.5 µm maintained at ambient temperature). The mobile phase consisted of 0.1% formic acid (pH 3.2) and acetonitrile (80 : 20) and a flow rate of 0.2 mL min<sup>-1</sup> for 4 min. The analytes were monitored by electrospray ionization in positive ion multiple reaction monitoring mode. The method provided a linear response ( $r = 0.9998$ ) from a quantitation range of 5 ng mL<sup>-1</sup> to at least 500 ng mL<sup>-1</sup>. The mean extraction recovery % of gemifloxacin from spiked human urine was  $101.33 \pm 2.58\%$ . The reproducibility of the method was reliable with the intra- and inter-day precision of <2% and accuracy within 2%. The

established method was reliably applied for the determination of gemifloxacin in volunteers' urine samples with the mean recoveries of gemifloxacin from Factive tablets 320mg > 97.0%.

**Keywords:** Gemifloxacin.

### 1356. HPLC and TLC-Densitometric Methods for the Determination of Some Antimigraine Drugs in Bulk Powder and in Pharmaceutical Preparations

Amr Mohamed Mohamed Badawey

*Research Journal of Pharmaceutical Dosage Forms and Technology*, 5 (5): 289-295(2013)

Two simple and accurate chromatographic methods were developed for the determination of zolmitriptan, and sumatriptan in raw material and in tablets. The first method uses isocratic high performance liquid chromatographic (HPLC) method. Analysis was performed on Agilent Zorbax C18 column using a mobile phase consisting of phosphate buffer pH3: acetonitrile: methanol (2:1:1, v/v/v) with a flow rate of 0.75 ml/min and UV detection at 253 nm. The second method uses thin-layer chromatographic (TLC) separation of sumatriptan, zolmitriptan and eletriptan from their impurities followed by densitometric measurements of drug spots at 254 nm. This separation was carried out on silica gel 60 F254 using chloroform: ethylacetate: methanol: ammonia (72:10:18:2, v/v/v/v) as mobile phase. The methods were validated according to ICH guidelines and the acceptance criteria for linearity, accuracy, precision, specificity and system suitability were met in all cases. The methods were linear in the range of 10-40 µg/ml and 10-50 µg/ml for zol. and sum. respectively by HPLC method and in range of 1-20 µg/spot, 1-20 µg/spot and 1-10 µg/spot for ele., sum. and zol. respectively by TLC method. The proposed methods were successfully applied for the determination of zol., sum. and ele. in bulk and tablets forms. The results were compared statistically at 95% confidence level with reported methods. There was no significant difference between the mean percentage recoveries and precision of the methods.

**Keywords:** Zolmitriptan; Sumatriptan; Eletriptan; Hplc; Tlc densitometry.

### 1357. Ion Selective Electrodes for Potentiometric Determination of Baclofen in Pharmaceutical Preparations

Safaa Mohamed Riad Mohany and Nadia M. Mostafa

*Analytical and Bioanalytical Electrochemistry*, 5: 494-505(2013)

Two different sets of baclofen sensors were developed for its potentiometric determination in pharmaceutical preparations, based on the fact that baclofen behaves as cation in acidic medium and anion in basic medium ( $pK_1=9.62$  and  $pK_2=3.87$ ; respectively). Six baclofen-selective electrodes were investigated using precipitation based technique with either sodium tetraphenyl borate as an anionic exchanger or 1, 10-ortho-phenanthrolineferrous as a cationic exchanger; respectively upon using polyvinyl chloride (PVC) matrix and dioctyl sebacate (DOS) as a plasticizer. The resultant sensors have different forms, either as membrane electrodes (sensors I&IV), coated wire electrodes (sensors II&V) or as micro sized graphite electrodes (sensors III&VI). Linear responses of 10-6-10-2 M with slopes of

43.05, 43.11, and 43.05 mv/decade within pH range 4-6 were obtained for sensors I, II and III. On the other hand, linear responses of  $10^{-7}$ - $10^{-3}$  M with slopes of 55.90, 57.13 and 57.37 mV/decade within pH 6-8 range were obtained for sensors IV, V and VI; respectively. All these sensors were prepared and fully characterized in terms of composition, life span, usable pH range, response time and temperature. The sensors show good selectivity to the drug in presence of a variety of inorganic and organic interferent substances. The proposed procedures were compared to the USP pharmacopoeial method and showed no significant difference. The proposed sensors displayed useful analytical characteristics for the potentiometric determination of baclofen in pure form and in pharmaceutical preparations.

**Keywords:** Baclofen; Selective electrodes; Sodium tetraphenyl Borate; 1; 10-Ortho-phenanthroline-ferrous and polyvinyl Chloride (PVC).

### 1358. Ion Selective Membrane Electrodes for Stability Indicating Determination of Benoxinate Hydrochloride in Pure form and in Drug Product

Eman Saad Hassan Elzanfaly and Marianne Nebsen

*Anal Bioanal Electrochem*, 5: 166-177 (2013)

This paper presents a comparative study between four sensors constructed to determine benoxinate hydrochloride (BX) in the presence of its hydrolysis induced degradation product using different ion association complexes and plasticizers. Precipitation based technique was used for sensors fabrication. The BX complexes with the cationic exchangers; BX-reinikate, BX-tetraphenylborate, BX-phosphotungstate, and BX-tetrakis were obtained in situ by soaking the PVC membranes in  $1 \times 10^{-2}$  BX solution. Dioctyl phthalate and nitrophenyl octyl ether were used as solvent mediators. The proposed sensors showed fast, stable Nernstian responses across a relatively wide BX concentration range ( $5 \times 10^{-5}$  to  $10^{-1}$  M) in the pH range of 4-6. The suggested sensors could be used for several weeks without any measurable change in sensitivity. They displayed good selectivity for BX in presence of its degradation product, common inorganic and organic species. The proposed sensors were successfully applied for the determination of BX in pure powder form and eye drops where good recoveries were obtained.

**Keywords:** Benoxinate hydrochloride; Stability indicating method; Reinikate; Tetraphenylborate; Phosphotungstate; Tetrakis.

### 1359. Ion Selective Membrane Electrodes for the Determination of Xylometazoline Hydrochloride in Rabbit Aqueous Humor Using 2 Hydroxy Propyl $\beta$ -Cyclodextrine and Calix[6]Arene as Ionophores

Ghada Mostafa Elsayed Elsayed, Marianne Nebsen, Mohammed Abdelkawy and Sona Zaki Elkhateeb

*Analytical and Bioanalytical Electrochemistry*, 5: 368-380 (2013)

Three novel Xylometazoline Hydrochloride (XYLO) selective electrodes were investigated with Dioctyl phthalate (DOP) as a plasticizer in a polymeric matrix of polyvinyl chloride (PVC). Sensor 1 was fabricated using Phosphomolybdic acid (PMA) as an anionic exchanger without incorporation of an ionophore. Sensor 2 used 2-hydroxy propyl  $\beta$ -cyclodextrin (hp  $\beta$ -CD) as an



ionophore while sensor 3 was constructed using calix[6]arene as an ionophore. Linear responses of XYLO within the concentration ranges of  $10^{-4}$  to  $10^{-2}$ ,  $10^{-5}$  to  $10^{-2}$  and  $10^{-5}$  to  $10^{-2}$  mol L<sup>-1</sup> were obtained using sensors 1, 2 and 3, respectively. Nernstian slopes of 49.78, 56.21 and 46.20 mV/decade over the pH range of 5–9 for sensors 1, 2 and 5–7 for sensor 3 were observed. The selectivity coefficients of the developed sensors indicated excellent selectivity for XYLO. The utility of 2-hydroxy propyl  $\beta$ -cyclodextrin and calix[6]arene as ionophores had a significant influence on increasing the membrane sensitivity and selectivity of sensors 2 and 3 compared to sensor 1. The proposed sensors displayed useful analytical characteristics for the determination of XYLO in bulk powder, different pharmaceutical formulations, and biological fluids (Rabbit aqueous humor) and in the presence of its degradation product (2, 6-dimethyl-4-tertbutyl-phenylacetic acid) and thus could be used as stability-indicating method.

**Keywords:** Xylometazoline; Hydroxypropyl  $\beta$  cyclodextrine; Calix [6] arene; Rabbit aqueous humor.

### 1360. LC-MS as a Stability-Indicating Method for Analysis of Hyoscine N-Butyl Bromide Under Stress Degradation Conditions with Identification of Degradation Products

Mohammed Abdelkawy Mohammed Ibrahim; Nouruddin W Ali and Mohammed Gamal

*Pharmaceutica Analytica Acta*, S7: (2013)

Hyoscine N-Butyl Bromide (HBB) was subjected to different ICH prescribed stress conditions. It showed extensive decomposition under base hydrolytic conditions, while it was less liable to stress acid hydrolytic conditions. It showed also moderate degradation in response to oxidation stress of hydrogen peroxide. The drug showed no changes under photolysis conditions. In total, a number of major degradation products were detected by HPLC and identified by LC-MS. For establishment of stability-indicating assay, the reaction solutions in which different degradation products were formed were prepared, and the separation was optimized by varying the HPLC conditions. An acceptable chromatogram was achieved using a C18 column using (water: methanol 50: 50 v/v, pH adjusted to 3.9 with trifluoroacetic acid) as a mobile phase with flow rate of 1.0 ml min<sup>-1</sup> and UV detection wavelength at 210 nm. The percent of degradation was calculated in each run by measuring the intensity of the peak area of the intact drug at 6.2 min. Complete degradation only occurred in case of 5 N NaOH indicates that the drug is very sensitive to alkaline hydrolysis. The LC-MS study was carried out to identify the major degradation products using a sunfire (waters) C-18 column and a mobile phase comprising of acetonitrile: 0.1M ammonium acetate (80:20, v/v) with flow rate of 1.0 ml min<sup>-1</sup>. MS measurements were acquired in positive ion full scan modes from 50 to 400 amu. The *m/z* values of the main peaks were investigated with the expected chemical structure of degradates.

### 1361. New Potentiometric Determination of Clindamycin Hydrochloride in Pharmaceuticals

Hanan Abd El-Monem A. Merey, Mohamed S. Rizk, Shereen M. Tawakkol and Mona N. Sweilam

*Research and Reviews In Electrochemistry*, 4 (5): 161-167 (2013)

A potentiometric membrane sensor responsive with satisfactory selectivity to clindamycin hydrochloride was prepared for simple and fast determination of this drug in pure form and pharmaceutical dosage forms without prior extraction process or separation from different dosage form excipients. The sensor was based on the formation of an ion association complex between clindamycin hydrochloride as a cationic drug and sodium phosphotungstate as anionic electroactive material. The produced ion association complex was incorporated in plasticized polyvinyl chloride membrane. The performance characteristics of this sensor were evaluated according to IUPAC recommendations-reveal fast, stable and near Nernstian response for  $3.16 \times 10^{-4}$  –  $1 \times 10^{-1}$  M for clindamycin hydrochloride. Statistical comparison between the results obtained by applying the proposed potentiometric method for the determination of the clindamycin hydrochloride and those obtained by applying the official method was done and no significant difference was found at *p* = 0.05. Validation of the method according to ICH guidelines shows the suitability of the sensor for quality control analysis of the cited drugs in pharmaceutical formulations. The proposed sensors can also be used as a detector for HPLC method.

**Keywords:** Clindamycin hydrochloride; Membrane sensor; Potentiometry; Sodium phosphotungstate.

### 1362. Novel Poly (Vinyl Chloride) Matrix Membrane Sensors for Determination of Cilostazol in Presence of its Degradation Product and in Plasma

Safaa Mohamed Riad and Nouruddin W. Ali

*Analytical and Bioanalytical Electrochemistry*, 5: 622-634 (2013)

Three novel techniques for selective determination of Cilostazol in presence of its oxidative degradation product were described. The three techniques involve the construction and studying of electrochemical response characteristics of novel poly (vinyl chloride) [PVC] matrix membrane sensors for cilostazol detection by using the ion-association complexes of this cation with sodium tetraphenyl borate (NaTPB), phosphotungstic acid (PTA) and ammonium reineckate (amm.RNC) counter anions as ion exchange sites in a plasticized PVC matrix, either as ion selective membranes, microcoated wire or as micro sized graphite selective sensors. The preparation and full characterization of these sensors, including composition, life span, usable pH range, response time and temperature were described. The electrodes were used for potentiometric determination of cilostazol in pure form, pharmaceutical products, plasma and in presence of its oxidative degradation product. These sensors showed near-Nernstian slopes of 56.14, 58.82, 56.23, 56.7, 59.14, 56.84, 58.72, 59.44 and 58.37 mV over the concentration ranges of  $1.0 \times 10^{-7}$ – $1.0 \times 10^{-2}$  M for NaTPB and PTA sensors and  $1.0 \times 10^{-6}$ – $1.0 \times 10^{-2}$  M for amm.RNC sensors. The electrodes show good selectivity for cilostazol relative to a large number of inorganic cations, organic cations, sugars and amino acids. The behavior of the three sensors in presence of human plasma was also studied and reasonable results were obtained. The methods were successfully applied for determination of the intact drug in bulk powder and in presence of its oxidative degradation product; therefore it can be used as stability indicating methods.

**Keywords:** Cilostazol; Sodium tetraphenyl borate (NaTPB); Phosphotungstic Acid (PTA); Ammonium reineckate (amm.RNC); PVC Sensors; Plasma.

### 1363. Potentiometric Determination of Clorazepate Dipotassium in Human Plasma

Nadia Mohamed Mostafa Hamoda and Safa'a M. Riad

*International Journal of Pharmacy and Pharmaceutical Sciences*, 5 (1): 299-305 (2013)

Three developed techniques for the selective determination of clorazepate dipotassium were described. The three techniques were investigated with dioctyl phthalate (DOP) as a plasticizer in a polymeric matrix of polyvinyl chloride (PVC). These sensors for clorazepate cation were based on the use of the ion-association complexes of this cation with tetraphenyl borate, phosphotungstic acid and ammonium reineckate counter anions as ions exchange sites in a plasticized PVC matrix, either as ion selective membranes (sensor 1, 1' and 1''), microcoated wire (sensor 2, 2' and 2'') or as micro-sized graphite sensor (sensor 3, 3' and 3''). All these sensors were prepared and fully characterized in terms of composition, life span, usable pH range, response time and temperature. These sensors showed near Nernstian responses with slopes in the range of 56.7-59.4 mV decade<sup>-1</sup> in a pH range of 4-7 over the concentration ranges of  $1.0 \times 10^{-3}$  -  $1.0 \times 10^{-7}$  M and  $1.0 \times 10^{-3}$  -  $1.0 \times 10^{-6}$  M for tetraphenyl borate sensors (1, 2 and 3) and the rest of the studied sensors; respectively. The electrodes exhibit good selectivity for clorazepate with respect to a large number of inorganic cations, sugars and many other exipients. The proposed sensors displayed useful analytical characteristics for the potentiometric determination of clorazepate in pure form, pharmaceutical preparation and in human plasma. The proposed electrodes offer the advantages of simplicity, accuracy and direct applicability to turbid and colored samples without any interference.

**Keywords:** Clorazepate dipotassium; Sodium tetraphenyl borate (NaTPB); Phosphotungstic Acid (PTA); Ammonium Reineckate (ARNC); Potentiometry and Plasma.

### 1364. Selective Determination of Midodrine Hydrochloride in the Presence of its Acidic Degradation Product

Mamdouh Reda Rezk Yousef, Osama Abdel Sattar, Amr M. Badawy and Omaima M. Khattab

*Analytical Chemistry, an Indian Journal*, 12 (5): 182-187 (2013)

Two stability-indicating methods were developed for determination of midodrine in the presence of its acidic degradation product (the metabolite). The degradation product was isolated via acid degradation and then characterized and structurally elucidated. The first method was the first derivative of the ratio spectra <sup>1</sup>DD. The second method was a high performance liquid chromatographic one. Selective quantification of midodrine in pure form, pharmaceutical formulation and/or in the presence of its degradant was demonstrated. The indication of stability was done under condition likely to be expected at normal storage condition.

**Keywords:** Midodrine; Stability; HPLC; Spectroscopy.

### 1365. Selective Spectrophotometric Methods for Quantification of Sitagliptin and Metformin

Safaa Mohamed Riad Mohany

*Analytical Chemistry an Indian Journal*, 12 (2): 41-47 (2013)

Four simple, accurate and precise spectrophotometric methods were developed and validated for the simultaneous determination of sitagliptin phosphate (STA) and metformin HCl (MTF) in their mixture. Among the developed methods were first derivative, second derivative, dual wavelength and ratio subtraction methods. The first derivative spectrophotometric method was used for the determination of STA in the range of 25-500 µg mL<sup>-1</sup>, while the second derivative spectrophotometric method was used for the determination of STA in the range of 25-500 µg mL<sup>-1</sup> in addition to MTF in the range of 2.5-35 µg mL<sup>-1</sup>. The dual wavelength and ratio subtraction methods were used for the determination of MTF in the range of 5-30 µg mL<sup>-1</sup> and 2.5-30 µg mL<sup>-1</sup>, respectively. The results were statistically compared with the reference ones. The developed methods were proved to be selective and accurate for the quality control and routine determination of the cited drugs in their mixture and in their pharmaceutical formulations. 2013 Trade Science Inc.- INDIA

**Keywords:** Metformin; Sitagliptin; First derivative; Second derivative; Dual wavelength; Ratio subtraction.

### 1366. Simultaneous Determination of Ezetimibe and Atorvastatin Calcium in Binary Mixture by Second Derivative (D<sup>2</sup>) Spectrofluorimetric Method

Medhat Ahmed A. Al-Ghobashy, Yehia Z. Baghdady, Abdel-Aziz E. Abdel-Aleem and Soheir A. Weshahy

*Australian Journal of Basic and Applied Sciences*, 7 (8): 842-850 (2013)

A method for the simultaneous determination of ezetimibe (EZB) and atorvastatin calcium (ATVC) was developed, based on the measurement of their native fluorescence signals, by using second-derivative spectrofluorimetry to resolve the mixture. EZB was measured at  $\lambda_{em} = 455.0$  nm, and ATVC was measured at  $\lambda_{em} = 394.0$  nm. Instrumental parameters were optimized, and the emission spectra were recorded between 380.0 and 470.0 nm, at  $\lambda_{ex} = 246.0$  nm and excitation and emission slit widths of 10.0 nm. The calibration graphs were linear over the ranges of 200 – 900 ng/mL for both EZB and ATVC, with a mean percentage recovery of  $99.64 \pm 0.88$  and  $99.88 \pm 0.61$ , respectively. Methods were validated according to ICH guidelines and successfully applied for analysis of bulk powder and pharmaceutical formulations. The results were statistically compared to a reported method and no significant difference was noticed regarding accuracy and precision.

**Keywords:** Ezetimibe; Atorvastatin calcium; Derivative spectrofluorimetry; Pharmaceutical preparation.

### 1367. Simultaneous Determination of Hyoscine Nbutyl Bromide and Paracetamol by RP-TLC Spectrodensitometric Method

Mohammed Abdelkawy M. Ibrahim, Nouruddin W Ali and Mohammed Gamal

*British Journal of Pharmaceutical Research*, 3: (2013)

**Aims:** A simple RP-TLC Spectrodensitometric method was developed for determination of Hyoscine N-Butyl Bromide (HBB) and Paracetamol (PAR) either in bulk powder or in their Pharmaceutical preparation.

**Study Design:** Validation study.

**Methodology:** In this method; HBB and PAR were separated on RP-18 W/ UV<sub>254</sub> TLC plates using developing mobile phase consisting of methanol: citrate buffer (pH=1.5) : trifluoroacetic acid (70:30:0.1, by volume) at room temperature. Experimental conditions such as band size, slit width, different developing systems and scanning wavelength were carefully studied and the optimum conditions were selected. The obtained bands were then scanned at 210 nm. The two drugs were satisfactorily resolved with  $R_F$  0.60  $\pm$  0.02 for HBB and 0.81  $\pm$  0.02 for PAR. The validation of spectrodensitometric method was done regarding linearity accuracy precision and specificity.

**Results:** Linearity of the proposed methods was evaluated and it was found to lie within the concentration range of 2.0-12.0  $\mu\text{g}\cdot\text{band}^{-1}$  for HBB and 2.0-14.0  $\mu\text{g}\cdot\text{band}^{-1}$  for PAR.

**Conclusion:** The proposed method was successfully applied for determination of HBB and PAR in pure form and in their different pharmaceutical formulations. The method proved to be specific, accurate and selective.

**Keywords:** RP-TLC; Spectrodensitometry; Hyoscine N-butyl bromide; Paracetamol.

### 1368. Simultaneous Determination of Omeprazole, Tinidazole and Clarithromycin in Bulk Powder and Helicure Tablets by TLC-densitometric Technique

Mamdouh Reda Rezk Yousef, Hesham Salem, Safa'a M. Riad and Kholoud Ahmed

*Journal of Pharmaceutical Education and Research (Jper)*, 4 (1): 34-40 (2013)

A sensitive and precise thin layer chromatographic method has been developed and validated for simultaneous determination of omeprazole, tinidazole and clarithromycin in bulk powder; laboratory prepared mixture and combined dosage form. The technique adopted for quantification is coupled TLC-densitometry. The mobile phase used was a mixture of methylene chloride, isopropyl alcohol, acetonitrile and ammonia (11: 1.2: 5: 0.2, v/v/v/v). The detection of spots was carried out densitometrically using a UV detector at 300 nm in absorbance mode. This system was found to give compact spots for omeprazole ( $R_F$  0.45), tinidazole ( $R_F$  0.67) and clarithromycin ( $R_F$  0.89). The method was linear in the range of 1-20  $\mu\text{g}$  spot<sup>-1</sup>, 1-10  $\mu\text{g}$  spot<sup>-1</sup>, and 1-20  $\mu\text{g}$  spot<sup>-1</sup> for omeprazole, tinidazole and clarithromycin respectively with significantly high value of correlation coefficient ( $r^2 > 0.99$ ). The selectivity of the proposed method was checked using laboratory prepared mixtures. The proposed method was found to be accurate, precise, reproducible and specific and can be applicable for the simultaneous determination of omeprazole, tinidazole and clarithromycin in tablet dosage form without interference from other additives.

**Keywords:** Omeprazole; Tinidazole; Clarithromycin; TLC-densitometry.

### 1369. Simultaneous Determination of Paracetamol and Metoclopramide in Antimigraine Pharmaceutical Formulations

Amr Mohamed M. Badawey, Abd El-Aziz B. Abd El-Aleem, Shaban M. Khalile and Omneya K. El-Naggar

*Research Journal of Pharmaceutical Dosage forms and Technology*, 5 (5): 270-274 (2013)

This paper describes sensitive, accurate and precise TLC-densitometric and high performance liquid chromatographic (HPLC) methods for simultaneous determination of paracetamol and metoclopramide in pharmaceutical formulation. The TLC method employed aluminum TLC plates precoated with silica gel F254 as the stationary phase and ethylacetate/ methanol/ammonia (85:10:5 v/v/v) as the mobile phase, where the chromatogram was scanned at 254 nm. The developed HPLC method used a Zorbax C18 column with isocratic elution. The mobile phase composed of phosphate buffer pH 4.0: methanol (75:25 v/v) at flow rate of 1.0 ml/min. Quantitation was achieved with UV detection at 273 nm. The methods were validated according to the International Conference on Harmonization (ICH) guidelines. The selectivity of the proposed methods was tested using laboratory-prepared mixtures. The developed methods were successfully applied for the determination of paracetamol and metoclopramide in bulk powder and combined dosage form.

**Keywords:** High-performance liquid chromatography; Thin layer chromatography; Antimigraine drugs; Paracetamol; Metoclopramide.

### 1370. Simultaneous Determination of Simvastatin and Sitagliptin in Tablets by New Univariate Spectrophotometric and Multivariate Factor Based Methods

Maha Abdel-Monem Aboseri Hegazy, Hayam Mahmoud Lotfy and Sherif Abdel Naby Abdel-Gawad

*European Journal of Chemistry*, 4 (4): 414-421 (2013)

Five simple, sensitive and precise spectrophotometric and chemometric methods were used for simultaneous determination of Simvastatin (SM) and Sitagliptin (SIT) in their pure powdered forms and in the tablets. The proposed methods are the extended ratio subtraction method (EXRSM), ratio difference method (RDSM), mean centering of ratio spectra method (MCR) and chemometric methods, namely principal component regression (PCR) and partial least squares (PLS). In EXRSM; SM was determined at 237.5 nm, while SIT was determined at 267 nm, in RDSM; the difference in amplitudes at 237.5 and 245.5 nm was used for SM and 263.5 and 248.0 nm for SIT, while in MCR; SM and SIT were determined at 239.0 and 273.0 nm, respectively. PCR and PLS are factor based multivariate methods which utilize the whole spectra of SM and SIT. The developed methods were successfully applied for the determination of the studied drugs in their bulk powder, laboratory prepared mixtures and in tablets. All validation parameters of the developed methods were determined. The obtained results were statistically compared with each other along with a reported method.

**Keywords:** Sitagliptin; Univariate; Simvastatin; Multivariate; Chemometrics; Spectrophotometry.

### 1371. Simultaneous Determination of Some Antihypertension Drugs in their Binary Mixtures by Simple Spectrophotometric Methods

Hala Elsayed Elsayed Zaazaa, Eglal A. Abdelaleem, Ibrahim A. Naguib and Mohammed E. Draz

*Asian Journal of Biomedical and Pharmaceutical Sciences*, 3: 5-12 (2013)

Two simple, accurate and cost effective dual wavelength (Method I) and mean centering of ratio spectra MCR (Method II) spectrophotometric methods are developed and validated for determination of two drug combinations. The first comprises Hydrochlorothiazide (HCZ) and Benazepril Hydrochloride (BZ) and the second comprises HCZ and Candesartan Cilexetil (CAN) in their bulk powder and pharmaceutical tablets. In method (I), two wavelengths were selected for each drug in such a way that the difference in absorbance was zero for the second drug. For BZ/HCZ, mixture (I), BZ had equal absorbance values at 224.2 and 252.9 nm, therefore these two wavelengths were used to determine HCZ. Similarly, 243.8 and 293.8 nm were selected to determine BZ, where HCZ had equal absorbance values. For CAN/HCZ, mixture (II), HCZ is determined at 242.2 and 264.4 nm while CAN is determined at 257.8 and 280 nm. In method (II), absorption spectra of each drug were recorded, divided by suitable divisor and the obtained ratio spectra were mean centered. The concentrations of the proposed drugs were then determined from the calibration curves obtained by measuring amplitudes at 274 and 240.2 nm for HCZ and BZ respectively for mixture (I) and 274 and 240.4 nm for HCZ and CAN respectively for mixture (II). The developed methods were validated according to ICH guidelines demonstrating good accuracy and precision. The results were statistically compared with those obtained by reported methods indicating no significant difference and ability of methods to be used for routine analysis of proposed drugs.

**Keywords:** Hydrochlorothiazide; Benazepril hydrochloride; Candesartan cilexetil; Dual wavelength; Mean centering of ratio spectra; Spectrophotometry.

### 1372. Simultaneous Spectrophotometric Determination of Metronidazole and Diiodohydroxyquine

Safaa Mohamed Riad Mohany, Hesham Salem, Mamdouh Reda and Kholoud Ahmed

*Analytical Chemistry an Indian Journal*, 13: 23-32 (2013)

Four sensitive and precise spectrophotometric methods were developed and validated for the simultaneous determination of metronidazole (MTR) and diiodohydroxyquinoline (DIQ) in their mixture and in their pharmaceutical formulations. Among the methods adopted were, second-derivative ( $^2D$ ), third-derivative ( $^3D$ ), derivative ratio spectroscopy ( $^1DD$ ) and isosbestic point technique. The selectivity of the proposed methods was checked using laboratory prepared mixtures. The proposed methods were simple, not expensive and applicable that make them suitable for the analysis of MTR and DIQ in their mixture and in pharmaceutical formulations for routine unknown analysis in quality control labs.

**Keywords:** Metronidazole; Diiodohydroxyquinoline; Determination; Spectrophotometry.

### 1373. Simultaneous UV- Spectrophotometric Techniques for Determination of Chlorpheniramine Maleate and Naphazoline Hydrochloride in Eye Drops

Mohamed Refaat Elsayed Elghobashy, Osama Mohamed Badran, Maissa Yacoub Salem and Khadiga Mohamed Kelani

*Analytical Chemistry an Indian Journal*, 13: 69-76 (2013)

A binary mixture of chlorpheniramine maleate (I) and naphazoline hydrochloride (II) was determined by four different UV techniques. The first one utilizes second ( $D_2$ ) derivative spectrophotometry at 266.2 nm for determination of (I), without interference from (II) and at 291.5 and 298.5 nm for determination of (II) without interference from (I). The second technique depends on the simultaneous use of the first derivative of the ratio spectra ( $DD_1$ ) with measurement at 245 nm and 263 nm for determination of (I) using the spectrum of  $20 \mu\text{g ml}^{-1}$  (II) as a divisor and measuring at 295.5 nm for the determination of (II) using the spectrum of  $20 \mu\text{g ml}^{-1}$  (I) as a divisor. The third method is mean centering of ratio spectra with measurement at 254.2 and 291.4 nm for (I) and (II) respectively. The fourth method depends on the predictive abilities of the principal component regression (PCR) and partial least squares (PLS) were examined for the simultaneous determination of the binary mixture. The suggested procedures were checked using laboratory prepared mixtures and were successfully applied for the analysis of their pharmaceutical preparations. The validity of the proposed methods was further assessed by applying the standard addition technique. The results obtained by applying the proposed methods were statistically analyzed and compared with a reported method.

**Keywords:** Chlorpheniramine maleate; Naphazoline hydrochloride; Derivative spectrophotometry; Derivative ratio spectrophotometry; Mean centering; Multivariate spectral analysis methods.

### 1374. Spectrofluorimetric Determination of Diiodohydroxyquinoline in Presence of Metronidazole in Pharmaceutical Formulation and Spiked Human Plasma

Mohammed Abdelkawy Mohammed Ibrahim, Hassan Y. Aboul-Enein, Nouruddin W Ali and Mohammed Gamal

*Gazi University Journal of Science*, 26: (2013)

Accurate and sensitive spectrofluorimetric method was developed for determination of diiodohydroxyquinoline in presence of metronidazole. In this method the native fluorescence of diiodohydroxyquinoline in water solvent at  $\lambda = 495$  nm when excitation was at 250 nm is used for its determination. Linear correlation was obtained in the concentration range of 400 to 900 ng mL $^{-1}$ . The proposed method was successfully applied for determination of diiodohydroxyquinoline in bulk powder with mean accuracy of  $100.21 \pm 1.13$  or in spiked human plasma with mean accuracy of  $100.53 \pm 1.42$  without interference of metronidazole.

**Keywords:** Spectrofluorimetry; Diiodohydroxyquinoline; Metronidazole.

### 1375. Spectrophotometric and Chromatographic Methods for the Determination of A Binary Mixture of Sodium Cromoglicate and Xylometazoline Hydrochloride

Hayam Mahmoud Lotfy Ibrahim, Sarah S. Saleh, Nagiba Y. Hassan and Samia M. Elgizawy

*Analytical Chemistry an Indian Journal*, 13(4): 152-160 (2013)

Simple, sensitive and precise spectrophotometric and chromatographic methods were developed for simultaneous

determination of Sodium cromoglicate (SCG) and Xylometazoline hydrochloride (XYLO) in their pure form and nasal solution. By applying the spectrophotometric methods, (SCG) was determined by direct spectrophotometry through measuring its zero-order ( $D_0$ ) absorption spectra at 325 nm; while (XYLO) was determined using two methods. The first method utilized the first derivative spectra ( $D^1$ ) of (XYLO) after prior separation of SCG from medium using 0.1 N HCl. The second method depends on derivative compensation ratio technique depending on the mean ratio of  $D^1$  peak amplitudes of SCG ( $D_{231.4}/D_{309.4}$ ). The chromatographic method utilized a Zorbax SB-C<sub>18</sub> column and a mobile phase of acetonitrile: 10 mM phosphate buffer (pH 4): triethylamine, in ratio (80: 19.9: 0.1 v/v/v), delivered at flow rate of 1.2 mL/min and the detections were done at 220 nm. The proposed methods were validated in compliance with the ICH guidelines and were successfully applied for the analysis of (SCG) and (XYLO) in the laboratory prepared mixtures and combined pharmaceutical dosage form.

**Keywords:** Sodium cromoglicate; Xylometazoline hydrochloride; Derivative spectrophotometry; Derivative compensation ratio technique; Chromatographic.

### 1376. Spectrophotometric and TLC-Densitometric Determination of Dantrolene Sodium in Presence of its Acid Degradates

Hebat Allah Mohammed Essam El-Din, Samah S. Abbas and Mohammad G. El-Bardicy

*Annaallyyttiiccaall Chemiisstryan Indian J., 12: 26-31 (2013)*

This work is concerned with determination of dantrolene sodium in presence of its acid degradates in bulk and in pharmaceutical formulations by two different techniques. The first one is the application of first derivative spectrophotometric technique which permits selective determination of dantrolene sodium at  $\lambda$  420.9 nm without interference. Beer's law was obeyed in the concentration range of 2-22  $\mu\text{g mL}^{-1}$  with mean percentage recovery of  $99.67 \pm 1.018$ . The second method depends on the quantitative densitometric evaluation of thin layer chromatogram of dantrolene sodium with ultraviolet detection at 388 nm using chloroform/acetone/ glacial acetic acid (85:15:1 by volume) as a developing system with no interference of its acid degradates. The calibration graph was linear in the range of 0.1-0.6  $\mu\text{g/band}$ . The suggested methods were used to determine the drug in presence of its acid degradates in both pure form and commercial capsules. The obtained results were statistically compared with those obtained by the manufacturer's method, showing no significant difference with respect to accuracy and precision.

**Keywords:** Dantrolene sodium; Derivative spectrophotometry; TLC-densitometry; Acid degradation.

### 1377. Spectrophotometric Determination of Diiodohydroxyquinoline in Presence of Metronidazole in Pharmaceutical Formulation

Mohammed Abdelkawy Mohammed Ibrahim, Nouruddin W Ali and Mohammed Gamal

*Int. J. of Analytical and Bioanalytical Chemistry, 3: (2013)*

Accurate and selective spectrophotometric method was developed for determination of Diiodohydroxyquinoline (DIHQ) in presence

of metronidazole (MTN). In this work, a spectrophotometric method based on reduction of ferric-phenanthroline (ferriin) to ferrous-phenanthroline (ferroin) by DIHQ is used where the absorption of the obtained orange-red color ferroin chelate was measured at  $\lambda_{\text{max}}$  510 nm. Linear correlation was obtained in the concentration range of 2.0 to 10.0  $\mu\text{g mL}^{-1}$ . The proposed method was successfully applied for determination of Diiodohydroxyquinoline in bulk powder with mean accuracy of  $100.15 \pm 0.538$  at 510 nm without interference of metronidazole.

**Keywords:** Spectrophotometry; O-Phenanthroline; Diiodohydroxyquinoline; Metronidazole.

### 1378. Stability Indicating Chemometric Methods for the Determination of Two Cephalosporin Drugs by Partial Least Squares and Principle Component Regression Multivariate Calibration Methods

Shereen Ahmed Hassan Boltia, Laila Abdel-fattah, Soheir A. Weshahy, Nagiba Y. Hassan and Nadia M. Mostafa

*Australian J. of Basic and Applied Sciences, 7: 285-292 (2013)*

In this study, Two multivariate calibration methods, including principal component regression (PCR) and partial least square (PLS), have been used for the determination of two cephalosporin drugs namely cefpodoxime and cefixime in the presence of their acidic and alkaline induced degradation products. Although the components show a large degree of spectral overlap, they have been determined simultaneously and rapidly requiring no separation step. The PCR and PLS techniques are useful chemometric approaches using UV spectral analysis due to the simultaneous inclusion of many spectral wavelengths instead of the single wavelength used in derivative spectrophotometry, thus a great improvement in the precision and predictive abilities of these multivariate calibrations is observed. Spectra of cefpodoxime and cefixime and their acidic and alkaline induced degradation products were recorded at several concentrations within their linear ranges and were used to compute the calibration mixture between wavelengths 200 and 400 nm at an interval of 1 nm in water. PLS and PCR were used for chemometric analysis of data and the parameters of the chemometric procedures were optimized. A calibration set was constructed for the mixture and the best model was used for the prediction of the concentration of the selected drug. The proposed procedures were successfully applied for the determination of cefpodoxime and cefixime in laboratory-prepared mixtures and in pharmaceutical formulations, with no interference from excipients as indicated by the recovery study results. The validity of the proposed methods was assessed using the standard addition technique.

**Keywords:** Stability indicating method; Degradation; Cefpodoxime proxetil; Cefixime trihydrate; Multivariate calibration methods.

### 1379. Stability Indicating Chromatographic Methods for the Determination of Trosipium Chloride

Nesrin Khamis Ramadan Selim, Lamia M. Abd El Halim, Hoda F. EL Sanabary and Maissa Y. Salem

*International Journal of Chemistry, 34: 1217-1224 (2013)*

Two precise, accurate and sensitive high-performance liquid chromatographic and thin-layer chromatographic methods were



developed and validated for the determination of Trosipium chloride in presence of its degradation products. Forced degradation studies were performed using HCl and NaOH. Separation of the drug from its degradation products by HPLC was achieved using a X- Bridge C18 column and acetonitrile/methanol/0.05M potassium dihydrogen phosphate/triethylamine in a ratio of (25:25:50:0.2 by volume) as a mobile phase, pH was adjusted to  $4 \pm 0.1$  with ortho-phosphoric acid. The flow rate was 1ml/min. Detection was performed at 215 nm. The linearity range was 0.5 to 18  $\mu\text{g/ml}$ . The mean percentage recovery was  $100.40 \pm 0.450 \%$ . The TLC method was used for separation of the drug from its degradation products using silica gel 60 F<sub>254</sub> plates; the optimized mobile phase was acetonitrile/glacial acetic acid (5:5 by volume). Quantitatively, the spots were scanned densitometrically at 215 nm. The linearity range was 2 to 16  $\mu\text{g/spot}$ . The mean percentage recovery was  $99.96 \pm 0.700 \%$ . The degradation products were obtained in acid and alkaline stress conditions were the same, therefore the alkaline degradation products were prepared, identified and compared with the standard ones. Statistical comparison between the results obtained by these methods and those obtained by the official method was done, and no significance difference was obtained.

**Keywords:** Trosipium chloride; Stability studies; Degradation; HPLC; TLC; Benizic acid.

### 1380. Stability Indicating Chromatographic Techniques for the Determination of Pipoxolan HCL

Hala Elsayed E. Zaazaa, Afaf O. Mohamed, Mohamed Abdelkawy and Maha A.Hawwam

*Journal of Applied Pharmaceutical Science*, 3: 66-73 (2013)

Two simple, accurate and sensitive methods were developed for the determination of pipoxolan HCl in presence of its degradation product. HPLC method (A), performed on C18 column using Acetonitrile: 1mM ammoniumacetate (80:20 v/v) as a mobile phase with a flow rate of 1.8ml/min. Detection was performed at 210 nm. TLC densitometric method (B), using silica gel 60 F<sub>254</sub> plates; the optimized mobile phase was chloroform: toluene: methanol: 10% ammonia (6:5:3:0.1 v/v). Quantitatively the spots were scanned densitometrically at 210 nm. Linearity ranges were 1 – 10  $\mu\text{g/ml}$  for method A and 2-20  $\mu\text{g/band}$  for method B, with mean percentage recoveries  $99.38 \pm 0.672\%$  and  $99.32 \pm 0.97\%$  for methods A and B, respectively. The proposed methods were found to be specific for pipoxolan HCl in presence of up to 90% of its degradation product. Statistical comparison between the results obtained by these methods and the manufacturer's method was done, and it was found that there was no significant differences between them.

**Keywords:** Pipoxolan HCL; HPLC; TLC-densitometric; Stability.

### 1381. Stability Indicating Methods for the Determination of Cefpodoxime Proxetil in the Presence of its Acid and Alkaline Degradation Products

Shereen Ahmed Hassan Boltia

*International Journal of Pharmaceutical and Biological Research (IJPBR)*, 3: 223-239 (2013)

Four different, accurate, sensitive and reproducible stability-indicating methods for the determination of cefpodoxime proxetil (CPD) in the presence of its acid and alkaline degradation products are presented. The first method is based on derivative spectrophotometry. Second derivative spectrophotometry was applied where CPD was determined at 261 nm in the presence of its acid degradation product and also third derivative spectrophotometry was applied where CPD was determined at 282 nm in the presence of its alkaline degradation product. The second method is based on the first derivative of ratio spectrophotometry (1DD) of CPD at 215 nm and 255 nm in the presence of its acid degradation product and at 243 nm in the presence of its alkaline degradation product. The third method is ratio subtraction spectrophotometry where the drug is determined at 232 nm in laboratory prepared mixtures of CPD and its acid or alkaline degradation product. Calibration graphs were established for 4.0-40.0  $\mu\text{g/ml}$  for CPD determination by the three spectrophotometric methods. The fourth method is an isocratic reversed-phase HPLC procedure, a Zorbax C8 column was used to separate CPD from its acid and alkaline degradation product using acetonitrile: water: triethylamine (60:40:1, v/v/v) as a mobile phase and detection at 232 nm. The suggested procedures were successfully applied for the analysis of CPD in bulk powder and in pharmaceutical preparations. The results obtained by applying the proposed methods were statistically analyzed and compared with those obtained by the official method.

**Keywords:** Cefpodoxime proxetil; Stability indicating method; Degradation; High-performance liquid chromatography.

### 1382. Stability Indicating Spectrophotometric and Chemometric Methods for Determination of Buflomedil in Presence of its Acid Induced Degradation Products

Maha Abdel-Monem Aboseri Hegazy, Azza Aziz Moustafa, Hesham Salem and Omnia Ali

*Analytical Chemistry Letters*, 3(5,6): 342-358 (2013)

Simple, accurate, sensitive, selective and validated UV spectrophotometric univariate and multivariate methods were developed for determination of Buflomedil (BFM) in presence of BFM degradation products (BFM Deg). The univariate methods includes mean centering of ratio spectra (MCR), ratio differences spectrophotometric method (RDSM) and H-point standard addition method (HPSAM); the first one used the amplitude at 235.7 nm, the second utilized the difference in amplitudes at 250 nm and 282 nm; while, the third method utilized the absorbance values at 247 and 282.4 nm. Linearity was obtained for the proposed methods in the ranges of 10-100  $\mu\text{g/mL}^{-1}$ . The percentage recoveries were  $100.06 \pm 0.963$ ,  $100.17 \pm 0.962$  and  $100.90 \pm 0.667$  for the three methods in a respective order. Multivariate methods involves the application of three chemometric techniques, and classical least square (CLS) principal component regression (PCR) and partial least-squares regression (PLS), which were used for the simultaneous determination of the BFM and its degradation products. The results obtained from the proposed methods, together with the reported one, were statistically compared using one-way analysis of variance (ANOVA). These methods are suitable as stability indicating methods for the determination of BFM in presence of its degradation products either in bulk powder or in pharmaceutical formulations.

**Keywords:** Buflomedil; Degradation products; Spectrophotometry; Chemometry.

### 1383. Stability Indicating Spectrophotometric and Spectrodensitometric Methods for Determination of Calcium Dobesilate in the Presence of its Impurity and/or Degradation Product

Maha Abdel-Monem Aboseri Hegazy, Nour W. Sayed, Eglal A. Abdel-Aleem, M. Abdelkawy and Rehab M. Abdelfatah

*International Journal of Pharmacy and Pharmaceutical Sciences*, 5 (3): 207-214 (2013)

**Objective:** To develop Two simple, specific, accurate and precise methods for determination of calcium dobesilate (CD) in the presence of its impurity and/ or degradation product namely hydroquinone (HQ).

**Methods:** Method A is an extended ratio subtraction one (EXRSM), while method B is a HPTLC-densitometric one using benzene: methanol: ethyl acetate: sodium lauryl sulphate (7: 2.5: 2: 0.05 v/v/v/w) as a developing system.

**Results:** The developed methods were successfully applied for determination of CD in the assay of raw material and tablets as well as quantitative determination of HQ with standard deviation values less than 1.5. The two methods are linear over the concentration range of 5-70  $\mu\text{g. mL}^{-1}$  for CD, and 5-60  $\mu\text{g. mL}^{-1}$  for HQ, methods were validated as per ICH guidelines; accuracy, precision and repeatability are found to be within the acceptable limits.

**Conclusion:** The two developed extended ratio subtraction method (EXRSM) and the HPTLC-densitometric one are valid for application in laboratories lacking liquid chromatographic instruments.

**Keywords:** Calcium dobesilate; Hydroquinone; Extended ratio subtraction; HPTLC-Densitometric; Stability.

### 1384. Stability Indicating Spectrophotometric Methods for Determination of Bumadizone in the Presence of its Alkaline Degradation Product

Hala Elsayed E. Zaazaa, Nouruddin W. Ali, Maimana A. Magdy and Mohamed Abdelkawy

*Drug Invention Today*, 5 (2): 139-147 (2013)

**Objectives:** Simple, selective and precise stability indicating spectrophotometric methods were adopted and validated for the quantitative determination of Bumadizone calcium semihydrate (BUM) in presence of its alkaline degradation product (DEG I).

**Methods:** **Method A** is based on the application of first derivative ( $^1\text{D}$ ) spectrophotometry, then measuring the amplitude of BUM at 245.4 nm. **Method B** depends on measuring the peak amplitude of the first derivative of the ratio spectra ( $^1\text{DD}$ ) at 242.6, 260 and 274 nm over a concentration range of 6-20  $\mu\text{g mL}^{-1}$ . **Method C** is isoabsorptive point spectrophotometry where total concentration of BUM and DEG I was calculated at their isoabsorptive point at 242.2 nm ( $\lambda_{\text{iso}}$ ) while DEG I concentration alone can be determined at  $\lambda_{\text{max}}$  320 nm, and then BUM concentration can be determined by subtraction. In **Method D** ratio subtraction spectrophotometry is applied.

**Results:** The four methods were found to be specific for determination BUM in presence of different concentrations of

DEG I and were successfully applied for the determination of BUM in Octomol tablets.

**Conclusion:** Statistical comparison between the results obtained by applying the proposed methods and that obtained by the manufacturer one for the determination of the drug was done, and it was found that there is no significant difference between them.

**Keywords:** Bumadizone; Derivative ratio spectrophotometry; First derivative of ratio; Spectra spectrophotometry; Isoabsorptive spectrophotometry; Ratio subtraction spectrophotometry.

### 1385. the Use of Calixarene as Ionophores in Potentiometric Ion-Selective Electrodes of Naftidrofuryl Oxalate Using Microsized Membrane Sensors for Kinetic Study of Naftidrofuryl (NFT) Degradation

Mohamed Abdalla Elsayed Aga

*European Journal of Chemistry*, 4 (2): 124-131 (2013)

Novel miniaturized polyvinyl chloride (PVC) membrane sensors in all-solid state graphite and platinum wire supports were developed, electrochemically evaluated and used for the assay of naftidrofuryl oxalate (NFT). The NFT sensors were based on the reaction between the drug cation and tetrakis (4-chlorophenyl) borate (TpCIPB) anionic exchanger as electro active material and sulfocalix-8-arene as ionophore dispersed in a PVC matrix. Linear responses of  $10^{-2}$ -  $10^{-6}$  M and  $10^{-2}$ - $10^{-5}$  M with cationic slopes of 56.9 mV and 54.1 mV over the pH range 2-5 were obtained by using the NFT-coated graphite (sensor 1) and platinum wire (sensor 2) membrane sensors, respectively. The utility of 4-sulfocalix-8-arene as ionophore had a significant influence on increasing the membrane sensitivity and selectivity. The methods were also used to determine the intact drug in the presence of its degradate in Praxilene tablets, plasma and cerebrospinal fluid (CSF) with good recovery. Sensor 1 was used to study the kinetics of NFT alkaline degradation that was found to follow a pseudo first-order reaction. The activation energy could be estimated from the Arrhenius plot to be 12.572 Kcal mol.

**Keywords:** Naftidrofuryl oxalate; Tetrakis (4-chlorophenyl) borate; 4-Sulfocalix-8-arene; Plasma; Cerebrospinal fluid; Reaction kinetics.

### 1386. Two New Spectrophotometric Approaches to the Simultaneous Determination of Ezetimibe and Atorvastatin Calcium

Medhat Ahmed A. Al-Ghobashy, Yehia Z. Baghdady, Abdel-Aziz E. Abdel-Aleem and Soheir A. Weshahy

*International Journal of Chemical Studies*, 1(2): 14-25 (2013)

Two rapid, simple and sensitive spectrophotometric methods for the quantitative analysis of ezetimibe (EZB) and atorvastatin calcium (ATVC) in bulk powder and combined tablet form have been developed and validated. The first method is bivariate calibration and the second method is ratio subtraction in conjunction with second derivative ( $\text{D}^2$ ) spectrophotometry. These methods are tested by analyzing synthetic binary mixtures of the above drugs and they are applied to commercial pharmaceutical preparation of the subjected drugs. Standard deviation is  $< 2$  in the assay of raw materials and tablets.

Methods are validated as per ICH guidelines and statistical comparison of the suggested methods with the reported spectrophotometric one using *F* and *t* tests showed no significant difference regarding both accuracy and precision.

**Keywords:** Ezetimibe; Atorvastatin calcium; Spectrophotometry; Bivariate calibration; Ratio subtraction; Derivative spectrophotometry.

### 1387. Univariate Versus Multivariate Spectrophotometric Methods for Simultaneous Determination of Complex Binary Mixtures with Overlapped Spectra: A Comparative Study

Hayam Mahmoud Lotfy Ibrahim, Sarah S. Saleh, Nagiba Y. Hassan and Samia M. Elgizawy

*Analytical Chemistry Letters*, 3 (2): 70-84 (2013)

Two novel simple and accurate univariate spectrophotometric methods were described for the determination of a binary mixture of Sodium cromoglicate (SCG) and Fluorometholone (FLU) namely; ratio subtraction coupled with extended ratio subtraction (RS-EXRSM) and constant center (CCSM) spectrophotometric methods. The methods were able to recover the zero order absorption spectra of both drugs from their binary mixture through simple mathematical calculations. The linearity ranges were found to be (2.5-25  $\mu\text{g/mL}$ ) and (4- 25  $\mu\text{g/mL}$ ) for SCG and FLU, respectively. A comparative study was conducted between the proposed univariate methods versus multivariate ones, based on using principle component regression (PCR) and partial least squares (PLS-2). Upon applying the methods for the determination of SCG and FLU in laboratory prepared mixtures, the (CCSM and PLS-2) proved to be of higher predictive ability rather than (RSEXRS and PCR) in prediction of mixtures containing low concentration of one of the components. The proposed methods were validated in compliance with the ICH guidelines. These methods could be alternative to different HPLC techniques in quality control laboratories lacking the required facilities for those expensive techniques.

**Keywords:** Constant center; Extended ratio subtraction; PLS; PCR; Chemometrics; Sodium cromoglicate; Fluorometholone.

### 1388. Validated Chromatographic methods for Determination of Paracetamol, Pseudoephedrin and Cetirizin in Pharmaceutical Formulation

Maha Abdel-Monem Aboseri Hegazy, Fatma E. Khattab and Basma M. Abdelhameed

*Analytical Chemistry in Indian Journal*, 12 (7): 248-255 (2013)

Two specific, sensitive and precise stability indicating chromatographic methods had been developed, optimized and validated for determination of Paracetamol (PAR), Pseudoephedrin (PS) and Cetirizin (CET) in their laboratory prepared mixtures and pharmaceutical formulations. The first method was based on thin layer chromatographic densitometry (TLC). The optimum separation was achieved using silica gel 60 F<sub>254</sub> Aluminum TLC plates and ethyl acetate: methanol: ammonia (75: 20: 5 by volume) as a developing system. Good correlations were obtained in the ranges of (1-12  $\text{mg mL}^{-1}$ ) for PAR and PS and (3-15  $\text{mg mL}^{-1}$ ) for CET. The second method was based on high performance liquid chromatography with

ultraviolet detection (HPLC-UV), at which the proposed components were separated on a reversed phase C18 column using phosphate buffer (pH 3.6): acetonitrile (1: 1.2 by volume) as the mobile phase, maintaining constant flow rate of 1  $\text{mL min}^{-1}$  and detection at 210 nm. Linear regressions were obtained in the ranges of 1.0-60, 1.0-50 and 0.1-60  $\mu\text{g mL}^{-1}$  for PAR, PS and CET, respectively.

Different parameters affecting the suggested methods had been optimized in order to obtain maximum separation of the cited components. System suitability parameters of the two developed methods were also tested. The suggested methods were successfully applied for determination of PAR, PS and CET in their commercial capsules. Both methods were validated in compliance with the ICH guidelines with satisfactory results. Also they were statistically compared to each other and to the reported method, no significant difference was found, providing their accuracy and precision.

**Keywords:** Paracetamol; Pseudoephedrin; Cetirizin; Thin layer chromatography; High performance liquid chromatography.

### 1389. Validated Stability Indicating Spectrophotometric Methods for the Determination of Lidocaine Hydrochloride, Calcium Dobesilate, and Dexamethasone Acetate in their Dosage forms

Hayam Mahmoud Lotfy Ibrahim, Shereen M. Tawakkol, Nesma M. Fahmy and Mostafa A. Shehata

*Analytical Chemistry Letters*, 3 (3): 208-225 (2013)

Simple, specific, accurate and precise spectrophotometric methods were developed for determination of lidocaine hydrochloride, and calcium dobesilate in their binary mixture, or combined with dexamethasone acetate as a ternary mixture; in the presence of hydroquinone, the degradation product of calcium dobesilate without prior separation. In binary mixture lidocaine hydrochloride was determined using novel mathematical methods namely amplitude subtraction and amplitude factor, in addition to ratio subtraction coupled with first derivative.

While dexamethasone acetate was assayed by first derivative method. Lidocaine and dexamethasone in ternary mixture could be determined by a novel resolution technique namely successive spectrophotometric resolution; including successive ratio subtraction coupled with either first derivative, or extended ratio subtraction for dexamethasone and ratio subtraction coupled with first derivative for lidocaine hydrochloride; and finally the calcium dobesilate could be determined by first derivative, derivative ratio and the novel modified amplitude subtraction methods.

The calibration curves are linear over the concentration range of 2-20  $\mu\text{g mL}^{-1}$  for both lidocaine hydrochloride and dexamethasone acetate, 2-19  $\mu\text{g mL}^{-1}$  or 6-50  $\mu\text{g mL}^{-1}$  for calcium dobesilate. The proposed methods could be successfully applied to commercial pharmaceutical preparations of the cited drugs.

The proposed methods were validated according to the ICH guidelines. The obtained results were statistically compared with those of the reference reported methods using student *t*-test, *F*-test, and one way ANOVA, showing no significant difference with respect to accuracy and precision.

**Keywords:** Successive spectrophotometric resolution; Lidocaine hydrochloride; Dexamethasone acetate; Calcium dobesilate; Hydroquinone.

**Dept. of BioChemistry**

**1390. Temporal Regulation of EGF Signalling Networks by the Scaffold Protein Shc1**

Yong Zheng, Cunjie Zhang, David R. Croucher, Mohamed A. Soliman, Nicole St-Denis, Adrian Pasculescu, Lorne Taylor, Stephen A. Tate, W. Rod Hardy, Karen Colwill, Anna Yue Dai, Rick Bagshaw, James W. Dennis, Anne-Claude Gingras, Roger J. Daly and Tony Pawson

*Nature*, 499: 166-171 (2013) IF: 38.597

Cell-surface receptors frequently use scaffold proteins to recruit cytoplasmic targets, but the rationale for this is uncertain. Activated receptor tyrosine kinases, for example, engage scaffolds such as Shc1 that contain phosphotyrosine (pTyr)-binding (PTB) domains. Using quantitative mass spectrometry, here we show that mammalian Shc1 responds to epidermal growth factor (EGF) stimulation through multiple waves of distinct phosphorylation events and protein interactions. After stimulation, Shc1 rapidly binds a group of proteins that activate pro-mitogenic or survival pathways dependent on recruitment of the Grb2 adaptor to Shc1 pTyr sites. Akt-mediated feedback phosphorylation of Shc1 Ser29 then recruits the Ptpn12 tyrosine phosphatase. This is followed by a sub-network of proteins involved in cytoskeletal reorganization, trafficking and signal termination that binds Shc1 with delayed kinetics, largely through the SgK269 pseudokinase/adaptor protein. Ptpn12 acts as a switch to convert Shc1 from pTyr/Grb2-based signalling to SgK269-mediated pathways that regulate cell invasion and morphogenesis. The Shc1 scaffold therefore directs the temporal flow of signalling information after EGF stimulation

**Keywords:** Protein-protein interaction networks; Growth signaling; Phosphorylation; Dynamic networks.

**1391. Requirement of NEMO/IKK $\gamma$  for Effective Expansion of KRAS-Induced Precancerous Lesions in the Pancreas**

Heba Hamed Salem, H. J. Maier, M. Wagner, T. G. Schips, B. Baumann and T. Wirth

*Oncogene*, 32: 2690-2695 (2013) IF: 7.357

Pancreatic carcinoma, a leading cause of cancer death, is thought to develop out of pancreatic intraepithelial neoplasia (PanIN). PanIN lesions have not yet attained the fully malignant phenotype, but show increased proliferation and dysplasia, and frequently bear an oncogenic KRAS mutation. Pancreatic cancer development is associated with increased activity of the transcription factor NF- $\kappa$ B. NEMO (IKK $\gamma$ ) is a subunit of the IKK complex essential for the activation of canonical NF- $\kappa$ B signaling and has been ascribed both oncogenic and tumor-suppressive roles in gastrointestinal tumors. Here, we wanted to address the function of NEMO in pancreatic tumorigenesis. We therefore conditionally ablated NEMO in a mouse model for pancreatic carcinoma based on the expression of oncogenic KRAS in pancreatic precursor cells. Mice were analyzed for PanIN lesions and for the activation of associated signaling pathways. NEMO ablation in the pancreas, while in itself not causing any overt pathology, led to a drastic (>93%) decrease in the prevalence of both low-grade and high-grade PanIN in 10-month-old mice expressing oncogenic KRAS. Also, the

inflammatory and fibrotic response associated with KRAS action in the pancreas was virtually abolished, including expression of inflammatory cytokines and activation of the interleukin-6/STAT3 axis. Moreover, the activation of MAPK signaling, Notch and KLF4 signaling normally observed in KRAS-induced PanIN was strongly reduced or absent when NEMO was ablated. Our study suggests that NEMO, an IKK subunit necessary for canonical NF- $\kappa$ B activation, is dispensable for normal pancreatic development and function, but essential for the propagation of KRAS-induced PanIN lesions.

**Keywords:** Pancreatic intraepithelial neoplasia; Pancreatic carcinoma; Animal model; KRAS; NEMO/IKK $\gamma$ .

**1392. Role of AKAP79/150 in  $\beta$ 1-Adrenergic Receptor Trafficking and Signaling in Mammalian Cells**

Mohammed Mostafa Nooh, Xin Li and Suleiman W. Bahouth

*Journal of Biological Chemistry*, 288: 33797-33812 (2013) IF: 4.65

AKAPs (A-kinase anchoring proteins) participate in the formation of macromolecular signaling complexes that include protein kinases, ion channels, effector enzymes and GPCRs. We examined the role of AKAP79/150 (AKAP5) in trafficking and signaling of the  $\beta$ 1-adrenergic receptor ( $\beta$ 1-AR). shRNA-mediated down-regulation of AKAP5 in HEK-293 cells inhibited the recycling of the  $\beta$ 1-AR. Recycling of the  $\beta$ 1-AR in AKAP5 knock-down cells was rescued by shRNA-resistant AKAP5. However, truncated mutants of AKAP5 with deletions in the domains involved in membrane targeting or in binding to calcineurin or PKA, failed to restore the recycling of the  $\beta$ 1-AR, indicating that full-length AKAP5 was required. Furthermore, recycling of the  $\beta$ 1-AR in rat neonatal cardiac myocytes was dependent on targeting the AKAP5/PKA complex to the carboxy-tail of the  $\beta$ 1-AR. To analyze the role of AKAP5 more directly, recycling of the  $\beta$ 1-AR was determined in ventricular myocytes from AKAP5 $^{-/-}$  mice. In AKAP5 $^{-/-}$  myocytes, the agonist-internalized  $\beta$ 1-AR did not recycle, except when full-length AKAP5 was reintroduced. These data indicate that AKAP5 exerted specific and profound effects on  $\beta$ 1-AR recycling in mammalian cells. Biochemical or real-time, FRET-based imaging of cyclic AMP revealed that deletion of AKAP5 sensitized the cardiac  $\beta$ 1-AR signaling pathway to isoproterenol. Moreover, isoproterenol-mediated increase in contraction rate, surface area and expression of  $\beta$ -myosin heavy chains was significantly greater in AKAP5 $^{-/-}$  myocytes than in AKAP5 $^{+/+}$  myocytes. These results indicate a significant role for the AKAP5 scaffold in signaling and trafficking of the  $\beta$ 1-AR in cardiac myocytes and mammalian cells.

**Keywords:** GPCR;  $\beta$ -adrenergic receptors; Anchoring protein; Trafficking; Confocal microscopy.

**1393. Carvedilol Alleviates Adjuvant-Induced Arthritis and Subcutaneous Air Pouch Edema: Modulation of Oxidative Stress and Inflammatory Mediators.**

Maha Mahmoud A. El-Sawalhi and Hany Hamdy A. Arab

*Toxicol Appl Pharm*, 268 (2): 241-248 (2013) IF: 3.975



Rheumatoid arthritis (RA) is a systemic inflammatory disease with cardiovascular complications as the leading cause of morbidity. Carvedilol is an adrenergic antagonist which has been safely used in treatment of several cardiovascular disorders. Given that carvedilol has powerful antioxidant/anti-inflammatory properties, we aimed to investigate its protective potential against arthritis that may add further benefits for its clinical usefulness especially in RA patients with concomitant cardiovascular disorders. Two models were studied in the same rat; adjuvant arthritis and subcutaneous air pouch edema. Carvedilol (10mg/kg/day p.o. for 21days) effectively suppressed inflammation in both models with comparable efficacy to the standard anti-inflammatory diclofenac (5mg/kg/day p.o.). Notably, carvedilol inhibited paw edema and abrogated the leukocyte invasion to air pouch exudates. The latter observation was confirmed by the histopathological assessment of the pouch lining that revealed mitigation of immuno-inflammatory cell influx. Carvedilol reduced/normalized oxidative stress markers (lipid peroxides, nitric oxide and protein thiols) and lowered the release of inflammatory cytokines (TNF- $\alpha$  & IL-6), and eicosanoids (PGE<sub>2</sub> & LTB<sub>4</sub>) in sera and exudates of arthritic rats. Interestingly, carvedilol, per se, didn't present any effect on assessed biochemical parameters in normal rats. Together, the current study highlights evidences for the promising anti-arthritic effects of carvedilol that could be mediated through attenuation of leukocyte migration, alleviation of oxidative stress and suppression of proinflammatory cytokines and eicosanoids.

**Keywords:** Carvedilol; Adjuvant arthritis; Air pouch edema; Oxidative stress; Inflammatory mediators

#### 1394. OSU-A9 Inhibits Angiogenesis in Human Umbilical Vein Endothelial Cells Via Disrupting AKT-Nf- $\kappa$ B and MAPK Signaling Pathways

Hany H. Arab, Hany A. Omar, El-Shaimaa A. Arafa, Samir A. Salama, Chieh-HsiWu and Jing-RuWeng

*Toxicology and Applied Pharmacology*, 272 (3): 616-624 (2013)  
IF: 3.975

Since the introduction of angiogenesis as a useful target for cancer therapy, few agents have been approved for clinical use due to the rapid development of resistance. This problem can be minimized by simultaneous targeting of multiple angiogenesis signaling pathways, a potential strategy in cancer management known as polypharmacology. The current study aimed at exploring the anti-angiogenic activity of OSU-A9, an indole-3-carbinol-derived pleiotropic agent that targets mainly Akt-nuclear factor-kappa B (NF- $\kappa$ B) signaling which regulates many key players of angiogenesis such as vascular endothelial growth factor (VEGF) and matrix metalloproteinases (MMPs). Human umbilical vein endothelial cells (HUVECs) were used to study the in vitro anti-angiogenic effect of OSU-A9 on several key steps of angiogenesis. Results showed that OSU-A9 effectively inhibited cell proliferation and induced apoptosis and cell cycle arrest in HUVECs. Besides, OSU-A9 inhibited angiogenesis as evidenced by abrogation of migration/invasion and Matrigel tube formation in HUVECs and attenuation of the in vivo neovascularization in the chicken chorioallantoic membrane assay. Mechanistically, Western blot, RT-PCR and ELISA analyses showed the ability of OSU-A9 to inhibit MMP-2 production and VEGF expression induced by hypoxia or phorbol-12-myristyl-13-acetate. Furthermore, dual inhibition of Akt-NF- $\kappa$ B and mitogen-

activatedprotein kinase (MAPK) signaling, the key regulators of angiogenesis, was observed. Together, the current study highlights evidences for the promising anti-angiogenic activity of OSU-A9, at least in part through the inhibition of Akt-NF- $\kappa$ B and MAPK signaling and their consequent inhibition of VEGF and MMP-2. These findings support OSU-A9's clinical promise as a component of anticancer therapy.

**Keywords:** OSU-A9; Angiogenesis; Akt-NF- $\kappa$ B; MAPKS; VEGF; MMP-2.

#### 1395. SAP97 Controls the Trafficking and Resensitization of the Beta-1-Adrenergic Receptor Through its PDZ2 and I3 Domains

Mohammed M. Nooh, Anjaparavanda P. Naren, Sung-Jin Kim, Yang K. Xiang and Suleiman W. Bahouth

*Plos One*, 8: 63379-63379 (2013) IF: 3.73

Previous studies have determined that the type-1 PDZ sequence at the extreme carboxy-terminus of the  $\beta$ 1-adrenergic receptor ( $\beta$ 1-AR) binds SAP97 and AKAP79 to organize a scaffold involved in trafficking of the  $\beta$ 1-AR. In this study we focused on characterizing the domains in SAP97 that were involved in recycling and resensitization of the  $\beta$ 1-AR in HEK-293 cells. Using a SAP97 knockdown and rescue strategy, we determined that PDZ-deletion mutants of SAP97 containing PDZ2 rescued the recycling and resensitization of the  $\beta$ 1-AR. Among the three PDZs of SAP97, PDZ2 displayed the highest affinity in binding to the  $\beta$ 1-AR. Expression of isolated PDZ2, but not the other PDZs, inhibited the recycling of the  $\beta$ 1-AR by destabilizing the macromolecular complex involved in trafficking and functional resensitization of the  $\beta$ 1-AR. In addition to its PDZs, SAP97 contains other protein interacting domains, such as the I3 sequence in the SRC homology-3 (SH3) domain, which binds to AKAP79. Deletion of I3 from SAP97 ( $\Delta$ I3-SAP97) did not affect the binding of SAP97 to the  $\beta$ 1-AR. However,  $\Delta$ I3-SAP97 could not rescue the recycling of the  $\beta$ 1-AR because it failed to incorporate AKAP79/PKA into the SAP97- $\beta$ 1-AR complex. Therefore, bipartite binding of SAP97 to the  $\beta$ 1-AR and to AKAP79 is necessary for SAP97-mediated effects on recycling, externalization and functional resensitization of the  $\beta$ 1-AR. These data establish a prominent role for PDZ2 and I3 domains of SAP97 in organizing the  $\beta$ 1-adrenergic receptosome involved in connecting the  $\beta$ 1-AR to trafficking and signaling networks.

**Keywords:** SAP97; Trafficking; Beta-1-adrenergic receptor; PDZ2; Domains.

#### 1396. Potential Therapeutic Effect of Nanobased Formulation of Rivastigmine on Rat Model of Alzheimer's Disease

Manal Fouad Ismail, Aliaa Nabil El-Meshad and Neveen Abdel-Hameed Salem

*International Journal of Nanomedicine*, 8: 393-406 (2013)  
IF: 3.463

**Background:** To sustain the effect of rivastigmine, a hydrophilic cholinesterase inhibitor, nanobased formulations were prepared. The efficacy of the prepared rivastigmine liposomes (RLs) in comparison to rivastigmine solution (RS) was assessed in an aluminium chloride (AlCl<sub>3</sub>)-induced Alzheimer's model.



**Methods:** Liposomes were prepared by lipid hydration (F1) and heating (F2) methods. Rats were treated with either RS or RLs (1 mg/kg/day) concomitantly with AlCl<sub>3</sub> (50 mg/kg/day).

**Results:** The study showed that the F1 method produced smaller liposomes (67.51 ± 14.2 nm) than F2 (528.7 ± 15.5 nm), but both entrapped the same amount of the drug (92.1% ± 1.4%). After 6 hours, 74.2% ± 1.5% and 60.8% ± 2.3% of rivastigmine were released from F1 and F2, respectively. Both RLs and RS improved the deterioration of spatial memory induced by AlCl<sub>3</sub>, with RLs having a superior effect. Further biochemical measurements proved that RS and RLs were able to lower plasma C-reactive protein, homocysteine and asymmetric dimethylarginine levels. RS significantly attenuated acetylcholinesterase (AChE) activity, whereas Na<sup>+</sup>/K<sup>+</sup>-adenosine triphosphatase (ATPase) activity was enhanced compared to the AlCl<sub>3</sub>-treated animals; however, RLs succeeded in normalization of AChE and Na<sup>+</sup>/K<sup>+</sup> ATPase activities. Gene-expression profile showed that cotreatment with RS to AlCl<sub>3</sub>-treated rats succeeded in exerting significant decreases in *BACE1*, *AChE*, and *IL1B* gene expression. Normalization of the expression of the aforementioned genes was achieved by coadministration of RLs to AlCl<sub>3</sub>-treated rats. The profound therapeutic effect of RLs over RS was evidenced by nearly preventing amyloid plaque formation, as shown in the histopathological examination of rat brain.

**Conclusion:** RLs could be a potential drug-delivery system for ameliorating Alzheimer's disease.

**Keywords:** Rivastigmine; Alzheimer's disease; Liposomes; Rats; Gene expression.

### 1397. Effect of Protein Malnutrition on the Metabolism and Toxicity of Cisplatin, 5-Fluorouracil and Mitomycin C in Rat Stomach

Tarek K. Motawi, Hanan M. Abd-Elgawad and Nancy N. Shahin

*Food and Chemical Toxicology*, 56: 467-482 (2013) IF: 3.01

This study investigated the effect of protein malnutrition on metabolism and toxicity of cisplatin (CP), 5-fluorouracil (FU) and mitomycin C (MMC) in rat stomach. Weanling male Wistar rats received a normal (24%) or low (2.5%) protein diet for 28 days and were allocated into: normally-fed control, protein-malnourished control (PM), 3 normally-fed drug-treated groups and 3 protein-malnourished drug-treated groups (PM-CP, PM-FU and PM-MMC). Cisplatin and MMC were injected intraperitoneally (8 mg/kg on day 26 and 1 mg/kg/day for 7 days, respectively). 5-Fluorouracil was given orally (50 mg/kg/day for 5 days). Compared with normally-fed counterparts, PM-CP rats exhibited higher glutathione S-transferase, aminopeptidase N and cysteine S-conjugate beta-lyase (CCBL) and lower gamma-glutamyltransferase activities, PM-FU rats exhibited decreased dihydropyrimidine dehydrogenase and cytochrome P450 1A1/2 activities and PM-MMC rats showed higher quinone reductase and depleted xanthine oxidase activities. Protein-malnourished drug-treated groups exhibited exacerbated gastrotoxicity, relative to normally-fed counterparts, manifested by lower mucus levels, higher permeability and histopathological deterioration, along with increased oxidative stress in PM-CP rats and exaggerated prostaglandin E<sub>2</sub> production in PM-MMC rats. Conclusively, protein malnutrition alters CP, FU and MMC metabolism in rat stomach by enhancing CCBL pathway for CP activation, delaying

FU elimination and activating two-electron reduction of MMC, potentiating their gastrotoxicity.

**Keywords:** Protein malnutrition; Cisplatin; 5-Fluorouracil; Mitomycin C; Stomach metabolizing enzymes; Gastric toxicity.

### 1398. Effect of Glycemic Control on Soluble RAGE and Oxidative Stress in Type 2 Diabetic Patients

Tarek Mohamed Kamal Motawi, Mohamed A. Abou-Seif, Ahmed M. A. Bader and Mohamed O. Mahmoud

*BMC Endocrine Disorders*, 13: 1-8 (2013) IF: 2.65

**Background:** The interaction of advanced glycation end products (AGEs) and its receptor (RAGE) has played an important role in the pathogenesis of diabetes and its complications. A soluble form of RAGE (sRAGE) has been reported as a decoy receptor for AGEs. Oxidative stress is demonstrated in pathological condition such as atherosclerosis and diabetes mellitus. It has been suggested to be involved in the pathogenesis of both macro- and microvascular complications. This study was designed to evaluate the effect of glycemic control on sRAGE and oxidative stress markers in type 2 diabetic patients.

**Methods:** Seventy patients with type 2 diabetes and 20 healthy subjects were recruited into the study. Blood glutathione (GSH) and plasma total nitric oxide (NO<sub>x</sub>) levels were measured using commercially available colorimetric kits, blood superoxide dismutase (SOD) activity was measured by the method of Marklund and Marklund, and plasma C-peptide, oxidized LDL (ox-LDL), sRAGE, and VCAM-1 levels were measured using competitive ELISA kits.

**Results:** Plasma sRAGE levels were significantly lower ( $p < 0.05$ ) while VCAM-1 levels were significantly higher ( $p < 0.05$ ) in poorly controlled diabetic patients compared with healthy control. Blood GSH levels were significantly lower in diabetic patients compared with healthy control ( $p < 0.05$ ). Plasma C-peptide, NO<sub>x</sub>, ox-LDL levels, and SOD activity were not significantly different in diabetic patients compared with healthy control. Plasma levels of sRAGE were negatively associated with circulating VCAM-1 levels in diabetic patients.

**Conclusion:** Poor glycemic control decreases plasma sRAGE and increases VCAM-1 levels while good glycemic control improves these abnormalities which provides benefit to diabetic patients.

**Keywords:** sRAGE, Oxidative stress; HbA<sub>1c</sub>, Type 2 DM.

### 1399. Genetic Variants in Vitamin D Pathway in Egyptian Asthmatic Children: A Pilot Study

Manal Fouad Ismail, Hala G. Elnady and Eman M. Fouda

*Human Immunology*, 74: 1659-1664 (2013) IF: 2.298

**Objectives:** Asthma is a genetically heterogeneous disease. Genetic variants in vitamin D pathway have been reported to be involved with asthma risk. The study aimed to test whether vitamin D binding protein (VDBP or GC-group component) and vitamin D receptor (VDR) gene polymorphisms were associated with asthma characteristics as well as vitamin D level in Egyptian children.

**Design and methods:** The study included 51 asthmatic children and 33 healthy controls of matched sex and age. All participants were genotyped for two SNPs; GC (rs2282679) and VDR (rs2228570) using Taq-Man allele discrimination assays.

**Results:** Genotype distribution of GC and VDR showed a significant association with asthma ( $P = 0.02, P = 0.002$ ). Children carrying the risk “G” allele for GC SNP are 2.22 times more prone to develop asthma [OR = 2.22, 95% CI (1.18–4.2)] whereas those carrying the risk “F” allele for VDR SNP are nearly twice and half times susceptible for asthma development [OR = 2.68, 95% CI (1.36–5.28)] than healthy individuals. For the GC SNP, homozygous children “GG” exhibited significant difference in pulmonary functions (FEV1, FEV1/FVC), asthma severity and asthma control, IgE and vitamin D levels compared to pooled cases of GT and TT genotypes. For the VDR SNP, no significant association between VDR variants and the tested characteristics except for the pulmonary functions where the FEV1/FVC in asthmatic children with “FF” genotype differ significantly from those carrying “FF” genotype.

**Conclusion:** GC and VDR variants may be implicated in asthma susceptibility; hence, further larger studies are still needed to extrapolate our findings to the general population.

**Keywords:** VDR; VDBP; Asthma; Gene polymorphism.

#### 1400. Modulatory Effect of Lycopene on Deltamethrin-Induced Testicular Injury in Rats

Manal Fouad Ismail and Hanaa M. Mohamed

*Cell Biochemistry and Biophysics*, 65: 425-432 (2013) IF: 1.912

**Aim:** of the current study was to investigate the ability of deltamethrin to induce testicular injury in rats and its possible attenuation with lycopene. Rats were divided into three groups: *Group I* (DEL) received deltamethrin, 5 mg/kg b.w./day orally, in corn oil. *Group II* (DEL + Lyc) received oral dose of lycopene (4 mg/kg b.w./day) in corn oil concurrently with deltamethrin following the same regimen as in group I. *Group III* (Control) received appropriate volume of corn oil. After 4 weeks, deltamethrin-treated rats showed decreased body weight, serum testosterone, luteinizing hormone and follicle-stimulating hormone levels. Testicular total oxidant capacity (TOC), nitrite/nitrate (NOx), poly (ADP-ribose) polymerase (PARP), and DNA damage were significantly increased. RT-PCR demonstrated significant up-regulation in testicular mRNA for glutathione-S-transferase and heat-shock protein-70 (HSP-70), whereas steroidogenic acute regulatory (StAR) protein was down-regulated after deltamethrin exposure. Lycopene was able to restore body weight, serum testosterone, StAR mRNA, TOC, NOx levels, and PARP activity with significant decrease in HSP-70 mRNA, and DNA damage. In conclusion, lycopene was able to counteract the deleterious effect of deltamethrin.

**Keywords:** Deltamethrin; Lycopene; Apoptosis; Testosterone; Gene expression.

#### 1401. Antioxidant and Antiapoptotic Effects of Proanthocyanidin and Ginkgo Biloba Extract Against Doxorubicin-Induced Cardiac Injury in Rats

Noha Ahmed M. El Boghdady

*Cell Biochemistry and Function*, 31: 344-351 (2013) IF: 1.854

Grape seed proanthocyanidins (GSPE) and ginkgo biloba extract (EGb761) are considered to have protective effects against several diseases. The cardiotoxicity of doxorubicin (DOX) has been reported to be associated with oxidative damage. This study was

conducted to evaluate the cardioprotective effects of GSPE and EGb761 against DOX-induced heart injury in rats. DOX was administered as a single i.p. dose (20 mg/kg<sup>-1</sup>) to adult male rats. DOX-intoxicated rats were orally administered GSPE (200 mg/kg<sup>-1</sup> day<sup>-1</sup>) or EGb761 (100 mg/kg<sup>-1</sup> day<sup>-1</sup>) for 15 consecutive days, starting 10 days prior to DOX injection. DOX-induced cardiotoxicity was evidenced by a significant increase in serum aspartate transaminase (AST), creatine phosphokinase isoenzyme (CK-MB), lactate dehydrogenase (LDH), total cholesterol (TC) and triglyceride (TG) activities and levels. Increased oxidative damage was expressed by the depletion of cardiac reduced glutathione (GSH), elevation of cardiac total antioxidant (TAO) level and accumulation of the lipid peroxidation product, malondialdehyde (MDA).

Significant rises in cardiac tumour necrosis factor- $\alpha$  (TNF- $\alpha$ ) and caspase-3 levels were noticed in DOX-intoxicated rats. These changes were ameliorated in the GSPE and EGb761-treated groups. Histopathological analysis confirmed the cardioprotective effects of GSPE and EGb761. In conclusion, GSPE and EGb761 mediate their protective effect against DOX-induced cardiac injury through antioxidant, anti-inflammatory and antiapoptotic mechanisms.

**Keywords:** Caspase-3; Doxorubicin; Ginkgo biloba extract; Grape seed proanthocyanidins; Heart injury; Oxidative stress; Tumour necrosis factor- $\alpha$ .

#### 1402. Chemopreventive Efficacy of Green Tea Drinking Against 1,2-Dimethyl Hydrazine-Induced Rat Colon Carcinogenesis

Nermin Abd Elhamid Sadik

*Cell Biochemistry and Function*, 31(3): 196-207 (2013) IF: 1.854

Colorectal cancer is one of the leading causes of tumour-related deaths. In the present study, the chemopreventive effect of green tea on 1,2-dimethylhydrazine (DMH)-induced colon carcinogenesis was studied in male Wistar rats. The DMH group received subcutaneous injections of DMH (30 mg kg<sup>-1</sup> body weight) once a week for 30 weeks, the normal group received the vehicle of DMH, and the DMH + green tea group received DMH simultaneously with 1% green tea as their sole source of drinking fluid throughout the experimental period.

In the DMH group treated with green tea, significant reductions in gene overexpressions of colonic nuclear factor  $\kappa$ B (NF- $\kappa$ B), tumour necrosis factor  $\alpha$ , inducible nitric oxide synthase and cyclooxygenase 2, and NF- $\kappa$ B immunostaining indicates the anti-inflammatory effect of green tea in attenuating colon cancer. Moreover, the anti-angiogenic and anti-invasiveness effects of green tea were revealed as reductions of both vascular endothelial growth factor and matrix metalloproteinase-7 mRNA expression levels.

These effects were confirmed by the significant reduction of serum tumour necrosis factor  $\alpha$ , C-reactive protein levels, inhibition of tumour incidence, and nearly normal survival rate and colonic architecture. It can be concluded that green tea exerts a potent chemopreventive effect on colon carcinogenesis possibly due to the inhibition of NF- $\kappa$ B.

**Keywords:** Colon cancer; Green tea; NF- $\kappa$ B; TNF- $\alpha$ ; COX-2; VEGF-C.

### 1403. Modulation of Age-Related Changes in Oxidative Stress Markers and Energy Status in the Rat Heart and Hippocampus: A Significant Role for Ozone Therapy

Hebatallah Abd El-Moeti Mohamed Darwish, Maha M. El-Sawalhi, Mohamed N. Mausouf and Amira A. Shaheen

*Cell Biochemistry and Function*, 31: 518-525 (2013) IF: 1.854

Oxidative stress emerges as a key player in the ageing process. Controlled ozone administration is known to promote an oxidative preconditioning or adaptation to oxidative stress. The present study investigated whether prophylactic ozone administration could interfere with the age-related changes in the heart and the hippocampus of rats. Four groups of rats, aged about 3months old, were used. Group 1 (Prophylactic ozone group) received ozone/oxygen mixture by rectal insufflations (0.6mg/kg) twice/week for the first 3months, then once/week till the age of 15months. Group 2 (Oxygen group) received oxygen as vehicle for ozone in a manner similar to group 1. Group 3 (Aged control group) was kept without any treatment until the age of 15months. A fourth group of rats (Adult control group) was evaluated at 3months of age to provide baseline data. Ozone alleviated age-associated redox state imbalance as evidenced by reduction of lipid and protein oxidation markers, lessening of lipofuscin deposition, restoration of glutathione levels in both tissues and normalization of glutathione peroxidase activity in the heart tissue. Ozone also mitigated age-associated energy failure in the heart and the hippocampus, improved cardiac cytosolic  $\text{Ca}^{2+}$  homeostasis and restored the attenuated  $\text{Na}^+$ ,  $\text{K}^+$ -ATPase activity in the hippocampus of aged rats. These data provide new evidence concerning the anti-ageing potential of prophylactic ozone administration.

**Keywords:** Ozone; Ageing; Oxidative stress; Energy status; Heart; Hippocampus.

### 1404. Angiotensin-Converting Enzyme Inhibition and Angiotensin AT1 Receptor Blockade Downregulate Angiotensin-Converting Enzyme Expression and Attenuate Renal Injury in Streptozotocin-Induced Diabetic Rats

Tarek K. Motawi, Shohda A. El-Maraghy and Mahmoud A. Senousy

*Journal of Biochemical And Molecular Toxicology*, 27 (7): 378-387 (2013) IF: 1.596

Angiotensin-converting enzyme (ACE) is upregulated in the diabetic kidney and contributes to renal injury. This study investigates the possible beneficial effects of the ACE inhibitor (ACEI), enalapril and the AT1 receptor blocker (ARB), valsartan, on renal ACE expression, renal structure, and function in streptozotocin (STZ)-induced diabetic rats. Male Wistar rats were allocated into four groups: control, STZ-diabetic rats, and STZ-diabetic rats treated with either enalapril (10 mg/kg/day) or valsartan (50 mg/kg/day) for 8 weeks. Enalapril and valsartan reduced renal ACE mRNA and protein expression,  $\text{Na}^+$ / $\text{K}^+$ -ATPase activity, oxidative stress, and serum transforming growth factor- $\beta$ 1 levels compared to the diabetic group. Both treatments normalized renal nitrate/nitrite levels and ameliorated the observed histopathological changes. In conclusion, ACE

downregulation by ACEI and ARB indicates that angiotensin II upregulates ACE through AT1 receptor. Prevention of diabetes-induced changes in ACE expression and  $\text{Na}^+$ / $\text{K}^+$ -ATPase activity could be a new explanation of the renoprotective effects of ACEIs and ARBs.

**Keywords:** ACE Expression; aCE Inhibitor; AT1 Receptor Blocker;  $\text{Na}^+$ / $\text{K}^+$  ATPase; Diabetic nephropathy; Oxidative stress.

### 1405. Naproxen and Cromolyn as New Glycogen Synthase Kinase $\beta$ Inhibitors for Amelioration of Diabetes and Obesity: an Investigation by Docking Simulation and Subsequent in Vitro/in Vivo Biochemical Evaluation

Tarek M. K. Motawi, Yasser Bustanji, Shohda A. EL-Maraghy, Mutasem O. Taha and Mohamed A. S. Al Ghusseini

*Journal of Biochemical and Molecular Toxicology*, 27: 425-436 (2013) IF: 1.596

Naproxen and cromolyn were investigated as new inhibitors of glycogen synthase kinase- $\beta$  (GSK- $\beta$ ) in an attempt to explain their hypoglycemic properties. Study included simulated docking experiments, in vitro enzyme inhibition assay, and in vivo validations. Both drugs not only were optimally fitted within a GSK- $\beta$  binding pocket via several attractive interactions with key amino acids but also exhibited potent in vitro enzymatic inhibitory activities of IC<sub>50</sub> 1.5 and 2.0  $\mu\text{M}$  for naproxen and cromolyn, respectively. In vivo experiments illustrated that both drugs significantly reduced serum glucose and increased hepatic glycogen- and serum insulin levels in normal and type II diabetic Balb/c mice models. In obese animal model, both drugs exhibited significant reduction in mice weights, serum glucose, and resistin levels along with significant elevation in serum insulin, C-peptide, and adiponectin values. It can be concluded that naproxen and cromolyn are novel GSK- $\beta$  inhibitors and can help in management of diabetes and obesity.

**Keywords:** Cromolyn; Docking simulation; Glycogen; Glycogen synthase kinase- $\beta$ ; Naproxen; Resistin.

### 1406. Increased Cardiac Endothelin 1 and Nitric Oxide in Adriamycin Induced Acute Cardiotoxicity: Protective Effect of *Ginkgo Biloba* Extract

Noha Ahmed M. El Boghdady

*Indian Journal of Biochemistry and Biophysics*, 50: 202-209 (2013) IF: 1.026

Cardiotoxicity and congestive heart failure are the major factors that limit the use of anti-neoplastic drug adriamycin (ADR). There is increasing experimental evidence that endothelin-1 (ET-1) and nitric oxide (NO) are vasoactive mediators that regulate cardiac performance. The present study was undertaken to investigate the role of ET-1 and NO in ADR-induced acute cardiotoxicity and to evaluate the protective effect of *Ginkgo biloba* extract (EGb761) in rats. A single dose of ADR (20 mg/kg i.p.) caused a significant increase in the cardiac enzyme activities of aspartate transaminases (AST), lactate dehydrogenase (LDH) and creatine phosphokinase isoenzyme (CK-MB) in the serum of animals. This was accompanied by significant increase in cardiac malondialdehyde (MDA), total antioxidant capacity (TAC), tumor necrosis factor- $\alpha$  (TNF- $\alpha$ ), ET-1 and nitrite/nitrate (NOx)

levels. On the other hand, reduced glutathione (GSH) was significantly depressed. Histopathological examination of heart tissues showed hyalinization of the myocardium, with interstitial edema and inflammatory exudates. Pre-treatment of the animals with EGb761 (100 mg/kg, orally) 10 days before and 5 days after ADR treatment reversed the cardiac enzyme levels to normal value, decreased cardiac MDA, TAC, TNF- $\alpha$ , ET-1 and NO(x), increased GSH and reversed the histopathological damage induced by ADR. In conclusion, the cardioprotective effects of EGb761 on markers of ADR-induced acute cardiotoxicity appeared to have been mediated by the regulation of inflammatory and vasoactive mediators, as well as the inhibition of membrane lipid peroxidation. Thus, EGb761 may find use as promising adjuvant therapy to ameliorate cardiotoxicity of ADR.

**Keywords:** Adriamycin; Endothelin-1; Ginkgo biloba extract; Cardiotoxicity; Nitric oxide; Tumor necrosis factor- $\alpha$ .

#### 1407. Mutational Analysis of the PTPN11 Gene in Egyptian Patients with Noonan Syndrome

Mona L. Essawi, Manal F. Ismail, Hanan H. Afifi, Maha M. Kobesiy, Ahmed El Kotoury and Maged M. Barakat

*Journal of the Formosan Medical Association*, 112: 707-712 (2013) IF: 1

**Background/ Purpose:** Noonan syndrome (NS) is inherited as an autosomal dominant disorder with dysmorphic facies, short stature, and cardiac defects, which can be caused by missense mutations in the protein tyrosine phosphatase nonreceptor type 11 (PTPN11) gene, which encodes src homology region 2 domain containing tyrosine phosphatase-2 (SHP-2), a protein tyrosine phosphatase that acts in signal transduction downstream to growth factors and cytokines. The current study aimed to study the molecular characterization of the PTPN11 gene among Egyptian patients with Noonan syndrome.

**Methods:** Eleven exons of the PTPN11 gene were amplified and screened by single stranded conformational polymorphism (SSCP). DNA samples showing band shift in SSCP were subjected to sequencing.

**Results:** Mutational analysis of the PTPN11 gene revealed T/C transition at position 854 in exon 8, predicting Phe285Ser substitution within PTP domain of SHP-2 protein, in one NS patient and e21C/T polymorphism in intron 7 in four other cases.

**Conclusion:** Knowing that NS is phenotypically heterogeneous, molecular characterization of the PTPN11 gene should serve to establish NS diagnosis in patients with atypical features, although lack of a mutation does not exclude the possibility of NS.

**Keywords:** Egyptian patients; Noonan syndrome; PTPN11; SHP-2, Mutational analysis.

#### 1408. Possible Involvement of Oxidative Stress in Diethylnitrosamine-Induced Hepatocarcinogenesis: Chemopreventive Effect of Curcumin

Hebatallah A. Darwish and Noha A. El-Boghdady

*Journal of Food Biochemistry*, 37: 553-561 (2013) IF: 0.756

This study investigated the effect of curcumin against diethylnitrosamine (DEN)-induced hepatocarcinogenesis. Rats were divided into three groups. The first group served as a

control. The second group received DEN (orally, 20 mg/kg) five times a week for 8 weeks, followed by 10 mg/kg for another 7 weeks.

The third group was supplemented with 2% curcumin diet simultaneously with DEN. The results showed normalization of serum level of total antioxidant capacity,  $\gamma$ -glutamyl transferase and aminotransferase activities along with deoxyribonucleic acid, ribonucleic acid and malondialdehyde levels, glutathione reductase and glutathione peroxidase activities in the liver of curcumin group.

Significant decreases in the elevated level of glutathione, glutathione-S-transferase and glucose-6-P dehydrogenase activities were observed. Serum alkaline phosphatase activity and the relative liver weight were not significantly altered. Concomitantly, the histopathological damage was attenuated by curcumin.

In conclusion, curcumin exerted a potential chemopreventive effect in DEN-induced hepatocarcinogenesis.

**Practical Applications:** Various therapeutic effects, such as anti-inflammatory, anti-cancer, anti-angiogenic and wound-healing effects, have been described for curcumin. The present study is an endeavor in the direction of determining its possible mechanism of protection in diethylnitrosamine-induced hepatocarcinogenesis in rats. Our study proved that curcumin exhibits a hepatoprotective potential, and hence, it can be used as value-added agents to limit both exposure to and the adverse health effects from dietary hepatocarcinogens.

**Keywords:** Curcumin; Diethylnitrosamine; Hepatocarcinogenesis; Oxidative Stress; Rat.

#### 1409. Insulin Resistance in Type II Diabetes Mellitus with Liver Cirrhosis

Amal A. Abd El-Fattah, Mohamed I. Hamed, Serag Eldin A. Sadek and Ahmed S. Abu-Elhana

*Global Journal of Pharmacology*, 7 (2): 109-117 (2013)

Diabetes Mellitus (DM) is a progressive disease characterized by elevation of fasting and post-prandial blood glucose level that may occur due to insulin deficiency, insulin resistance or both. In spite of high prevalence of DM in patients with liver cirrhosis few studies have focused on this association.

We investigated the glycemic profile of 61 candidate that were divided into three groups, diabetic group of 21 DM patients, diabetic cirrhotic group of 20 diabetic patients with cirrhosis and control group of 20 healthy volunteers that matches age and sex.

The findings of this study revealed that both fasting and post-prandial serum insulin levels of diabetic cirrhotic patients were significantly elevated than those of diabetic non cirrhotic patients ( $P < 0.01$ ). Also positive co-relation between serum Triglyceride (TG) and both serum fasting insulin and blood glucose levels were seen within the diabetic non cirrhotic group.

While there was a negative co-relation between serum Low Density Lipoprotein (LDL-C) and serum fasting insulin level of diabetic patients with cirrhosis. These results suggest that insulin resistance may consider as one of the clinical features in diabetic patients with cirrhosis probably related to hepatopathology.

**Keywords:** Insulin resistance; Liver cirrhosis; Diabetes mellitus.

**Dept. of Clinical Pharmacy**

**1410. Factors Affecting the Motivation of Healthcare Professionals Providing Care to Emiratis with Type 2 Diabetes**

Dalia Dawood, Layla Alhyas, Jessica D Jones Nielsen and Azeem Majeed

*Journal of the Royal Society of Medicine*, 4: 1-14 (2013)  
IF: 1.717

**Objective:** We aimed to identify facilitators of and barriers to healthcare professionals' motivation in a diabetes centre in the United Arab Emirates (UAE).

**Design:** A qualitative research approach was employed using semistructured interviews to assess perception of and attitudes regarding healthcare professionals' motivation in providing good quality diabetes care.

**Setting:** A diabetes centre located in Abu- Dhabi, UAE.

**Participants:** Healthcare professionals including specialist physicians, dieticians, podiatrists, health educators and nurses were recruited through purposive sampling.

**Main Outcome Measures:** After data collection, the audiotaped interviews were transcribed verbatim and subjected to content analysis.

**Results:** Nine semistructured interviews were conducted with healthcare professionals of various professional backgrounds. Important facilitators and barriers related to patient, professional, organization and cultural factors were identified. Barriers that related to heavy workload, disjointed care, lack of patient compliance and awareness, and cultural beliefs and attitudes about diabetes were common. Key facilitators included the patient's role in achieving therapeutic outcomes as well as compliance, cooperation and communication.

**Conclusion:** This qualitative study provides some unique insights about factors affecting healthcare professionals' motivation in providing good quality care. To improve the motivation of healthcare professionals in the management of diabetes and therefore the quality of diabetes care, several steps are needed. Importantly, the role of primary care should be reinforced and strengthened regarding the management of type 2 diabetes mellitus, privacy of the consultation time should be highly protected and regulated, and awareness of the Emirate culture and its impact on health should be disseminated to the healthcare professionals providing care to Emiratis with diabetes. Also, greater emphasis should be placed on educating Emiratis with diabetes on, and involving them in, the management of their condition.

**Keywords:** UAE; Factors; Motivation; Type 2 diabetes.

**1411. Vitamin D Levels in Egyptian HCV Patients (Genotype 4) Treated with Pegylated Interferon**

Nirmeen Ahmed Sabry, A. A. Mohamed, M. M. Abbassi, W.A. Ibrahim and Z. A. Ali-Eldin

*Acta Gastro-Enterologica Belgica*, 76: 38-44 (2013) IF: 0.628

**Background/Aim:** Vitamin D has been shown to play an important immunomodulatory role. Deficiency of vitamin D has been recently associated to the lack of response to interferon therapy in Hepatitis C virus genotype 1 infected patients. This study aims to evaluate serum level of vitamin D and verify

whether circulating vitamin D has any independent role in predicting the rates of HCV virologic response after the administration of pegylated interferon to Egyptian patients infected with genotype 4 HCV.

**Methods:** Fifty patients infected with HCV genotype 4 and not co-infected with neither Hepatitis B virus nor Human Immunodeficiency Virus were recruited for the study. They were treated with ribavirin-pegylated interferon alpha 2a. Viral titer was determined at baseline, at 12 weeks and at end of treatment (48 weeks). Vitamin D levels and a biochemical profile were obtained for the patients at baseline and at end of treatment. Vitamin D control group consisting of 20 healthy patients of similar age and weight to the study group were recruited to obtain vitamin D levels.

**Results:** Vitamin D levels in HCV infected patients were significantly lower than in healthy subjects. Responders to ribavirin plus pegylated interferon alpha 2a therapy had significantly higher vitamin D levels than non-responders.

**Conclusion:** Vitamin D deficiency predicts an unfavorable response to interferon-based treatment of HCV.

**Keywords:** Vitamin D; HCV; Genotype 4; Egyptian patient.

**1412. A Specially Tailored Vancomycin Continuous Infusion Regimen for Renally Impaired Critically Ill Patients**

Nirmeen Ahmed Sabry, Eman Mohamed Bahgat Eldemiry, Maggie M. Abbassi, Sanaa S. Abdel Shafy, Mohamed S. Mokhtar and Ahmed Abdel Bary

*Sage Open Medicine*, 1: 1-6 (2013)

**Background:** Vancomycin remains the gold standard for treatment of methicillin-resistant *Staphylococcus aureus*. Specially designed continuous infusion of vancomycin leads to better therapy.

**Methodology:** A total of 40 critically ill patients who suffered from pneumonia susceptible to vancomycin, had serum creatinine  $>1.4$  mg%, and oliguria  $<0.5$  mL/kg/h for 6 h were included in the study with respiratory culture sensitivity to vancomycin  $\leq 2$  mg/L. Patients' clinical, microbiological, and biological data were obtained by retrospective analysis of the corresponding medical files before and after vancomycin treatment. Patients with serum creatinine level  $\geq 4$  mg% and patients who received renal replacement therapy during the treatment period were excluded. The patients were divided into two groups—group 1 (intermittent dosing) and group 2 (continuous infusion) based on the following **Formula:** rate of vancomycin continuous infusion (g/day) =  $[0.0205 \text{ creatinine clearance (mL/min)} + 3.47] \times [\text{target vancomycin concentration at steady state (}\mu\text{g/mL)}] \times (24/1000)$ . Trough vancomycin serum levels were also assessed using high-performance liquid chromatographic technique. Patients' outcomes such as clinical improvement, adverse events, and 15-day mortality were reported.

**Results:** Group 2 showed significant reduction in blood urea nitrogen, creatinine serum levels, white blood cells, partial carbon dioxide pressure, body temperature, and Sequential Organ Failure Assessment score, while significant increase in partial oxygen pressure and saturated oxygen was also observed. A significantly shorter duration of treatment with a comparable vancomycin serum levels was also reported with group 2.

**Conclusion:** After treatment, comparison in patients' criteria supports the superiority of using continuous infusion of



vancomycin according to this equation in renally impaired patients.

**Keywords:** Vancomycin; Therapeutic drug monitoring; High-performance liquid chromatographic; Continuous infusion; Critically Ill.

### 1413. Community Pharmacists' Involvement in Breast Cancer Health Promotion in United Arab Emirates (UAE)

Osama Hussein Kamel and Rana M. Ibrahim

*American J. of Pharmacology; Toxicology*, 8: 155-163 (2013)

Breast cancer is the most common cancer in women in Middle East countries. Despite the continuous efforts to increase the public awareness of breast cancer via campaigns and public screening programs, breast cancer screening rate remains low. The participation of community pharmacists in the communication and dissemination of breast cancer screening information should have a significant positive impact. The objectives of this study were to assess the degree of community pharmacists' participation in breast cancer health promotion activities in United Arab Emirates (UAE), to evaluate their attitudes towards the involvement in breast cancer health promotion and receiving breast cancer continuous education. The study objectives were addressed in a cross-sectional survey distributed to community pharmacists in Sharjah, Dubai and Ajman Emirates (UAE). The survey measured the extent of community pharmacists' participation in breast cancer health promotion activities, their interest and comfort in providing breast cancer health promotion, and their perceived barriers for integrating breast cancer health promotion activities into their daily practice. Over a 24-week period, we collected 275 surveys out of 335 pharmacists approached (82% response rate). Ninety-six percent indicated that they never invited healthcare professionals to provide breast cancer education in the pharmacy, 67% said that they never distributed breast cancer educational materials and 47% reported that they never counseled patients about breast cancer. Nevertheless, more than 75% were highly interested in being engaged in breast cancer health promotion activities. In addition, 87% believed that discussing breast cancer awareness with female patients in the pharmacy was beneficial to patients. Yet pharmacists perceived many barriers for integrating breast cancer health promotion into their daily practice including lack of educational materials (87%) and lack of enough time (74%). Moreover, their breast cancer knowledge mean score was 51% with 87% expressing a high interest in receiving breast cancer continuous education. Despite their low participation in breast cancer health promotion, the mainstream of pharmacists was interested in educating patients about breast cancer. However, low breast cancer knowledge and other barriers can prevent actualizing this role.

**Keywords:** Community pharmacists; Breast cancer; Health promotion; United arab emirates.

### 1414. Comparison on Efficacy and Safety of Three Inpatient Insulin Regimens for Management of Non-Critical Patients with Type 2 Diabetes

Eman Said, Samar Farid, Nirmeen Sabry and May Fawzi

*Pharmacology and Pharmacy*, 4: 556-565 (2013)

**Background:** Hyperglycemia in hospitalized patients is associated with poor clinical outcomes. Scheduled Subcutaneous Insulin therapy has been recommended for better glycemic control.

**Aims:** To compare efficacy and safety of traditional sliding scale insulin (SSI) versus modified 70/30 insulin versus basal plus supplemental scale (SS) insulin regimens for glycemic control of inpatients with diabetes.

**Methods:** In a prospective trial, 62 patients with diabetes were randomized to receive either hospital SSI (N = 22), or twice daily 70/30 insulin plus supplemental lunchtime insulin for BG = 150 mg/dL (N = 21) or once every night glargine plus prandial glulisine for BG = 150 mg/dL (N = 19). 70/30 insulin and glargine were started respectively at 0.4 and 0.2 U/kg/day for BG = 200 mg/dL or 0.5 and 0.3 U/kg/day for BG above 200 mg/dL.

**Results:** Starting at BG level of  $204 \pm 68$ ,  $200 \pm 50$  and  $241 \pm 94$  mg/dL in SSI, 70/30 insulin and glargine/glulisine groups respectively, ( $F(2,35.47) = 1.467$ ,  $p = 0.244$ , Welch test), mean daily BG after first day of hospitalization was statistically significant ( $F(2,35.58) = 7.043$ ,  $p = 0.003$ , Welch test) lower in 70/30 insulin group ( $171 \pm 38$  mg/dL) compared to ( $218 \pm 71$  mg/dL) in SSI group ( $p = 0.026$ ) and ( $225 \pm 65$  mg/dL) in glargine/glulisine group ( $p = 0.01$ ). Conclusions: With poorly educated nursing staff, basal plus SS insulin failed to provide adequate glycemic control. However, tailored 70/30 insulin regimen resulted in statistically significant glycemic control compared to traditional SSI.

**Keywords:** Type 2 DM; Sliding scale insulin; 70/30 Insulin; Basal insulin; Supplemental insulin.

### Dept. of Microbiology and Immunology

### 1415. Genome-Scale Metabolic Reconstructions of Multiple Escherichia Coli Strains Highlight Strain-Specific Adaptations to Nutritional Environments

Jonathan M. Monk, Pep Charusanti, Ramy K. Aziz, Joshua A. Lerman, Ned Premyodhin, Jeffrey D. Orth, Adam M. Feist and Bernhard Ø. Palsson

*Proceedings of the National Academy of Sciences*, 110: 20338-20343 (2013) IF: 9.7

Genome-scale models (GEMs) of metabolism were constructed for 55 fully sequenced Escherichia coli and Shigella strains. The GEMs enable a systems approach to characterizing the pan and core metabolic capabilities of the E. coli species. The majority of pan metabolic content was found to consist of alternate catabolic pathways for unique nutrient sources. The GEMs were then used to systematically analyze growth capabilities in more than 650 different growth-supporting environments. The results show that unique strain-specific metabolic capabilities correspond to pathotypes and environmental niches. Twelve of the GEMs were used to predict growth on six differentiating nutrients, and the predictions were found to agree with 80% of experimental outcomes. Additionally, GEMs were used to predict strain-specific auxotrophies. Twelve of the strains modeled were predicted to be auxotrophic for vitamins niacin (vitamin B<sub>3</sub>), thiamin (vitamin B<sub>1</sub>), or folate (vitamin B<sub>9</sub>). Six of the strains modeled have lost biosynthetic pathways for essential amino acids methionine, tryptophan, or leucine. Genome-scale analysis of multiple strains of a species can thus be used to define the metabolic essence of a microbial species and delineate growth

differences that shed light on the adaptation process to a particular microenvironment.

**Keywords:** Microbiology; Systems biology; Metabolic reconstruction; *Escherichia coli*; Mathematical modeling; Computational biology.

#### 1416. Microevolution of Highly Pathogenic Avian Influenza A(H5N1) Viruses Isolated from Humans, Egypt, 2007–2011

Mary Younan, Mee Kian Poh, Emad Ellassal, Todd Davis, Pierre Rivailler, Amanda L. Balish, Natosha Simpson, Joyce Jones, Varough Deyde, Rosette Loughlin, Ije Perry, Larisa Gubareva, Maha A. ElBadry, Shaun Truelove, Anne M. Gaynor, Emad Mohareb, Magdy Amin, Claire Cornelius, Guillermo Pimentel, Kenneth Earhart, Amel Naguib, Ahmed S. Abdelghani, Samir Refaey, Alexander I. Klimov, Ruben O. Donis and Amr Kandeel

*Emerging Infectious Diseases*, 19 (1): 43-50 (2013) IF: 5.9

We analyzed highly pathogenic avian influenza A(H5N1) viruses isolated from humans infected in Egypt during 2007-2011. All analyzed viruses evolved from the lineage of subtype H5N1 viruses introduced into Egypt in 2006; we found minimal evidence of reassortment and no exotic introductions. The hemagglutinin genes of the viruses from 2011 formed a monophyletic group within clade 2.2.1 that also included human viruses from 2009 and 2010 and contemporary viruses from poultry; this finding is consistent with zoonotic transmission. Although molecular markers suggestive of decreased susceptibility to antiviral drugs were detected sporadically in the neuraminidase and matrix 2 proteins, functional neuraminidase inhibition assays did not identify resistant viruses. No other mutations suggesting a change in the threat to public health were detected in the viral proteomes. However, a comparison of representative subtype H5N1 viruses from 2011 with older subtype H5N1 viruses from Egypt revealed substantial antigenic drift.

**Keywords:** Influenza; H5N1; Egypt.

#### 1417. Adjunctive Corticosteroid Therapy Improves Lung Immunopathology and Survival During Severe Secondary Pneumococcal Pneumonia in Mice

Hazem Elsayed Ghoneim and Jonathan A. McCullers

*Journal of Infectious Diseases Advance Access*, 23: (2013) IF: 5.848

Secondary bacterial pneumonia is a significant cause of morbidity and mortality during influenza, despite routine use of standard antibiotics. Antibiotic-induced immunopathology associated with bacterial cell wall lysis has been suggested to contribute to these poor outcomes. Using *Streptococcus pneumoniae* in a well-established murine model of secondary bacterial pneumonia (SBP) following influenza, we stratified disease severity based on pneumococcal load in the lungs via *in vivo* bioluminescence imaging. Ampicillin treatment cured mice with mild pneumonia but was ineffective against severely pneumonic mice, despite effective bacterial killing. Adjunctive dexamethasone therapy improved ampicillin-induced immunopathology and improved outcomes in mice with severe SBP. However, early dexamethasone therapy during primary influenza infection

impaired lung adaptive immunity as manifest by increased viral titers, with an associated loss of its protective functions in SBP. These data support adjunctive clinical use of corticosteroids in severe cases of community-acquired pneumonia.

**Keywords:** Antibiotics; Corticosteroids; Dexamethasone; Immunomodulation; Influenza; Pneumonia; *Streptococcus pneumoniae*.

#### 1418. Depletion of Alveolar Macrophages During Influenza Infection Facilitates Bacterial Superinfections

Hazem E. Ghoneim, Paul G. Thomas and Jonathan A. McCullers

*Journal of Immunology*, 191: 1250-1259 (2013) IF: 5.52

Viruses such as influenza suppress host immune function by a variety of methods. This may result in significant morbidity through several pathways, including facilitation of secondary bacterial pneumonia from pathogens such as *Streptococcus pneumoniae*. PKH26-phagocytic cell labeling dye was administered intranasally to label resident alveolar macrophages (AMs) in a well-established murine model before influenza infection to determine turnover kinetics during the course of infection. More than 90% of resident AMs were lost in the first week after influenza, whereas the remaining cells had a necrotic phenotype. To establish the impact of this innate immune defect, influenza-infected mice were challenged with *S. pneumoniae*. Early AM-mediated bacterial clearance was significantly impaired in influenza-infected mice: ~50% of the initial bacterial inoculum could be harvested from the alveolar airspace 3 h later. In mock-infected mice, by contrast, >95% of inocula up to 50-fold higher was efficiently cleared. Coinfection during the AM depletion phase caused significant body weight loss and mortality. Two weeks after influenza, the AM population was fully replenished with successful re-establishment of early innate host protection. Local GM-CSF treatment partially restored the impaired early bacterial clearance with efficient protection against secondary pneumococcal pneumonia. We conclude that resident AM depletion occurs during influenza infection. Among other potential effects, this establishes a niche for secondary pneumococcal infection by altering early cellular innate immunity in the lungs, resulting in pneumococcal outgrowth and lethal pneumonia. This novel mechanism will inform development of novel therapeutic approaches to restore lung innate immunity against bacterial superinfections.

**Keywords:** Influenza; Pneumococcal pneumonia; Alveolar macrophage; GM-CSF; Bacterial superinfections.

#### 1419. Eye-Mediated Induction of Specific Immune Tolerance to Encephalitogenic Antigens

Hossam M. Ashour and Shukkur M. Farooq

*Cns Neuroscience and Therapeutics*, 19 (7): 503-510 (2013) IF: 4.458

**Aims:** Administration of antigens into the anterior chamber (AC) of the eye induces a form of antigen-specific immune tolerance termed anterior chamber-associated immune deviation (ACAID). This immune tolerance effectively impairs host delayed-type hypersensitivity (DTH) responses. We hypothesized that ACAID could be generated in BALB/c mice following AC inoculation of

the encephalitogenic antigens myelin oligodendrocyte glycoprotein (MOG) and myelin basic protein (MBP).

**Methods:** We used DTH assays and local adoptive transfer (LAT) assays to test whether MOG/MBP-induced ACAID following their administration into the AC, whether they elicited this immune tolerance via CD8<sup>+</sup> T cells, and whether their AC coadministration (MOG/MBP) induced specific immune tolerance to one or both antigens.

**Results:** We showed that MOG/MBP-induced AC-mediated specific immune tolerance, as evident from impaired DTH responses. This antigen-driven DTH suppression was solely mediated via splenic CD8<sup>+</sup> T cells as confirmed by LAT assays. Finally, a single AC injection with both antigens was sufficient to induce specific immune tolerance to these antigens, as evident from DTH and LAT assays.

**Conclusion:** ACAID T-cell regulation could be used as a therapeutic tool in the treatment of complicated autoimmune diseases that involve multiple antigens such as multiple sclerosis.

**Keywords:** Acaid; Multiple sclerosis; Peripheral tolerance; T regulatory cells.

#### 1420. Avian Influenza: Virology, Diagnosis and Surveillance

Hossam M. Ashour, Mohamed E. El-Zowalaty, Stephen A. Bustin and Mohamed I. Hussein

*Future Microbiology*, 8 (9): 1209-1227 (2013) IF: 4.018

Avian influenza virus (AIV) is the causative agent of a zoonotic disease that affects populations worldwide with often devastating economic and health consequences. Most AIV subtypes cause little or no disease in waterfowl, but outbreaks in poultry can be associated with high mortality. Although transmission of AIV to humans occurs rarely and is strain dependent, the virus has the ability to mutate or reassort into a form that triggers a life-threatening infection. The constant emergence of new influenza strains makes it particularly challenging to predict the behavior, spread, virulence or potential for human-to-human transmission. Because it is difficult to anticipate which viral strain or what location will initiate the next pandemic, it is difficult to prepare for that event. However, rigorous implementation of biosecurity, vaccination and education programs can minimize the threat of AIV. Global surveillance programs help record and identify newly evolving and potentially pandemic strains harbored by the reservoir host.

**Keywords:** Avian influenza; Diagnosis; Real-time PCR; Surveillance; Vaccines; Virus isolation; Waterfowl.

#### 1421. Applying Shannon's Information Theory to Bacterial and Phage Genomes and Metagenomes

Ramy K. Aziz, Sajia Akhter, Barbara A. Bailey, Peter Salamon, Ramy K. Aziz and Robert A. Edwards

*Scientific Reports*, 3: 1-7 (2013) IF: 2.927

All sequence data contain inherent information that can be measured by Shannon's uncertainty theory. Such measurement is valuable in evaluating large data sets, such as metagenomic libraries, to prioritize their analysis and annotation, thus saving computational resources. Here, Shannon's index of complete phage and bacterial genomes was examined. The information content of a genome was found to be highly dependent on the

genome length, GC content, and sequence word size. In metagenomic sequences, the amount of information correlated with the number of matches found by comparison to sequence databases. A sequence with more information (higher uncertainty) has a higher probability of being significantly similar to other sequences in the database. Measuring uncertainty may be used for rapid screening for sequences with matches in available database, prioritizing computational resources, and indicating which sequences with no known similarities are likely to be important for more detailed analysis.

**Keywords:** Bioinformatics; Information theory; Genomics; Metagenomics; Genometrics.

#### 1422. Emergence of Carbapenem-Resistant *Acinetobacter Baumannii* Harboring the OXA-23 Carbapenemase in Intensive Care Units of Egyptian Hospitals

Ahmed Sh. Attia, Mahmoud Fouad, Wael M. Tawakkol and Abdelgawad M. Hashem

*Int. J. of Infectious Diseases*, 17: 1252-1254 (2013) IF: 2.357

**Background:** Healthcare-associated infections are a worldwide threat to hospitalized patients, especially those in intensive care units. The prevalence of these infections in Egypt, and their antimicrobial resistance patterns and mechanisms, were investigated in this study.

**Methods:** A total of 547 cases of healthcare-associated infections were investigated. Causative agents were identified and antimicrobial susceptibility determined. Carbapenem-resistant *Acinetobacter baumannii* isolates were further investigated for their resistance mechanism via the modified Hodge test, inhibitor-potentiated disk diffusion test, synergy with carbonyl cyanide chlorophenylhydrazide, and PCR. Moreover, clonal linkage was examined via enterobacterial repetitive intergenic consensus (ERIC)-PCR.

**Results:** *Klebsiella* spp was the most prevalent species in the isolates examined (217; 40%). Although *A. baumannii* represented only 10% of the total isolates, it showed the highest percentage of carbapenem resistance (74%). PCR showed that 100% of the resistant isolates carried both bla<sub>OXA-51</sub> and bla<sub>OXA-23</sub> genes, 85% carried the class 1 integrase genes, and only 2.5% carried metallo-beta-lactamase (bla<sub>VIM</sub>). ERIC-PCR indicated that isolates from different hospitals were genetically linked.

**Conclusions:** These findings represent the first report of the alarming spread of OXA-23 carbapenemase in *A. baumannii* in Egyptian intensive care units. The spread of such strains has serious health consequences and requires the application of strict infection control measures.

**Keywords:** *Acinetobacter baumannii*; Carbapenem resistance; OXA-23 carbapenemase; Egypt.

#### 1423. A Molecular Investigative Approach to an Outbreak of Acute Hemorrhagic Conjunctivitis in Egypt, October 2010

Aymen S. Yassin, Ehab A. Ayoub, Caroline F. Shafik, Anne M. Gaynor, Emad W. Mohareb, Magdy A. Amin, Samir El-Refaey, Mohamed Genedy and Amr Kandeel

*Virology Journal*, 10: (2013) IF: 2

**Background:** During October 2010, Egypt reported an outbreak of acute hemorrhagic conjunctivitis (AHC). A total of 1831 cases were reported from three governorates; 1703 cases in El Daqahliya, 92 cases in Port Said, and 36 in Damietta. The purpose of this study was to identify and characterize the causative agent associated with this outbreak.

**Methods:** The U.S. Naval Medical Research Unit No.3 (NAMRU-3) was contacted by the Egyptian Ministry of Health and Population to perform diagnostic laboratory testing on eighteen conjunctival swabs from patients with conjunctivitis from El Daqahliya Governorate. Conjunctival swabs were tested by molecular methods for human adenovirus (HAdV) and enteroviruses (EV). Virus isolation was performed; the isolated virus was further characterized by molecular typing and phylogenetic analysis.

**Results:** The majority of the samples (17/18) were positive for enterovirus and all were negative for HAdV. Molecular typing and sequencing of the isolated virus revealed the presence of coxsackievirus A24 variant. Phylogenetic analysis based on the VP1 and 3C regions demonstrated that the Egyptian viruses belonged to Genotype IV and are closely related to coxsackievirus A24 variant, reported in a similar outbreak in China in August 2010.

**Conclusions:** This study strongly suggests that coxsackievirus A24 variant was associated with the acute hemorrhagic conjunctivitis outbreak reported in Egypt in October 2010. There is a possibility that the same strain of CV-A24v was implicated in the AHC outbreaks in both China and Egypt in 2010.

**Keywords:** Egypt; Outbreak; Coxsackievirus A24 variant; Phylogenetic analysis; Acute hemorrhagic conjunctivitis.

#### 1424. Scaling Up for the Industrial Production of Rifamycin B; Optimization of the Process Conditions in Bench-Scale Fermentor

Tamer M. Essam, Hewaida F. El-Sedawy, Manal M. M. Hussein, Ossama M. El-Tayeb and Fatma H.A. Mohammad

*Bulletin of Faculty of Pharmacy, Cairo University, 51: 43-48 (2013) IF: 1.75*

Optimization of fermentation process conditions using a gene amplified variant of *Amycolatopsis mediterranei* (NCH) was carried out.

The use of aeration level 1.5 vvm increased the yield by 16.6% (from 13.81 to 16.1 g/l) upon controlling the temperature at 28 °C. Adjustment of the aeration level at 1.5 vvm for 3 days then controlling the dissolved oxygen (DO) at 30% saturation further increased the yield to 17.8 g/l.

The optimum pH was 6.5 for 3 days then 7 thereafter when a production yield of 16.1 g/l was recorded using an aeration rate of 1.5 vvm.

Controlling the pH at constant value (6.5 or 7) all through the fermentation process decreased the yield by 5–21%. Controlling the temperature at 30 °C for 3 days then 28 °C thereafter slightly increased the yield by 5% upon using an aeration rate of 1 vvm while it decreased upon using an aeration rate of 1.5 vvm. Integration of the most optimum conditions increased the production yield by 22% from 13.81 to 17.8 g/l.

**Keywords:** *Amycolatopsis mediterranei*; Antibiotics; Fermentor; Rifamycin B; Scaling up.

#### 1425. Photosynthetic Based Algal-Bacterial Combined Treatment of Mixtures of Organic Pollutants and CO<sub>2</sub> Mitigation in A Continuous Photobioreactor

Tamer M. Essam, Marwa El-Rakaiby and Abdelgawad Hashem

*World Journal of Microbiology Biotechnology, 29: 969-974 (2013) IF: 1.26*

An algal-bacterial microcosm was synthetically constructed of *Chlorella vulgaris* MM1 and *Pseudomonas* MT1. This microcosm was able to treat simulated wastewater supplemented with mixtures of phenol and pyridine up to 4.6 and 4.4 mM, respectively, in a continuous stirred tank bioreactor (CSTR) using photosynthetic oxygenation. Complete pollutant removal and detoxification and 82 % removal of introduced chemical oxygen demand (COD) were achieved at a hydraulic retention time (HRT) of 2.7 days. Increasing the influent load to 5.3 and 6.3 mM reduced the removal of phenol, pyridine and COD to 78, 21 and 59 %, respectively. Fertilization of the photobioreactor with 24 mM NaHCO<sub>3</sub> restored the treatment and detoxification efficiencies. The system was able to additionally mitigate up to 72 mM NaHCO<sub>3</sub> at the same HRT. Although the fertilization increased the system treatment efficiency, the settleability of the algal-bacterial microcosm was significantly reduced. When the photobioreactor was operated at HRT of 2.7 days in a 12/12 h of dark/light cycle, complete removal of 4.7 mM phenol was recorded but only 11 % of 5.7 mM pyridine was removed. The COD removal efficiency and CO<sub>2</sub> mitigation were also reduced to 65 and 86 %, respectively, and the effluent retained significant toxicity where 73 % inhibition was recorded. Elongation of the illumination time to 48 h (HRT of 4 days at 12/12 h dark/light cycle) restored the treatment and detoxification efficiencies.

**Keywords:** Microalgae; Organic pollutants; Phenol; Photobioreactor; Pyridine.

#### 1426. Fluoroquinolone Resistant Mechanisms in Methicillin-Resistant *Staphylococcus Aureus* Clinical Isolates in Cairo, Egypt

Aymen S. Yassin, Rasha A. Hashem, Hamdallah H. Zedan and Magdy A. Amin

*The Journal of Infection in Developing Countries, 7: 796-803 (2013) IF: 1.2*

**Introduction:** Methicillin-resistant *Staphylococcus aureus* (MRSA) is a persistent problem in community and health care settings. Fluoroquinolones are among the drugs of choice used to treat MRSA infections. This study aims to identify different mechanisms of fluoroquinolone resistance in local MRSA random sampling isolates in Cairo, Egypt.

**Methodology:** A total of 94 clinical isolates of *S. aureus* were collected from two major University hospitals in Cairo. Identification was confirmed by appropriate morphological, cultural, and biochemical tests. The antibiotic susceptibility pattern was determined for all isolates. The possible involvement of efflux pumps in mediating fluoroquinolone resistance as well as changes in the quinolone resistance determining region (QRDR) of *gyrA* and *gyrB* genes were investigated.

**Results:** A total of 45 isolates were found to be MRSA, among which 26 isolates were found to be fluoroquinolone-resistant. The

MIC values of the tested fluoroquinolones in the presence of the efflux pump inhibitors omeprazole and piperine were reduced. Measuring the uptake of ciprofloxacin upon the addition of the efflux pump inhibitor omeprazole, an increased level of accumulation was observed. Non-synonymous and silent mutations were detected in the QRDR of *gyrA* and *gyrB* genes. **Conclusions:** These results shed light on some of the resistance patterns of MRSA strains isolated from local health care settings in Cairo, Egypt. The resistance of these MRSA towards fluoroquinolones does not depend only on mutation in target genes; other mechanisms of resistance such as the permeability effect, efflux pumps and decreased availability of quinolones at the target site can also be involved.

**Keywords:** Staphylococcus aureus; MRSA; Fluoroquinolones; National cancer institute; El damardash hospital; Efflux pumps.

#### 1427. Multiplex Polymerase Chain Reaction (PCR) for the Detection of Diarrheagenic Escherichia Coli and Shigella Directly From Stool

Omneya M. Moustafa, Y. M. Ragab and M. M. M. Hussein

*African Journal of Microbiology Research*, 7 (34): 4368-4372 (2013)

*Shigella* and diarrheagenic *Escherichia coli* (DEC) are the most common causes of diarrheal diseases in developing countries. A multiplex polymerase chain reaction (mPCR) was developed for identification of DEC infections caused by shiga toxin producing *E. coli* (STEC), enteropathogenic *E. coli* (EPEC), enterotoxigenic *E. coli* (ETEC), enteroinvasive *E. coli* (EIEC) and *Shigella* in fecal samples by simultaneous and specific detection of seven virulence genes (*eaeA*, *stx1*, *stx2*, *bfpA*, *LT*, *ST* and *ipaH*). The detection limit of the method was  $10^1$  to  $10^3$  cfu/PCR assay from pure cultures. When the multiplex PCR was tested with DNA purified from artificially spiked stool samples directly from stool or after overnight pre-enrichment in buffered peptone water, the detection limit was  $10^6$  cfu and  $10^1$ -  $10^5$  cfu/ gm stool, respectively. The developed mPCR is specific, sensitive, easy, rapid and of low cost method for detecting DEC in stool.

**Keywords:** Diarrheagenic *Escherichia coli*; *Shigella*; Shiga toxin producing *E. coli* (STEC); Enteroinvasive *E. coli* (EIEC); Enteropathogenic *E. coli* (EPEC); Enterotoxigenic *E. coli* (ETEC); Multiplex PCR.

#### 1428. The in Vitro Induction of Type II Collagen-Specific Immune Tolerance in Balb/C Mice

Hossam Mohamed Ashour and S. M. Frooq

*European Journal of Inflammation*, 11 (1): 169-178 (2013)

Type II collagen (CII) protein is the main component of hyaline cartilage. The clinical importance of CII in arthritis, aging, and osteoarthritis is significant, but its ability to induce specific immune tolerance has not been extensively studied before. We have recently proven that CII is capable of inducing Anterior Chamber Associated Immune Deviation (ACAID) when injected into the eye. Here, we hypothesized that ACAID-mediated tolerance could be induced in Balb/c mice that receive an intravenous administration of CII-induced in vitro-generated ocular-like antigen-presenting cells (APCs) or T regulatory cells (Tregs). Delayed hypersensitivity (DTH) assays were used to

examine the hypothesis. In mice injected with CII-specific ACAID APCs, the specific regulatory activities resided in the spleen cells, splenic T cells, and ACAID CD8<sup>+</sup> T cells, as proven by local adoptive transfer (LAT) assays. Conversely, there was a lack of regulatory activity in the CD4<sup>+</sup> CD25<sup>+</sup> T cell compartment of the recipient mice. Thus, ACAID CD8<sup>+</sup> Tregs generated in vitro could be directly responsible for the expression of CII-driven ACAID-mediated tolerance and could be used as potential therapeutic tools in the treatment of CII-associated autoimmune diseases.

**Keywords:** Anterior chamber; Immune tolerance; T regulatory cells; Collagen type II; Arthritis; Aging.

#### Dept. of Pharmaceutical Chemistry

#### 1429. Synthesis and Antiprotozoal Activity of Dicationic *m*-Terphenyl and 1,3-Dipyridylbenzene Derivatives

Reem Khidr Mohamed Arafa, Donald A. Patrick, Mohamed A. Ismail, Tanja Wenzler, Xiaohua Zhu, Trupti Pandharkar, Susan Kilgore Jones, Karl A. Werbovetz, Reto Brun, David W. Boykin and Richard R. Tidwell

*Journal of Medicinal Chemistry*, 56: 5473-5494 (2013) IF: 5.614

4,4''-Diamidino-*m*-terphenyl (1) and 36 analogues were prepared and assayed in vitro against *Trypanosoma brucei* rhodesiense, *Trypanosoma cruzi*, *Plasmodium falciparum*, and *Leishmania amazonensis*. Twenty-three compounds were highly active against *T. b. rhodesiense* or *P. falciparum*. Most noteworthy were amidines 1, 10, and 11 with IC<sub>50</sub> of 4 nM against *T. b. rhodesiense*, and dimethyltetrahydropyrimidinyl analogues 4 and 9 with IC<sub>50</sub> values of ≤ 3 nM against *P. falciparum*. Bipyridylimidamide derivative 31 was 25 times more potent than benzimidazole against *T. cruzi* and slightly more potent than amphotericin B against *L. amazonensis*. Terphenyldiamidine 1 and dipyridylbenzene analogues 23 and 25 each cured 4/4 mice infected with *T. b. rhodesiense* STIB900 with four daily 5 mg/kg intraperitoneal doses, as well as with single doses of ≤ 10 mg/kg. Derivatives 5 and 28 (prodrugs of 1 and 25) each cured 3/4 mice with four daily 25 mg/kg oral doses.

**Keywords:** Antiprotozoal activity; Dicationic *m*-terphenyl and 1,3-Dipyridylbenzene derivatives.

#### 1430. Design, Synthesis and QSAR Studies of Spiroindole Derivatives as New Antiproliferative Agents

Riham F. George, Nasser S. M. Ismail, Jacek Stawinski and Adel S. Girgis

*European Journal of Medicinal Chemistry*, 68: 339-351 (2013) IF: 3.499

A variety of 4'-aryl-3-(arylmethylidene)-1''-[(cyclic-amino)methylene]-1'-methyl-dispiro[cyclohexane-1,3'-rrolidine-2',3''[3H] indole]-2,2''(1'H)-diones 4a-u were prepared via reaction of 2E,6E-bis(arylidene)-1-cyclohexanones 1a-i with azomethine ylides, generated in situ via a decarboxylative condensation of isatins 2a-c and sarcosine (3). Single crystal X-ray study of 4a, revealed structural and stereochemical features of these derivatives. While most of the synthesized compounds exhibit



mild antitumor properties when tested against various human tumor cell lines (HEPG2 “liver”, HELA “cervical” and PC3 “prostate” cancers), three of them, 4d and 4p (active against HEPG2), and compound 4g (active against HELA), demonstrated higher activities, that were close or even higher than that of the reference standard Doxorubicin. QSAR studies revealed good predictive and statistically significant 3 descriptor models ( $r^2 = 0.903-0.812$ ,  $r^2_{\text{adjusted}} = 0.855-0.672$ ,  $r^2_{\text{prediction}} = 0.773-0.605$ ).

**Keywords:** 2, 6- Bis(arylidene)- 1- cyclohexanone; Spiropyrrrolidine- oxindole; Azomethine ylide; Antitumor; Qsar.

#### 1431. Novel Heterocyclic-Fused Pyrimidine Derivatives: Synthesis, Molecular Modeling and Pharmacological Screening

Reem Khidr M. Arafa, Mai S. Nour and Nehad A. El-Sayed

*European Journal of Medicinal Chemistry*, 69: 498-507 (2013)  
IF: 3.499

Novel heterocyclic-fused pyrimidines viz pyrrolo[1,2-c]pyrimidines 4-8, pyrimido [5,4-e] pyrrolo [1,2-c] pyrimidines 9-14, pyrimido [40,50:4,5] pyrimido [1,6-a] azepines 16-18, pyrrolo[10,20:1,6]pyrimido[4,5-d][1,3]thiazines 19a,b and 1,3-thiazino[40,50:4,5]pyrimido[1,6-a]-azepine 19c were designed and synthesized as potential anticancer agents. In this investigation all the newly synthesized compounds were subjected to cytotoxic screening against MCF-7 breast cancer cell line. Moreover, kinase inhibitory assay was done for compounds 5, 7, 9 and 18 against the non-receptor and receptor tyrosine kinases c-Src and VEGFR, respectively. The tested compounds were more potent against c-Src than VEGFR, and the highest activity was observed for 18 showing 81% c-Src activity inhibition. Finally, molecular docking was performed with c-Src and VEGFR in an attempt to simulate and understand the possible binding interactions underlying the association between these small molecules and the kinase enzyme ATP binding pocket essential amino acids.

**Keywords:** Fused pyrimidines; Antiproliferative agents; MCF-7 breast cancer cell line; C-Src and VEGFR Inhibition.

#### 1432. Synthesis and Anticancer Activity of Some Novel Trifluoromethylquinolines Carrying A Biologically Active Benzenesulfonamide Moiety

Yassin Mohammed Nissan, Mohammed S. Al-Dosari, Mostafa M. Ghorab, Mansour S. Alsaied and Abdulkareem B. Ahmed

*European Journal of Medicinal Chemistry*, 69: 373-383 (2013)  
IF: 3.499

Several trifluoromethylquinoline derivatives containing a biologically active benzenesulfonamide moiety **2-14**, **16**, urea derivatives **15**, **17**, 4-isothiocyanate **18** and the corresponding carbamimidothioic acid derivatives **19-30**, were synthesized from the strategic starting material 4-chloro-7-trifluoromethylquinoline **1**. The structures of the newly synthesized compounds were elucidated on the basis of elemental and spectral analyses. All the prepared compounds were evaluated for their in vitro anticancer activity against various cancer cell lines. Most of the synthesized compounds showed good activity, especially compound **15** which exhibited higher activity than the reference drug doxorubicin. In order to suggest the mechanism of action for their cytotoxic

activity, molecular docking for all synthesized compounds was done on the active site of PI3K and good results were obtained.

**Keywords:** Trifluoromethylquinoline; Sulfonamide; Carbamimidothioic acid; Anticancer activity.

#### 1433. Synthesis and Biological Evaluation of Novel Coumarinepyrazoline Hybrids Endowed with Phenylsulfonyl Moiety as Antitumor Agents

Kamilia Mahmoud Amin, Amal A.M. Eissa, Sahar M. Abou-Seri, Fadi M. Awadallah and Ghaneya S. Hassan

*European Journal of Medicinal Chemistry*, 60: 187-198 (2013)  
IF: 3.499

Two groups of coumarin-pyrazoline hybrids were synthesized. The target compounds were obtained by cyclization of the coumarin chalcones with various substituted hydrazines to produce the corresponding pyrazolines through 1,4-addition on  $\alpha,\beta$ -unsaturated carbonyl system. Selected compounds were investigated for their anticancer activity toward 60 cancer cell lines according to US NCI protocol where breast cancer MCF7 and colon cancer HCT-116 were the most susceptible to the influence of compounds **7d**, **8c** and **9c**. Encouraged by this, all final compounds were screened against colorectal cell line HCT-116. The tested compounds exhibited high potency with  $IC_{50}$  ranging from 0.01  $\mu$ M to 2.8  $\mu$ M. Moreover, compound **9c** which possessed the highest cytotoxicity proved to have weak enzyme inhibitory activity against PI3K ( $p110\alpha/p85\alpha$ ).

**Keywords:** Coumarins; Pyrazoline; Phenylsulfonyl derivatives; Antitumor activity.

#### 1434. Synthesis and in Vitro Antiproliferative Effect of Novel Quinoline-Based Potential Anticancer Agents

Gehan H. Hegazy, Reem K. Arafa, Gary A. Piazza, Ashraf H. Abadi

*European Journal of Medicinal Chemistry*, 63: 826-832 (2013)  
IF: 3.499

Several derivatives with a quinoline scaffold and a flexible, semi-flexible or rigid side chains at position 8 of the quinoline ring were synthesized and assessed for their in vitro activity versus the human colon cancer cell line HT29 and the human breast cancer cell line MDA-MB231. The HT29 cell line was more refractory to the cytotoxic activity of some compounds, meanwhile all the quinoline derivatives except one displayed high to moderate activity against MDA-MB231 with  $IC_{50}$  values ranging between 4.6 and 48.2  $\mu$ M. The most active derivative in this study against both tested cell lines was the Schiff's base **4e** with  $IC_{50}$  of 4.7 and 4.6  $\mu$ M against HT29 and MDA-MB231, respectively.

**Keywords:** Quinolines; Antiproliferative agents; Cytotoxicity; HT29 human colon cancer cell line; MDA-MB231 human breast cancer cell line.

#### 1435. Synthesis of Novel 1,3,4-Trisubstituted Pyrazoles as Anti-Inflammatory and Analgesic Agents

Hanan H. Georgey, Fatma A. Ragab, Nagwa M. Abdel Gawad and Mona F. Said

*European Journal of Medicinal Chemistry*, 63: 645-654 (2013)  
IF: 3.499

Some novel 1,3,4-trisubstituted pyrazoles were synthesized and screened for their anti-inflammatory and analgesic activities as well as their ulcerogenic liability. They showed anti-inflammatory and analgesic activities with better GIT tolerance than the standard drug phenylbutazone. In addition,  $IC_{50}$  values for **5e** and **8e** were recorded. Compound **5e** was found to be the most active one as anti-inflammatory and analgesic agent. On the other hand, COX-1/COX-2 isozyme selectivity was also done which showed equal inhibition to both isoforms.

**Keywords:** Pyrazole; Schiff's base; Pyrrole; Anti-inflammatory; Analgesic; COX inhibition.

#### 1436. Synthesis of Some Dihydropyrimidine-Based Compounds Bearing Pyrazoline Moiety and Evaluation of their Antiproliferative Activity

Fadi M. Awadallah, Gary A. Piazza, Bernard D. Gary, Adam B. Keeton and Joshua C. Canzoneri

*European Journal of Medicinal Chemistry*, 70: 273-279 (2013)  
IF: 3.499

Two series of 2-(3,5-diaryl-4,5-dihydropyrazol-1-yl)-1-methyl-6-oxo-4-phenyl-1,6-dihydropyrimidine-5- carbonitriles **5a-h** and 4-(4-chlorophenyl)- 2- (3,5-diaryl - 4, 5- dihydropyrazol-1-yl)-1-ethyl-6-oxo-1,6-dihydropyrimidine- 5- carbonitriles **6a-h** were synthesized via a cyclocondensation reaction of the corresponding 2- hydrazinopyrimidines **3a, b** with the appropriate 2 – propen-1-ones **4a-h**. The target compounds were screened for their antiproliferative activity against A 549 (lung), HT 29 (colon), MCF 7 and MDA-MB 231 (breast) cell lines. The two most susceptible cell lines were the colon (HT 29) and breast (MDA-MB 231). Generally, the 4 – unsubstituted phenyl pyrimidine derivatives **5a-h** were more active than their 4-chlorophenylpyrimidine analogs **6a-h**. Compounds **5e** and **5g**, showed high activity against three of the cell lines. The most active compound **5c** possessed  $IC_{50} = 1.76 \mu M$  against A 549 cell line.

**Keywords:** Antiproliferative activity; Human breast (MDA-MB 231) cell line; Human colon (HT 29) cell line; Pyrazoline; Pyrimidine.

#### 1437. Synthesis, Antitumor and Antibacterial Activities of Some Novel Tetrahydrobenzo [4,5]Thieno[2,3-d]Pyrimidine Derivatives

Safinaz E. Abbas, Nagwa M. Abdel Gawad, Riham F. George and Yahya A. Akar

*European Journal of Medicinal Chemistry*, 65: 195-204 (2013)  
IF: 3.499

Two series of new tetrahydrobenzo[4,5]thieno[2,3-d]pyrimidines namely 2,3-disubstituted derivatives **3a-z** and 2,4-disubstituted ones **6a-c** were prepared and tested for their antitumor and antibacterial activities. The structures of the prepared compounds were confirmed by spectral and elemental analyses. Compound **3z** exhibited the highest antitumor activity against breast MCF-7 with  $IC_{50} = 0.19 \mu M$  compared to Doxorubicin ( $IC_{50} = 5.46 \mu M$ ), while **3r** was the most active one against liver HEPG-2 cancer cell line with  $IC_{50} = 1.29 \mu M$  as regard to Doxorubicin ( $IC_{50} = 7.36 \mu M$ ). Concerning the antibacterial activity, compounds **3m** and **3z** exerted remarkable activity against the tested bacterial species

compared to Ampicillin, whereas compound **6c** showed good activity against only Gram positive species.

**Keywords:** Thieno [2,3-d] pyrimidines; Antitumor activity; Antibacterial activity; MCF-7; HEPG-2.

#### 1438. Monoamine Oxidase-A and B Inhibiting Effect and Molecular Modeling of Some Synthesized Coumarin Derivatives

Omaima M. Abdelhafez, Kamelia M. Amin, Hamed I. Ali, Mohamed M. Abdalla and Rasha Z. Batran

*Neurochemistry International*, 62: 198-209 (2013) IF: 2.659

New series of bioactive 7-oxy coumarin derivatives were synthesized and tested for their in vitro and in vivo monoamine oxidase (MAO) A and B inhibitory effect. In vitro studies revealed exceptionally potent and selective MAO- A inhibitors with  $K_i$  values on a picomolar range. The acetohydrazide (**3b**) and the dioxopyrrolidine derivative (**7b**) showed the most potent in vitro and in vivo MAO inhibition activity. Moreover, molecular modeling study of the synthesized compounds into MAO-A (PDB: 2Z5X) and MAO-B (PDB: 2XFN) binding sites exhibited direct correlation between AutoDock binding affinity and % inhibition MAO-A (pM) and MAO-B ( $\mu M$ ). In addition, the results of in vivo MAO inhibiting properties (ED<sub>50</sub>) of the tested compounds revealed better direct correlation.

**Keywords:** MAO- A and B; 7- Oxy coumarins; Acetohydrazides; Dioxopyrrolidines; Molecular modeling

#### 1439. Simultaneous Determination of Chlordiazepoxide and Selected Antidepressants Using CZE

Ehab F. El-Kady, Marwa F. Mansour, Nabawia M. El-Guindi, Samir M. El-Moghazy and Ann Van Schepdael

*Journal of Separation Science*, 36: 3432-3439 (2013) IF: 2.591

A simple CE method was developed and validated for the simultaneous determination of chlordiazepoxide (CHL), amitriptyline, and nortriptyline (mixture I) or the determination of CHL and imipramine (mixture II) using the same BGE. Sertraline and amitriptyline were used as internal standards for the first and second mixtures, respectively. The method allows amitriptyline to be completely separated from its impurity and main metabolite nortriptyline, which can be quantified from 0.2  $\mu g/mL$ . The separation was achieved using 20 mM potassium phosphate buffer pH 5 containing 12 mM  $\beta$ -cyclodextrin and 1 mM carboxymethyl- $\beta$ - cyclodextrin. UV detection was performed at 200 nm and a voltage of 15 kV was applied on an uncoated fused-silica capillary at 25°C. These experimental conditions allowed separation of the compounds to be obtained in 7 min. Calibration graphs proved the linearity up to 40  $\mu g/mL$  for CHL, up to 100  $\mu g/mL$  for amitriptyline and imipramine, and up to 5  $\mu g/mL$  for nortriptyline. The accuracy and precision of the method have been determined by analyzing synthetic mixtures and pharmaceutical formulations. The analytical results were quite good in all cases indicating that the method was linear, sensitive, precise, accurate, and selective for both mixtures.

**Keywords:** Amitriptyline hydrochloride; Capillary electrophoresis; Chlordiazepoxide; Imipramine hydrochloride; Quality control.

#### 1440. Synthesis and Biological Evaluation of Some Substituted-2-N-(5-Chloro-2-Methoxy-4-Methylbenzenesulphonyl) Glutamic Acid Derivatives Against Prostate Cancer Cell Line PC3

Ghaneya Sayed Hassan and Doaa Ezzat Abdel Rahman

*Chemical and Pharmaceutical Bulletin*, 61: 212-221 (2013) IF: 1.592

New series of substituted glutamine 5a-l and glutamic acid diamides, diureide and dihydrazide 7a-e were synthesized from parent glutamic acid compound 3 and evaluated for their cytotoxic activity against tumor cell line PC3 (prostate cancer cell line). Most of the tested compounds exploited potent growth inhibitory activity with  $IC_{50}$  values ranging 0.034–3.97  $\mu$ m. Particularly, compounds 5a, 3, 5j, 5b, 7c, 7e, 5l, and 5k exhibited superior potency ( $IC_{50}$ =0.034, 0.04, 0.05, 0.074, 0.25, 0.4, 0.49, 0.522  $\mu$ m, respectively) to the reference drug Doxorubicin ( $IC_{50}$ =0.63  $\mu$ m), while compound 7b showed  $IC_{50}$ , 0.71  $\mu$ m, comparable to that of Doxorubicin. In summary, the newly synthesized compounds provided promising new lead for the future redesign and development of glutamine and glutamic acid derivatives as novel antitumor agents. The quantitative structure–activity relationship (QSAR) study was applied to find a mathematical correlation between the structures of compounds and their activity against PC3 cell line expressed as  $IC_{50}$  values.

**Keywords:** Glutamate system; Glutamic acid; Glutamine; Prostate cancer (PC); PC3 cell line.

#### 1441. Design and Synthesis of Some 3-Substituted-2-[(2,4-Dichlorophenoxy)-Methyl]Quinazolin-4(3H)-One Derivatives as Potential Anticonvulsant Agents

Fadi Mohsen Awadallah, Safinaz El-Sayed Abbas, Nashwa Ahmed Ibrahim, Eman Gaber Said and Gihan Kamel

*Chemical Pharmaceutical Bulletin*, 61: 679-687 (2013) IF: 1.564

Series of 2,3-disubstituted quinazolinone derivatives and a [1,2,4]triazino[2,3-c]quinazolinone featuring the pharmacophoric elements of anticonvulsant drugs were designed and synthesized. Target compounds were screened for their anticonvulsant activity using the subcutaneous pentylenetetrazole (s.c. PTZ) and maximal electroshock (MES) models. The s.c. PTZ test showed that the most active compound was the amide derivative 9c having a protective dose 50 ( $PD_{50}$ ) of 200.53  $\mu$ mol/kg ( $PD_{50}$  of phenobarbitone=62.18  $\mu$ mol/kg); nevertheless, this low potency is outweighed by the much higher safety profile of 9c ( $LD_{50}$ >3000 mg/kg). In the MES screening, seven compounds were equal to or more active than phenytoin; some of these compounds were less neurotoxic than phenytoin. Few compounds such as 9c and 10 were effective in both models.  $LD_{50}$  for the most active compounds was calculated.

**Keywords:** Quinazolinone; Pentylenetetrazole model; Maximal electroshock model; Anticonvulsant activity;  $LD_{50}$ ; Neurotoxicity

#### 1442. Discovering Some Novel 7-Chloroquinolines Carrying A Biologically Active Benzenesulfonamide Moiety as A New Class of Anticancer Agents

Yassin Mohammed Nissan, Mohammed Salem Al-Dosari, Mostafa Mohamed Ghorab and Mansour Sulaiman Al-Said

*Chemical & Pharmaceutical Bulletin*, 61: 50-58 (2013) IF: 1.564

Based on the reported anticancer activity of quinolines, a new series of 7-chloroquinoline derivatives bearing the biologically active benzenesulfonamide moiety 2–17 and 19–25 were synthesized starting with 4,7-dichloroquinoline 1. Compound 17 was the most active compound with  $IC_{50}$  value 64.41, 75.05 and 30.71  $\mu$ m compared with Doxorubicin as reference drug with  $IC_{50}$  values 82.53, 88.32 and 73.72  $\mu$ m on breast cancer cells, skin cancer cells and neuroblastoma, respectively. All the synthesized compounds were evaluated for their in vitro anticancer activity on breast cancer cells, skin cancer cells and neuroblastoma cells. Most of the synthesized compounds showed moderate activity. In order to suggest the mechanism of action for their cytotoxic activity, molecular docking for all synthesized compounds was done on the active site of phosphoinositide kinase (PI3K) and good results were obtained.

**Keywords:** Quinoline; Sulfonamide; Anticancer activity.

#### 1443. Modulating the Cyclic Guanosine Monophosphate Substrate Selectivity of the Phosphodiesterase 3 Inhibitors by Pyridine, Pyrido[2,3-D]Pyrimidine Derivatives and their Effects Upon the Growth of Ht-29 Cancer Cell Line

Ashraf Hassan Abadi, Marwa Saeed Hany, Shimaa Awadain Elsharif, Amal Abdel Haleem Eissa, Bernard DeWayne Gary, Heather Nicole Tinsley, and Gary Anthony Piazza.

*Chemical and Pharmaceutical Bulletin*, 61(4): 405–410 (2013) IF: 1.564

Analogues with the scaffolds of 3-cyano-4-alkoxyphenyl-6-bromoaryl-2-pyridone and 2-amino-3-cyano-4-alkoxyphenyl-6-bromoarylpyridine were synthesized. Cyclization of the 2-amino derivatives with formic acid and formamide gave the corresponding pyrido[2,3-d]pyrimidin-4(3H)-one and the pyrido[2,3-d]pyrimidin-4-amine derivatives, respectively. Active phosphodiesterase 3 (PDE3) inhibitors were identified from each of the four aforementioned scaffolds. This is the first report that pyrido[2,3-d]pyrimidin-4(3H)-one and pyrido[2,3-d]pyrimidin-4-amine derivatives can inhibit PDE3. The analogues with the pyridine and pyrido[2,3-d]pyrimidin-4(3H)-one scaffolds inhibited both cAMP and cyclic guanosine monophosphate (cGMP) hydrolysis by PDE3, while the amine containing scaffolds were more selective for cGMP hydrolysis. This observation may set the base for substrate-selective pharmacological modulation of this important class of drug targets and with less side effects, particularly tachycardia. The dual inhibitors of PDE3 were more potent inhibitors towards the growth of HT-29 cancer cell lines.

**Key words:** phosphodiesterase 3; substrate-modulation; pyridine derivative

#### 1444. Synthesis, Quantitative Structure–Activity Relationship and Biological Evaluation of 1,3,4-Oxadiazole Derivatives Possessing Diphenylamine Moiety as Potential Anticancer Agents

Doaa Ezzat Abdel Rahman

*Chemical and Pharmaceutical Bulletin*, 61(2): 151-159 (2013) IF: 1.564

Synthesis of 2,5-disubstituted-1,3,4-oxadiazole (2a-c), 3-substituted aminomethyl-5-substituted-1,3,4-oxadiazole-2(3H)-thione (4a-m) and 2-substituted thio-5-substituted-1,3,4-oxadiazole (5a, b) had been described. All the synthesized derivatives were screened for anticancer activity against HT29 and MCF7 cancer cell lines using Sulfo-Rodamine B (SRB) standard method. Most of the tested compounds exploited potent antiproliferative activity against HT29 cancer cell line rather than MCF7 cancer cell line. Compounds 2a-c, 4f and 5a exhibited potent cytotoxicity ( $IC_{50}$  1.3–2.0  $\mu$ M) and selectivity against HT29 cancer cell line. Quantitative structure–activity relationship (QSAR) study was applied to find a correlation between the experimental antiproliferative activities of the newly synthesized oxadiazole derivatives with their physicochemical parameter and topological index.

**Keywords:** 1,3,4-Oxadiazole; Mannich base; Anticancer; HT29 cell line; MCF7 cell line; Quantitative structure–activity relationship study.

#### 1445. Pyrazolone Derivatives: Synthesis, Anti-Inflammatory, Analgesic, Quantitative Structure–Activity Relationship and *in Vitro* Studies

Hanan Hanna Georgey, Fatma Abdel-Fattah Ragab, Nagwa Mohamed Abdel-Gawad and Mona Fikry Said

*Chemical; Pharmaceutical Bulletin (Tokyo)*, 61: 834-845 (2013) IF: 1.56

Some 1-(4-chlorophenyl or benzenesulfonamide)-2,3- and/or 4-substituted-1H-pyrazol-5(4H)-one derivatives were synthesized and screened for their anti-inflammatory and analgesic activities, in addition to their ulcerogenic liability. They were found to be active as anti-inflammatory and analgesic agents. Compound 6b was found to be the most active as anti-inflammatory agent and compound 9b was found to be the most active one as anti-inflammatory and analgesic agent. On the other hand, cyclooxygenase-1/-2 (COX-1)/COX-2 isozyme selectivity was also done and the tested compounds showed equal inhibition to both isoforms. Moreover, 2D-quantitative structure–activity relationship (QSAR) studies revealed well predictive and statistically significant and cross validated QSAR model that helps to explore some expectedly potent compounds.

**Keywords:** Pyrazolone; Acetic acid; Quantitative structure–activity relationship; Cyclooxygenase Inhibition; Anti-inflammatory.

#### 1446. Synthesis of Novel Bis-Anthraquinone Derivatives and Their Biological Evaluation as Antitumor Agents

Gehan Hegazy Hegazy and Azza T. Taher

*Archives of Pharmacol Research*, 36: 573-578 (2013) IF: 1.538

Cancer has become a major worldwide problem and drug resistance now is one of the most important problems in treatment of cancer. Anthraquinone derivatives represent one of the most important drugs that can be used in treatment of many types of cancer. In this study two series of novel bis-anthraquinone derivatives have been synthesized. Five of these compounds were chosen to be evaluated for their antitumor activity against human cancer cell lines by the National Cancer Institute (NCI, USA).

Marked activity was shown for the tested compounds (2–6). The most active one was compound 6 with mean value 67.00 against all cell lines. Compounds 7 and 8 were found inactive.

**Keywords:** Anticancer DNA; Bis-anthraquinone derivatives.

#### 1447. Synthesis, Antimicrobial Activity and Molecular Modeling Study of Substituted 5-Aryl-Pyrimido[5,4-C] Quinoline-2,4-Diones

Reem Khidr Mohamed Arafa, Mohamed A. Ismail, Shar Al-Shihry and Usama El-Ayaan

*Journal of Enzyme Inhibition and Medicinal Chemistry*, 28: 530-538 (2013) IF: 1.495

A series of pyrimido[5,4-c]quinoline-2,4-dione derivatives **5a–k** were synthesized in moderate yields via a thermolysis reaction of equimolar ratio of 5-arylidine-1,3-dimethylbarbituric acid derivatives **3a–d** with aniline derivatives **4a–d** at 150–180 °C for 1–2 h. Eight of the synthesized compounds were chosen for a primary *in vitro* one-dose anticancer assay performed using the full NCI 60 cell panel. Only compound **5b** showed moderate GI% at the used dose (10  $\mu$ M) against four of the tested cell lines corresponding to leukemia SR (GI%: 51), non small-cell lung cancer HOP-92 (GI%: 63), melanoma UACC-62 (GI%: 53) and renal cancer UO-31 (GI%: 69). On the other hand, antimicrobial screening of the whole set of the synthesized compounds was performed against three Gram +ve and two Gram –ve bacterial strains. Results of the antimicrobial screening showed that compounds **5d**, **5e**, **5f**, **5h** and **5k** have broad spectrum antibacterial efficacy being moderately active against all the tested Gram +ve and two Gram –ve bacteria. Also, compound **5a** showed interesting results being only active against *Streptococcus faecalis* and both tested Gram –ve strains viz. *E. coli* and *P. aeruginosa*. In order to compare the binding mode of the most active compounds **5e** and **5f** along with the inactive compound **5c** we docked these compounds into the empty binding site of topoisomerase II DNA gyrase (PDB ID: 1KZN), and results were compared with the bound inhibitor Clorobiocin.

**Keywords:** Antimicrobial; Anticancer; 5-Arylidine-1,3-dimethylbarbituric acid; Pyrimido[5,4-C]quinoline-2,4-dione; Molecular modeling.

#### 1448. A Validated Spectrofluorimetric Method for the Determination of Nifuroxazide Through Coumarin Formation Using Experimental Design

Marianne Alphonse M. Ragheb and Asmaa Ahmed El-Zaher

*Chemistry Central Journal*, 7 (90): 1-12 (2013) IF: 1.31

**Background:** Nifuroxazide (NF) is an oral nitrofurantoin antibiotic, having a wide range of bactericidal activity against gram positive and gram negative enteropathogenic organisms. It is formulated either in single form, as intestinal antiseptic or in combination with drotaverine (DV) for the treatment of gastroenteritis accompanied with gastrointestinal spasm. Spectrofluorimetry is a convenient and sensitive technique for pharmaceutical quality control. The new proposed spectrofluorimetric method allows its determination either in single form or in binary mixture with DV. Furthermore, experimental conditions were optimized using the new approach: Experimental design, which has many advantages

over the old one, one variable at a time (OVAT approach).

**Results:** A novel and sensitive spectrofluorimetric method was designed and validated for the determination of NF in pharmaceutical formulation. The method was based upon the formation of a highly fluorescent coumarin compound by the reaction between NF and ethylacetoacetate (EAA) using sulfuric acid as catalyst. The fluorescence was measured at 390 nm upon excitation at 340 nm. Experimental design was used to optimize experimental conditions. Volumes of EAA and sulfuric acid, temperature and heating time were considered the critical factors to be studied in order to establish an optimum fluorescence. Each two factors were co-tried at three levels. Regression analysis revealed good correlation between fluorescence intensity and concentration over the range 20–400 ng mL<sup>-1</sup>. The suggested method was successfully applied for the determination of NF in pure and capsule forms. The procedure was validated in terms of linearity, accuracy, precision, limit of detection and limit of quantification. The selectivity of the method was investigated by analysis of NF in presence of the co-mixed drug DV where no interference was observed. The reaction pathway was suggested and the structure of the fluorescent product was proposed. Statistical comparison between the presented method and a reported spectrophotometric one was carried out on pure and pharmaceutical formulation and revealed no significant difference.

**Conclusion:** The proposed method was considered economic, accurate, precise and highly sensitive. It could be easily applied in laboratory quality control for the analysis of NF in pure form and in pharmaceutical dosage form.

**Keywords:** Nifuroxazide; Spectrofluorimetry; Experimental design; Coumarin; Ethylacetoacetate.

#### 1449. Different Validated Methods for Determination of Cefditoren Pivoxil

Ramzia Ismail I. El-Bagary, Nisreen F. Abo-Talib and M. Badawi N. Eldin

*Journal of Planner Chromatography*, 26 (1): 43-55 (2013)  
IF: 0.955

Six, sensitive, precise and accurate methods have been developed for the determination of cefditoren pivoxil (CP). The first two methods were based on the formation of charge transfer colored complex between CP and p-chloranilic acid (p-CA) or 2,3-dichloro-5,6-dicyano-1,4-benzoquinone (DDQ) in the concentration range of 50.00–225.00 µg mL<sup>-1</sup> and 75.00–250.00 µg mL<sup>-1</sup>, respectively. The influence of different parameters on color formation was studied to determine optimum conditions for the visible spectrophotometric methods. The other four methods were adopted for determination of the studied drug in the presence of its acid degradation products including two spectrophotometric methods, namely, first derivative (D<sup>1</sup>) and first derivative of ratio spectra (DD<sup>1</sup>), and two chromatographic methods, namely, thin-layer chromatography (TLC) and high-performance liquid chromatography (HPLC), as stability indicating techniques. The degradation products were identified by infrared and mass spectroscopy. All the proposed methods were validated and successfully applied for determination of CP in pure form and in pharmaceutical preparations with good recovery ranges between 99.19 and 100.62. The results obtained by applying the proposed methods were statistically analyzed and compared with those

obtained by the manufacturer method, and no significant difference was found.

**Keywords:** Cefditoren pivoxil; RP-HPLC; TLC; Derivative spectroscopy; Colorimetry.

#### 1450. Three Validated Methods for Simultaneous Determination of Ofloxacin and Dexamethasone in Binary Mixture

Ramzia Ismail I. El-Bagary, Hanan A. Ahmed, Bahia A. Moussa and Mahmoud N. Darwish

*Journal of Planner Chromatography*, 26 (1): 56-61 (2013)  
IF: 0.955

Three selective, precise, and accurate methods were developed and validated for the simultaneous determination of ofloxacin and dexamethasone in bulk powder and pharmaceutical formulation, namely, derivative ratio spectrophotometric, densitometric and HPLC method. The first method is based on the use of derivative ratio spectrophotometric technique which allows the determination of ofloxacin and dexamethasone at  $\lambda_{\max}$  286, 235 nm over concentration range 1–13.5 and 1–7 µg mL<sup>-1</sup> for ofloxacin and dexamethasone, respectively. The second method is a densitometric one which depended on the separation on silica gel plate using methanol–phosphate buffer (4:6 v/v) and pH adjusted to 5 with orthophosphoric acid as a developing system and the spots were scanned at 300 and 240 nm for ofloxacin and dexamethasone, respectively at the linearity range of 1–6 mg/spot for each cited drug. The last method is HPLC using acetonitrile–H<sub>2</sub>O (7:3 v/v) and pH adjusted to 6.08 with 0.1 M acetic acid as the mobile phase at a flow rate 1.5 mL/min and UV detection at 254 nm. Regression analysis showed good regression coefficient. The suggested methods were successfully applied for simultaneous determination of ofloxacin and dexamethasone in bulk, laboratory prepared mixtures and pharmaceutical dosage form with good accuracy and precision. The results obtained by applying the proposed methods were statistically analyzed and compared with those obtained by the official methods.

**Keywords:** Ratio derivative spectrophotometry; TLC–densitometry; HPLC; Ofloxacin; Dexamethasone.

#### 1451. A Novel Class of Substituted Spiro [Quinazoline-2,1'-Cyclohexane] Derivatives as Effective Parp-1 Inhibitors: Molecular Modeling, Synthesis, Cytotoxic and Enzyme Assay Evaluation

Kamilia Mahmoud Amin, Manal M. Anwar, Yasmin M. Syam, Mohammed Khedr, Mohsen M. Kamel and Emad M. M. Kassem

*Acta Poloniae Pharmaceutica- Drug Research*, 70: 687-708 (2013) IF: 0.465

Molecular docking simulation study was carried out to design a novel series of spiro [(2H, 3H) quinazoline-2,1'-cyclohexan]-4(1H)-one derivatives as a new class of effective PARP-1 inhibitors. Spiro [2H-3,1-benzoxazine-2,1'-cyclohexan]-4(1H)-one (5) was the starting compound to synthesize the target proposed analogues. The derivatives that showed the top scores and had the best fitting in the binding sites of the target protein were selected to evaluate their in vitro anti-proliferative activity against the cultured human breast carcinoma cell line (MCF-7)



using doxorubicin as a standard drug. Additionally, the compounds that exhibited the highest cytotoxic efficiency were further subjected to **PARP-1** enzyme assay taking 3-aminobenzamide as the reference drug. The structures of the novel derivatives were confirmed on the bases of microanalytical and spectral data.

**Keywords:** Anti-proliferative activity; Molecular docking; **PARP-1** inhibitors; Spiro [(2H, 3H) quinazoline- 2,1'-Cyclohexan]-4 (1H)- one.

#### 1452. Synthesis, Cytotoxic Evaluation and Molecular Docking Study of Novel Quinazoline Derivatives as Parp-1 Inhibitors

Kamilia Mahmoud Amin, Manal M. Anwar, Mohsen M. Kamel, Emad M. M. Kassem, Yasmin M. Syam and Samia A. Elseginy

*Acta Poloniae Pharm. Drug Res.*, 70: 833-849 (2013) IF: 0.465

Novel series of spiro[(2H,3H)-quinazoline-2,1'-cyclohexane] derivatives (I-XVI) were synthesized and biologically evaluated as cytotoxic agents against human breast carcinoma cell lines (MCF-7) using doxorubicin as a reference drug. Most of the tested compounds displayed promising cytotoxic activity, especially derivatives V, VIb and XIb.

The most active compounds were docked into the **PARP-1** enzyme binding site to predict the ligand-protein binding modes. Lipinski rule of five and ADME profile suggested strongly that compounds V and VIb are promising agents as breast cancer inhibitors with drug likeness approach that have **PARP-1** inhibitory activity. The structures of all newly synthesized compounds were confirmed by microanalysis and IR, <sup>1</sup>H-NMR and mass spectral data.

**Keywords:** Spiro quinazoline-cyclohexane derivatives; Cytotoxic activity; Molecular docking; **PARP-1** enzyme; Drug-likeness.

#### 1453. Anti-Breast Cancer of Some Novel Pyrrole and Pyrrolopyrimidine Derivatives Bearing A Biologically Active Sulfonamide Moiety

Yassin M. Nissan, Mostafa M. Ghorab and Mansour S. Alsaïd

*Life Science Journal*, 10: 2170-2183 (2013) IF: 0.165

Several novel pyrroles **5**, **6**, **11-15**, **20** and pyrrolopyrimidines **7-10**, **16-19**, **21-26** having a biologically active sulfonamide moieties were synthesized in order to study their anticancer activity.

The prepared compounds were characterized by elemental analyses, IR, <sup>1</sup>H-NMR and <sup>13</sup>C-NMR spectra, then screened as anticancer agents against human breast cancer cell line (MCF7). All the tested compounds showed good cytotoxic activity better than the reference drug Doxorubicin as reference drug with IC<sub>50</sub> values ranging between 6.46-7.86 µM except compounds **19** and **31** which showed comparable activity with IC<sub>50</sub> values of 8.30, 8.39 µM, respectively.

In order to predict the mechanism of action for their activity, molecular docking on the active site of c-Src kinase enzyme was performed and good results were obtained.

**Keywords:** Anticancer activity; Pyrrole; Pyrrolopyrimidine; Sulfonamides.

#### 1454. Application of Chromatographic and Spectrophotometric Methods for the Analysis of Aliskiren and Hydrochlorothiazide Antihypertensive Combination

Marwa Ahmed Elfeky, Menna I. Ezzeldin, Engy Shokry and Ramzia I. Elbagary

*International Journal of Advanced Chemistry*, 1: 13-20 (2013)

High performance liquid chromatographic (HPLC) and spectrophotometric methods developed for the simultaneous determination of Aliskiren (ALK) and Hydrochlorothiazide (HCT) combination in bulk powder and in tablets dosage form. Determination of ALK and HCT was achieved by chromatographic separation on Econosphere C-18 column using a mobile phase consisting of water (pH 7.5): acetonitrile (50:50) at a flow rate of 0.5 mL.min<sup>-1</sup> and UV detection at 208 nm. Method validation parameters were found to be acceptable over the concentrations range of 5-150 µg.mL<sup>-1</sup>, 1-50 µg.mL<sup>-1</sup> for ALK and HCT respectively. Regarding the spectrophotometric methods, two methods were employed. Simultaneous Equation method, absorbance readings are taken at two wavelengths 277.48 nm (for ALK) and 267.48 nm (for HCT) in methanol. Dual Wavelength method, the difference between absorbance readings are taken at two wavelengths 273.3 nm, 260 nm (for Aliskiren) and 270 nm, 280 nm (for HCT) in methanol. The applied spectrophotometric methods were found to be rapid, specific, precise and accurate over the concentration range of 5 – 150 µg.mL<sup>-1</sup> and 1 – 41 µg.mL<sup>-1</sup> for ALK and HCT respectively and can be applied for the routine analysis of these drugs in bulk, and combined dosage form without any interference by the excipients.

**Keywords:** High performance liquid chromatography; Simultaneous equation; Dual wavelength; Aliskiren; Hydrochlorothiazide.

#### 1455. Application of Chromatographic and Spectrophotometric Methods for the Analysis of Selected Antihypertensive Combinations

Marwa Ahmed Elfeky, Menna I. Ezzeldina, Engy Shokry and Ramzia I. Elbagary

*International Journal of Analytical, Pharmaceutical; Biomedical Sciences*, 2: 6-15 (2013)

High performance liquid chromatographic (HPLC) and spectrophotometric methods developed for the simultaneous determination of antihypertensive mixture namely Perindopril and Indapamide in bulk powder and in tablets dosage form. Chromatographic separation of Perindopril and Indapamide was achieved on the Econosphere C-18 column (150mm x 4.6mm, 5µm) using a mobile phase system consisting of acetonitrile: 5mM sodium phosphate buffer (pH 7.5) (50:50) at a flow rate of 0.5 mL/min with UV detection at 202 nm. Method validation parameters were found to be acceptable over the concentration ranges of 1-140 µg/mL and 1-40 µg/mL for Perindopril and Indapamide respectively. Regarding the spectrophotometric methods, two methods were employed, Ratio Subtraction and First Derivative methods. In Ratio Subtraction method, absorbance readings are taken at two wavelengths 277.48 nm (λ<sub>max</sub> of Aliskiren) and 315 nm (extended spectrum of Hydrochlorothiazide) in methanol. In First Derivative method,

absorbance readings are taken at two wavelengths 237.2 nm (for Aliskiren) and 275.8 nm (for Hydrochlorothiazide) in methanol. The applied spectrophotometric methods were found to be rapid, specific, precise and accurate over the concentration range of 5 – 150 µg/mL and 1 – 41 µg/mL for Aliskiren and Hydrochlorothiazide respectively.

**Keywords:** High performance liquid chromatography; Ratio subtraction; First derivative; Perindopril; Indapamide; Aliskiren; Hydrochlorothiazide.

#### 1456. Derivative and Derivative Ratio Spectrophotometric Methods for the Simultaneous Determination of Moxifloxacin Hydrochloride with Ketorolac Tromethamine and Ciprofloxacin Hydrochloride with Dexamethasone Sodium Phosphate in Bulk and Drop

Marwa Ahmed Elfeky, Ramzia I. El-Bagary, Fatma-Elzhray M. Khaled and Emad M. Hussien

*Journal of Chemical and Pharmaceutical Research*, 5: 155-164 (2013)

Two simple and rapid spectrophotometric methods were developed for the determination of two binary mixtures: moxifloxacin hydrochloride (MFH) with ketorolac tromethamine (KTM) and ciprofloxacin hydrochloride (CFH) with dexamethasone sodium phosphate (DSP). The first method, zero-crossing derivative spectrophotometry, depends on measuring the second derivative peak and trough values at 304 nm and 250.6 nm for MFH and KTM, respectively. The second method is a derivative ratio spectrophotometry. It depends on measuring the trough amplitude of the second derivative of the ratio spectra at 287.5 nm by dividing the spectra of CFH by the spectrum of 15.0 µg mL<sup>-1</sup> DSP. Also, DSP was determined by measuring the peak amplitude of the third derivative of the ratio spectra at 254.5 nm using 10.0 µg mL<sup>-1</sup> CFH as the divisor. The proposed methods were validated in compliance with the ICH guidelines and were successfully applied for determination of moxifloxacin, ciprofloxacin, ketorolac and dexamethasone in their laboratory prepared mixtures and pharmaceutical formulations.

**Keywords:** Moxifloxacin; Ciprofloxacin; Ketorolac; Dexamethasone; Derivative spectrophotometry; Derivative ratio spectrophotometry.

#### 1457. Derivative, Derivative of the Ratio Spectrophotometric and Stability-Indicating RP-HPLC Methods for the Determination of Mometasone Furoate and Miconazole Nitrate in Cream

Marwa Ahmed Elfeky, Ramzia I. El-Bagary, Manal A. El-Shaal and Enas H. Tolba

*Journal of Chemical Pharmaceutical Research*, 5: 368-378 (2013)

Three simple, selective and precise methods, namely, derivative, derivative of the ratio spectrophotometric and high performance liquid chromatographic (HPLC) methods were developed and validated for the simultaneous determination of mometasone furoate and miconazole nitrate in mixture. The first method

involves the use of derivative spectrophotometry with the zero-crossing technique where mometasone furoate was determined using its <sup>1</sup>D (λ = 8) amplitude at 270.5 nm and miconazole nitrate was determined using its <sup>3</sup>D (λ = 4) amplitude at 282.1 nm. The second method involves the application of the second derivative of the ratio spectrophotometric method where mometasone furoate and miconazole nitrate were determined using Δλ = 4 at 267.2 nm and 281.2 nm, respectively. The third method is based on gradient elution of mometasone furoate and its alkaline degradation products along with miconazole nitrate on reversed phase C18 column, (3.9 × 300 mm, 10 µm) - Waters, using a mobile phase consisting of 1.5% w/v aqueous ammonium acetate buffer, pH 7.6 and acetonitrile, at a flow rate of 2 mL/min.

Quantitation was achieved applying dual wavelength detection where mometasone furoate and its alkaline degradation products were detected at 240 nm and miconazole nitrate was detected at 230 nm at ambient temperature. In addition, products from alkaline degradation of mometasone furoate were verified by LC-MS. The methods were validated according to the International Conference on Harmonization (ICH) guidelines. The selectivity of the proposed methods was tested using laboratory-prepared mixtures. The developed methods were successfully applied for the determination of mometasone furoate and miconazole nitrate in bulk and in its pharmaceutical preparation.

**Keywords:** Mometasone furoate; Miconazole nitrate; Derivative spectrophotometry; Derivative of the ratio spectrophotometry; Stability-indicating HPLC.

#### 1458. Development and Validation of A Reversed Phase Liquid Chromatographic Method for the Determination of Three Gliptins and Metformin in the Presence of Metformin Impurity (1-Cyanoguanidine)

Ehab Farouk Elkady, Ramzia Ismail El-Bagary and Bassam Mahfouz Ayoub

*European Journal of Chemistry*, 4: 444-449 (2013)

A simple and precise liquid chromatographic method has been developed and validated for the determination of either sitagliptin (STG), vildagliptin (VLG) or saxagliptin HCL (SXX) and metformin HCL (MET) in the presence of metformin degradation product, 1-cyanoguanidine (CGN). Chromatographic separation was achieved on a Symmetry<sup>®</sup> cyanide column (150 mm × 4.6 mm, 5 µm). Isocratic elution using a mobile phase of potassium dihydrogen phosphate buffer (pH = 4.6) - acetonitrile (30:70, v:v) at a flow rate of 1 mL/min with UV detection at 210 nm was performed. The LC method was used for the simultaneous determination of STG, VLG, SXX and MET in the ranges of 5-200, 5-200, 0.5-80.0 and 20-800 µg/mL, respectively. The results were statistically compared with the reference method for each drug using one-way analysis of variance (ANOVA). The method developed was satisfactorily applied to the analysis of the pharmaceutical formulations and proved to be specific and accurate for the quality control of the cited drugs in pharmaceutical dosage forms.

**Keywords:** Sitagliptin; Metformin; Saxagliptin; Vildagliptin; Liquid chromatography; Stability indicating assay.

#### 1459. Development and Validation of A Stability Indicating HPLC Method for the Simultaneous Determination of Captopril and Indapamide

Marianne A. Ragheb, Bahia Abbas Moussa, Ashraf Hassan Abadi and Hanan Abou Youssef

*Analytical Chemistry, an Indian Journal*, 12 (6): 222-232 (2013)

A simple, selective, precise and stability indicating reversed phase HPLC method was developed and validated for the simultaneous determination of captopril (CAP) and indapamide (IN) in presence of their degradation products, using hydrochlorothiazide (HZ) as internal standard, in powder and tablets. The separation was achieved on an Agilent Zorbax C<sub>18</sub> column, with isocratic flow. The mobile phase consisted of methanol:water:triethylamine (42.5:57.5:0.028, v/v/v), adjusted with o-phosphoric acid to pH 2.5. The flow rate was maintained at 2 ml min<sup>-1</sup>. The UV detection was carried out at 220 nm for CAP, CAP oxidation product and IN degradation product (I) and 242 nm for IN and 272 nm for HZ. Linearity was demonstrated with good correlation coefficients (0.9998), over the concentration range of 27.5-550 µg.mL<sup>-1</sup> and 2.5- 50 µg.mL<sup>-1</sup>, in case of CAP and IN, respectively. The method was successfully validated in accordance to ICH guidelines. Individual drugs (CAP and IN) were exposed to hydrolytic and oxidative stress conditions. The method gave high resolution among the degradation products and the analytes. The proposed method is accurate, stability indicating and successfully applied for the determination of CAP and IN in synthetic mixtures and tablets.

**Keywords:** Captopril; Degradation; Indapamide; HPLC; Stability indicating method.

#### 1460. Improved Reversed Phase Liquid Chromatographic Method with Pulsed Electrochemical Detection For Tobramycin in Bulk and Pharmaceutical Formulation

Ehab Farouk Elkady, Vicky Manyanga, Jos Hoogmartens and Erwin Adams

*Journal of Pharmaceutical Analysis*, 3: 161-167(2013)

Tobramycin is one of the aminoglycoside antibiotics that lack a UV absorbing chromophore. However, the application of pulsed electrochemical detection (PED) has been used successfully for the analysis of this and similar antibiotics. This work describes an improved liquid chromatographic (LC) method combined with PED, which is able to separate much more impurities than before. Using a Discovery C-18 RP column (250 mm × 4.6 mm i.d., 5 µm), isocratic elution was carried out with a mobile phase containing sodium sulfate (35 g/L), sodium octane sulphonate (1 g/L), tetrahydrofuran (14 mL/L) and 0.2 M phosphate buffer pH 3.0 (50 mL/L). Using these experimental conditions, the limit of quantification (LOQ, S/N = 10) was 5 ng. The linearity was examined in the range LOQ-60 µg/mL and the coefficient of determination was 0.998. The method also proved to be repeatable and the recovery was close to 100%. The influence of the different chromatographic parameters on the separation was investigated by means of an experimental design. The proposed method is useful in quality control of tobramycin drug substances and drug products.

**Keywords:** Liquid; Chromatography- pulsed electrochemical detection; Tobramycin; Aminoglycoside antibiotics.

#### 1461. Novel Techniques for the Determination of Cisatracurium Besylate Alone or in the Presence of its Degradation Product

Ramzia Ismail I. El-Bagary, Nisreen F. Abo-Talib and Marwa A. El-Wahab Mohamed

*Am. J. Pharm Health Research*, 1 (9): 82-95 (2013)

Four simple, accurate and precise methods have been developed and validated for the determination of cisatracurium besylate in bulk and in its pharmaceutical preparation. The first method was a spectrofluorimetric method based on measuring the native fluorescence intensity (FI) of cisatracurium (CIS) in aqueous micellar medium at 317 nm upon excitation at 235 nm in the range of 0.2- 2.2 µg.mL<sup>-1</sup>. The other three methods were adopted for the determination of the studied drug in the presence of its alkaline degradation product including a spectrophotometric method namely, first derivative of ratio spectra (DD<sup>1</sup>) in the range of 8-38 µg.mL<sup>-1</sup> and two high pressure liquid chromatographic (HPLC) methods, one with diode array detector (DAD) and the other with fluorescence detector (FLD) in the ranges of 1.0- 40.0 µg.mL<sup>-1</sup> and 0.25-20.0 µg.mL<sup>-1</sup>, respectively. Separation was achieved on Supelco Discovery C<sub>18</sub> column (150 mm x 4.6 mm, 5 µm) and Agilent Zorbax SB-CN column (50 mm x 4.6 mm, 1.8 µm) for HPLC-DAD and HPLC- FLD methods, respectively. All the proposed methods were validated and successfully applied for the determination of CIS in bulk and in pharmaceutical preparation with good recovery ranges between 99.92- 100.71. The results obtained by applying the proposed methods were statistically analyzed and compared with those obtained by the manufacturer method, and no significant difference was found.

**Keywords:** Cisatracurium besylate; Diode-array detector; Fluorescence detector; Spectrofluorimetry and First derivative ratio of ratio spectroscopy.

#### 1462. On-Line Coupling of derivatization with pre-Concentration to Determine Trace Levels of Methotrexate

Ramzia Ismail I. El-Bagary, Samy Emara, Tsutomu Masujima, Walaa Zarad and Maha Kamal

*Journal of pharmaceutical analysis*, 3 (1): 28-35 (2013)

A new simple, sensitive and precise green analytical procedure using an automated packed-reactor derivatization technique coupled with on-line solid-phase enrichment (SPEn) has been developed and evaluated to determine trace levels of methotrexate (MTX). The method was based on injection of MTX into a flowing stream of phosphate buffer (0.04 M, pH 3.4), carried through the packed oxidant reactor of Cerium (IV) trihydroxyhydroperoxide for oxidative cleavage of the drug into highly fluorescent product, 2,4-diaminopteridine-6-carboxylic acid, followed by SPEn on a head of short ODS column (10 mm × 4.6 mm i.d., 5 µm particle size). The flow rate was 0.25 mL/min and packed reactor temperature was 40 °C. The trapped product was back-flush eluted from the ODS column to the detector by column-switching with an environmentally friendly mobile phase consisting of ethanol and phosphate buffer (0.04 M, pH 3.4) in the ratio of 5:95 (v/v). The eluent was monitored at emission and excitation wavelengths of 460 and 360 nm, respectively. The calibration curve was linear over the concentration range of 1.25-50 ng/mL with a detection limit of

0.08 ng/mL. The method was successfully applied to determine MTX in pharmaceutical formulations with mean percentage recovery ranging from 99.48 to 99.60.

**Keywords:** Methotrexate; Flow injection analysis; Cerium (IV) trihydroxyhydroperoxide; On-line solid phase enrichment; Fluorescence detection.

#### 1463. Simultaneous Determination of Sitagliptin and Metformin in Ternary Mixture with Sitagliptin Acid Degradation Product

Ehab Farouk Elkady, Ramzia Ismail El-Bagary and Bassam Mahfouz Ayoub

*European Journal of Chemistry, 4: 360-365 (2013)*

In this work, the acidic degradation product of sitagliptin phosphate monohydrate (STG) was synthesized, separated and its structure was elucidated. Additionally, two reversed-phase liquid chromatographic (RP-LC) methods have been developed for the determination of STG. The first method comprised the determination of STG in binary mixture with sitagliptin acid degradation product (SDP) in laboratory prepared mixtures, in plasma and in dosage form. This method was based on isocratic elution using a mobile phase consisting of potassium dihydrogen phosphate buffer (pH = 4.6)- acetonitrile (30:70, v:v) with fluorometric detection. The fluorometric detector was operated at 267 nm for excitation and 575 nm for emission. In the second method, the simultaneous determination of STG and metformin (MET) in the presence of SDP has been developed. In this method, the ternary mixture of STG, MET and SDP was separated using a mobile phase consisting of potassium dihydrogen phosphate buffer (pH = 4.6)- acetonitrile (15:85, v:v) with UV detection at 220 nm. Chromatographic separation in the two methods was achieved on a Symmetry® Waters C18 column (150 mm × 4.6 mm, 5 µm). The optimized methods were validated and proved to be specific, robust and accurate for the quality control of the cited drugs in pharmaceutical preparations.

**Keywords:** Metformin; Sitagliptin phosphate; Stability indicating assay; Pharmaceutical preparation; Sitagliptin degradation product; Reversed-phase liquid chromatography.

#### 1464. Spectrophotometric Determination of Oxybutynin Hydrochloride Via Charge- Transfer Complexation Reaction

Marianne A. Mahrouse, Sonia T. Hassib, Awatef E. Farag and Eman A. Mostafa

*International Journal of Pharmaceutical and Chemical Sciences, 2 (4): 2024-2033 (2013)*

Two simple, accurate and reproducible spectrophotometric methods were developed for the quantitative estimation of oxybutynin hydrochloride in pure form and in pharmaceutical preparation. The methods were based on the charge transfer complex formation of oxybutynin as *n*-electron donor with two  $\pi$ -electron acceptors: 2,3-dichloro-5,6-dicyano-*p*-benzoquinone (DDQ) (DDQ method) and 2,5-dichloro-3,6-dihydroxy-*p*-benzoquinone (*p*-chloranilic acid) (*p*-chloranilic acid method) in acetonitrile. Different variables affecting the reactions were investigated and optimized. Under the optimum reaction conditions, linear relationship with good correlation coefficients

(0.9998- 0.9999) was found between the absorbances at 457 nm and 520 nm and the concentrations of oxybutynin over the concentration ranges of 20- 80 µg mL<sup>-1</sup> and 30- 160 µg mL<sup>-1</sup>, for DDQ and *p*-chloranilic acid methods, respectively. The proposed methods were validated in accordance with ICH guidelines and were applied successfully to pharmaceutical formulation. The stoichiometric relationship determined by Job's continuous variation method was found to be 1:1 (drug: reagent) for both methods. Statistical comparison of the results obtained by applying the proposed methods and the reference method was carried out and revealed no significant difference between the results. Therefore, the charge transfer approach using DDQ and *p*-chloranilic acid can be applied successfully for the determination of oxybutynin in tablets in quality control laboratories.

**Keywords:** Oxybutynin hydrochloride; DDQ; *P*-chloranilic acid; Spectrophotometry.

#### 1465. Spectrophotometric Methods for the Determination of Linagliptin in Binary Mixture with Metformin Hydrochloride and Simultaneous Determination of Linagliptin and Metformin Hydrochloride Using High Performance Liquid Chromatography

Ehab Farouk Elkady, Ramzia I. El-Bagary and Bassam M. Ayoub

*International Journal of Biomedical Science, 9: 41-47 (2013)*

Simple, accurate and precise Zero order, first derivative spectrophotometric and chromatographic methods have been developed and validated for the determination of linagliptin (LNG) and metformin HCl (MET). The zero order and first derivative spectrophotometric methods were used for the determination of LNG in the range of 5-30 µg mL<sup>-1</sup> by measuring the absorbance at 299 nm and 311 nm respectively. Besides, a reversed-phase liquid chromatographic (RP-LC) method is described for the simultaneous determination of LNG and MET. Chromatographic separation was achieved on a Symmetry® Waters C18 column (150 mm × 4.6 mm, 5 µm). Isocratic elution based on potassium dihydrogen phosphate buffer pH (4.6) – methanol (30:70, v/v) at a flow rate of 1 mL min<sup>-1</sup> with UV detection at 260 nm was performed. Linearity, accuracy and precision were found to be acceptable over the concentration ranges of 0.125-4 µg mL<sup>-1</sup> and 20-800 µg mL<sup>-1</sup> for LNG and MET, respectively. The results were statistically compared using one-way analysis of variance (ANOVA). The optimized methods were validated and proved to be specific, robust, precise and accurate for the quality control of the drugs in their pharmaceutical preparation.

**Keywords:** Linagliptin; Metformin hydrochloride; Reversed-phase liquid chromatography; Spectrophotometry; Pharmaceutical preparation.

#### 1466. Stability Indicating Spectrophotometric and TLC Densitometric Methods for the Determination of Gemifloxacin Mesylate in Tablet Form

Marianne A. Mahrouse, Bahia Abbas Moussa, Mahmoud Ali Hassan and Michael Gamal Fawzy

*Analytical Chemistry, an Indian Journal, 12 (5): 165-176 (2013)*

Gemifloxacin mesylate (GEM), a novel fluoroquinolone used for respiratory tract infections, was determined by three simple, accurate and precise spectrophotometric methods and a TLC densitometric method, in presence of its acid degradation product. Method (A) was first derivative technique ( $^1D$ ) which allows the determination of GEM by measuring the peak amplitudes at 280 and 360 nm where the acid degradation product displays zero value. Method (B) was based on second derivative ratio technique ( $^2DD$ ) in which the peak amplitude was measured at 289.3 nm using  $10 \mu\text{g mL}^{-1}$  of the acid degradation product as divisor. Method (C) depends on the formation of a colored product between GEM and *p*-dimethylaminobenzaldehyde (DAB) reagent and the absorbance was measured at 400 nm. Method (D) depends on separation of GEM from its acid degradation product on TLC plates pre-sprayed with EDTA solution (3% w/v), using chloroform: methanol: ammonia solution (6:3:0.5, v/v/v) as developing system, followed by densitometric determination of GEM. The proposed methods were successfully applied to the analysis of GEM in pure and tablet forms, in addition to laboratory prepared mixtures (methods A, B and D). The methods were validated in accordance to ICH guidelines and compared with the reference method, revealing no significant difference.

**Keywords:** Gemifloxacin mesylate; First derivative; Second derivative ratio; *p*-dimethylaminobenzaldehyde; TLC.

#### 1467. Synthesis, Characterization and Antimicrobial Activity of Some Novel Isoindole-1,3-Dione Derivatives

Kamilia Mahmoud Amin, Afaf H. El-Masry, Neama A. Mohamed, Ghada E. A. Awad and Basma S. Habib

*Der Pharma Chemica*, 5: 97-108 (2013)

The present investigation, represents the synthesis of new derivatives containing 2-((4-acetyl phenylimino) methyl) isoindoline-1,3-dione moiety incorporated with different heterocycles such as pyrazoline, isoxazoline, pyrimidine, pyridones and iminopyridine. Spectral techniques of IR,  $^1H$  NMR, Mass spectroscopy and elemental analyses were used to characterize the synthesized compounds. Most of the synthesized compounds were tested for their antimicrobial activity against a variety of gram positive and gram negative bacteria as well as fungal isolates using Ciprofloxacin and Ketoconazole as reference drugs. Some of the tested compounds showed potent activity and could be considered as promising antibacterial and antifungal agents.

**Keywords:** Phthalimide; Heterocyclic derivatives; Antibacterial agents; Antifungal agents.

#### 1468. Validated Derivative Spectrophotometric and Chromatographic Methods for the Determination of Doxazosin Mesylate in Presence of its Degradation Product and/or Related Impurity

Marianne A. Mahrouse, Sonia T. Hassib, Awatef E. Farag and Eman A. Mostafa

*International Journal of Pharmaceutical Analysis, Recent Sciences Publications*, 38 (2): 1146-1155 (2013)

Doxazosin mesylate (DOX) is useful in the management of hypertension and urinary retention associated with benign

prostatic hyperplasia. DOX is prepared via a multistep synthesis, the possibility of by-product formation exists. Its potential impurities may also be formed due to spontaneous decomposition of the drug. Impurity may influence the efficacy and safety of the pharmaceutical products. Therefore, the aim of this investigation was the isolation and identification of the degradation product by spectroscopy and determination of DOX in presence of its potential impurities by specific methods. Four new validated spectrophotometric and chromatographic methods were developed for the determination of DOX in drug substance and drug product, in presence of its potential impurities. The first method, derivative difference spectrophotometry ( $\Delta^1D$  method), depends on derivatization of the pH-induced absorbance difference of the drug solution and measurement of the amplitude of the minimum at 289.6 nm (zero value of its related impurity: 6,7-dimethoxy-2,4(1H,3H)-quinazolinedione, DQD). In the second method, first derivative ratio spectrophotometry ( $^1DD$  method) was adopted in presence of up to 60 % DOX alkaline degradation product (Deg I). The intact drug was determined by measuring the peak amplitude at 292.2 nm over the concentration range  $4-16 \mu\text{g mL}^{-1}$ . The third method is based on TLC separation of doxazosin mesylate from its Deg I and DQD, using ethyl acetate: methanol: triethylamine (4: 0.4: 0.3, v/v/v) as developing system, followed by densitometric measurement of the spot at 345 nm. The fourth method is an isocratic reversed phase HPLC which allows the determination of DOX in presence of its Deg I and DQD. Good resolution with a chromatographic run time less than 4 min was achieved using methanol: acetonitrile: water: triethylamine (50: 30: 20: 0.2, v/v/v/v) as mobile phase and UV detection at 245 nm. Forced degradation under alkaline conditions was carried out, one of the degradation products was isolated and its structure was confirmed. The methods were validated in accordance to ICH guidelines. Statistical analysis revealed no significant difference between the results obtained and the reported one. The newly developed methods were found to be highly efficient, specific and sensitive.

**Keywords:** Doxazosin mesylate; Derivative ratio; Derivative.

#### 1469. Validated Difference Spectrophotometric and Stability Indicating HPLC Estimation of Linezolid in Tablets

Marianne A. Mahrouse, Bahia A. Moussa, Mahmoud A. Hassan and Michael G. Fawzy

*International Journal of Pharmaceutical Analysis, Recent Sciences Publications*, 38 (2): 1166-1173 (2013)

Three methods are presented for the determination of linezolid (LIN), a new antibacterial agent, in pharmaceutical dosage form. The first method, difference spectrophotometry ( $\Delta A$ ), was based on the principle that LIN exhibited two different absorption spectra in acidic and basic media. LIN was estimated by measuring the difference in absorbance of LIN in 0.1 N HCl relative to that of a solution of equal concentration in 0.1 N NaOH at 239.5 nm. The second method, differential derivative ( $\Delta^1D$ ) spectrophotometry, comprised of measurement of the peak amplitude at 250 nm in the first derivative of the difference absorption spectrum. The third method was based on HPLC separation of LIN from its alkaline degradation product using Kromasil  $C_{18}$  column, as stationary phase and sodium 1-octanesulfonate (20 mM): acetonitrile (70: 30, v/v) as mobile phase. The flow rate was maintained at  $1.5 \text{ mL min}^{-1}$ , isocratic



elution was applied throughout the analysis. UV detection was carried out at 257 nm. LIN alkaline degradation product was isolated and its structure was elucidated. The methods were linear over the concentration ranges of 10-40  $\mu\text{g ml}^{-1}$  for  $\Delta\text{A}$  and  $\Delta^1\text{D}$  methods and 20-200  $\mu\text{g ml}^{-1}$  for HPLC method. The proposed methods were validated according to ICH guidelines and successfully applied for the analysis of tablet dosage form. The newly developed methods could be applied for the analysis of LIN in quality control laboratories.

**Keywords:** Difference spectrophotometry; Differential derivative; Degradation; HPLC; Linezolid.

#### Dept. of Pharmaceutical Organic Chemistry

##### 1470. Synthesis and Anticancer Activity of Novel 2-Pyridyl Hexahydrocyclooctathieno [2,3-D]Pyrimidine Derivatives

Asmaa Elsayed A. Kassab and Ehab M. Gedawy

*European Journal of Medicinal Chemistry*, 63: 224-230 (2013)  
IF: 3.499

A series of new 2-pyridylhexahydrocycloocta[4,5]thieno[2,3-d]pyrimidines with different substituents as C-4 position were synthesized. The anticancer activity of the newly synthesized compounds were tested in vitro using a two stage process utilizing 60 different human tumor cell lines representing leukemia, melanoma and cancers of lung, colon, central nervous system, ovary, kidney, prostate as well as breast. Compounds 4a, 6a, 7a, 7d and 7g showed potent anticancer activity at low concentrations against most of the used human tumor cell lines comparable with doxorubicin as standard potent anticancer drug (average  $\log_{10} \text{GI}_{50}$  over all cell lines = -6.85). Also, compound 4b was selective against SNB-75 (CNS cancer)  $\log_{10} \text{GI}_{50}$  = -5.57. Interestingly, compound 7e exhibited promising selectivity against 13 tumor cell lines showing growth inhibition percentages between 54.05 and 89.23.

**Keywords:** 2-Pyridyl hexahydrocyclooctathieno [2,3-D] pyrimidines; 2-Pyridyl hexahydrocyclooctathieno[2,3-D]pyrimidin-4(3H) - ones; Synthesis; Anticancer activity.

##### 1471. Advances in the Discovery of Kinesin Spindle Protein (Eg5) Inhibitors as Antitumor Agents

Hala Bakr Ali El-Nassan

*European Journal of Medicinal Chemistry*, 62: 614-631 (2013)  
IF: 3.499

Cancer is considered as one of the most serious health problems. Despite the presence of many effective chemotherapeutic agents, their severe side effects together with the appearance of mutant tumors limit the use of these drugs and increase the need for new anticancer agents. Eg5 represents an attractive target for medicinal chemists since Eg5 is overexpressed in many proliferative tissues while almost no Eg5 is detected in nonproliferative tissues. Many Eg5 inhibitors displayed potent anticancer activity against some of the mutant tumors with limited side effects. The present review provides an overview about the progress in the discovery of Eg5 inhibitors especially from 2009 to 2012 as well as the clinical trials conducted on some of these inhibitors.

**Keywords:** Eg5; KSP; Inhibitors; Antimitotic agents.

##### 1472. Synthesis and Anticonvulsant Activity of New Phenytoin Derivatives

Nadia Abdalla Khalil, S. Botros, Bassem H. Naguib and Yara El-Dash

*European Journal of Medicinal Chemistry*, 60: 57-63 (2013)  
IF: 3.499

Hybrids between phenytoin and thiosemicarbazide, 1,3,4-oxadiazole, 1,3,4-thiadiazole or 1,2,4-triazole were synthesized and tested for anticonvulsant activity. Preliminary anticonvulsant screening was performed using standard maximal electroshock (MES) and subcutaneous pentylenetetrazole (scPTZ) screens in mice. The neurotoxicity was determined applying the rotarod test. Among these compounds, 4 and 5d showed the highest protection (80%) in the scPTZ test at a dose of 100 mg/kg, whereas the compound 5b displayed promising anticonvulsant effect in the MES model.

**Keywords:** Phenytoin; Oxadiazole; Thiadiazole; Triazole; Anticonvulsant activity.

##### 1473. Synthesis of Novel Chromene Derivatives of Expected Antitumor Activity

Aliaa Mohamed Amin, Manal M. Kandeel, Eman K. A. Abdelall and Heba A. H. Elshemy

*European Journal of Medicinal Chemistry*, 59: 183-193 (2013)  
IF: 3.499

Inhibition of tubulin polymerization is one of the important tactics in cancer therapy. Since 4-aryl-4H-chromene derivatives are found to be microtubule-binding agents via interfering with tubulin polymerization so we decide to concentrate our exploration efforts on the combination of this nucleus with 5-, 6-, and/or 7-membered heterocyclic moieties in a novel series of compounds to explore the effect that might result from this combination. Ten novel compounds were selected for anticancer screening assay against MCF-7 breast cancer cell line in comparison to colchicine as positive control and most of them showed excellent activity.

**Keywords:** Microtubule-binding agents; 4-Aryl-4H-chromenes; Heterocyclic moieties; Breast cancer; Cytotoxic activity.

##### 1474. Selective Sequential Cross-Coupling Reactions on Imidazole Towards Neurodazine and Analogues

Lisa-Maria Recnik, Mohammed Abd El Hameid, Maximilian Haider, Michael Schnürch and Marko D. Mihovilovic

*Synthesis*, 45: 1387-1405 (2013) IF: 2.5

Polysubstituted imidazoles represent a common structural motif in bioactive molecules. A modular and flexible strategy towards 2,4,5-triarylated imidazoles is reported applying a Suzuki-Miyaura cross-coupling protocol. Employing 1-protected 2,4,5-tribromoimidazole as starting material, both stepwise and one-pot protocols towards the title compounds are disclosed. The utility of the approach was demonstrated by synthesizing neurodazine, a biologically active molecule affecting neuronal cell differentiation.

**Keywords:** Heterocycles; Cross-coupling; Palladium; Regioselectivity; Homogeneous catalysis.

**1475. Novel 4-Substituted -2 (1H)-phthalazinone Derivatives: Synthesis, Molecular Modeling Study and their Effects On  $\alpha$ -Receptors**

Nadia A. Khalil, Eman M. Ahmed, Hosam A. Elshihawy and Sawsan A. Zaitone

*Medicinal Chemistry Research*, 22(3): 1057-1064 (2013) IF: 1.612

Novel 4-(4-bromophenyl) phthalazine derivatives connected via an alkyl spacer to amine or N-substituted piperazine were designed and synthesized as promising  $\alpha$ -adrenoceptor antagonists. The structures of the phthalazine derivatives were established using elemental and spectral analyses. Twelve of the tested compounds displayed significant  $\alpha$ -blocking activity. Molecular modeling studies were performed to rationalize the biological results. Among the tested compounds, 7j displayed the best-fitting score and the highest in vitro activity.

**Keywords:** Phthalazinones;  $\alpha$ -Adrenoceptor antagonists; Molecular modeling; Arylpiperazine.

**1476. Design and Synthesis of Some Thieno[2,3-C] Pyridazine Derivatives of Expected Anticancer Activity**

Aliaa Mohamed Kamal, Afaf K. El-Ansary and Mokhtar AbdHafiz Al-Ghorafi

*Medicinal Chemistry Research*, 22: 2589-2601 (2013) IF: 1.612

Design and synthesis of some new thienopyridazine derivatives as anticancer agents were the goal of this work. Accordingly, a series of novel compounds were synthesized via reacting thienopyridazine carboxylic acid hydrazide with different organic reagents. Twelve novel compounds were selected by National Cancer Institute for a full anticancer screening assay where seven of the investigated compounds showed non-selective broad spectrum and promising activity almost against all cancer cell lines. One of the most active compounds was chosen to be evaluated against 60-cell line panel at five concentration levels and revealed a remarkable growth inhibition activity.

**Keywords:** Antitumor agents; Thieno [2,3-C] pyridazines; Cytotoxic activity; Pharmacophores; Improving chemotherapy regimen.

**1477. Design and Synthesis of Thienopyridines as Novel Templates for Acetylcholinesterase Inhibitors**

Suzan Mohamed Aboel-Maaty, Mohga M. Badran, Maha Abdel Hakeem, Afaf El-Malah and Rania M. Abdel Salam

*Medicinal Chemistry Research*, 22: 4087-4095 (2013) IF: 1.612

New dual binding site acetylcholinesterase (AChE) inhibitors have been designed and synthesized as a new drug candidate for the treatment of Alzheimer's disease (AD) through the binding to both catalytic and peripheral sites of the enzyme. Therefore, a series of thienopyridine analogs of tacrine were synthesized and investigated for their ability to inhibit the activity of AChE in comparison with tacrine. All the compounds were found to inhibit AChE activity, especially compounds 7b and 11a, which were found to be more potent than tacrine.

**Keywords:** Synthesis; Thienopyridines; AChE inhibitors; Alzheimer's disease.

**1478. Synthesis, Characterization, and Biological Evaluation of Certain 1,3-Thiazolone Derivatives Bearing Pyrazoline Moiety as Potential Anti-Breast Cancer Agents**

Nadia Abdalla Khalil, Eman M. Ahmed and Hala B. El-Nassan

*Medicinal Chemistry Research*, 22: 1021-1027 (2013) IF: 1.612

A series of 5-arylidene-2-(3,5-diaryl-4,5-dihydro-1H-pyrazol-1-yl)-1,3-thiazol-4(5H)-ones were synthesized and screened for their in vitro antitumor activity against human breast adenocarcinoma cell line (MCF-7). Five of the test compounds exhibited good antitumor activity superior to the reference drug, doxorubicin, with IC<sub>50</sub> range 1.4–2.3  $\mu$ M. Among the test compounds, 2-[3,5-bis(4-chlorophenyl)-4,5-dihydro-1H-pyrazol-1-yl]-5-(2-methoxybenzylidene)-1,3-thiazol-4(5H)-one (3i) was found to show the most potent anticancer activity.

**Keywords:** Pyrazoline; 1,3-Thiazolone; Antitumor activity; MCF.

**1479. Synthesis and Biological Evaluation of New Heteroaryl Carboxylic Acid Derivatives as Anti-Inflammatory-Analgesic Agents**

Eman Mohamed Mostafa, Khaled Abouzid Mohamed, Nadia Abdalla Khalil and Sawsan Abo-Bakr Zaitone

*Chemical; Pharmaceutical Bulletin of Japan*, 61(2): 222-228 (2013) IF: 1.56

A series of nicotinic acid derivatives structurally related to niflumic acid and certain pyridazine-containing compounds have been synthesized and characterized by analytical and spectral data. All compounds were screened for their potential analgesic and anti-inflammatory activities. The compounds which displayed analgesic and anti-inflammatory activities were tested for ulcerogenicity and screened for in vivo inhibition of certain inflammatory cytokines such as tumor necrosis factor- $\alpha$  (TNF- $\alpha$ ), interleukin-6 (IL-6), and cyclooxygenase-2 (COX-2). Compounds 1c, 2a, 2b, and 5a have shown potent analgesic and anti-inflammatory activities.

**Keywords:** Nicotinic acid; Niflumic acid; Pyridazine; Analgesic; Anti-inflammatory.

**1480. Synthesis of New Nicotinic Acid Derivatives and their Evaluation as Analgesic and Anti-Inflammatory Agents**

Nadia Abdalla Khalil, Eman Mohamed Ahmed, Khaled Omar Mohamed and Sawsan Abo-Bakr Zaitone

*Chemical Pharmaceutical Bulletin (Japan)*, 61: 933-940 (2013) IF: 1.564

A series of 2-substituted phenyl derivatives of nicotinic acid 4a–l were synthesized and evaluated for their analgesic and anti-inflammatory activities. Compounds including 2-bromophenyl substituent, 4a, c, and d, proved to display distinctive analgesic and anti-inflammatory activities in comparison to mefenamic acid as a reference drug. Compound 4c could be identified as the most biologically active member within this study with an interesting dual anti-inflammatory analgesic profile. Effect of the compounds 4a–l on the serum level of certain inflammatory cytokines such as

tumor necrosis factor (TNF)- $\alpha$  and interleukin (IL)-6 was also determined.

**Keywords:** Nicotinic acid; Fenamate; Analgesic; Anti-inflammatory.

#### 1481. Synthesis of Some Novel Thieno [3,2-*d*] Pyrimidines as Potential Cytotoxic Small Molecules Against Breast Cancer

Mohammed Kamal Abdel Hameid, Manal Kandeel, Kamal Eman, and Madlen Berty Labib

*Chem. Pharm. Bull. (Tokyo)*, 61(6): 637-647 (2013) IF: 1.564

A variety of novel thieno[3,2-*d*]pyrimidines with different decorating functional groups were synthesized as a part of a study aiming to enrich the arsenal of chemotherapeutic agents for the treatment of cancer. The design of synthetic molecules based on DNA-interchelating properties by hydrogen bond formation. The reported compounds herein are: 4-aminothienopyrimidine derivatives 4a, b and their 4-substituted phenylamino analogues 8a, b; 4-thienopyrimidin-4-ones 5a, b; N-alkyl thienopyrimidin-4-ones 6a – g; 4-chloro- thienopyrimidines 7a, b and thienopyrimidoquinazolinones 9a, b which are the structural mimics of 8a, b. The synthesized molecules were evaluated for their in vitro cytotoxic activity against human breast cancer cell line (MCF-7). Biological screening revealed varying cytotoxic potencies of the tested molecules compared with Doxorubicin as a reference drug. The cytotoxicity results from the study suggested that the synthesized 2.04 nmol molecules are potential antitumor agents and compound 4a was the most potent with an IC<sub>50</sub>

**Keywords:** Heterocycle; Thieno[3,2-*d*] pyrimidine; Cytotoxic activity; Breast cancer.

#### 1482. 3-[(6-Arylamino)Pyridazinylamino]Benzoic Acids: Design, Synthesis and *in Vitro* Evaluation of Anticancer Activity

Nadia Abdalla Khalil, Khaled A. M. Abouzid, Eman M. Ahmed and Khaled Omar Mohamed

*Archives of Pharmacal Research*, 36: 41-50 (2013) IF: 1.538

A series of novel substituted 3,6-disubstituted pyridazines based on the structure of vatalanib (PTK787) were designed and synthesized. The cytotoxicity of the final compounds was tested in vitro on HT-29 colon cancer cell line. Compounds 2a and 2b with 4-chlorophenylamino moiety, exerted the highest cytotoxic activity with IC<sub>50</sub> values equal to 15.3 and 3.9  $\mu$ M respectively. The most promising compound, 2b, was found to be about fivefold more active than vatalanib against HT-29 colon cancer cell line.

**Keywords:** Pyridazine; Colon cancer; Vatalanib; Cytotoxic.

#### 1483. Novel 4-Substituted-2(1*H*)-Phthalazinone Derivatives: Synthesis, Molecular Modeling Study and Their Effects on $\alpha$ -Receptors

Eman Mohamed Ahmed, Nadia A. Khalil, Hosam A. Elshihawy and Sawsan A. Zaitone

*Archives of Pharmacal Research*, 36 (6): 671-683 (2013) IF: 1.538

Novel 4-(4-bromophenyl) phthalazine derivatives connected via an alkyl spacer to amine or N-substituted piperazine were designed and synthesized as promising  $\alpha$ -adrenoceptor antagonists. The structures of the phthalazine derivatives were established using elemental and spectral analyses. Twelve of the tested compounds displayed significant  $\alpha$ -blocking activity. Molecular modeling studies were performed to rationalize the biological results. Among the tested compounds, 7j displayed the best-fitting score and the highest in vitro activity.

**Keywords:** Phthalazinones;  $\alpha$ -Adrenoceptor antagonists; Molecular modeling; Arylpiperazine.

#### 1484. Synthesis of New 1,3,4-Benzotriazepin-5-One Derivatives and their Biological Evaluation as Antitumor Agents

Lamia Wagdy Mohamed and Azza T. Taher

*Archives of Pharmacal Research*, 36: 684-693 (2013) IF: 1.538

New derivatives of 1,3,4-benzotriazepin-5-one were designed and synthesized as structural analogues to the antitumor agents devazepide and asperlicin. An efficient and novel approach to the synthesis of 2-amino-1,3,4-benzotriazepin-5-one 2 was developed and its structure was confirmed. The newly synthesized derivatives were evaluated for their in vitro antitumor activity on 60 different cell lines. Compounds 8 and 9 displayed the most potent antitumor activity against several cell lines specifically ovarian cancer, renal cancer and prostate cancer, while compounds 5, 10 and 12 showed significant activities against UO-31 renal cancer cell line.

**Keywords:** 1,3,4- Benzotriazepin-5-one derivatives; Synthesis; Antitumor activity.

#### 1485. Synthesis and Binding Study of Certain 6-Arylalkanamides as Molecular Probes for Cannabinoid Receptor Subtypes

Azza T. Taher, Hanan H. Kadry, Marco Allarà, Vincenzo Di Marzo, Ashraf H. Abadi, and Khaled A. Abouzid

*Journal of Enzyme Inhibition and Medicinal Chemistry*, 28 (3): 436-439 (2013) IF: 1.495

Tetrahydrocannabinol and other mixed cannabinoid (CB) receptors CB<sub>1</sub>/CB<sub>2</sub> receptor agonists are well established to elicit antinociceptive effects and psychomimetic actions, however, their potential for abuse have dampened enthusiasm for their therapeutic development. In an effort to refine a semi-rigid structural framework for CB<sub>2</sub> receptors binding, we designed novel compounds based on aromatic moiety and flexible linker with various amides mimicking the outlook of the endogenous anandamide which could provide as CB<sub>2</sub> receptor ligand. In this direction, we developed and synthesized new aryl or arylidene hexanoic acid amides and aryl alkanolic acid diamide carrying different head groups. These new compounds were tested for their affinities for human recombinant CB receptors CB<sub>1</sub> and CB<sub>2</sub> and fatty acid amide hydrolase. Although, the preliminary screening of these compounds demonstrated weak binding activity towards CB receptor subtypes at 10  $\mu$ M, yet this template still could serve up as probes for further optimization and development of affinity ligand for CB receptors.

**Keywords:** Cannabinoid; Selective CB<sub>2</sub> Ligands; Synthesis.

#### 1486. Design, Synthesis and Cytotoxic Activity of Some Novel Compounds Containing Pyrazolo[3,4-*d*] Pyrimidines Nucleus

Manal Mustafa Kandeel, Sameha M. Roshdy, Eman K. A. Abdelall, Mohamed A. Abdelgawad and Phoebe F. Lamie

*Journal of Chemical Sciences*, 125 (5): 1029-1034 (2013)  
IF: 1.298

Novel pyrazolo [3,4-*d*] pyrimidines were designed and synthesized as antitumor agents against human breast cancer adenoma (MCF-7). Molecular modelling and pharmacological screening were performed against breast cancer cell line and also certain synthetic pathways were developed in order to introduce functionality onto C6 and N5 positions of pyrimidine moiety. Surprisingly, all the test compounds showed IC<sub>50</sub> lower than that of the standard olomoucine I, especially compounds 4b, 8a, 10b, 11a and b, which showed IC<sub>50</sub> between 0.009 and 0.004  $\mu$ M.

**Keywords:** Pyrazolo [3,4-*d*] pyrimidine derivatives; Cytotoxic activity; MCF-7; Cyclin-dependent kinase inhibitors (CDKI).

#### 1487. Design, Synthesis, and Cytotoxicity of Pyridine, Pyrazole, and Thiazole Derivatives Derived from N-Alkyl-4,5,6,7-Tetrahydro-1-Benzothiophene

Mona Monir Kamel, A. K. El-Ansary and Y. R. Milad

*Chemistry of Heterocyclic Compounds*, 49: 392-403 (2013)  
IF: 0.634

The reaction of 4,5,6,7-tetrahydro-1-benzothiophene derivatives with ethyl acetoacetate gave oxobutanamide derivatives. The reactivity of these products towards some chemical reagents was studied to afford new heterocyclic derivatives. The cytotoxicity of the newly synthesized compounds was evaluated against three human tumor cells lines and three normal cell lines. The results showed that some of these compounds exhibit high inhibitory effects towards the three tumor cell lines and the normal cell lines.

**Keywords:** Pyridine; Tetrahydro-1-benzothiophene; Thiazole; Thiophene; Cytotoxicity.

#### 1488. Design and Synthesis of Novel Pyrano [2,3-*C*] Pyrazoles and Related Fused Ring Systems and Evaluation of Antiinflammatory, Analgesic and Antipyretic Activities

Azza Taher Shalaby, Afaf K. El-Ansary, Ahmed Abd El-Hamed El-Rahmany, Wafaa El-Eraky and Sally A. El-Awdan

*Life Science Journal*, 10 (2): 904-914 (2013) IF: 0.165

A series of some new pyrano [2,3-*d*]pyrimidine derivatives were synthesized and evaluated for their antiinflammatory as well as analgesic and antipyretic activities. The results showed that all compounds possessed promising anti-inflammatory activity. Compounds 6a and 9b have shown a potent anti-inflammatory activity more than piroxicam reference drug. Whereas, compounds 6c, 8a, 9a and 10a,b exhibited equipotent analgesic activity compared to piroxicam and compound 10b showed excellent antipyretic activity more than piroxicam. None of the tested compounds showed an ulcerogenic effect.

**Keywords:** Pyrano [2,3-*C*] pyrazole; Pyrano[2,3-*d*] pyrimidine; Synthesis; Anti-inflammatory; Analgesic; Antipyretic.

#### 1489. Synthesis and Cytotoxic Activity of Certain Diaryl Cyclohexene Derivatives Structurally Related to Combretastatins

Mohammed Kamal Abdel Hameid, A. Aboul-Magd, M. M. Kandeel and S. Elmeligie

*International Journal of Medicine ;Pharmaceutical Sciences (Ijmps)*; 3: 63-75 (2013)

A series of compounds structurally based on 3,5-diarylcyclohexene core was synthesized aiming to enrich the arsenal of chemotherapeutic agents for the treatment of cancer. The synthetic pathways for the preparation of the target molecules passed via certain intermediates as 3,5-diaryl-2-cyclohexen-1-ones 3a-d which were prepared by decarboxylation of the esters 2a-d then reacting them with 2-cyanoacetic acid hydrazide to give 2-cyanoacetohydrazide derivatives 4a-d. The latter compounds were used in a series of reactions to afford the target molecules Mannich compounds 5a-d, acrylohydrazide derivatives 6a-d and the pyridine compounds 7a-c and 8a,b. All newly prepared compounds were subjected to in vitro cytotoxic activity against human breast carcinoma cell line (MCF-7). Cytotoxicity screening revealed different antitumor potencies in comparison to colchicine as a reference drug. Starting with 3,5-diarylcyclohexenone derivative 3d that was more potent than colchicine, Mannich derivatives 5a-d were less active than the reference drug, the acrylohydrazide derivatives 6a-d showed equal activity to colchicine. Pyridine derivatives 7a-c and 8a,b showed higher cytotoxic activity. Compound 8b was the most potent with an IC<sub>50</sub> of 2.35 nM.

**Keywords:** Cyclohexenones; Cyanoacetohydrazides; Tubulin; Breast carcinoma.

#### 1490. Synthesis and in Vitro Antitumor Activity of New Benzothiazole and Benzoxazole Derivatives

Mohammed Kamal Abdel Hameid, Manal M. Kandeel, Eman K. A. Abdelall, Mohammed K. Abd El Hamid, Mohamed A. Abdelgawad and John N. Philoppes

*Journal of Chemical and Pharmaceutical Research*, 5 (8): 16-21 (2013)

A series of benzothiazole and benzoxazole derivatives were synthesized from their parents whom bearing o-aminocyanogroups then functionalized on amino group or cyano group. Some of the newly formed compounds were evaluated, in vitro, for their antitumor activity against MCF-7. Compound 4b was the most potent, showing activity (0.011  $\mu$ M). IC<sub>50</sub>.

**Keywords:** Antitumor activity; Benzothiazoles; Benzoxazoles; MCF-7.

#### 1491. Synthesis and in Vitro Antitumor Activity of Some new Mannich Bases

Hanan Hassan Kadry, Manal M. Kandeel, Nadia A. Abdou and Rana M. El-Masry

*International Journal of Chemtech Research*, 5 (1): 401-408 (2013)

Two series of Novel Mannich bases has been synthesized from chalcones 3 and 7 and evaluated for their in vitro cytotoxic activity. Out of the newly synthesized compounds, four derivatives 4a, 4b, 4e, 4f were selected by the National Cancer Institute (NCI) to be evaluated for their in-vitro antitumor activity by in-vitrodisease-oriented human cells screening panel assay. All the tested compounds exhibited a broad spectrum of antitumor activity against renal cancer UO-31.

**Keywords:** Antitumor activity; Cytotoxicity; Chalcones; Mannich bases; Synthesis.

#### 1492. Synthesis of Certain Fused Pyrrolothieno [3, 2-E] Pyrazine Derivatives with Possible Anxiolytic Activity

Mohammed Kamal Abdel Hameid, Mohga M. Badran and Samhia M.A. Roshdy

*Organic Chemistry (An Indian Journal)*, 9 (11): 427-436 (2013)

The work comprises the synthesis of some newly 4-Substituted dopyrrolothienopyrazines (XIV) with possible anxiolytic effect by either cyclization of urea derivatives (XI) with phosphorus oxychloride or by reaction of 4-chloropyrrolothienopyrazine (XII) with morpholine. Also, 4-alkoxy pyrrolothienopyrazines (XIII) was prepared by heating of pyrrolothienopyrazin-4(5H)-one (VIII) with phosphorus oxychloride to afford 4-chloropyrrolothienopyrazine (XII) which upon reaction with certain alcohols in presence of sodium metal yielded alkoxy pyrrolothienopyrazines (XIII). Boiling of either compound (IV) or the azide (VII) with *o*-dichlorobenzene afforded pyrrolothienopyrazine-4(5H)-one (VIII).

In different yields Reaction of the acid hydrazide (VI) with sodium nitrite and concentrated hydrochloric acid afforded the new acyl azide (VII). Refluxing the acid (III) with thionyl chloride produced the intermediate 2-(pyrrol-1-yl)-3-thiophene carbonyl chloride (V) which upon heating with hydrazine hydrate gave the desired acid hydrazide (VI). Reaction of 2-(pyrrol-1-yl)-3-thiophene carboxylic acid (III) with ethyl chloroformate, triethylamine and diphenyl phosphoryl azide (DPPA) afforded the unexpected urea derivative (IV).

Open field test was done to determine changes of animal behaviors and as screening for antipsychotic activity for some of the prepared compounds, thus it can be concluded that some of the prepared compounds showed central sedative effects and possible anti-anxiety activity.

**Keywords:** 5-HT; Anxiolytic; Pyrrolothienopyrazine.

#### 1493. Synthesis, Antimicrobial and Cytotoxic Activity of Novel 4-Phenoxy and 4-(Substitutedamino) Pyrazolo [3, 4-d] Pyrimidine Derivatives

Mohammed Kamal Abd El Hameid, Hala Bakr El-Nassan and Khaled Omar Ahmed.

*Organic Chemistry an Indian Journal*, 9 (9): (2013)

A series of new pyrazolopyrimidines was synthesized. Antimicrobial screening was done for the novel molecules to discover their activity against some test organisms, *Staphylococcus aureus* (ATCC 25923) (as example for Gram-positive bacteria), *Escherichia coli* (ATCC 25922), *Enterobacter*

*cloacae* (ATCC 23048), *Klebsiella* (ATCC 23495), *Salmonella typhimurium* (as examples for Gram-negative bacteria) and *Candida albicans* (as example for fungi).

The antimicrobial screening results showed that some of these compounds exhibited a significant antimicrobial activity, where, compounds (5c) and (5e) showed the highest antimicrobial activity with MIC of 16 µg/mL, whilst, compounds (4d), (5g) and (5h) displayed antifungal activity against *Candida albicans*. Besides, eight of the newly synthesized compounds were selected by National Cancer Institute NCI (U.S.A) to be screened for their cytotoxic activity. The test compounds showed limited cytotoxic activity.

The cytotoxicity results suggested that substitution at position 4 of pyrazolo [3, 4-d] pyrimidine with aryloxy or substituted anilino moieties was preferred to aralkylamino moiety. Besides, introduction of small lipophilic group like methyl group in the para position of aryloxy or anilino moiety enhanced the cytotoxic activity. The results of cytotoxic screening were in good agreement with the calculated log P of the test compounds.

#### Dept. of Pharmaceutical Technology and Industrial Pharmacy

#### 1494. Fast-Dissolving Sublingual Films of Terbutaline Sulfate: Formulation and *in Vitro*/ *In Vivo* Evaluation

Howida Kamal Ibrahim, Soha Sayed and Mohamed Farid El-Milligi

*Molecular Pharmaceutics*, 10: 2942-2947 (2013) IF: 4.57

Terbutaline sulfate fast dissolving sublingual films were prepared using seven drug compatible film formers in different combinations and proportions.

The film polymers are maltodextrin, Na alginate, Carbowax 430, xanthan gum, HPMC E5, PVP K-25, and Na CMC. Propylene glycol and sorbitol were used as plasticizers and mannitol as filler. The optimum polymer concentrations and the plasticizer amount were selected on the basis of flexibility, tensile strength, and stickiness of the films.

The prepared films were evaluated for their tensile strength, thickness uniformity, disintegration time (in vitro and in vivo), in vitro dissolution, and moisture content. Polymer type rather than total polymer concentration or plasticizer amount showed a significant effect on the tested film properties.

A randomized, single dose, crossover study was conducted in four healthy volunteers to compare the pharmacokinetic profile of terbutaline sulfate from the prepared films and the conventional oral tablets.

The film formula of choice gave a significantly faster drug absorption rate and recorded a relative bioavailability of 204.08%. Sublingual films could be promising as a convenient delivery system for terbutaline sulfate in patients with swallowing problems. The improved extent of absorption (higher AUC(0-24)) indicates success in improving drug bioavailability, and the faster absorption rate could be promising for the management of acute episodes of asthma.

**Keywords:** Terbutaline sulfate; Sublingual; Fast dissolving film.



### 1495. Azithromycin to Prevent Bronchopulmonary Dysplasia in Ureaplasma-Infected Preterm Infants: Pharmacokinetics, Safety, Microbial Response, and Clinical Outcomes with A 20-Milligram-Per-Kilogram Single Intravenous Dose

Ahmed Abdelfattah Othman, Rose M. Viscardi, Hazem E. Hassan, Natalie D. Eddington, Elias Abebe, Michael L. Terrin, David A. Kaufman and Ken B. Waites

*Antimicrobial Agents and Chemotherapy*, 57 (5): 2127-2133 (2013) IF: 4.565

Ureaplasma respiratory tract colonization is associated with bronchopulmonary dysplasia (BPD) in preterm infants. Previously, we demonstrated that a single intravenous (i.v.) dose of azithromycin (10 mg/kg of body weight) is safe but inadequate to eradicate Ureaplasma spp. in preterm infants. We performed a nonrandomized, single-arm open-label study of the pharmacokinetics (PK) and safety of intravenous 20-mg/kg single-dose azithromycin in 13 mechanically ventilated neonates with a gestational age between 24 weeks 0 days and 28 weeks 6 days. Pharmacokinetic data from 25 neonates (12 dosed with 10 mg/kg i.v. and 13 dosed with 20 mg/kg i.v.) were analyzed using a population modeling approach. Using a two-compartment model with allometric scaling of parameters on body weight (WT), the population PK parameter estimates were as follows: clearance,  $0.21 \text{ liter/h} \times \text{WT}(\text{kg})^{0.75}$  [ $\text{WT}(\text{kg})^{0.75}$  indicates that clearance was allometrically scaled on body weight (in kilograms) with a fixed exponent of 0.75]; intercompartmental clearance,  $2.1 \text{ liters/h} \times \text{WT}(\text{kg})^{0.75}$ ; central volume of distribution (V),  $1.97 \text{ liters} \times \text{WT}(\text{kg})$ ; and peripheral V,  $17.9 \text{ liters} \times \text{WT}(\text{kg})$ . There was no evidence of departure from dose proportionality in azithromycin exposure over the tested dose range. The calculated area under the concentration-time curve over 24 h in the steady state divided by the MIC<sub>90</sub> (AUC<sub>24</sub>/MIC<sub>90</sub>) for the single dose of azithromycin (20 mg/kg) was 7.5 h. Simulations suggest that 20 mg/kg for 3 days will maintain azithromycin concentrations of >MIC<sub>50</sub> of 1 µg/ml for this group of Ureaplasma isolates for =96 h after the first dose. Azithromycin was well tolerated with no drug-related adverse events. One of seven (14%) Ureaplasma-positive subjects and three of six (50%) Ureaplasma-negative subjects developed physiologic BPD. Ureaplasma was eradicated in all treated Ureaplasma-positive subjects. Simulations suggest that a multiple-dose regimen may be efficacious for microbial clearance, but the effect on BPD remains to be determined.

**Keywords:** Azithromycin; Pharmacokinetics; Preterm infants; Bronchopulmonary dysplasia.

### 1496. Daptomycin Pharmacokinetics and Pharmacodynamics in A Pooled Sample of Patients Receiving Thrice-Weekly Hemodialysis

Noha Nabil Salama, Jill M. Butterfield, Bruce A. Mueller, Nimish Patel, Katie E. Cardone, Darren W. Grabe and Thomas P. Lodise

*Antimicrobial Agents and Chemotherapy*, 57: 864-872 (2013) IF: 4.565

While the pharmacokinetic (PK) properties of daptomycin in hemodialysis (HD) patients have been evaluated previously by three groups, resultant dosing recommendations have varied. To address this clinical conundrum, this study combined

concentration-time data from these PK evaluations and derived uniform dosing recommendations among patients on HD receiving daptomycin. A two-compartment model with separate HD and non-HD clearance terms was fit to the PK data from these studies by using BigNPAG. Embedded with PK parameters from the population PK analysis, 5,000-subject Monte Carlo simulations (MCS) were performed to identify HD dosing schemes that provided efficacy (cumulative and daily area under the concentration-time curve [AUC] values) and toxicity (trough concentrations of = 24.3 mg/liter) profiles comparable to those from simulations employing the daptomycin PK model derived from the Staphylococcus aureus bacteremia-infective endocarditis (SAB-IE) study. Separate HD dosing schemes were sought for the two weekly interdialytic periods (48 and 72 h). For the 48-h interdialytic period, intra- and post-HD dosing provided the most isometric cumulative and daily AUCs. For the 72-h interdialytic period, all HD dosing schemes provided noncumulative AUC values from 48 to 72 h (AUC<sub>48-72</sub>) that were <50% of the SAB-IE AUC<sub>48-72</sub> values. Increasing the parent dose by 50% intra- or post-HD 0.

\provided comparable AUC(48-72) values, while maintaining acceptable trough concentration (C<sub>min</sub>) values. When efficacy and toxicity profiles were evaluated for each individual study, higher probabilities for C<sub>min</sub> reaching = 24.3 mg/liter were observed in one of the three studies. Given the high probability of C<sub>min</sub> being = 24.3 mg/liter in one of the three studies, more intensive creatine phosphokinase (CPK) monitoring may be warranted in HD patients receiving daptomycin.

**Keywords:** Hemodialysis; Daptomycin; Pharmacokinetics.

### 1497. Pharmacokinetics of Levodopa, Carbidopa, and 3-O-Methyldopa Following 16-Hour Jejunal Infusion of Levodopa-Carbidopa Intestinal Gel in Advanced Parkinson'S Disease Patients

Ahmed Abdelfattah Othman, Dag Nyholm, Per Odin, Anders Johansson, Krai Chatamra, Charles Locke and Sandeep Dutta

*The Aaps Journal*, 15 (2): 316-323 (2013) IF: 4.386

Motor complications of Parkinson's disease (PD) are a consequence of pulsatile dopaminergic stimulation from standard oral levodopa therapy. Levodopa-carbidopa intestinal gel (LCIG) is infused continuously via an intrajejunal percutaneous gastrostomy tube. This was the first study designed to characterize the full pharmacokinetic profiles of levodopa, carbidopa, and levodopa metabolite, 3-O-methyldopa (3-OMD) poirewqyerw f with 16-h LCIG infusion. Nineteen advanced PD patients (mean age, 65 years) who were on LCIG therapy for =30 days were enrolled. Patients received their individualized LCIG infusion doses, and serial pharmacokinetic samples were collected. Eighteen patients completed the study; 19 were assessed for safety. Mean (SD) total levodopa and carbidopa doses were 1,580 (403) and 395 (101)?mg, respectively. Mean (SD) C<sub>avg</sub> (µg/mL) were 2.9 (0.84) for levodopa, 17.1 (4.99) for 3-OMD, and 0.22 (0.08) for carbidopa. The degree of fluctuation [defined as (C<sub>max</sub>?-?C<sub>min</sub>)/C<sub>avg</sub>] in levodopa, 3-OMD, and carbidopa plasma concentrations was very low (0.52, 0.21, and 0.96, respectively) during hours 2–16 of infusion. Accordingly, the within-subject coefficients of variation in levodopa, 3-OMD, and carbidopa concentrations were low (13%, 6%, and 19%, respectively). Three patients (16%) reported =1 treatment-emergent adverse event; none were considered severe.

Continuous intrajejunal LCIG infusion maintained stable plasma levodopa levels over 16 h. Consistent exposure has been shown to reduce motor and nonmotor complications associated with oral medications. LCIG was well tolerated, consistent with previous reports.

**Keywords:** Duodopa; Lcig; Levodopa-carbidopa intestinal gel; Parkinson's Disease; Pharmacokinetics.

#### 1498. An Oral TRPV1 Antagonist Attenuates Laser Radiant-Heat-Evoked Potentials and Pain Ratings From UV<sub>B</sub>-Inflamed and Normal Skin

Ahmed Abdelfattah Othman, Klaus Schaffler, Peter Reeh, W. Rachel Duan, Andrea E. Best, Connie R. Faltynek, Charles Locke and Wolfram Nothaft

*British Journal of Clinical Pharmacology*, 75 (2): 404-414(2013)  
IF: 3.578

**Aims:** Laser (radiant-heat) evoked potentials (LEPs) from vertex-EEG peak-to-peak (PtP) amplitude were used to determine acute antinociceptive/antihyperalgesic efficacy of ABT-102, a novel TRPV1 antagonist efficacious in preclinical pain models, compared with activecontrols and placebo in normal and UV<sub>B</sub>-inflamed skin.

**Methods:** This was a randomized, placebo- and active-controlled, double-blind, intra-individual, crossover trial. Twenty-four healthy subjects received six sequences of single doses of ABT-102 (0.5, 2, 6 mg), etoricoxib 90 mg, tramadol 100 mg and placebo. Painful stimuli were induced by CO<sub>2</sub>-laser on normal and UVB-inflamed skin. LEPs and visual analogue scale (VAS-pain) ratings were taken at baseline and hourly up to 8h post-dose from both skin types.

**Results:** Compared with placebo, significant mean decreases in the primary variable of LEP PtP-amplitude from UVB-inflamed skin were observed with ABT-102 6 mg ( $P < 0.001$ ), ABT-102 2 mg ( $P = 0.002$ ), tramadol 100 mg ( $P < 0.001$ ), and etoricoxib 90 mg ( $P = 0.001$ ) over the 8 h period; ABT-102 0.5 mg was similar to placebo. ABT-102 6 mg was superior to active controls over the 8 h period ( $P < 0.05$ ) whereas ABT-102 2 mg was comparable. Improvements in VAS scores compared with placebo were observed with ABT-102 6 mg ( $P < 0.001$ ) and ABT-102 2 mg ( $P = 0.002$ ). ABT-102 average plasma concentrations were 1.3, 4.4 and 9.4 ng ml<sup>-1</sup> for the 0.5, 2 and 6 mg doses, respectively. There were no clinically significant safety findings.

**Conclusions:** TRPV-1 antagonism appears promising in the management of clinical pain, but requires further investigation.

**Keywords:** Analgesia; Hyperalgesia; Laser evoked potentials; Phase 1; UV-Inflamed skin; Visual analogue scale.

#### 1499. Effects of the TRPV1 Antagonist ABT-102 on Body Temperature in Healthy Volunteers: Pharmacokinetic/ Pharmacodynamic Analysis of Three Phase 1 Trials

Ahmed A. Othman, Wolfram Nothaft, Walid M. Awni and Sandeep Dutta

*British Journal of Clinical Pharmacology*, 75 (4): 1029-1040 (2013) IF: 3.578

**Aim :** To characterize quantitatively the relationship between ABT-102, a potent and selective TRPV1 antagonist, exposure and

its effects on body temperature in humans using a population pharmacokinetic/pharmacodynamic modelling approach.

**Methods :** Serial pharmacokinetic and body temperature (oral or core) measurements from three double-blind, randomized, placebo-controlled studies [single dose (2, 6, 18, 30 and 40 mg, solution formulation), multiple dose (2, 4 and 8 mg twice daily for 7 days, solution formulation) and multiple-dose (1, 2 and 4 mg twice daily for 7 days, solid dispersion formulation)] were analyzed. nonmem was used for model development and the model building steps were guided by pre-specified diagnostic and statistical criteria. The final model was qualified using non-parametric bootstrap and visual predictive check.

**Results:** The developed body temperature model included additive components of baseline, circadian rhythm (cosine function of time) and ABT-102 effect (Emax function of plasma concentration) with tolerance development (decrease in ABT-102 Emax over time). Type of body temperature measurement (oral vs. core) was included as a fixed effect on baseline, amplitude of circadian rhythm and residual error. The model estimates (95% bootstrap confidence interval) were: baseline oral body temperature, 36.3 (36.3, 36.4)°C; baseline core body temperature, 37.0 (37.0, 37.1)°C; oral circadian amplitude, 0.25 (0.22, 0.28)°C; core circadian amplitude, 0.31 (0.28, 0.34)°C; circadian phase shift, 7.6 (7.3, 7.9) h; ABT-102 Emax, 2.2 (1.9, 2.7)°C; ABT-102 EC50, 20 (15, 28) ng/ml-1; tolerance T50, 28 (20, 43) h.

**Conclusions:** At exposures predicted to exert analgesic activity in humans, the effect of ABT-102 on body temperature is estimated to be 0.6 to 0.8°C. This effect attenuates within 2 to 3 days of dosing.

**Keywords:** Abt-102; Body temperature; Nonmem; Population modeling; Tolerance; TRPV1.

#### 1500. Safety, Tolerability and Pharmacokinetics of the Histamine H3 Receptor Antagonist, ABT-288, in Healthy Young Adults and Elderly Volunteers

Ahmed Abdelfattah Othman, George Haig, Hana Florian, Charles Locke, Jun Zhang and Sandeep Dutta

*British Journal of Clinical Pharmacology*, 75 (5): 1299-1311 (2013) IF: 3.578

**Aim:** The objective of this work was to characterize the safety, tolerability and pharmacokinetics of ABT-288, a highly selective histamine H3 receptor antagonist, in healthy young adults and elderly subjects following single and multiple dosing in a phase 1 setting.

**Methods:** Single doses (0.1, 0.3, 1, 3, 10, 20 and 40 mg ABT-288) and multiple doses (0.5, 1.5, 3 and 6 mg ABT-288 once-daily for 14 days) were evaluated in young adults and multiple doses (0.5, 1.5, 3 and 5 mg ABT-288 once-daily for 12 days) were evaluated in elderly subjects using randomized, double-blind, placebo-controlled, dose-escalating study designs. The effect of food on ABT-288 pharmacokinetics (5 mg single dose) was evaluated using an open label, randomized, crossover design.

**Results:** ABT-288 safety, tolerability and pharmacokinetics were comparable in young and elderly subjects. Single doses up to 40 mg and multiple doses up to 3 mg once-daily were generally safe and well tolerated. The most frequently reported adverse events were hot flush, headache, abnormal dreams, insomnia, nausea and dizziness. ABT-288 exposure (AUC) was dose-proportional over the evaluated dose ranges. The mean elimination half-life ranged from 40 to 61 h across dose groups.

Steady state was achieved by day 10 of once-daily dosing with 3.4- to 4.2-fold accumulation. Food did not have a clinically meaningful effect on ABT-288 exposure.

**Conclusions:** Based on the above results, 1 and 3mg once-daily doses of ABT-288 were advanced to phase 2 evaluation in Alzheimer's patients.

**Keywords:** ABT-288; Alzheimer's; Cognition; H3 Receptors; Pharmacokinetics; Tolerability.

### 1501. Brain Targeting of Olanzapine Via Intranasal Delivery of Core-Shell Difunctional Block Copolymer Mixed Nanomicellar Carriers: *in vitro* Characterization, *Ex Vivo* Estimation of Nasal Toxicity and *in Vivo* Biodistribution Studies

Ghada Ahmed Abdelbary and Mina Ibrahim Tadros

*International Journal of Pharmaceutics*, 452: 300-310 (2013)

IF: 3.458

Olanzapine (OZ) is atypical antipsychotic drug that suffers from low brain permeability due to efflux by P-glycoproteins and hepatic first-pass metabolism. The current work aimed to develop OZ-loaded micellar nanocarriers and investigate their nose-to-brain targeting potential. OZ-loaded (5 mg/ml) micelles (F1-F12) were prepared, using a Pluronic® mixture of L121 and P123, adopting thin-film hydration method. The micelles were evaluated for turbidity, particle size, morphology, drug-entrapment efficiency (EE%), drug-loading characteristics, *in vitro* drug release and *ex vivo* nasal toxicity in sheep. The *in vivo* biodistribution and pharmacokinetic studies in the brain/blood following intravenous (i.v.) and intranasal (i.n.) administrations of technetium-labeled OZ-loaded micelles and OZ-solution were evaluated in rats. Spherical micelles ranging in size from 18.97 to 380.70 nm were successfully developed. <sup>1</sup>H NMR studies confirmed OZ incorporation into micelle core. At a drug:Pluronic® L121:Pluronic® P123 ratio of 1:8:32 (F11), the micelles achieved a conciliation between kinetic and thermodynamic stability, high drug-EE%, controlled drug-release characteristics and evoked minor histopathological changes in sheep nasal mucosa. The significantly ( $P < 0.05$ ) higher values for F11 micelles (i.n.); brain/blood ratio (0.92), drug targeting index (5.20), drug targeting efficiency (520.26%) and direct transport percentage (80.76%) confirmed the development of a promising non-invasive OZ-loaded nose-to-brain delivery system.

**Keywords:** Olanzapine; Polymeric mixed micelles; Radiolabeling; Nose-to-brain delivery; *In vivo* biodistribution.

### 1502. Hydroxychloroquine Niosomes: A New Trend in Topical Management of Oral Lichen Planus

Ehab Rasmy Bendas, Hamoud Abdullah, Mohamed H.M. El-Komy and Mohamed A.A. Kassem

*International Journal of Pharmaceutics*, 458: 287-295 (2013)

IF: 3.458

The work aimed at studying a novel topical niosomal gel formulation of hydroxychloroquine for the management of oral lichen planus. Niosomes have been reported as conceivable vesicles to deliver drug molecules to the desired mucous membrane or skin layers. Hydroxychloroquine niosomes were designed using different methods of preparation. Tween 20 and

cholesterol in molar ratio (1:0.5) were used. The prepared systems were characterized for entrapment efficiency, particle size and *in vitro* drug release. Different factors affecting the encapsulation of hydroxychloroquine in niosomes were studied vs. varying the type of surfactant, the cholesterol:surfactant molar ratio and the amount of the drug. The selected niosome formulation was dispersed in different gel formulations and evaluated according to the *in vitro* drug release and the physical stability. The results showed that the type of surfactant, cholesterol ratio and incorporated amount of drug altered the entrapment efficiency and the *in vitro* release of hydroxychloroquine from niosomes. The optimum formulation was prepared by reverse phase evaporation technique using Brij 98:cholesterol molar ratio (1:1.5) and containing 20 mg of hydroxychloroquine and incorporated in 20% w/v Pluronic F-127 gel. A double-blind, controlled clinical study was performed using two groups of patients. Group A ( $n = 11$ ) who received hydroxychloroquine niosomal gel formulation, one application-a-day over 4 months showed 64.28% reduction in the size of lesions and the average score of pain was reduced from "4" to "1". Compared to placebo group B ( $n = 5$ ), who showed only 3.94% reduction in the lesion size and the average score of pain was remained "3". Our results suggest that these niosomal formulations could constitute a promising approach for the topical treatment of oral lichen planus in short time with less side effects and no recurrence after stopping the treatment.

**Keywords:** Hydroxychloroquine; Niosomes; Pluronic F-127 gel; Oral lichen planus; Clinical study.

### 1503. Microemulsion and Poloxamer Microemulsion-Based Gel for Sustained Transdermal Delivery of Diclofenac Epilamine Using in-Skin Drug Depot: *in Vitro/in Vivo* Evaluation

Emad Basalious Bashir Basalious, Shahinaze A. Fouada, Mohamed A. El-Nabarawib and Saadia A. Tayelb

*International Journal of Pharmaceutics*, 453: 569-578 (2013)

IF: 3.458

Microemulsion (ME) and poloxamer microemulsion-based gel (PMBG) were developed and optimized to enhance transport of diclofenac epilamine (DE) into the skin forming in-skin drug depot for sustained transdermal delivery of drug. D-optimal mixture experimental design was applied to optimize ME that contains maximum amount of oil, minimum globule size and optimum drug solubility. Three formulation variables; the oil phase X1 (Capryol®), Smix X2 (a mixture of Labrasol/Transcutol®, 1:2 w/w) and water X3 were included in the design. The systems were assessed for drug solubility, globule size and light absorbance. Following optimization, the values of formulation components (X1, X2, and X3) were 30%, 50% and 20%, respectively. The optimized ME and PMBG were assessed for pH, drug content, skin irritation, stability studies and *ex vivo* transport in rat skin. Contrary to PMBG and Flector® gel, the optimized ME showed the highest cumulative amount of DE permeated after 8 h and the *in vivo* anti-inflammatory efficacy in rat paw edema was sustained to 12 h after removal of ME applied to the skin confirming the formation of in-skin drug depot. Our results proposed that topical ME formulation, containing higher fraction of oil solubilized drug, could be promising for sustained transdermal delivery of drug.

**Keywords:** Diclofenac epilamine; In-skin depot; Sustained transdermal delivery; D-optimal design; Microemulsion.

**1504. Promising ION-Sensitive in Situ Ocular Nanoemulsion Gels of Terbinafine Hydrochloride: Design, in Vitro Characterization and in Vivo Estimation of the Ocular Irritation and Drug Pharmacokinetics in the Aqueous Humor of Rabbits**

Mina Ibrahim Tadros Ayad, Saadia Ahmed Tayel, Mohamed Ahmed El-Nabarawi and Wessam Hamdy Abd-Elsalam

*International Journal of Pharmaceutics*, 443 (1-2): 293-305 (2013) IF: 3.458

Terbinafine hydrochloride (T-HCl) is recommended for the management of fungal keratitis. To maintain effective aqueous humor concentrations, frequent instillation of T-HCl drops is necessary. This work aimed to develop alternative controlled-release in situ ocular drug-loaded nanoemulsion (NE) gels. Twelve pseudoternary-phase diagrams were constructed using oils (isopropyl myristate/Miglyol® 812), surfactants (Tween® 80/Cremophor® EL), a co-surfactant (polyethylene glycol 400) and water. Eight drug-loaded (0.5%, w/v) NEs were evaluated for thermodynamic stability, morphology, droplet size and drug release in simulated tear fluid (pH 7.4). Following dispersion in gellan gum solution (0.2%, w/w), the in situ NE gels were characterized for transparency, rheological behavior, mucoadhesive force, drug release and histopathological assessment of ocular irritation. Drug pharmacokinetics of sterilized F31 [Miglyol® 812, Cremophor® EL: polyethylene glycol 400 (1:2) and water (5, 55 and 40%, w/w, respectively)] in situ NE gel and oily drug solution were evaluated in rabbit aqueous humor. The NEs were thermodynamically stable and have spherical droplets (<30 nm). The gels were transparent, pseudoplastic, mucoadhesive and showed more retarded zero-order drug release rates. F31 in situ NE gel showed the least ocular irritation potential and significantly ( $P < 0.01$ ) higher  $C_{max}$ , delayed  $T_{max}$ , prolonged mean residence time and increased bioavailability.

**Keywords:** Terbinafine hydrochloride; Gellan gum; In situ gels; Nanoemulsions; Aqueous humor.

**1505. Transdermal Drug Delivery of Paroxetine Through Lipid-Vesicular Formulation to Augment its Bioavailability**

Randa Tag Abd El-rehim, Mohamed A. El-Nabarawi, Ehab R. Bendas and Mohammed Y.S. Abary

*International Journal of Pharmaceutics*, 443: 307-317 (2013) IF: 3.991

Paroxetine (PAX) is the most potent serotonin reuptake blocker antidepressant clinically available. This study is aimed to reduce the side effects accompanied with the initial high plasma concentration after oral administration of PAX and fluctuations in plasma levels and also to decrease the broad metabolism of the drug in the liver by developing and optimizing liposomal transdermal formulation of PAX in order to improve its bioavailability. PAX liposomes were prepared by reverse phase evaporation technique using lecithin phosphatidylcholine (LPC), cholesterol (CHOL) and drug in different molar ratios. The prepared liposomes were characterized for size, shape, entrapment efficiency and in vitro drug release. The studies demonstrated successful preparation of PAX liposomes. The

effect of using different molar ratios of (LPC:CHOL) on entrapment efficiency and on drug release was studied. Liposomes showed percentage entrapment efficiency (%EE) of  $81.22 \pm 3.08\%$  for optimized formula (F5) which composed of (LPC:CHOL, 7:7) and 20 mg of PAX, with average vesicle size of  $220.53 \pm 0.757$  nm. The selected formula F5 (7:7) was incorporated in gel bases of HPMC-E4M (2%, 4%, and 6%). The selected formula of PAX liposomal gel of HPMC-E4M (2% and 4%) were fabricated in the reservoir type of transdermal patches and evaluated through in vitro release. After that the selected formula of PAX liposomal gel transdermal patch was applied to rabbits for in vivo bioavailability study in comparison with oral administration of the marketed PAX tablet. An HPLC method was developed for the determination of PAX in plasma of rabbits after transdermal patch application and oral administration of the marketed PAX tablets of 20 mg dose. The intra- and inter-day accuracy and precision were determined as relative error and relative standard deviation, respectively. The linearity was assessed in the range of 5–200 ng/ml. Pharmacokinetic parameters were determined as the  $C_{max}$  of PAX liposomal transdermal patch was found to be 92.53 ng/ml at  $t_{max}$  of 12 h and AUC<sub>0–48</sub> was 2305.656 ng h/ml and AUC<sub>0–8</sub> was 3852.726 ng h/ml, compared to the  $C_{max}$  of 172.35 ng/ml after oral administration of the marketed PAX tablet with  $t_{max}$  of 6 h and AUC<sub>0–24</sub> was 1206.63 ng h/ml and AUC<sub>0–8</sub> was 1322.878 ng h/ml. These results indicate improvement of bioavailability of the PAX after liposomal transdermal patch application and sustaining of the therapeutic effects compared to oral administration.

**Keywords:** Liposomes; Paroxetine; Lecithin Phosphatidylcholine; Cholesterol; In vitro drug release; Liposomal gel; Transdermal patch; Hplc assay method; Bioavailability study.

**1506. Pharmaceutical and Medical Aspects of Hyaluronic Acid–Ketorolac Combination Therapy in Osteoarthritis Treatment: Radiographic Imaging and Bone Mineral Density**

Hanan Mohamed El Laithy, Alia A. Badawi, Demiana I. Nesseem and Shereen S. El-Husseny

*Journal of Drug Targeting*, 6: 551-563 (2013) IF: 2.995

The objective of this study was to formulate novel painless combined hyaluronic acid (HA)–ketorolac (KT) membrane for the management of osteoarthritis with rapid analgesic onset, thus avoiding HA frequent invasive intra-articular injections and KT gastrointestinal complaints associated with all non-steroidal anti-inflammatory drugs. HA was chemically crosslinked with carbodiimide/glutaraldehyde to yield membrane of low water content. Different in vitro aspects (mechanical properties, water content and in vitro release) were studied leading to an optimized soft, flexible K8 HA membrane containing 30mg KT that achieved the desired balance of excellent elasticity and low water content. Moreover, a successful retardation of KT release rate was achieved (82%) after 48 h with favored initial fast drug release in the first hour (32.7%) to attain rapid analgesic effect. The clinical assessments in arthritic rats revealed apparent improvement in joint space narrowing, highest increase in bone mineral density at the proximal tibia and distal femur joints with the absence of osteophytosis only in animal group treated with combined HA–KT membrane. Application of K8 membrane was able to preserve KT plasma concentration above its minimum effective concentration



for 48 h therefore, would be able to replace six commercial tablets each of 10 mg KT.

**Keywords:** Bone mineral density; Freund's complete adjuvant; Hyaluronic acid; Ketorolac tromethamine; Osteoarthritis; Radiography.

### 1507. Soluplus: A Novel Polymeric Solubilizer for Optimization of Carvedilol Solid Dispersions: Formulation Design and Effect of Method of Preparation

Rehab Nabil Mohamed and Mona Basha

*Powder Technology*, 237: 406-414 (2013) IF: 2.024

The aim of this work was to investigate the applicability of different industrially scalable techniques in the preparation of solid dispersions using a novel polyvinyl caprolactam-polyvinyl acetate-polyethylene glycol graft copolymer (Soluplus®) for preparing immediate-release formulations of a poorly water-soluble BCs class II drug. Carvedilol (CAR), a non-selective  $\beta$ -blocker, has been selected as poorly water-soluble model drug. The solid dispersions were prepared by three different techniques; solvent evaporation, freeze drying and spray drying in different CAR: Soluplus ratios using 32 full factorial design.

Among the formulations tested, CAR solid dispersion preparation using freeze drying method at ratio of 1:10 (CAR: Soluplus) showed the highest saturation solubility and was selected for further investigation. Solid state characterization was evaluated by differential scanning calorimetry (DSC) and X-ray diffraction study (XRD), scanning electron microscopy (SEM) and Fourier transformation infrared spectroscopy (FTIR). DSC and XRD analyses indicated the complete transformation of CAR in the solid dispersion from crystalline to amorphous state. Selected CAR solid dispersion was further incorporated into ODTs using three commercially mannitol-based fillers; Pearlitol Flash, Pharmaburst and Ludiflash.

The ODTs were evaluated for hardness, disintegration time and drug dissolution. Pearlitol Flash, and Pharmaburst ODTs showed shorter disintegration times (b1 min) and significantly higher dissolution profile (>90% within 30 min) compared to Ludiflash ODTs. Thus, the development of CAR solid dispersions using Soluplus as ODTs could be used as a promising approach for improving the solubility and oral bioavailability of poorly water-soluble drugs.

**Keywords:** Soluplus; Solid dispersion; Carvedilol.

### 1508. Design and Optimization of Surfactant-Based Nanovesicles for Ocular Delivery of Clotrimazole

Rehab Nabil Mohamed, Mona Basha, Sameh Hosam Abd El-Alim and Ghada E. A. Awad

*Journal of Liposome Research*, 23: 203-210 (2013) IF: 1.909

The objective of this study was to develop an efficient ocular nanovesicular carrier providing a controlled delivery of Clotrimazole (CLT); a water insoluble antifungal drug. The nanovesicular carriers were formulated using Span 60 with one of the following edge activators (EA): Tween 80 (TW80), sodium cholate (SC) or sodium deoxycholate (SDC). A 32 full factorial design was used to study the effect of two independent variables, namely, the type of EA and the ratio of Span 60 to EA. The effects

of these parameters on the mean particle size, entrapment efficiency (EE) and zeta potential (ZP) were investigated as dependent variables. Then, optimization was performed producing the best optimized formulation composed of SDC as an EA at the ratio of 90:10 (Span 60:EA) with an average diameter of 479.60 nm, EE of 87.92% and ZP of 33.7 mV. The optimized nanovesicular carriers appeared as spherical unilamellar vesicles with CLT in an amorphous state as evidenced by the differential scanning calorimetry study.

The antifungal activity against *Candida albicans* compared to niosomal formulation as well as the CLT suspension was determined. CLT-loaded nanovesicular carriers displayed sustained antifungal effect over 12 h. The AUC of the optimized formulation was 3.09 times more than that of drug suspension with no sign of irritation after testing for ocular tolerance. Therefore, the present study showed the feasibility of using non-ionic surfactant nanovesicles as carrier systems for prolonged ocular delivery of CLT.

**Keywords:** Clotrimazole; Edge activators; Nanovesicles; Ocular delivery.

### 1509. Transfersomal Lyophilized Gel of Buspirone HCl: Formulation, Evaluation and Statistical Optimization

Rehab Nabil Shamma and Ibrahim Elsayed

*Journal of Liposome Research*, 23: 244-254 (2013) IF: 1.909

**Context:** Buspirone HCl has very low oral bioavailability (4%) due to deactivation by extensive first pass effect. It also has very limited transdermal permeation due to its high hydrophilicity.

**Objective:** The aim of this study was to increase the transdermal permeation of buspirone HCl utilizing a stable dosage form.

**Methods:** Transfersomes were prepared using Tween-80 as a flexibility imparting agent to the vesicular walls. Oleic acid and/or ethanol, with different percentages, were utilized as a permeation enhancer. Formulations were characterized by analyzing particle size, polydispersity index, zeta potential, entrapment efficiency, in vitro release and ex vivo drug permeation. Factorial design (32) was planned for the optimization of formulations using Design-Expert software. Lyophilized transfersomal gel of the optimized formulation was prepared using hydroxypropyl methylcellulose (HPMC) K100, carboxymethyl cellulose or sodium alginate with or without mannitol as a cryoprotectant. Physical characterization of the transfersomes and the lyophilized gel were carried out using transmission and scanning electron microscopy respectively.

**Results:** The optimized formulation (T7), containing 35% oleic acid, had the highest desirability value (0.658) with high ex vivo drug flux (43.40 mg/h/cm<sup>2</sup>) through rat skin when compared with the aqueous drug solution and formula T1 (without oleic acid). The T7 transfersomal gel containing HPMC K100 (G2) had the highest desirability value (0.640) among the lyophilized formulations with decreased ex vivo drug flux (38.98 mg/h/cm<sup>2</sup>) in comparison with the original transfersomal formula (T7).

**Conclusions:** Lyophilized transfersomal gel containing oleic acid was considered as a promising transdermal delivery system for hydrophilic drugs.

**Keywords:** Ex vivo; Factorial design; Permeation; Transdermal.



### 1510. Positively Charged Polymeric Nanoparticle Reservoirs of Terbinafine Hydrochloride: Preclinical Implications for Controlled Drug Delivery in the Aqueous Humor of Rabbits

Mina Ibrahim Tadros, Saadia Ahmed Tayel, Mohamed Ahmed El-Nabarawi and Wessam Hamdy Abd-Elsalam

*Aaps Pharmscitech*, 14 (2): 782-793 (2013) IF: 1.584

Frequent instillation of terbinafine hydrochloride (T HCl) eye drops (0.25%, w/v) is necessary to maintain effective aqueous humor concentrations for treatment of fungal keratitis. The current approach aimed at developing potential positively charged controlled-release polymeric nanoparticles (NPs) of T HCl. The estimation of the drug pharmacokinetics in the aqueous humor following ocular instillation of the best-achieved NPs in rabbits was another goal. Eighteen drug-loaded (0.50%, w/v) formulae were fabricated by the nanoprecipitation method using Eudragit® RS100 and chitosan (0.25%, 0.5%, and 1%, w/v). Soybean lecithin (1%, w/v) and Pluronic® F68 (0.5%, 1%, and 1.5%, w/v) were incorporated in the alcoholic and aqueous phases, respectively. The NPs were evaluated for particle size, zeta potential, entrapment efficiency percentage (EE%), morphological examination, drug release in simulated tear fluid (pH 7.4), Fourier-transform IR (FT-IR), X-ray diffraction (XRD), physical stability (2 months, 4°C and 25°C), and drug pharmacokinetics in the rabbit aqueous humor relative to an oily drug solution. Spherical, discrete NPs were successfully developed with mean particle size and zeta potential ranging from 73.29 to 320.15 nm and +20.51 to +40.32 mV, respectively. Higher EE% were achieved with Eudragit® RS100-based NPs. The duration of drug release was extended to more than 8 h. FT-IR and XRD revealed compatibility between inactive formulation ingredients and T HCl and permanence of the latter's crystallinity, respectively. The NPs were physically stable, for at least 2 months, when refrigerated. F5-NP suspension significantly ( $P < 0.05$ ) increased drug mean residence time and improved its ocular bioavailability; 1.657-fold.

**Keywords:** Aqueous humor; Chitosan; Eudragit® RS100; Nanoparticles; Terbinafine hydrochloride.

### 1511. Sucrose Stearate-Enriched Lipid Matrix Tablets of Etodolac: Modulation of Drug Release, Diffusional Modeling and Structure Elucidation Studies

Ahmed Abd ElBary Abd ElRahman, Mina Ibrahim Tadros and Ahmed Adel Alaa-Eldin

*Aaps Pharmscitech*, 14: 656-668 (2013) IF: 1.584

Etodolac is a non-steroidal anti-inflammatory drug having an elimination half-life of 7 h; oral doses are given every 6–8 h. The aim of current work was the development of controlled-release etodolac lipid matrix tablets. The variables influencing design of these tablets (L1–L28) by the hot fusion method were investigated including; (1) lipid type (stearic acid, cetyl alcohol, cetostearyl alcohol, Imwitor 900K, Precirol ATO 5 and Compritol ATO 888), (2) drug/lipid ratio (1:0.25 and 1:0.50, respectively), (3) filler type (lactose, Avicel PH101 and their physical mixtures; 2:1, 1:1, and 1:2, respectively), (4) surfactant's HLB (5 and 11), and (5) drug/surfactant ratio (20:1 and 10:1, respectively).

Statistical analysis and kinetic modeling of drug release data were evaluated. The inner matrix of the tablet was visualized via scanning electron microscopy (SEM). An inverse correlation was observed between the drug/lipid ratio and the drug release rate. Precirol- and Compritol-containing formulae showed more retarded drug release rates. Lactose/Avicel physical mixture (1:1) was considered as a filler of choice where it minimized the burst effect observed with Avicel®-free formulae. The higher surfactant's HLB, the higher drug release rate. The similarity factor ( $f_2$ ) between the drug release profiles revealed similarity within the investigated drug/surfactant ratios. Sucrose stearate D1805-based matrix (L21) succeeded in delivering more than 90% of etodolac over 12 h, following anomalous (non-Fickian) controlled-release kinetics. SEM micrographs confirmed pore formation, within the latter matrix, upon contact with dissolution medium.

**Keywords:** Anti-inflammatory; Controlled release; Etodolac; Hot fusion method; Lipid matrix tablets; Precirol ATO 5; Sucrose stearate; Surfactant; Sustained release.

### 1512. Content Uniformity Testing: Suitability of Different Approaches for Marketed Low Dose Tablets

Mohamed Ahmed Mohi ElDin El Nabarawi, Magdi M. Abdel Hamid, Fars K. Alanazi, Magdy I. Mohamed and Adel A. Sakr

*Pharmaceutical Development and Technology*, 18: 1277-1287 (2013) IF: 1.333

**Context:** Content uniformity (CU) testing was developed and improved to control the effectiveness and safety of dosage units. Many modifications of compendial CU test have been introduced and several alternatives have been suggested.

**Objectives:** This study aims to evaluate the degree of suitability of current USP CU test for low dose tablets and to compare the performance of the current test with that of the former USP27-NF22 and other alternatives for different sample sizes.

**Methods:** All locally marketed risperidone (RSP) tablets were analyzed using newly developed and validated isocratic UPLC method. The CU results were statistically analyzed in groups with sample sizes comparable to the USP sampling plans.

**Results:** Seven out of eleven products failed the different requirements of the former and current USP <905> chapters as well as of several alternative CU tests with several substantial deviations.

**Conclusion:** The current USP <905> chapter was found to have some deficiencies that allowed such failed products to exist in the market. The dependence of compendial CU test on two-staged sampling plan and the use of arithmetic mean to calculate the reference and acceptance values were obvious shortcomings.

**Keywords:** Content uniformity; USP <905>; Uniformity of dosage units; Low dose tablets; Risperidone; UPLC.

### 1513. Development and Optimization of Lyophilized Orally Disintegrating Tablets Using Factorial Design

Rehab Nabil Shamma, Iman Saad Ahmed and Ragia Ali Shoukri

*Pharmaceutical Development and Technology*, 18: 935-943 (2013) IF: 1.333

The aim of this study was to evaluate the use of maltodextrin as a sugar-matrix former along with several cellulosic binders in the preparation of freeze-dried orally disintegrating tablets (ODT).

The ODT was prepared by freeze—drying an aqueous dispersion of nimesulide (NM) containing maltodextrin and a cellulosic binder. The influence of formulation parameters on the in vitro/in vivo disintegration time and in vitro dissolution of NM from ODTs along with other tablet characteristics was investigated using full factorial design. The optimized ODT contained 5% w/v maltodextrin DE 29, 2% w/v Methocel® E15, and 5% w/v NM, disintegrated in less than 10 s and showed more than 70% of NM in ODTs dissolved within 2 min, compared to only 1.52% of NM plain drug and 7.25% of NM in immediate release commercial tablet. Crystalline state evaluation of NM in the optimized ODT was conducted through differential scanning calorimetry, and X-ray powder diffraction. The study suggests that the optimized ODT formulation developed in this work may be an alternative to conventional formulations of NM inconvenient to the patients such as intramuscular or rectal administration.

**Keywords:** Maltodextrin; Freeze drying; Factorial design.

#### 1514. Effect of Fixed Aqueous Layer Thickness of Polymeric Stabilizers on Zeta Potential and Stability of Aripiprazole Nanosuspensions

Mohamed Ahmed Mohi El-Din El Nabarawi, Aly A. Abdelbary, Xiaoling Li, Abdelhalim Elassy and Bhaskara Jasti

*Pharmaceutical Development and Technology*, 18: 730-735 (2013) IF: 1.333

The aim of this study was to evaluate the effect of the thickness of adsorbed polymer layer (also known as Fixed Aqueous Layer Thickness, FALT) of polymeric stabilizers on zeta potential and stability of nanoparticles in a suspension. Aripiprazole, a poorly water soluble drug was used as a model drug to evaluate rationale for increased FALT and to understand the effect of hydrophilicity and hydrophobicity of polymeric stabilizers on FALT of aripiprazole nanosuspensions. The nanosuspensions were prepared by media milling and Pluronic F68, Pluronic F127, Hydroxypropyl methylcellulose (HPMC) and Hydroxypropyl cellulose (HPC) were used as polymeric stabilizers. The particle size (immediately after preparation and after 1 week of storage at 25°C) and zeta potential of aripiprazole nanosuspensions were determined. For Pluronics, FALT was determined theoretically whereas for HPMC and HPC it was calculated as Debye Huckel parameter from the zeta potential dependence on the ionic strength. An increase in FALT resulted in reduced zeta potential. With an increase in FALT of polymers used, the stability of nanosuspensions showed improvement. Furthermore, a linear correlation was shown to exist between the FALT and length of hydrophilic chains in Pluronics.

**Keywords:** Nanosuspensions; Falt; Pluronics; Zeta potential; Stability.

#### 1515. Microencapsulation of Hydroxyzine HCL by Thermal Phase Separation: *in Vitro* Release Enhancement and *in Vivo* Pharmacodynamic Evaluation

Randa Latif Aziz Salama, Christianne Mounir Zaki Rizkalla and Iman Ibrahim Soliman

*Pharmaceutical Development and Technology*, 18: 196-209 (2013) IF: 1.333

The systemic effect of hydroxyzine hydrochloride following its oral administration or topical application is associated with non compliant anticholinergic effect. Subsequently, the present study aims to prepare microcapsules loaded with hydroxyzine hydrochloride enabling its controlled release into the skin and reducing the side effect of its systemic absorption. The microcapsules were prepared by thermal phase separation method using ethylcellulose/cyclohexane. Optimization of the formulation parameters was carried out by: (1) varying the type and the concentration of the coacervation inducer with microcapsules prepared with three different core: wall ratios, (2) by using ethyl cellulose with two different viscosities, (3) and by the addition of pore inducers such as pregelatinized starch and sucrose in order to enhance the drug release. Microcapsules of 99% encapsulation efficiency were prepared using 1% w/v polyisobutylene, and 1:0.1 core: wall ratio. The highest percent of drug is released after 9 h from microcapsules prepared using 1:0.1 core : wall ratio. Almost 100% drug was released after 3 h, from the same microcapsules prepared with pregelatinized starch that acts as a core coated with the drug. The pharmacodynamic effect of the chosen preparation was tested on the shaved back of histamine sensitized rabbits. Histopathological studies were driven for the detection of the healing of inflamed tissues.

**Keywords:** Microcapsules; Thermal phase separation; Hydroxyzine HCL; Pore inducer; Ethylcellulose/cyclohexane; Polyisobutylene.

#### 1516. Rapidly Absorbed Orodispersible Tablet Containing Molecularly Dispersed Felodipine for Management of Hypertensive Crisis: Development, Optimization and *in Vitro/In Vivo* Studies

Emad Basalious Bashir Basalious, Wessam El-Sebaie and Omaima El-Gazayerly

*Pharmaceutical Development and Technology*, 18: 407-416 (2013) IF: 1.333

A liquisolid orodispersible tablet of felodipine, a BCS Class II drug, was developed to improve drug dissolution and absorption through the buccal mucosa for management of hypertensive crisis. A 24 full-factorial design was applied to optimize felodipine liquisolid systems (FLSs) having acceptable flow properties and possessing enhanced drug dissolution rates. Four formulation variables; The liquid type, X1 (PG or PEG), drug concentration, X2 (10% and 20%), type of coat, X3 (Aerosil® and Aeroperl®) and excipients ratio, X4 (10 and 20) were included in the design. The systems were assessed for dissolution and flow properties. Following optimization, the formulation components (X1, X2, X3 and X4) were PEG, 10%, Aerosil® and 20, respectively. The optimized FLS was compressed into felodipine liquisolid orodispersible tablet using Prosolv® as carrier material (FLODT-2). The in vitro and in vivo disintegration times of FLODT-2 were 9 and 7 s, respectively. The in vivo pharmacokinetic study using human volunteers showed a significant increase in dissolution and absorption rates of the formulation of FLODT-2 compared to soft gelatin capsules filled with felodipine solution in PEG under the same conditions. Our results proposed that the optimized FLODT formulation could be promising to manage hypertensive crisis.

**Keywords:** Felodipine; Optimization; Orodispersible tablet; Full-factorial design; Liquisolid.

### 1517. Self Nano-Emulsifying Simvastatin Based Tablets: Design and *in Vitro/in Vivo* Evaluation

Ghada Ahmed Abdelbary, Maha Amin and Salwa Salah

*Pharmaceutical Development and Technology*, 18: (2013)  
IF: 1.333

The aim of this work is to improve the oral bioavailability of poorly water soluble drug, simvastatin (SV) through combining the advantages of self-nanoemulsifying systems (SNEs) and tablets. Ternary phase diagram was constructed using Labrafil, Tween 80 and Transcutol, in order to evaluate self-nanoemulsification domain. The particle size distribution and zeta potential of the prepared systems were evaluated using Malvern Zetasizer. Liquisolid powders were prepared using Aeroperl® as a coating material and Avicel® or Starch 1500 as carrier materials, the powder flow properties were then evaluated. Compressed SV SNE based tablets were evaluated regarding their physical characteristics, in-vitro release properties as well as in-vivo pharmacokinetic evaluation in six healthy human volunteers using a validated LC/MS/MS method. The in-vitro release results revealed that the developed SNE based tablets improved the release of SV significantly, compared to commercially available SV tablets (Zocor®). The optimal SV SNE tablet formulation was S3St10 (10% Labrafil, 60% Tween 80, and 30% Transcutol). The in-vivo evaluation of S3St10 revealed that rapid and enhanced absorption of SV could be obtained from the SNE based tablet, with a 1.5 fold increase in bioavailability than that obtained after administration of Zocor®. Hence such an approach could be promising in improving the bioavailability of SV.

**Keywords:** Simvastatin; Liquisolid powder; Self-nanoemulsification; *In vivo* study; LC/MS/MS.

### 1518. Zero-Order Release Profile of Metoclopramide Hydrochloride Sublingual Tablet Formulation

Randa Latif Aziz Salama

*Pharmaceutical Development and Technology*, 18(6): 1372-1378 (2013) IF: 1.33

This report describes zero-order approximation for metoclopramide hydrochloride sublingual tablet formulation. Effects of type and concentration of excipients on release were investigated. Study revealed that highest rate of dissolution was attained with croscopolvidone and decreased in the order croscopolvidone > sodium starch glycolate > ac-di-sol. All formulations demonstrated flush release, except the one containing 10% croscopolvidone where a lagtime of 0.5 min. was depicted. Increasing the concentration of croscopolvidone from 5 to 10% gave the same half-life, whereas kinetics of release changed to zero order. Differential scanning calorimetry and infrared spectroscopy did not reveal any sign of physical or chemical interaction between drug and croscopolvidone. In order to study the alignment of polymeric network inside tablet matrix, scanning electron microscopy was performed on the tablet and its cross-section. Matrix with 10% croscopolvidone showed higher density of interconnections extending to the interior of core enabling fast and constant release. Hence physicochemical characteristics of croscopolvidone could be tailored by varying its concentration, in a way that provided a porous matrix with tight arrangement of polymeric chains, resembling to an assemblage of cylinders with

constant apertures, from which zero-order release was approached.

**Keywords:** Sublingual tablet; Zero order; Metoclopramide hydrochloride; Fast-disintegrating tablet; Superdisintegrants; Constant release profile.

### 1519. Formulation and Evaluation of Itopride Microcapsules in Human Volunteers

Aliaa Nabil Ahmed ElMeshad, S.A. Yehia, A.H. Elshafeey and H. Al-Bialeh

*Journal of Drug Delivery and Scientific Technology*, 23: 239-245(2013) IF: 1.088

In this study an attempt to sustain the oral release of itopride hydrochloride (ITO), a highly water-soluble drug, by microencapsulation using different polymers was carried out. The prepared microcapsules were characterized according to: particle size, encapsulation efficiency, and in vitro drug release and in vivo study in healthy human volunteers. Results showed that the particle size of microcapsules ranged from  $591 \pm 2$  to  $886 \pm 4$   $\mu\text{m}$  and the encapsulation efficiency of ITO inside microcapsules ranged from  $63 \pm 1$  to  $90 \pm 1$  %. The optimum formulation had a particle size of  $860 \pm 11$   $\mu\text{m}$  and was able to entrap  $90 \pm 1$  % ITO. The in vitro release study showed that  $88 \pm 1$  % of ITO was released from the optimum formulation after 12 h using Eudragit RS-100. The pharmacokinetic parameters of the optimum formulation in human volunteers showed that the maximum plasma concentration was  $1624 \pm 168$  ng/mL, AUC<sub>0-8</sub> was  $85835 \pm 6116$  ng.h/mL, AUC<sub>0-48</sub> was  $29728 \pm 761$  ng.h/mL, and the mean residence time was  $108 \pm 9$  h. The relative bioavailability of ITO from the optimum formulation compared to commercial oral tablets Ganaton as a reference standard was 317.9 %.

**Keywords:** Sustained release; Microencapsulation; Itopride hydrochloride; Solvent evaporation; Eudragit; Hydroxypropylmethyl cellulose.

### 1520. Buparlisib. Phosphatidylinositol 3-Kinase Alpha Inhibitor, Oncolytic. Monograph

Noha Nabil Salama Mohamed

*Drugs of The Future*, 38: 73-79 (2013) IF: 0.399

The PI3K signaling pathway is dysregulated in many tumor types, where it is associated with a poor prognosis and resistance to multiple therapies, and inhibition of PI3K is an emerging strategy in the treatment of cancer. Buparlisib (NVP-BKM-120) is a 2,6-dimorpholinopyrimidine derivative and a potent pan-PI3K inhibitor, inhibiting PI3K downstream signaling, including downregulation of p-Akt and p-S6R, and inducing apoptosis of cancer cells. In animal models, buparlisib inhibited tumor growth and metastasis of breast, lung, glioma, multiple myeloma, gastric and soft tissue sarcoma, and it synergized with other cytotoxic agents. Buparlisib is rapidly absorbed and highly bioavailable after oral administration, with a half-life of approximately 40 hours, mainly via hepatic clearance. The product is currently being tested in clinical trials in several solid tumors and was found to be well tolerated, preliminary data demonstrating variable clinical responses including partial response, stable disease and progressive disease.

**Keywords:** Buparlisib; PI3K signaling pathway; Treatment of Cancer; Pan-PI3K inhibitor; NVP-BKM-120

### 1521. Application of A Novel UPLC–MS/MS Method for the Pharmacokinetic/Bioequivalence Determination of Atorvastatin and Ezetimibe in Human Plasma

Ghada Ahmed Abdelbary and Marianne Nebesen

*Journal of Pharmacy Research*, 7: (2013)

**Aims :** The aim of this study is to determine the pharmacokinetic parameters of atorvastatin calcium (AT) and ezetimibe (EZ) in human volunteers following the administration of a single oral dose of two drug products containing both active ingredients.

**Materials and methods:** A novel, sensitive and selective ultra performance liquid chromatography coupled with tandem mass spectrometry (UPLC- MS/ MS) method was developed and validated for the quantification of AT and EZ in human plasma following administration of a single dose comprising AT 40 mg and EZ 10 mg, using a non-blind, two – treatment, two-period, randomized, crossover design, in twenty four healthy human volunteers. Atorvastatin, ezetimibe and the internal standard etilefrine (IS) were extracted from plasma and analyzed on a reversed-phase C18 column under gradient conditions.

**Results :** The ion transitions monitored in multiple reaction-monitoring mode were 440.4, 271.25, 164.02 m/z derived from 559.57, 408.43, 182.12 m/z for AT, EZ and IS respectively. Calibration curves were generated over the range of 0.1–20 ng mL<sup>-1</sup> for both drugs with values for coefficient of correlation greater than 0.999. The parametric point estimates and the 90% confidence intervals for ln-transformed AUC<sub>0–t</sub>, AUC<sub>0–8</sub>, and c<sub>max</sub>, were within commonly accepted bioequivalence range of 80–125% range, thus the results reveal that the bioequivalence between the two drug products could be concluded.

**Conclusion :** The method is very simple and allows obtaining a very good recovery of the analytes. The validated UPLC–MS/MS method has been applied to a pharmacokinetic/bioequivalence study.

**Keywords:** Atorvastatin; Ezetimibe; Pharmacokinetic; Bioequivalence study; Plasma; UPLC–MS/MS.

### 1522. Assessment of Bioavailability of Sumatriptan Transdermal Delivery Systems in Rabbits

Aliaa Nabil Ahmed ElMeshad, Mohamed El-Nabarawi and Mohamed Yousif Moutasim

*International Journal of Pharmacy and Pharmaceutical Sciences*, 5 (2): 225-240 (2013)

**Objectives:** The purpose of the study was development, characterization and assessing the bioavailability of sumatriptan transdermal films in male albino rabbits (n=15) using HPLC method of analysis.

**Method:** Films were prepared using 50mg sumatriptan, Eudragit® polymers, plasticizers, and penetration enhancers.

**Results:** Results proved that the best plasticizer was triacetin. Eucalyptus oil and oleic acid increased the amount of sumatriptan permeated through mice skin after 24h from 17.18% (without enhancer) to 74.45 and 58.72% respectively. The optimum formulation did not produce irritation to rabbit skin and the histological structure of the epidermis and dermis were intact (n=15). Following oral administration of Imigran® (GlaxoSmithKline), C<sub>max</sub> was 2.609±0.186µg/ml after 2h and

the AUC(0-24) was 18.60µg.h/ml. After transdermal administration of optimum formulation, C<sub>max</sub> was 2.892±0.106µg/ml after 2h and the AUC (0-24) was 26.42µg.h/ml.

**Conclusion:** There were no significant differences between the rate of drug bioavailability following transdermal and oral medications, but there was a significant difference between the extents of the bioavailability of sumatriptan, with the transdermal film higher in value (p<0.05).

**Keywords:** Transdermal; Sumatriptan; Eucalyptus oil; Skin irritation; Bioavailability.

### 1523. Evaluation of Sanazole Cytotoxicity in Human Drug-Sensitive and MDR Uterine Sarcoma Cells

Mariame Ali Hassan, Yukihiro Furusawa, Seisukei Okazawa, Kazuyuki Tobe and Takashi Kondo

*Pharmaceutica Analytica Acta*, 4: (2013)

Chemotherapy is one of the principle modes of cancer treatment. However, cells adapt to repeated chemotherapeutic exposures in several ways resulting in multidrug resistance (MDR). Therefore, it is mandatory to search for effective alternatives that are refractory to resistant mechanisms. In this study, we investigated the cytotoxicity of sanazole, a nitrotriazole derivative known for its hypoxic radio-sensitization, against a human MDR cell line highly expressing P-glycoprotein that functions as an efflux pump to lipophilic drugs. The results showed that MDR cells exhibited initial sensitivity to the drug compared to the parent sensitive cells. Sanazole action was independent of the degree of resistance and P-glycoprotein expression. Prolonged exposures (48 h) to the drug affected both cell phenotypes viability to a similar extent. However, cell cycle analysis revealed that the underlying pathways differed between cells with respect to their p53 status. For instance, cell cycle was halted in G1- and S-phase in parent and MDR cells, respectively. The (apoptotic) DNA fragmentation in MDR cells was dose-dependently higher compared to the parent cells. Sanazole treatment decreased polyploidy in a dose-dependent manner in MDR cells. The present study provides evidence on the possible potential of sanazole multidrug resistant cancer cells.

**Keywords:** Cytotoxicity; Multidrug resistance; Sanazole; P-glycoprotein; P53.

### 1524. Formulation and Evaluation of New Sildenafil Citrate-Caffeine Oral Disintegrating Tablets: *in Vitro* and *in Vivo* Evaluation

Sally Adel Abd el-Halim, El-Nabarawi M.A. and El Refaai K.I.

*Journal of Pharmaceutical Research and Opinion*, 3: 46-63 (2013)

Sildenafil citrate (SC) oral disintegrating tablets (ODTs) have been prepared by freeze drying technique (lyophilization) using various excipients for improving their oral disintegration, dissolution and bioavailability in order to treat erectile dysfunction (ED). Caffeine was added to the best selected formula of the prepared SC ODTs to maintain normal blood pressure and prevent its decrease caused by administration of SC. The physicochemical and solid-state properties as well as the dissolution behavior of all the prepared tablet formulae

were evaluated. Moreover, SC bioavailability in human volunteers from the prepared ODTs was compared to that of the market product oral tablet (Viagra). The effect of addition of caffeine to the best selected formula of SC ODTs on the blood pressure of human volunteers was also monitored. Using gelatin as a matrix former in oral disintegrating tablets together with tween80 as a solubilizer enhanced the dissolution rate and extent of SC with 100 % of drug being dissolved after 7 minutes. Moreover, the in vivo study showed that the AUC<sub>0-12</sub> of the lyophilized tablets SC ODTs and SC/Caffeine ODTs was higher than that of commercial oral product (Viagra®), with relative bioavailability values of 122 % and 125% respectively compared to the commercial oral product (Viagra®). Addition of caffeine to the best selected formula of SC ODTs maintain blood pressure and inhibit severe decrease in the blood pressure which caused by administration of the best selected formula of SC ODTs and commercial oral product (Viagra®). Therefore, SC/Caffeine ODT is a promising dosage form for treating erectile dysfunction with avoiding side effects.

**Keywords:** Sildenafil citrate; Erectile dysfunction; Oral disintegrating tablet; Lyophilization.

#### 1525. Formulation and Evaluation of Taste-Masked Orally Disintegrating Tablets of Nicergoline Based On $\beta$ -Cyclodextrin Inclusion Complexation

Ahmed Abd ElBary Abd ElRahman, Mohammed Ahmed El Nabarawi, Ahmed Mahmoud Abdelhaleem Ali and Amira Hosny Hassan

*International Journal of Drug Delivery*, 5: 110-120 (2013) IF: 1.02

Successfully to improve the drug's solubility, dissolution rate and hence per oral absorption. In addition, masking of the bitter taste was also achieved. The preparation of inclusion complexes was performed using two different techniques, namely; physical mixing and kneading. The apparent stability constant ( $K_c$ ) of the complex was calculated from the phase solubility analysis. Compatibility of nicergoline and  $\beta$ -CD complex with disintegrants and superdisintegrants were evaluated using powder x-ray diffractometry (PXRD), differential scanning calorimetry (DSC), and fourier transform infrared spectroscopy (FTIR). The morphology of complex particles was studied using scanning electron microscopy. Pharmaceutical characterization confirmed that all additives were compatible with the drug and no signs of physical or chemical interaction were detected. Orodispersible tablets (ODTs) of nicergoline complexed with  $\beta$ -CD and containing 7-9 % camphor had rapid disintegration time (7-12 seconds) and fast drug release profiles (90-100 % in 10 minutes). Therefore, nicergoline ODTs are considered a valuable choice dosage form with improved per oral absorption and taste acceptability.

**Keywords:**  $\beta$ -cyclodextrin; Inclusion complex; Nicergoline; Orodispersible; Sublimation.

#### 1526. Furosemide Loaded Superporous Hydrogel Composite as A Controlled Release Device: Different Strategies for Drug Loading

Randa Latif Aziz Salama, Abdel Halim S.A. and Abdel Kader O.M.

*Journal of Pharmaceutical Research and Opinion*, 3 (6): 28-35 (2013)

The aim of the present work was to develop controlled release, gastroretentive device using superporous hydrogel composite (SPHC). Furosemide was chosen as good candidate for such system due to its narrow absorption window, low bioavailability and short half-life. Plain hydrogel was evaluated with respect to swelling ratio, apparent density and floating time. Scanning electron micrographs of SPHC showed large interconnected pores and extensive capillary insertion. Prepared Microspheres were tested for drug content, and tablets evaluated with respect to quality control tests. All loaded formulae inside SPHC were tested for drug release profile. Microspheres, tablets and drug solutions were tested for loading inside SPHC. Kinetic treatment of release data revealed that soaked drug solution was unable to control drug release, where it gave a  $t_{1/2}$  (0.5hrs) very similar to that of the free drug (0.6hrs). Loaded microspheres showed only a slight retardation in release  $t_{1/2}$  to 1.06 hrs along with a high percent of flush (~30mg %). However, loaded tablet demonstrated a promising sustained effect corresponding to a release  $t_{1/2}$  = 6hrs and a low percent of initial flush (~1.2mg %). Therefore, the applicability of SPHC as a controlled release device proved to be largely dependent on the type of dosage form included.

**Keywords:** Controlled release formulation; Gastroretentive device; Super porous hydrogel composite; Furosemide.

#### 1527. Computed Tomographic Evaluation of Canal Shape Instrumented by Different Kinematics Rotary Nickel-Titanium Systems

Abeer M. Marzouk and Angie G. Ghoneim

*J. Endod. (JOE)*, 39 (7): 906-909 (2013)

**Introduction:** This study evaluated the effects of 2 different kinematics rotary nickel-titanium (NiTi) systems, Twisted File (TF), a continuous rotation full-sequence system, and WaveOne (WO), a reciprocating single-file system, on transportation, curvature, and volumetric changes of curved root canals by using cone-beam computed tomography.

**Methods:** Forty mesiobuccal canals of mandibular molars with angle of curvature ranging from 25°-35° were divided according to the NiTi rotary system used in canal preparation into 2 groups of 20 samples each, TF group and WO group. Canals were scanned by using an i-CAT cone-beam computed tomography scanner before and after instrumentation to evaluate canal transportation at coronal, middle, and apical thirds, canal curvature, and volumetric changes. The significance level was set at  $P \leq 0.05$ .

**Results:** TF system recorded significantly lower mean of canal transportation than WO group at all canal thirds (apical  $P = 0.034$ , middle  $P = 0.003$ , and coronal  $P = 0.012$ ). In both groups the apical third recorded the significantly least amount of transportation ( $P < 0.05$ ). There was no significant difference between the 2 groups in canal curvature and volumetric changes after instrumentation ( $P > 0.05$ ).

**Conclusion:** Both TF and WO NiTi systems can be safely used to the full working length, resulting in satisfactory preservation of the original canal shape.

**Keywords:** Canal transportation; Computed tomography; Root canal volume; Twisted file; Waveone file.



### 1528. Optimization for Glimepiride Dissolution Enhancement Utilizing Different Carriers and Techniques

Randa Latif Aziz Salama, Rana R. Makar, Ehab A. Hosni and Omaima N. El-Gazayerly

*Journal of Pharmaceutical Investigation*, 43: 115-131 (2013)

The present work is a comparative study that matches between carriers and techniques used to prepare solid mixtures with glimepiride. The study is directed toward elucidation of the most promising carrier capable of highly improving drug dissolution along with the most successful technique used for drug formulation. Mixtures were tested for drug content and dissolution. The most optimum formulae were characterized by DSC, IR and XRPD. Kinetic treatment of dissolution data was performed for physical and co-ground mixtures, solid dispersions and their adsorbates, triple solid dispersions and their adsorbates, microwave generated or treated solid dispersions. Results revealed that enhancing effect mostly reached maximum with ternary solid dispersion adsorbate (TSDads). The latter technique demonstrated a dramatic increase in drug dissolution rate which was reflected in the shortest half-life for most carriers at variable degrees. The highest dissolution rate was attained with pregelatinized starch and decreased to variable degrees with remaining carriers. Differences were ascribed to chemical nature as well as relative water solubility of carriers. The combined effects of incorporating surfactants, polymers and adsorbents to glimepiride contributed together to improve wetting, reduce crystallinity and caused substantial increase in the surface area which made TSDads the most promising technique for enhancing dissolution of glimepiride.

**Keywords:** Solid dispersion; Triple solid dispersion; Triple solid dispersion adsorbate; Dissolution enhancement; Glimepiride; Microwave solid dispersion; Water soluble polymers; Water insoluble polymers.

### 1529. Preparation, Characterization and Evaluation of Tenoxicam Gels and Microemulsion Gels for Topical Drug Delivery

Mai G. El-Hennawy, Sally A. Abdel Halim, Alia Badawy and Mohammed A. Effat

*Inventi Impact: Pharm Tech*, 257-267 (2013)

Gels and microemulsions are classes of dosage forms that have emerged as promising drug delivery system for the delivery of various drugs. The objective of this study is to prepare tenoxicam, a non-steroidal anti-inflammatory drug (NSAID), topical gel formulae using cellulose derivatives (Sodium carboxymethyl cellulose (NaCMC), Methyl cellulose (MC), Hydroxypropyl methyl cellulose (HPMC), Hydroxy ethyl cellulose (HEC), and Hydroxy propyl cellulose (HPC)) as gelling agents and to prepare topical microemulsions, microemulsion-gel formulae using (labrasol, tween 80 and tween 20) mainly as surfactants, (Oleic acid and isopropylmyristate (IPM)) as oils. Fifteen gel formulae were prepared (F1-F15) and evaluated for physical properties (color, clarity, homogeneity), rheological properties, pH measurements, in vitro drug permeation through cellulose dialysis membranes and in vitro drug permeation studies through natural rat skin. The gel formulae which showed best physical properties and highest drug permeation were chosen in the preparation of

microemulsion-gel formulae. Ten microemulsion formulae were prepared (M1-M10) and those with the broadest microemulsion region as shown by the phase diagrams and those with the maximum loading capacity of tenoxicam were chosen to be formulated into microemulsion-gel formulae. Nine microemulsion-gel formulae were prepared (S1-S9) and evaluated for physical properties (color, clarity, homogeneity), rheological properties, pH measurements, in vitro drug permeation through cellulose dialysis membranes and in vitro permeation studies through natural rat skin. In vivo rat-paw edema tests were carried out to evaluate the activity of gel formulae and microemulsion-gel formulae which showed maximum tenoxicam permeation through rat-skin, and compared them with market product Feldene® gel (Piroxicam 0.5%). The obtained results showed that S3 microemulsion-gel formula possesses the maximum drug permeation as well as anti-inflammatory activity which proved to be even greater than Feldene® gel. Therefore, S3 is effectively promising as topical anti-inflammatory dosage forms, due to the permeation enhancement caused by using microemulsions together with the gel base.

**Keywords:** Microemulsions; Tenoxicam; Gels.

### 1530. The Design and Evaluation of Novel Encapsulation Technique for Topical Application of Alpha Lipoic Acid

Ehab Rasmy Bendas, Saly Sherif and Sabry Badawy

*Journal of Advanced Pharmaceutical Research*, 4: 13-22 (2013)

Cubosomes are discrete, sub-micron, nanostructured particles of the bicontinuous cubic liquid crystalline phase. Such novel particles are utilized to encapsulate guest molecules which are either hydrophilic, lipophilic or amphiphilic, due to the compartmentalization of its structure. Cubosomes usually have been produced by means of time-consuming methods involving high energy input "Top-down approach". However, the application of high energy is regarded as a barrier to temperature sensitive ingredients and is difficult to scale up. As a result, it was useful to develop a process for producing cubosomes that requires no significant energy input as the "Bottom-up approach". The purpose of this study was to evaluate the efficiency of both approaches in fabrication of cubosomes. Dispersions were characterized by visual inspection, optical and transmission electron microscopy, encapsulation efficiency and in-vitro release. Results indicated that the bottom-up approach using less energy input was more efficient in generation of smaller cubosomes with higher encapsulation efficiency and slower release rate.

**Keywords:** Liquid crystals; Glyceryl monooleate; Alpha lipoic acid; Cubosomes; Bottom-up approach; Top-down approach.

### Dept. of Pharmacognosy

### 1531. Rice Bran Extract Protects from Mitochondrial Dysfunction in Guinea Pig Brains

Hesham Ibrahim El-Askary, Stephanie Hagl, Alexa Kocher, Christina Schiborr, Schamim H. Eckert, Ion Ciobanu, Marc Birringer, Amr Helal, Mohamed T. Khayyal, Jan Frank, Walter E. Muller and Gunter P. Eckert

*Pharmacological Research*, 76: 17-27 (2013) IF: 4.346

Mitochondrial dysfunction plays a major role in the development of age-related neurodegenerative diseases and recent evidence suggests that food ingredients can improve mitochondrial function. In the current study we investigated the effects of feeding a stabilized rice bran extract (RBE) on mitochondrial function in the brain of guinea pigs. Key components of the rice bran are oryzanols, tocopherols and tocotrienols, which are supposed to have beneficial effects on mitochondrial function. Concentrations of  $\alpha$ -tocotrienol and  $\gamma$ -carboxyethyl hydroxychroman (CEHC) but not  $\gamma$ -tocotrienol were significantly elevated in brains of RBE fed animals and thus may have provided protective properties. Overall respiration and mitochondrial coupling were significantly enhanced in isolated mitochondria, which suggests improved mitochondrial function in brains of RBE fed animals. Cells isolated from brains of RBE fed animals showed significantly higher mitochondrial membrane potential and ATP levels after sodium nitroprusside (SNP) challenge indicating resistance against mitochondrial dysfunction. Experimental evidence indicated increased mitochondrial mass in guinea pig brains, e.g. enhanced citrate synthase activity, increased cardiolipin as well as respiratory chain complex I and II and TIMM levels. In addition levels of Drp1 and fis1 were also increased in brains of guinea pigs fed RBE, indicating enhanced fission events. Thus, RBE represents a potential nutraceutical for the prevention of mitochondrial dysfunction and oxidative stress in brain aging and neurodegenerative diseases.

**Keywords:** Bioenergetics; Mitochondria; Brain; Nutrition; Respiration; Cardiolipin; Mitochondrial dynamics; Nitrosative stress; Oxidative stress; Rice bran extract.

### 1532. Acylated Pregnane Glycosides from *Caralluma Quadrangula*

Essam Abdel-Hamid Abdel-Sattar, Hossam M. Abdallah, Abdel-Moneim M. Osman and Hussein Almehdar

*Phytochemistry*, 88: 54-60 (2013) IF: 3.575

In a previous study, the methanolic extract as well as the chloroform fraction of the aerial parts of *Caralluma quadrangula* (Forssk.) N.E.Br. indigenous to Saudi Arabia showed significant in vitro cytotoxic activity against breast cancer (MCF7) cell line. In a biologically-guided fractionation approach, four acylated pregnane glycosides were isolated from the chloroform fraction of *C. quadrangula*. The structures of the isolated compounds were elucidated by the analysis of their MS and NMR data. The compounds were identified as 12,20-di-O-benzoylboucerin 3-O- $\beta$ -D-digitoxopyranosyl-(1  $\rightarrow$  4)- $\beta$ -D-canaropyranosyl-(1  $\rightarrow$  4)- $\beta$ -D-cymaropyranoside (1), 12,20-di-O-benzoylboucerin 3-O- $\beta$ -D-cymaropyranosyl-(1  $\rightarrow$  4)- $\beta$ -D-canaropyranosyl-(1  $\rightarrow$  4)- $\beta$ -D-cymaropyranoside (2), 12,20-di-O-benzoylboucerin 3-O- $\beta$ -D-glucopyranosyl-(1  $\rightarrow$  4)- $\beta$ -D-digitoxopyranosyl-(1  $\rightarrow$  4)- $\beta$ -D-canaropyranosyl-(1  $\rightarrow$  4)- $\beta$ -D-cymaropyranoside (3) and 12,20-di-O-benzoyl-3,5a,12 $\beta$ ,14 $\beta$ ,20-pentahydroxy-(20R)-pregn-6-ene 3-O- $\beta$ -D-glucopyranosyl-(1  $\rightarrow$  4)- $\beta$ -D-digitoxopyranosyl-(1  $\rightarrow$  4)- $\beta$ -D-canaropyranosyl-(1  $\rightarrow$  4)- $\beta$ -D-cymaropyranoside (4). The isolated compounds were tested for their cytotoxic activity against breast cancer (MCF7) cell line.

**Keywords:** *Caralluma quadrangula*; Asclepiadaceae; Pregnane glycosides; Cytotoxicity on breast cancer.

### 1533. Metabolomics Driven Analysis of Artichoke Leaf and its Commercial Products Via UHPLC-qTOF-MS and Chemometrics

Mohamed Ali Ali Farag, Sherweit H. El-Ahmady, Fatma S. Elian and Ludger A. Wessjohann

*Phytochemistry*, 95: 177-187 (2013) IF: 3.3

The demand to develop efficient and reliable analytical methods for the quality control of herbal medicines and nutraceuticals is on the rise, together with an increase in the legal requirements for safe and consistent levels of active principles. Here, we describe an ultra-high performance liquid chromatography method (UHPLC) coupled with quadrupole high resolution time of flight mass spectrometry (qTOF-MS) analysis for the comprehensive measurement of metabolites from three *Cynara scolymus* (artichoke) cultivars: American Green Globe, French Hyrious, and Egyptian Baladi. Under optimized conditions, 50 metabolites were simultaneously quantified and identified including: eight caffeic acid derivatives, six saponins, 12 flavonoids and 10 fatty acids. Principal component analysis (PCA) was used to define both similarities and differences among the three artichoke leaf cultivars. In addition, batches from seven commercially available artichoke market products were analysed and showed variable quality, particularly in caffeic acid derivatives, flavonoid and fatty acid contents. PCA analysis was able to discriminate between various preparations, including differentiation between various batches from the same supplier. To the best of our knowledge, this study provides the first approach utilizing UHPLC-MS based metabolite fingerprinting to reveal secondary metabolite compositional differences in artichoke leaf extracts.

**Keywords:** Artichoke; *Cynara scolymus* L. (Asteraceae); Principal component analysis; Quality control; UHPLC-MS.

### 1534. Phytochemical, Phylogenetic, and Anti-Inflammatory Evaluation of 43 *Urtica* Accessions (Stinging Nettle) Based on UPLC-Q-TOF-MS Metabolomic Profiles

Mohamed Ali Ali Farag, Maximilian Weigend, Federico Luebert, Grischa Brokamp and Ludger A. Wessjohann

*Phytochemistry*, 96: 170-183 (2013) IF: 3.3

Several species of the genus *Urtica* (especially *Urtica dioica*, Urticaceae), are used medicinally to treat a variety of ailments. To better understand the chemical diversity of the genus and to compare different accessions and different taxa of *Urtica*, 63 leaf samples representing a broad geographical, taxonomical and morphological diversity were evaluated under controlled conditions. A molecular phylogeny for all taxa investigated was prepared to compare phytochemical similarity with phylogenetic relatedness. Metabolites were analyzed via UPLC-PDA-MS and multivariate data analyses. In total, 43 metabolites were identified, with phenolic compounds and hydroxy fatty acids as the dominant substance groups. Principal component analysis (PCA) and hierarchical clustering analysis (HCA) provides a first structured chemotaxonomy of the genus. The molecular data present a highly resolved phylogeny with well-supported clades and subclades. *U. dioica* is retrieved as both para- and polyphyletic. European members of the *U. dioica* group and the North American subspecies share a rather similar metabolite

profile and were largely retrieved as one, nearly exclusive cluster by metabolite data. This latter cluster also includes- remotely related- *Urtica urens*, which is pharmaceutically used in the same way as *U. dioica*. However, most highly supported phylogenetic clades were not retrieved in the metabolite cluster analyses. Overall, metabolite profiles indicate considerable phytochemical diversity in the genus, which largely falls into a group characterized by high contents of hydroxy fatty acids (e.g., most Andean-American taxa) and another group characterized by high contents of phenolic acids (especially the *U. dioica*-clade). Anti-inflammatory in vitro COX1 enzyme inhibition assays suggest that bioactivity may be predicted by gross metabolic profiling in *Urtica*.

**Keywords:** *Urtica dioica* L.; Urticaceae; Metabolic profiling; UPLC-MS; Anti-inflammatory; Phylogeny.

### 1535. Cytotoxic Effect of Commercial Humulus Lupulus L. (HOP) Preparations – in Comparison to its Metabolomic Fingerprint

Mohamed Ali Farag and Ludger A. Wessjohann

*Journal of Advanced Research*, 4: 417-421 (2013) IF: 3.0

Hops (*Humulus lupulus* L. Cannabaceae) is an economically important crop, that has drawn more attention in recent years due to its potential pharmaceutical applications. Bitter acids (prenylated polyketides) and prenylflavonoids are the primary phytochemical components that account for hops resins medicinal value. We have previously reported on utilizing untargeted NMR and MS metabolomics for analysis of 13 hops cultivars, revealing for differences in  $\alpha$ - versus  $\beta$ -bitter acids composition in derived resins. In this study, effect of ratios of bitter  $\alpha$ - to  $\beta$ -acids in hop resins to cytotoxicity of hop resins was investigated. In vitro cell culture assays revealed that  $\beta$ -acids were more effective than  $\alpha$ -acids in growth inhibition of PC3 and HT29 cancer cell lines. Nevertheless, hop resins enriched in  $\beta$ -acids showed comparable growth inhibition patterns to  $\alpha$ -enriched resins and suggesting that bioactivity may not be easily predicted by metabolomics and/or gross metabolic profiling in hops.

**Keywords:** *Humulus lupulus* L.; Metabolomics; Humulones; Lupulones; Anticancer activity; Hops.

### 1536. Metabolome Classification of Brassica Napus L. Organs Via UPLC-QTOF-PDA-MS and Their Anti-Oxidant Potential

Mohamed Ali Farag, Mohamed G. Sharaf Eldin, Hanaa Kassem and Mohamed Abou el Fetouh

*Phytochemical Analysis*, 24: 277-287 (2013) IF: 2.5

**Introduction:** *Brassica napus* L. is a crop widely grown for its oil production and other nutritional components in the seed. In addition to the seed, other organs contain a wide range of phenolic metabolites although they have not been investigated to the same extent as in seeds.

**Objective:** To define and compare the phytochemical composition of *B. napus* L. organs, namely the root, stem, leaf, inflorescence and seeds.

**Method:** Non-targeted metabolomic analysis via UPLC-QTOF-MS was utilised in order to localise compounds belonging to various chemical classes (i.e. oxygenated fatty acids, flavonols, phenolic acids and sinapoyl choline derivatives).

**Results:** The vast majority of identified metabolites were flavonol glycosides that accumulated in most of the plant organs. Whereas other classes were detected predominantly in specific organs, i.e. sinapoyl cholines were present uniquely in seeds. Furthermore, variation in the accumulation pattern of metabolites from the same class was observed, particularly in the case of quercetin, kaempferol and isorhamnetin flavonols. Anti-oxidant activity, based on 2,2-diphenyl-1-picrylhydrazyl analysis was observed for all extracts, and correlated to some extent with total flavonoid content.

**Conclusion:** This study provides the most complete map for polyphenol composition in *B. napus* L. organs. By describing the metabolites profile in *B. napus* L., this study provides the basis for future investigations of seeds for potential health and/or medicinal use.

**Keywords:** UPLC-MS; Metabolite profiling; Nmr; Principal component analysis; Anti-oxidant; Flavonoids; *Brassica napus* L.

### 1537. Dynamic Chemical Communication Between Plants and Bacteria Through Airborne Signals: Induced Resistance by Bacterial Volatiles

Mohamed Ali Farag, Huiming Zhang and Choong-Min Ryu

*Journal of Chemical Ecology*, 39: 1007-1018 (2013) IF: 2.5

Certain plant growth-promoting rhizobacteria (PGPR) elicit induced systemic resistance (ISR) and plant growth promotion in the absence of physical contact with plants via volatile organic compound (VOC) emissions. In this article, we review the recent progress made by research into the interactions between PGPR VOCs and plants, focusing on VOC emission by PGPR strains in plants. Particular attention is given to the mechanisms by which these bacterial VOCs elicit ISR. We provide an overview of recent progress in the elucidation of PGPR VOC interactions from studies utilizing transcriptome, metabolome, and proteome analyses. By monitoring defense gene expression patterns, performing 2-dimensional electrophoresis, and studying defense signaling null mutants, salicylic acid and ethylene have been found to be key players in plant signaling pathways involved in the ISR response. Bacterial VOCs also confer induced systemic tolerance to abiotic stresses, such as drought and heavy metals. A review of current analytical approaches for PGPR volatile profiling is also provided with needed future developments emphasized. To assess potential utilization of PGPR VOCs for crop plants, volatile suspensions have been applied to pepper and cucumber roots and found to be effective at protecting plants against plant pathogens and insect pests in the field. Taken together, these studies provide further insight into the biological and ecological potential of PGPR VOCs for enhancing plant self-immunity and/or adaptation to biotic and abiotic stresses in modern agriculture.

**Keywords:** PGPR; ISR; IST; Volatile organic compounds; Headspace.

### 1538. Botanical and Genetic Characteristics of Farsetia Aegyptia Turra Growing in Egypt

Amira Ahmed Abdel Motaal, Walaa M. Ismail, Nadia M. Sokkar and Ahlam M. El-Fishawy

*Bulletin of Faculty of Pharmacy, Cairo University*, 51: 151-165 (2013) IF: 2.0

*Farsetia aegyptia* Turra is a perennial woody desert shrub native to Egypt. It is used by native Bedouins as an anti-diabetic and antispasmodic. Study of the botanical features was carried out for the root, young and old stems, leaf, fruit and seed of the plant. *F. aegyptia* Turra was characterized by the presence of myrosin cells and non-glandular branched unicellular two-armed hairs in the stem, leaves and fruit, while the root showed sclereids with a wide or narrow lumen and lignified pitted walls. Furthermore, the DNA of the plant was extracted from leaf samples and analysed using ten random decamer primers. A total of 58 random amplified polymorphic DNA (RAPD) markers were identified. Both the botanical study and the DNA fingerprint helped in the identification of the plant.

**Keywords:** Farsetia; Botanical study; DNA fingerprint.

### 1539. Phytochemical Analysis and Anti-Inflammatory Potential of *Hyphaene Thebaica* L. Fruit

Mohamed Ali Farag and Paul W. Paré

*Journal of Food Science*, 78: C1503-C1508 (2013) IF: 1.77

Metabolite profiling and biological activity are reported from organic and aqueous extracts of the fruit from the desert palm *Hyphaene thebaica*. Phenolics and oxylipids profiles were determined using UPLC-PDA-TOF (ultra performance-photodiode array-time of flight) high-resolution mass spectrometry in order to obtain the molecular formula and exact mass. Under optimized conditions, 17 compounds were simultaneously identified and quantified including 2 cinnamic acid derivatives, 5 flavonoids, 6 fatty acids, 2 sphingolipids, a lignan, and a stilbene. Sugars composition in the fruit was characterized and quantified by <sup>1</sup>H-NMR (nuclear magnetic resonance) with sucrose detected as the major component in fruit at a level of 219 mg/g. Fruit organic extracts anti-inflammatory potential was assessed in vitro by cyclooxygenase-1 enzyme inhibition.

**Keywords:** *Hyphaene thebaica* L.; NMR; UPLC/MS; Anti-inflammatory activity; Phenolics.

### 1540. Comparative Study of Volatile Oil Content and Antimicrobial Activity of Pecan Cultivars Growing in Egypt

Ali Mahmoud Ali Hassaneen El-Halawany, Seham S. El Hawary, Soumaya S. Zaghloul and Mahitab H. El Bishbishy

*Journal of Medicinal Foods*, 16: 1022-1029 (2013) IF: 1.642

The volatile oils obtained from the leaves of four pecan cultivars growing in Egypt were evaluated for their chemical composition and antimicrobial activity. The selected cultivars (cv.) were *Carya illinoensis* (Wangneh.) K. Koch. cv. Wichita, *C. illinoensis* cv. Western Schley, *C. illinoensis* cv. Cherokee, and *C. illinoensis* cv. Sioux. The gas chromatography-mass spectrometry analyses revealed that the volatile oils from samples of the different cultivars differ in composition and percentage of their components.  $\beta$ -Curcumene was found as the major constituent of the cv. Wichita oil, whereas germacrene D was the major component of cv. Sioux, cv. Cherokee, and cv. Western Schley. The antimicrobial activity was assayed using the Kirby-Bauer Method by measuring the zone of inhibition of growth. All

volatile oils displayed an antimicrobial activity against the tested bacterial strains. On the other hand, only the volatile oil of cv. Wichita showed an antifungal effect on *Aspergillus flavus*. This work has identified candidates of volatile oils for future in vivo studies to develop antibiotic substitutes for the diminution of human and animal pathogenic bacteria. Nevertheless, the variations of the volatile oil components and antimicrobial potencies of the different studied cultivars, necessitate identifying the cultivars used in future studies.

**Keywords:** Anti-bacterial; Anti-funga;  $\beta$ -curcumene; *Carya illinoensis*; germacrene D.

### 1541. A New Fatty Alcohol from *Terminalia Arjuna* Leaves

Ahlam Mahmoud Elfishawy, Samir A. Ross, Ataa Said, Usama W. Hawas, Babu L. Tekwani, Mohamed M. Radwan and Mohamed Aboelmagd

*Medicinal Chemistry Research*, 22 (12) 5844-5847 (2013)  
IF: 1.612

A new fatty alcohol (1) together with ten known compounds was isolated from the leaves of *Terminalia arjuna* Roxb. Their chemical structures were established on the basis of physical, chemical, and spectroscopic methods to be identified as (*E*)-3,5,7,16 tetramethylheptadeca-2-en-1-ol (1), apigenin, luteolin, vitexin, isovitexin, luteolin-3'-glucuronide, gallic acid, methyl gallate, ellagic acid, stigmaterol, and  $\beta$ -sitosterol-3-*O*-glucoside. Apigenin, vitexin, and isovitexin were isolated for the first time from this species, while luteolin-3'-glucuronide was isolated for the first time from the genus *Terminalia*. Compound 1 and its acetate derivative (2) showed good antileishmanial activity with IC<sub>50</sub> values of 9.0 and 2.0  $\mu$ g/mL, respectively.

**Keywords:** *Terminalia arjuna*; Fatty alcohol; Flavonoids; Antileishmanial.

### 1542. Screening of Immunomodulatory Activity of Total and Protein Extracts of Some Moroccan Medicinal Plants

Essam Abdel-Hamid Abdel-Sattar, Abdeljlil Daoudi and Lotfi Aarab

*Toxicology and Industrial Health Journal*, 29: 245-253 (2013)  
IF: 1.555

Herbal and traditional medicines are being widely used in practice in many countries for their benefits of treating different ailments. A large number of plants in Morocco were used in folk medicine to treat immunerelated disorders.

The objective of this study is to evaluate the immunomodulatory activity of protein extracts (PEs) of 14 Moroccan medicinal plants. This activity was tested on the proliferation of immune cells. The prepared total and PEs of the plant samples were tested using MTT (3-(4,5-dimethylthiazol-2-yl)-2,5-diphenyltetrazolium bromide) assay on the splenocytes with or without stimulation by concanavalin-A (Con-A), a mitogenic agent used as positive control.

The results of this study indicated different activity spectra. Three groups of activities were observed. The first group represented by *Citrullus colocynthis*, *Urtica dioica*, *Elettaria cardamomum*, *Capparis spinosa* and *Piper cubeba* showed a significant

immunosuppressive activity. The second group that showed a significant immunostimulatory activity was represented by *Aristolochia longa*, *Datura stramonium*, *Marrubium vulgare*, *Sinapis nigra*, *Delphinium staphysagria*, *Lepidium sativum*, *Ammi visnaga* and *Tetraclinis articulata*.

The rest of the plant extracts did not alter the proliferation induced by Con-A. This result was more important for the PE than for the total extract. In conclusion, this study revealed an interesting immunomodulating action of certain PEs, which could explain their traditional use.

The results of this study may also have implications in therapeutic treatment of infections, such as prophylactic and adjuvant with cancer chemotherapy.

**Keywords:** Immunomodulatory activity; Mtt assay; Total extract; Protein extract; *Citrullus colocynthis*; *Lepidium sativum*; *Datura stramonium*.

#### 1543. Anti-Estrogenic Activity of Mansonone G and Mansorin A Derivatives

Riham Salah El-Dine El Sayed, Ali M. El-Halawany and Masao Hattori

*Pharmaceutical Biology*, 51: 948-954 (2013) IF: 1.206

**Context:** Mansonone G and mansorin A are major bioactive constituents from *Mansonia gagei* Drumm (Sterculiaceae) wood, and their mild anti-estrogenic activity was reported previously by the authors.

**Objective:** In order to increase the potency of their anti-estrogenic effect and to clarify their binding way to estrogen receptor on a molecular level, several derivatives of both compounds will be prepared and a docking study of the original compounds and their derivatives on estrogen receptor alpha (ER $\alpha$ ) was carried out.

**Materials and methods:** The original compounds were isolated from the heartwood of *M. gagei*.

Nine alkyl derivatives were prepared by acetylation, methylation, or adding a basic side chain to the free hydroxyl group of both compounds.

The estrogenic/anti-estrogenic activities of the derivatives compared to the original compounds were carried out using ER $\alpha$  competitive binding screen and yeast two-hybrid assay expressing ER $\alpha$  and ER $\beta$  using concentrations ranging from 10 to 100  $\mu$ M.

**Results:** Acetyl mansonone G showed a 10-fold increase in its binding ability to ER $\alpha$  compared to mansonone G with an IC<sub>50</sub> 630  $\mu$ M. Similarly, methyl mansonone G and acetyl mansonone G showed 50% and 35% inhibition of 17 $\beta$ -estradiol-induced  $\beta$ -galactosidase activity at 10  $\mu$ M in the yeast expressing ER $\alpha$ , and 42% and 30%, respectively, at 10  $\mu$ M in the yeast expressing ER $\beta$ . Virtual docking of acetyl mansonone G to ER $\alpha$  showed that it binds, with its acetyl oxygen, in a similar way to the 17 $\beta$ -OH of estradiol.

**Discussion and conclusion:** The phenolic hydroxyl group in mansonones and mansorins was not essential for binding to estrogen receptors. In addition, acetyl mansonone G could represent a promising starting material for the synthesis of anti-estrogenic agents.

**Keywords:** Acetyl mansonone G; Docking study; ER $\alpha$  And ER $\beta$ ; *Mansonia gagei*; Tamoxifen.

#### 1544. Protective Effect of Echinops Galalensis Against CCL<sub>4</sub>-Induced Injury on the Human Hepatoma Cell Line (HUH7)

Shahira Mohammed Ezzat, Hossam M. Abdallah, Riham Salah El Dine, Essam Abdel-Sattar and Ashraf B. Abdel-Naim

*Phytochemistry Letters*, 6: 73-78 (2013) IF: 1.179

Phytochemical investigation of the flowering aerial parts of *Echinops galalensis* (Asteraceae) led to the isolation of a new taraxasteryl triterpene, 3 $\beta$ -acetoxy-taraxast-12, 20(30)-diene-11 $\alpha$ -21 $\alpha$ -diol (1), together with nine known metabolites,  $\alpha$ -amyrin (2),  $\beta$ -sitosterol (3), erythrodilol (4), lup-20(29)-ene-1,3-diol (5), 1,5-dicaffeoylquinic acid (6), 3,5-dicaffeoylquinic acid (7), 3,4-dicaffeoylquinic acid (8), 4,5-dicaffeoylquinic acid (9) and apigenin-7-O- $\beta$ -D-glucoside (10).

The structure of the new compound was determined by comprehensive analyses of their 1D and 2D NMR, mass spectral (HR-EI) data and comparison with previously known analogs. The effect of the methanol extract of *E. galalensis*, its fractions as well as compounds (1–10) on human hepatoma cell line (Huh7) was evaluated according to aspartate aminotransferase (AST), alanine transaminase (ALT), superoxide dismutase (SOD) activities and malondialdehyde (MDA) level before and after exposure of the cells to carbon tetrachloride (CCl<sub>4</sub>). It was found that pre-treatment of human hepatoma cell line (Huh7) with the tested samples (100  $\mu$ g/ml) prior to CCl<sub>4</sub> challenge protected against cell injury. The protective effect of *E. galalensis* was suggested to be mediated, at least partly, by its antioxidant activity.

**Keywords:** *Echinops galalensis*; 3 $\beta$ -Acetoxy-taraxast-12 20(30)-diene-11 $\alpha$ ,21 $\alpha$ -Diol; Hepatoprotective; Huh7 cell line.

#### 1545. Comparative Study of the Chemical Composition and Biological Activities of Magnolia Grandiflora and Magnolia Virginiana Flower Essential Oils

Mohamed Ali Farag and Dalia A. Al-Mahdy

*Natural Product Research*, 27: 1091-1097 (2013) IF: 1.05

The biological activities and the determined major volatile components in the *Magnolia grandiflora* and *M. virginiana* flowers extracts were compared. Volatile components were detected in the essential oil by dynamic headspace sampling (HS). 2-Phenylethanol (40% and 61%) was found as the main constituent in the essential oil and HS samples of *M. virginiana*, respectively.

In the *M. grandiflora* oil sample, (*E,E*)-farnesol (18%) and 2-phenylethanol (10%) were found as main constituents, whereas germacrene D (17%) and  $\beta$ -bisabolene (17%) were the main components of the HS sample. The essential oil in *M. virginiana* displayed a moderate antioxidant activity relative to vitamin E, whereas both essential oils were active against human lung carcinoma and breast carcinoma cell lines, even at concentrations higher than 200  $\mu$ g mL<sup>-1</sup>.

**Keywords:** *Magnolia grandiflora* L., *Magnolia virginiana* L.; Headspace volatiles; Essential oil; Antioxidant; Anticancer; GC-MS.



#### 1546. Metabolite Profiling Driven Analysis of *Salsola* Species and their Anti-Acetylcholinesterase Potential

Mohamed Ali Ali Farag, Dalia M. Rasheed, Soheir M. El Zalabani, Mahmoud A. Koheil and Hala M. El-Hefnawy

*Natural Product Research*, 27: 2320-2327 (2013) IF: 1.1

Over 100 species of the genus *Salsola* are distributed in dry, arid parts of Asia, Europe and Africa, of which many species are recognised as antifungal, anticancer, antihypertensive and anthelmintic agents. Egyptian *Salsola* received scant characterization of either its phytochemical composition or its biological effects.

In this study, the metabolite profiles of two *Salsola* species viz. *S. vermiculata* and *S. tetrandra* were characterised in the aerial portions and root via ultra-performance liquid chromatography high-resolution qTOF-MS and NMR. Identified metabolites belonged to various classes including hydroxycinnamic acid conjugates, flavonoids, oxygenated fatty acids and alkaloids. Principal component analysis of derived biochemical profiles was also used for species and/or organs classification.

Roots were enriched in hydroxycinnamic acid conjugates, whereas flavonoids were more abundant in aerial parts with kaempferol derivatives as major flavonoids in *S. tetrandra* versus quercetin in *S. vermiculata*. The root of *S. vermiculata* exhibited strong anti-acetylcholinesterase activity relative to eserine standard.

**Keywords:** *Salsola*; Metabolite profiling; Anticholinesterase; UPLC/MS; NMR; PCA.

#### 1547. Evaluation and Characterization of the Immunomodulatory Activity of the Protein Extract from *Citrullus Colocynthis* L

Essam Abdel-Hamid Abdel-Sattar, Abdeljlil Daoudi, Dalila Boustia and Lotfi Aarab

*Food and Agricultural Immunology*, 24: 47-57 (2013)  
IF: 0.73

*Citrullus colocynthis* L. is a plant widely used in Moroccan traditional medicine as a strong laxative and has many others uses. The aim of the present work is to evaluate the immunomodulatory activity of the protein extract (PE) from seeds of *C. colocynthis*.

The results of this study showed that the PE has an immunosuppressive activity in vitro. The activity was assessed through the evaluation of the proliferation of splenocytes induced by the mitogen concanavalin-A factor.

The PE showed no agglutination activity against rabbit erythrocytes, and was separated into two fractions F1 and F2 with molecular weight of 160 and 79 kDa, respectively. Fraction F1 showed the highest immunosuppressive activity (44.62%) in dose-dependent manner ( $IC_{50}$  60  $\mu$ g/mL) and is characterized into three sub-units of 53.65 kDa. The sub-units of F1 were determined by the polyacrylamide gel electrophoresis. The fraction F1 of the PE could be a promising immunosuppressing agent extracellular.

**Keywords:** *Citrullus colocynthis*; Concanavalin-A; Splenocytes; Gel electrophoresis; Immunomodulatory; Immunosuppressive.

#### 1548. Development and Validation of A High-Performance Liquid Chromatography Method for Standardization of the Bioactive Ethyl Acetate Fraction of *Alstonia Scholaris* (Linn.) R. Br. Growing in Egypt

Hesham Ibrahim El-Askary, Mahmoud M. El-Olemy, Maha M. Salama and Mahetab H. Amer

*Zeitschrift Fur Naturforschung C*, 68: 376-383 (2013) IF: 0.604

Bio-guided fractionation of the ethanolic extract of the leaves of *Alstonia scholaris* (Apocynaceae) growing in Egypt was carried out to evaluate its antihyperglycemic activity in alloxan-induced diabetic rats and its hepatoprotective activity against  $CCl_4$ -induced hepatotoxicity in rats. The ethyl acetate fraction of the ethanolic extract showed the highest antihyperglycemic [(133.6  $\pm$  4.2) mg/mL, relative to metformin with (92.3  $\pm$  2.7) mg/mL] and hepatoprotective [(37.9  $\pm$  1.4) U/L, relative to silymarin with (29.7  $\pm$  0.8) U/L] activities. Four compounds were isolated from this fraction, and identified by spectroscopic techniques and by comparison with reported data: caffeic acid and isoquercitrin for the first time from this plant, in addition to quercetin 3-*O*- $\beta$ -D-xylopyranosyl (1" $\rightarrow$ 2")- $\beta$ -D-galactopyranoside (major compound) and chlorogenic acid. A validated reversed phase-high-performance liquid chromatography (RP-HPLC) method was developed for the standardization of the bio active ethyl acetate fraction. The calibration curve showed good linearity ( $r^2 > 0.999$ ) within tested ranges. The relative standard deviation of the method was less than 3% for intra- (0.4 – 2.0%) and inter-day (1.9 – 2.8%) assays. Mean recovery of the method was within the range of 98.5 – 102.5%. The minimum detectable concentration of the analyte (LOD) was found to be 0.04  $\mu$ g/mL. This developed HPLC method was shown to be simple, rapid, precise, reproducible, robust, specific, and accurate for quality assessment of the bioactive fraction.

**Keywords:** Validated RP-HPLC method; Quercetin 3-*O*- $\beta$ -D-xylopyranosyl (1" $\rightarrow$ 2")- $\beta$ -dgalactopyranoside; *Alstonia scholaris*.

#### 1549. Hepatitis C Virus NS3-NS4A Protease Inhibitors from the Endophytic *Penicillium Chrysogenum* Isolated from the Red Alga *Liagora Viscida*

Ali Mahmoud Ali Hassaneen El-Halawany, Usama W. Hawas and Eman F. Ahmed

*Z. Naturforsch. C*, 68c: 355-366 (2013) IF: 0.604

Hepatitis C virus (HCV) NS3-NS4A protease is an attractive target for anti-HCV agents because of its important role in replication. In this work, we demonstrated that the ethyl acetate extract of the endophytic fungus *Penicillium chrysogenum* exhibited a potent activity against HCV NS3-NS4A protease with an  $IC_{50}$  value of 20  $\mu$ g/mL. The fungus was isolated from the red alga *Liagora viscida* and identified by its morphology and 18S rDNA. Largescale fermentation of the fungus in Czapek's peptone liquid medium followed by chromatographic purification of the active extract from the liquid medium allowed the isolation of twelve known metabolites. The biological properties of the isolated compounds were explored for anti-HCV protease as well as antimicrobial and anticancer activities. A computational docking study of the active isolated compounds against HCV

protease was used to formulate a hypothetical mechanism for the inhibitory activity of the active compounds on the tested enzymes.

**Keywords:** Red algae; Liagora viscid; Penicillium chrysogenum; HCV NS3-NS4A protease.

#### 1550. New Bioactive Metabolites from A Crown Gall Induced on an Eucalyptus Tereticornis Sm. Tree

Maha Mahmoud Salama, Shahira M. Ezzat, Riham Salah El Dine, Aly M. El-Sayed and Amany A. Sleem

*Zeitschrift Fur Naturforschung C*, 68: 461-47 (2013) IF: 0.604

Applying a bioactivity-guided isolation strategy for the ethanolic extract of crown gall tumours induced on an Eucalyptus tereticornis tree, two new compounds in addition to a known one were isolated. The new compounds were identified as an amino acid derivative named 1-ethyl-6-(1'-methyl-1'-phenylethyl) piperidin-2-one (1) and a lanostane tetracyclic triterpene named 3 $\beta$ -hydroxy-24-methyl-28,17(20),24(28)-trien-22-oic acid (2), together with stigmastrol-3-O-glucoside (3). The three compounds exhibited significant cytotoxic activity against two human cell lines, breast (MCF7) and colon (HCT116), with IC<sub>50</sub> values of 1.01, 1.54, and 2.15  $\mu$ g/ml, respectively, against MCF7 and 3.49, 3.83, and 3.39  $\mu$ g/ml, respectively, against HCT116. Furthermore, in rats elevated levels of blood cholesterol, triglycerides, and low-density lipoprotein (LDLc) were significantly reduced, while the level of high-density lipoprotein (HDLc) was significantly increased by administration of the ethanolic extract as well as of 3. These results support a correlation between the reduction of blood cholesterol levels and improvement of colorectal cancer.

**Keywords:** Crown gall; New amino acid derivatives; Colorectal cancer.

#### 1551. Antiosteoporotic Effect of Some Herbal Extracts Versus Alendronate on an Animal Model of Osteoporosis

Essam Abdel-Hamid Abdel-Sattar, Laila Sabry, Mai Abdul Sattar and Hanan Ali Amin

*Life Science Journal* 10, 10: 177-187 (2013) IF: 0.165

The aim of the present study was to investigate the rationale for the use of two herbal extracts of Sophora japonica and Calligonum comosum whether alone or in combination versus alendronate in treatment of osteoporosis. Female albino rats were randomly arranged in eleven groups; 8 rats each. First group served as normal control while the second was sham operated. The remaining nine groups were ovariectomized (OVX); the first of which was not treated and served as a control for the other OVX and treated groups, while the second group received only DMSO (vehicle). The third group was treated with alendronate. Fourth, fifth, sixth and seventh groups were treated with Sophora and Calligonum at two dose levels respectively. In addition, eighth and ninth groups were treated with both plants at two dose levels. Alendronate and the extract of the herbs were administered orally daily for three months. Body weight was measured, biochemical effects were evaluated and histomorphometrical examination of the distal parts of the tibia. The results obtained revealed that OVX – treated rats exhibited a dose- dependent improvement in all measured parameters; body

weight, biochemical markers, histomorphometric changes compared to non treated OVX-control group. Furthermore, combination of both plant extracts produced near results to that of alendronate improvement on biochemical markers and on cortical and trabecular bone thickness and this was a dose –dependent. Therefore, the present study clearly demonstrated that the extracts of Sophora Japonica and Calligonum Comosum have the potential for being used as alternative or supplement therapy for osteoporosis.

**Keywords:** Osteoporosis; Sophora japonica; Calligonum Comosum and alendronate.

#### 1552. Botanical and Genetic Characterization of Mentha Suaveolens Ehrh. Cultivated in Egypt

Zeinab Abdel Aziz Mohamed Kandil

*Pharmacognosy Journal*, 5: 228-237 (2013)

This paper deals with the detailed botanical study of the stems and leaves of Mentha suaveolens Ehrh. (Labiatae), a highly valued medicinal and fragrant plant. Mentha suaveolens Ehrh. is useful as a carminative, antispasmodic, diaphoretic, analgesic, anti-inflammatory and antimicrobial drug. It is also useful in case of nausea, bronchitis and anorexia. Botanical investigation of Mentha suaveolens Ehrh has not been reported so far. Therefore, The macro- and micromorphological characteristics of the stems and leaves of Mentha suaveolens Ehrh. cultivated in Egypt are presented, with the aim of finding out the diagnostic characters for identification and differentiation of this species either in the entire or powdered forms. The major microscopic features of the stems and leaves are the presence of both glandular and non-glandular trichomes. Labiateous glandular trichomes, a significant feature responsible for the secretion of volatile oil, are numerous on both stem and leaf surfaces. Also, the presence of diacytic stomata is another important diagnostic feature of the plant. Furthermore, the DNA of the plant was extracted and amplified using 10 decamer primers to reveal RAPD fragments. Each of the ten primers successfully directed the amplification of a genome-specific fingerprint of DNA fragment. A total of 65 different fragments have been generated by the two primers: OPC-07 and OPA-11 respectively, which can be used for the selective discrimination of M. suaveolens Ehrh. The highest numbers of fragments were 15 and 9 produced by the primers OPC-07 and OPA-11 respectively. The analysis of RAPD data, under the experimental conditions, can thus be used to distinguish the plant from other related species.

**Keywords:** Dna Fingerprinting; Macromorphological; Micromorphological; Mint.

#### 1553. Botanical Study, DNA Fingerprinting, Nutritional Values and Certain Proximates of Entada Rheedii Spreng

Mona Morad Mohamed Ibrahim Okba, Fathy M. Soliman<sup>1</sup>, Kadriya S. El-Deeb and Miriam F. Yousif

*International Journal of Pharmacy and Pharmaceutical Sciences*, 5: 311-329 (2013)

Entada rheedii Spreng. (Family Fabaceae) seeds are used in Egypt in folk medicine. Macro- and micro-morphological characters of E. rheedii Spreng. seeds imported from India together with that of

roots, stems and leaves cultivated in Egypt were presented with the aim of their identification in entire and powdered forms. Cultivation in Egypt gave a climbing plant instead of the huge fruiting trees bordering the Indian Ocean. Plant materials were fixed, freehand sectioned and stained with Safranin. Leaves are compound, bipinnate; their blades exhibit rubiaceous and few ranunculaceous stomata, non-glandular trichomes and dorsiventral mesophyll. The stem upper part is cylindrical with six ridges. The stem has relatively wide pith surrounded by open collateral vascular bundles. Study of Deoxyribonucleic acid (DNA) fingerprinting, total seed protein profiling, nutritional value and certain proximates was carried out in order to contribute to the identification of the plant material. A total of 53 different fragments have been recorded in DNA fingerprinting, produced mainly by (A-19) primer, showing 15 bands ranging from 1.337 Kbp to 0.356 Kbp. Eight bands were recorded in seed total protein banding profile of *E. rheedii* Spreng seed with molecular weights ranging from 52 to 9 KDa. High levels of Glutamic acid and Phenyl alanine amino acids were determined. Moisture, carbohydrates and ash percentages were 7.35, 16.47 and 2.83 respectively. Evaluation of macroelements (Ca, Na, K and P); and microelement (Fe) revealed that potassium (K) and phosphorous (P) occupied the highest positions (1264 and 1240 mg/100 g seeds respectively) among the macroelements, whereas the micro element Iron (Fe) level was 3.3 mg/100 g seeds.

**Keywords:** Entada; Macro and micro morphology; Nutritive Value; Amino acids; Macro and micro elements; Proximate analysis.

#### 1554. Chemical Composition and Biological Activities of Peels and Leaves Essential Oils of Four Cultivars of Citrus Deliciosa Var. Tangarina

Azza Ramy Abdel Monem, Seham S. El-hawary, Kamilia F. Taha, Farid N. Kirillos and Amira A. Mohamed

*American Journal of Essential Oil and Natural Product*, 2: 1-6 (2013)

The hydrodistilled essential oils of peels and leaves of four cultivars of *Citrus deliciosa* var. tangarina (Fina Clementine, Nour Clementine, Spinosa Clementine and Thornless Clementine) belonging to family Rutaceae were analyzed by GC/ MS. Limonene was the major constituent of all the oil samples under investigation except in case of Nour Clementine leaves, where sabinene was the major component. Generally, total hydrocarbons were of higher percentage than total oxygenated compounds, also total monoterpenes showed higher percentage than total sesquiterpenes. The studied essential oils showed a dose-dependent antioxidant activity. Thornless leaves oil showed the highest antioxidant potential, it recorded the same  $EC_{50}$  as ascorbic acid. The antimicrobial activity of Citrus peels and leaves oils was screened against Gram-positive and Gram-negative bacteria, yeast and fungi. Leaves oils showed higher antimicrobial activity than peels oils against all the tested microorganisms among them Thorny Clementine leaves oil was the most potent. Peels oils were tested for cytotoxic activity against liver, cervix, breast carcinoma and normal baby hamster kidney fibroblast cell lines. Peels oils showed potent cytotoxic activity against the tested carcinoma cell lines comparing to doxorubicin, while they exhibited no effect on normal baby hamster kidney fibroblast cell line which indicated their safety.

The antiviral activity of the studied essential oils was tested by hemagglutination test of washed chicken erythrocytes. The allantoic amniotic fluid of embryonic eggs inoculated with different Citrus essential oils under investigation, suspension of H5N1 virus and antibiotic gave a positive test, this indicates inactivated H5N1 virus.

**Keywords:** Citrus deliciosa var; Tangarina; Fina Clementine; Nour Clementine; Spinosa clementine; Thornless clementine; Antioxidant; Antimicrobial; Cytotoxic; Antiviral.

#### 1555. Comparative DNA Profiling, Phytochemical Investigation, and Biological Evaluation of Two Ficus Species Growing in Egypt

El-Sayed Ahmed Elkashoury, Mona H. Hetta, Nemat Z. Yassin, Hossam M. Hassan, Sally A. El-Awdan and Naglaa I. Afifi

*Pharmacognosy Research*, 5: 291-299 (2013)

**Aim and Background:** A comparison between two *Ficus* species, cultivated in Egypt, was carried out in this study. Their DNA analysis revealed that they are not closely related.

**Materials and Methods:** The pharmacopoeial constants of the leaves showed higher total ash and acid insoluble ash in *F. lyrata* than in *F. platypoda*. The other parameters were close in both species. Preliminary phytochemical screening revealed the presence of carbohydrate and/or glycosides, tannins, flavonoids, sterols, and triterpenes in their leaves and was detected in traces in their stems.

**Results:** Saponification of n-hexane extract of the leaves yielded 46% and 74.8% for the unsaponifiable matters and 20% and 15% for the fatty acids for *F. platypoda* and *F. lyrata*, respectively. n-Docosane (21.69%) and n-heptacosane (33.77%) were the major hydrocarbons in *F. platypoda* and *F. lyrata*, respectively. b-Sitosterol was the main sterol, palmitic (22.07%) and carboceric (35.72%) acids were the major identified saturated fatty acids in both species, while linoleic acid was the main unsaturated fatty acid (18.66% and 16.7%) in both species, respectively. The acute toxicity study revealed that the two species were safe up to 2 g/kg. The antioxidant activity using 1,1-diphenyl-2-picrylhydrazyl (DPPH) assay and pyrogallol as the standard was more significant for *F. platypoda* (232.6  $\mu$ g/ml) than for *F. lyrata*, (790.9  $\mu$ g/ml). The oral antihyperglycemic activity in diabetic rats using alloxan revealed that the 80% ethanolic extract of the leaves of *F. platypoda* was more active than that of the leaves of *F. lyrata* in decreasing the blood glucose level at 200 mg/kg/day (107.9  $\pm$  5.817, 127.2  $\pm$  4.359) and 400 mg/kg/day (64.11  $\pm$  4.358, 127.7  $\pm$  6.889), respectively, when compared with the diabetic control gliclazide (172.3  $\pm$  2.089).

**Conclusion:** The results of this study provide evidence that the two *Ficus* species have antioxidant and antihyperglycemic activity, in the order *F. platypoda* and then *F. lyrata*.

**Keywords:** Acute toxicity; Antihyperglycemic; Antioxidant; DNA; *Ficus platypoda*; *Ficus lyrata*.

#### 1556. Gas Chromatography-Mass Spectrometry Analysis, Hepatoprotective and Antioxidant Activities of the Essential Oils of Four Libyan Herbs

Shahira Mohammed Ezzat, S. EL-Hawary, A. EL-Shabrawy and F. EL-Shibany

*Journal of Medicinal Plants Research*, 7: 1746-1753 (2013)

Following an ethnobotanical survey for hepatoprotective remedies, four Libyan medicinal plants from family Lamiaceae; *Ajuga iva* (L.) Schreber, *Marrubium vulgare* L., *Rosmarinus officinalis* L. and *Thymus capitatus* Hoff. et Link growing widely in Beida, Libya, were selected for our study. The chemical composition of essential oils hydrodistilled from the dried aerial parts, were analyzed by gas chromatography-mass spectrometry (GC-MS). The major constituents of the essential oils of *A. iva* and *R. officinalis* were carvacrol (35.07%) and 1,8-cineol (35.21%), respectively, thymol was the major constituent of the essential oil of *M. vulgare* (20.11%) and *T. capitatus* (90.15%). The oil of *M. vulgare* had the most powerful antioxidant activity by restoring glutathione levels in the blood of alloxan-induced diabetic rats. The rats treated with the essential oils of *M. vulgare*, *R. officinalis* and *T. capitatus* (50 mg/kg) showed a significant decrease in liver enzymes which were elevated by  $\text{CCl}_4$  ( $p < 0.01$ ). The essential oil of *M. vulgare* had the most potent hepatoprotective activity.

**Keywords:** *Ajuga iva*; *Marrubium vulgare*; *Rosmarinus officinalis*; *Thymus capitatus* antioxidant; Hepatoprotective.

#### 1557. High-Throughput Screening of 75 Euphorbiaceae and Myrtaceae Plant Extracts for in-Vitro Antitumor and Pro-Apoptotic Activities on Human Tumor Cell Lines and Lethality to Brine Shrimp

Nabaweya Mostafa ALi El-fiky, May A. El Manawaty, Walid Fayad, Gamila M. Wassel and Bassem S. El-Menshaw

*International Journal of Pharmacy and Pharmaceutical Sciences*, 5(2): 178-183 (2013)

**Objective:** Various approaches are used for discovering cytotoxic anticancer therapeutics from plants. In this study 75 extracts representing 47 plant species belonging to families Euphorbiaceae and Myrtaceae were screened by three in-vitro bioassays, to detect extracts with possible antitumor activity.

**Methods:** The methanol plant extracts were screened over three bioassays viz., cytotoxicity on HepG2 human hepatocellular carcinoma cell line assessed by MTT method, pro-apoptotic activity on HCT116 human colon carcinoma cell line measured by the increase of M30 neo-epitope apoptosis biomarker through sandwich ELISA, as well as brine shrimp lethality (BSL) bioassay.

**Results:** 54 extracts were active in at least one bioassay. 43 extracts (57%) scored cytotoxic on HepG2, compared to 32 (43%) pro-apoptotic extracts in HCT116-M30 assay and 18 (24%) lethal extracts in BSL test. Out of the 43 cytotoxic extracts 15 (20%) possessed pro-apoptotic activity, which may be considered the ideal candidate agents.

**Conclusion:** The relatively high number of active extracts detected in the 3 bioassays may be attributed to the selected families being rich in reported bioactivities and folk medicinal uses. The extracts of *Melaleuca leucadendron* L. and *Callistemon rigidus* R.Br. were considered the most promising ( $\geq 90\%$  toxicity in HepG2 cytotoxicity and  $\geq 3$  fold increase in apoptotic background signal at 100 ppm); while the activity of *C. rigidus* is firstly to be recorded here and subsequent investigation for its active compounds is recommended. The three bioassay approach described could be useful in screening large numbers of extracts for detecting antitumor agents.

**Keywords:** Cytotoxicity; M30 apoptosense; HepG2 human hepatocellular carcinoma; HCT116 human colon carcinoma; Cancer therapeutics drug discovery.

#### 1558. In Vitro and in Vivo Anticancer Activity of the Fruit Peels of Solanum Melongena L. Against Hepatocellular Carcinoma

Maha Mahmoud Salama, Marawan M Shabana, Shahira M. Ezzat and Laila R. Ismail

*Journal of Carcinogenesis and Mutagenesis*, 4: 1-6 (2013)

**Background:** The fruit peels of *Solanum melongena* L. which is a common vegetable in Egypt, were investigated for biologically active metabolites in an approach to find any medicinal benefits from such waste products.

**Methods:** The Methanol Extract of the Peels (MEP) was subjected to fractionation and purification for the isolation of its major constituents. Identification of the compounds was carried out on the basis of physico-chemical properties and spectral analysis ( $^1\text{H}$  NMR,  $^{13}\text{C}$  NMR, COSY and HMBC). The MEP together with the isolated compounds were tested against five human cancer cell lines representing the most common types of cancer in Egypt: colon cancer cell line (HCT116), larynx cancer cell line (HEP2), breast cancer cell line (MCF7), cervix cancer cell line (HELA) and liver cancer cell line (HEPG2). MEP was tested in vivo against the  $\text{CCl}_4$ -induced hepatocellular carcinoma (HCC) in rats at two dose levels (100 and 200 mg/kg.b.wt).

**Results:** Five steroidal compounds; three steroidal alkaloids: solasodine ( $\text{S}_1$ ), solamargine ( $\text{S}_4$ ) and solasonine ( $\text{S}_5$ ) together with two steroidal glycosides:  $\beta$ -sitosterol-3-O- $\beta$ -D-glucoside ( $\text{S}_2$ ) and poriferasterol-3-O- $\beta$ -D-glucoside ( $\text{S}_3$ ) were isolated. The MEP and the five isolated compounds exhibited moderate to potent activities against the tested human cancer cell lines however their pronounced activity was revealed against HEPG2, accordingly, MEP was tested in vivo against the  $\text{CCl}_4$ -induced Hepatocellular Carcinoma (HCC) in rats. The MEP showed a dose-dependent anticancer activity through stabilization of the hepato-cells revealed by reduction in  $\alpha$ -fetoprotein (AFP) (which could be considered as tumor marker), it also restored the levels of AST, ALT and albumin in a dose dependent manner. Histopathology of liver tissues treated with MEP strongly supported our results. **Conclusion:** Our findings supported the reuse of such waste products as a new remedy for treating cancer.

**Keywords:** *S. melongena* L.; Peels; Hepatocellular carcinoma; Steroidal alkaloids.

#### 1559. In Vitro Antioxidant Potential and Antiprotozoal Activity of Methanolic Extract of Mentha Longifolia and Origanum Syriacum

Khalil H. Al-Ali, Hesham A. El-Beshbishy, Abdulaziz A. Alghaithy, Hossam Abdallah, Ayman A. El-Badry and Essam Abdel-Sattar

*Journal of Biological Sciences*, 13: 207-216 (2013)

Labiatae family is represented in Saudi Arabia. It is one of the most distinctive families of flowering plants with a great diversity. This study aimed to investigate in vitro antioxidant and antiprotozoal activities of methanolic extract of *Mentha longifolia* (ML) and *Origanum syriacum* (OS). OS exhibited high phenolic

contents (mg gallic acid equivalent g-1 weight)  $87 \pm 3.5$  mg GAE g-1. ML produced  $23 \pm 3.2$  mg GAE g-1. Using potassium ferricyanide method, OS exhibited high absorbance after 120 h ( $0.53 \pm 0.037$ ) that was directly proportional to the reducing power, however, ML produced lower absorbance ( $0.38 \pm 0.031$ ). Percentage scavenging activity against diphenyl-2-picryl-hydrazyl radical was 87% (OS) and 128% (ML). Absorbencies of ferric thiocyanate assay was 0.86 and 0.25 for ML and OS, respectively. Using phosphomolybdenum method, OS exhibited antioxidant activity (80%) followed by ML (55%). Percentage superoxide scavenging activities was 47 (OS) and 15% (ML). OS exhibited antimalarial activity against P. falciparum-K1 strain in contrast to ML. OS extract exhibited activity against T. cruzi. ML exhibited activity against T. cruzi. OS exhibited activity against T. b. brucei. However, ML showed no marked activity against T. b. brucei. ML and OS exhibited no marked activity against L. infantum. Both ML and OS exhibited no marked cytotoxic activity against MRC-5 cells. It was concluded that, ML and OS have the potency to act as powerful antioxidants and to some extent as antiprotozoal.

**Keywords:** Cytotoxicity; In Vitro; Antiprotozoal; Mentha; Antioxidant; Organum.

#### 1560. New Triterpenoid Acyl Derivatives and Biological Study of Manilkara Zapota (L.) Van Royen Fruits

Azza Ramy Abdel Monem, Nesrin M. Fayek, Mohamed Y. Mossa and Meselhy R. Meselhy

*Pharmacognosy Research*, 5: 55-59 (2013)

$\beta$ -amyrin-3-(3'-dimethyl) butyrate, a new natural compound was isolated from the fruits of Manilkara zapota (L.) Van Royen, in addition to lupeol-3-acetate and 4-caffeoylquinic acid (cryptochlorogenic acid). The structures of these compounds were identified using different spectral methods (IR, MS, UV,  $^1\text{H}$ -NMR,  $^{13}\text{C}$ -NMR and 2D-NMR). The alcoholic and aqueous extracts of the unripe fruits, in addition to their aqueous homogenate exhibited antioxidant, antihyperglycemic and hypocholesterolemic activities.

**Keywords:** 4-Caffeoylquinic acid; Antihyperglycemic; Antioxidant;  $\beta$ -Amyrin-3-(3'-dimethyl) butyrate; Hypocholesterolemic; Lupeol-3-acetate; Manilkara zapota.

#### 1561. Phenolic Content, Radical Scavenging Activity and Cytotoxicity of Tamarix Nilotica (Ehrenb.) Bunge Growing in Egypt

Rehab Mohamed Seif Eldin Ashour, Riham Omar Bakr and Mohamed Abd El-Aziz El Raey

*J. of Pharmacognosy and Phytotherapy*, 5 (3): 47-52 (2013)

The radical scavenging activity using 1,1-diphenyl, 2-picrylhydrazyl (DPPH) and cytotoxicity using sulphorhodamine B (SRB) assay of the aqueous methanolic extract of Tamarix nilotica (Ehrenb.) Bunge (Tamaricaceae) flowers and its subextracts ( $\text{CHCl}_3$ , EtOAc and Pet.ether) were evaluated. Total phenolic and flavonoid contents were estimated using colorimetric assays. Ethyl acetate (EtOAc) showed the highest free radical scavenging activity with inhibitory concentration ( $\text{IC}_{50}$ )  $7.25 \pm 0.86$   $\mu\text{g/ml}$  in addition to potential cytotoxic effect

on liver cell carcinoma (Huh-7) ( $\text{IC}_{50}$   $49.1 \pm 0.96$   $\mu\text{g/ml}$ ) whereas effect on lung cell carcinoma (A-549) was much lower ( $\text{IC}_{50}$ :  $137.9 \pm 1.85$   $\mu\text{g/ml}$ ). EtOAc had the highest flavonoid content ( $1.75 \pm 1.5$  mg/g QE) compared to other subextracts. These results indicated that ethyl acetate fraction contains bioactive compounds worthy of more sophisticated studies as free radical scavenger and cytotoxic agent.

**Keywords:** Tamarix nilotica; Cytotoxic activity; Sulphorhodamine B (SRB) assay; Scavenging activity; 1,1-Diphenyl, 2-picrylhydrazyl (DPPH) assay; Flavonoid; Phenolic.

#### 1562. Phytochemical and Biological Studies of Schinus Polygamus Growing in Egypt

Abeer Mohamed Ali El Sayed, Marwan M. Shabana, Ali M. El Sayed, Miriam F. Yousif and Amany A. Sleem

*International Journal of Traditional and Herbal Medicine*, 1(5): 136-146 (2013)

The leaf ethanol extract of Schinus polygamus (Cav.) Cabrera has evidenced medicinal value as hepatoprotective. It demonstrated inhibitory effects on standard microbes (approximated to) 50% potency of ofloxacin. The same extract evidenced in vitro cytotoxicity on human cell lines viz, liver carcinoma HEPG2, larynx carcinoma HEP2, and colon carcinoma HCT116 when compared to doxorubicin. The leaf ethanol extract of S. polygamus showed variable anti inflammatory, analgesic, and antipyretic activities. Analysis of the hydrolyzed methanol extract of S. polygamus by HPLC allowed the identification of four phenolic acids and five flavonoid aglycones. Gallic acid and chlorogenic acid were identified as major phenolic acids. Major identified flavonoid aglycones were luteolin, kaempferol, quercetin, naringenin, and apigenin. The anti-inflammatory, analgesic, and antimicrobial activities support scientifically the use of S. polygamus in folk medicine for the fore mentioned variable uses. The content of plant constituents as polyphenols of the leaves of S. polygamus justify to some extent the hepatoprotective, anti-inflammatory and analgesic activity with pain tolerance. DNA fingerprinting of the leaves of S. polygamus was carried out as a mean of identification of the genetic profile of the Egyptian plant.

**Keywords:** Schinus polygamus cabrera; Polyphenolics; Hepatoprotective activity; Antimicrobial activity; Cytotoxic effect.

#### 1563. Seasonal Variation in the Composition of Plectranthus Amboinicus (Lour.) Spreng Essential Oil and its Biological Activities

Azza Ramy Abdel Monem, Seham S. El-hawary, Rabie H. El-Sofany, Rehab S. Ashour and Amany A. Sleem

*American J. of Essential Oil and Natural Product*, 2: 11-18 (2013)

The effect of seasonal variation on the yield and composition of the essential oils of the leaves and stems of Plectranthus amboinicus (Lour.) Spreng, growing in Egypt, collected along the four seasons at three months intervals viz., January, April, July and October was studied. The highest yield of essential oils of both the leaves and stems was obtained during spring (0.12% and 0.13% v/w fresh weight, respectively). The GC/MS analysis of the essential oil samples revealed a qualitative and quantitative variation in chemical composition. Concerning the leaves,  $\delta$ -



cadinene was the major component in the oils of spring (18.66%) and autumn (12.52%), while,  $\beta$ -caryophyllene (12.65%) and thymol (8.75%) were the major components in the oils of winter and summer, respectively. Concerning stems,  $\alpha$ -humulene was the major component in the oil samples of winter (11.14%) and summer (12.70%), while,  $\beta$ -copaene-4- $\alpha$ -ol (9.37%) and thymol (13.02%) were the major constituents in the oil samples of spring and autumn respectively. Further analysis of GC/MS data revealed that, the total sesquiterpenes were of higher percentage than the total monoterpenes in both the oil samples along the four seasons. The total oxygenated compounds were found highest in the volatile oil of the leaves collected in summer (53.57%) and volatile oil of the stems collected in spring (55.99%). The volatile oils of the leaves and stems exhibited variable antioxidant, anti-inflammatory, analgesic, diuretic, cytotoxic and antimicrobial activities. The LD<sub>50</sub> of the volatile oils of both the leaves and stems were up to 0.05 ml/kg.

**Keywords:** Plectranthus amboinicus (Lour.) spreng; Essential oil; Seasonal variations; Antioxidant; Antiinflammatory; Analgesic; Diuretic; Cytotoxic; Antimicrobial.

#### 1564. Seasonal Variation of Essential Oil, Oxygenated Compounds Content and Antioxidant Capacities of Leaves and Ripe and Unripe Fruits of Fortunella Japonica Swingle (Kumquat)

Mostafa Aly Abdelkawy, Heba A. El-Gizawy, Samir M. Osman, Mahmoud A. Koheil, Ali M. El halawany and Mohammed A. Hussein

*World Journal of Medicine, 1 (4): 204-215 (2013)*

Hydrodistilled oils of the fresh leaves and peels of Fortunella japonica Swingle cultivated in Egypt were prepared from samples collected along the four seasons. Furthermore, antioxidant potential of the oils was tested by 2, 2-diphenyl-1-picrylhydrazyl (DPPH) assay, hydrogen peroxide scavenging and reducing antioxidant power methods. The percentage yields of these essential oils were 0.4%, 0.6%, 0.3%, and 0.8% of the dry weight for winter, spring, summer and autumn leaves samples & 0.5% and 0.9% for ripe and unripe fruits. GC/MS analyses of all samples revealed a qualitative and quantitative variability in the oil composition.

The total identified oxygenated compounds were constituted about 44.83%, 27.19%, 40.49%, 26.78%, 0.99% and 0.86% of the total composition of the leaves oils for winter, spring, summer, autumn, ripe and unripe peels, respectively. Limonene was the major constituent in ripe and unripe peels while aromadendrene was major constituent in leaves samples. The results showed that the concentration of the winter, spring, summer, autumn, unripe and ripe peels essential oil needed to scavenge 50% of DPPH<sup>•</sup>, were 62.25, 75.08, 75.11, 100.0, 133.17 and 124.38mg/ml, respectively and showed reducing ability on Fe<sup>3+</sup> radical (EC<sub>50</sub>=0.50, 0.62, 0.75, 0.84, 1.00 and 1.12mg/ml, respectively). This study showed that Fortunella japonica Swingle essential oils exhibited free radical scavenging activity in all tests and could be considered as a source of natural antioxidants. Also, Seasonal variations affect biosynthesis of different types of antioxidant compounds in Fortunella japonica Swingle. Thus, the medicinal and nutritional value of the plant will depend on harvesting season.

**Keywords:** Fortunella japonica swingle; Oxygenated compounds; Essential oils and DPPH.

#### Dept. of Pharmacology and Toxicology

#### 1565. Nicorandil Ameliorates Mitochondrial Dysfunction in Doxorubicin- Induced Heart Failure in Rats: Possible Mechanism of Cardioprotection

Lamiaa Ahmed Ahmed Attia Shams Eldin and Shohda A. EL-Maraghy

*Biochemical Pharmacology, 86: 1301-1310 (2013)*

IF: 4.576

Despite of its known cardiotoxicity, doxorubicin is still a highly effective anti-neoplastic agent in the treatment of several cancers. In the present study, the cardioprotective effect of nicorandil was investigated on hemodynamic alterations and mitochondrial dysfunction induced by cumulative administration of doxorubicin in rats. Doxorubicin was injected i.p. over 2 weeks to obtain a cumulative dose of 18 mg/kg. Nicorandil (3 mg/kg/day) was given orally with or without doxorubicin treatment. Heart rate and aortic blood flow were recorded 24 h after receiving the last dose of doxorubicin. Rats were then sacrificed and hearts were rapidly excised for estimation of caspase-3 activity, phosphocreatine and adenine nucleotides contents in addition to cytochrome c, Bcl2, Bax and caspase 3 expression.

Moreover, mitochondrial oxidative phosphorylation capacity, creatine kinase activity and oxidative stress markers were measured together with the examination of DNA fragmentation and ultrastructural changes. Nicorandil was effective in alleviating the decrement of heart rate and aortic blood flow and the state of mitochondrial oxidative stress induced by doxorubicin cardiotoxicity. Nicorandil also preserved phosphocreatine and adenine nucleotides contents by restoring mitochondrial oxidative phosphorylation capacity and creatine kinase activity. Moreover, nicorandil provided a significant cardioprotection via inhibition of apoptotic signaling pathway, DNA fragmentation and mitochondrial ultrastructural changes.

Interestingly, nicorandil did not interfere with cytotoxic effect of doxorubicin against the growth of solid Ehrlich carcinoma. In conclusion, nicorandil was effective against the development of doxorubicin-induced heart failure in rats as indicated by improvement of hemodynamic perturbations, mitochondrial dysfunction and ultrastructural changes without affecting its antitumor activity.

**Keywords:** Cardiotoxicity; Doxorubicin; Mitochondria; Nicorandil.

#### 1566. Additional Antiepileptic Mechanisms of Levetiracetam in Lithium-Pilocarpine Treated Rats

Dalaal Moustafa Abdallah, Muhammad Y. Al-Shorbagy and Bahia M. El-Sayeh

*Plos One, 8 (10): (2013) IF: 3.73*

Several studies have addressed the antiepileptic mechanisms of levetiracetam (LEV); however, its effect on catecholamines and the inflammatory mediators that play a role in epilepsy remain elusive. In the current work, lithium (Li) pretreated animals were administered LEV (500 mg/kg i.p) 30 min before the induction of convulsions by pilocarpine (PIL). Li-PIL-induced seizures were accompanied by increased levels of hippocampal prostaglandin (PG) E<sub>2</sub>, myeloperoxidase (MPO), tumor necrosis factor- $\alpha$ , and interleukin-10. Moreover, it markedly elevated hippocampal lipid

peroxides and nitric oxide levels, while it inhibited the glutathione content. Li-PIL also reduced hippocampal noradrenaline, as well as dopamine contents. Pretreatment with LEV protected against Li-PIL-induced seizures, where it suppressed the severity and delayed the onset of seizures in Li-PIL treated rats. Moreover, LEV reduced PGE2 and MPO, yet it did not affect the level of both cytokines in the hippocampus. LEV also normalized hippocampal noradrenaline, dopamine, glutathione, lipid peroxides, and nitric oxide contents. In conclusion, alongside its antioxidant property, LEV anticonvulsive effect involves catecholamines restoration, as well as inhibition of PGE2, MPO, and nitric oxide.

**Keywords:** PGE2; Levetiracetam; Lithium-pilocarpine; Noradrenaline; Seizures.

### 1567. Cerebrolysin Ameliorates Cognitive Deficits in Type III Diabetic Rats

Noha Nagah Soliman Nassar, Gehan S. Georgy, Hanaa A. Mansour and Dalaal M. Abdallah

*Plos One*, 8 (6): (2013) IF: 3.73

Cerebrolysin (CBL) a mixture of several active peptide fragments and neurotrophic factors including brain-derived neurotrophic factor (BDNF), is currently used in the management of cognitive alterations in patients with dementia.

Since Cognitive decline as well as increased dementia are strongly associated with diabetes and previous studies addressed the protective effect of BDNF in metabolic syndrome and type 2 diabetes; hence this work aimed to evaluate the potential neuroprotective effect of CBL in modulating the complications of hyperglycaemia experimentally induced by streptozotocin (STZ) on the rat brain hippocampus.

To this end, male adult Sprague Dawley rats were divided into (i) vehicle- (ii) CBL- and (iii) STZ diabetic-control as well as (iv) STZ+CBL groups. Diabetes was confirmed by hyperglycemia and elevated glycated haemoglobin (HbA1c%), which were associated by weight loss, elevated tumor necrosis factor (TNF)- $\alpha$  and decreased insulin growth factor (IGF)-1 $\beta$  in the serum. Uncontrolled hyperglycemia caused learning and memory impairments that corroborated degenerative changes, neuronal loss and expression of caspase (Casp)-3 in the hippocampal area of STZ-diabetic rats.

Behavioral deficits were associated by decreased hippocampal glutamate (GLU), glycine, serotonin (5-HT) and dopamine. Moreover, diabetic rats showed an increase in hippocampal nitric oxide and thiobarbituric acid reactive substances versus decreased non-protein sulphydryls. Though CBL did not affect STZ-induced hyperglycemia, it partly improved body weight as well as HbA1c%. Such effects were associated by enhancement in both learning and memory as well as apparent normal cellularity in CA1 and CA3 areas and reduced Casp-3 expression. CBL improved serum TNF- $\alpha$  and IGF-1 $\beta$ , GLU and 5-HT as well as hampering oxidative biomarkers. In conclusion, CBL possesses neuroprotection against diabetes-associated cerebral neurodegeneration and cognitive decline via anti-inflammatory, antioxidant and antiapoptotic effects.

**Keywords:** Cerebrolysin; Cognition; Diabetes; Inflammation; Insulin growth factor; Oxidative stress; Neurotransmitters; STZ; TNF- $\alpha$ .

### 1568. Phytol/ Phytanic Acid and Insulin Resistance: Potential Role of Phytanic Acid Proven by Docking Simulation and Modulation of Biochemical Alterations

Hanan Salah El-Din El-Abhar, Mohamed M. Elmazar, Mona F. Schaal and Nahla A. Farag

*Plos One*, 8 (1): (2013) IF: 3.73

Since activation of PPAR $\gamma$  is the main target for the antidiabetic effect of TZDs, especially when it heterodimerizes with RXR, we aimed to test the potential antidiabetic effect of phytol (250 mg/kg), the natural precursor of phytanic acid, a RXR ligand and/or pioglitazone (5 mg/kg) to diabetic insulin-resistant rats. Regarding the molecular docking simulation on PPAR $\gamma$ , phytanic acid, rather than phytol, showed a binding mode that mimics the crystal orientation of rosiglitazone and pioglitazone, forming H bonds with the same amino acids (S289, H 323, H 449 and Y 473), and the least energy level, which emphasizes their importance for PPAR $\gamma$  molecular recognition, activation, hence antidiabetic activity. In addition, docking on the RXR $\alpha$ /PPAR $\gamma$  heterodimer, revealed that phytanic acid has higher binding affinity and lesser energy score on RXR $\alpha$ , compared to the original ligand, retinoic acid. Phytanic acid binds by 3H bonds and shares retinoic acid in arginine (R 316). These results were further supported biochemically, where oral phytol and/or pioglitazone (5 mg/kg) improved significantly glucose homeostasis, lipid panel, raised serum adiponectin level and lowered TNF- $\alpha$ , reaching in most cases the effect of the 10 mg/kg pioglitazone. The study concluded that the insulin sensitizing/anti-diabetic effect of phytol is mediated by partly from activation of nuclear receptors and heterodimerization of RXR with PPAR $\gamma$  by phytanic acid.

**Keywords:** Phytol; Phytanic acid; Insulin; Docking; PPAR.

### 1569. Novel Effects of Ectoine, A Bacteria-Derived Natural Tetrahydropyrimidine in Experimental Colitis

Mohamed Taky El-Din Khayyal, Heba Abdel-Aziz, Walaa Wadie, Dalaal M. Abdallah and Georg Lentzen

*Phytomedicine*, 20: 585-591 (2013) IF: 2.972

Evidence suggests an important role of intestinal barrier dysfunction in the etiology of inflammatory bowel disease (IBD). Therefore stabilizing mucosal barrier function constitutes a new therapeutic approach in its management. Ectoine is a compatible solute produced by aerobic chemoheterotrophic and halophilic/halotolerant bacteria, where it acts as osmoprotectant and effective biomembrane stabilizer, protecting the producing cells from extreme environmental stress. Since this natural compound was also shown to prevent inflammatory responses associated with IBD, its potential usefulness was studied in a model of colitis. Groups of rats were treated orally with different doses of ectoine (30–300mg/kg) or sulfasalazine (reference drug) daily for 11 days. On day 8 colitis was induced by intracolonic instillation of 2,4,6-trinitrobenzenesulfonic acid, when overt signs of lesions develop within the next 3 days. On day 12, blood was withdrawn from the retro-orbital plexus of the rats and the animals were sacrificed. The colon was excised and examined macroscopically and microscopically. Relevant parameters of oxidative stress and inflammation were measured in serum and

colon homogenates. Induction of colitis led to marked weight loss, significant histopathological changes of the colon, and variable changes in levels of myeloperoxidase, reduced glutathione, malondialdehyde, and all inflammatory markers tested. Treatment with ectoine ameliorated the inflammatory changes in TNBS-induced colitis. This effect was associated with reduction in the levels of TNF- $\alpha$ , IL-1 $\beta$ , ICAM-1, PGE<sub>2</sub> and LTB<sub>4</sub>. The findings suggest that intestinal barrier stabilizers from natural sources could offer new therapeutic measures for the management of IBD.

**Keywords:** Inflammatory bowel disease; Trinitrobenzenesulfonic acid; Compatible solutes; Ectoines; Intestinal barrier.

#### 1570. Catechol Conjugates Are in Vivo Metabolites of Salicis Cortex

Mohamed Taky El Din Khayyal, Susanne Knuth, Rania M. Abdelsalam, Frank Schweda, Jörg Heilmann, Martin Georg Kees, Georg Mair, Frieder Kees and Guido Jürgenliemk

*Planta Medica*, 79: 1489-1494 (2013) IF: 2.348

After oral administration of 100 mg/kg b.w. (235.8  $\mu$ mol/kg) salicortin to Wistar rats, peak serum concentrations of 1.43 mg/L (13.0  $\mu$ M) catechol were detected after 0.5 h in addition to salicylic acid by HPLC-DAD after serum processing with  $\beta$ -glucuronidase and sulphatase. Both metabolites could also be detected in the serum of healthy volunteers following oral administration of a willow bark extract (Salicis cortex, Salix spec., Salicaceae) corresponding to 240 mg of salicin after processing with both enzymes. In humans, the  $c_{max}$  (1.46 mg/L, 13.3  $\mu$ M) of catechol was reached after 1.2 h. The predominant phase-II metabolite in humans and rats was catechol sulphate, determined by HPLC analysis of serum samples processed with only one kind of enzyme. Without serum processing with glucuronidase and sulphatase, no unconjugated catechol could be detected in human and animal serum samples. As catechol is described as an anti-inflammatory compound, these results may contribute to the elucidation of the mechanism of the action of willow bark extract.

**Keywords:** Salix; Salicaceae; Catechol; Salicortin; Metabolism; Conjugates; Salicylic acid; Pharmacokinetic study; In vivo.

#### 1571. The Selective 5-LOX Inhibitor 11-Keto- $\beta$ -Boswellic Acid Protects Against Myocardial Ischemia Reperfusion Injury in Rats: Involvement of Redox and Inflammatory Cascades

Noha Nagah Soliman nassar, Shima M. Elshazly and Dalia M. Abd El-Motteleb

*Naunyn-Schmiedeberg's Archives of Pharmacology*, 386 (9): 823-833 (2013) IF: 2.147

Myocardial ischemia induces 5-lipoxygenase (LOX) translocation and leukotriene production in the heart. Leukotrienes increase inflammatory responses aggravating, thereby, ischemia-reperfusion (I/R) injury. This study aimed to investigate whether the selective 5-LOX inhibitor 11-keto- $\beta$ -boswellic acid (11-keto BA), in three different dose levels, exert a protective effect on myocardial I/R injury in an in vivo rat heart model. Sixty male Wistar rats were used in this study and divided into five equal groups ( $n = 12$ ): GPI, sham-operated receiving normal saline; Gp

2, rats were subjected to 45 min left anterior descending coronary artery ligation followed by 4 h reperfusion to serve as I/R group. Gps 3–5 received 11-keto BA in doses 250, 500, 1,000 mg/kg, respectively, via an oral gavage for 7 days then were exposed to I/R. I/R injury induced a significant elevation in myeloperoxidase activity and gene expression of intracellular adhesion molecules, cyclooxygenase-2, 5-lipoxygenase, nuclear factor kappa-beta, tumor necrosis factor alpha, nuclear factor (erythroid-derived 2)-like 2, and hemeoxygenase-1 consequently with reduction in glutathione peroxidase in heart tissues. Furthermore, immunohistochemical examination of the heart tissues showed positive immunostaining for both 3-nitrotyrosine and caspase-3 with DNA-ladder formation in all diseased rats. 11-keto BA in three dose levels exerted dose dependent cardioprotective effect manifested by dose-dependent reduction in serum lactate dehydrogenase and infarct size through mechanisms related to enhancement of antioxidant capacity and prevention of inflammatory cascades.

**Keywords:** 11-Keto BA; Myocardial I/R; 5-LOX; NRF2; NF- $\kappa$ B; ICAM-1.

#### 1572. Antidiabetic Effects of A Standardized Egyptian Rice Bran Extract

Mohamed Taky El-Din Khayyal, Rebecca M. Kaup and Eugen J. Verspohl

*Phytotherapy Research*, 27: 264-271 (2013) IF: 2.068

An extract was prepared from Egyptian stabilized rice bran and standardized to contain 2%  $\gamma$ -oryzanol in addition to its content of other bioactives, notably tocotrienol and policosanol. The standardized extract was found to have a concentration-dependent effect on insulin release in vitro, which, however, is not mediated by  $\gamma$ -tocotrienol in rice bran (detected by HPLC) as could have been expected. Policosanol and  $\gamma$ -oryzanol have insulinotropic effects. The in vitro data of rice bran directly translate into in vivo data of rats by using a glucose tolerance test (increase in plasma insulin). Tocotrienols are well known for their apoptotic effect on tumor cells; nevertheless, an attempt was made to study glucose uptake in HEP-G2 cells, which needs to induce an insulin-resistant state by TNF- $\alpha$ . The Egyptian rice bran extract has an antidiabetic effect.  $\gamma$ -Oryzanol, which is a possible precursor of the insulinotropic compound ferulic acid, is a candidate for this effect. Therefore, it is reasonable to assume that the prevalence of diabetes or at least a prediabetic (type 2) situation can be ameliorated by the investigated rice bran extract. The potential usefulness of the extract as a nutraceutical is currently undergoing more thorough investigations.

**Keywords:** Rice bran; Diabetes; Tocotrienol; Policosanol.

#### 1573. Beneficial Effects of Co-Enzyme Q<sub>10</sub> and Rosiglitazone in Fructose-Induced Metabolic Syndrome in Rats

Hala Ahmed Fahmy Mohamed Zaki, Suzan M. Mansour and Ezz-El-Din S. El-Denshary

*Bulletin of faculty of pharmacy, Cairo university*, 51: 13-21 (2013) IF: 2

Increased fructose consumption is strongly associated with metabolic syndrome (MS). This study was performed to elucidate

the role of co-enzyme Q<sub>10</sub> (CoQ) and/or rosiglitazone (Rosi) in fructose induced MS. Four groups of rats ( $n = 8-10$ ) were fed on fructose-enriched diet (FED) for 16 weeks. One served as FED-control while the remaining groups were treated with CoQ (10 mg/kg/day), Rosi (4 mg/kg/day) or their combination during the last 6 weeks. Another group was fed on normal laboratory chow (normal control). At the end of the experiment, blood samples were collected for estimation of markers related to MS. In addition, histological examination of liver, kidney and pancreas samples was done. Induction of the MS was associated with increased body weight gain (34%) coupled with elevated levels of blood glucose (48%), insulin (86%), insulin resistance (270%), uric acid (69%), urea (155%), creatinine (129%) and blood lipids with different degrees. Fructose-induced MS also reduced plasma catalase (62%) and glutathione peroxidase (89%) activities parallel to increased serum leptin and tumor necrosis factor- $\alpha$  (TNF- $\alpha$ ) levels. These changes were coupled by marked histological changes in the examined tissues. Treatment with CoQ or Rosi attenuated most of MS-induced changes. Besides, the combination of both agents further reduced blood glucose, total cholesterol, triglycerides and urea levels, as well as, normalized serum levels of leptin and TNF- $\alpha$ . In addition, combined therapy of both agents elevated HDL-cholesterol level and glutathione peroxidase activity. In conclusion, the present study proves the benefits of co-supplementation of CoQ and Rosi in a fructose-induced model of insulin resistance.

**Keywords:** Rosiglitazone; Co-enzyme Q<sub>10</sub>; Leptin; Tumor necrosis factor; Insulin resistance.

#### 1574. Protective Effects of Atorvastatin and Quercetin on Isoprenaline-Induced Myocardial Infarction in Rats

Sanaa A Kenawy, Mai A. Zaaan, Hala F. Zaki and Amany I. El-Brairy

*Bulletin of Faculty of Pharmacy, Cairo University, 51: 35-41 (2013) IF: 2*

Myocardial infarction (MI) continues to be a major public health problem in the world. Statins exhibit cardio-protective effects by several mechanisms beyond their lipid lowering activity. Quercetin is a natural flavonoid that possesses significant anti-oxidant and anti-inflammatory activities. The present study aimed to investigate the effects of pretreatment with atorvastatin (10 mg/kg) and quercetin (50 mg/kg), as well as their combination on isoprenaline-induced MI in rats. Markers chosen to assess cardiac damage included serum activity of creatine kinase-MB (CK-MB) and serum level of cardiac troponin-I (cTn-I), as well as oxidative stress and inflammatory biomarkers including serum levels of C-reactive protein (CRP), tumor necrosis factor- $\alpha$  (TNF- $\alpha$ ), and interleukin-10 (IL-10) as well as cardiac contents of lipid peroxides, reduced glutathione (GSH), and nitrite. Furthermore, ECG monitoring and histological examinations of cardiac tissues were done. Isoprenaline increased serum CK-MB activity and cTn-I level as well as inflammatory and oxidative stress biomarkers. In addition, it produced ST-segment elevation and degenerative changes in heart tissues. Pretreatment with atorvastatin suppressed significantly the elevated levels of cTn-I, CRP, TNF- $\alpha$ , and IL-10 in serum coupled with reduction in cardiac lipid peroxides; however, it increased cardiac nitrite content. Quercetin decreased isoprenaline-induced changes in oxidative stress and inflammatory biomarkers with marked

improvement in ECG and histopathologic alterations. Combination of quercetin with atorvastatin resulted in similar protective effects. In conclusion, quercetin can be regarded as a promising cardio-protective natural agent in MI alone or combined with atorvastatin.

**Keywords:** Atorvastatin; Quercetin; Myocardial infarction; C-reactive protein; Cytokines.

#### 1575. Streptozotocin-Induced Vascular and Biochemical Changes in Rats: Effects of Rosiglitazone VS. Metformin

Aiman Saad El-Khatib, Dalia O. Saleh, Ayman R. Bayoumi and Wafaa I. El-Eraky

*Bulletin of Faculty of Pharmacy, Cairo University, 51: 131-138 (2013) IF: 2*

The aim was to investigate rosiglitazone and metformin effects on some vascular and biochemical changes associated with streptozotocin (55 mg/kg; i.p.)-induced hyperglycaemia in rats. Isolated aortas were used to evaluate their reactivity towards norepinephrine, acetylcholine, and sodium nitroprusside. Blood samples were used to assess the biochemical changes of some parameters viz., plasma lipid peroxides and nitric oxide levels and erythrocytic glutathione peroxidase activity. Hyperglycaemic animals orally received rosiglitazone (0.5 mg/kg) or metformin (150 mg/kg) daily for 2 weeks and their effects were determined 24 h after the last dose. Our results revealed that streptozotocin-induced hyperglycaemia is associated with impaired vascular reactivity towards various agents, increased lipid peroxides level, decreased glutathione peroxidase activity, and decreased nitric oxide level. Both drugs further decreased norepinephrine-induced contraction and improved acetylcholine and sodium nitroprusside-induced relaxations. Rosiglitazone restored the alterations in all tested biochemical parameters while metformin restored only glutathione peroxidase activity. In conclusion both drugs show beneficial effects against the vascular dysfunction associated with hyperglycaemia which might be related to their euglycaemic activity in addition to anti-oxidant property of rosiglitazone and a direct effect of metformin on vascular smooth muscle.

**Keywords:** Rosiglitazone; Metformin; Streptozotocin; Rat aorta; Oxidative stress.

#### 1576. Vinpocetine Protects Liver Against Ischemia-Reperfusion Injury

Hala A. Fahmy Zaki and Rania Mohsen Abdelsalam

*Canadian Journal of Physiology and Pharmacology, 91(12): 1064-1070 (2013) IF: 1.556*

Hepatic ischemia-reperfusion (IR) injury is a clinical problem that leads to cellular damage and organ dysfunction mediated mainly via production of reactive oxygen species and inflammatory cytokines. Vinpocetine has long been used in cerebrovascular disorders. This study aimed to explore the protective effect of vinpocetine in IR injury to the liver. Ischemia was induced in rats by clamping the common hepatic artery and portal vein for 30 min followed by 30 min of reperfusion. Serum transaminases and liver lactate dehydrogenase (LDH) activities, liver inflammatory cytokines, oxidative stress biomarkers, and liver histopathology were assessed. IR resulted in marked histopathology changes in

liver tissues coupled with elevations in serum transaminases and liver LDH activities. IR also increased the production of liver lipid peroxides, nitric oxide, and inflammatory cytokines interleukin-1 $\beta$  and interleukin-6, in parallel with a reduction in reduced glutathione and interleukin-10 in the liver. Pretreatment with vinpocetine protected against liver IR-induced injury, in a dose-dependent manner, as evidenced by the attenuation of oxidative stress as well as inflammatory and liver injury biomarkers. The effects of vinpocetine were comparable with that of curcumin, a natural antioxidant, and could be attributed to its antioxidant and anti-inflammatory properties.

**Keywords:** Liver ischemia-reperfusion; Vinpocetine; Curcumin; Cytokines; Oxidative stress.

### 1577. Effect of Celecoxib and L-Name on Global Ischemia-Reperfusion Injury in the Rat Hippocampus

Sarah A. Abd El-Aal, Maha M. El-Sawalhi, Mona Seif-El-Nasr, and Sanaa A. Kenawy

*Drug and Chemical Toxicology*, 36 (4) :385-395 (2013) IF: 1.293

Transient global ischemia continues to be an important clinical problem with limited treatment options. The present study aimed to investigate the possible protective effects of celecoxib [a selective cyclooxygenase (COX-2) inhibitor] and N-omega-nitro-L-arginine methyl ester (L-NAME) [a nonselective nitric oxide synthase (NOS) inhibitor] against global ischemia-reperfusion (IR) induced biochemical and histological alterations in the rat hippocampus. Global ischemia was induced by bilateral clamping of the common carotid arteries for 60 minutes. Hippocampal cysteinyl aspartate-specific protease-3 (caspase-3) activity, nitrite/ nitrate contents (NOX), as well as COX-2 immunoreactivity in the hippocampal Cornu Ammonis 1 (CA1) subregion were dramatically increased 24 hours after global ischemia. After 72-hour of reperfusion, ischemia induced a selective, extensive neuronal loss in the hippocampus CA1 subregion. Celecoxib (3 and 5 mg/kg, intraperitoneally; i.p.), administered 30 minutes before ischemia and at 6, 12, and 22 hours of 24-hour reperfusion, caused significant reductions in hippocampal caspase-3 activity as well as the number of COX-2 immunoreactive (COX-2 ir) neurons in the CA1 subregion. Further, celecoxib (3 or 5 mg/kg, i.p.), administered 30 minutes before ischemia and at 6, 12, 22, and 48 hours of 72-hour reperfusion, provided a notable histological protection of hippocampal CA1 neurons. Meanwhile, L-NAME (3 mg/kg, i.p.), administered twice (immediately after ischemia and 45 minutes after starting the reperfusion period), effectively reduced the elevated NOX level, decreased hippocampal caspase-3 activity and COX-2 immunoreactivity, and ameliorated ischemia-induced damage in the hippocampal CA1 subregion. The present study indicates that celecoxib and L-NAME might be neuroprotective agents of potential benefit in the treatment of cerebral ischemia.

### 1578. Chromium Picolinate and Rosiglitazone Improve Biochemical Derangement in A Rat Model of Insulin Resistance: Role of TNF- $\alpha$ and Leptin

Hala Ahmed Fahmy Mohamed Zaki, Suzan M. Mansour and Ezz EL-Din EL-Denshary

*Pharmacologia*, 4: 186-196 (2013)

**Objective:** Incidence of Metabolic Syndrome (MS) is strongly associated with increased fructose consumption. This study aimed to elucidate the role of rosiglitazone, Chromium Picolinate (CP) and their combination on fructose-induced MS.

**Materials and methods:** Four groups of rats (n = 10) were fed on Fructose-enriched Diet (FED) for 16 weeks. One served as FED-control while the remaining groups were treated with rosiglitazone (4 mg kg<sup>-1</sup> day<sup>-1</sup>), CP (80  $\mu$ g kg<sup>-1</sup> day<sup>-1</sup>) or their combination during the last 6 weeks. A fifth group was fed on normal diet (normal group). At the end, blood samples were collected for estimation MS-related markers.

**Results:** Histological examination of livers, kidneys and pancreases from all groups was done. Induction of MS was associated with increased weight gain and insulin resistance coupled with elevated levels of blood glucose, insulin, uric acid, urea, creatinine and lipids. FED also reduced plasma catalase and glutathione peroxidase activities parallel to increased serum leptin and TNF- $\alpha$  levels. This was coupled with marked histological changes in the livers, kidneys and pancreases. Treatment with rosiglitazone or CP attenuated most of the changes associated with MS. Besides, combination of both agents further improved disease markers and decreased hepatocytes fibrosis.

**Conclusion:** The present results reveal the benefits of co-supplementation of rosiglitazone and CP in MS.

**Keywords:** Fructose; Rosiglitazone; Chromium picolinate; Leptin-tumor necrosis factor; Insulin resistance.

### 1579. Gastroprotective Activity of Mirtazapine, Escitalopram and Venlafaxine in Depressed Rats

Hala A. Fahmy Zaki and Sally A. El-Awdan

*African Journal of Pharmacy and Pharmacology*, 7: 2701-2709 (2013)

The study investigated the gastro-protective effects of certain antidepressants in relation to ranitidine on indomethacin-induced ulcer in depressed rats. Animals were divided into 6 groups (n = 8). Induction of depression was done by clonidine (0.8 mg/kg; i.p.) for 10 days in all groups except the 1st one (normal control). Depressive-like behavior was confirmed by increased immobility time in forced swimming test. Groups 1 and 2 received saline (normal and depressed controls, respectively). Groups 3 to 6 received p.o. mirtazapine (10 mg/kg), escitalopram (10 mg/kg), venlafaxine (20 mg/kg) and ranitidine (50 mg/kg), respectively for 30 days. After the last treatment, gastric ulcer was induced using indomethacin (25 mg/kg; p.o.) in groups 2 to 6. An additional group received indomethacin alone (control indomethacin). Animals were sacrificed and ulcer scores were determined. Part of the stomach was preserved for histopathologic studies while the other part was used for determination of reduced glutathione (GSH), malondialdehyde (MDA), nitric oxide (NO), tumor necrosis factor-alpha (TNF- $\alpha$ ) and interleukin-10 (IL-10) contents. Pretreatment with all antidepressants used ameliorated indomethacin-induced changes in rat stomach. Biochemical findings were supported by histologic studies. In conclusion, the observed gastroprotective effects of mirtazapine, escitalopram and venlafaxine are possibly mediated by modulation of inflammatory cytokines and antioxidant effects.

**Keywords:** Mirtazapine; Escitalopram; Venlafaxine; Depression; Indomethacin.



### 1580. Grape (*Vitis Vinifera*) Seed Extract Inhibits the Cytotoxicity and Oxidative Stress in Liver of Rats Treated with Carbon Tetrachloride

Ghada M. A. Ragab, Ezzeldeen S. El-Denshary, Aziza M. Hassan, Sekena H. Abdel-Azeim, Nabila S. Hassan, Fathia A. Manna and Mosaad A. Abdel-Wahhab

*Global Journal of Pharmacology*, 7 (3): 258-269 (2013)

The present study examined the curative action of Grape seed extract (GSE) on experimentally induced hepatic damage in rats by carbon tetrachloride (CCl<sub>4</sub>). Rats were divided into six groups (8 rats/group) treated for 21 days and included the control group, Group 2 the group treated orally twice a week with CCl<sub>4</sub> (1.0 mg/kg b.w) in corn oil, Group 3 and 4 treated orally with GSE at low dose (100 mg/kg b.w) or high dose (200 mg/kg b.w) and Groups 5 and 6 treated with CCl<sub>4</sub> plus GSE at the two tested doses. At the end of experimental period, blood and liver samples were collected from all groups for the biochemical, histological, histochemical and cytogenetic analysis. The results indicated that CCl<sub>4</sub> induced hepatic damage in the rats as evidenced by a significant increase in serum AST, ALT, ALP, triglycerides, MDA, nitric oxide, LDH, CEA, total lipid, cholesterol, DNA fragmentation and NO accompanied with a significant decrease in total proteins, GPX, SOD, DNA and RNA content in the liver and Fas and TNF $\alpha$  gene expression in the liver. Treatment with GSE reversed the values of the biochemical parameters to near normal values and improved the content of nucleic acids in hepatic tissues, the gene expression and the histopathological and histochemical picture of the liver. It could be concluded that GSE may be used in protection against and/or the treatment of liver disease.

**Keywords:** Liver; Grape Seed Extract; Cytogenetic; Gene Expression; Oxidative Stress; Antioxidant.

### 1581. Impact of the Dopaminergic System on Mucosal Integrity in Indomethacin-Induced Gastric Ulcers in Rats: Possible Modulation by Ranitidine or L-carnitine

Sally A. El-Awdan, Hala F. Zaki, Omar M. Abdel Salam, Wafaa I. El-Iraqy and Sanaa A. Kenawy

*Pharmacologia*, 4 (1): (2013)

The present study aim to explore the impact of bromocriptine, or ziprasidone on rats mucosal integrity and the possible modulation by L-carnitine or ranitidine. Adult male Wistar rats were divided into 10 groups: the 1<sup>st</sup> and 2<sup>nd</sup> groups received 1% Tween 80 and served as normal and control groups, respectively. The remaining groups were treated as follows: 3-6 received bromocriptine (2.5 mg kg<sup>-1</sup>), L-carnitine (50 mg kg<sup>-1</sup>), ranitidine (50 mg kg<sup>-1</sup>) or ziprasidone (3 mg kg<sup>-1</sup>), respectively. Groups 7-10 received combinations of bromocriptine or ziprasidone with either L-carnitine or ranitidine. Drugs were daily administered (p.o.) for two weeks then all groups were subjected to pyloric ligation. Indomethacin (30 mg kg<sup>-1</sup>; p.o.) was immediately administered to all groups except the normal one. Rats were euthanized 4 h thereafter and stomachs were opened to evaluate the number and severity of the lesions. Gastric volume, acid output, peptic activity as well as mucin and gastric mucus concentrations were determined. Moreover, stomach content of lipid peroxides,

reduced glutathione, nitric oxide metabolites and tumor necrosis factor were also estimated. Indomethacin administration resulted in increased ulcer index and severity that was coupled by increased titratable acidity, acid output and disturbance in antioxidant status. Such effects were intensified by ziprasidone and ameliorated by bromocriptine, L-carnitine or ranitidine. Moreover, administration of L-carnitine or ranitidine with ziprasidone attenuated its damaging effect. In conclusion, dopamine agonists play a significant role in maintenance of gastric mucosal integrity; meanwhile, dopamine antagonists complicate indomethacin-induced ulcers, an effect that could be mitigated by combined treatment with L-carnitine or ranitidine.

### 1582. HLA Alloimmunization Inegyptian Aplastic Anemia Patients Receiving Exclusively Leukoreduced Blood Components

Azza Ahmed Aboul Enein, Nermeen Ahmed El Desoukey, Eiman Abdel Wahab Hussein, Mona Hamdi and Nada Adnan Jamjom

*Transfusion and Apheresis Science*, 48 (2): 213-218 (2013)

**Background:** The aim of the work was to detect the presence of anti-human leukocyte antigens (anti-HLAs) class I and II antibodies in sera of multitransfused aplastic anemia patients using two different techniques. The effect of the implemented transfusion practice on the frequency of these antibodies was studied as well as their effect on the patient's clinical condition.

**Methods:** Flow cytometry panel reactive antibodies (FlowPRA) for HLA class I and II were determined and compared to the results obtained by Complement-dependent cytotoxicity (CDC) assay.

**Results:** Over the past 3 years, 20 aplastic anemia patients received leukoreduced blood components, 5/20 patients received leukoreduced products exclusively throughout their disease (group 1), 15/20 patients had received non-leukoreduced components previously (group 2). None of the patients in group 1 was FlowPRA positive. Six patients from group 2 (40%) were FlowPRA positive, only four out of these six patients showed positive CDC test. Positive and negative predictive values of CDC were 44.4 and 81.4% respectively, with 65% accuracy. Platelet refractoriness was encountered in 13/20 patients; only 3 out of these 13 patients (23%) were FlowPRA positive (38 $\pm$ 18%). One refractory patient died from intracranial hemorrhage. His FlowPRA was 65.7% and CDC assay failed to detect it.

**Conclusion:** Leukoreduction of blood components minimizes the incidence of HLA alloimmunization. Further investigations for other immune causes of platelet refractoriness are recommended. FCM is a simple and reliable technique for detection of anti-HLA antibodies, while CDC assay lacks sensitivity and specificity.

**Keywords:** HLA Alloimmunization; Leukoreduction; Refractoriness; Single donor platelets.

### 1583. Possible Protection Against Isoniazid-Induced Hepatotoxicity by Certain Natural Agents

Ezz Eldin Saeed El-Denshary, Wessam H. Elesawy, Somaia A. Nada, Adel Bakeer and Naglaa Assaf

*International Journal of Pharmaceutical Research and Bioscience*, 2 (2): 345-361 (2013)

Isoniazid (INH), which is a first-line antimicrobial for tuberculosis, is adversely associated with hepatotoxicity. The aim of the current study was to evaluate the protective effect of  $\alpha$ -LA, I-carnitine, ginseng, and CoQ10 against isoniazid induced hepatotoxicity in rats. Thirty six male Sprague-Dawley (SD) rats were allocated into different groups and over a 3-week period, they were treated intraperitoneal (I.P) either with INH alone (100mg/kg b.w) or with INH after daily pretreatment orally with I-carnitine (250mg/kg b.w),  $\alpha$ -LA (50mg/kg b.w), CoQ10 (15mg/kg b.w) or I.P with ginseng (20mg/kg b.w). Biochemical and histopathological evaluations were done and INH-treated groups were compared with rats receiving no treatment and with rats given I-carnitine,  $\alpha$ -LA, ginseng and CoQ10. The results indicated that I.P administration of INH induced severe hepatic injury associated with oxidative stress. The combined treatment with INH plus one of the foregoing antioxidants resulted in a significant improvement in all evaluated parameters. It could be concluded that any of the previous antioxidants protect SD rats against the severe INH-induced hepatic toxic effects.

**Keywords:** Hepatotoxicity; Isoniazid; Herbal products.

#### 1584. Role of Serotonergic and Dopaminergic Neurotransmission in the Antidepressant Effects of Malt Extract

Hala A. Fahmy Zaki and Hanan A. Rizk

*African Journal of Pharmacy and Pharmacology*, 7 (46): 2960-2971 (2013)

The benefit of malt extract in clonidine-induced depression was previously reported. The present study aimed to explore its mechanism of action. Animals were classified into normal and depressed rats. Induction of depression was done by i.p. injection of clonidine (0.8 mg/kg) daily for 7 days. Depressed rats were sub-classified into 6 groups treated for one week as follows: Group I received 1% tween 80 p.o. (control group); the remaining groups received malt extract (1250 mg/kg; p.o) alone or preceded (30 min) by i.p. injection of spiperone (0.03 mg/kg), sulpiride (7.5 mg/kg), phentolamine (5 mg/kg) or propranolol (7.5 mg/kg), respectively. Forced swimming test (FST) was carried out 24 h thereafter. Brains were isolated for estimation of serotonin, dopamine and norepinephrine contents as well as inflammatory and oxidative stress biomarkers. Clonidine increased total immobility time and decreased struggling time in FST parallel to alterations in brain neurotransmitters, inflammatory and oxidative stress markers. Treatment with malt extract reversed clonidine-induced behavioral and neurochemical changes. Such effects were partly antagonized in groups pre-treated with spiperone or sulpiride. Serotonergic and dopaminergic transmission are involved in the antidepressant effects of malt extract in addition to its antioxidant and anti-inflammatory effects.

**Keywords:** Depression; Malt extract; Spiperone; Sulpiride; Neurotransmitters; Cytokines.

#### 1585. Stem Cells and Cardiac Repair: Alternative and Multifactorial Approaches

Lamiaa Ahmed A. Attia

*Journal of Regenerative Medicine and Tissue Engineering*, 2: 1-9 (2013)

Severe myocardial infarction can lead to ventricular remodelling and progressive contractile dysfunction with inability of the heart to maintain perfusion to vital organs. Pharmacological and surgical interventions can only alleviate symptoms or retard further disease progression. However, these interventions fail to regenerate dead myocardium. Stem cells have the potential to replace or repair dead or injured cells after myocardial infarction. Stem cells are either integrated by themselves or provide a platform to transmit molecular signals to a target tissue without actually integrating into the tissue itself.

Clinical studies, still in early stages, have reported that this therapeutic modality may lead to an overall improvement of cardiac function. Endogenous cell homing presents a promising approach that may represent an effective alternative to stem cell transplantation. Identifying factors and adequate regulation of signalling between bone marrow, peripheral circulation and infarcted myocardium are important in orchestrating the process of mobilization, incorporation, survival, differentiation and proliferation of stem cells.

Moreover, the potential for magnifying stem cell-mediated paracrine effects using “genetically engineered”, “preconditioned”, “targeted” or “combined stem cell therapies” can provide promising options for enhancing stem cell therapy success while limiting adverse effects. It is hoped that these experimental trials will be eventually translated into successful treatment strategies in the clinical field.

**Keywords:** Cardiac Repair; Homing; Mobilization; Regeneration; Stem cells.

### The National Cancer Institute

#### Dept. of Clinical Pathology

#### 1586. Detection of Bocavirus in Children Suffering from Acute Respiratory Tract Infections in Saudi Arabia

Ahmed S. Abdel-Moneim, Mahmoud M. Kamel, Abdullhamid S. Al-Ghamdi and Mater I. R. Al-Malky

*Plos One*, 8 (1): 1-4 (2013) IF: 3.73

Espiratory distress and/or diarrhea. To our knowledge, noprevious study has reported the existence of bocavirus in Saudi Arabia. Swabs samples from 80 children with respiratorytract infections were examined for the presence of HBoV. Real-time polymerase chain reaction was used as a sensitivemethod to detect the HBoV. Direct gene sequencing was used Human bocavirus (HBoV) was recently discovered in children with to determine the genotype of the detected virus isolates.HBoV was detected in 22.5% of the examined patients.

The NP1 partial gene sequence from all patients showed that thecirculated strains were related to HBoV-1 genotype. Most of HBoV infected patients showed evidence of mixed coinfectionwith other viral pathogens. The current study clearly demonstrated that genetically conserved HBoV1 circulates in SaudiArabia. Interestingly, most of the HBoV1 infected cases were associated with high rates of co-infections with other viruses.

**Keywords:** Bocavirus; Children; Acute respiratory tract infections; Saudi Arabia.

### 1587. CTLA-4 Polymorphism and Clinical Outcome Post Allogeneic Hematopoietic Stem Cell Transplantation

Ghada I. Mossallam and Mohamed A. Samra

*Human Immunology*, 74 (12): 1643-1648 (2013) IF: 2.298

CTLA-4 inhibitory molecule plays an important role in regulating T cell activation. It is considered a crucial element in keeping the immune balance and has been implicated in cancer, autoimmunity and transplantation immunology. Inconsistent observations are reported regarding its association with hematopoietic stem cell transplantation (HSCT). Genotyping of CTLA-4 was performed in recipients and their HLA-matched donors for +49A/G and CT60 polymorphisms (80 and 94 pairs, respectively) using PCR-RFLP. No association was encountered between both polymorphisms in patients and donors and acute or chronic graft versus host disease. Significant association was observed between recipient +49A/G G allele and lower disease-free survival and overall survival compared to AA genotype (HR: 2.17,  $p = 0.03$ , 95% CI: 1.05–4.48 and HR: 2.54,  $p = 0.01$ , 95% CI: 1.16–5.54), respectively. Our results suggest that CTLA-4 genotyping may predict outcome in patients post HSCT. To validate our results, further studies on a larger cohort are needed.

**Keywords:** CTLA-4; Allogeneic hematopoietic stem cell transplantation.

### 1588. Prognostic Significance of WT1 Expression at Diagnosis and End of Induction in Egyptian Adult Acute Myeloid Leukemia Patients

Ghada Ibrahim Mossallam, Thoraya M. Abdel Hamid and Hossam K. Mahmoud

*Hematology*, 18 (2): 69-74 (2013) IF: 1.393

**Background:** Wilms' tumor (WT1) gene overexpression has been reported in the majority of acute myeloid leukemia (AML) patients at diagnosis and has been evaluated as prognostic and minimal residual disease (MRD) marker.

**Patients and methods:** WT1 overexpression was evaluated in 68 adult AML patients at diagnosis and at the end of induction using quantitative real-time polymerase chain reaction (PCR).

**Results:** No significant associations were encountered between WT1 overexpression at diagnosis and other prognostic factors. Complete remission (CR) was achieved in 74% of the patients with WT1 overexpression compared to 80% of patients with normal levels ( $P = 0.5$ ). No significant associations were encountered between WT1 overexpression at diagnosis and disease-free survival (DFS) or overall survival (OS) ( $P = 0.6$  and  $0.3$ , respectively). At the end of induction, the median duration of DFS in patients achieving  $\geq 2$  log reduction was not reached compared to only 5 months (range: 2.1–7.9 months) in those attaining  $< 2$  log reduction ( $P = 0.2$ ). The median duration of OS in patients achieving  $\geq 2$  log reduction was 13 months (range: 0–33.3 months) compared to 7.5 months (5.4–9.6 months) in those attaining  $< 2$  log reduction ( $P = 0.2$ ). The survival at 1 year in patients achieving  $\geq 2$  log was double the group with  $< 2$  log reduction (67% compared to 33%).

**Conclusion:** Our results, although not reaching the level of significance, probably due to the small sample size, still suggest that the early assessment of WT1 transcript level at the end of

induction in patients in CR may have a prognostic significance on clinical outcome and may thus be a useful marker for risk stratification especially in patients lacking disease-specific marker.

**Keywords:** Acute myeloid leukemia; Wilms' tumor gene; Prognosis; Minimal residual disease.

### 1589. Peripheral Blood Mammaglobin Gene Expression for Diagnosis and Prediction of Metastasis in Breast Cancer Patients

Wafaa M. Radwan, Heba S. Moussa, Enas S. Essa, Samia H. Kandil and Azza M. Kamel

*Asia-Pacific Journal of Clinical Oncology*, 9 (9): 66-70 (2013) IF: 0.907

**Aim:** To evaluate the value of peripheral blood mammaglobin (MG) gene expression for diagnosis and prediction of metastasis in breast cancer patients.

**Methods:** MG expression was detected by nested reverse-transcription polymerase chain reaction in the peripheral blood of 46 females (32 breast cancer, 12 benign breast lesions, 2 no breast abnormalities). In total 28 breast cancer patients were followed up through a period of 34 months for the development of metastasis.

**Results:** MG expression was detected in 16/32 (50%) breast cancer patients but not in patients with benign lesions or healthy participants. Five patients had metastasis at diagnosis. During the 34 months of follow up, more MG-positive patients showed metastatic lesions and none of the MG negative patients who were followed up developed metastasis.

**Conclusion:** The study suggests blood MG expression is a specific molecular marker for detection of occult mammary carcinoma cells of patients with operable breast cancer. It might be of value as a predictor of subsequent metastasis. Large-scale studies and longer follow-up periods are needed.

**Keywords:** Breast cancer; Circulating tumor cell; Mammaglobin; Metastasis.

### 1590. Assessment to the Effects of Low Power Diode Laser on Wound Healing in Diabetic Rats

Ahmed. H. Osman, Mahmoud. M. Kamel, Mohamed. H. Wahdan and Mahmoud Al-gazaly

*Life Science Journal*, 10 (2): 1313-1321 (2013) IF: 0.165

**Objective:** Evaluation of the effect of low level laser therapy (LLLT) using diode laser 808 nm on wound healing in diabetic rats as experimental animal model. Background data: Delayed wound healing is reported by several medical care units as changing cases. One of the causes for chronic wounds and delayed wound healing is diabetes which sometime associated with suppuration, gangrene and may be ended by amputation. This is encountered in different medical specialities.

**Methods:** 40 male albino rats, each weighed 200-220 gm. Diabetes was chemically induced using streptozotocin, 40 mg/kg, dissolved in citrate buffer solution (pH 4.3) and administered as tail vein injection in all experimental rats groups except control group. Seven days after streptozotocin injection, blood glucose levels were measured by using a glucometer and test strips.

**Results:** Gross examination showed faster wound closure in the laser exposed groups with minimal scar tissue formation in

comparison with non-laser treated group. The clinical findings were confirmed by the histopathological study using Haematoxylin and Eosin and Masson's Trichrome stain that revealed moderate inflammatory reaction in the laser group versus severe suppurative inflammatory reaction with keloid formation in the control non-treated group. Laser group also showed earlier granulation tissue formation and re-epithelization than non-treated control group.

**Conclusion:** Low level laser therapy using diode laser 808 nm can be applied as an efficient method to accelerate wound healing in diabetic patient. Low level laser therapy has anti-inflammatory and antiseptic effects in addition to minimal scar tissue formation.

**Keywords:** Diode laser; Diabetes mellitus; Wound healing; Pathology.

### 1591. Association of Vitamin D Receptors Genes Polymorphism (*Apa I*, and *Taq I*) with Type 1 Diabetes in Saudi Arabia (KSA)

El-Sayed El-Badrawy, Zein S. Ibrahim, Amal Abedel Aziz, Mahmoud M Kamel, Gaber M Shehab and Ayman Kamal

*Life Science Journal*, 10 (3): 1555-1562 (2013) IF: 0.165

Type 1 diabetes mellitus (T1DM) results from an immune-mediated destruction of insulin-producing-cells in the pancreatic islets of Langerhans. There are clear differences in immunogenetic predisposition to type1 diabetes among countries. Studies have indicated that vitamin D supplementation in early childhood decreases the risk of T1DM. Vitamin D exerts its action via the nuclear vitamin D receptor (VDR), which shows an extensive polymorphism. VDR gene polymorphisms have been associated with altered gene expression or gene function. Four single nucleotide polymorphisms (SNPs) in the VDR gene produce variation in four recognition sites. These recognition sites variants include Fok I, Bsm I, APA I and Taq I. This study was conducted to investigate the relationship between VDR gene polymorphisms and the incidence of T1DM in Saudi people living in Taif region. APA I recognition site was found in low frequency in diabetic patient (7/37)18.9% while, its frequency was high(8/14) 57.1% among normal children. Taq I has two recognition sites. The first was found at nucleotide number 293 that was found in a frequency of (1/14) 7.1% in normal non-diabetic individuals while it was detected in (7/37) 18.9% in diabetic patients. The second Taq I recognition site was found at nucleotide number 494 without any differences between diabetic and normal individuals. This study indicates that there is an association between VDR genetic polymorphism and incidence of T1DM in Saudi people live in Taif region.

**Keywords:** Vit.D receptors; Polymorphism; Type 1 diabetes.

### 1592. Heat Shock Protein-70 and-27 Expressions as Parameters of Early Diagnosis and Disease Progression in Hepatocellular Carcinoma

Amal Fawzy, Hatem Attia, Fatma A Khalaf, Eman Abd El Sameea, Mahmoud A El Tahawy, Mohamed Farag and Fatma Younis

*Life Science Journal*, 10 (1): 262-268 (2013) IF: 0.165

Hepatocellular carcinoma (HCC) is one of the most common malignant tumors worldwide. Despite remarkable advances in diagnostic and therapeutic techniques, the incidence of HCC is still on the increase. The role of liver biopsy in diagnosis of HCC has declined. However, with recent advances in genomics and proteomics a great number of potential serum and tissue markers have been identified and are being developed as new candidate markers for both diagnosis and prognosis of HCC, and may increase the need for liver biopsy. The aim of this study is to investigate the role of HSP70 and HSP27 expressions in early detection of HCC and to find their relation to parameters of disease progression. The study was conducted on 76 patients, 42 have proved HCC and 34 patients with liver cirrhosis (LC) without HCC. Routine laboratory investigations were done including: liver function tests, complete blood counts, serum alpha fetoprotein (AFP), hepatitis B and HCV hepatitis markers, and HCV-RNA levels. HSP70 and 27 expressions were determined in liver sampling by Real-Time PCR. Overexpression of HSP70 was detected in 92.86% of HCC which is statistically significantly higher compared to LC (2.94%) cases, and overexpression of HSP27 was significantly increased in HCC cases (57.14%) as compared to LC patients (8.82%). The overexpression of HSP70 was associated with early HCC diagnostic parameters (tumour size) and prognostic criteria (vascular invasion and tumour grade, Overexpression of HSP27 was associated with tumor size and tumor number, but not associated with each of AFP, vascular invasion and tumor grade. Conclusion: From the above results, we conclude that, found expressions of HSP70 and HSP27 may play an important role in hepatocarcinogenesis, and especially HSP70 can contribute tumor progression. We thus suggest that HSP70 may represent a good molecular target for treatment of HCV-related HCC.

**Keywords:** Hepatocellular carcinoma; HSP70; HSP27; Expression; RT-PCR.

### 1593. Prognostic Markers in Pediatric T- Cell Lymphoblastic Leukemia/Lymphoma

Mohamed H.M. Hussein, Alaa M. El-Haddad, Heba S. Moussa and Ossama M. Maher

*Life Science Journal*, 10: 1804-1813 (2013) IF: 0.165

**Background:** Historically, the diagnosis of T-cell acute lymphoblastic leukemia (T-ALL) or T-cell lymphoblastic lymphoma (T-LBL) predicted a higher risk of induction failure, early relapse, and worse even t-free survival (EFS) compared with B-precursor childhood leukemia or lymphoma. Treatment intensification has dramatically improved the general prognosis of childhood T-cell precursor acute lymphoblastic leukaemia (T-ALL). Nevertheless, approximately 20–25% of cases still relapse early. Various prognostic parameters have been sought for better risk stratification and treatment adjustments for patients with markers of poor prognosis.

A task that has been considerably difficult, with conflicting results from different studies. In this study we aimed at highlighting prognostic parameters that would help in better risk stratification and treatment planning of pediatric T cell ALL and LBL patients.

**Material and methods:** 105 pediatric T-cell leukemia/lymphoma patients were enrolled in the study. T-ALL were 72 cases and 33 cases were T lymphoblastic Leukemia (LBL), stage III. Patients were diagnosed by thorough examination and extensive lab workup. Patients were further evaluated for response to therapy.

The T ALL cases at days 8, 14 and again at day 43, end of induction, together with the LBL cases. Patients were followed up for a median of 20 months and survival was correlated to parameters that could carry prognostic significance.

**Results:** The patients' mean age was 9.75 years and male : female ratio was 3.2:1. The 3 years overall survival (OS) was, for the whole 105 patients 77.4 ±5.1%, for the leukemia group 81.6±5%, and for the lymphoma group 77.6±8.1%. The disease free survival (DFS) was 60.42±5.6%, 93.3±6.4%, 47.1±8.6% and event free survival (EFS) was 50.71±8.3%, 48.5±6.2% and 59.2 ±9.2% respectively.

Age significantly correlated with OS of patients ( $p=0.04$ ). For T ALL, male gender, TLC  $<50 \times 10^9/L$  and good prednisone responders correlated with DFS ( $p=0.01$ ), ( $p<0.001$ ) and ( $p=0.02$ ) respectively. Also, male gender and good prednisone response correlated with EFS ( $p=0.05$ ) and ( $p<0.001$ ) respectively.

**Conclusion:** further studies are needed to establish concrete prognostic markers that would be used for better risk stratification of pediatric T-cell L/L and hence improve the management of pediatric T-cell ALL and LBL and achieve better outcome for the patients

**Keywords:** T-Cell All; T-Lbl; Prognostic parameters.

#### 1594. Detection of Mammaglobin mRNA in the Blood of Breast Cancer Egyptian Female Patients and its Relation to Established Prognostic Parameters

Dalia Kadry, Amal Fawzy, Iman A. Abdelgawad, Iman Loay H. Abulkheir and Fatma M.A. Abou El Kasem

*Life Science Journal*, 10 (2): 1133-1142 (2013) IF: 0.165

**Background:** Mammaglobin, also known secretoglobulin family 2A member 2 (SCGB2A2), is a member of the superfamily of secretoglobins. Its expression is highly specific of mammary tissue and has been shown to be overexpressed in breast tumor tissue, indicating that mammaglobin might confer a growth advantage to mammaglobin-expressing tumor cells.

**Methods:** The study included 46 breast cancer patients with 20 patients diagnosed to have benign breast tumors by clinical evaluation and fine needle aspiration cytology. Malignancy was ruled out by histopathological examination, and 10 apparently healthy volunteering females as normal controls using real-time RT-PCR.

**Results:** Mammaglobin was detected in 26% of peripheral blood of breast cancer patients studied but not in any of the benign or healthy individuals.

It showed statistically significant relations with the positivity of HER2 expression, the presence of distant metastasis and with CEA with  $p$ -value (0.0019), (0.013), (0.001) respectively. On the other hand, it was statistically non-significant for age, grade and stage, ER or PR positivity in breast cancer patients, size of the tumor, and Lymph node involvement.

**Conclusion:** So the study suggests that MG expression is a specific molecular marker for detection of occult mammary carcinoma cells in peripheral blood of patients with operable breast cancer. It might be of value as a predictor of subsequent metastasis.

**Keywords:** Mammaglobin; Breast cancer; PCR.

#### Dept. of Medical Oncology

#### 1595. Long-Term Effects of Continuing Adjuvant Tamoxifen to 10 Years Versus Stopping at 5 Years After Diagnosis of Oestrogen Receptor-Positive Breast Cancer: ATLAS, a Randomised Trial

Christina Davies, Hongchao Pan, Jon Godwin, Richard Gray, Rodrigo Arriagada, Vinod Raina, Mirta Abraham, Victor Hugo Medeiros Alencar, Atef Badran, Xavier Bonfi Il, Joan Bradbury, Michael Clarke, Rory Collins, Susan R Davis, Antonella Delmestri, John F Forbes, Peiman Haddad, Ming-Feng Hou, Moshe Inbar, Hussein Khaled, Joanna Kielanowska, Wing-Hong Kwan, Beela S Mathew, Indraneel Mittra, Bettina Müller, Antonio Nicolucci, Octavio Peralta, Fany Pernas, Lubos Petruzelka, Tadeusz Pienkowski, Ramachandran Radhika, Balakrishnan Rajan, Maryna T Rubach, Sera Tort, Gerard Urrutia, Miriam Valentini Yaochen Wang and Richard Peto

*The Lancet*, 9 (381): 805-816 (2013) IF: 36.427

**Background:** For women with oestrogen receptor (ER)-positive early breast cancer, treatment with tamoxifen for 5 years substantially reduces the breast cancer mortality rate throughout the first 15 years after diagnosis. We aimed to assess the further effects of continuing tamoxifen to 10 years instead of stopping at 5 years.

**Methods:** In the worldwide Adjuvant Tamoxifen: Longer Against Shorter (ATLAS) trial, 12 894 women with early breast cancer who had completed 5 years of treatment with tamoxifen were randomly allocated to continue tamoxifen to 10 years or stop at 5 years (open control). Allocation (1:1) was by central computer, using minimisation. After entry (between 1996 and 2005), yearly follow-up forms recorded any recurrence, second cancer, hospital admission, or death. We report effects on breast cancer outcomes among the 6846 women with ER-positive disease, and side-effects among all women (with positive, negative, or unknown ER status). Long-term follow-up still continues. This study is registered, number ISRCTN19652633.

**Findings:** Among women with ER-positive disease, allocation to continue tamoxifen reduced the risk of breast cancer recurrence (617 recurrences in 3428 women allocated to continue vs 711 in 3418 controls,  $p=0.002$ ), reduced breast cancer mortality (331 deaths vs 397 deaths,  $p=0.01$ ), and reduced overall mortality (639 deaths vs 722 deaths,  $p=0.01$ ). The reductions in adverse breast cancer outcomes appeared to be less extreme before than after year 10 (recurrence rate ratio [RR] 0.90 [95% CI 0.79–1.02] during years 5–9 and 0.75 [0.62–0.90] in later years; breast cancer mortality RR 0.97 [0.79–1.18] during years 5–9 and 0.71 [0.58–0.88] in later years). The cumulative risk of recurrence during years 5–14 was 21.4% for women allocated to continue versus 25.1% for controls; breast cancer mortality during years 5–14 was 12.2% for women allocated to continue versus 15.0% for controls (absolute mortality reduction 2.8%). Treatment allocation seemed to have no effect on breast cancer outcome among 1248 women with ER-negative disease, and an intermediate effect among 4800 women with unknown ER status. Among all 12 894 women, mortality without recurrence from causes other than breast cancer was little affected (691 deaths without recurrence in 6454 women allocated to continue versus 679 deaths in 6440 controls; RR 0.99 [0.89–1.10];  $p=0.84$ ). For the incidence (hospitalization or death) rates of specific diseases, RRs were as follows: pulmonary embolus 1.87 (95% CI 1.13–3.07,  $p=0.01$  [including 0.2% mortality in both treatment groups]), stroke 1.06



(0.83–1.36), ischaemic heart disease 0.76 (0.60–0.95,  $p=0.02$ ), and endometrial cancer 1.74 (1.30–2.34,  $p=0.0002$ ). The cumulative risk of endometrial cancer during years 5–14 was 3.1% (mortality 0.4%) for women allocated to continue versus 1.6% (mortality 0.2%) for controls (absolute mortality increase 0.2%).

**Interpretation:** For women with ER-positive disease, continuing tamoxifen to 10 years rather than stopping at 5 years produces a further reduction in recurrence and mortality, particularly after year 10. These results, taken together with results from previous trials of 5 years of tamoxifen treatment versus none, suggest that 10 years of tamoxifen treatment can approximately halve breast cancer mortality during the second decade after diagnosis.

**Keywords:** Long term; Tamoxifen.

### 1596. Developing Cancer Control Plans in Africa: Examples from Five Countries

Daniela Cristina Stefan, Ahmed M. Elzawawy, Hussein M. Khaled, Fabien Ntaganda, Anita Asimwe, Beatrice Wiafe Addai, Seth Wiafe and Isaac F. Adewole

*The Lancet Oncology*, 14 (4): 189-195 (2013) IF: 25.117

The creation and implementation of national cancer control plans is becoming increasingly necessary for countries in Africa, with the number of new cancer cases per year in the continent expected to reach up to 1.5 million by 2020. Examples from South Africa, Egypt, Nigeria, Ghana, and Rwanda describe the state of national cancer control plans and their implementation. Whereas in Rwanda the emphasis is on development of basic facilities needed for cancer care, in those countries with more developed economies, such as South Africa and Nigeria, the political will to fund national cancer control plans is limited, even though the plans exist and are otherwise well conceived. Improved awareness of the increasing burden of cancer and increased advocacy are needed to put pressure on governments to develop, fund, and implement national cancer control plans across the continent.

**Keywords:** Cancer control; Africa.

### 1597. Schistosomiasis and Cancer in Egypt: Review

Hussein Khaled

*Journal of Advanced Research*, 4: 461-466 (2013) IF: 3

Schistosomiasis is not known to be associated with any malignant disease other than bladder cancer. Bladder cancer is still the most common malignant tumor among males in Egypt and some African and Middle East countries. However, the frequency rate of bladder cancer has declined significantly during the last 25 years. This drop is mainly related to the control of Schistosomiasis. Many studies have elucidated the pathogenic events of Schistosoma-related bladder cancer with a suggested theory of pathogenesis. Furthermore, the disease presents with a distinct clinicopathologic profile that is quite different from bladder cancer elsewhere with younger age at presentation, more male predominance, more invasive stages, and occurrence of squamous cell carcinoma pathologic subtype. However, recent data suggest that this profile has been dramatically changed over the past 25 years leading to minimization of the differences between its features in Egypt and that in Western countries. Management of muscle-invasive localized disease is mainly surgery with 5-year survival rates of 30–50%. Although still a

debatable issue, adjuvant and neoadjuvant chemotherapy and radiotherapy have improved treatment outcomes including survival and bladder preservation rates in most studies. This controversy emphasizes the need of individualized treatment options based on a prognostic index or other factors that can define the higher risk groups where more aggressive therapy is needed. The treatment for locally advanced and/or metastatic disease has passed through a series of clinical trials since 1970s. These phase II and III trials have included the use of single agent and combination of chemotherapy and radiotherapy regimens. The current standard of systemic chemotherapy of generally fit patients is now the gemcitabine–cisplatin combination. In conclusion, a changing pattern of bladder cancer in Egypt is clearly observed. This is mainly due to the success in the control of Schistosomiasis. It may also be due to increased exposure to other etiologic factors that include smoking, pesticides, and/or other causative agents. This change will ultimately affect disease management.

**Keywords:** Schistosomiasis; Bilharziasis; Bladder cancer; Squamous cell carcinoma.

### 1598. Adherence of Non-Pharmaceutically Sponsored Oncology Trial Protocols to the International Conference on Harmonization (ICH) Guidelines in an Academic Institution outside the ICH Jurisdictions and the Impact of IRB Implementation on this Adherence

Ahmed A. Zeeneldin

*Journal of the Egyptian National Cancer Institute*, 25: 71-78 (2013) IF: 2

**Purpose:** To assess adherence of non-pharmaceutically sponsored trials (non-PSTs) to ICH protocol structure guidelines and to estimate the effect of implementing Institutional Review Board's (IRB) review on this adherence.

**Methods:** This is a retrospective exploratory study where 60 non-PST clinical trial protocols (CTPs) were reviewed and halved to IRB-reviewed CTPs (IRCTPs) and non-IRB-reviewed CTPs (non-IRCTPs). Adherence score (AS) was calculated as the number of fulfilled items or sub-items divided by their total number.

**Results:** Three adherence patterns were encountered: (1) items consistently present in both groups e.g. general and background information, objectives, inclusion criteria and intervention details, (2) items consistently absent in both groups and included contact information of investigators and trial sites, product accountability, randomization codes' management, interim analyses and many other statistical aspects, and (3) items variably present in both groups where the effect of IRB was verifiable. Trial site details, potential benefits, discontinuation and exclusion criteria, and follow up for adverse events were more encountered in IRCTPs than non-IRCTPs. Withdrawal criteria and monitoring of treatment compliance showed a reverse pattern ( $p < 0.05$  for all). The total AS, administrative AS and ethics AS for IRCTPs was 43%, 22% and 70% compared to 38%, 16% and 33% for non-IRCTPs ( $p < 0.003$ ,  $< 0.001$ ,  $0.004$ ), respectively. The scientific AS was 54% for both groups ( $p = 0.87$ ).

**Conclusions:** IRB implementation at NCI-Egypt improved ethical and administrative sections of academic protocols. However, this improvement is modest and needs further actions including adoption of protocol templates. Scientific sections were as good after IRB implementation as they were before that.

**Keywords:** Academic clinical trial protocols; Adherence; ICH Guidelines; IRB-Review; NCI-Egypt.

### 1599. Breast Cancer Laterality Among Egyptian Patients and Its Association with Treatments and Survival

Ahmed A. Zeeneldin, Mohamed Ramadan, Nehal Elmashad, Ibrahim Fakhr, Amira Diaa and Ehab Mosaad

*Journal of the Egyptian National Cancer Institute*, 25: 199-207 (2013) IF: 2.0

**Background and aim:** Breast cancers (BCs) involve the left side (LS) more than the right side (RS). Among the Egyptians, neither BC laterality nor its association with demographic factors, tumor locations, treatments and outcomes were previously reported.

**Patients and methods:** Laterality was analyzed among 5459 BCs from the Gharbiah population-based cancer registry covering > 5% of the Egyptian population. Cox proportional model was used to assess the independent effect of stage, ER, and laterality on overall survival (OS).

**Results:** In Egypt, BCs involve LS more than RS with LS-to-RS ratio (LRR) of 1.16. LS predominance was evident among men and women and both younger (<45 years) and older patients. HER2 over-expression and ductal cancers were significantly more in RSBCs while lobular cancers were significantly more in LSBCs. There were no significant differences in localization within the breast between LSBCs and RSBCs ( $p = 0.51$ ). LS predominance was noticed across all subgroups except in patients with HER2 positive tumors (LRR = 0.63;  $p = 0.02$ ). OS was significantly better in stage II and ER positive tumors than stage III and ER negative tumors. Despite OS of LSBCs being generally lower than RSBCs, this was not statistically significant. The significant impact of stage on OS was lost in LSBCs.

**Conclusions:** Among Egyptian patients, the left breast is at greater risk of cancer than the right one. Despite right-sided tumors seemed more aggressive, Left-sided ones tend to confer worse survival than right-sided tumors.

**Keywords:** Egypt; Breast cancer; Laterality; Therapy; Survival.

### 1600. Clinico-Pathological Features of Breast Carcinoma in Elderly Egyptian Patients: A Comparison with the Non-Elderly Using Population-Based Data

Ahmed Abdelmabood Zeeneldin, Mohamed Ramadan, Ayman Abdelsamee Gaber and Fatma Mohamed Taha

*Journal of the Egyptian National Cancer Institute*, 25: 5-11 (2013) IF: 2

**Background:** Breast cancer (BC) is a major worldwide health care problem that mostly afflicts the elderly population in the more developed countries. It is not known how common is breast cancer among elderly Egyptian patients and whether this differs from the disease in younger patients.

**Aims:** To study the clinico-pathological features of BC in elderly Egyptian patients (>65 years of age) among the population of an Egyptian Governorate, Gharbiah, and to compare these features with those of younger patients (<65 years).

**Methods:** This is a cross sectional study that compares elderly BC (EBC) and the non-elderly BC (NEBC) using the information

from the Gharbiah Population-based Cancer registry (GPCR) during the years 1999–2007.

**Results:** Out of 6078 BCs, 12% were EBCs and 88% were NEBCs. Between 1999 and 2007, the crude incidence rate (CIR, per 100,000 populations) of EBC increased from 47 to 71 and that of NEBC increased from 16 to 17. Compared to NEBC patients, EBC patients were more likely to have a positive family history and present with a distant disease and less likely to present with a localized disease. EBCs were more likely to have lung metastases and less likely to have liver metastases. Histology, grade, hormone and HER-2 receptor statuses were comparable in both groups. Apart from hormonal therapies, the elderly were less likely to receive surgery, radiotherapy or chemotherapy.

**Conclusion:** EBC patients in Egypt present with advanced disease and are less likely to receive surgery, radiotherapy or chemotherapy compared to NEBC patients.

**Keywords:** Elderly breast cancer; Incidence; Epidemiology; Egypt.

### 1601. Primary Gastrointestinal Lymphoma in An Egyptian District: A Study Using A Population-Based Cancer Registry

Magdy M. Saber, Ahmed A. Zeeneldin, Mohamed A. Samra and Sarah A. Farag

*Journal of the Egyptian National Cancer Institute*, 25: 95-101 (2013) IF: 2

**Introduction:** Gastrointestinal lymphoma (GIL) is the most common extranodal form of non-Hodgkin's lymphoma (NHL) with geographical and age variation of its various subtypes.

**Aim:** To study GIL in Gharbiah, Egypt and to recognize the treatments employed and their outcomes including survival.

**Methods:** This is a retrospective study. Between 2000 and 2002, 40 adult patients with GIL were identified in the Gharbiah population based cancer registry (GPBCR); 26 cases of whom were treated at Tanta Cancer Center (TCC).

**Results:** GIL in Gharbiah, Egypt represented 6.2% of all GIT cancers. The median age was 47 years with slight male predominance.

The commonest primary site was the stomach followed by the colon/rectum then the small intestine (67.5%, 25% and 7.5%, respectively). The commonest histological subtypes were the diffuse large B-cell (41.5%) followed by marginal zone B-cell (39%).

The commonest symptoms were abdominal pains followed by vomiting. Only 18% of GILs were surgically resected. Most patients (77%) received chemotherapy with a 60% complete response (CR) rate. Once in CR, relapses are occasional.

The median overall survival (OS) and progression free survival (PFS) were 31 and 14 months (95% CI, 13.2–48.7 and 6.4–21.6 months, respectively). Gastric primary site and diffuse large B cell subtype carry a non-significant worse OS and PFS than those of other sites and subtypes.

**Conclusions:** GILs in Gharbiah, Egypt are characterized by predominance of male gender, gastric site and marginal zone histology. Survival is worse for gastric and diffuse large B-cell GILs compared to other sites and histologies.

**Keywords:** Gastrointestinal lymphoma; Egypt; Gharbiah population-based cancer registry; Treatment; Outcomes; Survival.

### 1602. Role of Cyclins A and E in Endometrial Carcinogenesis in Breast Cancer Patients Under Tamoxifen Treatment

Ayman M. Metwally, Lobna A. Refaat, HebatAllah Shaaban, Somaia Megm, Mohamed Emara, Amany A. Tohamy, Eman Abou Sinna and Hussein Khaled

*Journal of the Egyptian National Cancer Institute*, 25: 193-198 (2013) IF: 2

**Purpose:** The objective of our study was to determine the relevance of cyclins A and E overexpression in endometrial carcinogenesis in hormone receptor-positive breast cancer patients under tamoxifen therapy. **Experimental design:** We assessed expression of cyclins A and E in Endometrial cytology samples collected from 36 ER and PR positive breast cancer patients; under tamoxifen treatment by using the Tao-brush non-invasive brushing cytology technique. Cyclins were detected in the collected samples by means of immuno-cytochemistry. The patients included in this study are a cohort of 36 breast cancer patients who were operated upon at the National Cancer Institute – Cairo University in the period from February 2006 to May 2008 and received tamoxifen (TAM) as part of their adjuvant treatment. **Results:** Cyclins A and E were expressed in 17 and 15 of the 36 collected endometrial cytology samples (47.2% and 41.6% respectively). Expression of cyclins A and E was highly correlated to Tamoxifen exposure duration (32 and 43 months respectively)  $p < 0.001$ . Tamoxifen median exposure duration was shortened to 21 months in cases showing positivity for either markers, while in cases showing positivity for both cyclins, the median exposure duration was longer (44.5 months) ( $p < 0.001$ ). Neither cyclin A nor E was detected before median tamoxifen exposure duration of 11 months. Endometrial carcinoma cases had the longest Tamoxifen exposure duration (60 months).

**Conclusion:** Cyclins A and E expression is involved in the carcinogenesis of endometrium in women with breast cancer and under tamoxifen treatment. Follow up of the patients using these 2 markers is highly recommended starting from the 12th month.

**Keywords:** Endometrial; Carcinogenesis; Cyclins A; E; Tamoxifen.

### 1603. Role of Ki67 in Predicting Resistance to Adjuvant Tamoxifen in Postmenopausal Breast Cancer Patients

Heba M. Elzawahry, Magdy M. Saber, Nadia M. Mokhtar, Ahmed A. Zeeneldin, Yahia M. Ismail and Nelly H. Alieldin

*Journal of the Egyptian National Cancer Institute*, 25: 181-191 (2013) IF: 2

**Introduction:** Breast cancer (BC) is a major health problem in Egypt and worldwide. Its prognosis depends not only on tumor stage but also on tumor biology.

**Aim:** To correlate the expression of Ki67 with the clinical outcomes of early hormone-receptor positive postmenopausal BC patients who are receiving tamoxifen.

**Methods:** This cohort study included 70 patients. They were followed up for a minimum of 2 years. Ki67 was assessed on paraffin-embedded blocks using immunohistochemistry methods.

**Results:** The median Ki67 value was 22.5% (IQR, 10%–50%). Ki67 was significantly higher in patients with HER2 positive

tumors compared to HER2 negative tumors. After a median follow up period of 53 months, 22 patients (31%) developed disease recurrence either loco-regional or distant in 5.7% and 30%, respectively.

Recurrent patients had significantly higher tumor stage, nodal stage and Ki67 values compared to non-recurrent cases. The 2-, 3- and 5-year overall survival (OS) and disease-free survival (DFS) rates were 100% & 91%, 98% & 84% and 77% & 59%, respectively. DFS was significantly worse with higher TNM stage, lower ER expression and higher Ki67 values. OS was significantly worse in patients with Ki67 values  $\geq 30\%$ . Ki67  $\geq 30\%$  was an independent predictor of recurrence, poor DFS and OS.

**Conclusion:** High Ki67 expression is predictive of poor prognosis and of resistance to adjuvant tamoxifen therapy in postmenopausal BC. We recommend considering Ki67 as one of the risk factors that guide adjuvant treatment decisions.

**Keywords:** Breast cancer; Adjuvant hormonal therapy; Tamoxifen; Postmenopausal; Ki67; National cancer institute; Egypt.

### 1604. Small Intestinal Cancers Among Adults in an Egyptian District: A Clinicopathological Study Using A Population-Based Cancer Registry

Ahmed A. Zeeneldin, Magdy M. Saber, Ibrahim A. Seif El-Din and Sara A. Frag

*Journal of the Egyptian National Cancer Institute*, 25: 107-114 (2013) IF: 2

**Background:** Small intestinal cancers (SICs) are very rare all over the world and little is known about them in Egypt.

**Methods:** This a retrospective study. Between 2000 and 2002, 30 cases with SICs were identified in the Gharbiah population based cancer registry (GPBCR); 17 cases of whom were treated at Tanta Cancer Center (TCC).

**Results:** The median age was 51 years with female predominance. The duodenum was the commonest site (43%) followed by the ileum then the jejunum. Adenocarcinoma (AC), carcinoids, gastrointestinal stromal tumors (GISTs), lymphoma and sarcoma represented 50%, 10%, 17%, 13% and 10% respectively.

Abdominal pain was the commonest symptom and localized disease was the commonest presentation. Surgery, chemotherapy and radiotherapy were employed in 65%, 35% and 0% of patients, respectively.

The median overall survival and progression free survival (OS, PFS) were 18 and 15 months (95% CI: 10.4–25.6 and 3.6–26.4), respectively. AC had inferior OS and PFS to other histologies ( $p = 0.08$  and  $0.12$ , respectively). Also, duodenum subsite was inferior in OS and PFS to other sites ( $p = 0.25$  and  $0.35$ , respectively).

**Conclusions:** SICs in Gharbiah, Egypt are characterized by predominance of female gender and adenocarcinoma histology. One year survival is 64% with a poor outcome for adenocarcinoma and duodenal subsite.

**Keywords:** Egypt; Gharbiah population-based cancer registry; Small intestinal neoplasms; Treatment; Survival.

### 1605. Transarterial Chemoembolization for the Treatment of Hepatocellular Carcinoma: A Single Center Experience Including 221 Patients

Ahmed Abdelmabood Zeeneldin, Salem Eid Salem, Reda Hassan Tabashy, Asmaa Ahmed Ibrahim and Nelly Hassan Alieldin

*Journal of the Egyptian National Cancer Institute*, 25: 143-150 (2013) IF: 2

**Background:** Hepatocellular carcinoma (HCC) is a major health problem in Egypt as well as in many countries. Transarterial chemoembolization (TACE) is a treatment modality applicable to locally advanced HCC beyond surgery or ablative therapies and is associated with survival improvements. The aim of this study was to assess the outcomes of TACE in our center over the past four years.

**Methods:** This is a retrospective cohort study that included 221 patients with locally advanced HCC treated with TACE in a single center between the years 2007 and 2010. The median age was 57 years with male predominance. Liver cirrhosis, viral hepatitis and Bilharziasis were encountered in 64%, 31% and 8% of patients, respectively. Abdominal pain was the most common presenting symptom (67%). Most cases were diagnosed based on radiology (57%) with a TNM stage I or II (73%) and a median AFP value of 150 ng/mL.

**Results:** 221 patients received 440 cycles of TACE with a median of 2 cycles per patient. Cisplatin and doxorubicin (50 mg per cycle, each) were the most commonly used drugs. Impaired liver function was the most common toxicity. Liver cell failure occurred in 17% of patients. An objective tumor response was achieved in 44% of cases. The median overall survival (OS) was 16 months (95% CI, 13–19 months) and the median progression free survival (PFS) was 6 months (95% CI, 4.3–7.8 months). Responding patients, Child-Pugh class A and patients receiving standard doses of chemotherapy had a significantly better OS than their counterparts. Only Child-Pugh class A was associated with significantly longer PFS ( $p < 0.001$ ).

**Conclusion:** TACE produces reasonable responses and fair survival rates in locally advanced HCC but with noticeable toxicities. Proper patients' selection and prompt liver support are mandates for improving TACE outcomes.

**Keywords:** Hepatocellular carcinoma; Transarterial chemoembolization; Treatment; National cancer institute; Egypt.

### 1606. Assessment of Diagnosis of Inflammatory Breast Cancer Cases at Two Cancer Centers in Egypt and Tunisia

Catherine Schairer, Amr S. Soliman, Sherif Omar, Hussein Khaled, Saad Eissa, Farhat Ben Ayed, Samir Khalafallah, Wided Ben Ayoub, Elizabeth D. Kantor, Sofia Merajver, Sandra M. Swain, Mitchell Gail and Linda Morris Brown

*Cancer Medicine Journal*, 2 (2): 178-184 (2013)

The diagnosis of inflammatory breast cancer (IBC) is largely clinical and therefore inherently somewhat subjective. The objective of this study was to evaluate the diagnosis of IBC at two centers in North Africa where a higher proportion of breast cancer is diagnosed as IBC than in the United States (U.S.). Physicians prospectively enrolled suspected IBC cases at the National Cancer

Institute (NCI) – Cairo, Egypt, and the Institut Salah Azaiz (ISA), Tunisia, recorded extent and duration of signs/symptoms of IBC on standardized forms, and took digital photographs of the breast. After second-level review at study hospitals, photographs and clinical information for confirmed IBC cases were reviewed by two U.S. oncologists. We calculated percent agreement between study hospital and U.S. oncologist diagnoses. Among cases confirmed by at least one U.S. oncologist, we calculated median extent and duration of signs and Spearman correlations. At least one U.S. oncologist confirmed the IBC diagnosis for 69% (39/50) of cases with photographs at the NCI-Cairo and 88% (21/24) of cases at the ISA. All confirmed cases had at least one sign of IBC (erythema, edema, peau d'orange) that covered at least one-third of the breast. The median duration of signs ranged from 1 to 3 months; extent and duration of signs were not statistically significantly correlated. From the above-mentioned outcomes, it can be concluded that the diagnosis of a substantial proportion of IBC cases is unambiguous, but a subset is difficult to distinguish from other types of locally advanced breast cancer. Among confirmed cases, the extent of signs was not related to delay in diagnosis.

**Keywords:** Edema; Egypt; Erythema; Inflammatory breast cancer; Peau d'orange; Tunisia.

### 1607. Effect of Mesenchymal Stem Cells and A Novel Curcumin Derivative On Notch1 Signaling in Hepatoma Cell Line

Mohamed T. Abdel Aziz, Hussien M. Khaled, Ali El Hindawi, Nagwa K. Roshdy, Laila A. Rashed, Dina Sabry, Amira A. Hassouna, Fatma Taha and Walaa I. Ali

*Biomed Research International Journal*, (2013)

This study was conducted to evaluate the effect of mesenchymal stem cells (MSCs) and a novel curcumin derivative (NCD) on HepG2 cells (hepatoma cell line) and to investigate their effect on Notch1 signaling pathway target genes. HepG2 cells were divided into HepG2 control group, HepG2 cells treated with MSC conditioned medium (MSCs CM), HepG2 cells treated with a NCD, HepG2 cells treated with MSCs CM and NCD, and HepG2 cells treated with MSCs CM (CM of MSCs pretreated with a NCD). Expression of Notch1, Hes1, VEGF, and cyclin D1 was assessed by real-time, reverse transcription-polymerase chain reaction (RT-PCR) in HepG2 cells. In addition, HepG2 proliferation assay was performed in all groups. Notch1 and its target genes (Hes1 and cyclin D1) were downregulated in all treated groups with more suppressive effect in the groups treated with both MSCs and NCD. Also, treated HepG2 cells showed significant decrease in cell proliferation rate. These data suggest that modulation of Notch1 signaling pathway by MSCs and/or NCD can be considered as a therapeutic target in HCC.

**Keywords:** Mesenchymal stem cell; Hepatoma cell line.

### 1608. Research Profile of the Egyptian National Cancer Institute (ENCI) in the Pubmed

Ahmed A. Zeeneldin

*Mediterranean Oncology Journal*, 3: 56-63 (2013)

**Background:** The Egyptian National Cancer Institute (enCI) is the largest cancer center in Egypt, Africa and the Middle East. It is



concerned not only with cancer treatment, but also with education and research. This study was conducted to assess the publications affiliated to enCI in the PubMed.

**Methods:** On the 29th of October 2012, the PubMed was searched for publications that are affiliated to the enCI, Cairo University, Egypt. Records were manually scrutinized to extract relevant information.

**Results:** 391 records were retrieved. Publication volume showed a giant step in 2004. Most enCI articles are hosted by the enCI journal. Departments of Surgery, Cancer Biology, Medical Oncology, Radiotherapy and Pathology made the greatest contribution to the publications of the Egyptian National Cancer Institute in the PubMed contributing 23%, 20%, 14%, 13% and 11%, respectively. One author from Cancer Biology Dept. topped enCI authors' lists. Cancers of the breast followed by the urinary bladder, head, neck & thyroid, leukemias and lymphomas were the most common diseases included in enCI publications in the PubMed representing 14%, 11%, 9.5%, 9%, and 7%, respectively. The main theme of the publications were the investigation of how tests perform in certain clinical settings (40%), of new techniques (e.g. surgical, radiotherapy, stem-cell transplantation; 27%), of drugs or drug regimens (12%) or the reporting of the epidemiologic features of cancers. Only 31 publications (7.9%) were reporting on clinical trials of which 18 were randomized clinical trials. We did not encounter a single phase I trial publication.

**Conclusion:** Research output of the enCI needs to be leveraged both in quality and volume. Research specific training programs as well as research strategic planning will be of great help. Supporting the new-laid enCI research center may be a step in the right direction.

**Keywords:** Egyptian national cancer institute; Cancer; Publication volume; PubMed.

#### Dept. of Pediatrics Oncology

##### 1609. Parental Trust in Health Care-a Prospective Study From the Children's Cancer Hospital in Egypt

Hanan El Malla, Ulrika Kreicbergs, Gunnar Steineck, Ulrica Wilderäng, Yasser El Sayed Elborai and Nathalie Ylitalo

*Psycho-Oncology*, 22: 548-554 (2013) IF: 3.506

**Objective:** Patient-physician communication and patient satisfaction are important elements of cancer care. Trust is considered to be crucial for the patient-physician relationship, yet little is to be found in the literature regarding what factors may influence trust.

**Methods:** We assessed predictors of trust in health-care professionals and in the medical care by administering two questionnaires, one at start of chemotherapy treatment and one at the time of the third chemotherapy cycle, to 304 parents of children with newly diagnosed cancer at the Children's Cancer Hospital in Cairo, Egypt.

**Results:** Parents' trust in the medical care at the time of the child's third chemotherapy cycle was significantly associated with the following at the start of treatment: having received at least moderate information about the disease (relative risk (RR) 13.2; 95% CI 7.8–22.3) and the treatment (RR 17.2; 95% CI 9.5–31.4), having the opportunity to communicate with the child's physicians (RR 21.3; 95% CI 11.7–38.8), being satisfied with the physicians' conversation style (RR 30.6; 95% CI 14.4–64.9),

having the emotional needs met (RR 22.2; 95% CI 11.8–41.9), and being met with care by the child's physicians (RR 32.0; 95% CI 15.2–67.7). After multivariable model selection, the strongest predictor of trust at the time of the third chemotherapy cycle was to be met with care at the start of treatment.

**Conclusion:** Parents being met with care by the child's physicians at the beginning of the child's chemotherapy treatment develop an increased trust in the medical care.

**Keywords:** Communication; Trust; Pediatric oncology; Cancer; Medical care.

##### 1610. Adherence to Medication: a Nation-Wide Study from the Children's Cancer Hospital, Egypt

Hanan El Malla, Nathalie Ylitalo Helm, Ulrica Wilderäng, Yasser El Sayed Elborai, Gunnar Steineck and Ulrika Kreicbergs

*World Journal of Psychiatry*, 3: 25-33 (2013)

**Aim:** To investigate adherence to medical regimen and predictors for non-adherence among children with cancer in Egypt.

**Methods:** We administered two study specific questionnaires to 304 parents of children diagnosed with cancer at the Children's Cancer Hospital in Cairo, Egypt, one before the first chemotherapy treatment and the other before the third. The questionnaires were translated to colloquial Egyptian Arabic, and due to the high illiteracy level in Egypt an interviewer read the questions in Arabic to each parent and registered the answers. Both questionnaires consisted of almost 90 questions each. In addition, a Case Report Form was filled in from the child's medical journal. The study period consisted of 7 mo (February until September 2008) and we had a participation rate of 97%. Descriptive statistics are presented and Fisher's exact test was used to check for possible differences between the adherent and non-adherent groups. A P-value below 0.05 was considered significant. Software used was SAS version 9.3 for Windows (SAS Institute Inc., Cary, NC, United States).

**Results:** Two hundred and eighty-one (90%) parents answered the second questionnaire, regarding their child's adherence behaviour. Approximately two thirds of the children admitted to their third chemotherapy treatment had received medical recommendations upon discharge from the first or second chemotherapy treatment (181/281, 64%). Sixty-eight percent (123/181) of the parents who were given medical recommendations reported that their child did not follow the recommendations. Two main predictors were found for non-adherence: child resistance (111/123, 90%) and inadequate information (100/123, 81%). In the adherent group, 20% of the parents (n = 12/58) reported trust in their child's doctor while 14 percent 8/58 reported trust in the other health-care professionals. Corresponding numbers for the non-adherent group are 8/123 (7%) for both their child's doctor and other health-care professionals. Almost all of the parents expressed a lack of optimism towards the treatment (116/121, 96%), yet they reported an intention to continue with the treatment for two main reasons, for the sake of their child's life (70%) (P = 0.005) and worry that their child would die if they discontinued the treatment (81%) (P < 0.0001).

**Conclusion:** Non-adherence to medical regimen is common among children diagnosed with cancer in Egypt, the main reasons being child resistance and inadequate information.



**Keywords:** Cancer; Adherence to medical regimen; Non-compliance; Patient-physician communication; Paediatric oncology; Psycho-oncology; Psychosocial.

#### Dept. of Surgical Oncology

##### 1611. Neobladder Long Term Follow-up

I. Fakhr, A.-M. Mohamed, A. Moustafa, M. Al-Sherbiny and M. Salama

*Journal of the Egyptian National Cancer Institute*, 25: 43-49 (2013) IF: 2.0

One of the commonest forms of orthotopic bladder substitution for bladder cancer survivors, used in our institute, is the use of ileocecal segment. Sometimes, the need for Indiana pouch heterotopic continent diversion arises.

**Aim:** To compare the long-term effect of orthotopic ileocecal bladder and heterotopic Indiana pouch following radical cystectomy in bladder cancer patients.

**Patients and methods:** Between January 2008 and December 2011, 91 patients underwent radical cystectomy/anterior pelvic exenteration and orthotopic ileocecal bladder reconstruction (61 patients) and Indiana pouch (30 patients), when orthotopic diversion could not be technically or oncologically feasible.

**Results:** Convalescence was uneventful in most patients. All minor and major urinary leakage cases, in both diversions groups, where successfully conservatively treated. Only one patient in the ileocecal group with major urinary leak required re-exploration with successful revision of uretero-colonic anastomosis. Only one patient in the Indiana pouch group had accidentally discovered sub-centimetric stone, which was simply expelled. The overall survival proportion of ileocecal group was 100% compared to 80% in the Indiana pouch group ( $p < 0.001$ ). The disease free survival proportion of ileocecal group was 90.8% compared to 80% in the Indiana pouch group ( $p = 0.076$ ). Effective comparative daytime and nighttime urinary continence as well as renal function deterioration were not statistically significant between both reconstruction types.

**Conclusion:** Both ileocecal bladder and Indiana pouch are safe procedures in regard to long-term effects over kidney function following radical cystectomy.

**Keywords:** Ileocecal bladder; Indiana pouch; Continence; Radical cystectomy.

##### 1612. Outcome of Fertility Preserving Surgery in Early Stage Ovarian Cancer

Ibrahim Fakhr, Mohamed Abd-Allah, Samy Ramzy, Abdel-Maksoud Mohamed and Amani Saber

*Journal of the Egyptian National Cancer Institute*, 25: 219-222 (2013) IF: 2.0

**Aim:** To assess the role of fertility preserving surgery in treatment of patients with stage IA, G1 or G2 ovarian carcinoma without adjuvant chemotherapy.

**Patients and methods:** From 2006 to 2008, a prospective non-randomized study recruited 150 women, with suspicious early malignant ovarian mass.

**Results:** Among the 150 explored patients, only 43 (28.6%) patients underwent exploration. Only 32/150 (21.3%) patients had proven stage IA, either G1 or G2, epithelial ovarian cancer.

Among the 32 patients, 22 (68.7%) patients were nullipara while 10 (32.1%) had one child. All patients had unilateral tumors; 26 (81.25%) patients had G1 and 6 (18.75%) patients had G2 tumors; 24/32 (75.0%) tumors were serous, 6/32 (18.7%) were mucinous and 2/32 (6.2%) were endometrioid, and none was clear cell type. The median follow up period was 58.5 months (ranged: 48–72 months). Two patients (6.7%) were lost during follow up; data will be presented for the remaining 30 patients. One patient, at 27th month of follow up, had open abdominal exploration to investigate abnormal pelvic mass on routine ultrasound follow up examination. Frozen section revealed recurrent invasive mucinous tumor. She underwent radical surgery with pelvic and para-aortic lymph node dissection, followed by adjuvant chemotherapy, and remained free of disease, for the remaining 29 months of the follow up period. Neither distant metastases nor mortality were reported among our patients.

**Conclusion:** Fertility preserving surgery can be considered a safe treatment strategy in patients with stage IA, G1 or G2 ovarian carcinoma.

**Keywords:** Fertility preserving surgery; Early stage ovarian carcinoma.

#### Dept. of Tumor Biology

##### 1613. Aberrant Overexpression of MiR-421 Downregulates ATM and Leads to A Pronounced DSB Repair Defect and Clinical Hypersensitivity in SKX Squamous Cell Carcinoma

Wael Y. Mansour, Natalia V. Bogdanova, Ulla Kasten-Pisula, Thorsten Rieckmann, Sabrina Köcher, Kerstin Borgmann, Michael Baumann, Mechtild Krause, Cordula Petersen, Hailiang Hu, Richard A. Gatti, Ekkehard Dikomey, Thilo Dörk and Jochen Dahm-Daphi

*Radiotherapy and Oncology*, 106: 147-154 (2013) IF: 4.52

**Background:** Cellular and clinical sensitivity to ionizing radiation (IR) is determined by DNA double-strand breaks (DSB) repair. Here, we investigate the molecular mechanism underlying the extreme response of a head and neck tumor case (SKX) to standard radiotherapy.

**Methods:** Immunofluorescence (IF) was used for the assessment of DSB repair, Western blot and real-time PCR for protein and mRNA expression, respectively.

**Results:** SKX cells exhibited a pronounced radiosensitivity associated with numerous residual  $\gamma$ -H2AX foci after IR. This was not associated with lacking canonical repair proteins. SKX cells did not express any ATM protein. Accordingly, immunoblotting revealed no ATM kinase activity toward substrates such as p-SMC1, p-Chk2 and p-KAP1. Sequencing of all 66 exons of ATM showed no mutation. ATM mRNA level was moderately reduced, which could be reverted by 5'-Aza-C treatment but without restoring protein levels. Importantly, we demonstrated a post-transcriptional regulation in SKX cells via 6-fold enhanced levels of miR-421, which targets the 3'-UTR of ATM mRNA. Transfection of SKX cells with either anti-miR-421 inhibitor or a microRNA-insensitive ATM vector recovered ATM expression and abrogated the hyper-radiosensitivity.

**Conclusion:** This is the first report describing microRNA-mediated down-regulation of ATM leading to clinically manifest tumor radiosensitivity.

**Keywords:** ATM; MIR421; Radiosensitivity.

#### 1614. The Absence of Ku But Not Defects in Classical Non-Homologous End-Joining Is Required To Trigger PARP1-Dependent End-joining

Wael Y. Mansour, K. Borgmann, C. Petersen, Ekkehard Dikomey and Jochen Dahm-Daphi

*Dna Repair*, 12: 1134-1142 (2013) IF: 4.274

Classical-non-homologous end-joining (C-NHEJ) is considered the main pathway for repairing DNA double strand breaks (DSB) in mammalian cells. When C-NHEJ is defective, cells may switch DSB repair to an alternative-end-joining, which depends on PARP1 and is more erroneous.

This PARP1-EJ is suggested to be active especially in tumor cells contributing to their genomic instability. Here, we define conditions under which cells would switch the repair to PARP1-EJ. Using the end joining repair substrate pEJ, we revealed that PARP1-EJ is solely used when Ku is deficient but not when either DNA-PKcs or Xrcc4 is lacking. In the latter case, DSB repair, however, could be shuttled to PARP1-EJ after additional Ku80 down-regulation, which partly rescued the DSB repair in these mutants.

We demonstrate here that PARP-EJ may work on DSB ends at high fidelity manner, as evident from the unchanged efficiency upon blocking end resection by either roscovitin or mirin. Furthermore, we demonstrate for that PARP-EJ is likewise involved in the repair of multiple DSBs (I-PpoI- and IR-induced). Importantly, we identified a chromatin signature associated with the switch to PARP1-EJ which is characterized by a strong enrichment of both PARP1 and LigIII at damaged chromatin. Together, these data indicate that Ku is the main regulator for the hierarchal organization between C-NHEJ and PARP1-EJ.

**Keywords:** Dsb repair; Non-homologous End-joining; Alternative end-Joining; PARP1-dependent end-Joining.

#### 1615. Potential Role of Curcumin and Taurine Combination Therapy on Human myeloid Leukemic Cells Propagated *in Vitro*

Motawa E. El-Houseini, Mohammed Osman Refaei, Ahmed Ibrahim Amin and Mahmoud A. Abol-Ftouh

*Leukemia and Lymphoma*, 1-7 (2013) IF: 2.301

Curcumin and taurine are natural products that have been used in this study evaluating their therapeutic effect on myeloid leukemic cells propagated *in vitro*. Sixty patients with myeloid leukemia and 30 healthy volunteers were enrolled in the study. All patient groups were admitted to the Medical Oncology Department of the National Cancer Institute, Cairo University.

There were statistically significant differences between treated leukemic cells compared to normal mononuclear leukocytes in cell density, interferon- $\gamma$  and immunophenotypic profile, mainly CD4, CD8 and CD25. This work highlights the possibility of using curcumin and taurine as a potential useful therapy in the management of patients suffering from chronic and acute myeloid leukemias.

**Keywords:** Acute myeloid leukemia (AML); Chronic myeloid leukemia (CML); Curcumin-taurine; Immunophenotypic profile.

#### 1616. Urinary High Molecular Weight Matrix Metalloproteinases as Non-Invasive Biomarker for Detection of Bladder Cancer

Mohammed A. Mohammed, Manar F. Seleim, Mohga S. Abdalla, Hayat M. Sharada and Abdel Hady A. Abdel Wahab

*Bmc Urology*, 13: 25-32 (2013) IF: 1.694

**Background:** Matrix Metalloproteinases (MMPs) are key molecules for tumor growth, invasion and metastasis. Over-expression of different MMPs in tumor tissues can disturb the homeostasis and increase the level of various body fluids. Many MMPs including high molecular weights (HMWs) were detected in the urine of prostate and bladder cancer patients. Our aim here is to assess the usefulness of HMW MMPs as non invasive biomarkers in bilharzial bladder cancer in Egyptian patients.

**Methods:** The activity of different MMPs including HMW species was determined using zymographic analysis technique in the urine samples procured from sixty six bladder cancer patients (bilharzial and non-bilharzial) as well as hundred healthy control subjects. Also, the correlation between these HMW MMPs activities and different clinico-pathological parameters was investigated.

**Results:** High frequency of urine MMPs (uMMPs) activity was determined in 63.6% of examined tumor cases, however, none of the control cases showed any uMMPs activity. MMP-9 had the highest activity (62%) followed by MMP-9/NGAL (60%), MMP-2 (54.5%), MMP-9 dimer (53%), ADAMTS (25.6%), and the lowest one was MMP-9/TIMP-1 (12%) only. There was no correlation between uMMPs and any of clinico-pathological parameters including age, gender, tumor size and type, bilharziasis, grade, lymph node involvement, and invasion to the prostate. A significant correlation was established only between MMP-9/TIMP-1 activities with the tumor size.

**Conclusions:** This study revealed that the detection of urinary MMPs including HMWs activity might be sensitive biomarkers for prediction of bladder cancer. It is also demonstrated that the detection of these urinary HMW gelatinases could not differentiate between bilharzial and non bilharzial bladder cancer subtypes.

**Keywords:** Bladder cancer; High molecular weight matrix metalloproteinases; Early detection; Biomarkers.

#### 1617. Resveratrol Inhibits Proliferation, Angiogenesis and Induces Apoptosis in Colon Cancer Cells: Calorie Restriction Is the Force to the Cytotoxicity

M. A. Fouad, A. M. Agha, M. M. Al Merzabani and S. A. Shouman

*Human and Experimental Toxicology*, 32: 1067-1080 (2013) IF: 1.453

The aim of this study was to examine the antitumor activity of resveratrol in human colorectal cancer cell lines (HCT116 and Caco2) and to explore its mechanism of action assuming that it is by calorie-restriction effect. Resveratrol inhibited the proliferation of colon cancer cells with half maximal inhibitory concentration (IC<sub>50</sub>) equal to 50 and 130  $\mu$ M for HCT116 and Caco2, respectively. Caco2 cells appeared with significant time-dependent increase in the glycolytic pathway, a behaviour that was absent in HCT116 cells. Resveratrol (100  $\mu$ M) significantly decreased the glycolytic enzymes (pyruvate kinase and lactate dehydrogenase)

in Caco2 cells, while an increase in citrate synthase activity and a decrease in glucose consumption were observed in both cell lines. Moreover, resveratrol downregulated the expressions of leptin and c-Myc, and decreased the content of vascular endothelial growth factor. The apoptotic markers, caspases 3 and 8, were activated and the Bax/Bcl2 ratio was increased. The study suggested a promising anticancer activity of resveratrol, calorie restriction pathway may be one of the driving forces for this activity.

**Keywords:** Resveratrol; Colorectal carcinoma; Calorie restriction; Apoptosis; Angiogenesis.

### 1618. Serum Talin-1 is a Potential Novel Biomarker For Diagnosis of Hepatocellular Carcinoma in Egyptian Patients

Mahmoud M. Youns, Abdel Hady A. Abdel Wahab, Zeinab A. Hassan and Mohamed S. Attia

*Asian Pacific Journal of Cancer Prevention, 14: 3819-3823 (2013) IF: 1.271*

**Background:** Hepatocellular carcinoma (HCC) is a major cause of cancer mortality worldwide. The outcome of HCC depends mainly on its early diagnosis. To date, the performance of traditional biomarkers is unsatisfactory. Talins were firstly identified as cytoplasmic protein partners of integrins but Talin-1 appears to play a crucial role in cancer formation and progression. Our study was conducted to assess the diagnostic value of serum Talin-1 (TLN1) compared to the most feasible traditional biomarker alpha-fetoprotein (AFP) for the diagnosis of HCC.

**Methods:** TLN1 was detected using enzyme linked immunosorbent assay (ELISA) in serum samples from 120 Egyptian subjects including 40 with HCC, 40 with liver cirrhosis (LC) and 40 healthy controls (HC).

**Results:** ROC curve analysis was used to create a predictive model for TLN1 relative to AFP in HCC diagnosis. Serum levels of TLN1 in hepatocellular carcinoma patients were significantly higher compared to the other groups ( $p < 0.0001$ ). The diagnostic accuracy of TLN1 was higher than that of AFP regarding sensitivity, specificity, positive predictive value and negative predictive value in diagnosis of HCC.

**Conclusions:** The present study showed for the first time that Talin-1 (TLN1) is a potential diagnostic marker for HCC, with a higher sensitivity and specificity compared to the traditional biomarker AFP.

**Keywords:** Hepatocellular carcinoma; Talin-1; Alpha; Fetoprotein; Liver cirrhosis; Marker.

### 1619. Evaluation of Vascular Endothelial Growth Factor (VEGF) Levels and Survival Among Triple-Negative Breast Cancer (TNBC) and Non-TNBC Cases

Mohamed A. El-Hefny, Arif M. Afandiyev, Sevil Karimova and Tarek Dardeer

*International Journal of Advanced Scientific and Technical Research, 6: 22-36 (2013)*

**Background:** Triple-negative breast cancer (TNBC) is characterized by early relapses, poor outcome, and having chemotherapy as the only therapeutic option. This study aims to determine the incidence of triple negative breast cancer in Azeri

women, to compare the serum levels of the vascular endothelial growth factor (VEGF), survival and clinical behavior in triple negative breast cancer patients (TNBC) with non-TNBC, and to find an optimal threshold discriminating non-TNBC from TNBC patients. **Methods:** Serum VEGF levels and survival were determined for 180 patients who received adjuvant chemotherapy at the New Oncology Center- Azerbaijan Medical University from 2005 to 2010. **Results:** Twenty seven patients (15%) were classified as TNBC, they had VEGF mean value of 890.63 pg/mL while non-TNBC had mean VEGF of 410.62 pg/mL, and the difference was highly significant ( $p < 0.001$ ). In addition, there were significant differences between patients with TNBC and non-TNBC in the overall survival (OS) (22 vs. 53 months), the time to death after chemotherapy (20 vs. 47 months), time from diagnosis to first relapse (17 vs. 31.5 months), and the time between first relapse and death (8.0 months vs. 17.0 months),  $p < 0.001$ . From ROC curve analysis, we found that 665 pg/mL was an optimal threshold discriminating non-TNBC from TNBC patients with sensitivity and specificity of 88.9% and 99.3%, respectively. **Conclusion:** The incidence of TNBC in present study was 15%. TNBC patient had higher serum VEGF levels and shorter survival compared with non-TNBC. The optimal cut-off value of VEGF was 665 ng/mL that might discriminate non-TNBC from TNBC patients.

**Keywords:** Vascular endothelial growth factor (VEGF); Survival; Triple-negative; Breast cancer.

### 1620. Ex Vivo Assessment of the Protective Effect of Curcumin and Taurine Against Human Hepatocarcinogenesis

Sherif H. Abdeen, Motawa E. EL-Houseini, Mamdouh EL-Sherbiny, Reda Tabashy and Amany Salah

*The Journal of Basic and Applied Zoology, 66: 180-187 (2013)*

Hepatocellular carcinoma (HCC) is the fifth most common malignant tumor all over the world. Although several treatments such as tumor resection and liver transplantation are used to treat HCC, there is no overall long-term survival benefit. Therefore, the need for therapy to prevent the recurrence of HCC is essential. Curcumin and taurine have been used to participate in cancer management such as HCC through activation of immune system. Mononuclear leukocytes (MNLs) obtained from cirrhotic patients ( $n = 25$ ), HCC patients ( $n = 25$ ) and healthy volunteers ( $n = 25$ ) were included in this study. Cell density and percentage of CD4<sup>+</sup>, CD8<sup>+</sup>, and CD25<sup>+</sup> of the MNLs treated with curcumin and taurine were performed in addition to IFN- $\gamma$  level determined in their cultured media. The results revealed that there was a highly significant increase in MNLs' density of cirrhotic patients treated with curcumin and taurine. Where in HCC patients there were high significant increases in MNLs treated with curcumin and/or taurine. IFN- $\gamma$  level showed no significant increase in HCC, cirrhotic patients and controls. There were high significant increases in percentage of CD8<sup>+</sup> of cirrhotic and HCC patients treated with curcumin and combination of curcumin and taurine. But, percentage of CD4<sup>+</sup> showed a high significant decrease in cirrhotic and HCC patients due to treatment with curcumin and/or taurine, on the contrary there were high significant increases in controls. Furthermore, there were high significant increases in percentage of CD25<sup>+</sup> of cirrhotic patients and healthy controls treated with curcumin and/or taurine, but HCC patients showed no significant increase in percentage of CD25<sup>+</sup> in MNLs treated with curcumin and/or taurine.

**Keywords:** Cirrhosis; Curcumin; Hepatocellular carcinoma Immunophenotypic profile; Interferon-gamma; Taurine.

### 1621. Phytochemical Investigation and Molecular Profiling By P21 and Nf- $\kappa$ B of Chorisia crispiflora Hexane Extract in Human Breast Cancer Cells in Vitro

Samar S. Azab, Abeer M. Ashmawy and Omayma A. Eldahshan

*British Journal of Pharmaceutical Research, 1: 78-89 (2013)*

**Aims:** The current study targets two main aims; 1st aim is the phytochemical investigation of the hexane extract of *Chorisia crispiflora* leaves. The 2nd aim is the evaluation of the invitro cytotoxic activity of the extract then examination of the molecular mechanisms underlying this cytotoxic effect.

**Study Design:** Isolation and identification of the compounds, cytotoxic activity investigation on breast cancer cell line and molecular mechanisms underlying the cytotoxic extract of *Chorisia crispiflora* which may interfere with several cell signaling pathways and insert anti-cancer effects through the suppression of NF- $\kappa$ B or activation of p21, on breast cancer cell lines MCF-7.

**Place and Duration of Study:** Faculty of Pharmacy, Ain Shams University and National Cancer Institute, Cairo University, Egypt. The study was completed within 10 months.

**Methodology:** n-hexane extract was tested against breast cancer cell line then investigated for its effect on NF- $\kappa$ B, p21 and DNA fragmentation. The compounds isolated were identified using different spectroscopic techniques.

**Results:** In this regard, three main compounds were isolated;  $\beta$ -sitosterol 1,  $\beta$ -sitosterol 3- glucoside 2 and stigmasterol 3- glucoside 3. The extract exhibited IC<sub>50</sub> values of 7 and 4.2  $\mu$ g/ml following 48 and 72 hrs of treatment; indicating its significant in-vitro cytotoxic activity. This cytotoxic activity was proven to be mediated through down regulation of NF- $\kappa$ B.

**Conclusion:** Our results suggest that n-hexane extract has potent cytotoxic effect on MCF7 cells in addition to down regulation of NF- $\kappa$ B. These findings consequently merit further exploration of the extract in subsequent in-vivo studies and later in controlled clinical trials.

**Keywords:** *Chorisia crispiflora*; Phytosterols; MCF7; NF- $\kappa$ B.

### Dept. of Tumor Pathology

### 1622. Role of Thyroid Transcription Factor-1 and P63 Immunocytochemistry in Cytologic Typing of Non-Small Cell Lung Carcinomas

Eman Abu Sinna, Noha Ezzat and Ghada M. Sherif

*Journal of the Egyptian National Cancer Institute, 25(4): 209-218 (2013) IF: 2*

**Purpose:** Evaluation of the value of thyroid transcription factor (TTF-1) and P63 in subtyping of non-small cell lung cancer in cytologic material.

**Patients and methods:** This is a retrospective study including 40 cases of primary lung lesions who underwent image guided FNAC from pulmonary nodules. The final histopathologic diagnosis was the gold standard. Cell blocks were stained with anti-TTF-1, and P63. Nuclear immunoreactivity for both markers was considered specific. Sensitivity, specificity, positive and

negative predictive values, of the cytologic diagnosis and of the two markers, as well as the accuracy of the combined markers were calculated.

**Results:** Cytomorphology achieved a sensitivity of 83.3%, specificity of 91%, PPV of 91%, and NPV of 83.3%, for the diagnosis of AC, and 91% sensitivity, 83.3% specificity, 83.3% PPV, and 91% NPV, for the diagnosis of SCC. The concordance between cytologic and histopathologic diagnoses of AC and SCC was 87%. TTF-1 achieved 87.5% sensitivity, 94.7% specificity, 95.5% PPV, and 85.7% NPV for AC, while P63 achieved 94.7% sensitivity, 95.8% specificity, 94.7% PPV, and 95.8% NPV for SCC. TTF-1 enhanced the sensitivity of cytomorphology for AC from 83.3% to 87.5%, and specificity from 91% to 94.7%. Similarly P63 enhanced the sensitivity for SCC from 91% to 94.7%, and specificity from 83.3% to 95.8%.

**Conclusion:** TTF-1 achieved moderate sensitivity, and high specificity in the diagnosis of AC, while P63 was highly sensitive and specific for the diagnosis of SCC. Immunocytochemistry raised the sensitivity and specificity of FNAC in diagnosing AC and SCC using TTF-1 and P63, respectively.

**Keywords:** FNAC; NSCLC; ICC; TTF-1; P63.

### 1623. Prognosis, Treatment, And Pathological Characteristics of Metaplastic Breast Carcinoma: the Experience from the Egyptian National Cancer Institute

Samy Elbadawya, Iman Goudab, HebatAllah M. Shaaban, Gerges Attiaa and Maha Eltahera

*Egyptian Journal of Pathology, (2013)*

**Background** Metaplastic breast carcinoma (MBC) comprises a histologically diverse group of malignancies that seem to have characteristics different from those of invasive duct carcinoma. The objective of this study was to describe the clinicopathological appearance of MBC and the prognostic outcome of patients with this disease in order to establish proper management.

**Methods:** A total of 38 patients were diagnosed with MBC between 1998 and 2009, at National Cancer Institute, Egypt. Patient medical records were revised, and the overall survival and disease-free survival were estimated. Tissue samples from 30 of these 38 patients were available, and immunostaining for estrogen receptor and progesterone receptor, epidermal growth factor receptor (EGFR), and Her2/neu was performed for all samples.

**Results:** The most common subtype was carcinosarcoma, of which grade III was reported in 20 patients. Immunohistochemically, all patients were negative for estrogen receptor and progesterone receptor, three were positive for Her2/neu overexpression, and 53.3% were positive for EGFR. Adjuvant chemotherapy was used in 31 patients and adjuvant radiotherapy in 25 patients. The mean follow-up was 32 months (5–59 months). Seventeen patients (44.7%) failed therapy, and nine of them died of disease. Locoregional failure was reported in three patients, distant failure in 10, and both were reported in four patients. The 4-year overall survival was  $59 \pm 13\%$ , and the disease-free survival was  $37 \pm 12\%$ .

**Conclusion:** MBC is a rare entity among cases of breast carcinomas in Egypt. The diagnosis is difficult in some cases and requires rigorous use of immunohistochemistry. Most patients present with poor prognostic indicators. A multicenter approach for large-scale studies is recommended to analyze the tendency for

EGFR expression in MBC. These findings have potential implications for the design of clinical trials involving.

**Keywords:** Disease-free survival; Epidermal growth factor receptor; Metaplastic breast carcinoma; Overall survival.

#### 1624. The Role of Arginase-1 and Glypican-3 in Differentiating Hepatocellular Carcinoma from Metastatic Carcinoma in Fine-Needle Aspiration Cytology

Neveen Tahoun and Noha Ezzat

*Egyptian Journal of Pathology*, 33(2): 157-164 (2013)

**Purpose :** The aim of the study was to evaluate the role of the novel marker arginase-1 in differentiating hepatocellular carcinoma (HCC) from metastatic adenocarcinoma and compare the results with those for glypican-3. Patients and methods This is a retrospective study including 124 cases with liver masses referred from the Radiology Department to the Cytology Unit, Pathology Department, NCI. The pathological diagnosis and/or radiological picture were the gold standard. From each cell block two slides were stained with anti-arginase-1 and glypican-3. Sensitivity, specificity, positive and negative predictive values, percentage of marker expression as well as intensity and distribution of both markers among different grades were evaluated, and comparison of these items between the two markers was made. Results The sensitivity and specificity of arginase-1 were 96.1 and 95.7%, respectively, and those for glypican-3 were 90.9 and 91.5%, respectively. Arginase-1 was expressed in 36 (97.3%) moderately differentiated and 30 (93.8%) poorly differentiated HCC cases, whereas glypican-3 expression was detected in 34 (91.9%) moderately and 28 (87.5%) poorly differentiated HCCs, respectively. All cases of well-differentiated HCC showed strong and diffuse staining for arginase-1, compared with seven (87.5%) cases for glypican-3. In the moderately.

**Keywords:** Arginase-1; Fine-needle aspiration cytology; Glypican-3; Hepatocellular carcinoma; ICC.

#### 1625. The Role of Fine-Needle Aspiration Cytology and Ultrasound Elastography in Predicting Malignancy in Thyroid Nodules

Nesreen H. Hafez, Neveen S. Tahoun and Omnia Mokhtar

*Egyptian Journal Of Pathology*, (2013)

**Background :** It is crucial to have a clear diagnostic approach to ensure patients presenting with thyroid nodules are managed appropriately. Fine-needle aspiration cytology (FNAC) is the best preoperative test used for differentiating malignant from benign nodules. Cytology has certain limitations that restrict its use as a single diagnostic test. Ultrasound elastography (USE) is a newly developed technique that uses ultrasound to provide an estimation of tissue stiffness under application of external force. The aim of this study was to assess whether USE improves the accuracy of FNAC in predicting malignancy in thyroid nodules.

**Patients and methods:** This prospective study included 96 patients with a solitary thyroid nodule or dominant nodule in the setting of multinodular goiter from January 2011 to July 2012. They were examined using USE at the Radiology Department, National cancer Institute, Cairo University. Tissue stiffness was scored from 1 (low stiffness over the entire nodule) to 5 (high

stiffness over the entire nodule and surrounding tissue). All patients were referred for FNAC at the Cytology Unit, Pathology Department. Cytological specimens were evaluated blindly (without knowing the scores of USE) and classified according to the recent Bethesda classification. All the studied patients underwent surgery and were evaluated for the final histopathological diagnoses.

**Results:** On FNAC, 46 of 61 cases (75.4%) with a final histopathological diagnosis of benign nodule had a negative diagnosis, whereas 34 of 35 cases (97.1%) with a final histopathological diagnosis of carcinoma had a positive diagnosis ( $P < 0.005$ ), with a sensitivity of 97.1%, a specificity of 75.4%, a positive predictive value (PPV) of 69.4%, a negative predictive value (NPV) of 97.9%, and diagnostic accuracy of 83.3%. On real-time USE, 57 of 61 benign nodules had a score of 1 or 2, whereas all malignant nodules had a score of 3–5 ( $P < 0.0001$ ), with a sensitivity of 100%, specificity of 93.4%, PPV of 89.7%, NPV of 100%, and diagnostic accuracy of 95.8%. In the 18 nodules with a cytological report of follicular neoplasm, USE was efficient in differentiating benign from malignant nodules ( $P < 0.0005$ ).

**Conclusion:** USE is a promising imaging technique that can assist in the differential diagnosis of thyroid nodules with higher sensitivity, specificity, PPV, NPV, and diagnostic accuracy compared with FNAC. Therefore, it may be useful to introduce it into the routine clinical practice in association with FNAC.

#### 1626. Value of Image-Guided Fine-Needle Aspiration Cytology in the Diagnosis of Bone Lesions

Ayman M. Metwally, Lobna A. Refaat, HebatAllah Shaaban, Somaia Megm, Mohamed Emara, Amany A. Tohamy, Eman Abou Sinna, Hussein Khaled

*Egyptian Journal Of Pathology*, 25 : 193-198 (2013)

**Purpose:** The objective of our study was to determine the relevance of cyclins A and E overexpression in endometrial carcinogenesis in hormone receptor-positive breast cancer patients under tamoxifen therapy.

**Experimental design:** We assessed expression of cyclins A and E in Endometrial cytology samples collected from 36 ER and PR positive breast cancer patients; under tamoxifen treatment by using the Tao-brush non-invasive brushing cytology technique. Cyclins were detected in the collected samples by means of immuno-cytochemistry. The patients included in this study are a cohort of 36 breast cancer patients who were operated upon at the National Cancer Institute Cairo University in the period from February 2006 to May 2008 and received tamoxifen (TAM) as part of their adjuvant treatment.

**Results:** Cyclins A and E were expressed in 17 and 15 of the 36 collected endometrial cytology samples (47.2% and 41.6% respectively). Expression of cyclins A and E was highly correlated to Tamoxifen exposure duration (32 and 43 months respectively)  $p < 0.001$ . Tamoxifen median exposure duration was shortened to 21 months in cases showing positivity for either markers, while in cases showing positivity for both cyclins, the median exposure duration was longer (44.5 months) ( $p < 0.001$ ). Neither cyclin A nor E was detected before median tamoxifen exposure duration of 11 months. Endometrial carcinoma cases had the longest Tamoxifen exposure duration (60 months).

**Conclusion:** Cyclins A and E expression is involved in the carcinogenesis of endometrium in women with breast cancer and under tamoxifen-treatment. Follow up of the patients using these 2 markers is highly recommended starting from the 12th month.



## Faculty of Physical Therapy

*Dept. of Physical Therapy for Neuromuscular Disorder*

### 1627. Comparison Between Trans-Cranial Electromagnetic Stimulation and Low-Level Laser On Modulation of Trigeminal Neuralgia

Yasser Ibrahim Seada, Reda Nofel and Hayam Mahmoud Sayed

*Journal of Physical Therapy Science*, 25 (8): 911-914 (2013)

IF: 0.175

**Purpose:** To determine which of the transcranial electromagnetic stimulation or low level laser therapy is more effective in the treatment of trigeminal neuralgia of multiple sclerosis patients.

**Methods:** Thirty multiple sclerosis patients of both sexes participated in this study. The age of the subjects ranged from 40 to 60 years and their mean age was (56.4–6.6). Participants were randomly selected from Dental and Neurology Outpatient Clinics at King Khalid Hospital, Najran University, Saudi Arabia. Patients were randomly divided into two equal groups of 15. The Laser group received a low level laser therapy, 830 nm wavelength, 10 Hz and 15 min duration, while the Electromagnetic group received repetitive transcranial electromagnetic stimulation at a frequency of 10 Hz, intensity of 50 mA and duration of 20 minutes. Patients were assessed pre and post treatment for degree of pain using a numerical rating scale, maximal oral mouth opening using a digital calibrated caliper, masseter muscle tension using a tensiometer and a compound action potentials of masseter and temporalis muscles. [Results] There were significant improvements after treatment in both groups, with a significant difference between the Electromagnetic and Laser groups, in favor of the Electromagnetic group. **Conclusion:** Repetitive transcranial electromagnetic stimulation at 10 Hz, 50 mA, and 20 minutes duration is more effective than low level laser therapy at reducing trigeminal pain, increasing maximum oral mouth opening, masseter and temporalis muscle tension in multiple sclerosis patients.

**Keywords:** Trigeminal neuralgia; Low level laser; Trans-cranial electromagnetic stimulation.

### 1628. Effect of Different Physical Therapy Modalities on Post-Operative Recovery Following Transverse Carpal Ligament Release: A Randomized Controlled Trial

Salah A. Sawan, Hayam M. Sayed Mahmoud and Maha M. Hussien

*Physiotherapy Practice and Research*, 34 (2): 75-82 (2013)

**Objective:** To compare between selected post-operatives physical therapy modalities after transverse carpal ligament release. **DESIGN:** Double blind, randomized controlled trial.

**Setting:** Health insurance hospital outpatient clinic in Cairo, Egypt **Subjects:** Forty-five female patients aged 25–45 years, following transverse carpal ligament release of the dominant hand, referred to the physical therapy outpatient clinic of a health insurance hospital, Egypt.

**Intervention:** Patients were randomly allocated to three equal groups of 15: Ultrasonic group received continuous ultrasound with nerve and tendon gliding exercises, Laser group received laser therapy and the same exercises, Exercise group received the

same exercises only. Treatment duration was six weeks, three times per week.

**Main Measure:** Visual analogue scale for pain intensity, pinch dynamometer for muscle strength, motor and sensory distal latencies for median nerve.

**Results:** There was significant improvement after treatment in all groups, with no significant difference between the Ultrasonic group and the Laser group; there was a highly significant difference between the Ultrasonic group and the Exercise group, and a significant difference between the Laser group and the Exercise group.

**Conclusion:** Continuous ultrasound accompanied with nerve and tendon gliding exercises is considered more effective in the post-operative treatment of transverse carpal ligament release, giving best results and percentage of improvements when compared either to Laser therapy with nerve and tendon gliding exercises or nerve and tendon gliding exercises only.

**Keywords:** Carpal tunnel syndrome; Laser therapy; Continuous ultrasound; Nerve gliding; Tendon exercise.

### 1629. Impact of Exercise Program on Functional Status among Pos T- Lumbar Laminectomy Patients

Labiba Abd kader Mohamed, Lamia Mohamed N. Ismail, Khairia Abo Bakr Elsawi and Salah Abd El-Monem Sawan

*Journal of Biology Agriculture and Healthcare*, 3 (10): 62-72 (2013)

A laminectomy is a surgical incision performed to remove herniated intervertebral discs. Strengthening and stretching exercise program helps post-laminectomy patients to move and do routine activities without putting extra strain on their backs, relieve their pain leading to improvement of functional status. **Aim:** to evaluate the impact of exercise program on functional status among post-lumbar laminectomy patients'. **Design:** quasi-experimental design.

**Setting:** This study was conducted at the neurosurgery department of El-Manial University Hospital, Cairo.

**Sample:** A purposive sample of 30 male and female adult patients undergoing lumbar laminectomy was recruited in this study.

**Tools:** data were collected utilizing the following tools: 1) The Structured Interview Questionnaire, including socio-demographic and related medical data. 2) Physical Assessment Sheet, and 3) Oswestry Low Back Pain Disability Questionnaire.

**Results:** the study findings revealed that the majority of study subjects were males, married and have normal musculoskeletal posture.

All participants had severe low back pain and high level of functional disabilities preoperatively. A significant difference in pain intensity and functional ability was evident between the preoperative period and six weeks postoperatively after implementing the exercise program. **Recommendations:** A written hospital clinical guideline on the common causes and safe post-laminectomy exercises is recommended to be established. Replication of this study on a larger sample and in different hospital settings with increasing the duration of implementing the postoperative exercise program treatment.

**Keywords:** Exercise program; Functional status; Lumbar laminectomy.

**Dept. of Physical Therapy for Basic Science**

**1630. Extension Traction Treatment for Patients with Discogenic Lumbosacral Radiculopathy: A Randomized Controlled Trial**

Ibrahim M Moustafa and Aliaa A Diab

*Clinical Rehabilitation*, 27 (1): 51-62 (2013) IF: 2.191

**Objective:** To investigate the effects of lumbar extension traction in patients with unilateral lumbosacral radiculopathy due to L5-S1 disc herniation. **Design:** A randomized controlled study with six-month follow-up. **Setting:** University research laboratory. **Subjects:** Sixty-four patients with confirmed unilateral lumbosacral radiculopathy due to L5-S1 disc herniation and a lumbar lordotic angle less than 39°, randomly assigned to traction or control group. **Interventions:** The control group (n = 32) received hot packs and interferential therapy, whereas the traction group (n = 32) received lumbar extension traction in addition to hot packs and interferential therapy.

**Main Outcome Measures:** Absolute rotatory angle, back and leg pain rating scale, Oswestry Disability Index, Modified Schober test, H-reflex (latency and amplitude) and intervertebral movements were measured for all patients three times (before treatment, after 10 weeks of treatment and at six-month follow-up).

**Results:** There was a significant difference between the traction group and the control group adjusted to baseline values at 10 weeks post treatment with respect to: absolute rotatory angle ( $P < 0.001$ ), Oswestry Disability Index ( $P = 0.002$ ), back and leg pain ( $P = 0.009$ ,  $P = 0.005$ ), Modified Schober test ( $P = 0.002$ ), latency and amplitude of H-reflex ( $P = 0.01$ ,  $P < 0.001$ ), intervertebral movements ( $P < 0.05$ ). At six-month follow-up there were statistically significant differences between the study and control groups for all the previous variables ( $P < 0.05$ ).

**Conclusion:** The traction group receiving lumbar extension traction in addition to hot packs and interferential therapy had better effects than the control group with regard to pain, disability, H-reflex parameters and segmental intervertebral movements

**Keywords:** Assessment; Lumbar radiculopathy; Randomized controlled trial; Rehabilitation; Traction.

**1631. The Efficacy of Lumbar Extension Traction for Sagittal Alignment in Mechanical Low Back Pain: A Randomized Trial**

Aliaa Attiah Mohamed Diab and Ibrahim Moustafa Moustafa

*Journal of Back Musculoskeletal Rehabilitation*, 26 (2): 312-320 (2013) IF: 0.613

**Background:** There is growing interest in the role of abnormal asymmetrical posture, which is considered one of the most important etiological factors reported to be associated with mechanical low back pain.

**Objective:** This study was conducted to investigate the effect of lumbar extension traction on the pain, function and whole spine sagittal balance as represented in lumbar curvature, thoracic curvature, C7 plumb line, and sacral slope.

**Methods:** Eighty patients with chronic mechanical low back pain (CMLBP) and definite hypolordosis were randomly assigned to traction or a control group. The control group (n=40) received

stretching exercises and infrared radiation, whereas the traction group (n=40) received lumbar extension traction in addition to stretching exercises and infrared radiation three times a week for 10 weeks. Back pain rating scale, Oswestry Disability Index, and radiological spine sagittal balance parameters in terms of lumbar lordosis, thoracic kyphosis, sacral slope, and positioning of C7 plumb line were measured for all patients at three intervals (before treatment, after 10 weeks of treatment, and at six months follow-up). **Results:** There was a significant difference between the traction and control groups adjusted to baseline value of outcome at 10 weeks post treatment with respect to lumbar lordotic curve ( $P=0.000$ ), thoracic kyphosis ( $P=0.013$ ), sacral slope ( $P=0.001$ ), C7 plumb line distance ( $p=0.001$ ), while there was no significant difference with respect to pain ( $p=0.29$ ) and Oswestry Disability Index (ODI) ( $p=0.1$ ). At 6-months follow-up, there were significant differences between both groups for all the previous variables ( $p < 0.05$ ). **Conclusion:** Lumbar extension traction in addition to stretching exercises and infrared radiation improved the spine sagittal balance parameters and decreased the pain and disability in CMLBP.

**Keywords:** Traction; Mechanical low back pain; Randomized controlled trial.

**Dept. of Physical Therapy of Surgery**

**1632. Effect of Pulsed Nd:YAG Laser in the Treatment of Neuropathic Foot Ulcers in Children with Spina Bifida: A Randomized Controlled Study**

Anwar Abdelgayed Ebid, Ehab Mohamed Abd El-Kafy and Mohamed Salaheldien M. Alayatt

*Photomedicine and Laser Surgery*, 31 (12): 565-570 (2013) IF: 1.634

**Objective:** This study assessed the effects of pulsed Nd:YAG laser treatment of neuropathic foot ulcers in children with spina bifida. Background data: Children with spina bifida face increased risk for developing neuropathic foot ulcers.

**Methods:** In a randomized controlled trial, 39 children and adolescents (ages 6–15 years) with spina bifida and stage III neuropathic foot ulcers were randomly assigned to the laser group or the placebo laser group.

The former received pulsed Nd:YAG laser treatments (i.e., total energy of 300–350 J during three sessions/week) plus standard wound care, and the latter received sham laser treatments plus standard wound care. Wound size and wound appearance were assessed for all patients at the beginning of the treatment, after 5 weeks, and after 10 weeks.

**Results:** The decrease in wound surface area at 5 and 10 weeks post-treatment was significantly greater in the laser group (i.e.,  $2.44 \pm 0.33$  and  $0.29 \pm 0.25$  cm<sup>2</sup>, respectively) than in the placebo group (i.e.,  $3.81 \pm 0.18$  and  $3.24 \pm 0.44$  cm<sup>2</sup>, respectively). Also, the decrease in the total score for the Pressure Sore Status Tool (PSST) at 5 and 10 weeks post-treatment was significantly different for the laser group (i.e.,  $32.76 \pm 2.30$  and  $17.52 \pm 1.66$ , respectively) than for the placebo group (i.e.,  $46.50 \pm 2.12$  and  $38.11 \pm 3.17$ , respectively).

**Conclusions:** Treatment with pulsed neodymium:yttrium aluminum garnet (Nd:YAG) laser combined with standard wound care decreases wound size and improves wound appearance for stage III neuropathic foot ulcers in children with spina bifida.

**Keywords:** Pulsed high intensity laser; Neuropathic foot ulcer; Wound healing.

### 1633. Effect of Neuromuscular Electrical Stimulation on Abdominal Muscle Strength and Pulmonary Function after Major Abdominal Surgery: A Randomized Controlled Trial

Anwar Abdelgayed Ebid, Ashraf Abdelaal Mohamed and Amira Hussin Draz

*Jokull Journal*, 63 (6): 320-338 (2013) IF: 1

**Objective:** To investigate the effects of 12-weeks neuromuscular electrical stimulation (NMES) program on abdominal muscle strength, abdominal and waist circumference and selected pulmonary function after major abdominal surgery. **Design:** Randomized controlled trial.

**Material and Methods:** Forty five patients participated in the study and were randomized into NMES group and placebo NMES group. NMES group received 12- weeks NMES program 5 times per week 20-45 minutes per session and placebo NMES group received placebo NMES five times per week.

**Main measures:** Isometric abdominal muscle strength, abdominal circumference, waist circumference, forced vital capacity (FVC) and forced expiratory volume in one second (FEV1) were measured at baseline, one month after surgery (midpoint) and after 12-weeks. **Results:** Patients in the NMES group showed a significant improvement as compared with those in the placebo NMES group. Abdominal strength and percentage of improvement after 12-weeks were  $94.47 \pm 1.62$  Nm (73.02%) for NMES group and  $58.04 \pm 2.14$  Nm (4.57 %) for the placebo NMES group. Abdominal and waist circumference and percentage of improvement were  $94.60 \pm 2.12$  cm (4.30%) and  $98.04 \pm 1.29$  cm (6.28%) for NMES group and  $98.13 \pm 1.75$  cm (1.00%) and  $103.64 \pm 1.13$  cm (0.73%) for the placebo NMES group. FVC and FEV1 and percentage of improvement for the NMES group was  $3.75 \pm 0.33$  liter (26.27 % and  $2.87 \pm 0.29$  liter (27.82%) and for the control group was  $3.25 \pm 0.27$  liter (10.9 %) and  $2.42 \pm 0.23$  liter (9.35%) respectively.

**Conclusions:** Participation in NMES program is effective for strength gain and improves pulmonary function in rehabilitation of post-surgical patients.

**Keywords:** Neuromuscular electrical stimulation; Abdominal muscle strength; Major surgery; Pulmonary function.

## Faculty of Nursing

### Dept. of Community Health Nursing

### 1634. Assessment of Factors that Hinder Early Detection of Breast Cancer among Females at Cairo University Hospital

Gehan M. Ismail, Azza A. Abd El Hamid and Amel G. Abd ElNaby

*World Applied Sciences Journal*, 23 (1): 99-108 (2013)

In Egypt, breast cancer ranks the first among cancer affecting females. The aim of this research was to assess factors that hinder early detection of breast cancer among females at Cairo University Hospital. A descriptive exploratory research design was adopted in this research. Females were selected from the surgical outpatient clinic and surgical inpatient wards at Cairo University Hospital. Sample of 120 females diagnosed as third

stage breast cancer. Tool for data collection was structured interview schedule developed by researchers. It included two parts; Part I: A) Sociodemographic characteristics; B) History of the sample and C) Knowledge about methods of breast cancer detection. Part II, factors that hinder early detection of breast cancer. Results revealed that, the most common factors that hinder early detection of breast cancer are; lack of awareness about breast cancer (79%), denying having breast cancer (72%) and financial problems (25%). Also, a statistically significance negative correlation was found between age of females and breast self- examination and mammogram, while, a statistically significant positive correlation was found between age of females and seeking medical help. Conclusion: delay in breast cancer diagnosis was influenced by interactions between many factors as lack of awareness about methods of early detection, financial problems, denial of having breast problems.

**Keywords:** Breast cancer; Females; Early detection.

### 1635. Assessment of Violence Among Primary School Children at Cairo Governorate

Hebe M. Share, Enass H. El-Shair and Gehan M. Ismail

*Middle-East Journal of Scientific Research*, 16 (2): 179-190 (2013)

At home, at school and in the community The aim of this research was to assess types of violence among primary school children at Cairo Governorate. A descriptive correlational design was adopted in this study. Three schools (two governmental and one experimental school) were selected randomly from south Cairo educational directorate. A samples of 216 students from 5th and 6th grade at the three schools were included in the study. Two tools were used to collect data pertinent to the study: 1) Structured interviewing questionnaire sheet to collect data about socio-demographic characteristics of the students as age, sex, gender, parental education, etc... 2) Violence assessment tool: it had 4 parts; a. School related violence, b. Physical abuse of students by their parents, c. Emotional abuse and negligence and d. Sexual abuse.

**Results:** revealed that, the most frequent type of violence was school-related violence, followed by physical abuse of students by their parents and the least type of violence found was emotional abuse. Regarding sexual abuse, it was found that (30%) of the students are exposed to some form of sexual abuse. A highly statistically significant difference was found between student's age and exposure to emotional and sexual abuse as well as school related violence. A statistically significant difference was found between number of family members and exposure to physical abuse by parents.

**Conclusion:** It was obvious from the results that violence and child abuse is a significant public health problem among th

**Keywords:** Violence; Primary school children; Parents

### 1636. Cerebrovascular Stroke Recurrence Among Critically Ill Patients at a Selected University Hospital in Egypt

Warda Youssef M. Morsy, Hanaa Ali Elfeky and Rasha Alsayed Ahmed

*Journal of Biology, Nagriculture and Healthcare*, 13: 22-33 (2013)

Cerebrovascular stroke (CVS) is a fatal disease. Literature review cited that, CVS recurrence is more devastating than the first attack. The risk of recurrent CVS is up to 15 times greater than the risk of CVS and is attributed to insufficient control of risk factors and non compliance with medical advice. So that, identification of risk factors of recurrence is an important role of the critical care nurses, plays an essential role in the prevention of further stroke.

**Aim:** to study the risk factors, frequency and severity of recurrent cerebrovascular stroke among adult critically ill patients admitted to intensive care units.

**Research questions:** Q1- What are the risk factors of recurrent cerebrovascular stroke among critically ill patients at a selected university hospital? Q2- What are the intervals of recurrence from the first attack of cerebrovascular stroke? Q3- What is the frequency of recurrent cerebrovascular stroke attacks among critically ill patients? Q4-What is the severity rate of recurrent cerebrovascular stroke among critically ill patients?. A descriptive exploratory research design was utilized in the current study. The study was conducted at different CVS intensive care units at a selected University Hospital. A sample of convenience including all adult patients admitted to the ICU with recurrent CVS over a period of six months (80 patients) was included. Three tools were used for data collection: socio-demographic and medical data sheet, CVS risks factors assessment sheet, and the National Institutes of Health Stroke Scale (NIHSS).

**Results:** The majority of the studied group admitted with the first recurrence of CVS, had different chronic illnesses such as hypertension (100%) & diabetes mellitus (95%). The duration of CVS recurrence ranged from two- < five years among 30% of the studied group. 36.25% of the studied group admitted with severe degree of CVS with a mean severity score of ( $X = 19.17 \pm SD = 1.255$ ).

**Conclusions:** uncontrollable risk factors (old age, male gender, marriage); life style risk factors (smoking, obesity, low income); chronic medical diseases (old CVS, hypertension, diabetes mellitus, ischemic heart disease, myocardial infarction, heart failure,... etc ); noncompliance with prescribed drugs of chronic illnesses, abnormal laboratory investigations (high cholesterol, triglyceride, low density lipoprotein) represented the common risk factors and contributed to recurrent cerebrovascular stroke with different severity.

**Keywords:** Cerebrovascular stroke; Recurrence; Critically Ill Patients; Risk factors; Severity.

### 1637. Factors Affecting Validity of Arterial Blood Gases Results Among Critically III Patients: Nursing Perspectives

Warda youssef, Ahmed Yahia, Nahla Shaaban Ali and Sameh Elhabashy

*Journal of Education and Practice, 4 (15) 47-56 (2013)*

Arterial blood gases sampling is one of the most common laboratory tests in intensive care units and might be corrupted by pre-analytical factors that influence the validity of results. Arterial blood gases are valuable only if obtained properly and measured carefully. Corrupted factors in arterial blood gas sampling change significantly the results and adversely affect patient-care decisions when the magnitude of the error is clinically important. Therefore the nurses' role is very important to control these factors. The aim of this study is to assess the different pre-

analytical factors affecting ABGs results' validity among critically ill patients at Cairo University Hospitals. The following research questions were formulated Q1: What do critical care nurses know about the different factors which can affect ABG results' validity?, Q2: What are the different practices performed by critical care nurses in relation to ABG results' validity? and Q3: What are the additional pre-analytical factors that might affect the ABG results?. A descriptive exploratory research design was utilized in this study. A sample of convenience of 68 bed side nurses were recruited from three intensive care units affiliated to Cairo University Hospitals which are; Surgical ICU, medical ICU, and Neurological ICU. Three tools were utilized to collect data; ABGs nurses' knowledge questionnaire that consists of two sections, the first section included Socio-demographic data and the second section constituted 17 questions that covered factors affecting ABGs' results, ABG withdrawal technique, and indications, and complications of sampling related questions. The second tool was ABGs observational checklist including arterial sampling practices through two main different methods; direct puncturing from radial or femoral sites and indirect puncturing from arterial line and finally assessment of pre-analytical factors that may affect validity of ABG results. Findings of the study showed that the all the studied subjects (100%) demonstrated unsatisfactory knowledge and practical level in relation to ABG sampling and controlling the different factors that might affect ABG results' validity. Moreover, There were no significant statistical difference between knowledge scores regarding educational level ( $F=2.73$ ;  $P=0.07$ ), working area ( $F=1.07$ ;  $P=0.34$ ), and gender ( $F=1.096$ ;  $P=0.29$ ) among the studied subjects. Results of the current study indicated a real gap between nurses' knowledge and practices as compared to the evidence based guidelines of American Association for Respiratory Care in management of ABG sampling. The current study recommends an enrichment of critical care nurses' knowledge and practices related to this essential procedure in addition to consideration of the different corrupting factors by hospital authorities to keep with the related evidence based guide lines that will be great benefits for patient, hospital, and all health professionals.

**Keywords:** Validity of arterial blood gases' results; Pre-analytical factors affecting.

### Dept. of Medical-Surgical Nursing

### 1638. Factors Predisposing to Organ (S) Dysfunction Among Critically

Fatma Abdelaziz Mohammed

*Advances in Life Science and Technology, 12: 22-32 (2013)*

Multiple organs dysfunction is one of the most challenging clinical problems in the intensive care units. It is one of the leading causes of morbidity and the main cause of mortality in critically ill patients. Therefore, requires efforts of of the health care team especially critical care nurses who are the healthcare providers and most closely involved in the daily care of critically ill patients. They have the opportunity to early detect and identify patients at risk for the development organs dysfunction.

**Aim of the study:** To identify factors predisposing to organ(s) dysfunction among critically ill adult patients at a selected university hospital. Research questions: Q1-What is the frequency of organ dysfunction among critically ill adult patients at a selected university hospital, in Egypt? Q2-What are diffrent

predisposing factors to organ dysfunction among critically ill adult patients at a selected university hospital, in Egypt?.

**Research design:** A descriptive/exploratory research design was utilized. **Sample:** A sample of convenience consisting of 110 adult male and female critically ill patients admitted to different intensive care units over a period of six months was included. **Tools of data collection:** Four tools were utilized for data collection: Sociodemographic and Medical data Sheet; Predisposing Factors to Organ (s) Dysfunction Assessment Sheet; Physical Assessment Sheet; and The Sequential Organ Failure Assessment score (SOFA).

**Results:** The current study revealed that: more than half (55.5%) of the studied sample had two organs dysfunction, of these (n=33/54.1%) were in age group from 58- < 68, with no significant statistical relationship between the age and frequency of organs dysfunction ( $\chi^2/P = 20.24/0.20$ ). Infection, heart failure, hypertension, and diabetes were the common predisposing factors to organ(s) dysfunction in percentages of 63.6%, 30.2%, & 22% respectively. Mild degree of organs dysfunction were most frequently noticed on admission, after 24 and 96 hours of admission to the ICU with mean SOFA scores of  $5.08 \pm 1.601$ ,  $4.87 \pm 1.86$ , &  $5.00 \pm 1.87$  respectively. The mean total and subtotal SOFA scores didn't differ significantly in different assessment times (F/ P= 1.29/0.35, 3.63/0.10, 2.69/0.72). The fate of the studied sample differed significantly in relation to the total mean SOFA scores ( $\chi^2 = 54.96$ ,  $p = 0.000$ ).

**Conclusion:** multi-organ(s) dysfunction was evident among critically ill patients. The most common predisposing factors were comorbidity diseases, infection on admission, after 48 and 96 hours of admission, having different types of shock, and trauma. So, identification and management of these predisposing factors may decrease the complication and improve patients' outcomes. **Recommendations:** Based on findings of the present study the following are recommended: strict application of universal precautions/infection control measures; prevention, and early detection of shock, sepsis, and so organ dysfunction; designing continuous practical educational programs about the application of the strict aseptic technique, the universal precautions and infection control for critical care nurses; Designing booklets and posters about early manifestation, predisposing factors, and importance of prevention of sepsis and organ dysfunction for critical care nurses; and utilization of SOFA scores in the management of patient with sepsis and organ dysfunction.

**Keywords:** Predisposing factors; Organ (S) dysfunction; Critically Ill patients; Sepsis; Sofa scores.

### 1639. Intensive Care Nurses' Knowledge and Practices Regarding Infection Control Standard Precautions at A Selected Egyptian Cancer Hospital

Hany Girgis Eskander, Warda Youssef M. Morsy and Hanaa Ali Ahmed Elfeky

*Journal of Education and Practice*, 4: 160-174 (2013)

Critical care nurses are the health care professionals who have the obligation to protect critically ill patients against infection especially those who are immune compromised, in order to enhance their recovery, prevent deterioration in their health, and achieve high quality nursing care. Therefore critical care nurses should have sound knowledge and strict adherence to infection control standard precautions.

**Aim of the study:** to assess nurses' knowledge and evaluate their practice regarding infection control standard precautions. **Research design:** A descriptive research design was utilized in this study. **Sample:** A sample of convenience including 77 ICU nurses was recruited in the current study. **Setting:** The study was carried out at the Intensive Care of a selected Cancer Hospital in Egypt.

**Tools of data collection:** Two tools were developed, tested for clarity and feasibility, and then used to collect data pertinent to the current: a- Structured Interview Questionnaire to assess nurses' knowledge regarding infection control standard precautions. b-Nurses' Performance Observational Checklist to evaluate nurses' practice/ utilization of infection control standard precautions.

**Results:** the current study revealed that, approximately two thirds (63.6%) of the studied sample had unsatisfactory knowledge level (<75%) with a mean total knowledge score of  $102.5 \pm 13.7$ . However, more than half (57.1%) of the studied sample had satisfactory performance level (>75%) with a mean total performance scores of  $77.3 \pm 4.4$ . Negative significant correlations were found between: mean knowledge scores, and age; mean knowledge scores and years of experience ( $r = -.323$  &  $r = -.325$  at  $P < 0.004$  respectively); between mean practice scores and age; and mean practice scores and years of experience ( $r = -.235$  &  $r = -.291$  at  $P < 0.39$ , 0.010 respectively). However, positive correlations were found between mean knowledge scores and mean practice scores; age and years of experience ( $r = 0.318$  &  $0.794$  at  $P < 0.005$  &  $0.000$  respectively).

**Conclusion:** Based on findings of the current study, it can be concluded that inspite of having satisfactory performance level regarding infection control standard precautions, critical care nurses had unsatisfactory knowledge level. **Recommendation:** updating knowledge and performance of ICU nurses through continuing in-service educational programs; emphasizing the importance of following the latest evidence-based practices of infection control in continuing education/ training programs; strict observation of nurses' performance/ utilization of infection control standard precautions and correction of poor practices by the infection control team are required; and providing training programs for newly joined ICU nurses about infection control standard precautions and at regular intervals.

**Keywords:** Infection control (IC); Standard precautions (SP); Intensive care unit (ICU); Knowledge; Practices.

### 1640. Nurses' Practices and Perception of Delirium in the Intensive Care Units of a Selected University Hospitals in Egypt

Hanaa Ali Elfeky and Fatma Shoeib Ali

*Journal of Education and Practice*, 19: 61-70 (2013)

Delirium is a common but frequently undetected complication in hospitalized critically ill patients leading to poor outcomes, prolonged hospital stays, and increased costs of care. Therefore, because of their daily contact with critically ill patients, critical care nurses are at the frontline of patients' care and are in a unique position to improve their outcomes through timely identification of individuals at risk, early detection of signs and symptoms of delirium, and providing the needed intervention.

**Aim of the study:** to assess critical care nurses' practices and perception of delirium among critically ill patients in different critical care settings. **Research Design:** A descriptive exploratory



research design was utilized in this study. **Research questions:** To achieve the aim of the present study, the following two research questions were formulated: 1-What is the current nurses' practice of delirium assessment in the critical care units 2- How critical care nurses perceive delirium among critically ill patients.

**Setting:** The study was carried out at different Critical Care Departments at Cairo University Hospitals, in Egypt. **Sample:** A sample of convenience including all nurses (120) working at different critical care departments was included in the current study. **Tools of data collection:** Two tools were used to collect data pertinent to the current study: **Socio demographic data sheet** (covers data such as gender, age, years of experience, attended staff development courses, working hours, etc.....); and Nursing practices and perceptions assessment sheet: was adopted from Devlin, et al., (2008). It covers data related to frequency of evaluating patients for level of sedation and presence of delirium; presence of delirium; frequency of using delirium assessment sheet; received education regarding ICU sedation assessment and ICU delirium assessment, and statements that pertain to delirium in the ICU.

**Results:** the current study revealed that inspite of having many years of experience in working with critically ill patients, all ICU nurses (100%) ranked delirium assessment as the fourth priority after level of conscious, pain assessment, handling agitation, and caring for devices. More than half of the studied nurses (54.2%) never assessed delirium, and 100% of nurses never received training about assessing and handling delirium.

**Conclusion:** delirium is an under diagnosed problem in the ICU; it is a common response to the ICU environment. It is challenging to be assessed among critically ill patients and represents a problem that requires active intervention on the part of caregivers. Recommendations: Incorporating cognitive assessment in general, and delirium assessment in particular into nursing education courses; Integration of delirium assessment and management into daily nursing care of critically ill patients, and training critical care nurses about early recognition of delirium among critically ill patients

**Keywords:** Delirium; Delirium assessment and nurses' perception; Practices.

#### 1641. Relationship between Body Mass Index and in-Hospital Outcomes of Acute Myocardial Infarction Patients at A Selected Critical Care Unit of A University Hospital- Egypt

Hanaa Ali Ahmed Elfeky

*Advances in Life Science and Technology, 14: 64-80 (2013)*

Myocardial infarction (MI) is acute and catastrophic event. It is one of the leading causes to morbidity and mortality worldwide. Multiple risk factors were found to be responsible for the occurrence of MI; among these factors are overweight and obesity. Therefore, the aim of the present study is to study the relationship between body mass index (BMI) and in-hospital outcomes among acute myocardial infarction patients at a selected critical care unit of a university hospital. Two research questions were formulated: 1- What is the body mass index profile of acute myocardial infarction patients admitted to a selected critical care unit of a university hospital; and 2: What is the relationship between body mass index and different in-hospital outcomes of acute myocardial infarction patients admitted to a selected critical care unit of a university hospital. A descriptive exploratory

research design was utilized. The current study was conducted at a selected critical care unit of a university hospital, in Egypt. A sample of convenience including 60 adult male and female patients was included in the current study. Two tools were developed by the researcher and utilized to collect data pertinent to the current study: Socio-demographic and medical data sheet which covers data about patients' age, gender, diagnosis, body weight, height, length of ICU stay, past medical history, current or recent smoking, and at home medications; and Patient's assessment sheet which was developed based on Acute Coronary Treatment and Intervention Outcomes Network (ACTION) Registry-Get with the Guidelines (GWTG). It covers data such as: patients' presentation; laboratory findings; reperfusion strategy; medications within 24 hours of admission and at discharge; discharge intervention and in- hospital outcomes. Results: males represented the great majority (90%) of the studied sample. They had different BMI categories: overweight, grade I, and grade II obesity, in percentages of 33.3%, 30%, and 25% respectively, with a mean BMI of 31.52+ 4.96. No significant statistical relationship was found between BMI and gender. The studied group admitted as a result of acute anterior MI, acute inferior MI, and acute unspecific MI, in percentages of 45%, 30% & 25% respectively. No significant statistical relationship was found between BMI and diagnosis. Around two thirds of the studied group (58.2%) experienced different in hospital **problems/outcomes:** recurrent MI attacks (26.7%), cardiogenic shock (18.3%), C.V.S (6.6%), and Death (6.6%). High significant statistical relationship was found between BMI and in-hospital outcomes (Chi square = 46.13 at p<0.004). Based on findings of the present study it can be concluded that the majority of acute myocardial infarction patients had above normal BMI values ranging from over weight to the third grade obesity (in the current study), and obviously was significantly related to the adverse in hospital outcomes. Therefore, the current study recommends, the important role of the critical care nurse in monitoring myocardial infarction patients' nutritional status through assessing their body mass index, thus providing individualized in hospital/ at discharge instructions, which could enhance patients' outcomes, and reduce complications.

**Keywords:** Acute myocardial infarction; Body mass index; Risk factors; In- hospital patients' outcomes.

#### Dept. of Nursing Administration

#### 1642. OSCE in Maternity and Community Health Nursing: Saudi Nursing Student'S Perspectivea

Abeer Eswi, Amany Samy and Halalia Shaliabe

*American Journal of Research Communication, 1(3): 143-162 (2013)*

**Objective:** Structured clinical examination (OSCE) has been increasingly used in medical and nursing education to provide a valid assessment of the clinical competencies for the students.

**Aim:** aim of the current study was to assess the Saudi nursing student's perception and feedback about OSCE examination.

**Methods:** A descriptive exploratory research design was utilized for the study as it suits its nature; the study was conducted in an institute of Nursing in Riyadh city, Saudi Arabia, A non probability convenience sample of 80 nursing students who completed their community health nursing as well as maternity nursing OSCE examination were recruited for the study. A self-administered structured questionnaire was utilized to gather

relevant data regarding perception and feedback of the students about the validity, reliability, fairness, and quality of OSCE as a test tool. Pierre OSCE evaluation questionnaire was used as a valid and reliable tool for collecting the study data.

**Results:** Results of the study revealed that the majority of the students in both courses provided positive feedback about the OSCE attributes as (95%) agreed that the OSCE was a realistic assessment for the course. In regards to the quality of OSCE performance, the majority of the students agreed that OSCE exam was fair (95%), covered a wide range of knowledge (90%), it was well administrated (96.3%).

**Conclusion:** OSCE is a realistic assessment for the nursing practical courses. It could assess a wide range of learned materials. the majority of the students agreed that OSCE exam was fair, covered a wide range of knowledge.

**Keywords:** OSCE; Maternity nursing; Community health nursing; Student's perspective.

### 1643. Cerebral Perfusion Pressure among Acute Traumatic Brain Injury Patients at Supine Versus Semi-Fowler Positions

Tahsien Mohamed Okasha, Khaled Samir Anbar and Yousria Abd El Salam Seloma

*Advances in Life Science and Technology, 12: 1-3 (2013)*

**Background:** Positioning is one of the most frequently performed nursing activities in the intensive care units. However literature review documented lack of knowledge about the relationship of cerebral dynamics and different body positions among acute traumatic brain injury patients.

**Aim:** the aim of this study is to assess the effect of supine and semi-fowler position on cerebral perfusion pressure among patients with acute traumatic brain injuries at Cairo University Hospital as indicated by: Glasgow coma score (GCS), arterial blood gases values (ABG), oxygen saturation and vital signs (pulse, blood pressure and respiratory rate).

**Research Questions:** What is the effect of supine position on cerebral perfusion pressure among patients with acute traumatic brain injuries? And what is the effect of semi fowler position on cerebral perfusion pressure among patients with acute traumatic brain injuries. **Sample:** Convenience sample of 39 patients admitted with acute traumatic brain injury. Design: Descriptive exploratory repeated measures study. Setting: University Hospital in Cairo.

**Tools:** Initial acute traumatic brain injury patient's assessment sheet, and cerebral oxygenation and physiological parameters assessment sheet for acute traumatic brain injury patients. Result: The mean age was  $28.5 \pm 7.9$  years. (74.4%) have normal body weight, (25.6%) were having cerebral contusion. Significant increase of CPP, Pao<sub>2</sub>, SaO<sub>2</sub>, SPO<sub>2</sub>, mean arterial pressure and systolic blood pressure, in 15 min post semi-fowler position assessment with a significant decrease of PaCo<sub>2</sub>. Significant decrease of pulse rate in supine position was evident. With no significant changes in diastolic blood pressure and GCS. **Conclusion:** Semi-fowler position was found to affect the ABG values, mean arterial pressure, respiratory rate, SpO<sub>2</sub> and CPP positively.

**Recommendation:** Studying the effect of side lying and prone position to establish data base about the optimal body position for acute traumatic head injury patients is highly recommended with replication of this study on larger probability sample.

**Keywords:** Supine Position; Semi-Fowler Position; Physiological Parameters; Cerebral Perfusion Pressure; Acute Traumatic Brain Injury.

### 1644. Impact of a Designed Nursing Intervention Protocol on Myocardial Infarction Patient's Outcome at A Selected University Hospital in Egypt

Abdelhameed Mahros Abdelhameed, Warda Youssef Mohamed, Yousria Abd El-salam Seloma and Hanan El-sayed Zaghlal

*Journal of Biology, Agriculture and Healthcare, 3 (17): 25-35 (2013)*

**Background:** Myocardial infarction is a life threatening disease that influences the physical, psychological and social dimensions of the individual. Improper lifestyle is one of the causes of this disease. The designing and implementing of nursing intervention protocol for MI patients could be one of the important and fundamental steps in improving MI patients outcomes.

**Aim:** The aim of this study was to examine the impact of a designed nursing intervention protocol on myocardial infarction patient's outcomes as indicated by higher post total mean knowledge scores, higher post total mean practices scores and high level of compliance to lifelong instruction.

**Research Hypotheses:** H1. Patients who will be exposed to a designed nursing intervention protocol will have a higher post total mean knowledge scores; H2. Patients who will be exposed to a designed nursing intervention protocol will have a higher post total mean practices scores; H3. Patients who will be exposed to a designed nursing intervention protocol will have a high level of compliance to lifelong instruction. **Design:** A quasi-experimental research design was utilized in this study **Sample:** A convenience sample of 40 adult male and female MI patients.

**Setting:** The cardiac care units at a selected Cairo University Hospital were recruited to fulfill the aim of this study. Tools: Four tools were formulated & tested to collect data pertinent to the study; Socio-demographic and medical data sheet, Pre/Post knowledge questionnaire sheet, an Observational checklist and Compliance assessment sheet. Structured interview, reviewing medical records and direct observation were utilized for data collection.

**Results:** The study results revealed that the post total mean knowledge scores of the studied subjects is increased significantly with value of  $t = 20.6$  at  $p = 0.000$ , higher post total practice scores among the studied subjects with  $t$  &  $p$  values ( $t = 5.6$  at  $p = 0.000$ ) also, studied subjects had mild to high compliance level regarding the lifelong instructions.

**Conclusion:** It can be concluded that, enrichment of patients' knowledge and practices in relation to their condition and utilization of the effective nursing intervention protocol as an approach of care could have a positive impact upon improvement of patients' outcome. Recommendations: The study recommended Conduction of further studies in order to assess the effectiveness of the designed protocol on patients' outcome regarding different cardiac disorders with replication of this study on a larger probability sample from different geographical locations at the Arab Republic of Egypt, in addition to establishment of cardiac rehabilitation center in the different health care organizations.

**Keywords:** Nursing intervention protocol; Myocardial infarction; Outcomes; Cardiac care units.

CAIRO UNIVERSITY

Publication  
in  
Book & Chapters

## Publication in Book/ Chapter

### Faculty of Medicine

#### Dept. of Andrology & Sexology

#### 1645. Klinefelter Syndrome

Ibrahim Mohamed Fahmy

Book: *Male Infertility Practice*, Chapter 32, Jaypee Brothers Medical Publishers, (2013)

In 1942, Dr Harry Klinefelter published a report on nineteen men with a constellation of features: testicular dysgenesis, elevated urinary gonadotropins, microorchidism, eunuchoidism, azoospermia, and gynecomastia.<sup>1</sup> It was believed to be an endocrine disorder of unknown etiology. In 1949, Barr and Bertram discovered dense chromatin bodies "Barr bodies" detected in smears of stained buccal mucosal cells of phenotypic females and not males. In 1956, Barr bodies were detected in seven patients with Klinefelter syndrome thus suggesting a genetic origin of the disorder.<sup>2</sup> In 1959, Jacobs et al.<sup>3</sup> recognized that Klinefelter syndrome was a chromosomal disorder, with an extra X chromosome resulting in the karyotype of 47,XXY. During the early 1970's, a number of centers began screening newborns for sex chromosomal abnormalities, because there was a need to obtain accurate information about childhood development in this condition.<sup>4</sup> Most, but not all XXY males, are infertile with small testicles, a relative increase in the numbers of Leydig cells, tubular sclerosis, and interstitial fibrosis of varying degrees.<sup>5</sup> Their ejaculate is usually azoospermic, and levels of testosterone are typically low to low-normal. At first it was believed that hypogonadism was due to failure of Sertoli cells of the testes, along with deficiency of second testicular hormone - X hormone - which regulates levels of pituitary gonadotropins (later known as inhibin).<sup>1</sup> The presence of an extra X chromosome is considered the fundamental etiologic factor of KS. The constant components of the disorder remain as Klinefelter et al. described, but in contrast to their hypothesis, Leydig cells are hypofunctional. However, testosterone levels may be well within normal range leading to varying degrees of virilization. The hypothesis concerning a second testicular hormone was correct, as shown by studies that inhibin B originating from testicular Sertoli cells correlate well with Sertoli cell function and are found in extremely low levels in KS patients.

**Keywords:** Klinefelter syndrome; Male infertility; Testes; IVF; ICSI. Premature ejaculation from etiology to diagnosis and Treatment.

#### 1646. The Management of Non-obstructive Azoospermia

Ahmed Mohamed Abdel

Book: *Male Infertility Practice*, Chapter 32, Jaypee Brothers Medical Publishers, (2013)

Azoospermia, the absence of spermatozoa in the ejaculate, is observed in 1% of the general population and in 10–15% of infertile men. Azoospermia may result from pre-testicular or testicular causes having adverse effects on spermatogenesis or post-testicular causes leading to obstruction of the genital tract. Pre-testicular causes are infrequent in infertility clinics and include lesions in the hypothalamus or pituitary gland leading to defective production of FSH and/or LH resulting in secondary

spermatogenic (testicular) failure. Testicular causes include all conditions leading to spermatogenic alteration other than hypothalamic and pituitary diseases. The severe forms of primary spermatogenic failure lead to azoospermia or severe oligozoospermia. Testicular causes of azoospermia are collectively referred to as non-obstructive azoospermia (NOA). The estimated prevalence of NOA in patients with severe male factor ranges between 40 and 60%.<sup>1</sup> In the past patients with proven NOA were considered hopeless.

Since testicular pathology is usually heterogeneous, foci of complete spermatogenesis might be present in a testis with severe impaired spermatogenesis. The introduction of ICSI opened the possibility to achieve pregnancy when only few spermatozoa could be retrieved from testicular biopsies in men having NOA with a reasonable probability of success.

#### 1647. Risks Factors in Premature Ejaculation: the Neurological Risk Factor and the Local Hypersensitivity

Ibrahim A. Abdel-Hamid, Moheb M. Abdel-Razek and Tarek Anis Emmanuele A. Jannini, Chris G. McMahon, Marcel D. and Waldinger (Edts)

Book: *Premature Ejaculation From Etiology to Diagnosis Treatment*, Chapter (14) : 167 -186 Springer, (2013)

Premature ejaculation (PE, sometimes referred to as rapid or early ejaculation) is the most common male sexual complaint [1]. Historically, attempts to explain the etiology of PE have included a diverse range of organic and psychological factors. Organic causes of PE are often categorized into genetic, neurological, endocrine and metabolic, urological, and drug-induced subsets [2]. The past two decades have seen advances in awareness of PE in neurological disorders, tools for the assessment of PE, and treatment options. Despite these advances, there remains a dearth of clear, evidence-based research as to its etiology. The condition may be a complication of many neurological risk factors that significantly impacts quality of life, and as such must be addressed and treated. In addition, prevention of PE begins with awareness of risk factors by patients and clinicians. This chapter provides an overview of the neurological risk factors and local penile hypersensitivity that appear to be involved in the pathogenesis of PE.

**Keywords:** Premature Ejaculation; Sexual Medicine; Male Sexual Dysfunction.

#### 1648. Ongoing and Future Research

Rany Mohamed Mahmoud Shamloul

Book: *Erectile Dysfunction*, Oxford University Press, (2013)

Advances in the understanding of the physiological mechanisms responsible for penile erection and pathophysiologicals resulting in erectile dysfunction (ED) have led to the development of novel treatments such as the oral phosphodiesterase-5 (PDE-5) inhibitor class of agents, which can, in the majority of cases, successfully treat ED. However, our knowledge of the underlying biological events that govern the erectile response remains incomplete; as new molecular targets or mechanisms are identified, the potential exists for refining or redefining treatments for compromised erectile function. This chapter examines ongoing research and provides a look into the "translational" future

of patient management, including such exciting opportunities for personalized and target-specific intervention as gene and growth factor therapy, stem cell and cell-based therapies, and regenerative medicine.

**Keywords:** Erectile dysfunction.

#### Dept. of Anesthesiology

##### 1649. Management of Brain Tumor in Pregnancy and Anesthesia Window

Hala Mostafa Goma

Book: *Clinical Management and Evolving Novel Therapeutic Strategies for Patients with Brain Tumors*, Intech, 556-568 (2013)

Brain tumor surgery during pregnancy has a great concern in Egypt now days. High prevalence of brain tumors during pregnancy was noticed. There is no accurate statistics for the prevalence.

The most common tumors are pituitary tumors, meningioma, gliomas, metastasis of breast carcinomas. Many problems affect anesthesia, as the interaction between many different factors, as the physiological changes during pregnancy, including, cardiovascular, respiratory changes [1].

Problems occur, during diagnosis, and treatment of tumors. Also problems during surgery are, drug interactions with the anesthesia drugs, blood loss and transfusion, prevention preterm labour, and anesthesia for urgent cesarean section during surgery for removal of brain tumor, in the chapter I tried to summarize all these factors from anesthesia point of view did many cases for brain resection during pregnancy. I hope to give this experience for any young anesthesiologist how may face such cases.

**Keywords:** Clinical Management and Evolving; Novel Therapeutic Strategies for Patients with Brain Tumors.

#### Dept. of Dermatology

##### 1650. Challenging Cases in Dermatology

Mohammad Aly Abdel-Qader El Darouti

(eBook) Springer London Heidelberg New York Dordrecht, (2013)

The cases presented in this book will guide the reader through the process of making a diagnosis based on logical thinking. The book provides a wealth of knowledge regarding diagnostic approaches and pearls of wisdom. In addition to unusual presentations of common diseases, it includes discussions about rare diseases, complex cases, surprising diagnoses, therapeutic challenges and other important features. Becoming acquainted with such unusual cases will provide the dermatologist with increased knowledge, a wider perspective, and innovative techniques that can be used to solve diagnostic dilemmas. Readers will improve their way of thinking and data analysis, and will be able to improve differential diagnoses. This book provides the unique feature of a strategic way of thinking while discussing each case, in order to reach a diagnosis.

The text includes comparisons of each case to other similar cases, pointing out the distinguishing features of conditions under consideration.

**Keywords:** Challenging Cases; Dermatology.

#### Dept. of Obstetrics and Gynecology

##### 1651. Evaluation of Infertility - Investigations and Diagnostic Interventions

Akmal Nabil El-Mazny

Lambert Academic Publishing, (2013)

Infertility can be defined as the failure to achieve a pregnancy within one year of regular unprotected intercourse. A specific male or female factor can be identified in approximately 80% of couples. Advances in the understanding of the causes of infertility have facilitated the development of increasingly complex diagnostic tools. The accurate detection of underlying reproductive abnormalities helps to guide management decisions and maximize treatment outcomes. A basic evaluation for infertility may be grouped into three main categories: semen analysis, assessment of ovulation, uterine and tubal evaluation. Uterine and tubal structures may be visualized using a variety of techniques, including hysterosalpingography, transvaginal sonography, sonohysterography, laparoscopy or hysteroscopy. This book provides a comprehensive overview of the current investigations and diagnostic interventions for the evaluation of infertility along with their indications and use; and also identifies areas for future research.

**Keywords:** Infertility; Investigations; Interventions.

##### 1652. Assisted Reproduction - Indications and Techniques

Akmal Nabil El-Mazny

Lambert Academic Publishing, (2013)

Assisted reproductive technologies (ARTs) include any procedure in which oocytes and spermatozoa, or embryos are manipulated in vitro for the purpose of establishing a pregnancy.

Intrauterine insemination, in which laboratory-prepared sperm are inserted into the uterine cavity through a cervical catheter, is indicated in mild-moderate male factor infertility along with a number of other diagnoses. In vitro fertilization (IVF) is an ART in which sperm and oocytes are retrieved and combined outside of the body where fertilization occurs, the embryos are then transferred to the uterus. Initially developed for tubal factor infertility, IVF is now indicated in a broad range of situations and is very successful. Multiple techniques are used to enable and improve ARTs including: intracytoplasmic sperm injection, gamete intrafallopian transfer, tubal embryo transfer, embryo cryopreservation, assisted hatching, and preimplantation genetic diagnosis. Hopefully this book will enhance your knowledge of ARTs along with their appropriate indications and use, and that you will be able to apply this information to your professional practice.

**Keywords:** Assisted Reproduction; Indications; Techniques.

##### 1653. Diabetes in Pregnancy - Risk Assessment and Management

Akmal Nabil El-Mazny

Lambert Academic Publishing, (2013)



Diabetes mellitus is a multisystem disease with both biochemical and anatomical consequences. Diabetes in pregnant women may be pregestational, where diabetes (type 1 or type 2) is diagnosed before pregnancy, or gestational, which refers to diabetes diagnosed during pregnancy. While planning the management of risk pregnancies, including those complicated by diabetes, two vital questions should be asked: "How will this disorder affect gestational outcome ", and "How will pregnancy affect maternal clinical status " Diabetes is associated with the most adverse fetal outcome, increased rates of miscarriage, congenital malformations, intrauterine fetal death, macrosomia, prematurity, and neonatal metabolic and respiratory disorders. in addition, the physiological changes associated with pregnancy can adversely impact maternal health.

Retinopathy, nephropathy, neuropathy, hypertension/preeclampsia, and cardiovascular disease can all affect and be affected by pregnancy. I hope that this book will provide a comprehensive review of diabetes in pregnancy along with its complications and management, and that you will be able to apply this information to your professional practice.

**Keywords:** Diabetes; Pregnancy; Complications; Management.

#### 1654. Medical Research : Scientific Writing and Publishing

Akmal Nabil El-Mazny

*Create Space Independent Publishing Platform, (2013)*

Scientific writing and publishing marks the endpoint of medical research that has been performed, completed, reviewed and accepted, and complements teaching and training, clinical service and patient care. This book instructs, in a very clear style, the guidelines authors should follow in order to improve the quality of their scientific papers.

Chapter I provides an overview on the application and implementation of internationally accepted principles for research practice.

Chapter II presents in details all the necessary steps of research design and scientific writing; including an essential introduction to evidence-based medicine and biomedical statistics.

Chapter III describes the uniform requirements of biomedical journals as well as the editorial and review processes for research publishing. Everything is easy when you know how – I hope that this book will provide the "know how" for all researchers, academicians and health-care professionals.

**Keywords:** Medical; Research; Scientific; Writing; Publishing.

#### 1655. Hysteroscopic Management of Endometrial Bleeding and IUD

Amr Hassan Hussein El Said Wahba

Book: *Nezhat's Video Assisted and Robotic Assisted Laparoscopy and Hysteroscopy*, (4th edition) Cambridge University Press, Chapter 7.9, (2013)

Hysteroscopy has become one of the valuable tools in the gynecological evaluation in modern practice. Its role in the assessment of cases with abnormal uterine bleeding in the IUD users is becoming well recognized. Abnormal uterine bleeding in IUD users can be caused by the IUD itself or may be due to coexisting pathologies. This chapter highlights the role of hysteroscopy in the evaluation and management of such cases.

**Keywords:** Hysteroscopy; Iud; Endometrial Bleeding.

**Dept. of Orthopaedic**

#### 1656. Animal Models of Orthopedic Implant-Related Infection

Ahmed Fouad Mohammed Seifeldin

Book: *Biomaterials Associated Infection Immunological Aspects and Antimicrobial Strategies*, Springer – Verlag, (2013)

Musculoskeletal infection remains a great challenge in orthopedic and trauma surgery. Despite best medical and surgical practice and significant advances in research and development, bone and implant associated infections are still difficult to diagnose, impossible to prevent in all cases and require invasive and debilitating treatment.

The development and safe clinical implementation of novel preventative, therapeutic or diagnostic strategies requires the use of animal models of infection, which provide crucial evidence regarding performance, cytocompatibility, biocompatibility, and safety prior to clinical implementation. Many animal models of musculoskeletal infection have been described in the literature; however, there remains a dearth of fully standardized or universally accepted reference models hindering advancement in the field. The following chapter provides an overview of the animal models available for the study of musculoskeletal infection, the latest advances that are expected to improve them, and some of the most important scientific output achieved using these models.

**Keywords:** Biomaterials; Immunology; Orthopaedic Implants; Animal Models; Biomedical Engineering.

**Dept. of Parasitology**

#### 1657. Intestinal Capillariasis

Nadia Aly Essa El-Dib and Thomas Weitzel

Book: *Parasitología Humana*, (2013)

Capillaria philippinensis is a tiny nematode parasite of fish-eating birds. It is a member of the genus Capillaria that includes up to 250 members parasitizing almost all types of animals. Its importance arises from its ability to infect humans and causes a serious illness that may end fatally if not diagnosed and treated in the proper time.

The first human case was detected in the Philippines in 1963. Reports showed that the infection was endemic in the Philippines with the appearance of few epidemics that caused deaths among infected patents. Experimental studies to reveal the mode of infection and the life cycle of the parasite have shown that infection occurs as a result of ingestion of infective larvae in the intestine of fresh or brackish-water fish eaten raw. The parasite has a unique life cycle. It inhabits the wall of the small intestine, produces immature thick-shelled eggs that pass in feces and infective larvae that cause internal autoinfection and hyperinfection leading to continuous deterioration of infected patients.

The thick-shelled eggs mature in water and infect the intestine of small fish, which is eaten raw and non-eviscerated in the Far East. Infection appeared later in different areas of the Far East and Middle East.

Thailand, Taiwan, Japan, Korea, China, Iran and Egypt. A case was detected in Italy, but was thought to get the infection from

Indonesia and a case was reported from Spain but the infection was suspected to be from Colombia. *Ixobrychus* spp., the bird reservoir host detected in the Far East, is also known in other countries and may have a role in maintenance of infection.

Birds do not know the country borders and can move to other countries at the times of migration carrying new infection to new places. Infection causes diarrhea, and malabsorption of all nutrients leading to loss of weight, cachexia and lower limb edema, ascites and/or pleural effusion due to low blood albumin. Death may occur as a result of electrolyte imbalance, mainly hypokalemia or concomitant bacterial infection. All the detected cases till now depended on accidental diagnosis by a Parasitologist.

Most of the cases suffered for a long duration and had to spend many expenses to be diagnosed, and some died due to late diagnosis or complications.

The parasite shows irregular shedding of parasite stages in feces; that is why the examination of several samples is needed in order to reach a final diagnosis. Treatment of cases depends on the use of albendazole for at least 10 days or mebendazole for about 28 days. It is also very important to treat the electrolyte imbalance as well as the hypoproteimemia.

**Keywords:** Capillaria Philippinensis; Intestinal Capillariasis; Hypoproteinaemia; Malabsorption; Chronic Diarrhea.

#### Dept. of Pediatrics

### 1658. Diabetic Ketoacidosis: Clinical Practice Guidelines

Shereen Abdelghaffar Khalil

Book: *Type 1 Diabetes*, Intech, (2013)

**Introduction:** Diabetic Ketoacidosis (DKA) the most common endocrinal emergency remains a life threatening condition despite improvements in diabetes care. The purpose of this chapter is to briefly review the pathophysiology of DKA and discuss recommended treatment protocols and current standards of care pertaining to children, adolescents and adults with type 1 or 2 diabetes presenting with DKA. The information provided is based on evidence from published studies and internationally accepted guidelines whenever possible and, when not, supported by expert opinion or consensus.

**Keywords:** Diabetic Ketoacidosis; Practice Guidelines; Evidence; Based.

### 1659. Childhood Obesity in Developing Countries

Ghada Mohammad Anwar

Book: *Auxology Studying Human Growth and Development*, Schweizerbart Science Publisher, (2013)

This new book is a comprehensive description of human physical growth and development (Auxology) with contributions by 56 internationally reputed experts. The entire spectrum of basic and advanced information on growth tracking, growth prediction, short-term-, catch-up- and rapid growth, nutritional and social factors influencing human growth, and issues related to preventive health care, growth in ethnic minorities and migrants, and growth in developing countries is presented. The text is generously illustrated by 270 colour figures and 89 comprehensive tables. The text also introduces new mathematical approaches to growth modelling and provides practical

information on how to use and interpret growth charts. Current national references for height, weight, body mass index (BMI) and head circumference for various countries (US, ARG, BRA, CAN, IND, BEL, GER, IT, NL, PL, SW, SWI, TUR, UK, WHO) are provided, as are growth references for twins, preterm infants and syndrome specific growth charts for clinical purposes.

The book is of greatest interest to all pediatricians, to medical students and students of human biology, health workers, nutritionists, medical staff and professionals interested in child and adolescent growth and development.

**Keywords:** Children; Obesity; Developing Countries.

### 1660. Studying Human Growth and Development

Mortada Hassan Fakhri El-Shabrawi

Book: *Auxology Studying Human Growth and Development*, Schweizerbart Science Publisher, (2013)

**Definition** Menarche is the occurrence of first menstruation; it is a unique and relatively late marker of female puberty. Menarche is the endpoint of a complex sequence of maturational events and it is highly significantly correlated with age at the appearance of breast buds which result from onset of estrogenic action. Menarche is the most widely used indicator of sexual maturation as it is the most accurately recalled indicator of puberty among girls. Timing of menarche in relation to pubertal stages: Menarche most commonly occurs during late stage 3–early stage 4 breast development [figure (1)].

Menarche usually occurs in the 6-month period preceding or following the fusion of the second and first distal phalanges and the appearance of the sesamoid bone. Peak bone mineral content velocity takes place at the age of menarche and 9 to 12 months after peak height velocity. Menarche occurs as a girl's body fat percentage reaches 17-22%. Menarche may not signal the institution of ovulation and menstrual cycling. Although ovulation, and hence potential fertility, may be present before menarche, in many females, regular ovulatory cycling does not occur for several months or years with 50% of cycles are anovulatory during the first two years after menarche; this decreases to 20% by five years post-menarche. After menarche, growth may range from 1 to 10 cm (average 5cm). Generally, the older a girl at menarche the greater the adult height.

**Keywords:** Menarch; Egypt; Developing Countries.

### 1661. Albuminuria in Pediatric Patients

Habby Kaiser Sawires

Book: *Albuminuria Symptoms, Causes and Treatment Options*, Nova Science Publishers, (2013)

Albuminuria may not only serve as an early marker of advanced disease, but may also serve as a predictor of disease progression and poor outcome. This fact makes the current book "Albuminuria: Symptoms, Causes and Treatment Options" very crucial and timely.

The book is composed of ten chapters written by experts from seven different countries. It is well classified to serve its purpose, divided in three broad sections. The first section deals with the clinical evaluation and implications of albuminuria. It also covers the molecular, cellular and biochemical basis of albuminuria. The second section is geared towards albuminuria noted in special clinical conditions; diabetic nephropathy, cardiovascular diseases,

resistant hypertension and following renal transplantation and exercise. The third and final section covers albuminuria among the extremes of age; both the pediatric and the fastest growing elderly group.

### 1662. Illustrated Pediatrics

Mostafa Zakaria Mohamed

*Lambert Academic Publishing, (2013)*

Illustrated Pediatrics is one of the most popular books in the Middle Eastern countries. The first edition appeared in the year 2000, and since then, It has become a well established textbook for undergraduate medical students for many years. It presents the pediatrics curriculum in the form of high quality photos, figures, tables and illustrations. In this new edition, the contents have been extensively updated and many new photos were added to better highlight the visual elements of teaching and learning pediatrics. Overall, Illustrated Pediatrics makes a great addition to any medical student's shelf.

**Keywords:** Illustrated; Pediatrics; Undergraduates; Medical Students.

### Dept. of Physiology of the nervous system - nerve disease

### 1663. Demyelinating and Sleep

Lamia Medhat Afifi

Book: *The Encyclopedia Sleep*, Academic press –Elsevier, (2013)

This chapter is about the different sleep disorders that may be seen in different demyelinating diseases, the most common of which is multiple sclerosis

**Keywords:** Sleep; Demyelinating; Multiple Sclerosis; Adem.

### Dept. of Rheumatology

### 1664. Behcet's disease and subclinical atherosclerosis

Tamer Mohamed Atef Mostafa Gheita

*Lambert Academic Publishing, (2013)*

Although the pathogenesis of the auto-inflammation in Behçet's disease remains controversial, this book provides a new insight that inflammation and subclinical atherosclerosis in BD may develop through different mechanisms from that involved with other rheumatic conditions. This book presents a comprehensive description of the basics of Behçet's disease and atherosclerosis with in-depth discussion of their association that is commonly overlooked by rheumatologists and primary care physicians. It provides advanced information of such a mysterious and interesting rheumatic disease. The book is designed to provide a useful and informative overview for rheumatology students and professionals and the material included is sufficiently comprehensive to serve as a reference for general practitioners dealing with Behçet's disease patients. The readers will take a worthy idea on the disease, updates in medical treatments and the team approach concepts in its management. This book should prove fruitful in completing the canvas of the role of

inflammation in atherosclerosis, and in translating these concepts to improve human health.

**Keywords:** Behçet's Disease; Subclinical; Atherosclerosis; Ultrasonography; Pathogenesis; Activity; Investigations; Management; Updates.

### Faculty of Pharmacy

### Dept. of Microbiology and Immunology

### 1665. Antibiotic Resistance Patterns Among Common Gram Positive and Gram Negative Pathogens in Clinical Isolates from Major Hospitals in Cairo, Egypt

Aymen Samir Mohamed Yassein

Book: *Worldwide Research Efforts in the Fighting against Microbial Pathogens: From Basic Research to Technological Developments*, Brown Walker Press, (2013)

Selected for this study. Clinical isolates were collected from hundreds of patients admitted to several hospitals in the greater Cairo area. Microscopic, cultural and biochemical tests were used to identify the isolates and confirm their proper classification. Antibigrams were carried out for the isolates against several antibiotics belonging to different classes. Minimum inhibitory concentrations were determined for the resistant isolates. Molecular approaches were followed to determine the presence of antibiotic resistance as well as virulence genes.

### 1666. Genomes, Metagenomes, and Microbiomes: A New Biology for a New Millennium

Ramy Karam Aziz

Book: *New Life Sciences: Science to Society*, Bibliotheca Alexandrina, (2013)

After centuries of biological research, it has only recently become common knowledge that the vast majority of life forms cannot be seen by the human eye, and a great proportion of them cannot be cultured in the laboratory with commonly used culturing techniques. The tremendous numbers of microbial cells and virus particles reflect an immense diversity of lifestyles that can adapt to nearly every environment on the surface of the Earth and in the depths of its oceans. Here we discuss the new sciences of genomics and metagenomics and their application on the human microbiome project.

### Dept. of Pharmaceutical Technology and Industrial Pharmacy

### 1667. Ultrasound as an Adjuvant Tool in drug delivery

Mariame Ali Hassan

Book: *Cellular Response to Physical Stress and Therapeutic Applications*, Nova Science Publishers, (2013)

The discovery of the mutual interaction between tissues and ultrasound waves was responsible for the introduction of ultrasound in the medical field as an indispensable tool in diagnosis and as a therapeutic tool as well. For therapeutic applications, ultrasound can offer a variety of scenarios to correct pathological conditions as in the case of physiotherapy, lithotripsy, wound and bone fracture healing, and cancer ablation. Moreover, ultrasound can enhance transdermal delivery, promote the (targeted) delivery of genes, macromolecules and drugs into tissues and cells, and affect the release kinetics of different dosage forms prepared to respond to the acoustic stimuli. Despite the growing literature on the usefulness of ultrasound as a physical delivery tool over the past decades, recent studies have contributed to expanding our knowledge about the mechanisms underlying the observed effects and, simultaneously, imposed a number of questions criticizing the efficiency of the ultrasound-aided delivery approach. In this chapter, the acoustic determinants of the effects of ultrasound and the biological responses to ultrasound exposure will be reviewed. Finally, the limitations of ultrasound-aided delivery approach will be discussed in a trial to redirect future investigations to resolve the boundaries against the translational research.

## Faculty of Nursing

### Dept. of Nursing Critical Care and Emergency

#### **1668. Cerebral Oxygenation among Acute Traumatic Brain Injury Patients**

Tahsin Mohamed Okasha

*Lambert Academic Publishing, (2013)*

Positioning is one of the most frequently performed nursing activities in the intensive care units. However literature review documented lack of knowledge about the relationship of cerebral dynamics and different body positions among acute traumatic brain injury patients. the aim of this study was to assess the effect of supine and semi-fowler position on cerebral oxygenations and physiological parameters among patients with acute traumatic brain injuries at Cairo University Hospitals as indicated by: Glasgow coma score (GCS), arterial blood gases values (ABG), oxygen saturation and vital signs (pulse, blood pressure and respiratory rate). Descriptive exploratory repeated measures design was used in this study. The study was conducted on 39 subjects admitted with acute traumatic brain injury within the first 48 hours of hospital admission. Result revealed that semi-Fowler position has positive effect on cerebral dynamics, arterial blood gases, and hemodynamic parameters it help in improving the cerebral perfusion pressure (CPP). Understanding the effect of positions on cerebral dynamics in traumatic brain injured patients helps in improve the prognosis and decrease the complication.

#### **1669. Factors Affecting Validity of Arterial Blood Gases Results**

Sameh El-Sayed Mohamed

*Lambert Academic Publishing, (2013)*

One of the most common laboratory tests in intensive care units is the arterial blood gases, sampling of arterial blood gases (as a critical care nursing responsibility) might be corrupted by pre-analytical factors that influence the validity of results. Arterial blood gases are valuable only if obtained properly and measured carefully. Corrupted factors in arterial blood gas sampling change significantly the results and adversely affect patient-care decisions when the magnitude of the error is clinically important. Validity of a laboratory finding has been defined as the 'degree of achieving the objective' to answer the question which the physician asks accuracy and specifically. Therefore, the study aimed to assess the factors affecting arterial blood gases results' validity among critically ill patients at Cairo University Hospital, as indicated by nurses' knowledge and practices, supplies and equipment, heprinization of the syringes, patients' variables, after withdrawal sample management, and documentation.

#### **1670. Organ Dysfunction Among Adults Critically Ill Patients Identification of Factors Predisposing to Organ Dysfunction**

Fatma Abdel-Aziz Mohamed

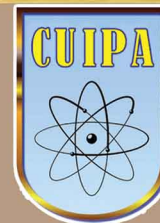
*Lambert Academic Publishing, (2013)*

Multiple organs dysfunction syndrome (MODS) is one of the most challenging clinical problems in the intensive care unit. MODS is the main cause of death in ICUs. Therefore the critical care nurse has an important role regarding identification and management of predisposing factors that may decrease the incidence of MODS and improve patients' outcomes. The current study aimed at identification of factors predisposing to organ(s) dysfunction among critically ill adult patients at a selected Cairo University Hospital and to suggest a nursing intervention protocol. Predisposing factors to organ(s) dysfunction were found to be as heart failure; hypertension; diabetes; and chest infection. Mild degree of organs dysfunction were most frequently noticed throughout ICU stay.





Cairo University



# **(4) Social & Humanity Sciences Sector**

**4-1 Faculty of Economics and Political Science**

**4-2 Faculty of Commerce**



CAIRO UNIVERSITY

Publication  
in  
Journals

## Faculty of Economics and Political Science

### Dept. of Application of Computer in Social Sciences

#### **1671. Logical Framework Analysis (LFA): Through the Current Information Systems to Promote the Mainstreaming of Global Environmental Issues in National Plans and Policies- Case of Egypt**

Nedal M. Elsaid, Ahmed E. Okasha and Abdalla A. Abdelghaly

*International J. of Science and Advanced Technology*, 3: (2013)

Dealing with the imperatives of sustainable development represents a growing challenge in the context of rapid globalization, persistent poverty and social inequality, and the changing patterns of production and consumption, climatic and environmental changes, and the changing roles of public and private sector institutions. The concept of sustainability for the industrialists and the businessmen in the past is to try to achieve coordination between the profits and a commitment to environmental considerations, but things become more complicated due to the world transformation into open and global market which it emerged under increasing pressure to meet environmental and social responsibilities, which continually expands its scope. Information and data are necessary in supporting and rationalizing decision making to build an Egyptian information society as well as the industrial sector which it will be able to pursuing and absorbing the great flow of advanced knowledge and aid cost savings. The current approach does not have an unified methodological framework, data collection and management is not standardize. Moreover, the existing set of environmental indicators is not comprehensive and does not respond to the information requirements. Limited environmental information is produced currently and it is not fed into the planning and policy making process, on the other hand available monitoring data is not shared among the agencies. Furthermore, there is no coordination and cooperation occur among the relevant institutions resulting in gaps and duplications. The current regulation is not comprehensive for the implementation of an adequate national environmental monitoring system. It is worth mentioning that monitoring and evaluation, particularly with regards to information management, is the "most significant constraint to effective environmental policy making and implementation in Egypt". In this regard, the need for a "unified methodological framework" for monitoring activities is identified as essential. Together with the need to synchronize data collection, storage, accessibility and usability.

**Keywords:** Is evaluation; Evaluation research; Software quality model; ISO 9126 standard; Information systems performance; Sustainable development.

#### **1672. Establish New Reports and New Inquires Through Usage of Business Intelligent Tools to Handle the Defects of the Current Reports and Inquires - Ministry of State for Environmental Affairs – Egypt**

Nedal M. Elsaid, Ahmed E. Okasha and Abdalla A. Abdelghaly

*International Journal of Engineering Research and Technology*, 2: 2883-2891 (2013)

Business intelligence (BI) systems combine operational data with analytical tools to present complex and competitive information to planners and decision makers. The objective is to improve the timeliness and quality of inputs to the decision process. Business Intelligence is used to understand the capabilities available in the firms and the institutions. Although business intelligence systems are widely used in industry, research about them is limited. This research is aiming to provide more insight that determines, analyses and solves the current reports and inquires defects for the ministry of state for environmental affairs which it is one of the most critical issues affect the decision makers.

**Keywords:** Data Warehouse; Data mart; BI Business intelligence; Methodology; Data framework; Establish; Reports; Inquires; Through; Usage; Business; Intelligent; Tools; To; Handle; Defects; Current; Reports; Inquires; Ministry; State; Environmental; Affairs; Egypt.

#### **1673. A Survey on Business Intelligence Application to Evaluate the Software Quality from End User Point of View**

Nedal M. Elsaid, Ahmed E. Okasha and Abdalla A. Abdelghaly

*International Journal of Scientific and Engineering Research*, 4: 1932-1940 (2013)

Information technology supports all major business processes and business functions. Software plays a very important role in the industry and society. So as the role of software in the industry and the society becomes vital, It becomes very crucial to develop high quality and easy to use software. This article deals with the software evaluation and it afford survey contains various models and metrics for measuring the software from the end users prospective. There are several software quality models that evaluate how easily users can use the software to carry out their required task. The article is also measured in terms of its capability to provide the user satisfaction and ability to fulfill the needs of the users by providing the user friendly interfaces.

**Keywords:** Information system evaluation; Software evaluation; ISO 9216; Business intelligence; Evaluation methodology.

#### **1674. Defining and Solving the Organizational Structure Problems to Improve the Performance of Ministry of State for Environmental Affairs - Egypt**

Nedal M. Elsaid, Ahmed E. Okasha and Abdalla A. Abdelghaly

*International Journal of Scientific and Research Publications*, 3: (2013)

The structured problem solving is important methodology in improve the organization performance. This study is aiming to provide more insight that determines the organizational problems solutions for the ministry of state for environmental affairs which it is one of the most critical issues effect the administration fields. Firstly, we discuss the concept of organization structured and organization structured types. Secondly, we focus on the signs of poor organizations structured which it indicate that the organization is deeply need to solve the mentioned problem. Thirdly, we discuss the base of structured problem solving is the Deming circle: And introduce the Bank's 6 steps process of the problem solving. then discuss the important of a create and maintain healthy organization structured manner using team in

problem solving. Finally, we discuss the arguments against using a structured problem solving.

**Keywords:** Organizational structure; Os types; Poor os; Healthy os; Os arguments; Os procedures.

#### Dept. of Economics

### 1675. Electricity Demand Analysis and Forecasting: A Panel Cointegration Approach

Alaa Essam El-Shazly

*Energy Economics*, 40: 251-258, (2013) IF: 2.538

This article analyzes the demand for electricity and provides out-of-sample forecasting at the sectoral level using a panel cointegration approach. The econometric model permits cross-sectional heterogeneity within a dynamic framework that incorporates information on relevant income and prices of domestic and foreign goods. Both the short-run dynamics and the long-run slope coefficients are allowed to vary across cross-sections. Also, the testing for unit roots and cointegration in panels allows for heterogeneous fixed effects and deterministic trends.

Using Egyptian data, it is shown that the empirical model produces reliable ex-post forecasts near the end of the full sample period. These pseudo forecasts are representative of what one would expect if the forecasting relationship is stationary. The long-run parameter estimates are then used to conduct ex-ante forecasting under plausible assumptions for policy making.

**Keywords:** Electricity demand analysis; Forecasting; Panel cointegration.

### 1676. Higher Education Externalities in Egyptian Labor Markets

Hanan Hussien Ramadan Nazier

*Advances In Management and Applied Economics*, 3: 193-217 (2013)

Augmenting a Mincerian earnings function with governorate level data, this paper estimated the external return to higher education for individuals in Egypt in 2010.

The results suggested that these externalities are negative and exist only for female workers, while for males these externalities were again negative but statistically insignificant. A unit increase in governorate average higher education is associated with a 68% decrease in females' hourly wage. This could be explained by the fact that education degrees are simply used as a device to signal higher ability without raising productivity. Another reason could be excess supply of higher education graduates in the Egyptian labor market. These results have been tested through a number of robustness checks. Results survived to the introduction of individual and governorate level variables; it is not due to imperfect substitutability across workers; it still holds when treating local human capital as endogenous variable and instrumented it.

**Keywords:** Human capital; Returns to education; Spillovers from education; Education externalities; Higher education; Wages.

### 1677. Assessing the Effects of Trade Liberalization on Wage Inequalities in Egypt: A Microsimulation Analysis

Chahir Raouf Zaki Tadros

*The International Trade Journal*, 27: 63-104 (2013)

This article aims at evaluating the liberalization policies' effects on wage inequality in Egypt. Gender, geographical, and skill dimensions are used to break down labor into eight segments. This article simulates the effect of a reduction of tariffs imposed on imports by 50%. Results show that the effect of trade liberalization policies depends on the characteristics of the individual and the working sector. Thanks to the expansion of textiles, garments, chemicals, and services, inequality decreases for urban and rural skilled men as well as skilled and unskilled women working in urban areas. By contrast, inequality increases among unskilled men and skilled women in rural areas.

**Keywords:** Trade liberalization; Microsimulation; Wage inequalities; Egypt.

### 1678. Trade Facilitation and Corruption: ACge Model of Egypt

Chahir Raouf Zaki Tadros

*The Journal of North African Studies*, 18: 70-111 (2013)

This paper extends a dynamic computable general equilibrium (CGE) model to introduce trade facilitation aspects. The contributions are twofold on both the theoretical and empirical levels. First, it attempts to explicitly model trade facilitation in two alternative ways. On the one hand, trade facilitation is considered as a pure deadweight loss and, on the other hand, as a rent-generating process that takes corruption into account. Concerning the empirical side, the tariff equivalent of red tape and related procedures are being estimated, not assumed, at the sectoral level in a companion paper and are introduced in the CGE model.

The Exter model is modified and calibrated on the Egyptian social accounting matrix of 2000/2001. The results show that trade facilitation boosts exports, imports and welfare in a significant way. Yet, when the cost and the tariff equivalent effect of trade facilitation are jointly modelled, the impact of such a process is reduced. Moreover, some sectors like processed food, garments, chemicals and high value-added products witness a significant expansion more than others. When the welfare gains coming from corruption are taken into account, the elimination of administrative barriers to trade is associated with lower, though positive, gains.

**Keywords:** Cge models; Trade facilitation; Trade liberalisation; Corruption; Egypt.

### 1679. Higher Education for Sustainable Consumption: Challenges and Opportunities

Marwa Mohamed Shibl Biltagy

*International Journal of Education and Research*, 1(9): 1-12 (2013)

This paper focuses on how higher education institutions can use the United Nations Decade of Education for Sustainable

Development (2005-2014) to promote sustainable consumption. Higher education has an important role to play concerning education for sustainable consumption and the construction of a learning society. What is especially significant about this paper is the emphasis on the role of higher education in sustainable consumption.

The results include innovative strategies to change curricula; to shape public opinion and national policies for sustainability; to make sure that research serves the needs of social and economic development that is sustainable and to enable students to develop their knowledge, values and skills that society will need for real progress towards sustainable consumption. The learning outcomes of this paper are the recommendations that lead to increased curriculum development, interdisciplinary research on sustainable consumption in higher education institutions and change in attitudes and behavior of individuals.

**Keywords:** Higher education; Sustainable consumption; Sustainable development; Challenges; Opportunities.

### 1680. Comparative Performance Study of Conventional and Islamic Banking in Egypt

Mona Esam Othman Fayed

*Journal of Applied Finance and Banking*, 3: 1-14, (2013)

The purpose of this empirical study is to analyze and compare the performance of Islamic and conventional banking in Egypt and to find out which of the banking streams is performing better than the other. To make appropriate comparative analysis, three Islamic banks (Faisal Islamic Bank, ElBarakaMisr, and National Bank for Development) and six conventional banks (National Bank of Egypt, BanqueMisr, Bank of Alexandria, National SocieteGenerale Bank, Arab African International Bank, Commercial International Bank) were used during the period from 2008 to 2010. Financial ratios were estimated from annual reports and financial statements. Seven financial ratios were used to gauge profitability, liquidity and credit risk; and a model known as "Bank-o-meter" was used to gauge solvency. Findings indicate the superiority of conventional banks over Islamic ones in profitability, liquidity, credit risk management as well as solvency.

**Keywords:** Performance evaluation; Islamic banking; Conventional banking; Profitability; Liquidity; Credit risk; Solvency.

### 1681. Trade Liberalization and Labor Demand Elasticities: Empirical Evidence for Egypt

Hanan Hussien Ramadan Nazier

*International Research Journal of Finance and Economics*, Issue 111: 30-45 (2013) IF: 0.4

This paper examined how trade liberalization affected employment and labor demand elasticities in the manufacturing sector in Egypt over the period from 1989-90 to 2009-2010. Theoretically, trade liberalization may affect labor demand through two channels: the direct effect and the indirect effect; via increasing labor demand elasticity. However, for the Egyptian case our findings did not support this theoretical hypothesis. Moreover, our results also suggested that openness did not have a direct effect on labor demand. This may contribute to explain the low employment response to trade liberalization reached by

several studies on developing countries neglecting the elasticity channel.

**Keywords:** Labormarkets; Labordeman delasticities ; Tradeliberalization.

### 1682. On the Determinants of Trade in Services: Evidence from the MENA Region

F. Karam and Chahir Raouf Zaki Tadros

*Applied Economics*, 33: 4662-4676 (2013)

This article examines the determinants of aggregate flows of service trade in MENA countries using an adapted version of the gravity model and a panel dataset covering the 2000 to 2009 period for 21 countries and 10 sectors. A new determinant of trade performance is introduced: the number of bound commitments undertaken by a sector in the WTO as well as the availability of those commitments by mode of supply. The results show that being a WTO member boosts trade in services. In addition, the number of bound commitments increases exports, imports and trade in services. This positive and significant effect remains robust even after controlling for several econometric issues, Namely, the selection bias related to the WTO membership and the endogeneity of commitments

**Keywords:** Trade in services; WTO commitments; Gravity models; Mena region.

### 1683. Why Don't Banks Lend to Egypt's Private Sector?

Santiago Herrera, Christophe Hurlin and Chahir Raouf Zaki Tadros

*Economic Modelling*, 33: 347-356, (2013) IF: 0.557

Bank credit to Egypt's private sector decreased over the last decade, despite a recapitalized banking system and high rates of economic growth. Recent macro-economic turmoil has reinforced the trend. This paper explains the decrease based on credit supply and demand considerations by 1) presenting stylized facts regarding the evolution of the banks' sources and fund use in 2005 to 2011, noting two different cycles of external capital flows, and 2) estimating private credit supply and demand equations using quarterly data from 1998 to 2011. The system of simultaneous equations is estimated both assuming continuous market clearing and allowing for transitory price rigidity entailing market disequilibrium. The main results are robust to the market clearing assumption. During the global financial crisis, a significant capital outflow stalled bank deposit growth, which in turn affected the private sector's credit supply. At the same time, the banking sector increased credit to the government. Both factors reduced the private sector's credit supply during the period under study. After the trough of the global crisis, capital flowed back into Egypt and deposit growth stopped being a drag on the supply side, but bank credit to the government continued to drive the decrease in the private sector's credit supply. Beginning in the final quarter of 2010, capital flows reversed in tandem with global

Capital markets, and in January 2011 the popular uprising that ousted President Hosni Mubarak added an Egypt-specific shock that accentuated the outflow. Lending capacity dragged again, accounting for 10% of the estimated fall in private credit. Credit to the government continued to drain resources, accounting for 70–

80% of the estimated total decline. Reduced economic activity contributed around 15% of the total fall in credit.

The relative importance of these factors contrasts with that of the preceding capital inflow period, when credit to the government accounted for 54% of the estimated fall, while demand factors accounted for a similar percentage.

**Keywords:** Private credit; Egypt; Supply; Demand system; Disequilibrium model.

#### **1684. On Informality and Productivity of Micro and Small Enterprises: Evidence from MENA Countries**

Rana Hendy and Chahir Raouf Zaki Tadros

*International Journal of Entrepreneurship and Small Business*, 19: 438-470 (2013)

The objective of this paper is twofold. First, it aims to examine the impact of informality on productivity in the Middle East and North Africa (MENA) in order to identify existing barriers to formality. Second, it pinpoints factors that boost productivity of micro and small enterprises (MSEs). Using firm-level micro data from the Egyptian and Turkish MSEs surveys, we first find that firm's age, entrepreneur's gender, age and education have a significant impact on the probability of belonging to the informal sector. In addition, we find a negative effect of informality on productivity in both Egypt and Turkey. While this result is sensitive to the estimation method for the Egyptian case, it remains robust for the Turkish one. Consequently, there is a clear and significant productivity differential between formal and informal firms in Turkey, but not in Egypt.

**Keywords:** Micro and small enterprises; Mses; Micro enterprises; Productivity; Informal entrepreneurship; Middle east; Egypt; Turkey; Mena region; Small firms; Gender; Age; Education Levels.

#### **1685. Crowding Out Effect of Public Borrowing: the Case of Egypt**

Mona Esam Othman Fayed

*International Research Journal of Finance and Economics*, 107: 28-38, (2013)

The relationship between government borrowing and private credit is usually thought of as a negative one in the policy discussions and financial media. However, at least on a theoretical level, the relationship is ambiguous. In light of the recent excessive public borrowing from domestic sources in Egypt, a cointegration approach is used to investigate the relationship between public borrowing and private credit. The paper sheds light on the "quantity channel" of crowding out of private investment in Egypt by focusing on the volume of private credit. It concludes that government borrowing from the domestic banks crowds in private credit. This is due the strong risk diversification effect because of safe government assets in banks portfolios. However, this positive impact may be reversed in the case of a substantial increase in Treasury bill rate, as compared to lending interest rate. This leads to a crowding out effect.

**Keywords:** Government borrowing; Private investment; Private Credit; Domestic banking sector; Crowding out; Crowding in; Risk diversification effect.

#### **1686. An Empirical Analysis of the Impact of Mobile Broadband on Economic Growth in Emerging Economies**

Mona Farid Mohamed Badran

*International Research Journal For Finance and Economics*, 108: 144-157 (2013) IF: 0.409

Mobile broadband penetration in developing countries is expected to reach 8.5 percent by the end of 2011, up from 5.3 percent recorded in 2010 (ITU 2012). It is also expected that emerging regions will surpass the developed world in terms of the number of mobile broadband connections in first half of 2013. Thus the impact of mobile broadband on economic growth in these countries is a vital issue that needs to be vigorously investigated. The contribution of the present paper is in the estimation of this impact with a focus on emerging economies from 2008-2011. Results reveal the positive and highly significant impact of mobile broadband on economic growth in emerging countries. Our analysis shows that in emerging countries, 1 percent increase in mobile broadband per household would lead to approximately 7 percent increase in GDP growth rate, ceteris paribus. Adding additional controls, such as the Global Competitiveness Index and the Independent Regulator, the conclusion reveals that these controls are statistically insignificant.

**Keywords:** Mobile broadband; Growth; Emerging countries; Panel data; Endogeneity; Instrumental variables.

#### **1687. Access to Finance and Financial Problems of Smes: Evidence from Egypt**

Hala El-saied, Mahmoud Al-Said and Chahir Zaki

*Int. J. Entrepreneurship and Small Business*, 20: 286-309 (2013)

Financial services seem to be under-utilised by small and medium sized enterprises (SMEs) as only 50% are dealing with banks and benefiting from an improved access to finance. In addition, these firms still face several constraints in terms of access to finance. Using an extensive census that has been recently done by the Egyptian Banking Institute, we try to examine the determinants of the access to finance of SMEs in Egypt as well as the determinants of having banking problems. The main findings of this paper show that legal form, economic activity, labour, capital, and sales turnover have a significant effect on having banking facilities. In addition, we found that the smaller the firm, the higher the probability of having banking problems. We run a battery of sensitivity analysis tests and found that these results remain robust.

**Keywords:** Small and medium sized enterprises; Smes; Access to finance; Entrepreneurship; Financial problems; Egypt.

#### **Dept. of Political Science**

#### **1688. Elections of the People's Assembly, Egypt 2011/12**

Mazen Abd El-Rahman Hassan

*Electoral Studies*, 32: 370-374 (2013) IF: 0.887

For more than two months – from 28 November 2011 till mid-January 2012–50 million eligible Egyptian voters were called to



cast their votes in the country's first parliamentary election since former president Hosni Mubarak was forced to resign on 11 February 2011 in the face of unprecedented mass protests. Up for competition were the lower house's 498 seats. The transitional period's Constitutional Declaration, passed by a public referendum in March 2011, not only made that house – The People's Assembly (PA) – the main law-making body, but also charged it with selecting a 100-member committee that would be responsible for writing a new draft constitution. This new constitution was to be put to a referendum before being adopted. The election was thus the first point on a transitional timeline that included eventually holding a presidential election in May/June 2012, which would then seal the transfer of power from the Supreme Council of Armed Forces (SCAF) to a civilian government.

**Keywords:** Egypt; Elections; People's assembly.

### 1689. Institutional Factors Affecting Party Systems In New Democracies: Endogenous or Exogenous Predictors?

Mazen Abd El-Rahman Hassan

*Democratization*, 20: 668-692 (2013) IF: 0.598

A major criticism of studies using the institutionalist approach to explain party systems' characteristics in new democracies is the endogeneity argument.

This is that parties design the surrounding institutional context and hence that context cannot be assumed to affect the same party system that devised it. Using a sample of 31 new democracies, this article challenges this argument both qualitatively and quantitatively.

The central assumption is that even if politicians/parties are driven during periods of institutional design by selfish, vote-maximizing tendencies, it is still very difficult for them to design electoral institutions that guarantee their subsequent electoral victory.

Three justifications for the argument are developed. First, absence of reliable information on how different institutional frameworks would interact with the electoral strengths and weaknesses of one's party means that the knowledge necessary to pick the most favourable electoral institutions in the first years of transitions is rarely available. Second, decision-making processes at periods of institutional design are also shown to result in compromises between participating parties which prevent any single party from attaining all of its objectives. Finally, it is shown empirically that many parties that were significant during periods of institutional design suffered electorally under the same institutional settings that they presumably helped to design.

**Keywords:** Endogeneity; Institutions; Party systems; New democracies; Eastern europe; Latin america.

### 1690. Rethinking the New ENP: A Vision for an Enhanced European Role in Arab Revolutions

Sally Khalifa Isaac

*Democracy and Security*, 9: 40-60 (2013)

This article assesses the new release of the European Neighborhood Policy by the European Union in May 2011.

**Keywords:** Enp; EMP; Arab revolutions; Euro Arab relations

### Dept. of Statistics

### 1691. A Semiparametric Mixed Model Approach to Phase I Profile Monitoring

Abdel-Salam Gomaa Abdel-Salam Abdel-Salam, Jeffrey B. Birch and Willis A. Jensen

*Quality and Reliability Engineering International*, 29: 555-569 (2013) IF: 0.68

Profile monitoring is an approach in quality control best used where the process data follow a profile (or curve). The majority of previous studies in profile monitoring focused on the parametric (P) modeling of either linear or nonlinear profiles, with both fixed and random effects, under the assumption of correct model specification. More recently, in the absence of an obvious P model, nonparametric (NP) methods have been employed in the profile monitoring context. For situations where a P model is adequate over part of the data but inadequate of other parts, we propose a semiparametric procedure that combines both P and NP profile fits. We refer to our semiparametric procedure as mixed model robust profile monitoring (MMRPM). These three methods (P, NP and MMRPM) can account for the autocorrelation within profiles and treat the collection of profiles as a random sample from a common population. For each approach, we propose a version of Hotelling's T<sup>2</sup> statistic for use in Phase I analysis to determine unusual profiles based on the estimated random effects and obtain the corresponding control limits. Simulation results show that our MMRPM method performs well in making decisions regarding outlying profiles when compared to methods based on a misspecified P model or based on NP regression. In addition, however, the MMRPM method is robust to model misspecification because it also performs well when compared to a correctly specified P model. The proposed chart is able to detect changes in Phase I data and has easily calculated control limits. We apply all three methods to the automobile engine data of Amiriet al.5 and find that the NP and the MMRPM methods indicate signals that did not occur in a P approach.

**Keywords:** T<sup>2</sup> control chart; Industrial application; Model robust regression; Model misspecification; Model robust profile monitoring.

### 1692. The Performance of the Adaptive Exponentially Weighted Moving Average Control Chart with Estimated Parameters

Nesma Aly Mahmoud Saleh, Mahmoud A. Mahmoud and Abdel-Salam G. Abdel-Salam

*Quality and Reliability Engineering International*, 29: 595-606 (2013) IF: 0.68

The adaptive exponentially weighted moving average (AEWMA) control chart has the advantage of detecting balance mixed range of mean shifts. Its performance has been studied under the assumption that the process parameters are known. Under this assumption, previous studies have shown AEWMA to provide superior statistical performance when compared with other different types of control charts. In practice, however, the process parameters are usually unknown and are required to be estimated. Using a Markov Chain approach, we show that the performance of the AEWMA control chart is affected when parameters are estimated compared with the known-parameter case. In addition,

we show the effect of different standard deviation estimators on the chart performance. Finally, a performance comparison is conducted between the exponentially weighted moving average (EWMA) chart and the AEWMA chart when the process parameters are unknown. We recommend the use of the AEWMA chart over the ordinary EWMA chart especially when a small number of Phase I samples is available to estimate the unknown parameters.

**Keywords:** Aewma; Estimation effect; Markov chain; Average run length; Statistical process control.

### 1693. Efficient Use of a Two-Stage Randomized Response Procedure

Sally Farid Abdel ghafarAbdel fatah, Reda Mazloun and Sarjinder Singh

*Brazilian Journal of Probability and Statistics*, 27 (4): 608-617 (2013) IF: 0.442

Towards the search for improving the randomized response models used to estimate a population proportion bearing a sensitive characteristic, a new model, based on the use of a two-stage randomized response procedure, is proposed. The condition under which the proposed estimator is more efficient than the Odumade and Singh [Comm. Statist. Theory Methods 38 (2009) 439-446] estimator has been obtained. An empirical study has also been performed to examine the relative efficiency of the proposed estimator with respect to the Odumade and Singh [Comm. Statist. Theory Methods 38 (2009) 439-446] estimator. Moreover, the proposed estimator can be easily adjusted to be more efficient than the Warner [J. Amer. Statist. Assoc. 60 (1965) 63-69], Mangat and Singh [Biometrika 77 (1990) 439-442], Mangat [J. R. Stat. Soc. Ser. B Stat. Methodol. 56 (1994) 93-95] and Odumade and Singh [Comm. Statist. Theory Methods 38 (2009) 439-446] estimators.

**Keywords:** Simple random sampling; Estimation of proportion; Randomized response sampling; Two-stage randomized response procedure; Four decks of cards.

### 1694. Evaluation of Driver Perception-Reaction Time under Rainy or Wet Roadway Conditions at Onset of Yellow Indication

Ihab El-Shawarby, Abdel-Salam G. Abdel-Salam and Hesham Rakha

*Transportation Research Record Journal of the Transportation Research Board*, 2394: 18-24 (2013) IF: 0.442

The research presented in this paper characterizes the impact of a wet pavement surface and rainy weather conditions on driver perception-reaction time (PRT) at the onset of the yellow indication on the approach to a high-speed signalized intersection. An in-vehicle differential Global Positioning System was used in a controlled field environment. Three hundred eighty-four data records for all drivers who stopped at the onset of the yellow indication were available for analysis. The minimum time to intersection (TTI) ranged from 2.35 s to 5.71 s. Statistical analyses were used to quantify the effects of the TTI, grade (uphill or downhill), gender, and age (<40 years, 40 to 59 years, and ≥60 years) on driver PRT. The study demonstrated that driver PRT increases as TTI increases. A longer PRT was found when

vehicles traveled along an upgrade section, given that the driver was typically accelerating when the yellow indication was initiated. No gender differences were found in PRT, and no statistically significant differences were found between different age groups. Furthermore, the study demonstrated that driver PRT increased under conditions of a wet pavement surface and rainy weather as compared with clear weather conditions over the entire TTI range.

### 1695. Selection of the Ridge Parameter Using Mathematical Programming

Ramadan Hamed, Ali El-Hefnawy and Aya Farag

*Communications In Statistics – Simulation and Computation*, 42: 1409-1432, (2013) IF: 0.295

Ridge regression solves multicollinearity problems by introducing a biasing parameter that is called ridge parameter; it shrinks the estimates and their standard errors in order to reach acceptable results. Selection of the ridge parameter was done using several subjective and objective techniques that are concerned with certain criteria. In this study, selection of the ridge parameter depends on other important statistical measures to reach a better value of the ridge parameter. The proposed ridge parameter selection technique depends on a mathematical programming model and the results are evaluated using a simulation study. The performance of the proposed method is good when the error variance is greater than or equal to one; the sample consists of 20 observations, the number of explanatory variables in the model is 2, and there is a very strong correlation between the two explanatory variables.

**Keywords:** Mean squared error; Nonlinear programming model; Ridge regression.

### 1696. The Effect of Methods for Handling Missing Values on the Performance of the Mewma Control Chart

Doaa F. Madbully, Petros E. Maravelakis and Mahmoud A. Mahmoud

*Communications in Statistics – Simulation and Computation*, 42: 1437-1454 (2013) IF: 0.294

This article is concerned with the effect of the methods for handling missing values in multivariate control charts. We discuss the complete case, mean substitution, regression, stochastic regression, and the expectation-maximization algorithm methods for handling missing values. Estimates of mean vector and variance-covariance matrix from the treated data set are used to build the multivariate exponentially weighted moving average (MEWMA) control chart. Based on a Monte Carlo simulation study, the performance of each of the five methods is investigated in terms of its ability to obtain the nominal in-control and out-of-control average run length (ARL). We consider three sample sizes, five levels of the percentage of missing values, and three types of variable numbers. Our simulation results show that imputation methods produce better performance than case deletion methods. The regression-based imputation methods have the best overall performance among all the competing methods.

**Keywords:** Average run length; Estimation effect; Mewma control chart; Missing values.

### 1697. Estimating and Planning Step Stress Accelerated Life Test for Generalized Logistic Distribution under Type-I Censoring

Hanan Mohamed Aly Hasan and Salma O. Bleed

*International Journal of Applied Mathematics and Statistical Sciences*, 2: 1-16 (2013)

This paper presents estimation and derivation of optimum test plan for time step stress accelerated life test (SSALT). The maximum likelihood (ML) method is applied to estimate the unknown parameters of the generalized logistic distribution, to construct the asymptomatic confidence intervals, and to predict the value of the scale parameter and the reliability function under the usual conditions. The scale parameter of the lifetime distribution is assumed to be an inverse power law function of the stress level. Moreover, we consider minimizing the determinant of Fisher information matrix to obtain the optimum time of changing stress point, and also the optimum censoring time. Finally, numerical simulation is introduced.

**Keywords:** Accelerated life test; Step stress; Type-I censoring; Maximum likelihood estimation; Fisher information matrix; Optimum test plan; Generalized logistic distribution.

### 1698. Bayesian Estimation for the Generalized Logistic Distribution Type-II Censored Accelerated Life Testing

Hanan Mohamed Aly Hasan and Salma O. Bleed

*International Journal of Contemporary Mathematical Sciences*, 8: 969-986 (2013)

This paper develops Bayesian analysis for Constant Stress Accelerated Life Test (CSALT) under Type-II censoring scheme. Failure times are assumed to distribute as the three-parameter Generalized Logistic (GL) distribution. The inverse power law model is used to represent the relationship between the stress and the scale parameter of a test unit. Bayes estimates are obtained using Markov Chain Monte Carlo (MCMC) simulation algorithm based on Gibbs sampling. Then, confidence intervals, and predicted values of the scale parameter and the reliability function under usual conditions are obtained. Numerical illustration and an illustrative example are addressed for illustrating the theoretical results. WinBUGS software package is used for implementing Markov Chain Monte Carlo (MCMC) simulation and Gibbs sampling.

**Keywords:** Accelerated life test; Constant stress; Type-II censoring; Bayesian method; Generalized logistic distribution; Markov chain Monte Carlo (MCMC); Gibbs samples.

## Faculty of Commerce

### Dept. of Accounting

### 1699. Do Analysts Follow Emerging Economy Firms With Higher Intangible Assets? Empirical Evidence from Egypt

Mohamed Abdel Salam Sayed Elbannan

*Advances in Accounting*, 29: 50-59 (2013) IF: 2

This paper tests whether analyst coverage and effort are related to the level of intangible assets reported by Egyptian listed firms. Intangible assets represent increasingly important investments for many firms, but most of these assets are not capitalized under prevailing accounting standards. Analysts reduce the information asymmetry by examining both financial reports and other information. Many Egyptian firms today seek access to foreign capital. I hypothesize that the larger the potential intangible assets of firms the more analysts will cover these firms and pursue private information about these firms. Sample consists of 435 firm-year observations over the period 1999–2007, and intangible assets are measured using eight different firm- and industry-level proxies. Consistent with prior research, results suggest that coverage is significantly associated with firm R&D, industry advertising expenses, firm size, and trading volume. Results also suggest that analyst effort is a function of firm and industry-level R&D expenses and firm size.

**Keywords:** Ias 38; Analyst coverage; Intangible assets; Analyst effort, Egypt.

### Dept. of Business Administration

### 1700. He Mystique of Macro-boycotting Behaviour: A Conceptual Framework

Ehab Mohamed Abou Aish, Sally McKechnie, Ibrahim Abosag and Salah Hassan

*International Journal of Consumer Studies*, 37: 165-171 (2013)

In spite of the aim of the World Trade Organization and other international organizations to foster international trade and development by lessening protectionism agendas worldwide, there has been a rise in consumer-boycotting behaviour at a macro level involving campaigns directed against foreign products from countries embroiled in conflicts in international relations, rather than against products from individual companies perceived to have engaged in a domestic egregious act. While campaigning at this level is becoming a more effective tool for consumer protest, as it negatively affects both the boycotted countries' macroeconomics and companies' micro-competitiveness, consumer motivation to participate in macro-level boycotts has so far been overlooked in the boycotting literature. This paper examines consumers' behavioural intentions to participate in macro-boycotting campaigns within the context of an Arab country, which has recently witnessed a number of campaigns of this nature. Using the theory of planned behaviour, the findings of an exploratory qualitative study of Egyptian consumers offer insights into the motives and barriers to individual macro-boycott participation. Findings are discussed together with managerial implications.

**Keywords:** Boycotting; Consumer behaviour; International Marketing; Country of origin; Egypt.

### 1701. Leadership Teaching Impact on Tourism Students' Attitudes and Perceptions towards Leadership in Developing Economies: the Case of Egypt

Hatem Osman Aly Salem El-Gohary

*Journal of Hospitality and Tourism Education*, 25: 180-192 (2013)

This study aims to investigate the influence of leadership teaching in developing economies (i.e., Egypt) on tourism students' attitudes and perceptions toward leadership and their leadership skills. The study validates a conceptual model utilizing a positivist approach, in which quantitative data were collected based on a survey strategy through questionnaires targeting a sample of 1,046 Egyptian final-year tourism undergraduate students. The findings indicate that teaching leadership in tourism undergraduate courses in Egypt has an impact on students' attitudes and perceptions toward leadership as well as their leadership skills. This study adds to the extremely limited number of empirical studies that have been conducted to investigate leadership teaching by Egyptian universities and has great benefits for practitioners, researchers, and educators though providing a clearer view and deeper understanding of the issues related to teaching leadership in tourism undergraduate courses in a developing economy (Egypt).

**Keywords:** Leadership; Leadership teaching; Tourism schools; Undergraduate tourism courses; Developing economies; Egypt.

### 1702. Choice of Export Entry Mode by Developing Economies Smes: an Empirical Investigation of Egyptian Smes

Hatem Osman Aly Salem El-Gohary

*Journal of Economic and Administrative Sciences*, 29: 113-133 (2013)

**Purpose:** The purpose of this paper is to add to the accumulative knowledge in the field through investigating the different factors affecting the choice of export entry mode by Egyptian SMEs. An organised examination of the literature related to export entry modes by SMEs is discussed to provide and develop a clear understanding about the different factors affecting the choice of export entry mode by Egyptian SMEs. Such investigation will help in achieving a deep and reflective understanding of current exporting practises by Egyptian SMEs. The findings indicated that there is very few research studies in the literature related to the choice of export entry mode in developing countries in general and there was no published studies related to the choice of export entry mode in Egypt.

**Design/methodology/approach:** The paper reviews the published literature related to choice of export entry mode by SMEs in general and to SMEs in developing countries (e.g. Egypt) in particular. Based on this review and the results of two focus groups, the paper validates a conceptual model utilising a positivist research philosophy with a quantitative approach, in which quantitative data are collected based on survey strategy through questionnaires to address different levels of the study.

**Findings:** The findings showed that Egyptian SMEs owners, marketing and sales managers have a limited knowledge in relation to the different available export entry modes. The

findings also illustrated that SME internal factors, local market factors and target market factors have different impacts on the choice of export entry mode and that only small number of Egyptian SMEs conducted an effective and efficient export activities.

**Research limitations/ implications:** The paper will provide great benefits for entrepreneurs, policy makers, practitioners, researchers and educators though providing a clearer view and deep understanding for the issues related to different factors affecting the choice of export entry mode by Egyptian SMEs.

**Originality/value:** The paper adds to the extremely limited number of empirical studies that has been conducted to investigate different factors affecting the choice of export entry mode by Egyptian and Developing Economies SMEs. Depending on this research, researchers and scholars in the field can have a clearer view to set their attitude towards suitable future research studies which in turn will contribute to the related accumulated knowledge in the field.

**Keywords:** Developing countries; Export; Market entry mode; Sme; Export marketing; Structural equation modelling (SEM); Survey research.

### 1703. Factors Affecting Egyptian Consumers' Intentions for Accepting Online Shopping

Osama Abdel khalek Elansary and Ahmed Samir Roushdy

*The Journal of American Academy of Business, Cambridge*, 19(1): 191-201 (2013)

The objective of this research is to highlight and explore factors affecting consumers' intentions for accepting online shopping. It is important to find out variables that impede Egyptian consumers' intentions for accepting online purchase. The research approached a convenient sample out of the internet consumers' population.

An online survey was administered to collect data. The initial interviews with Egyptian online vendors and literature review showed that the important independent factors that affect Egyptian consumers' intentions for accepting internet shopping, as dependent variable, were:

- (1) the trust in website,
- (2) e-service quality,
- (3) consumers attitude toward online shopping and the consumers demographic characteristics as moderating variables. The research findings pointed out that all the demographic characteristics had significant impact on the consumers' intentions for online shopping, Men were more oriented for accepting online shopping compared to women, consumers aged between 36 to 45 years old were having the highest intentions to accept online shopping, Consumers experience with the internet was a very significant factor and was positively correlated with the intentions for accepting online shopping, graduates were having more intentions for online shopping compared with MBA/MSC and PhD holders, and Trust, e-service quality and Consumers attitude toward online shopping were positively and significantly correlated to consumers' intentions.

#### 1704. The Impact of Hard Discount Control Mechanism on the Discount Volatility of UK Closed-End Funds

Ahmed Fouad Saleh Salhin

*Investment Management and Financial Innovations*, 10: 68-76 (2013)

The impact of hard discount control mechanisms on the discount volatility of UK closed-end funds is investigated. Using ten years data, the paper starts by analyzing the main factors that influence the variation in discount volatility across the sector.

Standard deviation of net asset value returns, market value and the percentage of unquoted assets in the fund's portfolio are found to be highly significant. As a robustness test, the whole period is split into two five years periods which has no effect on the significance of the variables.

The analysis is then extended to show that closed-end funds which commit to a hard discount control mechanism tend to have lower discount volatility. However, the last finding is not highly significant suggesting that in general hard discount control mechanisms could be used more effectively to control discount volatility.

**Keywords:** Discount; Discount volatility; Closed-end funds; Buybacks; Discount control mechanism.

#### 1705. Customer Relationship Management (CRM) Practices by Small Businesses in Developing Economies: A Case Study of Egypt

Hatem Osman Aly Salem El-Gohary

*International Journal of Customer Relationship Marketing and Management (IJCRMM)*, 4: 1-20 (2013)

This study investigates the different factors affecting Customer Relationship Management (CRM) adoption by Egyptian Small Business Enterprises (SBEs).

A systematic review of extant literature on CRM adoption by SBEs was conducted both holistically, and specifically in developing countries (e.g. Egypt).

The study then progresses to validate a conceptual framework of CRM practices utilising a positivist research philosophy augmented with a quantitative approach, using questionnaire survey data. Findings indicated the response rate of Egyptian SBEs was low and that SBEs' owners, marketing managers and sales managers lack knowledge about CRM practice and the different tools or forms related to it.

The findings also illustrated that SBE internal and external factors have a different impact upon CRM adoption. The study provides stakeholders (including entrepreneurs, policy makers, practitioners, researchers and educators) with an invaluable insight and a deeper understanding of issues related to CRM adoption by Egyptian SBEs.

This research makes an important contribution to the current dearth of empirical studies in this field. Research outcomes consolidate and clarify several pertinent issues and provide peers with direction for future research.

**Keywords:** CRM adoption; Customer relationship management (CRM); Developing economies; Egypt; Small business enterprises (SBES).

*Dept. of Mathematics and Insurance*

#### 1706. The Impact of Company-Specific and External Factors on Corporate Risk Taking: the Case of Egyptian Insurance Companies

Mohamed Sherif and Mahmoud Mohamed Elsayed Ahmed

*Corporate Ownership and Control Journal*, 10(3)Continued-I: 211-226 (2013)

Using a two-way panel regression analysis with fixed and random effects and the generalized method of moment (GMM), we investigate the impact of both firm-specific and external factors on the risk taking of Egyptian insurance companies. We use hand-collected data of Egyptian insurance companies over the period from 2006 to 2011 to estimate the relationship between total and systematic risks as risk measures and the independent variables. Following Eling and Mark (2011) the extent of risk taking is quantified through variations in stock prices and these are explained by firm-specific and external factors. We find that differences in company size, interest rate level and economic development affect variations in stock prices. The analysis also highlights differences between the life and non-life insurers, with the non-life insurers exhibiting a higher level of risk (market and premium) and board independence. The pattern of results are qualitatively the same for non-life insurers but different for life insurers when we use GMM method.

**Keywords:** Risk management; Corporate risk taking; Corporate governance; Insurance industry; Egypt.



CAIRO UNIVERSITY

Publication  
in  
Book & Chapters

## Publication in Book/ Chapter

### Faculty of Economics and Political Science

#### Dept. of Economics

#### 1707. Interest-Rate Spreads and Efficiency in the Banking Market: A Panel Data Analysis for Egypt (1984- 2007)

Mona Esam Othman Fayed

Lambert Academic Publishing, (2013)

This study investigates the efficiency of financial intermediation in the Egyptian banking market by determining the variables affecting the behavior of the interest-rate spread in Egypt for the period 1984-2007. It is shown that the dynamic approach is more appropriate than the static one and has richer results. This is clear in its result about mean reversion of the interest rate spread as expected from theory, as well as the error correction term, which gave information about the adjustment of the spread towards its equilibrium level. The study concluded that, in the long-run, bank policies that attempt to lower the overhead costs would have a positive effect on the efficiency of the intermediation process. The same applies to monetary policies that reduce the levels of the reserve requirement ratio and discount rates to the minimum safe levels that still protect depositors' funds. Also, the increased level of competition between banks would cause a reduction in interest-rate spread. On the macroeconomic level, financial liberalization and stability of the exchange rate would result in desirable effects in this aspect. However, in order to improve the intermediation efficiency of the banking sector in the short-run, the following findings have to be taken into considerations. First, an increase in the liquidity ratio leads to a decline in the interest-rate spread. Second, relatively stable inflation rates have a desirable impact on the level of interest rate spread. Third, it is a stylized fact that the spread has a mean-reverting behavior. Finally, more than half of the disequilibrium between the spread and the explanatory variables is made up in the subsequent period. The dynamic econometric approach has the advantage of taking these short term characteristics and so yields richer results than the static modeling approach.

**Keywords:** Banks intermediation efficiency; Static approach; Dynamic approach.

#### Dept. of Political Science

#### 1708. The Transatlantic Partnership and the AU. Complementary and Coordinated Efforts for Peace and Security in Africa

Sally Khalifa Isaac

AU-NATO Collaboration: Implications and Prospects, Nato Defense College, (2013)

This chapter touches on transatlantic cooperation in Sub-Saharan Africa. Thereby, the author maps out the various methods transatlantic allies (the US and European states) support security in Africa and assesses the level of complementarity among the existing efforts. He then presents recommendations for future transatlantic support for African security, including the development of a coordinating body, joint engagement by

transatlantic actors with the AU and outreach to non-transatlantic actors.

**Keywords:** Au; NATO; Eu; African security.

#### 1709. Civil Society Activism in Authoritarian Regimes

Mustapha Kamel AL-Sayyid

*Civil Society in Syria and Iran. Activism in Authoritarian Contexts*, Lynne Rienner Publishers, ISBN: 978-1-58826-881-5 (2013)

This is the concluding chapter of the book. It takes a stand against the "Transitology" School which confines political change in non-democratic countries to what happens during the transition phase. It claims that political change does take place in fact under authoritarian regimes. It supports this claim by examining changes in economic policies and in the composition of ruling groups in both Syria and Iran which are taken as two persisting authoritarian regimes in the Middle East.

Changes of economic policies in particular are relevant because the two countries were not subjected to external pressures of international financial institutions and foreign donors which pushed other countries to do so. The chapter also stresses the point that some non-governmental organizations, described in other countries as civil society actors were quite active in these two countries but did not call for democratization. This observation should temper enthusiasm in certain political science writings which hail such organizations in all cases as champions of democracy.

**Keywords:** Civil society; Authoritarianism; Political change; Economic policy; Composition of the elite.

#### 1710. What Went Wrong with Mubarak's Regime?

Mustapha Kamel AL-Sayyid

*Egypt's Tahrir Revolution*, Lynne Rienner Publishers, (2013)

This is the first chapter in this book. The author strives to find out what went wrong with Mubarak's regime that led to its downfall in February 2011. Two sets of explanations are offered, one relating to the unintended consequences of certain policies and institutions of the regime, and the second were serious errors of judgement committed voluntarily by its leaders. Mubarak's regime could not be blamed for expansion of education, though of mediocre quality, facilitating access to mass media, allowing a good degree of freedom of expression and maintaining autonomy of the armed forces.

These policies and institutional features enhanced consciousness by citizens of corruption within the regime and made it possible for the armed forces to decide which side to back when collective protest exploded into a popular revolution. Having been in power for three decades, it persisted in paving the way for family succession at the presidency, flagrant rigging of elections and harsh repressive measures. It also underestimated the power of the demonstration effect of the Tunisian revolution. Being oblivious to the changing environment surrounding it, it could not escape the downfall.

**Keywords:** Family succession; Autonomy of armed forces; Tunisian revolution; Khaled said.

### **1711. Rule of Law, Ideology and Human Rights in Egyptian Courts**

Mustapha Kamel AL-Sayyid

*The rule of Law, Islam and Constitutional Politics in Egypt and Iran, State University of New York Press, ISBN: 978-1-4384-4597-7 (2013)*

Does independence of the judiciary vs. executive authority that does not hesitate to infringe on citizens' rights ensure protection of such rights. This chapter argues that while this is definitely a necessary condition, it is by no means sufficient. The wording of constitutional and legal provisions is often too general as to leave the judge with no immediate clue on how to apply the relevant rule, particularly in controversial cases, which is often the situation in human rights disputes. The chapter analyses this dilemma by examining contradictory rulings of Egyptian judges in litigation concerning freedom of belief, fair trial and economic and social rights.

**Keywords:** Independence of Judiciary; Freedom of belief; Fair trial; Economic; Social rights.

## **Faculty of Commerce**

*Dept. of Business Administration*

### **1712. Critical Perspectives on the Accounting for Intangibles**

Mohamed Abdel Salam Sayed Elbannan

*Lambert Academic Publishing, (2013)*

This book deals with the economic consequences of the current financial reporting requirements for Research and development. The book contains two studies that shed light on the impact of R&D reporting in one developed (USA) and one less developed economy (Egypt). In the first analysis, I find that R&D productivity increases cost of capital and information risk factors directly and indirectly through motivating managerial accounting discretion. High R&D expenditure firms incur 23.4 (216) basis points higher cost of debt (equity) compared to low R&D expenditure firms. Also, R&D firms have relatively higher weight for the discretionary component of accruals quality compared to the innate component in cost of equity capital calculations. In the second analysis, I find that the larger the potential intangible assets of firms the more analysts will cover these firms and pursue private information about these firms.

*Dept. of Business Administration*

### **1713. E-Marketing in Developed and Developing Countries: Emerging Practices**

Hatem Osman Aly Salem El-Gohary

*IGI Global, (2013)*

While e-marketing has emerged as an aid in allowing businesses to reach a broader audience, evolutions in computer science and technology have made its comprehension a bit more complex. E-Marketing in Developed and Developing Countries: Emerging Practices aims to create a deeper understanding of the policies and

practices that are involved in a successful e-marketing environment. This publication highlights the strategies and applications currently being used in both developed and developing countries; proving to be beneficial for entrepreneurs, policy makers, researchers, and students wishing to expand their comprehensive knowledge in this field.

### **1714. Social Media Marketing: Prospects for Marketing Theory and Practice on the Social Web**

Abeer A. Mahrous

*E-Marketing in Developed and Developing Countries: Emerging Practices, IGI Global, Chapter 4 :56 -58 (2013)*

This chapter aims at shedding the light on the rising global phenomena of social media marketing either in the B2C or in the B2B markets. Specifically, the chapter provides a review and synthesis of the prominent literature on social media marketing as well as examining the best practices of companies that use social media platform to achieve marketing objectives. A special emphasis is given on delineating the effect of social media use on customer buying behavior. The chapter concludes with useful insights and tips that can help companies to develop social media marketing strategies in order to boost brand visibility and enhance sales.

**Keywords:** Social media marketing; Social media use; Egypt; Emerging markets.

### **1715. New Marketing Applications for the Internet**

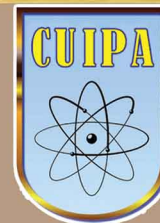
Hala Mohamed Labib

*E-Marketing in Developed and Developing Countries: Emerging Practices, IGI Global, (2013)*

The Internet is an important source for data and knowledge; hence, it currently plays a significant role in our daily lives. Internet applications have contributed tremendously in facilitating our work in terms of cost and effort cutting, expanding markets, changing the methods used to carry out activities, different applications, changing the quality required by customers, and consumer desires and behavior. Examples of these applications are online marketing, e-mail marketing, home business, and mobile marketing. E-research can also be considered as an Internet application. In fact, there are many terminologies related to this concept such as Internet research, online research, and Web research. This chapter provides an illustration of some of the new marketing applications of the Internet.



Cairo University



**(5)**

## **Humanity Sciences Sector**

**5-1 Faculty of Arts**

**5-2 Faculty of Archaeology**

**5-3 Faculty of Kindergarten**

**5-4 Faculty of African Research and Studies**



CAIRO UNIVERSITY

Publication  
in  
Journals



## Faculty of Arts

### Dept. of French Language and its Literature

#### 1716. L'habit Ne Fait Pas Le Révolutionnaire: L'histoire À Travers Le Prisme De L'ironie Dans Los Relámpagos De Agisto De Jorge Ibarguengoitia

Mona Saraya

*Inter-Textes*, 15: 91-101 (2013)

La révolution mexicaine a fait l'objet de plusieurs œuvres littéraires, Mais Los relámpagos de Agosto a particulièrement retenu notre attention étant donné qu'elle présente une réalité démythifiée, une écriture qui, par l'ironie, cherche à mettre à la surface ce qui est tu et occulté officiellement. Cette œuvre ne cherche pas à glorifier les héros de la Révolution, mais l'auteur dénonce leur envie de prendre en mains le pouvoir, les complots et les faveurs mutuelles. L'œuvre se présente comme étant les Mémoires d'un général nommé Arroyo qui les dicte à Ibarguengoitia.

C'est donc un texte qui appartient à la littérature de témoignage, autobiographique, réaliste, authentique et qui exprime le point de vue d'Arroyo sur les mêmes faits historiques mais distinct de celui des autres. C'est une parodie des autres Mémoires écrites par d'autres généraux comme Zapata, Orozco, Carranza ET Huerta. Nous distinguons entre ironie verbale basée sur l'hyperbole et la confrontation de deux idées contradictoires, et l'ironie situationnelle où il s'agit des tours que joue le Destin, de l'intertextualité et du collage.

**Keywords:** Ironie; Ibarguengoitia; Los relámpagos de agosto; Revoltuon mexicaine.

#### 1717. De La Caricature Egyptienne

Maha Ahmed Gad E-I Hak

*Ridiculosa*, 431-460 (2013)

Cette recherche se propose de suivre l'évolution du dessin de presse- en tant que produit culturel- en Egypte à travers l'analyse de quelques exemples représentatifs, depuis ses débuts, et jusqu'à nos jours.

Le rôle joué par les dessinateurs européens est indéniable dès la fin du XIX<sup>ème</sup> siècle, comme on peut le constater lorsqu'on étudie l'œuvre des dessinateurs étrangers auxquels les organes de presse égyptienne avaient eu recours: ceux-ci étaient aidés par les journalistes égyptiens responsables du texte, afin que le dessin de presse soit conforme au message à véhiculer, message appartenant à une autre culture que celle des dessinateurs. Peu à peu, la caricature devient une œuvre totalement égyptienne. Cet art est passé par de multiples formes, selon les dessinateurs et les écoles (usages différents de couleur, rapports texte /image variés...) L'étude de ces images dans leur contexte historique, permet de suivre l'évolution de cet art, de connaître les différentes influences européennes subies, ainsi que l'impact des transformations sociopolitiques du pays.

**Keywords:** Caricature; Dessins de presse égyptiens; Histoire culturelle.

#### 1718. Paris, Le Caire ET Sao Paulo A Travers Le Site De Tv5monde

Maha Ahmed El Said Gad El-Hak

*Dialogues et Cultures*, 59: 17-34 (2013)

Cette étude représente une analyse comparative de trois villes, Paris, Le Caire et Sao Paulo, à travers le site français TV5 Monde. Le corpus étudié figure dans la série intitulée "Les Cités du Monde". Ce site présente un exemple intéressant de dialogue interculturel, ainsi que de "dialogue" entre le texte et l'image. L'approche sémiotique basée sur l'analyse des discours verbal et iconique, permet de saisir le site en tant que produit culturel. Les habitants de chaque ville sont présentés dans leurs cadres spatio-culturels respectifs, ainsi que dans leurs rapports à la langue et à la culture française.

Des exemples représentatifs de différents types d'images- fixes telles que la photographie, et mobiles telles que les films d'animation- offrent un matériel important pour la découverte de ces villes, forgeant dans l'esprit des récepteurs une certaine représentation de chacune de ces villes et de ses habitants. A travers l'analyse des rapports complexes entre Soi et l'Autre, se dégage une facette importante de "la francophonie". Nous essayerons de cerner la "vision du monde" que véhiculent les divers discours sur le site de TV5 en général, ainsi que celui des "Cités du Monde".

**Keywords:** Image de paris; Le caire; Sao paulo, Francophonie; Tv5monde.

### Dept. of Japanese Language and its Literature

#### 1719. Listening Problems of Japanese Arabic Learners: With Special Emphasis on the Issue of /H/ and /H/

Hanan Rafik

*International Center for Japanese Studies*, 3: 121-134 (2013)

In this paper, I discuss the listening problems of Japanese Arabic learners focusing on the issue of /h/ and /h/. First, I introduce a contrastive phonetic analysis of Arabic and Japanese. Following this, I analyze learners' errors through listening investigations. These investigations show that the most difficult problems for Japanese Arabic learners are distinguishing between /t/ and /l/, /h/ and /h/, and pharyngealised and non- pharyngealised sounds.

In this paper, I also explain the phonetic feature of /h/ and /h/, and suggest an effective teaching methods of these two consonants for Japanese Arabic learners.

I conclude that despite the existence of /h/ in Japanese and the non-existence of /h/, /h/ is more difficult to the learner than /h/. I think that this result is due to the following reasons:

? The affection of Japanese allophone [çi] and on learners The affection of syllable final C and CC appearance in Arabic. So I suggest an allophone - level and syllable - level investigations in order to make the actual situation of Japanese Arabic learners even clearer for future studies.

**Keywords:** Japanese arabic learners; Phonetic feature of Arabic; Japanese; Learners; Errors.

**Dept. of Libraries, Documentation and Information**

**1720. A Proposed Knowledge Map for Library, Archives and Information Science from an Academic-Professional View Highlighting Cairo University**

Sherif Kamel Mahmoud Shaheen

*International Journal of Social Science*, 7(1): 110-129 (2013)

The paper aims at introducing a new Knowledge Map for library, archives and information science that can help library schools to evaluate their coverage of Academic courses syllabi topics and professional skills as well as their future needs for specialized academic disciplines.

The proposed Knowledge Map will be tested by applying it on the oldest library school in the Arab region, the department of library, archives and information technology at Cairo University on both the syllabi and Academic staff.

The study reviews several efforts concerning categorizing or classifying library, Archives and Information science, like: The JITA Classification Schema of Library and Information Science and some search tools like Portal: Library and Information science...etc. The proposed Knowledge Map will be used as a measurable tool to answer the following two questions: what is the subject distribution of courses provided at the library school? What is the specialization map for the faculty staff working at the library school? Also, the proposed knowledge map could be used to explore the balance of search efforts and trends in the library school.

The search efforts consist of both: Post graduate students' theses and dissertations subjects in addition to faculty staff published journal articles and conference papers.

**Keywords:** Knowledge map – cairo university; Dept. of library; Archives; It – specialization map – subject distribution of courses – knowledge sources classification – information theories.

**Dept. of Philosophy**

**1721. Galarza Y Su Amistad Con Intelectuales Egipcios\* Galarza and His Friendship with Some Egyptian Intellectuals**

Ahmed Abdel Halim Atteya

*Anaquel De Estudios Árabes*, 2471-79: 71-79 (2013)

Vicente Galarza y Pérez Castañeda (1878-1938), known in Egypt as the Count of Galarza, arrived in the country in 1905, he first engaged in archeological work and afterwards in teaching philosophy at the recently founded Egyptian University, for the years 1915-1921, and at the Higher School for Teachers Training, for the years 1921-1931. Through all these years he established friendship with personalities of the Egyptian political and intellectual life, and this article sheds light on the abovementioned relationship.

**Keywords:** Vicente galarza Y perez castañeda; Egyptian university; Theosophy.

**Dept. of Philosophy**

**1722. La Philosophie et La Religion En Egypte**

Ahmed Abdel Halim Atteya

*Dogma*, 2471-79: 1-22 (2013)

Au début, nous abordâmes la religion entre la philosophie et la modernité pour introduire l'analyse des écrits égyptiens sur la philosophie et la révolution. A notre avis, la révolution est la confirmation des principes de la modernité que l'humanité chercha à réaliser tout le long de son histoire. Le rationalisme, le progrès, la science, les Lumières, l'humanité, la liberté et la démocratie et la société humaine préoccupèrent la pensée philosophique. La révolution en général est l'incarnation des idéaux de la philosophie de la modernité.

**Keywords:** Révolution.

**Faculty of Archaeology**

**Dept. of Conservation**

**1723. Atherosclerosis across 4000 Years of Human History: the Horus Study of Four Ancient Populations**

Randall C. Thompson, Adel H. Allam, Guido P. Lombardi, L. Samuel Wann, M. Linda Sutherland, James D. Sutherland, Muhammad Al-Tohamy Soliman, Bruno Frohlich, David T. Mininberg, Janet M. Monge, Clide M. Vallodolid, Samantha L. Cox, Gomaa Abd el-Maksoud, Ibrahim Badr, Michael I. Miyamoto, Abd el-Halim Nur el-din, Jagat Narula, Caleb E. Finch and Gregory S. Thomas

*The Lancet*, 381: 1211-1222 (2013) IF: 39.06

**Summary Background:** Atherosclerosis is thought to be a disease of modern human beings and related to contemporary lifestyles. However, its prevalence before the modern era is unknown. We aimed to evaluate preindustrial populations for atherosclerosis.

**Methods:** We obtained whole body CT scans of 137 mummies from four different geographical regions or populations spanning more than 4000 years. Individuals from ancient Egypt, ancient Peru, the Ancestral Puebloans of southwest America, and the Unangan of the Aleutian Islands were imaged. Atherosclerosis was regarded as definite if a calcified plaque was seen in the wall of an artery and probable if calcifications were seen along the expected course of an artery.

**Findings:** Probable or definite atherosclerosis was noted in 47 (34%) of 137 mummies and in all four geographical populations: 29 (38%) of 76 ancient Egyptians, 13 (25%) of 51 ancient Peruvians, two (40%) of five Ancestral Puebloans, and three (60%) of five Unangan hunter gatherers (p=NS). Atherosclerosis was present in the aorta in 28 (20%) mummies, iliac or femoral arteries in 25 (18%), popliteal or tibial arteries in 25 (18%), carotid arteries in 17 (12%), and coronary arteries in six (4%). Of the five vascular beds examined, atherosclerosis was present in one to two beds in 34 (25%) mummies, in three to four beds in 11 (8%), and in all five vascular beds in two (1%).

Age at time of death was positively correlated with atherosclerosis (mean age at death was 43 [SD 10] years for mummies with atherosclerosis vs 32 [15] years for those without;

$p < 0.0001$ ) and with the number of arterial beds involved (mean age was 32 [SD 15] years for mummies with no atherosclerosis, 42 [10] years for those with atherosclerosis in one or two beds, and 44 [8] years for those with atherosclerosis in three to five beds;  $p < 0.0001$ ).

**Interpretation:** Atherosclerosis was common in four preindustrial populations including preagricultural huntergatherers. Although commonly assumed to be a modern disease, the presence of atherosclerosis in premodern human beings raises the possibility of a more basic predisposition to the disease.

**Funding:** National Endowment for the Humanities, Paleocardiology Foundation, The National Bank of Egypt, Siemens, and St Luke's Hospital Foundation of Kansas City.

**Keywords:** Mummies; Ancient populations; Atherosclerosis; CT scans.

#### 1724. in-Vitro Studies on Wood Degradation in Soil by Soft-Rot Fungi: *Aspergillus Niger* and *Penicillium Chrysogenum*

Safa Abdel-Kader Mohamed Hamed

*International Biodeterioration and Biodegradation*, 78: 98-102 (2013) IF: 2.059

This paper focuses on the biodegradation of wood by two soft-rot fungi, *Aspergillus niger* and *Penicillium chrysogenum*, in soil which was artificially infested. The structural changes of pine and sycamore wood were evaluated by scanning electron microscope (SEM). Surprisingly, soft-rot fungi tolerate low moisture to cause extensive decay in the wood samples. The micrographs showed differences in hyphae colonization and wood degradation patterns between soft-rot species under this study; *A. niger* produced soft-rot decay type I (cavity formation) and soft-rot decay type II (erosion), while *P. chrysogenum* caused only soft-rot decay type II.

**Keywords:** Pine wood; Sycamore wood; *Aspergillus niger*; *Penicillium chrysogenum*; Soil; SEM.

#### 1725. Characterization of *Streptomyces* Isolates Causing Colour Changes of Mural Paintings in Ancient Egyptian Tombs

M. E. F. Abdel-Halim, A. A. Sakr, M. F. Ali, M. F. Ghaly and C. Sohlenkamp

*Microbiological Research*, 168 (7): 428-437 (2013) IF: 1.993

Paintings in ancient Egyptian tombs often suffer colour changes due to microbial growth and colonization. *Streptomyces* strains were isolated from mural paintings of Tell Basta and Tanis tombs (East of Nile Delta, Egypt) and were identified using biochemical and molecular methods. The 16S rDNA sequences data indicated that isolated strains were closely related to *S. coelicolor*, *S. albidofuscus*, *S. ambofaciens*, *S. canarius*, *S. parvulus*, *S. corchorusii*, *S. albidofuscus* and *S. nigrifaciens*. It could be shown that *Streptomyces* strains are involved on a large scale in the colour changes of paintings and stone support by producing a wide range of metabolites such as acids (oxalic, citric and sulphuric acids), biopigments of melanin, carotenoids, and hydrogen sulphide.

**Keywords:** Azurite; Malachite; Mural paintings; *Streptomyces*; Tell Basta.

#### 1726. From Ptolemaic to Modern Inked Linen Via Laser Induced Breakdown Spectroscopy (LIBS)

Harby E. Ahmed and Olodia Aied Nassef

*Analytical Methods*, 5: 3114-3121 (2013) IF: 1.855

Laser Induced Breakdown Spectroscopy (LIBS) has been applied to inked linen textile that belongs to a mummy's linen wrapping dated back to the Ptolemaic period (330 BC: 30 AD). The rarity of the ancient archaeological piece introduced in this study has suggested the use of a model sample of currently manufactured linen for comparison purposes and optimization of the experimental conditions. The Nd:YAG laser operating at both wavelengths 532 and 1064 nm as our excitation source along with an Echelle spectrometer with an intensified charge-coupled device detector has been employed. Under the experimental conditions adopted throughout this work, the use of the visible 532 nm laser produced poorer S/B when compared to that produced by a 1064 nm laser which suggests the production of colder plasma leading to less atomization of the ablated material. Additionally, the 532 nm wavelength shows a negative behavior in ablating ink writings which was visually clear. Although, LIBS qualitative results are so comparable to that of SEM-EDX, some elements were detected only by LIBS which could be attributed to the irregularity of ink on linen. Thus, the capabilities of LIBS should be extensively exploited to the in situ measurements and analysis of archaeological ink and fabrics.

**Keywords:** LIBS; Textile; Historical; EDX.

#### 1727. Chemical Cleaning of Soiled Deposits and Encrustations on Archaeological Glass: A Diagnostic and Practical Study

Ramadan Awad Ramadan Abd-Allah

*Journal of Cultural Heritage*, 14 (2): 97-108 (2013) IF: 1.176

The aim of this study is practically to establish a chemical strategy for cleaning soiled deposits and encrustations on archaeological glasses. Investigations were performed on a series of Roman glass samples (Fragments and complete objects) coming from different excavations in northern Jordan. The chemical composition of the glass samples was determined by XRF analysis technique, whereas XRD and EDX methods were used to determine the mineralogical and elemental composition of the soiled deposits and encrustations on the glass surfaces. Furthermore, SEM examination and optical assessment were performed before and after cleaning glass. The glass samples were subjected to different cleaning protocols such as Calgon (Sodium hexametaphosphate), EDTA (Ethylenediaminetetraacetic acid) at different pH values, citric and tartaric acids and piranha solution (a solution of sulphuric acid and hydrogen peroxide). Sepiolite poultices soaked by chemical agents were the most suitable methods used for applying chemical solutions on the glass surface. It can be concluded that EDTA is generally accepted as the most effective chelating agents recommended for cleaning encrustations on durable glass. It was more effective and safe at neutral pH with low concentrations around 5-7 %. The calcareous crusts can safely be removed by using a piranha solution. Citric and tartaric acids appeared a moderate efficiency on cleaning weathered and stable glass. Calgon has a tendency to damage corroded and iridescent surfaces, and should be avoided when cleaning weathered glass.

**Keywords:** Archaeological glass; Soiled deposits; Encrustations; Examination; Chemical cleaning.

### 1728. Efficiency of Antibiotics and Gamma Irradiation in Eliminating Streptomyces Strains Isolated from Paintings of Ancient Egyptian Tombs

Mahmoud E. F. Abdel-Haliem, Mona F. Ali, Mohamed F. Ghaly and Akmal A. Sakr

*Journal of Cultural Heritage*, 14 (1): 45-50 (2013) IF: 1.176

Forty-six Streptomyces strains were isolated from paintings and stone surfaces from Tell Basta and Tanis tombs (80 km south-east Cairo, Egypt). Eight of these strains were selected to determine their sensitivity against 13 antibiotics. In general, high levels of resistance could be observed. Gentamycin, spiramycin and doxycycline were the most effective antibiotics against the majority of strains under study. Due to the observed antibiotic resistances, gamma irradiation was studied as a possible alternative to inhibit microbial growth. Isolated bacteria were exposed to different doses of gamma irradiation (5, 10, 15, 20 and 25 kGy). The growth of all Streptomyces isolates except *S. canarius* was completely inhibited at 25 kGy. The applied doses of gamma irradiation did not cause any observable alterations or colour changes to pigments and binding media (Arabic gum, animal glue and egg-yolk) used in the paintings.

**Keywords:** Azurite; Gamma irradiation; Hematite; Lamp black; Limonite; Malachite; Oserkon II; Streptomyces; 16S Rna gene; Tanis; Tell basta.

### 1729. Possibilities Application of Nanoscience and Nanotechnology in Conservation of Archaeological Wood: A Review

Safa Abdel-Kader Mohamed Hamed

*Jokull Journal*, 63 (12): 9-19 (2013) IF: 1

This article reviews the application of nanotechnology in the conservation of archaeological wood based on their structure and deterioration. Nanotechnology can be applied in deacidification, cleaning, and consolidation of archaeological wood. Soft Nanoscience (microemulsions and micelles) can be used to remove contaminants and polymers, used in previous treatments, and to clean the wood surface. Hard Nanoscience (hydroxides nanoparticles in non-aqueous solvents) can be applied to deacidify wood of ancient shipwrecks, for example. The author highlights ways of treatments that were applied to other cultural heritage items and could be applied to archaeological wood but not examined yet, especially in the case of polychrome wood according to its structure.

**Keywords:** Archaeological wood; Nanotechnology; Deacidification; Cleaning; Consolidation.

### 1730. Studying Irradiation Homogeneity in Light Aging for Historical Textile

Khaled Elnagar, Sameh M. Reda, Harby E. Ahmed and Shady Kamal

*Fibers and Polymers*, 14: 1581-1585 (2013) IF: 0.912

Instrumental light aging is one of the most important tools for restoration and conservation of historical textiles. It is used in testing stability of conservation materials, in addition to its lightening effect during the presentation in the museums. Light fading is an important tool for preparing the aged textile and other polymeric samples especially for archaeological conservation applications. Many fadometers do not give homogeneous exposure for all sample's areas. This work studies the color changes of silk fabric dyed with turmeric (*Curcuma longa* L.) mordanted with alum or ferric sulfate. Color change was studied for the exposure periods ranged from five to hundred hours. Three positions of different irradiance levels were measured on the same sample namely (bottom, middle and upper). Individual color change for each position was recorded and studied. The results showed that there is non-homogeneous irradiance distribution due to different positions in fadometer or mordant used.

**Keywords:** Light aging; Conservation; Silk; Mordant; Turmeric.

### 1731. Analytical Study of Coptic Wall Paintings in Egypt, El-Ba2939awat Necropolis, Kharga Oasis: A Case Study

Ahmed Abo El-Yamin, Hussein Marey Mahmoud and Atef Brania

*Periodico Di Mineralogia*, 82 (1): 25-40 (2013) IF: 0.776

The present study aims to analyze Coptic wall paintings dating back to the late third/early fourth to the seventh century AD from El-Bagawat necropolis, Kharga Oasis, Egypt. The analysis was carried out by means of optical microscopy (OM), scanning electron microscopy (SEM) equipped with an energy dispersive X-ray detector (EDS), X-ray diffraction analysis (XRD), Fourier transform infrared spectroscopy (FT-IR) and the petrographic examination. The results allowed the identification of the stratigraphic analysis of the wall paintings, their chemical composition and the painting technique employed. On the other hand, the results permitted a comparison between the Coptic wall paintings and those from the Pharaonic, Ptolemaic and Roman periods. The obtained results will enrich our knowledge concerning some painting materials from an important example of the Coptic art in Egypt.

**Keywords:** Coptic wall paintings; El-bagawat necropolis; Kharga oasis; SEM-EDS; XRD; FT-IR; Green earth.

### 1732. Raman Microscopic Analysis of a Multi-Pigmented Surface from the Theban Tomb (TT277), Luxor, Egypt

Hussein Hassan Marey Hassan Mahmoud

*Acta Physica Polonica A*, 123 (4): 782-785 (2013) IF: 0.531

In this study, the Raman microscopy technique was employed for identifying a multi-pigmented surface from the wall decorations of the Theban tomb (TT277), Luxor, Egypt. The Raman spectra were collected in the near infrared excitation line (785 nm Linefocus) of a diode laser source which enables mapping scan of specific areas in only few minutes. The microstructure and microanalysis of samples were performed by the aid of an environmental scanning electron microscopy coupled with an energy dispersive X-ray analysis system. The identified pigments were red ochre (haematite), yellow ochre (goethite) and carbon

black (from a vegetable origin). Traces of anatase were found in the yellow coloured areas which can be a contaminant in natural iron oxide deposits. The ground layer was identified as anhydrite with minor amounts of calcium carbonates detected in some samples. The results showed the capability of the Raman microscopy for direct and fast identification of multi-pigmented surfaces in wall paintings and other decorative objects.

**Keywords:** Theban tombs; Raman microscopy; Pigments.

### 1733. Application of CaCo3-Nanoparticles for Consolidation of Damaged Coptic Plasters in Egypt

Hussein Marey Mahmoud and Ayman El-Midany

*European Journal of Science and Theology*, 9 (3): 187-196 (2013) IF: 0.389

Egypt has the largest fortune of cultural heritage materials of different kinds which record the history of the Egyptian civilization. These materials are subjected to different deterioration factors causing several damages to the inner matrix as well as disfiguring the appearance of these materials. The present study aims to prepare and evaluate CaCO<sub>3</sub>-nanoparticles to consolidate damaged Coptic plasters collected from the monastery of Saint Simeon (Deir Anba Hatre), Aswan, Upper Egypt. The evaluation of the consolidation process was performed using scanning electron microscopy (SEM) in addition to measuring the physical and mechanical properties of the samples. The obtained results showed that the consolidation with CaCO<sub>3</sub>-nanoparticles was beneficial in improving the physical and mechanical properties of the treated samples.

**Keywords:** Coptic plasters; Saint simeon monastery; CaCO<sub>3</sub>-nanoparticles; Consolidation; SEM-eds.

### 1734. Color Alteration of Ancient Egyptian Blue Faience

Abubakr Moussa and Mona Fouad Ali

*International Journal of Architectural Heritage: Conservation, Analysis, and Restoration*, 7 (3): 261-274 (2013) IF: 0.37

Four different colored faience tiles were found in South Tomb of King Djoser in Saqqara, Egypt. The tiles suffer from various deterioration aspects, mainly color alteration, which occurred as a result of the reaction between present salts and the free copper ions of blue faience and changing it into greenish blue, dark green, and light green. The aim of this work is to study the color change phenomenon of ancient Egyptian blue faience, used in the construction and decoration of the walls in the south tomb of King Djoser-Saqqara by means of light optical microscope (LOM), x-ray diffraction spectroscopy (XRD), and scanning electron microscopy/energy dispersion X-ray (SEM EDX) analysis. The obtained results revealed that the pigment material cuprorivaite (CaCuSi<sub>4</sub>O<sub>10</sub>) was used in glazing the tiles and imparted the blue color. Other blue pigment materials were used in conjunction with Egyptian blue such as turquoise [CuAl<sub>6</sub>(PO<sub>4</sub>)<sub>4</sub>(OH)<sub>8</sub>·4H<sub>2</sub>O]. The results indicate that the first trials for producing Egyptian blue were not in the 4th dynasty as it has been declared by previous authors.

**Keywords:** Faience; X-ray diffraction (xrd) analysis; Scanning electron microscopy/energy dispersion X-ray (sem edx) analysis; Egyptian blue; Turquoise; Discoloring.

### 1735. A New Method for Cleaning Oil Paintings Using Zinc Oxide Nanoparticles by Osama El-Feky and Mohammad Hassan

By Osama El-Feky and Mohammad Hassan<sup>29</sup>

*E-Conservation*, 25: 115-126 (2013)

The cleaning of oil paintings using traditional methods, namely mechanical and chemical cleaning, is a critical process that presents serious risks to the painting such as chemical reactions with the paint and ground layer compounds. These cleaning techniques require a high level of training and experience. A new method for cleaning and removal of stains from oil paintings based on laboratory prepared zinc oxide nanoparticles suspended in distilled water at 0.5% concentration (w/v %) was investigated to overcome the disadvantages of the traditional methods. The nanoparticles suspension can be used for removal of soot, grease, wax, and house fly specks from oil paintings by covering the stains with the suspension and then subjecting it to UV radiation at 365 nm for a certain period of time. The stains can then be easily removed using a cotton swab. This new method allows a high control of the areas to be cleaned with no secondary effects.

### 1736. Investigation of Historical Egyptian Textile Using Laser – Induced Breakdown Spectroscopy (LIBS)- a Case Study

Harby Ezzeldin Hassan Ahmed

*Journal of Textiles Apparel. Technology and Management*, 8: 1-10 (2013)

This paper evaluates the use of Laser Induced Breakdown Spectroscopy (LIBS) for the analysis of Egyptian historical textiles. The chemical information provided by LIBS, as well as the detrimental effects of laser-induced damages were studied as a function of laser energy and the number of laser pulses used for analysis. The main elements in the metal fibers were Cu, Au, Ag, Cr, Mn, Zn and Ca. The results obtained through LIBS were confirmed by Scanning Electron Microscopy coupled to Energy-dispersive X-ray spectroscopy (SEM-EDX). The damage of the metal threads after LIBS application was monitored by SEM and Optical Microscopy. The textile samples used were obtained from the museum of the Faculty of Applied Arts, Helwan University, Egypt.

**Keywords:** Textile; Metal fiber; Historical; Libs; Sem; Edex; Elementals.

### 1737. Electrical Resistance Tomography (ERT) Subsurface Imaging for Non- Destructive Testing and Survey in Historical Buildings Preservation

Sayed Mohamed Sayed Mohamed Hemeda

*Australian Journal of Basic and Applied Sciences*, 7 (1): 344-357 (2013)

The paper presents the application of non-pervasive electrical resistance tomography (ERT) subsurface imaging surveys for the rehabilitation and strengthening of Habib Sakakini's Palace (1897 AC) in Cairo, Egypt. The use of several high-resolution geoelectrical methods derived from the fieldsurvey techniques



proved to be very effective in the Non-Destructive Testing and survey of architectural heritage. In particular the application of a tomographical approach allowed us to obtain subsurface images of the cross-sections of the bearing soil with complex layers and structures that clearly show the presence of eventual anomalies. Some experiments with geoelectrical tomographic techniques gave very interesting results also when working on historical buildings that seemed a hostile environment for geoelectrics. This is very interesting also due to the velocity of the measurements and of the data processing: this means short times and low costs. The use of microgeophysical techniques offers many advantages with respects to some "classical" techniques under different angles: velocity of execution, non-pervasiveness and costs. The results of ERT are compared to ground penetrating radar (GPR) – they are just as detailed but are often easier to interpret, at a lower cost.

**Keywords:** El-sakakini palace; Cairo; Electrical resistance tomography (ERT); Architectural heritage preservation; Non-Destructive testing; Survey.

### 1738. Geotechnical Characterization of Sakakini, S Palace Stones and Other Construction Materials, Cairo- Egypt

Sayed Mohamed Sayed Mohamed Hemeda

*Geomaterials*, 3 (1): 38-46 (2013)

The understanding of the geotechnical problems and failure mechanisms of stone structures of Sakakini palace (1897 after century) entails a comprehensive study on the mechanical behaviour of the stones and other construction materials. In addition to micro analysis, geological and geomorphologic interests, several investigations on stone deterioration and engineering geology were performed. First phase included more sophisticated techniques, which provided additional information on particular aspects of site deterioration and it included laser induced breakdown spectroscopy (LIBs), electron probe micro analysis, micro XRD and XRF analyses, scanning electron microscope analysis coupled with EDX probing, transmission electron microscopy and grain size distribution analysis, permeability and pore size distribution of stone, mortars, core binders and other construction materials. Second phase included the determination of mechanical properties of building stones, such as compressive strength, modulus of elasticity, tensile strength, and shear strength. To arrive at reliable values for these properties, a suitable number of samples should be extracted, prepared for testing, and properly tested. The test results are then analyzed to establish the investigated stone properties. The testing program includes extracting seven cylindrical cores from the basement stone walls of Sakakini's mansion in downtown Cairo. The cores are extracted using rotary cylindrical diamond blade coring machine.

The top and bottom surfaces of every core were prepared to be flat circular surfaces perpendicular to the vertical axis of the core. Because the palace is museum and attractive places for the tourists, core sampling could be carried out only at a limited number of locations under official permission. For the purpose, cylindrical specimens with a diameter of 42 - 44 mm and height of 90 - 100 mm, prepared by the use of a core drilling machine and some collected blocks from the archaeological site under investigation were taken to determine the bulk structure, physical, short and long-term mechanical properties of the stone

and other construction materials in the laboratory. A number of specimens prepared from these blocks were employed for testing. Furthermore, limitation due to the number of blocks was overcome by the determination of the in situ characteristics of the stones by Schmidt hammer tests, geo-tomographic investigations and rock mass classification on some stone rock structures where testing has been permitted. The objectives of the study are to provide a characterization of micro structures and the mechanical properties of the stones of Sakakini's Mansion; describe the required testing plan; describe the test results and conclude the values of the basic mechanical properties of the building stones. The following sections provide detailed descriptions of the steps taken to achieve the objectives of the study. The purpose of the present research is to provide recommendations regarding the strengthening and the safety of architectural heritage under long and short-term loading. For this purpose, a set of experimental tests and of advanced numerical analyses are to be carried out.

**Keywords:** Architectural heritage; Sakakini palace; Geotechnical; Investigations; Mechanical properties; Stone deterioration; Laser induced breakdown spectroscopy (LIBS).

### 1739. Laser Induced Breakdown Spectroscopy and Other Analytical Techniques Applied on Construction Materials at Kom El-Dikka, Alexandria, Egypt

Sayed Mohamed Sayed Mohamed Hemeda

*Mediterranean Archaeology and Archaeometry*, 13 (2): 103-119 (2013)

In order to retrofit and conserve the archeological site of Kom El-Dikka, Alexandria, Egypt, a systematic study of construction materials was applied. The samples of mortars, brick and limestone samples have been taken from the remains of ancient Auditorium, houses and baths (300 AD).

The analytical techniques showed that different qualities of mortars and brick were used for different purposes. Almost impermeable hydraulic mortars were found in contact with draining canals.

This was the initiative to start combining advanced analyses of mortars and other construction materials by determining their physical and chemical characteristics in order to find the textural features and the alterations of the structure and understand their resistance to weathering. Here samples were analyzed and examined by using Laser induced breakdown spectroscopy (LIBS), SEM attached with EDX, Polarizing microscope, Optical microscopy in transmitted polarized light, XRD, DTA-TGA, Grain Size Distribution, Pore Media Characterization, while some limestone and mortars were tested, to determine their uniaxial compressive strength, porosity, water absorption, proportion of constituents of cement mortars, and durability. The paper focuses on the interrelation of findings from the above-referred examinations. The use of reactive siliceous materials in combination with lime, as well as, the excellent gradation of aggregates used seems to be the ancient protocol of the good performance of the ancient mortars. It is concluded the high skillfulness of ancient masons of the classical period in construction materials.

**Keywords:** Kom el-dikka; Oolitic limestone; Ancient mortars, Brick; Durability; Protection; Libs; Analytical.

#### 1740. Assessment of Commonly Used Cleaning Methods on the Anatomical Structure of Archaeological Wood

Safa Abdel-Kader Mohamed Hamed, Mona Fuaad ALI and Nesrin Mohamed Nabil Elhadidi

*International Journal of Conservation Science*, 4: 153-160 (2013)

This study was conducted to diagnose and evaluate the effect of commonly used cleaning methods in Egypt on the anatomical structure of archaeological wood samples. Beech wood samples, which were taken from anonymous mashrabia, have been cleaned mechanically and chemically, then a scanning electron microscope (SEM) study was undertaken, to monitor any significant structural changes in wood samples due to cleaning processes. SEM data, however, show that cleaning procedures, both mechanical and chemical, affect the anatomical structure of wood, and do not achieve the best result. The main problem is that the effect of reagents cannot be easily removed from the wood structure. Ethyl alcohol proved to have the minimal effect on the wood structure in this study.

**Keywords:** Archaeological wood; Mechanical cleaning; Chemical cleaning; SEM.

#### 1741. Proactive Investigation Using Bioagents and Fungicide for Preservation of Egyptian Stone Sarcophagus

Maisa M. Mansour

*Journal of Applied Sciences Research*, 9 (3): 1917-1930 (2013)

A stone sarcophagus (excavated in 1992) from Behbeit el-Hager, El-Gharbieh, Egypt was selected for this study. Petrographic microscope (PM), Light microscope (LM), X-Ray Diffraction analysis (XRD), Scanning electron microscope (SEM), polymerase chain reaction (PCR), and ribosomal RNA (rRNA) were used to identify the stone composition and to measure the growth of the microorganisms and their effect on the stone composition. Polarizing, light and scanning electron microscopes were used to study the stone thin sections. The results achieved identified nine different fungal species belonging to *Cladosporium cladosporioides*, *Paecilomyces variotii* and *Curvularia lunata*. Moreover, *Bacillus megaterium* bacteria isolates were also determined. The deep penetration of the microorganisms through the stone and the resultant deterioration was investigated. *Cladosporium cladosporioides* colonies and hyphae penetrated through the pores and caused pitting of the stone structure causing deep pits to a depth of 216.5 m. Elemental analysis of the deteriorated stone Sarcophagus by fungi and bacteria indicated the decrease in calcium and magnesium. *Bacillus megaterium* led to the loss of calcium (from 57.6 to 50.0%) and the buildup of nitrogen in the deteriorated stone. Experimental studies on biocide application on the stone Sarcophagus were also carried out using essential oils (Tea tree oil, Lavender oil, Rosemary oil and Origanum oil), plant extracts (*Synadenium grantii* and *Codiaeum variegatum*) and fungicide (Tecto (Thiabendazole) 50% SC and Option 40% (cymoxanil WDG) in different concentrations.

The results of this study, indicated that Origanum oil in a concentration as low as 0.125% (v/v) successfully inhibited the fungal growth of the treated stone, while *Synadenium grantii* inhibited the growth at 4% wt/v and 100 ppm of Option 40%. The

antimicrobials used, were in compliance with our case study and with the proposed preservation solutions. All treatments were esthetically acceptable for archaeological objects, for instances; being colorless, transparent and safe. Furthermore, they were fairly stable and did not encounter any colour change with the time of experiment.

**Keywords:** Stone sarcophagus; Limestone; Colonization; Penetration; Microorganism; Biocides.

#### 1742. Spectroscopic Investigation on Paint Layers of Sabil-Kuttab Umm 'Abbas ceiling, Mohammed Ali Era in Cairo, Egypt: identification of unusual pigment and medium

Mona Hussien Abdel-Ghani

*Egyptian Journal of Archaeological and Restoration Studies "EJARS"*, 3: 95-105 (2013)

A comprehensive study has been undertaken into Sabil-Kuttab Umm 'Abbas ceiling (1867AD / 1284 H) in Cairo Egypt. The study included both organic and inorganic constituents comprising; the pigments, the paint media, the gold layer and the white ground layer. The analytical instruments chosen for the study were Raman microscopy, Fourier transform infrared spectroscopy coupled with attenuated total reflection (FTIR-ATR) and optical microscopy.

The pigments identified were ultramarine blue  $\text{Na}_6[\text{Al}_6\text{Si}_6\text{O}_{24}]$  Sn, indigo ( $\text{C}_{16}\text{H}_{10}\text{N}_2\text{O}_2$ ), Vermilion ( $\alpha\text{-HgS}$ ), red ochre ( $\text{Fe}_2\text{O}_3 + \text{clay} + \text{silica}$ ), barium white ( $\text{BaSO}_4$ ), lead white ( $2\text{PbCO}_3 \cdot \text{Pb}(\text{OH})_2$ ) and cobalt yellow ( $\text{K}_3[\text{Co}(\text{NO}_2)_6]$ ). The chromate mineral, hemihedrite ( $\text{ZnPb}_{10}(\text{CrO}_4)_6(\text{SiO}_4)_2\text{F}_2$ ), was detected for the first time as an artistic pigment in this study. The paint media revealed were animal glue admixed with linseed oil and mastic resin. The detection of mastic resin as a paint medium in Egyptian paintings is of interest. The white Ground layer was found to consist of calcium sulfate dihydrate ( $\text{CaSO}_4 \cdot 2\text{H}_2\text{O}$ ) and calcite ( $\text{CaCO}_3$ ) admixed with animal glue.

**Keywords:** Sabil; Kuttab; Umm abbas; Mohammad ali Era; Raman spectroscopy; FTIR.

#### 1743. Biodeterioration of Binding Media in Tempera Paintings by Streptomyces Isolated from Some Ancient Egyptian Paintings

Akmal A. Sakr, M. F. Ghaly, M. F. Ali and M. E. F. Abdel-Halim

*African Journal of Biotechnology*, 12 (14): 1644-1656 (2013)

Eight out of 46 *Streptomyces* isolates representing highest deterioration symptoms of disfiguration and scaling were isolated from mural paintings within tombs at Tell Basta and Tanis, Lower Egypt. These isolates were identified using traditional and 16S rDNA sequencing methods as *Streptomyces albidofuscus*, *Streptomyces ambofaciens*, *Streptomyces canarius*, *Streptomyces chibaensis*, *Streptomyces coelicolor*, *Streptomyces corchorusii*, *Streptomyces nigrificans* and *Streptomyces parvulus*. These identified *Streptomyces* isolates decomposed animal glue into amino acids with a high percentage of L-glutamic acid and ammonia as end product, depolymerized arabic gum into free mono-sugars, decomposed egg yolk into amino acids with low percentage of L-glutamic acid and ammonia and decomposed

bees wax enzymatically into short chains of stearic acid. Finally, these isolates caused flaking of paintings layers due to penetration of filamentous mycelium within painting layers with the assistance of enzymatic hydrolysis.

**Keywords:** Animal glue; Arabic gum; Bees wax; Biodeterioration; Egg yolk; Streptomyces; Tell basta; Tanis; Egyptian tombs.

#### **1744. The Use of Gamma Irradiation in the Sterilization of Streptomyces Colonizing the Tempa Paintings in Ancient Egyptian Tombs**

Akmal Ali Sakr, Mohamed Farouk Ghaly and Mona Foad Ali

*International Journal of Conservation Science*, 4 (3): 283-294 (2013)

Eight out of forty six Streptomyces strains from mural paintings at the Tell Basta and Tanis tombs were exposed to increasing doses (5, 10, 15, 20, 25kGy) of gamma irradiation. These strains varied in their resistance profile. *S. canarius* was the most resistant to gamma irradiation doses, as it was totally eliminated at 25kGy, whereas *S. chibaensis* and *S. albidofuscus* resisted to 20kGy and *S. ambofaciens* resisted 15kGy. The other strains under investigation showed a lower resistance to gamma irradiation.

Tricyclazole (5, 7, 10 µg/mL) inhibited melanin production after gamma irradiation at doses lower than lethal dose. Gamma irradiation with the previous doses enhanced the chitinase activity of irradiated Streptomyces strains, but *S. canarius* was the exception. No color change was observed either for pigments or for binding media, after gamma irradiation at the same doses.

**Keywords:** Gamma irradiation; Melanin; Mural paintings; Streptomyces; Tricyclazole.

#### **1745. The Relationship between Salts and Growth of Streptomyces Isolated from Mural Paintings in Some Ancient Egyptian Tombs**

Mona Fouad Ali Abdelghany

*Conservation Science in Cultural Heritage*, 13: 313-330 (2013)

Eight out of the forty-six samples of Streptomyces representing the most potent deteriorating isolates were taken from scaled and stained mural paintings in the tombs at Tell Basta and Tanis, Lower Egypt. These isolates were identified using conventional and 16S rDNA sequencing methods and attributed to *S. albidofuscus*, *S. ambofaciens*, *S. canarius*, *S. chibaensis*, *S. coelicolor*, *S. corchorusii*, *S. nigrifaciens* and *S. parvullus*. The different salts occurring on the ancient Egyptian tombs, such as sodium chloride, potassium chloride and magnesium sulphates enhanced the growth of Streptomyces isolates till 10% of these salts. Streptomyces isolates adapted/adopted different defense mechanisms such as pigmentation, osmotic balance and amino acid production.

The salts had a synergistic effect in the deterioration of the mural paintings through the cooperation of the mycelium of Streptomyces with salts in the mechanical deterioration of the stone surfaces.

**Keywords:** Tombs; Egypt; Streptomyces; Salts; Carotenoid.

#### **1746. Archaeometric Analysis of Pigments from the Tomb of Nakht-Djehuty (TT189), El-Qurna Necropolis, Upper Egypt**

Hussein Hassan Marey Hassan Mahmoud

*Archéosciences, Revue D'archéométrie.*, 37: 19-33 (2013)

The main objective of the present work is to characterize some pigments from the tomb of Nakht-Djehuty (TT189), time of Ramesses II (c. 1279-1212 BC), El-Assasif district, El-Qurna necropolis, Luxor (ancient Thebes), Upper Egypt. The characterization of the examined wall paintings was carried out by means of optical microscopy (OM), scanning electron microscopy (SEM) equipped with an energy dispersive X-ray detector (EDS), X-ray diffraction analysis (XRD), Fourier transform infrared spectroscopy (FT-IR) and visible reflectance spectroscopy. The results revealed the characterization of the stratigraphic structure of wall decorations of the tomb and their chemical composition. The analysis of the examined samples indicated that the blue pigment was identified as Egyptian blue (Cuprorivaite), the green pigment as Egyptian green, the red pigment as red ochre, the yellow pigment as yellow ochre and the white pigment as a mixture of gypsum and calcite. The obtained results helped in identifying the chromatic palette used in one of the tombs dating back to the Ramesside period in Ancient Egypt.

**Keywords:** Wall paintings; Tomb of nakht-djehuty; Ramesside period; El-qurna; Pigments; Egyptian blue; Sem-eds; Ft; Ir; Xrd.

#### **Faculty of Kindergarten**

##### **Dept. of Essential Sciences**

#### **1747. Understanding a Simple Arabic Stories Using Event Calculus**

Mohamed Abd El-Salam Ali El-Sheikh

*American Journal of Applied Sciences*, 10: 1298-1306 (2013)

This study investigates the use of event calculus for understanding stories written in Arabic natural language. System makes a representation for commonsense knowledge and story events and then performs a commonsense reasoning to infer the details events which are not explicitly described in the story; furthermore it manages changes in objects properties over time and handles the actions synchronizations problem.

**Keywords:** Story understanding; Animating story; Event calculus; Commonsense reasoning; Reasoning about action.

## Institute of African Research and Studies

### Dept. of Geography

#### 1748. Impacts of Rainfall and Growing Season Changes on Food Crops Yield in Katsina, Northern Nigeria

Attia Mahmoud Mohamed El-Tantawi

*Katsina Journal of Natural and Applied Sciences*, 3 (2): 128-143 (2013)

Commonly described as arid and semiarid climate, Katsina State has subjected to large inter-annual, intra-annual, and inter-decadal variability of rainfall over space and time from 1942 to 2008. The 66 years time series data was used to compute the temporal and spatial variability of rainfall and data of (1981-2010) used to analyze the onset of rainy season variability over the long-term period of 1942-2008 and over the recent short-term period from 1976-2008 which experienced the magnitude of climate change. The trend was however interrupted by multi-year anomalies and there is a reduction in rainfall over the study period. Rainfall index shows those bad years which experienced rainfall less than normal were more than the good years which experienced rainfall more than normal. Analysis of the growing season in the study area revealed considerable high variability, the number of days in between the onset date and the cessation date decreased over study period. The yield of food crops (Millet, maize, Sorghum) data were also used to investigate the possible impacts of rainfall on food crops yield in the study area. There is no clear pattern shown for the trend in onset dates. If the present downward trend in annual rainfall totals continues, a statistically significant shift in growing season may be expected, and then the impacts on food crop yield will be very high.

**Keywords:** Rainfall variability; Growing season; Food crops; Katsina; Nigeria.

### Dept. of Natural Resources

#### 1749. Rooting of White Shrub and Firebush Shrub Hardwood Cuttings Using Growth Regulators Quick Dip Treatments

Mohamed Said Abbas

*Journal of Food, Agriculture and Environment*, 11 (3,4): 2775-2780 (2013) IF: 0.435

Vegetative propagation through stem cuttings is the most vital method to reproduce plants and conserve their innate desirable characters. Sixty uniform hardwood cuttings of each species with the same number of nodes of 1 cm diameter were used to test the influence of indole-3-butyric acid (IBA) and naphthalene acetic acid (NAA) after quick dip for 5 seconds on induction, growth of adventitious roots and establishment of *Bougainvillea peruviana* cv. Shubra (BOPE) and *Hamelia patens* Jacquin (HAPA) species hardwood cuttings during vegetative propagation. Cuttings vitality expressed as bud break responded positively to growth regulators treatments. IBA at 2000 ppm resulted in higher bud break percentage (73.9% in BOPE and 59.2% in HAPA), higher rooting percentage (53.6% in BOPE and 28.4% in HAPA), greater number of roots per cutting (15.5 in BOPE and 24.8 in HAPA), higher root length per cutting (31.6 mm in BOPE and

27.2 mm in HAPA), higher roots fresh weight (9.5 g in BOPE and 8.8 g in HAPA) and higher roots dry weight (6.6 g in BOPE and 6.4 g in HAPA), and higher establishment percentage (60.3% in BOPE and 42.3% in HAPA), greater number of branches per cutting (3.6 in BOPE and 5.4 in HAPA), longer branches (139.2 mm in BOPE and 139.23 in HAPA mm), and greater number of leaves per cuttings (59.0 in BOPE and 50.1 in HAPA). The response of BOPE and HAPA species hard-wood cuttings to treatments was not consistent. To use a quick dip treatment method and achieve comparable results to soaking treatments for 12 and 24 h, a four-time increase in the treatment concentration is required.

**Keywords:** Growth regulators; Quick dip; Hard wood cuttings; Iba, Naa; Rooting; Establishment; Shubra white shrub; Firebush shrub.

#### 1750. Hydrocarbon Generating Basins and Migration Pathways in the Gulf of Suez, Egypt

Naglaa Saleh Mohamed Hassan

*Life Science Journal*, 10 (5s): 229-235 (2013) IF: 0.165

The study aims to investigate the influence of rifting on the processes of organic matter maturation, hydrocarbon generation, expulsion, and migration, as well as the influence of rifting on the preservation of accumulated hydrocarbons in the Gulf of Suez. The study identified the presence of sixteen generating and expelling troughs based on the results of thermal burial histories: Darag, Nebwi, Lagia, October, Fieran, Amer, Belayim, July, Ramadan, Morgan, West Zeit, East Zeit, Ashrafi, Ghara, Gamsa, and Sharm troughs. These names were given after geographic areas or known oil fields in the proximity to the respective trough or in its vicinity. All the source formations in the sixteen troughs reached top oil window and expelled their hydrocarbons at 10 million years before present (mybp) and continued till present. Such timing post-dates the Early Miocene Mid Clysmic or Mid Rudeis "disturbing" event and the Late Miocene Messinian "quiet" event, which suggest high Migration and accumulation efficiencies for hydrocarbons generated in these troughs. The Darag, Amer, Belayim, Ghara, and Sharm troughs are considered the highest in preservation as migration started the latest among other troughs (4.8 and 2.5 mybp relative to 10 to 6 mmybp for the July, Ramadan, Morgan, West Zeit, East Zeit, Ashrafi, and Gamsa troughs.). The suggested prospective areas for future exploration should be located updip and in the hydrocarbon migration pathway.

**Keywords:** Petroleum potential; Thermal burial History; Great african rift; Gulf of suez.

#### 1751. Effects of Sulfuric Acid and Hot Water Pre-Treatments on Seed Germination and Seedlings Growth of Cassia Fistula L.

Amira Shawky Ahmed El-Said Soliman

*American-Eurasian J. Agric. and Environ. Sci.*, 13 (1): 07-15 (2013)

This experiment is separated into two parts: dormancy breaking methods for Cassia fistula seeds using different pre-treatments and seedlings growth investigation during the two seasons of 2009/2010 and 2010/2011. The seeds were acid scarification by H

SO 2 4 (36N) for 2 minutes and hot water treatment (60, 80 and 100°C for 3, 6 and 9 minutes). Germination indices were determined. In the second part seedlings were kept in greenhouse to superior quality seedlings from different treatments and after 60 days growth parameters were also recorded in both seasons. The results showed that acid scarification for 2 minutes and then soaking in hot water at 100°C for 6 minutes was the best method for breaking dormancy of *Cassia fistula* which resulted in an increased germination percentage to 96% and gave highly quality of golden shower seedlings.

**Keywords:** *Cassia fistula*; Sulfuric acid; Hot water; Germination indices; Growth parameters.

### 1752. Response of *Adansonia Digitata* to Compost and Zeolite in Replacement of Chemical Fertilization

Amira Shawky Ahmed El-Said Soliman

*American-Eurasian J. Agric. and Environ. Sci.*, 13 (2): 198-206 (2013)

The unique cation exchange, adsorption, hydration-dehydration and catalytic properties of natural zeolite (as granules) loaded with micronutrients, have promoted their use in clean agriculture as soil amendments and slow-release fertilizers. This study was conducted in open field for two successive seasons 2011 and 2012 to investigate the effect of natural zeolite, organic fertilizer (compost) and combination of them on growth and chemical constituents of *Adansonia digitata* L. seedlings. The results indicated that zeolite loaded with micronutrients mixed with organic fertilizer led to significant increase in growth characters with reference to (fresh weight, dry weight, number of leaves, leaf area, as well as stem diameter) and chemical composition symbolized in (net photosynthesis, stomatal conductance, crude protein, water use efficiency, plant pigments, total carbohydrates, ascorbic acid, N, P, K, Zn, Fe, Mn, B, Ca, Mg) besides indigenous hormones such as indole acetic acid (IAA), gibberellic acid (GA3) and cytokinins (CK) in comparison with the recommended dose of chemical fertilizers NPK (as control) under the same conditions. These results undoubtedly confirm that zeolite and organic fertilizer (compost) mixture could replace the application of chemical fertilizers and consequently improve the quality and quantity of *Adansonia* tree. Generally, this application may have direct impacts on safety and efficacy of active constituents which entail for medicinal and aromatic products. Besides minimizing economic costs and pollution of agricultural environment.

**Keywords:** *Adansonia digitata*; Chemical composition; Compost; Growth characters; Zeolite.

### 1753. Effect of Nutritional Status on Growth Pattern of Stunted Preschool Children in Egypt

Hassan Mohamed Sobhy Hassan

*Academic Journal of Nutrition*, 2 (1): 1-9 (2013)

Growth retardation is highly prevalent among children in low-income countries. Infections and inadequate food intake are well-established causes of growth retardation; however, the possible specific role of micronutrient deficiencies in the etiology of growth retardation and other developmental and health outcomes has gained attention recently. The aim of the present study was to

provide information about nutritional status of stunted Egyptian preschool children and their dietary intake, which will help in designing a proper nutrition education messages & appropriate preventive strategies to improve linear growth. The study was designed as a case control study included (100) Egyptian children aged 2-6 years old, with delayed linear growth, proportionate stunted, randomly selected from the stunted outpatient clinic of National Nutrition Institute (NNI) and results were compared to (50) age, sex and socioeconomic matching control. All participants were subjected to the baseline assessment (Full history- clinical examination- anthropometric measurements including weight & height- lab investigation including hemoglobin concentration, serum Ca, Zn, Vit. A, TSH, T4, T3 & albumin and stool analysis - dietary intake including "Twenty four-hour recall" method & food frequency questionnaire. Results showed that mean height for age Z score is significantly lower among the stunted compared to the control group. Dietary intake analysis showed that mean intake of all minerals is significantly lower among stunted children as compared to control group. % intake of RDA from Ca was 57.2% for stunted as compared to 101.7% for control. Nearly the same pattern was noticed for Mg, while intake of all macronutrients was significantly lower among stunted compared to the control group. Vitamin A intake of stunted group represented only 67.5% of RDA as compared to 214.0% of control group; the difference was

highly significant between the two groups. All blood values of Albumin, TSH, T3, T4, Ca, Zn & Vit. A were significantly lower among stunted group as compared to control, although within normal range, according to cut off point of each parameter, while both groups were anaemic with no significant differences between the two groups. As a conclusion, it seemed that dietary intake deficiency of several micronutrients of stunted children (primarily Ca, Zn, Mg and vitamin A) & all macronutrients intake may play an important role in their linear growth retardation. Calcium intake level among stunted children was far below the recommended figures.

Nutrition education messages encouraging high consumption of dairy products are needed to counteract this pattern of low calcium intake. Preventive strategies to prevent stunting and promote healthy eating & milk consumption are recommended.

**Keywords:** Stunted growth; Body mass index (BMI); Nutritional status.

### 1754. Characterization of 6-Gingerol for in Vivo and in Vitro Ginger (*Zingiber Officinale*) Using High Performance Liquid Chromatography

Mohamed Said Abbas

*Global Journal of Botanical Science*, 1: 9-17 (2013)

Ginger (*Zingiber officinale* Rosco) belonging to the family Zingiberaceae is one of the world's most important spices and produces a pungent, aromatic rhizome that is valuable all over the world. Qualitative and quantitative analysis of 6-gingerol in different parts (in vivo and in vitro) of *Zingiber officinale* using thin layer chromatography (TLC) and high performance liquid chromatography (HPLC) have been performed. Data of TLC showed spots having identical R<sub>f</sub> value (0.15), according to the synthetic standards of 6-gingerol in all samples extract. 6-gingerol was detected in all extracts of different parts of ginger derived from in vivo and in vitro culture conditions. Quantitative



determination of 6-gingerol using HPLC technique was carried out. Comparing with the peaks of 6-gingerol in synthetic standards, in vivo rhizomes and in vitro cultures of different ginger parts was showed similar UV spectra characteristics. The quantity of 6-gingerol in rhizomes (in vivo and in vitro) and in vitro microrhizomes (45.37; 42.64; 28.11 mg/g respectively), were showed a higher value than that of in vitro calli, shoots and roots (7.89; 7.46; 6.40 mg/g respectively).

**Keywords:** Ginger; Rhizome; In vitro; Callus; TLC; HPLC.

#### **1755. A Comparison between Claypool and Schmoker Methods in a Quantitative Evaluation of Kharita and Khatatba Source Rocks, North Western Desert, Egypt**

Naglaa Saleh Mohamed Hassan

*Inventi Rapid: Energy&Power*, 2: 1-5 (2013)

By applying the hydrogen index values obtained from S2 versus TOC graph and mass balance calculations obtained from the results of Rock-Eval pyrolysis, the original hydrocarbon generative capacity and the amounts of the hydrocarbons generated are estimated. For calculations and comparison, two methods were applied (Claypool et al. 1998 and Schmoker 1994) for 30 organic rich samples representative Kharita and Khatatba formations, from wells IF 37-7 and S. Dabaa 11-1. Such formations are characterized by gas/oil prone source rock (Type III/II kerogen) with different thermal maturities. Calculation results indicate that the amounts of original hydrocarbons and the hydrocarbon generative capacities of the two methods are similar and not correlated with the results of the Rock-Eval pyrolysis.

**Keywords:** Hydrocarbons; Western desert; Maturities; Pyrolysis; Quantitative evaluation.

CAIRO UNIVERSITY

Publication  
in  
Book & Chapters

## Publication in Book/ Chapter

### Faculty of Arts

#### Dept. of Philosophy

#### 1756. Heraclitus Fragments A Text and Translation with a Commentary

Hoda Mohamed El-Sayed Elkholy

*Greek Foundation of Educational research and studies*, (2013)

Prof. El-khouly with her book on Heraclitus she renews even the recent research on the Ephesian philosopher, Through an unexpected focal extension and comprehension, i.e., in terms of logic, both in width and depth. The novelty of this work resides in interferences, corrections and interpretations concerning the Heraclitean fragments its author proceeds to, while in addition. she translates the Greek text into Arabic

#### Dept. of English Language and its Literature

#### 1757. Shakespeare's Festive World a Semiotic Study of Selected plays by Willian Shakespeare

Hihan Anwar Mahmoud

*Lambert Academic Publishing*, (2013)

The introduction highlights the concept of "festivity" and how it reached its peak in the Elizabethan age. It also discloses Bakhtin's concept of the "carnivalesque" and sheds light upon the Semiotic theory. The first chapter examines the festive elements in A Midsummer Night's Dream (1595) and As You Like It (1599) as comedies. The second chapter focuses on the festive elements in two of Shakespeare's great tragedies: Othello (1602-3) and King Lear (1605).

The third chapter discloses the festive elements in two of Shakespeare's late romances: The Winter's Tale (1610) and The Tempest (1611). The conclusion presents what is deduced from this research: In the comedies, festivity builds up until it reaches its peak with the marriages of the characters at the end. In the tragedies, Shakespeare employs festivity as a tool of intrigue. In the romances, the festive spirit reigns. Yet, the ambivalence of festivity remains as the most remarkable feature.

#### 1758. The rule of New Media in the Egyptian Revolution of 2011 : Visuality as an Agent of Change

Randa Aboubakr

*Popular Culture in the Middle East and North Africa: A Postcolonial Outlook*, Routledge, (2013)

The significant role played by new media in the Egyptian revolution of 2011 was an outcome of an underlying battle that had been going on for about a quarter of a century between repression on the official political and social levels and the relative freedom available in the virtual world. This paper explores the role played by visuality in new media during the revolution by scrutinising how the visual was adopted as an effective means of not only disseminating information and mobilising people during the early days of the revolution, but of political campaigning for even much longer.

**Keywords:** New media; Intervisuality; Hacktivism.

#### 1759. Literatur und Gesellschaft: eine Einschaeztung der Situation in Aegypten

Randa Aboubakr

*Zeitgenoessische Kuenstler: Arabische Welt*, Steidl Verlag, (2013)

It is perhaps a commonplace that literature, like any other form of artistic and intellectual production, is strongly linked to major social and political developments in a society. This is usually a two-way link. Literature is a reflection of social and political developments in as much as it is one of the forces contributing to ushering in those developments, as well as of consolidating them. Like the social and political scene in any society, the literary scene is in a state of constant flux, going through periods of major upheavals, which, in their turn, reflect crucial developments in the contemporary life of that society. The contemporary Egyptian literary field is not an exception. The social and political upheavals Egypt has been witnessing throughout the past two decades have both impacted the literary production of this period, and been impacted by it. When we move from examining the field of writing and reading in general to scrutinizing the literary field, we can observe that those changes have contributed to the emergence of 'new' writings by a young generation of writers, working side-by-side with more established writers. This essay seeks to examine the contemporary literary scene in Egypt, with particular emphasis on the young poetry scene.

**Keywords:** Egyptian literature; Literary field; Colloquial poetry.

#### 1760. Alternating Images: Simulacra of Ideology in Egyptian Advertisements

Maha F. El Said

*Popular Culture in the Middle East and North Africa: A Postcolonial Outlook*, (2013)

Globalization can be considered the ultimate manifestation of the postmodern condition: fragmented yet connected, similar yet different, global yet local. Globalization has no center; it creates images to be perused and realities to be substituted by the hyper-real. Globalization's ideology is consumerism, its cathedrals hyper-malls, its prophets advertisements. Egypt is a country that has seen many colonial eras, however, unlike many other colonized countries, we've always retained our cultural identity and our native language. In this chapter I attempt to trace the impact of advertisements on forming a false, fragile identity that shapes popular ideology—an ideology that limits itself to 'fashionable' ideologies without impacting true original identity. An exposition of the alternating popular ideologies starting with communism/socialism of the Nasser era, the Americanization of the Sadat Era, and the Islamization of the Mubarak era show how many Egyptian youngsters create their own 'false copy' of ideology in an attempt to belong to, and distinguish themselves in, the global village. Influenced by images and false copies of happiness, freedom, and faith offered by some system or the other created a simulacrum of ideology. Finally the need to synthesize all global influences and come up with our own definition of a modern way of life, that cherishes the authenticity of the local, that derives its force from root values and beliefs is highlighted.

**Keywords:** Popular culture; Globalization; Advertisements.

### 1761. Lexical Cohesion Shifts in the English and Arabic Versions of the United Nations Human Rights Declaration (UNHRD): A Contrastive Analysis

Nahla Mahmoud Helmy Nadeem

*New Research into Applied Linguistics and Language Learning*, MacroWorld publishing, (2013)

The present study aims at exploring lexical cohesion shifts in the UNHRD English and Arabic texts. The basic argument postulated in the paper is that every translation is bound to result in shifts both in the type and size of lexical cohesive devices which can shed light on the textual and rhetorical preferences in a specific register in the two languages and the translation strategies adopted. Drawing on studies in text linguistics, translation shifts and lexical cohesion (Baker, 1992; Blum- Kulka, 2000; Halliday and Hasan, 1991; Tanskanen, 2006), the study aims to detect and describe the various types of lexical cohesion shifts in the English- Arabic translation of the UNHR document in an attempt to explain the underlying factors which may have prompted these shifts. Through comparing and contrasting the rendering of lexical cohesion patterns in the two texts, the study concluded that those shifts might occur as a result of the text type at hand, the lexical patterning in the SL and TL or the translation strategies used which might in turn lead to explicitation? or implicitation? in the target text.

**Keywords:** Lexical cohesion; Translation shifts; Explicitation Hypothesis; Contrastive analysis; Translation strategies.

### 1762. Stories to Live By: An Exploration of Personal Experience Narrative in Hadith

Nahla Mahmoud Helmy Nadeem

*Reflections on Narrative Interdisciplinary Storytelling*, Inter-Disciplinary Press, (2013)

In this paper, I explore some of the features of the personal experience narrative (PEN) used in the sincerity hadith told by Prophet Muhammed. The hadith is classified in Riyad As-Sali'in under the theme of sincerity and the text itself is used for ethical/religious teaching. Using Labov's work on PEN structures the paper attempts to answer two key questions: a) whether or not the Labovian model applies to the PENs (PEN) used in the hadith and b) how effective the model can be in establishing the link between what was said (i.e. the stories told), how the narratives are structured and the Islamic concepts the hadith is meant to teach. The analysis shows that though the hadith belongs to a different language with assumedly different socio-linguistic narrative practices, the Labovian model works as an effective tool of analysis.

### 1763. Popular Culture in the Middle East and North Africa: A Postcolonial Outlook

Walid Abdel Aal Abdellah El Hamamsy

*Routledge*, (2013)

This book explores the body and the production process of popular culture in, and on, the Middle East and North Africa, Turkey, and Iran in the first decade of the 21<sup>st</sup> century, and up to

the current historical moment. Essays consider gender, racial, political, and cultural issues in film, cartoons, music, dance, photo-tattoos, graphic novels, fiction, and advertisements. Contributors to the volume span an array of specializations ranging across literary, postcolonial, gender, media, and Middle Eastern studies and contextualize their views within a larger historical and political moment, analyzing the emergence of a popular expression in the Middle East and North Africa region in recent years, and drawing conclusions pertaining to the direction of popular culture within a geopolitical context. The importance of this book lies in presenting a fresh perspective on popular culture, combining media that are not often combined and offering a topical examination of recent popular production, aiming to counter stereotypical representations of Islamophobia and otherness by bringing together the perspectives of scholars from different cultural backgrounds and disciplines. The collection shows that popular culture can effect changes and alter perceptions and stereotypes, constituting an area where people of different ethnicities, genders, and orientations can find common grounds for expression and connection.

**Keywords:** Post-colonial studies popular culture middle east studies.

### Dept. of German Language and its Literature

#### 1764. Frauen im Spiegel der Medien. Linguistische Analys werbespezifischer Sprachverwendung

Mona Rashad Noueshi

*Higher Humanities Education in the 21st Century*, Ministry of Education and Science of the Russian Federation, (2013)

The study looks at the advertisements as time-bound expressions, Analyzes the linguistic representation of the advertising specific image of women in the 50's that is possible to explain from the society and social structures. This verbal (text) and nonverbal information is taken into consideration. The article covers three areas: semiotics, advertising research and text linguistics.

**Keywords:** Semiotics; Advertising research; Text linguistics.

### Dept. of French Language and its Literature

#### 1765. Enjeux de l'intertextualité dans la littérature égyptienne d'expression française

Rania Mohamed Fathy Mohamed Abdou

*Trajectoires et dérivés de la littérature-monde*, Francopolyphonies, (2013)

Reproduisant les tonalités d'une polyphonie qui recueille les résonances les plus variées, l'intertextualité illustre, au plus haut degré, l'interaction entre le même et le divers. Le présent travail se propose d'analyser ses composantes dans deux récits autobiographiques de la littérature égyptienne d'expression française, celui de Gulpéire Effaltoun et de Azza Heikal. Elle s'attachera à mettre en évidence toute la richesse et la complexité des rapports entre mondes, identités et voix pluriels, dont témoigne l'intertextualité, et voir dans quelle mesure on peut parler, dans ces textes, de tension(s) définissant les liens entre multiples champs, ou de traversée de frontières caractérisant une écriture englobante et intégrante.

**Keywords:** Intertextualité; Littérature Égyptienne d'Expression française; Autobiographie; Identité; Histoire.

### 1766. Le jububier du patriarche", roman africain entre oralité et écriture

Shahenda Ezat Abdel-Kader

*Editions universitaires européennes, (2013)*

Les romans africains d'expression française sont une parfaite illustration de la rencontre de deux modes d'expression différents : l'oral et l'écrit. Nés d'un double héritage vu la scolarisation de leur auteur d'une part et la culture orale traditionnelle d'autre part, ces romans incarnent la survie de la tradition dans un contexte moderne. Ce livre se propose d'analyser les indices de l'oralité dans "Le jububier du patriarche", roman sénégalais écrit par Aminata SOW FALL et de souligner comment cette oralité qui se greffe sur le plan narratif, rhétorique et symbolique exerce son influence sur la poétique romanesque de cette auteure.

### 1767. Les concours d'écriture de jeunes en Égypte

Ghraa Hussien Mehna

*Approche Internationale Des Écrits Littéraires Des Jeunes Et Des Conditions De Leur Conservation, L'Harmattan, (2013)*

The research is entitled: "Writing Competitions of Children in Egypt," and was published in *Approche internationale des écrits littéraires des jeunes et des conditions de leur conservation*; a book by L'Harmattan. A number of children literature researchers and writers from different countries participated in this edited book. The chapter presenting the research discusses the poetry and story workshops that I had organized for children around their imitation of Mohammad Aziz Lahbabi's poem, which is entitled: "Sun." I have conducted this workshop for primary grade students at the Lycée School of Bab al-Luq, as one of the activities of the festival and poetry contest of Egyptian Association for French Professors (AEPF).

The second workshop was about rewriting the famous children's story: Red Riding Hood, where different narrations were written for the story, by either changing characters or places. This unleashed the children's imagination, as they invented different endings for the story. These writing workshops aimed at teaching French Language through different writing activities.

### 1768. L'impact des conflits sur la vie sociale de l'enfant

Ghraa Hussien Mehna

*L'image de l'enfant dans Les conflits, L'Harmattan, (2013)*

The research is entitled: "The Effect of Conflict on the Social Life of a Child," and was published by L'Harmattan in *L' image de l'enfant dans les conflits*, Paris, 2013. A number of researchers from different French and African universities participated in this book, including myself from Cairo. The chapter I have written discusses the effect of wars and conflicts on children, even if indirectly. The research studies two novels, namely, "The Big House" by the Algerian author Mohammad Dib and "I Saw Ramallah" by the Palestinian author Murid Barghouthi. Even

though the two novels are separated by a long timespan, both deal with occupation; whether the French occupation of Algeria or the Israeli occupation in Palestine, along three main lines. The first is the familial and social framework, the second is social realism and the third is the socio-political dimension. The novels exhibit how both children, Omar and Tamim, are affected by the occupation, which imprints their lives with feelings of loss and instability. A child, then, may be like a dummy that is moved by the surrounding events or a victim that experiences fear and hunger, and is exposed to danger. Both novels reflect the reality that these children lived under the occupation of their homelands.

## Faculty of Archaeology

### Dept. of Egyptian Archaeology

### 1769. The Unknown Horment and The Archive of his priests in the Ibiotaphion of the Tuna al-Gebel necropolis

Mahmoud Ebeid Shahat

*Tuna-Gebel-Band4, Verlag Patrick Brose, (2013)*

This study deals with the god Hormerti who was mentioned on some demotic papyri from the subterranean galleries of the sacred animal (Ibiotapheion) in the Tuna al-Gebel necropolis, and sheds light on the demotic archive of his priests from the same site. The god Hormerti is closely connected with the god Osiris-Bull in the necropolis of Pharbaithos, and it seems that this god belongs to the secret temple events inside the great Temple of Thoth in the Tuna al-Gebel necropolis. Perhaps he is connected with PA-Gm (the young [Thoth] -bull), the star god, star (bull) of the sky, the nocturnal form of Thoth united with Osiris as the bull of the sky belonging to this temple.

The identification of this archive and the real role of the god Hormerti and his priests in the Tuna al-Gebel necropolis may be modified, when the papyri referring to this god and his priests are fully studied.

### Dept. of Conservation

### 1770. Seismic Hazard Analysis for Archaeological Structures — A Case Study for EL Sakakini Palace Cairo, Egypt

Sayed Mohamed Sayed Mohamed Hemeda

*Engineering Seismology, Geotechnical and Structural Earthquake Engineering, The modern architectural heritage of Egypt is rich, and extensively variable. It covers all kinds, (2013)*

The modern architectural heritage of Egypt is rich, and extensively variable. It covers all kinds of monumental structures from palaces, public buildings, residential and industrial buildings, to bridges, springs, gardens and any other modern structure, which falls within the definition of a monument and belongs to the Egyptian cultural heritage. We present herein a comprehensive geophysical survey and seismic hazard assessment for the rehabilitation and strengthening of Habib Sakakini's Palace in Cairo, which is considered one of the most significant architectural heritage sites in Egypt. The palace located on an



ancient water pond at the eastern side of Egyptian gulf close to Sultan Bebris Al-Bondoqdary mosque, a place also called “Prince Qraja al-Turkumany pond”. That pond had been filled down by Habib Sakakini at 1892 to construct his famous palace in 1897.

## **Institute of African Research and Studies**

### ***Dept. of Natural Resources***

#### **1771. Improving Jatropha spp. In Egypt**

Amira Shawky Ahmed El-Said Soliman

*Lambert Academic Publishing, (2013)*

Jatropha is a genus of flowering plants in the spurge family, Euphorbiaceae. It has a great economic importance and can be utilized in several ways. It cited as one of the best candidates for future biodiesel production. It is resistant to drought and pests, and produces seeds containing 27-40% oil, averaging 34.4%. The remaining press cake of jatropha seeds after oil extraction could also be considered for energy production. However, despite their abundance and use as oil and reclamation plants, none of the Jatropha species have been properly domesticated and, as a result, their productivity is variable, and the long-term impact of their large-scale use on soil quality and the environment is unknown. Therefore, this study was carried out at the experimental laboratory of the Natural Resources Department, Institute of African Research and Studies, Cairo University, Egypt, for improving growth and chemical composition of Jatropha spp.

#### **1772. Hydrocarbon Generating Basins and Migration Pathways in the Gulf of Suez**

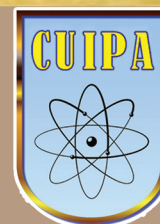
Naglaa Saleh Mohamed Hassan

*Lambert Academic Publishing, (2013)*

The well known oil province of the Gulf of Suez (GOS) represents the north of the Great East African Rift System in Egypt. Since the beginning of the last century, the GOS has been a highly prospective area for petroleum exploration, where the history of oil-producing fields started in 1886 with the discovery of Gemsa oil field. The process of rifting and the accompanying activities including faulting, deposition, uplift, and erosion are thought to have significantly affected the petroleum systems in the GOS. This book gives an idea about the influence of rifting on the processes of the organic matter maturation, hydrocarbon generation, expulsion and migration, as well as the control of rifting on preservation of accumulated hydrocarbons in the GOS. The time of petroleum expulsion and migration relative to the time of the main trap forming tectonic events is important, as the latter have a direct impact on petroleum accumulation and thus its preservation in the trap. Maturation and hydrocarbon generation, migration, and entrapment are affected and controlled by the events immediately preceding the stage of peak-generation of hydrocarbons and their expulsion.



Cairo University



# Authours' Index

## Authors' Index

### A

**Abada, Khairy:** 537, 538  
**Abadi, Ashraf:** 1459  
**Abadir, Magdi:** 712, 722  
**Abbas, Ikhliss:** 178  
**Abbas, Mohamed:** 1749, 1751, 1754  
**Abbas, Samah:** 1320, 1331, 1346, 1376  
**Abbassi, Maggie:** 1412  
**Abd Alfatah, Mohamed:** 1752  
**Abd El-Ghany, Wafaa:** 615  
**Abd El-Halim, Sally:** 1524, 1526, 1529  
**Abd-Elhameed, Waleed :** 283, 291  
**Abd El-Rahman, Yasser:** 271  
**Abd El-Wahab, Abeer:** 522  
**Abdalla, Khaled:** 881  
**Abdallah, Amany:** 513  
**Abdallah, Dalaal:** 1566, 1567, 1569  
**Abd-Allah, Foad:** 1255, 1256  
**Abdallah, Hossam:** 1532  
**Abdallah, Magda:** 191  
**Abdallah, Mahmoud:** 1306  
**Abdallah, Moatassem:** 884  
**Abd-Allah, Ramadan:** 1727  
**Abdeen, Mostafa:** 781, 805, 806, 808, 809, 810, 812, 824, 826, 833  
**Abdel-Baky, Abeer :** 545, 546  
**Abdel-Fattah, Amal:** 1409  
**Abdel-Harith, Mohamed:** 640, 641, 642, 647  
**Abdel-Riheem, Nadia:** 235  
**Abdelaal, Alaa:** 996  
**Abdelall, Yassmen:** 945, 951, 953  
**Abdelattah, Abdallah:** 940  
**Abdelaziz, Ahmed:** 1287  
**Abdelaziz, Ashraf:** 1096, 1103, 1115  
**Abdel-Aziz, Hend:** 483  
**Abdelaziz, Mohamed:** 1144, 1145, 1163  
**Abdel-Aziz, Mosaad:** 1084, 1085  
**Abdelaziz, Samy:** 543, 544  
**Abdelaziz, Wessameldin:** 654, 655, 657, 661  
**Abdelbary, Ghada:** 1501, 1517, 1521  
**Abdelfatah, Sally:** 1693  
**Abdel-Fattah, Khaled:** 876  
**Abdel-Fattah, Laila:** 1349, 1378, 1381  
**Abdel-Gaber, Rewaida:** 411  
**Abdelgawad,** 505  
**Abdelrahman:**  
**Abdel-Gawad, Essam:** 624

**Abd-Elgawad, Hanan:** 1397  
**Abdel-Gawad, Sherif:** 1344, 1370  
**Abdel-Ghaffar, Fathy:** 410, 414, 435, 679  
**Abdelghaffar, Shereen:** 1658  
**Abdelghaly, Abdalla:** 1671, 1672, 1673, 1674  
**Abdel-Ghani, Mona:** 1742  
**Abdel-Ghani, Nour:** 127, 128, 153, 155, 185, 196, 214  
**Abdelghany, Ismail:** 518  
**Abdel-Ghany, Mohamed:** 1256  
**Abdelghany, Mona:** 1725, 1728, 1734, 1740, 1743, 1744, 1745  
**Abd-El-Hafiz, Salwa:** 789, 811  
**Abdelhalim, Mona:** 1146  
**Abdel-Hameid, Mohammed:** 1474, 1481, 1489, 1490, 1492  
**Abdelhamid, Abdou:** 180, 200, 215, 219, 235, 236  
**Abdelhamid, Ismail:** 116  
**Abdelhamid, Mahmoud:** 642  
**Abdelkader, Ahmed:** 1030  
**Abdel-Kader, Fawzy:** 368, 375, 399  
**Abdelkader, Mahmoud:** 28, 32, 37, 47  
**Abdel-Kader, Neamat:** 768  
**Abdel-Kader, Nora:** 123, 232, 667  
**Abdel-Karim, Abeer:** 173  
**Abdel-Karim, Randa:** 869  
**Abdelkawy, Mohamed:** 1306, 1310, 1317, 1330, 1332, 1341, 1354, 1360, 1367, 1374, 1377, 1380, 1384  
**Abdelkawy, Mostafa:** 1564  
**Abdel-Khalek, Amr:** 420  
**Abdellatif, Galila:** 656  
**Abd-Elatif, Mohamed:** 1008  
**Abd-Elatif, Noha:** 1622, 1624  
**Abdelmageed, Haggag:** 474  
**Abdelmaguid, Tamer:** 841  
**Abdel-Maksoud, Gomaa:** 1723  
**Abdel-Malak, Raouf:** 562  
**Abdel-Mobdy, Yasmin:** 471  
**Abdel-Moein, Khaled:** 638  
**Abdel-Moety, Ezzat:** 1311  
**Abdelmoety, Ghada:** 1186  
**Abdelmonem, Nabil:** 710, 718, 719, 721, 723  
**Abdel-Moniem, Ebtsam:** 450  
**Abdelrahman, El-Sayed:** 276, 278  
**Abdelrohman, Mahmoud:** 1687, 1692, 1696  
**Abdel-Salam, Abdel-Salam:** 1691, 1692, 1694  
**Abdelsalam, Rania:** 1570, 1576  
**Abdel-Salam, Zinab:** 641  
**Abdel-Sattar, Essam:** 1532, 1542, 1544, 1547, 1551, 1559

<b>Abdelwahab, Abdel:</b>	1616, 1618	<b>Abuzeid, Ola:</b>	1146
<b>Abdel-Wahab, Yasser:</b>	304	<b>Adham, Fatma:</b>	243
<b>Abdel-Wahed, Naglaa:</b>	1303	<b>Adly, Amr:</b>	728, 730, 744, 750, 789, 811
<b>Abde-Raheem, Heba:</b>	1065	<b>Afifi, Lamia:</b>	1663
<b>Abdo, Ahmed:</b>	103, 107, 134, 321, 669, 674	<b>Afify, Abd El Moneim:</b>	450, 461, 464, 472
<b>Abdo, Tamer:</b>	744, 750	<b>Aga, Mohamed:</b>	1385
<b>Abdou, Manal:</b>	1280	<b>Agha, Aza:</b>	1617
<b>Abdou, Nadra-Elwgoud:</b>	564	<b>Agha, Hala:</b>	1226
<b>Abd-Rabou, Mahmoud:</b>	844	<b>Ahmad, Mohamed:</b>	465
<b>Abdulazim, Mohammed:</b>	1287, 1288	<b>Ahmad, Neveen:</b>	245, 251, 253, 254, 255
<b>Abdulmagead, Ibrahim:</b>	384, 392	<b>Ahmed, Ahmed:</b>	83, 108, 221
<b>Abdulrahman, Eiman:</b>	1032	<b>Ahmed, Ahmed:</b>	128, 136, 139, 141, 152, 153, 154, 155
<b>Abdulrazzak, Omar:</b>	1289	<b>Ahmed, Ahmed:</b>	156
<b>Abdulsalam, Hosni:</b>	673	<b>Ahmed, Amr:</b>	292, 293
<b>Abhar, Hanan:</b>	1568	<b>Ahmed, Ashour:</b>	158, 159
<b>Abo, Mennat:</b>	1025, 1031, 1037	<b>Ahmed, Dalia:</b>	1233
<b>Aboeleela, Magdy:</b>	739, 746	<b>Ahmed, Ekram:</b>	1238, 1241, 1244
<b>Aboelgheit, Samah:</b>	1271	<b>Ahmed, Eman:</b>	1475, 1478, 1479, 1480
<b>Aboelhassan, Diea:</b>	567	<b>Ahmed, Geraldine:</b>	1291
<b>Aboelross, Ehab:</b>	1304	<b>Ahmed, Hanan:</b>	1144, 1145
<b>Abo-Ezz, Eid:</b>	276	<b>Ahmed, Harby:</b>	1726, 1730, 1736
<b>Abo-Gabel, Mahasan:</b>	1046, 1052	<b>Ahmed, Hoda:</b>	131
<b>Abohadima, Samir:</b>	819	<b>Ahmed, Iman:</b>	1513
<b>Abo-Hegab, Al:</b>	420	<b>Ahmed, Mahmoud:</b>	1706
<b>Abo-Hegazy, Samir:</b>	507	<b>Ahmed, Mohamed:</b>	134, 357, 358, 359, 360, 363, 364, 366, 371, 374, 387, 389, 401
<b>Abo-Steit, Mahmoud:</b>	1196	<b>Ahmed, Mohamed:</b>	846, 850, 851
<b>Abo-Taleb, Noha:</b>	1303	<b>Ahmed, Nadia:</b>	99, 100, 122
<b>Abouaish, Ehab:</b>	1700	<b>Ahmed, Nadia:</b>	780, 792
<b>Abouelsaood, Ahmed:</b>	769	<b>Ahmed, Nawal:</b>	418, 424
<b>Abou-Khadra, Maha:</b>	1228, 1229, 1233	<b>Ahmed, Olfat:</b>	589
<b>Aboul-Ela, Nabil:</b>	268	<b>Ahmed, Osama:</b>	465, 471
<b>Aboulela, Waseem:</b>	1286	<b>Ahmed, Saher:</b>	391, 394, 403
<b>Aboul-Enein, Ahmed:</b>	449, 464, 692, 693	<b>Ahmed, Ali:</b>	946, 947, 948, 952
<b>Aboul-Enein, Khalid:</b>	447	<b>Ahmed, Samar:</b>	1272, 1280
<b>Aboulfotouh, Abdel-Nasser:</b>	398	<b>Ahmed, Samia:</b>	559
<b>Aboulfotouh, Abdou:</b>	536	<b>Ahmed, Wael:</b>	420
<b>Aboumoussa, Zinat:</b>	373, 378, 382	<b>Ahmed, Youssri:</b>	291
<b>Abou-Salem, Nermeen:</b>	1174, 1176, 1179	<b>Ahmed, Zakia:</b>	574, 626, 627
<b>Abou-Seri, Sahar:</b>	1433	<b>Alaasar, Mohamed:</b>	69, 72, 73, 132
<b>Abou-Youssef, Hazem:</b>	1024	<b>Al-Agaty, Ahmed:</b>	1009
<b>Abouzeid, Abdel-Zaher:</b>	858, 877	<b>Alalkamy, Essam:</b>	1245
<b>Abouzeid, Ayman:</b>	595, 607	<b>Alamein, Amal:</b>	1350
<b>Abu El-Ela, Faten:</b>	693	<b>Alanani, Naglaa:</b>	1225, 1240
<b>Abu Median, Ahmed:</b>	1039, 1042	<b>Albadri, Ahmed:</b>	1133
<b>Abuarab, Mohamed:</b>	487	<b>Algarem, Hasan:</b>	1099
<b>Abuelfadl, Tamer:</b>	754, 757	<b>Al-Ghobashy, Medhat:</b>	1305, 1307, 1347, 1366, 1386
<b>Abu-Elzahab, Helal:</b>	57, 425	<b>Al-Hameed, Salah:</b>	609
<b>Abulata, Nelly:</b>	1034	<b>Alharery, Mahmoud:</b>	570, 571, 573
<b>Abulkheir, Iman:</b>	1594	<b>Ali, Amr:</b>	1293
<b>Abu-Seida, Ashraf:</b>	617, 618, 620		
<b>Abutaleb, Ahmed S.:</b>	906, 911, 912		
<b>Abu-Taleb, Amira:</b>	59		

<b>Ali, Abdulaziz:</b>	875	<b>Amin, Omnia:</b>	1233
<b>Ali, Amany:</b>	429	<b>Amin, Rehab:</b>	645
<b>Ali, Fatma:</b>	1640	<b>Amin, Shaimaa:</b>	1253
<b>Ali, Galal:</b>	846, 849, 850, 851	<b>Amin, Yasser:</b>	1266, 1267, 1276, 1277
<b>Ali, Hoda:</b>	920	<b>Amir, Azza:</b>	432, 434, 437, 439, 441, 442, 444
<b>Ali, Hosam:</b>	503, 504	<b>Ammar, Rasha:</b>	1252
<b>Ali, Mahmoud:</b>	1404	<b>Anany, Mervat:</b>	1019
<b>Ali, Maisa:</b>	1741	<b>Anbar, Khaled:</b>	1643
<b>Ali, Mohamed:</b>	62	<b>Anis, Hussein:</b>	741
<b>Ali, Mohammed:</b>	1616	<b>Anis, Mohamed:</b>	1647
<b>Ali, Nahla:</b>	1637	<b>Ansary, Mervat:</b>	1021
<b>Ali, Rehab:</b>	446, 463, 467, 469	<b>Anwar, Ghada:</b>	1231, 1660
<b>Ali, Riham:</b>	105, 123	<b>Arab, Hany:</b>	1393
<b>Ali, Shimaa:</b>	103, 134, 669	<b>Arafa, Reem:</b>	1429, 1431, 1434, 1447
<b>Alieldin, Nelly:</b>	1603, 1605	<b>Aref, Mortada:</b>	258
<b>Al-Inany, Hesham:</b>	1172, 1173, 1178	<b>Aref, Wael:</b>	1122
<b>Alkhatib, Mohamed:</b>	1045, 1124, 1134	<b>Arnaout, Heba:</b>	1135
<b>Allah, Elham:</b>	619	<b>Ashmawey, Abeer:</b>	1621
<b>Allah, Mongy:</b>	1146	<b>Ashour, Hani:</b>	520
<b>Allah, Osama:</b>	1107, 1197	<b>Ashour, Hossam:</b>	1419, 1420, 1428
<b>Allam, Nashwa:</b>	1273	<b>Ashour, Rehab:</b>	1561, 1563
<b>Allam, Samy:</b>	369, 370, 380, 398	<b>Ashour, Zainab:</b>	1273
<b>Al-Sawaf, Ahmed:</b>	1181	<b>Assar, Salwa:</b>	958
<b>Alsharnoubi, Jehan:</b>	641, 663	<b>Atiya, Amir:</b>	791
<b>Al-Sherbiney, Heba:</b>	1292	<b>Atta, Nada:</b>	103, 107, 669
<b>Al-Sherbini, El-Sayed:</b>	646, 651	<b>Attaby, Fawzy:</b>	237, 239
<b>Al-Sherbiny, Magdy:</b>	1611	<b>Attalla, Ehab:</b>	48
<b>Al-Shorbagy, Muhammad:</b>	1566	<b>Atteya, Ahmed:</b>	1721, 1722
<b>Alsirafy, Samy:</b>	1049, 1050, 1051, 1056	<b>Attia, Ahmed:</b>	1422
<b>Altalbawy, Farag:</b>	644, 649	<b>Attia, Dina:</b>	1154
<b>Alwakeel, Hanan:</b>	1033	<b>Attia, Osama:</b>	267
<b>Aly, Ahmed:</b>	1115	<b>Attia, Wael:</b>	1242
<b>Aly, Mahmoud:</b>	863, 864, 865, 866, 868	<b>Attiaa, Gerges:</b>	1623
<b>Aly, Mohamed:</b>	475	<b>Awaad, Mohamed:</b>	616
<b>Aly, Salwa:</b>	555	<b>Awad, Hanan:</b>	246, 247, 252, 257
<b>Aly, Samir:</b>	1439	<b>Awad, Manal:</b>	817
<b>Aly, Wael:</b>	1009	<b>Awad, Mohamed:</b>	76, 77, 84, 87, 88
<b>Ameer, Magda:</b>	208	<b>Awadalla, Fayez:</b>	562, 563, 564
<b>Amer, Aziza:</b>	609	<b>Awadallah, Fadi:</b>	1433, 1436
<b>Amer, Dalal:</b>	1258	<b>Awadein, Ahmed:</b>	1187, 1189, 1191, 1193, 1194, 1195
<b>Amer, Hanaa:</b>	56, 57, 68	<b>Ayoub, Essam F.:</b>	897
<b>Amer, Wafaa:</b>	484	<b>Azab, Heba:</b>	1129
<b>Amin, Ahmed:</b>	1158, 1615	<b>Azeem, Mohsen:</b>	1009, 1013
<b>Amin, Amr:</b>	1041, 1043, 1045, 1046, 1052, 1054	<b>Azim, Fadwa:</b>	1030
<b>Amin, Heba:</b>	1391	<b>Aziz, Mohamed:</b>	1101, 1107, 1108, 1113
<b>Amin, Iman:</b>	1071	<b>Aziz, Nahla:</b>	246
<b>Amin, Kamilia:</b>	1433, 1438, 1451, 1452, 1467	<b>Aziz, Ramy:</b>	1415, 1421, 1666
<b>Amin, Magdy:</b>	664	<b>Aziz, Rasha:</b>	1139
<b>Amin, Magdy:</b>	1416, 1423, 1426	<b>Azzam, Omar:</b>	1065
<b>Amin, Maha:</b>	1517	<b>Azzouz, Iftitan:</b>	658, 660
<b>Amin, Mona:</b>	405, 419, 421, 685, 1136, 1137		



**B**

<b>Badawe, Mona:</b>	454
<b>Badawey, Amr:</b>	1307, 1309, 1322, 1334, 1338, 1347, 1356, 1365, 1366, 1369, 1386
<b>Badawey, Amr:</b>	1343, 1356, 1364, 1369
<b>Badawi, Alia:</b>	1506, 1529
<b>Badawy, Mohammed:</b>	86, 89, 169, 170
<b>Badawy, Mohamed:</b>	117, 130
<b>Badawy, Sahar:</b>	1008
<b>Bader, Ahmed:</b>	1398
<b>Badie, Adel:</b>	527, 528, 529, 530, 531
<b>Badran, Mohga:</b>	1477, 1492
<b>Badran, Mona:</b>	1686
<b>Bahaa, Sara:</b>	1059
<b>Bakeer, Adel:</b>	1583
<b>Bakhete, Mahmud:</b>	526
<b>Bakhoun, Sameh:</b>	1248
<b>Bakr, Mona.:</b>	660
<b>Baky, Heba:</b>	26
<b>Barakat, Dalia:</b>	520
<b>Barakat, Maged:</b>	1407
<b>Barsoum, Rashad:</b>	1093
<b>Bary, Ahmed:</b>	1412
<b>Basalious, Emad:</b>	1503, 1516
<b>Basha, Mohammad:</b>	361
<b>Bashtar, Abdel:</b>	408, 413, 679, 682
<b>Bashtar, Abdel-Rahman:</b>	373, 377, 378, 379, 382
<b>Bassal, Taha:</b>	249
<b>Bassiony, Heba:</b>	1136
<b>Bassiouny, Dalia:</b>	1065
<b>Bassiouny, Dalia:</b>	1065
<b>Bassyouni, Iman:</b>	1265, 1267, 1270
<b>Bastawros, Nabil:</b>	292, 293, 296, 299
<b>Basyoni, Maha:</b>	1209, 1210
<b>Baz, Alaa:</b>	1291
<b>Baz, Mohamed:</b>	1232
<b>Baz, Tamer:</b>	1092, 1093, 1099, 1109
<b>Bebawi, Hany:</b>	1309, 1334
<b>Belal, Dawlat:</b>	1132
<b>Belal, Ehab:</b>	1256
<b>Bendas, Ehab:</b>	1502, 1505, 1530
<b>Beshary, Tarek:</b>	777, 778, 815
<b>Beshlawy, Amal:</b>	1030, 1218, 1221, 1223, 1230
<b>Bichir, Salah:</b>	805, 808
<b>Biltagy, Marwa:</b>	1679
<b>Boghdady, Noha:</b>	1401, 1406, 1408
<b>Bohy, Abo:</b>	1280
<b>Boltia, Shereen:</b>	1349, 1378, 1381
<b>Bossiela, Manal:</b>	1073
<b>Brania, Atef:</b>	1731

**D**

<b>Daif, Emad Tawfik:</b>	1297, 1299, 1300, 1301
<b>Dardeer, Tarek:</b>	1619
<b>Darouti, Mohammad:</b>	1059, 1071, 1650
<b>Darweesh, Amira:</b>	1599
<b>Darweesh, Hanan:</b>	1273, 1275
<b>Darweesh, Mohammed:</b>	1213, 1214
<b>Darweesh, Samar:</b>	
<b>Darwish, Dalia:</b>	1048
<b>Darwish, Hany:</b>	1308, 1313, 1314, 1318, 1321, 1324, 1325, 1336, 1355
<b>Darwish, Hebatallah:</b>	1403, 1408
<b>Dawood, Dalia:</b>	1703
<b>Dawood, Kamal:</b>	91, 92, 176, 181, 198, 205, 227
<b>Dawoud, Mohamed:</b>	67
<b>Deeb, Kadriya:</b>	1553
<b>Deeb, Somaya:</b>	434, 437, 439, 442
<b>Dessouky, Ali:</b>	1695
<b>Diab, Aliaa:</b>	1630, 1631
<b>Doha, Eid:</b>	283, 288, 290, 291, 294, 297, 303, 305
<b>Dorgham, Dina:</b>	1059
<b>Dorrah, Hassen:</b>	746
<b>Dorrah, Moataza:</b>	249
<b>Doss, Essam:</b>	1212
<b>Doss, Waheed:</b>	1097, 1102, 1106
<b>Dwidar, Hany:</b>	12, 15

**E**

<b>Ebade, Abdelhay:</b>	1010
<b>Ebid, Anwar Abdelgayed:</b>	1632, 1633
<b>Eddin, Mohamad:</b>	1197
<b>Edmardash, Yusuf:</b>	245
<b>Effat, Dina:</b>	1041
<b>Eihusseiny, Mona:</b>	612
<b>Ei-Shaarawy, Abdel-Fattah:</b>	483
<b>Eishi, Nermine:</b>	1064, 1280
<b>Eissa, Ahmed:</b>	709, 720
<b>Eissa, Amal:</b>	1433, 1443
<b>Eissa, Mohamed:</b>	1286, 1287
<b>Eissa, Mohammed:</b>	1288
<b>Eissa, Saad:</b>	1606
<b>Ekladios, Sherif:</b>	1024
<b>El Hadidi, Nesrin:</b>	1740
<b>El Iraqi, Kassem:</b>	624
<b>El Refaee, Ehab:</b>	1167, 1171

<b>El Sherbini, Ashraf:</b>	398	<b>Eldin, Hanaa:</b>	1096
<b>El Sherbiny, Tharwat:</b>	370, 380, 398, 655	<b>El-Din, Hebat:</b>	1331, 1376
<b>El_Saadany, Zainab:</b>	1025, 1037, 1057	<b>El-Din, Hussein:</b>	738
<b>Elabhar, Ali:</b>	1012	<b>Eldin, Lamiaa:</b>	1565, 1585
<b>Elalla, Mostafa:</b>	1069	<b>Eldin, Mona:</b>	1099
<b>El-Anadouli, Bahgat:</b>	83, 84, 85, 87, 108, 221	<b>El-Fattah, Hussein:</b>	201, 232
<b>Elansary, Afaf:</b>	1476, 1487	<b>Elfeky, Hanaa:</b>	1636, 1638, 1639, 1640, 1641
<b>El-Ansary, Aida:</b>	232, 242, 667	<b>El-Feky, Osama:</b>	1735
<b>Elansary, Osama:</b>		<b>Elfeky, Souad:</b>	645
<b>El-Arnaouty, Sayed:</b>	519, 523	<b>El-Fiky, Nabaweya M.:</b>	1557
<b>El-Askary, Hesham:</b>	1531, 1548, 1552	<b>Elfishawy, Ahlam:</b>	1538, 1541
<b>Elassasy, Abdelhalim:</b>	1514	<b>El-Gamal, Mohamed:</b>	821
<b>El-Asser, Mohamed:</b>	518	<b>El-Gamel, Nadia:</b>	82, 124, 144
<b>Abd El-Aty, Abd El-Aty:</b>	594, 596, 597, 598, 599, 600, 601, 602, 603, 604, 605, 608	<b>El-Gawad, Karima:</b>	540, 541
<b>El-Awady, Basma:</b>	1166	<b>El-Gebaly, Hossam:</b>	390, 393, 400
<b>Elawwad, Abdelsalam:</b>	878	<b>El-Gendy, Essam:</b>	501
<b>Elazab, Nasser:</b>	284, 308, 314, 315	<b>El-Ghandour, Nasser:</b>	1168, 1169
<b>Elbadawy, Samy:</b>	1623	<b>El-Ghani, Monier:</b>	55
<b>El-Badry, Ayman:</b>	1207, 1208, 1211	<b>El-Ghar, Maha:</b>	128
<b>El-Bagary, Ramzia:</b>	1449, 1450, 1454, 1455, 1456, 1458, 1461, 1462, 1463, 1465	<b>El-Ghobary, Mohamed:</b>	1122
<b>El-Bana, Hesham:</b>	502	<b>El-Ghobashy, Mohamed:</b>	1320, 1342, 1373
<b>Elbanna, Elsayed:</b>	852, 860	<b>El-Ghor, Mohamed:</b>	417
<b>Elbannan, Mohamed:</b>	1699, 1712	<b>Elgayed, Sherein :</b>	592, 593, 618, 630, 634
<b>El-Bardicy, Mohammad:</b>	1331, 1376	<b>Elgindi, Abd:</b>	486
<b>Elbaroty, Gamal:</b>	451, 459, 462	<b>El-Gohry, Hatem:</b>	1701, 1702, 1705
<b>El-Bary, Mohamed:</b>	1088, 1113, 1155	<b>Elhabashy, Sameh:</b>	1637, 1669
<b>Elbasiouny, Mahmoud:</b>	662	<b>Elhaddad, Alaa:</b>	1593
<b>Elbatal, Ibrahim:</b>	943, 944, 956, 959, 961, 962, 963, 964, 965	<b>Elhadidi, Basman:</b>	705, 706, 707
<b>El-Batawy, Yasser:</b>	777, 778, 815	<b>Elhakim, Mahmoud:</b>	742
<b>Elbatt, Tamer:</b>	752, 756	<b>El-Halawany, Ali:</b>	1540, 1543, 1549
<b>Elbehairy, Ahmed:</b>	586, 588, 593	<b>El-Hammasy, Hassan:</b>	565
<b>El-Beltagi, Hossam:</b>	450, 452, 453, 454, 456	<b>El-Hawagry, Magdi:</b>	250
<b>El-Beltagy, Mohamed:</b>	782, 801, 816	<b>El-Hawary, Seham:</b>	1540, 1554, 1556, 1563
<b>El-Beshlawy, Mohamed:</b>	1111	<b>El-Hebeary, Mohamed:</b>	838, 842
<b>Elbialy, Nihal:</b>	23, 24, 27	<b>Elhefny, Mohamed:</b>	1619
<b>El-Boghdadi, Hatem:</b>	725	<b>Elhelf, Islam:</b>	1079, 1080
<b>Elborai, Yasser:</b>	1609, 1610	<b>El-Enbaawy, Mona:</b>	574, 577
<b>El-Dahshan, Ahmed:</b>	593, 634	<b>Elhelw, Rehab:</b>	577
<b>El-Deab, Mohamed:</b>	78, 83, 102, 108, 221	<b>Elhilali, Hala:</b>	1188
<b>Eldebss, Taha:</b>	92, 197	<b>Elhossainy, Salwa:</b>	1044
<b>El-Deeb, Heba:</b>	1292, 1293, 1296	<b>El-Idreesy, Tamer:</b>	235
<b>El-Deeb, Manal:</b>	1026	<b>Elkabbany, Farouk:</b>	362
<b>Eldeftar, Moteaa:</b>	181	<b>Elkader, Mohamed:</b>	1170
<b>El-Denshary, Ezz:</b>	1573, 1578, 1580, 1583	<b>Elkady, Ehab:</b>	1439, 1458, 1460, 1463, 1465
<b>El-desoukey, Nermeen:</b>	1582	<b>El-Kady, Maher:</b>	71
<b>El-Dessouky, Maher:</b>	171	<b>El-Kaffas, Khaled:</b>	1066
<b>El-Dib, Nadia:</b>		<b>El-Kafy, Ehab:</b>	1632
<b>El-Dien, Faten.:</b>	120, 211	<b>El-Karakasy, Hanaa:</b>	1234, 1243
<b>Eldin, Hala:</b>	1197	<b>Elkarakasy, Safa:</b>	1023
		<b>El-Kashif, Amr:</b>	1049
		<b>El-Kashoury, El-Sayeda:</b>	1552, 1555
		<b>El-Kashouty, Mohamed:</b>	270

<b>Elkassem, Mohamed:</b>	1177, 1182	<b>El-Rahman, Mahassen:</b>	1088, 1094, 1101, 1102, 1104
<b>Elkhateeb, Sona:</b>	1310	<b>El-Rahman, Hamed:</b>	192, 195
<b>El-Khatib, Aiman:</b>	1575	<b>El-Raziky, Maissa:</b>	1087, 1088, 1094, 1101, 1104, 1112, 1136, 1139, 1147, 1154, 1156
<b>El-Khayat, Waleed:</b>	1186	<b>El-Rehem, Fouad:</b>	446, 469
<b>El-Khayat, Yasser:</b>	999, 1006	<b>El-Rehim, Randa:</b>	1505
<b>Elkorany, Abeer:</b>	926	<b>Elroby, Mahmoud:</b>	1103
<b>El-Koussy, Mohamed:</b>	872, 873	<b>El-Rouby, Dalia:</b>	1302
<b>El-Laithy, Hanan:</b>	1506	<b>Elsaadany, Zinab:</b>	1031
<b>El-Lakkani, Ali:</b>	29, 46	<b>El-Sabaa, Abdel-Aleem:</b>	548, 1209
<b>Ellithi, Ali:</b>	325, 326, 327, 328, 329, 330, 331, 332, 333, 334, 335, 337, 340, 341, 342, 343, 344, 346, 347, 348, 349, 350, 351, 352, 355, 365, 376, 384, 390, 393, 400	<b>El-Said, Alyaa:</b>	432, 441, 444
<b>El-Mahallawi, Iman:</b>	872, 873, 874	<b>El-Said, Hany:</b>	1251, 1252
<b>El-Maksud, Tarek:</b>	392	<b>Elsakhawy, Mohamed:</b>	548
<b>Elmalek, Ehab:</b>	716, 717	<b>El-Sanousi, Ahmed:</b>	577
<b>Elmamlouk, Hussein:</b>	879	<b>El-Sawalhi, Maha:</b>	1393, 1403, 1577
<b>El-Maraghy, Shohda:</b>	1404, 1405, 1565	<b>Elsawi, Khairia:</b>	1629
<b>El-Marsafawy, Magdy:</b>	738	<b>Elsayed, Abir:</b>	1271
<b>El-Marsafy, Sahar:</b>	710, 718, 719	<b>Elsayed, Ahmed:</b>	279, 280
<b>El-Mazny, Ahmed:</b>	1130	<b>El-Sayed, Amr:</b>	556, 557, 558, 559, 560, 566
<b>El-Mazny, Akmal:</b>	1174, 1176, 1179, 1181, 1651, 1652, 1653, 1654	<b>Elsayed, Anwar:</b>	26, 38, 39
<b>Elmegeid, Marwa:</b>	362	<b>Elsayed, Gamal:</b>	521
<b>Elmelegie, Slawa:</b>	1489	<b>Elsayed, Ghada:</b>	1310
<b>El-Merzebany, Mahmoud:</b>	1617	<b>El-Sayed, Ibrahim:</b>	1645
<b>Elmeshad, Aliaa:</b>	1396, 1519, 1522	<b>Elsayed, Khaled A.:</b>	374
<b>Elmessery, Lobna:</b>	1031	<b>El-Sayed, Mohamed:</b>	782, 836
<b>Elmessiery, Medhat:</b>	817, 818	<b>Elsayed, Nehad:</b>	1431
<b>El-Midany, Ayman:</b>	853, 854, 855, 857, 859, 861, 862, 867, 1733	<b>El-Sayed, Aly:</b>	1550, 1562
<b>El-Mistikawy, Tarek:</b>	796, 823	<b>Elsayeh, Bahia:</b>	1566
<b>El-Mofty, Randa:</b>	1188	<b>Elsebaie, Hazem:</b>	1200, 1206
<b>El-Mofty, Salah:</b>	853, 862	<b>El-Sebaie, Wessam:</b>	1516
<b>El-Mofty, Sherine:</b>	1274	<b>El-Seidi, Eman:</b>	1164
<b>Elmoghy, Mohamed:</b>	249	<b>Elserafy, Magdy:</b>	1099, 1111
<b>Elmonem, Ahmed:</b>	24	<b>El-Shabrawi, Mortada:</b>	1220, 1222, 1225, 1235, 1240, 1243
<b>Elmougy, Mahamed:</b>	541	<b>El-Shabrawy, Abdel:</b>	1556
<b>Elnagar, Salah:</b>	525	<b>Elshafeey, Ahmed:</b>	1519
<b>Elnagdy, Sherif:</b>	49, 51, 53	<b>El-Shafei, Mohamed:</b>	1003
<b>Elnaggar, Sahar:</b>	787, 799	<b>El-Shafi, Mohamed:</b>	510, 515
<b>Elnahwy, Salah:</b>	792	<b>Elshahat, Khaled:</b>	585
<b>Elnasr, Hazem:</b>		<b>Elshahed, Mostafa:</b>	738
<b>El-Nassan, Hala:</b>	1471, 1478	<b>Elshair, Inass:</b>	1635
<b>El-Nokety, Mohammad:</b>	526, 527, 530	<b>Elshakhs, Neveen:</b>	1215, 1217, 1219
<b>Elragehy, Nariman:</b>	1306	<b>Elsharkawy, Aisha:</b>	1094, 1106
<b>El-Raghy, Saed M.:</b>	869	<b>El-Shazly, Alaa:</b>	1675
<b>Elrahman, Ahmed:</b>	1511, 1525	<b>El-Shazly, Mohamed:</b>	244
		<b>El-Shazly, Mohamed:</b>	844
		<b>Elshazly, Mostafa:</b>	1089
		<b>Elshehaby, Amal:</b>	1130
		<b>El-Sheikh, Mohamed:</b>	1747
		<b>El-Sheikh, Mohamed:</b>	525

<b>Elshemey, Wael:</b>	33, 34, 35, 36, 39, 48, 666	<b>Ezz, Heba:</b>	418, 424
<b>El-Shemy, Hany:</b>	447, 458, 688, 689, 690, 693	<b>Ezzat, Shahira:</b>	1544, 1550, 1556, 1558
<b>Elshenoufy, Hossam:</b>	1174, 1176	<b>F</b>	
<b>Elsherbiny, Mahmoud:</b>	930, 938	<b>Fadda, Samia:</b>	1281
<b>El-Sherbiny, Mahmoud:</b>	844	<b>Fadel, Osama:</b>	1135
<b>El-Sherbiny, Rami:</b>	880	<b>Faheem, Mena:</b>	555
<b>El-Sherbiny, Walid:</b>	1180	<b>Fahmay, Mohamed:</b>	125, 138, 168, 172, 174
<b>El-Sherif, Ahmed:</b>	90, 125, 137, 140, 142, 168, 172, 173, 174	<b>Fahmi, Abdel Gawad:</b>	94, 180, 236
<b>Elsherpieny, Elsayed:</b>	941, 942, 945, 949, 951, 953, 958	<b>Fahmy, Ahmed:</b>	903, 909
<b>Elshimy, Mohammed:</b>	1286, 1287, 1288, 1289	<b>Fahmy, Aly:</b>	1747
<b>El-Shkra, Mohamed:</b>	108, 113	<b>Fahmy, Ezzat:</b>	1047
<b>El-Soda, Mohamed:</b>	534	<b>Fahmy, Gamal:</b>	54
<b>El-Sofany, Rabie:</b>	1563	<b>Fahmy, Magdy:</b>	590
<b>El-Soud, Walid:</b>	52	<b>Fahmy, Yasser:</b>	1267, 1276, 1277
<b>Eltaher, Maha:</b>	1623	<b>Fakhr, Ibrahim M Y:</b>	1599, 1611, 1612
<b>Eltamawy, Mohamed:</b>	1254	<b>Farag, Ahmad:</b>	95, 104, 163, 181, 197, 205, 213
<b>El-Tantawi, Attia:</b>	1748	<b>Farag, Awatef:</b>	1464, 1468
<b>El-Tantawy, Shoukry:</b>	501	<b>Farag, Magdi:</b>	131
<b>El-Tayeb, El-Sayed:</b>	864	<b>Farag, Mohamed:</b>	1533, 1534, 1535, 1536, 1537, 1539, 1545, 1546
<b>El-Tawdy, Amira:</b>	1062, 1066, 1146	<b>Farag, Mohamed:</b>	353
<b>El-Tawil, Magdy:</b>	784, 825, 835	<b>Farag, Randa:</b>	75, 79
<b>Eltayeb, Osama:</b>	1424	<b>Farag, Sherif:</b>	742, 745
<b>El-Wahab, Azza:</b>	1210	<b>Faragg, Samy:</b>	74, 106, 114
<b>Elwahy, Ahmed:</b>	117, 118, 156	<b>Faramawey, Mohamed:</b>	1298
<b>El-Wakd, Mohammed:</b>	1265	<b>Faramawey, Amr:</b>	1016, 1017
<b>El-Zahab, Essam Abo:</b>	737, 747	<b>Farghali, Haithem:</b>	564
<b>El-Zaher, Asmaa:</b>	1448	<b>Farghaly, Thoraya:</b>	124, 149, 150, 151
<b>El-Zalabani, Soheir:</b>	1546	<b>Farhan, Marwa:</b>	1122
<b>Elzanfaly, Eman:</b>	1323, 1358	<b>Farid, Samar:</b>	1414
<b>Elzawahry, Heba:</b>	1603	<b>Farok, Alaa:</b>	1285
<b>El-Zawawy, Mohamed:</b>	306, 307, 675	<b>Farrag, Affaf:</b>	1111
<b>El-Zeany, Badr:</b>	1313, 1314	<b>Farrag, Azza:</b>	661
<b>Elzorkani, Bassel:</b>	1268, 1274	<b>Farrag, Mona:</b>	1235
<b>Emara, Aala:</b>	1298	<b>Fatah, Ahmed:</b>	1072, 1084
<b>Emara, Khalid:</b>	481, 482, 537	<b>Fatah, Dina:</b>	
<b>Emara, Mohamed:</b>	1602	<b>Fateen, Seif:</b>	711, 714, 715
<b>Esmael, Ihab:</b>	353	<b>Fathalah, Waleed:</b>	1104, 1112, 1113, 1116, 1118
<b>Esmat, Gamal:</b>	1087, 1088, 1090, 1091, 1092, 1093, 1094, 1095, 1098, 1100, 1101, 1104, 1106, 1109, 1110, 1112, 1114, 1136, 1137, 1154, 1156	<b>Fathi, Heba:</b>	1258
<b>Esmat, Samia:</b>	1070	<b>Fathy, Hesham:</b>	1082, 1083
<b>Essa, Khalid:</b>	277, 278	<b>Fathy, Mona:</b>	
<b>Essam, Mahmoud:</b>	832	<b>Fawaz, Lobna:</b>	1232
<b>Eswi, Abeer:</b>	1642	<b>Fawzi, Marwa:</b>	
<b>Ewais, Wael:</b>	1196	<b>Fawzy, Mai:</b>	1414
<b>Eweis, Essam:</b>	1256	<b>Fawzy, Yasser:</b>	662
		<b>Fayed, Adel:</b>	556, 566

<b>Fayed, Hatem:</b>	791
<b>Fayed, Mona:</b>	1680, 1685
<b>Fayek, Magda:</b>	724
<b>Fayek, Nesrin:</b>	1560
<b>Fayez, Ashraf:</b>	999
<b>Fayez, Mohamed:</b>	484, 695
<b>Fekry, Mostafa:</b>	
<b>Fitieh, Amira:</b>	21
<b>Foad, Marwa:</b>	1454, 1455, 1456, 1457
<b>Foda, Ayman:</b>	
<b>Fouad, Hanan:</b>	1139, 1163
<b>Fouad, Hany:</b>	1122
<b>Fouad, Mariam:</b>	1617
<b>Fouda, Mohamed:</b>	776, 790, 795, 798, 827
<b>Fouda, Ragai:</b>	1177
<b>Fouda, Usama:</b>	1177, 1182
<b>Frag, Eman:</b>	211, 222, 223

## G

<b>Gaafar, Hassan:</b>	1186
<b>Gaafar, Taghrid:</b>	1036
<b>Gaber, Ayman:</b>	1600
<b>Gaber, El-Sayed:</b>	1754
<b>Gaber, Wafaa:</b>	1269
<b>Gad, Ahmed:</b>	492
<b>Gadallah, Abdel-Sattar:</b>	659, 660
<b>Gad-Allah, Ahmed:</b>	192, 195
<b>Gahleb, Ahmed:</b>	673
<b>Galal, Fatma:</b>	522
<b>Galal, Hussein:</b>	571
<b>Galal, Khaled:</b>	1056
<b>Galal, Maha:</b>	1311
<b>Galal, Mona:</b>	543, 544, 561
<b>Galal, Nermeen:</b>	1037
<b>Gamal, Yosr:</b>	652, 656
<b>Gawad, Hamdy:</b>	284, 308, 314, 315, 319
<b>Gawad, Iman:</b>	1594
<b>Gawad, Nagwa:</b>	1435, 1445
<b>Gawad, Tarek:</b>	1258
<b>Gawad, Wissam:</b>	36, 46
<b>Gawdat, Heba:</b>	1070, 1073
<b>Gawwad, Adel:</b>	783
<b>Gazayerly, Omaila:</b>	1516, 1528
<b>Gazzar, Iman:</b>	1264
<b>Gazzawi, Nervina:</b>	247
<b>Gedawy, Ehab:</b>	1470
<b>Genidy, Gehad:</b>	109, 110, 120, 126, 129, 130, 171, 193, 194, 211, 222, 223, 241
<b>George, Riham:</b>	1430
<b>Georgey, Hanan:</b>	1435, 1445
<b>Gerguis, Emanuel:</b>	1017

<b>Ghallab, Noha:</b>	
<b>Ghamrawy, Mona:</b>	1133
<b>Ghanem, Hussein:</b>	983, 986, 987, 988, 989
<b>Ghany, Doaa:</b>	1440, 1444
<b>Ghany, Eman:</b>	1239
<b>Gharib, Hassan:</b>	
<b>Gheita, Tamer:</b>	1263, 1264, 1269, 1282, 1664
<b>Gheith, El-Sayed:</b>	516
<b>Gheith, Rasha:</b>	1023
<b>Ghobrial, Emad:</b>	1236, 1237
<b>Ghoneim, Angie:</b>	1527
<b>Ghoneim, Hazem:</b>	1417, 1418
<b>Ghoneim, Nahed:</b>	636, 638
<b>Ghoz, Emad:</b>	1257, 1258
<b>Gohar, Sherif:</b>	1257
<b>Goher, Nabila:</b>	1041
<b>Goma, Hala:</b>	1649
<b>Gomaa, Sobhy:</b>	177, 178, 182, 189, 190, 203, 204, 225, 233
<b>Gouda, Eman:</b>	543, 544
<b>Gouda, Heba:</b>	1027, 1038
<b>Gouda, Iman:</b>	1623
<b>Gouda, Ossama:</b>	731, 736
<b>Grace, Said R.:</b>	774, 788, 803, 807, 816, 828, 829, 835
<b>Guaily, Amr:</b>	771

## H

<b>Habib, Ahmed:</b>	1187
<b>Habib, Enmar:</b>	1286
<b>Hadhoud, Mayada:</b>	
<b>Hady, Ahmed:</b>	2, 3, 11
<b>Hafeez, Ahmed:</b>	1118
<b>Hafez, Amro:</b>	758
<b>Hafez, Hanan:</b>	1116, 1156
<b>Hafez, Rania:</b>	375
<b>Hafeza, Nesreen:</b>	1625
<b>Hafiz, Nagah:</b>	555
<b>Haidara, Mohamed:</b>	1249
<b>Hak, Maha:</b>	1717, 1718
<b>Hakam, Maha:</b>	1298
<b>Halim, Dalia:</b>	1071, 1074, 1075, 1077
<b>Hamad, Hanan:</b>	431
<b>Hamad, Heba:</b>	1635
<b>Hamad, Mohamed:</b>	261
<b>Hamdan, Mohamed:</b>	262, 264, 271
<b>Hamdy, Ahmed:</b>	863
<b>Hamdy, Mona:</b>	1034, 1038
<b>Hamdy, Rim:</b>	55
<b>Hamed, Dina:</b>	1122, 1133, 1139, 1145
<b>Hamed, Safaa:</b>	1724, 1729, 1740



<b>Hameed, Maha:</b>	1477	<b>Hatem, Mahmoud:</b>	577, 615
<b>Hamid, Azza:</b>	1634	<b>Hatem, Mohamed:</b>	490
<b>Hamid, Thoraya:</b>	1588	<b>Hay, Rania:</b>	1062, 1071, 1076, 1077
<b>Hammoud, Khaled:</b>	1287, 1289	<b>Heakal, Fakiha:</b>	206, 207
<b>Hamouda, Nadia:</b>	1349, 1357, 1363, 1378, 1381	<b>Hefnawi, Hala:</b>	1546
<b>Hamza, Haitham:</b>	929	<b>Hefny, Mohamed:</b>	207
<b>Hamza, Hala:</b>	1226, 1227, 1242	<b>Hefny, Shamel:</b>	1177, 1182
<b>Hamza, Nermin:</b>	934	<b>Hegazi, Ayman:</b>	536
<b>Hanafy, Riham:</b>	1007	<b>Hegazi, El-Saeed:</b>	536
<b>Hanna, Mariam:</b>	1126	<b>Hegazi, Nabil:</b>	484, 695, 696
<b>Haroum, Maged:</b>	1251	<b>Hegazy, Gehan:</b>	1434, 1446
<b>Haroun, Ehab:</b>	497, 498, 500	<b>Hegazy, Maha:</b>	1312, 1316, 1326, 1329, 1370, 1382, 1383, 1388
<b>Hasan, Hanan:</b>	1697, 1698	<b>Hegazy, Rania:</b>	1070
<b>Hasanin, Ahmed:</b>	1012	<b>Hegazy, Rehab:</b>	1058, 1059, 1061, 1064, 1066, 1069, 1070, 1071, 1072, 1074, 1075, 1077
<b>Hashem, Abdelgawad:</b>	1425	<b>Helal, Mohamed:</b>	289, 312, 313, 320, 322
<b>Hashem, Ahmed:</b>	1177, 1182	<b>Helal, Nahed:</b>	1224, 1239
<b>Hashem, Mohamed:</b>	540	<b>Helaly, Alexandra:</b>	524, 525
<b>Hashem, Mohamed:</b>	612	<b>Helaly, Mostafa:</b>	485
<b>Hashem, Rasha:</b>	1426	<b>Helmy, Shahinaz:</b>	528
<b>Hassaan, Mohamed:</b>	1298	<b>Hemayed, Elsayed Essa:</b>	724
<b>Hassaballah, Maha:</b>	1089, 1105	<b>Hemeda, Sayed:</b>	1737, 1738, 1739, 1770
<b>Hassan, Abdel-Karim:</b>	761	<b>Hilal, Rifaat:</b>	119, 158, 159, 186
<b>Hassan, Amal:</b>	950, 955	<b>Hilali, Mosaad:</b>	586, 587, 588
<b>Hassan, Walid:</b>	81, 98, 129, 130, 186, 199	<b>Hindawi, Ali:</b>	1107
<b>Hassan, Fayez:</b>	1294	<b>Hoda, El-Sayed:</b>	1756
<b>Hassan, Hanafy:</b>	743, 744, 747, 749, 750	<b>Hosny, Hosam:</b>	999
<b>Hassan, Hazem:</b>	468	<b>Hosny, Mohamed:</b>	1196
<b>Hassan, Hebatallah:</b>	404	<b>Hosny, Wafaa:</b>	168, 208, 209, 216, 668
<b>Hassan, Mariame:</b>	1523, 1667	<b>Hunter, Nahla:</b>	1066
<b>Hassan, Mazen:</b>	1688, 1689	<b>Hunter, Shereen:</b>	1111, 1155
<b>Hassan, Mohamed:</b>	832, 834	<b>Hussein, Abdel-Hamid:</b>	870, 871
<b>Hassan, Mohamed:</b>	1144, 1163	<b>Hussein, Ahmed:</b>	1747
<b>Hassan, Mohamed:</b>	1014	<b>Hussein, Bassem:</b>	360
<b>Hassan, Nagiba:</b>	1306, 1317, 1328, 1335, 1337, 1341, 1349, 1354, 1378, 1381, 1387	<b>Hussein, Ebtissam:</b>	535
<b>Hassan, Naglaa:</b>	1750, 1755	<b>Hussein, Hanaa:</b>	164, 165
<b>Hassan, Safaa:</b>	138	<b>Hussein, Hashem:</b>	535
<b>Hassan, Said:</b>	1313, 1314	<b>Hussein, Hussein:</b>	844
<b>Hassan, Salwa:</b>	1147	<b>Hussein, Mohamed:</b>	1593
<b>Hassan, Taghride:</b>	415, 416	<b>Hussein, Nagwa:</b>	1129, 1135
<b>Hassan, Zeinab:</b>		<b>Hussein, Rania:</b>	1163
<b>Hassaneen, Hamdi:</b>	155, 183, 210, 220	<b>Hussein, Rehab:</b>	426, 445
<b>Hassaneen, Huwaida:</b>	116, 151	<b>Hussein, Sherif:</b>	1131
<b>Hassanien, Aboul:</b>	915, 916, 917, 918, 920, 921, 922, 923, 924, 925, 926, 927, 928	<b>Hussien, Nahed:</b>	417
<b>Hassanien, Mostafa:</b>	1203, 1204	<b>Hussin, Hussin:</b>	626, 627
<b>Hassb-Elnaby, Salah:</b>	639		
<b>Hassib, Hekmat:</b>	242		
<b>Hassib, Sonia:</b>	1464, 1468		

## I

**Iamail, Hamida:** 428

<b>Ibrahem, Mai:</b>	549	<b>Kadry, Mohamed:</b>	430
<b>Ibrahem, Mohamed:</b>	1082, 1083	<b>Kamal, Ahmed:</b>	1188
<b>Ibrahim, Ahmed:</b>	529, 531	<b>Kamal, Aliaa:</b>	1473, 1476
<b>Ibrahim, Ahmed:</b>	268	<b>Kamel, Azza:</b>	1589
<b>Ibrahim, Asmaa:</b>	1605	<b>Kamel, Mona:</b>	1487
<b>Ibrahim, Dalia:</b>	61	<b>Kamel, Nermin:</b>	1027
<b>Ibrahim, Hamed:</b>	661	<b>Kamel, Osama:</b>	1413
<b>Ibrahim, Hayam:</b>	1309, 1316, 1319, 1328, 1334, 1335, 1337, 1339, 1343, 1370, 1375, 1387, 1389	<b>Kammar, Mohamed:</b>	269, 270
<b>Ibrahim, Heba:</b>	1195	<b>Kandeel, Ahmed:</b>	1044, 1055
<b>Ibrahim, Hend:</b>	478	<b>Kandeel, Manal:</b>	1473, 1481, 1490, 1491
<b>Ibrahim, Jehane:</b>	426	<b>Kandil, Zeinab:</b>	1552
<b>Ibrahim, Khaled:</b>	611, 612	<b>Kaoud, Hussein:</b>	593, 621, 622, 623, 628, 629, 630, 631, 632, 633, 634, 635, 700, 701, 702
<b>Ibrahim, Marwa:</b>	549		640
<b>Ibrahim, Mohamed:</b>	487	<b>Kasem, Mohamed:</b>	
<b>Ibrahim, Moheeb:</b>	883, 901	<b>Kasem, Rehab:</b>	
<b>Ibrahim, Nihal:</b>	792	<b>Kassab, Ahmed:</b>	663
<b>Ibrahim, Noha:</b>	1048, 1056	<b>Kassab, Asmaa:</b>	1470
<b>Ibrahim, Sahar:</b>	941, 942, 945, 949, 951, 953	<b>Kassem, Hanaa:</b>	1536
<b>Ibrahim, Sherif:</b>	406	<b>Kassem, Mohamed:</b>	1502
<b>Ibrashy, Ibrahim:</b>	1163	<b>Kassem, Rehab:</b>	1188
<b>Ibrahim, Ghaneya:</b>	1433, 1440	<b>Kawy, Wael:</b>	539
<b>Imam, Sahar:</b>	708	<b>Kelani, Khadiga:</b>	1342, 1373
<b>Isaac, Sally:</b>	1690, 1708	<b>Kenawy, Azza:</b>	1016, 1017
<b>Iskander, Marianne:</b>	1310, 1358, 1521	<b>Kenawy, Sanaa:</b>	1282, 1574, 1577, 1581
<b>Ismael, Eman:</b>	629	<b>Kesba, Hosny:</b>	485
<b>Ismail, Dina:</b>	1063, 1064	<b>Kesha, Hussein:</b>	1034
<b>Ismail, Hebat:</b>	499	<b>Khalaf, Ezz:</b>	259, 260, 265, 266
<b>Ismail, Ismail:</b>	22, 25	<b>Khalaf-Alaa, Perihan.:</b>	209, 216
<b>Ismail, Lamia:</b>	1629	<b>Khaled, Hussein:</b>	458, 1595, 1596, 1597, 1602, 1606
<b>Ismail, Mahmoud:</b>	763		112, 121, 131
<b>Ismail, Mahmoud:</b>	354, 376, 381, 390, 393, 400	<b>Khalial, Gamal:</b>	856
<b>Ismail, Manal:</b>	1396, 1399, 1400, 1407	<b>Khalifa, Waleed:</b>	758, 768
<b>Ismail, Somaya:</b>	427, 433, 436, 443	<b>Khalil, Ahmed:</b>	272
<b>Ismail, Taher:</b>	1153	<b>Khalil, Mohamed:</b>	1009, 1010, 1011, 1013
<b>Ismail, Walaa:</b>	1538	<b>Khalil, Mohamed:</b>	1472, 1475, 1478, 1479, 1480
<b>Ismial, Samir:</b>	463	<b>Khalil, Neveen:</b>	61, 63
<b>Issa, Yousry:</b>	160, 161, 201, 231	<b>Khalil, Wafaa:</b>	23
<b>Issac, Marianne:</b>	1024, 1248	<b>Khashab, Sahier:</b>	1123, 1125, 1126, 1127, 1128, 1132
<b>J</b>			34
<b>Jakee, Jakeen:</b>	571, 575, 576, 578	<b>Khater, Ibrahim:</b>	650, 653
<b>K</b>		<b>Khater, Mohamed:</b>	755
<b>Kadah, Yasser M.:</b>	910	<b>Khatab, Ahmed:</b>	839, 840, 845, 848
<b>Kadry, Hanan:</b>	1485, 1491	<b>Khatab, Aly:</b>	1353, 1388
		<b>Khatab, Fatma:</b>	1094, 1099, 1104, 1106, 1133, 1154
		<b>Khatab, Hany:</b>	1185
		<b>Khatab, Sherif:</b>	1569, 1570, 1572
		<b>Khayyal, Mohamed:</b>	104, 143, 148, 205
		<b>Kheder, Nabila:</b>	647, 648
		<b>Khedr, Amal:</b>	

<b>Khedr, Hesham:</b>	888
<b>Khedr, Mohamed:</b>	655
<b>Khodeir, Mostafa:</b>	1188
<b>Kholy, Amani:</b>	1019
<b>Khorshid, Ola:</b>	1025
<b>Khorshid, Omayma:</b>	1246
<b>Khorshied, Mervat:</b>	1025, 1034, 1035, 1037, 1038, 1065
<b>Khouisa, Mnia:</b>	1526
<b>Kirillos, Farid:</b>	1554
<b>Komy, Mohamed:</b>	1058, 1061, 1502
<b>Koofy, Nehal:</b>	1234
<b>Kord, Maimona:</b>	56, 68
<b>Kyrollos, Emmad:</b>	1047, 1053

## L

<b>Labib, Sameh:</b>	1106
<b>Leheta, Tahra:</b>	1077

## M

<b>Maamoun, Hoda:</b>	1124, 1132
<b>Maarouf, Ahmed:</b>	338
<b>Mabroke, Rania:</b>	497, 500
<b>Mabrouk, Walid:</b>	273, 274, 275
<b>Macky, Tamer:</b>	1190, 1192
<b>Madbuly, Doaa:</b>	1696
<b>Mady, Mohsen:</b>	40
<b>Magdi, Rania:</b>	1033
<b>Mahdy, Dali:</b>	1545
<b>Mahdy, Soliman:</b>	1016
<b>Maher, Manal:</b>	1424, 1427
<b>Maher, Osama:</b>	1593
<b>Mahgoub, Doaa:</b>	1061
<b>Mahgoub, Osama:</b>	745
<b>Mahmoud, Adel:</b>	502, 505
<b>Mahmoud, Ahmed:</b>	902, 904, 907, 908
<b>Mahmoud, Enas:</b>	1129
<b>Mahmoud, Gamalat:</b>	506, 513
<b>Mahmoud, Ghada:</b>	472
<b>Mahmoud, Hayam:</b>	1627, 1628
<b>Mahmoud, Hisham:</b>	374, 639
<b>Mahmoud, Hossam:</b>	1588
<b>Mahmoud, Hussein</b>	1731, 1732, 1733, 1746
<b>Hassan Marey:</b>	
<b>Mahmoud, Jelani:</b>	1262, 1271, 1275
<b>Mahmoud, Mahmoud:</b>	957, 960
<b>Mahmoud, Mona:</b>	1030
<b>Mahmoud, Nisreen:</b>	590
<b>Mahran, Khaled:</b>	547
<b>Maksoud, Abdel-</b>	1611, 1612

<b>Maksoud:</b>	
<b>Mandouh, Rasha:</b>	957
<b>Mandour, Iman:</b>	1231
<b>Mansour, Hesham:</b>	1086
<b>Mansour, Hesham:</b>	383, 385, 386, 388, 395, 396, 397, 402, 677
<b>Mansour, Suzan:</b>	1573, 1578
<b>Mansour, Wael:</b>	1613, 1614
<b>Marei, Waleed:</b>	579, 581, 583
<b>Marouf, Sherief:</b>	568, 571, 575, 578
<b>Marzouk, Abeer:</b>	1527
<b>Marzouk, Hanan:</b>	1155
<b>Marzouk, Mohamed:</b>	882, 883, 884, 885, 887, 892, 893, 896, 898, 900, 901
<b>Marzouk, Samar:</b>	1147, 1156
<b>Mashaly, Heba:</b>	1073
<b>Matter, Motawa:</b>	1615, 1620
<b>Mausouf, Mohamed:</b>	1403
<b>Mawgoud, Youssef:</b>	67
<b>Mazloun, Reda:</b>	1693
<b>Megahed, Mohammad:</b>	786
<b>Megahed, Said:</b>	837, 838, 843
<b>Meguid, Afaf:</b>	248, 257
<b>Mehaisen, Gamal M K:</b>	495
<b>Mehanni, Samah:</b>	1157
<b>Mehanny, Sameh S F:</b>	894
<b>Mehasseb, Marwa:</b>	1088, 1107
<b>Mekawy, Mohey:</b>	635
<b>Mekky, Ahmed:</b>	156
<b>Merey, Hanan:</b>	1311, 1323, 1333, 1348, 1361
<b>Meselhy, Meselhy:</b>	1560
<b>Metwalli, Naema:</b>	377
<b>Metwally, Ahmed:</b>	275, 672
<b>Metwally, Fadia:</b>	1317, 1341, 1354
<b>Metwally, Hala:</b>	1119, 1120
<b>Metwally, Hayman:</b>	17, 18
<b>Metwally, Nadia:</b>	179, 212
<b>Mikhail, Hany:</b>	1089
<b>Mikhail, Wafai:</b>	1753
<b>Mishriki, Amal:</b>	1248
<b>Moawad, Adel:</b>	580, 582, 584, 585
<b>Mobarak, Enas:</b>	1292, 1293, 1294, 1295, 1296
<b>Mofty, Hala:</b>	1197
<b>Mofty, Medhat:</b>	1073, 1074, 1075
<b>Mogawer, Mohamed:</b>	1021
<b>Mohamady, Ibrahim:</b>	1253
<b>Mohamed, Abdo:</b>	36
<b>Mohamed, Abeer:</b>	1096, 1103
<b>Mohamed, Ahmed:</b>	354
<b>Mohamed, Ahmed:</b>	1123, 1124, 1125, 1127, 1128, 1134

Mohamed, Ahmed:	571, 572	Mohsen, Rokaya:	514, 515
Mohamed, Ahmed:	1010	Mokhtar, Mohamed:	1234
Mohamed, Ali:	966	Mokhtar, Omnia:	1412
Mohamed, Amany:	115, 218	Mokhtar, Omnia:	1625
Mohamed, Amr:	249	Monem, Azza:	1554, 1560, 1563
Mohamed, Ayman:	390, 393, 400	Monem, Sayed:	440
Mohamed, Marwa:	211	Monib, Mohamed:	484
Mohamed, Ebtsam:	292	Morsy, Ahmed:	905
Mohamed, Ghada:	1262	Morsy, Hany:	1286, 1287, 1288, 1289
Mohamed, Heba:	1327	Mosaad, Ehab:	1599
Mohamed, Howida:	1494	Mossa, Mohamed:	1560
Mohamed, Hussein:	552, 553, 554	Mossallam, Ghada:	1587, 1588
Mohamed, Ibrahim:	1509	Mostafa, Azza:	1326, 1327, 1352, 1382
Mohamed, Khaled:	1480	Mostafa, Ehab:	487
Mohamed, Labiba:	1629	Mostafa, Fatma:	61
Mohamed, Lamia:	1484	Mostafa, Hanan:	1246
Mohamed, Magda:	417, 431	Mostafa, Mohamed:	992, 1003
Mohamed, Magdi:	1494, 1512	Mostafa, Taymour:	985, 992, 993, 994, 995, 996, 997, 1003, 1005
Mohamed, Mahmoud:	737		
Mohamed, Marwa:	496	Motaal, Amira:	1538
Mohamed, Mervat S.:	1151	Motawi, Tarek:	1397, 1398, 1404, 1405
Mohamed, Mohamed:	643	Mottaleb, Shady:	476
Mohamed, Mohamed:	1243	Moubasher, Hani:	58, 59
Mohamed, Mostafa:	1232, 1662	Mourad, Hebat-Allah:	763
Mohamed, Nadia:	1130	Mourad, Sherif:	895, 899
Mohamed, Noha:	1496, 1520	Mousa, Mahmoud:	1586, 1590, 1591
Mohamed, Rania:	1258	Mousa, Sabry:	561, 565
Mohamed, Saed:	1260	Moussa, Abubakr:	1734
Mohamed, Shaymaa:	548	Moussa, Bahia:	1450, 1459, 1466, 1469
Mohamed, Soheir:	1144	Moussa, Heba:	1589, 1593
Mohamed, Wael:	19, 20	Moussa, Sanaa:	60, 66
Mohamed, Waleed:	1096	Moussa, Tarek:	61
Mohamed, Warda:	1636, 1637, 1638, 1639, 1644	Moustafa, Ahmed:	1611
Mohamed, Zeinat:	50, 64	Moustafa, Gehan:	1634, 1635
Mohammed, Ammar:	932, 933, 934, 935, 936, 939	Moustafa, Ibrahim:	1630, 1631
Mohammed, Ammar:	931, 937	Moustafa, Mohamed:	739
Mohammed, Faten:	591	Moustafa, Omneya:	1427
Mohammed, Fatma:	1638, 1670	Moustafa, Yousry:	663
Mohammed, Haitham:	26, 38, 418, 665	Muhammed, Eman:	1238, 1241, 1244
Mohammed, Samih:	1288	Mukhtar, Ahmed:	1007, 1008, 1012, 1166
Mohammed, Waleed:	299	Mustafa, Hussien:	129, 130
Mohany, Safaa:	1322, 1338, 1345, 1353, 1357, 1362, 1363, 1365, 1368, 1372		
Mohareb, Rafat:	93, 97, 145, 146, 147, 166, 167, 187, 188, 202, 238	N	
Mohey, Abeer:	1269	Nabarawi, Mohammed:	1503, 1504, 1505, 1510, 1512, 1514, 1522, 1524, 1525
Mohsen, Adel:	794	Nabih, Mona:	1130
Mohsen, Amr:	662	Naby, Amal:	1634
Mohsen, Ashraf:	506, 507, 508, 509, 510, 511, 512, 513,	Nada, Mona:	415, 416
		Nafie, Mohammed:	753, 760, 762
		Naga, Mazen:	

<b>Naggar, Mona:</b>	818
<b>Naguib, Bassem:</b>	1472
<b>Naguib, Hala:</b>	112, 121
<b>Naguib, Mohamed:</b>	1117
<b>Nagy, Sayed:</b>	70
<b>Nashar, Rasha:</b>	80, 96, 101, 133
<b>Nasr, Aml:</b>	1020, 1026, 1180
<b>Nasr, Hatem:</b>	1054
<b>Nassar, Ahmed:</b>	721, 723
<b>Nassar, Mamdouh:</b>	210, 256
<b>Nassar, Mohamed:</b>	478
<b>Nassar, Mohamed:</b>	775, 783, 786
<b>Nassar, Noha:</b>	1567, 1571
<b>Nassef, Olodia:</b>	1726
<b>Nazier, Hanan:</b>	1676, 1681
<b>Negm, Hesham:</b>	1082, 1083
<b>Ngouly, Mayada:</b>	1089
<b>Nissan, Yassin:</b>	1432, 1442, 1453
<b>Nooh, Mohammed:</b>	1392, 1395
<b>Noueshi, Mona:</b>	1764
<b>Nurel-Din, Mohamed:</b>	1723

# O

<b>Okasha, Ahmed:</b>	1671, 1672, 1673, 1674
<b>Okasha, Hussein:</b>	
<b>Okasha, Tahsien:</b>	1643, 1668
<b>Okba, Mona:</b>	1553
<b>Omar, Aziza:</b>	257
<b>Omar, Rabab:</b>	1116, 1156
<b>Omar, Waleed:</b>	281
<b>Omran, Dalia:</b>	1105, 1111, 1117, 1118
<b>Oraby, Azza:</b>	1216
<b>Orban, Tamir:</b>	1288
<b>Osman, Heba:</b>	1115
<b>Osman, Kamelia:</b>	568, 569, 570, 573
<b>Osman, Mohamed:</b>	284, 308, 314, 315, 319
<b>Osman, Wafaa:</b>	375
<b>Othman, Ahmed:</b>	1495, 1497, 1498, 1499, 1500
<b>Owis, Ashraf H.:</b>	9, 10, 12, 13, 15, 16

P

**Prince, Abdel:** 556, 566

## R

**Raafat, Hala:** 1263  
**Rabou, Mohamed:** 548  
**Radwan, Ahmed:** 773, 776, 790, 793,

	795, 797, 798, 802, 820, 822, 827, 830
<b>Radwan, Mona:</b>	1129
<b>Radwan, Nasr:</b>	26, 38, 424
<b>Rafik, Hanan:</b>	1719
<b>Ragab, Fatma:</b>	1435, 1445
<b>Ragab, Gaafar:</b>	1131
<b>Ragab, Hisham:</b>	1204
<b>Ragab, Lamis:</b>	1030
<b>Ragab, Yasser:</b>	1427
<b>Rageh, Monira:</b>	27
<b>Ragheb, Marianne:</b>	1448, 1459, 1464, 1466, 1468, 1469
<b>Rahman, Dalia:</b>	1031
<b>Rahman, Khaled:</b>	247
<b>Rahoma, Walid:</b>	14
<b>Rakaiby, Marwa:</b>	1425
<b>Rakhawy, Mona:</b>	1259
<b>Ramadan, Hassan:</b>	478
<b>Ramadan, Nesrin:</b>	1327, 1351, 1352, 1379
<b>Ramadan, Shahira:</b>	1062
<b>Ramadan, Sohair:</b>	429, 438, 686
<b>Ramzy, Gihan:</b>	1254
<b>Rashad, Hassan:</b>	737
<b>Rashed, Laila:</b>	1062, 1063, 1064, 1069, 1122, 1145, 1152, 1157, 1159, 1253, 1558
<b>Rashed, Mhamed:</b>	450
<b>Rashed, Youssef:</b>	886, 889, 891
<b>Rasheed, Hoda:</b>	1061, 1069, 1070, 1146
<b>Ray, Lamis:</b>	1257
<b>Raziky, Mona:</b>	1030, 1142, 1234
<b>Reda, Wafaa:</b>	636
<b>Refaat, Lobna:</b>	1602
<b>Reheem, Nadia:</b>	1603
<b>Rehiem, Ayman:</b>	1089, 1107, 1113, 1116
<b>Rehim, Emam:</b>	452, 460
<b>Ridi, Rashika:</b>	407, 422, 687
<b>Riyadh, Sayed:</b>	143, 148, 177, 178
<b>Rizk, Hussien:</b>	1015, 1018
<b>Rizk, Mohamed:</b>	196, 222
<b>Rizkalla, Christianne:</b>	1515
<b>Robaa, Elsaid:</b>	4
<b>Romeih, Ehab:</b>	517
<b>Romeilah, Ramy:</b>	452, 461
<b>Roshdy, Nagwa:</b>	
<b>Roshdy, Samhia:</b>	1492

**S**

**Saad, Fawzy:** 510, 514  
**Saad, Mohamed:** 737



<b>Saber, Magdi:</b>	1601, 1603, 1604	<b>Samanoudy, Slwan.:</b>	1066
<b>Sabry, Hegazy:</b>		<b>Samer, Mohamed:</b>	488, 489, 490, 491
<b>Sabry, Nirmeen:</b>	1411, 1412, 1414	<b>Samra, Mohamed:</b>	1587, 1601
<b>Sabry, Randa:</b>	1269	<b>Sanad, Manar M.:</b>	486
<b>Sadik, Nermin:</b>	1141, 1402	<b>Saraya, Mona:</b>	1716
<b>Sadik, Nermin:</b>	1148	<b>Saroit, Iman:</b>	929
<b>Saed, Hala:</b>	1687	<b>Sawan, Salah:</b>	1628, 1629
<b>Safina, Sayed:</b>	506, 512	<b>Sawires, Happy:</b>	1661
<b>Said, Abeer:</b>	1008	<b>Sayed, Abeer:</b>	1562
<b>Said, Amal:</b>	1592, 1594	<b>Sayed, Ahmed:</b>	1285
<b>Said, Kareem:</b>	409, 412, 679, 680, 681	<b>Sayed, Ahmed:</b>	1180
<b>Said, Karim:</b>	1014	<b>Sayed, Alaa:</b>	298, 311, 317, 323, 324
<b>Said, Mohamed:</b>	713	<b>Sayed, Riham:</b>	1543, 1544, 1550
<b>Said, Naglaa:</b>		<b>Sayed, Yasmine:</b>	1189
<b>Said, Wael:</b>	1035	<b>Sayyoudh, Mohamed:</b>	864
<b>Sakr, Osama:</b>	493	<b>Seif, Abdulmoneim:</b>	739
<b>Salah Eldien, Mohamed:</b>	1632	<b>Seif, Walaa:</b>	339, 376, 381
<b>Salah, Salwa:</b>	1517	<b>Seifeldin, Ahmed:</b>	1656
<b>Salam, Omar:</b>	713, 717, 721, 723	<b>Seif-El-Nasr, Mona:</b>	1577
<b>Salam, Salwa:</b>	683, 684	<b>Seloma, Yousria:</b>	1643, 1644
<b>Salama, Maha:</b>	1548, 1550, 1558	<b>Senousy, Hoda:</b>	59
<b>Salama, Mohamed:</b>	1611	<b>Serror, Mohammed:</b>	888, 890
<b>Salama, Rabab:</b>	1104, 1112, 1156	<b>Setta, Ahmed:</b>	614
<b>Salama, Randa:</b>	1515, 1518, 1526, 1528	<b>Seyam, Reham:</b>	1295
<b>Salama, Walid:</b>	258	<b>Shaaban, Hebat:</b>	1035, 1602, 1623, 1626
<b>Salama, Zakaria:</b>	1108	<b>Shaaban, Mohamed:</b>	118
<b>Salamouny, Said:</b>	525	<b>Shaarawy, May:</b>	1190
<b>Saleem, Sahar:</b>	1078, 1081	<b>Shaarawy, Mohammed:</b>	1304
<b>Saleh, Doaa:</b>	1097, 1261	<b>Shaata, Elham:</b>	373, 382
<b>Saleh, Mahmoud:</b>	77, 84, 85, 87, 88	<b>Shabana, Marawan:</b>	1558, 1562
<b>Saleh, Marwah:</b>	1060, 1067	<b>Shabana, Reda:</b>	511
<b>Saleh, Mohammed:</b>	741	<b>Shady, Hoda:</b>	356
<b>Saleh, Nesma:</b>	1692	<b>Shaeer, Eman:</b>	991
<b>Saleh, Noha:</b>	24, 39	<b>Shaeer, Kamal:</b>	1006
<b>Saleh, Osiris:</b>	28, 30, 31, 41, 42, 43, 44, 45	<b>Shaeer, Osama:</b>	990, 991
<b>Saleh, Said:</b>	192, 195	<b>Shafik, Amani:</b>	1247
<b>Saleh, Samah:</b>	1021, 1022, 1028	<b>Shahat, Mahmoud:</b>	1769
<b>Salem, Hamed:</b>	895	<b>Shahba, Mohamed:</b>	1749
<b>Salem, Khaled:</b>	1198, 1201, 1205	<b>Shaheen, Amira:</b>	1403
<b>Salem, Maged:</b>	1040	<b>Shaheen, Iman Abdel</b>	1038
<b>Salem, Maissa:</b>	1311, 1313, 1314, 1333, 1342, 1348, 1351, 1373, 1379	<b>Mohsen:</b>	
<b>Salem, Manal:</b>	879, 880	<b>Shaheen, Noha:</b>	1123, 1124, 1125, 1126, 1127, 1128, 1134
<b>Salem, Mohamed:</b>	336	<b>Shaheen, Sherif:</b>	1720
<b>Salem, Mohamed:</b>	1222	<b>Shahin, Nancy:</b>	1397
<b>Salem, Mohamed:</b>	559	<b>Shahin, Rasha:</b>	1023
<b>Salem, Mohammed:</b>	1017	<b>Shaker, Olfat:</b>	1136, 1137, 1138, 1140, 1141, 1142, 1143, 1146, 1147, 1148, 1149, 1150, 1151, 1153, 1154, 1155, 1156, 1158, 1160, 1161, 1162, 1229
<b>Salem, Mostafa:</b>	1188	<b>Shalaby, Ahmad:</b>	1196
<b>Salem, Salem:</b>	1605		
<b>Salem, Suzan:</b>	1477		
<b>Salhin, Ahmed:</b>	1704		
<b>Salib, Samir:</b>	1472		

<b>Shalaby, Emad:</b>	65, 448, 457, 466, 470, 691, 692, 693, 694
<b>Shalaby, Mostafa:</b>	610, 611
<b>Shalash, Ahmed:</b>	759, 761, 762
<b>Shallaly, Nahla:</b>	261
<b>Shamloul, Rany:</b>	983, 984, 998, 999, 1000, 1001, 1002, 1004, 1648
<b>Shamloul, Reham:</b>	1256
<b>Shamma, Rehab:</b>	1507, 1508, 1509, 1513
<b>Shanab, Sanaa:</b>	65, 457
<b>Sharaf, Sahar:</b>	1024
<b>Shaurub, El-Sayed:</b>	248, 671
<b>Shawali, Ahmad:</b>	150, 162, 184, 191, 220
<b>Shawky, Doaa:</b>	770
<b>Shazly, Reem:</b>	1264, 1270
<b>Shehab, Gaber:</b>	465, 471, 1591
<b>Shehab, Ola:</b>	152
<b>Shehata, Mohamed:</b>	157, 191
<b>Shehata, Mostafa:</b>	1319, 1339, 1389
<b>Shehata, Said:</b>	540, 541, 542, 697, 698, 699
<b>Shehata, Samy:</b>	1612
<b>Shenawey, Abdelhameed:</b>	1644
<b>Sherif, Ghada:</b>	1622
<b>Sherif, Mohamed:</b>	1706
<b>Sherif, Sherif:</b>	93
<b>Sherif, Sherif:</b>	1272, 1274, 1281
<b>Shiba, Hala:</b>	1031
<b>Shibl, Mohamed:</b>	159
<b>Shohieb, Amal:</b>	1181
<b>Shokir, Eissa:</b>	876
<b>Shosha, Sherin:</b>	1196
<b>Shoukri, Raguia:</b>	1513
<b>Shouman, Samia:</b>	1617
<b>Shousha, Henda:</b>	1096, 1103
<b>Sidky, Mohamed:</b>	814
<b>Sinna, Eman:</b>	1602, 1622, 1626
<b>Slim, Tarek:</b>	839, 840, 845, 847, 848
<b>Sobhy, Hassan:</b>	504, 1753
<b>Sokkar, Nadia:</b>	1538
<b>Soliman, Ahmed:</b>	90, 142
<b>Soliman, Ahmed:</b>	1106, 1133
<b>Soliman, Ahmed:</b>	609
<b>Soliman, Ahmed M.:</b>	751, 765, 766, 820, 822
<b>Soliman, Amel:</b>	423, 425, 429, 438
<b>Soliman, Amin:</b>	1123, 1124, 1125, 1126, 1127, 1128, 1132, 1134
<b>Soliman, Amira:</b>	1751, 1752, 1771
<b>Soliman, Ashraf:</b>	55
<b>Soliman, Fathy:</b>	1553
<b>Soliman, Hesham:</b>	1199, 1202
<b>Soliman, Khalid:</b>	276

<b>Soliman, Manar:</b>	486
<b>Soliman, Mohamed:</b>	1390
<b>Soliman, Mohamed:</b>	1094
<b>Soliman, Mona:</b>	920
<b>Soliman, Mona:</b>	1122, 1133
<b>Soliman, Said:</b>	1285
<b>Suloma, Ashraf:</b>	485, 497, 498, 500
<b>Sweilam, Nasser:</b>	282, 285, 286, 287, 295, 300, 302, 310, 316, 318, 321, 674

## T

<b>Tabashy, Reda:</b>	1605, 1620
<b>Tadros, Chahir:</b>	1677, 1678, 1682, 1683, 1684, 1687
<b>Tadros, Mina:</b>	1501, 1504, 1510, 1511
<b>Taha, Dalia:</b>	636, 637
<b>Taha, Fatma:</b>	1600
<b>Taha, Sanaa:</b>	913, 914, 919
<b>Taher, Azza:</b>	1446, 1484, 1485
<b>Taher, Mona:</b>	905
<b>Tahoun, Neveen:</b>	1624, 1625
<b>Tahoun, Sameh:</b>	263
<b>Talaat, Neveen:</b>	477, 479, 480
<b>Taleb, Sawsan:</b>	483
<b>Tawadrous, Gamil:</b>	993, 1005
<b>Tawfek, Nehad:</b>	1026
<b>Tayeb, Tarek:</b>	246
<b>Tayel, Saadia:</b>	1503, 1504, 1510
<b>Tomerak, Rania:</b>	1038
<b>Torad, Faisal:</b>	619

## W

<b>Wadid, Magdy:</b>	100, 111, 135, 175, 670
<b>Wadie, Walaa:</b>	1569
<b>Wafa, Mohamed:</b>	801
<b>Wahab, Mohamed:</b>	1, 5, 8
<b>Wahab, Mohamed:</b>	423, 429
<b>Wahba, Amr:</b>	1655
<b>Wali, Iman:</b>	1164
<b>Wanas, Mamdouh:</b>	6, 7, 293
<b>Wassef, Mona:</b>	1032
<b>Weshahy, Soher:</b>	1346
<b>Wifi, Abdalla:</b>	841
<b>Wilson, Adel:</b>	1284

## Y

<b>Yamany, Samar:</b>	613
-----------------------	-----

<b>Yassin, Aymen:</b>	1423, 1426, 1665	<b>Zein, Haggag:</b>	532, 533
<b>Yehia, Ali:</b>	1315, 1326	<b>Zeineldin, Hatem:</b>	726, 727, 729, 732, 733, 734, 735, 740, 748
<b>Yehia, Soad:</b>	1519	<b>Zekri, Abdelrahman:</b>	956, 957, 1096, 1103
<b>Younan, Sandra:</b>	1250	<b>Zickri, Maha:</b>	1119, 1120, 1121
<b>Younis, Jehan:</b>	1043, 1054, 1055	<b>Zwam, Hamdy:</b>	1053
<b>Younis, Mohamed:</b>	772, 779, 785	<b>Zyton, Marwa:</b>	538
<b>Yousef, Hesham:</b>	249		
<b>Yousef, Mamdouh:</b>	1319, 1322, 1338, 1339, 1340, 1344, 1353, 1364, 1365, 1368, 1372		
<b>Yousef, Miriam:</b>	1553, 1562		
<b>Yousef, Randa:</b>	1074, 1075		
<b>Yousef, Shahinaz:</b>	664		
<b>Yousef, Yasmin:</b>	1097, 1099, 1101, 1107, 1108		
<b>Yousif, Ahmed:</b>	494, 499		
<b>Yousif, Tamer:</b>	1424, 1425		
<b>Youssef, Elhusseiny:</b>	56, 68		
<b>Youssef, Hanan:</b>	1459		
<b>Youssef, Helmy Mohamad:</b>	473		
<b>Youssef, Mira:</b>	982, 1253		
<b>Youssef, Mohamed:</b>	1172, 1183, 1184, 1185		
<b>Youssef, Mohamed:</b>	550, 551		
<b>Youssef, Tarek:</b>	650, 653		

## Z

<b>Zaazaa, Adham:</b>	984
<b>Zaazaa, Hala:</b>	1323, 1331, 1332, 1371, 1380, 1384
<b>Zaghla, Hanan:</b>	1644
<b>Zaher, Ahmed:</b>	1055
<b>Zaher, Effat:</b>	538
<b>Zaher, Hesham:</b>	1058, 1070
<b>Zakaria, Mohammed:</b>	1118
<b>Zaki, Hala:</b>	1573, 1574, 1576, 1578, 1579, 1581, 1584
<b>Zaki, Naglaa:</b>	1065
<b>Zaki, Sherif:</b>	982
<b>Zanaty, Fawzia:</b>	1007
<b>Zanaty, Taher:</b>	1020
<b>Zayed, Alia:</b>	244
<b>Zayed, Hania:</b>	1043
<b>Zayed, Naglaa:</b>	1096, 1101, 1102, 1103, 1105, 1155
<b>Zayed, Rania:</b>	1031
<b>Zayed, Shahira:</b>	1033
<b>Zedan, Hamdalaah:</b>	1426
<b>Zeeneldin, Ahmed:</b>	1598, 1599, 1600, 1601, 1603, 1604, 1605, 1608



General Scientific Research Department  
Phone: +(202)35704943 - 35676918 - 35675597  
Fax: +(202)37745324  
Web site: <http://gsrd.cu.edu.eg>.  
[www.cu.edu.eg](http://www.cu.edu.eg)  
E-mail: [resinfo@cu.edu.eg](mailto:resinfo@cu.edu.eg)